



# Contents

- 1. Cover**
- 2. Half Title**
- 3. Title Page**
- 4. Copyright Page**
- 5. Dedication**
- 6. Contents**
- 7. Preface to the Fifth Edition**
- 8. About the Authors**
- 9. PART 1 TRANSPORT PROCESSES:  
MOMENTUM, HEAT, AND MASS**
  - 1. Chapter 1 Introduction to Engineering Principles  
and Units**
    - 1. 1.0 Chapter Objectives**
    - 2. 1.1 Classification of Transport Processes and  
Separation Processes (Unit Operations)**
      - 3. 1.1A Introduction**
      - 2. 1.1B Fundamental Transport Processes**
      - 3. 1.1C Classification of Separation Processes**
      - 4. 1.1D Arrangement in Parts 1 and 2**
    - 3. 1.2 SI System of Basic Units Used in This Text  
and Other Systems**
      - 1. 1.2A SI System of Units**
      - 2. 1.2B CGS System of Units**
      - 3. 1.2C English FPS System of Units**
      - 4. 1.2D Dimensionally Homogeneous  
Equations and Consistent Units**



#### **4. 1.3 Methods of Expressing Temperatures and Compositions**

##### **1. 1.3A Temperature**

##### **2. 1.3B Mole Units and Weight or Mass Units**

##### **3. 1.3C Concentration Units for Liquids**

#### **5. 1.4 Gas Laws and Vapor Pressure**

##### **1. 1.4A Pressure**

##### **2. 1.4B Ideal Gas Law**

##### **3. 1.4C Ideal Gas Mixtures**

##### **4. 1.4D Vapor Pressure and Boiling Point of Liquids**

#### **6. 1.5 Conservation of Mass and Material Balances**

##### **1. 1.5A Conservation of Mass**

##### **2. 1.5B Simple Material Balances**

##### **3. 1.5C Material Balances and Recycle**

##### **4. 1.5D Material Balances and Chemical Reaction**

#### **7. 1.6 Energy and Heat Units**

##### **1. 1.6A Joule, Calorie, and Btu**

##### **2. 1.6B Heat Capacity**

##### **3. 1.6C Latent Heat and Steam Tables**

##### **4. 1.6D Heat of Reaction**

#### **8. 1.7 Conservation of Energy and Heat Balances**

##### **1. 1.7A Conservation of Energy**

##### **2. 1.7B Heat Balances**

#### **9. 1.8 Numerical Methods for Integration**

##### **1. 1.8A Introduction and Graphical Integration**

## **2. 1.8B Numerical Integration and Simpson's Rule**

### **10. 1.9 Chapter Summary**

## **2. Chapter 2 Introduction to Fluids and Fluid Statics**

### **1. 2.0 Chapter Objectives**

#### **2. 2.1 Introduction**

#### **3. 2.2 Fluid Statics**

##### **1. 2.2A Force, Units, and Dimensions**

##### **2. 2.2B Pressure in a Fluid**

##### **3. 2.2C Head of a Fluid**

##### **4. 2.2D Devices to Measure Pressure and Pressure Differences**

#### **4. 2.3 Chapter Summary**

## **3. Chapter 3 Fluid Properties and Fluid Flows**

### **1. 3.0 Chapter Objectives**

#### **2. 3.1 Viscosity of Fluids**

##### **1. 3.1A Newton's Law of Viscosity**

##### **2. 3.1B Momentum Transfer in a Fluid**

##### **3. 3.1C Viscosities of Newtonian Fluids**

#### **3. 3.2 Types of Fluid Flow and Reynolds Number**

##### **1. 3.2A Introduction and Types of Fluid Flow**

##### **2. 3.2B Laminar and Turbulent Flow**

##### **3. 3.2C Reynolds Number**

#### **4. 3.3 Chapter Summary**

## **4. Chapter 4 Overall Mass, Energy, and Momentum Balances**

### **1. 4.0 Chapter Objectives**

## **2. 4.1 Overall Mass Balance and Continuity Equation**

### **1. 4.1A Introduction and Simple Mass Balances**

### **2. 4.1B Control Volume for Balances**

### **3. 4.1C Overall Mass-Balance Equation**

### **4. 4.1D Average Velocity to Use in Overall Mass Balance**

## **3. 4.2 Overall Energy Balance**

### **1. 4.2A Introduction**

### **2. 4.2B Derivation of Overall Energy-Balance Equation**

### **3. 4.2C Overall Energy Balance for a Steady-State Flow System**

### **4. 4.2D Kinetic-Energy Velocity Correction Factor $\alpha$**

### **5. 4.2E Applications of the Overall Energy-Balance Equation**

### **6. 4.2F Overall Mechanical-Energy Balance**

### **7. 4.2G Bernoulli Equation for Mechanical-Energy Balance**

## **4. 4.3 Overall Momentum Balance**

### **1. 4.3A Derivation of the General Equation**

### **2. 4.3B Overall Momentum Balance in a Flow System in One Direction**

### **3. 4.3C Overall Momentum Balance in Two Directions**

### **4. 4.3D Overall Momentum Balance for a Free Jet Striking a Fixed Vane**

## **5. 4.4 Shell Momentum Balance and Velocity Profile in Laminar Flow**

**1. 4.4A Introduction**

**2. 4.4B Shell Momentum Balance Inside a Pipe**

**3. 4.4C Shell Momentum Balance for Falling Film**

**6. 4.5 Chapter Summary**

**5. Chapter 5 Incompressible and Compressible Flows in Pipes**

**1. 5.0 Chapter Objectives**

**2. 5.1 Design Equations for Laminar and Turbulent Flow in Pipes**

**1. 5.1A Velocity Profiles in Pipes**

**2. 5.1B Pressure Drop and Friction Loss in Laminar Flow**

**3. 5.1C Pressure Drop and Friction Factor in Turbulent Flow**

**4. 5.1D Pressure Drop and Friction Factor in the Flow of Gases**

**5. 5.1E Effect of Heat Transfer on the Friction Factor**

**6. 5.1F Friction Losses in Expansion, Contraction, and Pipe Fittings**

**7. 5.1G Friction Loss in Noncircular Conduits**

**8. 5.1H Entrance Section of a Pipe**

**9. 5.1I Selection of Pipe Sizes**

**3. 5.2 Compressible Flow of Gases**

**1. 5.2A Introduction and Basic Equation for Flow in Pipes**

**2. 5.2B Isothermal Compressible Flow**

**3. 5.2C Adiabatic Compressible Flow**

**4. 5.3 Measuring the Flow of Fluids**

- 1. 5.3A Pitot Tube**
- 2. 5.3B Venturi Meter**
- 3. 5.3C Orifice Meter**
- 4. 5.3D Flow-Nozzle Meter**
- 5. 5.3E Variable-Area Flow Meters  
(Rotameters)**
- 6. 5.3F Other Types of Flow Meters**
- 7. 5.3G Flow in Open Channels and Weirs**

## **5. 5.4 Chapter Summary**

## **6. Chapter 6 Flows in Packed and Fluidized Beds**

- 1. 6.0 Chapter Objectives**
- 2. 6.1 Flow Past Immersed Objects**
  - 1. 6.1A Definition of Drag Coefficient for Flow  
Past Immersed Objects**
  - 2. 6.1B Flow Past a Sphere, Long Cylinder,  
and Disk**
- 3. 6.2 Flow in Packed Beds**
- 4. 6.3 Flow in Fluidized Beds**
- 5. 6.4 Chapter Summary**

## **7. Chapter 7 Pumps, Compressors, and Agitation Equipment**

- 1. 7.0 Chapter Objectives**
- 2. 7.1 Pumps and Gas-Moving Equipment**
  - 1. 7.1A Introduction**
  - 2. 7.1B Pumps**
  - 3. 7.1C Gas-Moving Machinery**
  - 4. 7.1D Equations for Compression of Gases**
- 3. 7.2 Agitation, Mixing of Fluids, and Power  
Requirements**
  - 1. 7.2A Purposes of Agitation**

- 2. 7.2B Equipment for Agitation**
- 3. 7.2C Flow Patterns in Agitation**
- 4. 7.2D Typical “Standard” Design of a Turbine**
- 5. 7.2E Power Used in Agitated Vessels**
- 6. 7.2F Agitator Scale-Up**
- 7. 7.2G Mixing Times of Miscible Liquids**
- 8. 7.2H Flow Number and Circulation Rate in Agitation**
- 9. 7.2I Special Agitation Systems**
- 10. 7.2J Mixing of Powders, Viscous Materials, and Pastes**

#### **4. 7.3 Chapter Summary**

### **8. Chapter 8 Differential Equations of Fluid Flow**

#### **1. 8.0 Chapter Objectives**

#### **2. 8.1 Differential Equations of Continuity**

##### **1. 8.1A Introduction**

##### **2. 8.1B Types of Time Derivatives and Vector Notation**

##### **3. 8.1C Differential Equation of Continuity**

#### **3. 8.2 Differential Equations of Momentum Transfer or Motion**

##### **1. 8.2A Derivation of Equations of Momentum Transfer**

##### **2. 8.2B Equations of Motion for Newtonian Fluids with Varying Density and Viscosity**

##### **3. 8.2C Equations of Motion for Newtonian Fluids with Constant Density and Viscosity**

#### **4. 8.3 Use of Differential Equations of Continuity and Motion**

##### **1. 8.3A Introduction**

**2. 8.3B Differential Equations of Continuity and Motion for Flow Between Parallel Plates**

**3. 8.3C Differential Equations of Continuity and Motion for Flow in Stationary and Rotating Cylinders**

**5. 8.4 Chapter Summary**

**9. Chapter 9 Non-Newtonian Fluids**

**1. 9.0 Chapter Objectives**

**2. 9.1 Non-Newtonian Fluids**

**1. 9.1A Types of Non-Newtonian Fluids**

**2. 9.1B Time-Independent Fluids**

**3. 9.1C Time-Dependent Fluids**

**4. 9.1D Viscoelastic Fluids**

**5. 9.1E Laminar Flow of Time-Independent Non-Newtonian Fluids**

**3. 9.2 Friction Losses for Non-Newtonian Fluids**

**1. 9.2A Friction Losses in Contractions, Expansions, and Fittings in Laminar Flow**

**2. 9.2B Turbulent Flow and Generalized Friction Factors**

**4. 9.3 Velocity Profiles for Non-Newtonian Fluids**

**5. 9.4 Determination of Flow Properties of Non-Newtonian Fluids Using a Rotational Viscometer**

**6. 9.5 Power Requirements in Agitation and Mixing of Non-Newtonian Fluids**

**7. 9.6 Chapter Summary**

**10. Chapter 10 Potential Flow and Creeping Flow**

**1. 10.0 Chapter Objectives**

## **2. 10.1 Other Methods for Solution of Differential Equations of Motion**

### **1. 10.1A Introduction**

### **3. 10.2 Stream Function**

### **4. 10.3 Differential Equations of Motion for Ideal Fluids (Inviscid Flow)**

### **5. 10.4 Potential Flow and Velocity Potential**

### **6. 10.5 Differential Equations of Motion for Creeping Flow**

### **7. 10.6 Chapter Summary**

## **11. Chapter 11 Boundary-Layer and Turbulent Flow**

### **1. 11.0 Chapter Objectives**

### **2. 11.1 Boundary-Layer Flow**

#### **1. 11.1A Boundary-Layer Flow**

#### **2. 11.1B Boundary-Layer Separation and the Formation of Wakes**

#### **3. 11.1C Laminar Flow and Boundary-Layer Theory**

### **3. 11.2 Turbulent Flow**

#### **1. 11.2A Nature and Intensity of Turbulence**

#### **2. 11.2B Turbulent Shear or Reynolds Stresses**

#### **3. 11.2C Prandtl Mixing Length**

#### **4. 11.2D Universal Velocity Distribution in Turbulent Flow**

### **4. 11.3 Turbulent Boundary-Layer Analysis**

#### **1. 11.3A Integral Momentum Balance for Boundary-Layer Analysis**

### **5. 11.4 Chapter Summary**

## **12. Chapter 12 Introduction to Heat Transfer**



- 1. 12.0 Chapter Objectives**
- 2. 12.1 Energy and Heat Units**
  - 1. 12.1A Joule, Calorie, and Btu**
  - 2. 12.1B Heat Capacity**
  - 3. 12.1C Latent Heat and Steam Tables**
  - 4. 12.1D Heat of Reaction**
- 3. 12.2 Conservation of Energy and Heat Balances**
  - 1. 12.2A Conservation of Energy**
  - 2. 12.2B Heat Balances**
- 4. 12.3 Conduction and Thermal Conductivity**
  - 1. 12.3A Introduction to Steady-State Heat Transfer**
  - 2. 12.3B Conduction as a Basic Mechanism of Heat Transfer**
  - 3. 12.3C Fourier's Law of Heat Conduction**
  - 4. 12.3D Thermal Conductivity**
- 5. 12.4 Convection**
  - 1. 12.4A Convection as a Basic Mechanism of Heat Transfer**
  - 2. 12.4B Convective Heat-Transfer Coefficient**
- 6. 12.5 Radiation**
  - 1. 12.5A Radiation, a Basic Mechanism of Heat Transfer**
  - 2. 12.5B Radiation to a Small Object from Its Surroundings**
- 7. 12.6 Heat Transfer with Multiple Mechanisms/ Materials**
  - 1. 12.6A Plane Walls in Series**

**2. 12.6B Conduction Through Materials in Parallel**

**3. 12.6C Combined Radiation and Convection Heat Transfer**

**8. 12.7 Chapter Summary**

**13. Chapter 13 Steady-State Conduction**

**1. 13.0 Chapter Objectives**

**2. 13.1 Conduction Heat Transfer**

**1. 13.1A Conduction Through a Flat Slab or Wall (Some Review of Chapter 12)**

**2. 13.1B Conduction Through a Hollow Cylinder**

**3. 13.1C Multilayer Cylinders**

**4. 13.1D Conduction Through a Hollow Sphere**

**3. 13.2 Conduction Through Solids in Series or Parallel with Convection**

**1. 13.2A Combined Convection, Conduction, and Overall Coefficients**

**2. 13.2B Log Mean Temperature Difference and Varying Temperature Drop**

**3. 13.2C Critical Thickness of Insulation for a Cylinder**

**4. 13.2D Contact Resistance at an Interface**

**4. 13.3 Conduction with Internal Heat Generation**

**1. 13.3A Conduction with Internal Heat Generation**

**5. 13.4 Steady-State Conduction in Two Dimensions Using Shape Factors**

1. 13.4A Introduction and Graphical Method for Two-Dimensional Conduction
  2. 13.4B Shape Factors in Conduction
6. 13.5 Numerical Methods for Steady-State Conduction in Two Dimensions
  1. 13.5A Analytical Equation for Conduction
  2. 13.5B Finite-Difference Numerical Methods
7. 13.6 Chapter Summary
14. Chapter 14 Principles of Unsteady-State Heat Transfer
  1. 14.0 Chapter Objectives
  2. 14.1 Derivation of the Basic Equation
    1. 14.1A Introduction
    2. 14.1B Derivation of the Unsteady-State Conduction Equation
  3. 14.2 Simplified Case for Systems with Negligible Internal Resistance
    1. 14.2A Basic Equation
    2. 14.2B Equation for Different Geometries
    3. 14.2C Total Amount of Heat Transferred
  4. 14.3 Unsteady-State Heat Conduction in Various Geometries
    1. 14.3A Introduction and Analytical Methods
    2. 14.3B Unsteady-State Conduction in a Semi-infinite Solid
    3. 14.3C Unsteady-State Conduction in a Large Flat Plate
    4. 14.3D Unsteady-State Conduction in a Long Cylinder
    5. 14.3E Unsteady-State Conduction in a

## **Sphere**

### **6. 14.3F Unsteady-State Conduction in Two- and Three-Dimensional Systems**

### **7. 14.3G Charts for Average Temperature in a Plate, Cylinder, and Sphere with Negligible Surface Resistance**

## **5. 14.4 Numerical Finite-Difference Methods for Unsteady-State Conduction**

### **1. 14.4A Unsteady-State Conduction in a Slab**

### **2. 14.4B Boundary Conditions for Numerical Method for a Slab**

### **3. 14.4C Other Numerical Methods for Unsteady-State Conduction**

## **6. 14.5 Chilling and Freezing of Food and Biological Materials**

### **1. 14.5A Introduction**

### **2. 14.5B Chilling of Food and Biological Materials**

### **3. 14.5C Freezing of Food and Biological Materials**

## **7. 14.6 Differential Equation of Energy Change**

### **1. 14.6A Introduction**

### **2. 14.6B Derivation of Differential Equation of Energy Change**

### **3. 14.6C Special Cases of the Equation of Energy Change**

## **8. 14.7 Chapter Summary**

# **15. Chapter 15 Introduction to Convection**

## **1. 15.0 Chapter Objectives**

## **2. 15.1 Introduction and Dimensional Analysis in**

## **Heat Transfer**

- 1. 15.1A Introduction to Convection (Review)**
- 2. 15.1B Introduction to Dimensionless Groups**
- 3. 15.1C Buckingham Method**
- 3. 15.2 Boundary-Layer Flow and Turbulence in Heat Transfer**
  - 1. 15.2A Laminar Flow and Boundary-Layer Theory in Heat Transfer**
  - 2. 15.2B Approximate Integral Analysis of the Thermal Boundary Layer**
  - 3. 15.2C Prandtl Mixing Length and Eddy Thermal Diffusivity**
- 4. 15.3 Forced Convection Heat Transfer Inside Pipes**
  - 1. 15.3A Heat-Transfer Coefficient for Laminar Flow Inside a Pipe**
  - 2. 15.3B Heat-Transfer Coefficient for Turbulent Flow Inside a Pipe**
  - 3. 15.3C Heat-Transfer Coefficient for Transition Flow Inside a Pipe**
  - 4. 15.3D Heat-Transfer Coefficient for Noncircular Conduits**
  - 5. 15.3E Entrance-Region Effect on the Heat-Transfer Coefficient**
  - 6. 15.3F Liquid-Metals Heat-Transfer Coefficient**
- 5. 15.4 Heat Transfer Outside Various Geometries in Forced Convection**
  - 1. 15.4A Introduction**
  - 2. 15.4B Flow Parallel to a Flat Plate**

3. 15.4C Cylinder with Axis Perpendicular to Flow
4. 15.4D Flow Past a Single Sphere
5. 15.4E Flow Past Banks of Tubes or Cylinders
6. 15.4F Heat Transfer for Flow in Packed Beds
6. 15.5 Natural Convection Heat Transfer
  1. 15.5A Introduction
  2. 15.5B Natural Convection from Various Geometries
7. 15.6 Boiling and Condensation
  1. 15.6A Boiling
  2. 15.6B Condensation
8. 15.7 Heat Transfer of Non-Newtonian Fluids
  1. 15.7A Introduction
  2. 15.7B Heat Transfer Inside Tubes
  3. 15.7C Natural Convection
9. 15.8 Special Heat-Transfer Coefficients
  1. 15.8A Heat Transfer in Agitated Vessels
  2. 15.8B Scraped-Surface Heat Exchangers
  3. 15.8C Extended Surface or Finned Exchangers
10. 15.9 Chapter Summary
16. Chapter 16 Heat Exchangers
  1. 16.0 Chapter Objectives
  2. 16.1 Types of Exchangers
  3. 16.2 Log-Mean-Temperature-Difference Correction Factors

- 4. 16.3 Heat-Exchanger Effectiveness
- 5. 16.4 Fouling Factors and Typical Overall U Values
- 6. 16.5 Double-Pipe Heat Exchanger
- 7. 16.6 Chapter Summary
- 17. Chapter 17 Introduction to Radiation Heat Transfer
  - 1. 17.0 Chapter Objectives
  - 2. 17.1 Introduction to Radiation Heat-Transfer Concepts
    - 1. 17.1A Introduction and Basic Equation for Radiation
    - 2. 17.1B Radiation to a Small Object from Its Surroundings
    - 3. 17.1C Effect of Radiation on the Temperature Measurement of a Gas
  - 3. 17.2 Basic and Advanced Radiation Heat-Transfer Principles
    - 1. 17.2A Introduction and Radiation Spectrum
    - 2. 17.2B Derivation of View Factors in Radiation for Various Geometries
    - 3. 17.2C View Factors When Surfaces Are Connected by Reradiating Walls
    - 4. 17.2D View Factors and Gray Bodies
    - 5. 17.2E Radiation in Absorbing Gases
  - 4. 17.3 Chapter Summary
- 18. Chapter 18 Introduction to Mass Transfer
  - 1. 18.0 Chapter Objectives
  - 2. 18.1 Introduction to Mass Transfer and Diffusion

- 1. 18.1A Similarity of Mass, Heat, and Momentum Transfer Processes**
- 2. 18.1B Examples of Mass-Transfer Processes**
- 3. 18.1C Fick's Law for Molecular Diffusion**
- 4. 18.1D General Case for Diffusion of Gases A and B plus Convection**

### **3. 18.2 Diffusion Coefficient**

- 1. 18.2A Diffusion Coefficients for Gases**
- 2. 18.2B Diffusion Coefficients for Liquids**
- 3. 18.2C Prediction of Diffusivities in Liquids**
- 4. 18.2D Prediction of Diffusivities of Electrolytes in Liquids**
- 5. 18.2E Diffusion of Biological Solutes in Liquids**

### **4. 18.3 Convective Mass Transfer**

- 1. 18.3A Convective Mass-Transfer Coefficient**

### **5. 18.4 Molecular Diffusion Plus Convection and Chemical Reaction**

- 1. 18.4A Different Types of Fluxes and Fick's Law**
- 2. 18.4B Equation of Continuity for a Binary Mixture**
- 3. 18.4C Special Cases of the Equation of Continuity**

### **6. 18.5 Chapter Summary**

## **19. Chapter 19 Steady-State Mass Transfer**

- 1. 19.0 Chapter Objectives**
- 2. 19.1 Molecular Diffusion in Gases**
  - 1. 19.1A Equimolar Counterdiffusion in Gases**



2. 19.1B Special Case for A Diffusing Through Stagnant, Nondiffusing B
  3. 19.1C Diffusion Through a Varying Cross-Sectional Area
  4. 19.1D Multicomponent Diffusion of Gases
3. 19.2 Molecular Diffusion in Liquids
  1. 19.2A Introduction
  2. 19.2B Equations for Diffusion in Liquids
4. 19.3 Molecular Diffusion in Solids
  1. 19.3A Introduction and Types of Diffusion in Solids
  2. 19.3B Diffusion in Solids Following Fick's Law
  3. 19.3C Diffusion in Porous Solids That Depends on Structure
5. 19.4 Diffusion of Gases in Porous Solids and Capillaries
  1. 19.4A Introduction
  2. 19.4B Knudsen Diffusion of Gases
  3. 19.4C Molecular Diffusion of Gases
  4. 19.4D Transition-Region Diffusion of Gases
  5. 19.4E Flux Ratios for Diffusion of Gases in Capillaries
  6. 19.4F Diffusion of Gases in Porous Solids
6. 19.5 Diffusion in Biological Gels
7. 19.6 Special Cases of the General Diffusion Equation at Steady State
  1. 19.6A Special Cases of the General Diffusion Equation at Steady State
8. 19.7 Numerical Methods for Steady-State

## **Molecular Diffusion in Two Dimensions**

### **1. 19.7A Derivation of Equations for Numerical Methods**

### **2. 19.7B Equations for Special Boundary Conditions for Numerical Method**

### **9. 19.8 Chapter Summary**

## **20. Chapter 20 Unsteady-State Mass Transfer**

### **1. 20.0 Chapter Objectives**

### **2. 20.1 Unsteady-State Diffusion**

#### **1. 20.1A Derivation of a Basic Equation**

#### **2. 20.1B Diffusion in a Flat Plate with Negligible Surface Resistance**

#### **3. 20.1C Unsteady-State Diffusion in Various Geometries**

### **3. 20.2 Unsteady-State Diffusion and Reaction in a Semi-Infinite Medium**

#### **1. 20.2A Unsteady-State Diffusion and Reaction in a Semi-Infinite Medium**

### **4. 20.3 Numerical Methods for Unsteady-State Molecular Diffusion**

#### **1. 20.3A Introduction**

#### **2. 20.3B Unsteady-State Numerical Methods for Diffusion**

#### **3. 20.3C Boundary Conditions for Numerical Methods for a Slab**

### **5. 20.4 Chapter Summary**

## **21. Chapter 21 Convective Mass Transfer**

### **1. 21.0 Chapter Objectives**

### **2. 21.1 Convective Mass Transfer**

1. 21.1A Introduction to Convective Mass Transfer
2. 21.1B Types of Mass-Transfer Coefficients
3. 21.1C Mass-Transfer Coefficients for the General Case of A and B Diffusing and Convective Flow Using Film Theory
4. 21.1D Mass-Transfer Coefficients under High Flux Conditions
5. 21.1E Methods for Experimentally Determining Mass-Transfer Coefficients
3. 21.2 Dimensional Analysis in Mass Transfer
  1. 21.2A Introduction
  2. 21.2B Dimensional Analysis for Convective Mass Transfer
4. 21.3 Mass-Transfer Coefficients for Various Geometries
  1. 21.3A Dimensionless Numbers Used to Correlate Data
  2. 21.3B Analogies among Mass, Heat, and Momentum Transfer
  3. 21.3C Derivation of Mass-Transfer Coefficients in Laminar Flow
  4. 21.3D Mass Transfer for Flow Inside Pipes
  5. 21.3E Mass Transfer for Flow Outside Solid Surfaces
5. 21.4 Mass Transfer to Suspensions of Small Particles
  1. 21.4A Introduction
  2. 21.4B Equations for Mass Transfer to Small Particles
6. 21.5 Models for Mass-Transfer Coefficients

- 1. 21.5A Laminar Flow and Boundary-Layer Theory in Mass Transfer**
- 2. 21.5B Prandtl Mixing Length and Turbulent Eddy Mass Diffusivity**
- 3. 21.5C Models for Mass-Transfer Coefficients**

## **7. 21.6 Chapter Summary**

# **10. PART 2 SEPARATION PROCESS PRINCIPLES**

## **1. Chapter 22 Absorption and Stripping**

- 1. 22.0 Chapter Objectives**
- 2. 22.1 Equilibrium and Mass Transfer Between Phases**
  - 1. 22.1A Phase Rule and Equilibrium**
  - 2. 22.1B Gas–Liquid Equilibrium**
  - 3. 22.1C Single-Stage Equilibrium Contact**
  - 4. 22.1D Single-Stage Equilibrium Contact for a Gas–Liquid System**
  - 5. 22.1E Countercurrent Multiple-Contact Stages**
  - 6. 22.1F Analytical Equations for Countercurrent Stage Contact**
  - 7. 22.1G Introduction and Equilibrium Relations**
  - 8. 22.1H Concentration Profiles in Interphase Mass Transfer**
  - 9. 22.1I Mass Transfer Using Film Mass-Transfer Coefficients and Interface Concentrations**
  - 10. 22.1J Overall Mass-Transfer Coefficients and Driving Forces**
- 3. 22.2 Introduction to Absorption**

1. 22.2A Absorption
  2. 22.2B Equipment for Absorption and Distillation
4. 22.3 Pressure Drop and Flooding in Packed Towers
5. 22.4 Design of Plate Absorption Towers
6. 22.5 Design of Packed Towers for Absorption
  1. 22.5A Introduction to Design of Packed Towers for Absorption
  2. 22.5B Simplified Design Methods for Absorption of Dilute Gas Mixtures in Packed Towers
  3. 22.5C Design of Packed Towers Using Transfer Units
7. 22.6 Efficiency of Random-Packed and Structured Packed Towers
  1. 22.6A Calculating the Efficiency of Random-Packed and Structured Packed Towers
  2. 22.6B Estimation of Efficiencies of Tray and Packed Towers
8. 22.7 Absorption of Concentrated Mixtures in Packed Towers
9. 22.8 Estimation of Mass-Transfer Coefficients for Packed Towers
  1. 22.8A Experimental Determination of Film Coefficients
  2. 22.8B Correlations for Film Coefficients
  3. 22.8C Predicting Mass-Transfer Film Coefficients
10. 22.9 Heat Effects and Temperature Variations

## **in Absorption**

### **1. 22.9A Heat Effects in Absorption**

### **2. 22.9B Simplified Design Method**

## **11. 22.10 Chapter Summary**

## **2. Chapter 23 Humidification Processes**

### **1. 23.0 Chapter Objectives**

### **2. 23.1 Vapor Pressure of Water and Humidity**

#### **1. 23.1A Vapor Pressure of Water**

#### **2. 23.1B Humidity and a Humidity Chart**

#### **3. 23.1C Adiabatic Saturation Temperatures**

#### **4. 23.1D Wet Bulb Temperature**

### **3. 23.2 Introduction and Types of Equipment for Humidification**

### **4. 23.3 Theory and Calculations for Cooling-Water Towers**

#### **1. 23.3A Theory and Calculations for Cooling-Water Towers**

#### **2. 23.3B Design of Water-Cooling Tower Using Film Mass-Transfer Coefficients**

#### **3. 23.3C Design of Water-Cooling Tower Using Overall Mass-Transfer Coefficients**

#### **4. 23.3D Minimum Value of Air Flow**

#### **5. 23.3E Design of Water-Cooling Tower Using the Height of a Transfer Unit**

#### **6. 23.3F Temperature and Humidity of an Air Stream in a Tower**

#### **7. 23.3G Dehumidification Tower**

### **5. 23.4 Chapter Summary**

## **3. Chapter 24 Filtration and Membrane Separation Processes (Liquid–Liquid or Solid–Liquid Phase)**

- 1. 24.0 Chapter Objectives**
- 2. 24.1 Introduction to Dead-End Filtration**
  - 1. 24.1A Introduction**
  - 2. 24.1B Types of Filtration Equipment**
  - 3. 24.1C Filter Media and Filter Aids**
- 3. 24.2 Basic Theory of Filtration**
  - 1. 24.2A Introduction to the Basic Theory of Filtration**
  - 2. 24.2B Filtration Equations for Constant-Pressure Filtration**
  - 3. 24.2C Filtration Equations for Constant-Rate Filtration**
- 4. 24.3 Membrane Separations**
  - 1. 24.3A Introduction**
  - 2. 24.3B Classification of Membrane Processes**
- 5. 24.4 Microfiltration Membrane Processes**
  - 1. 24.4A Introduction**
  - 2. 24.4B Models for Microfiltration**
- 6. 24.5 Ultrafiltration Membrane Processes**
  - 1. 24.5A Introduction**
  - 2. 24.5B Types of Equipment for Ultrafiltration**
  - 3. 24.5C Flux Equations for Ultrafiltration**
  - 4. 24.5D Effects of Processing Variables in Ultrafiltration**
- 7. 24.6 Reverse-Osmosis Membrane Processes**
  - 1. 24.6A Introduction**
  - 2. 24.6B Flux Equations for Reverse Osmosis**
  - 3. 24.6C Effects of Operating Variables**

4. **24.6D Concentration Polarization in Reverse-Osmosis Diffusion Model**
5. **24.6E Permeability Constants for Reverse-Osmosis Membranes**
6. **24.6F Types of Equipment for Reverse Osmosis**
7. **24.6G Complete-Mixing Model for Reverse Osmosis**
8. **24.7 Dialysis**
  1. **24.7A Series Resistances in Membrane Processes**
  2. **24.7B Dialysis Processes**
  3. **24.7C Types of Equipment for Dialysis**
  4. **24.7D Hemodialysis in an Artificial Kidney**
9. **24.8 Chapter Summary**
4. **Chapter 25 Gaseous Membrane Systems**
  1. **25.0 Chapter Objectives**
  2. **25.1 Gas Permeation**
    1. **25.1A Series Resistances in Membrane Processes**
    2. **25.1B Types of Membranes and Permeabilities for Separation of Gases**
    3. **25.1C Types of Equipment for Gas-Permeation Membrane Processes**
    4. **25.1D Introduction to Types of Flow in Gas Permeation**
  3. **25.2 Complete-Mixing Model for Gas Separation by Membranes**
    1. **25.2A Basic Equations Used**
    2. **25.2B Solution of Equations for Design of a Complete-Mixing Case**



**3. 25.2C Minimum Concentration of Reject Stream**

**4. 25.3 Complete-Mixing Model for Multicomponent Mixtures**

**1. 25.3A Derivation of Equations**

**2. 25.3B Iteration Solution Procedure for Multicomponent Mixtures**

**5. 25.4 Cross-Flow Model for Gas Separation by Membranes**

**1. 25.4A Derivation of the Basic Equations**

**2. 25.4B Procedure for Design of Cross-Flow Case**

**6. 25.5 Derivation of Equations for Countercurrent and Cocurrent Flow for Gas Separation by Membranes**

**1. 25.5A Concentration Gradients in Membranes**

**2. 25.5B Derivation of Equations for Countercurrent Flow in Dense-Phase Symmetric Membranes**

**3. 25.5C Solution of Countercurrent Flow Equations in Dense-Phase Symmetric Membranes**

**4. 25.5D Derivation of Equations for Countercurrent Flow in Asymmetric Membranes**

**5. 25.5E Derivation of Equations for Cocurrent Flow in Asymmetric Membranes**

**6. 25.5F Effects of Processing Variables on Gas Separation**

**7. 25.6 Derivation of Finite-Difference Numerical**

## **Method for Asymmetric Membranes**

- 1. 25.6A Countercurrent Flow**
- 2. 25.6B Short-Cut Numerical Method**
- 3. 25.6C Use of a Spreadsheet for the Finite-Difference Numerical Method**
- 4. 25.6D Calculation of Pressure-Drop Effects on Permeation**

## **8. 25.7 Chapter Summary**

## **5. Chapter 26 Distillation**

- 1. 26.0 Chapter Objectives**
- 2. 26.1 Equilibrium Relations Between Phases**
  - 1. 26.1A Phase Rule and Raoult's Law**
  - 2. 26.1B Boiling-Point Diagrams and x-y Plots**
- 3. 26.2 Single and Multiple Equilibrium Contact Stages**
  - 1. 26.2A Equipment for Distillation**
  - 2. 26.2B Single-Stage Equilibrium Contact for Vapor-Liquid System**
- 4. 26.3 Simple Distillation Methods**
  - 1. 26.3A Introduction**
  - 2. 26.3B Relative Volatility of Vapor-Liquid Systems**
  - 3. 26.3C Equilibrium or Flash Distillation**
  - 4. 26.3D Simple Batch or Differential Distillation**
  - 5. 26.3E Simple Steam Distillation**
- 5. 26.4 Binary Distillation with Reflux Using the McCabe-Thiele and Lewis Methods**
  - 1. 26.4A Introduction to Distillation with**

## **Reflux**

- 2. 26.4B McCabe–Thiele Method of Calculation for the Number of Theoretical Stages**
- 3. 26.4C Total and Minimum Reflux Ratio for McCabe–Thiele Method**
- 4. 26.4D Special Cases for Rectification Using the McCabe–Thiele Method**

## **6. 26.5 Tray Efficiencies**

- 1. 26.5A Tray Efficiencies**
- 2. 26.5B Types of Tray Efficiencies**
- 3. 26.5C Relationship Between Tray Efficiencies**

## **7. 26.6 Flooding Velocity and Diameter of Tray Towers Plus Simple Calculations for Reboiler and Condenser Duties**

- 1. 26.6A Flooding Velocity and Diameter of Tray Towers**
- 2. 26.6B Condenser and Reboiler Duties Using the McCabe–Thiele Method**

## **8. 26.7 Fractional Distillation Using the Enthalpy–Concentration Method**

- 1. 26.7A Enthalpy–Concentration Data**
- 2. 26.7B Distillation in the Enriching Section of a Tower**
- 3. 26.7C Distillation in the Stripping Section of a Tower**

## **9. 26.8 Distillation of Multicomponent Mixtures**

- 1. 26.8A Introduction to Multicomponent Distillation**
- 2. 26.8B Equilibrium Data in Multicomponent**

## **Distillation**

- 3. 26.8C Boiling Point, Dew Point, and Flash Distillation**
- 4. 26.8D Key Components in Multicomponent Distillation**
- 5. 26.8E Total Reflux for Multicomponent Distillation**
- 6. 26.8F Shortcut Method for the Minimum Reflux Ratio for Multicomponent Distillation**
- 7. 26.8G Shortcut Method for Number of Stages at Operating Reflux Ratio**

## **10. 26.9 Chapter Summary**

## **6. Chapter 27 Liquid–Liquid Extraction**

- 1. 27.0 Chapter Objectives**
- 2. 27.1 Introduction to Liquid–Liquid Extraction**
  - 1. 27.1A Introduction to Extraction Processes**
  - 2. 27.1B Equilibrium Relations in Extraction**
- 3. 27.2 Single-Stage Equilibrium Extraction**
  - 1. 27.2A Single-Stage Equilibrium Extraction**
- 4. 27.3 Types of Equipment and Design for Liquid–Liquid Extraction**
  - 1. 27.3A Introduction and Equipment Types**
  - 2. 27.3B Mixer–Settlers for Extraction**
  - 3. 27.3C Spray Extraction Towers**
  - 4. 27.3D Packed Extraction Towers**
  - 5. 27.3E Perforated-Plate (Sieve-Tray) Extraction Towers**
  - 6. 27.3F Pulsed Packed and Sieve-Tray Towers**
  - 7. 27.3G Mechanically Agitated Extraction**

## **Towers**

### **5. 27.4 Continuous Multistage Countercurrent Extraction**

- 1. 27.4A Introduction**
- 2. 27.4B Continuous Multistage Countercurrent Extraction**
- 3. 27.4C Countercurrent-Stage Extraction with Immiscible Liquids**
- 4. 27.4D Design of Towers for Extraction**
- 5. 27.4E Design of Packed Towers for Extraction Using Mass-Transfer Coefficients**

### **6. 27.5 Chapter Summary**

## **7. Chapter 28 Adsorption and Ion Exchange**

- 1. 28.0 Chapter Objectives**
- 2. 28.1 Introduction to Adsorption Processes**
  - 1. 28.1A Introduction**
  - 2. 28.1B Physical Properties of Adsorbents**
  - 3. 28.1C Equilibrium Relations for Adsorbents**
- 3. 28.2 Batch Adsorption**
- 4. 28.3 Design of Fixed-Bed Adsorption Columns**
  - 1. 28.3A Introduction and Concentration Profiles**
  - 2. 28.3B Breakthrough Concentration Curve**
  - 3. 28.3C Mass-Transfer Zone**
  - 4. 28.3D Capacity of Column and Scale-Up Design Method**
  - 5. 28.3E Basic Models for Predicting Adsorption**
  - 6. 28.3F Processing Variables and Adsorption**

## **Cycles**

### **5. 28.4 Ion-Exchange Processes**

- 1. 28.4A Introduction and Ion-Exchange Materials**
- 2. 28.4B Equilibrium Relations in Ion Exchange**
- 3. 28.4C Use of Equilibrium Relations and Relative-Molar-Selectivity Coefficients**
- 4. 28.4D Concentration Profiles and Breakthrough Curves**
- 5. 28.4E Capacity of Columns and Scale-Up Design Method**

### **6. 28.5 Chapter Summary**

## **8. Chapter 29 Crystallization and Particle Size Reduction**

### **1. 29.0 Chapter Objectives**

### **2. 29.1 Introduction to Crystallization**

- 1. 29.1A Crystallization and Types of Crystals**
- 2. 29.1B Equilibrium Solubility in Crystallization**
- 3. 29.1C Yields, Material, and Energy Balances in Crystallization**
- 4. 29.1D Equipment for Crystallization**

### **3. 29.2 Crystallization Theory**

- 1. 29.2A Introduction**
- 2. 29.2B Nucleation Theories**
- 3. 29.2C Rate of Crystal Growth and the  $\Delta L$  Law**
- 4. 29.2D Particle Size Distribution of Crystals**
- 5. 29.2E Model for Mixed Suspension–Mixed Product Removal Crystallizer**

#### **4. 29.3 Mechanical Size Reduction**

##### **1. 29.3A Introduction**

##### **2. 29.3B Particle Size Measurement**

##### **3. 29.3C Energy and Power Required in Size Reduction**

##### **4. 29.3D Equipment for Particle Size Reduction**

#### **5. 29.4 Chapter Summary**

### **9. Chapter 30 Settling, Sedimentation, and Centrifugation**

#### **1. 30.0 Chapter Objectives**

#### **2. 30.1 Settling and Sedimentation in Particle–Fluid Separation**

##### **1. 30.1A Introduction**

##### **2. 30.1B Theory of Particle Movement Through a Fluid**

##### **3. 30.1C Hindered Settling**

##### **4. 30.1D Wall Effect on Free Settling**

##### **5. 30.1E Differential Settling and Separation of Solids in Classification**

##### **6. 30.1F Sedimentation and Thickening**

##### **7. 30.1G Equipment for Settling and Sedimentation**

#### **3. 30.2 Centrifugal Separation Processes**

##### **1. 30.2A Introduction**

##### **2. 30.2B Forces Developed in Centrifugal Separation**

##### **3. 30.2C Equations for Rates of Settling in Centrifuges**

##### **4. 30.2D Centrifuge Equipment for Sedimentation**

**5. 30.2E Centrifugal Filtration**

**6. 30.2F Gas–Solid Cyclone Separators**

**4. 30.3 Chapter Summary**

**10. Chapter 31 Leaching**

**1. 31.0 Chapter Objectives**

**2. 31.1 Introduction and Equipment for Liquid–Solid Leaching**

**1. 31.1A Leaching Processes**

**2. 31.1B Preparation of Solids for Leaching**

**3. 31.1C Rates of Leaching**

**4. 31.1D Types of Equipment for Leaching**

**3. 31.2 Equilibrium Relations and Single-Stage Leaching**

**1. 31.2A Equilibrium Relations in Leaching**

**2. 31.2B Single-Stage Leaching**

**4. 31.3 Countercurrent Multistage Leaching**

**1. 31.3A Introduction and Operating Line for Countercurrent Leaching**

**2. 31.3B Variable Underflow in Countercurrent Multistage Leaching**

**3. 31.3C Constant Underflow in Countercurrent Multistage Leaching**

**5. 31.4 Chapter Summary**

**11. Chapter 32 Evaporation**

**1. 32.0 Chapter Objectives**

**2. 32.1 Introduction**

**1. 32.1A Purpose**

**2. 32.1B Processing Factors**



### **3. 32.2 Types of Evaporation Equipment and Operation Methods**

#### **1. 32.2A General Types of Evaporators**

#### **2. 32.2B Methods of Evaporator Operations**

### **4. 32.3 Overall Heat-Transfer Coefficients in Evaporators**

### **5. 32.4 Calculation Methods for Single-Effect Evaporators**

#### **1. 32.4A Heat and Material Balances for Evaporators**

#### **2. 32.4B Effects of Processing Variables on Evaporator Operation**

#### **3. 32.4C Boiling-Point Rise of Solutions**

#### **4. 32.4D Enthalpy–Concentration Charts of Solutions**

### **6. 32.5 Calculation Methods for Multiple-Effect Evaporators**

#### **1. 32.5A Introduction**

#### **2. 32.5B Temperature Drops and Capacity of Multiple-Effect Evaporators**

#### **3. 32.5C Calculations for Multiple-Effect Evaporators**

#### **4. 32.5D Step-by-Step Calculation Methods for Triple-Effect Evaporators**

### **7. 32.6 Condensers for Evaporators**

#### **1. 32.6A Introduction**

#### **2. 32.6B Surface Condensers**

#### **3. 32.6C Direct-Contact Condensers**

### **8. 32.7 Evaporation of Biological Materials**

#### **1. 32.7A Introduction and Properties of**

## **Biological Materials**

### **2. 32.7B Fruit Juices**

### **3. 32.7C Sugar Solutions**

### **4. 32.7D Paper-Pulp Waste Liquors**

## **9. 32.8 Evaporation Using Vapor Recompression**

### **1. 32.8A Introduction**

### **2. 32.8B Mechanical Vapor-Recompression Evaporator**

### **3. 32.8C Thermal Vapor-Recompression Evaporator**

## **10. 32.9 Chapter Summary**

## **12. Chapter 33 Drying**

### **1. 33.0 Chapter Objectives**

### **2. 33.1 Introduction and Methods of Drying**

#### **1. 33.1A Purposes of Drying**

### **3. 33.2 Equipment for Drying**

#### **1. 33.2A Tray Dryer**

#### **2. 33.2B Vacuum-Shelf Indirect Dryers**

#### **3. 33.2C Continuous Tunnel Dryers**

#### **4. 33.2D Rotary Dryers**

#### **5. 33.2E Drum Dryers**

#### **6. 33.2F Spray Dryers**

#### **7. 33.2G Drying Crops and Grains**

### **4. 33.3 Vapor Pressure of Water and Humidity**

#### **1. 33.3A Vapor Pressure of Water**

#### **2. 33.3B Humidity and Humidity Chart**

#### **3. 33.3C Adiabatic Saturation Temperatures**

#### **4. 33.3D Wet Bulb Temperature**

### **5. 33.4 Equilibrium Moisture Content of**

## **Materials**

- 1. 33.4A Introduction**
- 2. 33.4B Experimental Data of Equilibrium Moisture Content for Inorganic and Biological Materials**
- 3. 33.4C Bound and Unbound Water in Solids**
- 4. 33.4D Free and Equilibrium Moisture of a Substance**

## **6. 33.5 Rate-of-Drying Curves**

- 1. 33.5A Introduction and Experimental Methods**
- 2. 33.5B Rate of Drying Curves for Constant-Drying Conditions**
- 3. 33.5C Drying in the Constant-Rate Period**
- 4. 33.5D Drying in the Falling-Rate Period**
- 5. 33.5E Moisture Movements in Solids During Drying in the Falling-Rate Period**

## **7. 33.6 Calculation Methods for a Constant-Rate Drying Period**

- 1. 33.6A Method for Using an Experimental Drying Curve**
- 2. 33.6B Method Using Predicted Transfer Coefficients for Constant-Rate Period**
- 3. 33.6C Effect of Process Variables on a Constant-Rate Period**

## **8. 33.7 Calculation Methods for the Falling-Rate Drying Period**

- 1. 33.7A Method Using Numerical Integration**
- 2. 33.7B Calculation Methods for Special Cases in Falling-Rate Region**

## **9. 33.8 Combined Convection, Radiation, and**

## **Conduction Heat Transfer in the Constant-Rate Period**

### **1. 33.8A Introduction**

### **2. 33.8B Derivation of the Equation for Convection, Conduction, and Radiation**

## **10. 33.9 Drying in the Falling-Rate Period by Diffusion and Capillary Flow**

### **1. 33.9A Introduction**

### **2. 33.9B Liquid Diffusion of Moisture in Drying**

### **3. 33.9C Capillary Movement of Moisture in Drying**

### **4. 33.9D Comparison of Liquid Diffusion and Capillary Flow**

## **11. 33.10 Equations for Various Types of Dryers**

### **1. 33.10A Through-Circulation Drying in Packed Beds**

### **2. 33.10B Tray Drying with Varying Air Conditions**

### **3. 33.10C Material and Heat Balances for Continuous Dryers**

### **4. 33.10D Continuous Countercurrent Drying**

## **12. 33.11 Freeze-Drying of Biological Materials**

### **1. 33.11A Introduction**

### **2. 33.11B Derivation of Equations for Freeze-Drying**

## **13. 33.12 Unsteady-State Thermal Processing and Sterilization of Biological Materials**

### **1. 33.12A Introduction**

### **2. 33.12B Thermal Death-Rate Kinetics of**

## **Microorganisms**

### **3. 33.12C Determination of Thermal Process Time for Sterilization**

### **4. 33.12D Sterilization Methods Using Other Design Criteria**

### **5. 33.12E Pasteurization**

### **6. 33.12F Effects of Thermal Processing on Food Constituents**

## **14. 33.13 Chapter Summary**

## **11. PART 3 APPENDIXES**

### **1. Appendix A.1 Fundamental Constants and Conversion Factors**

### **2. Appendix A.2 Physical Properties of Water**

### **3. Appendix A.3 Physical Properties of Inorganic and Organic Compounds**

### **4. Appendix A.4 Physical Properties of Foods and Biological Materials**

### **5. Appendix A.5 Properties of Pipes, Tubes, and Screens**

### **6. Appendix A.6 Lennard-Jones Potentials as Determined from Viscosity Data**

## **12. Notation**

## **13. Index**

# **Landmarks**

## **1. Cover**

## **2. Contents**

### **1. i**

### **2. ii**

### **3. iii**

4. iv
5. v
6. vi
7. vii
8. viii
9. ix
10. x
11. xi
12. xii
13. xiii
14. xiv
15. xv
16. xvi
17. xvii
18. xviii
19. xix
20. xx
21. xxi
22. xxii
23. xxiii
24. xxiv
25. xxv
26. xxvi
27. xxvii
28. xxviii
29. xxix
30. xxx
31. xxxi
32. xxxii
33. 1
34. 2
35. 3
36. 4
37. 5

38. 6  
39. 7  
40. 8  
41. 9  
42. 10  
43. 11  
44. 12  
45. 13  
46. 14  
47. 15  
48. 16  
49. 17  
50. 18  
51. 19  
52. 20  
53. 21  
54. 22  
55. 23  
56. 24  
57. 25  
58. 26  
59. 27  
60. 28  
61. 29  
62. 30  
63. 31  
64. 32  
65. 33  
66. 34  
67. 35  
68. 36  
69. 37  
70. 38  
71. 39

72. 40  
73. 41  
74. 42  
75. 43  
76. 44  
77. 45  
78. 46  
79. 47  
80. 48  
81. 49  
82. 50  
83. 51  
84. 52  
85. 53  
86. 54  
87. 55  
88. 56  
89. 57  
90. 58  
91. 59  
92. 60  
93. 61  
94. 62  
95. 63  
96. 64  
97. 65  
98. 66  
99. 67  
100. 68  
101. 69  
102. 70  
103. 71  
104. 72  
105. 73



**106. 74**  
**107. 75**  
**108. 76**  
**109. 77**  
**110. 78**  
**111. 79**  
**112. 80**  
**113. 81**  
**114. 82**  
**115. 83**  
**116. 84**  
**117. 85**  
**118. 86**  
**119. 87**  
**120. 88**  
**121. 89**  
**122. 90**  
**123. 91**  
**124. 92**  
**125. 93**  
**126. 94**  
**127. 95**  
**128. 96**  
**129. 97**  
**130. 98**  
**131. 99**  
**132. 100**  
**133. 101**  
**134. 102**  
**135. 103**  
**136. 104**  
**137. 105**  
**138. 106**  
**139. 107**

140. 108  
141. 109  
142. 110  
143. 111  
144. 112  
145. 113  
146. 114  
147. 115  
148. 116  
149. 117  
150. 118  
151. 119  
152. 120  
153. 121  
154. 122  
155. 123  
156. 124  
157. 125  
158. 126  
159. 127  
160. 128  
161. 129  
162. 130  
163. 131  
164. 132  
165. 133  
166. 134  
167. 135  
168. 136  
169. 137  
170. 138  
171. 139  
172. 140  
173. 141

174. 142  
175. 143  
176. 144  
177. 145  
178. 146  
179. 147  
180. 148  
181. 149  
182. 150  
183. 151  
184. 152  
185. 153  
186. 154  
187. 155  
188. 156  
189. 157  
190. 158  
191. 159  
192. 160  
193. 161  
194. 162  
195. 163  
196. 164  
197. 165  
198. 166  
199. 167  
200. 168  
201. 169  
202. 170  
203. 171  
204. 172  
205. 173  
206. 174  
207. 175

208. 176  
209. 177  
210. 178  
211. 179  
212. 180  
213. 181  
214. 182  
215. 183  
216. 184  
217. 185  
218. 186  
219. 187  
220. 188  
221. 189  
222. 190  
223. 191  
224. 192  
225. 193  
226. 194  
227. 195  
228. 196  
229. 197  
230. 198  
231. 199  
232. 200  
233. 201  
234. 202  
235. 203  
236. 204  
237. 205  
238. 206  
239. 207  
240. 208  
241. 209

242. 210  
243. 211  
244. 212  
245. 213  
246. 214  
247. 215  
248. 216  
249. 217  
250. 218  
251. 219  
252. 220  
253. 221  
254. 222  
255. 223  
256. 224  
257. 225  
258. 226  
259. 227  
260. 228  
261. 229  
262. 230  
263. 231  
264. 232  
265. 233  
266. 234  
267. 235  
268. 236  
269. 237  
270. 238  
271. 239  
272. 240  
273. 241  
274. 242  
275. 243

276. 244  
277. 245  
278. 246  
279. 247  
280. 248  
281. 249  
282. 250  
283. 251  
284. 252  
285. 253  
286. 254  
287. 255  
288. 256  
289. 257  
290. 258  
291. 259  
292. 260  
293. 261  
294. 262  
295. 263  
296. 264  
297. 265  
298. 266  
299. 267  
300. 268  
301. 269  
302. 270  
303. 271  
304. 272  
305. 273  
306. 274  
307. 275  
308. 276  
309. 277

310. 278  
311. 279  
312. 280  
313. 281  
314. 282  
315. 283  
316. 284  
317. 285  
318. 286  
319. 287  
320. 288  
321. 289  
322. 290  
323. 291  
324. 292  
325. 293  
326. 294  
327. 295  
328. 296  
329. 297  
330. 298  
331. 299  
332. 300  
333. 301  
334. 302  
335. 303  
336. 304  
337. 305  
338. 306  
339. 307  
340. 308  
341. 309  
342. 310  
343. 311

344. 312  
345. 313  
346. 314  
347. 315  
348. 316  
349. 317  
350. 318  
351. 319  
352. 320  
353. 321  
354. 322  
355. 323  
356. 324  
357. 325  
358. 326  
359. 327  
360. 328  
361. 329  
362. 330  
363. 331  
364. 332  
365. 333  
366. 334  
367. 335  
368. 336  
369. 337  
370. 338  
371. 339  
372. 340  
373. 341  
374. 342  
375. 343  
376. 344  
377. 345



**378. 346**

**379. 347**

**380. 348**

**381. 349**

**382. 350**

**383. 351**

**384. 352**

**385. 353**

**386. 354**

**387. 355**

**388. 356**

**389. 357**

**390. 358**

**391. 359**

**392. 360**

**393. 361**

**394. 362**

**395. 363**

**396. 364**

**397. 365**

**398. 366**

**399. 367**

**400. 368**

**401. 369**

**402. 370**

**403. 371**

**404. 372**

**405. 373**

**406. 374**

**407. 375**

**408. 376**

**409. 377**

**410. 378**

**411. 379**

**412. 380**

**413. 381**

**414. 382**

**415. 383**

**416. 384**

**417. 385**

**418. 386**

**419. 387**

**420. 388**

**421. 389**

**422. 390**

**423. 391**

**424. 392**

**425. 393**

**426. 394**

**427. 395**

**428. 396**

**429. 397**

**430. 398**

**431. 399**

**432. 400**

**433. 401**

**434. 402**

**435. 403**

**436. 404**

**437. 405**

**438. 406**

**439. 407**

**440. 408**

**441. 409**

**442. 410**

**443. 411**

**444. 412**

**445. 413**

446. 414  
447. 415  
448. 416  
449. 417  
450. 418  
451. 419  
452. 420  
453. 421  
454. 422  
455. 423  
456. 424  
457. 425  
458. 426  
459. 427  
460. 428  
461. 429  
462. 430  
463. 431  
464. 432  
465. 433  
466. 434  
467. 435  
468. 436  
469. 437  
470. 438  
471. 439  
472. 440  
473. 441  
474. 442  
475. 443  
476. 444  
477. 445  
478. 446  
479. 447

480. 448  
481. 449  
482. 450  
483. 451  
484. 452  
485. 453  
486. 454  
487. 455  
488. 456  
489. 457  
490. 458  
491. 459  
492. 460  
493. 461  
494. 462  
495. 463  
496. 464  
497. 465  
498. 466  
499. 467  
500. 468  
501. 469  
502. 470  
503. 471  
504. 472  
505. 473  
506. 474  
507. 475  
508. 476  
509. 477  
510. 478  
511. 479  
512. 480  
513. 481

**514. 482**

**515. 483**

**516. 484**

**517. 485**

**518. 486**

**519. 487**

**520. 488**

**521. 489**

**522. 490**

**523. 491**

**524. 492**

**525. 493**

**526. 494**

**527. 495**

**528. 496**

**529. 497**

**530. 498**

**531. 499**

**532. 500**

**533. 501**

**534. 502**

**535. 503**

**536. 504**

**537. 505**

**538. 506**

**539. 507**

**540. 508**

**541. 509**

**542. 510**

**543. 511**

**544. 512**

**545. 513**

**546. 514**

**547. 515**

548. 516  
549. 517  
550. 518  
551. 519  
552. 520  
553. 521  
554. 522  
555. 523  
556. 524  
557. 525  
558. 526  
559. 527  
560. 528  
561. 529  
562. 530  
563. 531  
564. 532  
565. 533  
566. 534  
567. 535  
568. 536  
569. 537  
570. 538  
571. 539  
572. 540  
573. 541  
574. 542  
575. 543  
576. 544  
577. 545  
578. 546  
579. 547  
580. 548  
581. 549

**582. 550**

**583. 551**

**584. 552**

**585. 553**

**586. 554**

**587. 555**

**588. 556**

**589. 557**

**590. 558**

**591. 559**

**592. 560**

**593. 561**

**594. 562**

**595. 563**

**596. 564**

**597. 565**

**598. 566**

**599. 567**

**600. 568**

**601. 569**

**602. 570**

**603. 571**

**604. 572**

**605. 573**

**606. 574**

**607. 575**

**608. 576**

**609. 577**

**610. 578**

**611. 579**

**612. 580**

**613. 581**

**614. 582**

**615. 583**

**616. 584**

**617. 585**

**618. 586**

**619. 587**

**620. 588**

**621. 589**

**622. 590**

**623. 591**

**624. 592**

**625. 593**

**626. 594**

**627. 595**

**628. 596**

**629. 597**

**630. 598**

**631. 599**

**632. 600**

**633. 601**

**634. 602**

**635. 603**

**636. 604**

**637. 605**

**638. 606**

**639. 607**

**640. 608**

**641. 609**

**642. 610**

**643. 611**

**644. 612**

**645. 613**

**646. 614**

**647. 615**

**648. 616**

**649. 617**



650. 618

651. 619

652. 620

653. 621

654. 622

655. 623

656. 624

657. 625

658. 626

659. 627

660. 628

661. 629

662. 630

663. 631

664. 632

665. 633

666. 634

667. 635

668. 636

669. 637

670. 638

671. 639

672. 640

673. 641

674. 642

675. 643

676. 644

677. 645

678. 646

679. 647

680. 648

681. 649

682. 650

683. 651

**684. 652**

**685. 653**

**686. 654**

**687. 655**

**688. 656**

**689. 657**

**690. 658**

**691. 659**

**692. 660**

**693. 661**

**694. 662**

**695. 663**

**696. 664**

**697. 665**

**698. 666**

**699. 667**

**700. 668**

**701. 669**

**702. 670**

**703. 671**

**704. 672**

**705. 673**

**706. 674**

**707. 675**

**708. 676**

**709. 677**

**710. 678**

**711. 679**

**712. 680**

**713. 681**

**714. 682**

**715. 683**

**716. 684**

**717. 685**

**718. 686**

**719. 687**

**720. 688**

**721. 689**

**722. 690**

**723. 691**

**724. 692**

**725. 693**

**726. 694**

**727. 695**

**728. 696**

**729. 697**

**730. 698**

**731. 699**

**732. 700**

**733. 701**

**734. 702**

**735. 703**

**736. 704**

**737. 705**

**738. 706**

**739. 707**

**740. 708**

**741. 709**

**742. 710**

**743. 711**

**744. 712**

**745. 713**

**746. 714**

**747. 715**

**748. 716**

**749. 717**

**750. 718**

**751. 719**

**752. 720**

**753. 721**

**754. 722**

**755. 723**

**756. 724**

**757. 725**

**758. 726**

**759. 727**

**760. 728**

**761. 729**

**762. 730**

**763. 731**

**764. 732**

**765. 733**

**766. 734**

**767. 735**

**768. 736**

**769. 737**

**770. 738**

**771. 739**

**772. 740**

**773. 741**

**774. 742**

**775. 743**

**776. 744**

**777. 745**

**778. 746**

**779. 747**

**780. 748**

**781. 749**

**782. 750**

**783. 751**

**784. 752**

**785. 753**

**786. 754**

**787. 755**

**788. 756**

**789. 757**

**790. 758**

**791. 759**

**792. 760**

**793. 761**

**794. 762**

**795. 763**

**796. 764**

**797. 765**

**798. 766**

**799. 767**

**800. 768**

**801. 769**

**802. 770**

**803. 771**

**804. 772**

**805. 773**

**806. 774**

**807. 775**

**808. 776**

**809. 777**

**810. 778**

**811. 779**

**812. 780**

**813. 781**

**814. 782**

**815. 783**

**816. 784**

**817. 785**

**818. 786**

**819. 787**

**820. 788**

**821. 789**

**822. 790**

**823. 791**

**824. 792**

**825. 793**

**826. 794**

**827. 795**

**828. 796**

**829. 797**

**830. 798**

**831. 799**

**832. 800**

**833. 801**

**834. 802**

**835. 803**

**836. 804**

**837. 805**

**838. 806**

**839. 807**

**840. 808**

**841. 809**

**842. 810**

**843. 811**

**844. 812**

**845. 813**

**846. 814**

**847. 815**

**848. 816**

**849. 817**

**850. 818**

**851. 819**

**852. 820**

**853. 821**

854. 822

855. 823

856. 824

857. 825

858. 826

859. 827

860. 828

861. 829

862. 830

863. 831

864. 832

865. 833

866. 834

867. 835

868. 836

869. 837

870. 838

871. 839

872. 840

873. 841

874. 842

875. 843

876. 844

877. 845

878. 846

879. 847

880. 848

881. 849

882. 850

883. 851

884. 852

885. 853

886. 854

887. 855

**888. 856**

**889. 857**

**890. 858**

**891. 859**

**892. 860**

**893. 861**

**894. 862**

**895. 863**

**896. 864**

**897. 865**

**898. 866**

**899. 867**

**900. 868**

**901. 869**

**902. 870**

**903. 871**

**904. 872**

**905. 873**

**906. 874**

**907. 875**

**908. 876**

**909. 877**

**910. 878**

**911. 879**

**912. 880**

**913. 881**

**914. 882**

**915. 883**

**916. 884**

**917. 885**

**918. 886**

**919. 887**

**920. 888**

**921. 889**



**922. 890**

**923. 891**

**924. 892**

**925. 893**

**926. 894**

**927. 895**

**928. 896**

**929. 897**

**930. 898**

**931. 899**

**932. 900**

**933. 901**

**934. 902**

**935. 903**

**936. 904**

**937. 905**

**938. 906**

**939. 907**

**940. 908**

**941. 909**

**942. 910**

**943. 911**

**944. 912**

**945. 913**

**946. 914**

**947. 915**

**948. 916**

**949. 917**

**950. 918**

**951. 919**

**952. 920**

**953. 921**

**954. 922**

**955. 923**

**956. 924**

**957. 925**

**958. 926**

**959. 927**

**960. 928**

**961. 929**

**962. 930**

**963. 931**

**964. 932**

**965. 933**

**966. 934**

**967. 935**

**968. 936**

**969. 937**

**970. 938**

**971. 939**

**972. 940**

**973. 941**

**974. 942**

**975. 943**

**976. 944**

**977. 945**

**978. 946**

**979. 947**

**980. 948**

**981. 949**

**982. 950**

**983. 951**

**984. 952**

**985. 953**

**986. 954**

**987. 955**

**988. 956**

**989. 957**

990. 958  
991. 959  
992. 960  
993. 961  
994. 962  
995. 963  
996. 964  
997. 965  
998. 966  
999. 967  
1000. 968  
1001. 969  
1002. 970  
1003. 971  
1004. 972  
1005. 973  
1006. 974  
1007. 975  
1008. 976  
1009. 977  
1010. 978  
1011. 979  
1012. 980  
1013. 981  
1014. 982  
1015. 983  
1016. 984  
1017. 985  
1018. 986  
1019. 987  
1020. 988  
1021. 989  
1022. 990  
1023. 991

1024. 992  
1025. 993  
1026. 994  
1027. 995  
1028. 996  
1029. 997  
1030. 998  
1031. 999  
1032. 1000  
1033. 1001  
1034. 1002  
1035. 1003  
1036. 1004  
1037. 1005  
1038. 1006  
1039. 1007  
1040. 1008  
1041. 1009  
1042. 1010  
1043. 1011  
1044. 1012  
1045. 1013  
1046. 1014  
1047. 1015  
1048. 1016  
1049. 1017  
1050. 1018  
1051. 1019  
1052. 1020  
1053. 1021  
1054. 1022  
1055. 1023  
1056. 1024  
1057. 1025

**1058. 1026**

**1059. 1027**

**1060. 1028**

**1061. 1029**

**1062. 1030**

**1063. 1031**

**1064. 1032**

**1065. 1033**

**1066. 1034**

**1067. 1035**

**1068. 1036**

**1069. 1037**

**1070. 1038**

**1071. 1039**

**1072. 1040**

**1073. 1041**

**1074. 1042**

**1075. 1043**

**1076. 1044**

**1077. 1045**

**1078. 1046**

**1079. 1047**

**1080. 1048**

**1081. 1049**

**1082. 1050**

**1083. 1051**

**1084. 1052**

**1085. 1053**

**1086. 1054**

**1087. 1055**

**1088. 1056**

**1089. 1057**

**1090. 1058**

**1091. 1059**

**1092. 1060**

**1093. 1061**

**1094. 1062**

**1095. 1063**

**1096. 1064**

**1097. 1065**

**1098. 1066**

**1099. 1067**

**1100. 1068**

**1101. 1069**

**1102. 1070**

**1103. 1071**

**1104. 1072**

**1105. 1073**

**1106. 1074**

**1107. 1075**

**1108. 1076**

**1109. 1077**

**1110. 1078**

**1111. 1079**

**1112. 1080**

**1113. 1081**

**1114. 1082**

**1115. 1083**

**1116. 1084**

**1117. 1085**

**1118. 1086**

**1119. 1087**

**1120. 1088**

**1121. 1089**

**1122. 1090**

**1123. 1091**

**1124. 1092**

**1125. 1093**

**1126. 1094**

**1127. 1095**

**1128. 1096**

**1129. 1097**

**1130. 1098**

**1131. 1099**

**1132. 1100**

**1133. 1101**

**1134. 1102**

**1135. 1103**

**1136. 1104**

**1137. 1105**

**1138. 1106**

**1139. 1107**

**1140. 1108**

**1141. 1109**

**1142. 1110**

**1143. 1111**

**1144. 1112**

**1145. 1113**

**1146. 1114**

**1147. 1115**

**1148. 1116**

**1149. 1117**

**1150. 1118**

**1151. 1119**

**1152. 1120**

**1153. 1121**

**1154. 1122**

**1155. 1123**

**1156. 1124**

**1157. 1125**

**1158. 1126**

**1159. 1127**

1160. 1128  
1161. 1129  
1162. 1130  
1163. 1131  
1164. 1132  
1165. 1133  
1166. 1134  
1167. 1135  
1168. 1136  
1169. 1137  
1170. 1138  
1171. 1139  
1172. 1140  
1173. 1141  
1174. 1142  
1175. 1143  
1176. 1144  
1177. 1145  
1178. 1146  
1179. 1147  
1180. 1148  
1181. 1149  
1182. 1150  
1183. 1151  
1184. 1152  
1185. 1153  
1186. 1154  
1187. 1155  
1188. 1156  
1189. 1157  
1190. 1158  
1191. 1159  
1192. 1160  
1193. 1161



1194. 1162  
1195. 1163  
1196. 1164  
1197. 1165  
1198. 1166  
1199. 1167  
1200. 1168  
1201. 1169  
1202. 1170  
1203. 1171  
1204. 1172  
1205. 1173  
1206. 1174  
1207. 1175  
1208. 1176  
1209. 1177  
1210. 1178  
1211. 1179  
1212. 1180  
1213. 1181  
1214. 1182  
1215. 1183  
1216. 1184  
1217. 1185  
1218. 1186  
1219. 1187  
1220. 1188  
1221. 1189  
1222. 1190  
1223. 1191  
1224. 1192  
1225. 1193  
1226. 1194  
1227. 1195

**1228. 1196**

**1229. 1197**

**1230. 1198**

**1231. 1199**

**1232. 1200**

**1233. 1201**

**1234. 1202**

**1235. 1203**

**1236. 1204**

**1237. 1205**

**1238. 1206**

**1239. 1207**

**1240. 1208**

**1241. 1209**

**1242. 1210**

**1243. 1211**

**1244. 1212**

**1245. 1213**

**1246. 1214**

**1247. 1215**

**1248. 1216**

## About This E-Book

EPUB is an open, industry-standard format for e-books. However, support for EPUB and its many features varies across reading devices and applications. Use your device or app settings to customize the presentation to your liking. Settings that you can customize often include font, font size, single or double column, landscape or portrait mode, and figures that you can click or tap to enlarge. For additional information about the settings and features on your reading device or app, visit the device manufacturer's Web site.

Many titles include programming code or configuration examples. To optimize

the presentation of these elements, view the e-book in single-column, landscape mode and adjust the font size to the smallest setting. In addition to presenting code and configurations in the reflowable text format, we have included images of the code that mimic the presentation found in the print book; therefore, where the reflowable format may compromise the presentation of the code listing, you will see a “Click here to view code image” link. Click the link to view the print-fidelity code image. To return to the previous page viewed, click the Back button on your device or app.

*Transport Processes and Separation  
Process Principles*

Fifth Edition

# ***Transport Processes and Separation Process Principles***

Fifth Edition

**CHRISTIE JOHN GEANKOPLIS**

**A. ALLEN HERSEL**

**DANIEL H. LEPEK**



Boston • Columbus • Indianapolis • New York • San Francisco • Amsterdam • Cape Town  
Dubai • London • Madrid • Milan • Munich • Paris • Montreal • Toronto • Delhi • Mexico City  
São Paulo • Sydney • Hong Kong • Seoul • Singapore • Taipei • Tokyo

Many of the designations used by manufacturers and sellers to distinguish their products are claimed as trademarks. Where those designations appear in this book, and the publisher was aware of a trademark claim, the designations have been printed with initial capital letters or in all capitals.

The authors and publisher have taken care in the preparation of this book, but make no expressed or implied warranty of any kind and assume no responsibility for errors or omissions. No liability is assumed for incidental or consequential damages in connection with or arising out of the use of the information or programs contained herein.

For information about buying this title in bulk quantities, or for special sales opportunities (which may include electronic versions; custom cover designs; and content particular to your business, training goals, marketing focus, or branding interests), please contact our corporate sales department at [corpsales@pearsoned.com](mailto:corpsales@pearsoned.com) or (800) 382-3419.

For government sales inquiries, please contact [governmentsales@pearsoned.com](mailto:governmentsales@pearsoned.com).

For questions about sales outside the U.S., please contact [intlcs@pearson.com](mailto:intlcs@pearson.com).

Visit us on the Web: [informit.com](http://informit.com)

Library of Congress Control Number:



2017956182

Copyright © 2018 Pearson Education,  
Inc.

All rights reserved. Printed in the United States of America. This publication is protected by copyright, and permission must be obtained from the publisher prior to any prohibited reproduction, storage in a retrieval system, or transmission in any form or by any means, electronic, mechanical, photocopying, recording, or likewise. For information regarding permissions, request forms and the appropriate contacts within the Pearson Education Global Rights & Permissions Department, please visit [www.pearsoned.com/permissions/](http://www.pearsoned.com/permissions/).

ISBN-13: 978-0-13-418102-8

ISBN-10: 0-13-418102-6

1 18

*To my mom, my wife, and my three sons*

*—Allen*

*To my family, friends, and the many  
students that I have taught*

*—Daniel*

# **Contents**

## **Preface to the Fifth Edition**

## **About the Authors**

### ***PART 1***

## **TRANSPORT PROCESSES: MOMENTUM, HEAT, AND MASS**

### ***Chapter 1* Introduction to Engineering Principles and Units**

#### **1.0 Chapter Objectives**

#### **1.1 Classification of Transport Processes and Separation Processes (Unit Operations)**

##### **1.1A Introduction**

**1.1B Fundamental Transport Processes**

**1.1C Classification of Separation Processes**

**1.1D Arrangement in Parts 1 and 2**

**1.2 SI System of Basic Units Used in This Text and Other Systems**

**1.2A SI System of Units**

**1.2B CGS System of Units**

**1.2C English FPS System of Units**

**1.2D Dimensionally Homogeneous Equations and Consistent Units**

**1.3 Methods of Expressing Temperatures and Compositions**

**1.3A Temperature**

**1.3B Mole Units and Weight or Mass Units**

**1.3C Concentration Units for Liquids**

**1.4 Gas Laws and Vapor Pressure**

**1.4A Pressure**

**1.4B Ideal Gas Law**

**1.4C Ideal Gas Mixtures**

**1.4D Vapor Pressure and Boiling Point of Liquids**

**1.5 Conservation of Mass and Material Balances**

**1.5A Conservation of Mass**

**1.5B Simple Material Balances**

**1.5C Material Balances and Recycle**

**1.5D Material Balances and Chemical Reaction**

**1.6 Energy and Heat Units**

**1.6A Joule, Calorie, and Btu**

**1.6B Heat Capacity**

**1.6C Latent Heat and Steam Tables**

**1.6D Heat of Reaction**

**1.7 Conservation of Energy and Heat Balances**

**1.7A Conservation of Energy**

**1.7B Heat Balances**

## **1.8 Numerical Methods for Integration**

### **1.8A Introduction and Graphical Integration**

### **1.8B Numerical Integration and Simpson's Rule**

## **1.9 Chapter Summary**

## ***Chapter 2* Introduction to Fluids and Fluid Statics**

## **2.0 Chapter Objectives**

### **2.1 Introduction**

### **2.2 Fluid Statics**

#### **2.2A Force, Units, and Dimensions**

#### **2.2B Pressure in a Fluid**



2.2C Head of a Fluid

2.2D Devices to Measure Pressure and Pressure Differences

2.3 Chapter Summary

## *Chapter 3* **Fluid Properties and Fluid Flows**

3.0 Chapter Objectives

3.1 Viscosity of Fluids

3.1A Newton's Law of Viscosity

3.1B Momentum Transfer in a Fluid

3.1C Viscosities of Newtonian Fluids

3.2 Types of Fluid Flow and Reynolds Number

3.2A Introduction and Types of Fluid Flow

3.2B Laminar and Turbulent Flow

3.2C Reynolds Number

**3.3 Chapter Summary**

## *Chapter 4* **Overall Mass, Energy, and Momentum Balances**

**4.0 Chapter Objectives**

**4.1 Overall Mass Balance and Continuity Equation**

4.1A Introduction and Simple Mass Balances

4.1B Control Volume for Balances

## 4.1C Overall Mass-Balance Equation

## 4.1D Average Velocity to Use in Overall Mass Balance

# 4.2 Overall Energy Balance

## 4.2A Introduction

## 4.2B Derivation of Overall Energy-Balance Equation

## 4.2C Overall Energy Balance for a Steady-State Flow System

## 4.2D Kinetic-Energy Velocity Correction Factor $\alpha$

## 4.2E Applications of the Overall Energy-Balance Equation

## 4.2F Overall Mechanical-Energy

## Balance

### 4.2G Bernoulli Equation for Mechanical-Energy Balance

## 4.3 Overall Momentum Balance

### 4.3A Derivation of the General Equation

### 4.3B Overall Momentum Balance in a Flow System in One Direction

### 4.3C Overall Momentum Balance in Two Directions

### 4.3D Overall Momentum Balance for a Free Jet Striking a Fixed Vane

## 4.4 Shell Momentum Balance and Velocity Profile in Laminar Flow

4.4A Introduction

4.4B Shell Momentum Balance Inside a Pipe

4.4C Shell Momentum Balance for Falling Film

**4.5 Chapter Summary**

## *Chapter 5* **Incompressible and Compressible Flows in Pipes**

**5.0 Chapter Objectives**

**5.1 Design Equations for Laminar and Turbulent Flow in Pipes**

5.1A Velocity Profiles in Pipes

5.1B Pressure Drop and Friction Loss in Laminar Flow

5.1C Pressure Drop and Friction Factor  
in Turbulent Flow

5.1D Pressure Drop and Friction Factor  
in the Flow of Gases

5.1E Effect of Heat Transfer on the  
Friction Factor

5.1F Friction Losses in Expansion,  
Contraction, and Pipe Fittings

5.1G Friction Loss in Noncircular  
Conduits

5.1H Entrance Section of a Pipe

5.1I Selection of Pipe Sizes

**5.2 Compressible Flow of Gases**

5.2A Introduction and Basic Equation

for Flow in Pipes

5.2B Isothermal Compressible Flow

5.2C Adiabatic Compressible Flow

**5.3 Measuring the Flow of Fluids**

5.3A Pitot Tube

5.3B Venturi Meter

5.3C Orifice Meter

5.3D Flow-Nozzle Meter

5.3E Variable-Area Flow Meters  
(Rotameters)

5.3F Other Types of Flow Meters

5.3G Flow in Open Channels and  
Weirs

## **5.4 Chapter Summary**

# ***Chapter 6* Flows in Packed and Fluidized Beds**

## **6.0 Chapter Objectives**

## **6.1 Flow Past Immersed Objects**

### **6.1A Definition of Drag Coefficient for Flow Past Immersed Objects**

### **6.1B Flow Past a Sphere, Long Cylinder, and Disk**

## **6.2 Flow in Packed Beds**

## **6.3 Flow in Fluidized Beds**

## **6.4 Chapter Summary**

# ***Chapter 7* Pumps, Compressors, and**



# **Agitation Equipment**

## **7.0 Chapter Objectives**

### **7.1 Pumps and Gas-Moving Equipment**

#### **7.1A Introduction**

#### **7.1B Pumps**

#### **7.1C Gas-Moving Machinery**

#### **7.1D Equations for Compression of Gases**

### **7.2 Agitation, Mixing of Fluids, and Power Requirements**

#### **7.2A Purposes of Agitation**

#### **7.2B Equipment for Agitation**

7.2C Flow Patterns in Agitation

7.2D Typical “Standard” Design of a Turbine

7.2E Power Used in Agitated Vessels

7.2F Agitator Scale-Up

7.2G Mixing Times of Miscible Liquids

7.2H Flow Number and Circulation Rate in Agitation

7.2I Special Agitation Systems

7.2J Mixing of Powders, Viscous Materials, and Pastes

**7.3 Chapter Summary**

# *Chapter 8*   **Differential Equations of Fluid Flow**

## **8.0**   Chapter Objectives

### **8.1**   Differential Equations of Continuity

#### 8.1A   Introduction

#### 8.1B   Types of Time Derivatives and Vector Notation

#### 8.1C   Differential Equation of Continuity

### **8.2**   Differential Equations of Momentum Transfer or Motion

#### 8.2A   Derivation of Equations of Momentum Transfer

## **8.2B Equations of Motion for Newtonian Fluids with Varying Density and Viscosity**

## **8.2C Equations of Motion for Newtonian Fluids with Constant Density and Viscosity**

# **8.3 Use of Differential Equations of Continuity and Motion**

## **8.3A Introduction**

## **8.3B Differential Equations of Continuity and Motion for Flow Between Parallel Plates**

## **8.3C Differential Equations of Continuity and Motion for Flow in Stationary and Rotating Cylinders**

# **8.4 Chapter Summary**

## *Chapter 9*   **Non-Newtonian Fluids**

### **9.0**   Chapter Objectives

### **9.1**   Non-Newtonian Fluids

#### **9.1A**   Types of Non-Newtonian Fluids

#### **9.1B**   Time-Independent Fluids

#### **9.1C**   Time-Dependent Fluids

#### **9.1D**   Viscoelastic Fluids

#### **9.1E**   Laminar Flow of Time-Independent Non-Newtonian Fluids

### **9.2**   Friction Losses for Non-Newtonian Fluids

#### **9.2A**   Friction Losses in Contractions, Expansions, and Fittings in Laminar

# Flow

## 9.2B Turbulent Flow and Generalized Friction Factors

## 9.3 Velocity Profiles for Non-Newtonian Fluids

## 9.4 Determination of Flow Properties of Non-Newtonian Fluids Using a Rotational Viscometer

## 9.5 Power Requirements in Agitation and Mixing of Non-Newtonian Fluids

## 9.6 Chapter Summary

# *Chapter 10* Potential Flow and Creeping Flow

## 10.0 Chapter Objectives

## **10.1 Other Methods for Solution of Differential Equations of Motion**

### **10.1A Introduction**

### **10.2 Stream Function**

### **10.3 Differential Equations of Motion for Ideal Fluids (Inviscid Flow)**

### **10.4 Potential Flow and Velocity Potential**

### **10.5 Differential Equations of Motion for Creeping Flow**

### **10.6 Chapter Summary**

## ***Chapter 11* Boundary-Layer and Turbulent Flow**

### **11.0 Chapter Objectives**

## **11.1 Boundary-Layer Flow**

### **11.1A Boundary-Layer Flow**

### **11.1B Boundary-Layer Separation and the Formation of Wakes**

### **11.1C Laminar Flow and Boundary-Layer Theory**

## **11.2 Turbulent Flow**

### **11.2A Nature and Intensity of Turbulence**

### **11.2B Turbulent Shear or Reynolds Stresses**

### **11.2C Prandtl Mixing Length**

### **11.2D Universal Velocity Distribution in Turbulent Flow**



## **11.3 Turbulent Boundary-Layer Analysis**

### **11.3A Integral Momentum Balance for Boundary-Layer Analysis**

## **11.4 Chapter Summary**

# ***Chapter 12* Introduction to Heat Transfer**

## **12.0 Chapter Objectives**

## **12.1 Energy and Heat Units**

### **12.1A Joule, Calorie, and Btu**

### **12.1B Heat Capacity**

### **12.1C Latent Heat and Steam Tables**

### **12.1D Heat of Reaction**

## **12.2 Conservation of Energy and Heat Balances**

### **12.2A Conservation of Energy**

### **12.2B Heat Balances**

## **12.3 Conduction and Thermal Conductivity**

### **12.3A Introduction to Steady-State Heat Transfer**

### **12.3B Conduction as a Basic Mechanism of Heat Transfer**

### **12.3C Fourier's Law of Heat Conduction**

### **12.3D Thermal Conductivity**

## **12.4 Convection**

## 12.4A Convection as a Basic Mechanism of Heat Transfer

## 12.4B Convective Heat-Transfer Coefficient

# 12.5 Radiation

## 12.5A Radiation, a Basic Mechanism of Heat Transfer

## 12.5B Radiation to a Small Object from Its Surroundings

# 12.6 Heat Transfer with Multiple Mechanisms/Materials

## 12.6A Plane Walls in Series

## 12.6B Conduction Through Materials in Parallel

## 12.6C Combined Radiation and Convection Heat Transfer

### 12.7 Chapter Summary

## *Chapter 13* **Steady-State Conduction**

### 13.0 Chapter Objectives

### 13.1 Conduction Heat Transfer

#### 13.1A Conduction Through a Flat Slab or Wall (Some Review of Chapter 12)

#### 13.1B Conduction Through a Hollow Cylinder

#### 13.1C Multilayer Cylinders

#### 13.1D Conduction Through a Hollow Sphere

## **13.2 Conduction Through Solids in Series or Parallel with Convection**

**13.2A Combined Convection, Conduction, and Overall Coefficients**

**13.2B Log Mean Temperature Difference and Varying Temperature Drop**

**13.2C Critical Thickness of Insulation for a Cylinder**

**13.2D Contact Resistance at an Interface**

## **13.3 Conduction with Internal Heat Generation**

**13.3A Conduction with Internal Heat Generation**

## **13.4 Steady-State Conduction in Two Dimensions Using Shape Factors**

### **13.4A Introduction and Graphical Method for Two-Dimensional Conduction**

### **13.4B Shape Factors in Conduction**

## **13.5 Numerical Methods for Steady-State Conduction in Two Dimensions**

### **13.5A Analytical Equation for Conduction**

### **13.5B Finite-Difference Numerical Methods**

## **13.6 Chapter Summary**

# ***Chapter 14 Principles of Unsteady-State Heat Transfer***

## **14.0 Chapter Objectives**

### **14.1 Derivation of the Basic Equation**

#### **14.1A Introduction**

#### **14.1B Derivation of the Unsteady-State Conduction Equation**

### **14.2 Simplified Case for Systems with Negligible Internal Resistance**

#### **14.2A Basic Equation**

#### **14.2B Equation for Different Geometries**

#### **14.2C Total Amount of Heat Transferred**

### **14.3 Unsteady-State Heat Conduction in Various Geometries**

## 14.3A Introduction and Analytical Methods

## 14.3B Unsteady-State Conduction in a Semi-infinite Solid

## 14.3C Unsteady-State Conduction in a Large Flat Plate

## 14.3D Unsteady-State Conduction in a Long Cylinder

## 14.3E Unsteady-State Conduction in a Sphere

## 14.3F Unsteady-State Conduction in Two- and Three-Dimensional Systems

## 14.3G Charts for Average Temperature in a Plate, Cylinder, and Sphere with Negligible Surface Resistance



## **14.4 Numerical Finite-Difference Methods for Unsteady-State Conduction**

### **14.4A Unsteady-State Conduction in a Slab**

### **14.4B Boundary Conditions for Numerical Method for a Slab**

### **14.4C Other Numerical Methods for Unsteady-State Conduction**

## **14.5 Chilling and Freezing of Food and Biological Materials**

### **14.5A Introduction**

### **14.5B Chilling of Food and Biological Materials**

### **14.5C Freezing of Food and Biological Materials**

## 14.6 Differential Equation of Energy Change

### 14.6A Introduction

### 14.6B Derivation of Differential Equation of Energy Change

### 14.6C Special Cases of the Equation of Energy Change

## 14.7 Chapter Summary

## *Chapter 15* **Introduction to Convection**

### 15.0 Chapter Objectives

### 15.1 Introduction and Dimensional Analysis in Heat Transfer

#### 15.1A Introduction to Convection

(Review)

15.1B Introduction to Dimensionless Groups

15.1C Buckingham Method

**15.2** Boundary-Layer Flow and Turbulence in Heat Transfer

15.2A Laminar Flow and Boundary-Layer Theory in Heat Transfer

15.2B Approximate Integral Analysis of the Thermal Boundary Layer

15.2C Prandtl Mixing Length and Eddy Thermal Diffusivity

**15.3** Forced Convection Heat Transfer Inside Pipes

15.3A Heat-Transfer Coefficient for  
Laminar Flow Inside a Pipe

15.3B Heat-Transfer Coefficient for  
Turbulent Flow Inside a Pipe

15.3C Heat-Transfer Coefficient for  
Transition Flow Inside a Pipe

15.3D Heat-Transfer Coefficient for  
Noncircular Conduits

15.3E Entrance-Region Effect on the  
Heat-Transfer Coefficient

15.3F Liquid-Metals Heat-Transfer  
Coefficient

**15.4** Heat Transfer Outside Various  
Geometries in Forced Convection

15.4A Introduction

15.4B Flow Parallel to a Flat Plate

15.4C Cylinder with Axis  
Perpendicular to Flow

15.4D Flow Past a Single Sphere

15.4E Flow Past Banks of Tubes or  
Cylinders

15.4F Heat Transfer for Flow in  
Packed Beds

**15.5** Natural Convection Heat Transfer

15.5A Introduction

15.5B Natural Convection from  
Various Geometries

**15.6** Boiling and Condensation

15.6A Boiling

15.6B Condensation

**15.7** Heat Transfer of Non-Newtonian  
Fluids

15.7A Introduction

15.7B Heat Transfer Inside Tubes

15.7C Natural Convection

**15.8** Special Heat-Transfer  
Coefficients

15.8A Heat Transfer in Agitated  
Vessels

15.8B Scraped-Surface Heat  
Exchangers

## 15.8C Extended Surface or Finned Exchangers

### 15.9 Chapter Summary

## *Chapter 16* **Heat Exchangers**

### 16.0 Chapter Objectives

### 16.1 Types of Exchangers

### 16.2 Log-Mean-Temperature-Difference Correction Factors

### 16.3 Heat-Exchanger Effectiveness

### 16.4 Fouling Factors and Typical Overall $U$ Values

### 16.5 Double-Pipe Heat Exchanger

### 16.6 Chapter Summary

# *Chapter 17*   **Introduction to Radiation Heat Transfer**

## **17.0**   Chapter Objectives

## **17.1**   Introduction to Radiation Heat- Transfer Concepts

### 17.1A   Introduction and Basic Equation for Radiation

### 17.1B   Radiation to a Small Object from Its Surroundings

### 17.1C   Effect of Radiation on the Temperature Measurement of a Gas

## **17.2**   Basic and Advanced Radiation Heat-Transfer Principles

### 17.2A   Introduction and Radiation Spectrum



17.2B Derivation of View Factors in  
Radiation for Various Geometries

17.2C View Factors When Surfaces  
Are Connected by Reradiating Walls

17.2D View Factors and Gray Bodies

17.2E Radiation in Absorbing Gases

**17.3** Chapter Summary

## *Chapter 18* **Introduction to Mass Transfer**

**18.0** Chapter Objectives

**18.1** Introduction to Mass Transfer and  
Diffusion

18.1A Similarity of Mass, Heat, and  
Momentum Transfer Processes

## 18.1B Examples of Mass-Transfer Processes

## 18.1C Fick's Law for Molecular Diffusion

## 18.1D General Case for Diffusion of Gases A and B plus Convection

# 18.2 Diffusion Coefficient

## 18.2A Diffusion Coefficients for Gases

## 18.2B Diffusion Coefficients for Liquids

## 18.2C Prediction of Diffusivities in Liquids

## 18.2D Prediction of Diffusivities of Electrolytes in Liquids

## 18.2E Diffusion of Biological Solutes in Liquids

### **18.3** Convective Mass Transfer

#### 18.3A Convective Mass-Transfer Coefficient

#### **18.4** Molecular Diffusion Plus Convection and Chemical Reaction

##### 18.4A Different Types of Fluxes and Fick's Law

##### 18.4B Equation of Continuity for a Binary Mixture

##### 18.4C Special Cases of the Equation of Continuity

### **18.5** Chapter Summary

# *Chapter 19*   **Steady-State Mass Transfer**

## **19.0**   Chapter Objectives

## **19.1**   Molecular Diffusion in Gases

### 19.1A   Equimolar Counterdiffusion in Gases

### 19.1B   Special Case for $A$ Diffusing Through Stagnant, Nondiffusing $B$

### 19.1C   Diffusion Through a Varying Cross-Sectional Area

### 19.1D   Multicomponent Diffusion of Gases

## **19.2**   Molecular Diffusion in Liquids

### 19.2A   Introduction

## 19.2B Equations for Diffusion in Liquids

### **19.3** Molecular Diffusion in Solids

#### 19.3A Introduction and Types of Diffusion in Solids

#### 19.3B Diffusion in Solids Following Fick's Law

#### 19.3C Diffusion in Porous Solids That Depends on Structure

### **19.4** Diffusion of Gases in Porous Solids and Capillaries

#### 19.4A Introduction

#### 19.4B Knudsen Diffusion of Gases

#### 19.4C Molecular Diffusion of Gases

19.4D Transition-Region Diffusion of Gases

19.4E Flux Ratios for Diffusion of Gases in Capillaries

19.4F Diffusion of Gases in Porous Solids

**19.5** Diffusion in Biological Gels

**19.6** Special Cases of the General Diffusion Equation at Steady State

19.6A Special Cases of the General Diffusion Equation at Steady State

**19.7** Numerical Methods for Steady-State Molecular Diffusion in Two Dimensions

19.7A Derivation of Equations for

# Numerical Methods

## 19.7B Equations for Special Boundary Conditions for Numerical Method

## 19.8 Chapter Summary

## *Chapter 20* **Unsteady-State Mass Transfer**

### 20.0 Chapter Objectives

### 20.1 Unsteady-State Diffusion

#### 20.1A Derivation of a Basic Equation

#### 20.1B Diffusion in a Flat Plate with Negligible Surface Resistance

#### 20.1C Unsteady-State Diffusion in Various Geometries

## **20.2 Unsteady-State Diffusion and Reaction in a Semi-Infinite Medium**

### **20.2A Unsteady-State Diffusion and Reaction in a Semi-Infinite Medium**

## **20.3 Numerical Methods for Unsteady-State Molecular Diffusion**

### **20.3A Introduction**

### **20.3B Unsteady-State Numerical Methods for Diffusion**

### **20.3C Boundary Conditions for Numerical Methods for a Slab**

## **20.4 Chapter Summary**

# ***Chapter 21* Convective Mass Transfer**



## **21.0 Chapter Objectives**

### **21.1 Convective Mass Transfer**

#### **21.1A Introduction to Convective Mass Transfer**

#### **21.1B Types of Mass-Transfer Coefficients**

#### **21.1C Mass-Transfer Coefficients for the General Case of A and B Diffusing and Convective Flow Using Film Theory**

#### **21.1D Mass-Transfer Coefficients under High Flux Conditions**

#### **21.1E Methods for Experimentally Determining Mass-Transfer Coefficients**

### **21.2 Dimensional Analysis in Mass**

# Transfer

## 21.2A Introduction

## 21.2B Dimensional Analysis for Convective Mass Transfer

## **21.3** Mass-Transfer Coefficients for Various Geometries

### 21.3A Dimensionless Numbers Used to Correlate Data

### 21.3B Analogies among Mass, Heat, and Momentum Transfer

### 21.3C Derivation of Mass-Transfer Coefficients in Laminar Flow

### 21.3D Mass Transfer for Flow Inside Pipes

## 21.3E Mass Transfer for Flow Outside Solid Surfaces

### **21.4** Mass Transfer to Suspensions of Small Particles

#### 21.4A Introduction

#### 21.4B Equations for Mass Transfer to Small Particles

### **21.5** Models for Mass-Transfer Coefficients

#### 21.5A Laminar Flow and Boundary-Layer Theory in Mass Transfer

#### 21.5B Prandtl Mixing Length and Turbulent Eddy Mass Diffusivity

#### 21.5C Models for Mass-Transfer Coefficients

## **21.6 Chapter Summary**

### ***PART 2***

## **SEPARATION PROCESS**

## **PRINCIPLES**

### ***Chapter 22 Absorption and Stripping***

#### **22.0 Chapter Objectives**

#### **22.1 Equilibrium and Mass Transfer Between Phases**

##### **22.1A Phase Rule and Equilibrium**

##### **22.1B Gas–Liquid Equilibrium**

##### **22.1C Single-Stage Equilibrium Contact**

##### **22.1D Single-Stage Equilibrium Contact for a Gas–Liquid System**

22.1E Countercurrent Multiple-Contact Stages

22.1F Analytical Equations for Countercurrent Stage Contact

22.1G Introduction and Equilibrium Relations

22.1H Concentration Profiles in Interphase Mass Transfer

22.1I Mass Transfer Using Film Mass-Transfer Coefficients and Interface Concentrations

22.1J Overall Mass-Transfer Coefficients and Driving Forces

**22.2** Introduction to Absorption

22.2A Absorption

## **22.2B Equipment for Absorption and Distillation**

### **22.3 Pressure Drop and Flooding in Packed Towers**

### **22.4 Design of Plate Absorption Towers**

### **22.5 Design of Packed Towers for Absorption**

#### **22.5A Introduction to Design of Packed Towers for Absorption**

#### **22.5B Simplified Design Methods for Absorption of Dilute Gas Mixtures in Packed Towers**

#### **22.5C Design of Packed Towers Using Transfer Units**

## **22.6 Efficiency of Random-Packed and Structured Packed Towers**

### **22.6A Calculating the Efficiency of Random-Packed and Structured Packed Towers**

### **22.6B Estimation of Efficiencies of Tray and Packed Towers**

## **22.7 Absorption of Concentrated Mixtures in Packed Towers**

## **22.8 Estimation of Mass-Transfer Coefficients for Packed Towers**

### **22.8A Experimental Determination of Film Coefficients**

### **22.8B Correlations for Film Coefficients**

## 22.8C Predicting Mass-Transfer Film Coefficients

## 22.9 Heat Effects and Temperature Variations in Absorption

### 22.9A Heat Effects in Absorption

### 22.9B Simplified Design Method

## 22.10 Chapter Summary

# *Chapter 23* **Humidification Processes**

## 23.0 Chapter Objectives

## 23.1 Vapor Pressure of Water and Humidity

### 23.1A Vapor Pressure of Water

### 23.1B Humidity and a Humidity Chart



## 23.1C Adiabatic Saturation Temperatures

## 23.1D Wet Bulb Temperature

## 23.2 Introduction and Types of Equipment for Humidification

## 23.3 Theory and Calculations for Cooling-Water Towers

### 23.3A Theory and Calculations for Cooling-Water Towers

### 23.3B Design of Water-Cooling Tower Using Film Mass-Transfer Coefficients

### 23.3C Design of Water-Cooling Tower Using Overall Mass-Transfer Coefficients

### 23.3D Minimum Value of Air Flow

23.3E Design of Water-Cooling Tower  
Using the Height of a Transfer Unit

23.3F Temperature and Humidity of an  
Air Stream in a Tower

23.3G Dehumidification Tower

**23.4 Chapter Summary**

*Chapter 24* **Filtration and Membrane  
Separation Processes (Liquid–Liquid  
or Solid–Liquid Phase)**

**24.0 Chapter Objectives**

**24.1 Introduction to Dead-End  
Filtration**

24.1A Introduction

24.1B Types of Filtration Equipment

## **24.1C Filter Media and Filter Aids**

## **24.2 Basic Theory of Filtration**

### **24.2A Introduction to the Basic Theory of Filtration**

### **24.2B Filtration Equations for Constant-Pressure Filtration**

### **24.2C Filtration Equations for Constant-Rate Filtration**

## **24.3 Membrane Separations**

### **24.3A Introduction**

### **24.3B Classification of Membrane Processes**

### **24.4 Microfiltration Membrane Processes**

24.4A Introduction

24.4B Models for Microfiltration

**24.5** Ultrafiltration Membrane  
Processes

24.5A Introduction

24.5B Types of Equipment for  
Ultrafiltration

24.5C Flux Equations for  
Ultrafiltration

24.5D Effects of Processing Variables  
in Ultrafiltration

**24.6** Reverse-Osmosis Membrane  
Processes

24.6A Introduction

24.6B Flux Equations for Reverse Osmosis

24.6C Effects of Operating Variables

24.6D Concentration Polarization in Reverse-Osmosis Diffusion Model

24.6E Permeability Constants for Reverse-Osmosis Membranes

24.6F Types of Equipment for Reverse Osmosis

24.6G Complete-Mixing Model for Reverse Osmosis

**24.7 Dialysis**

24.7A Series Resistances in Membrane Processes

24.7B Dialysis Processes

24.7C Types of Equipment for Dialysis

24.7D Hemodialysis in an Artificial  
Kidney

**24.8 Chapter Summary**

## *Chapter 25* **Gaseous Membrane Systems**

**25.0 Chapter Objectives**

**25.1 Gas Permeation**

25.1A Series Resistances in Membrane  
Processes

25.1B Types of Membranes and  
Permeabilities for Separation of Gases

## 25.1C Types of Equipment for Gas-Permeation Membrane Processes

### 25.1D Introduction to Types of Flow in Gas Permeation

## **25.2** Complete-Mixing Model for Gas Separation by Membranes

### 25.2A Basic Equations Used

### 25.2B Solution of Equations for Design of a Complete-Mixing Case

### 25.2C Minimum Concentration of Reject Stream

## **25.3** Complete-Mixing Model for Multicomponent Mixtures

### 25.3A Derivation of Equations

## 25.3B Iteration Solution Procedure for Multicomponent Mixtures

## **25.4** Cross-Flow Model for Gas Separation by Membranes

### 25.4A Derivation of the Basic Equations

### 25.4B Procedure for Design of Cross-Flow Case

## **25.5** Derivation of Equations for Countercurrent and Cocurrent Flow for Gas Separation by Membranes

### 25.5A Concentration Gradients in Membranes

### 25.5B Derivation of Equations for Countercurrent Flow in Dense-Phase Symmetric Membranes



25.5C Solution of Countercurrent Flow Equations in Dense-Phase Symmetric Membranes

25.5D Derivation of Equations for Countercurrent Flow in Asymmetric Membranes

25.5E Derivation of Equations for Cocurrent Flow in Asymmetric Membranes

25.5F Effects of Processing Variables on Gas Separation

**25.6** Derivation of Finite-Difference Numerical Method for Asymmetric Membranes

25.6A Countercurrent Flow

25.6B Short-Cut Numerical Method

25.6C Use of a Spreadsheet for the  
Finite-Difference Numerical Method

25.6D Calculation of Pressure-Drop  
Effects on Permeation

**25.7** Chapter Summary

## *Chapter 26* **Distillation**

**26.0** Chapter Objectives

**26.1** Equilibrium Relations Between  
Phases

26.1A Phase Rule and Raoult's Law

26.1B Boiling-Point Diagrams and  $x$ - $y$   
Plots

**26.2** Single and Multiple Equilibrium  
Contact Stages

26.2A Equipment for Distillation

26.2B Single-Stage Equilibrium  
Contact for Vapor–Liquid System

**26.3** Simple Distillation Methods

26.3A Introduction

26.3B Relative Volatility of Vapor–  
Liquid Systems

26.3C Equilibrium or Flash Distillation

26.3D Simple Batch or Differential  
Distillation

26.3E Simple Steam Distillation

**26.4** Binary Distillation with Reflux  
Using the McCabe–Thiele and Lewis  
Methods

26.4A Introduction to Distillation with Reflux

26.4B McCabe–Thiele Method of Calculation for the Number of Theoretical Stages

26.4C Total and Minimum Reflux Ratio for McCabe–Thiele Method

26.4D Special Cases for Rectification Using the McCabe–Thiele Method

**26.5** Tray Efficiencies

26.5A Tray Efficiencies

26.5B Types of Tray Efficiencies

26.5C Relationship Between Tray Efficiencies

## **26.6 Flooding Velocity and Diameter of Tray Towers Plus Simple Calculations for Reboiler and Condenser Duties**

### **26.6A Flooding Velocity and Diameter of Tray Towers**

### **26.6B Condenser and Reboiler Duties Using the McCabe–Thiele Method**

## **26.7 Fractional Distillation Using the Enthalpy–Concentration Method**

### **26.7A Enthalpy–Concentration Data**

### **26.7B Distillation in the Enriching Section of a Tower**

### **26.7C Distillation in the Stripping Section of a Tower**

## **26.8 Distillation of Multicomponent Mixtures**

### **26.8A Introduction to Multicomponent Distillation**

### **26.8B Equilibrium Data in Multicomponent Distillation**

### **26.8C Boiling Point, Dew Point, and Flash Distillation**

### **26.8D Key Components in Multicomponent Distillation**

### **26.8E Total Reflux for Multicomponent Distillation**

### **26.8F Shortcut Method for the Minimum Reflux Ratio for Multicomponent Distillation**

## 26.8G Shortcut Method for Number of Stages at Operating Reflux Ratio

### 26.9 Chapter Summary

## *Chapter 27* **Liquid–Liquid Extraction**

### 27.0 Chapter Objectives

### 27.1 Introduction to Liquid–Liquid Extraction

#### 27.1A Introduction to Extraction Processes

#### 27.1B Equilibrium Relations in Extraction

### 27.2 Single-Stage Equilibrium Extraction

## 27.2A Single-Stage Equilibrium Extraction

### 27.3 Types of Equipment and Design for Liquid–Liquid Extraction

#### 27.3A Introduction and Equipment Types

#### 27.3B Mixer–Settlers for Extraction

#### 27.3C Spray Extraction Towers

#### 27.3D Packed Extraction Towers

#### 27.3E Perforated-Plate (Sieve-Tray) Extraction Towers

#### 27.3F Pulsed Packed and Sieve-Tray Towers

#### 27.3G Mechanically Agitated



## Extraction Towers

### **27.4** Continuous Multistage Countercurrent Extraction

#### 27.4A Introduction

#### 27.4B Continuous Multistage Countercurrent Extraction

#### 27.4C Countercurrent-Stage Extraction with Immiscible Liquids

#### 27.4D Design of Towers for Extraction

#### 27.4E Design of Packed Towers for Extraction Using Mass-Transfer Coefficients

### **27.5** Chapter Summary

## *Chapter 28* Adsorption and Ion

# **Exchange**

## **28.0 Chapter Objectives**

### **28.1 Introduction to Adsorption Processes**

#### **28.1A Introduction**

#### **28.1B Physical Properties of Adsorbents**

#### **28.1C Equilibrium Relations for Adsorbents**

### **28.2 Batch Adsorption**

### **28.3 Design of Fixed-Bed Adsorption Columns**

#### **28.3A Introduction and Concentration Profiles**

28.3B Breakthrough Concentration Curve

28.3C Mass-Transfer Zone

28.3D Capacity of Column and Scale-Up Design Method

28.3E Basic Models for Predicting Adsorption

28.3F Processing Variables and Adsorption Cycles

## **28.4 Ion-Exchange Processes**

28.4A Introduction and Ion-Exchange Materials

28.4B Equilibrium Relations in Ion Exchange

28.4C Use of Equilibrium Relations  
and Relative-Molar-Selectivity  
Coefficients

28.4D Concentration Profiles and  
Breakthrough Curves

28.4E Capacity of Columns and Scale-  
Up Design Method

**28.5** Chapter Summary

## *Chapter 29* **Crystallization and Particle Size Reduction**

**29.0** Chapter Objectives

**29.1** Introduction to Crystallization

29.1A Crystallization and Types of  
Crystals

29.1B Equilibrium Solubility in  
Crystallization

29.1C Yields, Material, and Energy  
Balances in Crystallization

29.1D Equipment for Crystallization

## **29.2 Crystallization Theory**

29.2A Introduction

29.2B Nucleation Theories

29.2C Rate of Crystal Growth and the  
 $\Delta L$  Law

29.2D Particle Size Distribution of  
Crystals

29.2E Model for Mixed Suspension–  
Mixed Product Removal Crystallizer

## **29.3 Mechanical Size Reduction**

### **29.3A Introduction**

### **29.3B Particle Size Measurement**

### **29.3C Energy and Power Required in Size Reduction**

### **29.3D Equipment for Particle Size Reduction**

## **29.4 Chapter Summary**

## ***Chapter 30 Settling, Sedimentation, and Centrifugation***

### **30.0 Chapter Objectives**

### **30.1 Settling and Sedimentation in Particle–Fluid Separation**

30.1A Introduction

30.1B Theory of Particle Movement  
Through a Fluid

30.1C Hindered Settling

30.1D Wall Effect on Free Settling

30.1E Differential Settling and  
Separation of Solids in Classification

30.1F Sedimentation and Thickening

30.1G Equipment for Settling and  
Sedimentation

**30.2 Centrifugal Separation Processes**

30.2A Introduction

30.2B Forces Developed in Centrifugal

# Separation

## 30.2C Equations for Rates of Settling in Centrifuges

## 30.2D Centrifuge Equipment for Sedimentation

## 30.2E Centrifugal Filtration

## 30.2F Gas–Solid Cyclone Separators

## 30.3 Chapter Summary

## *Chapter 31 Leaching*

### 31.0 Chapter Objectives

### 31.1 Introduction and Equipment for Liquid–Solid Leaching

#### 31.1A Leaching Processes



31.1B Preparation of Solids for Leaching

31.1C Rates of Leaching

31.1D Types of Equipment for Leaching

**31.2** Equilibrium Relations and Single-Stage Leaching

31.2A Equilibrium Relations in Leaching

31.2B Single-Stage Leaching

**31.3** Countercurrent Multistage Leaching

31.3A Introduction and Operating Line for Countercurrent Leaching

**31.3B Variable Underflow in  
Countercurrent Multistage Leaching**

**31.3C Constant Underflow in  
Countercurrent Multistage Leaching**

**31.4 Chapter Summary**

## *Chapter 32* **Evaporation**

**32.0 Chapter Objectives**

**32.1 Introduction**

**32.1A Purpose**

**32.1B Processing Factors**

**32.2 Types of Evaporation Equipment  
and Operation Methods**

**32.2A General Types of Evaporators**

## **32.2B Methods of Evaporator Operations**

### **32.3 Overall Heat-Transfer Coefficients in Evaporators**

### **32.4 Calculation Methods for Single-Effect Evaporators**

#### **32.4A Heat and Material Balances for Evaporators**

#### **32.4B Effects of Processing Variables on Evaporator Operation**

#### **32.4C Boiling-Point Rise of Solutions**

#### **32.4D Enthalpy–Concentration Charts of Solutions**

### **32.5 Calculation Methods for Multiple-Effect Evaporators**

32.5A Introduction

32.5B Temperature Drops and  
Capacity of Multiple-Effect Evaporators

32.5C Calculations for Multiple-Effect  
Evaporators

32.5D Step-by-Step Calculation  
Methods for Triple-Effect Evaporators

**32.6** Condensers for Evaporators

32.6A Introduction

32.6B Surface Condensers

32.6C Direct-Contact Condensers

**32.7** Evaporation of Biological  
Materials

## 32.7A Introduction and Properties of Biological Materials

### 32.7B Fruit Juices

### 32.7C Sugar Solutions

### 32.7D Paper-Pulp Waste Liquors

## **32.8** Evaporation Using Vapor Recompression

### 32.8A Introduction

### 32.8B Mechanical Vapor-Recompression Evaporator

### 32.8C Thermal Vapor-Recompression Evaporator

## **32.9** Chapter Summary

## *Chapter 33*   **Drying**

### **33.0**   Chapter Objectives

### **33.1**   Introduction and Methods of Drying

#### 33.1A   Purposes of Drying

### **33.2**   Equipment for Drying

#### 33.2A   Tray Dryer

#### 33.2B   Vacuum-Shelf Indirect Dryers

#### 33.2C   Continuous Tunnel Dryers

#### 33.2D   Rotary Dryers

#### 33.2E   Drum Dryers

#### 33.2F   Spray Dryers

33.2G Drying Crops and Grains

**33.3** Vapor Pressure of Water and Humidity

33.3A Vapor Pressure of Water

33.3B Humidity and Humidity Chart

33.3C Adiabatic Saturation Temperatures

33.3D Wet Bulb Temperature

**33.4** Equilibrium Moisture Content of Materials

33.4A Introduction

33.4B Experimental Data of Equilibrium Moisture Content for Inorganic and Biological Materials

33.4C Bound and Unbound Water in Solids

33.4D Free and Equilibrium Moisture of a Substance

### **33.5 Rate-of-Drying Curves**

33.5A Introduction and Experimental Methods

33.5B Rate of Drying Curves for Constant-Drying Conditions

33.5C Drying in the Constant-Rate Period

33.5D Drying in the Falling-Rate Period

33.5E Moisture Movements in Solids During Drying in the Falling-Rate



Period

### **33.6** Calculation Methods for a Constant-Rate Drying Period

33.6A Method for Using an  
Experimental Drying Curve

33.6B Method Using Predicted  
Transfer Coefficients for Constant-Rate  
Period

33.6C Effect of Process Variables on a  
Constant-Rate Period

### **33.7** Calculation Methods for the Falling-Rate Drying Period

33.7A Method Using Numerical  
Integration

33.7B Calculation Methods for Special

## Cases in Falling-Rate Region

### **33.8** Combined Convection, Radiation, and Conduction Heat Transfer in the Constant-Rate Period

#### 33.8A Introduction

#### 33.8B Derivation of the Equation for Convection, Conduction, and Radiation

### **33.9** Drying in the Falling-Rate Period by Diffusion and Capillary Flow

#### 33.9A Introduction

#### 33.9B Liquid Diffusion of Moisture in Drying

#### 33.9C Capillary Movement of Moisture in Drying

## 33.9D Comparison of Liquid Diffusion and Capillary Flow

### **33.10** Equations for Various Types of Dryers

#### 33.10A Through-Circulation Drying in Packed Beds

#### 33.10B Tray Drying with Varying Air Conditions

#### 33.10C Material and Heat Balances for Continuous Dryers

#### 33.10D Continuous Countercurrent Drying

### **33.11** Freeze-Drying of Biological Materials

#### 33.11A Introduction

## 33.11B Derivation of Equations for Freeze-Drying

## **33.12** Unsteady-State Thermal Processing and Sterilization of Biological Materials

### 33.12A Introduction

### 33.12B Thermal Death-Rate Kinetics of Microorganisms

### 33.12C Determination of Thermal Process Time for Sterilization

### 33.12D Sterilization Methods Using Other Design Criteria

### 33.12E Pasteurization

### 33.12F Effects of Thermal Processing on Food Constituents

## **33.13 Chapter Summary**

### ***PART 3***

## **APPENDIXES**

### **Appendix A.1 Fundamental Constants and Conversion Factors**

### **Appendix A.2 Physical Properties of Water**

### **Appendix A.3 Physical Properties of Inorganic and Organic Compounds**

### **Appendix A.4 Physical Properties of Foods and Biological Materials**

### **Appendix A.5 Properties of Pipes, Tubes, and Screens**

### **Appendix A.6 Lennard-Jones Potentials as Determined from**

**Viscosity Data**

**Notation**

**Index**

## Preface to the Fifth Edition

In this updated fifth edition of *Transport Processes and Separation Process Principles*, the main objective was to reorganize the text into a new format that resembles contemporary transport phenomena and separations texts. Due to this overhaul, the total number of chapters has been increased from 14 to 33. Our hope is that the readability and the usage of the text have been improved for student learning. In addition, we have created numerous new homework problems, which can be found on our companion website (<https://www.trine.edu/transport5ed/>). Due to the prior widespread adoption of previous editions of the text, we made

small changes to the content of the fifth edition of the text so that many more readers could adapt to the new format.

Since chemical and other engineering students must study many different topics today, we have provided a more unified introduction to the transport processes of momentum, heat, and mass transfer, and to the application of separation processes. In this text, the principles of transport processes are covered first, and then the separation processes (unit operations) are covered later. To accomplish this, the text is divided into two major parts.

### **Part 1: Transport Processes: Momentum, Heat, and Mass**

This first part of the text deals with the fundamental principles of



transport phenomena.

**Fluid Mechanics:** 1. Introduction to Engineering Principles and Units; 2. Introduction to Fluids and Fluid Statics; 3. Fluid Properties and Fluid Flows; 4. Overall Mass, Energy, and Momentum Balances; 5. Incompressible and Compressible Flows in Pipes; 6. Flows in Packed and Fluidized Beds; 7. Pumps, Compressors, and Agitation Equipment; 8. Differential Equations of Fluid Flow; 9. Non-Newtonian Fluids; 10. Potential Flow and Creeping Flow; 11. Boundary-Layer and Turbulent Flow.

**Heat Transfer:** 12. Introduction to Heat Transfer; 13. Steady-State Conduction; 14. Principles of Unsteady-State Heat Transfer; 15. Introduction to

Convection; 16. Heat Exchangers; 17. Introduction to Radiation Heat Transfer.

**Mass Transfer:** 18. Introduction to Mass Transfer; 19. Steady-State Mass Transfer; 20. Unsteady-State Mass Transfer; 21. Convective Mass Transfer.

### **Part 2: Separation Process Principles (Includes Unit Operations)**

This part of the text deals with applications of transport processes and covers separation processes in the following chapters: 22.

Absorption and Stripping; 23.

Humidification Processes; 24.

Filtration and Membrane Separation Processes (Liquid–Liquid or Solid–Liquid Phase); 25. Gaseous

Membrane Systems; 26. Distillation;

27. Liquid–Liquid Extraction; 28.

Adsorption and Ion Exchange; 29. Crystallization and Particle Size Reduction; 30. Settling, Sedimentation, and Centrifugation; 31. Leaching; 32. Evaporation; 33. Drying.

In Chapter 1, elementary principles of mathematical and graphical methods, laws of chemistry and physics, material balances, and heat balances are reviewed. Many readers, especially chemical engineers, may be familiar with most of these principles, and may omit all or parts of the chapter.

This text may be used for a course of study that follows any of the five suggested plans noted below. In all plans, the inclusion of Chapter 1 is optional.

1. *Study of transport processes of momentum, heat, and mass, and separation processes.* In this plan, most of the text covers the principles of the transport processes in Part 1 and the separation processes in Part 2. This plan would be applicable primarily to chemical engineering as well as to other process-engineering fields in a one-and-one-half-year course of study at the junior and/or senior level.

2. *Study of transport processes of momentum, heat, and mass, and selected separation processes.* Only the elementary sections of Part 1 (the principles chapters, 1–21) are covered, plus selected separation processes topics from Part 2 that are applicable to a particular field, in a two-semester or three-quarter course.

3. *Study of transport processes of momentum, heat, and mass.* The purpose of this plan in a two-quarter or two-semester course is to obtain a basic understanding of the transport processes of momentum, heat, and mass transfer. This involves covering only the sections of Part 1 (Chapters 1-21) and omitting Part 2, the applied chapters on separation processes.

4. *Study of separation processes.* If the reader has had courses in the transport processes of momentum, heat, and mass, then Part 1 (Chapters 1–21) can be omitted and only the separation processes chapters in Part 2 are studied in a one-semester or two-quarter course. This plan could be used by chemical and certain other engineers.

5. *Study of mass transfer.* For those such as chemical and mechanical engineers who have had momentum and heat transfer, or those who desire only a background in mass transfer in a one-quarter or one-semester course, Chapters 12–19 would be covered. Additional chapters from Part 2 might be covered, depending on the needs of the reader or goals of the instructor.

While the SI system of units (Système International d'Unités) has been adopted by the scientific community, many of the example and homework problems are also given using English units.

*A. Allen Hersel*  
*Daniel H. Lepek*

Register your copy of *Transport*

*Processes and Separation Process Principles, Fifth Edition*, on the InformIT site for convenient access to updates and/or corrections as they become available. To start the registration process, go to [informit.com/register](http://informit.com/register) and log in or create an account. Enter the product ISBN (9780134181028) and click Submit. Look on the Registered Products tab for an Access Bonus Content link next to this product, and follow that link to access any available bonus materials. If you would like to be notified of exclusive offers on new editions and updates, please check the box to receive email from us.

---

## About the Authors

**Christie John Geankoplis** was a professor of chemical engineering and materials science at the University of Minnesota. His research involved transport processes, biochemical reactor engineering, mass transfer in liquid solutions, and diffusion and/or reaction in porous solids.

**A. Allen Hersel** is currently the vice president of academic affairs at Trine University in Angola, Indiana. He is also a professor in the department of chemical engineering, where he has taught transport phenomena and separations for the last 15 years. His research is in the area of bioseparations and engineering education. Before



entering academia, he worked for Koch Industries and Kellogg Brown & Root. He holds a Ph.D. in chemical engineering from Yale University.

**Daniel H. Lepek** is currently an associate professor of chemical engineering at The Cooper Union for the Advancement of Science and Art in New York, NY, where he has taught courses on transport phenomena, particle technology, and unit operations. His research is in the areas of particle technology, transport phenomena, and engineering education. He has also been a visiting professor at University College London in the United Kingdom and a Fulbright Scholar at Graz University of Technology in Austria. He holds a B.E. from The Cooper Union and a Ph.D. from New Jersey Institute

of Technology. He is currently an active member of the AIChE Education Division and the ASEE Chemical Engineering Division.

# **Part 1: Transport Processes: Momentum, Heat, and Mass**

# Chapter 1. Introduction to Engineering Principles and Units

## 1.0 Chapter Objectives

On completion of this chapter, a student should be able to:

- Describe what are unit operations and separation processes
- Identify industries in which unit operations and separation processes are commonly found
- Describe the principles of momentum, heat, and mass transfer
- Identify and use different units from the SI, English, and cgs systems
- Understand the concept of equations that are dimensionally homogeneous
- Provide examples of unit operations and separation processes
- Use and convert units involving temperature, composition,

and energy

- Describe and use the ideal gas law to solve vapor phase problems
- Describe the laws of conservation of mass and energy
- Solve problems involving material balances with and without recycle and chemical reaction
- Solve problems involving energy balances using the concepts of heat capacity, latent heat, heat of vaporization, and heat of reaction
- Understand the principles of numerical integration

## **1.1 Classification of Transport Processes and Separation Processes (Unit Operations)**

### **1.1A Introduction**

In the chemical and other physical processing industries, such as the food and biological processing industries, many similarities exist in the manner in which the entering feed materials are modified or processed into final products. We

can take these seemingly different chemical, physical, or biological processes and break them down into a series of separate and distinct steps. These steps are commonly called *unit operations*. However, the term “unit operations” has sometimes been superseded by the more descriptive term “separation processes.” These *separation processes* are common to all types of diverse process industries.

For example, the separation process *distillation* is used to purify or separate alcohol in the beverage industry and other types of hydrocarbons in the petroleum industry. The drying of grain and other foods is similar to the drying of lumber, filtered precipitates, and wool. The separation process *absorption*

occurs in the absorption of oxygen from air in a fermentation process or in a sewage treatment plant and in the absorption of hydrogen gas in a process for the liquid hydrogenation of oil. The evaporation of salt solutions in the chemical industry is similar to the evaporation of sugar solutions in the food industry. The settling and sedimentation of suspended solids in the sewage industry and the mining industry are similar. The flow of liquid hydrocarbons in the petroleum refinery and the flow of milk in a dairy plant are carried out in a similar fashion.

Many of these separation processes have certain fundamental and basic principles or mechanisms in common. For example, the mechanism of diffusion or mass transfer occurs in drying,

membrane separation, absorption, distillation, and crystallization. Heat transfer occurs in drying, distillation, and evaporation. The following classification of a more fundamental nature is often made, according to transfer or transport processes.

### **1.1B Fundamental Transport Processes**

*1. Momentum transfer.* This is concerned with the transfer of momentum that occurs in moving media, such as in the separation processes of fluid flow, sedimentation, mixing, and filtration. Momentum transfer is commonly called fluid mechanics in other disciplines.

*2. Heat transfer.* In this fundamental process, we are concerned with the



transfer energy in the form of heat from one place to another. It occurs in the separation processes of drying, evaporation, distillation, and many others.

*3. Mass transfer.* Here, material (or mass) is transferred from one phase to another distinct phase; the basic mechanism is the same whether the phases are gas, solid, or liquid.

Separation processes dependent on mass transfer include distillation, absorption, liquid–liquid extraction, membrane separation, adsorption, crystallization, and leaching.

### **1.1C Classification of Separation Processes**

The separation processes deal mainly with the transfer and change of energy and the transfer and

change of materials, primarily by physical means but also by physical–chemical means. The important separation processes, which can be combined in various sequences in a process and which are covered in this text, are described next.

*1. Evaporation.* This refers to the evaporation of a volatile solvent such as water from a nonvolatile solute such as salt or any other material in solution.

*2. Drying.* In this operation, volatile liquids, usually water, are removed from solid materials.

*3. Distillation.* This is an operation whereby components of a liquid mixture are separated by boiling because of their differences in vapor pressure.

4. *Absorption*. In this process, a component is removed from a gas stream by treatment with a liquid.

5. *Membrane separation*. This process involves the separation of a solute from a fluid by diffusion of this solute from a liquid or gas through a semipermeable barrier (i.e., the membrane) to another fluid.

6. *Liquid–liquid extraction*. In this case, a solute in a liquid solution is removed by contacting with another liquid solvent that is relatively immiscible with the solution.

7. *Adsorption*. In this process, a component of a gas or liquid stream is removed and adsorbed by a solid adsorbent.

8. *Ion exchange*. This process removes certain ions in solution from a liquid by the use of an ion-exchange solid.

9. *Liquid–solid leaching*. This process involves treating a finely divided solid with a liquid that dissolves out and removes a solute contained in the solid.

10. *Crystallization*. In this process, a solute, such as a salt, is removed from a solution by precipitating the solute from the solution.

11. *Mechanical–physical separations*. These processes involve the separation of solids, liquids, or gases by mechanical means, such as filtration, settling, centrifugation, and size reduction.

This text is arranged in two parts:

*Part 1: Transport Processes:*

*Momentum, Heat, and Mass.* These fundamental principles are covered extensively in Chapters 1 through 21 in order to provide the basis for study of separation processes in Part 2 of this text.

*Part 2: Separation Process Principles.*

The various separation processes and their applications to process areas are studied in Part 2 of this text.

There are a number of elementary engineering principles, mathematical techniques, and laws of physics and chemistry that are basic to a study of the principles of momentum, heat, and mass transfer, and the separation processes.

These are reviewed for the reader in this first chapter. Some readers, especially chemical engineers, agricultural engineers, civil engineers, and chemists, may be familiar with many of these principles and techniques, and may wish to omit all or parts of this chapter.

Homework problems at the end of each chapter are arranged in different sections, each corresponding to the number of a given section in the chapter.

## **1.2 SI System of Basic Units Used in This Text and Other Systems**

There are three main systems of basic units employed at present in engineering and science. The first and most important of these is the *SI* (Système International d'Unités) *system*, which has as its three basic

units the meter (m), the kilogram (kg), and the second (s). The other systems are the English foot (ft)–pound (lb)–second (s), or *English system*, and the centimeter (cm)–gram (g)–second (s), or *cgs system*.

At present, the SI system has been adopted officially for use exclusively in engineering and science, but the older English and cgs systems are still used. Much of the physical and chemical data, and empirical equations are given in these latter two systems. Hence, engineers should not only be proficient in the SI system, but must also be able to use the other two systems as well.

### **1.2A SI System of Units**

The basic quantities used in the SI system are as follows: the unit of

length is the meter (m); the unit of time is the second (s); the unit of mass is the kilogram (kg); the unit of temperature is the kelvin (K); and the unit of an element is the kilogram mole (kg mol). The other standard units are derived from these basic quantities.

The basic unit of force is the newton (N), defined as

$$1 \text{ newton (N)} = 1 \text{ kg} \cdot \text{m/s}^2$$

The basic unit of work, energy, or heat is the newton-meter, or joule (J).

$$1 \text{ joule (J)} = 1 \text{ newton} \cdot \text{m (N} \cdot \text{m)} = 1 \text{ kg} \\ \cdot \text{m}^2/\text{s}^2$$

Power is measured in joules/s or watts (W).



$$1 \text{ joule/s (J/s)} = 1 \text{ watt (W)}$$

The unit of pressure is the newton/m<sup>2</sup> or pascal (Pa).

$$1 \text{ newton/m}^2 \text{ (N/m}^2\text{)} = 1 \text{ pascal (Pa)}$$

The standard acceleration of gravity is defined as

$$1 \text{ } g = 9.80665 \text{ m/s}^2$$

A few of the standard prefixes for multiples of the basic units are as follows: giga (G) = 10<sup>9</sup>, mega (M) = 10<sup>6</sup>, kilo (k) = 10<sup>3</sup>, centi (c) = 10<sup>-2</sup>, milli (m) = 10<sup>-3</sup>, micro (μ) = 10<sup>-6</sup>, and nano (n) = 10<sup>-9</sup>.

Temperatures are defined in kelvin (K) as the preferred unit in the SI system. However, in practice, wide use is made

of the degree Celsius ( $^{\circ}\text{C}$ ) scale, which is defined by

$$T(^{\circ}\text{C}) = T(\text{K}) - 273.15$$

Note that  $1^{\circ}\text{C} = 1 \text{ K}$  and that in the case of temperature difference,

$$\Delta T(^{\circ}\text{C}) = \Delta T(\text{K})$$

The standard preferred unit of time is the second (s), but time can be in nondecimal units of minutes (min), hours (h), or days (d).

### **1.2B CGS System of Units**

The cgs system is related to the SI system as follows:

$$1 \text{ g mass (g)} = 1 \times 10^{-3} \text{ kg mass (kg)}$$

$$1 \text{ cm} = 1 \times 10^{-2} \text{ m}$$

1 dyne (dyn) = 1 g · cm/s<sup>2</sup> = 1 × 10<sup>-5</sup> newton (N)

1 erg = 1 dyn · cm = 1 × 10<sup>-7</sup> joule (J)

The standard acceleration of gravity is

$$g = 980.665 \text{ cm/s}^2$$

### **1.2C English FPS System of Units**

The English system is related to the SI system as follows:

1 lb mass (lb<sub>m</sub>) = 0.45359 kg

1 ft = 0.30480 m

1 lb force (lb<sub>f</sub>) = 4.4482 newton (N)

1 ft · lb<sub>f</sub> = 1.35582 newton · m (N · m) =  
1.35582 joules (J)

$$1 \text{ psia} = 6.89476 \times 10^3 \text{ newton/m}^2 \text{ (N/m}^2\text{)}$$

$$1.8^\circ\text{F} = 1 \text{ K} = 1^\circ\text{C (centigrade or Celsius)}$$

$$g = 32.174 \text{ ft/s}^2$$

The proportionality factor for Newton's law is

$$g_c = 32.174 \text{ ft} \cdot \text{lb}_m/\text{lb}_f \cdot \text{s}^2$$

The factor  $g_c$  in SI units and cgs units is 1.0 and is frequently omitted.

In Appendix A.1, convenient conversion factors for all three systems are tabulated. Further discussions and use of these relationships are given in various sections of the text.

This text uses the SI system as the primary set of units in the equations, example problems, and homework problems. However, the important equations derived in the text are given in a dual set of units, SI and English, when these equations differ. Some example problems and homework problems are also given using English units. In some cases, intermediate steps and/or answers in example problems are also stated in English units.

### **1.2D Dimensionally Homogeneous Equations and Consistent Units**

A dimensionally homogeneous equation is one in which all the terms have the same units. These units can be the base units or derived ones (i.e.,  $\text{kg/s}^2 \cdot \text{m}$  or Pa). Such an equation can be used with any system of units provided that the

same base or derived units are used throughout the equation. No conversion factors are needed when consistent units are used.

The reader should be careful about using any equation and should always check it for dimensional homogeneity. To do this, a system of units (SI, English, etc.) is first selected. Then, units are substituted for each term in the equation and like units in each term canceled out.

## **1.3 Methods of Expressing Temperatures and Compositions**

### **1.3A Temperature**

There are two temperature scales in common use in the chemical and biological industries. These are degrees Fahrenheit (abbreviated °F) and Celsius (°C). It is often

necessary to convert from one scale to the other. Both use the freezing point and boiling point of water at 1 atmosphere pressure as base points. Temperatures are often expressed as absolute degrees K (SI standard) or degrees Rankine ( $^{\circ}\text{R}$ ) instead of  $^{\circ}\text{C}$  or  $^{\circ}\text{F}$ . Table 1.3-1 shows the equivalences of the four temperature scales.

The difference between the boiling point of water and melting point of ice at 1 atm is  $100^{\circ}\text{C}$  or  $180^{\circ}\text{F}$ . Thus, a  $1.8^{\circ}\text{F}$  change is equal to a  $1^{\circ}\text{C}$  change.

Usually, the value of  $-273.15^{\circ}\text{C}$  is rounded to  $-273.2^{\circ}\text{C}$  and  $-459.67^{\circ}\text{F}$  to  $-460^{\circ}\text{F}$ . The following equations can be used to convert from one temperature scale to another:

$$^{\circ}\text{F}=32+1.8(^{\circ}\text{C})(1.3-1)$$

$$^{\circ}\text{C}=11.8(^{\circ}\text{F}-32)(1.3-2)$$

$$^{\circ}\text{R}=^{\circ}\text{F}+459.67(1.3-3)$$

$$\text{K}=^{\circ}\text{C}+273.15(1.3-4)$$

### **1.3B Mole Units and Weight or Mass Units**

There are many methods used to express compositions in gases, liquids, and solids. One of the most useful is molar units, since chemical reactions and gas laws are simpler to express in terms of molar units. A mole (mol) of a pure substance is defined as the amount of that substance whose mass is numerically equal to its molecular weight. Hence, 1 kg mol of methane  $\text{CH}_4$  contains 16.04 kg. Also, 1.0 lb mol of methane contains 16.04 lb<sub>m</sub>.



The mole fraction of a particular substance is simply the moles of this substance divided by the total number of moles. Likewise, the weight or mass fraction is the mass of the substance divided by the total mass. These two compositions, which hold for gases, liquids, and solids, can be expressed as follows for component *A* in a mixture:

Table 1.3-1. *Temperature Scales and Equivalents*



mole fraction of *A*) =  $\frac{\text{moles of } A}{\text{total moles}}$  (1.3-5)

mass or wt fraction of *A*) =  $\frac{\text{mass } A}{\text{total mass}}$  (1.3-6)

**EXAMPLE 1.3-1. Mole and Mass, or Weight Fraction of a Solution**

A container holds 50 g of water (*B*) and 50 g of NaOH (*A*). Calculate the weight fraction and mole fraction of NaOH. Also, calculate the lb<sub>m</sub> of NaOH (*A*) and H<sub>2</sub>O (*B*).

**Solution:** Taking as a basis for calculation 50 + 50 or 100 g of solution, the following data are calculated:

--

Hence,  $x_A = 0.310$ ,  $x_B = 0.690$ , and  $x_A + x_B = 0.310 + 0.690 = 1.00$ . Also,  $w_A + w_B = 0.500 + 0.500 = 1.00$ . To calculate the lb<sub>m</sub> of each component, **Appendix A.1** gives the conversion factor of 453.6 g per 1 lb<sub>m</sub>. Using this,

$$\text{lb mass of A} = 50 \text{ g A} / 453.6 \text{ g A/lbm A} = 0.1102 \text{ lbm A}$$

Note that the g of A in the numerator cancels the g of A in the denominator, leaving lb<sub>m</sub> of A in the numerator of the final answer. The reader is cautioned to put all units down in an equation and cancel those appearing in the numerator and denominator. In a similar manner, we obtain 0.1102 lb<sub>m</sub> B (0.0500 kg B).

The analyses of solids and liquids are usually given as a weight or mass fraction or a weight percent, and gases as a mole fraction or percent. Unless otherwise stated, analyses of solids and liquids will be assumed to be a weight (mass) fraction or percent, and those of gases to be a mole fraction or percent.

### 1.3C Concentration Units for Liquids

In general, when one liquid is mixed

with another miscible liquid, the volumes are not additive. Hence, compositions of liquids are usually not expressed as the volume percent of a component but as the weight or mole percent. Another convenient way to express concentrations of components in a solution is *molarity*, which is defined as g mol of a component per liter of solution.

Other methods used are kg/m<sup>3</sup>, g/liter, g/cm<sup>3</sup>, lb mol/ft<sup>3</sup>, lb<sub>m</sub>/ft<sup>3</sup>, and lb<sub>m</sub>/gallon. All of these concentrations depend on temperature, so the temperature must be specified.

The most common method of expressing total concentration per unit volume is density, kg/m<sup>3</sup>, g/cm<sup>3</sup>, or lb<sub>m</sub>/ft<sup>3</sup>. For example, the density of water at

277.2 K (4°C) is 1000 kg/m<sup>3</sup>, or 62.43 lb<sub>m</sub>/ft<sup>3</sup>. Sometimes the density of a solution is expressed as *specific gravity*, which is defined as the density of the solution at its given temperature divided by the density of a reference substance at its temperature. If the reference substance is water at 277.2 K, the specific gravity and density of the substance are numerically equal.

## 1.4 Gas Laws and Vapor Pressure

### 1.4A Pressure

There are numerous ways of expressing the pressure exerted by a fluid or system. An *absolute pressure* of 1.00 atm is equivalent to 760 mmHg at 0°C, 29.921 in. Hg, 0.760 m Hg, 14.696 lb force per square inch (psia), or 33.90 ft of water at 4°C. *Gage pressure* is the

pressure above the absolute pressure.

Hence, a pressure of 21.5 lb per square inch gage (*psig*) is 21.5 +

14.7 (rounded off), or 36.2 psia. In

SI units,  $1 \text{ psia} = 6.89476 \times 10^3$

pascal (Pa) =  $6.89476 \times 10^3$

newtons/m<sup>2</sup>. Also,  $1 \text{ atm} = 1.01325$

$\times 10^5 \text{ Pa}$ .

In some cases, particularly in

evaporation, one may express the

pressure as inches of mercury vacuum.

This means the pressure as inches of mercury measured “below” the absolute

barometric pressure. For example, a

reading of 25.4 in. Hg vacuum is 29.92

– 25.4, or 4.52 in. Hg absolute pressure.

Pressure conversion units are given in

Appendix A.1.

#### **1.4B Ideal Gas Law**

An *ideal gas* is defined as one that obeys simple laws. Also, in the ideal gas approximation, the gas molecules are considered as rigid spheres that occupy no volume and do not exert forces on one another. No real gases obey these laws exactly, but at ordinary temperatures and pressures of not more than several atmospheres, the ideal gas law gives answers within a few percent or less of the actual answers. Hence, for certain situations, this law is sufficiently accurate for engineering calculations.

The *ideal gas law* of Boyle states that the volume of a gas is directly proportional to the absolute temperature and inversely proportional to the absolute pressure. This is expressed as

$$pV=nRT(1.4-1)$$

where  $p$  is the absolute pressure in  $\text{N/m}^2$ ,  $V$  is the volume of the gas in  $\text{m}^3$ ,  $n$  is the kg mol of the gas,  $T$  is the absolute temperature in K, and  $R$  is the gas-law constant of  $8314.3 \text{ kg} \cdot \text{m}^2/\text{kg mol} \cdot \text{s}^2 \cdot \text{K}$ . When the volume is in  $\text{ft}^3$ ,  $n$  in lb moles, and  $T$  in  $^\circ\text{R}$ ,  $R$  has a value of  $0.7302 \text{ ft}^3 \cdot \text{atm}/\text{lb mol} \cdot ^\circ\text{R}$ . For cgs units (see Appendix A.1),  $V = \text{cm}^3$ ,  $T = \text{K}$ ,  $R = 82.057 \text{ cm}^3 \cdot \text{atm}/\text{g mol} \cdot \text{K}$ , and  $n = \text{g mol}$ .

In order that amounts of various gases may be compared, *standard conditions of temperature and pressure* (abbreviated STP or SC) are arbitrarily defined as 101.325 kPa (1.0 atm) abs and 273.15 K ( $0^\circ\text{C}$ ). Under these conditions, the volumes are as follows:

Volume of 1.0 g mol (SC)=22.414 L (liter)=22.414 cm<sup>3</sup>

**EXAMPLE 1.4-1. Gas-Law Constant**

Calculate the value of the gas-law constant  $R$  when the pressure is in psia, moles in lb mol, volume in ft<sup>3</sup>, and temperature in °R. Repeat for SI units.

**Solution:** At standard conditions,  $p = 14.7$  psia,  $V = 359$  ft<sup>3</sup>, and  $T = 460 + 32 = 492^\circ\text{R}$  (273.15 K). Substituting into Eq. (1.4-1) for  $n = 1.0$  lb mol and solving for  $R$ ,

$$\begin{aligned} R &= pVnT = (14.7 \text{ psia})(359 \text{ ft}^3)(1.0 \text{ lb mol}) \\ &\quad (492^\circ\text{R}) = 10.73 \text{ ft}^3 \cdot \text{psia} \cdot \text{lb mol}^{-1} \cdot \\ \text{°RR} &= pVnT = (1.01325 \times 10^5 \text{ Pa})(22.414 \text{ m}^3)(1.0 \text{ kg mol}) \\ &\quad (273.15 \text{ K}) = 8314 \text{ m}^3 \cdot \text{Pa} \cdot \text{kg mol}^{-1} \cdot \text{K} \end{aligned}$$

A useful relation can be obtained from Eq. (1.4-1) for  $n$  moles of gas at conditions  $p_1, V_1, T_1$ , and also at conditions  $p_2, V_2, T_2$ . Substituting into Eq. (1.4-1),

$$p_1 V_1 = nRT_1$$

$$p_2 V_2 = nRT_2$$

Combining gives



$$p_1 V_1 p_2 V_2 = T_1 T_2 (1.4-2)$$

### 1.4C Ideal Gas Mixtures

*Dalton's law* for mixtures of ideal gases states that the total pressure of a gas mixture is equal to the sum of the individual partial pressures:

$$P = p_A + p_B + p_C + \dots (1.4-3)$$

where  $P$  is total pressure and  $p_A$ ,  $p_B$ ,  $p_C$ , ... are the partial pressures of the components  $A$ ,  $B$ ,  $C$ , ... in the mixture.

Since the number of moles of a component is proportional to its partial pressure, the mole fraction of a component is

$$x_A = \frac{p_A}{P} = \frac{p_A}{p_A + p_B + p_C + \dots} (1.4-4)$$

The volume fraction is equal to the mole

fraction. Gas mixtures are almost always represented in terms of mole fractions and not weight fractions. For engineering purposes, Dalton's law is sufficiently accurate to use for actual mixtures at total pressures of a few atmospheres or less.

**EXAMPLE 1.4-2. Composition of a Gas Mixture**

A gas mixture contains the following components and partial pressures: CO<sub>2</sub>, 75 mmHg; CO, 50 mmHg; N<sub>2</sub>, 595 mmHg; and O<sub>2</sub>, 26 mmHg. Calculate the total pressure and the composition in mole fraction.

**Solution:** Substituting into Eq. (1.4-3),

$$P = p_A + p_B + p_C + p_D = 75 + 50 + 595 + 26 = 746 \text{ mmHg}$$

The mole fraction of CO<sub>2</sub> is obtained by using Eq. (1.4-4).

$$x_A (\text{CO}_2) = \frac{p_A}{P} = \frac{75}{746} = 0.101$$

In like manner, the mole fractions of CO, N<sub>2</sub>, and O<sub>2</sub> are calculated as 0.067, 0.797, and 0.035, respectively.

## 1.4D Vapor Pressure and Boiling Point of Liquids

When a liquid is placed in a sealed container, molecules of the liquid will evaporate into the space above

the liquid and fill it completely.

After a fixed amount of time, equilibrium is reached. This vapor will exert a pressure just like a gas and we call this pressure the *vapor pressure* of the liquid. The value of the vapor pressure is independent of the amount of liquid in the container as long as some is present.

If an inert gas such as air is also present in the vapor space, it will have very little effect on the vapor pressure. In general, the effect of total pressure on vapor pressure can be considered as negligible for pressures of a few atmospheres or less.

The vapor pressure of a liquid increases markedly with temperature. For example, from Appendix A.2 for water,

the vapor pressure at  $50^{\circ}\text{C}$  is 12.333 kPa (92.51 mmHg). At  $100^{\circ}\text{C}$ , the vapor pressure has increased greatly to 101.325 kPa (760 mmHg).

The *boiling point* of a liquid is defined as the temperature at which the vapor pressure of a liquid equals the total pressure. Hence, if the atmospheric total pressure is 760 mmHg, water will boil at  $100^{\circ}\text{C}$ . On top of a high mountain, where the total pressure is considerably less, water will boil at temperatures below  $100^{\circ}\text{C}$ .

A plot of vapor pressure  $P_A$  of a liquid versus temperature does not yield a straight line but a curve. However, for moderate temperature ranges, a plot of  $\log P_A$  versus  $1/T$  is a reasonably straight line, as follows:

$$\log P_A = m(1/T) + b(1.4-5)$$

where  $m$  is the slope,  $b$  is a constant for the liquid  $A$ , and  $T$  is the temperature in K.

## 1.5 Conservation of Mass and Material Balances

### 1.5A Conservation of Mass

One of the basic laws of physical science is the *law of conservation of mass*. This law, stated simply, says that mass cannot be created or destroyed (excluding, of course, nuclear or atomic reactions). Hence, the total mass (or weight) of all materials entering any process must equal the total mass of all materials leaving plus the mass of any materials accumulating or left in the process:

$$\text{input} = \text{output} + \text{accumulation} \quad (1.5-1)$$

In many cases, there will be no accumulation of materials in a process, and in those cases the input will simply equal the output. Stated in other words, “what goes in must come out.” We call this type of process a *steady-state process*:

$$\text{input} = \text{output (steady state)} \quad (1.5-2)$$

### **1.5B Simple Material Balances**

In this section, we do simple material (weight or mass) balances in various processes at steady state with no chemical reaction occurring. We can use units of kg, lb<sub>m</sub>, lb mol, g, kg mol, and so on, in our balances. The reader is cautioned to be consistent and not to mix several

units in a balance. When chemical reactions occur in the balances (as discussed in Section 1.5D), one should use kg mol units, since chemical equations relate moles reacting. In Chapter 4, overall mass balances will be covered in more detail and in Chapter 8, differential mass balances will be covered.

To solve a material-balance problem, it is advisable to proceed by a series of definite steps, as listed below:

1. *Sketch a simple diagram of the process.* This can be a simple box diagram showing each stream entering by an arrow pointing in and each stream leaving by an arrow pointing out. Include on each arrow the compositions, amounts, temperatures, and so on, of that stream. All pertinent data should be on this diagram.
2. *Write the chemical equations involved (if any).*
3. *Select a basis for calculation.* In most cases, the problem is concerned with a specific amount of one of the streams

in the process, which is selected as the basis.

4. *Make a material balance.* The arrows into the process will be input items and the arrows going out will be output items. The balance can be a total material balance as in Eq. (1.5-2) or a balance on each component present (if no chemical reaction occurs).

Typical processes that do not undergo chemical reactions are drying, evaporation, dilution of solutions, distillation, extraction, and so on. These can be solved by setting up material balances containing unknowns and solving these equations for the unknowns.

**EXAMPLE 1.5-1. Concentration of Orange Juice**

In the concentration of orange juice, a freshly extracted and strained juice containing 7.08 wt % solids is fed to a vacuum evaporator. In the evaporator, water is removed and the solids content increased to 58 wt % solids. For 1000 kg/h entering, calculate the amounts of the outlet streams of concentrated juice and water.

**Solution:** Following the four steps outlined, we make a process flow diagram (step 1), as shown in Fig. 1.5-1. Note that the letter  $W$  represents the unknown amount of water and  $C$  the amount of concentrated juice. No chemical reactions are given (step 2). Basis: 1000 kg/h entering juice (step 3).



To make the material balances (step 4), a total material balance will be made using Eq. (1.5-2):

$$1000 = W + C \quad (1.5-3)$$

This gives one equation and two unknowns. Hence, a component balance on solids will be made:

$$1000(7.08100) = W(0) + C(58100) \quad (1.5-4)$$

To solve these two equations, we solve Eq. (1.5-4) first for  $C$  since  $W$  drops out. We get  $C = 122.1$  kg/h concentrated juice.

Substituting the value of  $C$  into Eq. (1.5-3),

$$1000 = W + 122.1$$

and we obtain  $W = 877.9$  kg/h water.

As a check on our calculations, we can write a balance on the water component:

$$1000(100 - 7.08100) = 877.9 + 122.1(100 - 58100) \quad (1.5-5)$$

Solving,

$$929.2 = 877.9 + 51.3 = 929.2$$

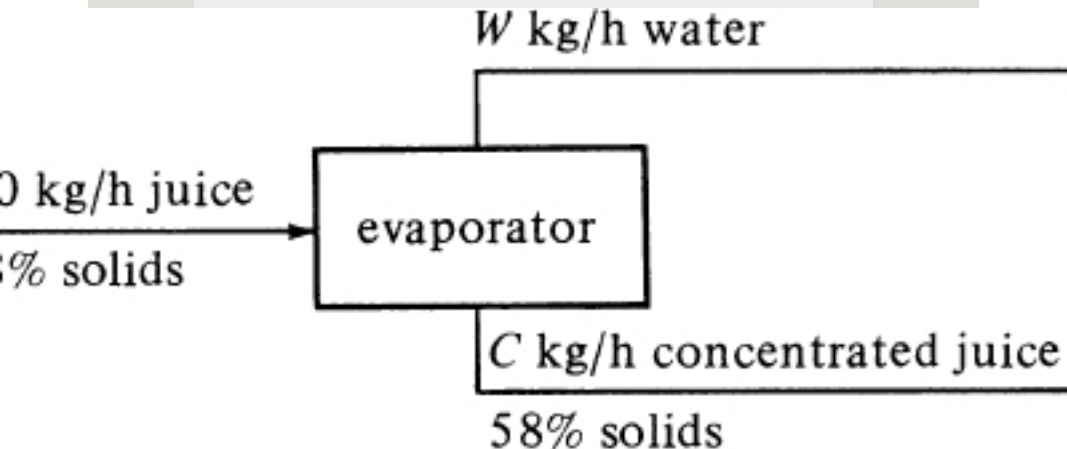


Figure 1.5-1. Process flow diagram for Example 1.5-1.

In Example 1.5-1, only one unit or separate process was involved. Often, a number of processes in series are involved. Then, we have a choice of making a separate balance over each separate process and/or a balance around the complete overall process.

### **1.5C Material Balances and Recycle**

Processes that have a recycle or feedback of part of the product into the entering feed are sometimes encountered. For example, in a sewage treatment plant, part of the activated sludge from a sedimentation tank is recycled back to the aeration tank where the liquid is treated. In some food-drying operations, the humidity of the entering air is controlled by

recirculating part of the hot, wet air that leaves the dryer. In chemical reactions, the material that did not react in the reactor can be separated from the final product and fed back to the reactor.

**EXAMPLE 1.5-2. Crystallization of  $\text{KNO}_3$  and Recycle**

In a process producing  $\text{KNO}_3$  salt, 1000 kg/h of a feed solution containing 20 wt %  $\text{KNO}_3$  is fed to an evaporator, which evaporates some water at 422 K to produce a 50 wt %  $\text{KNO}_3$  solution. This is then fed to a crystallizer at 311 K, where crystals containing 96 wt %  $\text{KNO}_3$  are removed. The saturated solution containing 37.5 wt %  $\text{KNO}_3$  is recycled to the evaporator. Calculate the amount of the recycle stream  $R$  in kg/h and the product stream of crystals  $P$  in kg/h.

**Solution:** Figure 1.5-2 gives the process flow diagram. As a basis, we shall use 1000 kg/h of fresh feed. No chemical reactions are occurring. We can make an overall balance on the entire process for  $\text{KNO}_3$  and solve for  $P$  directly:

$$1000(0.20) = W(0) + P(0.96)(1.5 - 6)P = 208.3 \text{ kg crystals/h}$$

To calculate the recycle stream, we can make a balance around the evaporator or the crystallizer. Using a balance on the crystallizer, since it now includes only two unknowns,  $S$  and  $R$ , we get for a total balance,

$$S = R + 208.3(1.5 - 7)$$

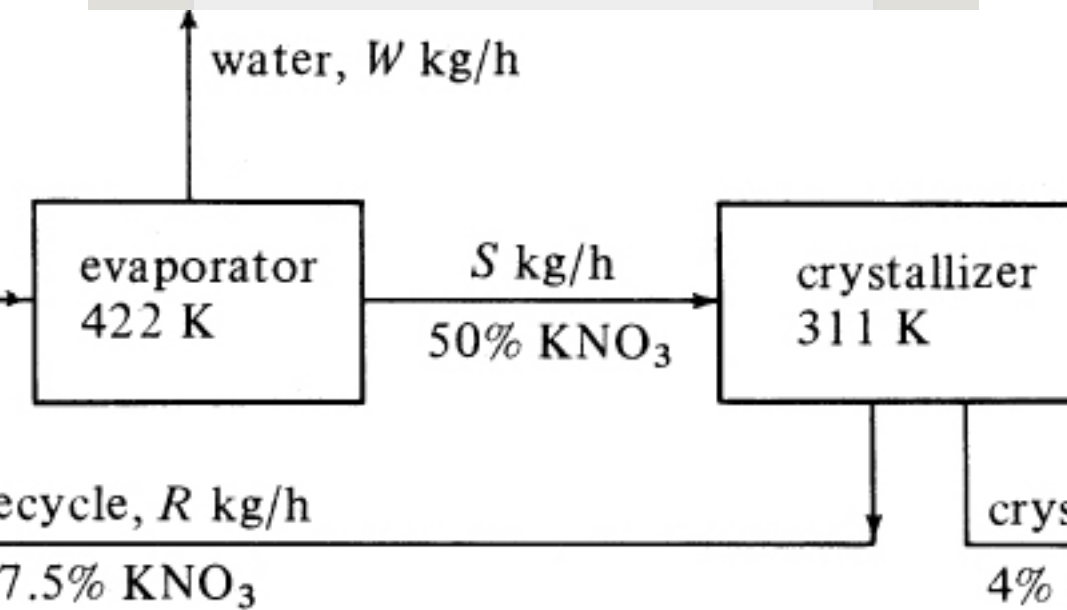


Figure 1.5-2. Process flow diagram for Example 1.5-2.

For a  $\text{KNO}_3$  balance on the crystallizer,

$$S(0.50) = R(0.375) + 208.3(0.96) \quad (1.5-8)$$

Substituting  $S$  from Eq. (1.5-7) into Eq. (1.5-8) and solving,  
 $R = 766.6 \text{ kg recycle/h}$  and  $S = 974.9 \text{ kg/h}$ .

### 1.5D Material Balances and Chemical Reaction

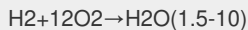
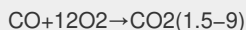
In many cases, the materials entering a process undergo chemical reactions in the process, so that the materials leaving are different from those entering. In these cases, it is usually convenient to make a molar

and not a weight balance on an individual component, such as kg mol H<sub>2</sub> or kg atom H, kg mol CO<sub>3</sub><sup>2-</sup> ion, kg mol CaCO<sub>3</sub>, kg atom Na<sup>+</sup>, kg mol N<sub>2</sub>, and so on. For example, in the combustion of CH<sub>4</sub> with air, balances can be made on kg mol of H<sub>2</sub>, C, O<sub>2</sub>, or N<sub>2</sub>.

**EXAMPLE 1.5-3. Combustion of a Fuel Gas**

A fuel gas containing 3.1 mol % H<sub>2</sub>, 27.2% CO, 5.6% CO<sub>2</sub>, 0.5% O<sub>2</sub>, and 63.6% N<sub>2</sub> is burned with 20% excess air (i.e., the air over and above that necessary for complete combustion to CO<sub>2</sub> and H<sub>2</sub>O). The combustion of CO is only 98% complete. For 100 kg mol of fuel gas, calculate the moles of each component in the exit flue gas.

**Solution:** First, the process flow diagram is drawn (Fig. 1.5-3). On the diagram, the components in the flue gas are shown. Let *A* be moles of air and *F* be moles of flue gas. Next, the chemical reactions are given:



An accounting of the total moles of O<sub>2</sub> in the fuel gas is as follows:

$$\text{mol O}_2 \text{ in fuel gas} = (1/2)(27.2)(\text{CO}) + 5.6(\text{CO}_2) + 0.5(\text{O}_2) = 19.7 \text{ mol O}_2$$

For all the H<sub>2</sub> to be completely burned to H<sub>2</sub>O, we need, from Eq. (1.5-10), 12 mol O<sub>2</sub> for 1 mol H<sub>2</sub>, or 3.1 (12)=1.55 total mol O<sub>2</sub>. For completely burning the CO from Eq.

(1.5-9), we need  $27.2(12)=13.6$  mol  $O_2$ . Hence, the amount of  $O_2$  we must add is, theoretically, as follows:

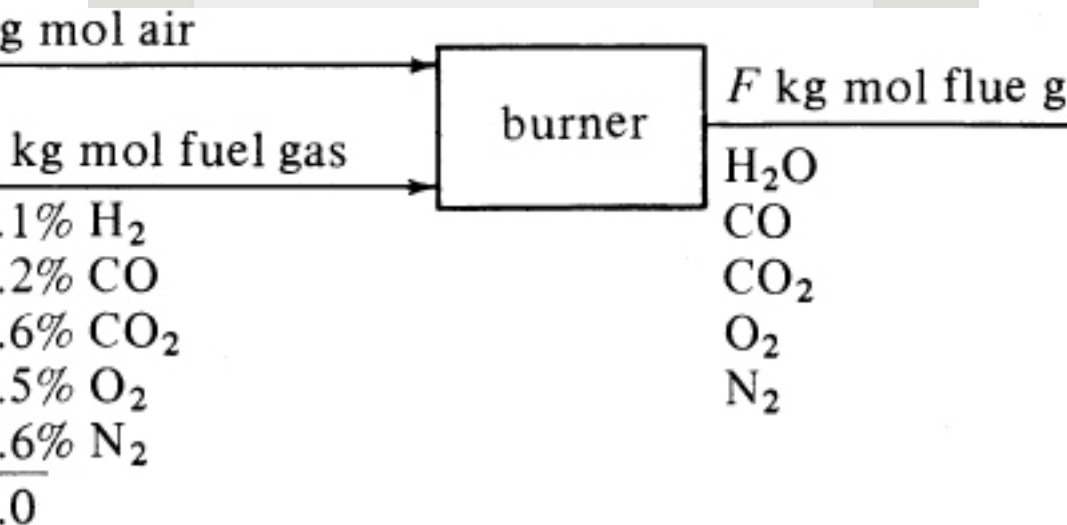


Figure 1.5-3. Process flow diagram for Example 1.5-3.

mol  $O_2$  theoretically needed =  $1.55 + 13.6 - 0.5$  (in fuel gas) =  $14.65$  mol  $O_2$

For a 20% excess, we add  $1.2(14.65)$ , or  $17.58$  mol  $O_2$ .

Since air contains 79 mol %  $N_2$ , the amount of  $N_2$  added is  $(79/21)(17.58)$ , or  $66.1$  mol  $N_2$ .

To calculate the moles in the final flue gas, all the  $H_2$  gives  $H_2O$ , or  $3.1$  mol  $H_2O$ . For  $CO$ , 2.0% does not react. Hence,  $0.02(27.2)$ , or  $0.54$  mol  $CO$  will be unburned.

A total carbon balance is as follows: inlet moles  $C = 27.2 + 5.6 = 32.8$  mol  $C$ . In the outlet flue gas,  $0.54$  mol will be as  $CO$  and the remainder of  $32.8 - 0.54$ , or  $32.26$  mol as  $CO_2$ .

For calculating the outlet mol  $O_2$ , we make an overall  $O_2$  balance:

$$O_2 \text{ in} = 19.7$$

$$\text{in fuel gas} + 17.58 \text{ (in air)} = 37.28 \text{ mol } O_2 \quad O_2 \text{ out} = (3.1/2) \text{ (in } H_2O) + (0.54/2) \text{ (in } CO) + 32.26 \text{ (in } CO_2) + \text{free } O_2$$

Equating inlet  $O_2$  to outlet, the free remaining  $O_2 = 3.2$  mol  $O_2$ . For the  $N_2$  balance, the outlet =  $63.6$  (in fuel gas) +

66.1 (in air), or 129.70 mol N<sub>2</sub>. The outlet flue gas contains 3.10 mol H<sub>2</sub>O, 0.54 mol CO, 32.26 mol CO<sub>2</sub>, 3.20 mol O<sub>2</sub>, and 129.7 mol N<sub>2</sub>.

In chemical reactions with several reactants, the limiting reactant component is defined as that compound that is present in an amount less than the amount necessary for it to react stoichiometrically with the other reactants. Then, the percent completion of a reaction is the amount of this limiting reactant actually converted, divided by the amount originally present, times 100.

## **1.6 Energy and Heat Units**

### **1.6A Joule, Calorie, and Btu**

In a manner similar to that used in making material balances on chemical and biological processes, we can also make energy balances

on a process. Often, a large portion of the energy entering or leaving a system is in the form of heat. Before such energy or heat balances are made, we must understand the various types of energy and heat units.

In the SI system, energy is given in joules (J) or kilojoules (kJ). Energy is also expressed in btu (British thermal units) or cal (calories). The calorie (abbreviated as cal) is defined as the amount of heat needed to heat 1.0 g water 1.0°C (from 14.5°C to 15.5°C). Also, 1 kcal (kilocalorie) = 1000 cal. The btu is defined as the amount of heat needed to raise 1.0 lb water 1°F. Hence, from Appendix A.1,

$$1 \text{ Btu} = 252.16 \text{ cal} = 1.05506 \text{ kJ} \quad (1.6-1)$$



## 1.6B Heat Capacity

The *heat capacity* of a substance is defined as the amount of heat necessary to increase the temperature by 1 degree. It can be expressed for 1 g, 1 lb, 1 g mol, 1 kg mol, or 1 lb mol of the substance.

For example, a heat capacity is expressed in SI units as J/kg mol · K; in other units as cal/g · °C, cal/g mol · °C, kcal/kg mol · °C, Btu/lb<sub>m</sub> · °F, or btu/lb mol · °F.

It can be shown that the actual numerical value of a heat capacity is the same in mass units or in molar units.

That is,

$$1.0 \text{ cal/g} \cdot \text{C}^\circ = 1.0 \text{ btu/lbm} \cdot \text{F}^\circ \quad (1.6-2)$$

$$1.0 \text{ cal/}$$

$$1 \text{ g mol} \cdot \text{C}^\circ = 1.0 \text{ btu/lb mol} \cdot \text{F}^\circ \quad (1.6-3)$$

For example, to prove this, suppose that a substance has a heat capacity of  $0.8 \text{ btu/lbm} \cdot \text{F}^\circ$ . The conversion is made using  $1.8^\circ\text{F}$  for  $1^\circ\text{C}$  or  $1 \text{ K}$ ,  $252.16 \text{ cal}$  for  $1 \text{ btu}$ , and  $453.6 \text{ g}$  for  $1 \text{ lbm}$ , as follows:

$$\begin{aligned} \text{heat capacity (cal g} \cdot \text{C}^\circ) &= (0.8 \text{ btu/lbm} \cdot \text{F}^\circ) \\ &\quad (252.16 \text{ cal/btu}) (453.6 \text{ g/lbm}) \\ &\quad (1.8 \text{ F}^\circ \cdot \text{C}^\circ) = 0.8 \text{ cal g} \cdot \text{C}^\circ \end{aligned}$$

The heat capacities of gases (also called *specific heat*) at constant pressure  $c_p$  are functions of temperature and, for engineering purposes, can often be assumed to be independent of pressure up to several atmospheres. In most process-engineering calculations, one is usually interested in the amount of heat

needed to heat a gas from one temperature  $t_1$  to another at  $t_2$ . Since the  $c_p$  varies with temperature, an integration must be performed or a suitable mean  $c_{pm}$  used. These mean values for gases have been obtained for  $T_1$  of 298 K or 25°C (77°F) and various  $T_2$  values, and are tabulated in Table 1.6-1 at 101.325 kPa pressure or less as  $c_{pm}$  in kJ/kg mol · K at various values of  $T_2$  in K or °C.

Table 1.6-1. *Mean Molar Heat Capacities of Gases Between 298 and  $T$  K (25 and  $T$ °C) at 101.325 kPa or Less (SI Units:  $c_p = \text{kJ/kg mol} \cdot \text{K}$ )*

*Mean Molar Heat Capacities of Gases Between 25 and  $T$ °C at 1 atm Pressure or Less (English Units:  $c_p = \text{btu/lb mol} \cdot$*

Source: O. A. Hougen, K. W. Watson, and R. A. Ragatz, *Chemical Process Principles*, Part I, 2nd ed. New York: John Wiley & Sons, Inc., 1954.

**EXAMPLE 1.6-1. Heating of N<sub>2</sub> Gas**

The gas N<sub>2</sub> at 1 atm pressure absolute is being heated in a heat exchanger. Calculate the amount of heat needed in J to heat 3.0 g mol N<sub>2</sub> in the following temperature ranges:

- 298–673 K (25–400°C)
- 298–1123 K (25–850°C)
- 673–1123 K (400–850°C)

**Solution:** For case (a), Table 1.6-1 gives  $c_{pm}$  values at 1 atm pressure or less, which can be used up to several atm pressures. For N<sub>2</sub> at 673 K,  $c_{pm} = 29.68$  kJ/kg mol · K or 29.68 J/g mol · K. This is the mean heat capacity for the range 298–673 K:

$$\text{heat required} = M \text{ g mol } (pmC \text{ Jg mol} \cdot \text{K}) (T_2 - T_1) \text{ K} \quad (1.6-4)$$

Substituting the known values,

$$\text{heat required} = (3.0)(29.68)(673 - 298) = 33\,390 \text{ J}$$

For case (b), the  $c_{pm}$  at 1123 K (obtained by linear interpolation between 1073 and 1173 K) is 31.00 J/g mol · K:

$$\text{heat required} = (3.0)(31.00)(1123 - 298) = 76\,725 \text{ J}$$

For case (c), there is no mean heat capacity for the interval 673–1123 K. However, we can use the heat required to heat the gas from 298 to 673 K in case (a) and subtract it

from case (b), which includes the heat required to go from 298 to 673 K plus 673 to 1123 K:

$$\text{heat required (673 – 1123 K)} = \text{heat required (298 – 1123 K)} \\ (1.6-5) - \text{heat required (298 – 673)}$$

Substituting the proper values into Eq. (1.6-5),

$$\text{heat required} = 76\,725 - 33\,390 = 43\,335 \text{ J}$$

When heating a gas mixture, the total heat required is determined by first calculating the heat required for each individual component and then adding the results to obtain the total.

The heat capacities of solids and liquids are also functions of temperature and independent of pressure. Data are given in Appendix A.2, Physical Properties of Water; A.3, Physical Properties of Inorganic and Organic Compounds; and A.4, Physical Properties of Foods and Biological Materials. More data are available in (P1) in the References section at the end of this chapter.

**EXAMPLE 1.6-2. Heating of Milk**

Rich cows' milk (4536 kg/h) at 4.4°C is being heated in a heat exchanger to 54.4°C by hot water. How much heat is needed?

**Solution:** From Appendix A.4, the average heat capacity of rich cows' milk is 3.85 kJ/kg · K. The temperature rise is  $\Delta T = (54.4 - 4.4)^\circ\text{C} = 50\text{ K}$ .

$$\text{heat required} = (4536 \text{ kg/h})(3.85 \text{ kJ/kg} \cdot \text{K})(1/3600 \text{ h/s})(50 \text{ K}) = 242.5 \text{ kW}$$

The enthalpy,  $H$ , of a substance in J/kg represents the sum of the internal energy plus the pressure–volume term. For no reaction and a constant-pressure process with a change in temperature, the heat change as computed from Eq. (1.6-4) is the difference in enthalpy,  $\Delta H$ , of the substance relative to a given temperature or base point. In other units,  $H = \text{btu/lb}_m$  or  $\text{cal/g}$ .

**1.6C Latent Heat and Steam Tables**

Whenever a substance undergoes a change of phase, relatively large

amounts of heat change are involved at a constant temperature. For example, ice at  $0^{\circ}\text{C}$  and 1 atm pressure can absorb  $6013.4 \text{ kJ/kg mol}$ . This enthalpy change is called the *latent heat of fusion*. Data for other compounds are available in various handbooks (P1, W1).

When a liquid phase vaporizes to a vapor phase under its vapor pressure at constant temperature, an amount of heat called the *latent heat of vaporization* must be added. For water at  $25^{\circ}\text{C}$  and a pressure of 23.75 mmHg, the latent heat is  $44\,020 \text{ kJ/kg mol}$ , and at  $25^{\circ}\text{C}$  and 760 mmHg,  $44\,045 \text{ kJ/kg mol}$ . Hence, the effect of pressure can be neglected in these types of engineering calculations. However, there is a large effect of temperature on the latent heat of water.

Also, the effect of pressure on the heat capacity of liquid water is small and can be neglected.

Since water is a very common chemical, the thermodynamic properties of it have been compiled in steam tables and are given in Appendix A.2 in SI and in English units.

**EXAMPLE 1.6-3. Use of Steam Tables**

Find the enthalpy change (i.e., how much heat must be added) for each of the following cases using SI and English units:

- Heating 1 kg (lb<sub>m</sub>) water from 21.11°C (70°F) to 60°C (140°F) at 101.325 kPa (1 atm) pressure
- Heating 1 kg (lb<sub>m</sub>) water from 21.11°C (70°F) to 115.6°C (240°F) and vaporizing at 172.2 kPa (24.97 psia)
- Vaporizing 1 kg (lb<sub>m</sub>) water at 115.6°C (240°F) and 172.2 kPa (24.97 psia)

**Solution:** For part (a), the effect of pressure on the enthalpy of liquid water is negligible. From Appendix A.2,

$$\begin{aligned}H &\text{ at } 21.11^\circ\text{C} = 88.60 \text{ kJ/kg or at } 70^\circ\text{F} = 38.09 \text{ btu/lbm} \\H &\text{ at } 60^\circ\text{C} = 251.13 \text{ kJ/kg or at } 140^\circ\text{F} = 107.96 \text{ btu/lbm} \\ \text{change in } H &= \Delta H = 251.13 - 88.60 = 162.53 \text{ kJ/kg} \\ &= 107.96 - 38.09 = 69.87 \text{ btu/lbm}\end{aligned}$$

In part (b), the enthalpy at 115.6°C (240°F) and 172.2 kPa



(24.97 psia) of the saturated vapor is 2699.9 kJ/kg or 1160.7 btu/lbm.

$$\begin{aligned}\text{change in } H &= \Delta H = 2699.9 - 88.60 = 2611.3 \text{ kJ/} \\ &\text{kg} = 1160.7 - 38.09 = 1122.6 \text{ btu/lbm}\end{aligned}$$

The latent heat of water at 115.6°C (240°F) in part (c) is

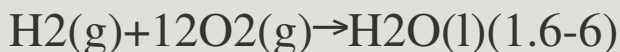
$$\begin{aligned}2699.9 - 484.9 &= 2215.0 \text{ kJ/kg} \\ 1160.7 - 208.44 &= 952.26 \text{ btu/} \\ &\text{lbm}\end{aligned}$$

## 1.6D Heat of Reaction

When chemical reactions occur, heat effects always accompany these reactions. This area where energy changes occur is often called *thermochemistry*. For example, when HCl is neutralized with NaOH, heat is given off and the reaction is exothermic. Heat is absorbed in an endothermic reaction. This heat of reaction is dependent on the chemical nature of each reacting material and product, and on their physical states.

For purposes of organizing data, we

define a standard heat of reaction  $\Delta H_0$  as the change in enthalpy when 1 kg mol reacts under a pressure of 101.325 kPa at a temperature of 298 K (25°C). For example, for the reaction



the  $\Delta H_0$  is  $-285.840 \times 10^3$  kJ/kg mol or  $-68.317$  kcal/g mol. The reaction is exothermic and the value is negative since the reaction loses enthalpy. In this case, the  $\text{H}_2$  gas reacts with the  $\text{O}_2$  gas to give liquid water, all at 298 K (25°C).

Special names are given to  $\Delta H_0$  depending upon the type of reaction. When the product is formed from the elements, as in Eq. (1.6-6), we call  $\Delta H_0$  the *heat of formation* of the product water,  $\Delta H_{f0}$ . For the combustion of  $\text{CH}_4$

to form  $\text{CO}_2$  and  $\text{H}_2\text{O}$ , we call it *heat of combustion*,  $\Delta H_{\text{c}0}$ . Data are given in Appendix A.3 for various values of  $\Delta H_{\text{c}0}$ .

**EXAMPLE 1.6-4. Combustion of Carbon**

A total of 10.0 g mol of carbon graphite is burned in a calorimeter held at 298 K and 1 atm. The combustion is incomplete and 90% of the C goes to  $\text{CO}_2$  and 10% to CO. What is the total enthalpy change in kJ and kcal?

**Solution:** From Appendix A.3, the  $\Delta H_{\text{c}0}$  for carbon going to  $\text{CO}_2$  is  $-393.513 \times 10^3 \text{ kJ/kg mol}$  or  $-94.0518 \text{ kcal/g mol}$ , and for carbon going to CO it is  $-110.523 \times 10^3 \text{ kJ/kg mol}$  or  $-26.4157 \text{ kcal/g mol}$ . Since 9 mol  $\text{CO}_2$  and 1 mol CO are formed,

$$\text{total } \Delta H = 9(-393.513) + 1(-110.523) = -3652 \text{ kJ} = 9(-94.0518) + 1(-26.4157) = -872.9 \text{ kcal}$$

If a table of heats of formation,  $\Delta H_{\text{f}0}$ , of compounds is available, the standard heat of the reaction,  $\Delta H_0$ , can be calculated by

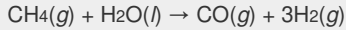
$$\Delta H_0 = \sum \Delta H_{\text{f}}(\text{products})_0 - \sum \Delta H_{\text{f}}(\text{reactants})_0 \quad (1.6-7)$$

In Appendix A.3, a short table of some

values of  $\Delta H_f$  is given. Other data are also available (H1, P1, S1).

**EXAMPLE 1.6-5. Reaction of Methane**

For the following reaction of 1 kg mol of CH<sub>4</sub> at 101.32 kPa and 298 K,



calculate the standard heat of reaction  $\Delta H^0$  at 298 K in kJ.

**Solution:** From Appendix A.3, the following standard heats of formation are obtained at 298 K:

Note that the  $\Delta H_f^0$  of all elements is, by definition, zero. Substituting into Eq. (1.6-7),

$$\begin{aligned}\Delta H^0 = & [-110.523 \times 103 - 3(0)] - (-74.848 \times 103 - 285.840 \times 103) = \\ & +250.165 \times 103 \text{ kJ/kg (endothermic)}\end{aligned}$$

## 1.7 Conservation of Energy and Heat Balances

### 1.7A Conservation of Energy

In making material balances, we used the law of conservation of mass, which states that the mass entering is equal to the mass leaving plus the mass left in the process. In a

similar manner, we can state the *law of conservation of energy*, which states that all energy entering a process is equal to that leaving plus that left in the process. In this section, elementary heat balances will be made.

Energy can appear in many forms. Some of the common forms are enthalpy, electrical energy, chemical energy (in terms of  $\Delta H$  reaction), kinetic energy, potential energy, work, and heat inflow.

In many cases in process engineering, which often takes place at constant pressure, electrical energy, kinetic energy, potential energy, and work either are not present or can be neglected. Then, only the enthalpy of the materials (at constant pressure), the

standard chemical-reaction energy ( $\Delta H_0$ ) at 25°C, and the heat added or removed must be taken into account in the energy balance. This is generally called a *heat balance*.

### 1.7B Heat Balances

In making a heat balance at steady state, we use methods similar to those used in making a material balance. The energy or heat coming into a process in the inlet materials plus any net energy added to the process are equal to the energy leaving in the materials. Expressed mathematically,

$$\sum H_R + (-\Delta H_{2980}) + q = \sum H_P \quad (1.7-1)$$

where  $\sum H_R$  is the sum of enthalpies of all materials entering the reaction

process relative to the reference state for the standard heat of reaction at 298 K and 101.32 kPa. If the inlet temperature is above 298 K, this sum will be positive.  $\Delta H_{2980}$  = standard heat of the reaction at 298 K and 101.32 kPa. The reaction contributes heat to the process, so the negative of  $\Delta H_{2980}$  is taken to be positive input heat for an exothermic reaction. Also,  $q$  = net energy or heat added to the system. If heat leaves the system, this item will be negative.  $\Sigma H_p$  = sum of enthalpies of all exiting materials referred to the standard reference state at 298 K (25°C).

Note that if the materials coming into a process are below 298 K,  $\Sigma H_R$  will be negative. Care must be taken not to confuse the signs of the items in Eq. (1.7-1). If no chemical reaction occurs,

then simple heating, cooling, or phase change is occurring. Use of Eq. (1.7-1) will be illustrated by several examples. For convenience, it is common practice to call the terms on the left-hand side of Eq. (1.7-1) input items, and those on the right, output items.

**EXAMPLE 1.7-1. Heating of a Fermentation Medium**

A liquid fermentation medium at 30°C is pumped at a rate of 2000 kg/h through a heater, where it is heated to 70°C under pressure. The waste heat water used to heat this medium enters at 95°C and leaves at 85°C. The average heat capacity of the fermentation medium is 4.06 kJ/kg · K, and that for water is 4.21 kJ/kg · K (Appendix A.2). The fermentation stream and the wastewater stream are separated by a metal surface through which heat is transferred and the streams do not physically mix with each other. Make a complete heat balance on the system. Calculate the water flow and the amount of heat added to the fermentation medium assuming no heat losses. The process flow is given in Fig. 1.7-1.

**Solution:** It is convenient to use the standard reference state of 298 K (25°C) as the datum to calculate the various enthalpies. From Eq. (1.7-1) the input items are as follows:

*Input items.*  $\Sigma H_R$  of the enthalpies of the two streams relative to 298 K (25°C) (note that  $\Delta t = 30 - 25^\circ\text{C} = 5^\circ\text{C} = 5\text{ K}$ ):

$$H(\text{liquid}) = (2000 \text{ kg/h})(4.06 \text{ kJ/kg} \cdot \text{K})(5 \text{ K}) = 4.060 \times 10^4 \text{ kJ}$$

$$hH(\text{water}) = W(4.21)(95 - 25) = 2.947 \times 10^2 (W = \text{kg/h})(-)$$

$$\Delta H_{2980} = 0 (\text{since there is no chemical reaction}) \quad q = 0 (\text{there are no heat losses or additions})$$



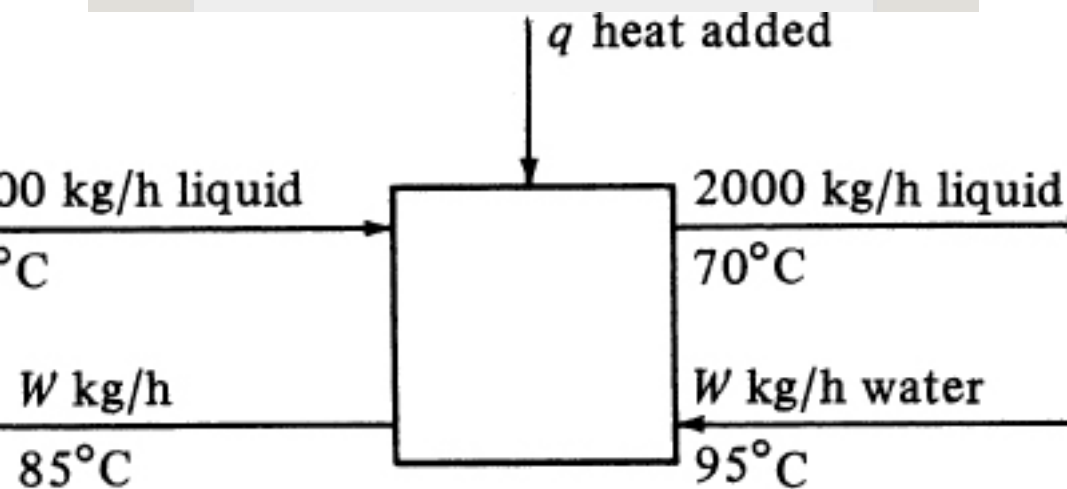


Figure 1.7-1. Process flow diagram for Example 1.7-1.

*Output items.*  $\Sigma H_P$  of the two streams relative to 298 K (25°C):

$$H(\text{liquid}) = 2000(4.06)(70 - 25) = 3.65 \times 10^5 \text{ kJ/h}$$

$$hH(\text{water}) = W(4.21)(85 - 25) = 2.526 \times 10^2 W \text{ kJ/h}$$

Equating input to output in Eq. (1.7-1) and solving for  $W$ ,

$$4.060 \times 10^4 + 2.947 \times 10^2 W = 3.654 \times 10^5 + 2.526 \times 10^2 W$$

$$W = 7720 \text{ kg/h water flow}$$

The amount of heat added to the fermentation medium is simply the difference of the outlet and inlet liquid enthalpies:

$$H(\text{outlet liquid}) - H(\text{inlet liquid}) = 3.654 \times 10^5 - 4.060 \times 10^4 = 3.248 \times 10^5 \text{ kJ/h}$$

$$(90.25 \text{ kW})$$

Note in this example that since the heat capacities were assumed constant, a simpler balance could have been written as follows:

$$\text{heat gained by liquid} = \text{heat lost by water}$$

$$2000(4.06)(70 - 30) = W(4.21)(95 - 85)$$

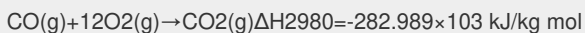
Then, solving,  $W = 7720 \text{ kg/h}$ . This simple balance works well when  $c_p$  is constant. However, when  $c_p$  varies with temperature and the material is a gas,  $c_{pm}$  values are only

available between 298 K (25°C) and  $T$  K, and the simple method cannot be used without obtaining new  $c_{pm}$  values over different temperature ranges.

### **EXAMPLE 1.7-2 Heat and Material Balance in Combustion**

The waste gas from a process of 1000 g mol/h of CO at 473 K is burned at 1 atm pressure in a furnace using air at 373 K. The combustion is complete and 90% excess air is used. The flue gas leaves the furnace at 1273 K. Calculate the heat removed in the furnace.

**Solution:** First, the process flow diagram is drawn in Fig. 1.7-2, and then a material balance is made:



(from Appendix A.3)

$$\begin{aligned} \text{mol CO} &= 1000 \text{ g mol/h} = \text{moles CO}_2 = 1.00 \text{ kg mol/h} \\ \text{mol O}_2 \text{ theoretically required} &= 12 (1.00) = 0.500 \text{ kg mol/h} \\ \text{mol O}_2 \text{ actually added} &= 0.500(1.9) = 0.95 \text{ kg mol/h} \end{aligned}$$

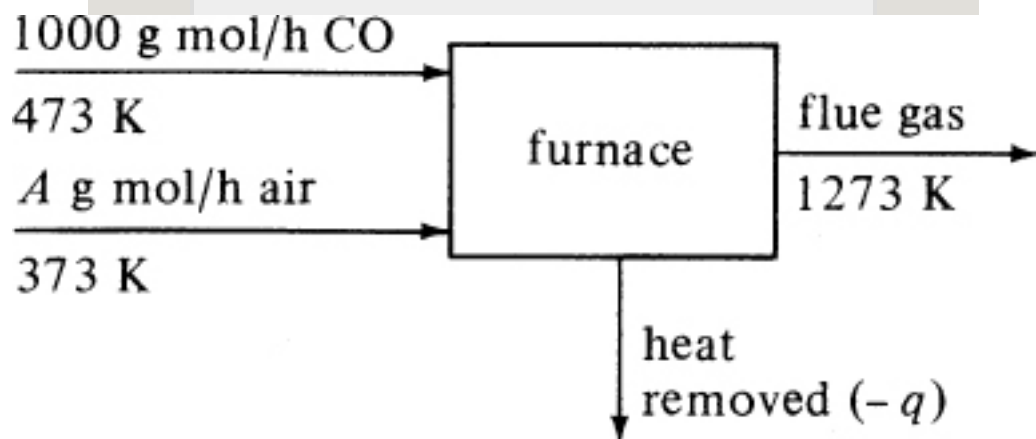


Figure 1.7-2. Process flow diagram for Example 1.7-2.

$$\begin{aligned} \text{mol N}_2 \text{ added} &= 0.95 \cdot 0.790 \cdot 21 = 3.570 \text{ kg mol/h} \\ \text{air added} &= 0.950 + 3.570 = 4.520 \text{ kg mol/h} \end{aligned}$$

$$h = \text{AO}_2 \text{ in outlet flue gas} = \text{added} - \text{used} = 0.950 - 0.500 = 0.450 \text{ kg mol/}$$

$$h\text{CO}_2 \text{ in outlet flue gas} = 1.00 \text{ kg mol/}$$

$$h\text{N}_2 \text{ in outlet flue gas} = 3.570 \text{ kg mol/h}$$

For the heat balance relative to the standard state at 298 K, we follow Eq. (1.7-1).

*Input items*

$$H(\text{CO}) = 1.00(c_{pm})(473 - 298) = 1.00(29.38)(473 - 298) = 5142 \text{ kJ/h}$$

(The  $c_{pm}$  of CO of 29.38 kJ/kg mol · K between 298 and 473 K is obtained from Table 1.6-1.)

$$H(\text{air}) = 4.520(c_{pm})(373 - 298) = 4.520(29.29)(373 - 298) = 9929 \text{ kJ/h} = \text{heat added, kJ/h}$$

(This will give a negative value here, indicating that heat was removed.)

$$-\Delta H_{2980} = (-282.989 \times 103 \text{ kJ/kg mol})(1.00 \text{ kg mol/h}) = 282\,990 \text{ kJ/h}$$

*Output items*

$$\begin{aligned} H(\text{CO}_2) &= 1.00(c_{pm})(1273 - 298) = 1.00(49.91)(1273 - 298) = 48\,660 \text{ kJ/h} \\ H(\text{O}_2) &= 0.450(c_{pm})(1273 - 298) = 0.450(33.25)(1273 - 298) = 14\,590 \text{ kJ/h} \\ hH(\text{N}_2) &= 3.570(c_{pm})(1273 - 298) = 3.570(31.43)(1273 - 298) = 109\,400 \text{ kJ/h} \end{aligned}$$

Equating input to output and solving for  $q$ ,

$$5142 + 9929 + q + 282\,990 = 48\,660 + 14\,590 + 109\,400 \quad q = -125\,411 \text{ kJ/h}$$

Hence, heat is removed:  $-34\,837 \text{ W}$ .

Often, when chemical reactions occur in a process and the heat capacities vary with temperature, the solution in a heat

balance can be trial and error if the final temperature is the unknown.

**EXAMPLE 1.7-3. Oxidation of Lactose**

In many biochemical processes, lactose is used as a nutrient, which is oxidized as follows:



The heat of combustion  $\Delta H_{\text{c0}}$  in Appendix A.3 at 25°C is  $-5648.8 \times 10^3 \text{ J/g mol}$ . Calculate the heat of complete oxidation (combustion) at 37°C, which is the temperature of many biochemical reactions. The  $c_{\text{pm}}$  of solid lactose is  $1.20 \text{ J/g} \cdot \text{K}$ , and the molecular weight is  $342.3 \text{ g mass/g mol}$ .

**Solution:** This can be treated as an ordinary heat-balance problem. First, the process flow diagram is drawn in Fig. 1.7-3. Next, the datum temperature of 25°C is selected and the input and output enthalpies calculated. The temperature difference  $\Delta T = (37 - 25)^\circ\text{C} = (37 - 25) \text{ K}$ .

*Input items*

$$\begin{aligned} H(\text{lactose}) &= (342.3 \text{ g})(c_{\text{pmJg}} \cdot \text{K})(37 - 25) \text{ K} = 342.3(1.20) \\ &\quad (37 - 25) = 4929 \text{ J} \\ H(\text{O}_2 \text{ gas}) &= (12 \text{ g mol}) \\ &\quad (c_{\text{pmJg mol}} \cdot \text{K})(37 - 25) \text{ K} = 12(29.38)(37 - 25) = 4230 \text{ J} \end{aligned}$$

(The  $c_{\text{pm}}$  of  $\text{O}_2$  was obtained from Table 1.6-1.)

$$-\Delta H_{250} = -(-5648.8 \times 10^3)$$

*Output items*

$$\begin{aligned} H(\text{H}_2\text{O liquid}) &= 11(18.02 \text{ g}) \\ &\quad (c_{\text{pmJg}} \cdot \text{K})(37 - 25) \text{ K} = 11(18.02)(4.18)(37 - 25) = 9943 \text{ J} \end{aligned}$$

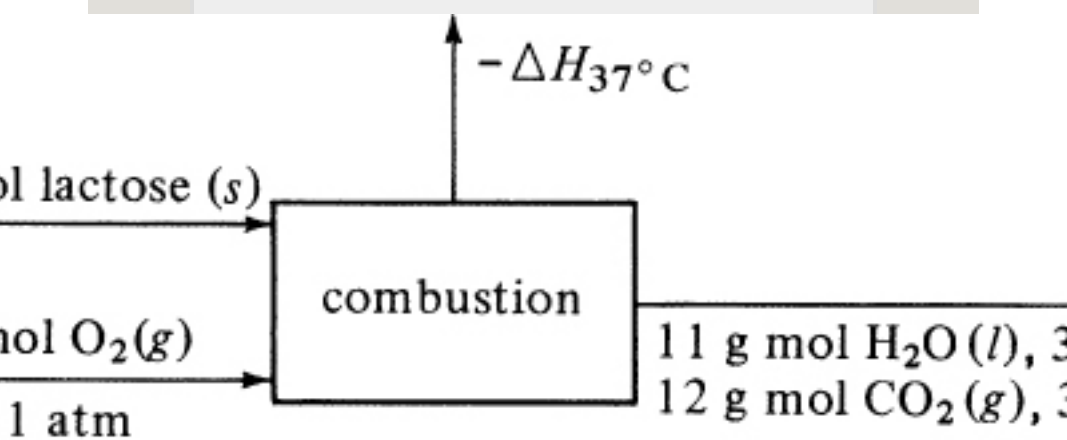


Figure 1.7-3. Process flow diagram for Example 1.7-3.

(The  $c_{pm}$  of liquid water was obtained from Appendix A.2.)

$$H(\text{CO}_2 \text{ gas}) = (12 \text{ g mol}) \\ (\text{cpmJ/g mol} \cdot \text{K}) (37 - 25) \text{ K} = 12(37.45)(37 - 25) = 5393 \text{ J}$$

(The  $c_{pm}$  of  $\text{CO}_2$  is obtained from Table 1.6-1.)

$\Delta H_{37^\circ\text{C}}$ : Setting input = output and solving,

$$4929 + 4230 + 5648.8 \times 103 = 9943 + 5393 - \\ \Delta H_{37^\circ\text{C}} \Delta H_{37^\circ\text{C}} = -5642.6 \times 103 \text{ J/g mol} = \Delta H_{310 \text{ K}}$$

## 1.8 Numerical Methods for Integration

### 1.8A Introduction and Graphical Integration

Often, the mathematical function  $f(x)$  to be integrated is too complex and we are not able to integrate it analytically. Or, in some cases, the

function is one that has been obtained from experimental data, and no mathematical equation is available to represent the data so that they can be integrated analytically. In these cases, we can use either numerical or graphical integration.

Integration of a function  $f(x)$  between the limits  $x = a$  to  $x = b$  can be represented by

$$\int_{x=a}^{x=b} f(x) dx \quad (1.8-1)$$

By plotting  $f(x)$  versus  $x$ , the area under the curve is equal to the value of the integral.

### **1.8B Numerical Integration and Simpson's Rule**

It is often desirable or necessary to perform a numerical integration by

computing the value of a definite integral from a set of numerical values of the integrand  $f(x)$ . This, of course, can be done graphically, but in most cases numerical methods suitable for the digital computer are desired.

The integral to be evaluated is Eq. (1.8-1), where the interval is  $b - a$ . The most generally used numerical method is the parabolic rule, often called *Simpson's rule*. This method divides the total interval  $b - a$  into an even number of subintervals  $m$ , where

$$m = \frac{b-a}{h} \quad (1.8-2)$$

The value of  $h$ , a constant, is the spacing used in  $x$ . Then, approximating  $f(x)$  by a parabola on each subinterval, Simpson's

rule is

$$\int_{x=a}^{x=b} f(x) dx = h \left[ \frac{f_0 + f_m}{2} + 4(f_1 + f_3 + f_5 + \dots + f_{m-1}) + 2(f_2 + f_4 + f_6 + \dots + f_{m-2}) \right] \quad (1.8-3)$$

where  $f_0$  is the value of  $f(x)$  at  $x = a$ ;  $f_1$  is the value of  $f(x)$  at  $x = x_1$ , ...;  $f_m$  is the value of  $f(x)$  at  $x = b$ . The reader should note that  $m$  must be an even number and the increments evenly spaced. This method is well suited for digital computation with a spreadsheet, since spreadsheets often have advanced numerical calculation methods built into their programs. Simpson's rule is a widely used numerical integration method.

In some cases, the available experimental data for  $f(x)$  are not at



equally spaced increments of  $x$ . Then, the numerical integration can be performed using the sum of the single-interval rectangles (trapezoidal rule) for the value of the interval. This is much less accurate than Simpson's rule. The trapezoidal-rule method becomes more accurate as the interval becomes smaller.

The experimental data for  $f(x)$  are sometimes spaced at large and/or irregular increments of  $x$ . These data can be smoothed by fitting a polynomial, exponential, logarithmic, or some other function to the data, which often can be integrated analytically. If the function is relatively complex, then it can be numerically integrated using Simpson's rule.

## **1.9 Chapter Summary**

In this chapter, we have introduced the concepts of transport processes, unit operations, and separation processes, which form the basis for this textbook. Many examples of different unit operations and separations processes from a range of chemical, biological, and process industries were provided.

Important elements necessary to solve transport and separation processes were discussed. First, an overview of the different types of units and parameters, such as temperature, pressure, mass, and composition was provided. Then, material and energy balances were introduced by using the laws of conservation and energy. Examples were shown that included recycle streams, chemical reactions, latent heat,

and heat of reaction. Finally, the principles of numerical introduction were described as a way to solve mathematical functions that are too complex to solve analytically.

## **Problems**

### **1.2-1. *Temperature of a Chemical***

***Process.*** The temperature of a chemical reaction was found to be 353.2 K. What is the temperature in °F, °C, and °R?

**Ans.** 176°F, 80°C, 636°R

### **1.2-2. *Temperature for Smokehouse***

***Processing of Meat.*** In smokehouse processing of sausage meat, a final temperature of 155°F inside the sausage is often used. Calculate this temperature in °C, K, and °R.

**1.3-1. *Molecular Weight of Air.*** For purposes of most engineering calculations, air is assumed to be composed of 21 mol % oxygen and 79 mol % nitrogen. Calculate the average molecular weight.

**Ans.** 28.9 g mass/g mol, lb mass/lb mol,  
or kg mass/kg mol

**1.3-2. *Oxidation of CO and Mole Units.***

The gas CO is being oxidized by O<sub>2</sub> to form CO<sub>2</sub>. How many kg of CO<sub>2</sub> will be formed from 56 kg of CO? Also, calculate the kg of O<sub>2</sub> theoretically needed for this reaction. (*Hint:* First, write the balanced chemical equation to obtain the mol O<sub>2</sub> needed for 1.0 kg mol CO. Then, calculate the kg mol of CO in 56 kg CO.)

**Ans.** 88.0 kg CO<sub>2</sub>, 32.0 kg O<sub>2</sub>

**1.3-3. *Composition of a Gas Mixture.*** A gaseous mixture contains 20 g of N<sub>2</sub>, 83 g of O<sub>2</sub>, and 45 g of CO<sub>2</sub>. Calculate the composition in mole fraction and the average molecular weight of the mixture.

**Ans.** Average mol wt = 34.2 g mass/g mol, 34.2 kg mass/kg mol

**1.3-4. *Composition of a Protein***

***Solution.*** A liquid solution contains 1.15 wt % of a protein, 0.27 wt % KCl, and the remainder is water. The average molecular weight of the protein by gel permeation is 525000 g mass/g mol. Calculate the mole fraction of each component in solution.

**1.3-5. *Concentration of NaCl Solution.***

An aqueous solution of NaCl has a concentration of 24.0 wt % NaCl with a density of 1.178 g/cm<sup>3</sup> at 25°C.

Calculate the following:

- Mole fraction of NaCl and water.
- Concentration of NaCl as g mol/liter, lbm/ft<sup>3</sup>, lbm/gal, and kg/m<sup>3</sup>.

### **1.4-1. *Conversion of Pressure***

***Measurements in Freeze Drying.*** In the experimental measurement of freeze drying of beef, an absolute pressure of 2.4 mmHg was held in the chamber. Convert this pressure to atm, in. of water at 4°C, μm of Hg, and Pa. (*Hint: See Appendix A.1 for conversion factors.*)

**Ans.**  $3.16 \times 10^{-3}$  atm, 1.285 in. H<sub>2</sub>O,  
2400 μm Hg, 320 Pa

**1.4-2. Compression and Cooling of Nitrogen Gas.** A volume of 65.0 ft<sup>3</sup> of N<sub>2</sub> gas at 90°F and 29.0 psig is compressed to 75 psig and cooled to 65°F. Calculate the final volume in ft<sup>3</sup> and the final density in lb<sub>m</sub>/ft<sup>3</sup>. [*Hint: Be sure to convert all pressures to psia first and then to atm. Substitute original conditions into Eq. (1.4-1) to obtain  $n$ , lb mol.*]

**1.4-3. Gas Composition and Volume.** A gas mixture of 0.13 g mol NH<sub>3</sub>, 1.27 g mol N<sub>2</sub>, and 0.025 g mol H<sub>2</sub>O vapor is contained at a total pressure of 830 mmHg and 323 K. Calculate the following:.

- Mole fraction of each component.
- Partial pressure of each component in mmHg.
- Total volume of mixture in m<sup>3</sup> and ft<sup>3</sup>.

**1.4-4. Evaporation of a Heat-Sensitive Organic Liquid.** An organic liquid is being evaporated from a liquid solution containing a few percent nonvolatile dissolved solids. Since it is heat-sensitive and may discolor at high temperatures, it will be evaporated under vacuum. If the lowest absolute pressure that can be obtained in the apparatus is 12.0 mmHg, what will be the temperature of evaporation in K? It will be assumed that the small amount of solids does not affect the vapor pressure, which is given as follows:

$$\log P_A = -2250(1/T) + 9.05$$

where  $P_A$  is in mmHg and  $T$  in K.

$$\text{Ans. } T = 282.3 \text{ K or } 9.1^\circ\text{C}$$

**1.5-1. Evaporation of Cane Sugar**



**Solutions.** An evaporator is used to concentrate cane sugar solutions. A feed of 10000 kg/d of a solution containing 38 wt % sugar is evaporated, producing a 74 wt % solution. Calculate the weight of solution produced and the amount of water removed.

**Ans.** 5135 kg/d of 74 wt % solution,  
4865 kg/d water

**1.5-2. Processing of Fish Meal.** Fish are processed into fish meal and used as a supplementary protein food. In the processing, the oil is first extracted to produce a wet fish cake containing 80 wt % water and 20 wt % bone-dry cake. This wet cake feed is dried in rotary-drum dryers to give a “dry” fish cake product containing 40 wt % water. Finally, the product is finely ground and

packed. Calculate the kg/h of wet cake feed needed to produce 1000 kg/h of “dry” fish cake product.

**Ans.** 3000 kg/h wet cake feed

**1.5-3. *Drying of Lumber.*** A batch of 100 kg of wet lumber containing 11 wt % moisture is dried to a water content of 6.38 kg water/1.0 kg bone-dry lumber. What is the weight of “dried” lumber and the amount of water removed?

**1.5-4. *Processing of Paper Pulp.*** A wet paper pulp contains 68 wt % water. After the pulp was dried, it was found that 55% of the original water in the wet pulp was removed. Calculate the composition of the “dried” pulp and its weight for a feed of 1000 kg/min of wet pulp.

### ***1.5-5. Two-Stage Production of Jam***

***from Crushed Fruit.*** In a process producing jam, crushed fruit containing 14 wt % soluble solids is combined with sugar (1.22 kg sugar/1.00 kg crushed fruit) and pectin (0.0025 kg pectin/1.00 kg crushed fruit) in a mixer. The resultant mixture is then evaporated in a kettle to produce a jam containing 67 wt % soluble solids. For a feed of 1000 kg crushed fruit, calculate the kg mixture from the mixer, kg water evaporated, and kg jam produced.

**Ans.** 2222.5 kg mixture, 189 kg water,  
2033.5 kg jam

### ***1.5-6. Drying of Cassava (Tapioca)***

***Root.*** Tapioca flour is used in many countries for bread and similar products. The flour is made by drying coarse

granules of the cassava root containing 66 wt % moisture to 5% moisture and then grinding to produce the flour. How many kg of granules must be dried and how much water removed to produce 5000 kg/h of flour?

**1.5-7. Processing of Soybeans in Three Stages.** A feed of 10000 kg of soybeans is processed in a sequence of three stages or steps (E1). The feed contains 35 wt % protein, 27.1 wt % carbohydrate, 9.4 wt % fiber and ash, 10.5 wt % moisture, and 18.0 wt % oil. In the first stage, the beans are crushed and pressed to remove oil, giving an expressed-oil stream and a stream of pressed beans containing 6% oil. Assume no loss of other constituents with the oil stream. In the second step, the pressed beans are extracted with

hexane to produce an extracted-meal stream containing 0.5 wt % oil and a hexane–oil stream. Assume no hexane in the extracted meal. Finally, in the last step the extracted meal is dried to give a dried meal of 8 wt % moisture.

Calculate the following:

- kg of pressed beans from the first stage.
- kg of extracted meal from the second stage.
- kg of final dried meal and the wt % protein in the dried meal.

**Ans.** (a) 8723 kg; (b) 8241 kg; (c) 7816 kg, 44.8 wt % protein

**1.5-8. *Recycle in a Dryer.*** A solid material containing 15.0 wt % moisture is dried so that it contains 7.0 wt % water by blowing fresh warm air mixed with recycled air over the solid in the dryer. The inlet fresh air has a humidity

of 0.01 kg water/kg dry air, the air from the drier that is recycled has a humidity of 0.1 kg water/kg dry air, and the mixed air to the dryer, 0.03 kg water/kg dry air. For a feed of 100 kg solid/h fed to the dryer, calculate the kg dry air/h in the fresh air, the kg dry air/h in the recycled air, and the kg/h of “dried” product.

**Ans.** 95.6 kg/h dry air in fresh air, 27.3 kg/h dry air in recycled air, and 91.4 kg/h “dried” product

**1.5-9. Crystallization and Recycle.** It is desired to produce 1000 kg/h of  $\text{Na}_3\text{PO}_4 \cdot 12\text{H}_2\text{O}$  crystals from a feed solution containing 5.6 wt %  $\text{Na}_3\text{PO}_4$  and traces of impurity. The original solution is first evaporated in an evaporator to a 35 wt %  $\text{Na}_3\text{PO}_4$  solution and then cooled to

293 K in a crystallizer, where the hydrated crystals and a mother-liquor solution are removed. One out of every 10 kg of mother liquor is discarded to waste to get rid of the impurities, and the remaining mother liquor is recycled to the evaporator. The solubility of  $\text{Na}_3\text{PO}_4$  at 293 K is 9.91 wt %.

Calculate the kg/h of feed solution and kg/h of water evaporated.

**Ans.** 7771 kg/h feed, 6739 kg/h water

**1.5-10. *Evaporation and Bypass in an Orange Juice Concentration.*** In a process for concentrating 1000 kg of freshly extracted orange juice (C1) containing 12.5 wt % solids, the juice is strained, yielding 800 kg of strained juice and 200 kg of pulpy juice. The strained juice is concentrated in a

vacuum evaporator to give an evaporated juice of 58% solids. The 200 kg of pulpy juice is bypassed around the evaporator and mixed with the evaporated juice in a mixer to improve the flavor. This final concentrated juice contains 42 wt % solids. Calculate the concentration of solids in the strained juice, the kg of final concentrated juice, and the concentration of solids in the pulpy juice bypassed. (*Hint:* First, make a total balance and then a solids balance on the overall process. Next, make a balance on the evaporator. Finally, make a balance on the mixer.)

**Ans.** 34.2 wt % solids in pulpy juice

**1.5-11. *Manufacture of Acetylene.*** To make 6000 ft<sup>3</sup> of acetylene (CHCH) gas at 70°F and 750 mmHg, solid calcium



carbide ( $\text{CaC}_2$ ), which contains 97 wt %  $\text{CaC}_2$  and 3 wt % solid inerts, is used along with water. The reaction is



The final lime slurry contains water, solid inerts, and  $\text{Ca}(\text{OH})_2$  lime. In this slurry, the total wt % solids of inerts plus  $\text{Ca}(\text{OH})_2$  is 20%. How many lb of water must be added and how many lb of final lime slurry is produced? [*Hint: Use a basis of 6000 ft<sup>3</sup> and convert to lb mol. This gives 15.30 lb mol  $\text{C}_2\text{H}_2$ , 15.30 lb mol  $\text{Ca}(\text{OH})_2$ , and 15.30 lb mol  $\text{CaC}_2$  added. Convert lb mol  $\text{CaC}_2$  feed to lb and calculate lb inerts added. The total lb solids in the slurry is then the sum of the  $\text{Ca}(\text{OH})_2$  plus inerts. In calculating the water added, remember that some is consumed in the reaction.]*

**Ans.** 5200 lb water added (2359 kg),  
5815 lb lime slurry (2638 kg)

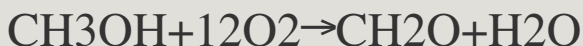
**1.5-12. Combustion of Solid Fuel.** A fuel analyzes 74.0 wt % C and 12.0% ash (inert). Air is added to burn the fuel, producing a flue gas of 12.4% CO<sub>2</sub>, 1.2% CO, 5.7% O<sub>2</sub>, and 80.7% N<sub>2</sub>. Calculate the kg of fuel used for 100 kg mol of outlet flue gas and the kg mol of air used. (*Hint:* First, calculate the mol O<sub>2</sub> added in the air, using the fact that the N<sub>2</sub> in the flue gas equals the N<sub>2</sub> added in the air. Then, make a carbon balance to obtain the total moles of C added.)

**1.5-13. Burning of Coke.** A furnace burns a coke containing 81.0 wt % C, 0.8% H, and the rest inert ash. The furnace uses 60% excess air (air over

and above that needed to burn all C to  $\text{CO}_2$  and H to  $\text{H}_2\text{O}$ ). Calculate the moles of all components in the flue gas if only 95% of the carbon goes to  $\text{CO}_2$  and 5% to CO.

### **1.5-14. *Production of Formaldehyde.***

Formaldehyde ( $\text{CH}_2\text{O}$ ) is made by the catalytic oxidation of pure methanol vapor and air in a reactor. The moles from this reactor are 63.1  $\text{N}_2$ , 13.4  $\text{O}_2$ , 5.9  $\text{H}_2\text{O}$ , 4.1  $\text{CH}_2\text{O}$ , 12.3  $\text{CH}_3\text{OH}$ , and 1.2  $\text{HCOOH}$ . The reaction is



A side reaction occurring is



Calculate the mol methanol feed, mol air feed, and percent conversion of

methanol to formaldehyde.

**Ans.** 17.6 mol  $\text{CH}_3\text{OH}$ , 79.8 mol air,  
23.3% conversion

**1.6-1. Heating of  $\text{CO}_2$  Gas.** A total of 250 g of  $\text{CO}_2$  gas at 373 K is heated to 623 K at 101.32 kPa total pressure. Calculate the amount of heat needed in cal, btu, and kJ.

**Ans.** 15050 cal, 59.7 btu, 62.98 kJ

**1.6-2. Heating a Gas Mixture.** A mixture of 25 lb mol  $\text{N}_2$  and 75 lb mol  $\text{CH}_4$  is being heated from  $400^\circ\text{F}$  to  $800^\circ\text{F}$  at 1 atm pressure. Calculate the total amount of heat needed in btu.

**1.6-3. Final Temperature in Heating Applesauce.** A mixture of 454 kg of applesauce at  $10^\circ\text{C}$  is heated in a heat

exchanger by adding 121300 kJ.

Calculate the outlet temperature of the applesauce. (*Hint: In Appendix A.4, a heat capacity for applesauce is given at 32.8°C. Assume that this is constant and use this as the average  $c_{pm}$ .*)

**Ans. 76.5°C**

**1.6-4. Use of Steam Tables.** Using the steam tables, determine the enthalpy change for 1 lb water for each of the following cases:

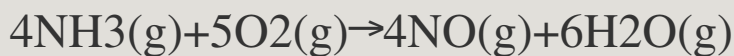
- Heating liquid water from 40°F to 240°F at 30 psia.  
(*Note: The effect of total pressure on the enthalpy of liquid water can be neglected.*)
- Heating liquid water from 40°F to 240°F and vaporizing at 240°F and 24.97 psia.
- Cooling and condensing a saturated vapor at 212°F and 1 atm abs to a liquid at 60°F.
- Condensing a saturated vapor at 212°F and 1 atm abs.

**Ans.** (a) 200.42 btu/lbm; (b) 1152.7 btu/lbm; (c) -1122.4 btu/lbm; (d) -970.3 btu/lbm, -2256.9 kJ/kg

**1.6-5. Heating and Vaporization Using Steam Tables.** A flow rate of 1000 kg/h of water at 21.1°C is heated to 110°C when the total pressure is 244.2 kPa in the first stage of a process. In the second stage at the same pressure, the water is heated further, until it is all vaporized at its boiling point. Calculate the total enthalpy change in the first stage and in both stages.

**1.6-6. Combustion of CH<sub>4</sub> and H<sub>2</sub>.** For 100 g mol of a gas mixture of 75 mol % CH<sub>4</sub> and 25% H<sub>2</sub>, calculate the total heat of combustion of the mixture at 298 K and 101.32 kPa, assuming that combustion is complete.

**1.6-7. Heat of Reaction from Heats of Formation.** For the reaction



calculate the heat of reaction,  $\Delta H$ , at 298 K and 101.32 kPa for 4 g mol of  $\text{NH}_3$  reacting.

**Ans.**  $\Delta H$ , heat of reaction =  $-904.7$  kJ

**1.7-1. Heat Balance and Cooling of Milk.** In the processing of rich cows' milk, 4540 kg/h of milk is cooled from  $60^\circ\text{C}$  to  $4.44^\circ\text{C}$  by a refrigerant. Calculate the heat removed from the milk.

**Ans.** Heat removed = 269.6 kW

**1.7-2. Heating of Oil by Air.** A flow of 2200 lb<sub>m</sub>/h of hydrocarbon oil at  $100^\circ\text{F}$

enters a heat exchanger, where it is heated to  $150^{\circ}\text{F}$  by hot air. The hot air enters at  $300^{\circ}\text{F}$  and is to leave at  $200^{\circ}\text{F}$ . Calculate the total lb mol air/h needed. The mean heat capacity of the oil is  $0.45 \text{ btu/lb}_m \cdot ^{\circ}\text{F}$ .

**Ans.** 70.1 lb mol air/h, 31.8 kg mol/h

**1.7-3. Combustion of Methane in a Furnace.** A gas stream of 10 000 kg mol/h of  $\text{CH}_4$  at 101.32 kPa and 373 K is burned in a furnace using air at 313 K. The combustion is complete and 50% excess air is used. The flue gas leaves the furnace at 673 K. Calculate the heat removed in the furnace. (*Hint:* Use a datum of 298 K and liquid water at 298 K. The input items will be the following: the enthalpy of  $\text{CH}_4$  at 373 K referred to 298 K; the enthalpy of the air



at 313 K referred to 298 K;  $-\Delta H_{c0}$ , the heat of combustion of  $\text{CH}_4$  at 298 K, which is referred to liquid water; and  $q$ , the heat added. The output items will include: the enthalpies of  $\text{CO}_2$ ,  $\text{O}_2$ ,  $\text{N}_2$ , and  $\text{H}_2\text{O}$  gases at 673 K referred to 298 K; and the latent heat of  $\text{H}_2\text{O}$  vapor at 298 K and 101.32 kPa from Appendix A.2. It is necessary to include this latent heat since the basis of the calculation and of the  $\Delta H_{c0}$ , is liquid water.)

**1.7-4. Preheating Air by Steam for Use in a Dryer.** An air stream at  $32.2^\circ\text{C}$  is to be used in a dryer and is first preheated in a steam heater to  $65.5^\circ\text{C}$ . The air flow is 1000 kg mol/h. The steam enters the heater saturated at  $148.9^\circ\text{C}$ , is condensed and cooled, and leaves as a liquid at  $137.8^\circ\text{C}$ . Calculate the amount of steam used in kg/h.

**Ans.** 450 kg steam/h

**1.7-5. Cooling Cans of Potato Soup After Thermal Processing.** A total of 1500 cans of potato soup undergo thermal processing in a retort at  $240^{\circ}\text{F}$ . Before being removed from the retort, the cans are then cooled to  $100^{\circ}\text{F}$  by cooling water, which enters at  $75^{\circ}\text{F}$  and leaves at  $85^{\circ}\text{F}$ . Calculate the lb of cooling water needed. Each can of soup contains 1.0 lb of liquid soup, and the empty metal can weighs 0.16 lb. The mean heat capacity of the soup is  $0.94 \text{ btu/lb}_m \cdot ^{\circ}\text{F}$  and that of the metal can is  $0.12 \text{ btu/lb}_m \cdot ^{\circ}\text{F}$ . A metal rack or basket which is used to hold the cans in the retort weighs 350 lb and has a heat capacity of  $0.12 \text{ btu/lb}_m \cdot ^{\circ}\text{F}$ . Assume that the metal rack is cooled from  $240^{\circ}\text{F}$  to  $85^{\circ}\text{F}$ , the temperature of the outlet

water. The amount of heat removed from the retort walls in cooling from 240 to 100°F is 10 000 btu. Radiation loss from the retort during cooling is estimated as 5000 btu.

**Ans.** 21320 lb water, 9670 kg

**1.8-1. Numerical Integration Using Simpson's Method.** The following experimental data for  $y = f(x)$  were obtained:



Determine the integral using Simpson's method:

$$A = \int_{x=0}^{x=0.6} f(x) dx$$

**Ans.**  $A = 38.45$

**1.8-2. Numerical Integration to Obtain Wastewater Flow.** The rate of flow of wastewater in an open channel has been measured and the following data obtained:

Determine the total flow in  $\text{m}^3$  for 120 min by numerical integration.

**Ans.** 92 350  $\text{m}^3$

### References

### Notation

# Chapter 2. Introduction to Fluids and Fluid Statics

## 2.0 Chapter Objectives

On completion of this chapter, a student should be able to:

- Explain the importance of fluid mechanics in multiple chemical and process industries
- Use both the English and SI units when solving fluid-statics problems
- Define what a fluid is, particularly in relation to the different phases of matter
- Explain the difference between incompressible and compressible fluids
- Explain the concept of a “continuum”
- Use Newton’s law of gravitation to determine the force exerted by an object or fluid
- Identify and use the units of force and pressure in different systems

- Explain the concept of pressure in a fluid
- Explain the concept of pressure drop, or pressure differential
- Distinguish between fluid pressure and pressure drop across a fluid
- Calculate the pressure in a fluid at different heights
- Convert pressure to a “head” of fluid
- Distinguish between atmospheric pressure and gage pressure
- Identify different pieces of equipment used to measure pressure drop
- Calculate the pressure drop from a U-tube manometer

## **2.1 Introduction**

The flow and behavior of fluids are important in many of the processes commonly found in different chemical industries. First, consider the petrochemical industry—millions of barrels of oil and other process fluids are transported

throughout the world through pipelines and other pieces of equipment. Second, consider the vast array of pipes and pumps used to transport water from reservoirs to houses and businesses. These are only two of the many industries that are heavily reliant on the transportation of fluids. Therefore, it is critical that chemical engineers understand the way in which fluids behave to properly transport them to homes and industries across the world.

In the process industries, many of the materials used and produced are commonly found in the fluid phase and must be properly stored, handled, pumped, and processed. Thus, it is necessary to become familiar with the

principles that govern the flow of fluids, as well as with the equipment commonly used to transport them.

Typical fluids frequently encountered in the process industries include water, air, CO<sub>2</sub>, oil, slurries, and thick syrups.

Before properly designing a system to transport fluids, it is important to first define what a fluid is.

A fluid may be defined as a substance that does not *permanently* resist deformation. Frequently, a fluid will change its shape when subjected to external forces. Consider the case of a child throwing a coin into a “wishing well.” When a coin is thrown into a “wishing well” full of water, ripples appear and the water changes shape in response to the force from the coin. Now, suppose that the well contained no



water and had a solid concrete bottom. If a coin was thrown onto this well, the coin would hit the bottom, ricochet, and there would be no displacement or deformation of the concrete bottom.

Technically, as the coin is falling through the well, the air would undergo displacement, though it is more difficult to visualize this deformation as compared to liquid water. In this text, gases, liquids, and saturated vapors are all considered to have the characteristics of fluids. Thus, they will obey many of the laws that govern fluid mechanics.

If a fluid is minimally affected by changes in pressure, it is said to be *incompressible*. Most liquids, such as water, are *incompressible* fluids, whereas most gases are considered to be *compressible* fluids. However, if gases

are subjected to minimal changes in pressure and temperature, they can be considered to be incompressible fluids as well since their density changes will also be small.

Like all physical matter, a fluid is composed of an extremely large number of molecules per unit volume. A theory such as the kinetic theory of gases or statistical mechanics treats the motions of molecules in terms of statistical groups and not in terms of individual molecules. In engineering, we are mainly concerned with the bulk or *macroscopic* behavior of a fluid rather than the individual molecular or microscopic behavior.

Thus, in momentum transfer we frequently treat a fluid as a continuous

distribution of matter, known as a “continuum.” This treatment as a continuum is valid when the smallest volume of fluid contains a number of molecules large enough that a statistical average is meaningful and the macroscopic properties of the fluid, such as density, pressure, and so on, vary smoothly or continuously from point to point.

The study of *momentum transfer*, or *fluid mechanics* as it is often called, can be divided into two branches: *fluid statics*, or fluids at rest, and *fluid dynamics*, or fluids in motion. In Section 2.2, we treat fluid statics; in Chapters 3–11, we treat fluid dynamics. Because momentum is being transferred in fluid dynamics, the term “momentum transfer” or “transport” is usually used.

In Section 18.1, momentum transfer is related to heat and mass transfer.

## **2.2 Fluid Statics**

### **2.2A Force, Units, and Dimensions**

For a static fluid, an important property is the pressure in the fluid. Pressure can be thought of as the surface force exerted by a fluid against the walls of its container. Also, pressure exists at any point in a volume of fluid.

In order to understand *pressure*, which is defined as force exerted per unit area, Newton's law of gravitation must be discussed. Newton's law of gravitation is used to calculate the force exerted by a mass under the influence of gravity and is given by

$$F = mg \quad (\text{SI units})(2.2-1)$$

where, in SI units,  $F$  is the force exerted in newtons n ( $\text{kg} \cdot \text{m}/\text{s}^2$ ),  $m$  the mass in kg, and  $g$  the standard acceleration of gravity, which is defined as  $9.80665 \text{ m}/\text{s}^2$ .

In English units, this equation is given by

$$F = mgg_c \quad (\text{English units})(2.2-1a)$$

where, in English units,  $F$  is in lbf,  $m$  is in lb<sub>m</sub>,  $g$  is  $32.1740 \text{ ft}/\text{s}^2$ , and  $g_c$  (a gravitational conversion factor) is  $32.147 \text{ lb}_m \cdot \text{ft}/\text{lbf} \cdot \text{s}^2$ . The gravitation conversion factor is necessary in English units since pounds can represent force *or* mass. It is defined such that  $g/g_c$  has a value of  $1.0 \text{ lbf}/\text{lb}_m$  and that  $1 \text{ lb}_m$  conveniently gives a force equal to 1

lbf. Often, when units of pressure are given, the word “force” is omitted, as in lb/in<sup>2</sup> (pounds per square inch, psi) instead of lbf/in<sup>2</sup>.

Another system of units sometimes used in Eq. (2.2-1) is one in which the  $g_c$  is omitted and the force ( $F = mg$ ) is given as lb<sub>m</sub> · ft/s<sup>2</sup>, a unit known as the *poundal*. Here, 1 lb<sub>m</sub> acted on by gravity will give a force of 32.174 poundals (lb<sub>m</sub> · ft/s<sup>2</sup>). If a mass of 1 g is used, the force ( $F = mg$ ) is expressed in terms of dynes (g-cm/s<sup>2</sup>). This is the centimeter–gram–second (cgs) systems of units.

Conversion factors for the different units of force and force per unit area (pressure) are given in Appendix A.1. Note that always in the SI system, and usually in the cgs system, the term  $g_c$  is

not used. However, it is frequently used in the English system to convert between pound force lbf and pound mass lb<sub>m</sub>, and is defined as 32.174 lb<sub>m</sub> ft/s<sup>2</sup>/lbf. In a similar way,  $g_c$  can be defined for SI units as 1 kg m/s<sup>2</sup> /N.

**EXAMPLE 2.2-1. Units and Dimensions of Force**

Calculate the force exerted by an object weighing 3 lb<sub>m</sub> in terms of the following:

- lb force (English units)
- Dynes (cgs units)
- Newtons (SI units)

**Solution:** For part (a), using Eq. (2.2-1a),

$$F (\text{force}) = mg_g = (3 \text{ lb}_m)(32.174 \text{ ft/s}^2) \\ (1 \text{ lbf} 32.174 \text{ lb}_m \cdot \text{ft/s}^2) = 3 \text{ lb force (lbf)}$$

For part (b), using Eq. (2.2-1),

$$F = mg = (3 \text{ lb}_m)(453.59 \text{ g/lb}_m) \\ (980.665 \text{ cm/s}^2) = 1.332 \times 10^6 \text{ g} \cdot \text{cm/s}^2 = 1.332 \times 10^6 \text{ dyn}$$

As an alternative method for part (b), using the conversion factors from Appendix A.1,

$$1 \text{ dyn} = 2.2481 \times 10^{-6} \text{ lbf} \\ (1 \text{ dyn} 2.2481 \times 10^{-6} \text{ lbf}) = 1.332 \times 10^6 \text{ dyn}$$

To calculate newtons in part (c), using Eq. (2.2-1),

$$F = mg = (3 \text{ lb}_m \times 1 \text{ kg} 2.2046 \text{ lb}_m) \\ (9.80665 \text{ m/s}^2) = 13.32 \text{ kg} \cdot \text{m/s}^2 = 13.32 \text{ N}$$

As an alternative method, using the conversion factors from

$$1 \text{ g} \cdot \text{cm/s}^2 (\text{dyn}) = 10^{-5} \text{ kg} \cdot \text{m/s}^2 (\text{newton}) \quad F = (1.332 \times 10^6 \text{ dyn}) \\ (10^{-5} \text{ newton/dyn}) = 13.32 \text{ N}$$

## 2.2B Pressure in a Fluid

In the previous section, it was shown that Eq. (2.2-1) can be used to calculate the force exerted by mass under the influence of gravity. Since pressure is defined as force per unit area, Eq. (2.2-1) can be extended to calculate the pressure in a fluid by taking into account the area.

In Fig. 2.2-1, a stationary column of fluid of height  $h_2$  (m) and constant cross-sectional area  $A$  ( $\text{m}^2$ ), where  $A = A_0 = A_1 = A_2$ , is shown. Note that  $h_2 = h_1 + h_3$ . The top plane of the fluid has a cross-sectional area of  $A_0$  and the pressure immediately above the fluid at the plane is  $P_0$  ( $\text{N/m}^2$ ), which could be



the pressure of the atmosphere directly above the fluid. The fluid at any depth, say  $h_1$ , must support all the fluid above it. It can be shown that the forces at any given horizontal point in a stationary or static fluid must be the same in all directions. Also, for a fluid at rest, the force/unit area, or pressure, is the same at all points with the same elevation. For example, at  $h_1$  (m) from the top, the pressure is the same at all points shown on the cross-sectional area  $A_1$ .

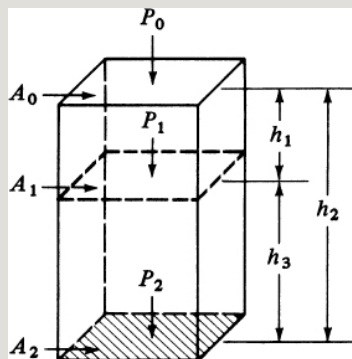


Figure 2.2-1. *Pressure in a static fluid.*

Eq. (2.2-1) can be used to calculate the

pressure at different depths (vertical points) in Fig. 2.2-1. First, it is necessary to calculate the mass of the fluid in the container. To calculate the mass of the fluid, its density  $\rho$  and volume  $V$  that it occupies must be known. Therefore, the mass of fluid occupying volume  $V$  can be calculated by

$$m = \rho V \quad (2.2-2)$$

For the fluid in Figure 2.2-1 of height  $h_2$ , the volume that it occupies is  $h_2 A$ . Therefore, the total mass of fluid that consists of height  $h_2$  m and density  $\rho$  kg/m<sup>3</sup> can be calculated by

$$\begin{aligned} m &= (\rho \text{ kg/m}^3)(h_2 \text{ m}) \\ (A \text{ m}^2) &= \rho h_2 A \text{ kg} \quad (2.2-2a) \end{aligned}$$

Substituting into Eq. (2.2-2a), the total

force  $F$  of the fluid on area  $A_2$  due to the fluid only is

$$F = mg = (\rho h^2 A \text{ kg})(g \text{ m/s}^2) = \rho g h^2 A \text{ kg} \cdot \text{ms}^{-2} \quad \text{or} \quad \text{N} \quad (2.2-3)$$

Since the pressure  $P$  is defined as force per unit area, it can be calculated using

$$P = F/A = (\rho g h^2 A) / A = \rho g h^2 \text{ N/m}^2 \quad \text{or} \quad \text{Pa} \quad (2.2-4)$$

This is the pressure exerted on cross-sectional area  $A_2$  due to the mass of the fluid above it. Here, the unit of pressure known as the Pascal (Pa) is defined as  $1 \text{ Pa} = 1 \text{ N/m}^2$ . This expression can be generalized for the pressure of the fluid at any depth  $h$  in the fluid, known as the *hydrostatic pressure*:

$$P = F/A = (\rho g h A) / A = \rho g h \text{ N/}$$

$$\text{m}^2 \quad \text{or} \quad \text{Pa} \quad (2.2-4a)$$

However, to calculate the total pressure on the fluid, it is necessary to take into account the atmospheric pressure or sometimes a greater external pressure acting on the fluid. By taking into account the atmospheric pressure at the top of the fluid,  $P_0$ , the total pressure  $P_2$  can be calculated by

$$P_2 = \rho g h_2 + P_0 \quad \text{N/m}^2 \quad \text{or} \quad \text{Pa} \quad (2.2-5)$$

Equation (2.2-5) is the fundamental equation for calculating the pressure in a fluid at any depth. For example, to calculate the pressure at depth  $h_1$ , the following equation can be used:

$$P_1 = \rho g h_1 + P_0 \quad (2.2-6)$$

Frequently, it is necessary to know the

*difference* in pressure between two depths (vertical points) in a fluid. For example, the pressure difference between points 2 and 1 is

$$\begin{array}{ll}
 P_2 - P_1 = (\rho g h_2 + P_0) - & \\
 (\rho g h_1 + P_0) = \rho g (h_2 - & \\
 h_1) & \text{(SI units)} \quad (2.2-7) \\
 P_2 - P_1 = \rho g g_c (h_2 - & \\
 h_1) & \text{(English units)}
 \end{array}$$

In the equation above,  $g_c$  is necessary because in English units, pressure is expressed in terms of pounds-force  $lbf$  and density  $\rho$  is calculated from mass expressed in pounds-mass  $lb_m$ .

It is important to note that since it is the depth of a fluid that determines the pressure in it, the shape of the vessel *does not* affect the pressure. For

example, in Fig. 2.2-2, if all three vessels are filled and open at the top, the pressure  $P_1$  at the bottom of all three vessels is the same and is equal to  $\rho gh_1 + P_0$ .

Another important type of pressure commonly used in chemical engineering calculations is known as *gage pressure*. Gage (or gauge) pressure is the pressure relative to atmospheric pressure and thus is essentially the pressure determined from a piece of equipment or pressure sensor that already takes into account the atmospheric pressure of the system. For example, if a pressure sensor at atmospheric conditions gives a pressure reading of  $P = 1$  atm, then the actual pressure of the fluid is technically 2 atm. Likewise, if a sensor gives a pressure reading of  $P = 0$  psig (or psi),

then the system is at atmospheric pressure (14.7 psia). Consider the case of a tire gage. If the gage reads 33 psig, then the absolute pressure of air in the tire would be 47.7 psia. Similarly, if the tire is completely deflated and reads 0 psig, the total absolute pressure is still 14.7 psia.

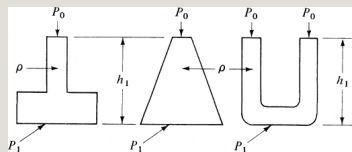


Figure 2.2-2. *Pressure in vessels of various shapes.*

#### **EXAMPLE 2.2-2. Pressure in a Storage Tank**

A large storage tank contains oil having a density of  $917 \text{ kg/m}^3$  ( $0.917 \text{ g/cm}^3$ ). The tank is  $3.66 \text{ m}$  ( $12.0 \text{ ft}$ ) tall and is vented (open) to the atmosphere with a pressure of  $1 \text{ atm}$  (abs) at the top. The tank is filled with oil to a depth of  $3.05 \text{ m}$  ( $10 \text{ ft}$ ) and also contains  $0.61 \text{ m}$  ( $2.0 \text{ ft}$ ) of water in the bottom of the tank. Calculate the absolute pressure in Pa and psia  $3.05 \text{ m}$  from the top of the tank (the oil/water interface) and at the bottom. Also calculate the gage pressure at the bottom of the tank.

**Solution:** First, a sketch is made of the tank, as shown in Fig. 2.2-3. The pressure  $P_0 = 1 \text{ atm}$  or  $14.696 \text{ psia}$  (from Appendix A.1). Also, the pressure  $P_0$  can be expressed in SI units, using conversion factors:

$$P_0 = 1.01325 \times 10^5 \text{ Pa}$$

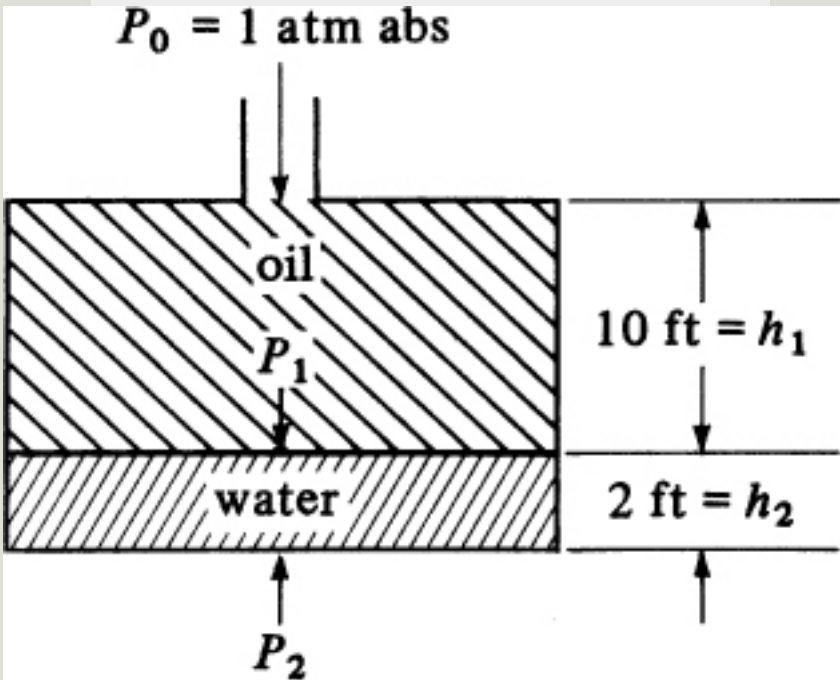


Figure 2.2-3. Storage tank in Example 2.2-2.

From Eq. (2.2-6), using English and then SI units,

$$P_1 = \rho_{\text{oil}} g h_1 + P_0 = (0.917 \times 62.43 \text{ lbm/ft}^3)(1.0 \text{ lbf/lbm})(10 \text{ ft}) \\ (1144 \text{ in.}^2/\text{ft}^2) + 14.696 \text{ lbf/in.}^2 = 18.68 \text{ psia} \\ P_1 = \rho_{\text{oil}} g h_1 + P_0 = (917 \text{ kg/m}^3)(9.8066 \text{ m/s}^2) \\ (3.05 \text{ m}) + 1.0132 \times 10^5 = 1.287 \times 10^5 \text{ Pa}$$

To calculate  $P_2$  at the bottom of the tank,  $\rho_{\text{water}} = 1000 \text{ kg/m}^3 = 1.00 \text{ g/cm}^3$  and

$$P_2 = \rho_{\text{water}} g h_2 + P_1 = (1.00 \times 62.43)(1.0)(2.0) \\ (1144) + 18.68 = 19.55 \text{ psia} = \rho_{\text{water}} g h_2 + P_1 = (1000)(9.8066) \\ (0.61) + 1.287 \times 10^5 = 1.347 \times 10^5 \text{ Pa}$$

The gage pressure at the bottom is equal to the absolute pressure  $P_2$  minus  $P_0$ :

$$P_{\text{gage}} = 19.55 \text{ psia} - 14.696 \text{ psia} = 4.85 \text{ psig}$$



## 2.2C Head of a Fluid

Pressures are given in many different sets of units, such as psia, dyn/cm<sup>2</sup>, and newtons/m<sup>2</sup>, and are given in Appendix A.1. However, a common method of expressing pressures is in terms of “head” in units of m or ft of a particular fluid. This height or head in meters or feet of the given fluid will exert the same pressure as the pressures it represents. Using Eq. (2.2-4a), which relates pressure  $P$  and height  $h$  of a fluid, the height or “head” of the given fluid can be expressed as

$$h \text{ (head)} = P \rho g \text{ m (SI)}$$
$$(2.2-8) \quad h = P g c_p g \text{ ft (English)}$$

**EXAMPLE 2.2-3. Conversion of Pressure to Head of a Fluid**

A fluid is observed to have a pressure of 1 standard atm or 101.325 kN/m<sup>2</sup> (Appendix A.1).

- Convert this pressure to “head” of fluid in m water at 4°C.
- Convert this pressure to “head” of fluid in mmHg at 0°C.

**Solution:** For part (a), the density of water at 4°C in Appendix A.2 is 1.000 g/cm<sup>3</sup>. From Appendix A.1, a density of 1.000 g/cm<sup>3</sup> equals 1000 kg/m<sup>3</sup>. Substituting these values into Eq. (2.2-8),

$$h(\text{head}) = P/\rho g = 101.325 \times 10^3 / (1000)(9.80665) = 10.33 \text{ m of water at } 4^\circ\text{C}$$

For part (b), the density of Hg in Appendix A.1 is 13.5955 g/cm<sup>3</sup>. Although the same procedure as part (a), can be used, there are alternative solutions. For example, for equal pressures  $P$  from different fluids, Eq. (2.2-8) can be rewritten as

$$P = \rho_{\text{Hg}} g h_{\text{Hg}} = \rho_{\text{H}_2\text{O}} g h_{\text{H}_2\text{O}} \quad (2.2-9)$$

Solving for  $h_{\text{Hg}}$  in Eq. (2.2-9) and substituting known values,

$$h_{\text{Hg}}(\text{head}) = \rho_{\text{H}_2\text{O}}/\rho_{\text{Hg}} h_{\text{H}_2\text{O}} = (1.000/13.5955)(10.33) = 760 \text{ mmHg}$$

## 2.2D Devices to Measure Pressure and Pressure Differences

In chemical and other industrial processing plants, it is often important to measure and control the pressure in a vessel or process. The pressure often impacts the liquid level in a vessel that may need to be

controlled. Also, since many fluids are flowing in a pipe or conduit, it is necessary to measure the rate at which the fluid is flowing. Many of these flow meters depend upon devices for measuring the pressure or a pressure difference (sometimes called a pressure “differential”). Some common devices are considered in the following paragraphs.

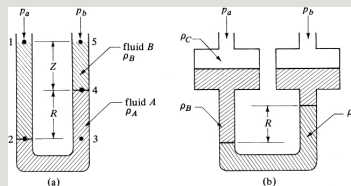


Figure 2.2-4. Manometers to measure pressure differences: (a) U tube; (b) two-fluid U tube.

*1. Simple U-tube manometer.* An example of a U-tube manometer is shown in Fig. 2.2-4a. The pressure  $p_a$  N/m<sup>2</sup> is exerted on one arm of the U tube

and the pressure  $p_b$  on the other arm. Both pressures  $p_a$  and  $p_b$  could be pressure taps from a fluid meter, or perhaps  $p_a$  could be a pressure tap and  $p_b$  the atmospheric pressure (or vice versa). The top of the manometer is filled with liquid  $B$ , having a density of  $\rho_B$  kg/m<sup>3</sup>, and the bottom with a fluid of higher density  $A$ , having a density of  $\rho_A$  kg/m<sup>3</sup>. Liquid  $A$  is immiscible with liquid  $B$ . To derive the relationship between  $p_a$  and  $p_b$ , we will use the fact that  $p_a$  is the pressure at point 1 and  $p_b$  at point 5. The pressure at point 2 is

$$p_2 = p_a + (Z + R)\rho_B g \text{ N/m}^2 \quad (2.2-10)$$

where  $R$  is the reading of the manometer in m. Since points 2 and 3 are at the same horizontal plane, the pressure at point 3 must be equal to that at point 2

by the principles of hydrostatics:

$$p_3 = p_2 \quad (2.2-11)$$

Therefore, the pressure at point 3 also equals the following:

$$p_3 = p_b + Z\rho_B g + R\rho_A g \quad (2.2-12)$$

Equating Eq. (2.2-10) to (2.2-12) and solving for the pressure difference,

$$p_a + (Z+R)\rho_B g = p_b + Z\rho_B g + R\rho_A g \quad (2.2-13)$$

$$p_a - p_b = R(\rho_A - \rho_B)g \quad (2.2-14)$$

The reader should note that since  $p_a$  and  $p_b$  are measured in the same horizontal plane, the distance  $Z$  does not affect the final result, nor do tube dimensions such

as radius.

**EXAMPLE 2.2-4. Pressure Difference in a Manometer**

A manometer, as shown in Fig. 2.2-4a, is being used to measure the differential head ("head loss") or pressure drop across a flow meter. The heavier fluid is mercury, with a density of  $13.6 \text{ g/cm}^3$ , and the top fluid is water, with a density of  $1.00 \text{ g/cm}^3$ . The reading on the manometer is  $R = 32.7 \text{ cm}$ . Calculate the pressure difference in  $\text{N/m}^2$  using SI units.

**Solution:** Converting  $R$  to m,

$$R = 32.7100 = 0.327 \text{ m}$$

Also converting  $\rho_A$  and  $\rho_B$  to  $\text{kg/m}^3$  and substituting into Eq. (2.2-14),

$$\begin{aligned} p_A - p_B &= R(\rho_A - \rho_B)g = (0.327 \text{ m})[(13.6 - 1.0)(1000 \text{ kg/m}^3)] \\ &= (9.8066 \text{ m/s}^2) = 4.040 \times 10^4 \text{ N/m}^2 \text{ (5.85 psia)} \end{aligned}$$

**2. Two-fluid U tube.** In Fig. 2.2-4b, a two-fluid U tube is shown, which is a sensitive device for measuring very small heads or pressure differences. Let  $A \text{ m}^2$  be the cross-sectional area of each of the large reservoirs and  $a \text{ m}^2$  be the cross-sectional area of each of the tubes forming the U. Proceeding and making a pressure balance for the U tube yields

the following expression for the pressure drop:

$$p_a - p_b = (R - R_0)(\rho_A - \rho_B + a/A \rho_B - a/A \rho_C)g \quad (2.2-15)$$

where  $R_0$  is the reading when  $p_a = p_b$ ,  $R$  is the actual reading,  $\rho_A$  is the density of the heavier fluid, and  $\rho_B$  is the density of the lighter fluid. Often,  $a/A$  is made sufficiently small as to be negligible and  $R_0$  is adjusted to zero. Using these approximations, the pressure drop can be found to be

$$p_a - p_b = R(\rho_A - \rho_B)g \quad (\text{SI}) \quad p_a - p_b = R(\rho_A - \rho_B)g \quad (\text{English}) \quad (2.2-16)$$

If  $\rho_A$  and  $\rho_B$  are close to each other, the reading  $R$  is magnified.

The U-tube manometer in Fig. 2.2-5a is used to measure the pressure  $p_A$  in a vessel containing a liquid with a density  $\rho_A$ . Derive the equation relating the pressure  $p_A$  and the reading on the manometer as shown.

**Solution:** At point 2, the pressure is

$$p_2 = p_{\text{atm}} + h_2 \rho_B g \quad (2.2-17)$$

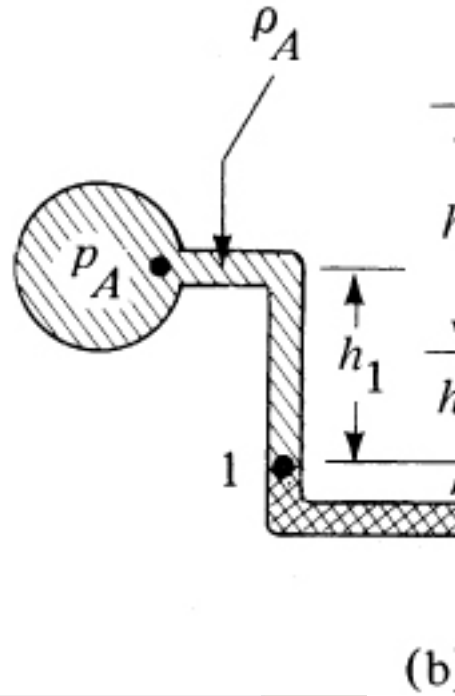
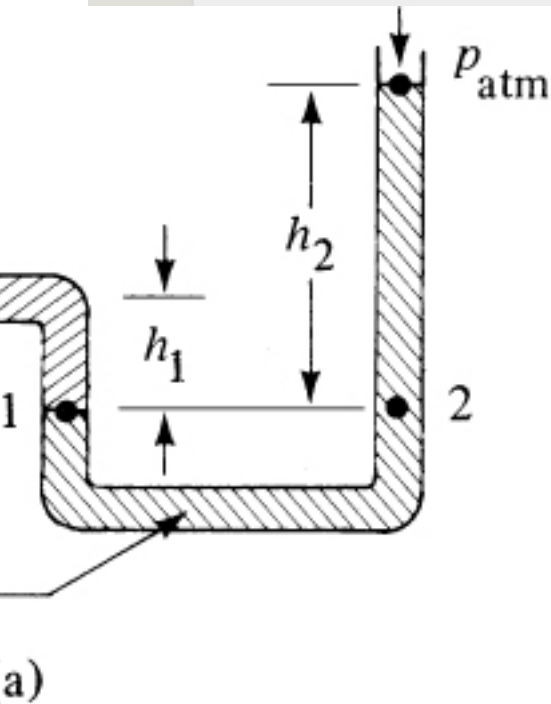


Figure 2.2-5. Measurements of pressure in vessels: (a) measurement of pressure in a vessel, (b) measurement of differential pressure.

At point 1, the pressure is

$$p_1 = p_A + h_1 \rho_A g \quad (2.2-18)$$

Equating  $p_1 = p_2$  by the principles of hydrostatics and rearranging,

$$p_A = p_{\text{atm}} + h_2 \rho_B g - h_1 \rho_A g \quad (2.2-19)$$



Another example of a U-tube manometer is shown in Fig. 2.2-5b. In this case, the device is used to measure the pressure difference between two vessels.

*3. Bourdon pressure gage.* Although manometers (including digital manometers) are commonly used to measure pressure differentials, another pressure-measuring device that is sometimes used is the mechanical Bourdon-tube pressure gage. A coiled hollow tube in the gage tends to straighten out when subjected to internal pressure, and the degree of straightening depends on the pressure difference between the inside and outside pressures. The tube is connected to a pointer on a calibrated dial.

4. *Gravity separator for two immiscible liquids.* Although gravity separators do not explicitly measure pressure, the device is used to separate liquids based on the principles of hydrostatics. In Fig. 2.2-6, a continuous gravity separator (decanter) is shown for the separation of two immiscible liquids, *A* (heavy liquid) and *B* (light liquid). The feed mixture of the two liquids enters at one end of the separator vessel, and the liquids flow slowly to the other end and separate into two distinct layers. Each liquid flows through a separate overflow line, as shown. Assuming the frictional resistance to the flow of the liquids is essentially negligible, the principles of fluid statics can be used to analyze the performance.

In Fig. 2.2-6, the depth of the layer of

heavy liquid  $A$  is  $h_{A1}$  m and that of  $B$  is  $h_B$ . The total depth  $h_T = h_{A1} + h_B$  and is fixed by position of the overflow line for  $B$ . The heavy liquid  $A$  discharges through an overflow leg  $h_{A2}$  m above the vessel bottom. Since the vessel and the overflow lines are both vented to the atmosphere, a hydrostatic balance gives

$$\rho_B g h_B + \rho_A g h_{A1} = \rho_A g h_{A2} \quad (2.2-20)$$

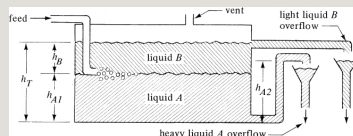


Figure 2.2-6. Continuous atmospheric gravity separator for immiscible liquids.

Substituting  $h_B = h_T - h_{A1}$  into Eq. (2.2-20) and solving for  $h_{A1}$ ,

$$h_{A1} = h_{A2} - h_T \rho_B / \rho_A \quad (2.2-21)$$

This shows that the position of the

interface or height  $h_{A1}$  depends on the ratio of the densities of the two liquids and on the elevations  $h_{A2}$  and  $h_T$  of the two overflow lines. Usually, the height  $h_{A2}$  is movable so that the interface level can be adjusted.

## 2.3 Chapter Summary

In this chapter, we have described the general properties of a fluid and identified chemical industries in which fluid transport is important. Fluids were defined as substances that do not *permanently* resist deformation. The difference between *compressible* and *incompressible* fluids was described in terms of pressure effects.

Newton's law of gravitation,

$$F=mg \quad (\text{SI units})(2.2-1)$$

$$F=mggc \quad (\text{English units})(2.2-1a)$$

was used to calculate the force exerted by a mass under the influence of gravity.

Since pressure is defined as the force exerted per unit area, we used Newton's law of gravitation to develop a general expression for the hydrostatic pressure of a fluid:

$$P=FA=(\rho ghA) \quad 1A=\rho gh \text{ N/m}^2 \quad \text{or} \quad \text{Pa}(2.2-4a)$$

where  $h$  is any depth in the fluid.

Various instruments used to measure the pressure or pressure drop in a fluid system were described, particularly the U-tube manometer. By using the

expression for the hydrostatic pressure of a fluid, which is a function of fluid height and fluid density, pressure drops in different manometer set-ups were explicitly calculated.

## Problems

### **2.2-1. *Gravitational constant.***

*Express the gravitational constant,  $g_c$  in terms of SI units.*

### **2.2-2a. *Pressure in a Spherical Tank.***

Calculate the pressure in psia and k N/m<sup>2</sup> at the bottom of an 8.0 ft spherical tank filled with oil. The top of the tank is vented to the atmosphere having a pressure of 14.72 psia. The density of the oil is 0.922 g/cm<sup>3</sup>.

**Ans.** 17.92 lbf/in.<sup>2</sup> (psia), 123.5 kN/m<sup>2</sup>

**2.2-2b. Pressure in a Spherical Tank (Revised).** Suppose that the spherical tank in the previous problem (2.2-2a) is submerged at the bottom of a pool of water that is 20 ft deep. Assuming that the oil and water are immiscible and that there is no pressure difference across the tank structure, calculate the pressure in psia and  $\text{kN/m}^2$  at the bottom of the oil tank located at the bottom of the pool.

**2.2-3. Pressure with Two Liquids, Hg and Water.** An open test tube at 293 K is filled at the bottom with 12.1 cm of Hg, and 5.6 cm of water is placed above the Hg. Calculate the pressure at the bottom of the test tube if the atmospheric pressure is 756 mmHg. Use a density of  $13.55 \text{ g/cm}^3$  for Hg and  $0.998 \text{ g/cm}^3$  for water. Give the answer in terms of  $\text{dyn/cm}^2$ , psia, and  $\text{kN/m}^2$ .

See Appendix A.1 for conversion factors.

**Ans.**  $1.175 \times 10^6$  dyn/cm<sup>2</sup>, 17.0 psia, 2.3 psig, 117.5 kN/m<sup>2</sup>

**2.2-4. *Head of a Fluid of Jet Fuel and***

***Pressure.*** The pressure at the top of a tank of jet fuel is 180.6 kN/m<sup>2</sup>. The depth of liquid in the tank is 6.4 m. The density of the fuel is 825 kg/m<sup>3</sup>.

Calculate the head of the liquid in m that corresponds to the absolute pressure at the bottom of the tank.

**2.2-5. *Measurement of Pressure.*** An open U-tube manometer similar to Fig.

2.2-4a is being used to measure the absolute pressure  $p_a$  in a vessel containing air. The pressure  $p_b$  is atmospheric pressure, which is 754



mmHg. The liquid in the manometer is water having a density of  $1000 \text{ kg/m}^3$ . Assume that the density of air is  $1.30 \text{ kg/m}^3$ . The reading  $R$  is  $0.415 \text{ m}$ . Calculate  $p_a$  in psia and kPa.

**Ans.**  $p_a = 15.17 \text{ psia}, 104.6 \text{ kPa}$

### **2.2-6. Two-fluid U-tube Manometer.**

Using pressure balances on the fluids found in Figure 2.2-4b, *explicitly* derive Equation 2.2-15.

### **2.2-7. Measurement of Small Pressure Differences.**

The two-fluid U-tube manometer is being used to measure the difference in pressure in a line containing air at  $1 \text{ atm abs}$  pressure. The value of  $R_0 = 0$  for equal pressures. The lighter fluid is a hydrocarbon with a density of  $812 \text{ kg/m}^3$  and the heavier

water has a density of  $998 \text{ kg/m}^3$ . The inside diameters of the U tube and reservoir are  $3.2 \text{ mm}$  and  $54.2 \text{ mm}$ , respectively. The reading  $R$  of the manometer is  $117.2 \text{ mm}$ . Calculate the pressure difference in  $\text{mmHg}$  and  $\text{Pa}$ .

**2.2-8. *Pressure in a Sea Lab.*** A sea lab  $5.0 \text{ m}$  high is to be designed to withstand submersion to  $150 \text{ m}$ , measured from sea level to the top of the sea lab. Calculate the pressure on top of the sea lab and also the pressure variation on the side of the container measured as the distance  $x$  in  $\text{m}$  from the top of the sea lab downward. The density of seawater is  $1020 \text{ kg/m}^3$ .

$$\text{Ans. } p = 10.00(150 + x)\text{kN/m}^2$$

**2.2-9. *Measurement of Pressure***

***Difference in Vessels.*** In Fig. 2.2-5b, the differential manometer is used to measure the pressure difference between two vessels. Derive the equation for the pressure difference  $p_A - p_B$  in terms of the liquid heights and densities.

***2.2-10. Design of a Settler–Separator for Immiscible Liquids.*** A vertical cylindrical settler–separator is to be designed for separating a mixture flowing at 20.0 m<sup>3</sup>/h and containing equal volumes of a light petroleum liquid ( $\rho_B = 875 \text{ kg/m}^3$ ) and a dilute solution of wash water ( $\rho_A = 1050 \text{ kg/m}^3$ ). Laboratory experiments indicate a settling time of 15 min is needed to adequately separate the two phases. For design purposes, use a 25-min settling time and calculate the size of the vessel needed, the liquid levels of the light and

heavy liquids in the vessel, and the height  $h_{A2}$  of the heavy-liquid overflow. Assume that the ends of the vessel are approximately flat, that the vessel diameter equals its height, and that one-third of the volume is vapor space vented to the atmosphere. Use the nomenclature given in Fig. 2.2-6.

**Ans.**  $h_{A2} = 1.537 \text{ m}$

### Notation

# Chapter 3. Fluid Properties and Fluid Flows

## 3.0 Chapter Objectives

On completion of this chapter, a student should be able to:

- Describe the difference between laminar flow and turbulent flow
- Explain the concept of fluid drag and shear stress
- Explain the basics of Newton's law of viscosity
- Describe the difference between solids and fluids in terms of rate of deformation
- Relate the shear stress to shear rate using Newton's law of viscosity
- Use Newton's law of viscosity to calculate the shear stress in a fluid
- Use both the American and SI units of energy when solving fluid dynamics problems
- Identify different units of measure for viscosity

- Know the difference between dynamic and kinematic viscosity
- Relate the concept of shear stress in a fluid to momentum transfer
- Explain the concept of a Newtonian fluid
- Describe the differences between Newtonian and non-Newtonian fluids
- Explain how temperature can affect the viscosity of liquids and gases
- Explain the concept of eddies as applied to turbulent flow
- Define the Reynolds number in terms of inertial and viscous forces
- Explain how the Reynolds number can be used to predict laminar and turbulent flow
- Explain the concept of the transition region for fluid flow
- Calculate the Reynolds number for a variety of fluid dynamics problems in different units

## **3.1 Viscosity of Fluids**

### **3.1A Newton's Law of Viscosity**

When a fluid is flowing through a

closed channel such as a pipe or between two flat plates, one of two main types of fluid flow behavior will usually occur. The type of fluid-flow behavior is dependent on the fluid's properties and the channel itself, but quite commonly the fluid velocity will be a deciding factor for the type of flow. At low velocities, the fluid tends to flow without lateral mixing, and adjacent layers slide past one another like playing cards. There are no cross-currents perpendicular to the direction of flow nor are there eddies, which are swirling packets of fluid. This flow regime or type of flow behavior is called *laminar flow*. At higher velocities, eddies form, which leads to lateral mixing. This is called *turbulent flow*. While both types of

fluid behavior are commonly observed in chemical engineering processes, the discussion in this section is limited to laminar flow.

A fluid can be distinguished from a solid by its behavior when subjected to an applied stress (force per unit area) or applied force. An elastic solid deforms by an amount proportional to the applied stress. When the applied stress to the solid is removed, so is the solid deformation. Fluids exhibit a different response to an externally applied stress. When fluids are subjected to a similar applied stress, they will *continue* to deform and flow. The fluid's velocity will also increase with increasing stress. Viscosity is that property of a fluid that gives rise to forces that resist the relative movement of adjacent layers in



the fluid. Sometimes, the property of viscosity is conceptualized as the fluid's "resistance" to flow, or deformation. These *viscous forces* arise from forces existing between the molecules in the fluid and are similar in character to the *shear forces* in solids.

The concepts above can be clarified by a more quantitative discussion of viscosity. In Fig. 3.1-1, a fluid is contained between two infinite (very long and very wide) parallel plates. Suppose that the bottom plate is moving parallel to the top plate and at a constant velocity  $\Delta v_z$  m/s faster relative to the top plate because of a steady force  $F$  (newtons) being applied. This force is called the *viscous drag force* and it arises from the viscous forces in the fluid. The plates are  $\Delta y$  m apart. Each

layer of liquid moves in the  $z$  direction. The layer immediately adjacent to the bottom plate is carried along at the velocity of this plate. The layer just above is at a slightly slower velocity and each layer moves at a slower velocity as we progress up in the  $y$  direction. This velocity profile is linear in the  $y$  direction, as shown in Fig. 3.1-1. An analogy to a fluid is a deck of playing cards where, if the bottom card is moved, all the other cards above it will slide to some extent.

It has been found experimentally that for many fluids the force  $F$ , in newtons, N, is directly proportional to the velocity  $\Delta v_z$  in m/s and to the area  $A$  in  $m^2$  of the plate used, and is inversely proportional to the distance  $\Delta y$  in m. When the flow is laminar, the force can be calculated

using *Newton's law of viscosity*:

$$FA = -\mu \Delta v_z \Delta y \quad (3.1-1)$$

where  $\mu$  is a proportionality constant called the *viscosity* (or *dynamic viscosity*) of the fluid, in  $\text{Pa} \cdot \text{s}$  or  $\text{kg/m} \cdot \text{s}$ . If we let  $\Delta y$  approach zero, then, using the definition of the derivative,

$$\tau_{yz} = -\mu \frac{dv_z}{dy} \quad (\text{SI units}) \quad (3.1-2)$$

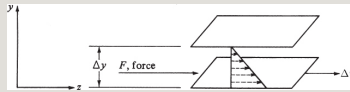


Figure 3.1-1. Fluid shear between two parallel plates.

where  $\tau_{yz} = F/A$  and is the shear stress or force per unit area exerted in the  $y$ -direction by fluid flowing in the  $z$ -direction in Newtons/ $\text{m}^2$  ( $\text{N/m}^2$ ). In the cgs system,  $F$  is in dynes,  $\mu$  is in  $\text{g/cm} \cdot \text{s}$ ,  $v_z$  in  $\text{cm/s}$ , and  $y$  is in  $\text{cm}$ . We can also

write Eq. (3.1-2) as

$$\tau_{yz} = -\mu \frac{dv_z}{dy} \quad (\text{English units}) \quad (3.1-3)$$

where  $\tau_{yz}$  is in units of  $\text{lb}_f/\text{ft}^2$ .

The unit of viscosity in the cgs system is  $\text{g}/\text{cm} \cdot \text{s}$ , which is also called *poise*.

More commonly, the unit *centipoise* is used for viscosity in the cgs system. In the SI system, viscosity is given in  $\text{Pa} \cdot \text{s}$  ( $\text{N} \cdot \text{s}/\text{m}^2$  or  $\text{kg}/\text{m} \cdot \text{s}$ ):

$$1 \text{ cp} = 1 \times 10^{-3} \text{ kg}/\text{m} \cdot \text{s} = 1 \times 10^{-3} \text{ Pa} \cdot \text{s} = 1 \times 10^{-3} \text{ N} \cdot \text{s}/\text{m}^2$$

$$\begin{aligned} 1 \text{ cp} &= 0.01 \text{ poise} = 0.01 \text{ g}/\text{cm} \cdot \text{s} \\ 1 \text{ cp} &= 6.7197 \times 10^{-4} \text{ lb}_m/\text{ft} \cdot \text{s} \end{aligned}$$

Other conversion factors for viscosity are given in Appendix A.1. Another form of viscosity, known as the *kinematic viscosity*,  $\mu/\rho$ , is given in  $\text{m}^2/\text{s}$

or  $\text{cm}^2/\text{s}$ , where  $\rho$  is the density of the fluid.

**EXAMPLE 3.1-1. Calculation of Shear Stress in a Liquid**

Referring to Fig. 3.1-1, the distance between plates is  $\Delta y = 0.5 \text{ cm}$ ,  $\Delta v_z = 10 \text{ cm/s}$ , and the fluid is ethyl alcohol at 273 K having a viscosity of 1.77 cp ( $0.0177 \text{ g/cm} \cdot \text{s}$ ).

- Calculate the shear stress  $\tau_{yz}$  and the velocity gradient or shear rate  $dv_z/dy$  using cgs units.
- Repeat, using lb force, s, and ft units (English units).
- Repeat, using SI units.

**Solution:** We can substitute directly into Eq. (3.1-1) or we can integrate Eq. (3.1-2). Using the latter method, rearranging Eq. (3.1-2), calling the bottom plate point 1, and integrating,

$$\tau_{yz} \int y_1 = 0 y_2 = 0.5 \text{ dy} = -\mu \int v_1 = 10 v_2 = 0 \text{ dv}_z \quad (3.1-4)$$

$$\tau_{yz} = \mu v_1 - v_2 y_2 - y_1 \quad (3.1-5)$$

Substituting the known values,

$$\begin{aligned} \tau_{yz} &= \mu v_1 - v_2 y_2 - y_1 = (0.0177 \text{ g/cm} \cdot \text{s})(10 - 0) \text{ cm}/ \\ &\quad \text{s}(0.5 - 0) \text{ cm} \quad (3.1-6) = 0.354 \text{ g} \cdot \text{cm}/ \\ &\quad \text{s}^2 \text{cm}^2 = 0.354 \text{ dyn/cm}^2 \end{aligned}$$

To calculate the shear rate  $dv_z/dy$ , since the velocity change is linear with  $y$ ,

$$\begin{aligned} \text{shear rate} &= dv_z/dy = \Delta v_z/\Delta y = (10 - 0) \text{ cm}/ \\ &\quad \text{s}(0.5 - 0) \text{ cm} = 20.0 \text{ s}^{-1} \quad (3.1-7) \end{aligned}$$

For part (b), using lb force units and the viscosity conversion factor from Appendix A.1,

$$\mu = (1.77 \text{ cp})(6.7197 \times 10^{-4} \text{ lbm/ft} \cdot \text{s/cp}) = (1.77)$$

$$(6.7197 \times 10^{-4}) \text{ lbm/ft}\cdot\text{s}$$

Integrating Eq. (3.1-3),

$$\tau_{yz} = \mu \text{ lbm/ft} \cdot \text{sgc lbf} \cdot \text{ft/lbf} \cdot \text{s}^2 (v_1 - v_2) \text{ft/s} (y_2 - y_1) \text{ft} \quad (3.1-8)$$

Substituting known values into Eq. (3.1-8) and converting  $\Delta v_z$  to ft/s and  $\Delta y$  to ft,  $\tau_{yz} = 7.39 \times 10^{-4} \text{ lbf/ft}^2$ . Also,  $dv_z/dy = 20 \text{ s}^{-1}$ .

For part (c),  $\Delta y = 0.5/100 = 0.005 \text{ m}$ ,  $\Delta v_z = 10/100 = 0.1 \text{ m/s}$ , and  $\mu = 1.77 \times 10^{-3} \text{ kg/m} \cdot \text{s} = 1.77 \times 10^{-3} \text{ Pa} \cdot \text{s}$ .

Substituting into Eq. (3.1-5),

$$\tau_{yz} = (1.77 \times 10^{-3})(0.10)/0.005 = 0.0354 \text{ N/m}^2$$

The shear rate will be the same at  $20.0 \text{ s}^{-1}$ .

### 3.1B Momentum Transfer in a Fluid

The shear stress  $\tau_{yz}$  in Eqs. (3.1-1)–(3.1-3) can also be interpreted as a *flux of z-directed momentum in the y direction*, which is the rate of momentum per unit area. The units of momentum are mass times velocity in  $\text{kg} \cdot \text{m/s}$ . Thus, the shear stress can also be written as

$$\tau_{yz} = \text{kg} \cdot \text{m/s}^2 \cdot \text{m}^2 \cdot \text{s} = \text{momentum} \cdot \text{m}^2 \cdot \text{s} \quad (3.1-9)$$

This gives the amount of momentum transferred per unit area per second.

This can be shown by considering the interaction between two adjacent layers of a fluid in Fig. 3.1-1 that have different velocities and, hence, different momentums in the  $z$  direction. The random motions of the molecules in the faster-moving layer send some of the molecules into the slower-moving layer, where they collide with the slower-moving molecules and tend to speed them up or increase their momentum in the  $z$  direction. In the same fashion, molecules in the slower layer also tend to retard those in the faster layer. This exchange of molecules between layers produces a transfer or flux of  $z$ -directed momentum from high-velocity to low-velocity layers. The negative sign in Eq.

(3.1-2) indicates that momentum is transferred down the gradient from high- to low-velocity regions. This is similar to the transfer of heat from high- to low-temperature regions.

### 3.1C Viscosities of Newtonian Fluids

Fluids that follow Newton's law of viscosity, which is represented by Eqs. (3.1-1)–(3.1-3), are called *Newtonian fluids*. For a Newtonian fluid, there is a linear relationship between the shear stress  $\tau_{yz}$  and the velocity gradient  $dv_z/dy$  (rate of shear). This means that the viscosity  $\mu$  is a constant and is independent of the rate of shear. Fluids that don't observe this behavior are known as *non-Newtonian fluids*. For non-Newtonian fluids, the relation between  $\tau_{yz}$  and  $dv_z/dy$  is not linear.



In this case, the viscosity  $\mu$  does not remain constant, but is often a function of the shear rate. Certain liquids—primarily pastes, slurries, high-molecular-weight polymers, and emulsions—do not obey Newton’s law. The science of the flow and deformation of these types of fluids is called *rheology*. A discussion of non-Newtonian fluids is presented later in Chapter 9.

Table 3.1-1. *Viscosities of Some Gases and Liquids at 101.32 kPa Pressure*

The viscosity of gases, which are Newtonian fluids, increases with increasing temperature and is approximately independent of pressure up to a pressure of about 1000 kPa. At

higher pressures, the viscosity of gases increases with increase in pressure. For example, the viscosity of N<sub>2</sub> gas at 298 K approximately doubles when going from 100 kPa to about  $5 \times 10^4$  kPa (R1). For liquids, the viscosity decreases with increasing temperature. Since liquids are essentially incompressible, their viscosities are usually not affected by pressure.

In Table 3.1-1, some experimental viscosity data are given for a few typical pure fluids at 101.32 kPa. The viscosities for gases are the lowest and do not differ markedly from gas to gas (about one order of magnitude), being about  $5 \times 10^{-6}$  to  $3 \times 10^{-5}$  Pa · s. The viscosities for liquids are much greater. The value for water at 293 K is about  $1 \times 10^{-3}$  Pa · s and for glycerol 1.069 Pa ·

s. At room temperature, the viscosity of water is approximately 1 cP. Hence, there are great differences between the viscosities of liquids at the same temperature. More complete tables of viscosities are given for water in Appendix A.2, for inorganic and organic liquids and gases in Appendix A.3, and for biological and food liquids in Appendix A.4. Extensive data are available in other references (P1, R1, W1, L1). Methods for estimating viscosities of gases and liquids when experimental data are not available are summarized elsewhere (R1). These estimation methods for gases at pressures below 100 kPa are reasonably accurate, with an error of about  $\pm 5\%$ , but the methods for liquids are often quite inaccurate.

## 3.2 Types of Fluid Flow and Reynolds Number

### 3.2A Introduction and Types of Fluid Flow

Whereas the principles of fluid statics, discussed in Section 2.2, are almost an exact science, the principles of fluid motions, or dynamics, are quite complex. The basic relations describing the motions of a fluid are the equations for the overall balances of mass, energy, and momentum, which will be covered in the following sections.

These overall or macroscopic balances will be applied to a control volume that is fixed in space. We use the term “overall” because we wish to apply these balances from outside the control volume. The changes inside the control volumes are determined in terms of the

properties of the streams entering and leaving as well as the exchanges of energy between the control volumes and their surroundings.

When making overall balances on mass, energy, and momentum, we are often not interested in the details of what occurs inside the enclosure. For example, in an overall balance, average inlet and outlet velocities are considered. However, in a differential balance, the velocity distribution inside an enclosure can be obtained by the use of Newton's law of viscosity.

In next section, we go into more detail regarding the two types of fluid flow that can occur: laminar flow and turbulent flow. Also, the Reynolds number will be introduced and used to

characterize the flow regimes.

### **3.2B Laminar and Turbulent Flow**

The type of flow occurring in a fluid moving in a channel is important for many fluid dynamics problems.

When fluids flow through a closed channel of any cross section (e.g., circular or rectangular), either of two distinct types of flow can be observed, according to the conditions present. These two types of flow can commonly be seen in a flowing open stream or river. When the velocity of the fluid is relatively slow, the flow patterns are smooth. However, when the velocity is quite high, an unstable pattern is observed. In this case, eddies, or small packets of fluid particles, are present, moving in all directions and at all

angles to the normal direction of flow.

The first type of flow, commonly observed at low velocities, where the layers of fluid seem to slide by one another without eddies or swirls being present, is called *laminar flow*.

Newton's law of viscosity holds for fluids in this regime, as discussed previously in Section 3.1A. The second type of flow, commonly observed at higher velocities, where eddies are present giving the fluid a fluctuating nature, is called *turbulent flow*.

The existence of laminar and turbulent flows is most easily visualized by the experiments of Reynolds, which are shown in Fig. 3.2-1. In his experiments, water was allowed to flow at a constant

flowrate through a transparent pipe. A thin, steady stream of dyed water was introduced from a fine jet, as shown, and its flow pattern observed. At low rates of water flow, the dye pattern was regular and formed a single line or stream similar to a thread, as shown in Fig.

3.2-1a. There was no lateral mixing of the fluid, and it flowed in streamlines down the tube. By putting in additional jets at other points in the pipe cross section, it was shown that there was no mixing in any parts of the tube and that the fluid flowed in straight, parallel lines. This type of flow is called laminar or *viscous flow*.

As the velocity was increased, it was found that at a definite velocity the thread of dye became dispersed and the pattern was very erratic, as shown in



Fig. 3.2-1b. This type of flow is known as *turbulent flow*. The velocity at which the flow changes from laminar flow to turbulent flow is known as the *critical velocity*.

### **3.2C Reynolds Number**

Studies have shown that the transition from laminar to turbulent flow in tubes is not only a function of velocity but also of the density and viscosity of the fluid, and the size of the tube's diameter. These variables can be combined into a dimensionless number known as the *Reynolds number*:

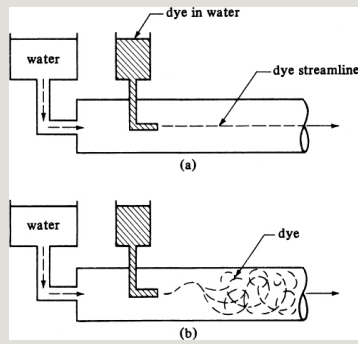


Figure 3.2-1. *Reynolds's experiment for different types of flow: (a) laminar flow; (b) turbulent flow.*

$$N_{Re} = Dv\rho\mu \quad (3.2-1)$$

where  $N_{Re}$  is the Reynolds number,  $D$  is the diameter in m,  $\rho$  is the fluid density in  $\text{kg/m}^3$ ,  $\mu$  is the fluid viscosity in  $\text{Pa} \cdot \text{s}$ , and  $v$  is the average velocity of the fluid in m/s (where average velocity is defined as the volumetric rate of flow divided by the cross-sectional area of the pipe). Units in the cgs system are  $D$  in cm,  $\rho$  in  $\text{g/cm}^3$ ,  $\mu$  in  $\text{g/cm} \cdot \text{s}$ , and  $v$  in cm/s. In the English system  $D$  is in ft,  $\rho$  is in  $\text{lb}_m/\text{ft}^3$ ,  $\mu$  is in  $\text{lb}_m/\text{ft} \cdot \text{s}$ , and  $v$  is in ft/s.

The instability of the flow that leads to disturbed or turbulent flow is determined by the ratio of the kinetic or inertial forces (i.e., the numerator) to the viscous forces (i.e., the denominator) in the fluid stream. The inertial forces are proportional to  $\rho v^2$  and the viscous forces to  $\mu_v/D$ , and the ratio  $\rho v^2/(\mu_v/D)$  is the Reynolds number.

For a straight circular pipe, when the value of the Reynolds number is less than 2100, the flow is always laminar. When the value is over 4000, the flow will be turbulent, except in very special cases. In between—called the *transition region*—the flow can be viscous or turbulent, depending upon the apparatus details, which cannot be predicted.

**EXAMPLE 3.2-1. Reynolds Number in a Pipe**

Water at 303 K is flowing at the rate of 10 gal/min in a pipe

having an inside diameter (ID) of 2.067 in. Calculate the Reynolds number using both English units and SI units.

**Solution:** From Appendix A.1, 7.481 gal = 1 ft<sup>3</sup>. The flow rate is calculated as

$$\begin{aligned}\text{flow rate} &= (10.0 \text{ gal/min}) (1 \text{ ft}^3 / 7.481 \text{ gal}) \\ &= (1 \text{ min} / 60 \text{ s}) = 0.0223 \text{ ft}^3 / \text{s} \\ \text{pipe diameter, } D &= 2.067 / 12 = 0.172 \text{ ft} \\ \text{cross-sectional area of pipe} &= \pi D^2 / 4 = \pi (0.172)^2 / 4 = 0.0233 \text{ ft}^2 \\ \text{velocity in pipe, } v &= (0.0223 \text{ ft}^3 / \text{s}) / (0.0233 \text{ ft}^2) = 0.957 \text{ ft/s}\end{aligned}$$

From Appendix A.2, for water at 303 K (30°C),

$$\begin{aligned}\text{density, } \rho &= 0.996 (62.43) \text{ lbm / ft}^3 \\ \text{viscosity, } \mu &= (0.8007 \text{ cp}) \\ &= (6.7197 \times 10^{-4} \text{ lbm / ft} \cdot \text{s}) = 5.38 \times 10^{-4} \text{ lbm / ft} \cdot \text{s}\end{aligned}$$

Substituting into Eq. (3.2-1),

$$\begin{aligned}N_{Re} &= D v \rho / \mu = (0.172 \text{ ft}) (0.957 \text{ ft/s}) (0.996 \times 62.43 \text{ lbm / ft}^3) \\ &= (5.38 \times 10^{-4} \text{ lbm / ft} \cdot \text{s}) = 1.905 \times 10^4\end{aligned}$$

Hence, the flow is turbulent. Using SI units,

$$\begin{aligned}\rho &= (0.996) (1000 \text{ kg/m}^3) = 996 \text{ kg/m}^3 \\ D &= (2.067 \text{ in.}) (1 \text{ ft} / 12 \text{ in.}) (1 \text{ m} / 3.2808 \text{ ft}) = 0.0525 \text{ m} \\ v &= (0.957 \text{ ft/s}) (1 \text{ m} / 3.2808 \text{ ft}) = 0.2917 \text{ m/s} \\ \mu &= (0.8007 \text{ cp}) (1 \times 10^{-3} \text{ kg / m} \cdot \text{s}) \\ &= (8.007 \times 10^{-4} \text{ kgm} \cdot \text{s}) = 8.007 \times 10^{-4} \text{ Pa} \cdot \text{s} \\ N_{Re} &= D v \rho / \mu = (0.0525 \text{ m}) (0.2917 \text{ m/s}) (996 \text{ kg/m}^3) / (8.007 \times 10^{-4} \text{ kg / m} \cdot \text{s}) = 1.905 \times 10^4\end{aligned}$$

### 3.3 Chapter Summary

In this chapter, we have described the two main types of fluid flows, *laminar flow* and *turbulent flow*, and how they are related to the fluid property of *viscosity*. We have shown how viscosity is related to the

shear stress in a fluid and the shear rate at which it deforms. This relationship was observed to follow Newton's law of viscosity,

$$\tau_{yz} = -\mu \frac{dv_z}{dy} \text{ (SI units)} \quad (3.1-2)$$

The relationship of shear stress in a fluid to the flux of momentum transferred was also described.

The fluid property of *viscosity* was described in terms of macroscopic behavior (i.e., deformation and “resistance to flow”) as well on the molecular level in the exchange of momentum between adjacent molecules. It was shown that fluid viscosity is temperature dependent, and the relationship between temperature and viscosity varies if the fluid is a liquid or

a gas.

The differences between *laminar flow* and *turbulent flow* were also described based on Reynolds's original experiment and a discussion on the formation of eddies, or swirling packets of fluids. In order to help predict the flow regime, the Reynolds number was described as the ratio of inertial forces to viscous forces and defined as:

$$N_{Re} = Dv\rho\mu \quad (3.2-1)$$

We also showed how the Reynolds number can be calculated from fluid and geometric properties, and how that value can be used to predict the flow behavior of the fluid.

## Problems

### 3.1-1. *Shear Stress in Soybean Oil.*

Using Fig. 3.1-1, the distance between the two parallel plates is 0.00914 m, and the lower plate is being pulled at a relative velocity of 0.366 m/s greater than the top plate. The fluid used is soybean oil with viscosity  $4 \times 10^{-2} \text{ Pa} \cdot \text{s}$  at 303 K (Appendix A.4).

- Calculate the shear stress  $\tau$  and the shear rate using lb force, ft, and s units.
- Repeat, using SI units.
- If glycerol at 293 K with a viscosity of  $1.069 \text{ kg/m} \cdot \text{s}$  is used instead of soybean oil, what relative velocity in m/s is needed using the same distance between plates so that the same shear stress is obtained as in part (a)? Also, what is the new shear rate?

**Ans.** (a) Shear stress =  $3.34 \times 10^{-2} \text{ lbf/ft}^2$ , shear rate =  $40.0 \text{ s}^{-1}$ ; (b)  $1.60 \text{ N/m}^2$ ; (c) relative velocity =  $0.01369 \text{ m/s}$ ,

$$\text{shear rate} = 1.50 \text{ s}^{-1}$$

**3.1-2 *Shear Stress and Shear Rate in Fluids.*** Using Fig. 3.1-1, the lower plate is being pulled at a relative velocity of 0.40 m/s greater than the top plate. The fluid used is water at 24°C.

- How far apart should the two plates be placed so that the shear stress  $\tau$  is 0.30 N/m<sup>2</sup>? Also, calculate the shear rate.
- If oil with a viscosity of  $2.0 \times 10^{-2}$  Pa · s is used instead at the same plate spacing and velocity as in part (a), what are the new shear stress and the shear rate?

**3.2-1. *Reynolds Number for Milk Flow.***

Whole milk at 293 K having a density of 1030 kg/m<sup>3</sup> and viscosity of 2.12 cp is flowing at the rate of 0.605 kg/s in a glass pipe having an inside diameter of 63.5 mm.

- Calculate the Reynolds number. Is this turbulent



flow?

- Calculate the flow rate needed in  $\text{m}^3/\text{s}$  for a Reynolds number of 2100 and velocity in  $\text{m/s}$ .

**Ans.** (a)  $N_{\text{Re}} = 5723$ , turbulent flow

### **3.2-2. Pipe Diameter and Reynolds**

**Number.** An oil is being pumped inside a 10.0 mm diameter pipe. The oil's density is  $855 \text{ kg/m}^3$  and its viscosity is  $2.1 \times 10^{-2} \text{ Pa} \cdot \text{s}$ . It is required that the flow remain in the laminar regime and thus the Reynolds number cannot exceed 2100.

- What is the maximum allowed velocity in the pipe?
- It is desired to maintain the same Reynolds number of 2100 and the same velocity as in part (a) using a second fluid with a density of  $925 \text{ kg/m}^3$  and a viscosity of  $1.5 \times 10^{-2} \text{ Pa} \cdot \text{s}$ . What pipe diameter should be used?

### **3.2-3. Reynolds Number for a**

**Petroleum Pipeline.** The Keystone

pipeline is a network of pipes and pumps used to transport Canadian crude oil to the United States. The average diameter of the pipeline can be assumed to be 30 inches in diameter and a maximum of 132,000 m<sup>3</sup> of crude oil can be transported per day through the pipes.

- Although the composition of crude oil can greatly affect its properties, if we assume the density of medium crude oil to be 0.85 g/cm<sup>3</sup> and the viscosity to be 10 cP, what is the velocity of crude oil flowing through the pipeline? What is the associated Reynolds number and is the flow in the laminar or turbulent flow regime?
- Suppose now that heavy crude oil with a density of 0.95 g/cm<sup>3</sup> and viscosity of 800 cP is being transported; calculate the Reynolds number and determine if the flow is in the laminar or turbulent regime.

**3.2-4. *Rate of Drawing Blood.*** You have recently visited your doctor for a physical examination and are required to

have blood work performed. Although blood is a complex fluid, we will assume it's a Newtonian fluid with a kinematic viscosity to be  $3 \cdot 10^{-6} \text{ m}^2/\text{s}$ . If a 7-gauge syringe (ID = 0.15 in) is used to draw blood, what is the maximum allowable flowrate possible, such that the fluid flow remains in the laminar flow regime?

**3.2-5. *Microfluidics*.** In this chapter, we have described how fluid velocity can greatly affect whether a fluid is flowing in the laminar or turbulent flow regime. However, other properties may affect fluid behavior. Consider the area of microfluidics—a branch of fluid dynamics that deals with fluids being transported in small chambers, often on the micro- or nano- scale. For these systems, what flow regime usually

dominates—laminar or turbulent flow?  
Explain your reasoning.

### References

### Notation

# Chapter 4. Overall Mass, Energy, and Momentum Balances

## 4.0 Chapter Objectives

On completion of this chapter, a student should be able to:

- Perform a simple mass balance on a fluid process
- Specify a control volume for solving fluid-mechanics problems
- Derive the overall mass-balance equation
- Derive the energy balance based on thermodynamic principles
- Explain the concept of the kinetic-energy correction factor
- Use the kinetic-energy correction factor for different flow regimes and problems
- Apply the energy balance to the design of a pump
- Extend the overall energy balance to derive the overall mechanical-energy balance

- Explain how the concept of work and energy is applied to pumps and piping systems
- Calculate the energy needed to operate a pump in a piping system
- Derive the Bernoulli equation
- Explain the limitations of the Bernoulli equation
- Use the Bernoulli equation to calculate the fluid discharge rate from a tank
- Derive the overall momentum balance and describe each force term in the balance
- Apply the overall momentum balance to solve fluid mechanics problems in one and two dimensions
- Explain the concept of a shell momentum balance
- Apply a shell momentum balance on a fluid element flowing in a circular pipe
- Use the shell momentum balance approach to determine the velocity profile for internal and external fluid mechanics problems

## **4.1 Overall Mass Balance and Continuity Equation**

### **4.1A Introduction and Simple Mass Balances**

In all fluid dynamics situations, fluids are in motion. Generally, they are moved from place to place and flow through systems of piping and/or process equipment by means of mechanical devices such as pumps or blowers, by gravity head, or by pressure. The first step in the solution of flow problems is generally to apply the principles of the conservation of mass to the whole system or to any part of the system. First, we will consider an elementary balance on a simple geometry, and later we will derive the general mass-balance equation.

Simple mass or material balances were introduced in Section 1.5, where

$$\text{input} = \text{output} + \text{accumulation} \quad (1.5-1)$$

Since, in fluid flow, we are usually working with rates of flow and usually at steady state where the rate of accumulation is zero, we obtain

$$\text{rate of input} = \text{rate of output (steady state)} \quad (4.1-1)$$

In Fig. 4.1-1, a simple flow system is shown where fluid enters section 1 with an average velocity  $v_1$  m/s and density  $\rho_1$  kg/m<sup>3</sup>.

The cross-sectional area is  $A_1$  m<sup>2</sup>. The fluid leaves section 2 with average velocity  $v_2$ . The mass balance, Eq. (4.1-1), becomes

$$m = \rho_1 A_1 v_1 = \rho_2 A_2 v_2 \quad (4.1-2)$$

where  $m$  = kg/s. Often,  $\rho v$  is expressed as  $G = \rho v$ , where  $G$  is mass velocity or



mass flux in  $\text{kg/s} \cdot \text{m}^2$ . In English units,  $v$  is in  $\text{ft/s}$ ,  $\rho$  is in  $\text{lb}_\text{m}/\text{ft}^3$ ,  $A$  is in  $\text{ft}^2$ ,  $m$  is in  $\text{lb}_\text{m}/\text{s}$ , and  $G$  is in  $\text{lb}_\text{m}/\text{s} \cdot \text{ft}^2$ .

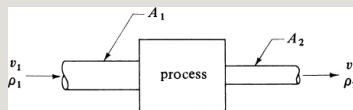


Figure 4.1-1. *Mass balance on a flow system.*

**EXAMPLE 4.1-1. Flow of Crude Oil and Mass Balance**

A petroleum crude oil having a density of  $892 \text{ kg/m}^3$  is flowing through the piping arrangement shown in Fig. 4.1-2 at a total rate of  $1.388 \times 10^{-3} \text{ m}^3/\text{s}$  entering pipe 1.

The flow divides equally in each of the pipes labeled “3”. The steel pipes are Schedule 40 pipe (see Appendix A.5 for actual dimensions). Calculate the following, using SI units:

- The total mass flow rate  $m$  in pipe 1 and pipes 3
- The average velocity  $v$  in 1 and 3
- The mass velocity  $G$  in 1

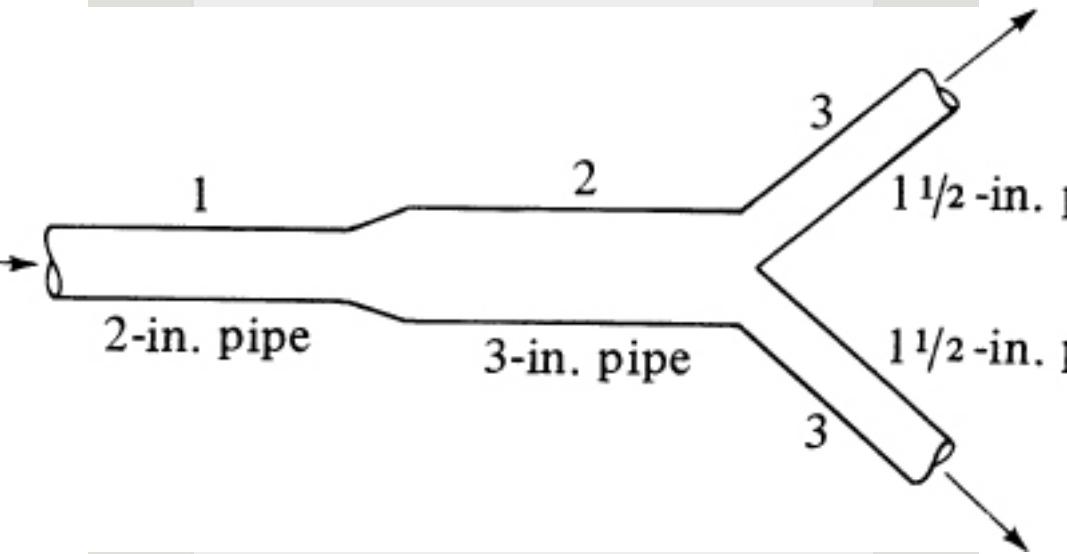


Figure 4.1-2. Piping arrangement for Example 4.1-1.

**Solution:** From Appendix A.5, the dimensions of the pipes are as follows: 2-in. pipe:  $D_1$  (ID) = 2.067 in.; cross-sectional area

$$A_1 = 0.02330 \text{ ft}^2 = 0.02330(0.0929) = 2.165 \times 10^{-3} \text{ m}^2$$

1 1/2-in. pipe:  $D_3$  (ID) = 1.610 in.; cross-sectional area

$$A_3 = 0.01414 \text{ ft}^2 = 0.01414(0.0929) = 1.313 \times 10^{-3} \text{ m}^2$$

The total mass flow rate is the same through pipes 1 and 2 and is

$$\dot{m}_1 = (1.388 \times 10^{-3} \text{ m}^3/\text{s})(892 \text{ kg}/\text{m}^3) = 1.238 \text{ kg}/\text{s}$$

Since the flow divides equally in each of pipes 3,

$$\dot{m}_3 = \dot{m}_2 = 1.238/2 = 0.619 \text{ kg}/\text{s}$$

For part (b), using Eq. (2.6-2) and solving for  $v$ ,

$$\begin{aligned} v_1 &= \dot{m}_1 / \rho_1 A_1 = 1.238 \text{ kg}/\text{s} / (892 \text{ kg}/\text{m}^3) \\ (2.165 \times 10^{-3} \text{ m}^2) &= 0.641 \text{ m}/\text{s} \\ v_3 &= \dot{m}_3 / \rho_3 A_3 = 0.619 / (892) \\ (1.313 \times 10^{-3}) &= 0.528 \text{ m}/\text{s} \end{aligned}$$

For part (c),

#### 4.1B Control Volume for Balances

The laws for the conservation of mass, energy, and momentum are all stated in terms of a system; these laws help govern the interaction of a system with its surroundings. A *system* is defined as a collection of fluid (sometimes called *fluid particles*) of fixed identity. However, for the flow of fluids, individual particles are not easily identifiable. As a result, attention is focused on a given space through which the fluid flows rather than on a given mass of fluid. The method used, which is more convenient, is to select a control volume, a region fixed in space through which the fluid flows.

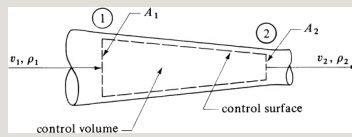


Figure 4.1-3. *Control volume for flow through a conduit.*

In Fig. 4.1-3, the case of a fluid flowing through a conduit is shown. The control surface, indicated by a dashed line, is the surface surrounding the control volume. In most problems, part of the control surface will coincide with some boundary, such as the wall of the conduit. The remaining part of the control surface is a hypothetical surface through which the fluid can flow, shown as point 1 and point 2 in Fig. 4.1-3. The control-volume representation is analogous to the open system of thermodynamics.

#### **4.1C Overall Mass-Balance Equation**

In deriving the general equation for

the overall balance of the property mass, the law of conservation of mass may be stated as follows for a control volume where no mass is being generated; this is similar to Eq. (1.5-1):

$$[N] - [\text{CONSUMPTION}] = [\text{ACCUMULATION}] \quad (4.1-3a)$$

This can be written on a rate basis for the case of no mass generation as,

$$(\text{rate of mass accumulation in control volume}) = 0 \quad (\text{rate of mass generation}) \quad (4.1-3b)$$

We now consider the general control volume fixed in space and located in a fluid flow field, as shown in Fig. 4.1-4. For a small element of area  $dA$  m<sup>2</sup> on the control surface, the rate of mass efflux from this element =  $(\rho v)(dA \cos$

$\alpha$ ), where ( $dA \cos \alpha$ ) is the area  $dA$  projected in a direction normal to the velocity vector  $\mathbf{v}$ ,  $\alpha$  is the angle between the velocity vector  $\mathbf{v}$  and the outward-directed unit, normal vector  $\mathbf{n}$  to  $dA$ , and  $\rho$  is the density in  $\text{kg/m}^3$ . The quantity  $\rho \mathbf{v}$  has units of  $\text{kg/s} \cdot \text{m}^2$  and is called a *flux* or *mass velocity*,  $G$ .

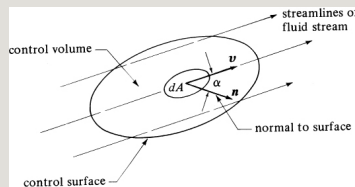


Figure 4.1-4. Flow through a differential area  $dA$  on a control surface.

From vector algebra, we recognize that  $(\rho \mathbf{v}) (dA \cos \alpha)$  is the scalar or dot product  $\rho(\mathbf{v} \cdot \mathbf{n}) dA$ . If we now integrate this quantity over the entire control surface  $A$ , we have the net outflow of mass across the control surface, or the net mass efflux in  $\text{kg/s}$  from the entire

control volume  $V$ :

$$\dot{m} = \int \int A v \rho \cos \alpha \, dA = \int \int A \rho (\mathbf{v} \cdot \mathbf{n}) \, dA \quad (4.1-4)$$

We should note that if mass is entering the control volume, that is, flowing inward across the control surface, the net efflux of mass in Eq. (4.1-4) is negative, since  $\alpha > 90^\circ$  and  $\cos \alpha$  is negative. Hence, there is a net influx of mass. If  $\alpha < 90^\circ$ , there is a net efflux of mass.

The rate of accumulation of mass within the control volume  $V$  can be expressed as follows:

$$\frac{d}{dt} \int \int_V \rho \, dV = \frac{dM}{dt} \quad (4.1-5)$$

where  $M$  is the mass of fluid in the volume in kg. Substituting Eqs. (4.1-4) and (4.1-5) into Eq. (4.1-3), we obtain

the general form of the overall mass balance:

$$\int \int A \rho (\mathbf{v} \cdot \mathbf{n}) dA + \frac{\partial}{\partial t} \int \int A \int \rho dV = 0 \quad (4.1-6)$$

The use of Eq. (4.1-6) can be shown for a common situation of steady state, one-dimensional flow, where all the flow inward is normal to  $A_1$  and outward is normal to  $A_2$ , as shown in Fig. 4.1-3.

When the velocity  $v_2$  leaving (Fig. 4.1-3) is normal to  $A_2$ , the angle  $\alpha_2$  between the normal to the control surface and the direction of the velocity is  $0^\circ$ , and  $\cos \alpha_2 = 1.0$ . Where  $v_1$  is directed inward,  $\alpha_1 > \pi/2$ , and for the case in Fig. 4.1-3,  $\alpha_1$  is  $180^\circ$  ( $\cos \alpha_1 = -1.0$ ). Since  $\alpha_2$  is  $0^\circ$  and  $\alpha_1$  is  $180^\circ$ , using Eq. (4.1-4),



$$\int \int A v_p \cos \alpha \, dA = \int \int A v_p \cos \alpha^2 \, dA \\ + \int \int A_1 v_p \cos \alpha_1 \, dA = v_2^2 \rho_2 A_2 - \\ v_1 \rho_1 A_1 \quad (4.1-7)$$

For steady state,  $dM/dt = 0$  in Eq. (4.1-5), and Eq. (4.1-6) becomes

$$m = \rho_1 A_1 v_1 = \rho_2 A_2 v_2 \quad (4.1-2)$$

which is Eq. (4.1-2), derived earlier.

In Fig. 4.1-3 and Eqs. (4.1-3)–(4.1-7), we were not concerned with the composition of any of the streams.

These equations can easily be extended to represent an overall mass balance for component  $i$  in a multicomponent system. For the case shown in Fig.

4.1-3, we combine Eqs. (4.1-5), (4.1-6), and (4.1-7), add a generation term, and obtain

$$m_{i2} - m_{i1} + dM_i/dt = R_i \quad (4.1-8)$$

where  $m_{i2}$  is the mass flow rate of component  $i$  leaving the control volume, and  $R_i$  is the rate of generation of component  $i$  in the control volume in kg per unit time. (Diffusion fluxes are neglected here or are assumed to be negligible.) In some cases, of course,  $R_i = 0$  for no generation. Often, it is more convenient to use Eq. (4.1-8) written in molar units.

**EXAMPLE 4.1-2. Overall Mass Balance in Stirred Tank**

Initially, a tank holds 500 kg of salt solution containing 10% salt. At point (1) in the control volume in Fig. 4.1-5, a stream enters at a constant flow rate of 10 kg/h containing 20% salt. A stream leaves at point (2) at a constant rate of 5 kg/h. The tank is well stirred. Derive an equation relating the weight fraction  $w_A$  of the salt in the tank at any time  $t$  in hours.

**Solution:** First, we make a total mass balance using Eq. (4.1-7) for the net total mass efflux ( $[IN] - [OUT]$ ) from the control volume:

$$\int \rho \mathbf{v} \cdot \mathbf{n} dA = m_2 - m_1 = 5 - 10 = -5 \text{ kg solution/h} \quad (4.1-9)$$

The accumulation can be determined from Eq. (4.1-5),

where  $M$  is total kg of solution in control volume at time  $t$ ,

$$\frac{\partial}{\partial t} \int_V \rho \, dV = \frac{dM}{dt} \quad (4.1-5)$$

Substituting Eqs. (4.1-5) and (4.1-9) into (4.1-6), and then integrating,

$$-5 + \frac{dM}{dt} = 0 \quad M = 500 \quad \frac{dM}{dt} = 5 \quad t = 0 \quad \frac{dM}{dt} \quad (4.1-10)$$

$$M = 5t + 500 \quad (4.1-11)$$

Equation (4.1-11) relates the total mass  $M$  in the tank at any time to  $t$ .

Next, making a component  $A$  salt balance, let  $w_A$  = weight fraction of salt in the tank at time  $t$  and also the concentration in the stream  $m_2$  leaving at time  $t$ . Again, using Eq. (4.1-7) a species mass balance ( $[IN] - [OUT]$ ) can be expressed as,

$$\int_V \rho \cos \alpha \, dA = (5)w_A - 10(0.20) = 5w_A = -2 \text{ kg salt/h} \quad (4.1-12)$$

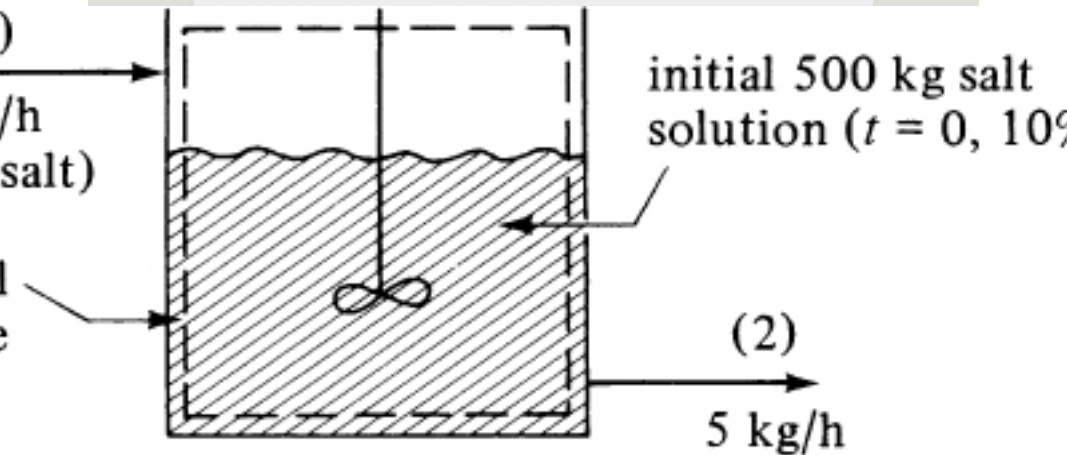


Figure 4.1-5. Control volume for flow in a stirred tank for Example 4.1-2.

Using Eq. (4.1-5) for a salt balance, the accumulation can be determined from

$$\frac{\partial}{\partial t} \int_V \rho \, dV = \frac{d}{dt} (Mw_A) = M \frac{dw_A}{dt} + w_A \frac{dM}{dt} \quad \text{salt/h} \quad (4.1-13)$$

Substituting Eqs. (4.1-12) and (4.1-13) into (4.1-6),

$$5w_A - 2 + M \frac{dw_A}{dt} + w_A \frac{dM}{dt} = 0 \quad (4.1-14)$$

Substituting the value for  $M$  from Eq. (4.1-11) into (4.1-14), separating variables, integrating, and solving for  $w_A$ ,

$$\begin{aligned} 5w_A - 2 + (500 + 5t) \frac{dw_A}{dt} \\ + w_A \frac{d(500 + 5t)}{dt} = 0 \end{aligned} \quad (4.1-15)$$

$$w_A = -0.1(100 + 100 + t)^2 + 0.20 \quad (4.1-16)$$

Note that Eq. (4.1-8) for component  $i$  could have been used for the salt balance with  $R_i = 0$  (no generation).

#### 4.1D Average Velocity to Use in Overall Mass Balance

In solving the case in Eq. (4.1-7), we assumed a constant velocity  $v_1$  at section 1 and constant velocity  $v_2$  at section 2. If the velocity is not constant but varies across the surface area, an average or bulk velocity is defined by

$$v_{av} = \frac{1}{A} \int \int A v \, dA \quad (4.1-17)$$

for a surface over which  $v$  is normal to  $A$  and the density  $\rho$  is assumed constant.

**EXAMPLE 4.1-3. Variation of Velocity Across Control Surface and Average Velocity**

For the case of incompressible flow ( $\rho$  is constant) through a circular pipe of radius  $R$ , the velocity profile is parabolic for laminar flow as follows:

$$v = v_{\max} [1 - (r/R)^2] \quad (4.1-18)$$

where  $v_{\max}$  is the maximum velocity at the center where  $r = 0$  and  $v$  is the velocity at a radial distance  $r$  from the center. Derive an expression for the average or bulk velocity  $v_{\text{av}}$  to use in the overall mass-balance equation.

**Solution:** The average velocity is represented by Eq. (4.1-17). In Cartesian coordinates,  $dA$  is  $dx dy$ . However, using polar coordinates, which are more appropriate for a pipe,  $dA = r dr d\theta$ , where  $\theta$  is the angle in polar coordinates. Substituting Eq. (4.1-18),  $dA = r dr d\theta$ , and  $A = \pi R^2$  into Eq. (4.1-17) and integrating,

$$\begin{aligned} v_{\text{av}} &= \frac{1}{\pi R^2} \int_0^{2\pi} \int_0^R v_{\max} [1 - (r/R)^2] r dr d\theta \\ &= \frac{v_{\max}}{\pi R^2} \int_0^{2\pi} \left[ \frac{R^2}{2} - \frac{r^3}{3} \right]_0^R d\theta \\ &= \frac{v_{\max}}{\pi R^2} \int_0^{2\pi} \left( \frac{R^2}{2} - \frac{R^3}{3} \right) d\theta \quad (4.1-19) \end{aligned}$$

$$v_{\text{av}} = \frac{v_{\max}}{2} \quad (4.1-20)$$

In this discussion, overall or macroscopic mass balances were made because we wish to describe these balances from outside the enclosure. In this section on overall mass balances,

some of the equations presented may have seemed quite obvious. However, the purpose was to develop the methods that should be helpful in the next sections. Overall balances will also be made on energy and momentum in the next sections. These overall balances do not tell us the details of what happens inside. However, in Section 4.4, a shell momentum balance will be made in order to obtain these details, which will give us the velocity distribution and pressure drop. To further study these details of the processes occurring inside the enclosure, differential balances rather than shell balances can be written; these are discussed later in Chapter 8 on differential equations of continuity and momentum transfer.

## **4.2 Overall Energy Balance**

## 4.2A Introduction

The second property to be considered in the overall balances on a control volume is energy. We shall apply the principle of the conservation of energy to a control volume fixed in space in much the same manner as the principle of conservation of mass was used to obtain the overall mass balance. The energy-conservation equation will then be combined with the first law of thermodynamics to obtain the final overall energy-balance equation.

We can write the first law of thermodynamics as

$$\Delta E = Q - W \quad (4.2-1)$$

where  $E$  is the total energy per unit mass of fluid,  $Q$  is the heat *absorbed* per unit mass of fluid, and  $W$  is the work of all kinds done per unit mass of fluid *upon* the surroundings. In the calculations, each term in the equation must be expressed in the same type of units, such as J/kg (SI), btu/lb<sub>m</sub>, or ft · lbf/lb<sub>m</sub> (English).

Since mass carries with it associated energy due to its position, motion, or physical state, we will find that each of these types of energy will appear in the energy balance. In addition, we can also transport energy across the boundary of the system without transferring mass.

#### **4.2B Derivation of Overall Energy-Balance Equation**

The overall balance for a conserved quantity such as energy is similar to



Eq. (4.1-3a) and Eq. (4.13b), and is as follows for a control volume:

$$[IN] - [CONSUMPTION] = [ACCUMULATION] \quad (4.1-3a)$$

$$\text{rate of entity output} - \text{rate of entity input} + \text{rate of entity accumulation} = 0 \quad (4.2-2)$$

The energy  $E$  present within a system can be classified in three ways:

1. *Potential energy*  $zg$  of a unit mass of fluid is the energy present because of the position of the mass in a gravitational field  $g$ , where  $z$  is the relative height in meters from a reference plane. The units for  $zg$  in the SI system are  $m \cdot m/s^2$ . Multiplying and dividing by kg mass, the units can be expressed as  $(kg \cdot m/s^2) \cdot (m/kg)$ , or J/kg. In English units, the potential energy is  $zg/g_c$  in  $ft \cdot lbf/lb_m$ .
2. *Kinetic energy*  $v^2/2$  of a unit mass of fluid is the energy present because of translational or rotational motion of the mass, where  $v$  is the velocity in m/s relative to the boundary of the system at a given point. Again, in the SI system, the units of  $v^2/2$  are J/kg. In the English system, the kinetic energy is  $v^2/2g_c$  in  $ft \cdot lbf/lb_m$ .

3. *Internal energy*  $U$  of a unit mass of a fluid is all of the other energy present, such as rotational and vibrational energy in chemical bonds. Again, the units are in J/kg or  $\text{ft} \cdot \text{lbf}/\text{lb}_m$ .

The total energy of the fluid per unit mass is then

$$E = U + \frac{v^2}{2} + zg \quad (\text{SI}) \quad E = U + \frac{v^2}{2g_c} + \frac{zg}{g_c} \quad (\text{English}) \quad (4.2-3)$$

The rate of accumulation of energy within the control volume  $V$  in Fig. 4.1-4 is

$$\text{accumulation in control volume} = \frac{\partial}{\partial t} \int_V (U + \frac{v^2}{2} + zg) \rho \, dV \quad (4.2-4)$$

Next, we consider the rate of energy input and output associated with mass in the control volume. The mass added or removed from the system carries internal, kinetic, and potential energy. In

addition, energy is transferred when mass flows into and out of the control volume. Net work is done by the fluid as it flows into and out of the control volume. This pressure–volume work per unit mass fluid is  $pV$ . The contribution of shear work is usually neglected. The  $pV$  term and  $U$  term are combined using the definition of enthalpy,  $H$ :

$$H=U+pV(4.2-5)$$

Hence, the total energy carried with a unit mass is  $(H + v^2/2 + zg)$ .

For a small area  $dA$  on the control surface in Fig. 4.1-4, the rate of energy efflux is  $(H + v^2/2 + zg)(\rho v)(dA \cos \alpha)$ , where  $(dA \cos \alpha)$  is the area  $dA$  projected in a direction normal to the velocity vector  $v$ , and  $\alpha$  is the angle

between the velocity vector  $\mathbf{v}$  and the outward-directed unit normal vector  $\mathbf{n}$ .

We now integrate this quantity over the entire control surface to obtain

$$(\text{net energy efflux from control volume}) = \iint_A (H + \frac{1}{2}v^2 + zg)(\rho v) \cos \alpha \, dA \quad (4.2-6)$$

Now, we have accounted for all energy associated with mass in the system and moving across the boundary in the energy balance, Eq. (4.2-2). Next, we take into account heat and work energy that transfers across the boundary and is not associated with mass. The term  $q$  is the heat transferred per unit time across the boundary to the fluid because of a temperature gradient. Heat absorbed by the system is positive by convention.

The work  $\dot{W}$ , which is energy per unit

time, can be divided into  $\dot{W}_S$ , purely mechanical shaft work identified with a rotating shaft crossing the control surface, and the pressure–volume work, which has been included in the enthalpy term  $H$  in Eq. (4.2-6). By convention, work done by the fluid upon the surroundings, that is, work out of the system, is positive.

To obtain the overall energy balance, we substitute Eqs. (4.2-4) and (4.2-6) into the entity balance Eq. (4.2-2) and equate the resulting equation to  $\dot{q} - \dot{W}_S$ :

$$\begin{aligned} \iint_A (H + v^2/2 + zg)(\rho v) \cos \alpha \, dA \\ + \partial/\partial t \iiint_V (U + v^2/2 + zg) \rho \, dV = \dot{q} - \dot{W}_S \end{aligned} \quad (4.2-7)$$

#### 4.2C Overall Energy Balance for a Steady-State Flow System

A common special case of the

overall or macroscopic energy balance is that of a steady-state system with one-dimensional flow across the boundaries, a single inlet, a single outlet, and negligible variation of height  $z$ , density  $\rho$ , and enthalpy  $H$  across either inlet or outlet area. This is shown in Fig. 4.2-1. To determine the overall energy balance for this system, we can consider the following: since the angle between the velocity vector and unit normal vector is  $\alpha = 0$  and since the accumulation term is 0 at steady state, Eq. 4.2-7 can be reduced to

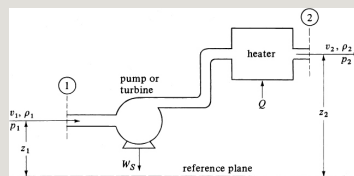


Figure 4.2-1. *Steady-state flow system for a fluid.*

$$\iint A(H + \frac{v^2}{2} + zg)(\rho v) dA = q - W \cdot S \quad (4.2-7a)$$

Integrating along the path of the fluid (from point 1 to point 2) yields the following expression:

$$H_2 m_2 - H_1 m_1 + m_2 (\frac{v_2^2}{2})_{av} - \frac{v_2^2}{2} m_2 - m_1 (\frac{v_1^2}{2})_{av} + \frac{v_1^2}{2} m_1 + g m_2 z_2 - g m_1 z_1 = q - W S \quad (4.2-8)$$

To arrive at this expression, it was necessary to integrate the kinetic-energy term. A derivation and explanation how this is performed is covered in the following section, 4.2D.

Note that for steady state,  $m_1 = \rho_1 v_1 A_1 = m_2 = m$ . Dividing through by  $m$  so that the equation is on a unit mass basis,

$$H_2 - H_1 + \frac{1}{2} [(v_2^2)_{av} - \frac{v_2^2}{2} - (\frac{v_1^2}{2})_{av} + \frac{v_1^2}{2}] + z_2 - z_1 = \frac{q}{g} - \frac{W}{g}$$

$$\frac{(v_3)_{av}}{2} + g(z_2 - z_1) = Q - WS \quad (\text{SI}) \quad (4.2-9)$$

The term  $(v_3)_{av}/(2v_{av})$  can be replaced by  $v_{2av}/2\alpha$ , where  $\alpha$  is the kinetic-energy velocity correction factor and is equal to  $v_{3av}/(v_3)_{av}$ . The term  $\alpha$  has been evaluated for various flows in pipes and is 12 for laminar flow and close to 1.0 for turbulent flow. Hence, Eq. (4.2-9) becomes

$$H_2 - H_1 + 12\alpha(v_{2av}^2 - v_{1av}^2) + g(z_2 - z_1) = Q - WS \quad (\text{SI})$$

$$H_2 - H_1 + 12\alpha g c(v_{2av}^2 - v_{1av}^2) + g g c(z_2 - z_1) = Q - WS \quad (\text{English})$$

$$(4.2-10)$$

Some useful conversion factors from Appendix A.1 are as follows:

$$1 \text{ hp} = 550 \text{ ft} \cdot \text{lbf} / \text{s} = 778.17 \text{ ft} \cdot \text{lbf} = 1055.06 \text{ J} = 1.05506 \text{ kJ}$$

$$1 \text{ ft} \cdot \text{lbf} / \text{lbm} = 2.9890 \text{ J} / \text{lbm}$$



$$1 \text{ kg} \cdot 1 \text{ N} \cdot \text{m} = 1 \text{ kg} \cdot \text{m}^2/\text{s}^2$$

#### 4.2D Kinetic-Energy Velocity Correction Factor $\alpha$

*1. Introduction.* In obtaining Eq. (4.2-8), it was necessary to integrate the kinetic-energy term

$$\text{kinetic energy} = \iint_A (v^2) (\rho v) \cos \alpha \, dA \quad (4.2-11)$$

that appeared in Eq. (4.2-7). To do this, we first take  $\rho$  as a constant and  $\cos \alpha = 1.0$ . Then, multiplying the numerator and denominator by  $v_{\text{av}} A$ , where  $v_{\text{av}}$  is the bulk or average velocity, and noting that  $m = \rho v_{\text{av}} A$ , Eq. (4.2-11) becomes

$$v_{\text{av}} A \iint_A (v^3) \, dA = m^2 v_{\text{av}} \frac{1}{A} \iint_A (v^3) \, dA \quad (4.2-12)$$

Dividing through by  $m$  so that Eq. (4.2-12) is on a unit mass basis,

$$\int_A (v^3) dA = (v^3)_{av} \int_A dA = (v^3)_{av} A = \alpha \int_A v^2 dA \quad (4.2-13)$$

where  $\alpha$  is defined as

$$\alpha = \frac{(v^3)_{av}}{\int_A v^2 dA} \quad (4.2-14)$$

and  $(v^3)_{av}$  is defined as follows:

$$(v^3)_{av} = \frac{1}{A} \int_A v^3 dA \quad (4.2-15)$$

The local velocity  $v$  varies across the cross-sectional area of a pipe. To evaluate  $(v^3)_{av}$  and, hence, the value of  $\alpha$ , we must have an equation relating  $v$  as a function of position in the cross-sectional area.

*2. Laminar flow.* In order to determine the value of  $\alpha$  for laminar flow, we first combine Eqs. (4.1-18) and (4.1-20) for laminar flow to obtain  $v$  as a function of position  $r$ :

$$v = 2v_{av} [1 - (r/R)^2] \quad (4.2-16)$$

Substituting Eq. (4.2-16) into (4.2-15) and noting that  $A = \pi R^2$  and  $dA = r \, dr \, d\theta$  (see Example 4.1-3), Eq. (4.2-15) becomes

$$\begin{aligned} (v^3)_{av} &= \frac{1}{\pi R^2} \int_0^{2\pi} \int_0^R [2v_{av}(1 - r^2/R^2)]^3 r \, dr \, d\theta \\ &= (2\pi) \frac{2^3 v_{av}^3}{3\pi R^2} \int_0^R (R^2 - r^2)^3 R^6 r \, dr \\ &= 16v_{av}^3 \frac{8}{8} \int_0^R (R^2 - r^2)^3 r \, dr \quad (4.2-17) \end{aligned}$$

Integrating Eq. (4.2-17) and rearranging,

$$\begin{aligned} (v^3)_{av} &= 16v_{av}^3 \frac{8}{8} \int_0^R (R^6 - 3r^2 R^4 + 3r^4 R^2 - r^6) r \, dr \\ &= 2v_{av}^3 (4.2-18) \end{aligned}$$

Substituting Eq. (4.2-18) into (4.2-14),

$$\alpha = v_{av}^3 (v^3)_{av} = v_{av}^3 2v_{av}^3 = 0.50 \quad (4.2-19)$$

Hence, for laminar flow the value of  $\alpha$  to

use in the kinetic-energy term of Eq. (4.2-10) is 0.50.

3. *Turbulent flow.* For turbulent flow, a relationship is needed between  $v$  and position. This can be approximated by the following expression:

$$v = v_{\max} (R - r/R)^{1/7} \quad (4.2-20)$$

where  $r$  is the radial distance from the center. Eq. (4.2-20) is substituted into Eq. (4.2-15) and the resultant integrated to obtain the value of  $(v^3)_{\text{av}}$ . Next, Eq. (4.2-20) is substituted into Eq. (4.1-17) and this equation integrated to obtain  $v_{\text{av}}$  and  $(v_{\text{av}})^3$ . Combining the results for  $(v^3)_{\text{av}}$  and  $(v_{\text{av}})^3$  into Eq. (4.2-14), the value of  $\alpha$  is 0.945 (see Problem 4.2-1 for the solution). The value of  $\alpha$  for turbulent flow varies from about 0.90 to

0.99. In most cases (except for precise work), the value of  $\alpha$  is taken to be 1.0.

#### **4.2E Applications of the Overall Energy-Balance Equation**

The total energy balance, Eq. (4.2-10), in the form given is not often used when appreciable enthalpy changes occur or appreciable heat is added (or subtracted), since the kinetic- and potential-energy terms are usually small and can be neglected. As a result, when appreciable heat is added or subtracted, or large enthalpy changes occur, the methods for performing heat balances described in Section 1.7B are generally used. Examples will be given to illustrate this and other cases.

**EXAMPLE 4.2-1. Energy Balance on a Steam Boiler**

Water enters a boiler at 18.33°C and 137.9 kPa through a pipe at an average velocity of 1.52 m/s. Exit steam at a height of 15.2 m above the liquid inlet leaves at 137.9 kPa, 148.9°C, and 9.14 m/s in the outlet line. At steady state, how much heat must be added per kg mass of steam? The flow in the two pipes is turbulent.

**Solution:** The process flow diagram is shown in Fig. 4.2-2. Rearranging Eq. (4.2-10) and setting  $\alpha = 1$  for turbulent flow and  $Ws = 0$  (no external work),

$$Q = (z_2 - z_1)g + v_2^2 - v_1^2 + (H_2 - H_1) \quad (4.2-21)$$

To solve for the kinetic-energy terms,

$$v_1^2 = (1.52)^2 = 2.31 \text{ J/kg} \quad v_2^2 = (9.14)^2 = 83.5 \text{ J/kg}$$

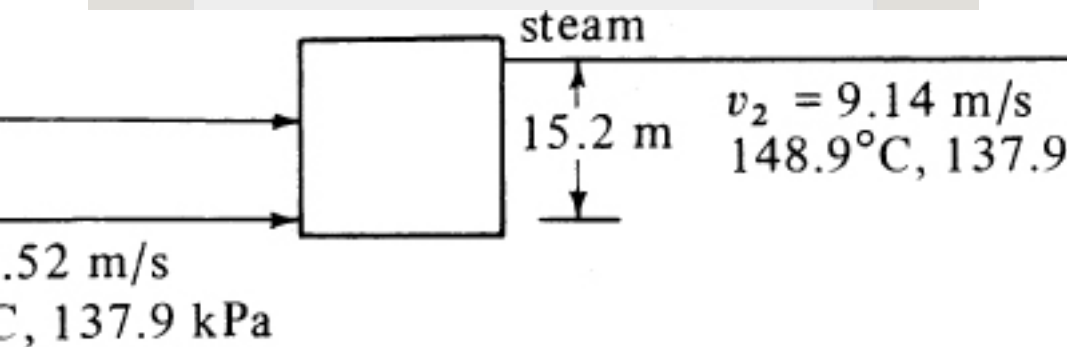


Figure 4.2-2. Process flow diagram for Example 4.2-1.

Taking the datum height  $z_1$  at point 1,  $z_2 = 15.2$  m. Then,

$$z_2 g = (15.2)(9.80665) = 149.1 \text{ J/kg}$$

From Appendix A.2, steam tables in SI units,  $H_1$  at 18.33°C = 76.97 kJ/kg,  $H_2$  of superheated steam at 148.9°C = 2771.4 kJ/kg, and

$$H_2 - H_1 = 2771.4 - 76.97 = 2694.4 \text{ kJ/kg} = 2.694 \times 10^6 \text{ J/kg}$$

Substituting these values into Eq. (4.2-21),

$$Q = (149.1 - 0) + (41.77 - 1.115) + 2.694 \times 106 Q = 189.75 + 2.694 \times 106 = 2.6942 \times 106 \text{ J/kg}$$

Hence, the kinetic-energy and potential-energy terms totaling 189.75 J/kg are negligible compared to the enthalpy change of water. This 189.75 J/kg would raise the temperature of liquid water about 0.0453°C, a negligible amount.

#### **EXAMPLE 4.2-2. Energy Balance in a Flow Calorimeter**

A flow calorimeter is being used to measure the enthalpy of steam. The calorimeter, which is a horizontal insulated pipe, consists of an electric heater immersed in a fluid flowing at steady state. Liquid water at 0°C at a rate of 0.3964 kg/min enters the calorimeter at point 1. The liquid is vaporized completely by the heater, where 19.63 kW is added, and steam leaves point 2 at 250°C and 150 kPa absolute. Calculate the exit enthalpy  $h_2$  of the steam if the liquid enthalpy at 0°C is set arbitrarily as 0. The kinetic-energy changes are small and can be neglected. (It will be assumed that pressure has a negligible effect on the enthalpy of the liquid.)

**Solution:** The process flow diagram is shown in Figure 4.2-3. For this case,  $W_s = 0$  since there is no shaft work between points 1 and 2. Also,  $(v_2^2/2\alpha - v_1^2/2\alpha) = 0$  and  $g(z_2 - z_1) = 0$ . For steady state,  $m_1 = m_2 = 0.3964/60 = 6.607 \times 10^{-3} \text{ kg/s}$ . Since heat is added to the system,

$$Q = 19.63 \text{ kJ/s} / 6.607 \times 10^{-3} \text{ kg/s} = 2971 \text{ kJ/kg}$$

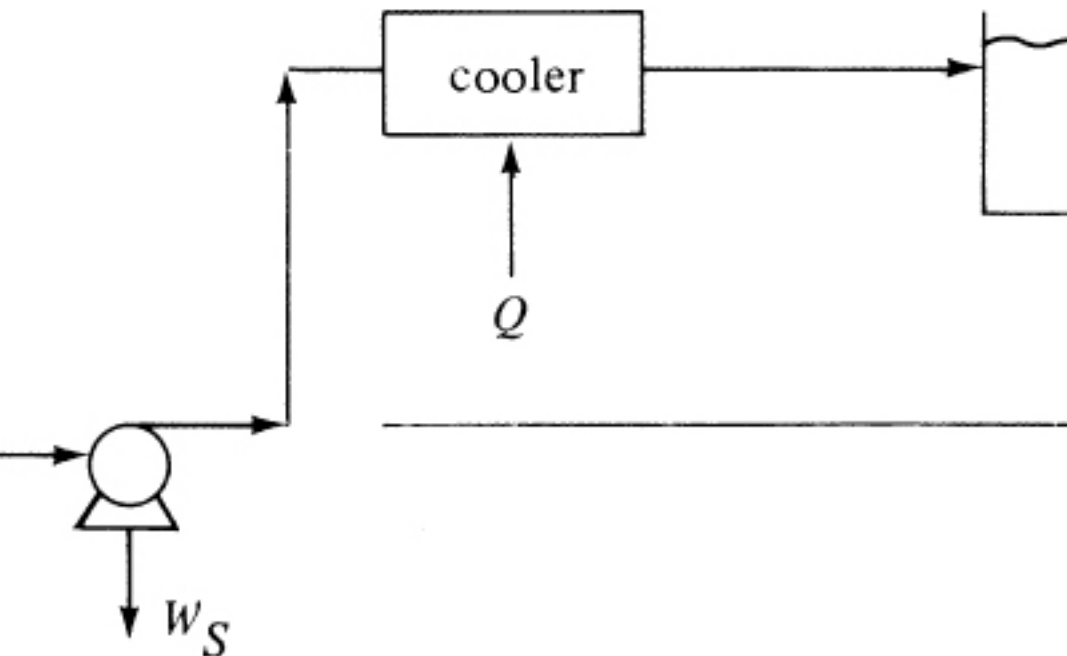


Figure 4.2-3. *Process flow diagram for energy balance for Example 4.2-2.*

The value of  $H_1 = 0$ . Equation (4.2-10) becomes

$$H_2 - H_1 + 0 + 0 = Q - 0$$

The final equation for the calorimeter is

$$H_2 = Q + H_1 \quad (4.2-22)$$

Substituting  $Q = 2971 \text{ kJ/kg}$  and  $H_1 = 0$  into Eq. (4.2-22),  $H_2 = 2971 \text{ kJ/kg}$  at  $250^\circ\text{C}$  and  $150 \text{ kPa}$ , which is close to the value from the steam table of  $2972.7 \text{ kJ/kg}$ .

## 4.2F Overall Mechanical-Energy Balance

A more useful type of energy balance for flowing fluids, especially



liquids, is a modification of the total energy balance to deal with mechanical energy. Engineers are often concerned with this special type of energy, called *mechanical energy*, which includes the work term, kinetic energy, potential energy, and the flow work part of the enthalpy term. Mechanical energy is a form of energy that is either work or a form that can be directly converted into work. The other terms in the energy-balance equation (4.2-10), heat terms and internal energy, do not permit simple conversion into work because of the second law of thermodynamics and the efficiency of conversion, which depends on the temperatures. Mechanical-energy terms have no such limitation and can be converted

almost completely into work. Energy converted to heat or internal energy is lost work or a loss in mechanical energy caused by frictional resistance to flow.

It is convenient to write an energy balance in terms of this loss,  $\Sigma F$ , which is the sum of all frictional losses per unit mass. For the case of steady-state flow, when a unit mass of fluid passes from inlet to outlet, the batch work done by the fluid,  $W'$ , is expressed as

$$W' = \int V_1 V_2 p \, dV - \Sigma F \quad (\Sigma F > 0) \quad (4.2-23)$$

This work  $W'$  differs from the  $W$  of Eq. (4.2-1), which also includes kinetic- and potential-energy effects. Writing the first law of thermodynamics for this case,

where  $\Delta E$  becomes  $\Delta U$ ,

$$\Delta U = Q - W' \quad (4.2-24)$$

The equation defining enthalpy, Eq. (4.2-5), can be written as

$$\Delta H = \Delta U + \Delta pV = \Delta U + \int_{V_1}^{V_2} p \, dV + \int_{p_1}^{p_2} V \, dp \quad (4.2-25)$$

Substituting Eq. (4.2-23) into (4.2-24) and then combining the resultant with Eq. (4.2-25), we obtain

$$\Delta H = Q + \Sigma F + \int_{p_1}^{p_2} V \, dp \quad (4.2-26)$$

Finally, we substitute Eq. (4.2-26) into (4.2-10) and  $1/\rho$  for  $V$ , to obtain the overall mechanical-energy-balance equation:

$$12\alpha[v_2^2 - v_1^2] + g(z_2 -$$

$$z_1) + \int p_1 p_2 dp + \Sigma F + WS = 0 \quad (4.2-27)$$

For English units, the kinetic- and potential-energy terms of Eq. (4.7-27) are divided by  $g_c$ .

The value of the integral in Eq. (4.2-27) depends on the equation of state of the fluid and the path of the process. If the fluid is an incompressible liquid, the integral becomes  $(p_2 - p_1)/\rho$  and Eq. (4.2-27) becomes

$$\frac{1}{2} \alpha (v_2^2 - v_1^2) + g(z_2 - z_1) + \frac{p_2 - p_1}{\rho} + \Sigma F + WS = 0 \quad (4.2-28)$$

**EXAMPLE 4.2-3. Mechanical-Energy Balance on a Pumping System**

Water with a density of 998 kg/m<sup>3</sup> is flowing at a steady mass flow rate through a uniform-diameter pipe. The entrance pressure of the fluid is 68.9 kN/m<sup>2</sup> abs in the pipe, which connects to a pump that actually supplies 155.4 J/kg of fluid flowing in the pipe. The exit pipe from the pump is the same diameter as the inlet pipe. The exit section of the pipe is 3.05 m higher than the entrance, and the exit pressure is 137.8 kN/m<sup>2</sup> abs. The Reynolds number in the pipe is above 4000 in the system. Calculate the frictional

loss  $\Sigma F$  in the pipe system.

**Solution:** First, a flow diagram of the system is drawn (Fig. 4.2-4), with 155.4 J/kg mechanical energy added to the fluid. Hence,  $W_s = -155.4$ , since the work done by the fluid is positive.

Setting the datum height,  $z_1 = 0$ ,  $z_2 = 3.05$  m. Since the pipe is of constant diameter,  $v_1 = v_2$ . Also, for turbulent flow  $\alpha = 1.0$  and

$$12(1)(v_2^2 - v_1^2) = 0$$

$$z_2 g = (3.05 \text{ m})(9.806 \text{ m/s}^2) = 29.9 \text{ J/kg}$$

Since the liquid can be considered incompressible, Eq. (4.2-28) is used:

$$p_1 = 68.9 \times 1000998 = 69.0 \text{ J/kg}$$

$$p_2 = 137.8 \times 1000998 = 138.0 \text{ J/kg}$$

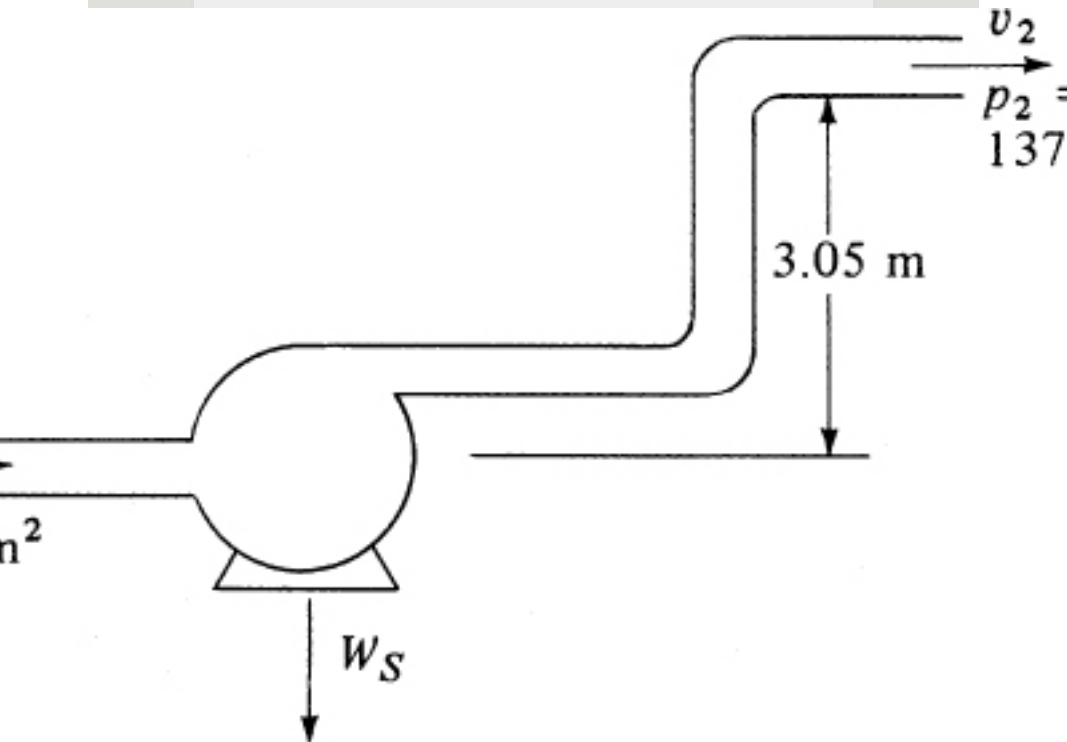


Figure 4.2-4. Process flow diagram for Example 4.2-3.

Using Eq. (4.2-28) and solving for  $\Sigma F$ , the frictional losses,

$$\Sigma F = -WS + 12\alpha(v_1^2 - v_2^2) + g(z_1 - z_2) + p_1 - p_2 \quad (4.2-29)$$

Substituting the known values, and solving for the frictional losses,

$$\Sigma F = -(-155.4) + 0 - 29.9 + 69.0 - 138.0 = 56.5 \text{ J/kg} \quad (18.9 \text{ ft-lbf/lbm})$$

#### **EXAMPLE 4.2-4. Pump Horsepower in a Flow System**

A pump draws 69.1 gal/min of a liquid solution having a density of 114.8 lb<sub>m</sub>/ft<sup>3</sup> from an open storage feed tank with a large cross-sectional area through a 3.068-in.-ID suction line. The pump discharges its flow through a 2.067-in.-ID line to an open overhead tank. The end of the discharge line is 50 ft above the level of the liquid in the feed tank. The friction losses in the piping system are  $\Sigma F = 10.0$  ft-lb force/lb mass. What pressure must the pump develop and what is the horsepower of the pump if its efficiency is 65% ( $\eta = 0.65$ )? The flow is turbulent.

**Solution:** First, a flow diagram of the system is drawn (Fig. 4.2-5). Equation (4.2-28) will be used. The term  $Ws$  in Eq. (4.2-28) becomes

$$WS = -\eta W_p \quad (4.2-30)$$

where  $-Ws$  = mechanical energy actually delivered to the fluid by the pump or net mechanical work,  $\eta$  = fractional efficiency, and  $W_p$  is the energy or shaft work delivered to the pump.

From Appendix A.5, the cross-sectional area of the 3.068-in. pipe is 0.05134 ft<sup>2</sup> and of the 2.067-in. pipe, 0.0233 ft<sup>2</sup>. The flow rate is

$$\begin{aligned} \text{flow rate} &= (69.1 \text{ gal/min})(1 \text{ min}/60 \text{ s}) \\ (1 \text{ ft}^3/7.481 \text{ gal}) &= 0.1539 \text{ ft}^3/\text{s} \quad v_2 = (0.1539 \text{ ft}^3/\text{s}) \\ &\quad (0.0233 \text{ ft}^2) = 6.61 \text{ ft/s} \end{aligned}$$

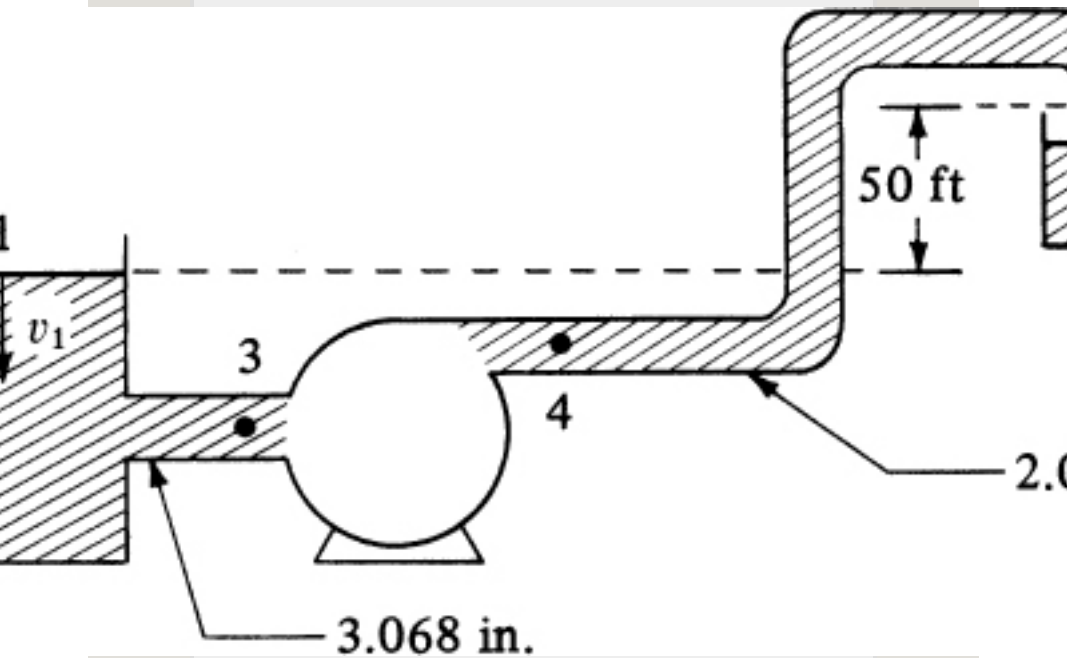


Figure 4.2-5. Process flow diagram for Example 4.2-4.

$v_1 = 0$ , since the tank is very large. Then,  $v_1^2/2gc = 0$ . The pressure  $p_1 = 1 \text{ atm}$  and  $p_2 = 1 \text{ atm}$ . Also,  $\alpha = 1.0$  since the flow is turbulent. Hence,

$$p_1 \rho - p_2 \rho = 0 + \frac{v_2^2}{2gc} = (6.61)^2 / (2 \cdot 32.174) = 0.678 \text{ ft} \cdot \text{lb} / \text{ft}^3 \cdot \text{bm}$$

Using the datum of  $z_1 = 0$ , we have

$$z_2 \rho = (50.0) \cdot 32.174 = 1608.7 \text{ ft} \cdot \text{lb} / \text{ft}^3 \cdot \text{bm}$$

Using Eq. (4.2-28), solving for  $W_s$ , and substituting the known values,

$$\begin{aligned} W_s &= z_1 \rho - z_2 \rho + \frac{v_1^2}{2gc} - \frac{v_2^2}{2gc} + p_1 \rho - p_2 \rho \\ \Sigma F &= 0 - 1608.7 + 0 - 0.678 + 0 = -1609.4 \text{ ft} \cdot \text{lb} / \text{ft}^3 \cdot \text{bm} \end{aligned}$$

Using Eq. (4.2-30) and solving for  $W_p$ ,

$$W_p = -$$

$$\begin{aligned} W_s \eta &= 1609.4 \text{ ft} \cdot \text{lb} / \text{ft}^3 \cdot \text{bm} = 93.3 \text{ ft} \cdot \text{lb} / \text{ft}^3 \cdot \text{bm} \\ \text{mass flow rate} &= (0.1539 \text{ ft}^3 / \text{s}) \\ &= (114.81 \text{ lb} / \text{ft}^3) = 17.65 \text{ lb} / \text{s} \\ \text{pump horsepower} &= (17.65 \text{ lb} / \text{s}) \\ &= (93.3 \text{ ft} \cdot \text{lb} / \text{ft}^3 \cdot \text{bm}) (1 \text{ hp} / 550 \text{ ft} \cdot \text{lb} / \text{s}) = 3.00 \text{ hp} \end{aligned}$$

To calculate the pressure the pump must develop, Eq.

(4.2-28) must be written over the pump itself between points 3 and 4 as shown on the diagram:

$$v_3 = (0.1539 \text{ ft}^3/\text{s}) / (10.05134 \text{ ft}^2) = 3.00 \text{ ft/s} \quad v_4 = v_3 = 3.00 \text{ ft/s}$$

Since the difference in level between  $z_3$  and  $z_4$  of the pump itself is negligible, it will be neglected. Rewriting Eq.

(4.2-28) between points 3 and 4 and substituting known values ( $\Sigma F = 0$ , since frictional losses through the pump are handled by the efficiency term),

$$\begin{aligned} p_4 - p_3 &= \rho(z_3 - z_4) + \frac{\rho}{2}(v_3^2 - v_4^2) - \rho \sum F \\ &= 0 + (3.00)^2(32.174) - \\ &= (6.61)^2(32.174) + 60.678 - 0 = 0 + 0.140 - 0.678 + 60.678 = 60.14 \text{ ft} \cdot \text{lbf/lbm} \\ p_3 &= (60.14 \text{ ft} \cdot \text{lbf/lbm}) (114.81 \text{ lbm/ft}^3) (1/144 \text{ in}^2/\text{ft}^2) = 48.0 \text{ lb force/in}^2 \\ &= 48.0 \text{ psia (pressure developed by pump)} \quad (331 \text{ kPa}) \end{aligned}$$

## 4.2G Bernoulli Equation for Mechanical-Energy Balance

In the special case where no mechanical energy is added ( $W_s = 0$ ) and for no friction ( $\Sigma F = 0$ ), then Eq. (4.2-28) becomes the Bernoulli equation, Eq. (4.2-32), for turbulent flow, which is of sufficient importance to deserve further discussion:

$$\begin{aligned} z_1 g + \frac{v_1^2}{2} + \frac{p_1}{\rho} &= z_2 g + \frac{v_2^2}{2} + \frac{p_2}{\rho} \quad (4.2-32) \end{aligned}$$



This equation covers many situations of practical importance and is often used in conjunction with the mass-balance equation (4.2-2) for steady state:

$$m = \rho_1 A_1 v_1 = \rho_2 A_2 v_2 \quad (4.1-2)$$

Several examples of its use will be given.

**EXAMPLE 4.2-5. Rate of Flow from Pressure Measurements**

A liquid with a constant density  $\rho$  kg/m<sup>3</sup> is flowing at an unknown velocity  $v_1$  m/s through a horizontal pipe of cross-sectional area  $A_1$  m<sup>2</sup> at a pressure  $p_1$  N/m<sup>2</sup>, and then it passes to a section of the pipe in which the area is reduced gradually to  $A_2$  m<sup>2</sup> and the pressure is  $p_2$ . Assuming no friction losses, calculate the velocities  $v_1$  and  $v_2$  if the pressure difference ( $p_1 - p_2$ ) is measured.

**Solution:** In Fig. 4.2-6, the flow diagram is shown with pressure taps to measure  $p_1$  and  $p_2$ . From the mass-balance continuity equation (4.1-2), for constant  $\rho$  where  $\rho_1 = \rho_2 = \rho$ ,

$$v_2 = v_1 A_1 / A_2 \quad (4.2-33)$$

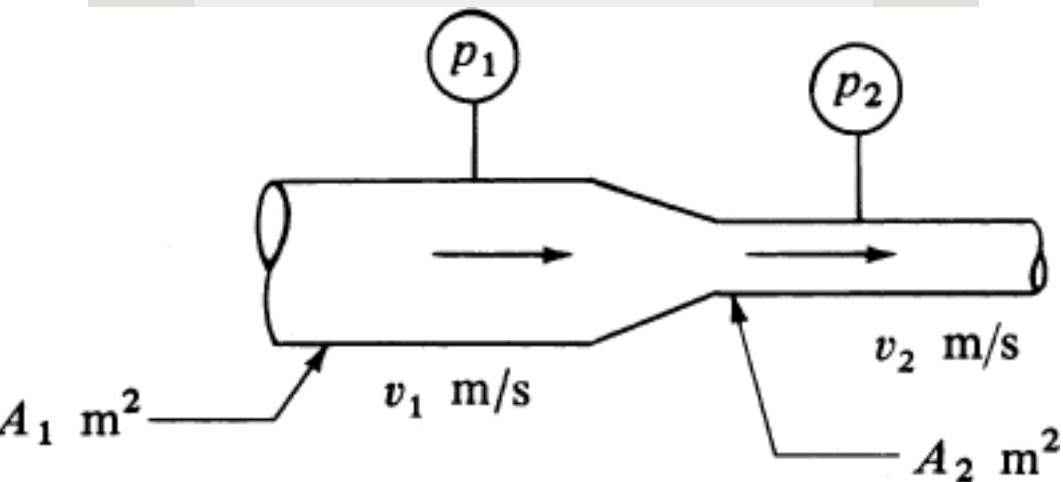


Figure 4.2-6. Process flow diagram for Example 4.2-5.

For the items in the Bernoulli equation (4.2-32) for a horizontal pipe,

$$z_1 = z_2 = 0$$

Then, Eq. (4.2-32) becomes, after substituting Eq. (4.2-33) for  $v_2$ ,

$$0 + v_1^2/2 + p_1/\rho = 0 + v_1^2 A_1^2 / A_2^2 + p_2/\rho \quad (4.2-34)$$

Rearranging,

$$p_1 - p_2 = \rho v_1^2 [(A_1/A_2)^2 - 1] \quad (4.2-35)$$

$$v_1 = \sqrt{\frac{p_1 - p_2}{\rho [(A_1/A_2)^2 - 1]}} \quad (4.2-36)$$

Performing the same derivation but in terms of  $v_2$ ,

$$v_2 = \sqrt{\frac{p_1 - p_2}{\rho [1 - (A_2/A_1)^2]}} \quad (4.2-37)$$

#### EXAMPLE 4.2-6. Rate of Flow from a Nozzle in a Tank

A nozzle of cross-sectional area  $A_2$  is discharging to the atmosphere and is located in the side of a large tank, in

which the open surface of the liquid in the tank is  $H$  m above the center line of the nozzle. Calculate the velocity  $v_2$  in the nozzle and the volumetric rate of discharge if no friction losses are assumed.

**Solution:** The nozzle flow is shown in Fig. 4.2-7, with point 1 taken in the liquid at the entrance to the nozzle and point 2 at the exit of the nozzle.

Since  $A_1$  is very large compared to  $A_2$ ,  $v_1 \cong 0$ . The pressure  $p_1$  is greater than 1 atm (101.3 kN/m<sup>2</sup>) by the head of fluid of  $H$  m. The pressure  $p_2$ , which is at the nozzle exit, is at 1 atm. Using point 2 as a datum,  $z_2 = 0$  and  $z_1 = 0$  m. Rearranging Eq. (4.2-32),

$$z_1 g + v_1^2/2 + p_1/\rho = z_2 g + v_2^2/2 + p_2/\rho \quad (4.2-38)$$

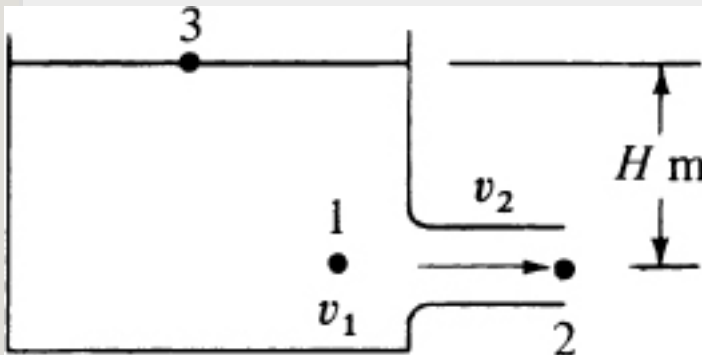


Figure 4.2-7. Nozzle flow diagram for Example 4.2-6.

Substituting the known values,

$$0 + 0 + p_1/\rho - p_2/\rho = 0 + v_2^2/2 \quad (4.2-39)$$

Solving for  $v_2$ ,

$$v_2 = \sqrt{2(p_1 - p_2)/\rho} \quad \text{m/s} \quad (4.2-40)$$

Since  $p_1 - p_2 = H\rho g$  and  $p_2 = p_3$  (both at 1 atm),

$$H = v_2^2 / 2g \quad \text{m} \quad (4.2-41)$$

where  $H$  is the head of liquid with density  $\rho$ . Then, Eq. (4.2-40) becomes

$$v^2 = 2gH \quad (4.2-42)$$

The volumetric flow rate is

$$\text{flow rate} = vA \quad \text{m}^3/\text{s} \quad (4.2-43)$$

To illustrate the fact that different points can be used in the balance, points 3 and 2 will be used. Writing Eq. (4.2-32),

$$z_2 g + \frac{v_2^2}{2} + \frac{p_2}{\rho} = z_3 g + \frac{v_3^2}{2} + \frac{p_3}{\rho} \quad (4.2-44)$$

Since  $p_2 = p_3 = 1 \text{ atm}$ ,  $v_3 = 0$ , and  $z_2 = 0$ ,

$$v^2 = 2gz_3 = 2gH \quad (4.2-45)$$

## 4.3 Overall Momentum Balance

### 4.3A Derivation of the General Equation

A momentum balance can be written for the control volume shown in Fig. 4.1-3, which is somewhat similar to the overall mass-balance equation. Momentum, in contrast to mass and energy, is a vector quantity. The total linear momentum vector  $\mathbf{P}$  of the total mass  $M$  of a moving fluid having a velocity of  $\mathbf{v}$  is

$$P=Mv(4.3-1)$$

The term  $Mv$  is the momentum of this moving mass  $M$  enclosed at a particular instant in the control volume shown in Fig. 4.1-4. The units of  $Mv$  are  $\text{kg} \cdot \text{m/s}$  in the SI system.

Starting with Newton's second law, we will develop the integral momentum-balance equation for linear momentum. Angular momentum will not be considered here. Newton's second law may be stated: The time rate of change of momentum of a system is equal to the summation of all forces acting on the system and takes place in the direction of the net force:

$$\sum F = dP/dt = dMv/dt(4.3-2)$$

where  $F$  is force. In the SI system,  $F$  is

in newtons (N) and  $1 \text{ N} = 1 \text{ kg} \cdot \text{m/s}^2$ .

Note that in the SI system,  $g_c$  is not needed, but it is needed in the English system.

The equation for the conservation of momentum with respect to a control volume can be written as follows:

$$\text{accumulation of momentum in control volume} = \sum \text{momentum in} - \sum \text{momentum out} + \sum \text{momentum generated} \quad (4.3-3)$$

This is in the same form as the general mass-balance equation (4.1-3), with the sum of the forces as the generation rate term. Hence, momentum is not conserved, since it is generated by external forces on the system. If external forces are absent, momentum is conserved.

Using the general control volume shown

in Fig. 4.1-4, we shall evaluate the various terms in Eq. (4.3-3), using methods very similar to the development of the general mass balance. For a small element of area  $dA$  on the control surface, we write

$$\text{rate of momentum efflux} = v(\rho v) (dA \cos \alpha) \quad (4.3-4)$$

Note that the rate of mass efflux is  $(\rho v) (dA \cos \alpha)$ . Also, note that  $(dA \cos \alpha)$  is the area  $dA$  projected in a direction normal to the velocity vector  $v$ , and  $\alpha$  is the angle between the velocity vector  $v$  and the outward-directed-normal vector  $n$ . From vector algebra, the product in Eq. (4.3-4) becomes

$$v(\rho v)(dA \cos \alpha) = \rho v(v \cdot n) dA \quad (4.3-5)$$

Integrating over the entire control

surface  $A$ ,

$$\text{me}) = \iint A v(\rho v) \cos \alpha \, dA = \iint A \rho v(v \cdot n) \, dA \quad (4.3-6)$$

The net efflux represents the first two terms on the right-hand side of Eq. (4.3-3).

Similarly to Eq. (4.1-5), the rate of accumulation of linear momentum within the control volume  $V$  is

$$\text{in control volume}) = \frac{\partial}{\partial t} \int \int_V \rho v \, dV \quad (4.3-7)$$

Substituting Equations (4.3-2), (4.3-6), and (4.3-7) into (4.3-3), the overall linear momentum balance for a control volume becomes

$$\begin{aligned} \sum F = & \int \int A \rho v(v \cdot n) \, dA \\ & + \frac{\partial}{\partial t} \int \int_V \rho v \, dV \end{aligned} \quad (4.3-8)$$



We should note that  $\Sigma \mathbf{F}$  in general may have a component in any direction, and that  $\mathbf{F}$  is the force the surroundings exert on the control-volume fluid. Since Eq. (4.3-8) is a vector equation, we may write the component scalar equations for the  $x$ ,  $y$ , and  $z$  directions:

$$\begin{aligned} \Sigma F_x = & \int \int A v_x \rho v \cos \alpha \, dA \\ & + \frac{\partial}{\partial t} \int V \rho v_x \, dV \text{ (SI)} \\ & + \frac{\partial}{\partial t} \iiint V \rho g c v_x \, dV \text{ (English)} \end{aligned} \quad (4.3-9)$$

$$\begin{aligned} \Sigma F_y = & \iiint A v_y \rho v \cos \alpha \, dA \\ & + \frac{\partial}{\partial t} \iiint V \rho v_y \, dV \end{aligned} \quad (4.3-10)$$

$$\begin{aligned} \Sigma F_z = & \int \int A v_z \rho v \cos \alpha \, dA \\ & + \frac{\partial}{\partial t} \int \int V \rho v_z \, dV \end{aligned} \quad (4.3-11)$$

The force term  $\Sigma F_x$  in Eq. (4.3-9) is composed of the sum of several forces. These are given as follows:

1. *Body force.* The body force  $F_{xg}$  is the  $x$ -directed force caused by gravity acting on the total mass  $M$  in the control volume. This force,  $F_{xg}$ , is  $Mg_x$ . It is zero if the  $x$  direction is horizontal.
2. *Pressure force.* The force  $F_{xp}$  is the  $x$ -directed force caused by the pressure forces acting on the surface of the fluid system. When the control surface cuts through the fluid, the pressure is taken to be directed inward and perpendicular to the surface. In some cases, part of the control surface may be a solid, and this wall is included inside the control surface. Then, there is a contribution to  $F_{xp}$  from the pressure on the outside of this wall, which typically is atmospheric pressure. If gage pressure is used, the integral of the constant external pressure over the entire outer surface can be automatically ignored.
3. *Friction force.* When the fluid is flowing, an  $x$ -directed shear or friction force  $F_{xs}$  is present, which is exerted on the fluid by a solid wall when the control surface cuts between the fluid and the solid wall. In some or many cases, this frictional force may be negligible compared to the other forces and is neglected.
4. *Solid surface force.* In cases where the control surface cuts through a solid, there is present force  $R_x$ , which is the  $x$  component of the resultant of the forces acting on the control volume at these points. This occurs typically when the control volume includes a section of pipe and the fluid it contains. This is the force exerted by the solid surface on the fluid.

The force terms of Eq. (4.3-9) can then be represented as

$$\sum F_x = F_{xg} + F_{xp} + F_{xs} + R_x \quad (4.3-12)$$

Similar equations can be written for the  $y$  and  $z$  directions. Then, Eq. (4.3-9) becomes, for the  $x$  direction,

$$\begin{aligned} \sum F_x = & F_{xg} + F_{xp} + F_{xs} \\ & + R_x = \int \int A v_x p \cos \alpha \, dA \\ & + \frac{\partial}{\partial t} \int \int V \int \rho v_x \, dV \end{aligned} \quad (4.3-13)$$

#### **4.3B Overall Momentum Balance in a Flow System in One Direction**

A quite common application of the overall momentum-balance equation is the case of a section of a conduit with its axis in the  $x$  direction. The fluid will be assumed to be flowing at steady state in the control volume shown in Fig. 4.3-1 and in Fig.

4.1-3. Since  $v = v_x$ , Eq. (4.3-13) for the  $x$  direction becomes as follows:

$$\begin{aligned} \sum F_x = & F_{xg} + F_{xp} + F_{xs} \\ + R_x = & \int \int A v_x p v_x \cos \alpha \, dA \end{aligned} \quad (4.3-14)$$

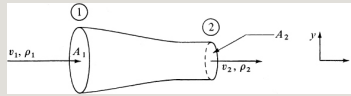


Figure 4.3-1. Flow through a horizontal nozzle in the  $x$  direction only.

Integrating, with  $\cos \alpha = \pm 1.0$  and  $\rho A = m/v_{av}$ ,

$$\begin{aligned} & F_{xg} + F_{xp} + F_{xs} \\ + R_x = & m(v_{x2})_{av} v_{x2} - \\ & m(v_{x1})_{av} v_{x1} \end{aligned} \quad (4.3-15)$$

where, if the velocity is not constant and varies across the surface area,

$$(v_{x2})_{av} = \frac{1}{A} \int \int A v_{x2} \, dA \quad (4.3-16)$$

The ratio  $(v_x^2)_{av}/v_{x\ av}$  is replaced by  $\beta v_{x\ av}$  where  $\beta$ , which is the momentum velocity correction factor, has a value of 1.00 to 1.10 for turbulent flow and 4/3 for laminar flow. For most applications in turbulent flow,  $(v_x^2)_{av}/v_{x\ av}$  is replaced by  $v_{x\ av}$ , the average bulk velocity. Note that the subscript  $x$  on  $v_x$  and  $F_x$  can be dropped, since  $v_x = v$  and  $F_x = F$  for one-directional flow.

The term  $F_{xp}$ , which is the force caused by the pressures acting on the surface of the control volume, is

$$F_{xp} = p_1 A_1 - p_2 A_2 \quad (4.3-17)$$

The friction force will be neglected in Eq. (4.3-15), so  $F_{xs} = 0$ . The body force  $F_{xg} = 0$  since gravity is acting only in the  $y$  direction. Substituting  $F_{xp}$  from

Eq. (4.3-17) into (4.3-15), replacing  $(v_x^2)_{av}/v_{x\ av}$  by  $\beta v$  (where  $v_{x\ av} = v$ ), setting  $\beta = 1.0$ , and solving for  $R_x$  in Eq. (4.3-15),

$$R_x = mv^2 - mv_1 + p_2 A_2 - p_1 A_1 \quad (4.3-18)$$

where  $R_x$  is the force exerted by the solid on the fluid. The force of the fluid on the solid (reaction force) is the negative of this, or  $-R_x$ .

**EXAMPLE 4.3-1. Momentum Velocity Correction Factor  $\beta$  for Laminar Flow**

The momentum velocity correction factor  $\beta$  is defined as follows for flow in one direction, where the subscript  $x$  is dropped:

$$(v^2)_{av} v_{av} = \beta v_{av}^2 \quad (4.3-19)$$

$$\beta = (v^2)_{av} / (v_{av})^2 \quad (4.3-20)$$

Determine  $\beta$  for laminar flow in a tube.

**Solution:** Using Eq. (4.3-16),

$$(v^2)_{av} = \frac{1}{A} \int_A v^2 dA \quad (4.3-21)$$

Substituting Eq. (4.2-16) for laminar flow into Eq. (4.3-21) and noting that  $A = \pi R^2$  and  $dA = r\ dr\ d\theta$ , we obtain (see Example 4.1-3)

$$(v_2)_{av} = \frac{1}{\pi R_2^2} \int_0^{2\pi} \int_{R_2}^{R_1} 2v_{av} (1 - \frac{r^2}{R_2^2}) r dr d\theta = (2\pi) \frac{2v_{av}}{2\pi R_2^2} \int_{R_2}^{R_1} (R_2^2 - r^2) r dr \quad (4.3-22)$$

Integrating Eq. (4.3-22) and rearranging,

$$(v_2)_{av} = 8v_{av} \frac{R_1^4 - R_2^4}{R_1^4 - R_2^4 + R_2^4} = 4.3v_{av} \quad (4.3-23)$$

Substituting Eq. (4.3-23) into (4.3-20),  $\beta = 4.3$ .

### **EXAMPLE 4.3-2. Momentum Balance for a Horizontal Nozzle**

Water is flowing at a rate of 0.03154 m<sup>3</sup>/s through a horizontal nozzle shown in Fig. 4.3-1 and discharges to the atmosphere at point 2. The nozzle is attached at the upstream end at point 1 and frictional forces are considered negligible. The upstream ID is 0.0635 m and the downstream 0.0286 m. Calculate the resultant force on the nozzle. The density of the water is 1000 kg/m<sup>3</sup>.

**Solution:** First, the mass flow and average or bulk velocities at points 1 and 2 are calculated. The area at point 1 is  $A_1 = (\pi/4)(0.0635)^2 = 3.167 \times 10^{-3}$  m<sup>2</sup> and  $A_2 = (\pi/4)(0.0286)^2 = 6.424 \times 10^{-4}$  m<sup>2</sup>. Then,

$$m_1 = m_2 = m = (0.03154)(1000) = 31.54 \text{ kg/s}$$

The velocity at point 1 is  $v_1 = 0.03154/(3.167 \times 10^{-3}) = 9.96$  m/s, and  $v_2 = 0.03154/(6.424 \times 10^{-4}) = 49.1$  m/s.

To evaluate the upstream pressure  $p_1$ , we use the mechanical-energy-balance equation (4.2-28), assuming no frictional losses and turbulent flow. (This can be checked by calculating the Reynolds number.) This equation then becomes, for  $\alpha = 1.0$ ,

$$v_1^2 + p_1/\rho = v_2^2 + p_2/\rho \quad (4.3-24)$$

Setting  $p_2 = 0$  gage pressure,  $\rho = 1000$  kg/m<sup>3</sup>,  $v_1 = 9.96$  m/s,  $v_2 = 49.1$  m/s, and solving for  $p_1$ ,

$$p_1 = (1000)(49.1^2 - 9.96^2) = 1.156 \times 10^6 \text{ N/m}^2 (\text{gage pressure})$$

For the x direction, the momentum-balance equation

(4.3-18) is used. Substituting the known values and solving for  $R_x$ ,

$$R_x = 31.54(49.10 - 9.96) + 0 - (1.156 \times 106) \\ (3.167 \times 10^{-3}) = -2427 \text{ N } (-546 \text{ lbf})$$

Since the force is negative, it is acting in the negative  $x$  direction, or to the left. This is the force of the nozzle on the fluid. The force of the fluid on the solid is  $-R_x$ , or  $+2427 \text{ N}$ .

### 4.3C Overall Momentum Balance in Two Directions

Another application of the overall momentum balance is shown in Fig. 4.3-2 for a flow system with fluid entering a conduit at point 1, inclined at an angle of  $\alpha_1$  relative to the horizontal  $x$  direction, and leaving a conduit at point 2 at an angle  $\alpha_2$ . The fluid will be assumed to be flowing at steady state and the frictional force  $F_{xs}$  will be neglected. Then, Eq. (4.3-13) for the  $x$  direction becomes as follows for no accumulation:

$$F_{xg} + F_{xp}$$



$$+R_x = \int \int A v_x \rho v \cos \alpha \, dA \quad (4.3-25)$$

Integrating the surface (area) integral,

$$\begin{aligned} & F_{xg} + F_{xp} \\ +R_x &= m(v_2^2)_{av} v_{2av} \cos \alpha_2 - \\ & m(v_1^2)_{av} v_{1av} \cos \alpha_1 \quad (4.3-26) \end{aligned}$$

The term  $(v^2)_{av}/v_{av}$  can again be replaced by  $v_{av}/\beta$ , with  $\beta$  being set at 1.0. From Fig. 4.3-2, the term  $F_{xp}$  is

$$\begin{aligned} F_{xp} &= p_1 A_1 \cos \alpha_1 - \\ & p_2 A_2 \cos \alpha_2 \quad (4.3-27) \end{aligned}$$

Then, Eq. (4.3-26) becomes as follows after solving for  $R_x$ :

$$\begin{aligned} R_x &= m v_2^2 \cos \alpha_2 - \\ & m v_1^2 \cos \alpha_1 + p_2 A_2 \cos \alpha_2 - \\ & p_1 A_1 \cos \alpha_1 \quad (4.3-28) \end{aligned}$$

The term  $F_{xg} = 0$  in this case.

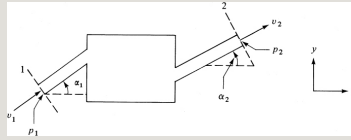


Figure 4.3-2. Overall momentum balance for flow system with fluid entering at point 1 and leaving at point 2.

For  $R_y$  the body force  $F_{yg}$  is in the negative  $y$  direction and  $F_{yg} = -m_t g$ , where  $m_t$  is the total mass fluid in the control volume. Replacing  $\cos \alpha$  by  $\sin \alpha$ , the equation for the  $y$  direction becomes

$$R_y = m v_2 \sin \alpha_2 - m v_1 \sin \alpha_1 + p_2 A_2 \sin \alpha_2 - p_1 A_1 \sin \alpha_1 + m_t g \quad (4.3-29)$$

**EXAMPLE 4.3-3. Momentum Balance in a Pipe Bend**

Fluid is flowing at steady state through a reducing pipe bend, as shown in Fig. 4.3-3. Turbulent flow will be assumed with frictional forces negligible. The volumetric flow rate of the liquid and the pressure  $p_2$  at point 2 are known, as are the pipe diameters at both ends. Derive the equations to calculate the forces on the bend. Assume that

the density  $\rho$  is constant.

**Solution:** The velocities  $v_1$  and  $v_2$  can be obtained from the volumetric flow rate and the areas. Also,  $m = \rho_1 v_1 A_1 = \rho_2 v_2 A_2$ . As in Example 4.3-2, the mechanical-energy-balance equation (4.3-24) is used to obtain the upstream pressure,  $p_1$ . For the  $x$  direction, Eq. (4.3-28) is used for the momentum balance. Since  $\alpha_1 = 0^\circ$ ,  $\cos \alpha_1 = 1.0$ , Equation (4.3-28) becomes

$$R_x = m v_2 \cos \alpha_2 - m v_1 + p_2 A_2 \cos \alpha_2 - p_1 A_1 \quad (\text{SI})$$

$$R_x = m g v_2 \cos \alpha_2 - m g v_1 + p_2 A_2 \cos \alpha_2 - p_1 A_1 \quad (\text{English}) \quad (4.3-30)$$

For the  $y$  direction, the momentum-balance equation (4.3-29) is used, where  $\sin \alpha_1 = 0$ :

$$R_y = m v_2 \sin \alpha_2 + p_2 A_2 \sin \alpha_2 + m g \quad (\text{SI}) \quad (4.3-31)$$

where  $m$  is total mass fluid in the pipe bend. The pressures at points 1 and 2 are gage pressures since the atmospheric pressures acting on all surfaces cancel. The magnitude of the resultant force of the bend acting on the control volume fluid is

$$|R| = \sqrt{R_x^2 + R_y^2} \quad (4.3-32)$$

The angle this makes with the vertical is  $\theta = \arctan(R_x/R_y)$ . The gravity force  $F_{yg}$  is often small compared to the other terms in Eq. (4.3-31) and is neglected.

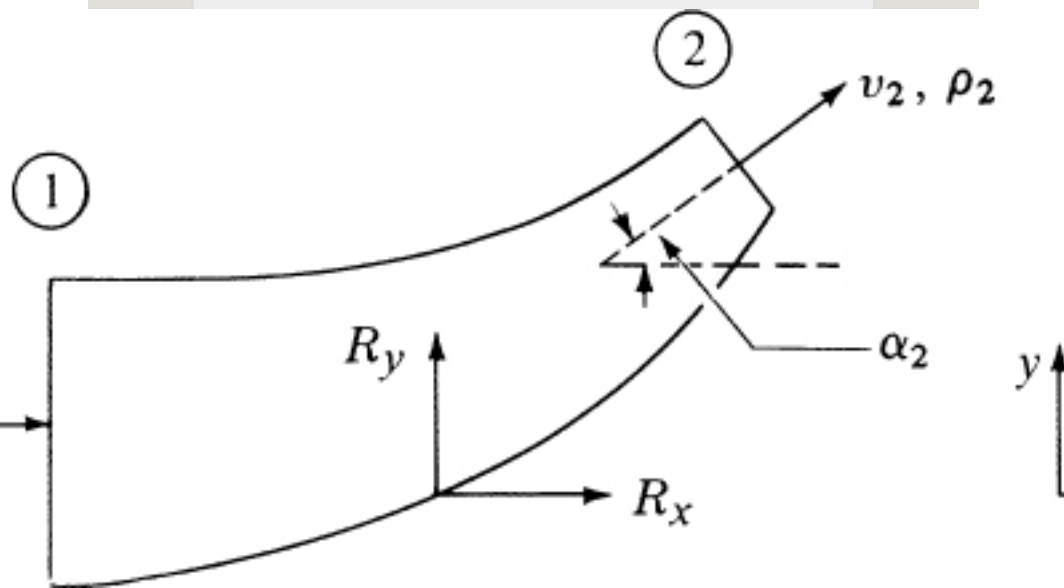


Figure 4.3-3. Flow through a reducing bend in Example 4.3-3.

#### **EXAMPLE 4.3-4. Friction Loss in a Sudden Enlargement**

A mechanical-energy loss occurs when a fluid flows from a small pipe to a large pipe through an abrupt expansion, as shown in Fig. 4.3-4. Use the momentum balance and mechanical-energy balance to obtain an expression for the loss for a liquid. (*Hint:* Assume that  $p_0 = p_1$  and  $v_0 = v_1$ , and make a mechanical-energy balance between points 0 and 2, and a momentum balance between points 1 and 2. It will be assumed that  $p_1$  and  $p_2$  are uniform over the cross-sectional area.)

**Solution:** The control volume is selected so that it does not include the pipe wall and  $R_x$  drops out. The boundaries selected are points 1 and 2. The flow through plane 1 occurs only through an area  $A_0$ . The frictional drag force will be neglected, and all the loss is assumed to be from eddies in this volume. Making a momentum balance between points 1 and 2 using Eq. (4.3-18) and noting that  $p_0 = p_1$ ,  $v_1 = v_0$ , and  $A_1 = A_2$ ,

$$p_1 A_2 - p_2 A_2 = m v_2 - m v_1 \quad (4.3-33)$$

The mass flow rate is  $m = v_0 \rho A_0$  and  $v_2 = (A_0/A_2) v_0$ .  
Substituting these terms into Eq. (4.3-33) and rearranging gives us

$$v_0^2 A_0 A_2 (1 - A_0 A_2) = p_2 - p_1 \rho \quad (4.3-34)$$

Applying the mechanical-energy-balance equation (4.2-28) to points 1 and 2,

$$v_0^2 - v_2^2 - \sum F = p_2 - p_1 \rho \quad (4.3-35)$$

Finally, combining Eqs. (4.3-34) and (4.3-35),

$$\sum F = v_0^2 (1 - A_0 A_2)^2 \quad (4.3-36)$$

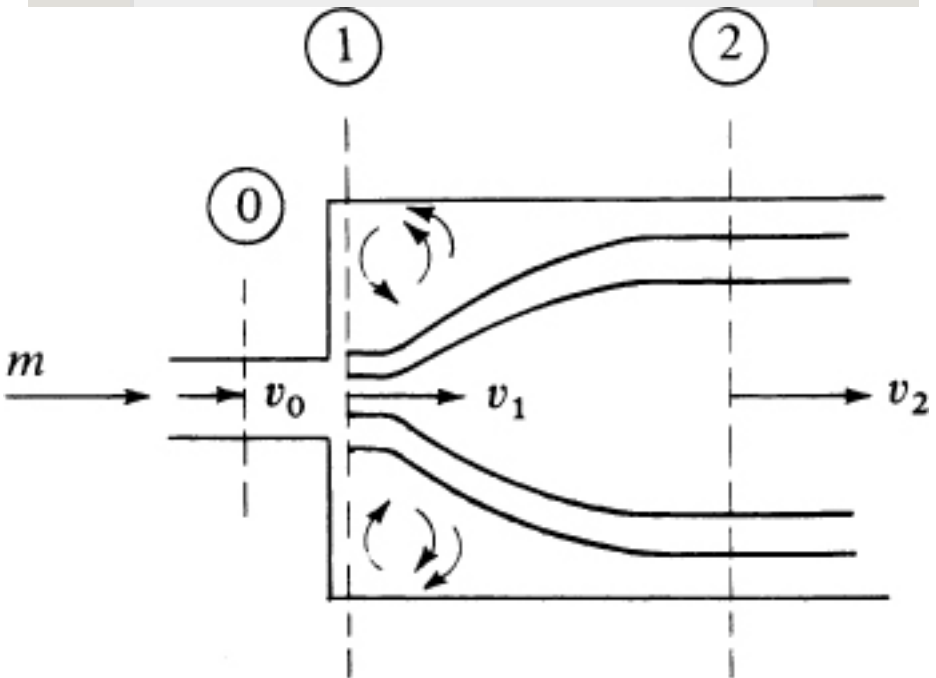


Figure 4.3-4. Losses in expansion flow.

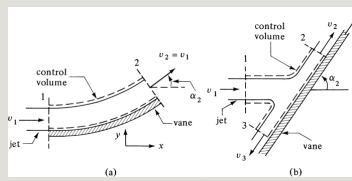


Figure 4.3-5. Free jet impinging on a fixed vane: (a) smooth, curved vane, (b) smooth, flat vane.

### 4.3D Overall Momentum Balance for a Free Jet Striking a Fixed Vane

When a free jet impinges on a fixed smooth vane as in Fig. 4.3-5, the overall momentum balance can be applied to determine the force on the vane. Since there are no changes in elevation or pressure before and after impact, there is no loss in energy, and application of the Bernoulli equation shows that the magnitude of the velocity is unchanged. Losses due to impact are neglected. The frictional resistance between the jet and the smooth vane is also neglected. The velocity is assumed

to be uniform throughout the jet upstream and downstream. Since the jet is open to the atmosphere, the pressure is the same at all ends of the vane.

In making a momentum balance for the control volume shown for the curved vane in Fig. 4.3-5a, Eq. (4.3-28) is written as follows for steady state, where the pressure terms are zero,  $v_1 = v_2$ ,  $A_1 = A_2$ , and  $m = v_1 A_1 \rho_1 = v_2 A_2 \rho_2$ :

$$R_x = mv_2 \cos \alpha_2 - mv_1 \cos \alpha_1 = mv_1 (\cos \alpha_2 - \cos \alpha_1) \quad (4.3-37)$$

Using Eq. (4.3-29) for the y direction and neglecting the body force,

$$R_y = mv_2 \sin \alpha_2 - mv_1 \sin \alpha_1 = mv_1 (\sin \alpha_2 - \sin \alpha_1) \quad (4.3-38)$$

Hence,  $R_x$  and  $R_y$  are the force

components of the vane on the control volume fluid. The force components on the vane are  $-R_x$  and  $-R_y$ .

**EXAMPLE 4.3-5. Force of a Free Jet on a Curved, Fixed Vane**

A jet of water having a velocity of 30.5 m/s and a diameter of  $2.54 \times 10^{-2}$  m is deflected by a smooth, curved vane, as shown in Fig. 4.3-5a, where  $\alpha = 60^\circ$ . What is the force of the jet on the vane? Assume that  $\rho = 1000$  kg/m<sup>3</sup>.

**Solution:** The cross-sectional area of the jet is  $A_1 = \pi(2.54 \times 10^{-2})^2/4 = 5.067 \times 10^{-4}$  m<sup>2</sup>. Then,  $m = v_1 A_1 \rho = 30.5 \times 5.067 \times 10^{-4} \times 1000 = 15.45$  kg/s. Substituting into Eqs. (4.3-37) and (4.3-38),

$$R_x = 15.45 \times 30.5 (\cos 60^\circ - 1) = -235.6 \text{ N } (-52.97 \text{ lbf}) \quad R_y = 15.45 \times 30.5 \sin 60^\circ = 408.1 \text{ N } (91.74 \text{ lbf})$$

The force on the vane is  $-R_x = +235.6$  N and  $-R_y = -408.1$  N. The resultant force is calculated using Eq. (4.3-32).

In Fig. 4.3-5b, a free jet at velocity  $v_1$  strikes a smooth, inclined flat plate and the flow divides into two separate streams whose velocities are all equal ( $v_1 = v_2 = v_3$ ) since there is no loss in energy. It is convenient to make a momentum balance in the  $p$  direction parallel to the plate. No force is exerted



on the fluid by the flat plate in this direction; that is, there is no tangential force. Then, the initial momentum component in the  $p$  direction must equal the final momentum component in this direction. This means  $\Sigma F_p = 0$ . Writing an equation similar to Eq. (4.3-26), where  $m_1$  is kg/s entering at 1 and  $m_2$  leaves at 2 and  $m_3$  at 3:

$$\begin{aligned}\Sigma F_p = 0 &= m_2 v_2 - m_1 v_1 \cos \alpha \\ m_3 v_3 &= m_2 v_1 - m_1 v_1 \cos \alpha \\ &= m_3 v_1\end{aligned}\quad (4.3-39)$$

By the continuity equation,

$$m_1 = m_2 + m_3 \quad (4.3-40)$$

Combining and solving,

$$\begin{aligned}m_2 &= m_1 \frac{1 + \cos \alpha}{2}, m_3 = m_1 \frac{1 - \cos \alpha}{2} \\ &\quad (4.3-41)\end{aligned}$$

The resultant force exerted by the plate on the fluid must be normal to it. This means the resultant force is simply  $m_1 v_1 \sin \alpha_2$ . Alternatively, the resultant force on the fluid can be calculated by determining  $R_x$  and  $R_y$  from Eqs. (4.3-28) and (4.3-29), and then using Eq. (4.3-32). The force on the bend is the opposite of this.

## **4.4 Shell Momentum Balance and Velocity Profile in Laminar Flow**

### **4.4A Introduction**

In Section 4.3, we analyzed momentum balances using an overall, macroscopic control volume. From this, we obtained the total or overall changes in momentum crossing the control surface. However, this overall momentum balance did not tell us the details of

what happens inside the control volume. In this section, we analyze a small control volume and then shrink this control volume to differential size. In doing so, we make a shell momentum balance using the momentum-balance concepts of the preceding section, and then, using the equation for the definition of viscosity, we obtain an expression for the velocity profile inside the enclosure and the pressure drop. The equations are derived for flow systems of simple geometry in laminar flow at steady state.

In many engineering problems, a knowledge of the complete velocity profile is not needed, but a knowledge of the maximum velocity, the average velocity, or the shear stress on a surface

is needed. In this section, we show how to obtain these quantities from the velocity profiles.

#### **4.4B Shell Momentum Balance Inside a Pipe**

Engineers often deal with the flow of fluids inside a circular conduit or pipe. In Fig. 4.4-1, we have a horizontal section of pipe in which an incompressible Newtonian fluid is flowing in one-dimensional, steady-state, laminar flow. The flow is fully developed; that is, it is not influenced by entrance effects and the velocity profile does not vary along the axis of flow in the  $x$  direction.

The cylindrical control volume is a shell with an inside radius  $r$ , thickness  $\Delta r$ , and length  $\Delta x$ . At steady state, the

conservation of momentum, Eq. (4.3-3), becomes as follows: sum of forces acting on control volume = rate of momentum out – rate of momentum into volume. The pressure forces become, from Eq. (4.3-27),

$$\begin{aligned} \text{pressure forces} = & pA|_x - pA|_{x+\Delta x} \\ & + \Delta x = p(2\pi r \Delta r)|_x - p(2\pi r \Delta r)|_{x+\Delta x} \quad (4.4-1) \end{aligned}$$

The shear force or drag force acting on the cylindrical surface at the radius  $r$  is the shear stress  $\tau_{rx}$  times the area  $2\pi r \Delta x$ . Here, the shear stress  $\tau_{rx}$  has two subscripts that refer to the viscous flux of  $x$ -momentum in the  $r$ -direction. However, this can also be considered as the rate of momentum flow into the cylindrical surface of the shell as described by Eq. (3.1-9). Hence, the net

rate of momentum efflux is the rate of momentum out – the rate of momentum in and is

$$\text{net efflux} = (\tau_{rx} 2\pi r \Delta x)|_{r+\Delta r} - (\tau_{rx} 2\pi r \Delta x)|_r \quad (4.4-2)$$

The net convective momentum flux across the annular surface at  $x$  and  $x + \Delta x$  is zero, since the flow is fully developed and the terms are independent of  $x$ . This is true since  $v_x$  at  $x$  is equal to  $v_x$  at  $x + \Delta x$ .

Equating Eq. (4.4-1) to (4.4-2) and rearranging,

$$(\tau_{rx})|_{r+\Delta r} - (\tau_{rx})|_r = r(p|_x - p|_{x+\Delta x}) \Delta x \quad (4.4-3)$$

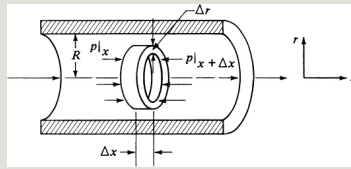


Figure 4.4-1. Control volume for shell momentum balance on a fluid flowing in a circular tube.

In fully developed flow, the pressure gradient ( $\Delta p / \Delta x$ ) is constant and becomes ( $\Delta p / L$ ), where  $\Delta p$  is the pressure drop for a pipe of length  $L$ . Letting  $\Delta r$  approach zero, we obtain

$$d(r\tau r x) dr = (\Delta p L) r \quad (4.4-4)$$

Separating variables and integrating,

$$\tau r x = (\Delta p L) r^2 + C_1 r \quad (4.4-5)$$

The constant of integration  $C_1$  must be zero if the momentum flux is not infinite at  $r = 0$ . Hence,

$$\tau r x = (\Delta p 2L) r = p_0 - p_L 2L r \quad (4.4-6)$$

This means that the momentum flux varies linearly with the radius, as shown in Fig. 4.4-2, and the maximum value occurs at  $r = R$  at the wall.

Substituting Newton's law of viscosity

$$\tau_{rx} = -\mu \frac{dv_x}{dr} \quad (4.4-7)$$

into Eq. (4.4-6), we obtain the following differential equation for the velocity:

$$\frac{dv_x}{dr} = -\frac{p_0 - p_L}{2\mu L} r \quad (4.4-8)$$

Integrating using the boundary condition at the wall,  $v_x = 0$  at  $r = R$ , we obtain the equation for the velocity distribution:

$$v_x = \frac{p_0 - p_L}{4\mu L} R^2 \left[ 1 - \left( \frac{r}{R} \right)^2 \right] \quad (4.4-9)$$

This result shows us that the velocity distribution is parabolic, as shown in



Fig. 4.4-2.

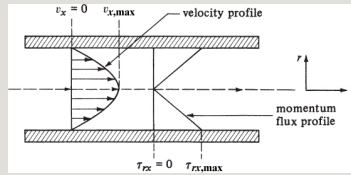


Figure 4.4-2. *Velocity and momentum flux profiles for laminar flow in a pipe.*

The average velocity  $v_{x\text{ av}}$  for a cross section is found by summing up all the velocities over the cross section and dividing by the cross-sectional area, as in Eq. (4.1-17). Following the procedure given in Example 4.1-3, where  $dA = r\,dr\,d\theta$  and  $A = \pi R^2$ ,

$$2\pi \int_0^R v_x r\,dr\,d\theta = \pi R^2 \int_0^R v_x \frac{2\pi r\,dr}{\pi R^2} \quad (4.4-10)$$

Combining Eqs. (4.4-9) and (4.4-10) and integrating,

$$v_{x\text{ av}} = \frac{(p_0 - p_L) R^2}{8\mu L} = \frac{(p_0 - p_L) R^2}{8\mu L}$$

$$\frac{p_0 - p_L}{4\mu L} D^2 \quad (4.4-11)$$

where diameter  $D = 2R$ . Hence, Eq. (4.4-11), which is known as the *Hagen–Poiseuille equation*, relates the pressure drop and average velocity for laminar flow in a horizontal pipe.

The maximum velocity for a pipe is found from Eq. (4.4-9) and occurs at  $r = 0$ :

$$v_{x \max} = \frac{p_0 - p_L}{4\mu L} R^2 \quad (4.4-12)$$

Combining Eqs. (4.4-11) and (4.4-12), we find that

$$v_{x \text{ av}} = \frac{v_{x \max}}{2} \quad (4.4-13)$$

Also, dividing Eq. (4.4-9) by (4.4-11),

$$\frac{v_x}{v_{x \text{ av}}} = 2[1 - (r/R)^2] \quad (4.4-14)$$

#### 4.4C Shell Momentum Balance for Falling Film

For the case of laminar flow of a fluid film down a vertical surface, we now use an approach similar to the one previously used for laminar flow inside a pipe. Falling films have been used to study various phenomena in mass transfer, including coatings on surfaces. The control volume for the falling film is shown in Fig. 4.4-3a, where the shell of fluid considered is  $\Delta x$  thick and has a length of  $L$  in the vertical  $z$  direction. This region is sufficiently far from the entrance and exit regions so that the flow is not affected by these regions. This means the velocity  $v_z(x)$  does not depend on position  $z$ .

To start, we set up a momentum balance in the  $z$  direction over a system  $\Delta x$  thick,

bounded in the  $z$  direction by the planes  $z = 0$  and  $z = L$ , and extending a distance  $W$  in the  $y$  direction. First, we consider the momentum flux due to molecular transport. The rate of momentum out – the rate of momentum in is the momentum flux at point  $x + \Delta x$  minus that at  $x$  times the area  $LW$ :

$$\text{net efflux} = LW(\tau_{xz})|_{x+\Delta x} - LW(\tau_{xz})|_x \quad (4.4-15)$$

The net convective momentum flux is the rate of momentum leaving the area  $\Delta x W$  at  $z = L$  minus that entering at  $z = 0$ . This net efflux is equal to 0, since  $v_z$  at  $z = 0$  is equal to  $v_z$  at  $z = L$  for each value of  $x$ :

$$\text{net efflux} = \Delta x W v_z(\rho v_z)|_{z=L} - \Delta x W v_z(\rho v_z)|_{z=0} = 0 \quad (4.4-16)$$

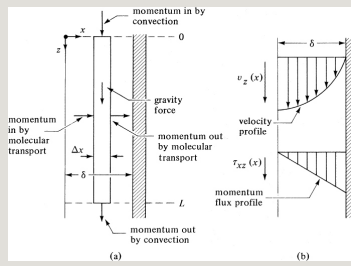


Figure 4.4-3. Vertical laminar flow of a liquid film: (a) shell momentum balance for a control volume  $\Delta x$  thick; (b) velocity and momentum flux profiles.

The gravity force acting on the fluid is

$$\text{gravity force} = \Delta x W L (\rho g) \quad (4.4-17)$$

Then, using Eq. (4.3-3) for the conservation of momentum at steady state,

$$\Delta x W L (\rho g) = L W (\tau_{xz})|_{x+\Delta x} - L W (\tau_{xz})|_x \quad (4.4-18)$$

Rearranging Eq. (4.4-18) and letting  $\Delta x \rightarrow 0$ ,

$$\tau_{xz}|_{x+\Delta x} - \tau_{xz}|_x \Delta x = \rho g \Delta x \quad (4.4-19)$$

$$\frac{d\tau_{xz}}{dx} = \rho g \quad (4.4-20)$$

Integrating using the boundary conditions at  $x = 0$ ,  $\tau_{xz} = 0$  at the free liquid surface and at  $x = x$ ,  $\tau_{xz} = \tau_{xz}$ ,

$$\tau_{xz} = \rho g x \quad (4.4-21)$$

This means the momentum-flux profile is linear, as shown in Fig. 4.4-3b, and the maximum value is at the wall. For a Newtonian fluid using Newton's law of viscosity,

$$\tau_{xz} = -\mu \frac{dv_z}{dx} \quad (4.4-22)$$

Combining Eqs. (4.4-21) and (4.4-22), we obtain the following differential equation for the velocity:

$$\frac{dv_z}{dx} = -\left(\frac{\rho g}{\mu}\right)x \quad (4.4-23)$$

Separating variables and integrating gives

$$v_z = -(\rho g / 2\mu)x^2 + C_1 \quad (4.4-24)$$

To evaluate the integration constant  $C_1$ , it is necessary to identify the boundary condition at this point. At the surface,  $x = \delta$  and the velocity is 0. This is known as the “no-slip” condition.

Using this boundary condition that  $v_z = 0$  at  $x = \delta$ ,  $C_1 = (\rho g / 2\mu)\delta^2$ . Hence, the velocity-distribution equation becomes

$$v_z = \rho g \delta^2 / 2\mu [1 - (x/\delta)^2] \quad (4.4-25)$$

This means the velocity profile is parabolic, as shown in Fig. 4.4-3b. The maximum velocity occurs at  $x = 0$  in Eq. (4.4-25) and is

$$v_{z \max} = \frac{\rho g \delta^2}{2\mu} \quad (4.4-26)$$

The average velocity can be found by using Eq. (4.1-17):

$$\delta \int_0^W \int_0^\delta v_z dx dy = W \delta \int_0^\delta v_z dx \quad (4.4-27)$$

Substituting Eq. (4.4-25) into (4.4-27) and integrating,

$$v_{z \text{ av}} = \frac{\rho g \delta^2}{3\mu} \quad (4.4-28)$$

Combining Eqs. (4.4-26) and (4.4-28), we obtain  $v_{z \text{ av}} = \frac{2}{3} v_{z \max}$ . The volumetric flow rate  $q$  is obtained by multiplying the average velocity  $v_{z \text{ av}}$  times the cross-sectional area  $\delta W$ :

$$q = \frac{\rho g \delta^3 W}{3\mu} \text{ m}^3/\text{s} \quad (4.4-29)$$

In falling films, the mass flow rate per unit width of wall  $\Gamma$  in  $\text{kg/s} \cdot \text{m}$  is often



defined as  $\Gamma = \rho \delta v_{z \text{ av}}$  and a Reynolds number is defined as

$$N_{\text{Re}} = 4\Gamma\mu = 4\rho\delta v_{z \text{ av}}\mu \quad (4.4-30)$$

Laminar flow occurs for  $N_{\text{Re}} < 1200$ .

Laminar flow with rippling present occurs for  $N_{\text{Re}} > 25$ .

**EXAMPLE 4.4-1. Falling Film Velocity and Thickness**

A 1.7-mm-thick oil film is flowing down a vertical wall. The oil density is  $820 \text{ kg/m}^3$  and the viscosity is  $0.20 \text{ Pa} \cdot \text{s}$ . Calculate the mass flow rate  $\Gamma$  needed per unit width of wall, and the associated Reynolds number. Also calculate the average velocity.

**Solution:** The film thickness is  $\delta = 0.0017 \text{ m}$ . Substituting Eq. (4.4-28) into the definition of  $\Gamma$ ,

$$\Gamma = \rho \delta v_{z \text{ av}} = (\rho \delta) \frac{g \delta^2}{3\mu} = \frac{\rho g \delta^3}{3\mu} = \frac{(820)(9.806)(1.7 \times 10^{-3})^3}{3(0.20)} = 0.05399 \text{ kg/s} \cdot \text{m} \quad (4.4-31)$$

Using Eq. (4.4-30),

$$N_{\text{Re}} = 4\Gamma\mu = 4(0.05399)(0.20) = 1.080$$

Hence, the film is in laminar flow. Using Eq. (4.4-28),

$$v_{z \text{ av}} = \frac{g \delta^2}{3\mu} = \frac{820(9.806)(1.7 \times 10^{-3})^2}{3(0.20)} = 0.03873 \text{ m/s}$$

## 4.5 Chapter Summary

In this chapter, we have described and derived the most common balance equations found in fluid dynamics situations. Starting with the law of conservation of mass,

$$\text{control volume})=0 \quad (\text{rate of mass generation}) \quad (4.1-3b)$$

we were able to derive the most general form of the mass balance equation:

$$\int \int_A \rho(\mathbf{v} \cdot \mathbf{n}) \, dA + \frac{\partial}{\partial t} \int \int_V \rho \, dV = 0 \quad (4.1-6)$$

For steady-state problems, where  $dM/dt = 0$ , we showed that this reduces to

$$\dot{m} = \rho_1 A_1 v_1 = \rho_2 A_2 v_2 \quad (4.1-2)$$

Starting with the first law of thermodynamics,

$$\Delta E = Q - W \quad (4.2-1)$$

and doing an entity balance on a control volume,

$$\begin{aligned} &\text{rate of entity output} - \text{rate of entity input} \\ &+ \text{rate of entity accumulation} = 0 \quad (4.2-2) \end{aligned}$$

we were able to derive the most general form of the energy balance:

$$\begin{aligned} &\iint_A (H + v^2/2 + zg)(\rho v) \cos \alpha \, dA \\ &+ \partial/\partial t \iiint_V (U + v^2/2 + zg) \rho \, dV = Q - \\ &W \quad (4.2-7) \end{aligned}$$

We also extended this equation to derive the overall mechanical energy balance:

$$\begin{aligned} &\frac{1}{2} \alpha [v_2^2 - v_1^2] + g(z_2 - z_1) + \int p_1 p_2 dp + \Sigma F + W = 0 \quad (4.2-27) \end{aligned}$$

By simplifying the overall mechanical

energy balance for cases where there is no mechanical added and no friction, we were able to transform this equation into the Bernoulli equation:

$$z_1 g + \frac{v_1^2}{2} + \frac{p_1}{\rho} = z_2 g + \frac{v_2^2}{2} + \frac{p_2}{\rho} \quad (4.2-32)$$

This equation was shown to be very useful in solving many fluid dynamics problems.

Newton's law

$$\sum F = \frac{dP}{dt} = \frac{dMv}{dt} \quad (4.3-2)$$

and the conservation of momentum around a control volume

$$\text{accumulation of momentum in control volume} \quad (4.3-3)$$

was used to derive the overall linear momentum balance for a control volume:

$$\sum \mathbf{F} = \int \int \mathbf{A} \rho \mathbf{v} (\mathbf{v} \cdot \mathbf{n}) dA + \frac{\partial}{\partial t} \int \int \mathbf{V} \int \rho \mathbf{v} dV \quad (4.3-8)$$

Lastly, the concept of a shell momentum balance was introduced and applied to a control fluid element, and then used to derive the velocity profiles found in various fluid dynamics problems.

## Problems

**4.1-1. *Average Velocity for Mass Balance in a Flow Down a Vertical Plate.*** For a layer of liquid flowing in laminar flow in the  $z$  direction down a vertical plate or surface, the velocity profile is

$$v_z = \frac{\rho g \delta^2}{2\mu} [1 - (x/\delta)^2]$$

where  $\delta$  is the thickness of the layer,  $x$  is the distance from the free surface of the liquid toward the plate, and  $v_z$  is the velocity at a distance  $x$  from the free surface.

- What is the maximum velocity  $v_{z \text{ max}}$ ?
- Derive the expression for the average velocity  $v_{z \text{ av}}$  and also relate it to  $v_{z \text{ max}}$ .

**Ans.** (a)  $v_{z \text{ max}} = \rho g \delta^2 / 2\mu$ , (b)  $v_{z \text{ av}} = \frac{2}{3} v_{z \text{ max}}$

**4.1-2. Flow of Liquid in a Pipe and Mass Balance.** A hydrocarbon liquid enters a simple flow system shown in Fig. 4.1-1 at an average velocity of 1.282 m/s, where  $A_1 = 4.33 \times 10^{-3} \text{ m}^2$  and  $\rho_1 = 902 \text{ kg/m}^3$ . The liquid is heated in the process and the exit density is 875 kg/m<sup>3</sup>. The cross-sectional area at point 2 is  $5.26 \times 10^{-3} \text{ m}^2$ . The process is

steady state.

- Calculate the mass flow rate  $m$  at the entrance and exit.
- Calculate the average velocity  $v$  at 2 and the mass velocity  $G$  at 1.

**Ans.** (a)  $m_1 = m_2 = 5.007 \text{ kg/s}$ , (b)  $G_1 = 1156 \text{ kg/s} \cdot m_2$

**4.1-3. Average Velocity for Mass Balance in a Turbulent Flow.** For turbulent flow in a smooth, circular tube with a radius  $R$ , the velocity profile varies according to the following expression at a Reynolds number of about  $10^5$ :

$$v = v_{\max} (R - r/R)^{1/7}$$

where  $r$  is the radial distance from the center and  $v_{\max}$  the maximum velocity at the center. Derive the equation

relating the average velocity (bulk velocity)  $v_{av}$  to  $v_{max}$  for an incompressible fluid. (*Hint: The integration can be simplified by substituting  $z$  for  $R - r$ .*)

**Ans.**  $v_{av} = (4/3)v_{max} = 0.667v_{max}$

**4.1-4. Bulk Velocity for Flow Between Parallel Plates.** A fluid flowing in laminar flow in the  $x$  direction between two parallel plates has a velocity profile given by the following:

$$v_x = v_{x \max} [1 - (y/y_0)^2]$$

where  $2y_0$  is the distance between the plates,  $y$  is the distance from the center line, and  $v_x$  is the velocity in the  $x$  direction at position  $y$ . Derive an equation relating  $v_{x \text{ av}}$  (bulk or average velocity) to  $v_{x \max}$ .



$$\text{Ans. } v_x \text{ av} = 23 \text{ } v_x \text{ max}$$

**4.1-5. Overall Mass Balance for a Dilution Process.** A well-stirred storage vessel contains 10000 kg of solution of a dilute methanol solution ( $w_A = 0.05$  mass fraction of alcohol). A constant flow of 500 kg/min of pure water is suddenly introduced into the tank and a constant rate of withdrawal of 500 kg/min of solution is started. These two flows are continued and remain constant. Assuming that the densities of the solutions are the same and that the total contents of the tank remain constant at 10000 kg of solution, calculate the time for the alcohol content to drop to 1.0 wt%.

$$\text{Ans. } 32.2 \text{ min}$$

**4.1-6. Overall Mass Balance for an Unsteady-State Process.** A storage vessel is well stirred and contains 500 kg of total solution with a concentration of 5.0% salt. A constant flow rate of 900 kg/h of salt solution containing 16.67% salt is suddenly introduced into the tank and a constant withdrawal rate of 600 kg/h is also started. These two flows remain constant thereafter. Derive an equation relating the outlet withdrawal concentration as a function of time. Also, calculate the concentration after 2.0 h.

**4.1-7. Mass Balance for Flow of a Sucrose Solution.** A 20 wt % sucrose (sugar) solution having a density of 1074 kg/m<sup>3</sup> is flowing through the same piping system as in Example 4.1-1 (Fig. 4.1-2). The flow rate entering pipe 1 is

1.892 m<sup>3</sup>/h. The flow divides equally in each of pipes 3. Calculate the following:

- The velocity in m/s in pipes 2 and 3
- The mass velocity  $G$  kg/m<sup>2</sup> · s in pipes 2 and 3

#### **4.2-1. *Kinetic-Energy Velocity***

##### ***Correction Factor for Turbulent Flow.***

Derive the equation to determine the value of  $\alpha$ , the kinetic-energy velocity correction factor, for turbulent flow. Use Eq. (4.2-20) to approximate the velocity profile and substitute this into Eq.

(4.2-15) to obtain  $(v_3)_{av}$ . Then, use Eqs. (4.2-20), (4.1-17), and (4.2-14) to obtain  $\alpha$ .

**Ans.**  $\alpha = 0.9448$

#### **4.2-2. *Flow Between Parallel Plates and Kinetic-Energy Correction Factor.***

The equation for the velocity profile of a

fluid flowing in laminar flow between two parallel plates is given in Problem 4.1-4. Derive the equation to determine the value of the kinetic-energy velocity correction factor  $\alpha$ . [*Hint*: First, derive an equation relating  $y$  to  $v$  to  $v_{av}$ . Then, derive the equation for  $(v^3)_{av}$ . And, finally, relate these results to  $\alpha$ .]

### ***4.2-3. Temperature Drop in a Throttling Valve and Energy Balance.***

Steam is flowing through an adiabatic throttling valve (no heat loss or external work). Steam enters point 1 upstream of the valve at 689 kPa abs and 171.1°C, and leaves the valve (point 2) at 359 kPa. Calculate the temperature  $t_2$  at the outlet. [*Hint*: Use Eq. (4.2-21) for the energy balance and neglect the kinetic-energy and potential-energy terms as shown in Example 4.2-1. Obtain the

enthalpy  $H_1$  from the steam tables in Appendix A.2. For  $H_2$ , linear interpolation of the values in the table will have to be done to obtain  $H = 4.57$  m. Use SI units.

**Ans.**  $t_2 = 160.6^\circ\text{C}$

**4.2-4. Energy Balance on a Heat Exchanger and a Pump.** Water at  $93.3^\circ\text{C}$  is being pumped from a large storage tank at 1 atm abs at a rate of  $0.189 \text{ m}^3/\text{min}$  by a pump. The motor that drives the pump supplies energy to the pump at the rate of 1.49 kW. The water is pumped through a heat exchanger, where it gives up 704 kW of heat and is then delivered to a large open storage tank at an elevation of 15.24 m above the first tank. What is the final temperature of the water to the

second tank? Also, what is the gain in enthalpy of the water due to the work input? (*Hint:* Be sure to use the steam tables for the enthalpy of the water. Neglect any kinetic-energy changes but not potential-energy changes.)

**Ans.**  $t_2 = 38.2^\circ\text{C}$ , work input gain =  
0.491 kJ/kg

**4.2-5. Steam Boiler and Overall Energy Balance.** Liquid water under pressure at 150 kPa enters a boiler at  $24^\circ\text{C}$  through a pipe at an average velocity of 3.5 m/s in turbulent flow. The exit steam leaves at a height of 25 m above the liquid inlet at  $150^\circ\text{C}$  and 150 kPa absolute, and the velocity in the outlet line is 12.5 m/s in turbulent flow. The process is steady state. How much heat must be added per kg of steam?

#### ***4.2-6. Energy Balance on a Flow***

##### ***System with a Pump and Heat***

***Exchanger.*** Water is stored in a large, well-insulated storage tank at  $21.0^{\circ}\text{C}$  and atmospheric pressure is being pumped at steady state from this tank by a pump at the rate of  $40 \text{ m}^3/\text{h}$ . The motor driving the pump supplies energy at the rate of  $8.5 \text{ kW}$ . The water is used as a cooling medium and passes through a heat exchanger, where  $255 \text{ kW}$  of heat is added to the water. The heated water then flows to a second large, vented tank, which is  $25 \text{ m}$  above the first tank. Determine the final temperature of the water delivered to the second tank.

#### ***4.2-7. Mechanical-Energy Balance in***

***Pumping Soybean Oil.*** Soybean oil is being pumped through a uniform-diameter pipe at a steady mass-flow rate.

A pump supplies 209.2 J/kg mass of fluid flowing. The entrance abs pressure in the inlet pipe to the pump is 103.4 kN/m<sup>2</sup>. The exit section of the pipe downstream from the pump is 3.35 m above the entrance and the exit pressure is 172.4 kN/m<sup>2</sup>. The exit and entrance pipes are the same diameter. The fluid is in turbulent flow. Calculate the friction loss in the system. See Appendix A.4 for the physical properties of soybean oil. The temperature is 303 K.

**Ans.**  $\Sigma F = 101.3 \text{ J/kg}$

**4.2-8. Pump Horsepower in a Brine System.** A pump transports 0.200 ft<sup>3</sup>/s of brine solution having a density of 1.15 g/cm<sup>3</sup> from an open feed tank having a large cross-sectional area. The suction line has an inside diameter of 3.548 in.



and the discharge line from the pump has a diameter of 2.067 in. The discharge flow goes to an open overhead tank, and the open end of this line is 75 ft above the liquid level in the feed tank. If the friction losses in the piping system are  $18.0 \text{ ft} \cdot \text{lbf/lbm}$ , what pressure must the pump develop and what is the horsepower of the pump if the efficiency is 70%? The flow is turbulent.

**4.2-9. Pressure Measurements from Flows.** Water having a density of  $998 \text{ kg/m}^3$  is flowing at the rate of  $1.676 \text{ m/s}$  in a 3.068-in.-diameter horizontal pipe at a pressure  $p_1$  of 68.9 kPa abs. It then passes to a pipe having an inside diameter of 2.067 in.

- Calculate the new pressure  $p_2$  in the 2.067-in. pipe. Assume no friction losses.
- If the piping is vertical and the flow is upward,

calculate the new pressure  $p_2$ . The pressure tap for  $p_2$  is 0.457 m above the tap for  $p_1$ .

**Ans.** (a)  $p_2 = 63.5 \text{ kPa}$ ; (b)  $p_2 = 59.1 \text{ kPa}$

**4.2-10. Draining Cottonseed Oil from a Tank.** A cylindrical tank 1.52 m in diameter and 7.62 m high contains cottonseed oil having a density of  $917 \text{ kg/m}^3$ . The tank is open to the atmosphere. A discharge nozzle of inside diameter 15.8 mm and cross-sectional area  $A_2$  is located near the bottom of the tank. The surface of the liquid is located at  $H = 6.1 \text{ m}$  above the center line of the nozzle. The discharge nozzle is opened, draining the liquid level from  $H = 6.1 \text{ m}$  to  $H = 4.57 \text{ m}$ . Calculate the time in seconds to do this. [Hint: The velocity on the surface of the reservoir is small and can be neglected.]

The velocity  $v_2$  m/s in the nozzle can be calculated for a given  $H$  by Eq. (4.2-36). However,  $H$ , and hence  $v_2$ , are varying. Set up an unsteady-state mass balance as follows: The volumetric flow rate in the tank is  $(A_t dH)/dt$ , where  $A_t$  is the tank's cross section in  $m^2$  and  $A_t dH$  is the  $m^3$  liquid flowing in  $dt$  s. This rate must equal the negative of the volumetric rate in the nozzle, or  $-A_2 v_2 m^3/s$ . Based on the overall balance equation, the negative sign is present since  $dH$  is the negative of  $v_2$ . Rearrange this equation and integrate between  $H = 6.1$  m at  $t = 0$  and  $H = 4.57$  m at  $t = t_F$ .]

**Ans.**  $t_F = 1388$  s

#### **4.2-11. Friction Loss in a Turbine**

**Water-Power System.** Water is stored in an elevated reservoir. To generate

power, water flows from this reservoir down through a large conduit to a turbine and then through a second, similar-sized conduit. At a point in the conduit 89.5 m above the turbine, the pressure is 172.4 kPa, and at a level 5 m below the turbine, the pressure is 89.6 kPa. The water flow rate is 0.800 m<sup>3</sup>/s. The output of the shaft of the turbine is 658 kW. The water density is 1000 kg/m<sup>3</sup>. If the efficiency of the turbine in converting the mechanical energy given up by the fluid to the turbine shaft is 89% ( $\eta_t = 0.89$ ), calculate the friction loss in the turbine in J/kg. Note that in the mechanical-energy-balance equation, the  $W_s$  is equal to the output of the shaft of the turbine over  $\eta_t$ .

$$\text{Ans.} = F = 85.3 \text{ J/kg}$$

#### **4.2-12. Pipeline Pumping of Oil.**

A pipeline laid cross-country carries oil at the rate of  $795 \text{ m}^3/\text{d}$ . The pressure of the oil is  $1793 \text{ kPa}$  gage leaving pumping station 1. The pressure is  $862 \text{ kPa}$  gage at the inlet to the next pumping station, 2. The second station is  $17.4 \text{ m}$  higher than the first station. Calculate the lost work  $0.1133 \text{ m}^3/\text{s}$ . friction loss) in  $\text{J/kg}$  mass oil. The oil density is  $769 \text{ kg/m}^3$ .

#### **4.2-13. Test of a Centrifugal Pump and Mechanical-Energy Balance.**

A centrifugal pump is being tested for performance, and during the test the pressure reading in the  $0.305\text{-m}$ -diameter suction line just adjacent to the pump casing is  $-20.7 \text{ kPa}$  (vacuum below atmospheric pressure). In the discharge line with a diameter of  $0.254 \text{ m}$  at a point  $2.53 \text{ m}$  above the suction

line, the pressure is 289.6 kPa gage. The flow of water from the pump is measured as 0.1133 m<sup>3</sup>/s. (The density can be assumed as 1000 kg/m<sup>3</sup>.) Calculate the kW input of the pump.

**Ans.** 38.11 kW

**4.2-14. Friction Loss in a Pump and Flow System.** Water at 20°C is pumped from the bottom of a large storage tank where the pressure is 310.3 kPa gage to a nozzle that is 15.25 m above the tank bottom and discharges to the atmosphere with a velocity in the nozzle of 19.81 m/s. The water flow rate is 45.4 kg/s. The efficiency of the pump is 80% and 7.5 kW are furnished to the pump shaft. Calculate the following:

- The friction loss in the pump
- The friction loss in the rest of the process

**4.2-15. Power for Pumping in a Flow System.** Water is being pumped from an open water reservoir at the rate of 2.0 kg/s at 10°C to an open storage tank 1500 m away. The pipe used is Schedule 40 312-in. pipe and the frictional losses in the system are 625 J/kg. The surface of the water reservoir is 20 m above the level of the storage tank. The pump has an efficiency of 75%.

- What is the kW power required for the pump?
- If the pump is not present in the system, will there be a flow?

**Ans.** (a) 1.143 kW

**4.3-1. Momentum Balance in a Reducing Bend.** Water is flowing at steady state through the reducing bend in Fig. 4.3-3. The angle  $\alpha_2 = 90^\circ$  (a right-angle bend). The pressure at point

2 is 1.0 atm abs. The flow rate is 0.020 m<sup>3</sup>/s and the diameters at points 1 and 2 are 0.050 m and 0.030 m, respectively. Neglect frictional and gravitational forces. Calculate the resultant forces on the bend in newtons and lb force. Use  $\rho = 1000 \text{ kg/m}^3$ .

**Ans.**  $-R_x = +450.0 \text{ N}$ ,  $-R_y = -565.8 \text{ N}$ .

**4.3-2. Forces on Reducing Bend.** Water is flowing at steady state and 363 K at a rate of 0.0566 m<sup>3</sup>/s through a 60° reducing bend ( $\alpha_2 = 60^\circ$ ) in Fig. 4.3-3. The inlet pipe diameter is 0.1016 m and the outlet 0.0762 m. The friction loss in the pipe bend can be estimated as  $v^2/5$ . Neglect gravity forces. The exit pressure  $p_2 = 111.5 \text{ kN/m}^2$  gage. Calculate the forces on the bend in newtons.



**Ans.**  $-R_x = +1344 \text{ N}$ ,  $-R_y = -1026 \text{ N}$

**4.3-3. Force of a Water Stream on a Wall.** Water at 298 K discharges from a nozzle and travels horizontally, hitting a flat, vertical wall. The nozzle has a diameter of 12 mm and the water leaves the nozzle with a flat velocity profile at a velocity of 6.0 m/s. Neglecting frictional resistance of the air on the jet, calculate the force in newtons on the wall.

**Ans.**  $-R_x = 4.059 \text{ N}$

**4.3-4. Flow Through an Expanding Bend.** Water at a steady-state rate of  $0.050 \text{ m}^3/\text{s}$  is flowing through an expanding bend that changes direction by  $120^\circ$ . The upstream diameter is 0.0762 m and the downstream diameter is 0.2112 m. The upstream pressure is

68.94 kPa gage. Neglect energy losses within the elbow and calculate the downstream pressure at 298 K. Also calculate  $R_x$  and  $R_y$ .

#### **4.3-5. *Force of a Stream on a Wall.***

Repeat Problem 4.3-3 for the same conditions except that the wall is inclined  $45^\circ$  to the vertical. The flow is frictionless. Assume no loss in energy. The amount of fluid splitting in each direction along the plate can be determined by using the continuity equation and a momentum balance. Calculate this flow division and the force on the wall.

**Ans.**  $m_2 = 0.5774 \text{ kg/s}$ ,  $m_3 = 0.09907 \text{ kg/s}$ ,  $-R_x = 2.030 \text{ N}$ ,  $-R_y = -2.030 \text{ N}$   
(force on wall).

**4.3-6. Momentum Balance for a Free Jet on a Curved, Fixed Vane.** A free jet having a velocity of 30.5 m/s and a diameter of  $5.08 \times 10^{-2}$  m is deflected by a curved, fixed vane as in Fig. 4.3-5a. However, the vane is curved downward at an angle of  $60^\circ$  instead of upward. Calculate the force of the jet on the vane. The density is 1000 kg/m<sup>3</sup>.

$$\text{Ans. } -R_x = 942.8 \text{ N}, -R_y = 1633 \text{ N}$$

**4.3-7. Momentum Balance for Free Jet on a U-Type, Fixed Vane.** A free jet having a velocity of 30.5 m/s and a diameter of  $1.0 \times 10^{-2}$  m is deflected by a smooth, fixed vane as in Fig. 4.3-5a. However, the vane is in the form of a U so that the exit jet travels in a direction exactly opposite to the entering jet. Calculate the force of the jet on the

vane. Use  $\rho = 1000 \text{ kg/m}^3$ .

$$\text{Ans. } -R_x = 146.1 \text{ N}, -R_y = 0$$

#### ***4.3-8. Momentum Balance on a Reducing Elbow and Friction Losses.***

Water at  $20^\circ\text{C}$  is flowing through a reducing bend, where  $\alpha_2$  (see Fig. 4.3-3) is  $120^\circ$ . The inlet pipe diameter is 1.829 m, the outlet is 1.219 m, and the flow rate is  $8.50 \text{ m}^3/\text{s}$ . The exit point  $z_2$  is 3.05 m above the inlet and the inlet pressure is 276 kPa gage. Friction losses are estimated as  $0.5v^2/2$  and the mass of water in the elbow is 8500 kg.

Calculate the forces  $R_x$  and  $R_y$  and the resultant force on the control-volume fluid.

#### ***4.3-9. Momentum Velocity Correction Factor $\beta$ for Turbulent Flow.***

Determine the momentum velocity correction factor  $\beta$  for turbulent flow in a tube. Use Eq. (4.2-20) for the relationship between  $v$  and position.

**4.4-1. *Film of Water on a Wetted-Wall Tower.*** Pure water at 20°C is flowing down a vertical wetted-wall column at a rate of 0.124 kg/s · m. Calculate the film thickness and the average velocity.

$$\text{Ans. } \delta = 3.370 \times 10^{-4} \text{ m, } v_{z \text{ av}} = 0.3687 \text{ m/s}$$

**4.4-2. *Shell Momentum Balance for Flow Between Parallel Plates.*** A fluid of constant density is flowing in laminar flow at steady state in the horizontal  $x$  direction between two flat and parallel plates. The distance between the two plates in the vertical  $y$  direction is  $2y_0$ .

Using a shell momentum balance, derive the equation for the velocity profile within this fluid and the maximum velocity for a distance  $L$  m in the  $x$  direction. [*Hint*: See the method used in Section 4.4B to derive Eq. (4.4-9). One boundary condition used is  $dv_x/dy = 0$  at  $y = 0$ .]

$$\text{Ans. } v_x = \frac{p_0 - p_L}{2\mu L} y^2 [1 - (y/Y_0)^2]$$

**4.4-3. Velocity Profile for a Non-Newtonian Fluid.** The stress rate of shear for a non-Newtonian fluid is given by

$$\tau_{rx} = K (-dv_x/dr)^n$$

where  $K$  and  $n$  are constants. Find the relation between velocity and radial position  $r$  for this incompressible fluid at steady state. [*Hint*: Combine the

equation given here with Eq. (4.4-6). Then, raise both sides of the resulting equation to the  $1/n$  power and integrate.]

$$\text{Ans. } v_x = \frac{n+1}{n} (p_0 - p_L) \frac{2K_L}{n} \left( \frac{R_0}{n} \right)^{n+1} \left[ 1 - \left( \frac{r}{R_0} \right)^{n+1} \right]^{1/n}$$

#### ***4.4-4. Shell Momentum Balance for a Flow Down an Inclined Plane.***

Consider the case of a Newtonian fluid in steady-state laminar flow down an inclined-plane surface that makes an angle  $\theta$  with the horizontal. Using a shell momentum balance, find the equation for the velocity profile within the liquid layer having a thickness  $L$  and the maximum velocity of the free surface. (*Hint:* The convective-momentum terms cancel for fully developed flow, and the pressure-force terms also cancel because of the

presence of a free surface. Note that there is a gravity force on the fluid.)

$$\mathbf{Ans.} \ v_{x \max} = \rho g L^2 \sin \theta / 2\mu$$

**Notation**



# Chapter 5. Incompressible and Compressible Flows in Pipes

## 5.0 Chapter Objectives

On completion of this chapter, a student should be able to:

- Identify the important geometrical properties used to describe flows in pipes
- Explain what is meant by the term *schedule pipe size*
- Differentiate and describe the velocity profile in a pipe for laminar and turbulent flow
- Explain why the velocity profile isn't uniform for flows in pipes
- Explain and calculate the maximum and average velocities for flows in pipes
- Calculate the pressure drop and frictional losses for flows in pipes
- Explain the concept of the friction factor
- Use the friction factor to determine pressure drop and

## frictional losses for flows in pipes

- Derive the expression for the friction factor for laminar flows in pipes
- Use friction-factor charts to determine the friction factor for flows in pipes
- Explain how pipe roughness affects the flows in pipes
- Calculate relative roughness for different pipe diameters and materials of construction
- Explain how heat transfer can affect fluid-flow behavior in a pipe
- Describe and calculate frictional losses associated with sudden expansions, contractions, and pipe fittings
- Apply frictional losses to the mechanical energy-balance equation to solve piping problems
- Describe how to account for frictional losses in noncircular ducts
- Explain the concept of entrance length in a pipe and how it is related to boundary layers
- Explain the difference between incompressible and compressible flows
- Calculate frictional losses for compressible fluids in a pipe
- Calculate the maximum velocity for adiabatic

compressible flow and explain how it is related to the Mach number

- Describe why it is necessary to measure and control the amount of fluid flows in a plant
- Describe the operational characteristics of pitot tubes, venturi meters, orifice meters, flow-nozzle meters and rotameters
- Calculate pressure drops and losses associated with flows in fluid metering devices

## **5.1 Design Equations for Laminar and Turbulent Flow in Pipes**

### **5.1A Velocity Profiles in Pipes**

One of the most important applications of fluid flow is the flow of fluids inside circular conduits, pipes, and tubes. Often, the flow behavior of fluids in these types of conduits is dependent on the size (e.g., diameter) of the conduits. As a reference, Appendix A.5 gives examples of commercial standard

steel-pipe sizes. Of those sizes, Schedule 40 pipe is a common standard. As a comparison, Schedule 80 pipe has a thicker wall and will withstand about twice the pressure of Schedule 40 pipe. The schedule number of a pipe refers to pipe thickness, or the difference between the outer and inner diameters. For example, 1-inch Schedule 40 and Schedule 80 pipes have the same *outer* diameter, but will have different *inner* diameters due to the different pipe thicknesses. Since both have the same outside diameter, they can use the same fittings. Sizes of tubing are generally given by the outside diameter and wall thickness. Perry and Green (P1) give detailed tables of various types of tubing and pipes.

When a fluid is flowing in a circular pipe and the velocities are measured at different distances from the pipe wall to the center of the pipe, it has been shown that for both laminar and turbulent flow, the fluid in the center of the pipe is moving faster than the fluid near the walls.

Figure 5.1-1 is a plot of the relative distance from the center of the pipe versus the fraction of maximum velocity  $v/v_{\max}$ , where  $v$  is local velocity at the given radial position and  $v_{\max}$  the maximum velocity at the center of the pipe. For viscous or laminar flow, the velocity profile is a true parabola, as derived in Eq. (4.4-9). The velocity at the wall is zero.

In many engineering applications, the

relation between the average velocity  $v_{av}$  in a pipe and the maximum velocity  $v_{max}$  is useful, since in some cases only the  $v_{max}$  at the center point of the tube is measured. Hence, from only one point measurement, this relationship between  $v_{max}$  and  $v_{av}$  can be used to determine  $v_{av}$ .

In Fig. 5.1-2, experimentally measured values of  $v_{av}/v_{max}$  are plotted as a function of the Reynolds numbers  $Dv_{av} \rho/\mu$  and  $Dv_{max} \rho/\mu$ .

The average velocity over the whole cross section of the pipe is precisely 0.5 times the maximum velocity at the center as given by the shell momentum balance in Eq. (4.4-13) for laminar flow. On the other hand, for turbulent flow, the curve is somewhat flattened in the

center (see Fig. 5.1-1) and the average velocity is about 0.8 times the maximum. This value of 0.8 varies slightly, depending upon the Reynolds number, as shown in the correlation in Fig. 5.1-2. (*Note:* See Problem 4.1-3, where a value of 0.817 is derived using the 17-power law.)

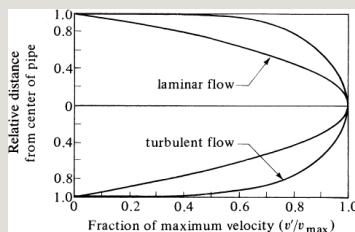


Figure 5.1-1. Velocity distribution of a fluid across a pipe.

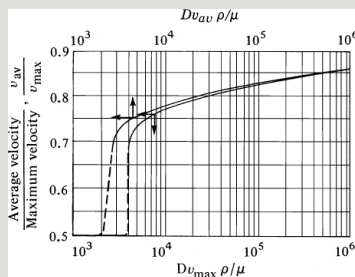


Figure 5.1-2. Ratio  $v_{av}/v_{max}$  as a function of different Reynolds number for pipes.

## 5.1B Pressure Drop and Friction Loss in Laminar Flow

*1. Pressure drop and loss due to friction.* When the fluid in a pipe is flowing at steady-state in the laminar flow regime, then, for a Newtonian fluid, the shear stress is given by Eq. (3.1-2), which is rewritten for change in radius  $dr$  rather than distance  $dy$ , as follows:

$$\tau_{rz} = -\mu dv_z/dr \quad (5.1-1)$$

Using this relationship and making a shell momentum balance on the fluid over a cylindrical shell, the Hagen–Poiseuille equation (4.4-11) for laminar flow of a liquid in a circular tube is obtained. This can be written as

$$\Delta p_f = (p_1 - p_2)_f = \frac{32\mu v(L^2 - L_1^2)}{D^2} \quad (5.1-2)$$



where  $p_1$  is upstream pressure at point 1, N/m<sup>2</sup>;  $p_2$  is pressure at point 2;  $v$  is average velocity in tube, m/s;  $D$  is inside diameter, m; and  $(L_2 - L_1)$  or  $\Delta L$  is length of the straight tube, m. For English units, the right-hand side of Eq. (5.1-2) is divided by  $g_c$ . The quantity  $(p_1 - p_2)_f$  or  $\Delta p_f$  is the pressure loss due to skin friction caused by the flowing fluid. Then, for constant  $\rho$ , the friction loss  $F_f$  is

$$F_f = \frac{(p_1 - p_2)_f}{\rho} = \frac{N \cdot m}{kg} \text{ (SI)} \quad F_f = \frac{ft \cdot lb_f}{lb_m} \text{ (English)}$$

(5.1-3)

This is the mechanical energy loss due to skin friction for the pipe in N · m/kg of fluid and is part of the  $\Sigma F$  term for frictional losses in the mechanical-energy-balance equation (4.2-28). This

term  $(p_1 - p_2)_f$  for skin-friction loss is different from the  $(p_1 - p_2)$  term, owing to velocity head or potential head changes in Eq. (4.2-28). That part of  $\Sigma F$  that arises from friction within the channel itself by laminar or turbulent flow is discussed in Sections 5.1B and 5.1C. The part of friction loss due to fittings (valves, elbows, etc.), bends, and the like, which sometimes constitute a large part of the friction, is discussed in Section 5.1F. Note that if Eq. (4.2-28) is applied to steady flow in a straight, horizontal tube, we obtain  $(p_1 - p_2)/\rho = \Sigma F$ .

One of the uses of Eq. (5.1-2) is in the experimental measurement of the viscosity of a fluid by measuring the pressure drop and volumetric flow rate through a tube of known length and

diameter. Often, slight corrections for kinetic energy and entrance effects are usually necessary in practice. Also, Eq. (5.1-2) is frequently used in the metering of small liquid flows.

**EXAMPLE 5.1-1. Metering of Small Liquid Flows**

A small capillary with an inside diameter of  $2.22 \times 10^{-3}$  m and a length 0.317 m is being used to continuously measure the flow rate of a liquid having a density of 875 kg/m<sup>3</sup> and a viscosity of  $1.13 \times 10^{-3}$  Pa · s. The pressure drop reading across the capillary during flow is 0.0655 m water (the density of water can be assumed to be 996 kg/m<sup>3</sup>). What is the flow rate in m<sup>3</sup>/s if end-effect corrections are neglected?

**Solution:** Assuming that the flow is laminar, Eq. (5.1-2) will be used. First, to convert the height  $h$  of 0.0655 m water to a pressure drop, use Eq. (2.2-4),

$$\Delta p_f = h \rho g = (0.0655 \text{ m}) (996 \text{ kg/m}^3) (9.80665 \text{ m/s}^2) = 640 \text{ kg} \cdot \text{m/s}^2 \cdot \text{m}^2 = 640 \text{ N/m}^2$$

Substituting into Eq. (5.1-2) the values  $\mu = 1.13 \times 10^{-3}$  Pa · s,  $L_2 - L_1 = 0.317$  m,  $D = 2.22 \times 10^{-3}$  m, and  $\Delta p_f = 640$  N/m<sup>2</sup>, and solving for  $v$ ,

$$\Delta p_f = 32 \mu v (L_2 - L_1) / D^2 \quad 640 = 32(1.13 \times 10^{-3})(v)(0.317) / (2.22 \times 10^{-3})^2 \quad v = 0.275 \text{ m/s}$$

The volumetric rate is then given as

$$\text{volumetric flow rate} = v \pi D^2 L / 4 = 0.275(\pi) (2.22 \times 10^{-3})^2 (0.317) / 4 = 1.066 \times 10^{-6} \text{ m}^3/\text{s}$$

Since it was assumed that laminar flow is occurring, the Reynolds number will be calculated to check this:

$$N_{Re} = D v \rho / \mu = (2.22 \times 10^{-3})(0.275)(875) / 1.13 \times 10^{-3} = 473$$

2. *Use of friction factor for friction loss in laminar flow.* A common parameter used in laminar and especially in turbulent flow is the *Fanning friction factor*,  $f$ , which is defined as the drag force per wetted surface unit area (shear stress  $\tau_s$  at the surface) divided by the product of density times velocity head, or  $12\rho v^2$ . Thus, the drag force is  $\Delta p f$  times the cross-sectional area  $\pi R^2$  and the wetted surface area is  $2\pi R\Delta L$ . Hence, the relation between the pressure drop due to friction and  $f$  is as follows for both laminar and turbulent flow:

$$\Delta p f = \tau_s \frac{2\pi R \Delta L}{\pi R^2} = 2\Delta L \frac{\tau_s}{R} = 2\Delta L \frac{\rho v^2}{2} = \rho v^2 \Delta L \quad (5.1-4)$$

Rearranging Eq. (5.1-4) and using  $D = 2R$  yields

$$f_p = 4 \frac{\Delta P}{L} \frac{D}{v^2} \quad (\text{SI}) \quad f_p = 4 \frac{\Delta P}{L} \frac{D}{v^2} \quad (\text{English}) \quad (5.1-5)$$

$$f_p = 4 \frac{\Delta P}{L} \frac{D}{v^2} \quad (\text{SI}) \quad f_p = 4 \frac{\Delta P}{L} \frac{D}{v^2} \quad (\text{English}) \quad (5.1-6)$$

For laminar flow only, combining Eqs. (5.1-2) and (5.1-5) yields the following expression for the friction factor,

$$f = \frac{16}{N_{Re}} = \frac{16 \mu}{D v} \quad (5.1-7)$$

Equations (5.1-2), (5.1-5), (5.1-6), and (5.1-7) for laminar flow are valid for Reynolds numbers up to around 2100. Beyond that, at a  $N_{Re}$  value above 2100, Eqs. (5.1-2) and (5.1-7) do not hold for turbulent flow. However, for turbulent flow, Eqs. (5.1-5) and (5.1-6), are used extensively along with empirical methods for predicting the friction factor  $f$ , as discussed in the next section.

### EXAMPLE 5.1-2. Use of Friction Factor in Laminar Flow

Assume the same known conditions as in Example 5.1-1 except that the velocity of 0.275 m/s is known and the pressure drop  $\Delta p_f$  is to be predicted. Use the Fanning friction factor method.

**Solution:** The Reynolds number is, as before,

$$N_{Re} = Dv\rho\mu = (22.2 \times 10^{-3} \text{ m})(0.275 \text{ m/s})(875 \text{ kg/m}^3) / (1.13 \times 10^{-3} \text{ kg/m}\cdot\text{s}) = 473$$

From Eq. (5.1-7) the friction factor  $f$  is

$$f = 16/N_{Re} = 16/473 = 0.0338 \quad (\text{dimensionless})$$

Using Eq. (5.1-5) with  $\Delta L = 0.317 \text{ m}$ ,  $v = 0.275 \text{ m/s}$ ,  $D = 2.22 \times 10^{-3} \text{ m}$ , and  $\rho = 875 \text{ kg/m}^3$ ,

$$\Delta p_f = 4 f \rho \Delta L D v^2 = 4(0.0338)(875)(0.317)(0.275)^2 / (2.22 \times 10^{-3}) = 640 \text{ N/m}^2$$

This, of course, agrees with the value in Example 5.1-1.

When the fluid is a gas and not a liquid, the Hagen–Poiseuille equation (5.1-2) can be written as follows for laminar flow:

$$\begin{aligned} m &= \pi D^4 M (p_1^2 - p_2^2) / (128 (2RT) \mu (L_2 - L_1)) \\ (\text{SI}) \quad m &= \pi D^4 g_c M (p_1^2 - p_2^2) / (128 (2RT) \mu (L_2 - L_1)) \quad (\text{English}) \\ & \quad (5.1-8) \end{aligned}$$

where  $m = \text{kg/s}$ ,  $M = \text{molecular weight in kg/kg mol}$ ,  $T = \text{absolute temperature in K}$ , and  $R = 8314.3 \text{ N} \cdot \text{m/kg mol} \cdot \text{K}$ . In English units,  $R = 1545.3 \text{ ft} \cdot \text{lb/lb mol} \cdot ^\circ\text{R}$ .

## 5.1C Pressure Drop and Friction Factor in Turbulent Flow

In turbulent flow, as in laminar flow, the friction factor also depends on the Reynolds number. However, it is

not possible to theoretically predict the Fanning friction factor  $f$  for turbulent flow as was shown previously for laminar flow. The friction factor must be determined empirically (experimentally), and it not only depends upon the Reynolds number but also on the pipe's surface roughness. In laminar flow, the roughness has essentially no effect. Dimensional analysis can also be used to show the dependence of the friction factor on these factors.

A large number of experimental data on friction factors for both smooth pipes and pipes with varying degrees of equivalent roughness have been obtained and correlated. For design purposes, to predict the friction factor  $f$  and, hence, the frictional pressure drop

for round pipes, the friction-factor chart in Fig. 5.1-3 can be used. It is a log–log plot of  $f$  versus  $N_{Re}$ . The friction factor  $f$  is then used in Eqs. (5.1-5) and (5.1-6) to predict the friction loss  $\Delta p_f$  or  $F_f$ :

$$\Delta p_f = 4 f \frac{L}{D} \frac{\rho v^2}{2} \quad (\text{SI}) \quad \Delta p_f = 4 f \frac{L}{D} \frac{\rho v^2}{2} g_c \quad (\text{English}) \quad (5.1-5)$$

$$F_f = 4 f \frac{L}{D} \frac{\rho v^2}{2} \quad (\text{SI}) \quad F_f = 4 f \frac{L}{D} \frac{\rho v^2}{2} g_c \quad (\text{English}) \quad (5.1-6)$$

For the region with a Reynolds number below 2100, the line is the same as given in Eq. (5.1-7). For a Reynolds number above 4000 for turbulent flow, the lowest line in Fig. 5.1-3 represents the friction-factor line for smooth pipes and tubes, such as glass tubes and drawn copper and brass tubes. The other lines, for higher friction factors, represent



lines for different relative roughness factors,  $\varepsilon/D$ , where  $D$  is the inside pipe diameter in m and  $\varepsilon$  is a roughness parameter, which represents the average height in m of roughness projections from the wall (M1). In Fig. 5.1-3, values for the equivalent roughness of new pipes are given (M1). The most common pipe, commercial steel, has a roughness of  $\varepsilon = 4.6 \times 10^{-5}$  m ( $1.5 \times 10^{-4}$  ft).

The reader should be cautioned about using friction factors  $f$  from other sources. The Fanning friction factor  $f$  in Eq. (5.1-6) is the one used here. Others use a friction factor (i.e., Darcy friction factor) that may be four times larger.

**EXAMPLE 5.1-3. Use of Friction Factor in Turbulent Flow**

A liquid is flowing through a horizontal straight pipe at a velocity of 4.57 m/s. The pipe used is commercial steel,

Schedule 40, 2 in. nominal diameter. The viscosity of the liquid is 4.46 cp and its density is 801 kg/m<sup>3</sup>. Calculate the mechanical-energy friction loss  $F_f$  in J/kg and the pressure drop in kPa for a 36.6 m section of pipe.

**Solution:** The following data are given: From Appendix A.5,  $D = 0.0525$  m,  $v = 4.57$  m/s,  $\rho = 801$  kg/m<sup>3</sup>,  $\Delta L = 36.6$  m and

$$\mu = (4.46 \text{ cp})(1 \times 10^{-3}) = 4.46 \times 10^{-3} \text{ kg/m} \cdot \text{s}$$

The Reynolds number is calculated as

$$\text{NRe} = Dv\rho/\mu = 0.0525(4.57)(801)/4.46 \times 10^{-3} = 4.310 \times 10^4$$

Hence, the flow is turbulent. For commercial steel pipe from the table in Fig. 5.1-3, the equivalent roughness is  $4.6 \times 10^{-5}$  m:

$$\epsilon D = 4.6 \times 10^{-5} \text{ m} / 0.0525 \text{ m} = 0.00088$$

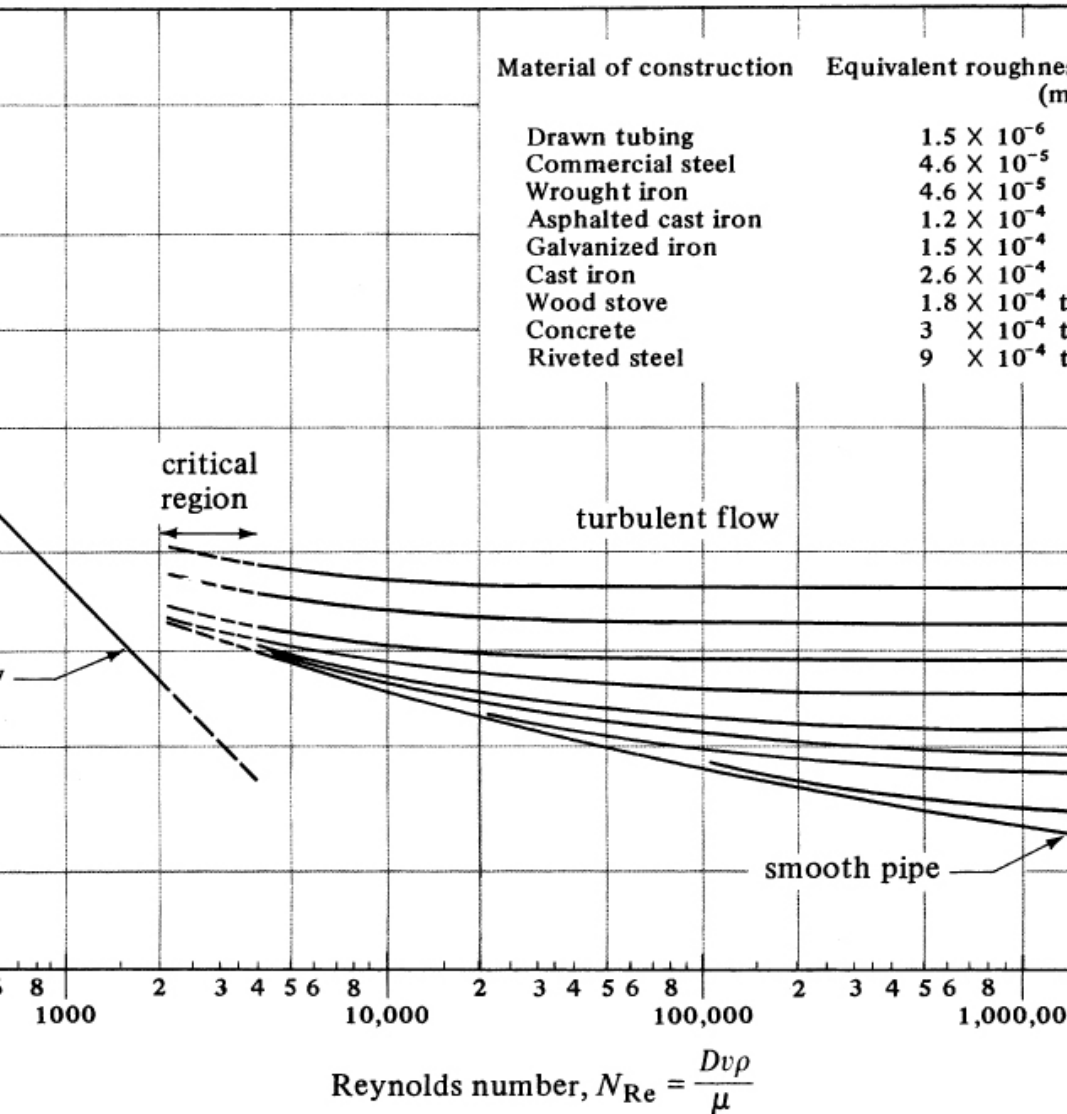


Figure 5.1-3. Friction factors for fluids inside pipes. Based on L. F. Moody, Trans. A.S.M.E., 66, 671 (1944): Mech. Eng. 69, 1005 (1947). With permission.

For a  $N_{Re}$  of  $4.310 \times 10^4$ , the friction factor from Fig. 5.1-3 is  $f = 0.006$ . Substituting into Eq. (5.1-6), the friction loss is

$$Ff = 4f\Delta LDv^2 = 4(0.006)(36.6)(4.57)^2(0.0525) \\ (2) = 174.8 \text{ J/kg} (58.5 \text{ ft} \cdot \text{lb} / \text{bm})$$

The previously calculated friction factor can be used to

calculate the pressure drop in Eq. 5.1-5:

$$\Delta p_f = 4f\rho\Delta L D v^2 = 4(0.006)(801)(36.6)(0.0525) \\ (4.57)^2(2)\Delta p_f = 139948 \text{ Pa} \approx 140 \text{ kPa} \text{ (20.3 psi)}$$

In problems involving the friction loss  $F_f$  in pipes,  $F_f$  is usually the unknown, with the diameter  $D$ , velocity  $v$ , and pipe length  $\Delta L$  known. For these problems, a direct solution is possible, as in Example 5.1-3. However, in some cases, the friction loss  $F_f$  is already set by the available head of liquid. Then, if the volumetric flow rate and pipe length are set, the unknown to be calculated is the diameter. This solution must be determined by trial and error, since the velocity  $v$  appears in both  $N_{Re}$  and  $f$ , which are unknown. In another case, with  $F_f$  again being already set, the diameter and pipe length are specified. This solution is also determined by trial and error, to calculate the velocity.

Example 5.1-4 presents the method to be used to calculate the pipe diameter with  $F_f$  set. Others (M2) give a convenient chart to aid in these types of calculations.

#### **EXAMPLE 5.1-4. Trial-and-Error Solution to Calculate Pipe Diameter**

Water at 4.4°C is to flow through a horizontal, commercial steel pipe having a length of 305 m at the rate of 150 gal/min. If a head of water of 6.1 m is available to overcome the friction loss  $F_f$ , calculate the pipe diameter.

**Solution:** From Appendix A.2, the density  $\rho = 1000 \text{ kg/m}^3$  and the viscosity  $\mu$  is

$$\mu = (1.55 \text{ cp})(1 \times 10^{-3}) = 1.55 \times 10^{-3} \text{ kg/m} \cdot \text{s} \\ \text{friction loss } F_f = (6.1 \text{ m})g = (6.1)(9.80665) = 59.82 \text{ J/kg} \\ \text{flow rate} = (150 \text{ gal/min})(1 \text{ ft}^3/7.481 \text{ gal})(1 \text{ min}/60 \text{ s}) \\ (0.028317 \text{ m}^3/\text{ft}^3) = 9.46 \times 10^{-3} \text{ m}^3/\text{s} \\ \text{sarea of pipe} = \pi D^2/4 \text{ m}^2 \quad (D \text{ is unknown}) \\ \text{velocity } v = (9.46 \times 10^{-3} \text{ m}^3/\text{s})/(\pi D^2/4 \text{ m}^2) = 0.01204/D^2 \text{ m/s}$$

The solution is by trial and error since  $v$  appears in  $N_{Re}$  and  $f$ . Assume that  $D = 0.089 \text{ m}$  for the first trial.

$$N_{Re} = Dv\rho\mu = (0.089)(0.01204)(1000) \\ (0.089)^2(1.55 \times 10^{-3}) = 8.730 \times 10^4$$

For commercial steel pipe and using Fig. 5.1-3,  $\varepsilon = 4.6 \times 10^{-5}$  m. Then,

$$\varepsilon/D = 4.6 \times 10^{-5} / 0.089 \text{ m} = 0.00052$$

From Fig. 5.1-3 for  $N_{Re} = 8.730 \times 10^4$  and  $\varepsilon/D = 0.00052$ ,  $f = 0.0051$ . Substituting into Eq. (5.1-6),

$$Ff = 59.82 = 4f\Delta L D v^2 = 4(0.0051)(305)D(2)(0.01204)^2 D^4$$

Solving for  $D$ ,  $D = 0.0945$  m. This does not agree with the assumed value of 0.089 m.

For the second trial,  $D$  will be assumed to be 0.0945 m.

$$N_{Re} = (0.0945)0.01204(0.0945)^2 1000 / 1.55 \times 10^{-3} = 8.220 \times 10^4 \quad \varepsilon/D = 4.6 \times 10^{-5} / 0.0945 = 0.00049$$

From Fig. 5.1-3,  $f = 0.0052$ . It can be seen that  $f$  does not change much with  $N_{Re}$  in the turbulent region:

$$Ff = 59.82 = 4(0.0052)(305)D(2)(0.01204)^2 D^4$$

Solving,  $D = 0.0954$  m or 3.75 in. Hence, the solution agrees closely with the assumed value of  $D$ .

## 5.1D Pressure Drop and Friction Factor in the Flow of Gases

The equations and methods discussed in this section for turbulent flow in pipes hold for incompressible liquids. They also hold for a gas if the density (or the pressure) changes by less than 10%. Then, an average density  $\rho_{av}$  in  $\text{kg/m}^3$ , should be used and the errors involved will be less

than the uncertainty limits in the friction factor  $f$ . For gases, Eq. (5.1-5) can be rewritten as follows for laminar and turbulent flow:

$$(p_1 - p_2)f = 4f\Delta LG^2 D^2 \rho_{av} \quad (5.1-9)$$

where  $\rho_{av}$  is the density at the average pressure,  $p_{av} = (p_1 + p_2)/2$ . Also, the  $N_{Re}$  used is  $DG/\mu$ , where  $G$  has units of  $\text{kg}/\text{m}^2 \cdot \text{s}$  and is a constant independent of the density and velocity variations for the gas unless the diameter changes along the length of piping. Equation (5.1-5) can also be written for gases as

$$\begin{aligned} p_1 - p_2 &= 4f\Delta LG^2 RTDM \quad (\text{SI}) \\ p_1 - p_2 &= 4f\Delta LG^2 RTgcDM \quad (\text{English}) \end{aligned} \quad (5.1-10)$$

where  $R$  is  $8314.3 \text{ J/kg mol} \cdot \text{K}$  or  $1545.3 \text{ ft} \cdot \text{lbf/lb mol} \cdot ^\circ\text{R}$  and  $M$  is the

molecular weight.

The derivation of Eqs. (5.1-9) and (5.1-10) applies only to cases with gases where the relative pressure change is small enough that large changes in velocity do not occur. If the exit velocity becomes large, the kinetic energy term, which has been omitted, becomes important. For pressure changes above about 10%, compressible flow is occurring, and the reader should refer to Section 5.2. In adiabatic flow in a uniform pipe, the velocity in the pipe cannot exceed the velocity of sound.

**EXAMPLE 5.1-5. Flow of Gas in Line and Pressure Drop**

Nitrogen gas at 25°C is flowing in a smooth tube having an inside diameter of 0.010 m at a flux of  $9.0 \text{ kg/s} \cdot \text{m}^2$ . The tube is 200 m long and the flow can be assumed to be isothermal. The pressure at the entrance to the tube is  $2.0265 \times 10^5 \text{ Pa}$ . Calculate the outlet pressure.

**Solution:** The viscosity of the gas from Appendix A.3 is  $\mu = 1.77 \times 10^{-5} \text{ Pa} \cdot \text{s}$  at  $T = 298.15 \text{ K}$ . Inlet gas pressure is  $p_1 = 2.0265 \times 10^5 \text{ Pa}$ ,  $G = 9.0 \text{ kg/s} \cdot \text{m}^2$ ,  $D = 0.010 \text{ m}$ ,  $M = 28.02 \text{ kg/kg mol}$ ,  $\Delta L = 200 \text{ m}$ , and  $R = 8314.3 \text{ J/kg mol} \cdot \text{K}$ .

Assuming that Eq. (5.1-10) holds for this case and that the pressure drop is less than 10%, the Reynolds number is

$$\text{NRe} = \frac{DG\mu}{0.010(9.0)1.77 \times 10^{-5}} = 5085$$

Hence, the flow is turbulent. Using Fig. 5.1-3,  $f = 0.0090$  for a smooth tube. Substituting into Eq. (5.1-10),

$$\begin{aligned} p_{12} - p_{22} &= 4f \Delta L G^2 R T D M (2.0265 \times 10^5)^2 - p_{22} = 4(0.0090)(200) \\ &\quad (9.0)^2 (8314.3)(298.15) 0.010 (28.02) 4.1067 \times 10^{10} - \\ &\quad p_{22} = 0.5160 \times 10^{10} \end{aligned}$$

Solving,  $p_2 = 1.895 \times 10^5$  Pa. Hence, Eq. (5.1-10) can be used, since the pressure drop is less than 10%.

### 5.1E Effect of Heat Transfer on the Friction Factor

The friction factor  $f$  in Fig. 5.1-3 is given for isothermal flow, that is, no heat transfer. When a fluid is being heated or cooled, the temperature gradient will cause a change in the physical properties of the fluid, especially its viscosity. For engineering practice, the following method of Sieder and Tate (S3) can be used to predict the friction factor for nonisothermal flow for liquids and gases:



1. Calculate the mean bulk temperature  $t_a$  as the average of the inlet and outlet bulk-fluid temperatures.
2. Calculate the  $N_{Re}$  using the viscosity  $\mu_a$  at  $t_a$  and use Fig. 5.1-3 to obtain  $f$ .
3. Using the tube wall temperature  $t_w$ , determine  $\mu_w$  at  $t_w$ .
4. Calculate  $\psi$  for the appropriate case:

$$\psi = (\mu_a \mu_w)^{0.17} \text{ (heating) } N_{Re} > 2100 \text{ (5.1-11)}$$

$$\psi = (\mu_a \mu_w)^{0.11} \text{ (cooling) } N_{Re} > 2100 \text{ (5.1-12)}$$

$$\psi = (\mu_a \mu_w)^{0.38} \text{ (heating) } N_{Re} < 2100 \text{ (5.1-13)}$$

$$\psi = (\mu_a \mu_w)^{0.23} \text{ (cooling) } N_{Re} < 2100 \text{ (5.1-14)}$$

5. The final friction factor is obtained by dividing  $f$  from step 2 by  $\psi$  from step 4.

Hence, when the liquid is being heated,  $\psi$  is greater than 1.0 and the final  $f$  decreases. The reverse occurs when cooling the liquid.

### 5.1F Friction Losses in Expansion, Contraction, and Pipe Fittings

Skin-friction losses in fluid flow through straight pipes are calculated

by using the Fanning friction factor. However, if the velocity of the fluid is changed in direction or magnitude, additional friction losses may occur. These result from further turbulence that develops because of vortices and other factors. Methods for estimating these losses are discussed below.

*1. Sudden enlargement losses.* If the cross section of a pipe enlarges very gradually, few or no extra losses are incurred. If the change is sudden, it results in additional losses due to eddies formed by the jet expanding in the enlarged section. This friction loss can be calculated by applying Eq. (4.3-36), which was derived for flows involving sudden enlargements:

$$h_{ex} = \frac{(v_1 - v_2)^2}{2g} \alpha = (1 -$$

$$\frac{A_1}{A_2} \left( \frac{v_1^2}{v_2^2} - 1 \right) = K_{ex} \alpha \quad (5.1-15)$$

where  $h_{ex}$  is the friction loss in J/kg,  $K_{ex}$  is the expansion-loss coefficient and equals  $(1 - A_1/A_2)^2$ ,  $v_1$  is the upstream velocity in the smaller area in m/s,  $v_2$  is the downstream velocity, and  $\alpha = 1.0$ . If the flow is laminar in both sections, the factor  $\alpha$  in the equation becomes 12. For English units, the right-hand side of Eq. (5.1-15) is divided by  $g_c$ . Also,  $h = \text{ft} \cdot \text{lbf/lbm}$ .

2. *Sudden contraction losses.* When the cross section of the pipe is suddenly reduced, the stream cannot follow around the sharp corner and additional frictional losses due to eddies occur. For turbulent flow, this is given by

$$h_c = 0.55 \left( 1 - \frac{A_2}{A_1} \right) \frac{v_1^2}{2}$$

$$A_2/A_1) v_2^2 \alpha = K_c v_2^2 \alpha / g_c \quad (5.1-16)$$

where  $h_c$  is the friction loss,  $\alpha = 1.0$  for turbulent flow,  $v_2$  is the average velocity in the smaller or downstream section, and  $K_c$  is the contraction-loss coefficient (P1) and approximately equals  $0.55(1 - A_2/A_1)$ . For laminar flow, the same equation can be used with  $\alpha = 12$  (S2). For English units, the right side is divided by  $g_c$ .

*3. Losses in fittings and valves.* Pipe fittings and valves also disturb the normal flow lines in a pipe and cause additional friction losses. In a short pipe with many fittings, the friction loss from these fittings could be greater than in the straight pipe. The friction loss for fittings and valves is given by the following equation:

$$h_f = K_f v^2 \quad (5.1-17)$$

where  $K_f$  is the loss factor for the fitting or valve and  $v$  is the average velocity in the pipe leading to the fitting.

Experimental values for  $K_f$  are given in Table 5.1-1 for turbulent flow (P1) and in Table 5.1-2 for laminar flow.

As an alternative method, some texts and references (B1) give data for losses in fittings as an equivalent pipe length in pipe diameters. These data, also given in Table 5.1-1, are presented as  $L_e/D$ , where  $L_e$  is the equivalent length of straight pipe having the same frictional loss as the fitting, and  $D$  is the inside pipe diameter. The  $K$  values in Eqs. (5.1-15) and (5.1-16) can be converted to as  $L_e/D$  values by multiplying the  $K$  by 50 (P1). The  $L_e$  values for the fittings

are simply added to the length of the straight pipe to get the total length of equivalent straight pipe to use in Eq. (5.1-6).

Table 5.1-1. *Friction Loss for Turbulent Flow Through Valves and Fittings*

--

Source: R. H. Perry and C. H. Chilton, *Chemical Engineers' Handbook*, 5th ed. New York: McGraw-Hill Book Company, 1973. With permission.

Table 5.1-2. *Friction Loss for Laminar Flow Through Valves and Fittings (K1)*

--

4. *Frictional losses in the mechanical-energy-balance equation.* The frictional losses due to the friction in the straight pipe (Fanning friction factor), enlargement losses, contraction losses, and losses in fittings and valves are all

incorporated into the  $\Sigma F$  term of Eq. (4.2-28) for the mechanical-energy balance, so that

$$f\Delta L D v^2/2 + K_{ex} v_1^2/2 + K_{cv} v^2/2 + K_{fv} v^2/2 \quad (5.1-18)$$

If all the velocities,  $v$ ,  $v_1$ , and  $v_2$  are the same, then by factoring, Eq. (5.1-18) becomes, for this special case,

$$\Sigma F = (4f\Delta L D + K_{ex} + K_{cv} + K_{fv}) v^2/2 \quad (5.1-19)$$

The use of the mechanical-energy-balance equation (4.2-28) along with Eq. (5.1-18) will be shown in the following examples.

**EXAMPLE 5.1-6. Friction Losses and Mechanical Energy Balance**

An elevated storage tank contains water at 82.2°C, as shown in Fig. 5.1-4. It is desired to have a discharge rate at point 2 of 100 gal/min (0.223 ft<sup>3</sup>/s). What must be the height  $H$  in ft of the water's surface in the tank relative to the discharge point? The pipe used is commercial steel pipe,

Schedule 40, and the lengths of the straight portions of the pipe are shown.

**Solution:** The mechanical-energy-balance equation (4.2-28) is written between points 1 and 2.

$$z_1 g g_c + v_1^2 / 2 \alpha g_c + (p_1 / \rho - p_2 / \rho) - W_S = z_2 g g_c + v_2^2 / 2 \alpha g_c + \sum F \quad (5.1-20)$$

From Appendix A.2, for water,  $\rho = 0.970(62.43) = 60.52$  lbm/ft<sup>3</sup> and  $\mu = 0.347$  cp =  $0.347 (6.7197 \times 10^{-4}) = 2.33 \times 10^{-4}$  lbm/ft · s. The diameters of the pipes are:

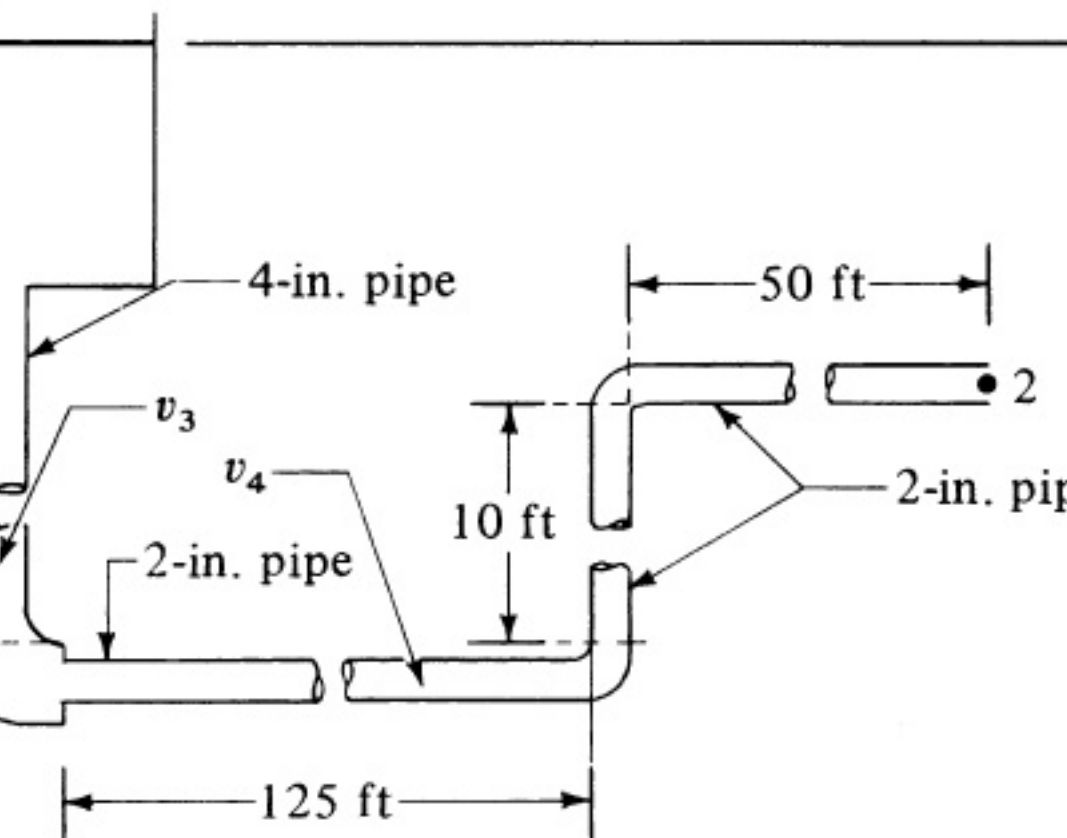


Figure 5.1-4. Process flow diagram for Example 5.1-6.

For 4-in. pipe:  $D_3 = 4.02612 = 0.3353$  ft;  $A_3 = 0.0884$  ft<sup>2</sup> For 2-



$$\text{in. pipe: } D_4 = 2.06712 = 0.1722 \text{ ft; } A_4 = 0.02330 \text{ ft}^2$$

The velocities in the 4-in. and 2-in. pipe are

$$v_3 = 0.223 \text{ ft/s} \quad v_4 = 0.2230.02330 = 9.57 \text{ ft/s} \quad (4\text{-in. pipe})$$

The  $\Sigma F$  term for frictional losses in the system includes the following: (1) contraction loss at tank exit, (2) friction in the 4-in. straight pipe, (3) friction in 4-in. elbow, (4) contraction loss from 4-in. to 2-in. pipe, (5) friction in the 2-in. straight pipe, and (6) friction in the two 2-in. elbows. Calculations for the six items are as follows:

1. *Contraction loss at tank exit.* From Eq. (5.1-16), for contraction from  $A_1$  to  $A_3$  cross-sectional area, since  $A_1$  of the tank is very large compared to  $A_3$ ,

$$K_c = 0.55(1 - A_3/A_1) = 0.55(1 - 0) = 0.55$$

$$h_{c3} = K_c v_3^2 / 2g = 0.55(2.523)^2 / (2 \times 32.174) = 0.054 \text{ ft} \cdot \text{lbf/lbm}$$

2. *Friction in the 4-in. pipe.* The Reynolds number is

$$N_{Re} = D_3 v_3 \rho / \mu = 0.3353(2.523)(60.52) / 2.33 \times 10^{-4} = 2.193 \times 10^5$$

Hence, the flow is turbulent. From Fig. 5.1-3,  $\varepsilon = 4.6 \times 10^{-5} \text{ m}$  ( $1.5 \times 10^{-4} \text{ ft}$ ).

$$\varepsilon / D_3 = 0.000150.3353 = 0.000448$$

Then, for  $N_{Re} = 219300$ , the Fanning friction factor  $f = 0.0047$ . Substituting into Eq. (5.1-6) for  $\Delta L = 20.0 \text{ ft}$  of 4-in. pipe,

$$F_f = 4f \Delta L D v_3^2 / 2g = 4(0.0047)20.00.3353(2.523)^2 / (2 \times 32.174) = 0.111 \text{ ft} \cdot \text{lbf/lbm}$$

3. *Friction in 4-in. elbow.* From Table 5.1-1,  $K_f = 0.75$ .

Then, substituting into Eq. (5.1-17),

$$h_f = K_f v_3^2 / 2g = 0.75(2.523)^2 / (2 \times 32.174) = 0.074 \text{ ft} \cdot \text{lbf/lbm}$$

4. *Contraction loss from 4- to 2-in. pipe.* Using Eq. (5.1-16) again for contraction from  $A_3$  to  $A_4$  cross-sectional area,

$$K_c = 0.55(1 - A_4/A_3) = 0.55(1 - 0.023300.0884) = 0.405$$

$$h_{c4} = K_c v_4^2 / 2g = 0.405(9.57)^2 / (2 \times 32.174) = 0.575 \text{ ft} \cdot \text{lbf/lbm}$$

5. *Friction in the 2-in. pipe.* The Reynolds number is

$$\text{NRe} = D_4 v_4 \rho \mu = 0.1722(9.57) \\ (60.52)2.33 \times 10^{-4} = 4.280 \times 10^5 \varepsilon D = 0.000150.1722 = 0.00087$$

The Fanning friction factor from Fig. 5.1-3 is  $f = 0.0048$ . The total length  $\Delta L = 125 + 10 + 50 = 185$  ft. Substituting into Eq. (5.1-6),

$$F_f = 4f \Delta L D v^2 g_c = 4(0.0048)185(9.57)^2(0.1722)(2) \\ (32.174) = 29.4 \text{ ft} \cdot \text{lb}_f/\text{lb}_m$$

6. *Friction in the two 2-in. elbows.* For a  $K_f = 0.75$  and two elbows,

$$h_f = 2K_f v^2 g_c = 2(0.75)(9.57)^2(32.174) = 2.136 \text{ ft} \cdot \text{lb}_f/\text{lb}_m$$

The total frictional loss  $\Sigma F$  is the sum of steps (1) through (6):

$$\Sigma F = 0.054 + 0.111 + 0.074 + 0.575 + 29.4 + 2.136 = 32.35 \text{ ft} \cdot \text{lb}_f/\text{lb}_m$$

Using as a datum level  $z_2$ ,  $z_1 = H$  ft,  $z_2 = 0$ . Since turbulent flow exists,  $\alpha = 1.0$ . Also,  $v_1 = 0$  and  $v_2 = v_4 = 9.57$  ft/s. Since  $p_1$  and  $p_2$  are both at 1 atm abs pressure and  $p_1 = p_2$ ,

$$p_1 \rho - p_2 \rho = 0$$

Also, since no pump is used,  $W_s = 0$ . Substituting these values into Eq. (5.1-20),

$$H g g_c + 0 + 0 - 0 = 0 + 1(9.57)^2(32.174) + 32.35$$

Solving,  $H(g/g_c) = 33.77 \text{ ft} \cdot \text{lb}_f/\text{lb}_m$  (100.9 J/kg) and  $H$  is 33.77 ft (10.3 m), the height of the water level above the discharge outlet.

### **EXAMPLE 5.1-7. Friction Losses with a Pump in the Mechanical Energy Balance**

Water at 20°C is being pumped from a tank to an elevated tank at the rate of  $5.0 \times 10^{-3} \text{ m}^3/\text{s}$ . All of the piping in Fig. 5.1-5 is 4-in. Schedule 40 pipe. The pump has an efficiency of 65%. Calculate the kW power needed for the pump.

**Solution:** The mechanical-energy-balance equation

(4.2-28) is written between points 1 and 2, with point 1 being the reference plane:

$$12\alpha(v_2^2 - v_1^2) + g(z_2 - z_1) + p_2 - p_1 + \Sigma F + WS = 0 \quad (4.2-28)$$

From Appendix A.2 for water,  $\rho = 998.2 \text{ kg/m}^3$  and  $\mu = 1.005 \times 10^{-3} \text{ Pa} \cdot \text{s}$ . For 4-in. pipe from Appendix A.5,  $D = 0.1023 \text{ m}$  and  $A = 8.219 \times 10^{-3} \text{ m}^2$ . The velocity in the pipe is  $v = 5.0 \times 10^{-3} / (8.219 \times 10^{-3}) = 0.6083 \text{ m/s}$ . The Reynolds number is

$$N_{Re} = Dv\rho/\mu = 0.1023(0.6083)(998.2)/1.005 \times 10^{-3} = 6.181 \times 10^4$$

Hence, the flow is turbulent.

The  $\Sigma F$  term for frictional losses includes the following: (1) contraction loss at the tank exit, (2) friction in the straight pipe, (3) friction in the two elbows, and (4) expansion loss at the tank entrance.

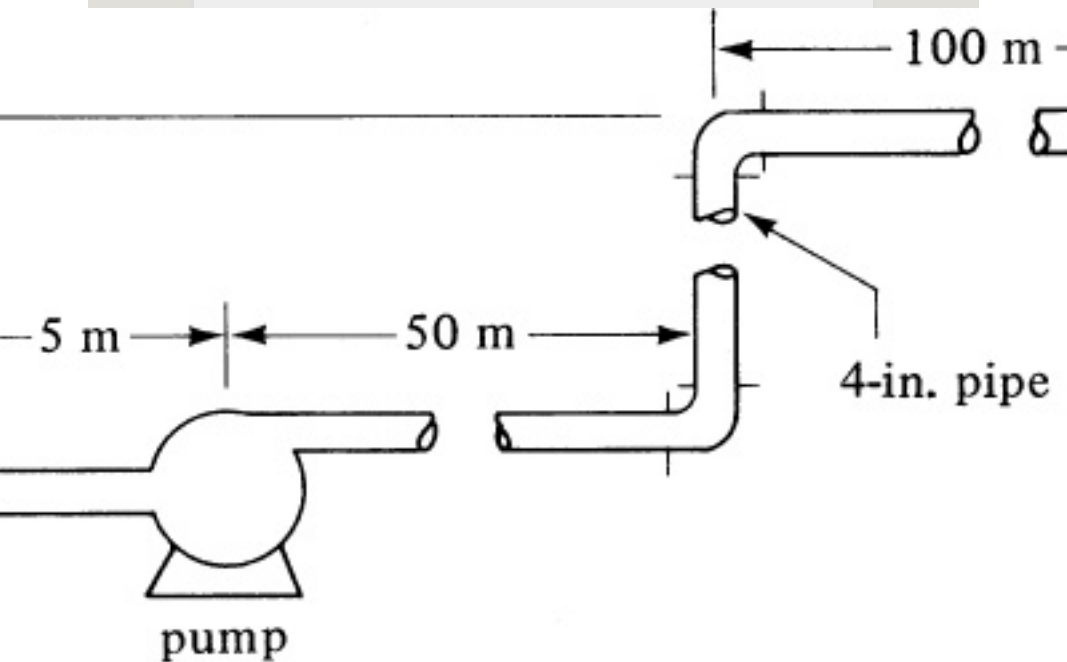


Figure 5.1-5. Process flow diagram for Example 5.1-7.

1. *Contraction loss at the tank exit.* From Eq. (5.1-16), for contraction from a large  $A_1$  to a small  $A_2$ ,

$$K_c = 0.55(1 - A_2/A_1) = 0.55(1 - 0) = 0.55$$

$$h_{K_c} = K_c v^2 / 2\alpha = (0.55) (0.6083)^2 (1.0) = 0.102 \text{ J/kg}$$

2. *Friction in the straight pipe.* From Fig. 5.1-3,  $\varepsilon = 4.6 \times 10^{-5} \text{ m}$  and  $\varepsilon/D = 4.6 \times 10^{-5} / 0.1023 = 0.00045$ . Then, for  $N_{Re} = 6.181 \times 10^4$ ,  $f = 0.0051$ . Substituting into Eq. (5.1-6) for  $\Delta L = 5 + 50 + 15 + 100 = 170 \text{ m}$ ,

$$F_f = 4f \Delta L D v^2 = 4(0.0051) 170 (0.1023) (0.6083)^2 = 6.272 \text{ J/kg}$$

3. *Friction in the two elbows.* From Table 5.1-1,  $K_r = 0.75$ . Then, substituting into Eq. (5.1-7) for two elbows,

$$h_f = 2K_r v^2 = 2(0.75) (0.6083)^2 = 0.278 \text{ J/kg}$$

4. *Expansion loss at the tank entrance.* Using Eq. (5.1-15),

$$K_{ex} = (1 - A_1/A_2)^2 = (1 - 0)^2 = 1.0$$

$$h_{K_{ex}} = K_{ex} v^2 = 1.0 (0.6083)^2 = 0.185 \text{ J/kg}$$

The total frictional loss is  $\sum F$ :

$$\sum F = 0.102 + 6.272 + 0.278 + 0.185 = 6.837 \text{ J/kg}$$

Substituting into Eq. (4.2-28), where  $(v_2^2 - v_1^2) = 0$  and  $(p_2 - p_1) = 0$ ,

$$0 + 9.806(15.0 - 0) + 0 + 6.837 + W_s = 0$$

Solving,  $W_s = 153.93 \text{ J/kg}$ . The mass flow rate is  $m = 5.0 \times 10^{-3} (998.2) = 4.991 \text{ kg/s}$ . Using Eq. (4.2-30),

$$W_s = -\eta W_p - 153.93 = 0.65 W_p$$

Solving,  $W_p = 236.8 \text{ J/kg}$ . The pump kW power is

$$\text{pump kW} = m W_p = 4.991 (236.8) = 1.182 \text{ kW}$$

## 5.1G Friction Loss in Noncircular Conduits

The friction loss in long, straight channels or conduits of a noncircular

cross section can be estimated by using the same equations employed for circular pipes if the diameter in the Reynolds number and in the friction-factor equation (5.1-6) is taken as the equivalent diameter.

The equivalent diameter  $D$  is defined as four times the hydraulic radius  $r_H$ .

The hydraulic radius is defined as the ratio of the cross-sectional area of the channel to the wetted perimeter of the channel for turbulent flow only. Hence,

$$D = 4r_H = 4 \frac{\text{cross-sectional area of channel}}{\text{wetted perimeter of channel}} \quad (5.1-21)$$

For example, for a circular tube,

$$D = 4 \left( \frac{\pi D^2 / 4}{\pi D} \right) = D$$

For an annular space with outside

diameter  $D_1$  and inside diameter  $D_2$ ,

$$D = 4(\pi D_1^2/4 - \pi D_2^2/4) / \pi D_1 + \pi D_2 = D_1 - D_2 \quad (5.1-22)$$

For a rectangular duct of sides  $a$  and  $b$  ft,

$$D = 4(ab) / (2a + 2b) = 2ab / (a + b) \quad (5.1-23)$$

For open channels and partly filled ducts in turbulent flow, the equivalent diameter and Eq. (5.1-6) are also used (P1). For a rectangle with depth of liquid  $y$  and width  $b$ ,

$$D = 4(by) / (b + 2y) \quad (5.1-24)$$

For a wide, shallow stream of depth  $y$ ,

$$D = 4y \quad (5.1-25)$$

For laminar flow in ducts running full and in open channels with various cross-sectional shapes other than circular, equations are given elsewhere (P1).

### **5.1H Entrance Section of a Pipe**

If the velocity profile at the entrance region of a tube is flat, a certain length of tube is necessary for the velocity profile to be fully established. This length for the establishment of fully developed flow is called the transition length or entry length. This is shown in Fig. 5.1-6 for laminar flow. At the entrance, the velocity profile is flat; that is, the velocity is the same at all positions. As the fluid progresses down the tube, the thickness of the boundary layers increases until finally they meet at the center of the

pipe and the parabolic velocity profile is fully established.

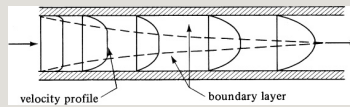


Figure 5.1-6. *Velocity profiles near a pipe entrance for laminar flow.*

The approximate entry length  $L_e$  of a pipe of diameter  $D$  for a fully developed velocity profile to be formed in laminar flow is (L2)

$$L_e D = 0.0575 \text{ NRe} \quad (5.1-26)$$

For turbulent flow, no relation is available to accurately predict the entry length for a fully developed turbulent velocity profile to form. As an approximation, the entry length is nearly independent of the Reynolds number and is fully developed after 50 diameters downstream.



**EXAMPLE 5.1-8. Entry Length for a Fluid in a Pipe**

Water at 20°C is flowing through a tube of diameter 0.010 m at a velocity of 0.10 m/s.

- Calculate the entry length.
- Calculate the entry length for turbulent flow.

**Solution:** For part (a), from Appendix A.2,  $\rho = 998.2 \text{ kg/m}^3$ ,  $\mu = 1.005 \times 10^{-3} \text{ Pa} \cdot \text{s}$ . The Reynolds number is

$$\text{NRe} = Dv\rho/\mu = 0.010(0.10)(998.2)/1.005 \times 10^{-3} = 993.2$$

Using Eq. (5.1-26) for laminar flow,

$$\text{LeD} = \text{Le}0.01 = 0.0575(993.2) = 57.1$$

Hence,  $L_e = 0.571 \text{ m}$ .

For turbulent flow in part (b),  $L_e = 50(0.01) = 0.50 \text{ m}$ .

The pressure drop or friction factor in the entry length is greater than in fully developed flow. For laminar flow, the friction factor is highest at the entrance ( $L_2$ ) and then decreases smoothly to the fully developed flow value. For turbulent flow, there will be some portion of the entrance over which the boundary layer is laminar and the friction-factor profile is difficult to express. As an approximation, the

friction factor for the entry length can be taken as two to three times the value of the friction factor in fully developed flow.

Table 5.1-3. *Representative Ranges of Velocities in Steel Pipes*

**5.11 Selection of Pipe Sizes**

In large or complex process piping systems, the optimum size of pipe to use for a specific situation depends upon the relative costs of capital investment, power, maintenance, and so on. Charts are available for determining these optimum sizes (P1). However, for small installations, approximations are usually sufficiently accurate.

Representative values for ranges of

velocity in pipes are shown in Table 5.1-3. For stainless-steel pipes, recent data (D1) show that the velocities in Table 5.1-3 for process lines or pump discharge should be increased by 70%.

## **5.2 Compressible Flow of Gases**

### **5.2A Introduction and Basic Equation for Flow in Pipes**

When pressure changes that are greater than about 10% occur in gases, the friction-loss equations (5.1-9) and (5.1-10) may be erroneous since compressible flow is occurring. For these situations, the solution of the energy balance is more complicated because of the variation of the density or specific volume with changes in pressure. The field of compressible flow is

very large and covers a very wide range of variation in geometry, pressure, velocity, and temperature. In this section, we restrict our discussion to isothermal and adiabatic flow in uniform, straight pipes. Compressible flow in nozzles is not covered here, but is discussed in some detail in other references (M2, P1).

The general mechanical-energy-balance equation (4.2-27) can be used as a starting point to model compressible fluid flow behavior in pipes. Assuming turbulent flow ( $\alpha = 1.0$ ), and no shaft work ( $W_s = 0$ ) and writing the equation for a differential length  $dL$ , Eq. (4.2-27) becomes

$$v dv + g dz + d p / \rho + d F = 0 \quad (5.2-1)$$

For a horizontal duct,  $dz = 0$ . Using only the wall shear frictional term for  $dF$  and writing Eq. (5.1-6) in differential form,

$$v dv + V dp + 4f v^2 dL / 2D = 0 \quad (5.2-2)$$

where the specific volume can be written as  $V = 1/\rho$ . Assuming steady-state flow and a uniform pipe diameter, the mass flow rate  $G$  is constant, and can be written as

$$G = v\rho = vV \quad (5.2-3)$$

$$dv = G dV \quad (5.2-4)$$

Substituting Eqs. (5.2-3) and (5.2-4) into (5.2-2) and rearranging,

$$G^2 dV / V + dp + 2f G^2 dL / D = 0 \quad (5.2-5)$$

This is the basic differential equation

that is to be integrated. To do this, the relation between  $V$  and  $p$  must be known so that the integral of  $dp/V$  can be evaluated. This integral depends upon the nature of the flow. Often, the two most common flow conditions found in pipes are isothermal and adiabatic flow.

### **5.2B Isothermal Compressible Flow**

To integrate Eq. (5.2-5) for isothermal flow, an ideal gas will be assumed, where the ideal gas law can be expressed as

$$pV = 1MRT \quad (5.2-6)$$

Solving for  $V$  in Eq. (5.2-6), and substituting it into Eq. (5.2-5) allows for the elimination of  $V$  from the pressure term. Therefore, integrating assuming  $f$  is constant, yields,

$$G_2 \int \frac{1}{V} dV + \frac{MRT}{p_1} \int \frac{1}{p} dp + 2fG_2 D \int \frac{1}{L} dL = 0 \quad (5.2-7)$$

$$G_2 \ln \frac{V_2}{V_1} + \frac{MRT}{p_1} (p_2 - p_1) + 2fG_2 D \Delta L = 0 \quad (5.2-8)$$

Substituting  $p_1/p_2$  for  $V_2/V_1$  and rearranging,

$$p_1 - p_2 = 4f \Delta L G_2 R T D M + 2G_2 R T M \ln \frac{p_1}{p_2} \quad (5.2-9)$$

where  $M$  = molecular weight in kg mass/kg mol,  $R = 8314.34 \text{ N} \cdot \text{m/kg mol} \cdot \text{K}$ , and  $T$  = temperature K. The quantity  $RT/M = p_{\text{av}}/\rho_{\text{av}}$ , where  $p_{\text{av}} = (p_1 + p_2)/2$  and  $\rho_{\text{av}}$  is the average density at  $T$  and  $p_{\text{av}}$ . In English units,  $R = 1545.3 \text{ ft} \cdot \text{lb}_f/\text{lb mol} \cdot ^\circ\text{R}$  and the right-hand terms are divided by  $g_c$ . Equation (5.2-9) then becomes

$$(p_1 - p_2) = 4f \Delta L G^2 / 2 D p_{av} + G^2 p_{av} \ln p_1 / p_2 \quad (5.2-10)$$

The first term on the right-hand side in Eqs. (5.2-9) and (5.2-10) represents the frictional loss as given by Eqs. (5.1-9) and (5.1-10). The last term in both equations is generally negligible in ducts of appreciable length unless the pressure drop is very large.

**EXAMPLE 5.2-1. Compressible Flow of a Gas in a Pipe Line**

Natural gas, which is essentially methane, is being pumped through a 1.016-m-ID pipeline for a distance of  $1.609 \times 10^5$  m ( $D_1$ ) at a rate of 2.077 kg mol/s. It can be assumed that the line is isothermal at 288.8 K. The pressure  $p_2$  at the discharge end of the line is  $170.3 \times 10^3$  Pa absolute. Calculate the pressure  $p_1$  at the inlet of the line. The viscosity of methane at 288.8 K is  $1.04 \times 10^{-5}$  Pa · s.

**Solution:**  $D = 1.016$  m,  $A = \pi D^2/4 = \pi(1.016)^2/4 = 0.8107$  m<sup>2</sup>. Then,

$$G = (2.077 \text{ kg mol/s})(16.0 \text{ kg/kg mol}) \\ (10.8107 \text{ m}^2) = 41.00 \text{ kg} \cdot \text{m}^2/\text{s} \quad \text{Re} = DG\mu = 1.016(41.00)/1.04 \times 10^{-5} = 4.005 \times 10^6$$

From Fig. 5.1-3,  $\varepsilon = 4.6 \times 10^{-5}$  m.

$$\varepsilon D = 4.6 \times 10^{-5} (1.016) = 0.0000453$$

The friction factor  $f = 0.0027$ .



In order to solve for  $p_1$  in Eq. (5.2-9), trial and error must be used. Estimating  $p_1$  at  $620.5 \times 10^3$  Pa,  $R = 8314.34 \text{ N} \cdot \text{m} / \text{kg mol} \cdot \text{K}$ , and  $\Delta L = 1.609 \times 10^5 \text{ m}$ . Substituting into Eq. (5.2-9),

$$\begin{aligned} p_1^2 - p_2^2 &= 4(0.0027)(1.609 \times 10^5)(41.00)^2(8314.34) \\ &\quad (288.8)1.016(16.0) + 2(41.00)^2(8314.34)(288.8) \\ (16.0) \ln 620.5 \times 10^3 / 170.3 \times 10^3 &= 4.375 \times 10^{11} + 0.00652 \times 10^{11} = 4.382 \times 10^{11} (\text{Pa})^2 \end{aligned}$$

Since  $P_2 = 170.3 \times 10^3$  Pa is specified, substituting this into the equation above and solving for  $p_1$ ,  $p_1 = 683.5 \times 10^3$  Pa. Substituting this new value of  $p_1$  into Eq. (5.2-9) again and solving for  $p_1$  the final result is  $p_1 = 683.5 \times 10^3$  Pa. Therefore, the solution has converged.

When the upstream pressure  $p_1$  remains constant, the mass flow rate  $G$  changes as the downstream pressure  $p_2$  is varied. From Eq. (5.2-9), when  $p_1 = p_2$ ,  $G = 0$ , and when  $p_2 = 0$ ,  $G = 0$ . This indicates that at some intermediate value of  $p_2$ , the flow  $G$  must be at a maximum. This means that the flow is at a maximum when  $dG/dp_2 = 0$ . Performing this differentiation on Eq. (5.2-9) for constant  $p_1$  and  $f$ , and solving for  $G$ ,

$$G_{\max} = M p_1^2 \sqrt{2RT} \quad (5.2-11)$$

Using Eqs. (5.2-3) and (5.2-6),

$$v_{\max} = \sqrt{RTM} = \sqrt{p_2 V_2} \quad (5.2-12)$$

This is the equation for the velocity of sound in the fluid at the conditions for isothermal flow. Thus, for isothermal compressible flow there is a maximum flow for a given upstream  $p_1$ , and further reduction of  $p_2$  will not give any further increase in flow. Further details as to the length of pipe and the pressure at maximum flow conditions are discussed elsewhere ( $D_1$ ,  $M_2$ ,  $P_1$ ).

**EXAMPLE 5.2-2. Maximum Flow for Compressible Flow of a Gas**

For the conditions of Example 5.2-1, calculate the maximum velocity that can be obtained and the velocity of sound at these conditions. Compare with Example 5.2-1.

**Solution:** Using Eq. (5.2-12) and the conditions in Example 5.2-1,

$$v_{\max} = \sqrt{RTM} = 8314(288.8)^{16.0} = 387.4 \text{ m/s}$$

This is the maximum velocity obtainable if  $p_2$  is decreased. This is also the velocity of sound in the fluid at the

conditions for isothermal flow. To compare with Example 5.2-1, the actual velocity at the exit pressure  $p_2$  is obtained by combining Eqs. (5.2-3) and (5.2-6) to give

$$v_2 = \frac{RTGp_2 M}{(170.3 \times 10^3) 16.0} = 36.13 \text{ m/s} \quad (5.2-13)$$

## 5.2C Adiabatic Compressible Flow

When the heat transfer through the wall of a pipe is negligible, the flow of gas in compressible flow in a straight pipe of constant cross section is adiabatic. Equation (5.2-5) has been integrated for adiabatic flow and details are given elsewhere (D1, M1, P1). Convenient charts for solving this case are also available (P1). The results for adiabatic flow often deviate very little from isothermal flow, especially in long pipes. For very short pipes and relatively large pressure drops, the adiabatic flow rate is greater than the isothermal, but the maximum

possible difference is about 20% (D1). For pipes of a length about 1000 diameters or longer, the difference is generally less than 5%. Equation (5.2-8) can also be used when the temperature change over the conduit is small by using an arithmetic-average temperature.

Using the same procedures for finding maximum flow that were used in the isothermal case, maximum flow occurs when the velocity at the downstream end of the pipe is the sonic velocity for adiabatic flow. This is

$$v_{\max} = \gamma p^{1/\gamma} V_2 = \gamma R T_M \quad (5.2-14)$$

where,  $\gamma = c_p/c_v$ , the ratio of heat capacities. For air,  $\gamma = 1.4$ . Hence, the maximum velocity for adiabatic flow is

about 20% greater than for isothermal flow. In practice, the rate of flow may not be limited by the flow conditions in the pipe, but by the development of sonic velocity in a fitting or valve in the pipe. Hence, care should be used in the selection of fittings for such pipes for compressible flow. Further details as to the length of pipe and pressure at maximum flow conditions are given elsewhere (D1, M2, P1).

A convenient parameter often used in compressible-flow equations is the Mach number,  $N_{Ma}$ , which is defined as the ratio of  $v$ , the speed of the fluid in the conduit, to  $v_{max}$ , the speed of sound in the fluid at the actual flow conditions:

$$N_{Ma} = \frac{v}{v_{max}} \quad (5.2-15)$$

At a Mach number of 1.0, the flow is sonic. At a value less than 1.0, the flow is subsonic, and supersonic at a number above 1.0.

### **5.3 Measuring the Flow of Fluids**

It is important to be able to measure and control the amount of materials entering and leaving a chemical or other processing plant. Since many of these materials are in the form of fluids, they are flowing in pipes or conduits. Many different types of devices are used to measure the flow of fluids. The simplest are those that directly measure the volume of the fluids, such as ordinary gas and water meters, and positive-displacement pumps. Other meters that are currently used are those that make use of an element, such as a

propeller or cups on a rotating arm, which rotates at a speed determined by the velocity of the fluid passing through it. Other devices that are widely used for fluid metering are the pitot tube, venturi meter, orifice meter, and open-channel weir.

### **5.3A Pitot Tube**

The pitot tube is used to measure the local velocity at a given point in the flow stream and not the average velocity in the pipe or conduit. In Fig. 5.3-1a, a sketch of this simple device is shown. One tube, the impact tube, has its opening normal to the direction of flow, while the static tube has its opening parallel to the direction of flow.

The fluid flows into the opening at point

2; pressure builds up and then remains stationary at this point, called the *stagnation point*. The difference in the stagnation pressure at point 2 and the static pressure measured by the static tube represents the pressure rise associated with the deceleration of the fluid. The manometer measures this small pressure rise. If the fluid is incompressible, we can write the Bernoulli equation (4.2-32) between point 1, where the velocity  $v_1$  is undisturbed before the fluid decelerates, and point 2, where the velocity  $v_2$  is zero:

$$\frac{v_1^2}{2} - \frac{v_2^2}{2} + p_1 - p_2 = 0 \quad (5.3-1)$$

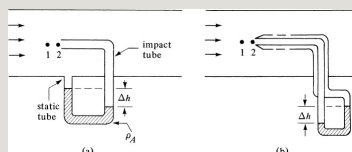


Figure 5.3-1. Diagram of pitot tube: (a) simple tube, (b) tube with static pressure holes.



Setting  $v_2 = 0$  and solving for  $v_1$ ,

$$v = C_p \sqrt{2(p_2 - p_1) / \rho} \quad (5.3-2)$$

where  $v$  is the velocity  $v_1$  in the tube at point 1 in m/s,  $p_2$  is the stagnation pressure,  $\rho$  is the density of the flowing fluid at the static pressure  $p_1$ , and  $C_p$  is a dimensionless coefficient to take into account deviations from Eq. (5.3-1) that generally varies between about 0.98 and 1.0. For accurate use, the coefficient should be determined by calibration of the pitot tube. This equation applies to incompressible fluids but can be used to approximate the flow of gases at moderate velocities and pressure changes of about 10% or less of the total pressure.

The value of the pressure drop  $p_2 - p_1$  or

$\Delta p$  in Pa is related to  $\Delta h$ , the reading on the manometer, by Eq. (2.2-14) as follows:

$$\Delta p = \Delta h(\rho_A - \rho)g \quad (5.3-3)$$

where  $\rho_A$  is the density of the fluid in the manometer in  $\text{kg/m}^3$  and  $\Delta h$  is the manometer reading in m. In Fig. 5.3-1b, a more compact design is shown with concentric tubes. In the outer tube, static pressure holes are parallel to the direction of flow. Further details are given elsewhere (P1).

Since the pitot tube measures velocity at only one point in the flow, several methods can be used to obtain the average velocity in the pipe. In the first method, the velocity is measured at the exact center of the tube to obtain  $v_{\text{max}}$ .

Then, by using Fig. 5.1-2, the  $v_{av}$  can be obtained. Care should be taken to have the pitot tube at least 100 diameters downstream from any pipe obstruction. In the second method, readings are taken at several known positions in the pipe cross section and then, using Eq. (4.1-17), a graphical or numerical integration is performed to obtain  $v_{av}$ .

**EXAMPLE 5.3-1. Flow Measurement Using a Pitot Tube**

A pitot tube similar to Fig. 5.3-1a is used to measure the air flow in a circular duct 600 mm in diameter. The flowing air temperature is 65.6°C. The pitot tube is placed at the center of the duct and the reading  $\Delta h$  on the manometer is 10.7 mm of water. A static-pressure measurement obtained at the pitot tube position is 205 mm of water above atmospheric. The pitot tube coefficient  $C_p = 0.98$ .

- Calculate the velocity at the center and the average velocity.
- Calculate the volumetric flow rate of the flowing air in the duct.

**Solution:** For part (a), the properties of air at 65.6°C from Appendix A.3 are  $\mu = 2.03 \times 10^{-5} \text{ Pa} \cdot \text{s}$ , and  $\rho = 1.043 \text{ kg/m}^3$  (at 101.325 kPa). To calculate the absolute static pressure, the manometer reading  $\Delta h = 0.205 \text{ m}$  of water indicates the pressure above 1 atm abs. Using Eq. (2.2-14), the water density as 1000 kg/m<sup>3</sup>, and assuming 1.043 kg/m<sup>3</sup> as the air density,

$$\Delta p = 0.205(1000 - 1.043)9.80665 = 2008 \text{ Pa}$$

Then, the absolute static pressure  $p_1 = 1.01325 \times 10^5 + 0.02008 \times 10^5 = 1.0333 \times 10^5$  Pa. The correct air density in the flowing air is  $(1.0333 \times 10^5 / 1.01325 \times 10^5) (1.043) = 1.063 \text{ kg/m}^3$ . This correct value, when used instead of 1.043, would have a negligible effect on the recalculation of  $p_1$ .

To calculate  $\Delta p$  for the pitot tube, Eq. (5.3-3) is used:

$$\Delta p = \Delta h(\rho_A - \rho)g = 10.71000(1000 - 1.063)(9.80665) = 104.8 \text{ Pa}$$

Using Eq. (5.3-2), the maximum velocity at the center is

$$v = 0.98 \sqrt{2(104.8)/1.063} = 13.76 \text{ m/s}$$

The Reynolds number, using the maximum velocity, is

$$N_{Re} = Dv_{max}\rho/\mu = 0.600(13.76)(1.063)/2.03 \times 10^{-5} = 4.323 \times 10^5$$

From Fig. 5.1-2,  $v_{av}/v_{max} = 0.85$ . Then,  $v_{av} = 0.85(13.76) = 11.70 \text{ m/s}$ .

To calculate the flow rate for part (b), the cross-sectional area of the duct,  $A = (\pi/4)(0.600)^2 = 0.2827 \text{ m}^2$ . The flow rate  $= 0.2827(11.70) = 3.308 \text{ m}^3/\text{s}$ .

### 5.3B Venturi Meter

A *venturi meter*, shown in Fig. 5.3-2, is usually inserted directly into a pipeline. A manometer or other device is connected to the two pressure taps shown and measures the pressure difference  $p_1 - p_2$  between points 1 and 2. The average velocity at point 1 where the

diameter is  $D_1$  m is  $v_1$  m/s, and at point 2 or the throat, the velocity is  $v_2$  and the diameter  $D_2$ . Since the narrowing down from  $D_1$  to  $D_2$  and the expansion from  $D_2$  back to  $D_1$  is gradual, little frictional loss due to contraction and expansion is incurred.

To derive the equation for the venturi meter, friction is neglected and the pipe is assumed to be horizontal. Assuming turbulent flow and writing the mechanical-energy-balance equation (4.2-28) between points 1 and 2 for an incompressible fluid,

$$v_1^2/2 + P_1/\rho = v_2^2/2 + P_2/\rho \quad (5.3-4)$$

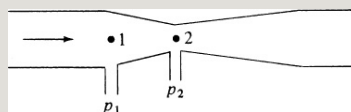


Figure 5.3-2. Venturi flow meter.

The continuity equation for constant  $p$  is

$$v_1 \pi D_1^2 = v_2 \pi D_2^2 \quad (5.3-5)$$

Combining Eqs. (5.3-4) and (3.2-5) and eliminating  $v_1$ ,

$$v_2 = \frac{1}{\beta^4} \sqrt{\frac{2(p_1 - p_2)}{\rho}} \quad (5.3-6)$$

In the expression above, the diameter ratio  $D_2/D_1$  is commonly called the  $\beta$  ratio, where  $\beta = D_2/D_1$ .

To account for the small friction loss, an experimental coefficient  $C_v$  is introduced to give

$$v_2 = C_v \frac{1}{\beta^4} \sqrt{\frac{2(p_1 - p_2)}{\rho}} \quad (5.3-7)$$

This holds for liquids and very small pressure drops in gases of less than 1%. For many meters and a Reynolds number  $> 10^4$  at point 1,  $C_v$  is about 0.98 for pipe diameters below 0.2 m and 0.99 for larger sizes. However, these coefficients can vary, and individual calibration is recommended if the manufacturer's calibration is not available.

To calculate the volumetric flow rate, the velocity  $v_2$  is multiplied by the area  $A_2$ :

$$\text{flow rate} = v_2 \pi D^2 / 4 \quad \text{m}^3/\text{s} \quad (5.3-8)$$

For measuring a compressible flow of gases, the adiabatic expansion from  $p_1$  to  $p_2$  pressure must be accounted for in Eq. (5.3-7). A similar equation and the

same coefficient  $C_v$  are used along with the dimensionless expansion correction factor  $Y$  (shown in Fig. 5.3-3 for air) as follows:

$$m = C_v A_2 Y \sqrt{1 - (D_2/D_1)^4} \sqrt{(p_1 - p_2) \rho_1} \quad (5.3-9)$$

where  $m$  is flow rate in kg/s,  $\rho_1$  is density of the fluid upstream at point 1 in kg/m<sup>3</sup>, and  $A_2$  is cross-sectional area at point 2 in m<sup>2</sup>.

The pressure difference  $p_1 - p_2$  occurs because the velocity is increased from  $v_1$  to  $v_2$ . However, farther down the tube, the velocity returns to its original value of  $v_1$  for liquids. Because of frictional losses, some of the difference  $p_1 - p_2$  is not fully recovered downstream from the original  $p_1$ . In a properly designed



venturi meter, the permanent loss is about 10% of the differential  $p_1 - p_2$ , and this represents power loss. A venturi meter is often used to measure flows in large lines, such as city water systems.

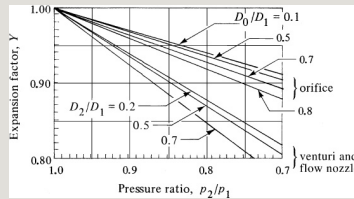


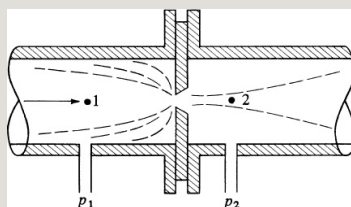
Figure 5.3-3. Expansion factor for air in venturi, flow nozzle, and orifice. Calculated from equations and data in references (M2, S3).

### 5.3C Orifice Meter

For ordinary installations in a process plant, the venturi meter has several disadvantages. It occupies a lot of space and is expensive. Also, the throat diameter is fixed, so that if the flow-rate range is changed considerably, inaccurate pressure differences may result. The *orifice*

*meter* overcomes these objections but at the price of a much larger permanent head or power loss.

A typical sharp-edged orifice is shown in Fig. 5.3-4. A machined and drilled plate having a hole of diameter  $D_0$  is mounted between two flanges in a pipe of diameter  $D_1$ . Pressure taps at points 1 upstream and 2 downstream measure  $p_1 - p_2$ . The exact positions of the two taps are somewhat arbitrary: in one type of meter, the taps are installed about 1 pipe diameter upstream and 0.3 to 0.8 pipe diameter downstream. The fluid stream, once past the orifice plate, forms a vena contracta or free-flowing jet.



The equation for the orifice is similar to Eq. (5.3-7):

$$v_0 = C_0 \sqrt{1 - (D_0/D_1)^4} \sqrt{2(p_1 - p_2)/\rho} \quad (5.3-10)$$

where  $v_0$  is the velocity in the orifice in m/s,  $D_0$  is the orifice diameter in m, and  $C_0$  is the dimensionless orifice coefficient. The orifice coefficient  $C_0$  is always determined experimentally. If the  $N_{Re}$  at the orifice is above 20000 and  $D_0/D_1$  is less than about 0.5, the value of  $C_0$  is approximately constant and has the value 0.61, which is adequate for design for liquids or gases (M2, P1). Below 20000, the coefficient rises sharply and then drops, and a correlation for  $C_0$  is given elsewhere (P1).

As in the case of the venturi, for

measuring the compressible flow of gases in an orifice, a correction factor  $Y$  given in Fig. 5.3-3 for air is used as follows:

$$m = C_0 A_0 Y \sqrt{1 - (D_0/D_1)^4} \sqrt{p_1 - p_2} \rho_1 \quad (5.3-11)$$

where  $m$  is flow rate in kg/s,  $\rho_1$  is upstream density in kg/m<sup>3</sup>, and  $A_0$  is the cross-sectional area of the orifice. For liquids,  $Y$  is 1.0.

The permanent pressure loss is much higher than for a venturi because of the eddies formed when the jet expands below the vena contracta. This loss depends on  $D_0/D_1$  and is as follows:

$$(p_1 - p_4) = (1 - \beta^4)(p_1 - p_2) \quad (5.3-12)$$

where  $\beta = D_0/D_1$  ( $P_1$ ) and  $p_4$  is the fully

recovered pressure 4–8 pipe diameters downstream. For  $\beta = 12$ , this power loss is 75% of  $p_1 - p_2$ .

**EXAMPLE 5.3-2. Metering Oil Flow by an Orifice**

A sharp-edged orifice having a diameter of 0.0566 m is installed in a 0.1541-m pipe through which oil having a density of 878 kg/m<sup>3</sup> and a viscosity of 4.1 cp is flowing. The measured pressure difference across the orifice is 93.2 kN/m<sup>2</sup>. Calculate the volumetric flow rate in m<sup>3</sup>/s. Assume that  $C_0 = 0.61$ .

**Solution:**

$$p_1 - p_2 = 93.2 \text{ kN/m}^2 = 9.32 \times 10^4 \text{ N/m}^2$$

$$D_1 = 0.1541 \text{ m} \quad D_0 = 0.0566 \text{ m} \quad D_1 = 0.0566/0.1541 = 0.368$$

Substituting into Eq. (5.3-10),

$$v_0 = C_0 \left( \frac{D_0}{D_1} \right)^{1/2} \sqrt{(p_1 - p_2) / \rho} = 0.61 \sqrt{(93.2 \times 10^3 \text{ N/m}^2) / (878 \text{ kg/m}^3)}$$

$$v_0 = 8.97 \text{ m/s}$$

$$\text{The volumetric flow rate} = v_0 \pi D_0^2 / 4 = (8.97)(\pi)(0.0566)^2 / 4 = 0.02257 \text{ m}^3/\text{s} \quad (0.797 \text{ ft}^3/\text{s})$$

The  $Re$  is calculated to see if it is greater than  $2 \times 10^4$  for  $C_0 = 0.61$ :

$$Re = D_0 v_0 \rho / \mu = (0.0566)(8.97)(878) / (4.1 \times 10^{-3}) = 1.087 \times 10^5$$

Hence, the Reynolds number is above  $2 \times 10^4$ .

### 5.3D Flow-Nozzle Meter

A typical *flow nozzle* is shown in Fig. 5.3-5. It is essentially a short

cylinder with the approach being elliptical in shape. This meter has characteristics similar to those of the venturi meter but is shorter and much less expensive. The length of the straight portion of the throat is about one-half the diameter of the throat,  $D_2$ . The upstream pressure tap  $p_1$  is 1 pipe diameter from the inlet-nozzle face, and the downstream tap  $p_2$  is 12 pipe diameter from the inlet-nozzle face.

The equation for flow of liquids is the same as Eq. (5.3-7) for the venturi, with the coefficient  $C_n$  for the flow nozzle replacing  $C_v$  for the venturi. Also, the equation for compressible flow of gases for the flow nozzle is the same as Eq. (5.3-9) for the venturi, with the coefficient  $C_n$ . The expansion factor  $Y$  is

the same for the flow nozzle and the venturi.

For the flow nozzle, the coefficient  $C_n$  ranges from 0.95 at a pipe Reynolds number of  $10^4$ , 0.98 at  $10^5$ , and 0.99 at  $10^6$  or above (P1, S3). The permanent pressure loss ( $p_1 - p_4$ ) is as follows, where  $p_4$  is the final, fully recovered downstream pressure:

$$(p_1 - p_4) = 1 - \beta^2 + \beta^2(p_1 - p_2) \quad (5.3-13)$$

where  $\beta = D_2/D_1$ . This loss is greater than that for venturi meters and less than that for orifice meters. For  $\beta = 12$ , this power loss is 60% of  $p_1 - p_2$ .

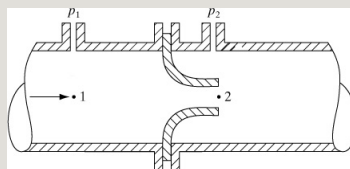


Figure 5.3-5. Flow-nozzle meter.

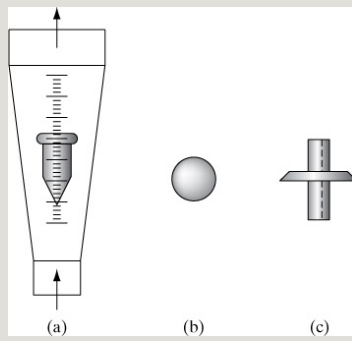


Figure 5.3-6. Rotameter: (a) flow diagram with glass tube, (b) spherical float, (c) viscosity-insensitive float.

### 5.3E Variable-Area Flow Meters (Rotameters)

In Fig. 5.3-6, a variable-area flow meter is shown. The fluid enters at the bottom of the tapered glass tube, flows through the annular area around the tube, and exits at the top. The float remains stationary. The differential head or pressure drop is held constant. At a higher flow rate, the float rises and the annular area increases to maintain a constant pressure drop. The height of rise in the tube is calibrated with the flow rate, and the relation between the



meter reading and the flow rate is approximately linear.

For a given float of density  $\rho_f$  and a fluid density  $\rho_A$ , the mass flow rate  $m_A$  is given by

$$m_A = q_A \rho_A = K(\rho_f - \rho_A) \rho_A \quad (5.3-14)$$

where  $q_A$ , the volumetric flow rate, is the reading on the rotameter, and  $K$  is a constant that is determined experimentally. If a fluid  $\rho_B$  is used instead of  $\rho_A$ , at the same height or reading of  $q_A$  on the rotameter and assuming  $K$  does not vary appreciably, the following approximation can be used:

$$m_A m_B = q_A \rho_A q_B \rho_B = (\rho_f - \rho_A) \rho_A (\rho_f - \rho_B) \rho_B \quad (5.3-15)$$

For gases where  $\rho_f \gg \rho_A$  and  $\rho_B$ ,  $q_B = q_A \rho_A / \rho_B$ . Note that the reading on the rotameter is usually taken at the widest point of the float.

### 5.3F Other Types of Flow Meters

Many other types of flow meters are available; the more important ones are discussed briefly as follows:

*1. Turbine- and paddle-wheel meters.* A turbine wheel or a paddle wheel is placed inside a pipe, and the rotary speed depends on the flow rate of the fluid.

*2. Thermal-gas mass flow meters.* Gas flowing in a tube is divided into a constant ratio because of laminar flow into a main stream and a small stream in a sensor tube. A small but constant

amount of heat is added to the sensor tube flow. By measuring the temperature rise, the output temperature rise can be related to the gas mass flow rate. These meters are mass flow meters and are unaffected by temperature and pressure.

*3. Magnetic flow meters.* A magnetic field is generated across the conductive fluid flowing in a pipe. Using Faraday's law of electromagnetic inductance, the induced voltage is directly proportional to the flow velocity (D3). The meter is insensitive to changes in density and viscosity. The meter cannot be used with most hydrocarbons because of their low conductivity.

*4. Coriolis mass flow meter.* This meter is insensitive to operating conditions of viscosity, density, type of fluid, and

slurries. Fluid from the main flow enters two U-tube side channels (D3). The fluid induces a Coriolis force according to Newton's second law. The tubes then twist slightly, and the measured twist angle is proportional to the mass flow rate.

*5. Vortex-shedding flow meter.* When a fluid flows past a blunt object, the fluid forms vortices or eddies (D3). The vortices are counted and the signal is proportional to the flow rate.

*6. Positive displacement flow meter.* When a fluid flows past mechanical elements, the flow rate is calculated based on the proportion by which the fluid mechanically displaces the measuring elements. Nutating disk meters and piston meters are two

common types. Residential and industrial gas and water meters are often positive displacement flow meters.

### 5.3G Flow in Open Channels and Weirs

In many instances in process engineering and in agriculture, liquids are flowing in open channels rather than closed conduits. To measure the flow rates, weir devices are often used. A *weir* is a dam over which the liquid flows. The two main types of weirs are the rectangular weir and the triangular weir, as shown in Fig. 5.3-7. The liquid flows over the weir and the height  $h_0$  (weir head) in m is measured above the flat base or the notch, as shown. This head should be measured at a distance of about  $3h_0$  m upstream of the weir by a

level or float gage.

The equation for the volumetric flow rate  $q$  in  $\text{m}^3/\text{s}$  for a rectangular weir is given by

$$q=0.415(L-0.2h_0)h_0^{1.52}g^{0.5} \quad (5.3-16)$$

where  $L$  = crest length in m,  $g = 9.80665 \text{ m/s}^2$ , and  $h_0$  = weir head in m. This is called the *modified Francis weir formula* and it agrees with experimental values within 3% if  $L > 2h_0$ , velocity upstream  $< 0.6 \text{ m/s}$ ,  $h_0 > 0.09 \text{ m}$ , and the height of the crest above the bottom of the channel  $> 3h_0$ . In English units,  $L$  and  $h$  are in ft,  $q$  is in  $\text{ft}^3/\text{s}$ , and  $g = 32.174 \text{ ft/s}^2$ .

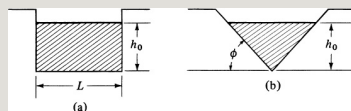


Figure 5.3-7. Types of weirs: (a) rectangular, (b) triangular.

For the triangular notch weir,

$$q=0.31h^{0.5}\tan\phi\sqrt{2g}\quad(5.3-17)$$

Both Eqs. (5.3-16) and (5.3-17) apply only to water. For other liquids, see data given elsewhere (P1).

## **5.4 Chapter Summary**

In this chapter, we have described the different types of pipes and fluid flows associated with incompressible and compressible flows in pipes.

First, we discussed their different types of construction materials and how the schedule size is important in terms of withstanding fluid pressure.

The different flow profiles and velocity distributions for laminar and turbulent flows were described and

shown in Figure 5.1-1.

When a fluid flows in a pipe, it experiences frictional losses that cause a drop in pressure. Based on the Hagen-Poiseuille equation, the pressure drop due to frictional losses was shown to be

$$\Delta p_f = (p_1 - p_2)_f = \frac{32\mu v (L_2 - L_1)}{D^2} \quad (5.1-2)$$

It was also shown that the friction loss could be calculated based on the pressure drop by

$$F_f = (p_1 - p_2)_f = \begin{cases} \text{N} \cdot \text{m} & \text{kg or J} \\ \text{kg} & \text{(SI)} \\ \text{ft} \cdot \text{lb} & \text{ft} \cdot \text{lb} \\ \text{ft} \cdot \text{lb} & \text{ft} \cdot \text{lb} \end{cases} \quad (5.4-2)$$

The concept of the Fanning friction factor was introduced and shown to be related to the pressure drop and



frictional losses for fluid flowing in a pipe. Therefore, the pressure drop and frictional losses can be calculated from the Fanning friction factor by

$$\Delta p_f = 4 f_F \Delta L D v^2 / 2g_c \quad \text{(SI)} \quad \Delta p_f = 4 f_F \Delta L D v^2 / 2g_c \quad \text{(English)} \quad (5.1-5)$$

$$f_F = 4 f \Delta L D v^2 / 2g_c \quad \text{(SI)} \quad f_F = 4 f \Delta L D v^2 / 2g_c \quad \text{(English)} \quad (5.1-6)$$

For laminar flow cases, the following expression for calculating the friction factor was derived:

$$f = 16 / \text{Re} = 16 \mu / D v \rho \quad (5.1-7)$$

For turbulent flow cases, it was shown that the friction factor chart (Figure 5.1-3) can be used to determine the friction factor for varying pipes of different relative roughness.

Correlations were provided for calculating friction losses in sudden expansions, contractions, and other types of pipe fittings. It was shown that all of these losses could be incorporated into the mechanical energy balance equation to determine the total frictional loss. The following expression was derived to take into account all losses in the mechanical energy balance equation:

$$\Delta L D v^2 + K_{ex} v^2 + K_{cv} v^2 + K_{fv} v^2 \quad (5.1-18)$$

Early in the chapter, the velocity profiles of fluids flowing in the laminar and turbulent flow regimes were shown. The concept of the entry length and fully-developed flow was discussed later in Section 5.1H, and the change in velocity profile in a pipe was shown in Figure 5.1-6.

Although the beginning of this chapter focused on incompressible fluids, Section 5.2 introduced the basic equations of compressible flow (where pressure changes greater than 10% occur in gases). The basic differential equation that describes compressible flow was derived as

$$G^2 dV/V + dp + 2fG^2 D dL = 0 \quad (5.2-5)$$

Specific examples of isothermal and adiabatic compressible flow were provided.

This chapter concluded with a review of common fluid metering devices in Section 5.3. The most common examples discussed were pitot tubes, venturi meters, orifice meters, and rotameters. Diagrams illustrating their

operation and expressions to calculate pressure drops in these meters were provided.

## Problems

**5.1-1. Viscosity Measurement of a Liquid.** One use of the Hagen–Poiseuille equation (5.1-2) is in determining the viscosity of a liquid by measuring the pressure drop and velocity of the liquid in a capillary of known dimensions. The liquid used has a density of  $912 \text{ kg/m}^3$ , and the capillary has a diameter of  $2.222 \text{ mm}$  and a length of  $0.1585 \text{ m}$ . The measured flow rate is  $5.33 \times 10^{-7} \text{ m}^3/\text{s}$  of liquid and the pressure drop is  $131 \text{ mm}$  of water (density  $996 \text{ kg/m}^3$ ). Neglecting end effects, calculate the viscosity of the liquid in  $\text{Pa} \cdot \text{s}$ .

$$\text{Ans. } \mu = 9.06 \times 10^{-3} \text{ Pa} \cdot \text{s}$$

**5.1-2. *Frictional Pressure Drop in a Flow of Olive Oil.***

Calculate the frictional pressure drop in pascals for olive oil at 293 K flowing through a commercial pipe having an inside diameter of 0.0525 m and a length of 76.2 m. The velocity of the fluid is 1.22 m/s. Use the friction-factor method. Is the flow laminar or turbulent? Use physical data from Appendix A.4.

**5.1-3. *Frictional Loss in Straight Pipe and the Effect of a Type of Pipe.***

A liquid having a density of 801 kg/m<sup>3</sup> and a viscosity of  $1.49 \times 10^{-3} \text{ Pa} \cdot \text{s}$  is flowing through a horizontal straight pipe at a velocity of 4.57 m/s. The commercial steel pipe is 112-in. nominal pipe size, Schedule 40. For a length of

pipe of 61 m, do as follows:

- Calculate the friction loss  $F_f$ .
- For a smooth tube of the same inside diameter, calculate the friction loss. What is the percent reduction of  $F_f$  for the smooth tube?

**Ans.** (a) 348.9 J/kg; (b) 274.2 J/kg (91.7 ft · lb<sub>f</sub>/lb<sub>m</sub>), 21.4% reduction

#### **5.1-4. Trial-and-Error Solution for**

**Hydraulic Drainage.** In a hydraulic project, a cast-iron pipe having an inside diameter of 0.156 m and a 305-m length is used to drain wastewater at 293 K.

The available head is 4.57 m of water.

Neglecting any losses from fittings and joints in the pipe, calculate the flow rate in m<sup>3</sup>/s. (*Hint:* Assume the physical properties of pure water. The solution is trial and error, since the velocity appears in  $N_{Re}$ , which is needed to determine the

friction factor. As a first trial, assume that  $v = 1.7 \text{ m/s}$ .)

**5.1-5. Mechanical-Energy Balance and Friction Losses.** Hot water is being discharged from a storage tank at the rate of  $0.223 \text{ ft}^3/\text{s}$ . The process flow diagram and conditions are the same as given in Example 5.1-6, except for different nominal pipe sizes of Schedule 40 steel pipe as follows: The 20-ft-long outlet pipe from the storage tank is 112-in. pipe instead of 4-in. pipe. The other piping, which was 2-in. pipe, is now 2.5-in. pipe. Note that a sudden expansion now occurs after the elbow in the 112-in. pipe to a 212-in. pipe.

**5.1-6. Friction Losses and Pump Horsepower.** Hot water in an open storage tank at  $82.2^\circ\text{C}$  is being pumped

at the rate of  $0.379 \text{ m}^3/\text{min}$  from the tank. The line from the storage tank to the pump suction is  $6.1 \text{ m}$  of 2-in. Schedule 40 steel pipe and it contains three elbows. The discharge line after the pump is  $61 \text{ m}$  of 2-in. pipe and contains two elbows. The water discharges to the atmosphere at a height of  $6.1 \text{ m}$  above the water level in the storage tank.

- Calculate all frictional losses  $\Sigma F$ .
- Make a mechanical-energy balance and calculate  $W_s$  of the pump in J/kg.
- What is the kW power of the pump if its efficiency is 75%?

**Ans.** (a)  $\Sigma F = 122.8 \text{ J/kg}$ ; (b)  $W_s = -186.9 \text{ J/kg}$ ; (c)  $1.527 \text{ kW}$

### ***5.1-7. Pressure Drop of a Flowing Gas.***

Nitrogen gas is flowing through a 4-in.



Schedule 40 commercial steel pipe at 298 K. The total flow rate is  $7.40 \times 10^{-2}$  kg/s and the flow can be assumed as isothermal. The pipe is 3000 m long and the inlet pressure is 200 kPa. Calculate the outlet pressure.

**Ans.**  $p_2 = 188.5$  kPa

### ***5.1-8. Entry Length for Flow in a Pipe.***

Air at 10°C and 1.0 atm abs pressure is flowing at a velocity of 2.0 m/s inside a tube having a diameter of 0.012 m.

- Calculate the entry length.
- Calculate the entry length for water at 10°C and the same velocity.

***5.1-9. Friction Loss in Pumping Oil to a Pressurized Tank.*** An oil having a density of 833 kg/m<sup>3</sup> and a viscosity of  $3.3 \times 10^{-3}$  Pa · s is pumped from an

open tank to a pressurized tank held at 345 kPa gage. The oil is pumped from an inlet at the side of the open tank through a line of commercial steel pipe having an inside diameter of 0.07792 m at the rate of  $3.494 \times 10^{-3} \text{ m}^3/\text{s}$ . The length of straight pipe is 122 m, and the pipe contains two elbows ( $90^\circ$ ) and a globe valve half open. The level of the liquid in the open tank is 20 m above the liquid level in the pressurized tank. The pump efficiency is 65%. Calculate the kW power of the pump.

**5.1-10. *Flow in an Annulus and Pressure Drop.*** Water flows in the annulus of a horizontal, concentric-pipe heat exchanger and is being heated from  $40^\circ\text{C}$  to  $50^\circ\text{C}$  in the exchanger, which has a length of 30 m of equivalent straight pipe. The flow rate of the water

is  $2.90 \times 10^{-3} \text{ m}^3/\text{s}$ . The inner pipe is 1-in. Schedule 40 and the outer is 2-in. Schedule 40. What is the pressure drop? Use an average temperature of  $45^\circ\text{C}$  for bulk physical properties. Assume that the wall temperature is an average of  $4^\circ\text{C}$  higher than the average bulk temperature so that a correction can be made for the effect of heat transfer on the friction factor.

### ***5.2-1. Derivation of Maximum Velocity for Isothermal Compressible Flow.***

Starting with Eq. (5.2-9), derive Eqs. (5.2-11) and (5.2-12) for the maximum velocity in isothermal compressible flow.

***5.2-2. Pressure Drop in Compressible Flow.*** Methane gas is being pumped through a 305-m length of 52.5-mm-ID

steel pipe at the rate of  $41.0 \text{ kg/m}^2 \cdot \text{s}$ .  
The inlet pressure is  $p_1 = 345 \text{ kPa abs}$ .  
Assume isothermal flow at  $288.8 \text{ K}$ .

- Calculate the pressure  $p_2$  at the end of the pipe. The viscosity is  $1.04 \times 10^{-5} \text{ Pa} \cdot \text{s}$ .
- Calculate the maximum velocity that can be attained at these conditions and compare with the velocity in part (a).

**Ans.** (a)  $p_2 = 298.4 \text{ kPa}$ ; (b)  $v_{\text{max}} = 387.4 \text{ m/s}$ ,  $v_2 = 20.62 \text{ m/s}$

**5.2-3. Pressure Drop in Isothermal Compressible Flow.** Air at  $288 \text{ K}$  and  $275 \text{ kPa abs}$  enters a pipe and is flowing in isothermal compressible flow in a commercial pipe having an ID of  $0.080 \text{ m}$ . The length of the pipe is  $60 \text{ m}$ . The mass velocity at the entrance to the pipe is  $165.5 \text{ kg/m}^2 \cdot \text{s}$ . Assume 29 for the molecular weight of air. Calculate the pressure at the exit. Also, calculate the

maximum allowable velocity that can be attained and compare with the actual.

**5.3-1. Flow Measurement Using a Pitot Tube.** A pitot tube is used to measure the flow rate of water at 20°C in the center of a pipe having an inside diameter of 102.3 mm. The manometer reading is 78 mm of carbon tetrachloride at 20°C. The pitot-tube coefficient is 0.98.

- Calculate the velocity at the center and the average velocity.
- Calculate the volumetric flow rate of the water.

**Ans.** (a)  $v_{\max} = 0.9372 \text{ m/s}$ ,  $v_{\text{av}} = 0.773 \text{ m/s}$ ; (b)  $6.35 \times 10^{-3} \text{ m}^3/\text{s}$

**5.3-2. Gas Flow Rate Using a Pitot Tube.** The flow rate of air at 37.8°C is being measured at the center of a duct

having a diameter of 800 mm by a pitot tube. The pressure-difference reading on the manometer is 12.4 mm of water. At the pitot-tube position, the static-pressure reading is 275 mm of water above 1 atm abs. The pitot-tube coefficient is 0.97. Calculate the velocity at the center and the volumetric flow rate of the air.

**5.3-3. Pitot-Tube Traverse for Flow-Rate Measurement.** In a pitot-tube traverse of a pipe having an inside diameter of 155.4 mm in which water at 20°C is flowing, the following data were obtained:

The pitot-tube coefficient is 0.98.

- Calculate the maximum velocity at the center.

- Calculate the average velocity. [*Hint:* Use Eq. (4.1-17) and do a numerical or a graphical integration.]

### ***5.3-4. Metering Flow by a Venturi.***

A venturi meter having a throat diameter of 38.9 mm is installed in a line having an inside diameter of 102.3 mm. It meters water having a density of 999 kg/m<sup>3</sup>. The measured pressure drop across the venturi is 156.9 kPa. The venturi coefficient  $C_v$  is 0.98. Calculate the gal/min and m<sup>3</sup>/s flow rate.

**Ans.** 330 gal/min, 0.0208 m<sup>3</sup>/s

### ***5.3-5. Use of a Venturi to Meter Water Flow.***

Water at 20°C is flowing in a 2-in. Schedule 40 steel pipe. Its flow rate is measured by a venturi meter having a throat diameter of 20 mm. The manometer reading is 214 mm of mercury. The venturi coefficient is 0.98.

Calculate the flow rate.

**5.3-6. Metering of an Oil Flow by an Orifice.** A heavy oil at  $20^{\circ}\text{C}$  having a density of  $900\text{ kg/m}^3$  and a viscosity of  $6\text{ cp}$  is flowing in a 4-in. Schedule 40 steel pipe. When the flow rate is  $0.0174\text{ m}^3/\text{s}$ , it is desired to have a pressure-drop reading across the manometer equivalent to  $0.93 \times 10^5\text{ Pa}$ . What size orifice should be used if the orifice coefficient is assumed as  $0.61$ ? What is the permanent pressure loss?

**5.3-7. Water Flow Rate in an Irrigation Ditch.** Water is flowing in an open channel in an irrigation ditch. A rectangular weir having a crest length  $L = 1.75\text{ ft}$  is used. The weir head is measured as  $h_0 = 0.47\text{ ft}$ . Calculate the flow rate in  $\text{ft}^3/\text{s}$  and  $\text{m}^3/\text{s}$ .



**Ans.** Flow rate = 1.776 ft<sup>3</sup>/s, 0.0503 m<sup>3</sup>/

s

**5.3-8. Sizing a Flow Nozzle.** A flow nozzle is to be sized for use in a pipe having an internal diameter of 1.25 in. to meter 0.60 ft<sup>3</sup>/min of water at 25°C. A pressure drop of 10.0 in. of water is to be used. Calculate the size of the flow nozzle and the permanent power loss in hp. Assume the coefficient  $C_n = 0.96$ .

**Ans.**  $D_2 = 0.506$  in., power =  $6.796 \times 10^{-4}$  hp

### References

### Notation

# Chapter 6. Flows in Packed and Fluidized Beds

## 6.0 Chapter Objectives

On completion of this chapter, a student should be able to:

- Explain the concept of drag
- Identify flows around solids, as opposed to flows inside conduits and pipes
- Distinguish between skin drag and form drag
- Sketch and explain flow behavior around an immersed object
- Explain how boundary-layer separation is observed in flows around solids
- Calculate the drag coefficient and drag force for flows around solids
- Explain how flow behavior can vary if the solid object is a cylinder, sphere, or disk
- Identify industrial examples of flows around immersed

objects

- Explain the concept of a packed bed
- Calculate the voidage and solid-volume fraction of a packed bed
- Use the Blake–Kozeny equation to calculate the pressure drop in a packed bed for laminar flow
- Use the Burke–Plummer equation to calculate the pressure drop in a packed bed for turbulent flow
- Use the Ergun equation to calculate the pressure drop in a packed bed
- Explain the concept of equivalent diameters
- Explain the concept of shape factors, in particular, sphericity
- Explain the difference between a fluidized and a packed bed
- Explain the differences between particulate and bubbling fluidization
- Calculate the minimum fluidization velocity for a fluidized bed
- Calculate the voidage of a fluidized bed at different fluidization velocities
- Calculate the minimum bubbling velocity for a fluidized

## 6.1 Flow Past Immersed Objects

### 6.1A Definition of Drag Coefficient for Flow Past Immersed Objects

#### *1. Introduction and types of drag.* In

Chapter 5, we were primarily concerned with momentum transfer and the frictional losses for flow of fluids inside conduits or pipes. In this section, we consider, in some detail, the flow of fluids around solid, immersed objects.

The flow of fluids outside of immersed bodies appears in many chemical engineering and processing applications. For example, these occur in flow past spheres in settling, flow through packed beds in drying and filtration, and flow past tubes in heat exchangers, as well as in many other applications. Often it is

useful to be able to predict the frictional losses and/or the force on the submerged objects in these various applications.

In the examples of fluid friction inside conduits that we considered in Chapter 5, the transfer of momentum perpendicular to the surface resulted in a tangential shear stress or drag on the smooth surface parallel to the direction of flow. This force exerted by the fluid on the solid in the direction of flow is called *skin* or *wall drag*. For any surface in contact with a flowing fluid, skin friction will exist. In addition to skin friction, if the fluid is not flowing parallel to the surface but must change direction to pass around a solid body such as a sphere, significant additional frictional losses will occur; this is called *form drag*.

In Fig. 6.1-1a, the flow of fluid is parallel to the smooth surface of the flat, solid plate. The force  $F$  in newtons on an element of area  $dA$  m<sup>2</sup> of the plate is the wall shear stress  $\tau_w$  times the area  $dA$ , or  $\tau_w dA$ . The total force is the sum of the integrals of these quantities evaluated over the entire area of the plate. Here, the transfer of momentum to the surface results in a tangential stress or skin drag on the surface.

In many cases, however, the immersed body is a blunt-shaped solid, which presents various angles to the direction of the fluid flow. As shown in Fig. 6.1-1b, the free-stream velocity is  $v_0$  and is uniform on approaching the blunt-shaped body suspended in a very large duct. Lines called *streamlines* represent the path of fluid elements around the

suspended body. The thin boundary layer adjacent to the solid surface is shown as a dashed line; at the edge of this layer, the velocity is essentially the same as the bulk fluid velocity adjacent to it. At the front center of the body, called the *stagnation point*, the fluid velocity will be zero; boundary-layer growth begins at this point and continues over the surface until the layer separates. The tangential stress on the body because of the velocity gradient in the boundary layer is the skin friction. Outside the boundary layer, the fluid changes direction to pass around the solid and also accelerates near the front and then decelerates. Because of these effects, an additional force is exerted by the fluid on the body. This phenomenon, called *form drag*, is in addition to the skin drag in the boundary layer.

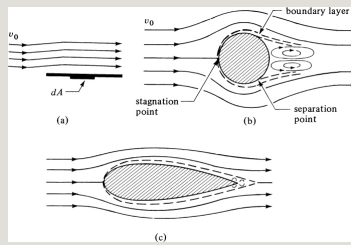


Figure 6.1-1. *Flow past immersed objects: (a) flat plate, (b) sphere, (c) streamlined object.*

In Fig. 6.1-1b, as shown, a separation of the boundary layer occurs and a wake, covering the entire rear of the object, occurs where large eddies are present and contribute to the form drag. The point of separation depends on the shape of the particle, Reynolds number, and other parameters.

The form drag for bluff bodies (e.g., cylinders and spheres) can be minimized by streamlining the body (Fig. 6.1-1c), which forces the separation point toward the rear of the body, greatly reducing the size of the wake. Additional discussion



of turbulence and boundary layers is given in Chapter 11.

2. *Drag coefficient.* From the preceding discussion, it is evident that the geometry of the immersed solid is a major factor in determining the amount of total drag force exerted on the body. Correlations of the geometry and flow characteristics for solid objects suspended or held in a free stream (immersed objects) are similar in concept and form to the friction factor–Reynolds number correlation given for flow inside conduits. In flow through conduits, the friction factor was defined as the ratio of the drag force per unit area (shear stress) to the product of density times the velocity head, as given in Eq. (5.1-4).

In a similar manner, for flow past immersed objects, the drag coefficient  $C_D$  is defined as the ratio of the total drag force per unit area to  $\rho v_0^2/2$ :

$$C_D = F_D / A_p \rho v_0^2 / 2 \quad (\text{SI}) \quad C_D = F_D / A_p \rho v_0^2 / 2 g_c \quad (\text{English}) \quad (6.1-1)$$

where  $F_D$  is the total drag force in N,  $A_p$  is an area in  $\text{m}^2$ ,  $C_D$  is dimensionless,  $v_0$  is free-stream velocity in  $\text{m/s}$ , and  $\rho$  is density of fluid in  $\text{kg/m}^3$ . In English units,  $F_D$  is in  $\text{lbf}$ ,  $v_0$  is in  $\text{ft/s}$ ,  $\rho$  is in  $\text{lbm/ft}^3$ , and  $A_p$  is in  $\text{ft}^2$ . The area  $A_p$  used is the area obtained by projecting the body on a plane perpendicular to the line of flow. For a sphere,  $A_p = \pi D_p^2/4$ , where  $D_p$  is sphere diameter; for a cylinder whose axis is perpendicular to the flow direction,  $A_p = L D_p$ , where  $L$  = cylinder length. Solving Eq. (6.1-1) for

the total drag force,

$$F_D = C_D v_0^2 \frac{\rho A_p}{2} \quad (6.1-2)$$

The Reynolds number for a given solid immersed in a flowing liquid is

$$N_{Re} = \frac{D_p v_0 \rho}{\mu} = \frac{D_p G_0}{\mu} \quad (6.1-3)$$

where  $G_0 = v_0 \rho$ .

#### **6.1B Flow Past a Sphere, Long Cylinder, and Disk**

For each particular shape of object and orientation of the object with respect to the direction of flow, a different relation of  $C_D$  versus  $N_{Re}$  exists. Correlations of drag coefficient versus Reynolds number are shown in Fig. 6.1-2 for spheres, long cylinders, and disks. The face of the disk and the axis of the

cylinder are perpendicular to the direction of flow. These curves have been determined experimentally. However, in the laminar region for very low Reynolds numbers (less than about 1.0), the experimental drag force for a sphere is the same as the theoretical Stokes' law equation as follows:

$$F_D = 3\pi\mu Dpv_0 \quad (6.1-4)$$

Combining Eqs. (6.1-2) and (6.1-4) and solving for  $C_D$ , the drag coefficient predicted by Stokes' law is

$$C_D = 24Dpv_0\rho/\mu = 24N_{Re} \quad (6.1-5)$$

The variation of  $C_D$  with  $N_{Re}$  (Fig. 6.1-2) is quite complicated because of the interaction of the factors that control skin drag and form drag. For a sphere,

as the Reynolds number is increased beyond the Stokes' law range, boundary layer separation occurs and a wake is formed. Further increases in  $N_{Re}$  cause shifts in the separation point. At about  $N_{Re} = 3 \times 10^5$ , the sudden drop in  $C_D$  is the result of the boundary layer becoming completely turbulent and the point of separation moving downstream. In the region of  $N_{Re}$ , about  $1 \times 10^3$  to  $2 \times 10^5$ , the drag coefficient is approximately constant for each shape and  $C_D = 0.44$  for a sphere. Above  $N_{Re}$ , about  $5 \times 10^5$ , the drag coefficients are again approximately constant, with  $C_D$  being 0.13 for a sphere, 0.33 for a cylinder, and 1.12 for a disk. Additional discussions and theory concerning flow past spheres are given in Section 10.5.

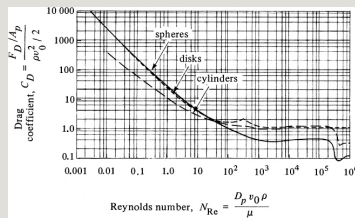


Figure 6.1-2. Drag coefficients for flow past immersed spheres, long cylinders, and disks. Reprinted with permission from C. E. Lapple and C. B. Shepherd, *Ind. Eng. Chem.*, **32**, 606 (1940). *The American Chemical Society*.

For derivations of theory and detailed discussions of the drag force for flow parallel to a flat plate, Chapter 11 on boundary-layer flow and turbulence should be consulted. The flow of fluids normal to banks of cylinders or tubes occurs in heat exchangers and other processing applications. The banks of tubes can be arranged in a number of different geometries. Because of the many possible geometric tube configurations and spacings, it is not possible to have one correlation for the data on pressure drop and friction

factors. Details of the many correlations available are given elsewhere (P1).

**EXAMPLE 6.1-1. Force on a Submerged Sphere**

Air at 37.8°C and 101.3 kPa absolute pressure flows at a velocity of 23 m/s past a sphere having a diameter of 42 mm. What is the drag coefficient  $C_D$  and the force on the sphere?

**Solution:** From Appendix A.3, for air at 37.8°C,  $\rho = 1.137$  kg/m<sup>3</sup> and  $\mu = 1.90 \times 10^{-5}$  Pa · s. Also,  $D_p = 0.042$  m and  $v_0 = 23.0$  m/s. Using Eq. (6.1-3),

$$NRe = D_p v_0 \rho / \mu = 0.042(23.0)(1.137) / 1.90 \times 10^{-5} = 5.781 \times 10^4$$

From Fig. 6.1-2 for a sphere,  $C_D = 0.47$ . Substituting into Eq. (6.1-2), where  $A_p = \pi D_p^2 / 4$  for a sphere,

$$F_D = C_D v_0^2 \rho A_p = (0.47)(23.0)^2 (1.137)(\pi)(0.042)^2 / 4 = 0.1958 \text{ N}$$

**EXAMPLE 6.1-2. Force on a Cylinder in a Tunnel**

Water at 24°C is flowing past a long cylinder at a velocity of 1.0 m/s in a large tunnel. The axis of the cylinder is perpendicular to the direction of flow. The diameter of the cylinder is 0.090 m. What is the force per meter length on the cylinder?

**Solution:** From Appendix A.2, for water at 24°C,  $\rho = 997.2$  kg/m<sup>3</sup> and  $\mu = 0.9142 \times 10^{-3}$  Pa · s. Also,  $D_p = 0.090$  m,  $L = 1.0$  m, and  $v_0 = 1.0$  m/s. Using Eq. (6.1-3),

$$NRe = D_p v_0 \rho / \mu = 0.090(1.0)(997.2) / 0.9142 \times 10^{-3} = 9.817 \times 10^4$$

From Fig. 6.1-2 for a long cylinder,  $C_D = 1.4$ . Substituting into Eq. (6.1-2), where  $A_p = L D_p = 1.0(0.090) = 0.090$  m<sup>2</sup>,

$$F_D = C_D v_0^2 \rho A_p = (1.4)(1.0)^2 (997.2)(0.09) = 62.82 \text{ N}$$

## 6.2 Flow in Packed Beds

*1. Introduction.* A system of considerable importance in chemical and other process engineering fields is the packed bed or packed column, which is used for a fixed-bed catalytic reactor, adsorption of a solute, absorption, filter bed, and other similar applications. The packing material in the bed may be spheres, irregular particles, cylinders, or various kinds of commercial packings. In the discussion to follow, it is assumed that the packing is everywhere uniform and that little or no channeling occurs. The ratio of diameter of the tower to packing diameter should be a minimum of 8:1 to 10:1 for wall effects to be small. In some theoretical



approaches, the packed column is modeled as a bundle of crooked tubes of varying cross-sectional area (B2). The theory developed for single straight tubes is used to develop the results for the bundle of crooked tubes.

*2. Laminar flow in packed beds.* In describing and modeling flow in packed beds, it is necessary to define certain geometric relations that are dependent on the fluid and particle volume distribution. For example, one of the most important parameters in packed beds is the void fraction  $\epsilon$ , or porosity, which is defined as

$$\epsilon = \frac{\text{void volume of bed}}{\text{total volume of bed (voids plus solids)}} \quad (6.2-1)$$

The specific surface of a particle  $a_v$  in  $\text{m}^{-1}$  is defined as

$$a_v = \frac{S_p}{V_p} \quad (6.2-2)$$

where  $S_p$  is the surface area of a particle in  $\text{m}^2$  and  $V_p$  is the volume of a particle in  $\text{m}^3$ . For a spherical particle,

$$a_v = \frac{6}{D_p} \quad (6.2-3)$$

where  $D_p$  is diameter in m. For a packed bed of nonspherical particles, the effective particle diameter  $D_p$  is defined as

$$D_p = \frac{6}{a_v} \quad (6.2-4)$$

Since  $(1 - \varepsilon)$  is the volume fraction of particles (sometimes called the *solid volume fraction*  $\phi$ ) in the bed,

$$a = \frac{a_v}{1 - \epsilon} = \frac{6D_p}{1 - \epsilon} \quad (6.2-5)$$

where  $a$  is the ratio of total surface area in the bed to total volume of bed (void volume plus particle volume) in  $m^{-1}$ .

**EXAMPLE 6.2-1. Surface Area in a Packed Bed of Cylinders**

A packed bed is composed of cylinders having a diameter  $D = 0.02$  m and a length  $h = D$ . The bulk density of the overall packed bed is  $962 \text{ kg/m}^3$  and the density of the solid cylinders is  $1600 \text{ kg/m}^3$ .

- Calculate the void fraction  $\epsilon$ .
- Calculate the effective diameter  $D_p$  of the particles.
- Calculate the value of  $a$  in Eq. (6.2-5).

**Solution:** For part (a), taking  $1.00 \text{ m}^3$  of packed bed as a basis, the total mass of the bed is  $(962 \text{ kg/m}^3)(1.00 \text{ m}^3) = 962 \text{ kg}$ . This mass of  $962 \text{ kg}$  is also the mass of the solid cylinders. Hence, volume of cylinders  $= 962 \text{ kg} / (1600 \text{ kg/m}^3) = 0.601 \text{ m}^3$ . Using Eq. (6.2-1),

$$\epsilon = \frac{\text{volume of voids in bed}}{\text{total volume of bed}} = \frac{1.000 - 0.601}{1.000} = 0.399$$

For the effective particle diameter  $D_p$  in part (b), for a cylinder where  $h = D$ , the surface area of a particle is

$$S_p = (2)\pi D^2/4 (\text{ends}) + \pi D(D) (\text{sides}) = 3\pi D^2/2$$

The volume  $V_p$  of a particle is

$$V_p = \pi D^2/4 (D) = \pi D^3/4$$

Substituting into Eq. (6.2-2),

$$a_v = \frac{S_p}{V_p} = \frac{3\pi D^2/2}{\pi D^3/4} = \frac{6}{D}$$

Finally, substituting into Eq. (6.2-4),

$$D_p = 6av = 66/D = D = 0.02 \text{ m}$$

Hence, the effective diameter to use is  $D_p = D = 0.02 \text{ m}$ .

For part (c), using Eq. (6.2-5),

$$a = 6D_p(1-\epsilon) = 6(0.02)(1-0.399) = 180.3 \text{ m}^{-1}$$

The average interstitial velocity in the bed is  $v \text{ m/s}$  and is related to the superficial velocity  $v'$  based on the cross section of the empty container by

$$v' = \epsilon v \quad (6.2-6)$$

The hydraulic radius  $r_H$  for flow defined in Eq. (5.1-21) is modified as follows (B2):

$$r_H = \frac{\text{cross-sectional area available for flow}}{\text{total wetted surface of solids} = \frac{\text{volume of voids}}{\text{volume of bed}} \frac{\text{wetted surface}}{\text{volume of bed}}} = \epsilon a \quad (6.2-7)$$

Combining Eqs. (6.2-5) and (6.2-7),

$$r_H = \frac{\epsilon}{6(1-\epsilon)} D_p \quad (6.2-8)$$

Since the equivalent diameter  $D$  for a channel is  $D = 4r_H$ , the Reynolds number for a packed bed is as follows, using Eq. (6.2-8) and  $v' = \epsilon v$ :

$$\begin{aligned} N_{Re} &= (4r_H) v \rho \mu = 4 \frac{\epsilon}{6(1-\epsilon)} D_p v \rho \mu \\ &= \frac{4}{6} \frac{\epsilon}{1-\epsilon} D_p v' \rho \mu \quad (6.2-9) \end{aligned}$$

For packed beds, Ergun (E1) defined the Reynolds number as shown above but without the  $4/6$  term:

$$N_{Re,p} = D_p v' \rho (1-\epsilon) \mu = D_p G' (1-\epsilon) \mu \quad (6.2-10)$$

where  $G' = v' \rho$ .

For laminar flow, the Hagen–Poiseuille

equation (5.1-2) can be combined with Eq. (6.2-8) for  $r_H$  and Eq. (6.2-6) to give

$$\Delta p = 32\mu v \Delta L D^2 = 32\mu (v'/\epsilon) \Delta L (4r_H)^2 = (72)\mu v' \Delta L (1-\epsilon)^2 \epsilon^3 D_p^2 \quad (6.2-11)$$

The true  $\Delta L$  is larger because of the tortuous path, and use of the hydraulic radius predicts too large a  $v'$ .

Experimental data show that the constant should be 150, which gives the *Blake-Kozeny equation* for laminar flow, void fractions less than 0.5, effective particle diameter  $D_p$ , and  $N_{Re,p} < 10$ :

$$\Delta p = 150\mu v' \Delta L D_p^2 (1-\epsilon)^2 \epsilon^3 \quad (6.2-12)$$

*3. Turbulent flow in packed beds.* For turbulent flow, we use the same procedure by starting with Eq. (5.1-5)

and substituting Eqs. (6.2-6) and (6.2-8) into this equation to obtain

$$\Delta p = 3f \rho (v')^2 \Delta L D_p^{1-\epsilon} \epsilon^3 \quad (6.2-13)$$

For highly turbulent flow, the friction factor should approach a constant value. Also, it is assumed that all packed beds should have the same relative roughness. Experimental data indicate that  $3f = 1.75$ . Hence, the final equation for turbulent flow for  $N_{Re,p} > 1000$ , which is called the *Burke–Plummer equation*, becomes

$$\Delta p = 1.75 \rho (v')^2 \Delta L D_p^{1-\epsilon} \epsilon^3 \quad (6.2-14)$$

Adding Eq. (6.2-12) for laminar flow and Eq. (6.2-14) for turbulent flow, Ergun (E1) proposed the following general equation, known as the *Ergun equation* for low, intermediate, and high

Reynolds numbers, which has been tested experimentally:

$$\Delta p = 150 \mu v' \Delta L D_p^{-2} (1 - \epsilon)^2 \epsilon^3 + 1.75 \rho (v')^2 \Delta L D_p^{-1} (1 - \epsilon) \epsilon^3 \quad (6.2-15)$$

Rewriting Eq. (6.2-15) in terms of dimensionless groups,

$$\Delta p \rho (G')^2 D_p \Delta L \epsilon^3 (1 - \epsilon) = 150 N_{Re,p} + 1.75 \quad (6.2-16)$$

See also Eq. (6.3-5) for another form of Eq. (6.2-16). This form of the Ergun equation (6.2-16) can be used for gases by taking the density  $\rho$  of the gas as the arithmetic average of the inlet and outlet pressures. The velocity  $v'$  changes throughout the bed for a compressible fluid, but  $G'$  is a constant. At high values of  $N_{Re,p}$ , Eqs. (6.2-15) and (6.2-16) reduce to Eq. (6.2-14), and to Eq.



(6.2-12) for low values. For large pressure drops with gases, Eq. (6.2-15) can be written in differential form (P1).

**EXAMPLE 6.2-2. Pressure Drop and Flow of Gases in a Packed Bed**

Air at 311 K is flowing through a packed bed of spheres having a diameter of 12.7 mm. The void fraction  $\varepsilon$  of the bed is 0.38 and the bed has a diameter of 0.61 m and a height of 2.44 m. The air enters the bed at 1.10 atm abs at the rate of 0.358 kg/s. Calculate the pressure drop of the air in the packed bed. The average molecular weight of air is 28.97.

**Solution:** From Appendix A.3, for air at 311 K,  $\mu = 1.90 \times 10^{-5}$  Pa · s. The cross-sectional area of the bed is  $A = (\pi/4)D^2 = (\pi/4)(0.61)^2 = 0.2922$  m<sup>2</sup>. Hence,  $G' = 0.358/0.2922 = 1.225$  kg/m<sup>2</sup> · s (based on an empty cross section of the container or bed).  $D_p = 0.0127$  m,  $\Delta L = 2.44$  m, and inlet pressure  $p_1 = 1.1(1.01325 \times 10^5) = 1.15 \times 10^5$  Pa.

From Eq. (6.2-10),

$$NRe_p = \frac{D_p G' (1 - \varepsilon)}{\mu} = \frac{0.0127(1.225)(1 - 0.38)}{(1.90 \times 10^{-5})} = 1321$$

To use Eq. (6.2-16) for gases, the density  $\rho$  to use is the average at the inlet  $p_1$  and outlet  $p_2$  pressures, or at  $(p_1 + p_2)/2$ . This is trial and error since  $p_2$  is unknown. Assuming that  $\Delta p = 0.05 \times 10^5$  Pa,  $p_2 = 1.115 \times 10^5 - 0.05 \times 10^5 = 1.065 \times 10^5$  Pa. The average pressure is  $p_{av} = (1.115 \times 10^5 + 1.065 \times 10^5)/2 = 1.090 \times 10^5$  Pa. The average density to use is

$$\rho_{av} = \frac{MRT p_{av}}{Z} = \frac{28.97(1.090 \times 10^5)}{8314.34(311)} = 1.221 \text{ kg/m}^3 \quad (6.2-17)$$

Substituting into Eq. (6.2-16) and solving for  $\Delta p$ ,

$$\Delta p (1.221)^2 (1.225)^2 20.0127^2 2.44 (0.38)^{31-0.38} = 1501321 + 1.75$$

Solving,  $\Delta p = 50.0497 \times 10^5 \text{ Pa}$ . This is close enough to the assumed value, so a second trial is not needed.

*4. Shape factors.* Many particles in packed beds are often irregular in shape. Therefore, equivalent diameters are often used to help model nonspherical particles. Multiple equivalent diameters exist that are based on different geometry conditions. For example, the equivalent volume diameter of a particle is defined as the diameter of a sphere having the same volume as this particle. Another way to account for nonspherical particles is to use particle *sphericity*. The sphericity (shape factor)  $\phi_s$  of a particle is the ratio of the surface area of this sphere having the same volume as the particle to the actual surface area of the particle. For a sphere, the surface area  $S_p = \pi D_p^2$  and the volume  $v_p = \pi D_p^3/6$ . Hence, for any

particle,  $\phi S = \pi D_p^2 / S_p$ , where  $S_p$  is the actual surface area of the particle and  $D_p$  is the diameter (equivalent diameter) of the sphere having the same volume as the particle. Then

$$S_p v_p = \pi D_p^2 / \phi S \pi D_p^3 / 6 = 6 \phi S D_p \quad (6.2-18)$$

From Eq. (6.2-2),

$$a v = S_p v_p = 6 \phi S D_p \quad (6.2-19)$$

Then, Eq. (6.2-5) becomes

$$a = 6 \phi S D_p (1 - \epsilon) \quad (6.2-20)$$

For a sphere,  $\phi_s = 1.0$ . For a cylinder where diameter = length,  $\phi_s$  is calculated to be 0.874, and for a cube,  $\phi_s$  is calculated to be 0.806. For granular materials, it is difficult to

measure the actual volume and surface area to obtain the equivalent diameter. Hence,  $D_p$  is usually taken to be the nominal size from a screen analysis or visual length measurements. The surface area is determined by adsorption measurements or measurement of the pressure drop in a bed of particles. Then, Eq. (6.2-18) is used to calculate  $\phi_s$  (Table 6.2-1). Typical values for many crushed materials are between 0.6 and 0.7. For convenience, for the cylinder and the cube, the nominal diameter is sometimes used (instead of the equivalent diameter), which then gives a shape factor of 1.0.

Table 6.2-1. *Shape Factors (Sphericity) of Some Materials*

--

5. *Mixtures of particles.* For mixtures of particles of various sizes, we can define a *mean specific surface*  $a_{vm}$  as

$$a_{vm} = \sum x_i a_{vi} \quad (6.2-21)$$

where  $x_i$  is the volume fraction.

Combining Eqs. (6.2-19) and (6.2-21),

$$D_{pm} = 6a_{vm} = 6 \sum x_i (6 / \phi S D_{pi}) = 1 \sum x_i / (\phi S D_{pi}) \quad (6.2-22)$$

where  $D_{pm}$  is the effective mean diameter for the mixture.

**EXAMPLE 6.2-3. Mean Diameter for a Particle Mixture**

A mixture contains three different types of particles. The mixture is 25% by volume of 25 mm size, 40% of 50 mm size, and 35% of 75 mm size. It is assumed that the sphericity for all particles is 0.68. Calculate the effective mean diameter.

**Solution:** The following data are given:  $x_1 = 0.25$ ,  $D_{p1} = 25$  mm;  $x_2 = 0.40$ ;  $D_{p2} = 50$ ;  $x_3 = 0.35$ ,  $D_{p3} = 75$ ;  $\phi_s = 0.68$ . Substituting into Eq. (6.2-22),

$$D_{pm} = 10.25 / (0.68 \times 25) + 0.40 / (0.68 \times 50) + 0.35 / (0.68 \times 75) = 30.0 \text{ mm}$$

6. *Darcy's empirical law for laminar flow*. Equation (6.2-12) for laminar flow in packed beds shows that the flow rate is proportional to  $\Delta p$  and inversely proportional to the viscosity  $\mu$  and length  $\Delta L$ . This is the basis for *Darcy's law*, as follows, for purely viscous flow in consolidated porous media:

$$v' = q'A = -k\mu\Delta p\Delta L \quad (6.2-23)$$

where  $v'$  is superficial velocity based on the empty cross section in cm/s,  $q'$  is the flow rate in cm<sup>3</sup>/s,  $A$  is the empty cross-sectional area in cm<sup>2</sup>,  $\mu$  is viscosity in cp,  $\Delta p$  is the pressure drop in atm,  $\Delta L$  is the length in cm, and  $k$  is the permeability in (cm<sup>3</sup> flow/s) · (cp) · (cm length)/(cm<sup>2</sup> area) · (atm pressure drop). The units used for  $k$  in cm<sup>2</sup> · cp/s · atm are often given in darcy or in millidarcy

(1/1000 darcy). Hence, if a porous medium has a permeability of 1 darcy, a fluid of 1 cp viscosity will flow at 1 cm<sup>3</sup>/s per 1 cm<sup>2</sup> cross section with a  $\Delta p$  of 1 atm per cm length. This equation is often used in measuring permeabilities of underground oil reservoirs.

### **6.3 Flow in Fluidized Beds**

*1. Types of fluidization behavior in fluidized beds.* In a packed bed of small particles, when a fluid enters at sufficient velocity from the bottom and passes up through the particles, the particles are pushed upward and the bed expands and becomes fluidized. Two general types of fluidization, *particulate fluidization* and *bubbling fluidization*, can occur.

In *particulate fluidization*, as the fluid

velocity is increased, the bed continues to expand and remains homogeneous for a time. The particles move farther apart and their motion becomes more rapid. The average bed density at a given velocity is the same in all regions of the bed. An example of this type of fluidization is catalytic cracking catalysts fluidized by gases. This type of fluidization is very desirable in promoting intimate contact between the gas and solids. Particulate fluidization can also be observed when liquids are used to fluidize the bed.

In *bubbling fluidization*, the gas passes through the bed as voids or bubbles, which may contain few particles. In this case, only a small percentage of the gas passes in the spaces between individual particles. As the gas velocity is



increased, the expansion of the bed is minimal. Since most of the gas is used in forming bubbles, little contact occurs between the individual particles and the bubbles.

Particles, while fluidized, that exhibit the type of behavior described above, have been classified by Geldart (G2) into different classes. Those called Type A, which exhibit particulate fluidization in gases, fall into the following approximate ranges: For  $\Delta\rho = (\rho_p - \rho) = 2000 \text{ kg/m}^3$ ,  $D_p = 20 - 125 \text{ }\mu\text{m}$ ;  $\Delta\rho = 1000$ ,  $D_p = 25 - 250$ ;  $\Delta\rho = 500$ ,  $D_p = 40 - 450$ ;  $\Delta\rho = 200$ ,  $D_p = 100 - 1000$ . For those called Type B, which exhibit bubbling fluidization, approximate ranges are as follows:  $\Delta\rho = 2000$ ,  $D_p = 125 - 700 \text{ }\mu\text{m}$ ;  $\Delta\rho = 1000$ ,  $D_p = 250 - 1000$ ;  $\Delta\rho = 500$ ,  $D_p = 450 - 1500$ ;  $\Delta\rho =$

200,  $D_p = 1000 - 2000$ .

Another type of behavior, called *slugging*, can occur in bubbling since the bubbles tend to coalesce and grow as they rise in the bed. If the column is small in diameter with a deep bed, bubbles can become large, filling the entire cross section and traveling up the tower separated by slugs of solids.

*2. Minimum velocity and porosity for particulate fluidization.* When a fluid flows upward through a packed bed of particles at low velocities, the particles remain stationary. As the fluid velocity is increased, the pressure drop increases according to the Ergun equation (6.2-15). Upon further increases in velocity, conditions finally occur where the force of the pressure drop times the

cross-sectional area equals the gravitational force on the mass of particles (also known as the “weight of the bed.” At this point, the particles begin to move and the onset of fluidization or minimum fluidization is reached. The fluid velocity at which fluidization begins is known as the *minimum fluidization velocity*  $v_{mf}$ , based on the empty cross section of the tower (superficial velocity).

Table 6.3-1. *Void Fraction,  $\epsilon_{mf}$ , at Minimum Fluidization Conditions (L2)*

The porosity of the bed when true fluidization occurs is the minimum porosity for fluidization,  $\epsilon_{mf}$ . Some typical values of  $\epsilon_{mf}$  for various materials are given in Table 6.3-1. The

bed expands to this voidage or porosity before particle motion appears. This minimum voidage can be determined experimentally by subjecting the bed to a rising gas stream and measuring the height of the bed  $L_{mf}$  in m. Generally, it appears best to use gas as the fluid rather than a liquid, since liquids give somewhat higher values of  $\varepsilon_{mf}$ .

As stated previously for the case of packed beds, the pressure drop increases as the gas velocity is increased until the onset of minimum fluidization. Then, as the velocity is further increased, the pressure drop decreases very slightly, and then it remains practically unchanged as the bed continues to expand or increase in porosity with increases in velocity. At high velocities, the bed may resemble a boiling liquid.

As the bed expands with increasing velocity, it continues to retain its top horizontal surface. Eventually, as the velocity is increased much further, entrainment (or loss) of particles from the actual fluidized bed surface becomes appreciable.

The relation between bed height  $L$  and porosity  $\varepsilon$  is as follows for a bed having a uniform cross-sectional area  $A$ . Since the volume  $LA(1 - \varepsilon)$  is equal to the total volume of solids if they existed as one control volume,

$$L_1 A(1 - \varepsilon_1) = L_2 A(1 - \varepsilon_2) \quad (6.3-1)$$

$$L_1 L_2 = \frac{1 - \varepsilon_2}{1 - \varepsilon_1} \quad (6.3-2)$$

where  $L_1$  is the height of the bed with porosity  $\varepsilon_1$  and  $L_2$  is the height of the bed with porosity  $\varepsilon_2$ .

3. *Pressure drop and minimum fluidizing velocity.* As a first approximation, the pressure drop at the start of fluidization can be determined as follows. The force obtained from the pressure drop times the cross-sectional area must equal the gravitational force exerted by the mass of the particles minus the buoyant force of the displaced fluid:

$$\Delta p A = L_m f A (1 - \epsilon_m f) (\rho_p - \rho) g \quad (6.3-3)$$

Hence,

$$\begin{aligned} \Delta p L_m f &= (1 - \epsilon_m f) (\rho_p - \rho) g \\ \Delta p L_m f &= (1 - \epsilon_m f) (\rho_p - \rho) g \end{aligned} \quad (6.3-4)$$

Since we often have irregular-shaped particles in the bed, and it is more convenient to use the particle size and

shape factor (sphericity) in the equations. First, for the effective mean diameter  $D_p$ , we substitute the term  $\phi_s D_P$ , where  $D_P$  now represents the particle size of a sphere having the same volume as the particle and  $\phi_s$  the shape factor. Often, the value of  $D_P$  is approximated by using the nominal size from a sieve analysis. Then, Eq. (6.2-15) for pressure drop in a packed bed becomes

$$\Delta p L = 150 \mu v' \phi_s^2 D_P^2 (1 - \epsilon)^2 \epsilon^3 + 1.75 \rho (v')^2 \phi_s D_P (1 - \epsilon) \epsilon^3 \quad (6.3-5)$$

where  $\Delta L = L$ , bed length in m.

Equation (6.3-5) can now be used by a small extrapolation for packed beds to calculate the minimum fluid velocity  $v_{mf}'$  at which fluidization begins by

substituting  $\nu_{mf}'$  for  $\nu'$ ,  $\varepsilon_{mf}$  for  $\varepsilon$ , and  $L_{mf}$  for  $L$ , and combining the result with Eq. (6.3-4) to give

$$1.75 DP^2 (\nu_{mf}')^2 \rho^2 \phi S \varepsilon_{mf}^3 \mu^2 + 150 (1 - \varepsilon_{mf}) DP \nu_{mf}' \rho \phi S^2 \varepsilon_{mf}^3 \mu - DP^3 \rho (\rho_p - \rho) g \mu^2 = 0 \quad (6.3-6)$$

Defining a Reynolds number as

$$N_{Re,mf} = DP \nu_{mf}' \rho \mu \quad (6.3-7)$$

Eq. (6.3-6) becomes

$$1.75 (N_{Re,mf})^2 \phi S \varepsilon_{mf}^3 + 150 (1 - \varepsilon_{mf}) (N_{Re,mf}) \phi S^2 \varepsilon_{mf}^3 - DP^3 \rho (\rho_p - \rho) g \mu^2 = 0 \quad (6.3-8)$$

When  $N_{Re,mf} < 20$  (small particles), the first term of Eq. (6.3-8) can be dropped, and when  $N_{Re,mf} > 1000$  (large



particles), the second term drops out.

If the terms  $\varepsilon_{mf}$  and/or  $\phi_s$  are not known, Wen and Yu (W4) found for a variety of systems that

$$S\phi\varepsilon_{mf}^3 \cong 114, 1 - \varepsilon_{mf}\phi S^2\varepsilon_{mf}^3 \cong 11 \quad (6.3-9)$$

Substituting into Eq. (6.3-8), the following simplified equation is obtained:

$$N_{Re,mf} = [(33.7)^2 + 0.0408 D P^3 \rho (\rho_p - \rho) g \mu^2]^{1/2} - 33.7 \quad (6.3-10)$$

This equation holds for a Reynolds number range of 0.001 to 4000.

Alternative equations are available in the literature (K1, W4).

**EXAMPLE 6.3-1. Minimum Velocity for Fluidization**

Solid particles having a size of 0.12 mm, a sphericity shape factor  $\phi_s$  of 0.88, and a density of 1000 kg/m<sup>3</sup> are to be

fluidized using air at 2.0 atm abs and 25°C. The voidage at minimum fluidizing conditions is 0.42.

- If the cross section of the empty bed is 0.30 m<sup>2</sup> and the bed contains 300 kg of solid, calculate the minimum height of the fluidized bed.
- Calculate the pressure drop at minimum fluidizing conditions.
- Calculate the minimum velocity for fluidization.
- Use Eq. (6.3-10) to calculate  $vmf'$  assuming that data for  $\phi_s$  and  $\epsilon_{mf}$  are not available.

**Solution:** For part (a), the volume of solids = 300 kg/(1000 kg/m<sup>3</sup>) = 0.300 m<sup>3</sup>. The height the solids would occupy in the bed if  $\epsilon_1 = 0$  is  $L_1 = 0.300 \text{ m}^3 / (0.30 \text{ m}^2 \text{ cross section}) = 1.00 \text{ m}$ . Using Eq. (6.3-2) and calling  $L_{mf} = L_2$  and  $\epsilon_{mf} = \epsilon_2$ ,

$$L_1 L_{mf} = 1 - \epsilon_{mf} - \epsilon_1 L_{mf} = 1 - 0.421 - 0$$

Solving,  $L_{mf} = 1.724 \text{ m}$ .

The physical properties of air at 2.0 atm and 25°C (Appendix A.3) are  $\mu = 1.845 \times 10^{-5} \text{ Pa} \cdot \text{s}$ ,  $\rho = 1.187 \times 2 = 2.374 \text{ kg/m}^3$ , and  $p = 2.0265 \times 10^5 \text{ Pa}$ . For the particle,  $DP = 0.00012 \text{ m}$ ,  $\rho_P = 1000 \text{ kg/m}^3$ ,  $\phi_s = 0.88$ , and  $\epsilon_{mf} = 0.42$ .

For part (b), using Eq. (6.3-4) to calculate  $\Delta p$ ,

$$\Delta p = L_{mf}(1 - \epsilon_{mf})(\rho_P - \rho)g = 1.724(1 - 0.42)(1000 - 2.374)(9.80665) = 0.0978 \times 10^5 \text{ Pa}$$

To calculate  $vmf'$  for part (c), Eq. (6.3-8) is used:

$$1.75(NRe_{mf})^2(0.88)(0.42)^3 + 150(1 - 0.42)(NRe_{mf})(0.88)^2(0.42)^3 - (0.00012)^3 \frac{2.374(1000 - 2.374)(9.80665)}{(1.845 \times 10^{-5})^2} = 0$$

Solving,

$$NRe_{mf} = 0.07764 = DP_{vmf} \rho \mu = 0.00012 (vmf') (2.374) 1.845 \times 10^{-5} = 0.005029 \text{ m/s}$$

Using the simplified Eq. (6.3-10) for part (d),

$$NRe_{mf} = [(33.7)^2 + 0.0408(0.00012)^3 (2.374)(1000 - 2.374)(9.80665)(1.845 \times 10^{-5})^2]^{1/2} = 33.7 = 0.07129$$

4. *Expansion of fluidized beds.* For the case of small particles and where  $NRe_f = D_p v' \rho / \mu < 20$ , we can estimate the variation of porosity or bed height  $L$  as follows. We assume that Eq. (6.3-8) applies over the whole range of fluid velocities, with the first term being neglected. Then, solving for  $v'$ ,

$$v' = \frac{D_p^2 (\rho_p - \rho) g \phi S}{150 \mu \epsilon^{3/2}} - \frac{\epsilon}{K \epsilon^{3/2 - \epsilon}} \quad (6.3-11)$$

We find that all terms except  $\epsilon$  are constant for the particular system, and  $\epsilon$  depends upon  $v'$ . This equation can be used with liquids to estimate  $\epsilon$  with  $\epsilon < 0.80$ . However, because of clumping and other factors, errors can occur when used for gases.

The flow rate in a fluidized bed is limited on the one hand by the minimum  $v_{mf}'$  and on the other by entrainment of solids from the bed. This maximum allowable velocity is approximated as the terminal settling velocity  $v_t'$  of the particles. Approximate equations for calculating the operating range are as follows (P2). For fine solids and  $N_{Re,f} < 0.4$ ,

$$v_t' v_{mf}' \cong 901 \quad (6.3-12)$$

For large solids and  $N_{Re,f} > 1000$ ,

$$v_t' v_{mf}' \cong 91 \quad (6.3-13)$$

**EXAMPLE 6.3-2. Expansion of a Fluidized Bed**

Using the data from Example 6.3-1, estimate the maximum allowable velocity  $v_t'$ . Using an operating velocity of 3.0 times the minimum, estimate the voidage of the bed.

**Solution:** From Example 6.3-1,  $N_{Re, mf} = 0.07764$ ,  $v_{mf}' = 0.005029$  m/s, and  $\epsilon_{mf} = 0.42$ . Using Eq. (6.3-12), the maximum allowable velocity is

$$vt' \approx 90(vmf') = 90(0.005029) = 0.4526 \text{ m/s}$$

Using an operating velocity  $v'$  of 2.0 times the minimum,

$$v = 2.0(vmf') = 2.0(0.005029) = 0.01006 \text{ m/s}$$

To determine the voidage at this new velocity, we substitute into Eq. (6.3-11) using the known values at minimum fluidizing conditions to determine  $K_1$ :

$$0.005029 = K_1(0.42)^{31-0.42}$$

Solving,  $K_1 = 0.03938$ . Then, using the operating velocity in Eq. (6.3-11),

$$0.01006 = (0.03938)\epsilon^{31-\epsilon}$$

Solving, the voidage of the bed at the operating velocity is  $\epsilon = 0.503$ .

*5. Minimum bubbling velocity.* The fluidization velocity at which bubbles are first observed is called the *minimum bubbling velocity*,  $v_{mb}'$ . For Group B particles, which exhibit bubbling fluidization,  $v_{mb}'$  is reasonably close to  $vmf'$ . For Group A particles,  $v_{mb}'$  is substantially greater than  $vmf'$ . The following equation (G3) can be used to calculate  $v_{mb}'$ :

$$v_{mb}' = 33D_p(\mu/\rho) - 0.1 \quad (6.3-14)$$

where  $v_{mb}'$  is minimum bubbling velocity in m/s,  $\mu$  is viscosity in  $\text{Pa} \cdot \text{s}$ , and  $\rho$  is gas density in  $\text{kg/m}^3$ . If the calculated  $v_{mf}'$  is greater than the calculated  $v_{mb}'$  by Eq. (6.3-14), then the  $v_{mf}'$  should be used as the minimum bubbling velocity (G4).

**EXAMPLE 6.3-3. Minimum Bubbling Velocity**

Using data from Example 6.3-1, calculate the  $v_{mb}'$ .

**Solution:** Substituting into Eq. (6.3-14),

$$v_{mb}' = 33(0.00012)(1.845 \times 10^{-5}/2.374) - 0.1 = 0.01284 \text{ m/s}$$

This is substantially greater than the  $v_{mf}'$  of 0.005029 m/s.

## 6.4 Chapter Summary

In this chapter, we have described the different flows and applications associated with flows past immersed objects—particularly pipes, tubes, spheres, flat plates, and disks. First, we discussed the flow behavior in

terms of boundaries layers, and streamlines, as well as stagnation and separation points. Based on the flow behavior, we were able to define and calculate drag forces and drag coefficients associated with these types of flows. For flows passed immersed objects, we defined the drag coefficient as

$$C_D = F_D / \frac{\rho v_0^2 A}{2} \quad (6.1-1)$$

For low Reynolds-number flow (Stokes' flow) past spheres, the drag force was shown to be calculated from

$$F_D = 3\pi\mu D v_0 \quad (6.1-4)$$

and the drag coefficient calculated from

$$C_D = \frac{24\mu}{\rho v_0 D} = \frac{24}{Re} \quad (6.1-5)$$

Packed beds were described as an ensemble of particles contained in a tube or column. Processes that use packed beds require a liquid to pass through the void space between the particles (known as the voidage). The voidage, also known as the void fraction, or porosity, can be calculated from

$$\text{voidage} = \frac{\text{void volume of bed}}{\text{total volume of bed (voids plus solids)}} \quad (6.2-1)$$

Two different models were described that relate the flow behavior of packed beds to pressure drop. For laminar flow, the Blake–Kozeny model is used, whereas for turbulent flow, the Burke–Plummer model is used. Both models were shown to be combined to form the Ergun equation, which holds for all types of flow and is given as



$$\Delta p = 150 \mu v' \Delta L D_p^2 (1 - \epsilon)^2 \epsilon^3 + 1.75 \rho (v')^2 \Delta L D_p^{1 - \epsilon} \epsilon^3 \quad (6.2-15)$$

For particles that are nonspherical, we considered different equivalent diameters and shape factors, in particular, sphericity.

We described two main types of fluidization behavior: particulate fluidization, characterized by uniform expansion, and bubbling fluidization, characterized by bubbles and gas bypassing. The minimum fluidization velocity was defined as the velocity where a packed bed transitions to a fluidized bed and the particles begin to “lift.” Different correlations were provided to calculate the minimum fluidization velocity and the minimum bubbling velocity. In addition, the way

in which bed voidage changes during bed expansion was also discussed and modeled.

## Problems

**6.1-1. *Force on a Cylinder in a Wind Tunnel.*** Air at 101.3 kPa absolute and 25°C is flowing at a velocity of 10 m/s in a wind tunnel. A long cylinder having a diameter of 90 mm is placed in the tunnel and the axis of the cylinder is held perpendicular to the air flow. What is the force on the cylinder per meter length?

**Ans.**  $C_D = 1.3$ ,  $F_D = 6.94 \text{ N}$

**6.1-2. *Wind Force on a Steam-Boiler Stack.*** A cylindrical steam-boiler stack has a diameter of 1.0 m and is 30.0 m

high. It is exposed to a wind at  $25^{\circ}\text{C}$  having a velocity of 50 miles/h. Calculate the force exerted on the boiler stack.

**Ans.**  $C_D = 0.33$ ,  $F_D = 2935 \text{ N}$

**6.1-3. *Effect of Velocity on Force on a Sphere and Stokes' Law.*** A sphere having a diameter of 0.042 m is held in a small wind tunnel, where air at  $37.8^{\circ}\text{C}$  and 1 atm abs and various velocities is forced past it.

- Determine the drag coefficient and force on the sphere for a velocity of  $2.30 \times 10^{-4} \text{ m/s}$ . Use Stokes' law here if it is applicable.
- Also determine the force for velocities of  $2.30 \times 10^{-3}$ ,  $2.30 \times 10^{-2}$ ,  $2.30 \times 10^{-1}$ , and  $2.30 \text{ m/s}$ . Make a plot of  $F_D$  versus velocity.

**6.1-4. *Drag Force on a Bridge Pier in a River.*** A cylindrical bridge pier 1.0 m in

diameter is submerged to a depth of 10 m. Water in the river at 20°C is flowing past at a velocity of 1.2 m/s. Calculate the force on the pier.

**6.2-1. *Surface Area in a Packed Bed.*** A packed bed is composed of cubes 0.020 m on a side and the bulk density of the packed bed is 980 kg/m<sup>3</sup>. The density of the solid cubes is 1500 kg/m<sup>3</sup>.

- Calculate  $\varepsilon$ , effective diameter  $D_p$ , and  $a$ .
- Repeat for the same conditions but for cylinders having a diameter of  $D = 0.02$  m and a length  $h = 1.5D$ .

**Ans.** (a)  $\varepsilon = 0.3467$ ,  $D_p = 0.020$  m,  $a = 196.0 \text{ m}^{-1}$

**6.2-2. *Derivation for the Number of Particles in a Bed of Cylinders.*** For a packed bed containing cylinders, where the diameter  $D$  of the cylinders is equal

to the length  $h$ , do as follows for a bed having a void fraction  $\varepsilon$ :

- Calculate the effective diameter.
- Calculate the number of cylinders,  $n$ , in 1 m<sup>3</sup> of the bed.

**Ans.** (a)  $D_p = D$

**6.2-3. Derivation of Dimensionless Equation for a Packed Bed.** Starting with Eq. (3.1-20), derive the dimensionless equation (3.1-21). Show all steps in the derivation.

**6.2-4. Flow and Pressure Drop of Gases in a Packed Bed.** Air at 394.3 K flows through a packed bed of cylinders having a diameter of 0.0127 m and length the same as the diameter. The bed void fraction is 0.40 and the length of the packed bed is 3.66 m. The air enters

the bed at 2.20 atm abs at the rate of 2.45 kg/m<sup>2</sup> · s based on the empty cross section of the bed. Calculate the pressure drop of air in the bed.

$$\text{Ans. } \Delta p = 0.1547 \times 10^5 \text{ Pa}$$

**6.2-5. *Flow of Water in a Filter Bed.***

Water at 24°C is flowing by gravity through a filter bed of small particles having an equivalent diameter of 0.0060 m. The void fraction of the bed is measured as 0.42. The packed bed has a depth of 1.50 m. The liquid level of water above the bed is held constant at 0.40 m. What is the water velocity  $v'$  based on the empty cross section of the bed?

**6.2-6. *Mean Diameter of Particles in a Packed Bed.*** A mixture of particles in a

packed bed contains the following volume percent of particles and sizes: 15%, 10 mm; 25%, 20 mm; 40%, 40 mm; and 20%, 70 mm. Calculate the effective mean diameter,  $D_{pm}$ , if the shape factor is 0.74.

$$\text{Ans. } D_{pm} = 18.34 \text{ mm}$$

**6.2-7. *Permeability and Darcy's Law.*** A sample core of porous rock obtained from an oil reservoir is 8 cm long and has a diameter of 2.0 cm. It is placed in a core holder. With a pressure drop of 1.0 atm, the water flow at 20.2°C through the core is measured as 2.60 cm<sup>3</sup>/s. What is the permeability in darcy?

**6.3-1. *Minimum Fluidization and Expansion of a Fluid Bed.*** Particles

having a size of 0.10 mm, a shape factor of 0.86, and a density of 1200 kg/m<sup>3</sup> are to be fluidized using air at 25°C and 202.65 kPa abs pressure. The void fraction at minimum fluidizing conditions is 0.43. The bed diameter is 0.60 m and the bed contains 350 kg of solids.

- Calculate the minimum height of the fluidized bed.
- Calculate the pressure drop at minimum fluidizing conditions.
- Calculate the minimum velocity for fluidization.
- Using 4.0 times the minimum velocity, estimate the porosity of the bed.

**Ans.** (a)  $L_{mf} = 1.810$  m; (b)  $\Delta p = 0.1212 \times 10^5$ ; (c)  $v_{mf}' = 0.004374$  m/s; (d)  $\varepsilon = 0.604$

**6.3-2. Minimum Fluidization Velocity Using a Liquid.** A tower having a



diameter of 0.1524 m is being fluidized with water at 20.2°C. The uniform spherical beads in the tower bed have a diameter of 4.42 mm and a density of 1603 kg/m<sup>3</sup>. Estimate the minimum fluidizing velocity and compare with the experimental value of 0.02307 m/s found by Wilhelm and Kwauk (W5).

### **6.3-3. *Fluidization of a Sand-Bed***

**Filter.** To clean a sand-bed filter, it is fluidized at minimum conditions using water at 24°C. The round sand particles have a density of 2550 kg/m<sup>3</sup> and an average size of 0.40 mm. The sand has the properties given in Table 3.1-2.

- The bed diameter is 0.40 m and the desired height of the bed at these minimum fluidizing conditions is 1.75 m. Calculate the amount of solids needed.
- Calculate the pressure drop at these conditions and the minimum velocity for fluidization.

- Using 4.0 times the minimum velocity, estimate the porosity and height of the expanded bed.

**Ans.** (a) 325.2 kg solids; (b)  $1.546 \times 10^4$  Pa

## References

## Notation

# Chapter 7. Pumps, Compressors, and Agitation Equipment

## 7.0 Chapter Objectives

On completion of this chapter, a student should be able to:

- Explain why it is often necessary to have a driving force to transport a fluid
- Explain why mechanical energy is supplied for horizontal flows
- Distinguish between pumps, fans, blowers, and compressors
- Explain how the compressibility of a fluid impacts the method for transporting it
- Calculate the actual (brake) and theoretical horsepower of a pump
- Calculate the electrical power needed to operate a pump
- Explain the process of cavitation and why it can be

damaging to pumps

- Calculate the net positive suction head required to operate a pump
- Interpret data from a pump's characteristic curve
- Distinguish between centrifugal and positive-displacement pumps
- Use the mechanical energy balance and thermodynamic relations to solve isothermal and adiabatic compression problems
- Explain why agitation is commonly used in the chemical and process industries and provide examples
- Describe different types of agitators and impellers used for mixing and agitation
- Explain why geometrical similarity is used for scale-up of agitation and mixing vessels
- Calculate the power and Reynolds number associated with agitation equipment
- Calculate the mixing time for agitation systems
- Explain why different agitation systems are needed for solid-fluid and solid-solid systems

## **7.1 Pumps and Gas-Moving Equipment**

## 7.1A Introduction

In order to make a fluid flow from one point to another in a closed conduit or pipe, it is necessary to have a driving force. Sometimes this force is caused by gravity, where differences in elevation cause a gradient in the potential energy of the fluid. For horizontal flows, the energy or driving force is commonly supplied by a mechanical device such as a pump or blower, which increases the mechanical energy of the fluid. This energy may be used to increase the velocity (i.e., move the fluid), the pressure, or the elevation of the fluid, as seen in the mechanical-energy-balance equation (4.2-28), which relates  $v$ ,  $p$ ,  $\rho$ , and work. The most common methods of adding energy are by positive

displacement or centrifugal action.

Generally, the word “pump” designates a machine or device for moving an incompressible liquid. Fans, blowers, and compressors are devices for moving gas (usually air). Fans discharge large volumes of gas at low pressures on the order of several hundred mm of water. Blowers and compressors discharge gases at higher pressures. With pumps and fans, the density of the fluid does not change appreciably and incompressible flow can be assumed. Compressible flow theory is used for blowers and compressors.

### **7.1B Pumps**

*1. Power and work required.* Using the total mechanical-energy-balance equation (4.2-28) on a pump and

piping system, the actual or theoretical mechanical energy  $W_s$  J/kg added by the pump to the fluid can be calculated. Example 4.2-5 shows such an example of this situation. If  $\eta$  is the fractional efficiency and  $W_p$  the shaft work delivered to the pump by the motor, Eq. (4.2-30) gives

$$W_p = -W_s \eta \quad (7.1-1)$$

The actual or brake power of a pump, which is also the power required from the motor to the pump, can be calculated as follows:

$$\begin{aligned}
 \text{brake kW} &= W_p m 1000 = \\
 &= -W_s m \eta \times 1000 \text{ (SI)} \quad \text{brake hp} = W_p m 550 = \\
 &= -W_s m \eta \times 550 \text{ (English)} \quad (7.1-2)
 \end{aligned}$$

where  $W_p$  is J/kg,  $m$  is the flow rate in

kg/s, 1000 is the conversion factor W/kW, and 550 is the conversion from lbf-ft/s to hp. In English units,  $Ws$  is in ft · lbf/lbm and  $m$  is in lbm/s. The theoretical or fluid power is

$$\text{theoretical power} = (\text{brake kW})(\eta) \quad (7.1-3)$$

The mechanical energy  $Ws$  in J/kg added to the fluid is often expressed as the developed head  $H$  of the pump in m of fluid being pumped, where

$$-WS = Hg(\text{SI}) \quad -WS = Hggc(\text{English}) \quad (7.1-4)$$

To calculate the power of a fan where the pressure difference is on the order of a few hundred mm of water, a linear average density of the gas between the inlet and outlet of the fan is used to



calculate  $W_s$  and brake kW or horsepower.

2. *Electric motor efficiency.* Since most pumps are driven by electric motors, the efficiency of the electric motor must be taken into account to determine the total electric power to the motor. Typical efficiencies  $\eta_e$  of electric motors are as follows: 77% for 12-kW motors, 82% for 2 kW, 85% for 5 kW, 88% for 20 kW, 90% for 50 kW, 91% for 100 kW, and 93% for 500 kW and larger. Hence, the total electric power input equals the brake power divided by the electric motor drive efficiency  $\eta_e$ :

$$\text{electric power input (kW)} = \text{brake kW} \eta_e = -\frac{W_{Sm} \eta_e \cdot 1000}{\eta_e} \quad (7.1-5)$$

3. *Suction lift of pumps (NPSH).* The

power calculated by Eq. (7.1-4) depends on the differences in pressures and not on the actual pressures being above or below atmospheric pressure. However, the lower limit of the absolute pressure in the suction (inlet) line to the pump is fixed by the vapor pressure of the liquid at the temperature of the liquid in the suction line. If the pressure on the liquid in the suction line drops below the vapor pressure, some of the liquid flashes into vapor, a process known as *cavitation*, which can be damaging to pumps. Then no liquid can be drawn into the pump, and vibration can occur.

To avoid flashes of vapor or cavitation, the pressure at the inlet of the pump must be greater than this vapor pressure and exceed it by a value termed the *net positive suction head required*, or

(NPSH)<sub>R</sub>. Pump manufacturers measure these values experimentally and include those values with the pumps that they sell.

For water below 100°C at 1750 rpm and for centrifugal pumps, typical values of (NPSH)<sub>R</sub> are as follows (P4): For pressures 3500 kPa (500 psig) or below: up to 200 gpm, 1.5 m (5 ft); up to 500 gpm, 2.1 m (7 ft); up to 1000 gpm, 3 m (10 ft); and up to 2000 gpm, 5.5 m (18 ft). At pressures of 7000 kPa (1000 psig), the values are doubled at 200 gpm or less and at 2000 gpm they are increased by 20%. At an rpm of 3550, the (NPSH)<sub>R</sub> increases by about a factor of 2.2.

To calculate the net positive suction head that will be available (NPSH)<sub>A</sub> at

the pump suction for the system shown in Fig. 7.1-1, Eq. (7.1-6) can be used:

$$\begin{aligned}
 (\text{NPSH})_A = & p_1 / \rho g - p_{vp} / \rho g + z_1 - v_2^2 / 2g - \sum F \quad (\text{SI}) \\
 (\text{NPSH})_A = & p_1 / g c \rho g - p_{vp} / g c \rho g + z_1 - v_2^2 / 2g c - \sum F \quad (\text{English})
 \end{aligned}
 \tag{7.1-6}$$

where  $(\text{NPSH})_A$  is in m (ft),  $\rho$  is the density of liquid in  $\text{kg/m}^3$  ( $\text{lb}_m/\text{ft}^3$ ),  $p_1$  is the pressure above the liquid's surface in  $\text{N/m}^2$  ( $\text{lb}_f/\text{ft}^2$ ),  $p_{vp}$  is the vapor pressure of a fluid at the given temperature in  $\text{N/m}^2$  ( $\text{lb}_f/\text{ft}^2$ ),  $z_1$  is the height of the open surface of a liquid above the pump's centerline in m (ft),  $\sum F$  is the friction loss in the suction line to the pump from Eq. (5.1-18) in  $\text{J/kg}$  ( $\text{ft lb}_f/\text{lb}_m$ ), and  $v_2^2/2$  is the velocity head in  $\text{J/kg}$  ( $v_2^2/2g_c$  is  $\text{ft lb}_f/\text{lb}_m$ ). Note that in Eq. (7.1-6), for SI units, the  $(\text{NPSH})_A$  in m is multiplied by  $g$  to give

units of J/kg.

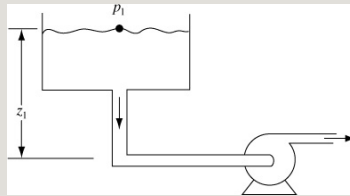


Figure 7.1-1. Diagram for  $(NPSH)_A$  available in a pumping system.

For cold water and the case where all the terms in Eq. (7.1-6) are small except  $p_1$ , at atmospheric pressure the  $(NPSH)_A$  is 10.3 m (33.9 ft). However, a practical limit is about 7.5 m (24.6 ft). The available NPSH for a given pump should be at least 1 m (3 ft) more than that required by the manufacturer.

**EXAMPLE 7.1-1.  $(NPSH)_A$  Available for a Pump**

Water at 50°C is stored in an open tank at atmospheric pressure. The pump is 3.0 m above the open tank level. The velocity in the pipe is 0.9 m/s. The friction head loss in the pipe has been calculated as 1.0 m. The required  $(NPSH)_R$  for this pump is 2.0 m. Calculate the available  $(NPSH)_A$ .

**Solution:** From Appendix A.2-3,  $\rho = 988.07 \text{ kg/m}^3$ . Also, the vapor pressure  $p_{vp} = 12.349 \text{ kPa}$  from A.2-9 and  $p_1 =$

$1.01325 \times 10^5$  Pa. Substituting into Eq. (3.3-6) and noting that  $z_1$  is negative and that the friction loss head of 1.0 m is multiplied by  $g$ ,

$$65(\text{NPSH})_A = 1.01325 \times 10^5 988.07 - 12.349 \times 10^3 988.07 - 9.80665(3.0) - 0.922 - 9.80665(1.0) \text{ Solving, } (\text{NPSH})_A = 5.14$$

Hence, the available  $(\text{NPSH})_A$  of 5.14 m is sufficiently greater than that required of 2.0 m.

*4. Centrifugal pumps.* Process industries commonly use centrifugal pumps. They are available in sizes of about 0.004 to 380 m<sup>3</sup>/min (1 to 100000 gal/min) and for discharge pressures from a few m of head to 5000 kPa or so. A centrifugal pump in its simplest form consists of an impeller rotating inside a casing. Figure 7.1-2 shows a schematic diagram of a simple centrifugal pump.

The liquid enters the pump axially at point 1 in the suction line and then enters the rotating eye of the impeller, where it spreads out radially. On spreading radially, it enters the channels

between the vanes at point 2 and flows through these channels to point 3 at the periphery of the impeller. From there, it is collected in the volute chamber at point 4 and flows out of the pump discharge at point 5. The rotation of the impeller imparts a high-velocity head to the fluid, which is changed to a pressure head as the liquid passes into the volute chamber, also known as the casing, and out the discharge. Some pumps are also made as two-stage or even multistage pumps.

Many complicating factors determine the actual efficiency and performance characteristics of a pump. Hence, the actual experimental performance of the pump is usually employed. The performance is usually expressed by the pump manufacturer in terms of

*characteristic curves*, which are usually for water. The head produced,  $H$  in m, will be the same for any liquid of the same viscosity. The pressure produced,  $p = H\rho g$ , will be in proportion to the density. Viscosities of less than  $0.05 \text{ Pa} \cdot \text{s}$  (50 cp) have little effect on the head produced. The brake kW varies directly with the density.

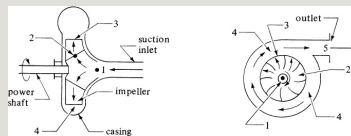


Figure 7.1-2. *Simple centrifugal pump.*

*Pump efficiencies* typical of centrifugal pumps at rated capacities are as follows: 50% for  $0.075 \text{ m}^3/\text{min}$  (20 gal/min), 62% for  $0.19 \text{ m}^3/\text{min}$  (50 gal/min), 68% for  $0.38 \text{ m}^3/\text{min}$  (100 gal/min), 75% for  $0.76 \text{ m}^3/\text{min}$  (200 gal/min), 82% for  $1.89 \text{ m}^3/\text{min}$  (500 gal/min), and 85% for



3.8 m<sup>3</sup>/min (1000 gal/min).

As rough approximations, the following relationships, called *affinity laws*, can be used for a given pump. The *capacity*  $q_1$  in m<sup>3</sup>/s is directly proportional to the rpm  $N_1$  or

$$q_1 q_2 = N_1 N_2 \quad (7.1-7)$$

The *head*,  $H_1$ , is proportional to  $q_1^2$ , or

$$H_1 H_2 = q_1^2 q_2^2 = N_1^2 N_2^2 \quad (7.1-8)$$

The *power consumed*,  $W_1$ , is proportional to the product of  $H_1 q_1$ , or

$$W_1 W_2 = H_1 q_1 H_2 q_2 = N_1^3 N_2^3 \quad (7.1-9)$$

A given pump can be modified when needed for a different capacity by changing the impeller size. Then, the

*affinity laws* for a constant-rpm  $N$  are as follows: The capacity  $q$  is proportional to the diameter  $D$ , the head  $H$  is proportional to  $D^2$ , and the brake horsepower  $W$  is proportional to  $D^3$ .

In most pumps, the speed is generally not varied. Characteristic curves for a typical single-stage centrifugal pump operating at a constant speed are given in Fig. 7.1-3 Most pumps are usually rated on the basis of head and capacity at the point of peak efficiency. The efficiency reaches a peak at about 50 gal/min flow rate. As the discharge rate in gal/min increases, the developed head drops. The brake hp increases, as expected, with flow rate.

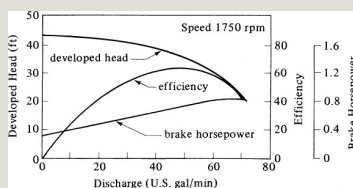


Figure 7.1-3. Characteristic curves for a single-stage centrifugal pump with water. From W. L. Badger and J. T. Banchero, *Introduction to Chemical Engineering*, New York: McGraw-Hill Book Company, 1955. With permission.

**EXAMPLE 7.1-2. Calculation of the Brake Horsepower of a Pump**

In order to see how the brake-hp curve is determined, calculate the brake hp at a 40 gal/min flow rate for the pump in Fig. 7.1-3.

**Solution:** At 40 gal/min, the efficiency  $\eta$  from the curve is about 60% and the head  $H$  is 38.5 ft. A flow rate of 40 gal/min of water with a density of 62.4 lb mass/ft<sup>3</sup> is

$$m = (40 \text{ gal/min} \times 60 \text{ s/min}) (1 \text{ ft}^3 / 7.48 \text{ gal}) (62.4 \text{ lb mass/ft}^3) = 5.56 \text{ lb mass/s}$$

The work  $Ws$  is as follows, from Eq. (7.1-4):

$$Ws = H g c = 38.5 \text{ ft} \cdot \text{lb mass/ft}^3 \cdot \text{s}$$

The brake hp from Eq. (7.1-2) is

$$\text{brake hp} = \frac{Ws}{m \times 550} = \frac{38.5 (5.56)}{0.60 (550)} = 0.65 \text{ hp} \quad (0.48 \text{ kW})$$

This value agrees with the value on the curve in Fig. 7.1-3.

**5. Positive-displacement pumps.** In this class of pumps, a definite volume of liquid is drawn into a chamber and then forced out of the chamber at a higher pressure. There are two main types of positive-displacement pumps. In the

*reciprocating pump*, the chamber is a stationary cylinder and liquid is drawn into the cylinder by withdrawal of a piston in the cylinder. Then, the liquid is forced out by the piston on the return stroke. In the *rotary pump*, the chamber moves from inlet to discharge and back again. In a gear rotary pump, two intermeshing gears rotate, and liquid is trapped in the spaces between the teeth and forced out the discharge.

Reciprocating and rotary pumps can be used up to very high pressures, whereas centrifugal pumps are limited in their head and are used for lower pressures. Centrifugal pumps deliver liquid at a uniform pressure without shocks or pulsations and can handle liquids with large amounts of suspended solids. In general, centrifugal pumps are primarily

used in chemical and biological processing plants.

Equations (7.1-1)–(7.1-5) hold for calculating the power of positive-displacement pumps. At a constant speed, the flow capacity will remain constant with different liquids. In general, the discharge rate will be directly dependent upon the speed. While power increases directly as the head increases, the discharge rate remains nearly constant as the head increases.

*Pump efficiencies  $\eta$*  of reciprocating pumps used to calculate brake horsepower are as follows: 55% at 2.2 kW (3 hp), 70% at 7.5 kW (10 hp), 77% at 14.9 kW (20 hp), 85% at 37 kW (50 hp), and 90% at 373 kW (500 hp).

## 7.1C Gas-Moving Machinery

*Gas-moving machinery* comprises mechanical devices used for compressing and moving gases.

They are often classified or considered from the standpoint of the pressure heads produced and they include fans for low pressures, blowers for intermediate pressures, and compressors for high pressures.

*1. Fans.* The most common method for moving small volumes of gas at low pressures is by means of a *fan*. Large fans are usually centrifugal and their operating principle is similar to that of centrifugal pumps. The discharge heads are low, from about 0.1 m to 1.5 m H<sub>2</sub>O. However, in some cases much of the added energy of the fan is converted to velocity energy and a small amount to

the pressure head.

In a centrifugal fan, the centrifugal force produced by the rotor causes a compression of the gas, called the *static pressure head*. Also, since the velocity of the gas is increased, a velocity head is produced. Both the static-pressure-head increase and velocity-head increase must be included in estimating efficiency and power. Operating efficiencies are in the range 40–70%. The operating pressure of a fan is generally given as an inches-of-water gage and is the sum of the velocity head and the static pressure of the gas leaving the fan. Incompressible flow theory can be used to calculate the power of fans.

When the rpm or speed of centrifugal fans varies, the performance equations

are similar to Eqs. (7.1-7)–(7.1-9) for centrifugal pumps.

**EXAMPLE 7.1-3. Brake-kW Power of a Centrifugal Fan**

It is desired to use 28.32 m<sup>3</sup>/min of air (metered at a pressure of 101.3 kPa and 294.1 K) in a process. This amount of air, which is at rest, enters the fan suction at a pressure of 741.7 mmHg and a temperature of 366.3 K, and is discharged at a pressure of 769.6 mmHg and a velocity of 45.7 m/s. A centrifugal fan having a fan efficiency of 60% is to be used. Calculate the brake-kW power needed.

**Solution:** Incompressible flow can be assumed, since the pressure drop is only  $(27.9/741.7)100$ , or 3.8% of the upstream pressure. The average density of the flowing gas can be used in the mechanical-energy-balance equation.

The density at the suction, point 1, is

$$\rho_1 = (28.97 \text{ kg air/kg mol})(1 \text{ kg mol}/22.414 \text{ m}^3)(273.2/366.3) \\ (741.7/760) = 0.940 \text{ kg/m}^3$$

(The molecular weight of 28.97 for air, the volume of 22.414 m<sup>3</sup>/kg mol at 101.3 kPa, and 273.2 K were obtained from Appendix A.1.) The density at the discharge, point 2, is

$$\rho_2 = (0.940) 769.6/741.7 = 0.975 \text{ kg/m}^3$$

The average density of the gas is

$$\rho_{av} = \rho_1 + \rho_2/2 = 0.940 + 0.975/2 = 0.958 \text{ kg/m}^3$$

The mass flow rate of the gas is

$$\dot{m} = (28.32 \text{ m}^3/\text{min})(1 \text{ min}/60 \text{ s})(1 \text{ kg mol}/22.414 \text{ m}^3) \\ (273.2/366.3)(28.97 \text{ kg/kg mol}) = 0.5663 \text{ kg/s}$$

The developed pressure head is

$$p_2 - p_1/\rho_{av} = (769.6 - 741.7) \text{ mm Hg}/760 \text{ mm/} \\ \text{atm} (1.01325 \times 10^5 \text{ N/m}^2/\text{atm})/(0.958 \text{ kg/m}^3) = 3883 \text{ J/kg}$$



The developed velocity head for  $v_1 = 0$  is

$$v_2^2 = (45.7)^2 = 2094 \text{ J/kg}$$

Writing the mechanical-energy-balance equation (4.2-28),

$$z_1 g + v_1^2 + p_1 \rho + W_S = z_2 g + v_2^2 + p_2 \rho + \sum F$$

Setting  $z_1 = 0$ ,  $z_2 = 0$ ,  $v_1 = 0$ , and  $\sum F = 0$ , and solving for  $W_S$ ,

$$-W_S = p_2 \rho + v_2^2 = 3883 + 2094 = 5977 \text{ J/kg}$$

Substituting into Eq. (7.1-2),

$$\text{brake kW} =$$

$$W_{Sm} \eta \cdot 1000 = 5977 (0.5663) 0.60 (1000) = 4.65 \text{ kW (6.23 hp)}$$

*2. Blowers and compressors.* For handling gas volumes at higher pressure rises than fans can accommodate, several distinct types of equipment are used. *Turboblowers* or *centrifugal compressors* are widely used to move large volumes of gas for pressure rises from about 5 kPa to several thousand kPa. The principles of operation for a turboblower are the same as for a centrifugal pump. The turboblower resembles the centrifugal pump in appearance, the main difference being

that the gas in the blower is compressible. The head of the turboblower, as in a centrifugal pump, is independent of the fluid handled. Multistage turboblowers are often used to go to the higher pressures.

Rotary blowers and compressors are machines of the positive-displacement type and are essentially constant-volume flow-rate machines with variable discharge pressures. Changing the speed will change the volume flow rate. Details of construction of the various types (P1) vary considerably, and pressures up to about 1000 kPa can be obtained, depending on the type.

Reciprocating compressors, which are of the positive displacement type that use pistons, are available for higher

pressures. Multistage machines are also available for pressures up to 10000 kPa or more.

### 7.1D Equations for Compression of Gases

In blowers and compressors, pressure changes are large and compressible flow occurs. Since the density changes markedly, the mechanical-energy-balance equation must be written in differential form and then integrated to obtain the work of compression. In the compression of gases, the static-head terms, velocity-head terms, and friction terms are dropped and only the work term  $dW$  and the  $dp/\rho$  term remain in the differential form of the mechanical-energy equation; or,

$$dW = dp/\rho \quad (7.1-10)$$

Integration between the suction pressure  $p_1$  and discharge pressure  $p_2$  gives the work of compression:

$$W = \int_{p_1}^{p_2} v dp \quad (7.1-11)$$

*1. Isothermal compression.* To integrate Eq. (7.1-11) for a perfect gas, either isothermal or adiabatic compression is assumed. For isothermal compression, where the gas is cooled as it is compressed,  $p/v$  is a constant equal to  $RT/M$ , where  $R = 8314.3 \text{ J/kg mol} \cdot \text{K}$  in SI units and  $1545.3 \text{ ft} \cdot \text{lbf/lb mol} \cdot ^\circ\text{R}$  in English units. Then,

$$pv = p_1 v_1 = p_2 v_2 \quad (7.1-12)$$

Solving for  $v$  in Eq. (7.1-12) and substituting it in Eq. (7.1-11), the work for isothermal compression is

$$p_2/p_1 = \ln p_2/p_1 = 2.3026 R T_1/M \log p_2/p_1 \quad (7.1-13)$$

Also,  $T_1 = T_2$ , since the process is isothermal.

*2. Adiabatic compression.* For adiabatic compression, the fluid follows an isentropic path and

$$p_1 \rho^\gamma = (p_2 \rho_2)^\gamma \quad (7.1-14)$$

where  $\gamma = c_p/c_v$ , the ratio of heat capacities. By combining Eqs. (7.1-11) and (7.1-14), and integrating,

$$-W_S = \frac{\gamma}{\gamma-1} R T_1 M [(p_2/p_1)^{(\gamma-1)/\gamma} - 1] \quad (7.1-15)$$

The adiabatic temperatures are related by

$$T_2/T_1 = (p_2/p_1)^{(\gamma-1)/\gamma} \quad (7.1-16)$$

To calculate the brake power when the efficiency is  $\eta$ ,

$$\text{brake kW} = W_s m (\eta) (1000) \quad (7.1-17)$$

where  $m = \text{kg gas/s}$  and  $W_s = \text{J/kg}$ .

The values of  $\gamma$  are approximately 1.40 for air, 1.31 for methane, 1.29 for  $\text{SO}_2$ , 1.20 for ethane, and 1.40 for  $\text{N}_2$  (P1).

For a given compression ratio, the work for isothermal compression in Eq.

(7.1-13) is less than the work for adiabatic compression in Eq. (7.1-15).

Hence, cooling is sometimes used in compressors to maintain isothermal conditions.

**EXAMPLE 7.1-4 Compression of Methane**

A single-stage compressor is used to compress  $7.56 \times 10^{-3}$  kg mol/s of methane gas at  $26.7^\circ\text{C}$  and 137.9 kPa abs to

551.6 kPa abs.

- Calculate the power required if the mechanical efficiency is 80% and the compression is adiabatic.
- Repeat part (a), but for the case of isothermal compression.

**Solution:** For part (a),  $p_1 = 137.9$  kPa,  $p_2 = 551.6$  kPa,  $M = 16.0$  kg mass/kg mol, and  $T_1 = 273.2 + 26.7 = 299.9$  K. The mass flow rate per sec is

$$\dot{m} = (7.56 \times 10^{-3} \text{ kg mol/s})(16.0 \text{ kg/kg mol}) = 0.121 \text{ kgs}$$

Substituting into Eq. (7.1-15) for  $\gamma = 1.31$  for methane and  $p_2/p_1 = 551.6/137.9 = 4.0/1$ ,

$$\begin{aligned} -W_S &= \gamma \gamma - 1 RT_1 M [(p_2/p_1)^{(\gamma-1)/\gamma} - 1] = (1.31 - 1) 8314.3 \\ &\quad (299.9) 16.0 [(4.0)^{(1.31-1)/1.31} - 1] = 256 \ 300 \text{ J/kg} \end{aligned}$$

Using Eq. (7.1-17),

$$\begin{aligned} \text{brake kW} &= - \\ W_S \dot{m} \eta \cdot 1000 &= (256 \ 300) 0.121 0.80 (1000) = 38.74 \text{ kW (52.0 hp)} \end{aligned}$$

For part (b), using Eq. (7.1-13) for isothermal compression,

$$\begin{aligned} -W_S &= 2.3026 RT_1 M \log p_2/p_1 = 2.3026 (8314.3) \\ &\quad (299.9) 16.0 \log 4.0 = 216 \ 000 \text{ J/kg} \\ \text{brake kW} &= - \\ W_S \dot{m} \eta \cdot 1000 &= (216 \ 000) 0.121 0.80 (1000) = 38.67 \text{ kW (43.8 hp)} \end{aligned}$$

Hence, isothermal compression uses 15.8% less power.

*3. Polytropic compression.* In large compressors, neither isothermal nor adiabatic compression is achieved. This polytropic path is

$$p_1 p_2 = (p_1 \rho)^n \quad (7.1-18)$$

For isothermal compression,  $n = 1.0$  and for adiabatic,  $n = \gamma$ . The value of  $n$  is found by measuring the pressure  $p_1$  and density  $\rho_1$  at the inlet, and  $p_2$  and  $\rho_2$  at the discharge, and then substituting these values into Eq. (7.1-18).

*4. Multistage compression ratios.* Water cooling is used between each stage in multistage compressors to reduce the outlet temperature to near the inlet temperature for a minimum power requirement. The compression ratios should be the same for each stage so that the total power is a minimum. This gives the same power in each stage. Hence, for  $n$  stages, the compression ratio ( $p_b/p_a$ ) for each stage is

$$p_b/p_a = (p_2/p_1)^{1/n} \quad (7.1-19)$$



where  $p_1$  is the inlet pressure and  $p_n$  the outlet pressure from  $n$  stages. For two stages, the compression ratio is  $p_n/p_1$ .

## **7.2 Agitation, Mixing of Fluids, and Power Requirements**

### **7.2A Purposes of Agitation**

In the chemical and other processing industries, many operations are dependent to a great extent on effective agitation and mixing of fluids. Generally, *agitation* refers to forcing a fluid by mechanical means to flow in a circulatory or similar pattern inside a vessel. *Mixing* usually implies taking two or more separate phases, such as a fluid and a powdered solid or two fluids, and causing them to be randomly distributed through one another.

There are a number of purposes for agitating fluids, some of which are briefly summarized:

1. Blending of two miscible liquids, such as ethyl alcohol and water
2. Dissolving solids in liquids, such as salt in water
3. Dispersing a gas in a liquid as fine bubbles, such as oxygen from air in a suspension of microorganisms for fermentation or for the activated-sludge process in waste treatment
4. Suspending fine solid particles in a liquid, as in the catalytic hydrogenation of a liquid, where solid catalyst particles and hydrogen bubbles are dispersed in the liquid
5. Agitating a fluid to increase heat transfer between the fluid and a coil or jacket in the vessel wall

## **7.2B Equipment for Agitation**

Generally, liquids are agitated in a cylindrical vessel that can be closed or open to the air. The height of the liquid is approximately equal to the tank diameter. An impeller mounted

on a shaft is driven by an electric motor. A typical agitator assembly is shown in Fig. 7.2-1.

*1. Three-blade propeller agitator.* There are several types of agitators that are widely used. A common type, shown in Fig. 7.2-1, is a three-bladed marine-type propeller similar to the propeller blade used to drive boats. The propeller can be a side-entering type in a tank or be clamped on the side of an open vessel in an off-center position. These propellers turn at high speeds of 400 to 1750 rpm (revolutions per minute) and are used for liquids of low viscosity (e.g., water). The flow pattern in a baffled tank with a propeller positioned on the center of the tank is shown in Fig. 7.2-1. This type of flow pattern is called *axial flow* since the fluid flows axially down the center axis

or propeller shaft and up the sides of the tank as shown.

2. Paddle agitators. Various types of paddle agitators are often used at low speeds, between about 20 and 200 rpm. Two-bladed and four-bladed flat paddles are common, as shown in Fig. 7.2-2a. The total length of the paddle impeller is usually 60–80% of the tank diameter and the width of the blade is 16 to 110 of its length. At low speeds, mild agitation is obtained in an unbaffled vessel. At higher speeds, baffles are used, since without baffles, the liquid is simply swirled around with little actual mixing. The paddle agitator is ineffective for suspending solids, since good radial flow is present, but there is little vertical or axial flow. An anchor or gate paddle, shown in Fig. 7.2-2b, is

often used. It sweeps or scrapes the tank walls and sometimes the tank bottom. It is used with viscous liquids where deposits on walls can occur and to improve heat transfer to the walls. However, it is a poor agitator for uniform mixing quality. Paddle agitators are often used to process starch pastes, paints, adhesives, and cosmetics.

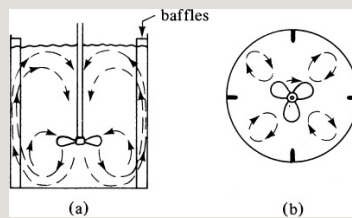


Figure 7.2-1. Baffled tank and three-blade propeller agitator with axial-flow pattern: (a) side view, (b) bottom view.

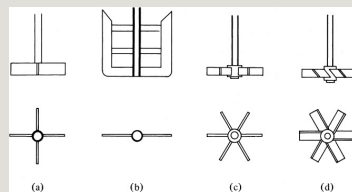


Figure 7.2-2. Various types of agitators: (a) four-blade paddle, (b) gate or anchor paddle, (c) six-blade open turbine, (d) pitched-blade ( $45^\circ$ ) turbine.

3. Turbine agitators. Turbines that resemble multibladed paddle agitators with shorter blades are used at high speeds for liquids with a very wide range of viscosities. The diameter of a turbine is normally between 30 and 50% of the tank diameter. The turbines usually have four or six blades. Figure 7.2-3 shows a flat six-blade turbine agitator with a disk. In Fig. 7.2-2c, a flat six-blade open turbine is shown. The turbines with flat blades give radial flow, as shown in Fig. 7.2-3. They are also useful for good gas dispersion; the gas is introduced just below the impeller at its axis and is drawn up to the blades and chopped into fine bubbles. In the pitched-blade turbine shown in Fig. 7.2-2d, with the blades at  $45^\circ$ , some axial flow is imparted so that a combination of axial and radial flow is

present. This type is useful in suspending solids since the currents flow downward and then sweep up the solids.

Often, a pitched-blade turbine with only four blades is used in suspension of solids. A high-efficiency, three-blade impeller (B6, F2) is similar to a four-blade pitched turbine; however, it features a larger pitch angle of  $30\text{--}60^\circ$  at the hub and a smaller angle of  $10\text{--}30^\circ$  at the tip. This axial-flow impeller produces more fluid motion and mixing per unit of power and is very useful in the suspension of solids.

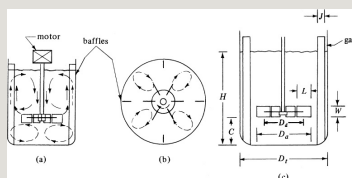


Figure 7.2-3. Baffled tank with six-blade turbine agitator with disk showing flow patterns: (a) side view, (b) bottom view, (c) dimensions of turbine and tank.

4. *Helical-ribbon agitators*. This type of agitator is used in highly viscous solutions and operates at a low rpm in the laminar region. The ribbon is formed in a helical path and is attached to a central shaft. The liquid moves in a tortuous flow path down the center and up along the sides in a twisting motion. Similar types are the double-helical-ribbon agitator and the helical-screw impeller.

5. Agitator selection and viscosity ranges. The viscosity of the fluid is one of several factors affecting the selection of the type of agitator. Indications of the viscosity ranges of these agitators are as follows: propellers are used for fluid viscosities below approximately  $3 \text{ Pa} \cdot \text{s}$  (3000 cp); turbines can be used below



approximately  $100 \text{ Pa} \cdot \text{s}$  ( $100\,000 \text{ cp}$ ); modified paddles such as anchor agitators can be used from  $50 \text{ Pa} \cdot \text{s}$  to about  $500 \text{ Pa} \cdot \text{s}$  ( $500\,000 \text{ cp}$ ); and helical and ribbon-type agitators are often used above this range to approximately  $1000 \text{ Pa} \cdot \text{s}$ , and have been used up to  $25\,000 \text{ Pa} \cdot \text{s}$ . For viscosities greater than  $2.5\text{--}5 \text{ Pa} \cdot \text{s}$  ( $5000 \text{ cp}$ ) and above, baffles are not needed since little swirling is present above these viscosities.

### **7.2C Flow Patterns in Agitation**

The flow patterns in an agitated tank depend upon the fluid properties, the geometry of the tank, the types of baffles in the tank, and the agitator itself. If a propeller or other agitator is mounted vertically in the center of a tank with no baffles, a swirling

flow pattern usually develops. Generally, this is undesirable, because of excessive air entrainment, development of a large vortex, and surging, especially at high speeds. To prevent this, an angular off-center position can be used with propellers with small horsepower. However, for vigorous agitation at higher power, unbalanced forces can become severe and limit the use of higher power.

For vigorous agitation with vertical agitators, baffles are generally used to reduce swirling and still promote good mixing. Baffles installed vertically on the walls of the tank are shown in Fig. 7.2-3. Usually four baffles are sufficient, with their width being about  $1/12$  of the tank diameter for turbines and

propellers. The turbine impeller drives the liquid radially against the wall, where it divides, with one portion flowing upward near the surface and back to the impeller from above and the other flowing downward. Sometimes, in tanks with large liquid depths much greater than the tank diameter, two or three impellers are mounted on the same shaft, each acting as a separate mixer. The bottom impeller is about 1.0 impeller diameter above the tank bottom.

In an agitation system, the volume flow rate of fluid moved by the impeller, or the circulation rate, is important in sweeping out the whole volume of the mixer in a reasonable time. Also, turbulence in the moving stream is important for mixing, since it entrains

the material from the bulk liquid in the tank into the flowing stream. Some agitation systems require high turbulence with low circulation rates, while others require low turbulence with high circulation rates. This often depends on the types of fluids being mixed and on the degree of mixing needed.

#### **7.2D Typical “Standard” Design of a Turbine**

The turbine agitator shown in Fig. 7.2-3 is the most commonly used agitator in the process industries. For the design of an ordinary agitation system, this type of agitator is often used in the initial design. The geometric proportions of the agitation system that are considered as a typical “standard” design are given in Table 7.2-1. These relative

proportions are the basis for the major correlations of agitator performance in numerous publications (see Fig. 7.2-3c for nomenclature).

In some cases,  $W/D_a = 18$  for agitator correlations. The number of baffles is four in most uses. The clearance or gap between the baffles and the wall is usually  $0.10\text{--}0.15 J$  to ensure that liquid does not form stagnant pockets next to the baffle and wall. In a few correlations, the ratio of baffle to tank diameter is  $J/D_t = 110$  instead of 112.

### **7.2E Power Used in Agitated Vessels**

In the design of an agitated vessel, an important factor is the power required to drive the impeller. Since the power required for a given

system cannot be predicted theoretically, empirical correlations have been developed to predict the power required. The presence or absence of turbulence can be correlated with the impeller's Reynolds number,  $NRe'$ , defined as

$$NRe' = Da^2 N \rho \mu \quad (7.2-1)$$

Table 7.2-1. *Geometric Proportions for a "Standard" Agitation System*



where  $Da$  is the impeller (agitator) diameter in m,  $N$  is the rotational speed in rev/s,  $\rho$  is the fluid density in  $\text{kg/m}^3$ , and  $\mu$  is the viscosity in  $\text{kg/m} \cdot \text{s}$ . The flow is laminar in the tank for  $NRe' < 10$ , turbulent for  $NRe' > 10^4$ , and, for a range between 10 and  $10^4$ , the flow is

transitional, being turbulent at the impeller and laminar in remote parts of the vessel.

Power consumption is related to fluid density  $\rho$ , fluid viscosity  $\mu$ , rotational speed  $N$ , and impeller diameter  $D_a$  by plots of power number  $N_p$  versus  $NRe'$ . The power number is defined as

$$N_p = \frac{P}{\rho N^3 D_a^5} \text{ (SI)} \quad N_p = \frac{P}{g_c \rho N^3 D_a^5} \text{ (English)} \quad (7.2-2)$$

where  $P$  = power in J/s or W. In English units,  $P$  = ft · lbf/s.

Figure 7.2-4 is a correlation (B3, R1) for frequently used impellers with Newtonian liquids contained in baffled, cylindrical vessels. Dimensional measurements of baffle, tank, and impeller sizes are given in Fig. 7.2-3c.

These curves may also be used for the same impellers in unbaffled tanks when  $NRe'$  is 300 or less (B3, R1). When  $NRe'$  is above 300, the power consumption for an unbaffled vessel is considerably less than for a baffled vessel. Curves for other impellers are also available (B3, R1).

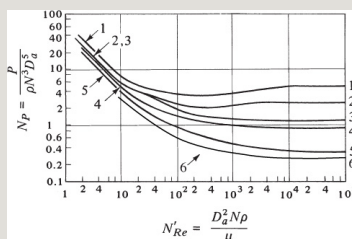


Figure 7.2-4. Power correlations for various impellers and baffles (see Fig. 7.2-3c for dimension  $Da$ ,  $D_t$ ,  $J$ , and  $W$ ). Data from D. W. Dodge and A. B. Metzner. A.I.Ch.E. J., **5**, 189, © 1959 American Institute of Chemical Engineers.

*Curve 1. Flat six-blade turbine with disk (like Fig. 7.2-3 but six blades);  $Da/W = 5$ ; four baffles each  $D_t/J = 12$ .*

*Curve 2. Flat six-blade open turbine*



*(like Fig. 7.2-2c);  $D_a/W = 8$ ; four baffles each  $D_t/J = 12$ .*

*Curve 3. Six-blade open turbine (pitched-blade) but blades at  $45^\circ$  (like Fig. 7.2-2d);  $D_a/W = 8$ ; four baffles each  $D_t/J = 12$ .*

*Curve 4. Propeller (like Fig. 7.2-1); pitch =  $2D_a$ ; four baffles each  $D_t/J = 10$ ; also holds for same propeller in angular off-center position with no baffles.*

*Curve 5. Propeller; pitch =  $D_a$ ; four baffles each  $D_t/J = 10$ ; also holds for same propeller in angular off-center position with no baffles.*

*Curve 6. High-efficiency impeller; four baffles each  $D_t/J = 12$ .*

*Curves 1, 2, and 3 reprinted with permission from R. L. Bates. P. L. Fondy, and R. R. Corpstein, Ind. Eng. Chem. Proc. Des. Dev., 2, 310 (1963). Copyright by the American Chemical Society. Curves 4 and 5 from J. H. Rushton, E. W. Costich, and H. J. Everett, Chem. Eng. Progr., 46, 395, 467 (1950). With permission.*

The power-number curve for  $N_p$  for the high-efficiency, three-blade impeller is shown as curve 6 in Fig. 7.2-4.

**EXAMPLE 7.2-1. Power Consumption in an Agitator**

A flat-blade turbine agitator with a disk having six blades is installed in a tank similar to Fig. 7.2-3. The tank diameter  $D_t$  is 1.83 m, the turbine diameter  $D_a$  is 0.61 m,  $D_t = H$ , and the width  $W$  is 0.122 m. The tank contains four baffles, each having a width  $J$  of 0.15 m. The turbine is operated at 90 rpm and the liquid in the tank has a viscosity of 10 cp and a density of 929 kg/m<sup>3</sup>.

- Calculate the required kW of the mixer.
- For the same conditions, except for the solution having a viscosity of 100000 cp, calculate the

required kW.

**Solution:** For part (a), the following data are given:  $D_a = 0.61$  m,  $W = 0.122$  m,  $D_t = 1.83$  m,  $J = 0.15$  m,  $N = 90/60 = 1.50$  rev/s,  $\rho = 929$  kg/m<sup>3</sup>, and

$$\mu = (10.0 \text{ cp})(1 \times 10^{-3}) = 0.01 \text{ kgm} \cdot \text{s} = 0.01 \text{ Pa} \cdot \text{s}$$

Using Eq. (7.2-1), the Reynolds number is

$$NRe' = Da^2 N \rho \mu = (0.61)^2 (1.50) 929 / 0.01 = 5.185 \times 10^4$$

Using curve 1 in Fig. 7.2-4, since  $Da/W = 5$  and  $D_t/J = 12$ ,  $NP = 5$  for  $NRe' = 5.185 \times 10^4$ . Solving for  $P$  in Eq. (7.2-2) and substituting known values,

$$P = NP \rho N^3 Da^5 = 5(929)(1.50)^3 (0.61)^5 = 1324 \text{ J/s} \\ = 1.324 \text{ kW (1.77 hp)}$$

For part (b),

$$\mu = 100 \ 000 (1 \times 10^{-3}) = 100 \text{ kgm} \cdot \text{s} \\ NRe' = (0.61)^2 (1.50) 929 / 100 = 5.185$$

This is in the laminar flow region. From Fig. 7.2-4,  $NP = 14$ .

$$P = 14(929)(1.50)^3 (0.61)^5 = 3707 \text{ J/s} = 3.71 \text{ kW (4.98 hp)}$$

Hence, a 10000-fold increase in viscosity only increases the power from 1.324 to 3.71 kW.

Variations of various geometric ratios from the “standard” design can have different effects on the power number  $NP$  in the turbulent region of the various turbine agitators as follows (B3):

1. For the flat six-blade open turbine,  $NP \propto (W/D_a)^{1.0}$ .

2. For the flat six-blade open turbine, varying  $D_a/D_t$  from 0.25 to 0.50 has practically no effect on  $NP$ .
3. With two six-blade open turbines installed on the same shaft and the spacing between the two impellers (vertical distance between the bottom edges of the two turbines) being at least equal to  $D_a$ , the total power is 1.9 times a single flat-blade impeller. For two six-blade pitched-blade ( $45^\circ$ ) turbines, the power is also about 1.9 times that of a single pitched-blade impeller.
4. A baffled, vertical square tank or a horizontal cylindrical tank has the same power number as a vertical cylindrical tank. However, marked changes in the flow patterns occur.

The power number for a plain anchor-type agitator similar to Fig. 7.2-2b but without the two horizontal crossbars is as follows for  $NRe' < 100$  (H2):

$$NP = 215(NRe')^{-0.955} \quad (7.2-3)$$

where  $D_a/D_t = 0.90$ ,  $W/D_t = 0.10$ , and  $C/D_t = 0.05$ .

The power number for a helical-ribbon

agitator for very viscous liquids for  $NRe' < 20$  is as follows (H2):

$$N_p = 186(NRe')^{-1} (\text{agitator pitch} / \text{tank diameter} = 1.0) \quad (7.2-4)$$

$$N_p = 290(NRe')^{-1} (\text{agitator pitch} / \text{tank diameter} = 0.5) \quad (7.2-5)$$

The typical dimensional ratios used are  $D_a/D_t = 0.95$ , with some ratios as low as 0.75, and  $W/D_t = 0.095$ . The agitator pitch is the vertical distance of a single flight of the helix in a  $360^\circ$  rotation (B6).

## 7.2F Agitator Scale-Up

*1. Introduction.* In the process industries, experimental data are often available for a laboratory-size or pilot-unit-size agitation system, and it is desired to scale up the

results to design a full-scale unit. Since the processes to be scaled up are very diverse, no single method can handle all types of scale-up problems, and many approaches to scale-up exist. Geometric similarity is, of course, important and the simplest to achieve. Kinematic similarity can be defined in terms of ratios of velocities or of times ( $R_2$ ). Dynamic similarity requires fixed ratios of viscous, inertial, or gravitational forces. Even if geometric similarity is achieved, dynamic and kinematic similarity often cannot be obtained at the same time. Hence, it is frequently up to the designer to rely on judgment and experience in the scale-up.

In many cases, the main objectives

usually present in an agitation process are as follows: *equal liquid motion*, such as in liquid blending, where the liquid motion or corresponding velocities are approximately the same in both cases; *equal suspension of solids*, where the levels of suspension are the same; and *equal rates of mass transfer*, where mass transfer is occurring between a liquid and a solid phase, between liquid–liquid phases, and so on, and the rates are the same.

2. *Scale-up procedure*. A suggested step-by-step procedure to follow in the scale-up is detailed as follows for scaling up from the initial conditions, where the geometric sizes given in Table 7.2-1 are  $D_{a1}$ ,  $DT_1$ ,  $H_1$ ,  $W_1$ , and so on, to the final conditions of  $D_{a2}$ ,  $DT_2$ , and so on:

1. Calculate the scale-up ratio  $R$ . Assuming that the original vessel is a standard cylinder with  $DT_1 = H_1$ , the volume  $V_1$  is

$$V_1 = (\pi DT_1^2 H_1) = (\pi DT_1^3) (7.2-6)$$

Then, the ratio of the volumes is

$$V_2/V_1 = \pi DT_2^3 / 4 \pi DT_1^3 / 4 = DT_2^3 / DT_1^3 (7.2-7)$$

The scale-up ratio is then

$$R = (V_2/V_1)^{1/3} = DT_2/DT_1 (7.2-8)$$

2. Using this value of  $R$ , apply it to all of the dimensions in Table 7.2-1 to calculate the new dimensions. For example,

$$Da_2 = R Da_1, J_2 = R J_1, \dots (7.2-9)$$

3. Then, a scale-up rule must be selected and applied to determine the agitator speed  $N_2$  to be used to duplicate the small-scale results using  $N_1$ . This equation is as follows ( $R_2$ ):

$$N_2 = N_1 (1/R)^n = N_1 (DT_1/DT_2)^n (7.2-10)$$

where  $n = 1$  for equal liquid motion,  $n = 3/4$  for equal suspension of solids, and  $n = 2/3$  for equal rates of mass transfer (which is equivalent to equal power per unit volume). This value of  $n$  is based on empirical and theoretical considerations.



4. Knowing  $N_2$ , the power required can be determined using Eq. (7.2-2) and Fig. 7.2-4.

**EXAMPLE 7.2-2. Derivation of a Scale-Up-Rule Exponent**

For the scale-up-rule exponent  $n$  in Eq. (7.2-10), show the following for turbulent agitation:

- When  $n = 23$ , the power per unit volume is constant in the scale-up.
- When  $n = 1.0$ , the tip speed is constant in the scale-up.

**Solution:** For part (a), from Fig. 7.2-4,  $NP$  is constant for the turbulent region. From Eq. (7.2-2),

$$P_1 = NP_1 N_1^3 D_1^{15} \quad (7.2-11)$$

Then, for equal power per unit volume,  $P_1/V_1 = P_2/V_2$ ; or, using Eq. (7.2-6),

$$P_1 V_1 = P_1 \pi D_1^3 L_1 = P_2 V_2 = P_2 \pi D_2^3 L_2 \quad (7.2-12)$$

Substituting  $P_1$  from Eq. (7.2-11) together with a similar equation for  $P_2$  into Eq. (7.2-12) and combining with Eq. (7.2-8).

$$N_2 = N_1 (1/R)^{2/3} \quad (7.2-13)$$

For part (b), using Eq. (7.2-10) with  $n = 1.0$ , rearranging, and multiplying by  $\pi$ ,

$$N_2 = N_1 (D_1/D_2)^{1.0} \quad (7.2-14)$$

$$\pi D_2 N_2 = \pi D_1 N_1 \quad (7.2-15)$$

where  $\pi D N$  is the tip speed in m/s.

To aid the designer of new agitation

systems as well as to serve as a guide for evaluating existing systems, some approximate guidelines are given as follows for liquids of normal viscosities (M2): for mild agitation and blending, 0.1 to 0.2 kW/m<sup>3</sup> of fluid (0.0005 to 0.001 hp/gal); for vigorous agitation, 0.4 to 0.6 kW/m<sup>3</sup> (0.002 to 0.003 hp/gal); for intense agitation or where mass transfer is important, 0.8 to 2.0 kW/m<sup>3</sup> (0.004 to 0.010 hp/gal). This power in kW is the actual power delivered to the fluid as given in Fig. 7.2-4 and Eq. (7.2-2). This does not include the power used in the gear boxes and bearings. Typical efficiencies of electric motors are given in Section 7.1B. As an approximation, the power lost in the gear boxes and bearings, and in inefficiency of the electric motor is approximately 30–40% of  $P$ , the actual

# power input to the fluid.

## **EXAMPLE 7.2-3. Scale-Up of Turbine Agitation System**

An existing agitation system is the same as given in Example 7.2-1, part (a), for a flat-blade turbine with a disk and six blades. The given conditions and sizes are  $D_{T1} = 1.83$  m,  $D_{a1} = 0.61$  m,  $W_1 = 0.122$  m,  $J_1 = 0.15$  m,  $N_1 = 90/60 = 1.50$  rev/s,  $\rho = 929$  kg/m<sup>3</sup>, and  $\mu = 0.01$  Pa · s. It is desired to scale up these results for a vessel whose volume is 3.0 times as large. Do this for the following two process objectives:

- Where an equal rate of mass transfer is desired
- Where equal fluid motion is needed

**Solution:** Since  $H_1 = D_{T1} = 1.83$  m, the original tank volume  $V_1 = (\pi D_{T1}^2 H_1)/4 = \pi(1.83)^3/4 = 4.813$  m<sup>3</sup>. Volume  $V_2 = 3.0(4.813) = 14.44$  m<sup>3</sup>. Following the steps in the scale-up procedure, and using Eq. (7.2-8),

$$R = (V_2/V_1)^{1/3} = (14.44/4.813)^{1/3} = 1.442$$

The dimensions of the larger agitation system are as follows:  $D_{T2} = R D_{T1} = 1.442(1.83) = 2.64$  m,  $D_{a2} = 1.442(0.61) = 0.880$  m,  $W_2 = 1.442(0.122) = 0.176$  m, and  $J_2 = 1.442(0.15) = 0.216$  m.

For part (a), for equal mass transfer,  $n = 23$  in Eq. (7.2-10).

$$N_2 = N_1 (1/R)^{2/3} = (1.50)(1/1.442)^{2/3} = 1.175 \text{ rev/s (70.5 rpm)}$$

Using Eq. (7.2-1),

$$N Re' = Da_2 N \rho \mu = (0.880)^2 (1.175) 929 (0.01) = 8.453 \times 10^4$$

Using  $N_P = 5.0$  in Eq. (7.2-2),

$$P_2 = N_P \rho N^3 D_a^5 = 5.0 (9.29) (1.175)^3 (0.880)^5 = 3977 \text{ J/s} = 3.977 \text{ kW}$$

The power per unit volume is

$$P_1/V_1 = 1.3244/4.813 = 0.2752 \text{ kW/m}^3 \\ P_2/V_2 = 3.977/14.44 = 0.2752 \text{ kW/m}^3$$

The value of  $0.2752 \text{ kW/m}^3$  is somewhat lower than the approximate guidelines of 0.8 to 2.0 for mass transfer.

For part (b), for equal fluid motion,  $n = 1.0$ .

$$\begin{aligned} N_2 &= (1.50)(11.442)^{1.0} = 1.040 \text{ rev/s} \\ P_2 &= 5.0(929) \\ &\quad (1.040)^3 (0.880)^5 = 2757 \text{ J} \\ s &= 2.757 \text{ kW} \\ P_2 V_2 &= 2.757(14.44) = 0.1909 \text{ kW/m}^3 \end{aligned}$$

## 7.2G Mixing Times of Miscible Liquids

In one method used to study the blending or mixing time for two miscible liquids, an amount of HCl acid is added to an equivalent amount of NaOH and the time required for the indicator to change color is noted. This is a measure of molecule–molecule mixing. Other experimental methods are also used. Rapid mixing takes place near the impeller, with slower mixing, which depends on the pumping circulation rate, in the outer zones.

In Fig. 7.2-6, a correlation of mixing

time is given for a turbine agitator (B5, M5, N1). The dimensionless mixing factor  $f_t$  is defined as

$$f_t = tT(NDa^2)^{2/3}g^{1/6}Da^{1/2}H^{1/2}Dt^{3/2} \quad (7.2-16)$$

where  $tT$  is the mixing time in seconds. For  $NRe' > 1000$ , since  $f_t$  is approximately constant, then  $tTN^{2/3}$  is constant. For some other mixers, it has been shown that  $tTN$  is approximately constant. For scaling up from vessel 1 to a larger vessel, 2, with similar geometry and with the same power/unit volume in the turbulent region, the mixing times are related by

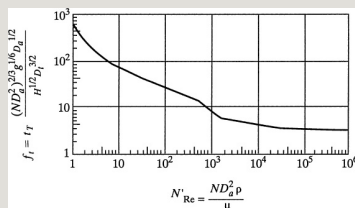


Figure 7.2-6. Correlation of mixing time for miscible liquids using a turbine in a baffled tank (for a plain turbine, a turbine with a disk, and a pitched-

$$t_{T2}/t_{T1} = (Da_2/Da_1)^{11/18} \quad (7.2-17)$$

Hence, the mixing time increases for the larger vessel. For scaling up while keeping the same mixing time, the power/unit volume  $P/V$  markedly increases:

$$(P_2/V_2)/(P_1/V_1) = (Da_2/Da_1)^{11/4} \quad (7.2-18)$$

Usually, in scaling up to large-size vessels, a somewhat larger mixing time is used so that the power/unit volume does not increase markedly.

The mixing time for a helical-ribbon agitator is as follows for  $NRe' < 20$  (H2):

$$NtT = 126(\text{agitator pitch}/\text{tank diameter} = 1.0)(7.2-19)$$

$$NtT = 90(\text{agitator pitch}/\text{tank diameter} = 0.5)(7.2-20)$$

For very viscous liquids, the helical-ribbon mixer gives a much smaller mixing time than a turbine for the same power/unit volume (M5). However, for nonviscous liquids, it gives longer times.

For a propeller agitator in a baffled tank, a mixing-time correlation is given by Biggs (B5), and that for an unbaffled tank by Fox and Gex (F1).

For a high-efficiency impeller in a baffled tank, mixing-time correlations are given by reference (F2), which shows that mixing times are lower than

# for pitched-blade agitators.

## **EXAMPLE 7.2-4. Scale-Up of Mixing Time in a Turbine Agitation System**

Using the existing conditions for the turbine with a disk as in Example 7.2-1, part (a), perform the following:

- Calculate the mixing time.
- Calculate the mixing time for a smaller vessel with a similar geometric ratio, where  $D_t$  is 0.30 m instead of 1.83 m. Do this for the same power per unit volume as used in part (a).
- Using the same mixing time calculated for the smaller vessel in part (b), calculate the new power per unit volume for the larger vessel in part (a).

**Solution:** In part (a),  $D_t = 1.83$  m,  $D_a = 0.16$  m,  $D_t = H$ ,  $N = 90/60 = 1.50$  rev/s,  $\rho = 929$  kg/m<sup>3</sup>, and  $\mu = 10$  cp = 0.01 Pa · s. From Example 7.2-1,  $NRe' = 5.185 \times 10^4$ ,  $N_P = 5$ ,  $P_1 = 1.324$  kW. For the tank volume,

$$V_1 = \pi(1.83)^2 (1.83)/4 = 4.813 \text{ m}^3$$

The power per unit volume is

$$P_1/V_1 = 1.324/4.813 = 0.2751 \text{ kW/m}^3$$

From Fig. 7.2-6 for  $NRe' = 5.185 \times 10^4$ ,  $f_t = 4.0$ . Substituting into Eq. (7.2-16),

$$f_t = 4.0 = tT(N_1 D_1^2)^{2/3} g_1^{1/6} D_1^{11/2} H_1^{1/2} D_1^{13/2} = tT(1.5 \times 0.61^2)^{2/3} (9.80665)^{1/6} (0.61)^{1/2} (1.831/2)^{11/2} (1.83)^{13/2} tT = 17.30 \text{ s}$$

For part (b), the scale-down ratio  $R$  from Eq. (7.2-8) is

$$R = D_2/D_1$$

$$D_2 = 0.30/1.83 = 0.1639 \text{ m} \quad D_2 = R D_1 = 0.1639(0.61) = 0.1000 \text{ m}$$

Also,  $H_2 = D_2 = 0.300$  m. Using the same  $P_1/V_1 = P_2/V_2 = 0.2751$  kW/m<sup>3</sup> in the turbulent region, and Eq. (7.2-17),

$$t_2 t_1^{-1} = (D_2^2/D_1^2)^{11/18} t_1 = 17.30(0.1000/0.61)^{11/18}$$



Hence,  $t_{r2} = 5.73$  s. This shows that the larger vessel has a marked increase in mixing time from 5.73 to 17.30 s for equal power per unit volume.

For part (c), using the same mixing time of 5.73 s for the smaller vessel, the power per unit volume of the larger vessel is calculated from Eq. (7.2-18) for equal mixing times:

$$\frac{P_2}{V_2} \frac{P_1}{V_1} = (Da_2 Da_1)^{11/40} \cdot 2751 \frac{P_1}{V_1}$$

$$V_1 = (0.10000 \cdot 6100)^{11/4}$$

Solving,  $P_1/V_1 = 39.73$  kW/m<sup>3</sup>. This, of course, is a very large and impractical increase.

## 7.2H Flow Number and Circulation Rate in Agitation

An agitator acts like a centrifugal pump impeller without a casing and gives a flow at a certain pressure head. This circulation rate  $Q$  in m<sup>3</sup>/s from the edge of the impeller is the flow rate perpendicular to the impeller discharge area. Fluid velocities have been measured in mixers and have been used to calculate the circulation rates. Data for baffled vessels have been correlated using the dimensionless

flow number  $N_Q$  ( $U_1$ ):

$$N_Q = Q N D a^3 (7.2-21)$$

$N_Q = 0.5$  marine propeller (pitch = diameter)  $N_Q = 0.75$  six-

blade turbine with disk ( $W/Da = 15$ )  $N_Q = 0.5$  six-

blade turbine with disk ( $W/Da = 18$ )  $N_Q = 0.75$  pitched-

blade turbine ( $W/Da = 15$ )

## 7.2I Special Agitation Systems

*1. Suspension of solids.* In some agitation systems, a solid is suspended in the agitated liquid.

Examples are when a finely dispersed solid is to be dissolved in the liquid, microorganisms are suspended in fermentation, a homogeneous liquid–solid mixture is to be produced for feed to a process,

and a suspended solid is used as a catalyst to speed up a reaction. The suspension of solids is somewhat similar to a fluidized bed. In the agitated system, circulation currents of the liquid keep the particles in suspension. The amount and type of agitation needed depend mainly on the terminal settling velocity of the particles, which can be calculated using the equations found in Chapter 30. Empirical equations for predicting the power required to suspend particles are given in references (M2, W1). Equations for pitched-blade turbines and high-efficiency impellers are given by Corpstein et al. (C4).

*2. Dispersion of gases and liquids in liquids.* In gas–liquid dispersion

processes, the gas is introduced below the impeller, which chops the gas into very fine bubbles. The type and degree of agitation affect the size of the bubbles and the total interfacial area. Typical of such processes are aeration in sewage treatment plants, hydrogenation of liquids by hydrogen gas in the presence of a catalyst, absorption of a solute from the gas by the liquid, and fermentation. Correlations are available for predicting the bubble size, holdup, and kW power needed (C3, L1, Z1). For liquids dispersed in immiscible liquids, see reference (T1). The power required for the agitator in gas–liquid dispersion systems can be as much as 10–50% less than that required when no gas is present (C3, T2).

*3. Motionless mixers.* The mixing of two

fluids can be accomplished in motionless mixers in a pipe with no moving parts. In such commercial devices, stationary elements inside a pipe successively divide portions of the stream and then recombine these portions.

Laminar-flow mixers are used to mix highly viscous mixtures. One type of static mixer has a series of fixed helical elements, as shown in Fig. 7.2-7. (Note that most mixers have from six to 20 elements.) In the first element, the flow is split into two semicircular channels and the helical shape gives the streams a  $180^\circ$  twist. The next and successive elements are placed at  $90^\circ$  relative to each other and split the flows into two for each element. Each split in flow creates more interfacial area between

layers. When these layers become sufficiently thin, molecular diffusion will eliminate concentration differences remaining. When each element divides the flow into two flow channels (M6),

$$dD=12n(7.2-22)$$

where  $n$  is the number of elements in series,  $d$  is the maximum striation thickness, and  $D$  is the pipe diameter. When  $n = 20$ , then about  $10^6$  divisions occur and  $d$  is a very small thickness, which enhances the rate of diffusion.

In another commercial type of static mixer (K3), the stream is divided four times for each element. Each element has interacting bars or corrugated sheets placed lengthwise in the pipe and at a  $45^\circ$  angle to the pipe's axis. The lengths

$L$  of the various types of elements vary from about 1.0 to 1.5 times the pipe diameter. These mixers are also used in turbulent-flow mixing.

In laminar flow with helical mixers, the pressure drop (and, hence, power required) is approximately six times as large as that in the empty pipe. In turbulent flow, because of energy losses due to changes of direction, the pressure drop can be up to several hundred times as large (M6, P1). The power loss is typically about 10% of the power of a dynamic mixer (K3). Motionless mixers are also used for heat transfer, chemical reactions, and dispersion of gases in liquids.

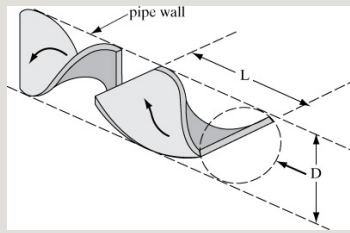


Figure 7.2-7. Two-element helical motionless mixer with element length  $L$  and pipe diameter  $D$  (M2, M6).

## 7.2J Mixing of Powders, Viscous Materials, and Pastes

*1. Powders.* For mixing solid particles or powders, it is necessary to displace parts of the powder mixture with respect to other parts. The simplest class of devices suitable for gentle blending is the tumbler. However, it is not usually used for breaking up agglomerates. A common type of tumbler is the *double-cone blender*, in which two cones are mounted with their open ends fastened together and rotated, as shown in Fig. 7.2-8a. Baffles can also be used internally. If an internal



rotating device is also used in the double cone, agglomerates can also be broken up. Other geometries used are a cylindrical drum with internal baffles or a twin-shell V type.

Tumblers used specifically for breaking up agglomerates are rotating cylindrical or conical shells charged with metal or porcelain steel balls or rods.

Another class of devices for blending solids is the *stationary shell device*, in which the container is stationary and the material displacement is accomplished by single or multiple rotating inner devices. In the ribbon mixer in Fig. 7.2-8b, a shaft with two open helical screws, numbers 1 and 2, attached to it rotates. One screw is left-handed and one right-handed. As the shaft rotates,

sections of powder move in opposite directions and mixing occurs. Other types of internal rotating devices are available for special situations (P1). Also, in some devices both the shell and the internal device rotate.

*2. Doughs, pastes, and viscous materials.* For mixing doughs, pastes, and viscous materials, large amounts of powder are required as the material is divided, folded, or recombined, and as different parts of the material are displaced relative to each other so that fresh surfaces recombine as often as possible. Some machines may require jacketed cooling to remove the heat generated.

The first type of device for this purpose is somewhat similar to those for

agitating fluids, with an impeller slowly rotating in a tank. The impeller can be a close-fitting anchor agitator as in Fig.

7.2-2b, where the outer sweep assembly may have scraper blades. A gate impeller can also be used that has horizontal and vertical bars to cut the paste at various levels and at the wall, which may have stationary bars. A modified gate mixer is the shear-bar mixer, which contains vertical rotating bars or paddles passing between vertical stationary fingers. Other modifications of these types are those where the can or container will rotate as well as the bars and scrapers. These are called *change-can mixers*.

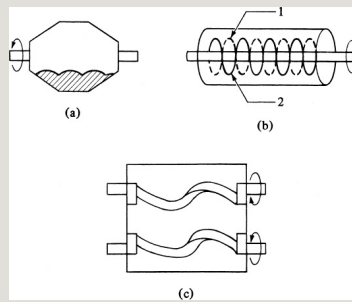


Figure 7.2-8. Mixers for powders and pastes: (a) double-cone powder mixer, (b) ribbon powder mixer with two ribbons, (c) kneader mixer for pastes.

The most commonly used mixer for heavy pastes and doughs is the *double-arm kneader mixer*. The mixing action is bulk movement, smearing, stretching, dividing, folding, and recombining. The most widely used design employs two counterrotating arms of sigmoid shape that may rotate at different speeds, as shown in Fig. 7.2-8c.

### 7.3 Chapter Summary

In this chapter, we have described and considered different systems that use pumps, compressors, blowers,

and fans, as well as those that use agitation and mixing devices. In all cases, we seek to move fluids, whether throughout a chemical plant, or within a closed vessel.

First, we considered systems where fluids need to move horizontally and vertically by applying mechanical energy. Different pumps were described and the power needed to operate these pumps was calculated. We showed that the actual or brake power necessary to operate a pump can be calculated from

$$\begin{aligned}\text{brake kW} &= W_{pm} / 1000 = - \\ & W S m \eta \times 1000 (\text{SI}) \text{brake hp} = W_{pm} / 550 = - \\ & W S m \eta \times 550 (\text{English})\end{aligned}\quad (7.3-1)$$

We also considered operational issues such as electric power, pump efficiency,

and electric motor efficiency. For cases where cavitation can occur, the net positive suction head required was calculated. The geometries and properties of centrifugal and positive-displacement pumps were also described. For systems that use compressible fluids, it was shown how to modify thermodynamic relations for work, density, and pressure to account for isothermal and adiabatic compression.

Later in the chapter, we considered systems that use agitation. These systems may use agitation to improve rates of heat or mass transfer, or to promote other desired characteristics, such as uniform mixing. Many examples were provided for systems that use agitation and mixing. All of these

systems use some type of agitator or impeller to promote fluid motion.

Different types of agitators, such as paddles and turbines, were described.

Models were derived to calculate the Reynolds number and the power inputted into agitation systems using different impellers. Operational issues such as scale-up and dimensional similarity were described. Finally, special agitation systems were discussed for situations involving solids and other types of very viscous materials, such as doughs and pastes.

## **Problems**

**7.1-1. *Brake Horsepower of a Centrifugal Pump.*** Using Fig. 7.1-2 and a flow rate of 60 gal/min, do as follows:

- Calculate the brake hp of the pump using water with

a density of  $62.4 \text{ lb}_m/\text{ft}^3$ . Compare with the value from the curve.

- Do the same for a nonviscous liquid having a density of  $0.85 \text{ g/cm}^3$ .

**Ans. (b) 0.69 brake hp (0.51 kW)**

### **7.1-2. *kW Power of a Fan.*** A

centrifugal fan will be used to take a flue gas at rest (zero velocity) and at a temperature of  $352.6 \text{ K}$  and a pressure of  $749.3 \text{ mmHg}$ , and discharge this gas at a pressure of  $800.1 \text{ mmHg}$  and a velocity of  $38.1 \text{ m/s}$ . The volume flow rate of gas is  $56.6 \text{ std m}^3/\text{min}$  of gas (at  $294.3 \text{ K}$  and  $760 \text{ mmHg}$ ). Calculate the brake kW of the fan if its efficiency is  $65\%$  and the gas has a molecular weight of  $30.7$ . Assume incompressible flow.

**7.1-3. *Adiabatic Compression of Air.*** A compressor operating adiabatically is to



compress  $2.83 \text{ m}^3/\text{min}$  of air at  $29.4^\circ\text{C}$  and  $102.7 \text{ kN/m}^2$  to  $311.6 \text{ kN/m}^2$ .

Calculate the power required if the efficiency of the compressor is 75%.

Also, calculate the outlet temperature.

**7.1-4.  $(NPSH)_R$  for Feed to a**

***Distillation Tower.*** A feed rate of 200 gpm of a hydrocarbon mixture at  $70^\circ\text{C}$  is being pumped from a tank at 1 atm abs pressure to a distillation tower. The density of the feed is  $46.8 \text{ lb}_m/\text{ft}^3$  and its vapor pressure is 8.45 psia. The velocity in the inlet line to the pump is 3 ft/s and the friction loss between the tank and pump is 3.5 ft of fluid. The net positive suction head required is 6 ft.

- How far below the liquid level in the tank must the pump be to obtain this required  $(NPSH)_R$ ?
- If the feed is at the boiling point, calculate the pump position.

**Ans.** (a)  $z_1 = -9.57 \text{ ft } (-2.92 \text{ m})$

**7.2-1. Power for Liquid Agitation.** It is desired to agitate a liquid having a viscosity of  $1.5 \times 10^{-3} \text{ Pa} \cdot \text{s}$  and a density of  $969 \text{ kg/m}^3$  in a tank having a diameter of  $0.91 \text{ m}$ . The agitator will be a six-blade open turbine having a diameter of  $0.305 \text{ m}$  operating at  $180 \text{ rpm}$ . The tank has four vertical baffles, each with a width  $J$  of  $0.076 \text{ m}$ . Also,  $W = 0.0381 \text{ m}$ . Calculate the required kW. Use curve 2, Fig. 7.2-4.

**Ans.**  $NP = 2.5$ , power =  $0.172 \text{ kW}$   
( $0.231 \text{ hp}$ )

**7.2-2. Power for Agitation and Scale-Up.** A turbine agitator having six flat blades and a disk has a diameter of  $0.203 \text{ m}$  and is used in a tank having a

diameter of 0.61 m and height of 0.61 m. The width  $W = 0.0405$  m. Four baffles are used having a width of 0.051 m. The turbine operates at 275 rpm in a liquid having a density of  $909 \text{ kg/m}^3$  and viscosity of  $0.020 \text{ Pa} \cdot \text{s}$ .

- Calculate the kW power of the turbine and  $\text{kW/m}^3$  of volume.
- Scale up this system to a vessel having a volume of 100 times the original for the case of equal mass-transfer rates.

**Ans.** (a)  $P = 0.1508 \text{ kW}$ ,  $P/V = 0.845 \text{ kW/m}^3$ ; (b)  $P_2 = 15.06 \text{ kW}$ ,  $P_2/V_2 = 0.845 \text{ kW/m}^3$

### ***7.2-3. Scale-down of a Process***

***Agitation System.*** An existing agitation process operates using the same agitation system and fluid as described in Example 7.2-1a. It is desired to design a small pilot unit with a vessel

volume of 2.0 liters so that the effects of various process variables on the system can be studied in the laboratory. The rates of mass transfer appear to be important in this system, so the scale-down should be on this basis. Design the new system specifying sizes, rpm, and kW power.

**7.2-4. *An Anchor Agitation System.*** An anchor-type agitator similar to that described for Eq. (7.2-3) is to be used to agitate a fluid having a viscosity of  $100 \text{ Pa} \cdot \text{s}$  and a density of  $980 \text{ kg/m}^3$ . The vessel size is  $D_t = 0.90 \text{ m}$  and  $H = 0.90 \text{ m}$ . The rpm is 50. Calculate the power required.

**7.2-5. *Design of an Agitation System.*** An agitation system is to be designed for a fluid having a density of  $950 \text{ kg/m}^3$

and a viscosity of  $0.005 \text{ Pa} \cdot \text{s}$ . The vessel volume is  $1.50 \text{ m}^3$  and a standard six-blade open turbine with blades at  $45^\circ\text{C}$  (curve 3, Fig. 7.2-4) is to be used with  $Da/W = 8$  and  $Da/D_t = 0.35$ . For the preliminary design, a power of  $0.5 \text{ kW/m}^3$  volume will be used. Calculate the dimensions of the agitation system, rpm, and kW power.

**7.2-6. Scale-Up of Mixing Times for a Turbine.** For scaling up a turbine-agitated system, do as follows:

- Derive Eq. (7.2-17) for the same power/unit volume.
- Derive Eq. (7.2-18) for the same mixing times.

**7.2-7. Mixing Time in a Turbine-Agitated System.** Do as follows:

- Predict the time of mixing for the turbine system in Example 7.2-1a.

- Using the same system as part (a) but with a tank having a volume of  $10.0 \text{ m}^3$  and the same power/unit volume, predict the new mixing time.

**Ans.** (a)  $f_t = 4.0$ ,  $t_T = 17.3 \text{ s}$

**7.2-8. *Effect of Viscosity on Mixing Time.*** Using the same conditions for the turbine mixer as in Example 7.2-4, part (a), except for a viscous fluid with a viscosity of  $100 \text{ Pa} \cdot \text{s}$  ( $100000 \text{ cp}$ ), calculate the mixing time. Compare this mixing time with that for the viscosity of  $10 \text{ cp}$ . Also, calculate the power per unit volume.

**Ans.**  $t_T = 562 \text{ s}$

**7.2-9. *Mixing Time in a Helical Mixer.***

A helical mixer with an agitator pitch/tank diameter = 1.0 and with  $D_t = 1.83 \text{ m}$  and  $D_a/D_t = 0.95$  is being used to agitate a viscous fluid having a viscosity

of 200000 cp and a density of 950 kg/m<sup>3</sup>. The value of  $N = 0.3$  rev/s.

Calculate the mixing time and the power per unit volume.

**Ans.**  $t_T = 420$  s

### References

### Notation

# Chapter 8. Differential Equations of Fluid Flow

## 8.0 Chapter Objectives

On completion of this chapter, a student should be able to:

- Distinguish between different types of derivatives (partial derivative, total derivative, substantial derivative)
- Distinguish and explain the differences between scalars, vectors, and tensors
- Identify different fluid properties and parameters such as scalars, vectors, and tensors
- Derive the equation of continuity for a volume element of fluid
- Simplify the equation of continuity for steady-state systems and systems of constant density
- Identify the equation of continuity in Cartesian, cylindrical, and spherical coordinates
- Derive the equation of motion (momentum balance) for a volume element of fluid



- Simplify the equation of motion for steady-state systems and systems with constant density and viscosity
- Identify the equation of motion in Cartesian, cylindrical, and spherical coordinates
- Derive the velocity profile for fluid systems using the equation of motion and the equation of continuity in Cartesian, cylindrical, and spherical coordinates

## 8.1 Differential Equations of Continuity

### 8.1A Introduction

In Chapter 4, overall mass, energy, and momentum balances allowed us to solve many elementary problems in fluid flow. These balances were performed on an arbitrary finite volume sometimes called a *control volume*. In these total-energy, mechanical-energy, and momentum balances, we only needed to know the state of the inlet and outlet streams, and the exchanges with the

surroundings.

These overall balances were powerful tools in solving various flow problems because they did not require knowledge of what goes on inside the finite control volume. Also, in the simple shell-momentum balances made in Section 4.4, expressions were obtained for the velocity distribution and pressure drop. However, to advance in our study of these flow systems, we must investigate in greater detail what goes on inside this finite control volume. To do this, we now use a differential element for a control volume. The differential balances will be similar to the overall and shell balances, but now we will make the balance in a single phase and integrate up to the phase boundary using the specified boundary conditions. In the

balances done previously, a balance was made for each new system studied. It is not necessary to formulate new balances for each new flow problem. It is often easier to start with the general forms of the differential equations for the conservation of mass (equation of continuity) and the conservation of momentum. These equations are then simplified by eliminating unneeded terms for each particular problem.

The differential-momentum-balance equation to be derived is based on Newton's second law and allows us to determine how velocity varies with position and time, as well as the pressure drop in laminar flow. The equation of momentum balance can be used for turbulent flow with certain modifications.

These conservation equations are often called the *equations of change*, since they describe the variations in the properties of the fluid with respect to position and time. Before we derive these equations, a brief review of the different types of derivatives with respect to time that occur in these equations and a brief description of vector notation will be given.

### **8.1B Types of Time Derivatives and Vector Notation**

*1. Partial time derivative.* Various types of time derivatives are used in the derivations to follow. The most common type of derivative is the partial time derivative. For example, suppose that we are interested in the mass concentration or density  $\rho$  in kg/m<sup>3</sup> in a flowing stream as a function of position  $x, y, z$ , and time

$t$ . The partial time derivative of  $\rho$  is  $\partial\rho/\partial t$ . This is the local change of density with time at a fixed point  $x$ ,  $y$ ,  $z$ .

2. *Total time derivative.* Suppose that we want to measure the density in the stream while we are moving about in the stream with velocities in the  $x$ ,  $y$ , and  $z$  directions of  $dx/dt$ ,  $dy/dt$ , and  $dz/dt$ , respectively. The total derivative  $d\rho/dt$  is

$$d\rho/dt = \partial\rho/\partial t + \partial\rho/\partial x \, dx/dt + \partial\rho/\partial y \, dy/dt + \partial\rho/\partial z \, dz/dt \quad (8.1-1)$$

This means that the density is a function of  $t$  and of the velocity components  $dx/dt$ ,  $dy/dt$ , and  $dz/dt$  at which the observer is moving.

3. *Substantial time derivative.* Another

useful type of time derivative is obtained if the observer floats along with the velocity  $\mathbf{v}$  of the flowing stream and notes the change in density with respect to time. This is called the derivative that follows the motion, or the *substantial time derivative*,  $D\rho/Dt$ :

$$D\rho/Dt = \partial\rho/\partial t + v_x\partial\rho/\partial x + v_y\partial\rho/\partial y + v_z\partial\rho/\partial z = \partial\rho/\partial t + (\mathbf{v} \cdot \nabla\rho) \quad (8.1-2)$$

where  $v_x$ ,  $v_y$ , and  $v_z$  are the velocity components of the stream velocity  $\mathbf{v}$ , which is a vector. This substantial derivative is applied to both scalar and vector variables. The term  $(\mathbf{v} \cdot \nabla\rho)$  will be discussed in part 6 of Section 8.1B.

**4. Scalars.** The physical properties encountered in momentum, heat, and mass transfer can be placed into three

main categories: scalars, vectors, and tensors. Scalars are quantities such as concentration, temperature, length, volume, time, and energy. They have magnitude but no direction and are considered to be zero-order tensors. The common mathematical algebraic laws hold for the algebra of scalars. For example,  $bc = cb$ ,  $b(cd) = (bc)d$ .

5. *Vectors*. Velocity, force, momentum, and acceleration are considered vectors since they have magnitude *and direction*. They are also regarded as first-order tensors and are written in boldface letters in this text, such as  $\mathbf{v}$  for velocity. The addition of two vectors  $\mathbf{B} + \mathbf{C}$  by parallelogram construction and the subtraction of two vectors  $\mathbf{B} - \mathbf{C}$  are shown in Fig. 8.1-1. The vector  $\mathbf{B}$  is represented by its three projections  $B_x$ ,

$B_y$ , and  $B_z$  on the  $x$ ,  $y$ , and  $z$  axes, and

$$\mathbf{B} = iB_x + jB_y + kB_z \quad (8.1-3)$$

where  $\mathbf{i}$ ,  $\mathbf{j}$ , and  $\mathbf{k}$  are unit vectors along the axes  $x$ ,  $y$ , and  $z$ , respectively.

In multiplying a scalar quantity  $r$  or  $s$  by a vector  $\mathbf{B}$ , the following identities hold:

$$r\mathbf{B} = \mathbf{B}r \quad (8.1-4)$$

$$(rs)\mathbf{B} = r(s\mathbf{B}) \quad (8.1-5)$$

$$r\mathbf{B} + s\mathbf{B} = (r+s)\mathbf{B} \quad (8.1-6)$$

The following identities also hold:

$$(\mathbf{B} \cdot \mathbf{C}) = (\mathbf{C} \cdot \mathbf{B}) \quad (8.1-7)$$

$$\mathbf{B} \cdot (\mathbf{C} + \mathbf{D}) = (\mathbf{B} \cdot \mathbf{C}) + (\mathbf{B} \cdot \mathbf{D}) \quad (8.1-8)$$

$$(\mathbf{B} \cdot \mathbf{C})\mathbf{D} \neq \mathbf{B}(\mathbf{C} \cdot \mathbf{D}) \quad (8.1-9)$$



$$(\mathbf{B} \cdot \mathbf{C}) = BC \cos \phi_{BC} \quad (8.1-10)$$

where  $\phi_{BC}$  is the angle between two vectors, and is less than  $180^\circ$ .

Second-order tensors  $\boldsymbol{\tau}$  arise primarily in momentum transfer and have nine components. They are discussed elsewhere (B2).

*6. Differential operations with scalars and vectors.* The gradient or “grad” of a scalar field is given as

$$\nabla \rho = \mathbf{i} \partial \rho / \partial x + \mathbf{j} \partial \rho / \partial y + \mathbf{k} \partial \rho / \partial z \quad (8.1-11)$$

where  $\rho$  is a scalar such as density.

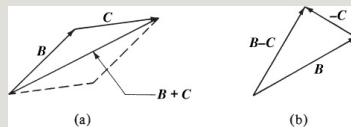


Figure 8.1-1. Addition and subtraction of vectors: (a) addition of vectors,  $\mathbf{B} + \mathbf{C}$ ; (b) subtraction of vectors,  $\mathbf{B} - \mathbf{C}$ .

The divergence or “div” of a vector  $\mathbf{v}$  is

$$(\nabla \cdot \mathbf{v}) = \frac{\partial v_x}{\partial x} + \frac{\partial v_y}{\partial y} + \frac{\partial v_z}{\partial z} \quad (8.1-12)$$

where  $\mathbf{v}$  is a vector of components  $v_x$ ,  $v_y$ , and  $v_z$ .

The Laplacian of a scalar field is

$$\nabla^2 \rho = \frac{\partial^2 \rho}{\partial x^2} + \frac{\partial^2 \rho}{\partial y^2} + \frac{\partial^2 \rho}{\partial z^2} \quad (8.1-13)$$

Other operations that may be useful are

$$\nabla(r s) = r \nabla s + s \nabla r \quad (8.1-14)$$

$$(\nabla \cdot s \mathbf{v}) = (\nabla s \cdot \mathbf{v}) + s (\nabla \cdot \mathbf{v}) \quad (8.1-15)$$

$$(\mathbf{v} \cdot \nabla s) = v_x \frac{\partial s}{\partial x} + v_y \frac{\partial s}{\partial y} + v_z \frac{\partial s}{\partial z} \quad (8.1-16)$$

## 8.1C Differential Equation of Continuity

### *1. Derivation of equation of*

*continuity*. A mass balance will be made for a pure fluid flowing through a stationary volume element  $\Delta x \Delta y \Delta z$  that is fixed in space, as in Fig. 8.1-2. The mass balance for the fluid with a density (mass concentration) of  $\rho$  is

$$(\text{rate of mass out}) = (\text{rate of mass accumulation}) \quad (8.1-17)$$

In the  $x$  direction, the rate of mass entering the face at  $x$  having an area of  $\Delta y \Delta z$  is  $(\rho v_x)_x \Delta y \Delta z$  kg/s, and that leaving at  $x + \Delta x$  is  $(\rho v_x)_{x+\Delta x} \Delta y \Delta z$ . The term  $(\rho v_x)$  is a mass flux in kg/s  $\cdot$  m<sup>2</sup>. Mass entering and mass leaving in the  $y$  and  $z$  directions are also shown in Fig. 8.1-2.

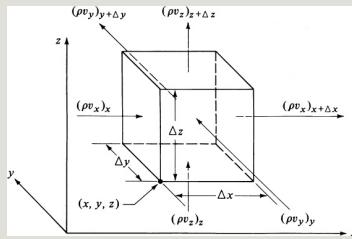


Figure 8.1-2. Mass balance for a pure fluid flowing through a fixed volume  $\Delta x \Delta y \Delta z$  in space.

The rate of mass accumulation in the volume  $\Delta x \Delta y \Delta z$  is

$$\text{of mass accumulation} = \Delta x \Delta y \Delta z \frac{\partial \rho}{\partial t} \quad (8.1-18)$$

Substituting all these expressions into Eq. (8.1-17) and dividing both sides by  $\Delta x \Delta y \Delta z$ ,

$$\begin{aligned} & [(\rho v_x)_x - (\rho v_x)_{x+\Delta x}] \Delta x + [(\rho v_y)_y - (\rho v_y)_{y+\Delta y}] \Delta y + [(\rho v_z)_z - (\rho v_z)_{z+\Delta z}] \Delta z \\ & = \frac{\partial \rho}{\partial t} \Delta x \Delta y \Delta z \end{aligned} \quad (8.1-19)$$

Taking the limit as  $\Delta x$ ,  $\Delta y$ , and  $\Delta z$  approach zero, we obtain the equation of continuity or conservation of mass for a

pure fluid:

$$\frac{\partial \rho}{\partial t} = -[\frac{\partial (\rho v_x)}{\partial x} + \frac{\partial (\rho v_y)}{\partial y} + \frac{\partial (\rho v_z)}{\partial z}] = -(\nabla \cdot \rho \mathbf{v}) \quad (8.1-20)$$

The vector notation on the right side of Eq. (8.1-20) comes from the fact that  $\mathbf{v}$  is a vector. Equation (8.1-20) tells us how the density  $\rho$  changes with time at a fixed point resulting from the changes in the mass velocity vector  $\rho \mathbf{v}$ .

We can convert Eq. (8.1-20) into another form by carrying out the actual partial differentiation:

$$\frac{\partial \rho}{\partial t} = -\rho(\frac{\partial v_x}{\partial x} + \frac{\partial v_y}{\partial y} + \frac{\partial v_z}{\partial z}) - (v_x \frac{\partial \rho}{\partial x} + v_y \frac{\partial \rho}{\partial y} + v_z \frac{\partial \rho}{\partial z}) \quad (8.1-21)$$

Rearranging Eq. (8.1-21),

$$\frac{\partial \rho}{\partial t} + v_x \frac{\partial \rho}{\partial x} + v_y \frac{\partial \rho}{\partial y} + v_z \frac{\partial \rho}{\partial z} = -$$

$$\rho(\partial v_x \partial x + \partial v_y \partial y + \partial v_z \partial z) \quad (8.1-22)$$

The left-hand side of Eq. (8.1-22) is the same as the substantial derivative in Eq. (8.1-2). Hence, Eq. (8.1-22) becomes

$$D\rho/Dt = -\rho(\partial v_x \partial x + \partial v_y \partial y + \partial v_z \partial z) = -\rho(\nabla \cdot \mathbf{v}) \quad (8.1-23)$$

*2. Equation of continuity for constant density.* In engineering problems with liquids that are relatively incompressible, the density  $\rho$  is assumed to be essentially constant. Then  $\rho$  remains constant for a fluid element as it moves along a path following the fluid motion, or  $D\rho/Dt = 0$ . Hence, Eq. (8.1-23) becomes, for a fluid of constant density at steady or unsteady state,

$$(\nabla \cdot \mathbf{v}) = \partial v_x \partial x + \partial v_y \partial y + \partial v_z \partial z = 0 \quad (8.1-24)$$

At steady state,  $\partial\rho/\partial t = 0$  in Eq. (8.1-22).

**EXAMPLE 8.1-1. Flow over a Flat Plate**

An incompressible fluid flows past one side of a flat plate. The flow in the  $x$  direction is parallel to the flat plate. At the leading edge of the plate, the flow is uniform at the free stream velocity  $v_{x0}$ . There is no velocity in the  $z$  direction. The  $y$  direction is the perpendicular distance from the plate. Analyze this case using the equation of continuity.

**Solution:** For this case where  $\rho$  is constant, Eq. (8.1-24) holds:

$$\partial v_x \partial x + \partial v_y \partial y + \partial v_z \partial z = 0 \quad (8.1-24)$$

Since there is no velocity in the  $z$  direction, we obtain

$$\partial v_x \partial x = -\partial v_y \partial y \quad (8.1-25)$$

At a given small value of  $y$  close to the plate, the value of  $v_x$  must decrease from its free stream velocity  $v_{x0}$  as it passes the leading edge in the  $x$  direction because of fluid friction. Hence,  $\partial v_x / \partial x$  is negative. Then, from Eq. (8.1-25),  $\partial v_y / \partial y$  is positive and there is a component of velocity away from the plate.

*3. Continuity equation in cylindrical and spherical coordinates.* It is often convenient to use cylindrical coordinates to solve the equation of continuity if a fluid is flowing in a cylinder (or a similar geometric system).

The coordinate system as related to rectangular coordinates is shown in Fig. 8.1-3a. The relations between rectangular  $x, y, z$  and cylindrical  $r, \theta, z$  coordinates are

$$\begin{aligned} x &= r \cos \theta & y &= r \sin \theta & z &= z \\ r &= \sqrt{x^2 + y^2} & \theta &= \tan^{-1} \frac{y}{x} \end{aligned} \quad (8.1-26)$$

Using the relations from Eq. (8.1-26) with Eq. (8.1-20), the equation of continuity in cylindrical coordinates is

$$\begin{aligned} \frac{\partial \rho}{\partial t} + \frac{1}{r} \frac{\partial (\rho r v_r)}{\partial r} + \frac{1}{r} \frac{\partial (\rho v_\theta)}{\partial \theta} \\ + \frac{\partial (\rho v_z)}{\partial z} = 0 \end{aligned} \quad (8.1-27)$$

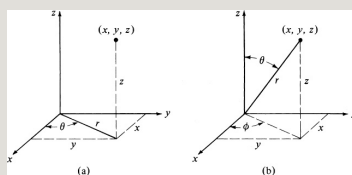


Figure 8.1-3. Curvilinear coordinate systems: (a) cylindrical coordinates, (b) spherical coordinates.



For spherical coordinates, the variables  $r$ ,  $\theta$ , and  $\phi$  are related to  $x$ ,  $y$ ,  $z$  by the following, as shown in Fig. 8.1-3b:

$$\begin{aligned} x &= r \sin \theta \cos \phi & y &= r \sin \theta \sin \phi & z &= r \cos \theta \\ r &= \sqrt{x^2 + y^2 + z^2} & \theta &= \tan^{-1} \frac{\sqrt{x^2 + y^2}}{z} & \phi &= \tan^{-1} \frac{y}{x} \end{aligned} \quad (8.1-28)$$

The equation of continuity in spherical coordinates becomes

$$\begin{aligned} & \frac{\partial \rho}{\partial t} + \frac{1}{r^2} \frac{\partial (\rho r^2 v_r)}{\partial r} \\ & + \frac{1}{r \sin \theta} \frac{\partial (\rho v_\theta \sin \theta)}{\partial \theta} \\ & + \frac{1}{r \sin \theta} \frac{\partial (\rho v_\phi)}{\partial \phi} = 0 \end{aligned} \quad (8.1-29)$$

## 8.2 Differential Equations of Momentum Transfer or Motion

### 8.2A Derivation of Equations of Momentum Transfer

The *equation of motion* is really the conservation-of-momentum equation (4.3-3), which we can write as

$$\begin{aligned} & \text{(rate of momentum in)-} \\ \text{on system)} &= \text{(rate of momentum accumulation)} \\ & \quad (8.2-1) \end{aligned}$$

We will make a balance on an element as in Fig. 8.1-2. First, we will consider only the  $x$  component of each term in Eq. (8.2-1). The  $y$  and  $z$  components can be described in an analogous manner.

The rate at which the  $x$  component of momentum enters the face at  $x$  in the  $x$  direction by convection is  $(\rho v_x v_x)_x \Delta y \Delta z$ , and the rate at which it leaves at  $x + \Delta x$  is  $(\rho v_x v_x)_{x+\Delta x} \Delta y \Delta z$ . The quantity  $(\rho v_x)$  is the mass flux, and it is multiplied by  $v_x$  to give the momentum flux.

The  $x$  component of momentum entering the face at  $y$  is  $(\rho v_y v_x)_y \Delta x \Delta z$ , and leaving at  $y + \Delta y$ , it is  $(\rho v_y v_x)_y$

$+\Delta y\Delta x\Delta z$ . For the face at  $z$ , we have  $(\rho v_z v_x)_z \Delta x \Delta y$  entering, and at  $z + \Delta z$  we have  $(\rho v_z v_x)_{z+\Delta z} \Delta x \Delta y$  leaving. Hence, the net convective  $x$  momentum flow into the volume element  $\Delta x \Delta y \Delta z$  is

$$\begin{aligned} & [(\rho v_x v_x)_x - (\rho v_x v_x)_{x+\Delta x}] \Delta y \Delta z \\ & + [(\rho v_y v_x)_y - (\rho v_y v_x)_{y+\Delta y}] \Delta x \Delta z \\ & + [(\rho v_z v_x)_z - (\rho v_z v_x)_{z+\Delta z}] \Delta x \Delta y \quad (8.2-2) \end{aligned}$$

Momentum flows in and out of the volume element by the mechanisms of convection or bulk flow is given in Eq. (8.2-2) and also by molecular transfer (by virtue of the velocity gradients in laminar flow). The rate at which the  $x$  component of momentum enters the face at  $x$  by molecular transfer is  $(\tau_{xx})_x \Delta y \Delta z$ , and the rate at which it leaves the surface at  $x + \Delta x$  is  $(\tau_{xx})_{x+\Delta x} \Delta y \Delta z$ .

$+\Delta x \Delta y \Delta z$ .  $(\tau_{xx})_x$  is the viscous flux of  $x$ -momentum in the  $x$ -direction. The rate at which it enters the face at  $y$  is  $(\tau_{yx})_y \Delta x \Delta z$ , and it leaves at  $y + \Delta y$  at a rate of  $(\tau_{yx})_{y+\Delta y} \Delta x \Delta z$ . Note that  $\tau_{yx}$  is the viscous flux of  $x$  momentum through the face perpendicular to the  $y$  axis. Writing a similar equation for the remaining faces, the net  $x$  component of momentum by molecular transfer is

$$[(\tau_{xx})_x - (\tau_{xx})_{x+\Delta x}] \Delta y \Delta z + [(\tau_{yx})_y - (\tau_{yx})_{y+\Delta y}] \Delta x \Delta z + [(\tau_{zx})_z - (\tau_{zx})_{z+\Delta z}] \Delta x \Delta y \quad (8.2-3)$$

These molecular fluxes of momentum may be considered as shear stresses and normal stresses. Hence,  $\tau_{yx}$  is the  $x$ -direction shear stress on the  $y$  face and  $\tau_{zx}$  is the shear stress on the  $z$  face. Also,  $\tau_{xx}$  is the normal stress on the  $x$  face.

The net fluid-pressure force acting on the element in the  $x$  direction is the difference between the forces acting at  $x$  and  $x + \Delta x$ :

$$(p_x - p_{x+\Delta x}) \Delta y \Delta z \quad (8.2-4)$$

The gravitational force  $g_x$  acting on a unit mass in the  $x$  direction is multiplied by the mass of the element to give

$$\rho g_x \Delta x \Delta y \Delta z \quad (8.2-5)$$

where  $g_x$  is the  $x$  component of the gravitational vector  $\mathbf{g}$ .

The rate of accumulation of  $x$  momentum in the element is

$$\Delta x \Delta y \Delta z \frac{\partial(\rho v_x)}{\partial t} \quad (8.2-6)$$

Substituting Eqs. (8.2-2)–(8.2-6) into

(8.2-1), dividing by  $\Delta x \Delta y \Delta z$ , and taking the limit as  $\Delta x$ ,  $\Delta y$ , and  $\Delta z$  approach zero, we obtain the  $x$  component of the differential equation of motion:

$$\begin{aligned} \partial(\rho v_x) \partial t = & -[\partial(\rho v_x v_x) \partial x + \partial(\rho v_y v_x) \partial y \\ & + \partial(\rho v_z v_x) \partial z] - (\partial \tau_{xx} \partial x + \partial \tau_{yx} \partial y \\ & + \partial \tau_{zx} \partial z) - \partial p \partial x + \rho g_x \end{aligned} \quad (8.2-7)$$

The  $y$  and  $z$  components of the differential equation of motion are, respectively,

$$\begin{aligned} \partial(\rho v_y) \partial t = & -[\partial(\rho v_x v_y) \partial x + \partial(\rho v_y v_y) \partial y \\ & + \partial(\rho v_z v_y) \partial z] - (\partial \tau_{xy} \partial x + \partial \tau_{yy} \partial y \\ & + \partial \tau_{zy} \partial z) - \partial p \partial y + \rho g_y \end{aligned} \quad (8.2-8)$$

$$\begin{aligned} \partial(\rho v_z) \partial t = & -[\partial(\rho v_x v_z) \partial x + \partial(\rho v_y v_z) \partial y \\ & + \partial(\rho v_z v_z) \partial z] - (\partial \tau_{xz} \partial x + \partial \tau_{yz} \partial y \\ & + \partial \tau_{zz} \partial z) - \partial p \partial z + \rho g_z \end{aligned} \quad (8.2-9)$$

We can use Eq. (8.1-20), which is the

continuity equation, and Eq. (8.2-7) to obtain an equation of motion for the  $x$  component and also do the same for the  $y$  and  $z$  components as follows:

$$\rho(\partial v_x \partial t + v_x \partial v_x \partial x + v_y \partial v_x \partial y + v_z \partial v_x \partial z) = -[\partial \tau_{xx} \partial x + \partial \tau_{yx} \partial y + \partial \tau_{zx} \partial z] + \rho g_x - \partial p \partial x \quad (8.2-10)$$

$$\rho(\partial v_y \partial t + v_x \partial v_y \partial x + v_y \partial v_y \partial y + v_z \partial v_y \partial z) = -[\partial \tau_{xy} \partial x + \partial \tau_{yy} \partial y + \partial \tau_{zy} \partial z] + \rho g_y - \partial p \partial y \quad (8.2-11)$$

$$\rho(\partial v_z \partial t + v_x \partial v_z \partial x + v_y \partial v_z \partial y + v_z \partial v_z \partial z) = -[\partial \tau_{xz} \partial x + \partial \tau_{yz} \partial y + \partial \tau_{zz} \partial z] + \rho g_z - \partial p \partial z \quad (8.2-12)$$

Adding vectorially, we obtain the following *equation of motion* for a pure fluid:

$$\rho D\mathbf{v}/Dt = -(\nabla \cdot \boldsymbol{\tau}) - \nabla p + \rho \mathbf{g} \quad (8.2-13)$$

We should note that Eqs. (8.2-7)–(8.2-13) are valid for any continuous medium.

### **8.2B Equations of Motion for Newtonian Fluids with Varying Density and Viscosity**

In order to use Eqs. (8.2-7)–(8.2-13) to determine velocity distributions, expressions must be used for the various stresses in terms of velocity gradients and fluid properties. For Newtonian fluids, the expressions for the stresses  $\tau_{xx}$ ,  $\tau_{yx}$ ,  $\tau_{zx}$ , and other similar stresses have been related to the velocity gradients and the fluid viscosity  $\mu$  (B2), and are as follows:

*1. Shear-stress components for Newtonian fluids in rectangular coordinates:*



$$\tau_{xx} = -2\mu \partial v_x \partial x + 23\mu (\nabla \cdot \mathbf{v}) \quad (8.2-14)$$

$$\tau_{yy} = -2\mu \partial v_y \partial y + 23\mu (\nabla \cdot \mathbf{v}) \quad (8.2-15)$$

$$\tau_{zz} = -2\mu \partial v_z \partial z + 23\mu (\nabla \cdot \mathbf{v}) \quad (8.2-16)$$

$$\tau_{xy} = \tau_{yx} = -\mu (\partial v_x \partial y + \partial v_y \partial x) \quad (8.2-17)$$

$$\tau_{yz} = \tau_{zy} = -\mu (\partial v_y \partial z + \partial v_z \partial y) \quad (8.2-18)$$

$$\tau_{zx} = \tau_{xz} = -\mu (\partial v_z \partial x + \partial v_x \partial z) \quad (8.2-19)$$

$$(\nabla \cdot \mathbf{v}) = (\partial v_x \partial x + \partial v_y \partial y + \partial v_z \partial z) \quad (8.2-20)$$

*2. Shear-stress components for Newtonian fluids in cylindrical coordinates:*

$$\tau_{rr} = -\mu [2 \partial v_r \partial r - 23(\nabla \cdot \mathbf{v})] \quad (8.2-21)$$

$$\tau_{\theta\theta} = -\mu [2(1r \partial v_\theta \partial \theta + v_{rr}) - 23(\nabla \cdot \mathbf{v})]$$

$$(8.2-22)$$

$$\tau_{zz} = -\mu[2 \frac{\partial v_z}{\partial z} - 2/3(\nabla \cdot \mathbf{v})] \quad (8.2-23)$$

$$\tau_{\theta\theta} = \tau_{\theta r} = -\mu[r \frac{\partial (v_\theta/r)}{\partial r} + 1/r \frac{\partial v_r}{\partial \theta}] \quad (8.2-24)$$

$$\tau_{\theta z} = \tau_{z\theta} = -\mu[\frac{\partial v_\theta}{\partial z} + 1/r \frac{\partial v_z}{\partial \theta}] \quad (8.2-25)$$

$$\tau_{zr} = \tau_{rz} = -\mu[\frac{\partial v_z}{\partial r} + \frac{\partial v_r}{\partial z}] \quad (8.2-26)$$

$$(\nabla \cdot \mathbf{v}) = 1/r \frac{\partial (rv_r)}{\partial r} + 1/r \frac{\partial v_\theta}{\partial \theta} + \frac{\partial v_z}{\partial z} \quad (8.2-27)$$

*3. Shear-stress components for  
Newtonian fluids in spherical  
coordinates:*

$$\tau_{rr} = -\mu[2 \frac{\partial v_r}{\partial r} - 2/3(\nabla \cdot \mathbf{v})] \quad (8.2-28)$$

$$\tau_{\theta\theta} = -\mu[2(1/r \partial v_{\theta} / \partial \theta + v_{rr}) - 2/3(\nabla \cdot \mathbf{v})] \quad (8.2-29)$$

$$\tau_{\phi\phi} = -\mu[2(1/r \sin \theta \partial v_{\phi} / \partial \phi + v_{rr} + v_{\theta} \cot \theta / r) - 2/3(\nabla \cdot \mathbf{v})] \quad (8.2-30)$$

$$\tau_{r\theta} = \tau_{\theta r} = -\mu[r \partial (v_{\theta} / r) / \partial r + 1/r \partial v_r / \partial \theta] \quad (8.2-31)$$

$$\tau_{\theta\phi} = \tau_{\phi\theta} = -\mu[\sin \theta r \partial (v_{\phi} / \sin \theta) / \partial \theta + 1/r \sin \theta \partial v_{\theta} / \partial \phi] \quad (8.2-32)$$

$$\tau_{r\phi} = \tau_{\phi r} = -\mu[1/r \sin \theta \partial v_r / \partial \phi + r \partial (v_{\phi} / r) / \partial r] \quad (8.2-33)$$

$$\begin{aligned} (\nabla \cdot \mathbf{v}) = & 1/r^2 \partial (r^2 v_r) / \partial r \\ & + [1/r \sin \theta \partial (v_{\theta} \sin \theta) / \partial \theta \\ & + 1/r \sin \theta \partial v_{\phi} / \partial \phi] \end{aligned} \quad (8.2-34)$$

*4. Equation of motion for Newtonian fluids with varying density and viscosity.*  
After Eqs. (8.2-14)–(8.2-20) for shear-

stress components are substituted into Eq. (8.2-10) for the  $x$  component of momentum, we obtain the general equation of motion for a Newtonian fluid with varying density and viscosity:

$$\rho \frac{Dv_x}{Dt} = \frac{\partial}{\partial x} [2\mu \frac{\partial v_x}{\partial x} - \frac{2}{3}\mu(\nabla \cdot \mathbf{v})] + \frac{\partial}{\partial y} [\mu(\frac{\partial v_x}{\partial y} + \frac{\partial v_y}{\partial x})] + \frac{\partial}{\partial z} [\mu(\frac{\partial v_x}{\partial z} + \frac{\partial v_z}{\partial x})] - \frac{\partial p}{\partial x} + \rho g_x \quad (8.2-35)$$

Similar equations are obtained for the  $y$  and  $z$  components of momentum.

### **8.2C Equations of Motion for Newtonian Fluids with Constant Density and Viscosity**

The equations given in Section 8.2B are seldom used in their complete forms. When the density  $\rho$  and the viscosity  $\mu$  are constant where  $(\Delta \cdot \mathbf{v}) = 0$ , the equations are simplified and we obtain the equations of motion for Newtonian fluids. These

equations are also called the *Navier–Stokes equations*.

*1. Equation of motion in rectangular coordinates.* For Newtonian fluids for constant  $\rho$  and  $\mu$  for the  $x$  component,  $y$  component, and  $z$  component, we obtain, respectively,

$$\rho(\partial v_x \partial t + v_x \partial v_x \partial x + v_y \partial v_x \partial y + v_z \partial v_x \partial z) = \mu(\partial^2 v_x \partial x^2 + \partial^2 v_x \partial y^2 + \partial^2 v_x \partial z^2) - \partial p \partial x + \rho g_x \quad (8.2-36)$$

$$\rho(\partial v_y \partial t + v_x \partial v_y \partial x + v_y \partial v_y \partial y + v_z \partial v_y \partial z) = \mu(\partial^2 v_y \partial x^2 + \partial^2 v_y \partial y^2 + \partial^2 v_y \partial z^2) - \partial p \partial y + \rho g_y \quad (8.2-37)$$

$$\rho(\partial v_z \partial t + v_x \partial v_z \partial x + v_y \partial v_z \partial y + v_z \partial v_z \partial z) = \mu(\partial^2 v_z \partial x^2 + \partial^2 v_z \partial y^2 + \partial^2 v_z \partial z^2) - \partial p \partial z + \rho g_z \quad (8.2-38)$$

Combining the three equations for the

three components, we obtain

$$\rho D\mathbf{v}/Dt = -\nabla p + \rho \mathbf{g} + \mu \nabla^2 \mathbf{v} \quad (8.2-39)$$

*2. Equation of motion in cylindrical coordinates.* These equations are as follows for Newtonian fluids for constant  $\rho$  and  $\mu$  for the  $r$ ,  $\theta$ , and  $z$  components, respectively:

$$\begin{aligned} \rho(\partial v_r/\partial t + v_r \partial v_r/\partial r + v_\theta r \partial v_r/\partial \theta - v_\theta^2/r \\ + v_z \partial v_r/\partial z) = -\partial p/\partial r \\ + \mu[\partial/\partial r(1/r \partial(rv_r)/\partial r) + 1/r^2 \partial^2 v_r/\partial \theta^2 - 2/r^2 \partial v_\theta/\partial \theta \\ + \partial^2 v_r/\partial z^2] + \rho g_r \quad (8.2-40) \end{aligned}$$

$$\begin{aligned} \rho(\partial v_\theta/\partial t + v_r \partial v_\theta/\partial r + v_\theta r \partial v_\theta/\partial \theta + v_r v_\theta/r \\ + v_z \partial v_\theta/\partial z) = -1/r \partial p/\partial \theta \\ + \mu[\partial/\partial r(1/r \partial(rv_\theta)/\partial r) + 1/r^2 \partial^2 v_\theta/\partial \theta^2 + 2/r^2 \partial v_r/\partial \theta \\ + \partial^2 v_\theta/\partial z^2] + \rho g_\theta \quad (8.2-41) \end{aligned}$$

$$\begin{aligned} \rho(\partial v_z/\partial t + v_r \partial v_z/\partial r + v_\theta r \partial v_z/\partial \theta \\ + v_z \partial v_z/\partial z) = -\partial p/\partial z \end{aligned}$$

$$r \frac{\partial v_z}{\partial r} + \frac{1}{r^2} \left[ \frac{\partial^2 v_z}{\partial \theta^2} + \frac{\partial^2 v_z}{\partial z^2} \right] + \rho g_z \quad (8.2-42)$$

3. *Equation of motion in spherical coordinates.* The equations for Newtonian fluids are given below for constant  $\rho$  and  $\mu$  for the  $r$ ,  $\theta$ , and  $\phi$  components, respectively:

$$\begin{aligned} & \rho \left( \frac{\partial v_r}{\partial t} + v_r \frac{\partial v_r}{\partial r} + v_\theta r \frac{\partial v_r}{\partial \theta} \right. \\ & \left. + v_\phi r \sin \theta \frac{\partial v_r}{\partial \phi} - v_\theta^2 + v_\phi^2 \right) = -\frac{\partial p}{\partial r} \\ & - 2r^2 v_\theta \cot \theta - 2r^2 \sin \theta \frac{\partial v_\phi}{\partial \phi} + \rho g_r \quad (8.2-43) \end{aligned}$$

$$\begin{aligned} & \rho \left( \frac{\partial v_\theta}{\partial t} + v_r \frac{\partial v_\theta}{\partial r} + v_\theta r \frac{\partial v_\theta}{\partial \theta} \right. \\ & \left. + v_\phi r \sin \theta \frac{\partial v_\theta}{\partial \phi} + v_r v_\theta r - \right. \\ & \left. v_\phi^2 \cot \theta \right) = -\frac{1}{r} \frac{\partial p}{\partial \theta} + \mu \left( \nabla^2 v_\theta - \right. \\ & \left. + 2r^2 \frac{\partial v_r}{\partial \theta} - \right. \\ & \left. \sin^2 \theta - 2r^2 \cos \theta \sin^2 \theta \frac{\partial v_\phi}{\partial \phi} \right) + \rho g_\theta \quad (8.2-44) \end{aligned}$$

$$\begin{aligned} & \rho \left( \frac{\partial v_\phi}{\partial t} + v_r \frac{\partial v_\phi}{\partial r} + v_\theta r \frac{\partial v_\phi}{\partial \theta} \right. \\ & \left. + v_\phi r \sin \theta \frac{\partial v_\phi}{\partial \phi} + v_\phi V_{rr} \right. \\ & \left. + v_\theta v_\phi r \cot \theta \right) = -\frac{1}{r \sin \theta} \frac{\partial p}{\partial \phi} \end{aligned}$$

$$\begin{aligned}
& +\mu(\nabla^2 v_\phi - v_\phi/r^2 \sin^2 \theta \\
& + 2r^2 \sin \theta \partial v_r / \partial \phi \\
& + 2 \cos \theta r^2 \sin^2 \theta \partial v_\theta / \partial \phi) + \rho g_\phi \quad (8.2-45)
\end{aligned}$$

where in the three equations above, the Laplacian is given as

$$\begin{aligned}
& + 1/r^2 \sin \theta \partial / \partial \theta (\sin \theta \partial / \partial \theta) + 1/r^2 \sin^2 \theta (\partial^2 / \partial \phi^2) \\
& \quad (8.2-46)
\end{aligned}$$

Significant advantages and uses arise in the transformation from rectangular coordinates to cylindrical coordinates. For example, in Eq. (8.2-40), the term  $\rho v_\theta^2/r$  is the centrifugal force. This gives the force in the  $r$  direction (radial) resulting from the motion of the fluid in the  $\theta$  direction. Note that this term is obtained automatically as a result of the transformation from rectangular to cylindrical coordinates. It does not have



to be added to the equation on physical grounds.

The Coriolis force,  $\rho v_r v_\theta / r$ , also arises automatically in the transformation of coordinates in Eq. (8.2-41). It is the effective force in the  $\theta$  direction when there is flow in both the  $r$  and the  $\theta$  directions, as in the case of flow near a rotating disk.

## **8.3 Use of Differential Equations of Continuity and Motion**

### **8.3A Introduction**

The purpose and uses of the differential equations of motion and continuity, as mentioned previously, are to apply these equations to any viscous-flow problem. For a given specific problem, the terms that are zero or near zero are simply

discarded and the remaining equations are used to solve for the velocity, density, and pressure distributions. Of course, it is necessary to know the initial conditions and the boundary conditions to solve the equations. Several examples will be given to illustrate the general methods used.

We will consider cases for flow in specific geometries that can easily be described mathematically, such as flow between parallel plates and in cylinders.

### **8.3B Differential Equations of Continuity and Motion for Flow Between Parallel Plates**

Two examples will be considered, one for horizontal plates and one for vertical plates.

***EXAMPLE 8.3-1. Laminar Flow Between Horizontal Parallel Plates***

Derive the equation giving the velocity distribution at steady state for laminar flow of a constant-density fluid with constant viscosity flowing between two flat and parallel plates. The velocity profile desired is at a point far from the inlet or outlet of the channel. The two plates will be considered to be fixed and of infinite width, with the flow driven by the pressure gradient in the  $x$  direction.

**Solution:** Assuming that the channel is horizontal, Fig. 8.3-1 shows the axes selected, with flow in the  $x$  direction and the width in the  $z$  direction. Since the flow is only in the  $x$  direction, the velocities  $v_y$  and  $v_z$  are therefore zero. The plates are a distance  $2y_0$  apart.

The continuity equation (8.1-24) for constant density is

$$\partial v_x \partial x + \partial v_y \partial y + \partial v_z \partial z = 0 \quad (8.1-24)$$

Since  $v_y$  and  $v_z$  are zero, Eq (8.1-24) becomes

$$\partial v_x \partial x = 0 \quad (8.3-1)$$

The Navier–Stokes equation for the  $x$  component is

$$\rho(\partial v_x \partial t + v_x \partial v_x \partial x + v_y \partial v_x \partial y + v_z \partial v_x \partial z) = \mu(\partial^2 v_x \partial x^2 + \partial^2 v_x \partial y^2 + \partial^2 v_x \partial z^2) - \partial p \partial x + \rho g_x \quad (8.2-36)$$

This can be simplified using the following:  $\partial v_x / \partial t = 0$  for steady state and  $v_y = 0$ ,  $v_z = 0$ . From the equation of continuity, it can be shown that  $\partial v_x / \partial x = 0$ . We can see that  $\partial^2 v_x / \partial x^2 = 0$ , since there is no change of  $v_x$  with  $x$ . Then,  $\partial^2 v_x / \partial z^2 = 0$ . Making these substitutions into Eq. (8.1-36), we obtain

$$\partial p \partial x - \rho g_x = \mu \partial^2 v_x \partial y^2 \quad (8.3-2)$$

In fluid-flow problems, we will be concerned with gravitational force only in the vertical direction for  $g_x$ , which is  $g$ , the gravitational force. We shall combine the static pressure  $p$  and the gravitational force and call them simply  $p$ , as follows (note that  $g_x = 0$  for the present case of a horizontal pipe but is not zero for the general case of a nonhorizontal pipe):

$$p = p + \rho g h \quad (8.3-3)$$

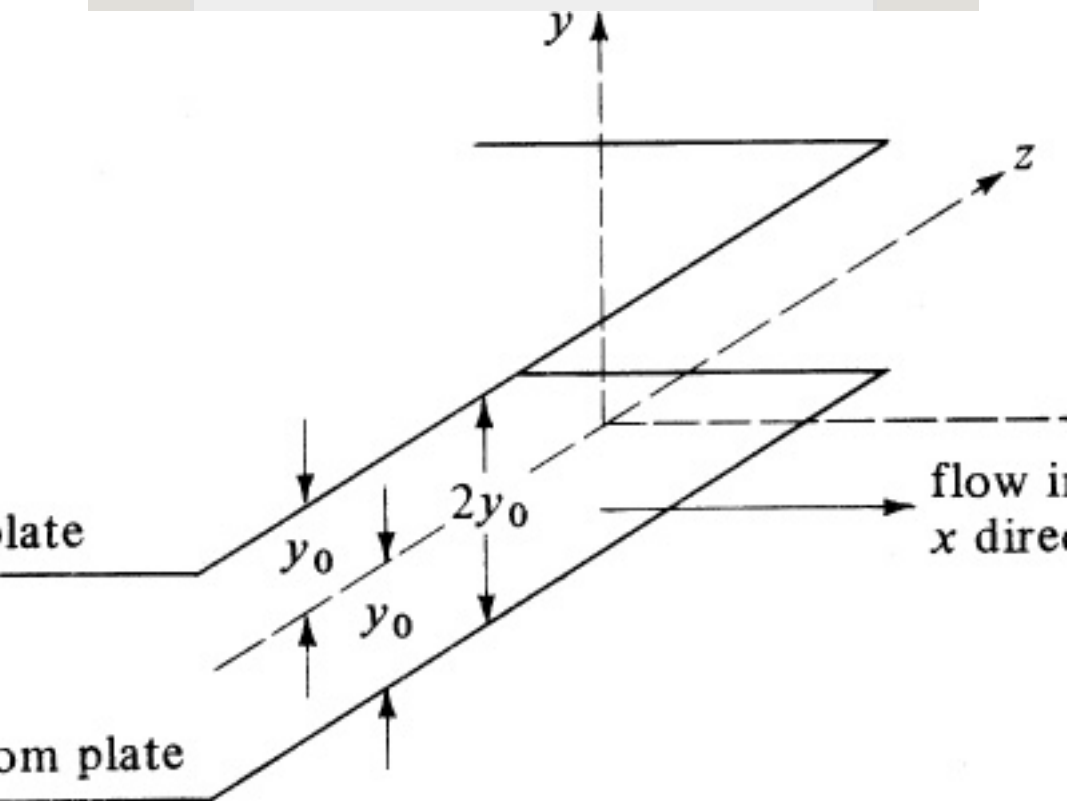


Figure 8.3-1. Flow between two parallel plates in Example 8.3-1.

where  $h$  is the distance upward from any chosen reference plane ( $h$  is in the direction opposed to gravity). Then, Eq. (8.3-2) becomes

$$\frac{\partial p}{\partial x} = \mu \frac{\partial^2 v_x}{\partial y^2} \quad (8.3-4)$$

We can see that  $p$  is not a function of  $z$ . Also, assuming that  $2y_0$  is small,  $p$  is not a function of  $y$ . (Some references avoid this problem and simply use  $p$  as a dynamic pressure, which is rigorously correct since dynamic pressure gradients cause flow. In a fluid at rest, the total pressure gradient is the hydrostatic pressure gradient, and the dynamic pressure gradient is zero.) Also,  $\frac{\partial p}{\partial x}$  is a constant in this problem, since  $v_x$  is not a function of  $x$ . Then, Eq. (8.3-4) becomes an ordinary differential equation:

$$d^2v_x/dy^2 = 1/\mu \quad dp/dx = \text{const} \quad (8.3-5)$$

Integrating Eq. (8.3-5) once, using the condition  $dv_x/dy = 0$  at  $y = 0$  for symmetry,

$$dv_x/dy = (1/\mu \quad dp/dx)y \quad (8.3-6)$$

Integrating again, using  $v_x = 0$  at  $y = y_0$ ,

$$v_x = 12\mu \quad dp/dx \quad (y_0^2 - y^2)/2 \quad (8.3-7)$$

The maximum velocity in Eq. (8.3-7) occurs when  $y = 0$ , giving

$$v_{x \text{ max}} = 12\mu \quad dp/dx \quad (-y_0^2)/2 \quad (8.3-8)$$

Combining Eqs. (8.3-7) and (8.3-8), we obtain the velocity profile in terms of the maximum velocity as

$$v_x = v_{x \text{ max}} [1 - (y/y_0)^2] \quad (8.3-9)$$

Hence, a parabolic velocity profile is obtained. This result was also obtained in Eq. (4.4-9) when using a shell-momentum balance.

The results obtained in Example 8.3-1 could also have been obtained by making a force balance on a differential element of fluid and using the symmetry of the system to omit certain terms.

**EXAMPLE 8.3-2. Laminar Flow Between Vertical Plates with One Plate Moving**

A Newtonian fluid is confined between two parallel and vertical plates as shown in Fig. 8.3-2 (W6). The surface on the left is stationary and the other is moving vertically at a

constant velocity  $v_0$ . Assuming that the flow is laminar, solve for the velocity profile.

**Solution:** The equation to use is the Navier–Stokes equation for the  $y$  coordinate, Eq. (8.2-37):

$$\rho(\partial v_y/\partial t + v_x \partial v_y/\partial x + v_y \partial v_y/\partial y + v_z \partial v_y/\partial z) = \mu(\partial^2 v_y/\partial x^2 + \partial^2 v_y/\partial y^2 + \partial^2 v_y/\partial z^2) - \partial p/\partial y + \rho g_y \quad (8.2-37)$$

At steady-state,  $\partial v_y/\partial t = 0$ . The velocities  $v_x$  and  $v_z = 0$ . Also,  $\partial v_y/\partial y = 0$  from the continuity equation,  $\partial v_y/\partial z = 0$ , and  $\rho g_y = -\rho g$ . The partial derivatives become derivatives and Eq. (8.2-37) becomes

$$\mu d^2 v_y/dx^2 - dp/dy - \rho g = 0 \quad (8.3-10)$$

This is similar to Eq. (8.3-2) in Example 8.3-1. The pressure gradient  $dp/dy$  is constant. Integrating Eq. (8.3-10) once yields

$$dv_y/dx - x\mu(dp/dy + \rho g) = C_1 \quad (8.3-11)$$

Integrating again gives

$$v_y - x^2/2\mu(dp/dy + \rho g) = C_1 x + C_2 \quad (8.3-12)$$

The boundary conditions are at  $x = 0$ ,  $v_y = 0$ , and at  $x = H$ ,  $v_y = v_0$ . Solving for the constants,  $C_1 = v_0/H - (H/2\mu)(dp/dy + \rho g)$  and  $C_2 = 0$ . Hence, Eq. (8.3-12) becomes

$$v_y = -12\mu(dp/dy + \rho g)(Hx - x^2)/H^2 + v_0 x/H \quad (8.3-13)$$

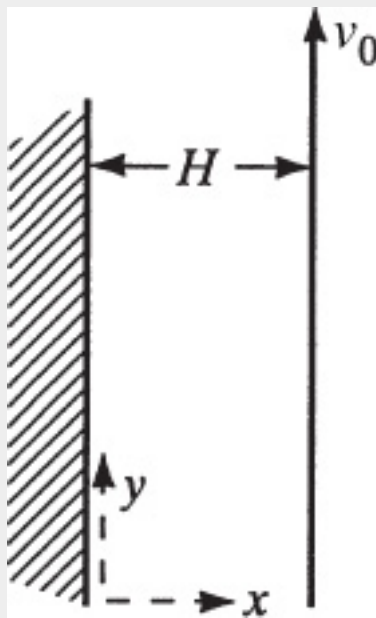


Figure 8.3-2. *Flow between vertical parallel plates in Example 8.3-2.*

### 8.3C Differential Equations of Continuity and Motion for Flow in Stationary and Rotating Cylinders

Several examples will be given for flow in stationary and rotating cylinders.

#### **EXAMPLE 8.3-3. Laminar Flow in a Circular Tube**

Derive the equation for steady-state viscous flow in a horizontal tube of radius  $r_0$ , where the fluid is far from the tube inlet. The fluid is incompressible and  $\mu$  is a constant. The flow is driven in one direction by a constant-pressure gradient.

**Solution:** The fluid will be assumed to flow in the  $z$  direction in the tube, as shown in Fig. 8.3-3. The  $y$  direction is vertical and the  $x$  direction horizontal. Since  $v_x$  and  $v_y$  are zero, the continuity equation becomes  $\partial v_z / \partial z = 0$ . For steady state,  $\partial v_z / \partial t = 0$ . Then, substituting into Eq. (8.2-38) for the  $z$  component, we obtain

$$\frac{dp}{dz} = \mu (\partial^2 v_z / \partial x^2 + \partial^2 v_z / \partial y^2) \quad (8.3-14)$$

To solve Eq. (8.3-14), we can use cylindrical coordinates from Eq. (8.1-26), giving

$$\begin{aligned} z &= z \\ x &= r \cos \theta \\ y &= r \sin \theta \\ r &= \sqrt{x^2 + y^2} \\ \theta &= \tan^{-1} y/x \end{aligned} \quad (8.1-26)$$

Substituting these into Eq. (8.3-14),

$$\frac{1}{\mu} \frac{dp}{dz} = \text{const} = \frac{d^2 v_z}{dr^2} + \frac{1}{r} \frac{dv_z}{dr} + \frac{1}{r^2} \frac{d^2 v_z}{d\theta^2} \quad (8.3-15)$$

The flow is symmetrical about the  $z$  axis, so  $\partial^2 v_z / \partial \theta^2$  is zero in Eq. (8.3-15). As before,  $dp/dz$  is a constant, and Eq. (8.3-15) becomes

$$\frac{1}{\mu} \frac{dp}{dz} = \text{const} = \frac{d^2 v_z}{dr^2} + \frac{1}{r} \frac{dv_z}{dr} = \frac{1}{r} \frac{d}{dr} (r \frac{dv_z}{dr}) \quad (8.3-16)$$



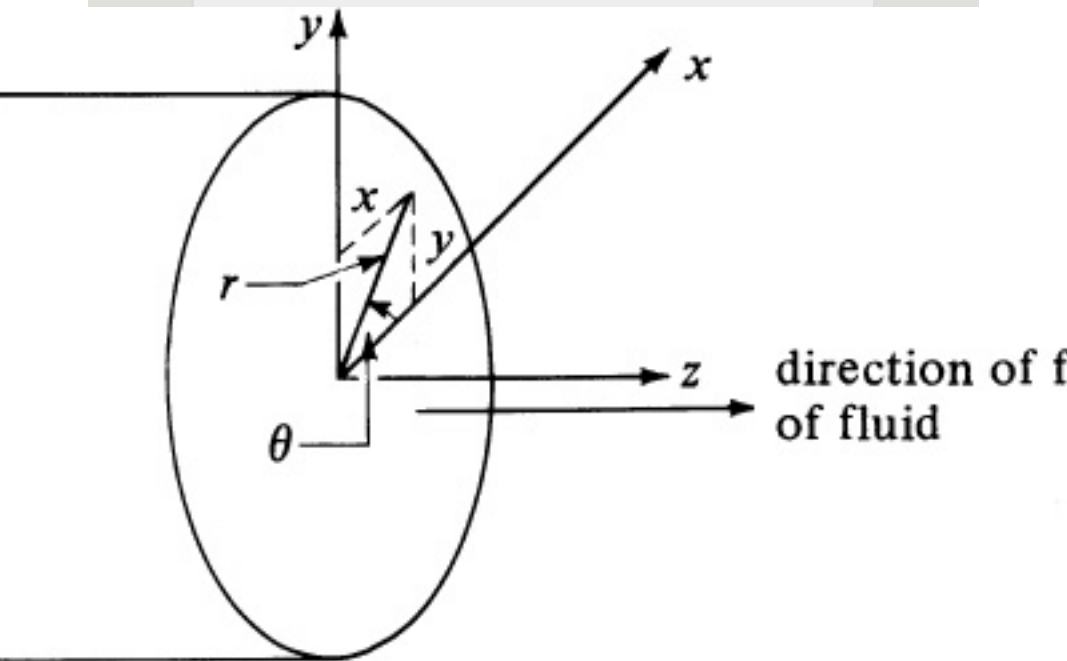


Figure 8.3-3. Horizontal flow in a tube in Example 8.3-3.

Alternatively, Eq. (8.2-42) in cylindrical coordinates can be used for the  $z$  component and the terms that are zero discarded:

$$\rho(\partial v_z / \partial t + v_r \partial v_z / \partial r + v_\theta \partial v_z / \partial \theta + v_z \partial v_z / \partial z) = -\partial p / \partial z + \mu(1/r \partial/\partial r (r \partial v_z / \partial r) + 1/r^2 \partial^2 v_z / \partial \theta^2 + \partial^2 v_z / \partial z^2) + \rho g_z \quad (8.2-42)$$

As before,  $\partial v_z / \partial t = 0$ ,  $\partial v_z^2 / \partial \theta^2 = 0$ ,  $v_r = 0$ ,  $\partial v_z / \partial \theta = 0$ , and  $\partial v_z / \partial z = 0$ . Then, Eq. (8.2-42) becomes identical to Eq. (8.3-16).

The boundary conditions for the first integration are  $dv_z/dr = 0$  at  $r = 0$ . For the second integration,  $v_z = 0$  at  $r = r_0$  (tube radius). The result is

$$v_z = \frac{1}{4\mu} \frac{dp}{dz} (r_0^2 - r^2) \quad (8.3-17)$$

Converting to the maximum velocity as before,

$$v_z = v_{z \max} [1 - (r/r_0)^2] \quad (8.3-18)$$

If Eq. (8.3-17) is integrated over the pipe cross section using Eq. (4.4-10) to give the average velocity  $v_{z \text{ av}}$ ,

$$v_z \, av = -r_0^2 8\mu \, dp/dz \quad (8.3-19)$$

This is found to be 50% of the maximum velocity in the tube. Integrating to obtain the pressure drop from  $z = 0$  for  $p = p_1$  to  $z = L$  for  $p = p_2$ , we obtain

$$p_1 - p_2 = 8\mu v_z \, av \, L \quad r_0^2 = 32\mu v_z \, av \, L \quad (8.3-20)$$

where  $D = 2r_0$ . This is the *Hagen–Poiseuille equation*, derived previously as Eq. (4.4-11).

#### EXAMPLE 8.3-4. Laminar Flow in a Cylindrical Annulus

Derive the equation for steady-state laminar flow inside the annulus between two concentric horizontal pipes. This type of flow occurs often in concentric-pipe heat exchangers.

**Solution:** In this case, Eq. (8.3-16) also still holds. However, the velocity in the annulus will reach a maximum at some radius  $r = r_{\max}$ , which is between  $r_1$  and  $r_2$ , as shown in Fig. 8.3-4. For the first integration of Eq. (8.3-16), the boundary conditions are  $dv_z/dr = 0$  at  $r = r_{\max}$ , which gives

$$r \, dv_z/dr = (1/\mu) dp/dz (r^2 - r_{\max}^2) \quad (8.3-21)$$

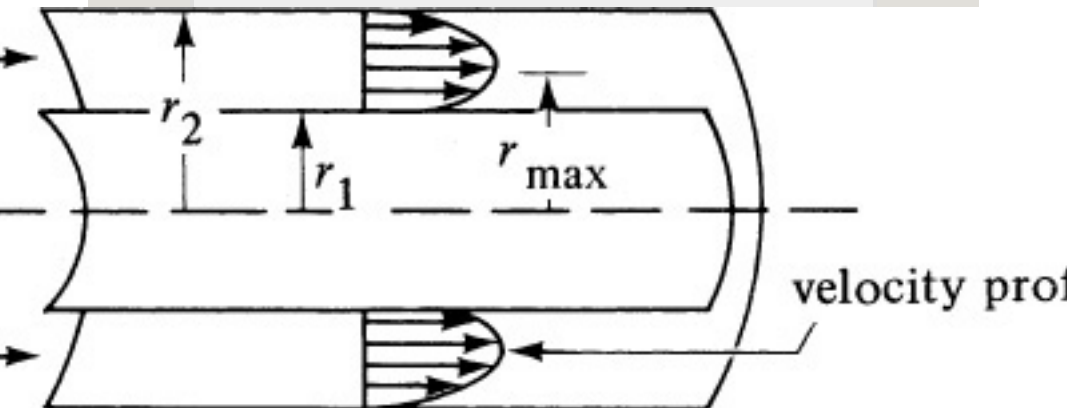


Figure 8.3-4. Flow through a cylindrical annulus.

Also, for the second integration of Eq. (8.3-21),  $v_z = 0$  at the inner wall where  $r = r_1$ , giving

$$v_z = (12\mu \frac{dp}{dz})(r_2^2 - r_1^2 - r_{\max}^2 \ln \frac{r}{r_1}) \quad (8.3-22)$$

Repeating the second integration but for  $v_z = 0$  at the outer wall where  $r = r_2$ , we obtain

$$v_z = (12\mu \frac{dp}{dz})(r_2^2 - r^2 - r_{\max}^2 \ln \frac{r}{r_2}) \quad (8.3-23)$$

Combining Eqs. (8.3-22) and (8.3-23) and solving for  $r_{\max}$ ,

$$r_{\max} = \frac{1}{2} \ln \left( \frac{r_2}{r_1} \right) (r_2^2 - r_1^2) \quad (8.3-24)$$

In Fig. 8.3-4, the velocity profile predicted by Eq. (8.3-23) is plotted. For the case where  $r_1 = 0$ ,  $r_{\max}$  in Eq. (8.3-24) becomes zero and Eq. (8.3-23) reduces to Eq. (8.3-17) for a single circular pipe.

### ***EXAMPLE 8.3-5. Velocity Distribution for Flow Between Coaxial Cylinders***

Tangential laminar flow of a Newtonian fluid with constant density is occurring between two vertical coaxial cylinders in which the outer one is rotating (S4) with an angular velocity of  $\omega$ , as shown in Fig. 8.3-5. It can be assumed that end effects can be neglected. Determine the velocity and the shear-stress distributions for this flow.

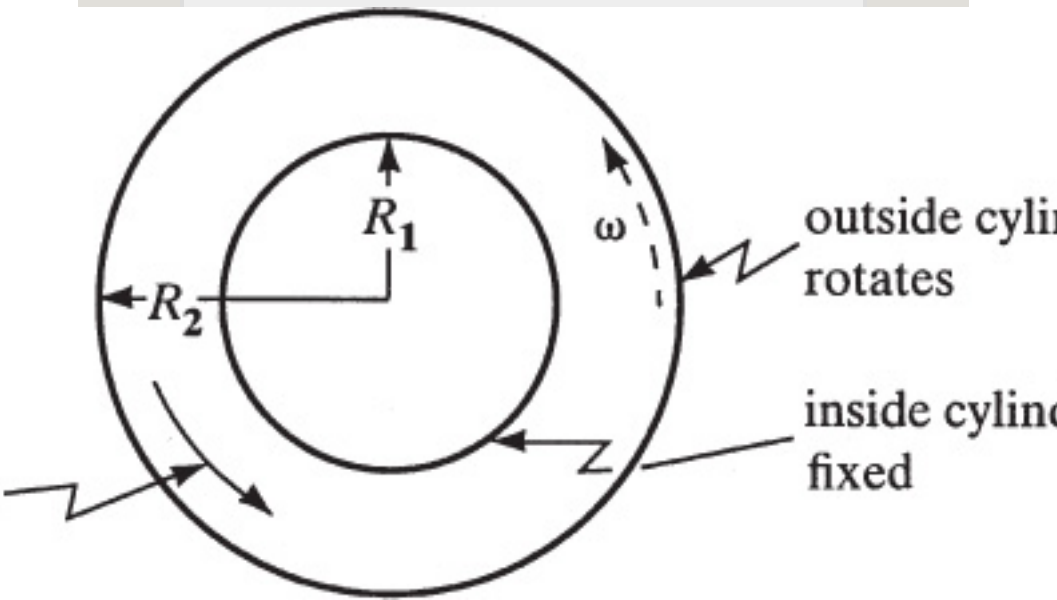


Figure 8.3-5. Laminar flow in the region between two coaxial cylinders in Example 8.3-5.

**Solution:** On physical grounds, the fluid moves in a circular motion; the velocity  $v_r$  in the radial direction is zero and  $v_z$  in the axial direction is zero. Also,  $\partial p / \partial t = 0$  at steady state. There is no pressure gradient in the  $\theta$  direction. The equation of continuity in cylindrical coordinates as derived before is

$$\frac{\partial \rho}{\partial t} + \frac{1}{r} \frac{\partial (\rho r v_r)}{\partial r} + \frac{1}{r} \frac{\partial (\rho v_\theta)}{\partial \theta} + \frac{\partial (\rho v_z)}{\partial z} = 0 \quad (8.1-27)$$

All terms in this equation are zero.

The equations of motion in cylindrical coordinates, Eqs. (8.2-40), (8.2-41), and (8.2-42), reduce to the following, respectively:

$$-\rho v_\theta^2 / r = -\partial p / \partial r \quad (r\text{-component}) \quad (8.3-25)$$

$$0 = \frac{d}{dr} \left( \frac{1}{r} \frac{d(r v_\theta)}{dr} \right) \quad (\theta\text{-component}) \quad (8.3-26)$$

$$0 = -\partial p / \partial z + \rho g_z \quad (z\text{-component}) \quad (8.3-27)$$

Integrating Eq. (8.3-26),

$$v_\theta = C_1 r + C_2 r \quad (8.3-28)$$

To solve for the integration constants  $C_1$  and  $C_2$ , the following boundary conditions are used: at  $r = R_1$ ,  $v_\theta = 0$ ; at  $r = R_2$ ,  $v_\theta = \omega R_2$ . The final equation is

$$v_\theta = \omega (R_2^2 - R_1^2) / (R_2^2 - R_1^2) [R_1 r - r R_1] \quad (8.3-29)$$

Using the shear-stress component for Newtonian fluids in cylindrical coordinates,

$$\tau_{r\theta} = -\mu [r \partial (v_\theta / r) / \partial r + 1/r \partial v_r / \partial \theta] \quad (8.2-31)$$

The last term in Eq. (8.2-31) is zero. Substituting Eq. (8.3-29) into (8.2-31) and differentiating gives

$$\tau_{r\theta} = -2\mu \omega R_2^2 (1/r^2) [R_1^2 / R_2^2 - R_1^2 / R_2^2] \quad (8.3-30)$$

The torque  $T$  that is necessary to rotate the outer cylinder is the product of the force times the lever arm:

$$T = (2\pi R_2 H) (-\tau_{r\theta})|_{r=R_2} = 4\pi \mu H \omega R_2^2 [R_1^2 / R_2^2 - R_1^2 / R_2^2] \quad (8.3-31)$$

where  $H$  is the length of the cylinder. This type of device has been used to measure fluid viscosities from observations of angular velocities and torque, and has also been used as a model for some friction bearings.

### **EXAMPLE 8.3-6. Rotating Liquid in a Cylindrical Container**

A Newtonian fluid of constant density is in a vertical cylinder of radius  $R$  (Fig. 8.3-6) with the cylinder rotating about its axis at angular velocity  $\omega$  (B2). Find the shape of the free surface at steady state.

**Solution:** The system can be described in cylindrical coordinates. As in Example 8.3-5, at steady state,  $v_r = v_z = 0$  and  $g_r = g_\theta = 0$ . The final equations in the cylindrical coordinates given below are the same as Eqs. (8.3-25)–(8.3-27) for Example 8.3-5, except that  $g_z = -g$  in Eq. (8.3-27):

$$\rho v_{\theta} 2r = \partial p \partial r (8.3-32)$$

$$0 = \mu \partial \partial r (1r \partial (rv_{\theta}) \partial r) (8.3-33)$$

$$\partial p \partial z = -\rho g (8.3-34)$$

Integration of Eq. (8.3-33) gives the same equation as in Example 8.3-5:

$$v_{\theta} = C_1 r + C_2 r (8.3-28)$$

The constant  $C_2$  must be zero since  $v_{\theta}$  cannot be infinite at  $r = 0$ . At  $r = R$ , the velocity  $v_{\theta} = R\omega$ . Hence,  $C_1 = \omega$  and we obtain

$$v_{\theta} = \omega r (8.3-35)$$

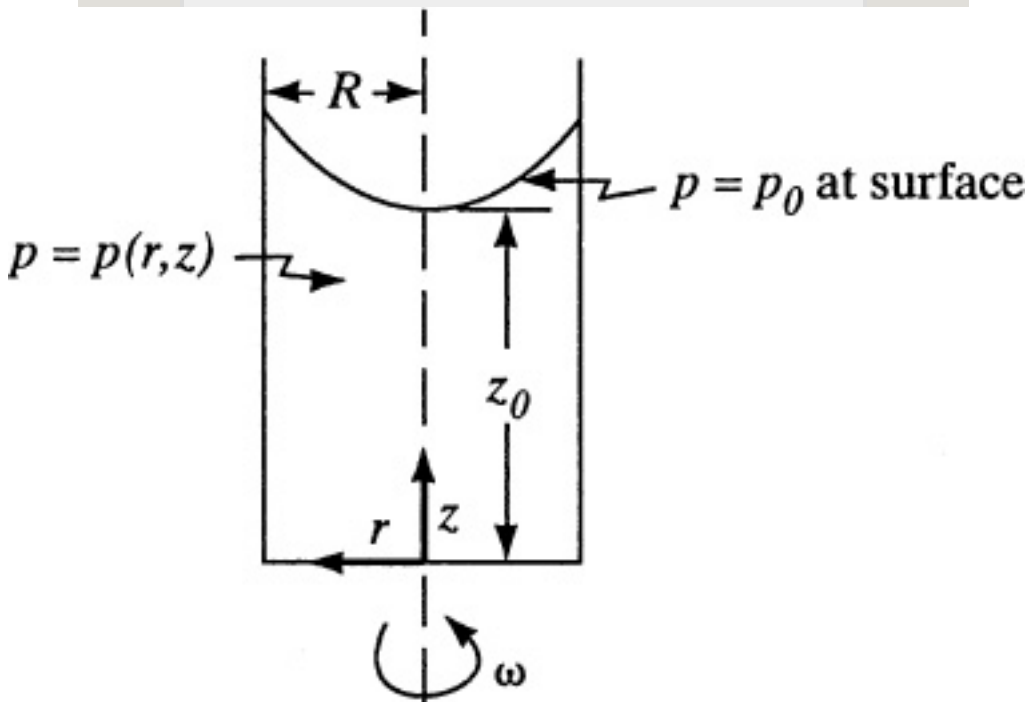


Figure 8.3-6. Liquid being rotated in a container with a free surface in Example 8.3-6.

Combining Eqs. (8.3-35) and (8.3-32),

$$\partial p / \partial r = \rho \omega^2 r \quad (8.3-36)$$

Hence, we see that Eqs. (8.3-36) and (8.3-34) show that pressure depends upon  $r$  because of the centrifugal force and upon  $z$  because of the gravitational force:

$$\partial p / \partial z = -\rho g \quad (8.3-34)$$

Since the term  $p$  is a function of position, we can write the total differential of pressure as

$$dp = \partial p / \partial r dr + \partial p / \partial z dz \quad (8.3-37)$$

Combining Eqs. (8.3-34) and (8.3-36) with (8.3-37) and integrating,

$$p = \rho \omega^2 r^2 / 2 - \rho g z + C \quad (8.3-38)$$

The constant of integration can be determined, since  $p = p_0$  at  $r = 0$  and  $z = z_0$ . The equation becomes

$$p - p_0 = \rho \omega^2 r^2 / 2 + \rho g (z_0 - z) \quad (8.3-39)$$

The free surface consists of all points on this surface at  $p = p_0$ . Hence,

$$z - z_0 = (\omega^2 / 2g) r^2 \quad (8.3-40)$$

This shows that the free surface is in the shape of a parabola.

## 8.4 Chapter Summary

In this chapter, we have described the main types of differential equations commonly found when

solving fluid-dynamics problems. Initially, we reviewed the different types of derivatives commonly found, including the local and substantial derivative. The differences between scalar, vectors, and tensors were described, and we identified important fluid parameters that can be represented as scalar, vector, and tensor quantities.

By considering a fluid element, we performed a mass balance and were able to derive the equation of continuity as

$$\frac{D\rho}{Dt} = -\rho(\partial v_x \partial x + \partial v_y \partial y + \partial v_z \partial z) = -\rho(\nabla \cdot \mathbf{v}) \quad (8.1-23)$$

in Cartesian coordinates, and showed that this reduces to

$$(\nabla \cdot \mathbf{v}) = \partial v_x \partial x + \partial v_y \partial y$$



$$+\partial v_z \partial z = 0 \quad (8.1-24)$$

for a fluid of constant density at steady-state.

Similarly, by considering a fluid element, we performed a momentum balance and were able to derive the equation of motion (or the Navier–Stokes equation) with the general form of

$$\rho D\mathbf{v}/Dt = -(\nabla \cdot \boldsymbol{\tau}) - \nabla p + \rho \mathbf{g} \quad (8.2-13)$$

Multiple forms of this equation were shown in Cartesian, cylindrical, and spherical coordinates systems. The equation was also simplified for cases of constant density and viscosity, and for cases at steady-state.

Finally, we used the equation of motion

and the equation of continuity to solve for velocity profiles for fluid dynamics problems in different geometrical coordinates.

## Problems

**8.1-1. *Equation of Continuity in a Cylinder.*** Fluid having a constant density  $\rho$  is flowing in the  $z$  direction through a circular pipe with axial symmetry. The radial direction is designated by  $r$ .

- Using a cylindrical shell balance with dimensions  $dr$  and  $dz$ , derive the equation of continuity for this system.
- Use the equation of continuity in cylindrical coordinates to derive the equation.

**8.1-2. *Change of Coordinates for Continuity Equation.*** Using the general equation of continuity given in rectangular coordinates, convert it to Eq.

(8.1-27), which is the equation of continuity in cylindrical coordinates. Use the relationships in Eq. (8.1-26) to do this.

**8.2-1. Combining Equations of Continuity and Motion.** Using the continuity equation and the equations of motion for the  $x$ ,  $y$ , and  $z$  components, derive Eq. (8.2-13).

**8.3-1. Average Velocity in a Circular Tube.** Using Eq. (8.3-17) for the velocity in a circular tube as a function of radius  $r$ ,

$$v_z = 14\mu \frac{dp}{dz} (r_0^2 - r^2) \quad (8.3-17)$$

derive Eq. (8.3-19) for the average velocity:

$$v_{z,av} = -\frac{r_0^2}{8\mu} \frac{dp}{dz} \quad (8.3-19)$$

**8.3-2. Laminar Flow in a Cylindrical Annulus.** Derive all the equations given in Example 8.3-4 and show all the steps. Also, derive the equation for the average velocity  $v_{z \text{ av}}$ . Finally, integrate to obtain the pressure drop from  $z = 0$  for  $p = p_0$  to  $z = L$  for  $p = p_L$ .

**Ans.**  $v_{z \text{ av}} = -\frac{1}{8\mu} \frac{dp}{dz} [r_2^2 + r_1^2 - r_2^2 - r_1^2 \ln(r_2/r_1)]$ ,  $v_{z \text{ av}} = \frac{p_0 - p_L}{8\mu L} [r_2^2 + r_1^2 - r_2^2 - r_1^2 \ln(r_2/r_1)]$

**8.3-3. Velocity Profile in Wetted-Wall Tower.** In a vertical wetted-wall tower, the fluid flows down the inside as a thin film  $\delta$  m thick in laminar flow in the vertical  $z$  direction. Derive the equation for the velocity profile  $v_z$ , as a function of  $x$ , the distance from the liquid surface toward the wall. The fluid is at a large distance from the entrance. Also, derive

expressions for  $v_{z \text{ av}}$  and  $v_{\text{max}}$ . (*Hint: At  $x = \delta$ , which is at the wall,  $v_z = 0$ . At  $x = 0$ , the surface of the flowing liquid,  $v_z = v_{z \text{ max}}$ .) Show all steps.*

$$\text{Ans. } v_z = (\rho g \delta^2 / 2\mu)[1 - (x/\delta)^2], \quad v_{z \text{ av}} = \rho g \delta^2 / 3\mu, \quad v_{z \text{ max}} = \rho g \delta^2 / 2\mu$$

### ***8.3-4. Velocity Profile in Falling Film and Differential Momentum Balance.***

A Newtonian liquid is flowing as a falling film on an inclined flat surface. The surface makes an angle  $\beta$  with the vertical. Assume that in this case, the section being considered is sufficiently far from both ends that there are no end effects on the velocity profile. The thickness of the film is  $\delta$ . The apparatus is similar to Fig. 4.4-3 but is not vertical. Do as follows:

- Derive the equation for the velocity profile of  $v_z$  as a

function of  $x$  in this film using the differential momentum-balance equation.

- Determine the maximum velocity and the average velocity.
- Determine an expression for the momentum flux distribution of  $\tau_{xz}$ . [*Hint*: Can Eq. (8.2-19) be used here?]

**Ans.** (a)  $v_z = (\rho g \delta^2 \cos \beta / 2\mu)[1 - (x/\delta)^2]$ ;  
(c)  $\tau_{xz} = \rho g x \cos \beta$

**8.3-5. Velocity Profiles for Flow Between Parallel Plates.** In Example 8.3-2, a fluid is flowing between vertical parallel plates with one plate moving. Do as follows:

- Determine the average velocity and the maximum velocity.
- Make a sketch of the velocity profile for three cases where the surface is moving upward, moving downward, and stationary.

**8.3-6. Conversion of Shear Stresses in**

***Terms of Fluid Motion.*** Starting with the  $x$  component of motion, Eq. (8.2-10), which is in terms of shear stresses, convert it to the equation of motion, Eq. (8.2-36), in terms of velocity gradients for a Newtonian fluid with constant  $\rho$  and  $\mu$ . Note that  $(\nabla \cdot \mathbf{v}) = 0$  in this case. Also, the use of Eqs. (8.2-14)–(8.2-20) should be considered.

### ***8.3-7. Derivation of Equation of Continuity in Cylindrical Coordinates.***

By means of a mass balance over a stationary element whose volume is  $r \Delta r \Delta \theta \Delta z$ , derive the equation of continuity in cylindrical coordinates.

### ***8.3-8. Flow Between Two Rotating Coaxial Cylinders.***

The geometry of two coaxial cylinders is the same as in Example 8.3-5. In this case, however,

both cylinders are rotating, with the inner rotating with an angular velocity of  $\omega_1$  and the outer at  $\omega_2$ . Determine the velocity and the shear-stress distributions using the differential equation of momentum.

**Ans.** 
$$v_\theta = \frac{R_2^2 \omega_2 - R_1^2 \omega_1}{R_2^2 - R_1^2} \left[ r \left( \frac{R_2^2 - R_1^2}{r^2} \right) - R_1^2 R_2^2 \right] - R_1^2 R_2^2 (\omega_2 - \omega_1)$$

### References

### Notation



# Chapter 9. Non-Newtonian Fluids

## 9.0 Chapter Objectives

On completion of this chapter, a student should be able to:

- Distinguish between Newtonian and non-Newtonian fluids
- Identify common types of non-Newtonian fluids
- Distinguish between Bingham plastic fluids, pseudoplastic fluids, dilatant fluids, time-dependent fluids, and viscoelastic fluids
- Determine the type of non-Newtonian fluid from a shear diagram (shear stress vs. shear rate)
- Use the generalized Reynolds number equation to calculate the limits of the laminar flow regime
- Calculate the pressure drop for power-law fluids flowing in laminar flow in a pipe
- Calculate the pressure drop for power-law fluids flowing in turbulent flow by using friction-factor charts

- Determine the flow profile for pseudoplastic and dilatant fluids in laminar flow
- Determine the flow profile for Bingham plastic fluids in laminar flow
- Calculate the pressure drop and volumetric flow of time-independent fluids based on their flow profiles
- Explain the concept of a rotational viscometer and how it is used to determine the flow properties of non-Newtonian fluids
- Calculate the flow properties of non-Newtonian fluids from data obtained with a rotational viscometer
- Explain the concept of apparent viscosity as applied to non-Newtonian fluids
- Calculate the Reynolds number associated with agitating and mixing non-Newtonian fluids
- Calculate the power necessary to agitate and mix non-Newtonian fluids

## **9.1 Non-Newtonian Fluids**

### **9.1A Types of Non-Newtonian Fluids**

As discussed in Section 3.1, Newtonian fluids are those types of fluids that follow Newton's law of

viscosity, Eq. (9.1-1):

$$\tau = -\mu \frac{dv}{dr} \text{ (SI)} \quad \tau = -\mu g_c \frac{dv}{dr} \text{ (English)} \quad (9.1-1)$$

where  $\mu$  is the viscosity and is a constant independent of shear rate. In Fig. 9.1-1, a plot is shown of shear stress  $\tau$  versus shear rate  $-dv/dr$ . The line for a Newtonian fluid is straight, with the slope being  $\mu$ .

If a fluid does not follow Eq. (9.1-1), it is a non-Newtonian fluid. For non-Newtonian fluids, a plot of  $\tau$  versus  $-dv/dr$  is not linear through the origin. Non-Newtonian fluids can be divided into two broad categories on the basis of their shear-stress/shear-rate behavior: those whose shear stress is independent of time or duration of shear (time-

independent), and those whose shear stress is dependent on time or duration of shear (time-dependent). Some non-Newtonian fluids exhibit elastic (rubberlike) behavior, which is also a function of time; they are called *viscoelastic fluids*. These fluids exhibit normal stresses perpendicular to the direction of flow in addition to the usual tangential stresses. Most of the emphasis here will be put on the time-independent class, which includes the majority of non-Newtonian fluids.

### 9.1B Time-Independent Fluids

*1. Bingham plastic fluids.* Bingham plastics are fluids that require a finite shear stress  $\tau_0$  (called the *yield stress*) to initiate flow. If the shear stress applied to the fluid is less than the yield stress, then the fluid won't

flow. However, once the applied stress is greater than the yield stress, it will flow. Often the flow behavior exhibits a Newtonian relationship between the shear stress and shear rate when the fluid is flowing.

However, for some types of Bingham plastics, the plot of  $\tau$  versus  $-dv/dr$  can be curved upward or downward, but this departure from exact Bingham plasticity is often small. Examples of fluids with a yield stress are drilling muds, peat slurries, yogurt, ketchup, chocolate mixtures, greases, shampoo, grain–water suspensions, toothpaste, paper pulp, and sewage sludge.

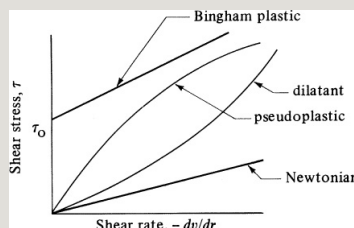


Figure 9.1-1. *Shear diagram for Newtonian and time-independent non-Newtonian fluids.*

2. *Pseudoplastic fluids.* The majority of non-Newtonian fluids are in this category and are also known as shear-thinning fluids. Examples of these fluids include polymer solutions or melts, greases, mayonnaise, biological fluids, detergent slurries, dispersion media in certain pharmaceuticals, and paints. The shape of the flow curve is shown in Fig. 9.1-1, and it generally can be represented by a power-law equation (sometimes called the *Ostwald–de Waele equation*):

$$\tau = K(-dv/dr)^n \quad (n < 1) \quad (9.1-2)$$

where  $K$  is the consistency index in  $\text{N} \cdot \text{s}/\text{m}^2$  or  $\text{lbf} \cdot \text{s}/\text{ft}^2$ , and  $n$  is the flow behavior index, dimensionless. The

apparent viscosity  $\mu_a$  in Eq. (9.1-3) is obtained from Eqs. (9.1-1) and (9.1-2) and decreases with increasing shear rate:

$$\mu_a = K(-dv/dr)^{n-1} \quad (9.1-3)$$

*3. Dilatant fluids.* These fluids are far less common than pseudoplastic fluids, and their flow behavior (Fig. 9.1-1) shows an increase in apparent viscosity with increasing shear rate. The power-law equation (9.1-2) is often applicable, but with  $n > 1$ :

$$\tau = K(-dv/dr)^n \quad (n > 1) \quad (9.1-4)$$

For a Newtonian fluid,  $n = 1$ . Solutions showing dilatancy are some corn flour–sugar solutions, wet beach sand, cornstarch in water, potassium silicate in water, and some solutions containing high concentrations of powder in water.

## 9.1C Time-Dependent Fluids

1. *Thixotropic fluids*. These fluids exhibit a reversible decrease in shear stress with time at a constant rate of shear. This shear stress approaches a limiting value that depends on the shear rate. Examples include some polymer solutions, shortening, some food materials, and paints. At present, the theory for time-dependent fluids is still not completely developed.

2. *Rheopectic fluids*. These fluids are quite rare in occurrence and exhibit a reversible increase in shear stress with time at a constant rate of shear. Examples are bentonite clay suspensions, certain sols, and gypsum suspensions. In design procedures for thixotropic and rheopectic fluids for



steady flow in pipes, the limiting flow-property values at a constant rate of shear are sometimes used (S2, W3).

### **9.1D Viscoelastic Fluids**

Viscoelastic fluids exhibit elastic recovery from the deformations that occur during flow. They show both viscous and elastic properties. Part of the deformation is recovered upon removal of the stress. Examples are flour dough, napalm, polymer melts, bitumens, and Silly Putty.

### **9.1E Laminar Flow of Time-Independent Non-Newtonian Fluids**

*1. Flow properties of a fluid.* In determining the flow properties of a time-independent non-Newtonian fluid, a capillary-tube viscometer is often used. The pressure drop  $\Delta P$  N/m<sup>2</sup> for a given flow rate  $q$  m<sup>3</sup>/s is

measured in a straight tube of length  $L$  m and diameter  $D$  m. This is repeated for different flow rates or average velocities  $\bar{v}$  m/s. If the fluid is time-independent, these flow data can be used to predict the flow in any other pipe size.

A plot of  $D\Delta p/4L$ , which is equal to  $\tau_w$ , the shear stress at the wall in N/m<sup>2</sup>, versus  $8\bar{v}/D$  which is proportional to the shear rate at the wall, is shown in Fig. 9.1-2 for a power-law fluid following Eq. (9.1-5):

$$\tau_w = D\Delta p/4L = K'(8\bar{v}/D)^{n'} \quad (9.1-5)$$

where  $n'$  is the slope of the line when the data are plotted on logarithmic coordinates and  $K'$  has units of  $\text{N} \cdot \text{s}_n$

$\text{Pa}\cdot\text{s}/\text{m}^2$ .

For  $n' = 1$ , the fluid is Newtonian; for  $n' < 1$ , pseudoplastic, or Bingham plastic if the curve does not go through the origin; and for  $n' > 1$ , dilatant. The  $K'$ , the consistency index in Eq. (9.1-5), is the value of  $D\Delta p/4L$  for  $8v_w/D = 1$ . The shear rate at the wall,  $(-dv/dr)_w$ , is

$$(-dv/dr)_w = (3n' + 1) \left( \frac{8v_w}{D} \right)^{1/n'} \quad (9.1-6)$$

Also,  $K' = \mu$  for Newtonian fluids.

Equation (9.1-5) is simply another statement of the power-law model of Eq. (9.1-2) applied to flow in circular tubes, and is more convenient to use for pipe-flow situations (D2). Hence, Eq. (9.1-5)

defines the flow characteristics just as completely as Eq. (9.1-2). It has been found experimentally (M3) that for most fluids,  $K'$  and  $n'$  are constant over wide ranges of  $8\bar{V}/D$  or  $D\Delta p/4L$ . However, for some fluids this is not the case, and  $K'$  and  $n'$  can vary. For those cases, the particular values of  $K'$  and  $n'$  used must be valid for the actual  $8\bar{v}/D$  or  $D\Delta p/4L$  with which one is dealing in a design problem. This method using flow in a pipe or tube is often used to determine the flow properties of a non-Newtonian fluid.

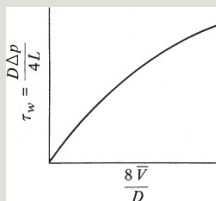


Figure 9.1-2. General flow curve for a power-law fluid in laminar flow in a tube.

In many cases, the flow properties of a fluid are determined using a rotational viscometer. The flow properties  $K$  and  $n$  in Eq. (9.1-2) are determined in this manner. A discussion of the rotational viscometer is given in Section 9.4.

When the flow properties are constant over a range of shear stresses that occurs for many fluids, the following equations hold (M3):

$$n' = n \quad (9.1-7)$$

$$K' = K(3n' + 14n')n' \quad (9.1-8)$$

Often, a generalized viscosity coefficient  $\gamma$  is defined as

$$\gamma = K' 8n'^{-1} \text{ (SI)} \quad \gamma = \frac{K'}{8n'} \text{ (English)} \quad (9.1-9)$$

where  $\gamma$  has units of  $\text{N} \cdot \text{s}_n'/\text{m}^2$  or  $\text{lb}_m/\text{ft} \cdot \text{s}_{2-n}'$ .

Typical flow-property constants (rheological constants) for some fluids are given in Table 9.1-1. Some data give  $\gamma$  values instead of  $K'$  values, but Eq. (9.1-9) can be used to convert these values if necessary. In some cases in the literature,  $K$  or  $K'$  values are given as  $\text{dyn} \cdot \text{s}_n'/\text{cm}^2$  or  $\text{lbf} \cdot \text{s}_n'/\text{ft}^2$ . From Appendix A.1, the conversion factors are

$$\begin{aligned} 1 \text{ lbf} \cdot \text{s}_n'/\text{ft}^2 &= 47.880 \text{ N} \cdot \text{s}_n'/ \\ &\quad \text{m}^2 \\ 1 \text{ dyn} \cdot \text{s}_n'/\text{cm}^2 &= 2.0886 \times 10^{-3} \text{ lbf} \cdot \text{s}_n'/\text{ft}^2 \end{aligned}$$

Table 9.1-1. *Flow-Property Constants for Non-Newtonian Fluids*

--

## 2. Equations for flow in a tube. In

order to predict the frictional pressure drop  $\Delta p$  in laminar flow in a tube of radius  $R_0$  and diameter  $D$ , Eq. (9.1-5) is solved for  $\Delta p = (p_0 - p_L)$ :

$$\Delta p = K' 4LD (8VD)^{n'} \quad (9.1-10)$$

If the average velocity is desired, Eq. (9.1-5) can be rearranged to give

$$V = D 8(\Delta p / K' 4L)^{1/n'} \quad (9.1-11)$$

If the equations are desired in terms of  $K$  instead of  $K'$ , Eqs. (9.1-7) and (9.1-8) can be substituted into (9.1-10) and (9.1-11). Substituting Eqs. (9.1-7) and (9.1-8) into Eq. (9.1-11) and noting that  $V = v_{x \text{ av}}$ ,

$$V = v_{x \text{ av}} = \frac{(n+1)(p_0 - p_L)^{1/n}}{2K L R_0^{(n+1)/n}} \quad (9.1-12)$$

However, to use this equation, the flow must be laminar. The generalized Reynolds number, which can be used to predict when the non-Newtonian flow becomes turbulent, has been defined as

$$N_{Re,gen} = \frac{D^n V^{2-n} \rho g}{K' 8^{n-1}} = \frac{D^n V^{2-n} \rho g}{K' 8^{n-1} (3n + 14n)^n (SI)} \quad (9.1-13)$$

### 3. *Friction-factor method.*

Alternatively, the pressure drop in Laminar flow can be predicted using the Fanning friction-factor method given in Eqs. (5.1-5)–(5.1-7) for Newtonian fluids, but using the generalized Reynolds numbers:

$$f = 16 N_{Re,gen} \quad (9.1-14)$$

$$\Delta p = 4 f_{LD} \frac{V^2}{g_c} \quad (SI) \quad \Delta p = 4 f_{LD} \frac{V^2}{g_c} \quad (English)$$



**EXAMPLE 9.1-1. Pressure Drop of Power-Law Fluid in Laminar Flow**

A power-law fluid having a density of  $1041 \text{ kg/m}^3$  is flowing through  $14.9 \text{ m}$  of a tubing with an inside diameter of  $0.0524 \text{ m}$  at an average velocity of  $0.0728 \text{ m/s}$ . The rheological or flow properties of the fluid are  $K' = 15.23 \text{ N} \cdot \text{s}/\text{m}^2$  ( $0.318 \text{ lbf} \cdot \text{s}/\text{ft}^2$ ) and  $n' = 0.40$ .

- Calculate the pressure drop and friction loss using Eq. (9.1-10) for laminar flow. Check the generalized Reynolds number to make sure that the flow is laminar.
- Repeat part (a) but use the friction-factor method.

**Solution:** The known data are as follows:  $K' = 15.23$ ,  $n' = 0.40$ ,  $D = 0.0524 \text{ m}$ ,  $V = 0.0728 \text{ m/s}$ ,  $L = 14.9 \text{ m}$ , and  $\rho = 1041 \text{ kg/m}^3$ . For part (a), using Eq. (9.1-10),

$$\Delta p = K' 4LD (8VD)^{n'} = 15.23(4)(14.9)(0.0524)(8 \times 0.0728 \times 0.0524)^{0.4} = 45,390 \text{ N/m}^2$$

Also, to calculate the friction loss,

$$F_f = \Delta p p = 45,390/1041 = 43.60 \text{ J/kg}$$

Using Eq. (9.1-13),

$$\text{NRe}_{\text{gen}} = Dn'V^2 - n'pK'gn^{-1} = (0.0524)(0.40)(0.0728)^{1.60} / (1041)(15.23)(8)^{-0.6} = 1.106$$

Hence, the flow is laminar.

For part (b), using Eq. (9.1-14)

$$f = 16\text{NRe}_{\text{gen}} = 16(1.106) = 14.44$$

Substituting into Eq. (9.1-15),

$$\Delta p = 4fp LD V^2 = 4(14.44)$$

## 9.2 Friction Losses for Non-Newtonian Fluids

### 9.2A Friction Losses in Contractions, Expansions, and Fittings in Laminar Flow

Since non-Newtonian power-law fluids flowing in conduits are often in laminar flow because of their usually high effective viscosity, losses in sudden changes of velocity and fittings are important in laminar flow.

*1. Kinetic energy in laminar flow.* In application of the total mechanical-energy balance in Eq. (4.2-28), the average kinetic energy per unit mass of fluid is needed. For fluids, this is (S2)

$$\text{average kinetic energy/} \\ \text{kg} = V^2 \alpha (9.2-1)$$

For Newtonian fluids,  $\alpha = 12$  for laminar flow. For power-law non-Newtonian fluids,

$$\alpha = (2n+1)(5n+3)3(3n+1)2(9.2-2)$$

For example, if  $n = 0.50$ ,  $\alpha = 0.585$ . If  $n = 1.00$ ,  $\alpha = 12$ . For turbulent flow for Newtonian and non-Newtonian fluids,  $\alpha = 1.0$  (D1).

## *2. Losses in contractions and fittings.*

Skelland (S2) and Dodge and Metzner (D2) state that when a fluid leaves a tank and flows through a sudden contraction to a pipe of diameter  $D_2$  or flows from a pipe of diameter  $D_1$  through a sudden contraction to a pipe of  $D_2$ , a vena contracta is usually formed downstream from the contraction. General indications are that the frictional

pressure losses for pseudoplastic and Bingham plastic fluids are very similar to those for Newtonian fluids at the same generalized Reynolds numbers in laminar and turbulent flow for contractions as well as for fittings and valves.

For contraction losses, Eq. (5.1-16) can be used, where  $\alpha = 1.0$  for turbulent flow; and for laminar flow, Eq. (9.2-2) can be used to determine  $\alpha$  since  $n$  is not 1.00.

For fittings and valves, friction losses should be determined using Eq. (5.1-17) and the values from Table 5.1-1.

*3. Losses in sudden expansion.* For the friction loss for a non-Newtonian fluid in laminar flow through a sudden

expansion from  $D_1$  to  $D_2$  diameter,  
Skelland (S2) gives

$$h_{ex} = \frac{3n+1}{2n+1} V^{1/2} \left[ n+3 \frac{D_1^2}{D_2^2} - \frac{(D_1 D_2)^2}{4} + 3(3n+1)^2 \frac{D_1^2}{D_2^2} + 3 \right]^{1/2} \quad (9.2-3)$$

where  $h_{ex}$  is the friction loss in J/kg. In English units, Eq. (9.2-3) is divided by  $g_c$  and  $h_{ex}$  is in ft · lbf/lbm.

Equation (5.1-15) for laminar flow with  $\alpha = 12$  for a Newtonian fluid gives values reasonably close to those of Eq. (9.2-3) for  $n = 1$  (Newtonian fluid). For turbulent flow, the friction loss can be approximated by Eq. (5.1-15), with  $\alpha = 1.0$  for non-Newtonian fluids (S2).

### 9.2B Turbulent Flow and Generalized Friction Factors

In turbulent flow of time-

independent fluids the Reynolds number at which turbulent flow occurs varies with the flow properties of the non-Newtonian fluid. In a comprehensive study, Dodge and Metzner (D2) derived a theoretical equation for turbulent flow of non-Newtonian fluids through smooth, round tubes. The final equation is plotted in Fig. 9.2-1, where the Fanning friction factor is plotted versus the generalized Reynolds number,  $N_{Re,gen}$ , given in Eq. (9.1-13). Power-law fluids with flow-behavior indexes  $n'$  between 0.36 and 1.0 were experimentally studied at Reynolds numbers up to  $3.5 \times 10^4$  and the derivation was confirmed.

The curves for different  $n'$  values break

off from the laminar line at different Reynolds numbers to enter the transition region. For  $n' = 1.0$  (Newtonian), the transition region starts at  $N_{Re,gen} = 2100$ . Since many non-Newtonian power-law fluids have high effective viscosities, they are often in laminar flow. The correlation for a smooth tube also holds for a rough pipe in laminar flow.

For rough commercial pipes with various values of roughness  $\epsilon/D$ , Fig. 9.2-1 cannot be used for turbulent flow, since it is derived for smooth tubes. The functional dependence of the roughness values  $\epsilon/D$  on  $n'$  requires experimental data, which are not yet available.

Metzner and Reed (M3, S3) recommend the use of the existing relationship, Fig. 5.1-3, for Newtonian fluids in rough tubes using the generalized Reynolds

number  $N_{\text{Re, gen}}$ . This is somewhat conservative, since preliminary data indicate that friction factors for pseudoplastic fluids may be slightly smaller than for Newtonian fluids. This is also consistent with Fig. 9.2-1 for smooth tubes, which indicates lower  $f$  values for fluids with  $n'$  below 1.0 (S2).

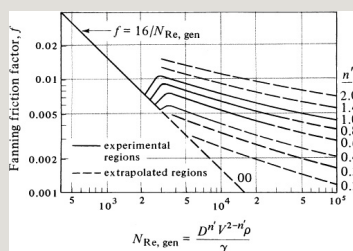


Figure 9.2-1. Fanning friction factor versus generalized Reynolds number for time-independent non-Newtonian and Newtonian fluids flowing in smooth tubes.

#### EXAMPLE 9.2-1. Turbulent Flow of a Power-Law Fluid

A pseudoplastic fluid that follows the power law, having a density of  $961 \text{ kg/m}^3$ , is flowing through a smooth, circular tube having an inside diameter of  $0.0508 \text{ m}$  at an average velocity of  $6.10 \text{ m/s}$ . The flow properties of the fluid are  $n' = 0.30$  and  $K' = 2.744 \text{ N} \cdot \text{s}/\text{m}^2$ . Calculate the frictional pressure drop for a tubing  $30.5 \text{ m}$  long.



**Solution:** The data are as follows:  $K' = 2.744$ ,  $n' = 0.30$ ,  $D = 0.0508$  m,  $V = 6.10$  m/s,  $\rho = 961$  kg/m<sup>3</sup>, and  $L = 30.5$  m. Using the general Reynolds-number Eq. (9.1-13),

$$N_{Re,gen} = D n' V^2 - n' \rho K' 8 n' \\ f' = (0.0508)^{0.3} (6.10)^{17} (961)^{2.744} (8 - 0.7) = 1.328 \times 10^4$$

Hence, the flow is turbulent. Using Fig. 9.2-1 for  $N_{Re,gen} = 1.328 \times 10^4$  and  $n' = 0.30$ ,  $f = 0.032$ .

Substituting into Eq. (9.1-15),

$$\Delta p = 4 f \rho L D V^2 = 4(0.032)(961)(30.5)(0.0508) \\ (6.10)^2 = 137.4 \text{ kN/m}^2 \quad (2870 \text{ lbf/ft}^2)$$

## 9.3 Velocity Profiles for Non-Newtonian Fluids

### 1. Pseudoplastic and dilatant fluids.

For pipe flow, Eq. (9.1-2) can be written as

$$\tau_{rx} = K(-dv_x/dr)^n \quad (9.3-1)$$

Equation (4.4-6) holds for all fluids:

$$\tau_{rx} = (p_0 - p_L) r / 2L \quad (4.4-6)$$

which relates  $\tau_{rx}$  with the radial distance  $r$  from the center. Equating the above

two equations and integrating between  $r = 0$  and  $r = R_0$  where  $v_x = 0$ ,

$$v_x = \frac{n}{n+1} (p_0 - p_L)^{1/n} \frac{R_0^{n+1}}{n} \left[ 1 - \left( \frac{r}{R_0} \right)^{n+1} \right] \quad (9.3-2)$$

At  $r = 0$ ,  $v_x = v_{x \max}$  and Eq. (9.3-2) becomes

$$v_x = v_{x \max} \left[ 1 - \left( \frac{r}{R_0} \right)^{n+1} \right] \quad (9.3-3)$$

The average velocity  $v_{x \text{ av}}$  is given by Eq. (9.1-12):

$$v_{x \text{ av}} = \frac{1}{R_0} \int_0^{R_0} v_x r \, dr = \frac{1}{R_0} \int_0^{R_0} \frac{n}{n+1} (p_0 - p_L)^{1/n} \frac{R_0^{n+1}}{n} \left[ 1 - \left( \frac{r}{R_0} \right)^{n+1} \right] r \, dr \quad (9.1-12)$$

Dividing Eq. (9.3-2) by (9.1-12),

$$\frac{v_x}{v_{x \text{ av}}} = \frac{3n+1}{n+1} \left[ 1 - \left( \frac{r}{R_0} \right)^{n+1} \right] \quad (9.3-4)$$

Using Eq. (9.3-4), the velocity profile can be calculated for laminar flow of a Newtonian fluid for  $n = 1$  to show the parabolic profile in Fig. 9.3-1. The velocity profiles for pseudoplastic fluids ( $n < 1$ ) show a flatter profile compared to the velocity profile for a Newtonian fluid. For extreme pseudoplastic behavior for  $n = 0$ , plug flow is obtained across the entire pipe. For dilatant behavior ( $n > 1$ ), the velocity profile is more pointed and narrower. For extreme dilatant fluids ( $n = \infty$ ), the velocity profile is a linear function of the radius.

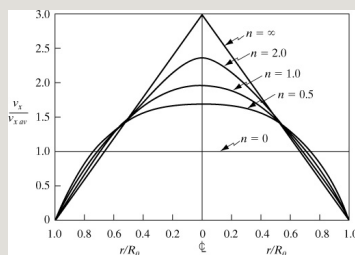


Figure 9.3-1. Dimensionless velocity profile  $v_x/v_{x,av}$  for power-law non-Newtonian fluids.

2. *Bingham plastic fluids*. For Bingham plastic fluids, a finite yield stress  $\tau_0$  in N/m<sup>2</sup> is needed to initiate flow, as given in Eq. (9.3-5):

$$\tau_{rx} = \tau_0 + \mu(-dv_x/dr) \quad (9.3-5)$$

The velocity profile for this fluid is more complex than that for non-Newtonian fluids. This velocity profile for Bingham plastic fluids is shown in Fig. 9.3-2.

Note the plug-flow region  $r = 0$  to  $r = r_0$ . In this region,  $dv_x/dr = 0$  because the momentum flux or shear stress  $\tau_{rx}$  is less than the yield value  $\tau_0$ .

In Table 9.3-1, some typical values for the rheological constants for Bingham plastic fluids are given.

To derive the equation for pipe flow, note that Eq. (4.4-6) holds for all fluids:

$$\tau_{rx}=(p_0-p_L)r^2/2L \quad (4.4-6)$$

Substituting Eq. (4.4-6) into (9.3-5),

$$(p_0-p_L)r^2/2L=\tau_0+\mu(-dv_x/dr) \quad (9.3-6)$$

Rearranging and integrating, where  $v_x = v_x$  at  $r = r$  and  $v_x = 0$  at  $r = R$ ,

$$v_x=(p_0-p_L/4\mu L)R^2[1-(r/R)^2]-\tau_0\mu R[1-r/R] \quad (9.3-7)$$

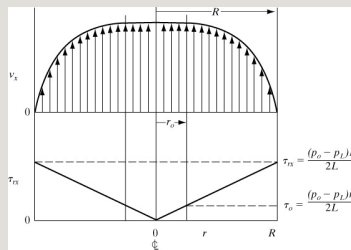


Figure 9.3-2. Velocity profile and shear diagram for flow of a Bingham plastic fluid in a pipe.

## Table 9.3-1. Rheological Constants for Bingham Plastic Fluids

The equation holds for the region where  $r > r_0$  and up to  $r = R$ . For the plug-flow region,  $r \leq r_0$ ,  $dv_x/dr = 0$ . In this region, using Eq. (4.4-6) and setting  $\tau_a = \tau_0$  at  $r_0$ ,

$$\tau_0 = (p_0 - p_L) r_0^2 / 2L \quad (9.3-8)$$

Substituting Eq. (9.3-8) into (9.3-7) for  $r = r_0$ , where plug flow occurs,

$$v_x = (p_0 - p_L) R^2 / 4\mu L [1 - (r_0/R)^2] \quad (9.3-9)$$

To obtain the flow rate  $Q$  in  $m^3/s$ , the following integral must be evaluated:

$$Q = 2\pi \int_{r_0}^R r v_x dr + 2\pi \int_0^{r_0} r v_x dr \quad (9.3-10)$$

Substituting Eq. (9.3-9) into the first part of Eq. (9.3-10) and (9.3-7) into the last part and integrating,

$$Q = \pi(p_0 - p_L)R^4 / 8\mu L [1 - 4.35 \tau_0 \tau_R + 13 (\tau_0 \tau_R)^4] \quad (9.3-11)$$

where  $\tau_R = (p_0 - p_L)R/2L$ , the momentum flux at the wall. This is known as the Buckingham–Reiner equation.

When  $\tau_0$  is zero, Eq. (9.3-11) reduces to the Hagen–Poiseuille equation, (4.4-11), for Newtonian fluids.

**EXAMPLE 9.3-1. Flow Rate of a Bingham Plastic Fluid**

A printing-pigment solution with properties similar to those in Table 9.3-1 is flowing in a 1.0-cm-diameter pipe that is 10.2 m long. A pressure driving force of 4.35 kN/m<sup>2</sup> is being used. Calculate the flow rate  $Q$  in m<sup>3</sup>/s.

**Solution:** From Table 9.3-1,  $\tau_0 = 0.4$  N/m<sup>2</sup> and  $\mu = 0.25$  Pa · s. Also,  $(p_0 - p) = 4.35$  kN/m<sup>2</sup> = 4350 N/m<sup>2</sup>,  $L = 10.2$  m, and  $R = 1.0/2$  cm = 0.005 m. Substituting into Eq. (9.3-8),

$$\tau_0 = 0.4 \text{ N/m}^2 = (p_0 - p_L)r/2L = (4350)r/2(10.2)$$

Solving,

$$r = 0.400(2)(10.2)/4350 = 0.001876 \text{ m} = 0.1876 \text{ cm}$$

Substituting into the following for  $\tau_R$ ,

$$\tau_R = (p_0 - p_L)R^2/L = (4350)(0.005)^2/(10.2) = 1.066 \text{ N/m}^2$$

Finally, substituting into Eq. (9.3-11),

$$Q = \pi(4350)(0.005)48(0.25)(10.2)$$

$$[1 - 430.41.066 + 13(0.41.066)4]Q = 2.120 \times 10^{-7} \text{ m}^3/$$

$$\text{svx av} = Q\pi R^2 = 2.120 \times 10^{-7} \pi (0.005)^2 = 2.700 \times 10^{-3} \text{ m/s}$$

## 9.4 Determination of flow Properties of Non-Newtonian Fluids Using a Rotational Viscometer

The flow-property or rheological constants of non-Newtonian fluids can be measured using pipe flow, as discussed in Section 9.1E. Another, more important method for measuring flow properties is by using a rotating concentric-cylinder viscometer, first described by Couette in 1890. In this device, a concentric rotating cylinder (spindle) spins at a constant rotational speed inside another cylinder. Generally, there is a very small gap between the walls. This annulus is filled with the fluid. The torque needed to maintain this constant rotation rate of the



inner spindle is measured by means of a torsion wire from which the spindle is suspended. A typical commercial instrument of this type is the Brookfield viscometer. Some types rotate the outer cylinder as well.

The shear stress at the wall of the bob or spindle is given by

$$\tau_w = \frac{T}{2\pi R_b^2 L} \quad (9.4-1)$$

where  $\tau_w$  is the shear stress at the wall, N/m<sup>2</sup> or kg · m/s<sup>2</sup>;  $T$  is the measured torque, kg · m<sup>2</sup>/s<sup>2</sup>;  $R_b$  is the radius of the spindle, m; and  $L$  is the effective length of the spindle, m. Note that Eq. (9.4-1) holds for Newtonian and non-Newtonian fluids.

The shear rate at the surface of the

spindle for non-Newtonian fluids is as follows (M6) for  $0.5 < R_b/R_c < 0.99$ :

$$(-dv/dr)_w = 2\omega n [1 - (R_b/R_c)^{2/n}] \quad (9.4-2)$$

where  $R_c$  is the radius of the outer cylinder or container, m; and  $\omega$  is the angular velocity of the spindle, rad/s. Also,  $\omega = 2\pi N/60$ , when  $N$  is expressed in RPM. Results calculated using Eq. (9.4-2) give values very close to those using the more complicated equation of Krieger and Maron (K2), also given in (P4, S2).

The power-law equation is given as

$$\tau = K(-dv/dr)^n \quad (9.1-2)$$

where  $K = N \cdot s_n/m^2$ ,  $kg \cdot s_{n-2}/m$ .

Substituting Eqs. (9.4-1) and (9.4-2) into (9.1-2) gives

$$T = 2\pi R b^2 L K [2n \{1 - (R_b/R_c)^2 / n\}]^n \omega^n \quad (9.4-3)$$

or,

$$T = A \omega^n \quad (9.4-4)$$

where

$$A = 2\pi R b^2 L K [2n \{1 - (R_b/R_c)^2 / n\}]^n \quad (9.4-5)$$

Experimental data are obtained by measuring the torque  $T$  at different values of  $\omega$  for a given fluid. The flow-property constants may be evaluated by plotting  $\log T$  versus  $\log \omega$ . The parameter  $n$  is the slope of the straight line and the intercept is  $\log A$ . The consistency factor  $K$  is now easily evaluated from Eq. (9.4-5).

Various special cases can be derived for Eq. (9.4-2):

1. *Newtonian fluid. ( $n = 1$ )*

$$(-dv/dr)_w = 2\omega [1 - (R_b/R_c)^2] \quad (9.4-6)$$

2. *Very large gap ( $R_b/R_c < 0.1$ ).* This is the case of a spindle immersed in a large beaker of test fluid. Equation (9.4-2) becomes

$$(-dv/dr)_w = 2\omega n \quad (9.4-7)$$

Substituting Eqs. (9.4-1) and (9.4-7) into (9.1-2),

$$T = 2\pi R_b^2 L K (2n)^n \omega^n \quad (9.4-8)$$

Again, as before, the flow-property constants can be evaluated by plotting  $\log T$  versus  $\log \omega$ .

3. *Very narrow gap* ( $R_b/R_c > 0.9$ ). This is similar to flow between parallel plates. Taking the shear rate at radius  $(R_b + R_c)/2$ ,

$$(-dv/dr)_w \cong \Delta v / \Delta r = 2\omega [1 - (R_b/R_c)^2] \quad (9.4-9)$$

This equation, then, is the same as Eq. (9.4-6).

## 9.5 Power Requirements in Agitation and Mixing of Non-Newtonian Fluids

For correlating the power requirements in agitation and mixing of non-Newtonian fluids, the power number  $NP$  is defined by Eq. (7.2-2), which is also the equation used for Newtonian fluids. However, the definition of the Reynolds number is much more complicated than for Newtonian fluids, since the apparent

viscosity is not constant for non-Newtonian fluids, but varies with the shear rates or velocity gradients in the vessel. Several investigators (G1, M1) have used an average apparent viscosity  $\mu_a$ , which is used in the Reynolds number as follows:

$$N'_{Re,n} = Da^2 N_p \mu_a \quad (9.5-1)$$

The average apparent viscosity can be related to the average shear rate or average velocity gradient by the following method. For a power-law fluid,

$$\tau = K(-dv/dy)_a v^n \quad (9.5-2)$$

For a Newtonian fluid,

$$\tau = \mu_a (-dv/dy)_a v \quad (9.5-3)$$

Combining Eqs. (9.5-2) and (9.5-3),

$$\mu_a = K \left( -dv/dy \right)_{av}^{n-1} \quad (9.5-4)$$

Metzner and others (G1, M1) found experimentally that the average shear rate  $(dv/dy)_{av}$  for pseudoplastic liquids ( $n < 1$ ) varies approximately as follows with the rotational speed:

$$(dv/dy)_{av} = 1.1N \quad (9.5-5)$$

Hence, combining Eqs. (9.5-4) and (9.5-5),

$$\mu_a = (1.1N)^{n-1} K \quad (9.5-6)$$

Substituting into Eq. (9.5-1),

$$N' Re_{n=Da} = 2N^{2-n} \rho^{1-n} K^{n-1} \quad (9.5-7)$$

Equation (9.5-7) has been used to

correlate data for a flat six-blade turbine with a disk in pseudoplastic liquids, and the dashed curve in Fig. 3.5-6 shows the correlation (M1). The solid curve applies to Newtonian fluids (R1). Both sets of data were obtained for four baffles with  $D_t/J = 10$ ,  $D_a/W = 5$ , and  $L/W = 54$ . However, since it has been shown that the difference in results for  $D_t/J = 10$  and  $D_t/J = 12$  is very slight (R1), this Newtonian line can be considered the same as curve 1 in Fig. 7.2-5. The curves in Fig. 9.5-1 show that the results are identical for the Reynolds number range 1–2000, except that they differ only in the Reynolds number range 10–100, where the pseudoplastic fluids use less power than the Newtonian fluids. The flow patterns for the pseudoplastic fluids show much greater velocity-gradient changes than



do the Newtonian fluids in the agitator. The fluid far from the impeller may be moving in slow laminar flow with a high apparent viscosity. Data for fan turbines and propellers are also available (M1).

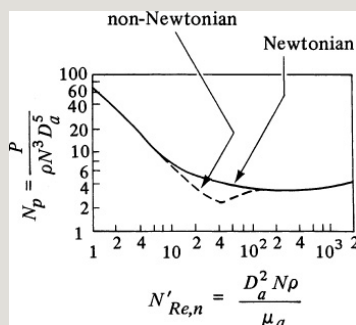


Figure 9.5-1. Power correlation in agitation for a flat, six-blade turbine with disk in pseudoplastic non-Newtonian and Newtonian fluids (G1, M1, R1):  $Da/W = 5$ ,  $L/W = 5/4$ ,  $D_t/J = 10$ .

## 9.6 Chapter Summary

In this chapter, we have introduced the concept of non-Newtonian fluids—fluids whose flow behavior (shear stress versus shear rate) does not follow Newton's law of viscosity.

Non-Newtonian fluids were classified into three main categories: time-independent fluids, time-dependent fluids, and viscoelastic fluids. Much of this chapter was focused on time-independent fluids, which can be classified into three main categories: Bingham plastic fluids, pseudoplastic fluids, and dilatant fluids. Bingham plastic fluids are unique in that a yield stress must be overcome to initiate flow. Pseudoplastic and dilatant fluids exhibit flow behavior that can be presented by a power-law equation,

$$\tau = K(-dv/dr)^n \quad (9.1-2)$$

For the equation above, pseudoplastic fluids hold for the case when  $n < 1$  and dilatant fluids hold for the case when  $n$

> 1.

For time-independent non-Newtonian fluids, we showed that for laminar flow, the pressure drop in a circular tube can be determined by two ways: using the equation for flow in a tube, and the friction-factor method. In both cases, it is necessary to determine the limit at which laminar flow is observed, which can be found by calculating the generalized Reynolds number:

$$N_{Re,gen} = D n' V^{2-n'} \rho g = D n' V^{2-n'} \rho K' 8^{n'-1} = D n V^{2-n} \rho K 8^{n-1} (3n + 14n)^n (9.1-13)$$

Based on this definition, the frictional pressure drop for a fluid flow in a tube in laminar can be found from

$$\Delta p = K' 4 L D (8 V D)^{n'} (9.1-10)$$

or, by using the friction-factor method:

$$\Delta p = 4f_p \frac{L}{D} \frac{V^2}{2} \quad (9.1-15)$$

where

$$f = \frac{16}{\text{Re}} \quad (9.1-14)$$

For cases of turbulent flow, we explained that these relations are no longer valid and other approaches must be followed to determine friction factor and pressure drop. For example, Figure 9.2-1 can be used to find the friction factor of power-law fluids flowing in smooth pipes.

The power-law relation for a time-independent fluid was used to theoretically determine the flow profiles in laminar flow. Similarly, flow profiles were also determined for Bingham

plastic fluids.

Rotational viscometers were introduced as a method to determine the flow properties of non-Newtonian fluids. This piece of equipment consists of two concentric cylinders in which a fluid is allowed to shear in the annular space. The relation between the torque needed to cause the shear stress required to flow at different values of angular velocity provides the characteristics necessary to model the non-Newtonian flow behavior.

Lastly, a discussion on the power requirements to agitate and mix non-Newtonian fluids was provided.

## **Problems**

### ***9.2-1. Pressure Drop of a Power-Law***

**Fluid, Banana Purée.** A power-law biological fluid, banana purée, is flowing at  $23.9^{\circ}\text{C}$ , with a velocity of  $1.018\text{ m/s}$ , through a smooth tube  $6.10\text{ m}$  long having an inside diameter of  $0.01267\text{ m}$ . The flow properties of the fluid are  $K = 6.00\text{ N} \cdot \text{s}^{0.454}/\text{m}^2$  and  $n = 0.454$ . The density of the fluid is  $976\text{ kg}/\text{m}^3$ .

- Calculate the generalized Reynolds number and also the pressure drop using Eq. (9.1-9). Be sure to convert  $K$  to  $K'$  first.
- Repeat part (a), but use the friction-factor method.

**Ans.** (a)  $N_{\text{Re,gen}} = 63.6$ ,  $\Delta p = 245.2\text{ kN}/\text{m}^2 (5120\text{ lbf}/\text{ft}^2)$

**9.2-2. Pressure Drop of Pseudoplastic Fluid.** A pseudoplastic power-law fluid having a density of  $63.2\text{ lb}_\text{m}/\text{ft}^3$  is flowing through  $100\text{ ft}$  of pipe having an

inside diameter of 2.067 in. at an average velocity of 0.500 ft/s. The flow properties of the fluid are  $K = 0.280 \text{ lbf} \cdot \text{s}_n/\text{ft}^2$  and  $n = 0.50$ . Calculate the generalized Reynolds number and also the pressure drop, using the friction-factor method.

### ***9.2-3. Turbulent Flow of a Non-Newtonian Fluid, Applesauce.***

Applesauce having the flow properties given in Table 9.1-1 is flowing in a smooth tube with an inside diameter of 50.8 mm and a length of 3.05 m at a velocity of 4.57 m/s.

- Calculate the friction factor and the pressure drop in the smooth tube.
- Repeat, but for a commercial pipe having the same inside diameter with a roughness of  $\epsilon = 4.6 \times 10^{-5} \text{ m}$ .

**Ans.** (a)  $N_{Re,gen} = 4855$ ,  $f = 0.0073$ ; (b)  $f = 0.0100$

**9.3-1. Velocity Profile of a Bingham Plastic Fluid.** For the conditions of Example 9.3-1, do as follows:

- Calculate the velocity for the plug-flow region at  $r = r_0$ .
- Calculate the velocity for values of  $r$  of 0.35 cm, 0.45 cm, and 0.50 cm and plot the complete velocity profile versus radial position.

**9.3-2. Pressure Drop for a Bingham Plastic Fluid.** A Bingham plastic fluid has a value of  $\tau_0 = 1.2 \text{ N/m}^2$  and a viscosity  $\mu = 0.4 \text{ Pa} \cdot \text{s}$ . The fluid is flowing at  $5.70 \times 10^{-5} \text{ m}^3/\text{s}$  in a pipe 2.5 m long with an internal diameter of 3.0 cm. Calculate the pressure drop ( $p_0 - p_L$ ) in  $\text{N/m}^2$  and  $r_0$ . (*Hint: This is a trial-and-error solution. As a first trial, assume  $\tau_0 = 0$ .*)



$$\text{Ans. } (p_0 - p_L) = 3400 \text{ N/m}^2$$

**9.4-1. Flow Properties of a Non-Newtonian Fluid from Rotational Viscometer Data.** Following are data obtained on a fluid using a Brookfield rotational viscometer:



The diameter of the inner concentric rotating spindle is 25.15 mm, the outer cylinder diameter is 27.62 mm, and the effective length is 92.39 mm. Determine the flow properties of this non-Newtonian fluid.

$$\text{Ans. } n = 0.870$$

**9.5-1. Agitation of a Non-Newtonian Liquid.** A pseudoplastic liquid having the properties  $n = 0.53$ ,  $K = 26.49 \text{ N} \cdot$

$s_n'/m^2$  and  $\rho = 975 \text{ kg/m}^3$  is being agitated in a system such as in Fig. 9.3-1, where  $D_t = 0.304 \text{ m}$ ,  $D_a = 0.151 \text{ m}$ , and  $N = 5 \text{ rev/s}$ . Calculate  $\mu_a, N_{Re,n'}$ , and the kW power for this system.

**Ans.**  $\mu_a = 4.028 \text{ Pa} \cdot \text{s}$ ,  $N_{Re,n} = 27.60$ ,  $N_P = 3.1$ ,  $P = 0.02966 \text{ kW}$

### References

### Notation

# Chapter 10. Potential Flow and Creeping Flow

## 10.0 Chapter Objectives

On completion of this chapter, a student should be able to:

- Describe systems that exhibit inviscid, potential, and creeping flow
- Simplify the Navier–Stokes equations to model inviscid and potential flow
- Describe the stream function
- Use the stream function to solve inviscid flow problems
- Generate plots of streamlines using the stream function
- Describe the velocity potential or potential function
- Use the velocity function to solve inviscid and potential flow problems
- Determine the velocity components of a flow problem using the stream function and velocity potential

- Simplify the Navier–Stokes equation to model creeping flow
- Describe how to solve creeping flow problems

## **10.1 Other Methods for Solution of Differential Equations of Motion**

### **10.1A Introduction**

In Section 8.3, we considered examples where the Navier–Stokes differential equations of motion could be solved analytically. These cases were used when the Navier–Stokes equations could be simplified so that only one non-vanishing component of the velocity remained. However, for cases in which two or three velocity components remain, the solutions to these cases can be complex and may require advanced mathematical techniques.

In this chapter, we will consider some

new approximations that allow us to simplify the differential equations in order to obtain analytical solutions. Often, terms that are quite small compared to the other terms will be omitted. Throughout this chapter, we will consider cases in which the solution of simplified Navier–Stokes equations may be obtained by using a stream function  $\psi(x, y)$  and/or a velocity potential  $\phi(x, y)$  rather than the terms of the velocity components  $v_x$ ,  $v_y$ , and  $v_z$ .

Three cases will be considered in this section: inviscid flow, potential flow, and creeping flow. The fourth case, boundary-layer flow, will be considered in Chapter 11.

## 10.2 Stream Function

The stream function  $\psi(x, y)$  is a

convenient parameter by which we can model systems that exhibit two-dimensional, steady, incompressible flow. The stream function  $\psi$  in  $\text{m}^2/\text{s}$  is related to the velocity components  $v_x$  and  $v_y$  by

$$v_x = \frac{\partial \psi}{\partial y}, v_y = -\frac{\partial \psi}{\partial x} \quad (10.2-1)$$

These definitions of  $v_x$  and  $v_y$  can then be used in the  $x$  and  $y$  components of the differential equation of motion, Eqs. (8.2-36) and (8.2-37), together with  $v_z = 0$ , to obtain a differential equation for  $\psi$  that is equivalent to the Navier–Stokes equation.

The stream function is very useful because of its physical significance. In steady flow, lines defined by  $\psi = \text{constant}$  are known as *streamlines*,

which are the actual curves traced out by the particles of fluid as it flows. A stream function exists for all two-dimensional, steady, incompressible flow whether the fluid is viscous or inviscid and whether the flow is rotational or irrotational.

**EXAMPLE 10.2-1. Stream Function and Streamlines**

The stream function relationship is given as  $\psi = xy$ . Find the equations for the components of velocity. Also plot the streamlines for a constant  $\psi = 4$  and  $\psi = 1$ .

**Solution:** Using Eq. (10.2-1),

$$v_x = \partial\psi/\partial y = \partial(xy)/\partial y = x \quad v_y = -\partial\psi/\partial x = -\partial(xy)/\partial x = -y$$

To determine the streamline for  $\psi = \text{constant} = 1 = xy$ , assume that  $y = 0.5$  and solve for  $x$ :

$$\psi = 1 = xy = x(0.5)$$

Hence,  $x = 2$ . The same procedure can be repeated for for  $y = 1$ ,  $x = 1$ ; for  $y = 2$ ,  $x = 0.5$ ; for  $y = 5$ ,  $x = 0.2$ , and so on. Doing the same for  $\psi = \text{constant} = 4$ , the streamlines for  $\psi = 1$  and  $\psi = 4$  are plotted in Fig. 10.2-1. A possible flow model is flow around a corner.

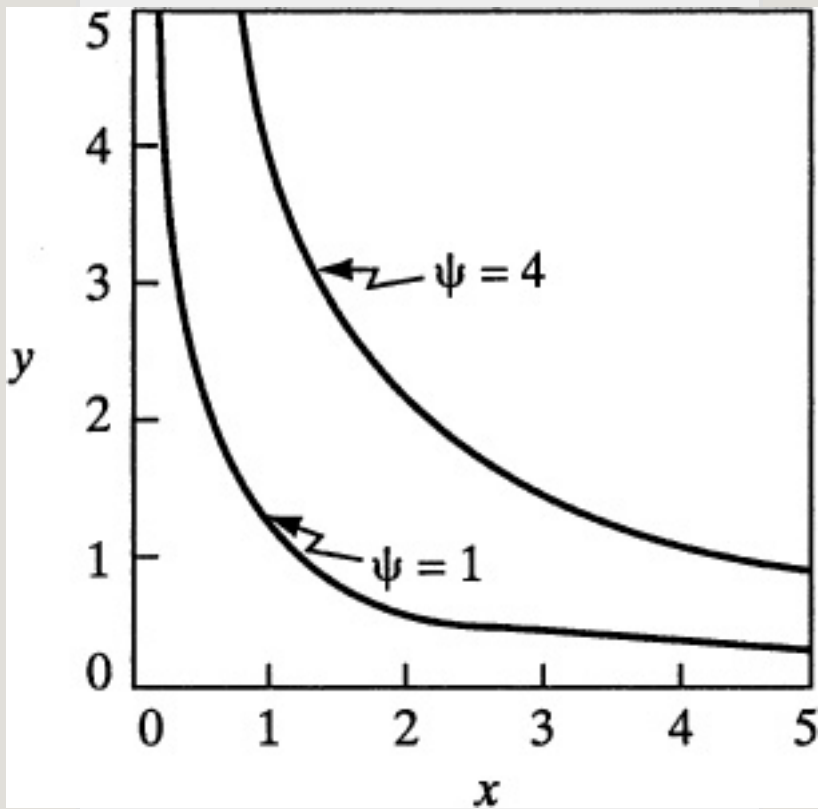


Figure 10.2-1. Plot of streamlines for  $\psi = xy$  for Example 10.2-1.

### 10.3 Differential Equations of Motion for Ideal Fluids (Inviscid Flow)

Special equations for *ideal or inviscid fluids* can be obtained for a fluid having a constant density and zero viscosity. These are called the *Euler equations*. For fluids of



constant density with zero viscosity, Eqs. (8.2-36)–(8.2-38) for the  $x$ ,  $y$ , and  $z$  components of momentum become

$$\rho(\partial v_x \partial t + v_x \partial v_x \partial x + v_y \partial v_x \partial y + v_z \partial v_x \partial z) = -\partial p \partial x + \rho g_x \quad (10.3-1)$$

$$\rho(\partial v_y \partial t + v_x \partial v_y \partial x + v_y \partial v_y \partial y + v_z \partial v_y \partial z) = -\partial p \partial y + \rho g_y \quad (10.3-2)$$

$$\rho(\partial v_z \partial t + v_x \partial v_z \partial x + v_y \partial v_z \partial y + v_z \partial v_z \partial z) = -\partial p \partial z + \rho g_z \quad (10.3-3)$$

At very high Reynolds numbers, the viscous forces are quite small compared to the inertia forces and the viscosity can be assumed as zero. These equations are useful in calculating the pressure distribution at the outer edge of the thin boundary layer in flow past immersed bodies. Away from the surface outside

the boundary layer, this assumption of an ideal fluid is often valid. This is discussed more in Chapter 11.

## 10.4 Potential Flow and Velocity Potential

The velocity potential or potential function  $\phi(x, y)$  in  $\text{m}^2/\text{s}$  is another useful parameter that is commonly used to solve inviscid flow problems and is defined as

$$v_x = \partial\phi/\partial x \quad v_y = \partial\phi/\partial y \quad v_z = \partial\phi/\partial z \quad (10.4-1)$$

This potential function exists only for a flow with zero angular velocity; thus, this potential function is for flows that are irrotational. This type of flow of an ideal or inviscid fluid ( $\rho = \text{constant}$ ,  $\mu = 0$ ) is called *potential flow*. Additionally, the velocity potential  $\phi$  exists for three-dimensional flows, whereas the stream

function does not. Another parameter that is used to describe the rotational behavior of fluid flows is *vorticity*.

The vorticity of a fluid is defined as follows:

$$\partial v_y / \partial x - \partial v_x / \partial y = 2\omega_z \quad (10.4-2)$$

or,

$$\partial^2 \psi / \partial x^2 + \partial^2 \psi / \partial y^2 = -2\omega_z \quad (10.4-3)$$

where  $2\omega_z$  is the vorticity and  $\omega_z$  in  $s^{-1}$  is angular velocity about the  $z$  axis. If  $2\omega_z = 0$ , the flow is irrotational and a potential function exists.

Using Eq. (8.1-24), the conservation-of-mass equation for flows in the  $x$  and  $y$  directions is as follows for constant density:

$$\partial v_x / \partial x + \partial v_y / \partial y = 0 \quad (10.4-4)$$

Differentiating  $v_x$  in Eq. (10.4-1) with respect to  $x$ , and  $v_y$  with respect to  $y$ , and substituting into Eq. (10.4-4),

$$\partial^2 \phi / \partial x^2 + \partial^2 \phi / \partial y^2 = 0 \quad (10.4-5)$$

This is Laplace's equation in rectangular coordinates. If suitable boundary conditions exist or are known, Eq. (10.4-5) can be solved to give  $\phi(x, y)$ . Then, the velocity at any point can be obtained using Eq. (10.4-1). Techniques for solving this equation include using numerical analysis, conformal mapping, and functions of a complex variable. Euler's equations can then be used to find the pressure distribution.

When the flow is inviscid and irrotational, a similar type of Laplace

equation is obtained from Eq. (10.4-3) for the stream function:

$$\frac{\partial^2 \psi}{\partial x^2} + \frac{\partial^2 \psi}{\partial y^2} = 0 \quad (10.4-6)$$

Lines of constant  $\phi$  are called equal potential lines, and for potential flow, they are everywhere perpendicular (orthogonal) to lines of constant  $\psi$ . This can be proved as follows:

A line of constant  $\psi$  would be such that the change in  $\phi$  is zero:

$$d\psi = \frac{\partial \psi}{\partial x} dx + \frac{\partial \psi}{\partial y} dy = 0 \quad (10.4-7)$$

Then, substituting Eq. (10.2-1) into the above,

$$\left(\frac{dy}{dx}\right)_{\psi=\text{constant}} = \frac{v_y}{v_x} \quad (10.4-8)$$

Also, for lines of constant  $\phi$ ,

$$d\phi = \frac{\partial \phi}{\partial x} dx + \frac{\partial \phi}{\partial y} dy = 0 \quad (10.4-9)$$

$$\left(\frac{dy}{dx}\right)\phi = \text{constant} = -\frac{v_x}{v_y} \quad (10.4-10)$$

Hence,

$$\left(\frac{dy}{dx}\right)\phi = \text{constant} = -1 \left(\frac{dy}{dx}\right)\psi = \text{constant} \quad (10.4-11)$$

An example of the use of the stream function is in obtaining the flow pattern for inviscid, irrotational flow past a cylinder of infinite length. The fluid approaching the cylinder has a steady and uniform velocity of  $v_\infty$  in the  $x$  direction. Laplace's equation (10.4-6) can be converted to cylindrical coordinates to give

$$\frac{\partial^2 \psi}{\partial r^2} + \frac{1}{r} \frac{\partial \psi}{\partial r} + \frac{1}{r^2} \frac{\partial^2 \psi}{\partial \theta^2} = 0 \quad (10.4-12)$$

where the velocity components are given by

$$v_r = \frac{1}{r} \frac{\partial \psi}{\partial \theta} \quad v_\theta = -\frac{1}{r} \frac{\partial \psi}{\partial r} \quad (10.4-13)$$

Using the four boundary conditions that are required and the method of separation of variables, the stream function  $\psi$  can be obtained. Converting to rectangular coordinates,

$$\psi = v_\infty y (1 - R^2 x^2 + y^2) \quad (10.4-14)$$

where  $R$  is the cylinder radius. The streamlines and the constant-velocity-potential lines are plotted in Fig. 10.4-1 as a flow net.

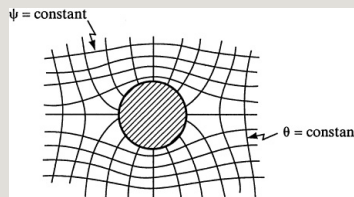


Figure 10.4-1. Streamlines ( $\psi = \text{constant}$ ) and constant velocity

*potential lines ( $\phi = \text{constant}$ ) for the steady and irrotational flow of an inviscid and incompressible fluid about an infinite circular cylinder.*

**EXAMPLE 10.4-1. Stream Function for a Flow Field**

The velocity components for a flow field are as follows:

$$v_x = a(x^2 - y^2) \quad v_y = -2axy$$

Prove that it satisfies the conservation of mass and determine  $\psi$ .

**Solution:** First, we determine  $\partial v_x / \partial x = 2ax$  and  $\partial v_y / \partial y = -2ax$ . Substituting these values into Eq. (8.1-24), the conservation of mass for two-dimensional flow,

$$\partial v_x / \partial x + \partial v_y / \partial y = 0 \text{ or } 2ax - 2ax = 0$$

Then, using Eq. (10.2-1),

$$v_x = \partial \psi / \partial y = a(x^2 - y^2) \quad v_y = \partial \psi / \partial x = -2axy \quad (10.4-15)$$

Integrating Eq. (10.4-15) for  $v_x$ ,

$$\psi = ax^2y - ay^3/3 + f(x) \quad (10.4-16)$$

Integrating Eq. (10.4-15) for  $v_y$ ,

$$-\psi = -2axy^2/2 + f(y) \quad (10.4-17)$$

Equating Eq. (10.4-16) to (10.4-17),

$$ax^2y - ay^3/3 + f(x) = -2axy^2 + f(y) \quad (10.4-18)$$

Canceling like terms,

$$-ay^3/3 + f(x) = -f(y) \quad (10.4-19)$$

Hence,  $f(x) = 0$  and  $f(y) = ay^3/3$ . Substituting  $f(x) = 0$  into Eq. (10.4-16),



$$\psi = ax^2y - ay^3 \quad (10.4-20)$$

**EXAMPLE 10.4-2. Stream Function and Velocities from Potential Function**

The potential function for a two-dimensional, irrotational, incompressible flow field is given as  $\phi = x^2 - 2y - y^2$ . Find the stream function  $\psi$  and the velocity components  $v_x$  and  $v_y$ .

**Solution:** Using Eqs. (10.2-1) and (10.4-1),

$$v_x = \partial\psi/\partial y = \partial\phi/\partial x = 2x \quad v_y = \partial\psi/\partial x = \partial\phi/\partial y = -2$$

Combining,

$$\partial\phi/\partial x = \partial\psi/\partial y = 2x \quad \partial\phi/\partial y = \partial\psi/\partial x = -2 \quad (10.4-21)$$

Differentiating the potential function with respect to  $x$  and equating the result to  $\partial\psi/\partial y$  from Eq. (10.4-21),

$$\partial\phi/\partial x = 2x - 0 = 2x = \partial\psi/\partial y \quad (10.4-22)$$

Differentiating the potential function with respect to  $y$  and equating the result to  $-\partial\psi/\partial x$  from Eq. (10.4-21),

$$\partial\phi/\partial y = 0 - 2 - 2y = -2 - 2y = -\partial\psi/\partial x \quad (10.4-23)$$

Integrating Eq. (10.4-22),

$$\psi = 2xy + f(x) \quad (10.4-24)$$

Integrating Eq. (10.4-23),

$$\psi = 2x + 2xy + f(y) \quad (10.4-25)$$

Equating Eq. (10.4-24) to (10.4-25),

$$\psi = 2xy + f(x) = 2x + 2xy + f(y) \quad (10.4-26)$$

Hence, after canceling  $2xy$  from both sides,

$$f(x) = 2x + f(y) \quad (10.4-27)$$

Therefore,  $f(x) = 2x$  and  $f(y) = 0$ . Substituting  $f(x) = 2x$  into Eq. (10.4-24),

$$\psi = 2xy + 2x \quad (10.4-28)$$

The velocities are, from Eqs. (10.4-22) and (10.4-23),

$$\partial\psi/\partial y = v_x = 2x \quad \partial\psi/\partial x = v_y = 2 - 2y \quad (10.4-29)$$

In potential flow, the stream function and potential function are used to represent the flow in the main body of the fluid. These ideal fluid solutions do not satisfy the condition that  $v_x = v_y = 0$  on the wall surface. Near the wall, viscous drag exists and boundary-layer theory, where we obtain approximate solutions for the velocity profiles in this thin boundary layer by taking into account viscosity, can be used. This is discussed in Chapter 11. Then, we combine this solution with the ideal flow solution that describes the flow outside the boundary layer.

## 10.5 Differential Equations of Motion for Creeping Flow

At very low Reynolds numbers, below approximately  $N_{Re} = 1$ , the term *creeping flow* is used to describe flow at very low velocities. This type of flow applies for the fall or settling of small particles through a viscous fluid. Stokes' law is derived using this type of flow in problems of settling and sedimentation.

In flows around a sphere, for example, the fluid changes velocity and direction in a complex manner. If the inertia effects in this case were important, it would be necessary to keep all the terms in the three Navier–Stokes equations. Experiments show that at a Reynolds

number below about 1, the inertia effects are small and therefore can be omitted. Hence, the equations of motion, Eqs. (8.2-36)–(8.2-38) for creeping flow of an incompressible fluid, can be simplified to become

$$\partial p / \partial x = \mu (\partial^2 v_x / \partial x^2 + \partial^2 v_x / \partial y^2 + \partial^2 v_x / \partial z^2) \quad (10.5-1)$$

$$\partial p / \partial y = \mu (\partial^2 v_y / \partial x^2 + \partial^2 v_y / \partial y^2 + \partial^2 v_y / \partial z^2) \quad (10.5-2)$$

$$\partial p / \partial z = \mu (\partial^2 v_z / \partial x^2 + \partial^2 v_z / \partial y^2 + \partial^2 v_z / \partial z^2) \quad (10.5-3)$$

For flow past a sphere, the stream function  $\psi$  can be used in the Navier–Stokes equation in spherical coordinates to obtain the equation for the stream function as well as the velocity distribution and pressure

distribution over the sphere. Then, by integration over the whole sphere, the form drag, caused by the pressure distribution, and the skin friction or viscous drag, caused by the shear stress at the surface, can be combined to give the total drag:

$$F_D = 3\pi\mu D_p v \quad (\text{SI}) \quad F_D = 3\pi\mu D_p v_{gc} \quad (\text{English})$$

(10.5-4)

where  $F_D$  is total drag force in N,  $D_p$  is particle diameter in m,  $v$  is free stream velocity of fluid approaching the sphere in m/s, and  $\mu$  is viscosity in kg/m · s. This is Stokes' equation for the drag force on a sphere.

Often, Eq. (10.5-4) is rewritten as follows:

$$F_D = C_D v^2 \rho A \quad (\text{SI}) \quad F_D = C_D v^2 g_c \rho A \quad (\text{English})$$

where  $C_D$  is a drag coefficient, equal to  $24/N_{Re}$  for Stokes' law, and  $A$  is the projected area of the sphere,  $\pi D_p^2/4$ . This is discussed in more detail in Section 6.1 for flow past spheres.

## 10.6 Chapter Summary

In this chapter, we have described systems that exhibit inviscid, potential, and creeping flow. Inviscid flow occurs when the viscosity of fluid is close to zero, or if viscous effects are negligible compared to other effects such as inertia. Two-dimensional systems that exhibit inviscid flow can be modeled and solved using a parameter known as the stream function  $\psi$  that is related

to the velocity components  $v_x$  and  $v_y$  by

$$v_x = \frac{\partial \psi}{\partial y}, v_y = -\frac{\partial \psi}{\partial x} \quad (10.2-1)$$

Using the stream function, the solution to the Navier–Stokes equations can be simplified. In addition, by determining the stream function, lines that describe the flow of the fluid, streamlines, can be generated.

Another parameter that often appears in inviscid flow problems is the vorticity, which describes whether the flow is rotational or irrotational. The vorticity of a fluid is defined as follows:

$$\frac{\partial v_y}{\partial x} - \frac{\partial v_x}{\partial y} = 2\omega_z \quad (10.4-2)$$

If the inviscid flow is irrotational, it is also known as potential flow. The

velocity potential, or potential function, is a parameter similar to the stream function, which can be used to solve inviscid potential flow systems. The velocity potential or potential function  $\phi(x, y)$  is defined as

$$v_x = \frac{\partial \phi}{\partial x} \quad v_y = \frac{\partial \phi}{\partial y} \quad v_z = \frac{\partial \phi}{\partial z} \quad (10.4-1)$$

Multiple examples have shown how to use the stream function and velocity potential to solve inviscid and potential flow problems.

Lastly, we described systems that exhibit creeping flow, which occurs when viscous effects dominate and inertial effects become negligible. For these systems, the Navier–Stokes equations can also be simplified. Mathematical techniques are available



to solve creeping flow problems. Due to the strong viscous effects, drag is commonly observed in creeping flow systems.

## Problems

### 10.2.1. *Stream Function and Velocity*

**Vector.** Flow of a fluid in two dimensions is given by the stream function  $\psi = Bxy$ , where  $B = 50 \text{ s}^{-1}$  and the units of  $x$  and  $y$  are in cm. Determine the value of  $v_x$ ,  $v_y$ , and the velocity vector at  $x = 1 \text{ cm}$  and  $y = 1 \text{ cm}$ .

**Ans.**  $v = 70.7 \text{ cm/s}$

**10.2-2. *Plot of Streamlines.*** For Ex. (10.4-2), plot the streamlines for  $\psi = 0$  and  $\psi = 2$  when  $x > 0$ .

### 10.2-3. *Stream Function for Two-*

**Dimensional Flow.** Find the stream function of the two-dimensional flow with constant density, where  $v_x = U[(y/L)^2 - (y/L)]$  and  $v_y = 0$ . The flow is between two parallel plates spaced  $L$  distance apart. Also, plot the velocity profile of  $v_x$  versus  $y$ .

$$\text{Ans. } \psi = UL[13(y/L)^3 - 12(y/L)^2]$$

#### **10.2-4. Velocity Field from Stream**

**Function.** Given the stream function  $\psi = 3x^2 + 2y^2$ , calculate  $v_x$  and  $v_y$  and draw the streamlines for  $\psi = 1$  and  $\psi = 2$ .

$$\text{Ans. } v_x = 4y, \quad v_y = -6x$$

**10.2-5. Streamline from Velocities.** The velocity  $v_x = x^2$  and  $v_y = -2xy$ . Determine the stream function  $\psi$ .

$$\text{Ans. } \psi = x^2y$$

**10.3-1. Euler's Equation of Motion for an Ideal Fluid.** Using the Euler equations (10.3-1)–(10.3-3) for ideal fluids with constant density and zero viscosity, obtain the following equation:

$$\rho D\mathbf{v}/Dt = -\nabla p + \rho \mathbf{g}$$

**10.4-1. Potential Function.** The potential function  $\phi$  for a given flow situation is  $\phi = C(x^2 - y^2)$ , where  $C$  is a constant. Check to see if it satisfies Laplace's equation. Determine the velocity components  $v_x$  and  $v_y$ .

**Ans.**  $v_x = 2Cx$ ,  $v_y = -2Cy$  ( $C = \text{constant}$ )

**10.4-2. Determining the Velocities from the Potential Function.** The potential function for flow is given as  $\phi = Ax + By$ , where  $A$  and  $B$  are constants. Determine the velocities  $v_x$  and  $v_y$ .

**10.4-3. Stream Function and Potential Function.** A liquid is flowing parallel to the  $x$  axis. The flow is uniform and is represented by  $v_x = U$  and  $v_y = 0$ .

- Find the stream function  $\psi$  for this flow field and plot the streamlines.
- Find the potential function and plot the potential lines.

**Ans.** (a)  $\psi = Uy$

**10.4-4. Velocity Components and Stream Function.** A liquid is flowing in a uniform manner at an angle of  $\beta$  with respect to the  $x$  axis. Its velocity components are  $v_x = U \cos \beta$  and  $v_y = U \sin \beta$ . Find the stream function and the potential function.

**Ans.**  $\psi = Uy \cos \beta - Ux \sin \beta$

**10.4-5. Flow Field with Concentric**

**Streamlines.** The flow of a fluid that has concentric streamlines has a stream function represented by  $\psi = 1/(x^2 + y^2)$ . Find the components of velocity  $v_x$  and  $v_y$ . Also, determine if the flow is rotational and, if so, determine the vorticity,  $2\omega_z$ .

**10.4-6. Potential Function and Velocity Field.** In Example 10.4-1 the velocity components were given. Show if a velocity potential exists and, if so, also determine  $\phi$ .

$$\text{Ans. } \phi = ax^3/3 - axy^2$$

**10.4-7. Stream and Potential Functions and Plots of These Functions.**

Determine the stream function  $\psi$  when the velocities are  $v_x = 2x$  and  $v_y = -2y$ . Also, determine the potential function

$\phi$ . Plot the stream function for  $\psi = 1$  and  $\psi = 2$ . Also, plot the equal potential lines for  $\phi = 1$  and  $\phi = 4$ .

**Ans.**  $\psi = 2xy, \phi = x^2 - y^2$

**10.4-8. Stream Function from Velocity Potential.** Find the stream function  $\psi$  from the velocity potential  $\phi = UL[(x/L)^3 - (3xy^2)/L^3]$ , where  $U$  and  $L$  are constants. Also, find  $v_x$  and  $v_y$ .

**Ans.**  $v_x = 3UL^2[x^2 - y^2], v_y = -6UxyL^2$

**Notation**

# Chapter 11. Boundary-Layer and Turbulent Flow

## 11.0 Chapter Objectives

On completion of this chapter, a student should be able to:

- Describe the concept of the boundary layer
- Sketch the profile of a boundary layer for flow past a flat plate
- Describe how the thickness of a boundary layer increases with distance from the leading edge
- Calculate and use the Reynolds number to determine if the flow past a flat plate is in the laminar or turbulent flow regime
- Explain the behavior of friction and drag for flows near the surface of a flat plate
- Simplify the equation of continuity and the Navier–Stokes equations to model boundary-layer flow
- Calculate the boundary-layer thickness, shear stress at the surface, and drag force for laminar flows past a flat plate

- Explain the concept of an eddy and how it is used to help describe turbulent flow-behavior
- Explain and show how the instantaneous velocity can be broken down into the time-averaged (mean) velocity and velocity fluctuations
- Explain the concept of intensity of turbulence and how it is related to velocity fluctuations
- Develop expressions for the time-averaged equation of continuity and Navier–Stokes equations
- Show how turbulent Reynolds stresses are obtained from the time-averaged Navier–Stokes equations
- Explain the concept of the Prandtl mixing length
- Determine the universal velocity profile for fluids in turbulent flow in pipes
- Use the von Kármán momentum integral balance to calculate the boundary-layer thickness, shear stress at the surface, and drag force for turbulent flows past a flat plate

## **11.1 Boundary-Layer Flow**

### **11.1A Boundary-Layer Flow**

In Section 8.3, the Navier–Stokes equations were used to find relations that described laminar flow behavior



between flat plates and inside circular tubes. In Chapter 10, these equations were modified to model both inviscid flow and creeping flow. In this section, the flow of fluids around objects will be considered in more detail, with particular attention being given to the region close to the solid surface, called the *boundary layer*.

In the boundary-layer region near the solid, the fluid motion is greatly affected by friction at this solid surface. In the bulk of the fluid far away from the boundary layer, the flow can often be adequately described by the theory of ideal fluids with zero viscosity.

However, in the thin boundary layer, viscosity is important. Since the region is thin, simplified solutions can be

obtained for the boundary-layer region. Prandtl originally suggested this division of the problem into two parts, which has been used extensively in fluid dynamics since its development.

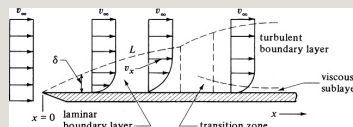
In order to help explain boundary layers, an example of boundary-layer formation in the steady-state flow of a fluid past a flat plate is given in Fig. 11.1-1. The velocity of the fluid upstream of the leading edge at  $x = 0$  of the plate is uniform across the entire fluid stream and has the value  $v_{\infty}$ . The velocity of the fluid at the interface is zero and the velocity  $v_x$  in the  $x$  direction increases as one goes farther away from the plate. The velocity  $v_x$  asymptotically approaches the velocity  $v_{\infty}$  of the bulk of the stream.

The dashed line  $L$  is drawn so that the velocity at that point is 99% of the bulk velocity  $v_{\infty}$ . The layer or zone between the plate and the dashed line constitutes the *boundary layer*. When the flow is laminar, the thickness  $\delta$  of the boundary layer increases with  $x$  as we move in the  $x$  direction. Here, the Reynolds number is defined as  $N_{\text{Re},x} = x v_{\infty} \rho / \mu$ , where  $x$  is the distance downstream from the leading edge. When the Reynolds number is less than  $2 \times 10^5$ , the flow is laminar, and the associated boundary layer is shown in Fig. 11.1-1.

The transition from laminar to turbulent flow on a smooth plate occurs in the Reynolds-number range  $2 \times 10^5$  to  $3 \times 10^6$ , as shown in Fig. 11.1-1. When the boundary layer is turbulent, a thin, viscous sublayer persists next to the

plate. The drag caused by the viscous shear in the boundary layers is called *skin friction* and is the only drag present for flow past a flat plate.

The type of drag occurring when fluid flows by a bluff or blunt shape such as a sphere or cylinder, which is mostly caused by a pressure difference, is termed *form drag*. This drag predominates in flow past such objects at all except low values of the Reynolds number. Often, a wake is present. Skin friction and form drag both occur in flow past a bluff shape, and the total drag is the sum of the skin friction and the form drag (see also Section 6.1).



### **11.1B Boundary-Layer Separation and the Formation of Wakes**

We discussed the growth of the boundary layer at the leading edge of a plate, as shown in Fig. 11.1-2.

However, some important phenomena also occur at the trailing edge of this plate and other objects. At the trailing edge or rear edge of the flat plate, the boundary layers are present at the top and bottom sides of the plate. On leaving the plate, the boundary layers gradually intermingle and disappear.

If the direction of flow is at right angles to the plate, as shown in Fig. 11.1-2, a boundary layer forms, as before, in the fluid that is flowing over the upstream face. Once at the edge of the plate,

however, the momentum in the fluid prevents it from making the abrupt turn around the edge of the plate, and it separates from the plate. A zone of decelerated fluid is present behind the plate and large eddies (vortices), called the *wake*, are formed in this area. The eddies consume large amounts of mechanical energy. This separation of boundary layers occurs when the change in velocity of the fluid flowing past an object is too large in direction or magnitude for the fluid to adhere to the surface.

Since formation of a wake causes large losses in mechanical energy, it is often necessary to minimize or prevent boundary-layer separation by streamlining the objects or by other means. This is also discussed in Section

## 6.1A for flow past immersed objects.

### 11.1C Laminar Flow and Boundary-Layer Theory

*1. Boundary-layer equations.* When laminar flow is occurring in a boundary layer, certain terms in the Navier–Stokes equations become negligible and can be neglected. The thickness of the boundary layer  $\delta$  is arbitrarily taken as the distance away from the surface where the velocity reaches 99% of the free-stream velocity. The concept of a relatively thin boundary layer leads to some important simplifications of the Navier–Stokes equations.

For two-dimensional laminar flow in the  $x$  and  $y$  directions of a fluid having a constant density, Eqs. (8.2-36) and (8.2-37) become as follows for flow at

steady state, as shown in Figure 11.1-1 when we neglect the body forces  $g_x$  and  $g_y$ :

$$v_x \frac{\partial v_x}{\partial x} + v_y \frac{\partial v_x}{\partial y} = -\frac{1}{\rho} \frac{\partial p}{\partial x} + \mu \left( \frac{\partial^2 v_x}{\partial x^2} + \frac{\partial^2 v_x}{\partial y^2} \right) \quad (11.1-1)$$

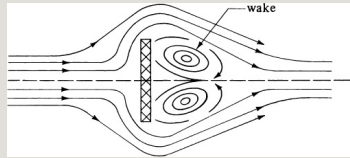


Figure 11.1-2. Flow perpendicular to a flat plate and boundary-layer separation.

$$v_x \frac{\partial v_y}{\partial x} + v_y \frac{\partial v_y}{\partial y} = -\frac{1}{\rho} \frac{\partial p}{\partial y} + \mu \left( \frac{\partial^2 v_y}{\partial x^2} + \frac{\partial^2 v_y}{\partial y^2} \right) \quad (11.1-2)$$

The continuity equation for two-dimensional flow becomes

$$\frac{\partial v_x}{\partial x} + \frac{\partial v_y}{\partial y} = 0 \quad (11.1-3)$$

In Eq. (11.1-1), the term  $(\mu/\rho)(\partial^2 v_x/\partial x^2)$



is negligible in comparison with the other terms in the equation. Also, it can be shown that all the terms containing  $v_y$  and its derivatives are small. Hence, the final two boundary-layer equations to be solved are Eq. (11.1-3) and

$$\begin{aligned} v_x \frac{\partial v_x}{\partial x} + v_y \frac{\partial v_x}{\partial y} = -\frac{1}{\rho} \frac{dp}{dx} \\ + \mu \frac{\partial^2 v_x}{\partial y^2} \end{aligned} \quad (11.1-4)$$

*2. Solution for laminar boundary layer on a flat plate.* An important case in which an analytical solution has been obtained for the boundary-layer equations is for the laminar boundary layer on a flat plate in steady flow, as shown in Fig. 11.1-1. A further simplification can be made in Eq. (11.1-4) in that  $dp/dx$  is zero since  $v_\infty$  is constant.

The final boundary-layer equations reduce to the equation of motion for the  $x$  direction and the continuity equation as follows:

$$\rho v_x \frac{\partial v_x}{\partial x} + \rho v_y \frac{\partial v_x}{\partial y} = \mu \frac{\partial^2 v_x}{\partial y^2} \quad (11.1-5)$$

$$\frac{\partial v_x}{\partial x} + \frac{\partial v_y}{\partial y} = 0 \quad (11.1-3)$$

The boundary conditions are  $v_x = v_y = 0$  at  $y = 0$  ( $y$  is distance from plate), and  $v_x = v_\infty$  at  $y = \infty$ .

The solution of this problem for laminar flow over a flat plate giving  $v_x$  and  $v_y$  as a function of  $x$  and  $y$  was first obtained by Blasius, and later elaborated by Howarth (B1, B2, S3). Although the mathematical details of the solution are quite tedious and complex, and will not be given here, the general procedure

will be outlined. Blasius reduced the two equations to a single ordinary differential equation, which is nonlinear. The equation could not be solved to give a closed form, but a series solution was obtained.

The results of the work by Blasius are given as follows. The boundary-layer thickness  $\delta$ , where  $v_x = 0.99v_\infty$ , is given approximately by

$$\delta = 5.0 \sqrt{x} \sqrt{\nu / v_\infty} = 5.0 \mu \sqrt{x} / \sqrt{\rho v_\infty} \quad (11.1-6)$$

where  $N_{Re,x} = x v_\infty \rho / \mu$ . Hence, as previously stated, the thickness  $\delta$  varies as  $x$ .

The drag in flow past a flat plate consists only of skin friction and is calculated from the shear stress at the surface at  $y = 0$  for any  $x$  as follows:

$$\tau_0 = \mu \left( \frac{\partial v_x}{\partial y} \right)_{y=0} \quad (11.1-7)$$

From the relation of  $v_x$  as a function of  $x$  and  $y$  obtained from the series solution, Eq. (11.1-7) becomes

$$\tau_0 = 0.332 \mu v \infty \rho v \infty \mu x \quad (11.1-8)$$

The total drag is given by the following for a plate of length  $L$  and width  $b$  is

$$F_D = b \int_0^L \tau_0 dx \quad (11.1-9)$$

Substituting Eq. (11.1-8) into (11.1-9) and integrating yields,

$$F_D = 0.664 b \mu \rho v \infty 3L \quad (11.1-10)$$

The drag coefficient  $C_D$  related to the total drag on one side of the plate having an area  $A = bL$  is defined as

$$F_D = C_D v \infty 22 \rho A (11.1-11)$$

Substituting the value for  $A$  and Eq. (11.1-10) into (11.1-11) yields

$$C_D = 1.328 \mu L v \infty \rho = 1.32,8 N_{Re,L}^{1/2} (11.1-12)$$

where  $N_{Re,L} = Lv \infty \rho / \mu$ . A form of Eq. (11.1-11) is used in Section 30.1 for motion of a particle through a fluid. Note that the definition of  $C_D$  in Eq. (11.1-12) is similar to the definition for Fanning friction factor  $f$  for pipes.

The equation derived for  $C_D$  applies to the laminar boundary layer only for  $N_{Re,L}$  less than about  $5 \times 10^5$ . Also, the results are valid only for positions where  $x$  is sufficiently far from the leading edge so that  $x$  or  $L$  is much greater than  $\delta$ . Experimental results on the drag coefficient to a flat plate confirm the

validity of Eq. (11.1-12). Boundary-layer flow past many other shapes has been successfully analyzed using similar methods.

## **11.2 Turbulent Flow**

### **11.2A Nature and Intensity of Turbulence**

*1. Nature of turbulence.* Since turbulent flow is important in many areas of engineering, the nature of turbulence has been extensively investigated. Measurements of the velocity fluctuations of the eddies in turbulent flow have helped explain the theory behind turbulence.

For turbulent flow, there are no exact solutions to flow problems as there are in laminar flow, since the approximate equations used depend on many assumptions. However, useful relations

have been obtained by combining experimental data and theory. Some of these relations will be discussed here.

Turbulence can be generated by the contact between two layers of fluid moving at different velocities or by a flowing stream in contact with a solid boundary, such as a wall or sphere.

When a jet of fluid from an orifice flows into a mass of fluid, turbulence can arise. In turbulent flow at a given place and time, large eddies are continually being formed that break down into smaller eddies and finally disappear.

Eddies can be as small as about 0.1–1 mm and as large as the smallest dimension of the turbulent stream. Flow inside an eddy is laminar because of its large size.

In turbulent flow, the velocity is fluctuating in all directions. In Fig. 11.2-1, a typical plot of the variation of the instantaneous velocity  $v_x$  in the  $x$  direction at a given point in turbulent flow is shown. The velocity  $v_x'$  is the deviation of the velocity from the mean velocity  $\bar{v}_x$  in the  $x$  direction of the stream's flow. Similar relations also hold for the  $y$  and  $z$  directions:

$$v_x = \bar{v}_x + v_x', v_y = \bar{v}_y + v_y', v_z = \bar{v}_z + v_z' \quad (11.2-1)$$

$$\bar{v}_x = \frac{1}{t} \int_0^t v_x dt \quad (11.2-2)$$

where the mean velocity  $\bar{v}_x$  is the time-averaged velocity for time  $t$ ,  $v_x$  the instantaneous total velocity in the  $x$  direction, and  $v_x'$  the instantaneous deviating or fluctuating velocity in the  $x$



direction. These fluctuations can also occur in the  $y$  and  $z$  directions. The value of  $v_x'$  fluctuates about zero as an average and, thus, the time-averaged values are  $\bar{v_x'}=0$ ,  $\bar{v_y'}=0$ ,  $\bar{v_z'}=0$ . However, the values of  $v_x'^2$ ,  $v_y'^2$ , and  $v_z'^2$  as well as their time-averaged values will not be zero. Similar expressions can also be written for pressure, which also fluctuates.

*2. Intensity of turbulence.* The time average of the fluctuating components vanishes over a time period of a few seconds. However, the time average of the squares of the fluctuating components is a positive value. Since the fluctuations are random, the data have been analyzed by statistical methods. The level or intensity of turbulence can be related to the square

root of the sum of the mean squares of the fluctuating components. This intensity of turbulence is an important parameter in the testing of models and the theory of boundary layers.

The intensity of turbulence  $I$  can be defined mathematically as

$$I = \frac{1}{\bar{u}} \sqrt{\frac{1}{3}(\bar{u}'^2 + \bar{v}'^2 + \bar{w}'^2)} \quad (11.2-3)$$

This parameter  $I$  is quite important. Such factors as boundary-layer transition, separation, and heat- and mass-transfer coefficients depend upon the intensity of turbulence. Simulation of turbulent flows in the testing of models requires that the Reynolds number and the intensity of turbulence be the same. One method used to measure intensity of turbulence is to use

a hot-wire anemometer.

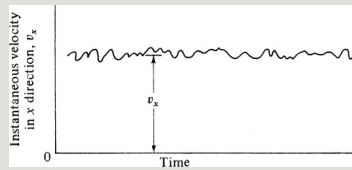


Figure 11.2-1. *Velocity fluctuations in turbulent flow.*

### 11.2B Turbulent Shear or Reynolds Stresses

In a fluid flowing in turbulent flow, shear forces occur wherever there is a velocity gradient across a shear plane, and these are much larger than those occurring in laminar flow. The velocity fluctuations in Eq. (11.2-1) give rise to turbulent shear stresses. The equations of motion and the continuity equation are still valid for turbulent flow. For an incompressible fluid having a constant density  $\rho$  and viscosity  $\mu$ , the continuity equation (8.1-24)

holds:

$$\partial v_x \partial x + \partial v_y \partial y + \partial v_z \partial z = 0 \quad (8.1-24)$$

Also, the  $x$  component of the equation of motion, Eq. (8.2-36), can be written as follows if Eq. (8.1-24) holds:

$$\begin{aligned} \partial(\rho v_x) \partial t + \partial(\rho v_x v_x) \partial x + \partial(\rho v_x v_y) \partial y \\ + \partial(\rho v_x v_z) \partial z = \mu(\partial^2 v_x \partial x^2 + \partial^2 v_x \partial y^2 + \partial^2 v_x \partial z^2) - \\ \partial p \partial x + p g_x \quad (11.2-4) \end{aligned}$$

We can rewrite the continuity equation (8.1-24) and Eq. (11.2-4) by replacing  $v_x$  by  $\bar{v}_x + v_x'$ ,  $v_y$  by  $\bar{v}_y + v_y'$ ,  $v_z$  by  $\bar{v}_z + v_z'$ , and  $p$  by  $\bar{p} + p'$ :

$$\begin{aligned} \partial(\bar{v}_x + v_x') \partial x + \partial(\bar{v}_y + v_y') \partial y + \partial(\bar{v}_z \\ + v_z') \partial z = 0 \quad (11.2-5) \end{aligned}$$

$$\begin{aligned} \partial[\rho(\bar{v}_x + v_x')] \partial t + \partial \rho[(\bar{v}_x + v_x')(\bar{v}_x \\ + v_x')] \partial x + \partial[\rho(\bar{v}_x + v_x')(\bar{v}_y + v_y')] \partial y \end{aligned}$$

$$+\partial[\rho(v^{-}x+vx')(v^{-}z+vz')]\partial z=\mu\nabla^2(v^{-}x+vx')-\partial(p^{-}+p')\partial x+\rho g_x(11.2-6)$$

Now, we use the fact that the time-averaged value of the fluctuating velocities is zero ( $v^{-}x', v^{-}y', v^{-}z'$  are zero), and that the time-averaged product  $v x' v y'^{-}$  is not zero. Then, Eqs. (11.2-5) and (11.2-6) become

$$\partial v^{-}x \partial x + \partial v^{-}y \partial y + \partial v^{-}z \partial z = 0(11.2-7)$$

$$\begin{aligned} & \partial(\rho v^{-}x) \partial t + \partial(\rho v^{-}x v^{-}x) \partial x \\ & + \partial(\rho v^{-}x v^{-}y) \partial y + \partial(\rho v^{-}x v^{-}z) \partial z + [\partial(\rho v x' \\ & \quad 'v x'^{-}) \partial x + \partial(\rho v x' v y'^{-}) \partial y + \partial(\rho v x' v z' \\ & \quad '^{-}) \partial z] = \mu \nabla^2 v^{-}x - \partial p^{-} \partial x + \rho g_x(11.2-8) \end{aligned}$$

By comparing these two time-smoothed equations with Eqs. (8.1-24) and (11.2-4), we see that the time-smoothed values everywhere replace the instantaneous values. However, in Eq.

(11.2-8) new terms arise in the set of brackets that are related to turbulent velocity fluctuations. For convenience, we use the notation

$$\begin{aligned}\bar{\tau}_{xxt} &= \rho \overline{v_x' v_x'}, \bar{\tau}_{yxt} = \rho \overline{v_x' v_y'} \\ \bar{\tau}_{zxt} &= \rho \overline{v_x' v_z'}\end{aligned}\quad (11.2-9)$$

These are the components of the turbulent momentum flux and are called *Reynolds stresses*.

### 11.2C Prandtl Mixing Length

The equations derived for turbulent flow must be solved to obtain the velocity profiles for turbulent flow. To do this, more simplifications must be made before the expressions for the Reynolds stresses can be evaluated. A number of semi-empirical equations have been used.

For example, the eddy-diffusivity model of Boussinesq is one of the earliest attempts to evaluate these stresses. By using the analogy to the equation for shear stress in laminar flow,  $\tau_{yx} = -\mu(dv_x/dy)$ , the turbulent shear stress can be written as

$$\tau_{yx} = -\eta_t dv_x/dy \quad (11.2-10)$$

where  $\eta_t$  is a turbulent or eddy viscosity, which is a strong function of position and flow. This equation can also be written as follows:

$$\tau_{yx} = -\rho \epsilon_t dv_x/dy \quad (11.2-11)$$

where  $\epsilon_t = \eta_t/\rho$  is eddy diffusivity of momentum, by analogy to the momentum diffusivity  $\mu/\rho$  for laminar flow.

In his mixing-length model, Prandtl developed an expression to evaluate these stresses by assuming that eddies move in a fluid in a manner similar to the movement of molecules in a gas. The eddies move a distance called the mixing length  $L$  before they lose their identity. However, in the definition of the Prandtl mixing length  $L$ , this small packet of fluid is assumed to retain its identity while traveling the entire length  $L$  and then lose its identity or be absorbed in the host region.

Prandtl assumed that the velocity fluctuation  $v_x'$  is due to a “lump” of fluid moving a distance  $L$  in the  $y$  direction and retaining its mean velocity. At point  $L$ , the lump of fluid will differ in mean velocity from the adjacent fluid by  $v_x|_{y+L} - v_x|_y$ . Thus,



the value of  $v_x'$  is

$$v_x|_{y'} = v_x|_{y+L} - v_x|_y \quad (11.2-12)$$

The length  $L$  is small enough that the velocity difference can be written as

$$v_x|_{y'} = v_x|_{y+L} - v_x|_y \\ = L dv_x/dy \quad (11.2-13)$$

Hence,

$$v_x' = L dv_x/dy \quad (11.2-14)$$

Prandtl also assumed that  $v_x' \approx v_y'$ .

Using this identity, the time average,  $\overline{v_x' v_y'}$ , can be expressed as

$$\overline{v_x' v_y'} = -L^2 |dv_x/dy| dv_x/dy \quad (11.2-15)$$

The minus sign and the absolute value were used to make the quantity  $\overline{v_x' v_y'}$

agree with experimental data.

Substituting Eq. (11.2-15) into (11.2-9),

$$\tau_{yx} = -\rho L^2 \frac{dv_x}{dy} \frac{dv_x}{dy} \quad (11.2-16)$$

Comparing with Eq. (11.2-11),

$$\epsilon_t = L^2 \frac{dv_x}{dy} \frac{dv_x}{dy} \quad (11.2-17)$$

### **11.2D Universal Velocity Distribution in Turbulent Flow**

To determine the velocity distribution for turbulent flow at steady state inside a circular tube, we divide the fluid inside the pipe into two regions: (1) a central core where the Reynolds stress approximately equals the shear stress; and (2) a thin, viscous sublayer adjacent to the wall where the shear stress is due only to viscous shear and where the turbulence effects are assumed

negligible. Later, we identify a third region known as the *buffer zone*, where both stresses are important.

Dropping the subscripts and superscripts on the shear stresses and velocity, and considering the thin, viscous sublayer, we can write

$$\tau_0 = -\mu dv/dy \quad (11.2-18)$$

where  $\tau_0$  is assumed constant in this region. Upon integration,

$$\tau_0 y = \mu v \quad (11.2-19)$$

Defining a friction velocity  $v^*$  as follows and substituting into Eq. (11.2-19),

$$v^* = \tau_0 / \mu \quad (11.2.20)$$

$$v^+ = y^+ \mu / \rho (11.2-21)$$

The dimensionless velocity ratio on the left can be written as

$$v^+ = v \rho \tau_0 / \mu \quad (\text{SI}) \quad v^+ = v \rho \tau_0 g_c / \mu \quad (\text{English})$$

(11.2-22)

The dimensionless number on the right can be written as

$$y^+ = \tau_0 \rho \mu y \quad (\text{SI}) \quad y^+ = \tau_0 g_c \rho \mu y \quad (\text{English})$$

(11.2-23)

where  $y$  is the distance from the wall of the tube. For a tube of radius  $r_0$ ,  $y = r_0 - r$ , where  $r$  is the distance from the center. Hence, for the viscous sublayer, the velocity distribution is

$$v^+ = y^+ (11.2-24)$$

Next, considering the turbulent core where any viscous stresses are neglected, Eq. (11.2-16) becomes

$$\tau = \rho L^2 \left( \frac{dv}{dy} \right)^2 \quad (11.2-25)$$

where  $dy/dy$  is always positive and the absolute value sign is dropped. Prandtl assumed that the mixing length is proportional to the distance from the wall, or

$$L = Ky \quad (11.2-26)$$

and that  $\tau = \tau_0 = \text{constant}$ . Equation (11.2-25) now becomes

$$\tau_0 = \rho K^2 y^2 \left( \frac{dv}{dy} \right)^2 \quad (11.2-27)$$

Hence,

$$v^* = Ky \frac{dv}{dy} \quad (11.2-28)$$

Upon integration,

$$v^* \ln y = K v + K_1 \quad (11.2-29)$$

where  $K_1$  is a constant. The constant  $K_1$  can be found by assuming that  $y$  is zero at a small value of  $y$ , for example  $y_0$ :

$$v v^* = v + = 1 K \ln y y_0 \quad (11.2-30)$$

Introducing the variable  $y_+$  by multiplying the numerator and denominator of the term  $y/y_0$  by  $v^*/v$ , where  $v = \mu/\rho$ , we obtain

$$v + = 1 K (\ln y v^* v - \ln y_0 V^* v) \quad (11.2-31)$$

$$v + = 1 K \ln y + + C_1 \quad (11.2-32)$$

A large amount of velocity distribution data by Nikuradse and others for a range of Reynolds numbers of 4000 to  $3.2 \times$

106 have been obtained, and the data fit Eq. (11.2-24) in the region up to  $y^+$  of 5 and also fit Eq. (11.2-32) above  $y^+$  of 30, with  $K$  and  $C_1$  being universal constants. For the region of  $y^+$  from 5 to 30, which is defined as the buffer region, an empirical equation of the form of Eq. (11.2-32) fits the data. In Fig. 11.2-2, the following relations that are valid are plotted to give a universal velocity profile for fluids flowing in smooth, circular tubes:

$$v^+ = y^+ \quad (0 < y^+ < 5) \quad (11.2-33)$$

$$v^+ = 5.0 \ln y^+ - 3.05 \quad (5 < y^+ < 30) \quad (11.2-34)$$

$$v^+ = 2.5 \ln y^+ + 5.5 \quad (30 < y^+) \quad (11.2-35)$$

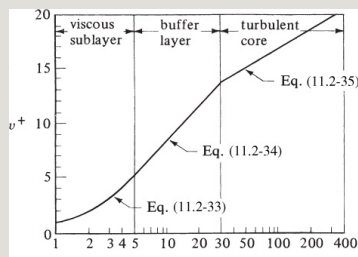


Figure 11.2-2. *Universal velocity profile for turbulent flow in smooth circular tubes.*

Three distinct regions are apparent in Fig. 11.2-2. The first region next to the wall is the *viscous sublayer* (historically called “laminar” sublayer), given by Eq. (11.2-33), where the velocity is proportional to the distance from the wall. The second region, called the *buffer layer*, is given by Eq. (11.2-34) and is a region of transition between the viscous sublayer with practically no eddy activity and the violent eddy activity in the *turbulent core region* given by Eq. (11.2-35). These equations can then be used and related to the Fanning friction factor discussed earlier



in this chapter. They can also be used in solving turbulent boundary-layer problems. Note that the values for  $y_+ = 5$  and  $y_+ = 30$  are approximately the same, regardless of which expression is used.

## **11.3 Turbulent Boundary-Layer Analysis**

### **11.3A Integral Momentum Balance for Boundary-Layer Analysis**

*1. Introduction and derivation of integral expression.* In the solution for the laminar boundary layer on a flat plate, the Blasius solution is quite restrictive, since it is only for laminar flow over a flat plate. Other systems, which may be more complex, cannot be solved by this method. An approximate method developed by von Kármán can be used when the configuration is more complicated or if the flow is

turbulent. This is an approximate momentum integral analysis of the boundary layer using an empirical or assumed velocity distribution.

In order to derive the basic equation for a laminar or turbulent boundary layer, a small control volume in the boundary layer on a flat plate is used, as shown in Fig. 11.3-1. The depth in the  $z$  direction is  $b$ . Flow is only through the surfaces  $A_1$  and  $A_2$ , as well as from the top curved surface at  $\delta$ . An overall integral momentum balance using Eq. (4.3-8) and overall integral mass balance using Eq. (4.1-6) are applied to the control volume inside the boundary layer at steady state, and the final integral expression by von Kármán is (B2, S3)

$$\tau_0 = \frac{d}{dx} \int_0^\delta \rho v_x (v_\infty - v_x) dy \quad (11.3-1)$$

where  $\tau_0$  is the shear stress at the surface  $y = 0$  at point  $x$  along the plate. Also,  $\delta$  and  $\tau_0$  are functions of  $x$ .

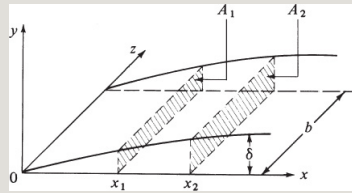


Figure 11.3-1. Control volume for integral analysis of the boundary-layer flow.

Equation (11.3-1) is an expression whose solution requires knowledge of the velocity  $v_x$  as a function of the distance from the surface,  $y$ . The accuracy of the results will, of course, depend on how closely the assumed velocity profile approaches the actual profile.

## 2. Integral momentum balance for a

*laminar boundary layer*. Before we use Eq. (11.3-1) for the turbulent boundary layer, this equation will be applied to the laminar boundary layer over a flat plate so that the results can be compared with the exact Blasius solution in Eqs. (11.1-6)–(11.1-12).

In this analysis, certain boundary conditions must be satisfied in the boundary layer:

$$v_x = 0 \text{ at } y = 0 \quad v_x \cong v_\infty \text{ at } y = \delta \quad v_x dy \cong 0 \text{ at } y = \delta \quad (11.3-2)$$

The conditions above are fulfilled using the following simple, assumed velocity profile:

$$v_x v_\infty = 3/2 y \delta - 1/2 (y/\delta)^3 \quad (11.3-3)$$

The shear stress  $\tau_0$  at a given  $x$  can be

obtained from

$$\tau_0 = \mu \left( \frac{dv_x}{dy} \right)_{y=0} \quad (11.3-4)$$

Differentiating Eq. (11.3-3) with respect to  $y$  and setting  $y = 0$ ,

$$\left( \frac{dv_x}{dy} \right)_{y=0} = 3v \propto 2\delta \quad (11.3-5)$$

Substituting Eq. (11.3-5) into (11.3-4),

$$\tau_0 = 3\mu v \propto 2\delta \quad (11.3-6)$$

Substituting Eq. (11.3-3) into Eq. (11.3-1) and integrating between  $y = 0$  and  $y = \delta$ , we obtain

$$\frac{d\delta}{dx} = \frac{28039}{9} \tau_0 v \propto 2\rho \quad (11.3-7)$$

Combining Eqs. (11.3-6) and (11.3-7), and integrating between  $\delta = 0$  and  $\delta = \delta$ , and  $x = 0$  and  $x = L$ ,

$$\delta = 4.64 \mu L \rho v \propto (11.3-8)$$

where the length of plate is  $x = L$ .

Proceeding in a manner similar to Eqs. (11.1-6)–(11.1-12), the drag coefficient is

$$C_D = 1.292 \mu L v \propto \rho = 1.292 N \text{Re} L^{1/2} (11.3-9)$$

A comparison of Eq. (11.1-6) with (11.3-8) and Eq. (11.1-12) with (11.3-9) shows the success of this method. Only the numerical constants differ slightly. This method can be used with reasonable accuracy for cases where an exact analysis is not feasible.

*3. Integral momentum analysis for turbulent boundary layer.* The procedures used for the integral momentum analysis for a laminar boundary layer can be applied to the

turbulent boundary layer on a flat plate. A simple empirical velocity distribution for pipe flow that is valid up to a Reynolds number of  $10^5$  can be adapted for the boundary layer on a flat plate, to become

$$v/v_\infty = (y/\delta)^{1/7} \quad (11.3-10)$$

This is known as the Blasius 1/7-power-law velocity profile, which is often used in turbulent-flow modeling.

Equation (11.3-10) is substituted into the integral relation equation (11.3-1):

$$\frac{d}{dx} \int_0^\delta v_\infty \left[ 2 \left( \frac{y}{\delta} \right)^{1/7} - \left( \frac{y}{\delta} \right)^{2/7} \right] dy = \frac{\tau_0}{\rho} \quad (11.3-11)$$

The power-law equation does not hold as  $y$  goes to zero at the wall. Another useful relation is the Blasius correlation

for shear stress for pipe flow, which is consistent at the wall for the wall shear stress  $\tau_0$ . For boundary-layer flow over a flat plate, it becomes

$$\tau_0 \rho v \propto 2 = 0.023 (\delta v \propto \rho \mu)^{-1/4} \quad (11.3-12)$$

Integrating Eq. (11.3-11), combining the result with Eq. (11.3-12), and integrating between  $\delta = 0$  and  $\delta = \delta$ , and  $x = 0$  and  $x = L$ ,

$$76 (L v \propto \rho \mu)^{-1/5} L = 0.376 L N_{Re,L}^{1/5} \quad (11.3-13)$$

Integration of the drag force as before yields

$$C_D = 0.072 N_{Re,L}^{-1/2} \quad (11.3-14)$$

In this development, the turbulent boundary layer was assumed to extend to  $x = 0$ . However, a certain length at the



front leading edge has a laminar boundary layer. Experimental data agree with Eq. (11.3-14) reasonably well from a Reynolds number of  $5 \times 10^5$  to  $10^7$ . More accurate results at higher Reynolds numbers can be obtained by using a logarithmic velocity distribution, Eqs. (11.2-33)–(11.2-35).

## **11.4 Chapter Summary**

In this chapter, we have introduced the concepts of boundary layers and turbulent flow. Boundary layers were introduced as characteristic of fluid flow past a flat plate. It was shown that the region near the surface of a flat plate can be modeled using boundary-layer theory and that the region far from the surface can be modeled using inviscid flow. Models based on Blasius were used to

calculate the boundary-layer thickness, shear stress, drag force, and drag coefficient as a function of distance from the leading edge.

The concept of turbulent flow was introduced by decomposing the instantaneous fluid velocity into a time-average mean velocity and a velocity fluctuation. This decomposition was used to develop time-averaged forms of the equation of continuity and the Navier–Stokes equation to model flow behavior in turbulent flow. Furthermore, these models were extended to determine the universal velocity profiles in pipes.

Finally, the integral momentum balance approach of von Kármán was introduced to determine turbulent boundary-layer

characteristics, such as boundary-layer thickness, shear stress, and drag force at the surface.

## Problems

**11.1-1. *Laminar Boundary Layer on Flat Plate.*** Water at 20°C is flowing past a flat plate at 0.914 m/s. The plate is 0.305 m wide.

- Calculate the Reynolds number 0.305 m from the leading edge to determine if the flow is laminar.
- Calculate the boundary-layer thickness at  $x = 0.152$  and  $x = 0.305$  m from the leading edge.
- Calculate the total drag on the 0.305-m-long plate.

**Ans.** (a)  $N_{Re,L} = 2.77 \times 10^5$ ; (b)  $\delta = 0.0029$  m at  $x = 0.305$  m

**11.1-2. *Air Flow Past a Plate.*** Air at 294.3 K and 101.3 kPa is flowing past a flat plate at 6.1 m/s. Calculate the

thickness of the boundary layer at a distance of 0.3 m from the leading edge and the total drag for a 0.3-m-wide plate.

**11.1-3. *Boundary-Layer Flow Past a Plate.*** Water at 293 K is flowing past a flat plate at 0.5 m/s. Do as follows:

- Calculate the boundary-layer thickness in m at a point 0.1 m from the leading edge.
- At the same point, calculate the point shear stress  $\tau_0$ . Also calculate the total drag coefficient.

**11.3-1. *Transition Point to a Turbulent Boundary Layer.*** Air at 101.3 kPa and 293 K is flowing past a smooth, flat plate at 100 ft/s. The turbulence in the air stream is such that the transition from a laminar to a turbulent boundary layer occurs at  $N_{Re,L} = 5 \times 10^5$ .

- Calculate the distance from the leading edge where

the transition occurs.

- Calculate the boundary-layer thickness  $\delta$  at a distance of 0.5 ft and 3.0 ft from the leading edge. Also calculate the drag coefficient for both distances  $L = 0.5$  and 3.0 ft.

## References

## Notation

# Chapter 12. Introduction to Heat Transfer

## 12.0 Chapter Objectives

On completion of this chapter, a student should be able to:

- Use both the American and SI units of energy when solving heat-transfer problems
- Apply the principle of conservation of energy (i.e., energy balance) for reacting and nonreacting systems
- Recognize that a temperature difference is the driving potential for heat transfer
- Know the difference between a heat flux and a heat rate
- Realize that heat transfer may occur by one of the three basic mechanisms of heat transfer: conduction, convection, and radiation
- Understand the basics of Fourier's law and its similarity to other rate-transfer processes
- Explain the physical significance of thermal conductivity and its basic mechanisms in gases, liquids, and solids

- Use Newton's Law of Cooling to solve for heat flux generated by convection
- Explain the physical significance of a heat-transfer coefficient
- Use the Stefan–Boltzmann equation to solve for the heat flux generated by radiation
- Solve problems in which heat is transferred by conduction in different materials/fluids in series or in parallel

## **12.1 Energy and Heat Units**

### **12.1A Joule, Calorie, and Btu**

In a manner similar to that used in preforming material balances on chemical and biological processes, we can also preform energy balances on a process. Often, a large portion of the energy entering or leaving a system is in the form of heat. Before such energy or heat balances are made, we must understand the various types of energy and heat units.

In the SI system, energy is given in joules (J) or kilojoules (kJ). Energy is also expressed in btu (British thermal units) or cal (calories). The calorie (abbreviated as cal) is defined as the amount of heat needed to heat 1.0 g water 1.0°C (from 14.5°C to 15.5°C). Also, 1 kcal (kilocalorie) = 1000 cal. The btu is defined as the amount of heat needed to raise 1.0 lb water 1°F. Hence, from the conversion factors given in Appendix A.1,

$$1 \text{ btu} = 252.16 \text{ cal} = 1.05506 \text{ kJ} \quad (12.1-1)$$

### 12.1B Heat Capacity

The *heat capacity* of a substance is defined as the amount of energy necessary to raise its temperature by 1 degree. It can be expressed for 1 g, 1 lb, 1 g mol, 1 kg mol, or 1 lb mol



of the substance. For example, heat capacity can be expressed in SI units as  $\text{J/kg mol} \cdot \text{K}$ ; in other units, it can be expressed as  $\text{cal/g} \cdot ^\circ\text{C}$ ,  $\text{cal/g mol} \cdot ^\circ\text{C}$ ,  $\text{kcal/kg mol} \cdot ^\circ\text{C}$ ,  $\text{btu/lb}_m \cdot ^\circ\text{F}$ , or  $\text{btu/lb mol} \cdot ^\circ\text{F}$ .

It can be shown that the actual numerical value of a heat capacity is the same in mass units or in molar units. That is,

$$1.0 \text{ cal/g} \cdot ^\circ\text{C} = 1.0 \text{ btu/lb}_m \cdot ^\circ\text{F} \quad (12.1-2)$$

$$1.0 \text{ cal/g mol} \cdot ^\circ\text{C} = 1.0 \text{ btu/lb mol} \cdot ^\circ\text{F} \quad (12.1-3)$$

For example, to prove this, suppose that a substance has a heat capacity of  $0.8 \text{ btu/lb}_m \cdot ^\circ\text{F}$ . The conversion is made using  $1.8^\circ\text{F}$  for  $1^\circ\text{C}$  or  $1 \text{ K}$ ,  $252.16 \text{ cal}$  for  $1 \text{ btu}$ , and  $453.6 \text{ g}$  for  $1 \text{ lb}_m$ , as

follows:

$$\begin{aligned}\text{heat capacity}[\text{cal g}^{-1}\cdot^{\circ}\text{C}^{-1}] &= (\text{cal g}^{-1}\cdot^{\circ}\text{C}^{-1}) = (0.8\text{bm}^{\circ}\text{F}) \\ & (252.16\text{calbm}^{-1})(1453.6\text{g/bm}) \\ & (1.8^{\circ}\text{F}^{\circ}\text{C}^{-1}) = 0.8\text{cal g}^{-1}\cdot^{\circ}\text{C}^{-1}\end{aligned}$$

The heat capacities of gases (sometimes called *specific heat*) at constant pressure  $c_p$  are functions of temperature and for engineering purposes can be assumed to be independent of pressure up to several atmospheres. In most process engineering calculations, one is usually interested in the amount of heat needed to heat a gas from one temperature  $t_1$  to another at  $t_2$ . Since the  $c_p$  varies with temperature, an integration must be performed or a suitable mean  $c_{pm}$  used. These mean values for gases have been obtained for  $T_1$  of 298 K or 25°C (77°F) and various  $T_2$  values, and are tabulated

in Table 12.1-1 at 101.325 kPa pressure or less as  $c_{pm}$  in kJ/kg mol · K at various values of  $T_2$  in K or °C.

---

**EXAMPLE 12.1-1. Heating of N<sub>2</sub> Gas**

The gas N<sub>2</sub> at 1 atm pressure absolute is being heated in a heat exchanger. Calculate the amount of heat needed in J to heat 3.0 g mol N<sub>2</sub> in the following temperature ranges:

- 298–673 K (25–400°C)
- 298–1123 K (25–850°C)
- 673–1123 K (400–850°C)

**Solution:** For case (a), Table 12.1-1 gives  $c_{pm}$  values at 1 atm pressure or less, which can be used up to several atm pressures. For N<sub>2</sub> at 673 K,  $c_{pm} = 29.68$  kJ/kg mol · K or 29.68 J/g mol · K. This is the mean heat capacity for the range 298–673 K:

$$\Delta H = m C_{pm} \Delta T = \text{heat required} = M \text{ g mol } (c_{pm} \text{ J/g mol } \cdot \text{K}) (T_2 - T_1) \text{ K} \quad (12.1-4)$$

Substituting the known values,

$$\begin{aligned} \text{heat required} &= (3 \text{ mole}) (29.68 \text{ J/mole} \cdot \text{K}) \\ &\quad (673 \text{ K} - 298 \text{ K}) = 33\,390 \text{ J} \end{aligned}$$

For case (b), the  $c_{pm}$  at 1123 K (obtained by linear interpolation between 1073 and 1173 K) is 31.00 J/g mol · K:

$$\begin{aligned} \text{heat required} &= (3 \text{ mole}) (31.00 \text{ J/mole} \cdot \text{K}) \\ &\quad (1123 \text{ K} - 298 \text{ K}) = 76\,725 \text{ J} \end{aligned}$$

For case (c), there is no mean heat capacity for the interval 673–1123 K. However, we can use the heat required to heat the gas from 298 to 673 K in case (a) and subtract it from case (b), which includes the heat to go from 298 to

673 K plus 673 to 1123 K:

heat required (673-1123K)=heat required (298-1123K)– heat required (298-673K)

Substituting the proper values into Eq. (12.1-5),

$$\text{heat required} = 76\,725\text{ J} - 33\,390\text{ J} = 43\,335\text{ J}$$

---

**Table 12.1-1. *Mean Molar Heat Capacities of Gases Between 298 and TK (25 and T°C) at 101.325 kPa or Less (SI Units:  $c_p = \text{kJ/kg mol} \cdot \text{K}$ )***

***Mean Molar Heat Capacities of Gases Between 25 and T°C at 1 atm Pressure or Less (English Units:  $c_p = \text{btu/lb mol } \mu \text{ } ^\circ\text{F}$ )***

*Source:* O. A. Hougen, K. W. Watson, and R. A. Ragatz, *Chemical Process Principles*, Part I, 2nd ed. New York: John Wiley & Sons, Inc., 1954.

When heating a gas mixture, the total

heat required is determined by first calculating the heat required for each individual component and then adding the results to obtain the total.

The heat capacities of solids and liquids are also functions of temperature and independent of pressure. Data are given in Appendix A.2, Physical Properties of Water; A.3, Physical Properties of Inorganic and Organic Compounds; and A.4, Physical Properties of Foods and Biological Materials. More data are available in (P1).

**EXAMPLE 12.1-2. Heating of Milk**

Rich cows' milk (4536 kg/h) at 4.4°C is being heated in a heat exchanger to 54.4°C by hot water. How much heat is needed?

**Solution:** From Appendix A.4, the average heat capacity of rich cows' milk is 3.85 kJ/kg · K. Temperature rise  $\Delta T = (54.4 - 4.4)^\circ\text{C} = 50 \text{ K}$ .

$$\text{heat required} = (4536 \text{ kg/h})(3.85 \text{ kJ/kg} \cdot \text{K})(1/3600 \text{ h/s})(50 \text{ K}) = 242.5 \text{ kW}$$

The enthalpy,  $H$ , of a substance in J/kg represents the sum of the internal energy plus the pressure–volume term. For no reaction and a constant-pressure process with a change in temperature, the heat change as computed from Eq. (12.1-4) is the difference in enthalpy,  $\Delta H$ , of the substance relative to a given temperature or base point. In other units,  $H = \text{btu/lb}_m$  or  $\text{cal/g}$ .

### 12.1C Latent Heat and Steam Tables

Whenever a substance undergoes a change of phase, relatively large amounts of heat change are involved at a constant temperature. For example, ice at  $0^\circ\text{C}$  and 1 atm pressure can absorb  $6013.4 \text{ kJ/kg mol}$ . This enthalpy change is called the *latent heat of fusion*. Data for other compounds are available in

various handbooks (P1, W1).

When a liquid phase vaporizes to a vapor phase under its vapor pressure at constant temperature, an amount of heat called the *latent heat of vaporization* must be added. Tabulations of latent heats of vaporization are given in various handbooks. For water at 25°C and a pressure of 23.75 mm Hg, the latent heat is 44 020 kJ/kg mol, and at 25°C and 760 mm Hg, 44 045 kJ/kg mol. Hence, the effect of pressure can be neglected in engineering calculations. However, there is a large effect of temperature on the latent heat of water. Also, the effect of pressure on the heat capacity of liquid water is small and can also be neglected.

Since water is a very common chemical,

its thermodynamic properties have been compiled in steam tables and are given in Appendix A.2 in SI and in English units.

**EXAMPLE 12.1-3. Use of Steam Tables**

Find the enthalpy change (i.e., how much heat must be added) for each of the following cases using SI and English units:

- Heating 1 kg (lbm) water from 21.11°C (70°F) to 60°C (140°F) at 101.325 kPa (1 atm) pressure.
- Heating 1 kg (lbm) water from 21.11°C (70°F) to 115.6°C (240°F) and vaporizing at 172.2 kPa (24.97 psia).
- Vaporizing 1 kg (lbm) water at 115.6°C (240°F) and 172.2 kPa (24.97 psia).

**Solution:** For part (a), the effect of pressure on the enthalpy of liquid water is negligible. From Appendix A.2,

$$\begin{aligned} H \text{ at } 21.11^\circ\text{C} &= 88.60 \text{ kJ/kg or at } 70^\circ\text{F} = 38.09 \text{ btu/lbm} \\ H \text{ at } 60^\circ\text{C} &= 251.13 \text{ kJ/kg or at } 140^\circ\text{F} = 107.96 \text{ btu/lbm} \\ \text{change in } H &= \Delta H = 251.13 - 88.60 = 162.53 \text{ kJ/kg} \\ &= 107.96 - 38.09 = 69.87 \text{ btu/lbm} \end{aligned}$$

In part (b), the enthalpy at 115.6°C (240°F) and 172.2 kPa (24.97 psia) of the saturated vapor is 2699.9 kJ/kg or 1160.7 btu/lbm.

$$\begin{aligned} \text{change in } H &= \Delta H = 2699.9 - 88.60 = 2611.3 \text{ kJ/kg} \\ &= 1160.7 - 38.09 = 1122.6 \text{ btu/lbm} \end{aligned}$$

The latent heat of water at 115.6°C (240°F) in part (c) is

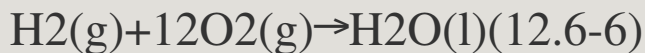
$$\begin{aligned} &2699.9 - 484.9 = 2215.0 \text{ kJ/kg} \\ &1160.7 - 208.44 = 952.26 \text{ btu/lbm} \end{aligned}$$



## 12.1D Heat of Reaction

When chemical reactions occur, heat effects always accompany these reactions. This area where energy changes occur is often called *thermochemistry*. For example, when HCl is neutralized with NaOH, heat is given off and the reaction is exothermic. Heat is absorbed in an endothermic reaction. This heat of reaction is dependent on the chemical nature of each reacting material and product, and on their physical states.

For purposes of organizing data, we define a standard heat of reaction  $\Delta H_0$  as the change in enthalpy when 1 kg mol reacts under a pressure of 101.325 kPa at a temperature of 298 K (25°C). For example, for the reaction



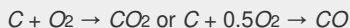
the  $\Delta H_0$  is  $-285.840 \times 10^3 \text{ kJ/kg mol}$  or  $-68.317 \text{ kcal/g mol}$ . The reaction is exothermic and the value is negative since the reaction loses enthalpy. In this case, the  $\text{H}_2$  gas reacts with the  $\text{O}_2$  gas to give liquid water, all at 298 K (25°C).

Special names are given to  $\Delta H_0$  depending upon the type of reaction. When the product is formed from the elements, as in Eq. (12.1-6), we call the  $\Delta H_0$  the *heat of formation* of the product water,  $\Delta H_{f0}$ . For the combustion of  $\text{CH}_4$  to form  $\text{CO}_2$  and  $\text{H}_2\text{O}$ , we call it the *heat of combustion*,  $\Delta H_{c0}$ . Data are given in Appendix A.3 for various values of  $\Delta H_{c0}$ .

**EXAMPLE 12.1-4. Combustion of Carbon**

A total of 10.0 g mol of carbon graphite is burned in a

calorimeter held at 298 K and 1 atm. The combustion is incomplete and 90% of the C goes to CO<sub>2</sub> and 10% goes to CO. What is the total enthalpy change in kJ and kcal?



**Solution:** From Appendix A.3 the  $\Delta H_f^\circ$  for carbon going to CO<sub>2</sub> is  $-393.513 \times 10^3$  kJ/kg mol or  $-94.0518$  kcal/g mol, and for carbon going to CO, it is  $-110.523 \times 10^3$  kJ/kg mol or  $-26.4157$  kcal/g mol. Since 9 mol CO<sub>2</sub> and 1 mol CO are formed,

$$\begin{aligned} \text{Total } \Delta H &= 9 \text{ gmo1}(-393.513 \text{ kJ/gmo1}) + 1 \text{ gmo1}(-110.523 \text{ kJ/g mol}) \\ &= -3652 \text{ kJ} = 9(-94.0518) + 1(-26.4157) = -872.9 \text{ kcal} \end{aligned}$$

If a table of heats of formation,  $\Delta H_f^\circ$  of compounds is available, the standard heat of the reaction,  $\Delta H^\circ$ , can be calculated by

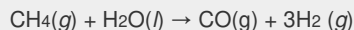
$$\Delta H^\circ = \sum \Delta H_f^\circ(\text{products}) - \sum \Delta H_f^\circ(\text{reactants}) \quad (12.1-7)$$

In Appendix A.3, a short table of some values of  $\Delta H_f^\circ$  is given. Other data are also available (H1, P1, S1).

**EXAMPLE 12.1-5. Reaction of Methane**

For the following reaction of 1 kg mol of CH<sub>4</sub> at 101.32 kPa

and 298 K,



calculate the standard heat of reaction  $\Delta H^\circ$  at 298 K in kJ.

**Solution:** From Appendix A.3, the following standard heats of formation are obtained at 298 K:

$$\Delta H_f^\circ (\text{kJ/kg mol}) \begin{matrix} \text{CH}_4(g) & -74.848 & \times 10^3 \\ \text{H}_2\text{O}(l) & -285.840 & \times 10^3 \\ \text{H}_2(g) & 0 & \end{matrix}$$

Note that the  $\Delta H_f^\circ$  of all elements is, by definition, zero. Substituting into Eq. (12.1-7),

$$\begin{aligned} \Delta H^\circ &= [-110.523 \times 10^3 - 3(0)] - \\ &(-74.848 \times 10^3 - 285.840 \times 10^3) = +250.165 \times 10^3 \text{ kJ} \\ &\text{kg mol CH}_4 \text{ (endothermic)} \end{aligned}$$

## 12.2 Conservation of Energy and Heat Balances

### 12.2A Conservation of Energy

In making material balances, we used the law of conservation of mass, which states that the mass entering is equal to the mass leaving plus the mass left in the process. In a similar manner, we can state the *law of conservation of energy*, which says that all energy entering a process is equal to that leaving plus

that left in the process. In this section, elementary heat balances will be made.

Energy can appear in many forms. Some of the common forms are enthalpy, electrical energy, chemical energy (in terms of  $\Delta H$  reaction), kinetic energy, potential energy, work, and heat inflow.

$$\Delta H + \Delta E_k + \Delta E_p = q - W \quad (12.2-1)$$

In many cases in process engineering, which often take place at constant pressure, electrical energy, kinetic energy, potential energy, and work either are not present or can be neglected. Then, only the enthalpy of the materials (at constant pressure), the standard chemical reaction energy ( $\Delta H_0$ ) at 25°C, and the heat added or removed

must be taken into account in the energy balance. This is generally called a *heat balance*.

$$\Delta H = q \quad (12.2-2)$$

### 12.2B Heat Balances

To make a heat balance at steady state we use methods similar to those used to make a material balance. The energy or heat coming into a process in the inlet materials, plus any net energy added to the process, are equal to the energy leaving the materials. Expressed mathematically,

$$\sum H_R + (-\Delta H_{2980}) + q = \sum H_P \quad (12.2-3)$$

where  $\sum H_R$  is the sum of enthalpies of all materials entering the reaction process relative to the reference state for

the standard heat of reaction at 298 K and 101.32 kPa. If the inlet temperature is above 298 K, this sum will be positive.  $\Delta H_{2980}$  = the standard heat of the reaction at 298 K and 101.32 kPa.

The reaction contributes heat to the process, so the negative of  $\Delta H_{2980}$  is taken to be positive input heat for an exothermic reaction. Also,  $q$  = net energy or heat added to the system. If heat leaves the system, this item will be negative.  $\Sigma H_R$  = sum of enthalpies of all leaving materials referred to the standard reference state at 298 K (25°C).

Note that if the materials coming into a process are below 298 K,  $\Sigma H_R$  will be negative. Care must be taken not to confuse the signs of the items in Eq. (12.2-3). If no chemical reaction occurs,

then simple heating, cooling, or phase change is occurring. Use of Eq. (12.2-3) will be illustrated by several examples. For convenience, it is common practice to call the terms on the left side of Eq. (12.2-3) input items, and those on the right, output items.

**EXAMPLE 12.2-1. Heating of Fermentation Medium**

A liquid fermentation medium at 30°C is pumped at a rate of 2000 kg/h through a heater, where it is heated to 70°C under pressure. The waste-heat water used to heat this medium enters at 95°C and leaves at 85°C. The average heat capacity of the fermentation medium is 4.06 kJ/kg · K, and that for water is 4.21 kJ/kg · K (Appendix A.2). The fermentation stream and the wastewater stream are separated by a metal surface through which heat is transferred and they do not physically mix with each other. Make a complete heat balance on the system. Calculate the water flow and the amount of heat added to the fermentation medium assuming no heat losses. The process flow is given in Fig. 12.2-1.



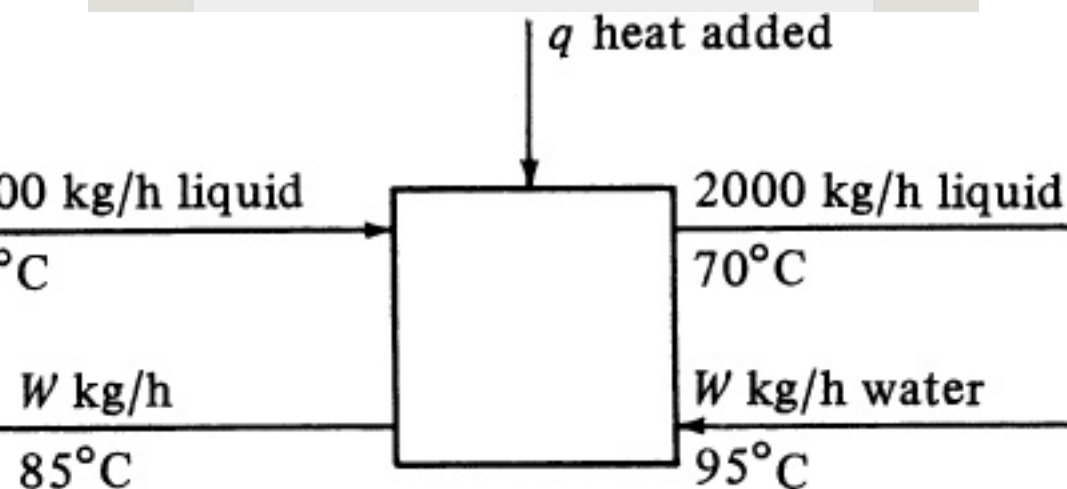


Figure 12.2-1. Process flow diagram for Example 12.2-1.

**Solution:** It is convenient to use the standard reference state of 298 K (25°C) as the datum to calculate the various enthalpies. From Eq. (12.2-3) the input items are as follows:

*Input items.*  $\Sigma H_R$  of the enthalpies of the two streams relative to 298 K (25°C) (note that  $\Delta t = 30 - 25^\circ\text{C} = 5^\circ\text{C} = 5\text{K}$ ):

$$H(\text{liquid}) = (2000 \text{ kg/h})(4.06 \text{ kJ/kg} \cdot \text{K})(5 \text{ K}) = 4.060 \times 10^4 \text{ kJ/h}$$

$$H(\text{water}) = W(4.21)(95 - 25) = 2.947 \times 10^2 \text{ kJ/kg}(W), \text{ where } (W [=] \text{ kg/h})$$

$$\Delta H_{2980} = 0 \text{ (since there is no chemical reaction)} \quad q = 0 \text{ (there are no heat losses or additions)}$$

*Output items.*  $\Sigma H_R$  of the two streams relative to 298 K (25°C):

$$H(\text{liquid}) = 2000(4.06)(70 - 25) = 3.65 \times 10^5 \text{ kJ/h}$$

$$H(\text{water}) = W(4.21)(85 - 25) = 2.526 \times 10^2 W \text{ kJ/h}$$

Equating input to output in Eq. (12.1-1) and solving for  $W$ ,

$$4.060 \times 10^4 + 2.947 \times 10^2 W = 3.654 \times 10^5 + 2.526 \times 10^2 W \quad W = 7720 \text{ kg/h}$$

The amount of heat added to the fermentation medium is simply the difference between the outlet and inlet liquid enthalpies:

$$H(\text{outlet liquid}) - H(\text{inlet liquid}) = 3.654 \times 105 - 4.060 \times 104 = 3.248 \times 105 \text{ kJ/h} (90.25 \text{ kW})$$

Note in this example that since the heat capacities were assumed constant, a simpler balance could have been written as follows:

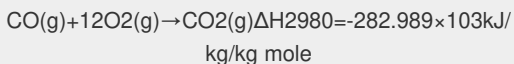
$$\text{heat gained by liquid} = \text{heat lost by water} \\ (70-30) = W(4.21)(95-85)$$

Then, solving,  $W = 7720 \text{ kg/h}$ . This simple balance works well when  $c_p$  is constant. However, when  $c_p$  varies with temperature and the material is a gas,  $c_{pm}$ , values are only available between 298 K (25°C) and  $t$  K, and the simple method cannot be used without obtaining new  $c_{pm}$  values over different temperature ranges.

### **EXAMPLE 12.2-2. Heat and Material Balance in Combustion**

The waste gas from a process of 1000 g mol/h of CO at 473 K is burned at 1 atm pressure in a furnace using air at 373 K. The combustion is complete and 90% excess air is used. The flue gas leaves the furnace at 1273 K. Calculate the heat removed in the furnace.

**Solution:** First, the process flow diagram is drawn in Fig. 12.2-2, and then a material balance is made:



(From Appendix A.3)

$$\begin{aligned} \text{mol CO} &= 1000 \text{ g mol/h} = \text{mol CO}_2 = 1.00 \text{ kg mol/h} \\ \text{mol O}_2 \text{ theoretically required} &= 12(1.00) = 0.500 \text{ kg mol/h} \\ \text{mol O}_2 \text{ actually added} &= 12(1.9) = 0.950 \text{ kg mol/h} \\ \text{mol N}_2 \text{ added} &= 0.950(79.0/21) = 3.570 \text{ kg mol/h} \\ \text{air added} &= 0.950 + 3.570 = 4.520 \text{ kg mol/h} \\ \text{O}_2 \text{ in outlet flue gas} &= \text{added} - \text{used} = 0.950 - 0.500 = 0.450 \text{ kg mol/h} \\ \text{CO}_2 \text{ in outlet flue gas} &= 1.00 \text{ kg mol/h} \\ \text{N}_2 \text{ in outlet flue gas} &= 3.570 \text{ kg mol/h} \end{aligned}$$

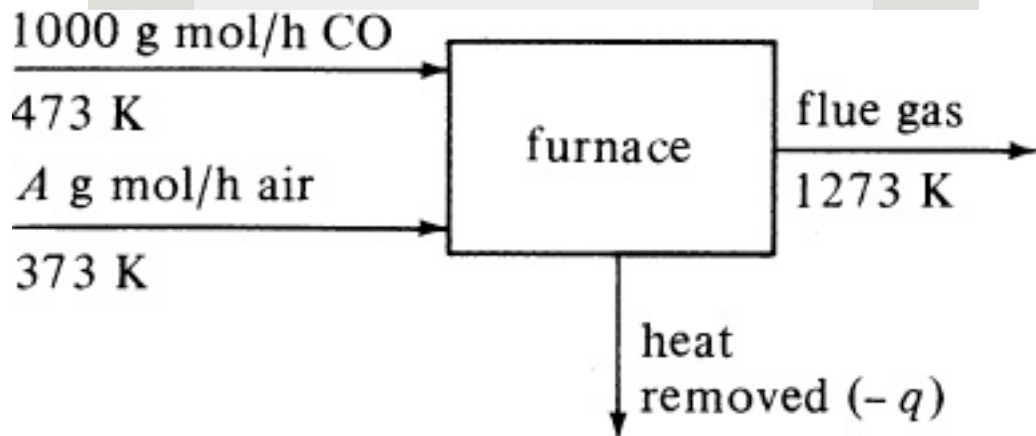


Figure 12.2-2. Process flow diagram for Example 12.2-2.

For the heat balance relative to the standard state at 298 K, we follow Eq. (12.2-1).

*Input items*

$$H(\text{CO}) = 1.00(c_{pm})(473 - 298) = 1.00(29.38)(473 - 298) = 5142 \text{ kJ/h}$$

(The  $c_{pm}$  of CO of 29.38 kJ/kg mole.K between 298 and 473 K is obtained from Table 12.1-1.)

$$H(\text{air}) = 4.520(c_{pm})(373 - 298) = 4.520(29.29)(373 - 298) = 9929 \text{ kJ/h} = \text{heat added, kJ/h}$$

(This will give a negative value here, indicating that heat was removed.)

$$-\Delta H_{2980} = -(-282.989 \times 103 \text{ kJ/kg mol})(1.00 \text{ kg mole/h}) = 282\,990 \text{ kJ/h}$$

*Output items*

$$\begin{aligned} H(\text{CO}_2) &= 1.00(c_{pm})(1273 - 298) = 1.00(49.91)(1273 - 298) = 48\,660 \text{ kJ/h} \\ H(\text{O}_2) &= 0.450(c_{pm})(1273 - 298) = 0.450(33.25)(1273 - 298) = 14\,590 \text{ kJ/h} \\ hH(\text{N}_2) &= 3.570(c_{pm})(1273 - 298) = 3.570(31.43)(1273 - 298) = 109\,400 \text{ kJ/h} \end{aligned}$$

Equating input to output and solving for  $q$ ,

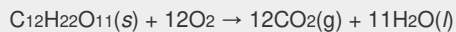
$$5142 + 9929 + q + 282990 = 48\,600 + 14\,590 + 109\,400q = -125\,411 \text{ kJ/h}$$

Hence, heat is removed:  $-34\,837 \text{ W}$ .

Often, when chemical reactions occur in the process and the heat capacities vary with temperature, the solution in a heat balance can be trial and error if the final temperature is the unknown.

#### **EXAMPLE 12.2-3. Oxidation of Lactose**

In many biochemical processes, lactose is used as a nutrient that is oxidized as follows:



The heat of combustion  $\Delta H_{\text{c}0}$  in **Appendix A.3** at  $25^\circ\text{C}$  is  $-5648.8 \times 10^3 \text{ J/g mol}$ . Calculate the heat of complete oxidation (combustion) at  $37^\circ\text{C}$ , which is the temperature of many biochemical reactions. The  $c_{\text{pm}}$  of solid lactose is  $1.20 \text{ J/g} \cdot \text{K}$ , and the molecular weight is  $342.3 \text{ g mass/g mol}$ .

**Solution:** This can be treated as an ordinary heat-balance problem. First, the process flow diagram is drawn in **Fig. 12.2-3**. Next, the datum temperature of  $25^\circ\text{C}$  is selected and the input and output enthalpies calculated. The temperature difference  $\Delta t = (37 - 25)^\circ\text{C} = (37 - 25) \text{ K}$ .

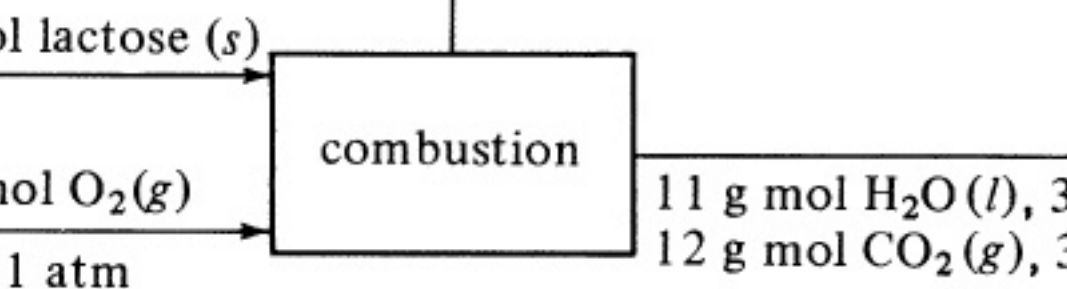


Figure 12.2-3. Process flow diagram for Example 12.2-3.

#### Input items

$$\begin{aligned} H(\text{lactose}) &= (342.3\text{g})(\text{cpmJg}\cdot\text{K})(37-25)\text{K} = 342.3(1.20) \\ &(37-25) = 4929 \text{ J} \\ H(\text{O}_2 \text{ gas}) &= (12\text{gmo1})(\text{cpmJgmo1}\cdot\text{K}) \\ &(37-25)\text{K} = 12(29.38)(37-25) = 4230 \text{ J} \end{aligned}$$

(The  $c_{pm}$  of  $\text{O}_2$  was obtained from Table 12.1-1.)

$$-\Delta H_{250} = -(-5648.8 \times 103\text{J/g mol - Lactose})$$

#### Output items

$$\begin{aligned} H(\text{H}_2\text{O liquid}) &= 11(18.02\text{g})(\text{cpmJg}\cdot\text{K}) \\ &(37-25)\text{K} = 11(17.02)(4.18)(37-25) = 9943 \text{ J} \end{aligned}$$

(The  $c_{pm}$  of liquid water was obtained from Appendix A.2.)

$$\begin{aligned} H(\text{CO}_2 \text{ gas}) &= (12\text{gmo1})(\text{cpmJgmo1}\cdot\text{K}) \\ &(37-25)\text{K} = 12(37.45)(37-25) = 5393 \text{ J} \end{aligned}$$

(The  $c_{pm}$  of  $\text{CO}_2$  is obtained from Table 12.1-1.)

$\Delta H_{37^\circ\text{C}}$ :

Setting input = output and solving,

$$\begin{aligned} 4929 + 4230 + 5648.8 \times 103 &= 9943 + 5393 - \\ \Delta H_{37^\circ\text{C}} \Delta H_{37^\circ\text{C}} &= -5642.6 \times 103\text{J/g} \end{aligned}$$

## 12.3 Conduction and Thermal Conductivity

### 12.3A Introduction to Steady-State Heat Transfer

The transfer of energy in the form of heat occurs in many chemical and other types of processes. Heat transfer often occurs in combination with other separation processes, such as drying lumber or foods, alcohol distillation, burning fuel, and evaporation. The heat transfer occurs because of a temperature-difference driving force and heat flows from the high- to the low-temperature region.

In calculating the rates of transport in a system using the molecular transport equation, it is necessary to account for the amount of this property being transported in the entire system. This is done by writing a general property

balance or conservation equation for the property (momentum, thermal energy, or mass) at unsteady state.

$$\text{Accumulation} = \text{In} - \text{Out} + \text{Generation} - \text{Consumption} \quad (12.3.1)$$

Equation (12.3-1) can then be written specifically for heat transfer,

$$\text{Rate of change of heat} = (\text{rate of heat in}) - (\text{rate of heat out}) + (\text{gen of heat} - \text{cons of heat}) \quad (12.3.2)$$

Assuming the rate of transfer of heat occurs only by conduction, we can insert *Fourier's law* (more description in Section 12.3C), for the in/out terms as

$$q_x A = -k dT/dx \quad (12.3-3)$$

Making an unsteady-state heat balance for the  $x$  direction only on the element

of volume or control volume in Fig. 12.3-1 by using Eqs. (12.3-1) and (12.3-2), with the cross-sectional area being  $A \text{ m}^2$  and the consumption term ignored,

$$\begin{aligned} \text{Accumulation} = \text{In} - \text{Out} + \text{Generation} \\ - \text{Consumption} \quad \frac{\partial E}{\partial t} = q_{x/x} - q_{x/x} + D_x \\ + q(\Delta x \cdot A) \end{aligned} \quad (12.3-4)$$

When only considering energy changes caused by a difference in temperature ( $\Delta E = \Delta H = m c_p \Delta T$ ), thus ignoring potential and kinetic energy changes,

$$\frac{\partial E}{\partial t} = \rho c_p \frac{\partial T}{\partial t} (\Delta x \cdot A) \quad (12.3-5)$$

Substituting back into Eq. (12.3-4),

$$\begin{aligned} \rho c_p \frac{\partial T}{\partial t} (\Delta x \cdot A) = q_{x/x} - q_{x/x} + \Delta x + q. \\ (\Delta x \cdot A) \end{aligned} \quad (12.3-6)$$



where  $q$  is rate of heat generated per unit volume. Assuming no heat generation and also assuming steady-state heat transfer, where the rate of accumulation is zero, Eq. (12.3-6) becomes

$$q_x|_x = q_x|_{x+\Delta x} \quad (12.3-7)$$

This means the rate of heat input by conduction = the rate of heat output by conduction; or  $q_x$  is a constant with time for steady-state heat transfer.

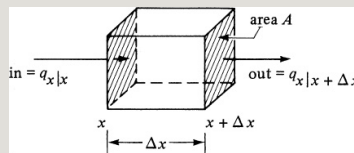


Figure 12.3-1. *Unsteady-state balance for heat transfer in control volume.*

In this chapter, we are concerned with a control volume where the rate of accumulation of heat is zero and we have steady-state heat transfer. The rate

of heat transfer is then constant with time, and the temperatures at various points in the system do not change with time. To solve problems in steady-state heat transfer, various mechanistic expressions in the form of differential equations for the different modes of heat transfer such as Fourier's law are integrated. Expressions for the temperature profile and heat flux are then obtained in this chapter.

In Chapter 14, the conservation-of-energy equations (4.2-2) and (12.3-6) will be used again when the rate of accumulation is not zero and unsteady-state heat transfer occurs. The mechanistic expression for Fourier's law in the form of a partial differential equation will be used where the temperature at various points and the

rate of heat transfer change with time. In Section 14.6, a general differential equation of energy change will be derived and integrated for various specific cases to determine the temperature profile and heat flux.

### **12.3B Conduction as a Basic Mechanism of Heat Transfer**

Heat transfer may occur by any one or more of the three basic mechanisms of heat transfer: conduction, convection, and radiation. In this section, we will focus on conduction.

*Conduction.* In conduction, heat can be conducted through solids, liquids, and gases. The heat is conducted by the transfer of the energy of motion between adjacent molecules. In a gas, the “hotter” molecules, which have greater

energy and motions, impart energy to the adjacent molecules at lower energy levels. This type of transfer is present to some extent in all solids, gases, or liquids in which a temperature gradient exists. In conduction, energy can also be transferred by “free” electrons, which is quite important in metallic solids. Examples of heat transfer mainly by conduction are heat transfer through walls of exchangers or a refrigerator, heat treatment of steel forgings, freezing of the ground during the winter, and so on.

### **12.3C Fourier’s Law of Heat Conduction**

As discussed previously for the general molecular transport equation, all three main types of rate-transfer processes—momentum transfer, heat transfer, and mass

transfer—are characterized by the same general type of equation. The transfer of electric current can also be included in this category. This basic equation is as follows:

$$\text{rate of a transfer process} = \frac{\text{driving force}}{\text{resistance}} \quad (12.3-8)$$

This equation states what we know intuitively: that in order to transfer a property such as heat or mass, we need a driving force to overcome a resistance.

The transfer of heat by conduction also follows this basic equation and is written as Fourier's law for heat conduction in fluids or solids:

$$q_x A = -k A \frac{dT}{dx} \quad (12.3-3)$$

where  $q_x$  is the heat-transfer rate in the  $x$  direction in watts (W),  $A$  is the cross-

sectional area normal to the direction of flow of heat in  $m^2$ ,  $T$  is temperature in K,  $x$  is distance in m, and  $k$  is the thermal conductivity in  $W/m \cdot K$  in the SI system. The quantity  $q_x/A$  is called the heat flux in  $W/m^2$ . The quantity  $dT/dx$  is the temperature gradient in the  $x$  direction. The minus sign in Eq. (12.3-3) is required because if the heat flow is positive in a given direction, the temperature decreases in this direction.

The units in Eq. (12.3-3) may also be expressed in the cgs system, with  $q_x$  in cal/s,  $A$  in  $cm^2$ ,  $k$  in  $cal/s \cdot ^\circ C \cdot cm$ ,  $T$  in  $^\circ C$ , and  $x$  in cm. In the English system,  $q_x$  is in btu/h,  $A$  in  $ft^2$ ,  $T$  in  $^\circ F$ ,  $x$  in ft,  $k$  in  $btu/h \cdot ^\circ F \cdot ft$ , and  $q_x/A$  in  $btu/h \cdot ft^2$ . From Appendix A.1, the conversion factors for thermal conductivity are

$$\text{Btu/h}\cdot\text{ft}^2\cdot^\circ\text{F}=4.1365\times 10^3\text{cal/} \\ \text{s}\cdot\text{cm}\cdot^\circ\text{C}\quad(12.3-9)$$

$$1\text{ Btu/h}\cdot\text{ft}\cdot^\circ\text{F}=1.73073\text{ W/} \\ \text{m}\cdot\text{K}\quad(12.3-10)$$

For heat flux and power,

$$1\text{ Btu/h}\cdot\text{ft}^2=3.1546\text{ W/m}^2\quad(12.3-11)$$

$$1\text{ Btu/h}=0.29307\text{ W}\quad(12.3-12)$$

Fourier's law, Eq. (12.3-3), can be integrated for the case of steady-state heat transfer through a flat wall of constant cross-sectional area  $A$ , where the inside temperature is  $T_1$  at point 1 and  $T_2$  at point 2, a distance of  $x_2 - x_1$  m away. Rearranging Eq. (12.3-3),

$$q_x A \int_{x_1}^{x_2} dx = - \\ k \int_{T_1}^{T_2} dT\quad(12.3-13)$$

Integrating, assuming that  $k$  is constant and does not vary with temperature, and dropping the subscript  $x$  on  $q_x$  for convenience,

$$qA = kx_2 - x_1(T_1 - T_2) \quad (12.3-14)$$

**EXAMPLE 12.3-1. Heat Loss Through an Insulating Wall**

Calculate the heat loss per  $m^2$  of surface area for an insulating wall composed of 25.4-mm-thick fiber insulating board, where the inside temperature is 352.7 K and the outside temperature is 297.1 K.

**Solution:** From Appendix A.3, the thermal conductivity of fiber insulating board is  $0.048 \text{ W/m} \cdot \text{K}$ . The thickness  $x_2 - x_1 = 0.0254 \text{ m}$ . Substituting into Eq. (12.3-14),

$$\begin{aligned} qA &= kx_2 - x_1(T_1 - T_2) = 0.048(0.0254)(352.7 - 297.1) = 105.1 \text{ W/m}^2 \\ &= (105.1 \text{ W/m}^2)(1.055 \text{ kcal/W} \cdot \text{h}) = 110.9 \text{ kcal/h} \cdot \text{m}^2 \end{aligned}$$

### 12.3D Thermal Conductivity

The defining equation for thermal conductivity is given as Eq. (12.3-3), and with this definition, experimental measurements have been made to determine the thermal



conductivity of different materials.

In Table 12.3-1, thermal conductivities of a few materials are given for the purpose of comparison. More-detailed data are given in Appendix A.3 for inorganic and organic materials and Appendix A.4 for food and biological materials. As seen in Table 12.3-1, gases have quite low values of thermal conductivity, liquids have intermediate values, and solid metals have very high values.

Table 12.3-1. *Thermal Conductivities of Some Materials at 101.325 kPa (1 Atm) Pressure ( $k$  in  $W/m \cdot K$ )*



1. *Gases.* In gases, the mechanism of thermal conduction is relatively simple.

The molecules are in continuous random motion, colliding with one another and exchanging energy and momentum. If a molecule moves from a high-temperature region to a region of lower temperature, it transports kinetic energy to this region and gives up this energy through collisions with lower-energy molecules. Since smaller molecules move faster, gases such as hydrogen should have higher thermal conductivities, as shown in Table 12.3-1.

Theories to predict thermal conductivities of gases are reasonably accurate and are given elsewhere (R1). However, for completeness, the predictive model developed by Chapman–Enskog for gases is given below,

$$k = 0.0829 T M W \sigma^2 \Omega_k \quad (12.3-15)$$

Where  $k$  is thermal conductivity ( $\text{Wm}\cdot\text{K}$ ),  $\sigma$  is the molecular diameter ( $\text{\AA}$ ),  $T$  is temperature (K),  $MW$  is the molecular weight, and  $\Omega_k$  is the Lennard-Jones collision integral.

Molecular diameter ( $\sigma$ ) can be found in Appendix A.6.  $\Omega_k$  can be approximated from the equation proposed by Neufeld et al. (N1),

$$\Omega_k(T^*) = 0.14874 + 0.52487 \exp(-0.77329 T^*) + 2.16178 \exp(-1.5 T^*) \quad (12.3-16)$$

where

$$T^* = k T \epsilon \quad (12.3-17)$$

Thermal conductivity increases approximately as the square root of the absolute temperature and is independent

of pressure up to a few atmospheres. At very low pressures (vacuum), however, the thermal conductivity approaches zero.

**EXAMPLE 12.3-2. Chapman–Enskog for the Prediction of Thermal Conductivity of  $H_2$**

Use Eqs. 12.3-16, 12.3-17, and 12.3-18 to calculate the thermal conductivity of  $H_2$  at 273 K and 1 atm, and then compare that value to the one in Table 12.3-1.

$T = 273\text{K}$ ,  $MW = 2$ , from Appendix A.6  $\sigma = 2.827 \text{ \AA}$ , and  $\epsilon/k = 59.7$ ; thus

$$T^* = kT\epsilon = 27359.7 = 4.6$$

Then, using Eq. 12.3-17,

$$\Omega k = 1.16145(4.6)^{-0.14874} + 0.52487 \exp(-0.77329 \cdot 4.6) + 2.16178 \exp(-2.43787 \cdot 4.6) \quad \Omega k = 0.941$$

Substituting the values above back into Eq. 12.3-16,

$$k = 0.0829(273/2)(2.827)^2 \cdot 0.941 = 0.129 \text{ W}\cdot\text{m}\cdot\text{K}^{-1}$$

This is lower than the  $0.167 \text{ W/m}\cdot\text{K}$  obtained from Table 12.3-1, so use the correlation with caution.

**2. Liquids.** The physical mechanism of energy conduction in liquids is somewhat similar to that of gases, where higher-energy molecules collide with lower-energy molecules. However, the

molecules are packed so closely together that molecular force fields exert a strong effect on the energy exchange. Since an adequate molecular theory of liquids is not available, most correlations to predict the thermal conductivities are empirical. Reid et al. (R1) discuss these in detail. The thermal conductivity of liquids varies moderately with temperature and often can be expressed as a linear variation.

$$k=a+bT(12.3-18)$$

where  $a$  and  $b$  are empirical constants. Thermal conductivities of liquids are essentially independent of pressure.

Water has a high thermal conductivity compared to organic-type liquids such as benzene. As shown in Table 12.3-1,

the thermal conductivities of most unfrozen foodstuffs, such as skim milk and applesauce, which contain large amounts of water, have thermal conductivities near that of pure water.

*3. Solids.* The thermal conductivity of homogeneous solids varies quite widely, as may be seen for some typical values in Table 12.3-1. The metallic solids of copper and aluminum have very high thermal conductivities, while some insulating nonmetallic materials such as rock wool and corkboard have very low conductivities.

Heat or energy is conducted through solids by two mechanisms. In the first, which applies primarily to metallic solids, heat, like electricity, is conducted by free electrons that move through the

metal lattice. In the second mechanism, present in all solids, heat is conducted by the transmission of energy due to vibration between adjacent atoms.

Thermal conductivities of insulating materials such as rock wool approach that of air since the insulating materials contain large amounts of air trapped in void spaces. Superinsulations for insulating cryogenic materials such as liquid hydrogen are composed of multiple layers of highly reflective materials separated by evacuated insulating spacers. Values of thermal conductivity are considerably lower than for air alone.

Ice has a thermal conductivity much greater than water. Hence, the thermal conductivities of frozen foods such as

lean beef and salmon given in Table 12.3-1 are much higher than for unfrozen foods.

## **12.4 Convection**

### **12.4A Convection as a Basic Mechanism of Heat Transfer**

The transfer of heat by convection implies the transfer of heat by bulk transport and the mixing of macroscopic elements of warmer portions with cooler portions of a gas or liquid. It also often refers to the energy exchange between a solid surface and a fluid. A distinction must be made between forced-convection heat transfer, where a fluid is forced to flow past a solid surface by a pump, fan, or other mechanical means, and natural or free convection, where warmer or



cooler fluid next to the solid surface causes a circulation because of a density difference resulting from the temperature differences in the fluid. Examples of heat transfer by convection are heat loss from a car radiator where air is circulated by a fan, stirring foods being cooked in a vessel, blowing across the surface of a hot cup of coffee to cool it, and so on.

Table 12.4-1. *Approximate Magnitude of Some Heat-Transfer Coefficients*

#### **12.4B Convective Heat-Transfer Coefficient**

It is well known that a hot piece of material will cool faster when air is blown or forced past the object. When the fluid outside the solid

surface is in forced or natural convective motion, we express the rate of heat transfer from the solid to the fluid, or vice versa, by the following equations:

$$q=hA(T_w-T_f) \text{ or } q=hA(T_f-T_w) \\ (12.4-1)$$

where  $q$  is the heat-transfer rate in W,  $A$  is the area in  $m^2$ ,  $T_w$  is the temperature of the solid surface in K,  $T_f$  is the average or bulk temperature of the fluid flowing past in K, and  $h$  is the convective heat-transfer coefficient in  $W/m^2 \cdot K$ . In English units,  $h$  is in  $btu/h \cdot ft^2 \cdot ^\circ F$ .

The coefficient  $h$  is a function of the system geometry, fluid properties, flow velocity, and temperature difference. In

many cases, empirical correlations are available to predict this coefficient, since it often cannot be predicted theoretically. Because we know that when a fluid flows past a surface there is a thin, almost stationary layer or film of fluid adjacent to the wall that presents most of the resistance to heat transfer, we often call the coefficient  $h$  a *film coefficient*.

In Table 12.4-1, some order-of-magnitude values of  $h$  for different convective mechanisms of free or natural convection, forced convection, boiling, and condensation are given. Water gives the highest values of the heat-transfer coefficients.

To convert the heat-transfer coefficient  $h$  from English to SI units,

$$1 \text{ btu/h} \cdot \text{ft}^2 \cdot ^\circ\text{F} = 5.6783 \text{ W/m}^2 \cdot \text{K}$$

**EXAMPLE 12.4-1. Heat Loss Through Convection**

The forced convective heat-transfer coefficient of flowing hot water (393 K) over a cold steel surface (283 K) is 1000  $\text{W/m}^2\cdot\text{K}$ . Determine the heat transfer rate per unit surface area ( $\text{W/m}^2$ ) from the water to the steel surface.

**Solution:** Use Eq. (12.4-1),  $q = hA(T_f - T_w)$ , and then move the area over to get  $qA = h(T_f - T_w)$ , so

$$qA = 1000 \text{ W/m}^2\cdot\text{K}(393\text{K} - 283\text{K}) = 110,000 \text{ W/m}^2$$

## 12.5 Radiation

### 12.5A Radiation, a Basic Mechanism of Heat Transfer

Radiation differs from heat transfer by conduction and convection in that no physical medium is needed for its propagation. Radiation is the transfer of energy through space by means of electromagnetic waves in much the same way as electromagnetic light waves transfer light. The same laws that govern the transfer of light govern the radiant transfer of heat.

Solids and liquids tend to absorb the radiation being transferred through them, so that radiation is important primarily in transfer through space or gases. The most important example of radiation is the transport of heat to the earth from the sun. Other examples are cooking food by placing it below red-hot electric heaters, heating fluids in coils of tubing inside a combustion furnace, and so on.

*1. Nature of radiant heat transfer.* In the preceding sections of this chapter, we have studied conduction and convection heat transfer. In conduction, heat is transferred from one part of a body to another, and the intervening material is heated. In convection, heat is transferred by the actual mixing of materials and by

conduction. In radiant heat transfer, the medium through which the heat is transferred usually is not heated. Again, radiation heat transfer is the transfer of heat by electromagnetic radiation.

Thermal radiation is a form of electromagnetic radiation similar to X rays, light waves, gamma rays, and so on, differing only in wavelength. It obeys the same laws as light: it travels in straight lines, can be transmitted through space and vacuum, and so on. It is an important mode of heat transfer and is especially important where large temperature differences occur, as, for example, in a furnace with boiler tubes, in radiant dryers, or in an oven baking food. Radiation often occurs in combination with conduction and convection. An elementary discussion of

radiant heat transfer will be given here, with a more advanced and comprehensive discussion provided in Chapter 17.

In an elementary sense, the mechanism of radiant heat transfer is composed of three distinct steps or phases:

1. The thermal energy of a hot source, such as the wall of a furnace at  $T_1$ , is converted into energy in the form of electromagnetic-radiation waves.
2. These waves travel through the intervening space in straight lines and strike a cold object at  $T_2$ , such as a furnace tube containing water to be heated.
3. The electromagnetic waves that strike the body are absorbed by it and converted back to thermal energy or heat.

*2. Absorptivity and black bodies.* When thermal radiation (such as light waves) falls upon a body, a portion is absorbed by the body in the form of heat, a portion is reflected back into space, and

a portion may actually be transmitted through the body. For most cases in process engineering, bodies are opaque to transmission, so this will be neglected. Hence, for opaque bodies,

$$\alpha + \rho = 1.0 \text{ (12.5-1)}$$

where  $\alpha$  is absorptivity or fraction absorbed and  $\rho$  is reflectivity or fraction reflected.

A *black body* is defined as one that absorbs all radiant energy and reflects none. Hence,  $\rho = 0$  and  $\alpha = 1.0$  for a black body. Actually, in practice there are no perfect black bodies, but a close approximation is a small hole in a hollow body, as shown in Fig. 12.5-1. The inside surface of the hollow body is blackened by charcoal. The radiation



enters the hole and impinges on the rear wall; a portion is absorbed there and a portion is reflected in all directions. The reflected rays impinge again, a portion is absorbed, and the process continues.

Hence, essentially all of the energy entering is absorbed and the area of the hole acts as a perfect black body. The surface of the inside walls is “rough” and rays are scattered in all directions, unlike a mirror, where they are reflected at a definite angle.

As stated previously, a black body absorbs all radiant energy falling on it and reflects none. Such a black body also emits radiation, depending on its temperature, and does not reflect any. The ratio of the emissive power of a surface to that of a black body is called *emissivity*  $\epsilon$  and is 1.0 for a black body.

Kirchhoff's law states that at the same temperature  $T_1$ ,  $\alpha_1$  and  $\epsilon_1$  of a given surface are the same, or

$$\alpha_1 = \epsilon_1 \quad (12.5-2)$$

Eq. (12.5-2) holds for any black or nonblack solid surface.

### *3. Radiation from a body and emissivity.*

The basic equation for heat transfer by radiation from a perfect black body with an emissivity  $\epsilon = 1.0$  is

$$q = A\sigma T^4 \quad (12.5-3)$$

where  $q$  is heat flow in W,  $A$  is  $m^2$  surface area of the body,  $\sigma$  is a constant  $5.676 \times 10^{-8} \text{ W/m}^2 \cdot \text{K}^4$  ( $0.1714 \times 10^{-8} \text{ btu/h} \cdot \text{ft}^2 \cdot ^\circ\text{R}^4$ ), and  $T$  is temperature of the black body in K ( $^\circ\text{R}$ ).

For a body that is not a black body and has an emissivity  $\epsilon < 1.0$  the emissive power is reduced by  $\epsilon$ , or

$$q = A\epsilon\sigma T^4 \quad (12.5-4)$$

Substances that have emissivities of less than 1.0 are called *gray bodies* when the emissivity is independent of the wavelength. All real materials have an emissivity  $\epsilon < 1$ .

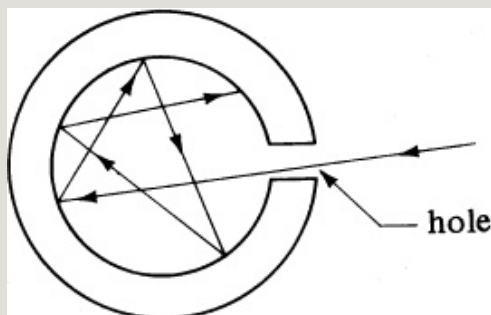


Figure 12.5-1. Concept of a perfect black body.

Table 12.5-1. *Total Emissivity,  $\epsilon$ , of Various Surfaces*

Since the emissivity  $\epsilon$  and absorptivity  $\alpha$  of a body are equal at the same temperature, the emissivity, like absorptivity, is low for polished metal surfaces and high for oxidized metal surfaces. Typical values are given in Table 12.5-1, but they do vary some with temperature. Most nonmetallic substances have high values. Additional data are tabulated in Appendix A.3.

#### **12.5B Radiation to a Small Object from Its Surroundings**

In the case of a small gray object of area  $A_1$  at temperature  $T_1$  in a large enclosure at a higher temperature  $T_2$ , there is a net radiation to the small object. The small body emits an amount of radiation to the enclosure given by

Eq. (12.5-4) as  $A_1 \epsilon_1 \sigma T_1^4$ . The emissivity  $\epsilon_1$  of this body is taken at  $T_1$ . The small body also absorbs an amount of energy from its surroundings at  $T_2$  given by  $A_1 \alpha_{12} \sigma T_2^4$ . The  $\alpha_{12}$  is the absorptivity of body 1 for radiation from the enclosure at  $T_2$ . The value of  $\alpha_{12}$  is approximately the same as the emissivity of this body at  $T_2$ . The net heat of absorption is then, by the Stefan–Boltzmann equation,

$$q = A_1 \epsilon_1 \sigma T_1^4 - A_1 \alpha_{12} \sigma T_2^4 = A_1 \sigma (\epsilon_1 T_1^4 - \alpha_{12} T_2^4) \quad (12.5-5)$$

A further simplification of Eq. (12.5-5) is usually made for engineering purposes by using only one emissivity for the small body, at temperature  $T_2$ .

Thus,

$$q = A_1 \epsilon \sigma (T_1^4 - T_2^4) \quad (12.5-6)$$

**EXAMPLE 12.5-1. Radiation to a Metal Tube**

A small oxidized horizontal metal tube with an OD of 0.0254 m (1 in.), 0.61 m (2 ft) long, and with a surface temperature at 588 K (600°F) is in a very large furnace enclosure with firebrick walls and the surrounding air at 1088 K (1500°F). The emissivity of the metal tube is 0.60 at 1088 K and 0.46 at 588 K. Calculate the heat transfer to the tube by radiation using SI and English units.

**Solution:** Since the large-furnace surroundings are very large compared to the small enclosed tube, the surroundings, when viewed from the position of the small body, appear black even if they are actually gray, and Eq. (12.5-6) is applicable. Substituting given values into Eq. (12.5-6) with an  $\epsilon$  of 0.6 at 1088 K,

$$\begin{aligned} A_1 &= \pi D L = \pi (0.0254 \text{ m}) \\ &(0.61 \text{ m}) = 0.049 \text{ m}^2 \\ q &= A_1 \epsilon \sigma (T_1^4 - T_2^4) = (0.049 \text{ m}^2)(0.6) \\ &(5.676 \times 10^{-8} \text{ W m}^{-2} \text{ K}^{-4}) [(588 \text{ K})^4 - (1088 \text{ K})^4] \\ q &= -2125 \text{ W} \end{aligned}$$

Other examples of small objects in large enclosures that occur in the process industries are a loaf of bread in an oven receiving radiation from the walls around it, a package of meat or food radiating heat to the walls of a freezing enclosure, a hot ingot of solid iron

cooling and radiating heat in a large room, and a thermometer measuring the temperature in a large duct.

## **12.6 Heat Transfer with Multiple Mechanisms/Materials**

### **12.6A Plane Walls in Series**

In the case where there is a multilayer wall of more than one material present, as shown in Fig. 12.6-1, we proceed as follows. The temperature profiles in the three materials  $A$ ,  $B$ , and  $C$  are shown. Since the heat flow  $q$  must be the same in each layer, we can write Fourier's equation for each layer as

$$q = k_A A \Delta x_A (T_1 - T_2) = k_B A \Delta x_B (T_2 - T_3) = k_C A \Delta x_C (T_3 - T_4) \quad (12.6-1)$$

Solving each equation for  $\Delta T$ ,

$$T_1 - T_2 = q \Delta x_A / k_A A$$

$$T_2 - T_3 = q \Delta x_B / k_B A$$

$$T_3 - T_4 = q \Delta x_C / k_C A \quad (12.6-2)$$

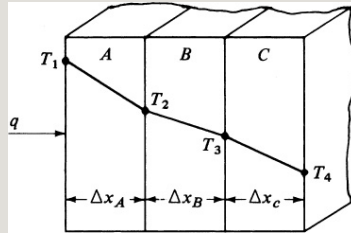


Figure 12.6-1. Heat flow through a multilayer wall.

Adding the equations for  $T_1 - T_2$ ,  $T_2 - T_3$ , and  $T_3 - T_4$ , the internal temperatures  $T_2$  and  $T_3$  drop out and the final rearranged equation is

$$q = \frac{T_1 - T_4}{\Delta x_A / (k_A A) + \Delta x_B / (k_B A) + \Delta x_C / (k_C A)} = T_1 - T_4 R_A + R_B + R_C \quad (12.6-3)$$

where the resistance  $R_A = \Delta x_A / k_A A$ , and so on.



Hence, the final equation is in terms of the overall temperature drop,  $T_1 - T_4$ , and the total resistance,  $R_A + R_B + R_C$ .

**EXAMPLE 12.6-1. Heat Flow Through an Insulated Wall of a Cold Room**

A cold-storage room is constructed of an inner layer of 12.7 mm of pine, a middle layer of 101.6 mm of cork board, and an outer layer of 76.2 mm of concrete. The wall surface temperature is 255.4 K inside the cold room and 297.1 K at the outside surface of the concrete. Use conductivities from Appendix A.3 for pine, 0.151; for cork board, 0.0433; and for concrete, 0.762 W/m · K. Calculate the heat loss in W for 1 m<sup>2</sup> and the temperature at the interface between the wood and cork board.

**Solution:** Calling  $T_1 = 255.4$ ,  $T_4 = 297.1$  K, pine as material A, cork as B, and concrete as C, a tabulation of the properties and dimensions is as follows:

$$k_A = 0.151 \text{ k}_B = 0.0433 \text{ k}_C = 0.762 \Delta x_A = 0.0127 \Delta x_B = 0.1016 \text{ m} \Delta x_C = 0.0762 \text{ m}$$

From Eq. (12.6-3), the resistances for each material are for an area of 1 m<sup>2</sup>,

$$\begin{aligned} R_A &= \Delta x / k_A = 0.0127 / 0.151 (1) = 0.0841 \text{ K/W} \\ R_B &= \Delta x / k_B = 0.1016 / 0.0433 (1) = 2.346 \text{ K/W} \\ R_C &= \Delta x / k_C = 0.0762 / 0.762 (1) = 0.100 \text{ K/W} \end{aligned}$$

Substituting into Eq. (12.6-3),

$$\begin{aligned} q &= (T_1 - T_4) / (R_A + R_B + R_C) = (255.4 - 297.1) / (0.0841 + \\ &2.346 + 0.100) = -41.72 / 2.530 = -16.48 \text{ W} \quad (-56.23 \text{ btu/h}) \end{aligned}$$

Since the answer is negative, heat flows in from the outside.

To calculate the temperature  $T_2$  at the interface between the pine and cork,

$$q = (T_1 - T_2) / R_A$$

Substituting the known values and solving,

$$-16.48 = 255.4 -$$

$T_2 = 256.79 \text{ K}$  at the interface

An alternative procedure for calculating  $T_2$  is to use the fact that the temperature drop is proportional to the resistance:

$$T_1 - T_2 = R_A + R_B + R_C (T_1 - T_4) \quad (12.6-4)$$

Substituting,

$$255.4 - T_2 = 0.0841(255.4 - 297.1) / 2530 = -1.39 \text{ K}$$

Hence,  $T_2 = 256.79 \text{ K}$ , as calculated before.

## 12.6B Conduction Through Materials in Parallel

Suppose that two plane solids,  $A$  and  $B$ , are placed side by side in parallel, and the direction of heat flow is perpendicular to the plane of the exposed surface of each solid. Then the total heat flow is the sum of the heat flow through solid  $A$  plus that through solid  $B$ . Writing Fourier's equation for each solid and summing,

$$q_T = q_A + q_B = k_A A_A \Delta x_A (T_1 -$$

$$T_2) + k_B A_B \Delta x_B (T_3 - T_4) \quad (12.6-5)$$

where  $q_T$  is total heat flow,  $T_1$  and  $T_2$  are the front and rear surface temperatures for solid  $A$ , and  $T_3$  and  $T_4$  are those for solid  $B$ .

If we assume that  $T_1 = T_3$  (front temperatures the same for  $A$  and  $B$ ) and  $T_2 = T_4$  (equal rear temperatures),

$$q_T = T_1 - T_2 \Delta x_A / k_A A_A + T_1 - T_2 \Delta x_B / k_B A_B = (1/R_A + 1/R_B)(T_1 - T_2) \quad (12.6-6)$$

An example would be an insulated wall ( $A$ ) of a brick oven where steel reinforcing members ( $B$ ) are in parallel and penetrate the wall. Even though the area  $A_B$  of the steel would be small compared to the insulated brick area  $A_A$ , the higher conductivity of the metal (which could be several hundred times

larger than that of the brick) could allow a large portion of the heat lost to be conducted by the steel.

Another example is a method of increasing heat conduction to accelerate the freeze-drying of meat. Spikes of metal in the frozen meat conduct heat more rapidly to the meat's interior.

It should be mentioned that in certain cases some two-dimensional heat flow can occur if the thermal conductivities of the materials in parallel differ markedly. Then, the results using Eq. (12.6-6) would be affected somewhat.

### **12.6C Combined Radiation and Convection Heat Transfer**

When radiation heat transfer occurs from a surface, it is usually accompanied by convective heat

transfer, unless the surface is in a vacuum. When the radiating surface is at a uniform temperature, we can calculate the heat transfer for natural or forced convection using the methods described in the previous sections of this chapter. The radiation heat transfer is calculated by the Stefan–Boltzmann equation, (12.5-6). Then, the total rate of heat transfer is the sum of convection plus radiation.

As discussed before, the heat-transfer rate by convection and the convective coefficient are given by

$$q_{\text{conv}} = h_c A_1 (T_1 - T_2) \quad (12.6-7)$$

where  $q_{\text{conv}}$  is the heat-transfer rate by convection in W,  $h_c$  the natural or forced

convection coefficient in  $\text{W/m}^2 \cdot \text{K}$ ,  $T_1$  the temperature of the surface, and  $T_2$  the temperature of the air and the enclosure. A radiation heat-transfer coefficient  $h_r$  in  $\text{W/m}^2 \cdot \text{K}$  can be defined as

$$q_{\text{rad}} = h_r A_1 (T_1 - T_2) \quad (12.6-8)$$

where  $q_{\text{rad}}$  is the heat-transfer rate by radiation in W. The total heat transfer is the sum of Eqs. (12.6-7) and (12.6-8):

$$q = q_{\text{conv}} + q_{\text{rad}} = (h_c + h_r) A_1 (T_1 - T_2) \quad (12.6-9)$$

To obtain an expression for  $h_r$ , we equate Eq. (12.5-6) to Eq. (12.6-8) and solve for  $h_r$ :

$$h_r = \epsilon \sigma (T_1^4 - T_2^4) / (T_1 - T_2) = \epsilon (5.676) (T_1/100)^4 - (T_2/100)^4 / (T_1 - T_2)$$

$$(SI) h_r = \epsilon (0.1714) (T_1/100)^4 - (T_2/100)^4 \quad (English) (12.6-10)$$

A convenient chart giving values of  $h_r$  in English units calculated from Eq. (12.6-10) with  $\epsilon = 1.0$  is given in Fig. 12.6-2. To use values from this figure, the value obtained from the figure should be multiplied by  $\epsilon$  to give the value of  $h_r$  to use in Eq. (12.6-9). If the air temperature is not the same as  $T_2$  of the enclosure, Eqs. (12.6-7) and (12.6-8) must be used separately and not combined as in Eq. (12.6-9).

**EXAMPLE 12.6-2. Combined Convection Plus Radiation from a Tube**

Recalculate Example 12.6-1 for combined radiation plus natural convection ( $h_c = 15.64 \text{ W/m}^2\text{-K}$ ) to the horizontal 0.0254-m tube.

**Solution:** Using Eq. (12.6-10) and  $\epsilon = 0.6$ ,

$$h_r = (0.60)(5.676) (1088/100)^4 - (588/100)^4 = 87.3 \text{ W/m}^2\text{-K}$$

Substituting into Eq. (12.6-9),

$$q = (h_c + h_r)A_1(T_1 - T_2) = (15.64 \text{ W/m}^2 \cdot \text{K} + 87.3 \text{ W/m}^2 \cdot \text{K})(0.0487 \text{ m}^2)(588 \text{ K} - 1088 \text{ K}) = -2507 \text{ W}$$

Hence, the heat loss of  $-2125 \text{ W}$  for radiation is increased to only  $-2507 \text{ W}$  when natural convection is also considered. In this case, because of the large temperature difference, radiation is the most important factor.

Perry and Green (P1, pp. 10–14) give a convenient table of natural convection plus radiation coefficients ( $h_c + h_r$ ) from single, horizontal, oxidized steel pipes as a function of the outside diameter and temperature difference. The coefficients for insulated pipes are about the same as those for a bare pipe (except that lower surface temperatures are involved for the insulated pipes), since the emissivity of cloth insulation wrapping is about that of oxidized steel, approximately 0.8. A more detailed discussion of radiation will be given in Chapter 17.



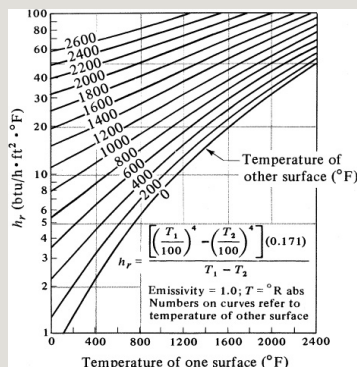


Figure 12.6-2. Radiation heat-transfer coefficient as a function of temperature. From R. H. Perry and C. H. Chilton, *Chemical Engineers' Handbook*, 5th ed. New York: McGraw-Hill Book Company, 1973. With permission.

## 12.7 Chapter Summary

When starting heat-transfer problems it is often beneficial/crucial to perform an overall energy balance:

$$\Delta H + \Delta E_k + \Delta E_p = q - W \quad (12.2-1)$$

However, in many cases seen in process engineering, they often take place at constant pressure, with electrical energy, kinetic energy, potential energy, and work either not present or neglected.

Thus the overall energy balance becomes:

$$\Delta H = q(12.2-2)$$

Next, the three mechanisms of heat transfer were discussed in the chapter: conduction, convection and radiation.

### **Conduction (Fourier's Law)**

$$qA = -k \frac{dT}{dx} (12.3-3)$$

After integration and assuming a plane wall with a constant cross-sectional area, Eq. 12.3-3 becomes:

$$qA = k(x_2 - x_1)(T_1 - T_2) (12.3-14)$$

Thermal conductivity ( $k$ ) was then discussed for gases, liquids, and solids. In general, the thermal conductivity of

solids is greater than that of liquids, which in turn is greater than that of gases.

$$k_{solids} > k_{liquids} > k_{gases}$$

## **Convection**

When the fluid outside the solid surface is in forced or natural convective motion, we express the rate of heat transfer from the solid to the fluid, or vice versa, by the following equation:

$$q = hA(T_w - T_f) \quad (12.4-1)$$

## **Radiation**

The basic equation for heat transfer by radiation from a grey body with an emissivity  $1.0 > \epsilon > 0$  is

$$q=A\epsilon\sigma T^4 \quad (12.5-4)$$

In the case of a small gray object of area  $A_1$  m<sup>2</sup> at temperature  $T_1$  in a large enclosure at a higher temperature, there is a net radiation to the small object that is described by the following equation:

$$q=A_1\epsilon\sigma(T_1^4-T_2^4) \quad (12.5-6)$$

Finally, heat transfer with multiple mechanisms/materials was introduced. For multiple materials, the example of a plane wall with constant cross-sectional area was used to calculate the heat flux with the following equation.

$$qA=\Delta T \Sigma R$$

For multiple mechanisms, the example of radiation and convective heat transfer was used where:

The total heat transfer is

$$q = q_{\text{conv}} + q_{\text{rad}} = (h_c + h_r) A_1 (T_1 - T_2) \quad (12.6-9)$$

where  $h_r$

$$\begin{aligned} h_r &= \epsilon \sigma (T_1^4 - T_2^4) / (T_1 - T_2) = \epsilon (5.676) \\ &\quad (T_1/100)^4 - (T_2/100)^4 / (T_1 - T_2) \\ &\quad (\text{SI}) \quad h_r = \epsilon (0.1714) (T_1/100)^4 - \\ &\quad (T_2/100)^4 / (T_1 - T_2) \quad (\text{English}) \end{aligned} \quad (12.6-10)$$

## Problems

**12.1-1. Heating of CO<sub>2</sub> Gas.** A total of 250 g of CO<sub>2</sub> gas at 373 K is heated to 623 K at 101.32 kPa total pressure. Calculate the amount of heat needed in cal, btu, and kJ.

**Ans.** 15050 cal, 59.7 btu, 62.98 kJ

**12.1-2. Fitting a Polynomial to Heat**

**Air.** Using the data on Table 12.1-1 and Excel to fit the  $c_p$  values of air as a function of temperature to a second-order polynomial ( $c_p = aT^2 + bT + c$ ). Use this polynomial to calculate the heat needed to heat 1000 kg of air from 30°C to 1000°C.

**12.1-3. Heating a Gas Mixture.** A mixture of 25 lb mol  $N_2$  and 75 lb mol  $CH_4$  is being heated from 400°F to 800°F at 1 atm pressure. Calculate the total amount of heat needed in btu.

**12.1-4. Final Temperature in Heating Applesauce.** A mixture of 454 kg of applesauce at 10°C is heated in a heat exchanger by adding 121 300 kJ. Calculate the outlet temperature of the applesauce. (*Hint:* In Appendix A.4 a heat capacity for applesauce is given at

32.8°C. Assume that this is constant and use this as the average  $c_{pm}$ .)

**Ans. 76.5°C**

### **12.1-5. *Energy Required to Heat***

***Methanol and Water.*** A mixture of 500 kg/s each of methanol and water 20°C is heated in a heat exchanger to 50°C.

Calculate the energy needed (kW) to heat the mixture. Heat capacities are not given and must be found in the appendix or elsewhere at a temperature between 20°C and 50°C.

**12.1-6. *Use of Steam Tables.*** Using the steam tables, determine the enthalpy change for 1 lb of water for each of the following cases:

- Heating liquid water from 40°F to 240°F at 30 psia. (Note that the effect of total pressure on the enthalpy of liquid water can be neglected.)

- Heating liquid water from 40°F to 240°F and vaporizing at 240°F and 24.97 psia.
- Cooling and condensing a saturated vapor at 212°F and 1 atm abs to a liquid at 60°F.
- Condensing a saturated vapor at 212°F and 1 atm abs.

**Ans.** (a) 200.42 btu/lbm; (b) 1152.7 btu/lbm; (c) -1122.4 btu/lbm; (d) -970.3 btu/lbm, -2256.9 kJ/kg

### **12.1-7. *Heating and Vaporization***

***Using Steam Tables.*** A flow rate of 1000 kg/h of water at 21.1°C is heated to 110°C when the total pressure is 244.2 kPa in the first stage of a process. In the second stage at the same pressure, the water is heated further until it is all vaporized at its boiling point. Calculate the total enthalpy change in both stages.

### **12.1-8. *Combustion of CH<sub>4</sub> and H<sub>2</sub>.***

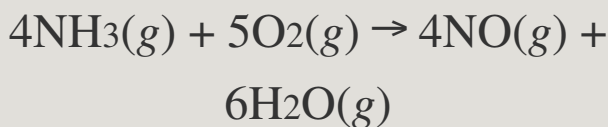
For 100 g mol of a gas mixture of 75



mol % CH<sub>4</sub> and 25% H<sub>2</sub>, calculate the total heat of combustion of the mixture at 298 K and 101.32 kPa, assuming that combustion is complete.

**12.1-9. *Combustion of CO.*** For 100 g mol of CO, calculate the total heat for combustion at 400 K and 101.32 kPa, assuming that combustion is complete. Assume a constant C<sub>pm</sub> for the gas 0.029 kJ/(mole\*K).

**12.1-10. *Heat of Reaction from Heats of Formation.*** For the reaction



calculate the heat of reaction,  $\Delta H$ , at 298 K and 101.32 kPa for 4 g mol of NH<sub>3</sub> reacting.

**Ans.**  $\Delta H$ , heat of reaction =  $-904.7 \text{ kJ}$

**12.1-11. Heat of Reaction from Heats of Formation.** Lime ( $\text{CaO}$ ) can be made from the decomposition of limestone ( $\text{CaCO}_3$ ):



Calculate the heat of reaction,  $\Delta H$ , at 298 K and 101.32 kPa for 10 kg mol reacting.

**12.2-1. Heat Balance and Cooling of Milk.** In the processing of rich cows' milk, 4540 kg/h of milk is cooled from  $60^\circ\text{C}$  to  $4.44^\circ\text{C}$  by a refrigerant. Calculate the heat removed from the milk.

**Ans.** Heat removed =  $269.6 \text{ kW}$

**12.2-2. Heating of Oil by Air.** A flow of 2200 lb<sub>m</sub>/h of hydrocarbon oil at 100°F enters a heat exchanger, where it is heated to 150°F by hot air. The hot air enters at 300°F and is to leave at 200°F. Calculate the total lb mol air/h needed. The mean heat capacity of the oil is 0.45 btu/lb<sub>m</sub> · °F.

**Ans.** 70.1 lb mol air/h, 31.8 kg mol/h

**12.2-3. Preheating Air by Steam for Use in a Dryer.** An air stream at 32.2°C is to be used in a dryer and is first preheated in a steam heater, where it is heated to 65.5°C. The air flow is 1000 kg mol/h. The steam enters the heater saturated at 148.9°C, is condensed and cooled, and leaves as a liquid at 137.8°C. Calculate the amount of steam used in kg/h.

**Ans.** 450 kg steam/h

**12.2-4. *Cooling of Cans of Potato Soup After Thermal Processing.*** A total of

1500 cans of potato soup undergo thermal processing in a retort at  $240^{\circ}\text{F}$ . The cans are then cooled to  $100^{\circ}\text{F}$  in the retort before being removed from the retort by cooling water, which enters at  $75^{\circ}\text{F}$  and leaves at  $85^{\circ}\text{F}$ . Calculate the lb of cooling water needed. Each can of soup contains 1.0 lb of liquid soup, and the empty metal can weighs 0.16 lb. The mean heat capacity of the soup is  $0.94 \text{ btu/lb}_m \cdot ^{\circ}\text{F}$  and that of the metal can is  $0.12 \text{ btu/lb}_m \cdot ^{\circ}\text{F}$ . A metal rack or basket that is used to hold the cans in the retort weighs 350 lb and has a heat capacity of  $0.12 \text{ btu/lb}_m \cdot ^{\circ}\text{F}$ . Assume that the metal rack is cooled from  $240^{\circ}\text{F}$  to  $85^{\circ}\text{F}$ , the temperature of the outlet water. The

amount of heat removed from the retort walls in cooling from 240 to 100°F is 10000 btu. Radiation loss from the retort during cooling is estimated as 5000 btu.

**Ans.** 21320 lb water, 9670 kg

### ***12.2-5. Double-Pipe Heat Exchanger.***

A 95% ethanol solution ( $C_p=0.62\text{BTU/lb}\cdot\text{R}$ ) at 150°F is pumped at a flow rate of 15 lb/s. Your job is to design a double-pipe heat exchanger that will cool the 95% ethanol mixture to 100°F by using cooling water ( $C_p=1.0\text{BTU/lb}\cdot\text{R}$ ) that is available at 50°F. Assume a 30°F cooling water approach to the outlet of the 95% ethanol solution. How much cooling water is needed?

### ***12.3-1. Insulation in a Cold Room.***

Calculate the heat loss per  $\text{m}^2$  of surface area for a temporary insulating wall of a food cold storage room where the outside temperature is  $299.9\text{ K}$  and the inside temperature  $276.5\text{ K}$ . The wall is composed of  $25.4\text{ mm}$  of corkboard having a  $k$  of  $0.0433\text{ W/m} \cdot \text{K}$ .

**Ans.**  $39.9\text{ W/m}^2$

**12.3-2. Determination of Thermal Conductivity.** In determining the thermal conductivity of an insulating material, the temperatures were measured on both sides of a flat slab of  $25\text{ mm}$  of the material and were  $318.4$  and  $303.2\text{ K}$ . The heat flux was measured as  $35.1\text{ W/m}^2$ . Calculate the thermal conductivity in  $\text{btu/h} \cdot \text{ft} \cdot ^\circ\text{F}$  and in  $\text{W/m} \cdot \text{K}$ .

### **12.3-3. *Variation of Thermal***

***Conductivity.*** A flat plane of thickness  $\Delta x$  has one surface maintained at  $T_1$  and the other at  $T_2$ . If the thermal conductivity varies according to temperature as

$$k = A + bT + cT^3$$

where  $A$ ,  $b$ , and  $c$  are constants, derive an expression for the one-dimensional heat flux  $q/A$ .

### **12.3-4. *Heat Transfer Through a Thick***

***Slab.*** Determine the steady-state rate of heat transfer per unit area ( $qA$ ) through a 5.0-cm-thick homogenous slab with its two faces maintained at uniform temperatures of  $40^\circ\text{C}$  and  $20^\circ\text{C}$ .

Thermal conductivity of the material is  $0.20 \text{ Wm}\cdot\text{K}$ .

**12.3-5. Conduction with Variable Thermal Conductivity.** You have a very long block of stainless steel that is losing heat at a rate  $2000 \text{ W/m}^2$ . If the temperature on the far left of the block is  $300^\circ\text{C}$ , plot the temperature profile as  $x$  varies from 0 to 1 m by 0.01 m increments with the following thermal conductivity:  $k(T) = 8 + 8.0 \times 10^{-3}T$ ,  $k(T)$  [=]  $\text{Wm}\cdot^\circ\text{C}$ . Solve Fourier's law analytically to get  $T$  as a function of  $x$  [ $T(x)$ ].

**12.3-6. Predicting Gaseous Thermal Conductivity.** Using the Chapman–Enskog equation, estimate the thermal conductivity of ammonia at 373 K and compare this value to the one given in the appendix (A.3-10).

**12.4-1. Forced Convection: Hot Fluid**



***Flowing Over a Cool Surface.*** The forced convective heat-transfer coefficient for a hot fluid flowing over a cool surface is  $300 \text{ W/m}^2 \cdot ^\circ\text{C}$ . The fluid temperature is  $200^\circ\text{C}$  and the surface is held at  $20^\circ\text{C}$ . Determine the heat transfer rate per unit surface area ( $q_A$ ) from the fluid to the surface.

***12.4-2. Forced Convection: Cold Fluid Flowing Over a Hot Surface.*** The forced convective heat-transfer coefficient for a cold fluid flowing over a hot surface is  $0.015 \text{ BTU/ft}^2 \cdot ^\circ\text{F} \cdot \text{S}.$  The fluid temperature is  $70^\circ\text{F}$  and the surface is held at  $400^\circ\text{F}$ . Determine the heat transfer rate per unit surface area ( $q_A$ ) from the fluid to the surface.

***12.4-3. Calculating the Convective Heat-Transfer Coefficient.*** A large tub

of water whose surface temperature is at  $40^{\circ}\text{F}$  is in contact with hot air at  $95^{\circ}\text{F}$ . Since the tub is large, initially it is losing heat at a steady rate of  $1000 \text{ BTU/ft}^2\cdot\text{s}$ . The area of the tub is  $100 \text{ ft}^2$ . What is the value of the initial convective heat-transfer coefficient?

#### **12.4-4. *Calculating Surface***

***Temperature.*** The steady-state heat flux toward a surface was  $1300 \text{ W/m}^2$ , the fluid temperature was  $100^{\circ}\text{C}$  and it was predicted that the heat-transfer coefficient was  $99.8 \text{ W/m}^2\cdot\text{K}$ . What was the surface/wall temperature?

#### **12.5-1. *Radiation to a Tube from a***

***Large Enclosure.*** Repeat Example

12.5-1 but use the slightly more accurate Eq. (12.5-5) with two different emissivities.

**Ans.**  $q = -2171 \text{ W } (-7410 \text{ btu/h})$

**12.5-2. *Baking a Loaf of Bread in an Oven.*** A loaf of bread having a surface temperature of 373 K is being baked in an oven whose walls and the interior air are at 477.4 K. The bread moves continuously through the large oven on an open chain-belt conveyor. The emissivity of the bread is estimated as 0.85, and the loaf can be assumed to be a rectangular solid 114.3 mm high  $\times$  114.3 mm wide  $\times$  330 mm long. Calculate the radiation heat-transfer rate to the bread, assuming that it is small compared to the oven and neglecting natural convection heat transfer.

**Ans.**  $q = 278.4 \text{ W } (950 \text{ btu/h})$

**12.5-3. *Radiant Energy Received from***

***a Wall.*** Radiant energy can be sensed by a person standing near a wall (area =  $7 \text{ m}^2$ ). The wall has a surface temperature around  $50^\circ\text{C}$ , and an emissivity value around 0.94. What would be the radiant energy loss from the wall at this temperature?

**12.5-4. *Surface Temperature.*** A spherical space ball of 0.5 cm diameter dissipates heat at 10 W. If the ball has an emissivity of 0.91 and it does not receive any appreciable radiation from any other surface, what is its surface temperature?

**12.6-1. *Insulation Needed for Food Cold Storage Room.*** A food cold storage room is to be constructed of an inner layer of 19.1 mm of pine, a middle layer of cork board, and an outer layer

of 50.8 mm of concrete. The inside wall surface temperature is  $-17.8^{\circ}\text{C}$  and the outside surface temperature is  $29.4^{\circ}\text{C}$  at the outer concrete surface. The mean conductivities are for pine, 0.151; cork, 0.0433; and concrete,  $0.762 \text{ W/m} \cdot \text{K}$ . The total inside surface area of the room to use in the calculation is approximately  $39 \text{ m}^2$  (neglecting corner and end effects). What thickness of cork board is needed to keep the heat loss to 586 W?

**Ans.** 0.128 m thickness

**12.6-2. *Insulation of a Furnace.*** A wall of a furnace 0.244 m thick is constructed of material having a thermal conductivity of  $1.30 \text{ W/m} \cdot \text{K}$ . The wall will be insulated on the outside with material having an average  $k$  of 0.346

$\text{W/m} \cdot \text{K}$ , so the heat loss from the furnace will be equal to or less than  $1830 \text{ W/m}^2$ . The inner surface temperature is  $1588 \text{ K}$  and the outer surface is  $299 \text{ K}$ . Calculate the thickness of insulation required.

**Ans.**  $0.179 \text{ m}$

### ***12.6-3. Heat Loss Through***

#### ***Thermopane Double Window.*** A

double-glazed window called

Thermopane is one in which two layers of glass are separated by a layer of dry, stagnant air. In a given window, each of the glass layers is  $6.35 \text{ mm}$  thick separated by a  $6.35\text{-mm}$  space of stagnant air. The thermal conductivity of the glass is  $0.869 \text{ W/m} \cdot \text{K}$  and that of air is  $0.026$  over the temperature range used. For a temperature drop of  $27.8 \text{ K}$

over the system, calculate the heat loss for a window  $0.914 \text{ m} \times 1.83 \text{ m}$ . (*Note:* This calculation neglects the effect of the convective coefficient on one outside surface of one side of the window, the convective coefficient on the other outside surface, and convection inside the window.)

**12.6-4. *Temperature Profile.*** A brick wall consists of a 5-inch-thick facing brick  $k=0.8 \text{ BTU} \cdot \text{hr} \cdot \text{ft} \cdot ^\circ\text{F}$  as the outside layer, a 6-inch-thick common brick  $k=0.45 \text{ BTU} \cdot \text{hr} \cdot \text{ft} \cdot ^\circ\text{F}$  as the middle layer, and 1-inch-thick gypsum plaster  $k=0.24 \text{ BTU} \cdot \text{hr} \cdot \text{ft} \cdot ^\circ\text{F}$  as the inside layer. If the steady-state heat flux through the wall is  $10 \text{ BTU} \cdot \text{hr} \cdot \text{ft}^2$ , what are the temperatures at all the material interfaces ( $T_2$  &  $T_3$ ) and surface temperature ( $T_4$ ) of the gypsum plaster

assuming the surface temperature of the facing brick is  $95^{\circ}\text{F}$  ( $T_1$ )? See Fig. 12.6-3.

**12.6-5. *Composite Materials in Parallel.*** A composite wall is to be constructed of 5-inch brick,  $k=0.8\text{Btuhr}\cdot\text{ft}\cdot\text{F}$ , 4 in. of corkboard  $k=0.025\text{Btuhr}\cdot\text{ft}\cdot\text{F}$ , and 1 in. of plastic  $k=1.5\text{Btuhr}\cdot\text{ft}\cdot\text{F}$ .

- Determine the thermal resistance of this wall ( $A = 1\text{ ft}^2$ ) if it is bolted together by  $\frac{3}{4}$ -inch bolts in which there are 4 bolts/ $\text{ft}^2$  of wall surface:  
 $k_{\text{Bolts}}=10\text{Btuhr}\cdot\text{ft}\cdot\text{F}$ . (Hint the bolts and the material together have a cross-sectional area of  $1\text{ m}^2$ .)
- In the situation above, if the outside temperature is  $92^{\circ}\text{F}$  and the inside is a cool  $70^{\circ}\text{F}$  what is the heat flow rate ignoring any convective fluxes?

**12.6-6. *Radiation and Convection from a Steam Pipe.*** A horizontal oxidized steel pipe carrying steam and having an OD of  $0.1683\text{ m}$  has a surface



temperature of 374.9 K and is exposed to air at 297.1 K in a large enclosure. Calculate the heat loss for 0.305 m of pipe from natural convection ( $h_c = 6.12 \text{ W/m}^2 \cdot \text{K}$ ) plus radiation. For the steel pipe, use an  $\epsilon$  of 0.79.

**Ans.**  $q = 163.3 \text{ W}$  (557 btu/h)

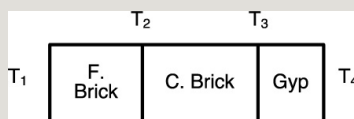


Figure 12.6-3. Figure for problem 12.6-4.

**12.6-7. Heat Loss from a Pipe.** A bare stainless-steel tube having an outside diameter of 76.2 mm and an  $\epsilon$  of 0.55 is placed horizontally in air at 294.2 K. The pipe surface temperature is 366.4 K and ( $h_c = 5.00 \text{ W/m}^2 \cdot \text{K}$ ). Calculate the value of  $h_r$  for radiation and the heat loss for 3 m of pipe.

## References

## Notation

# Chapter 13. Steady-State Conduction

## 13.0 Chapter Objectives

On completion of this chapter, a student should be able to:

- Solve steady-state conduction problems for each of the three common geometries (plane, cylinder, and sphere)
- Solve problems in which heat is transferred by conduction and convection in different materials/fluids in series or in parallel
- Derive equations for conduction in multilayer cylinders to solve heat-transfer problems
- Derive and solve conduction problems with a uniformly distributed heat source
- Use graphical and numerical methods to solve two-dimensional steady-state conduction problems

## 13.1 Conduction Heat Transfer

### 13.1A Conduction Through a Flat Slab or Wall (Some Review of Chapter 12)

In this section, Fourier's equation (12.3-3) will be used to obtain equations for one-dimensional steady-state conduction of heat through some simple geometries. For a flat slab or wall where the cross-sectional area  $A$  and  $k$  in Eq. (12.3-3) are constant, we obtained Eq. (12.3-14), which we rewrite as

$$qA = kx_2 - x_1(T_1 - T_2) = k\Delta x(T_1 - T_2) \quad (13.1-1)$$

This is shown in Fig. 13.1-1, where  $\Delta x = x_2 - x_1$ . Eq. (13.1-1) indicates that if  $T$  is substituted for  $T_2$  and  $x$  for  $x_2$ , the temperature varies linearly with distance, as shown in Fig. 13.1-1b.

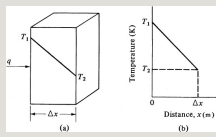


Figure 13.1-1. *Heat conduction in a flat wall: (a) geometry of wall, (b) temperature plot.*

If the thermal conductivity is not constant but varies linearly with temperature ( $k = a + bT$ ), then substituting Eq. (12.3-18) into Eq. (12.3-3) and integrating from  $T_1$  to  $T_2$  to drop the minus sign, then

$$qA = (a + bT) dT dx \quad (13.1-2)$$

where

$$\begin{aligned} qA \int_{x_1}^{x_2} dx &= \int_{T_1}^{T_2} (a + bT) dT \\ qA(x_2 - x_1) &= (aT_1 + bT_1^2/2) - (aT_2 + bT_2^2/2) \\ qA &= (a(T_1 - T_2) + b(T_1^2 - T_2^2)/2) / (x_2 - x_1) \\ &= k_m \Delta x (T_1 - T_2) \end{aligned} \quad (13.1-3)$$

where

$$k_m = a + b(T_1 + T_2)/2 \quad (13.1-4)$$

This means that the mean value of  $k$  (i.e.,  $k_m$ ) to use in Eq. (13.1-3) is the value of  $k$  evaluated at the linear average of  $T_1$  and  $T_2$ .

As stated in the introduction to transport processes, the rate of a transfer process equals the driving force over the resistance. Equation (13.1-1) can be rewritten in that form:

$$q = \frac{T_1 - T_2}{R} = \frac{\Delta T}{R}$$

$R = \text{driving force} / \text{resistance}$

where  $R = \Delta x / kA$  and is the resistance in K/W or  $h \cdot ^\circ\text{F}/\text{btu}$ .

### 13.1B Conduction Through a Hollow Cylinder

In many instances in the process industries, heat is being transferred through the walls of a thick-walled cylinder, such as a pipe that may or may not be insulated. Consider the hollow cylinder in Fig. 13.1-2 with an inside radius of  $r_1$ , where the temperature is  $T_1$ , an outside radius of  $r_2$  having a temperature of  $T_2$ , and a length of  $L$ . Heat is flowing radially from the inside surface to the outside. Rewriting Fourier's law, Eq. (12.3-3), with distance  $dr$  instead of  $dx$ ,

$$qA = -k dT dr \quad (13.1-5)$$

The cross-sectional area normal to the heat flow is

$$A = 2\pi r L \quad (13.1-6)$$

Substituting Eq. (13.1-6) into (13.1-5), rearranging, and integrating,

$$q 2\pi L \int_{r_1}^{r_2} \frac{dr}{r} = -k \int_{T_1}^{T_2} \frac{dT}{T} \quad (13.1-7)$$

$$q = \frac{k 2\pi L (T_1 - T_2)}{\ln(r_2/r_1)} \quad (13.1-8)$$

Multiplying numerator and denominator by  $(r_2 - r_1)$ ,

$$q = \frac{k A_1 m (T_1 - T_2) (r_2 - r_1)}{\ln(r_2/r_1) (r_2 - r_1)} = \frac{k A_1 m (T_1 - T_2) R}{\ln(r_2/r_1)} \quad (13.1-9)$$

where

$$A_1 m = \frac{(2\pi L r_2) - (2\pi L r_1) \ln(2\pi L r_2 / 2\pi L r_1)}{\ln(r_2/r_1)} = \frac{A_2 - A_1 \ln(A_2/A_1)}{\ln(r_2/r_1)} \quad (13.1-10)$$

$$R = \frac{r_2 - r_1}{k A_1 m} = \frac{\ln(r_2/r_1)}{2\pi k L} \quad (13.1-11)$$



The log mean area is  $A_{lm}$ . In engineering practice, if  $A_2/A_1 < 1.5/1$ , the linear mean area of  $(A_1 + A_2)/2$  is within 1.5% of the log mean area. From Eq. (13.1-8), if  $r$  is substituted for  $r_2$  and  $T$  for  $T_2$ , the temperature is seen to be a linear function of  $\ln r$  instead of  $r$ , as in the case of a flat wall. If the thermal conductivity varies with temperature as in Eq. (12.3-14), it can be shown that the mean value to use in a cylinder is still  $k_m$  of Eq. (13.1-3).

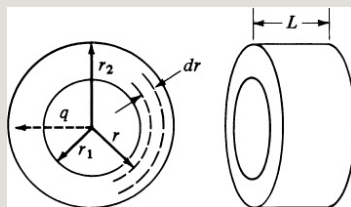


Figure 13.1-2. *Heat conduction in a cylinder.*

**EXAMPLE 13.1-1. Length of Tubing for a Cooling Coil**

A thick-walled cylindrical tubing of hard rubber having an inside radius of 5 mm and an outside radius of 20 mm is being used as a temporary cooling coil in a bath. Ice water is flowing rapidly inside, and the inside wall temperature is

274.9 K. The outside surface temperature is 297.1 K. A total of 14.65 W must be removed from the bath by the cooling coil. How many m of tubing are needed?

**Solution:** From Appendix A.3, the thermal conductivity at 0°C (273 K) is  $k = 0.151 \text{ W/m} \cdot \text{K}$ . Since data at other temperatures are not available, this value will be used for the range of 274.9 to 297.1 K.

$$r_1 = 51000 = 0.005 \text{ m}, r_2 = 201000 = 0.02 \text{ m}$$

The calculation will be done first for a length of 1.0 m of tubing. Solving for the areas  $A_1$ ,  $A_2$ , and  $A_{lm}$  in Eq. (13.1-10),

$$\begin{aligned} A_1 &= 2\pi L r_1 = 2\pi(1.0) \\ (0.005) &= 0.0314 \text{ m}^2 \\ A_2 &= 0.1257 \text{ m}^2 \\ A_{lm} &= A_2 - A_1 \ln(A_2/A_1) \\ &= 0.1257 - 0.0314 \ln(0.1257/0.0314) = 0.0680 \text{ m}^2 \end{aligned}$$

Substituting into Eq. (13.1-9) and solving,

$$\begin{aligned} q &= k A_{lm} (T_1 - T_2) / r_1 - r_2 = 0.151(0.0682) \\ (274.9 - 297.1) / (0.02 - 0.005) &= -15.2 \text{ W} \end{aligned}$$

An alternative solution not using  $A_{lm}$  is equally valid. Starting with Eq. 13.1-8,

$$\begin{aligned} q &= 2k\pi L \ln(r_2/r_1) (T_1 - T_2) \\ &= 2(0.151 \text{ W/m} \cdot \text{K}) \pi (1.0) \ln(0.02/0.005) \\ (297.1 \text{ K} - 274.9 \text{ K}) &= 14.65 \text{ W} \end{aligned}$$

The negative sign indicates that the heat flow is from  $r_2$  on the outside to  $r_1$  on the inside. Since 15.2 W is removed for a 1-m length, the needed length is

$$\text{length} = 14.65 \text{ W} / 15.2 \text{ W/m} = 0.964 \text{ m}$$

Note that the thermal conductivity of rubber is quite small. Generally, metal cooling coils are used since the thermal conductivity of metals is quite high. The liquid film resistances in this case are quite small and are neglected.

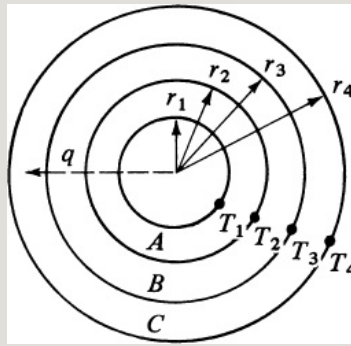


Figure 13.1-3. *Radial heat flow through multiple cylinders in series.*

### 13.1C Multilayer Cylinders

In the process industries, heat transfer often occurs through multilayers of cylinders, as for example when heat is being transferred through the walls of an insulated pipe. Figure 13.1-3 shows a pipe with two layers of insulation around it, that is, a total of three concentric hollow cylinders. The temperature drop is  $T_1 - T_2$  across material A,  $T_2 - T_3$  across B, and  $T_3 - T_4$  across C.

The heat-transfer rate  $q$  will, of course, be the same for each layer, since we are at steady state. Writing an equation similar to Eq. (13.1-9) for each concentric cylinder,

$$q = \frac{T_1 - T_2}{\frac{r_2 - r_1}{k_A A_{A1m}}} = \frac{T_2 - T_3}{\frac{r_3 - r_2}{k_B A_{B1m}}} = \frac{T_3 - T_4}{\frac{r_4 - r_3}{k_C A_{C1m}}} \quad (13.1-12)$$

where

$$\begin{aligned} A_{A1m} &= A_2 - A_1 \ln(A_2/A_1) \\ A_{B1m} &= A_3 - A_2 \ln(A_3/A_2) \\ A_{C1m} &= A_4 - A_3 \ln(A_4/A_3) \end{aligned} \quad (13.1-13)$$

Using the same method of combining the equations to eliminate  $T_2$  and  $T_3$  as was done for the flat walls in series, the final equations are

$$q = \frac{T_1 - T_4}{\frac{(r_2 - r_1)}{(k_A A_1 m)} + \frac{(r_3 - r_2)}{(k_B A_2 m)} + \frac{(r_4 - r_3)}{(k_C A_3 m)}} \quad (13.1-14)$$

$$q = \frac{T_1 - T_4}{R_A + R_B + R_C} = \frac{T_1 - T_4}{\sum R} \quad (13.1-15)$$

Hence, the overall resistance is again the sum of the individual resistances in series.

**EXAMPLE 13.1-2. Heat Loss from an Insulated Pipe**

A thick-walled tube of stainless steel (*A*) having a  $k = 21.63 \text{ W/m} \cdot \text{K}$  with dimensions of 0.0254 m ID and 0.0508 m OD is covered with a 0.0254-m-thick layer of an insulation (*B*),  $k = 0.2423 \text{ W/m} \cdot \text{K}$ . The inside-wall temperature of the pipe is 811 K and the outside surface of the insulation is at 310.8 K. For a 0.305-m length of pipe, calculate the heat loss and also the temperature at the interface between the metal and the insulation.

**Solution:** Calling  $T_1 = 811 \text{ K}$ ,  $T_2$  the interface, and  $T_3 = 310.8 \text{ K}$ , the dimensions are

$$r_1 = 0.0254/2 = 0.0127 \text{ m} \quad r_2 = 0.0508/2 = 0.0254 \text{ m} \quad r_3 = 0.0508 \text{ m}$$

The areas are as follows for  $L = 0.305 \text{ m}$ :

$$\begin{aligned} A_1 &= 2\pi L r_1 = 2\pi(0.305) \\ &(0.0127) = 0.0243 \text{ m}^2 \\ A_2 &= 2\pi L r_2 = 2\pi(0.305) \\ &(0.0254) = 0.0487 \text{ m}^2 \\ A_3 &= 2\pi L r_3 = 2\pi(0.305) \\ &(0.0508) = 0.0974 \text{ m}^2 \end{aligned}$$

From Eq. (13.1-13), the log mean areas for the stainless steel ( $A$ ) and insulation ( $B$ ) are

$$A_{1m} = \frac{A_2 - A_1 \ln(A_2/A_1)}{0.0487 - 0.0243 \ln(0.0487/0.0243)} = 0.0351 \text{ m}^2$$

$$A_{2m} = \frac{A_3 - A_2 \ln(A_3/A_2)}{0.0974 - 0.0487 \ln(0.0974/0.0487)} = 0.0703 \text{ m}^2$$

From Eq. (13.1-14), the resistances are

$$R_A = \frac{r_2 - r_1}{k_A A_{1m}} = \frac{0.012721}{1.63(0.0351)} = 0.01673 \text{ K/W}$$

$$R_B = \frac{r_3 - r_2}{k_B A_{2m}} = \frac{0.02540}{0.2423(0.0703)} = 1.491 \text{ K/W}$$

Hence, the heat-transfer rate is

$$q = \frac{T_1 - T_3}{R_A + R_B} = \frac{811 - 310}{0.01673 + 1.491} = 331.7 \text{ W} \quad (1132 \text{ Btu/h})$$

To calculate the temperature  $T_2$ ,

$$q = \frac{T_1 - T_2}{R_A} \quad \text{or} \quad 331.7 = \frac{811 - T_2}{0.01673}$$

Solving,  $811 - T_2 = 5.5 \text{ K}$  and  $T_2 = 805.5 \text{ K}$ . Only a small temperature drop occurs across the metal wall because of its high thermal conductivity.

### 13.1D Conduction Through a Hollow Sphere

Heat conduction through a hollow sphere is another case of one-dimensional conduction. Using Fourier's law for constant thermal conductivity with distance  $dr$ , where  $r$  is the radius of the sphere,

$$q_A = -k dT/dr \quad (13.1-5)$$

The cross-sectional area normal to the heat flow is

$$A=4\pi r^2 \quad (13.1-16)$$

Substituting Eq. (13.1-12) into Eq. (13.1-5), rearranging, and integrating,

$$\frac{q}{4\pi k} \int_{r_1}^{r_2} \frac{dr}{r^2} = -\frac{1}{k} \int_{T_1}^{T_2} T dt \quad (13.1-17)$$

$$q = 4\pi k (T_1 - T_2) \left( \frac{1}{r_1} - \frac{1}{r_2} \right) = \frac{T_1 - T_2}{\left( \frac{1}{r_1} - \frac{1}{r_2} \right) / 4\pi k} \quad (13.1-18)$$

it can easily be shown that the temperature varies hyperbolically with the radius (see Problem 13.1-4).

Hence, the overall resistance is again the sum of the individual resistances in series.

## 13.2 Conduction Through Solids in Series or Parallel with Convection

### 13.2A Combined Convection, Conduction, and Overall Coefficients

In many practical situations, the surface temperatures (or boundary conditions at the surface) are not known, but there is a fluid on both sides of the solid surfaces. Consider the plane wall in Fig. 13.2-1a, with a hot fluid at temperature  $T_1$  on the inside surface and a cold fluid at  $T_4$  on the outside surface. The convective coefficient on the outside is  $h_o$  W/m<sup>2</sup> · K, and  $h_i$  on the inside. (Methods for predicting the convective  $h$  will be given in Chapter 15.)

The heat-transfer rate using Eqs. (12.4-1) and (12.6-1) is given as



$$q = h_i A (T_1 - T_2) = k_A A \Delta x_A (T_2 - T_3) = h_o A (T_3 - T_4) \quad (13.2-1)$$

Expressing  $1/h_i A$ ,  $\Delta x_A/k_A A$ , and  $1/h_o A$  as resistances, and combining the equations as before,

$$q = \frac{T_1 - T_4}{1/h_i A + \Delta x_A/k_A A + 1/h_o A} = \frac{T_1 - T_4}{\sum R} \quad (13.2-2)$$

The overall heat transfer by combined conduction and convection is often expressed in terms of an overall heat-transfer coefficient  $U$  defined by

$$q = U A \Delta T_{\text{overall}} \quad (13.2-3)$$

where  $\Delta T_{\text{overall}} = T_1 - T_4$  and  $U$  is

$$U = \frac{1}{1/h_i + \Delta x_A/k_A + 1/h_o} \quad \text{W/m}^2 \cdot \text{K} \text{ (btuh/ft}^2 \cdot \text{°F)} \quad (13.2-4)$$

A more important application is heat transfer from a fluid outside a cylinder, through a metal wall, to a fluid inside the tube, as often occurs in heat exchangers. In Fig. 13.2-1b, such a case is shown.

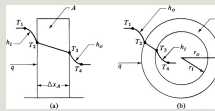


Figure 13.2-1. *Heat flow with convective boundaries: (a) plane wall, (b) cylindrical wall.*

Using the same procedure as before, the overall heat-transfer rate through the cylinder is

$$q = \frac{T_1 - T_2}{\frac{1}{h_1 A_i} + \frac{\ln(r_o/r_i)}{k A_{lm}} + \frac{1}{h_2 A_o}} \quad (13.2-5)$$

where  $A_i$  represents  $2\pi L r_i$ , the inside area of the metal tube;  $A_{lm}$  the log mean area of the metal tube; and  $A_o$  the

outside area.

The overall heat-transfer coefficient  $U$  for the cylinder may be based on the inside area  $A_i$  or the outside area  $A_o$  of the tube. Hence,

$$q = U_j A_j (T_1 - T_4) = U_o A_o (T_1 - T_4) = \frac{T_1 - T_4}{\sum R} \quad (13.2-6)$$

$$U_j = \frac{1}{\frac{1}{h_i} + \frac{(r_o - r_i)}{k} \frac{A_i}{A_o} + \frac{1}{h_o}} \quad (13.2-7)$$

$$U_o = \frac{1}{\frac{A_o}{A_i} \frac{1}{h_i} + \frac{(r_o - r_i)}{k} + \frac{1}{h_o}} \quad (13.2-8)$$

**EXAMPLE 13.2-1. Heat Loss by Convection and Conduction and Overall  $U$**

Saturated steam at 267°F is flowing inside a 34-in. steel pipe having an ID of 0.824 in. and an OD of 1.050 in. The pipe is insulated with 1.5 in. of insulation on the outside. The convective coefficient for the inside steam surface of the pipe is estimated as  $h_i = 1000 \text{ btu/h} \cdot \text{ft}^2 \cdot ^\circ\text{F}$ , and the convective coefficient on the outside of the lagging is estimated as  $h_o = 2 \text{ btu/h} \cdot \text{ft}^2 \cdot ^\circ\text{F}$ . The mean thermal conductivity of the metal is 45 W/m · K or 26 btu/h · ft · °F and 0.064 W/m · K, or 0.037 btu/h · ft · °F for the insulation.

- Calculate the heat loss for 1 ft of pipe using resistances if the surrounding air is at 80°F.
- Repeat, using the overall  $U_i$  based on the inside area  $A_i$ .

**Solution:** Calling  $r_i$  the inside radius of the steel pipe,  $r_1$  the outside radius of the pipe, and  $r_o$  the outside radius of the lagging, then

$$r_i = 0.41212 \text{ ft} \quad r_1 = 0.52512 \text{ ft} \quad r_o = 2.02512 \text{ ft}$$

For 1 ft of pipe, the areas are as follows:

$$A_j = 2\pi L r_i = 2\pi(1)(0.41212) = 0.2157 \text{ ft}^2 \quad A_1 = 2\pi L r_1 = 2\pi(1)(0.52512) = 0.2750 \text{ ft}^2 \quad A_o = 2\pi L r_o = 2\pi(1)(2.02512) = 1.060 \text{ ft}^2$$

From Eq. (13.1-13), the log mean areas for the steel ( $A$ ) pipe and lagging ( $B$ ) are

$$A_{A1m} = A_1 - A_i \ln(A_1/A_i) = 0.2750 - 0.2157 \ln(0.2750/0.2157) = 0.245 \text{ ft}^2$$

$$A_{B1m} = A_o - A_1 \ln(A_o/A_1) = 1.060 - 0.2750 \ln(1.060/0.2750) = 0.583 \text{ ft}^2$$

From Eq. (13.2-5) the various resistances are

$$R_i = 1/h_i A_i = 1/1000(0.2157) = 0.00464 \text{ ft}^2/\text{Btu h}$$

$$R_{A1} = r_1 - r_i / k A_{A1m} = (0.525 - 0.412) / (1226)(0.245) = 0.00148 \text{ ft}^2/\text{Btu h}$$

$$R_{B1} = r_o - r_1 / k A_{B1m} = (2.025 - 0.525) / (120)(0.583) = 5.80 \text{ ft}^2/\text{Btu h}$$

$$R_o = 1/h_o A_o = 1/12(1.060) = 0.472 \text{ ft}^2/\text{Btu h}$$

Using an equation similar to Eq. (13.2-5),

$$q = T_i - T_o / (R_i + R_{A1} + R_{B1} + R_o) = 267 - 800 / (0.00464 + 0.00148 + 5.80 + 0.472) = 267 - 806.278 = 29.8 \text{ Btu h}^{-1}$$

For part (b), the equation relating  $U_i$  to  $q$  is Eq. (13.2-6), which can be equated to Eq. (13.2-9):

$$q = U_j A_j (T_i - T_o) = T_i - T_o / \sum R \quad (13.2-10)$$

Solving for  $U_i$ ,

$$U_j = 1/A_i \sum R \quad (13.2-11)$$

Substituting known values,

$$U_j = 10.2157 / (6.278) = 0.738 \text{ Btu h}^{-1} \text{ ft}^2/\text{Btu h}^{-1}$$

Then, to calculate  $q$ ,

$$q = U_j A_j (T_i - T_o) = 0.738 (0.2157) (267 - 80) = 29.8 \text{ bm/h} (8.73 \text{ W})$$

### 13.2B Log Mean Temperature Difference and Varying Temperature Drop

Equations (12.4-1) and (13.2-2) as written apply only when the temperature drop ( $T_i - T_o$ ) is constant for all parts of the heating surface. Hence, the equation

$$q = U_j A_j (T_i - T_o) = U_o A_o (T_i - T_o) = UA(\Delta T) \quad (13.2-12)$$

only holds at one point in the apparatus when the fluids are being heated or cooled. However, as the fluids travel through the heat exchanger, they become heated or cooled and either  $T_i$  or  $T_o$ , or both, vary. Then,  $(T_i - T_o)$  or  $\Delta T$  varies with position, and some mean  $\Delta T_m$

must be used over the whole apparatus.

In a typical heat exchanger, a hot fluid inside a pipe is cooled from  $T_1'$  to  $T_2'$  by a cold fluid that is flowing on the outside in a double pipe countercurrently (in the reverse direction) and is heated from  $T_2$  to  $T_1$ , as shown in Fig. 13.2-2a. The  $\Delta T$  shown is varying with distance. Hence,  $\Delta T$  in Eq. (13.2-12) varies as the area  $A$  goes from 0 at the inlet to  $A$  at the outlet of the exchanger.

For countercurrent flow of the two fluids, as in Fig. 13.2-2a, the heat-transfer rate is

$$q = UA\Delta T_m \quad (13.2-13)$$

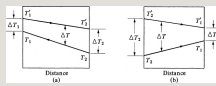


Figure 13.2-2. *Temperature profiles for one-pass double-pipe heat exchangers: (a) countercurrent flow; (b) cocurrent or parallel flow.*

where  $\Delta T_m$  is a suitable mean temperature difference to be determined. For a  $dA$  area, a heat balance on the hot and the cold fluids gives

$$dq = -m'c_p' dT' = mc_p dT \quad (13.2-14)$$

where  $m$  is flow rate in kg/s. The values of  $m$ ,  $m'$ ,  $c_p$ ,  $c_p'$ , and  $U$  are assumed constant.

Also,

$$dq = U(T' - T)dA \quad (13.2-15)$$

from Eq. (13.2-14),  $dT' = -dq/m'c_p'$  and  $dT = dq/mc_p$ . Then,

$$dT' - dT = d(T' - T) = -dq(1m'c_p + 1mc_p) \quad (13.2-16)$$

Substituting Eq. (13.2-15) into (13.2-16),

$$d(T' - T)T - T = -U(1m'c'p + 1mc_p)dA \quad (13.2-17)$$

Integrating between points 1 and 2,

$$\ln(T_2' - T_2 T_1' - T_1) = -UA(1m'c'p + 1mc_p) \quad (13.2-18)$$

Making a heat balance between the inlet and outlet,

$$q = m'c_p'(T_1' - T_2') = mc_p(T_2 - T_1) \quad (13.2-19)$$

Solving for  $m'c_p'$  and  $mc_p$  in Eq. (13.2.-19) and substituting into Eq.



(13.2-18),

$$q=UA[(T_1'-T_2)-(T_1'-T_1)]\ln[(T_2''-T_2)/(T_1'-T_1)] \quad (13.2-20)$$

Comparing Eqs. (13.2-13) and (13.2-20), we see that  $\Delta T_m$  is the log mean temperature difference  $\Delta T_{1m}$ . Hence, in the case where the overall heat-transfer coefficient  $U$  is constant throughout the equipment and the heat capacity of each fluid is constant, the proper temperature driving force to use over the entire apparatus is the log mean driving force,

$$q=UA\Delta T_{1m} \quad (13.2-21)$$

where

$$\Delta T_{1m} = \frac{\Delta T_2 - \Delta T_1}{\ln(\Delta T_2 / \Delta T_1)} \quad (13.2-22)$$

It can be also shown that for parallel flow, as pictured in Fig. 13.2-2b, the log mean temperature difference should be used. In some cases, where steam is condensing,  $T_1'$  and  $T_2'$  may be the same. The equations still hold for this case. When  $U$  varies with distance or other complicating factors occur, other references should be consulted (B1, P1, W1).

**EXAMPLE 13.2-2. Heat-Transfer Area and Log Mean Temperature Difference**

A heavy hydrocarbon oil that has a  $c_{pm} = 2.30 \text{ kJ/kg} \cdot \text{K}$  is being cooled in a heat exchanger from  $371.9 \text{ K}$  to  $349.7 \text{ K}$  and flows inside the tube at a rate of  $3630 \text{ kg/h}$ . A flow of  $1450 \text{ kg water/h}$  enters at  $288.6 \text{ K}$  for cooling and flows outside the tube.

- Calculate the water outlet temperature and heat-transfer area if the overall  $U_i = 340 \text{ W/m}^2 \cdot \text{K}$  and the streams are countercurrent.
- Repeat for parallel flow.

**Solution:** Assume a  $c_{pm} = 4.187 \text{ kJ/kg} \cdot \text{K}$  for water. The water inlet  $T_2 = 288.6 \text{ K}$ , outlet =  $T_1$ ; oil inlet  $T_1' = 371.9$ , outlet  $T_2' = 349.7$ . Calculating the heat lost by the oil,

$$q = (3630 \text{ kg/h})(2.30 \text{ kJ/kg} \cdot \text{K})(371.9 - 349.7) \text{ K} = 185400 \text{ kJ/h or } 51490 \text{ W (175700 btu/h)}$$

By a heat balance, the  $q$  must also equal the heat gained

by the water:

$$q = 185\,400 \text{ kJ/h} = (1450 \text{ kg/h})(4.187 \text{ kJ/kg}\cdot\text{K})(T_1 - 288.6) \text{ K}$$

Solving,  $T_1 = 319.1 \text{ K}$ .

To solve for the log mean temperature difference,

$$\begin{aligned}\Delta T_2 &= T_2' - T_2 = 349.7 - 288.6 = 61.1 \text{ K}, \Delta T_1 = T_1' - \\ T_1 &= 371.9 - 319.1 = 52.8 \text{ K}.\end{aligned}$$

Substituting into Eq. (13.2-22),

$$\begin{aligned}\Delta T_{1m} &= \Delta T_2 - \Delta T_1 \ln(\Delta T_2 / \\ \Delta T_1) &= 61.1 - 52.8 \ln(61.1/52.8) = 56.9 \text{ K}\end{aligned}$$

Using Eq. (13.2-21),

$$q = U_j A_j \Delta T_{1m} = 51\,490 = 340(A_j)(56.9)$$

Solving,  $A_j = 2.66 \text{ m}^2$ .

For part (b), the water outlet is still  $T_1 = 319.1 \text{ K}$ . Referring to Fig. 13.2-2b,  $\Delta T_2 = 371.9 - 288.6 = 83.3 \text{ K}$  and  $\Delta T_1 = 349.7 - 319.1 = 30.6 \text{ K}$ . Again, using Eq. (13.2-22) and solving,  $\Delta T_{1m} = 52.7 \text{ K}$ . Substituting into Eq. (13.2-21),  $A_i = 2.87 \text{ m}^2$ . This is a larger area than for counterflow. This occurs because counterflow gives larger temperature driving forces, and it is usually preferred over parallel flow for this reason.

### 13.2C Critical Thickness of Insulation for a Cylinder

In Fig. 13.2-3, a layer of insulation is installed around the outside of a cylinder whose radius  $r_1$  is fixed and with a length  $L$ . The cylinder has a high thermal conductivity and the

inner temperature  $T_1$  at point  $r_1$  outside the cylinder is fixed. An example is the case where the cylinder is a metal pipe with saturated steam inside. The outer surface of the insulation at  $T_2$  is exposed to an environment at  $T_0$  where convective heat transfer occurs. It is not obvious if adding more insulation with a thermal conductivity of  $k$  will decrease the heat-transfer rate.

At steady state, the heat-transfer rate  $q$  through the cylinder and the insulation equals the rate of convection from the surface:

$$q = h_o A (T_2 - T_0) \quad (13.2-23)$$

As insulation is added, the outside area,

which is  $A = 2\pi r_2 L$ , increases, but  $T_2$  decreases. However, it is not apparent whether  $q$  increases or decreases. To determine this, an equation similar to Eq. (13.2-5), with the resistance of the insulation represented by Eq. (13.1-11), is written using the two resistances:

$$q = \frac{2\pi L(T_1 - T_0)}{\ln(r_2/r_1)k + 1/r_2 h_0} \quad (13.2-24)$$

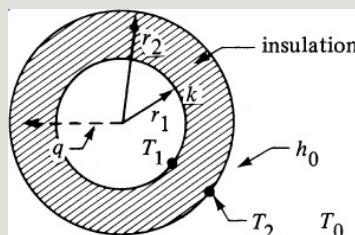
To determine the effect of the thickness of insulation on  $q$ , we take the derivative of  $q$  with respect to  $r_2$ , equate this result to zero, and obtain the following for maximum heat flow:

$$\frac{dq}{dr_2} = -2\pi L(T_1 - T_0) \left( \frac{1}{r_2^2 k} - \frac{1}{r_2^2 h_0} \right) \frac{1}{\ln(r_2/r_1)k + 1/r_2 h_0} = 0 \quad (13.2-25)$$

Solving,

$$(r_2)_{cr} = \frac{k}{h_o} \quad (13.2-26)$$

where  $(r_2)_{cr}$  is the value of the critical radius when the heat-transfer rate is a maximum. Hence, if the outer radius  $r_2$  is less than the critical value, adding more insulation will actually increase the heat-transfer rate  $q$ . Also, if the outer radius is greater than the critical, adding more insulation will decrease the heat-transfer rate. Using values of  $k$  and  $h_o$  typically encountered, the critical radius is only a few mm. As a result, adding insulation on small electrical wires could increase the heat loss. Adding insulation to large pipes decreases the heat-transfer rate.



**EXAMPLE 13.2-3. Insulating an Electrical Wire and Critical Radius**

An electric wire having a diameter of 1.5 mm and covered with a plastic insulation (thickness = 2.5 mm) is exposed to air at 300 K and  $h_o = 20 \text{ W/m}^2 \cdot \text{K}$ . The insulation has a  $k$  of  $0.4 \text{ W/m} \cdot \text{K}$ . It is assumed that the wire's surface temperature is constant at 400 K and is not affected by the covering.

- Calculate the value of the critical radius.
- Calculate the heat loss per m of wire length with no insulation.
- Repeat (b) for the presence of insulation.

**Solution:** For part (a), using Eq. (13.2-26),

$$(r_2)_{cr} = k/h_o = 0.4/20 = 0.020 \text{ m} = 20 \text{ mm}$$

For part (b),  $L = 1.0 \text{ m}$ ,  $r_2 = 1.5/(2 \times 1000) = 0.75 \times 10^{-3} \text{ m}$ ,  $A = 2\pi r_2 L$ . Substituting into Eq. (13.2-23),

$$q = h_o A (t_2 - T_0) = (20)(2\pi \times 0.75 \times 10^{-3} \times 1)(400 - 300) = 9.42 \text{ W}$$

For part (c) with insulation,  $r_1 = 1.5/(2 \times 1000) = 0.75 \times 10^{-3} \text{ m}$ ,  $r_2 = (2.5 + 1.5/2)/1000 = 3.25 \times 10^{-3} \text{ m}$ . Substituting into Eq. (13.2-24),

$$\begin{aligned} q &= 2\pi(1.0) \\ & (400 - 300.) \ln(3.25 \times 10^{-3} / 0.75 \times 10^{-3}) / 0.4 + 1/(325 \times 10^{-3}) \\ & (20) = 32.98 \text{ W} \end{aligned}$$

Hence, adding insulation greatly increases the heat loss.

## 13.2D Contact Resistance at an Interface

In the equations derived in this

section for conduction through solids in series (see Fig. 12.6-1), it has been assumed that the adjacent touching surfaces are at the same temperature so that completely perfect contact is made between the surfaces. For many engineering designs in industry, this assumption is reasonably accurate. However, in cases such as in nuclear power plants, where very high heat fluxes are present, a significant drop in temperature may be present at the interface. This interface resistance, called *contact resistance*, occurs when the two solids do not fit tightly together and a thin layer of stagnant fluid is trapped between the two surfaces. At some points, the solids touch at peaks in the surfaces and at other points, the fluid occupies the



open space.

This interface resistance is a complex function of the roughness of the two surfaces, the pressure applied to hold the surfaces in contact, the interface temperature, and the interface fluid.

Heat transfer takes place by conduction, radiation, and convection across the trapped fluid as well as by conduction through the points of contact of the solids. No completely reliable empirical correlations or theories are available to predict contact resistances for all types of materials. See references (C3, R1) for more detailed discussions.

The equation for the contact resistance is often given as

$$q = hcA\Delta T = \Delta T / R_c = \Delta T / R_c \quad (13.2-27)$$

where  $h_c$  is the contact-resistance coefficient in  $\text{W/m}^2 \cdot \text{K}$ ,  $\Delta T$  the temperature drop across the contact resistance in  $\text{K}$ , and  $R_c$  the contact resistance. The contact resistance  $R_c$  can be added to the other resistances in Eq. (12.6-3) to include this effect for solids in series. For contact between two ground-metal surfaces,  $h_c$  values on the order of magnitude of about  $0.2 \times 10^4$  to  $1 \times 10^4 \text{ W/m}^2 \cdot \text{K}$  have been obtained.

An approximation of the maximum contact resistance can be obtained if the maximum gap  $\Delta x$  between the surfaces can be estimated. Then, assuming that the heat transfer across the gap is by conduction only through the stagnant fluid,  $h_c$  is estimated as

$$h_c = k \Delta x \quad (13.2-28)$$

If any actual convection, radiation, or point-to-point contact is present, it will reduce this assumed resistance.

### **13.3 Conduction with Internal Heat Generation**

#### **13.3A Conduction with Internal Heat Generation**

In certain systems, heat is generated inside the conducting medium; that is, a uniformly distributed heat source is present. Examples of this are electric-resistance heaters and nuclear fuel rods. Also, if a chemical reaction is occurring uniformly in a medium, a heat of reaction is given off. In the agricultural and sanitation fields, compost heaps and trash heaps in which biological activity is occurring will give off heat.

Other important examples are in food

processing, where the heat of respiration of fresh fruits and vegetables is present. These heats of generation can be as high as 0.3 to 0.6 W/kg or 0.5 to 1 btu/h · lb<sub>m</sub>.

*1. Heat generation in a plane wall.* In Fig. 13.3-1, a plane wall is shown with internal heat generation. Heat is conducted only in the  $x$  direction. The other walls are assumed to be insulated. The temperature  $T_w$  in K at  $x = L$  and  $x = -L$  is held constant. The volumetric rate of heat generation is  $qW/m^3$  and the thermal conductivity of the medium is  $k$  W/m · K.

To derive the equation for this case of heat generation at steady state, we start with Eq. (12.3-6) but drop the accumulation term:

$$qx|_x + q \cdot (\Delta x \cdot A) = qx|_{x+\Delta x} + 0 \quad (13.3-1)$$

where  $A$  is the cross-sectional area of the plate. Rearranging, dividing by  $\Delta x$ , and letting  $\Delta x$  approach zero,

$$-dq/dx + q \cdot A = 0 \quad (13.3-2)$$

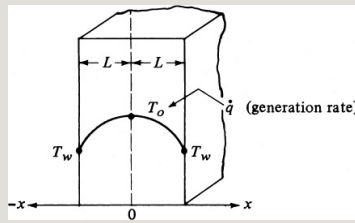


Figure 13.3-1. *Plane wall with internal heat generation at steady state.*

Substituting Eq. (12.3-3) for  $q$ ,

$$d^2T/dx^2 + q/k = 0 \quad (13.3-3)$$

Integration gives the following for  $q$ , constant:

$$T = -q/2k x^2 + C_1 x + C_2 \quad (13.3-4)$$

where  $C_1$  and  $C_2$  are integration constants. The boundary conditions are at  $x = L$  or  $-L$ ,  $T = T_w$ , and at  $x = 0$ ,  $T = T_0$  (center temperature). Then, the temperature profile is

$$T = -q \cdot 2kx^2 + T_0 \quad (13.3-5)$$

The center temperature is

$$T_0 = q \cdot L^2 / 2k + T_w \quad (13.3-6)$$

The total heat lost from the two faces at steady state is equal to the total heat generated,  $q \cdot T$ , in W:

$$qT = q \cdot (2LA) \quad (13.3-7)$$

where  $A$  is the cross-sectional area (surface area at  $T_w$ ) of the plate.

*2. Heat generation in a cylinder.* In a

similar manner, an equation can be derived for a cylinder of radius  $R$  with uniformly distributed heat sources and constant thermal conductivity. The heat is assumed to flow only radially, that is, the ends are neglected or insulated. The final equation for the temperature profile is

$$T = \frac{q}{4k}(R^2 - r^2) + T_w \quad (13.3-8)$$

where  $r$  is distance from the center. The center temperature  $T_0$  is

$$T_0 = \frac{q}{4k}R^2 + T_w \quad (13.3-9)$$

**EXAMPLE 13.3-1. Heat Generation in a Cylinder**

An electric current of 200 A is passed through a stainless-steel wire having a radius  $R$  of 0.001268 m. The wire is  $L = 0.91$  m long and has a resistance  $R$  of 0.126 ohms. The outer surface temperature  $T_w$  is held at 422.1 K. The average thermal conductivity is  $k = 22.5$  W/m · K. Calculate the center temperature.

**Solution:** First, the value of  $q$  must be calculated. Since power =  $I^2R$ , where  $I$  is current in amps and  $R$  is resistance in ohms,

$$I^2R = \text{watts} = q \cdot \pi R^2 L$$

Substituting known values and solving,

$$(200)^2(0.126) = q \cdot \pi (0.01268)^2 (0.91) \quad q = 1.096 \times 10^9 \text{ W/m}^2$$

Substituting into Eq. (13.3-9) and solving,  $T_0 = 441.7 \text{ K}$ .

## 13.4 Steady-State Conduction in Two Dimensions Using Shape Factors

### 13.4A Introduction and Graphical Method for Two-Dimensional Conduction

In previous sections of this chapter, we discussed steady-state heat conduction in one direction. In many cases, however, steady-state heat conduction is occurring in two directions, that is, two-dimensional conduction is occurring. The two-dimensional solutions are more involved and in most cases analytical solutions are not available. One important approximate method for solving such problems is to use a numerical method discussed in detail



in Section 13.5. Another important approximate method is the graphical method, which is a simple procedure that can provide reasonably accurate answers for the heat-transfer rate and is particularly applicable to systems having isothermal boundaries.

In the graphical method, we first note that for one-dimensional heat conduction through a flat slab (see Fig. 13.1-1) the direction of the heat flux or flux lines is always perpendicular to the isotherms. The graphical method for two-dimensional conduction is also based on the requirement that the heat-flux lines and isotherm lines intersect each other at right angles while forming a network of curvilinear squares. This means, as shown in Fig. 13.4-1, that we can sketch the isotherms and also the

flux lines until they intersect at right angles (are perpendicular to each other). With care and experience, we can obtain reasonably accurate results. General steps to use in this graphical method are as follows:

1. Draw a model to scale of the two-dimensional solid.  
Label the isothermal boundaries. In Fig. 13.4-1,  $T_1$  and  $T_2$  are isothermal boundaries.
2. Select a number  $N$  that is the number of equal temperature subdivisions between the isothermal boundaries. In Fig. 13.4-1,  $N = 4$  subdivisions between  $T_1$  and  $T_2$ . Sketch in the isotherm lines and the heat-flow or -flux lines so that they are perpendicular to each other at the intersections. Note that isotherms are perpendicular to adiabatic (insulated) boundaries and also to lines of symmetry.
3. Keep adjusting the isotherm and flux lines until, for each curvilinear square, the condition  $\Delta x = \Delta y$  is satisfied.

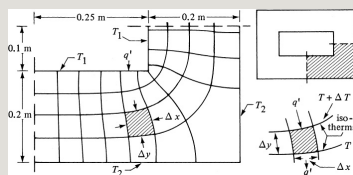


Figure 13.4-1. Graphical curvilinear-square method for two-dimensional heat conduction in a rectangular flue.

In order to calculate the heat flux using the results of the graphical plot, we first assume unit depth of the material. The heat flow  $q'$  through the curvilinear section shown in Fig. 13.4-1 is given by Fourier's law:

$$q' = -kA \frac{dT}{dy} = k(\Delta x \cdot 1) \frac{\Delta T}{\Delta y} \quad (13.4-1)$$

This heat flow  $q'$  will be the same through each curvilinear square within this heat-flow lane. Since  $\Delta x = \Delta y$ , each temperature subdivision  $\Delta T$  is equal. This temperature subdivision can be expressed in terms of the overall temperature difference  $T_1 - T_2$  and  $N$ , the number of equal subdivisions:

$$\Delta T = \frac{T_1 - T_2}{N} \quad (13.4-2)$$

Also, the heat flow  $q'$  through each lane is the same, since  $\Delta x = \Delta y$  in the

construction and in Eq. (13.4-1). Hence, the total heat transfer  $q$  through all of the lanes is

$$q = Mq' = Mk \Delta T \quad (13.4-3)$$

where  $M$  is the total number of heat-flow lanes as determined by the graphical procedure. Substituting Eq. (13.4-2) into (13.4-3),

$$q = MNk(T_1 - T_2) \quad (13.4-4)$$

**EXAMPLE 13.4-1. Two-Dimensional Conduction by Graphical Procedure**

Determine the total heat transfer through the walls of the flue shown in Fig. 13.4-1 if  $T_1 = 600$  K,  $T_2 = 400$  K,  $k = 0.90$  W/m · K, and  $L$  (length of flue) = 5 m.

**Solution:** In Fig. 13.4-1,  $N = 4$  temperature subdivisions and  $M = 9.25$ . The total heat-transfer rate through the four identical sections with a depth or length  $L$  of 5 m is obtained by using Eq. (13.4-4):

$$q = 4[MNkL(T_1 - T_2)] = 4[9.254(0.9)(5.0)(600 - 400)]$$

## 13.4B Shape Factors in Conduction

In Eq. (13.4-4), the factor  $M/N$  is called the conduction shape factor  $S$ , where

$$S = MN \quad (13.4-5)$$

$$q = kS(T_1 - T_2) \quad (13.4-6)$$

This shape factor  $S$  has units of m and is used in two-dimensional heat conduction where only two temperatures are involved. The shape factors for a number of geometries have been obtained and some are given in Table 13.4-1.

For a three-dimensional geometry such as a furnace, separate shape factors are used to obtain the heat flow through the edge and corner sections. When each of the interior dimensions is greater than one-fifth of the wall thickness, the shape

factors are as follows for a uniform wall thickness  $T_w$ :

$$1 = A/T_w \quad S_{\text{edge}} = 0.54L \quad S_{\text{corner}} = 0.15T_w \quad (13.4-7)$$

where  $A$  is the inside area of wall and  $L$  the length of inside edge. For a completely enclosed geometry, there are six wall sections, 12 edges, and eight corners. Note that for a single flat wall,  $q = kS_{\text{wall}}(T_1 - T_2) = k(A/T_w)(T_1 - T_2)$ , which is the same as Eq. (13.1-1) for conduction through a single flat slab.

For a long, hollow cylinder of length  $L$  such as that in Fig. 13.1-2,

$$S = 2\pi L \ln(r_2/r_1) \quad (13.4-8)$$

For a hollow sphere, from Eq. (13.1-18),

$$S = 4\pi r_1 r_2 / (r_2 - r_1) \quad (13.4-9)$$

Table 13.4-1. *Conduction Shape Factors*  
for  $q = kS(T_1 - T_2)^*$

\* The thermal conductivity of the medium is  $k$ .

## 13.5 Numerical Methods for Steady-State Conduction in Two Dimensions

### 13.5A Analytical Equation for Conduction

In Section 13.4, we discussed methods for solving two-dimensional heat-conduction problems using graphical procedures and shape factors. In this section, we consider analytical and numerical methods.

The equation for conduction in the  $x$  direction is as follows:

$$q_x = -kA \frac{\partial T}{\partial x} \quad (13.5-1)$$

Now, we shall derive an equation for steady-state conduction in two directions,  $x$  and  $y$ . Referring to Fig. 13.5-1, a rectangular block  $\Delta x$  by  $\Delta y$  by  $L$  is shown. The total heat input to the block is equal to the output:

$$q_x|_x + q_y|_y = q_x|_{x+\Delta x} + q_y|_{y+\Delta y} \quad (13.5-2)$$

Now, from Eq. (13.5-1),

$$q_x|_x = -k(\Delta y L) \frac{\partial T}{\partial x} \bigg|_x \quad (13.5-3)$$

Writing similar equations for the other three terms and substituting into Eq. (13.5-2),

$$\begin{aligned} -k(\Delta y L) \frac{\partial T}{\partial x} \bigg|_x &+ -k(\Delta x L) \frac{\partial T}{\partial x} \bigg|_y = \\ &-k(\Delta y L) \frac{\partial T}{\partial x} \bigg|_{x+\Delta x} + -k(\Delta x L) \frac{\partial T}{\partial x} \bigg|_{y+\Delta y} \end{aligned}$$



Dividing through by  $\Delta x \Delta y L$  and letting  $\Delta x$  and  $\Delta y$  approach zero, we obtain the final equation for steady-state conduction in two directions:

$$\frac{\partial^2 T}{\partial x^2} + \frac{\partial^2 T}{\partial y^2} = 0 \quad (13.5-5)$$

This is called the *Laplace's equation*.

There are a number of analytical methods for solving this equation. In the method of separation of variables, the final solution is expressed as an infinite Fourier series (H1, G1, K1). We consider the case shown in Fig. 13.5-2. The solid is called a semi-infinite solid since one of its dimensions is  $\infty$ . The two edges or boundaries at  $x = 0$  and  $x = L$  are held constant at  $T_1$  K. The edge at  $y = 0$  is held at  $T_2$ . And at  $y = \infty$ ,  $T = T_1$ . The solution relating  $T$  to position  $y$  and  $x$  is

$$T - T_1 T_2 - T_1 = 4\pi \left[ 11e^{-(\pi/L)y} \sin 1\pi x/L + 13e^{-(\pi/L)y} \sin 3\pi x/L + \dots \right] \quad (13.5-6)$$

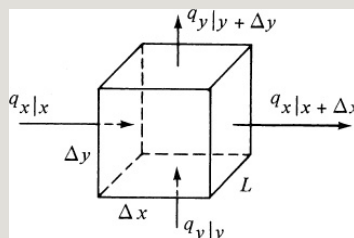


Figure 13.5-1. *Steady-state conduction in two directions.*

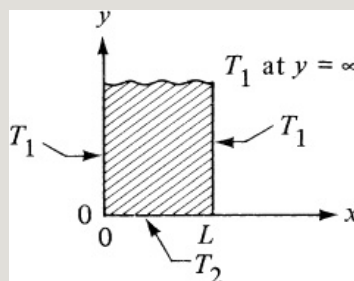


Figure 13.5-2. *Steady-state heat conduction in two directions in a semi-infinite plate.*

Other analytical methods are available and are discussed in many texts (C1, H1, G1, K1). A large number of such analytical solutions have been given in the literature. However, there are many

practical situations where the geometry or boundary conditions are too complex for analytical solutions, so that finite-difference numerical methods are used. These are discussed in the next section.

### 13.5B Finite-Difference Numerical Methods

*1. Derivation of the method.* Since the advent of fast digital computers, solutions to many complex two-dimensional heat-conduction problems by numerical methods are readily possible. In deriving the equations, we can start with the partial differential equation, (13.5-5). Setting up the finite difference of  $\partial^2 T / \partial x^2$ ,

$$\begin{aligned} \partial^2 T / \partial x^2 &= \partial(\partial T / \partial x) / \partial x = (T_{n+1,m} - T_{n,m}) / \Delta x - (T_{n,m} - T_{n-1,m}) / \Delta x \\ &= (T_{n+1,m} - 2T_{n,m} + T_{n-1,m}) / (\Delta x)^2 \quad (13.5-7) \end{aligned}$$

where the index  $m$  stands for a given value of  $y$ ,  $m + 1$  stands for  $y + 1 \Delta y$ , and  $n$  is the index indicating the position of  $T$  on the  $x$  scale. This is shown in Fig. 13.5-3. The two-dimensional solid is divided into squares. The solid inside a square is imagined to be concentrated at the center of the square, and this concentrated mass is a “node.” Imagine that each node is connected to the adjacent nodes by a small conducting rod as shown.

The finite difference of  $\partial^2 T / \partial y^2$  is written in a similar manner:

$$\frac{\partial^2 T}{\partial y^2} = \frac{T_{n,m+1} - 2T_{n,m} + T_{n,m-1}}{(\Delta y)^2} \quad (13.5-8)$$

Substituting Eqs. (13.5-7) and (13.5-8) into Eq. (13.5-5), and setting  $\Delta x = \Delta y$ ,

$$k\Delta y\Delta x(T_{n-1,m}-T_{n,m})+k\Delta y\Delta x(T_{n+1,m}-T_{n,m})+k\Delta x\Delta y(T_{n,m+1}-T_{n,m})+k\Delta x\Delta y(T_{n,m-1}-T_{n,m})=0$$

This equation states that the net heat flow into any point or node is zero at steady state. The shaded area in Fig. 13.5-3 represents the area on which the heat balance was made. Alternatively, Eq. (13.5-9) can be derived by making a heat balance on this shaded area. The total heat in for unit thickness is

$$k\Delta y\Delta x(T_{n-1,m}-T_{n,m})+k\Delta y\Delta x(T_{n+1,m}-T_{n,m})+k\Delta x\Delta y(T_{n,m+1}-T_{n,m})+k\Delta x\Delta y(T_{n,m-1}-T_{n,m})=0$$

Rearranging, this becomes Eq. (13.5-9). In Fig. 13.5-3, the rods connecting the nodes act as fictitious heat-conducting rods.

To use the numerical method, Eq. (13.5-9) is written for each node or point. Hence, for  $N$  unknown nodes,  $N$  linear algebraic equations must be written and the system of equations solved for the various node temperatures. For a hand calculation using a modest number of nodes, the iteration method can be used to solve the system of equations.

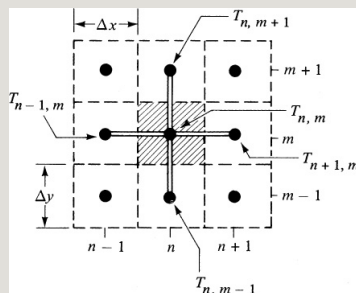


Figure 13.5-3. *Temperatures and arrangement of nodes for two-dimensional steady-state heat conduction.*

**2. Iteration method of solution.** In using the iteration method, the right-hand side of Eq. (13.5-9) is set equal to a residual

$q^-_{n,m}$ :

$$q^-_{n,m} = T_{n,m+1} + T_{n,m-1} + T_{n+1,m} + T_{n-1,m} - 4T_{n,m} \quad (13.5-11)$$

Since  $q^-_{n,m} = 0$  at steady state, solving for  $T_{n,m}$  in Eq. (13.5-11) or (13.5-9),

$$T_{n,m} = T_{n,m+1} + T_{n,m-1} + T_{n+1,m} + T_{n-1,m} \quad (13.5-12)$$

Equations (13.5-11) and (13.5-12) are the final equations to be used. Their use is illustrated in the following example.

**EXAMPLE 13.5-1. Steady-State Heat Conduction in Two Directions**

Figure 13.5-4 shows a cross section of a hollow rectangular chamber with inside dimensions  $4 \times 2$  m and outside dimensions  $8 \times 8$  m. The chamber is 20 m long. The inside walls are held at 600 K and the outside at 300 K. The  $k$  is  $1.5 \text{ W/m} \cdot \text{K}$ . For steady-state conditions, find the heat loss per unit chamber length. Use grids  $1 \times 1$  m.

**Solution:** Since the chamber is symmetrical, one-fourth of the chamber (shaded part) will be used. Preliminary estimates will be made for the first approximation:

$$T_{1,2} = 450 \text{ K}, \quad T_{2,2} = 400, \quad T_{3,2} = 400, \quad T_{3,3} = 400, \quad T_{3,4} = 450,$$

$T_{3,5} = 500$ ,  $T_{4,2} = 325$ ,  $T_{4,3} = 350$ ,  $T_{4,4} = 375$ , and  $T_{4,5} = 400$ . Note that  $T_{0,2} = T_{2,2}$ ,  $T_{3,6} = T_{3,4}$ , and  $T_{4,6} = T_{4,4}$ , by symmetry.

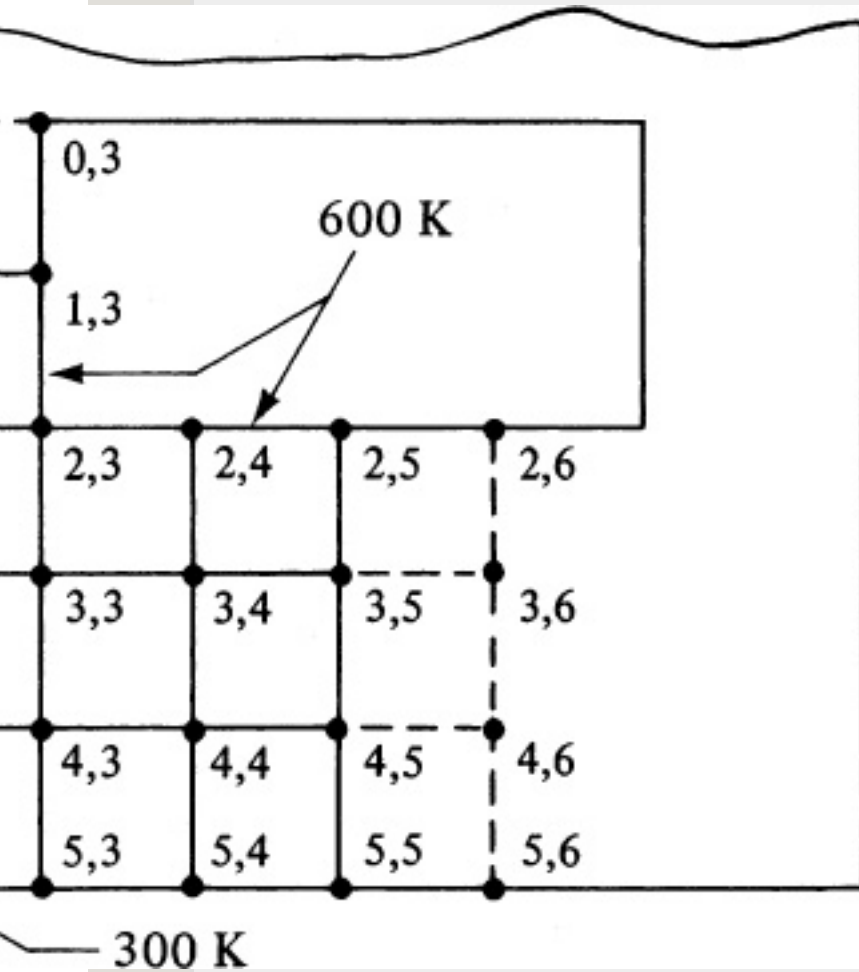


Figure 13.5-4. Square grid pattern for Example 13.5-1.

To start the calculation, one can select any interior point, but it is usually better to start near a boundary. Using  $T_{1,2}$ , we calculate the residual  $q_{1,2}$  using Eq. (13.5-11):

$$q_{1,2} = T_{1,1} + T_{1,3} + T_{0,2} + T_{2,2} - 4T_{1,2} = 300 + 600 + 400 + 400 - 4(450) = -100$$



Hence,  $T_{1,2}$  is not at steady state. Next, we set  $q_{1,2}$  to 0 and calculate a new value of  $T_{1,2}$  using Eq. (13.5-12):

$$T_{1,2} = T_{1,1} + T_{1,3} + T_{0,2} + T_{2,2} = 300 + 600 + 400 + 400 = 425$$

This new value for  $T_{1,2}$  of 425 K will replace the old one of 450 and be used to calculate the other nodes. Next,

$$q_{2,2} = T_{2,1} + T_{2,3} + T_{1,2} + T_{3,2} - 4T_{2,2} = 300 + 600 + 425 + 400 - 4(400) = 125$$

Setting  $q_{1,2}$  to zero and using Eq. (13.5-12),

$$T_{2,2} = T_{2,1} + T_{2,3} + T_{1,2} + T_{3,2} = 300 + 600 + 425 + 400 = 431$$

Continuing for all the rest of the interior nodes,

$$q_{3,2} = 300 + 400 + 431 + 325 - 4(400) = 214 \quad q_{3,2} = 300 + 400 + 431 + 325 - 4(400) = -144$$

Using Eq. (13.5-12),  $T_{3,2} = 364$ ,

$$q_{4,2} = 300 + 479 + 600 + 400 - 4(500) = -42 \quad T_{3,5} = 489 \quad q_{4,2} = 300 + 350 + 364 + 300 - 4(325) = 14 \quad T_{4,2} = 329 \quad q_{4,3} = 329 + 375 + 441 + 300 - 4(400) = 144$$

Having completed one sweep across the grid map, we can start a second approximation, using, of course, the new values calculated. We can start again with  $T_{1,2}$  or we can select the node with the largest residual. Starting with  $T_{1,2}$  again,

$$q_{1,2} = 300 + 600 + 431 + 431 - 4(425) = 62 \quad T_{1,2} = 440 \quad q_{2,2} = 300 + 600 + 440 + 364 - 4(431) = -20 \quad T_{2,2} = 426$$

This is continued until the residuals are as small as desired. The final values are as follows:

$$T_{1,2} = 441, T_{2,2} = 432, T_{3,2} = 384, T_{3,3} = 461, T_{3,4} = 485, T_{3,5} = 490, T_{4,2} = 340, T_{4,3} = 372, T_{4,4} = 387, T_{4,5} = 391$$

To calculate the total heat loss from the chamber per unit chamber length, we use Fig. 13.5-5. For nodes  $T_{2,4}$  to  $T_{3,4}$  with  $\Delta x = \Delta y$  and 1 m deep,

$$q = kA \Delta T \Delta x = k[\Delta x(1)] \Delta x (T_{2,4} - T_{3,4}) = k(T_{2,4} - T_{3,4}) \quad (13.5-13)$$

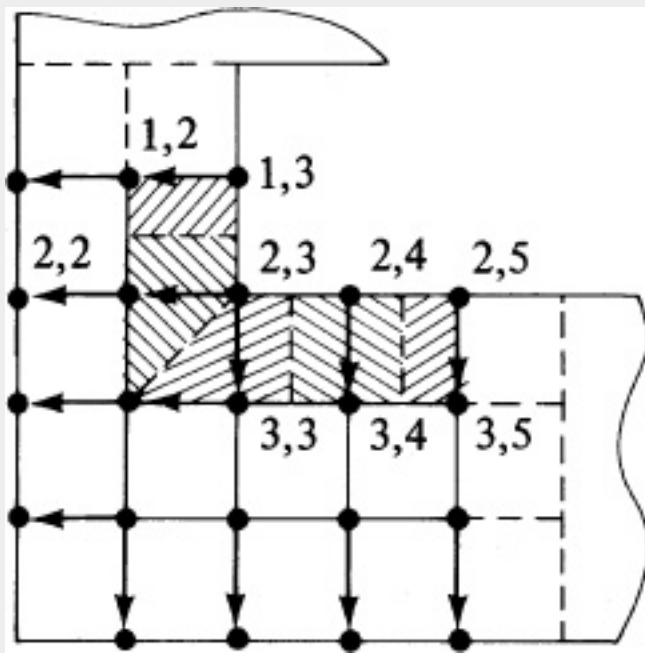


Figure 13.5-5. Drawing for calculation of total heat conduction.

The heat flux for nodes  $T_{2,5}$  to  $T_{3,5}$  and for  $T_{1,3}$  to  $T_{1,2}$  should be multiplied by 12 because of symmetry. The total heat conducted is the sum of the five paths for one-fourth of the solid. For four duplicate parts,

$$q_l = 4k[12(T_{1,3} - T_{1,2}) + (T_{2,3} - T_{2,2}) + (T_{2,4} - T_{3,4}) + 12(T_{2,5} - T_{3,5})]$$

$$(13.5-14) = 4(1.5)$$

$$600-441) + (600-432) + (600-461) + (600-485) + 12(600-490)] = 3340 \text{ W per 1.0 m deep}$$

Also, the total heat conducted can be calculated using the nodes at the outside, as shown in Fig. 13.5-5. This gives  $q_{ll} = 3430 \text{ W}$ . The average value is

$$q_{av} = 3340 + 3430 / 2 = 3385 \text{ W per 1.0 m deep}$$

If a larger number of nodes, that is, a smaller grid size, is used, a more

accurate solution can be obtained. Using a grid size of 0.5 m instead of 1.0 m for Example 13.5-1, a  $q_{av}$  of 3250 W is obtained. If a very fine grid is used, more accuracy can be obtained, but a digital computer would be needed for the large number of calculations. Matrix methods are also available for solving a set of simultaneous equations on a computer; an example can be found on the book's web site. The iteration method used here is often called the Gauss–Seidel method. The simplest and most convenient method is to use a spreadsheet program. This avoids the complication of using complex matrix methods and so forth.

*3. Equations for other boundary conditions.* In Example 13.5-1, the conditions at the boundaries were such

that the node points were known and constant.

For the case where there is convection at the boundary to a constant temperature  $T_\infty$ , a heat balance on the node  $n, m$  in Fig. 13.5-6a is as follows, where heat in = heat out (K1):

$$k\Delta y\Delta x(T_{n-1,m}-T_{n,m})+k\Delta x\frac{\Delta x}{2}\Delta y(T_{n,m}+1-T_{n,m})+k\Delta x\frac{\Delta x}{2}\Delta y(T_{n,m-1}-T_{n,m})=h\Delta y(T_{n,m}-T_\infty)\lim_{\Delta x\rightarrow 0}(13.5-15)$$

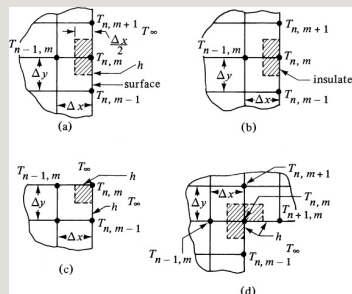


Figure 13.5-6. Other types of boundary conditions: (a) convection at a boundary, (b) insulated boundary, (c) exterior corner with convective boundary, (d) interior corner with convective boundary.

Setting  $\Delta x = \Delta y$ , rearranging, and setting the resultant equation  $q^-_{n,m}$  residual, the following results:

- For convection at a boundary,

$$h\Delta x k T_{\infty} + 12(T_{n-1,m} + T_{n,m+1} + T_{n,m-1}) - T_{n,m}(h\Delta x k + 2) = q^-_{n,m} \quad (13.5-16)$$

In a similar manner, for the cases in Fig. 13.5-6:

- For an insulated boundary,

$$12(T_{n,m+1} + T_{n,m-1}) + T_{n-1,m} - 2T_{n,m} = q^-_{n,m}$$

- For an exterior corner with convection at the boundary,

$$h\Delta x k T_{\infty} + 12(T_{n-1,m} + T_{n,m-1}) - (h\Delta x k + 1)T_{n,m} = q^-_{n,m} \quad (13.5-18)$$

- For an interior corner with convection at the boundary,

$$h\Delta x k T_{\infty} + T_{n-1,m} + T_{n,m+1} + 12(T_{n+1,m} + T_{n,m-1}) - (3 + h\Delta x k)T_{n,m} = q^-_{n,m} \quad (13.5-19)$$

For curved boundaries and other types of boundaries, see (C2, K1). To use Eqs. (13.5-16)–(13.5-19), the residual  $q^-_{n,m}$

is first obtained using the proper equation. Then,  $q_{n,m}^-$  is set equal to zero and  $T_{n,m}$  solved for in the resultant equation.

## 13.6 Chapter Summary

### Conduction (Fourier's Law)

$$q_A = -kA \frac{dT}{dx} \quad (12.3-3)$$

In Section 13.1, equations were derived and examples solved when thermal conductivity ( $k$ ) was a function of temperature when applied to Fourier's Law:

$$\begin{aligned} q_A \int_{x_1}^{x_2} \frac{dx}{k} &= \int_{T_2}^{T_1} \frac{dT}{aT + b} \\ q_A (x_2 - x_1) &= \frac{k}{a} \ln \left( \frac{aT_1 + b}{aT_2 + b} \right) \\ q_A &= \frac{k \Delta x}{x_2 - x_1} \ln \left( \frac{aT_1 + b}{aT_2 + b} \right) \end{aligned} \quad (13.1-3)$$

In addition, conduction problems where area was not constant were derived and solved for various geometries. For example:

- Conduction through a hollow cylinder:

$$q = k2\pi L \ln(r_2/r_1)(T_1 - T_2) \quad (13.1-8)$$

- Conduction through a hollow sphere:

$$q = 4\pi k(T_1 - T_2) \frac{1/r_1 - 1/r_2}{1/r_1 - 1/r_2} = T_1 - T_2 (1/r_1 - 1/r_2) / 4\pi k \quad (13.1-18)$$

- Multilayer cylinders:

$$q = T_1 - T_4 \frac{1}{R_A + R_B + R_C} = T_1 - T_4 \sum R \quad (13.1-15)$$

In Section 13.2, overall heat transfer by combined conduction and convection is often expressed in terms of an overall heat-transfer coefficient  $U$  defined by

$$q = UA\Delta T_m \quad (13.2-13)$$

where  $U$  is

$$U = \frac{1}{\frac{1}{h_i} + \frac{\Delta x}{k} + \frac{1}{h_o}} \quad \text{W/m}^2 \cdot \text{K} \quad (\text{Btu/h} \cdot \text{ft}^2 \cdot ^\circ\text{F}) \quad (13.2-4)$$

When dealing with heat exchangers, where temperatures change as the fluid travels through the exchanger, the  $\Delta T_{\text{overall}}$  is replaced with  $\Delta T_{\text{lm}}$  where:

$$\Delta T_{\text{lm}} = \frac{\Delta T_2 - \Delta T_1}{\ln(\Delta T_2 / \Delta T_1)} \quad (13.2-22)$$

The last two sections of the chapter dealt with steady-state conduction in two dimensions. In the first section 13.4, an approximate method called the graphical method was introduced. This method is a simple method that can provide reasonably accurate answers for the heat-transfer rate. The conduction equation becomes:

$$q = kS(T_1 - T_2) \quad (13.4-6)$$



In Section 13.5, both an analytical and a numerical method (finite-difference) were presented.

## Problems

**13.1-1. *Mean Thermal Conductivity in a Cylinder.*** Prove that if the thermal conductivity varies linearly with temperature as in Eq. (12.3-18), the proper mean value  $k_m$  to use in the cylindrical equation is given by Eq. (13.1-4) as in a slab.

**13.1-2. *Heat Removal of a Cooling Coil.*** A cooling coil of 1.0 ft of 304 stainless-steel tubing having an inside diameter of 0.25 in. and an outside diameter of 0.40 in. is being used to remove heat from a bath. The temperature at the inside surface of the tube is 40°F and is 80°F on the outside.

The thermal conductivity of 304 stainless steel is a function of temperature:

$$k = 7.75 + 7.78 \times 10^{-3}T$$

where  $k$  is in  $\text{btu/h} \cdot \text{ft} \cdot ^\circ\text{F}$  and  $T$  is in  $^\circ\text{F}$ . Calculate the heat removal in  $\text{btu/s}$  and watts.

**Ans.** 1.225  $\text{btu/s}$ , 1292 W

**13.1-3. *Removal of Heat from a Bath.***

Repeat Problem 13.1-2 but calculate for a cooling coil made of 308 stainless steel having an average thermal conductivity of  $15.23 \text{ W}/(\text{m} \cdot \text{K})$ .

**13.1-4. *Temperature Distribution in a Hollow Sphere.*** Derive Eq. (13.1-18)

for the steady-state conduction of heat in a hollow sphere. Also, derive an

equation that shows that the temperature varies hyperbolically with the radius  $r$ .

$$\text{Ans. } T - T_1 = \frac{T_2 - T_1}{r_2 - r_1} (1 - r_1/r)$$

### 13.2-1. *Heat Loss from a Steam*

**Pipeline.** A steel pipeline, 2-in.

Schedule 40 pipe, contains saturated steam at  $121.1^\circ\text{C}$ . The line is covered with 25.4 mm of insulation. Assuming that the inside surface temperature of the metal wall is at  $121.1^\circ\text{C}$  and the outer surface of the insulation is at  $26.7^\circ\text{C}$ , calculate the heat loss for 30.5 m of pipe. Also, calculate the kg of steam condensed per hour in the pipe due to the heat loss. The average  $k$  for steel from Appendix A.3 is  $45 \text{ W/m} \cdot \text{K}$  and the  $k$  for the insulation is 0.182.

$$\text{Ans. } 5384 \text{ W, } 8.81 \text{ kg steam/h}$$

### 13.2-2. Heat Loss with a Trial-and-

**Error Solution.** The exhaust duct from a heater has an inside diameter of 114.3 mm with ceramic walls 6.4 mm thick. The average  $k = 1.52 \text{ W/m} \cdot \text{K}$ . Outside this wall, an insulation of rock wool 102 mm thick is installed. The thermal conductivity of the rock wool is  $k = 0.046 + 1.56 \times 10^{-4} T^{\circ}\text{C} \text{ (W/m} \cdot \text{K)}$ . The inside surface temperature of the ceramic is  $T_1 = 588.7 \text{ K}$ , and the outside surface temperature of the insulation is  $T_3 = 311 \text{ K}$ . Calculate the heat loss for 1.5 m of duct and the interface temperature  $T_2$  between the ceramic and the insulation. [*Hint:* The correct value of  $k_m$  for the insulation is that evaluated at the mean temperature of  $(T_2 + T_3)/2$ . Hence, for the first trial assume a mean temperature of, say, 448 K. Then, calculate the heat loss and  $T_2$ . Using this

new  $T_2$ , calculate a new mean temperature and proceed as before.]

**13.2-3. Heat Loss by Convection and Conduction.** A glass window with an area of  $0.557 \text{ m}^2$  is installed in the wooden outside wall of a room. The wall dimensions are  $2.44 \times 3.05 \text{ m}$ . The wood has a  $k$  of  $0.1505 \text{ W/m} \cdot \text{K}$  and is  $25.4 \text{ mm}$  thick. The glass is  $3.18 \text{ mm}$  thick and has a  $k$  of  $0.692$ . The inside room temperature is  $299.9 \text{ K}$  ( $26.7^\circ\text{C}$ ) and the outside air temperature is  $266.5 \text{ K}$ . The convection coefficient  $h_i$  on the inside wall of the glass and the wood is estimated as  $8.5 \text{ W/m}^2 \cdot \text{K}$ ; the outside  $h_o$  is also estimated as  $8.5$  for both surfaces. Calculate the heat loss through the wooden wall, through the glass, and the total.

**Ans.** 569.2 W (wood) (1942 btu/h), 77.6 W (glass) (265 btu/h), 646.8 W (total) (2207 btu/h)

### **13.2-4. Convection, Conduction, and**

**Overall  $U$ .** A gas at 450 K is flowing inside a 2-in. steel pipe, Schedule 40.

The pipe is insulated with 51 mm of lagging having a mean  $k = 0.0623 \text{ W/m} \cdot \text{K}$ .

The convective heat-transfer coefficient of the gas inside the pipe is  $30.7 \text{ W/m}^2 \cdot \text{K}$  and the convective coefficient on the outside of the lagging is 10.8. The air is at a temperature of 300 K.

- Calculate the heat loss per unit length of 1 m of pipe using resistances.
- Repeat, using the overall  $U_o$  based on the outside area  $A_o$ .

### **13.2-5. Heat Transfer in a Steam**

**Heater.** Water at an average of  $70^{\circ}\text{F}$  is flowing in a 2-in. steel pipe, Schedule 40. Steam at  $220^{\circ}\text{F}$  is condensing on the outside of the pipe. The convective coefficient for the water inside the pipe is  $h = 500 \text{ btu/h} \cdot \text{ft}^2 \cdot ^{\circ}\text{F}$  and the condensing steam coefficient on the outside is  $h = 1500$ .

- Calculate the heat loss per unit length of 1 ft of pipe using resistances.
- Repeat, using the overall  $U_i$  based on the inside area  $A_i$ .
- Repeat, using  $U_o$ .

**Ans.** (a)  $q = 26\,710 \text{ btu/h}$  (7.828 kW),  
 (b)  $U_i = 329.1 \text{ btu/h} \cdot \text{ft}^2 \cdot ^{\circ}\text{F}$  (1869  $\text{W/m}^2 \cdot \text{K}$ ), (c)  $U_o = 286.4 \text{ btu/h} \cdot \text{ft}^2 \cdot ^{\circ}\text{F}$  (1626  $\text{W/m}^2 \cdot \text{K}$ )

**13.2-6. Heat Loss from Temperature Measurements.** A steel pipe carrying

steam has an outside diameter of 89 mm. It is lagged with 76 mm of insulation having an average  $k = 0.043 \text{ W/m} \cdot \text{K}$ . Two thermocouples, one located at the interface between the pipe wall and the insulation and the other at the outer surface of the insulation, give temperatures of  $115^\circ\text{C}$  and  $32^\circ\text{C}$ , respectively. Calculate the heat loss in W per m of pipe.

**13.2-7. *Effect of Convective Coefficients on Heat Loss in a Double Window.*** Repeat Problem 12.6-3 for heat loss in the double window. However, include a convective coefficient of  $h = 11.35 \text{ W/m}^2 \cdot \text{K}$  on one outside surface of one side of the window and an  $h$  of 11.35 on the other outside surface. Also calculate the overall  $U$ .



**Ans.**  $q = 106.7 \text{ W}$ ,  $U = 2.29 \text{ W/m}^2 \cdot \text{K}$

### **13.2-8. Critical Radius for Insulation.**

A metal steam pipe having an outside diameter of 30 mm has a surface temperature of 400 K and is to be insulated with an insulation having a thickness of 20 mm and a  $k$  of  $0.08 \text{ W/m} \cdot \text{K}$ . The pipe is exposed to air at 300 K and a convection coefficient of  $30 \text{ W/m}^2 \cdot \text{K}$ .

- Calculate the critical radius and the heat loss per m of length for the bare pipe.
- Calculate the heat loss for the insulated pipe assuming that the surface temperature of the pipe remains constant.

**Ans.** (b)  $q = 54.4 \text{ W}$

**13.2-9. Heat-Transfer Area and Use of Log Mean Temperature Difference.** A reaction mixture having a  $c_{pm} = 2.85 \text{ kJ/}$

kg · K is flowing at a rate of 7260 kg/h and is to be cooled from 377.6 K to 344.3 K. Cooling water at 288.8 K is available and the flow rate is 4536 kg/h. The overall  $U_o$  is 653 W/m<sup>2</sup> · K.

- For counterflow, calculate the outlet water temperature and the area  $A_o$  of the exchanger.
- Repeat for cocurrent flow.

**Ans.** (a)  $T_1 = 325.2$  K,  $A_o = 5.43$  m<sup>2</sup>; (b)  
 $A_o = 6.46$  m<sup>2</sup>

**13.2-10. Heating Water with Hot Gases and Heat-Transfer Area.** Water flowing at the rate of 13.85 kg/s is to be heated from 54.5 to 87.8°C in a heat exchanger by 54430 kg/h of hot gas flowing counterflow and entering at 427°C ( $c_{pm} = 1.005$  kJ/kg · K). The overall  $U_o = 69.1$  W/m<sup>2</sup> · K. Calculate the exit-gas temperature and the heat-transfer area.

**Ans.**  $T = 299.5^{\circ}\text{C}$

**13.2-11. Cooling Oil and Overall  $U$ .** Oil flowing at the rate of 7258 kg/h with a  $c_{pm} = 2.01 \text{ kJ/kg} \cdot \text{K}$  is cooled from 394.3 K to 338.9 K in a counterflow heat exchanger by water entering at 294.3 K and leaving at 305.4 K. Calculate the flow rate of the water and the overall  $U_i$  if the  $A_i$  is 5.11 m<sup>2</sup>.

**Ans.** 17 420 kg/h,  $U_i = 686 \text{ W/m}^2 \cdot \text{K}$

**13.3-1. Uniform Chemical Heat Generation.** Heat is being generated uniformly by a chemical reaction in a long cylinder of radius 91.4 mm. The generation rate is constant at 46.6 W/m<sup>3</sup>. The walls of the cylinder are cooled so that the wall temperature is held at 311.0 K. The thermal conductivity is 0.865 W/

m · K. Calculate the center-line temperature at steady state.

$$\text{Ans. } T_o = 311.112 \text{ K}$$

**13.3-2. Heat of Respiration of a Food Product.** A fresh-food product is held in cold storage at 278.0 K. It is packed in a container in the shape of a flat slab with all faces insulated except for the top flat surface, which is exposed to the air at 278.0 K. For estimation purposes, the surface temperature will be assumed to be 278 K. The slab is 152.4 mm thick and the exposed surface area is 0.186 m<sup>2</sup>. The density of the foodstuff is 641 kg/m<sup>3</sup>. The heat of respiration is 0.070 kJ/kg · h and the thermal conductivity is 0.346 W/m · K. Calculate the maximum temperature in the food product at steady state and the total heat given off

in W. (*Note:* It is assumed in this problem that there is no air circulation inside the foodstuff. Hence, the results will be conservative, since circulation during respiration will reduce the temperature.)

**Ans.** 278.42 K, 0.353 W (1.22 btu/h)

**13.3-3. *Temperature Rise in a Heating Wire.*** A current of 250 A is passing through a stainless-steel wire having a diameter of 5.08 mm. The wire is 2.44 m long and has a resistance of 0.0843  $\Omega$ . The outer surface is held constant at 427.6 K. The thermal conductivity is  $k = 22.5 \text{ W/m} \cdot \text{K}$ . Calculate the center-line temperature at steady state.

**13.4-1. *Curvilinear-Squares Graphical Method.*** Repeat Example 13.4-1 but

with the following changes:

- Select the number of equal temperature subdivisions between the isothermal boundaries to be five instead of four. Draw in the curvilinear squares and determine the total heat flux. Also calculate the shape factor  $S$ . Label each isotherm with the actual temperature.
- Repeat part (a), but in this case the thermal conductivity is not constant but  $k = 0.85 (1 + 0.00040T)$ , where  $T$  is temperature in K. [Note: To calculate the overall  $q'$ , the mean value of  $k$  at the mean temperature is used. The spacing of the isotherms is independent of how  $k$  varies with  $T$  (M1). However, the temperatures corresponding to the individual isotherms are a function of how the value of  $k$  depends upon  $T$ . Write the equation for  $q'$  for a given curvilinear section using the mean value of  $k$  over the temperature interval. Equate this to the overall value of  $q$  divided by  $M$  or  $q/M$ . Then solve for the isotherm temperature.]

### **13.4-2. Heat Loss from a Furnace.**

A rectangular furnace with inside dimensions of  $1.0 \times 1.0 \times 2.0$  m has a wall thickness of 0.20 m. The  $k$  of the walls is  $0.95 \text{ W/m} \cdot \text{K}$ . The inside of the

furnace is held at 800 K and the outside at 350 K. Calculate the total heat loss from the furnace.

$$\text{Ans. } q = 25\,171 \text{ W}$$

### **13.4-3. Heat Loss from a Buried Pipe.**

A water pipe whose wall temperature is 300 K has a diameter of 150 mm and a length of 10 m. It is buried horizontally in the ground at a depth of 0.40 m measured to the center line of the pipe. The ground surface temperature is 280 K and  $k = 0.85 \text{ W/m} \cdot \text{K}$ . Calculate the loss of heat from the pipe.

$$\text{Ans. } q = 451.2 \text{ W}$$

**13.5-1. Temperatures in a Semi-Infinite Plate.** A semi-infinite plate is similar to that in Fig. 13.5-2. At the surfaces  $x = 0$  and  $x = L$ , the temperature is held

constant at 200 K. At the surface  $y = 0$ , the temperature is held at 400 K. If  $L = 1.0$  m, calculate the temperature at the point  $y = 0.5$  m and  $x = 0.5$  m at steady state.

**13.5-2. Heat Conduction in a Two-Dimensional Solid.** For two-dimensional heat conduction as given in Example 13.5-1, derive the equation to calculate the total heat loss from the chamber per unit length using the nodes at the outside. There should be eight paths for one-fourth of the chamber. Substitute the actual temperatures into the equation and obtain the heat loss.

$$\text{Ans. } q = 3426 \text{ W}$$

**13.5-3. Steady-State Heat Loss from a Rectangular Duct.** A chamber that is in



the shape of a long, hollow, rectangular duct has outside dimensions of  $3 \times 4$  m and inside dimensions of  $1 \times 2$  m. The walls are 1 m thick. The inside surface temperature is constant at 800 K and the outside constant at 200 K. The  $k = 1.4$  W/m  $\cdot$  K. Calculate the steady-state heat loss per unit m of length of duct. Use a grid size of  $\Delta x = \Delta y = 0.5$  m. Also, use the outside nodes to calculate the total heat conduction. Use a spreadsheet for the calculation.

**Ans.**  $q = 7428$  W

**13.5-4. Two-Dimensional Heat Conduction and Different Boundary Conditions.** A very long, solid piece of material 1 by 1 m square has its top face maintained at a constant temperature of 1000 K and its left face at 200 K. The

bottom face and right face are exposed to an environment at 200 K and have a convection coefficient of  $h = 10 \text{ W/m}^2 \cdot \text{K}$ . The  $k = 10 \text{ W/m} \cdot \text{K}$ . Use a grid size of  $\Delta x = \Delta y = 13 \text{ m}$  and calculate the steady-state temperatures of the various nodes.

**13.5-5. Nodal Point at Exterior Corner Between Insulated Surfaces.** Derive the finite-difference equation for the case for the nodal point  $T_{n,m}$  at an exterior corner between insulated surfaces. The diagram is similar to Fig. 13.5-6c except that the two boundaries are insulated.

**Ans.**  $q_{nm}^- = \frac{1}{2}(T_{n-1,m} + T_{n,m-1}) - T_{n,m}$

## References

## Notation



# Chapter 14. Principles of Unsteady-State Heat Transfer

## 14.0 Chapter Objectives

On completion of this chapter, a student should be able to:

- Derive the equation for unsteady-state conduction with and without internal heat-generation
- Calculate the Biot number ( $N_{Bi}$ ), which compares the relative values of internal conduction resistance and surface convective resistance to heat transfer
- Use the Biot number as a guide when choosing the appropriate solution method to solve unsteady state problems
- Use the lumped capacity method to solve unsteady state problems where  $N_{Bi} < 0.1$
- Use equations to solve unsteady state problems with larger Biot numbers for a flat plat of thickness  $2H$  or for a semi-infinite solid
- Use convenient charts to help solve unsteady state

problems, with moderate Biot numbers where both internal and external resistances apply

- Apply numerical, finite-difference methods for unsteady-state conduction problems
- Derive the differential equation of energy change

## **14.1 Derivation of the Basic Equation**

### **14.1A Introduction**

In Chapters 12 and 13, we considered various heat-transfer systems in which the temperature at any given point and the heat flux were always constant over time, that is, at steady state. In this chapter, we will study processes in which the temperature at any given point in the system changes with time, that is, when heat transfer is in unsteady state or transient.

Before steady-state conditions can be

reached in a process, some time must elapse after the heat-transfer process is initiated to allow the unsteady-state conditions to disappear. For example, in Section 13.1A, we determined the heat flux through a wall at steady state. We did not consider the period during which one side of the wall was being heated up and the temperatures were increasing.

Unsteady-state heat transfer is important because of the large number of heating and cooling problems occurring industrially. In metallurgical processes, it is necessary to predict cooling and heating rates for various geometries of metals in order to predict the time required to reach certain temperatures. In food processing, for example, and specifically the canning industry, perishable canned foods are heated by

immersion in steam baths or chilled by immersion in cold water. In the paper industry, logs are immersed in steam baths before processing. In most of these processes, the material is suddenly immersed in a fluid of higher or lower temperature.

#### **14.1B Derivation of the Unsteady-State Conduction Equation**

To derive the equation for unsteady-state conduction in one direction in a solid, we refer to Fig. 14.1-1. Heat is being conducted in the  $x$  direction in the cube  $\Delta x$ ,  $\Delta y$ ,  $\Delta z$  in size. For conduction in the  $x$  direction, we write

$$q_x = -kA \frac{\partial T}{\partial x} \quad (14.1-1)$$

The term  $\partial T / \partial x$  means the partial or derivative of  $T$  with respect to  $x$ , with

the other variables,  $y$ ,  $z$ , and time  $t$ , being held constant. Next, making a heat balance on the cube, we can write

$$\text{heat output} + \text{rate of heat accumulation} \quad (14.1-2)$$

The rate of heat input to the cube is

$$\begin{aligned} \text{rate of heat input} &= q_x|_x = \\ &= -k(\Delta y \Delta z) \frac{\partial T}{\partial x} \bigg|_x \quad (14.1-3) \end{aligned}$$

Also,

$$\begin{aligned} \text{rate of heat input} &= q_x|_x \Delta x = \\ &= -k(\Delta y \Delta z) \frac{\partial T}{\partial x} \bigg|_{x+\Delta x} \quad (14.1-4) \end{aligned}$$

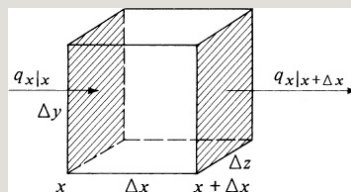


Figure 14.1-1. *Unsteady-state conduction in one direction.*

The rate of accumulation of heat in the



volume  $\Delta x \Delta y \Delta z$  in time  $\partial t$  is

$$\text{heat accumulation} = (\Delta x \Delta y \Delta z) \rho c_p \frac{\partial T}{\partial t} \quad (14.1-5)$$

The rate of heat generation in volume  $\Delta x \Delta y \Delta z$  is

$$\text{rate of heat accumulation} = (\Delta x \Delta y \Delta z) q \quad (14.1-6)$$

Substituting Eqs. (14.1-3)–(14.1-6) into (14.1-2) and dividing  $\Delta x \Delta y \Delta z$ ,

$$q_x - k \left( \frac{\partial T}{\partial x} \bigg|_{x+\Delta x} - \frac{\partial T}{\partial x} \bigg|_x \right) = \rho C_p \frac{\partial T}{\partial t} \quad (14.1-7)$$

Letting  $\Delta x$  approach zero, we have the second partial of  $T$  with respect to  $x$  or  $\partial^2 T / \partial x^2$  on the left side. Then, rearranging,

$$= k \rho c_p \frac{\partial^2 T}{\partial x^2} + q \cdot \rho c_p = \alpha \frac{\partial^2 T}{\partial x^2} + q \cdot \rho c_p \quad (14.1-8)$$

where  $\alpha$  is  $k/\rho c_p$ , thermal diffusivity.

This derivation assumes constant  $k$ ,  $\rho$ , and  $c_p$ . In SI units,  $\alpha = m^2/s$ ,  $T = K$ ,  $t = s$ ,  $k = W/m \cdot K$ ,  $\rho = kg/m^3$ ,  $q = W/m^3$ , and  $c_p = J/kg \cdot K$ . In English units,  $\alpha = ft^2/h$ ,  $T = ^\circ F$ ,  $t = h$ ,  $k = btu/h \cdot ft \cdot ^\circ F$ ,  $\rho = lb_m/ft^3$ ,  $q = btu/h \cdot ft^3$  and  $c_p = btu/lb_m \cdot ^\circ F$ .

For conduction in three dimensions, a similar derivation gives

$$\frac{\partial T}{\partial t} = \alpha (\frac{\partial^2 T}{\partial x^2} + \frac{\partial^2 T}{\partial y^2} + \frac{\partial^2 T}{\partial z^2}) + \frac{q}{\rho c_p} \quad (14.1-9)$$

In many cases, unsteady-state heat conduction is occurring but the rate of heat generation is zero. Then, Eqs. (14.1-8) and (14.1-9) become

$$\frac{\partial T}{\partial t} = \alpha \frac{\partial^2 T}{\partial x^2} \quad (14.1-10)$$

$$\frac{\partial T}{\partial t} = \alpha (\frac{\partial^2 T}{\partial x^2} + \frac{\partial^2 T}{\partial y^2} + \frac{\partial^2 T}{\partial z^2}) \quad (14.1-11)$$

Equations (14.1-10) and (14.1-11) relate the temperature  $T$  with position  $x$ ,  $y$ , and  $z$  and time  $t$ . The solutions of Eqs. (14.1-10) and (14.1-11) for certain specific cases as well as for the more general cases are considered in much of the remainder of this chapter.

## **14.2 Simplified Case for Systems with Negligible Internal Resistance**

### **14.2A Basic Equation**

We begin our treatment of transient heat conduction by analyzing a simplified case. In this situation, we consider a solid that has a very high thermal conductivity or a very low internal conductive resistance compared to the external surface resistance, where convection occurs from the external fluid to the surface of the solid. Since the internal

resistance is very small, the temperature within the solid is essentially uniform at any given time.

An example would be a small, hot cube of steel at  $T_0(K)$  at time  $t = 0$ , suddenly immersed in a large bath of cold water at  $T_\infty$  that is held constant with time.

Assume that the heat-transfer coefficient  $h$  in  $W/m^2 \cdot K$  is constant with time.

Making a heat balance on the solid object for a small time interval of time  $dt$  (s), the heat transfer from the bath to the object must equal the change in internal energy of the object:

$$hA(T_\infty - T)dt = c_p \rho V dT \quad (14.2-1)$$

where  $A$  is the surface area of the object in  $m^2$ ,  $T$  is the average temperature of

the object at time  $t$  in s,  $\rho$  is the density of the object in  $\text{kg/m}^3$ , and  $V$  is the volume in  $\text{m}^3$ . Rearranging the equation and integrating between the limits of  $T = T_0$  when  $t = 0$ , and  $T = T$  when  $t = t$ ,

$$\int_{T_0}^T \frac{dT}{T - T_\infty} = -\frac{hA}{c_p \rho V} \int_{t=0}^t dt \quad (14.2-2)$$

$$T - T_\infty = (T_0 - T_\infty) e^{-(hA/c_p \rho V)t} \quad (14.2-3)$$

This equation describes the time–temperature history of the solid object. The term  $c_p \rho V$  is often called the *lumped thermal capacitance* of the system. This type of analysis is often called the *lumped capacity method* or the *Newtonian heating or cooling method*.

#### 14.2B Equation for Different Geometries

When using Eq. (14.2-3), the

surface/volume ratio of the object must be known. The basic assumption of negligible internal resistance was made in the derivation. This assumption is reasonably accurate when

$$N_{Bi} = h x_c / k \quad (14.2-4)$$

where  $h x_c / k$  is called the Biot number  $N_{Bi}$ , which is dimensionless, and  $x_c$  is a characteristic dimension of the body obtained from  $x_c = V/A$ . The Biot number compares the relative values of internal conduction resistance and surface convective resistance to heat transfer.

For a sphere,

$$x_c = V/A = 4\pi r^3 / 3 \cdot 4\pi r^2 = r \quad (14.2-5)$$

For a long cylinder,

$$x_c = V A = \pi D^2 L / 4 \pi D L = D/4 = r/2 \quad (14.2-6)$$

For a long square rod,

$$x_c = V A = (2x)^2 L / 4(2x)L = x^2/(x) = x/2 \quad (\text{half thickness}) \quad (14.2-7)$$

**EXAMPLE 14.2-1. Cooling of a Steel Ball**

A steel ball having a radius of 1.0 in. (25.4 mm) is at a uniform temperature of 800°F (699.9 K). It is suddenly plunged into a medium whose temperature is held constant at 250°F (394.3 K). Assuming a convective coefficient of  $h = 2.0 \text{ btu/h} \cdot \text{ft}^2 \cdot ^\circ\text{F}$  ( $11.36 \text{ W/m}^2 \cdot \text{K}$ ), calculate the temperature of the ball after 1 h (3600 s). The average physical properties are  $k = 25 \text{ btu/h} \cdot \text{ft} \cdot ^\circ\text{F}$  ( $43.3 \text{ W/m} \cdot \text{K}$ ),  $\rho = 490 \text{ lbm/ft}^3$  ( $7849 \text{ kg/m}^3$ ), and  $c_p = 0.11 \text{ btu/lbm} \cdot ^\circ\text{F}$  ( $0.4606 \text{ kJ/kg} \cdot \text{K}$ ). Use SI and English units.

**Solution:** For a sphere from Eq. (14.2-5),

$$x_c = V A = r/3 = 1 \text{ in} / 3 = 0.33 \text{ in} = 1 \text{ ft} / 12 \text{ in} = 0.028 \text{ ft} = 8.467 \times 10^{-3} \text{ m}$$

From Eq. (14.2-4) for the Biot number,

$$\begin{aligned} \text{NBi} &= h x_c k = (2.0 \text{ btu/h} \cdot \text{ft}^2 \cdot ^\circ\text{F}) (0.028 \text{ ft}) (25 \text{ btu/h} \cdot \text{ft} \cdot ^\circ\text{F}) = 0.00222 \\ \text{NBi} &= h x_c k = (11.36 \text{ W/m}^2 \cdot \text{K}) (8.467 \times 10^{-3} \text{ m}) (43.3 \text{ W/m} \cdot \text{K}) = 0.00222 \end{aligned}$$

This value is  $< 0.1$ ; hence, the lumped capacity method can be used. Then,

$$\begin{aligned} h A c_p \rho V &= h c_p \rho x_c = (2.0 \text{ btu/h} \cdot \text{ft}^2 \cdot ^\circ\text{F}) (0.11 \text{ btu/lbm} \cdot ^\circ\text{F}) (490 \text{ lbm/ft}^3) \\ & (0.028 \text{ ft}) = 1.335 \text{ h}^{-1} \\ h c_p \rho x_c &= (11.36 \text{ W/m}^2 \cdot \text{K}) (4606 \text{ J/kg} \cdot \text{K}) \\ & (7849 \text{ kg/m}^3) (8.47 \times 10^{-3} \text{ m}) = 3.71 \cdot 10^{-4} \text{ s}^{-1} = 1.335 \text{ h}^{-1} \end{aligned}$$

Substituting into Eq. (14.2-3) for  $t = 1.0$  h and solving for  $T$ ,

$$\begin{aligned} T - T_{\infty} &= T_0 - T_{\infty} e^{-(hA/c\rho V)t} \\ (1.335 \text{ h})(1 \text{ h}) &= 3950 \text{ F} - 394.3 \text{ K} \frac{699.9 \text{ K} - 394.3 \text{ K}}{e^{-(hA/c\rho V)t} - 1} \\ &= (3.71 \times 10^{-4} \text{ s})(3600 \text{ s}) = 474.9 \text{ K} \end{aligned}$$

## 14.2C Total Amount of Heat Transferred

The temperature of the solid at any time  $t$  can be calculated from Eq. (14.2-3). At any time  $t$ , the instantaneous rate of heat transfer  $q(t)$  in W from the solid of negligible internal resistance can be calculated from

$$q(t) = hA(T - T_{\infty}) \quad (14.2-8)$$

Substituting the instantaneous temperature  $T$  from Eq. (14.2-3) into Eq. (14.2-8),

$$q(t) = hA(T_0 - T_{\infty}) e^{-(hA/c\rho V)t} \quad (14.2-9)$$



To determine the total amount of heat  $Q$  in  $W \cdot s$  or  $J$  transferred from the solid from time  $t = 0$  to  $t = t$ , we can integrate Eq. (14.2-9):

$$Q = \int_{t=0}^{t=t} q(t) dt = \int_{t=0}^{t=t} hA(T_0 - T)e^{-(hA/c\rho V)t} dt \quad (14.2-10)$$

$$Q = c\rho V(T_0 - T_\infty)[1 - e^{-(hA/c\rho V)t}] \quad (14.2-11)$$

#### **EXAMPLE 14.2-2. Total Amount of Heat in Cooling**

For the conditions in Example 14.2-1, calculate the total amount of heat removed up to time  $t = 3600$  s.

**Solution:** From Example 14.2-1,  $hA/c\rho V = 3.71 \times 10^{-4} s^{-1}$ . Also  $V = 4\pi r^3/3 = 4(\pi)(0.0254)^3/3 = 6.864 \times 10^{-5} m^3$ .

Substituting into Eq. (14.2-11),

$$Q = (4606 J/kg \cdot K)(7849 kg/m^3)(6.864 \times 10^{-5} m^3) (699.9 K - 394.3 K)[1 - e^{-(3.71 \times 10^{-4})(3600)}] Q = 5.589 \times 10^4 J$$

## **14.3 Unsteady-State Heat Conduction in Various Geometries**

### **14.3A Introduction and Analytical Methods**

In Section 14.2, we considered a

simplified case of negligible internal resistance where the object has a very high thermal conductivity. Now we will consider the more general situation where the internal resistance is not small, and hence the temperature is not constant in the solid. The first case that we shall consider is one where the surface convective resistance is negligible compared to the internal resistance. This could occur because of a very large heat-transfer coefficient at the surface or because of a relatively large conductive resistance in the object.

To illustrate an analytical method of solving this first case, we will derive the equation for unsteady-state conduction in the  $x$  direction only in a flat plate of

thickness  $2H$  as shown in Fig. 14.3-1.

The initial profile of the temperature in the plate at  $t = 0$  is uniform at  $T = T_0$ . At time  $t = 0$ , the ambient temperature is suddenly changed to  $T_1$  and held there. Since there is no convection resistance, the temperature of the surface is also held constant at  $T_1$ . Because this is conduction in the  $x$  direction, Eq. (14.1-10) holds:

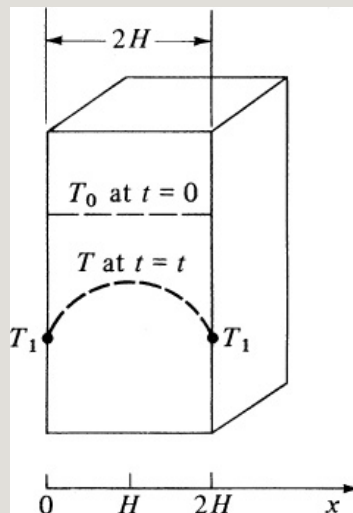


Figure 14.3-1. *Unsteady-state conduction in a flat plate with negligible surface resistance.*

$$\frac{\partial T}{\partial t} = \alpha \frac{\partial^2 T}{\partial x^2} \quad (14.1-10)$$

The initial and boundary conditions are

$$T = T_0, t = 0, x = 0 \quad T = T_1, t = t, x = 0 \quad T = T_1, t = t, x = 2H \quad (14.3-1)$$

Generally, it is convenient to define a dimensionless temperature  $Y$  so that it varies between 0 and 1. Hence,

$$Y = \frac{T - T_0}{T_1 - T_0} \quad (14.3-2)$$

Substituting Eq. (14.3-2) into (14.1-10),

$$\frac{\partial Y}{\partial t} = \alpha \frac{\partial^2 Y}{\partial x^2} \quad (14.3-3)$$

Redefining the boundary and initial conditions,

$$Y = 0, t = 0, x = 0 \quad Y = 1, t = t, x = 0 \quad Y = 1, t = t, x = 2H$$

$$Y = 0, t = t, x = 0$$

$$(14.3-4) Y = T_1 - T_0 = 0, t = t, x = 2H$$

A convenient procedure to use to solve Eq. (14.3-3) is the method of separation of variables, which leads to a product solution

$$Y = e^{-a^2 \alpha t} (A \cos ax + B \sin ax)$$

where  $A$  and  $B$  are constants and  $a$  is a parameter. Applying the boundary and initial conditions of Eq. (14.3-4) to solve for these constants in Eq. (14.3-5), the final solution is an infinite Fourier series (G1):

$$T - T_s = \frac{T_0 - T_s}{4H^2} \sum_{n=1}^{\infty} \frac{1}{n^2} \exp(-n^2 \pi^2 \alpha t / 4H^2) \sin(n\pi x / 2H) \quad n = 1, 3, 5, \dots$$

(14.3-6)

Hence, from Eq. (14.3-6), the temperature  $T$  at any position  $x$  and time

$t$  can be determined. However, these types of equations are very time-consuming to use and convenient charts have been prepared that are discussed in Sections 14.3B, 14.3C, 14.3D, and 14.3E, where a surface resistance is present.

#### **14.3B Unsteady-State Conduction in a Semi-Infinite Solid**

In Fig. 14.3-2, a semi-infinite solid is shown that extends to in the  $+x$  direction. Heat conduction occurs only in the  $x$  direction. Originally, the temperature in the solid is uniform at  $T_0$ . At time  $t = 0$ , the solid is suddenly exposed to or immersed in a large mass of ambient fluid at temperature  $T_1$ , which is constant. The convection coefficient  $h$  in  $\text{W/m}^2 \cdot \text{K}$  or  $\text{btu/h} \cdot \text{ft}^2 \cdot ^\circ\text{F}$  is present and is constant; that is, a surface resistance is present. Hence, the

temperature  $T_s$  at the surface is not the same as  $T_1$ .

The solution of Eq. (14.1-10) for these conditions has been obtained (S1) and is

$$\frac{T - T_0}{T_1 - T_0} = 1 - Y = \operatorname{erfc} \frac{x}{2\sqrt{\alpha t}} - \exp\left[-\frac{h\alpha k}{k_1}\left(x\sqrt{\alpha t} + \frac{h\alpha k_1}{k}\right)\right] \operatorname{erf}\left(\frac{x}{2\sqrt{\alpha t}} + \frac{h\alpha k}{k_1}\right) \quad (14.3-7)$$

where  $x$  is the distance into the solid from the surface in m (SI units),  $t$  = time in s, and  $\alpha = k/\rho c_p$  in  $\text{m}^2/\text{s}$ . In English units,  $x$  = ft,  $t$  = h, and  $\alpha = \text{ft}^2/\text{h}$ . The function  $\operatorname{erfc}$  is  $(1 - \operatorname{erf})$ , where  $\operatorname{erf}$  is the error function and numerical values are tabulated in standard tables and texts (G1, P1, S1);  $Y$  is the fraction of unaccomplished change  $(T_1 - T)/(T_1 - T_0)$ ; and  $1 - Y$  is the fraction of change.

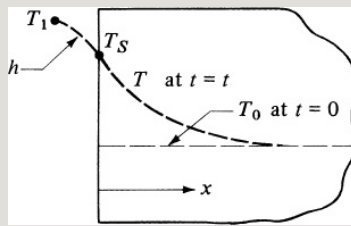


Figure 14.3-2. *Unsteady-state conduction in a semi-infinite solid.*

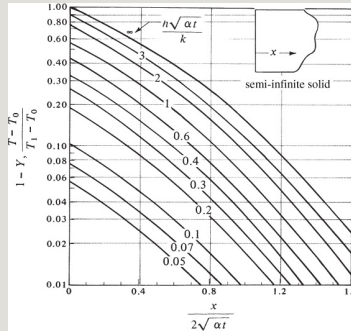


Figure 14.3-3. *Unsteady-state heat conducted in a semi-infinite solid with surface convection. Calculated from Eq. (14.3-7), (S1).*

Figure 14.3-3, calculated using Eq. (14.3-7), is a convenient plot used for unsteady-state heat conduction into a semi-infinite solid with surface convection. If conduction into the solid is slow enough or  $h$  is very large, the top line with  $h\alpha t/k=1.2$  is used.



### EXAMPLE 14.3-1. Freezing Temperature in the Ground

The depth in the earth's soil at which freezing temperatures penetrate is often of importance in agriculture and construction. On a certain fall day, the soil temperature is constant at  $15.6^{\circ}\text{C}$  ( $60^{\circ}\text{F}$ ) to a depth of several meters. A cold wave suddenly reduces the air temperature from  $15.6$  to  $-17.8^{\circ}\text{C}$  ( $0^{\circ}\text{F}$ ). The convective coefficient above the soil is  $11.36 \text{ W/m}^2 \cdot \text{K}$  ( $2 \text{ btu/h} \cdot \text{ft}^2 \cdot ^{\circ}\text{F}$ ). The soil properties can be assumed as  $\alpha = 4.65 \times 10^{-7} \text{ m}^2/\text{s}$  ( $0.018 \text{ ft}^2/\text{h}$ ) and  $k = 0.865 \text{ W/m} \cdot \text{K}$  ( $0.5 \text{ btu/h} \cdot \text{ft} \cdot ^{\circ}\text{F}$ ). Neglect any latent heat effects. Use SI and English units.

- What is the surface temperature after 5 h?
- To what depth in the soil will the freezing temperature of  $0^{\circ}\text{C}$  ( $32^{\circ}\text{F}$ ) penetrate in 5 h?

**Solution:** This is a case of unsteady-state conduction in a semi-infinite solid. For part (a), the value of  $x$ , which is the distance from the surface, is  $x = 0 \text{ m}$ . Then, the value of  $x/2\alpha t$  is calculated as follows for  $t = 5 \text{ h}$ ,  $\alpha = 4.65 \times 10^{-7} \text{ m}^2/\text{s}$ ,  $k = 0.865 \text{ W/m} \cdot ^{\circ}\text{C}$ , and  $h = 11.36 \text{ W/m}^2 \cdot ^{\circ}\text{C}$ . Using SI and English units,

$$x/2\alpha t = 0.2465 \times 10^{-7} \text{ m}^2/\text{s} \times 3600 \text{ s} / 2 \times 0.018 \text{ ft}^2/\text{h} \times 5 \text{ h}$$

Also,

$$\begin{aligned} h\alpha t/k &= 11.36 \text{ W/m}^2 \cdot \text{K} (4.65 \times 10^{-7} \text{ m}^2/\text{s}) \\ (5 \times 3600 \text{ s}) / 0.865 \text{ W/m} \cdot \text{K} &= 1.2 \\ h\alpha t/k &= 2 \text{ btu/h} \cdot \text{ft}^2 \cdot ^{\circ}\text{F} / (0.018 \text{ ft}^2/\text{h}) \\ (5 \text{ h}) / 0.5 \text{ btu/h} \cdot \text{ft} \cdot ^{\circ}\text{F} &= 1.2 \end{aligned}$$

Using Fig. 14.3-3, for  $x/2\alpha t = 0$  and  $h\alpha t/k = 1.2$  the value of  $1 - Y = 0.63$  is read off the curve. Converting temperatures to K,  $T_0 = 15.6^{\circ}\text{C} + 273.2 = 288.8 \text{ K}$  ( $60^{\circ}\text{F}$ ) and  $T_1 = -17.8^{\circ}\text{C} + 273.2 = 255.4 \text{ K}$  ( $0^{\circ}\text{F}$ ). Then,

$$1 - Y = T - T_0 / T_1 - T_0 = 0.63 = T - 288.8 / 255.4 - 288.8$$

Solving for  $T$  at the surface after 5 h,

$$T = 267.76 \text{ K or } -5.44^{\circ}\text{C} \text{ (} 22.2^{\circ}\text{F)}$$

For part (b),  $T = 273.2 \text{ K}$  or  $0^{\circ}\text{C}$ , and the distance  $x$  is unknown. Substituting the known values,

$$T - T_0 / T_1 - T_0 = 273.2 - 288.8 / 255.4 - 288.8 = 0.467$$

From Fig. 14.3-3 for  $(T - T_0)/(T_1 - T_0) = 0.467$  and  $h\alpha t/k = 1.2$ , a value of 0.16 is read off the curve for  $x/2\alpha t$ . Hence,

$$x/2\alpha t = 0.16 \Rightarrow x = 0.16 \times 2\alpha t = 0.16 \times 2 \times 10^{-7} \times (5 \times 3600) = 0.576 \times 10^{-3} \text{ m} = 0.576 \text{ mm}$$

Solving for  $x$ , the distance the freezing temperature penetrates in 5 h is

$$x = 0.0293 \text{ m (0.096 ft)}$$

### 14.3C Unsteady-State Conduction in a Large Flat Plate

A geometry that often occurs in heat-conduction problems is a flat plate of thickness  $2x_1$  in the  $x$  direction with large or infinite dimensions in the  $y$  and  $z$  directions, as shown in Fig. 14.3-4. Heat is being conducted only from the two flat and parallel surfaces in the  $x$  direction. The original uniform temperature of the plate is  $T_0$ ; at time  $t = 0$ , the solid is exposed to an environment at temperature  $T_1$  and unsteady-state conduction occurs. A surface resistance is present.

The numerical results of this case are presented graphically in Figs. 14.3-5 and 14.3-6. Figure 14.3-5, from Gurney and Lurie (G2), is a convenient chart for determining the temperatures at any position in the plate and at any time  $t$ . The dimensionless parameters used in this and subsequent unsteady-state charts in this section are given in Table 14.3-1 ( $x$  is the distance from the center of the flat plate, cylinder, or sphere;  $x_1$  is one-half the thickness of the flat plate, radius of cylinder, or radius of sphere; and  $x =$  distance from the surface for a semi-infinite solid.)

When  $n = 0$ , the position is at the center of the plate in Fig. 14.3-5. Often the temperature history at the center of the plate is quite important. A more accurate chart for determining only the

center temperature is given in Fig. 14.3-6, the Heisler (H1) chart. Heisler (H1) has also prepared multiple charts for determining the temperatures at other positions.

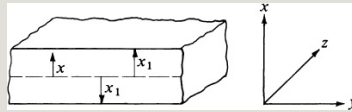


Figure 14.3-4. *Unsteady-state conduction in a large flat plate.*

**EXAMPLE 14.3-2. Heat Conduction in a Slab of Butter**

A rectangular slab of butter which is 46.2 mm thick at a temperature of 277.6 K (4.4°C) in a cooler is removed and placed in an environment at 297.1 K (23.9°C). The sides and bottom of the butter container can be considered to be insulated by the container side walls. The flat top surface of the butter is exposed to the environment. The convective coefficient is constant at  $8.52 \text{ W/m}^2 \cdot \text{K}$ . Calculate the temperature in the butter at the surface, at 25.4 mm below the surface, and at 46.2 mm below the surface at the insulated bottom after 5 h of exposure.

**Solution:** The butter can be considered as a large, flat plate with conduction vertically in the  $x$  direction. Since heat is entering only at the top face and the bottom face is insulated, the 46.2 mm of butter is equivalent to a half plate with thickness  $x_1 = 46.2 \text{ mm}$ . In a plate with two exposed surfaces, as in Fig. 14.3-4, the center at  $x = 0$  acts as an insulated surface, and both halves are mirror images of each other.

Table 14.3-1. *Dimensionless Parameters for Use in Unsteady-State Conduction Charts*

--	--

The physical properties of butter from Appendix A.4 are  $k = 0.197 \text{ W/m} \cdot \text{K}$ ,  $c_p = 2.30 \text{ kJ/Kg} \cdot \text{K} = 2300 \text{ J/kg} \cdot \text{K}$ , and  $\rho = 998 \text{ kg/m}^3$ . The thermal diffusivity is

$$\alpha = \frac{k}{\rho c_p} = \frac{0.197 \text{ W/m} \cdot \text{K}}{998 \text{ kg/m}^3 \cdot 2300 \text{ J/kg} \cdot \text{K}} = 8.58 \times 10^{-8} \text{ m}^2/\text{s}$$

Also,  $x_1 = 46.2 \text{ mm}$  or  $0.0462 \text{ m}$ .

The parameters needed for use in Fig. 14.3-5 are

$$m = \frac{k}{h x_1} = \frac{0.197 \text{ W/m} \cdot \text{K}}{8.52 \text{ W/m}^2 \cdot \text{K} \cdot 0.0462 \text{ m}} = 0.5 \quad X = \frac{\alpha t}{x_1^2} = \frac{8.58 \times 10^{-8} \text{ m}^2/\text{s} (5 \times 3600 \text{ s})}{(0.0462 \text{ m})^2} = 0.72$$

For the top surface, where  $x = x_1 = 0.0462 \text{ m}$ ,

$$n = \frac{x}{x_1} = \frac{0.0462}{0.0462} = 1.0$$

Then, using Fig. 14.3-5,

$$Y = 0.25 = \frac{T_1 - T}{T_1 - T_0} = \frac{297.1 - T}{297.1 - 277.6}$$

Solving,  $T = 292.2 \text{ K}$  ( $19.0^\circ\text{C}$ ).

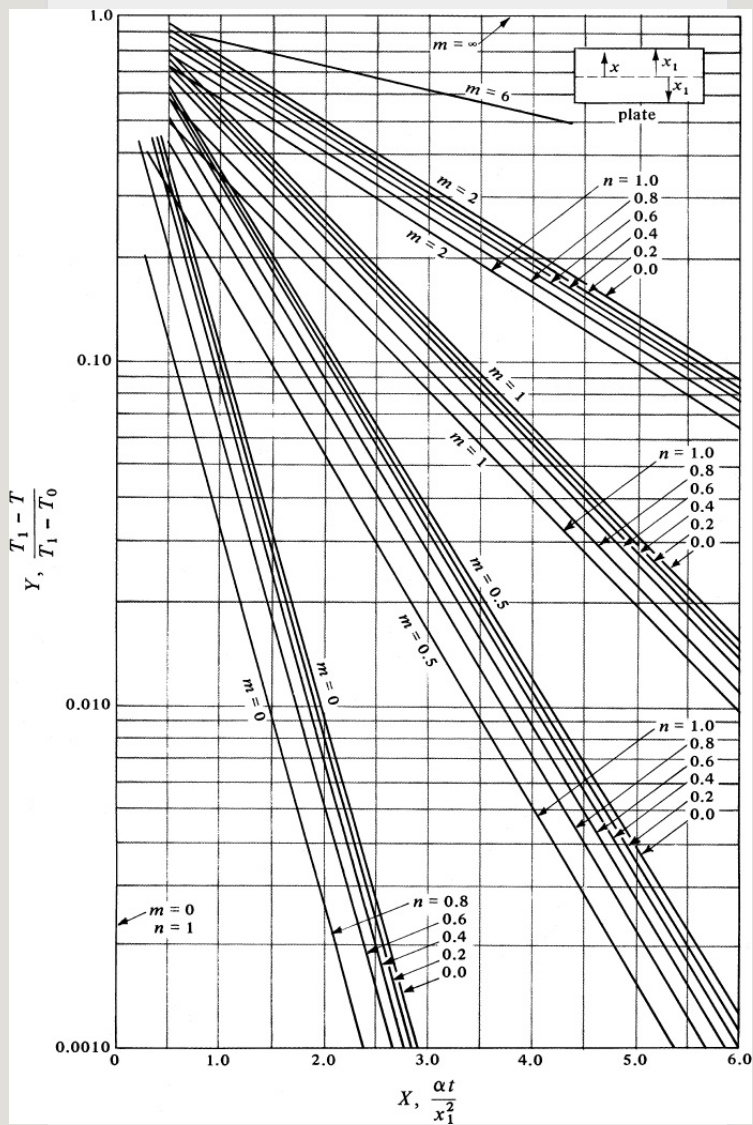


Figure 14.3-5. *Unsteady-state heat conduction in a large flat plate. From H. P. Gurney and J. Lurie, Ind. Eng. Chem., 15, 1170 (1923).*

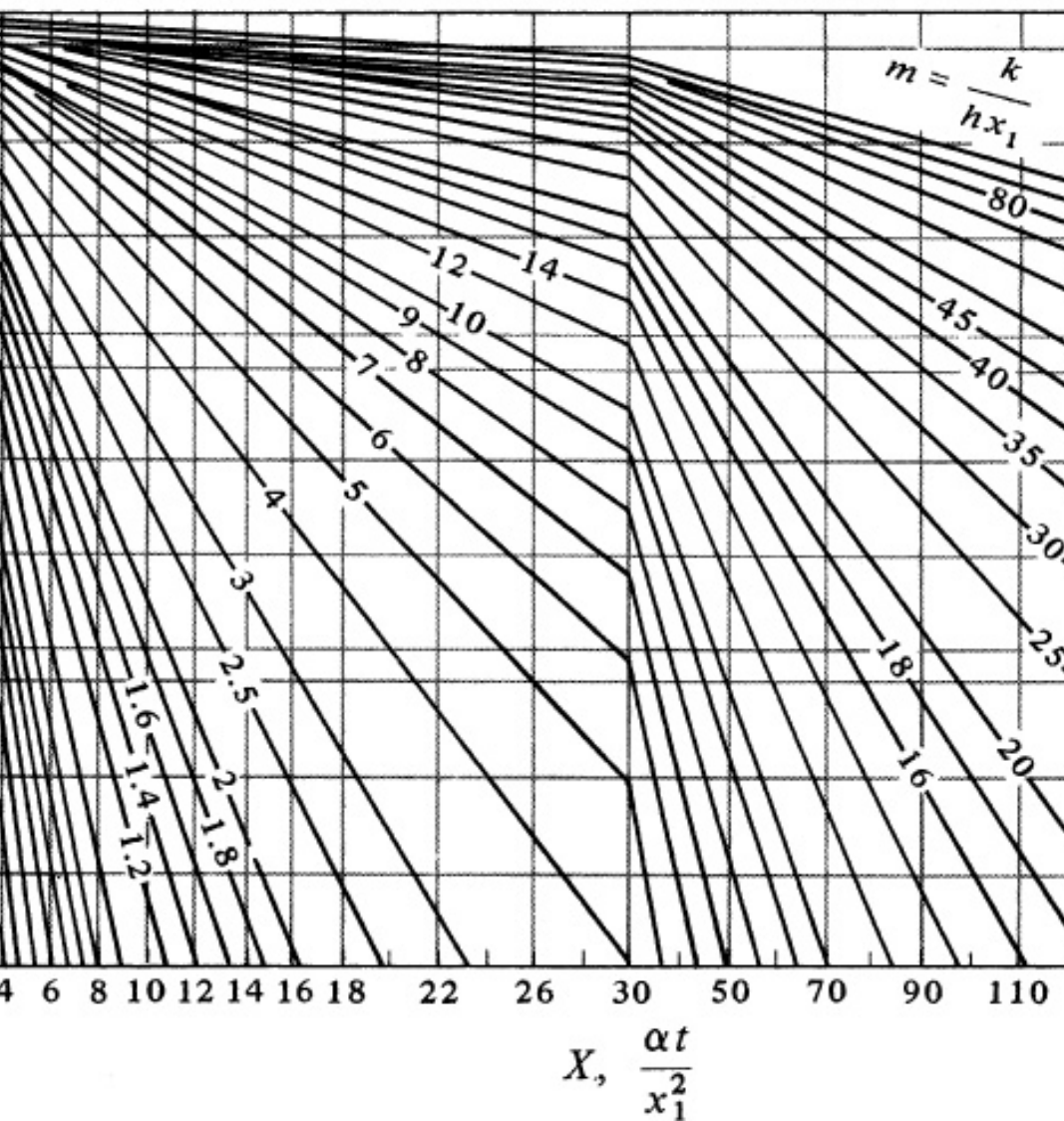


Figure 14.3-6. Chart for determining temperature at the center of a large flat plate for unsteady-state heat conduction. From H. P. Heisler, Trans. A.S.M.E., 69, 227 (1947). With permission.

At the point 25.4 mm from the top surface, or 20.8 mm from the center,  $x = 0.0208$  m, and

$$n = x/x_1 = 0.0208/0.0462 = 0.45$$

From Fig. 14.3-5,

$$Y=0.45=T_1-TT_1-T_0=297.1-T297.1-277.6$$

Solving,  $T = 288.2 \text{ K}$  ( $15.1^\circ\text{C}$ ).

For the bottom point, or  $0.0462 \text{ m}$  from the top,  $x = 0$  and

$$n=xx_1=0x_1=0$$

Then, from Fig. 14.3-5,

$$Y=0.50=T_1-TT_1-T_0=297.1-T297.1-277.6$$

Solving,  $T = 287.4 \text{ K}$  ( $14.2^\circ\text{C}$ ). Alternatively, using Fig.

14.3-6, which is only for the center point,  $Y = 0.53$  and  $T = 286.8 \text{ K}$  ( $13.6^\circ\text{C}$ ).

### 14.3D Unsteady-State Conduction in a Long Cylinder

Now we consider unsteady-state conduction in a long cylinder where conduction occurs only in the radial direction. The cylinder is long so that either conduction at the ends can be neglected or the ends are insulated. Charts for this case are presented in Fig. 14.3-7 for determining the temperatures at any position and in Fig. 14.3-8 for the center temperature only.



**EXAMPLE 14.3-3. Transient Heat Conduction in a Can of Pea Purée**

A cylindrical can of pea purée (C2) has a diameter of 68.1 mm and a height of 101.6 mm, and is initially at a uniform temperature of 29.4°C. The cans are stacked vertically in a retort, and steam at 115.6°C is admitted. For a heating time of 0.75 h at 115.6°C, calculate the temperature at the center of the can. Assume that the can is in the center of a vertical stack of cans and that it is insulated on its two ends by the other cans. The heat capacity of the metal wall of the can will be neglected. The heat-transfer coefficient of the steam is estimated as 4540 W/m<sup>2</sup> · K. Physical properties of purée are  $k = 0.830$  W/m · K and  $\alpha = 2.007 \times 10^{-7}$  m<sup>2</sup>/s.

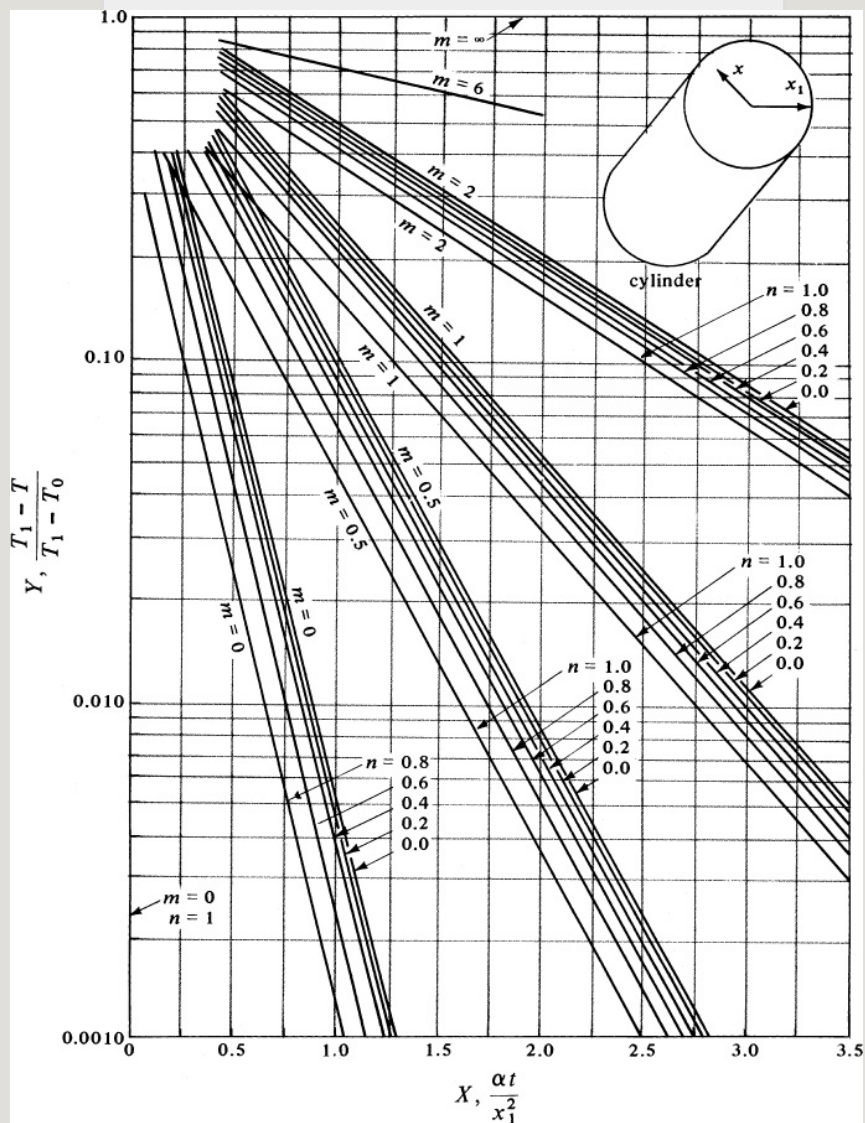


Figure 14.3-7. *Unsteady-state heat conduction in a long cylinder.* From H. P. Gurney and J. Lurie, *Ind. Eng. Chem.*, **15**, 1170 (1923).

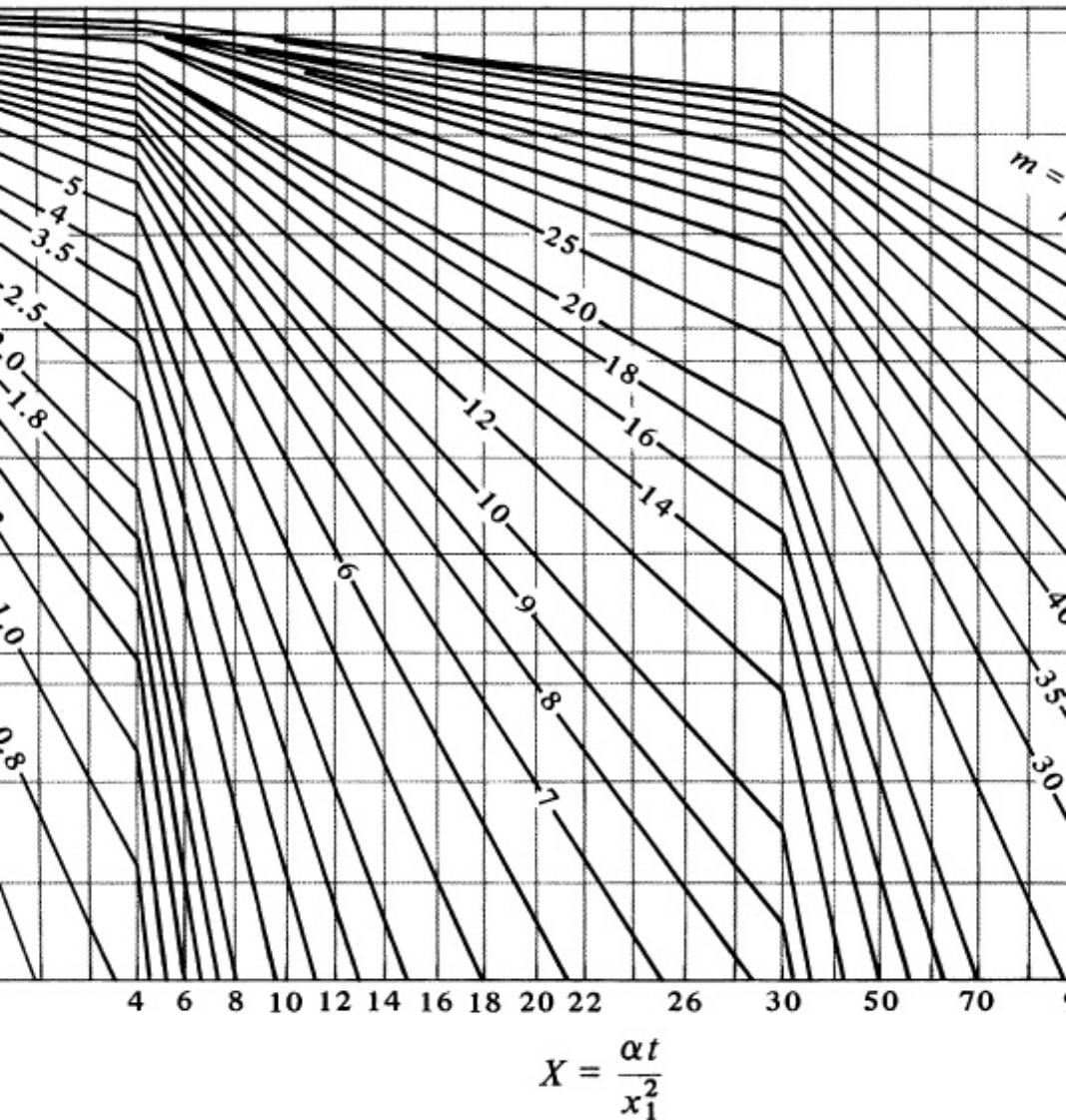


Figure 14.3-8. Chart for determining temperature at the center of a long cylinder for unsteady-state heat conduction. From H. P. Heisler, Trans. A.S.M.E., 69, 227 (1947). With permission.

**Solution:** Since the can is insulated at both ends, we can consider it as a long cylinder. The radius is  $x_1 = 0.0681/2 = 0.03405$  m. For the center with  $x = 0$ ,

$$n = x/x_1 = 0/x_1 = 0$$

Also,

$$m = khx_1 = 0.8 \cdot 304540(0.03405) = 0.00537X = \alpha x_1^2 = (2.007 \times 10^{-7}) \\ (0.75 \times 3600)(0.03405)^2 = 0.468$$

Using Fig. 14.3-8 from Heisler for the center temperature,

$$Y = 0.13 = T_1 - T_{T1} - T_0 = 115.6 - T_{115.6} - 29.4$$

Solving,  $T = 104.4^\circ\text{C}$ .

### 14.3E Unsteady-State Conduction in a Sphere

Figure 14.3-9 shows a chart by Gurney and Lurie (G2) for determining the temperatures at any position in a sphere. Figure 14.3-10 is a chart by Heisler (H1) for determining only the center temperature in a sphere.

### 14.3F Unsteady-State Conduction in Two- and Three-Dimensional Systems

The heat-conduction problems considered so far have been limited to one dimension. However, many practical problems involve simultaneous unsteady-state

conduction in two and three directions. We shall illustrate how to combine one-dimensional solutions to yield solutions for several-dimensional systems.

Newman (N1) used the principle of superposition and showed mathematically how to combine the solutions for one-dimensional heat conduction in the  $x$ , the  $y$ , and the  $z$  direction into an overall solution for simultaneous conduction in all three directions. For example, a rectangular block with dimensions  $2x_1$ ,  $2y_1$ , and  $2z_1$  is shown in Fig. 14.3-11. For the  $Y$  value in the  $x$  direction, as before,

$$Y_x = T_1 - T_x \quad T_1 - T_0 \quad (14.3-8)$$

where  $T_x$  is the temperature at time  $t$  and

position  $x$  is the distance from the center line, as before. Also,  $n = x/x_1$ ,  $m = k/hx_1$ , and  $X_x = \alpha t/x_1^2$ , as before. Then, for the  $y$  direction,

$$Y_y = T_1 - T_y T_1 - T_0 \quad (14.3-9)$$

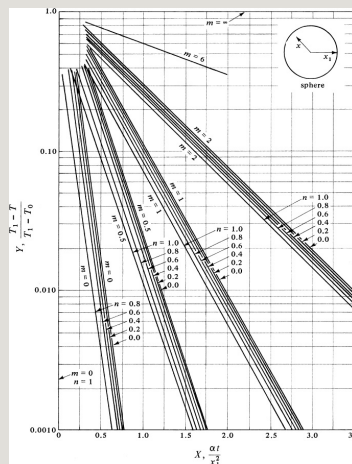


Figure 14.3-9. *Unsteady-state heat conduction in a sphere.* From H. P. Gurney and J. Lurie, *Ind. Eng. Chem.*, **15**, 1170 (1923).

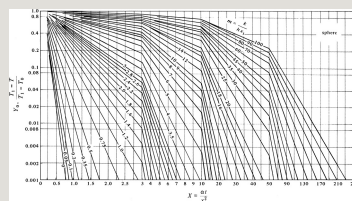


Figure 14.3-10. *Chart for determining the temperature at the center of a sphere for unsteady-state heat conduction.* From H. P. Heisler, *Trans. A.S.M.E.*, **69**, 227 (1947). With permission.

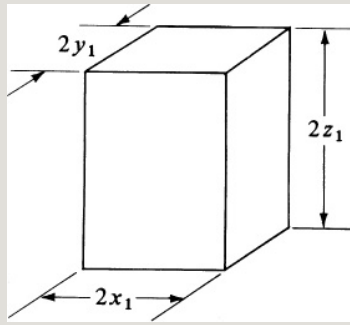


Figure 14.3-11. Unsteady-state conduction in three directions in a rectangular block.

and  $n = y/y_1$ ,  $m = k/hy_1$ , and  $X_y = \alpha t/y_1^2$ . Similarly, for the  $z$  direction,

$$Y_z = \frac{T_1 - T_z}{T_1 - T_0} \quad (14.3-10)$$

Then, for simultaneous transfer in all three directions,

$$Y_{x,y,z} = (Y_x)(Y_y)(Y_z) = \frac{T_1 - T_{x,y,z}}{T_1 - T_0} \quad (14.3-11)$$

where  $T_{x,y,z}$  is the temperature at the point  $x, y, z$  from the center of the

rectangular block. The value of  $Y_x$  for the two parallel faces is obtained from Figs. 14.3-5 and 14.3-6 for conduction in a flat plate. The values of  $Y_y$  and  $Y_z$  are similarly obtained from the same charts.

For a short cylinder with radius  $x_1$  and length  $2y_1$ , the following procedure is followed: First  $Y_x$  for the radial conduction is obtained from the figures for a long cylinder. Then  $Y_y$  for conduction between two parallel planes is obtained from Fig. 14.3-5 or 14.3-6 for conduction in a flat plate. Then,

$$Y_{x,y} = (Y_x)(Y_y) = \frac{T_1 - T_{x,y}}{T_1 - T_0} \quad (14.3-12)$$

**EXAMPLE 14.3-4. Two-Dimensional Conduction in a Short Cylinder**

Repeat Example 14.3-3 for transient conduction in a can of pea purée but assume that conduction also occurs from the



can's two flat ends.

**Solution:** The can, which has a diameter of 68.1 mm and a height of 101.6 mm, is shown in Fig. 14.3-12. The given values from Example 14.3-3 are  $x_1 = 0.03405$  m,  $y_1 = 0.1016/2 = 0.0508$  m,  $k = 0.830$  W/m · K,  $\alpha = 2.007 \times 10^{-7}$  m<sup>2</sup>/s,  $h = 4540$  W/m<sup>2</sup> · K, and  $t = 0.75(3600) = 2700$  s.

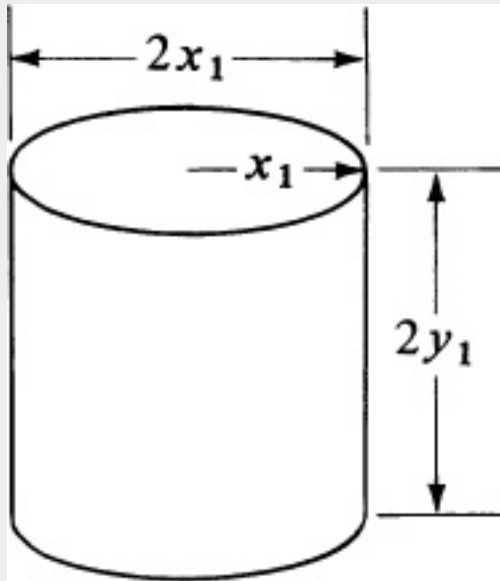


Figure 14.3-12. Two-dimensional conduction in a short cylinder in Example 14.3-4.

For conduction in the  $x$  (radial) direction as calculated previously,

$$n = x_1 = 0.03405 \text{ m}, m = khx_1 = 0.830 \text{ W/m} \cdot \text{K} \cdot 4540 \text{ W/m}^2 \cdot \text{K} \cdot 0.03405 \text{ m} = 0.00537 \text{ X} = \alpha x_1^2 = 2.007 \times 10^{-7} \text{ m}^2/\text{s} (0.75 \times 3600 \text{ s}) (0.03405 \text{ m})^2 = 0.468$$

From Fig. 14.3-8 for the center temperature,

$$Y_x = 0.13$$

For conduction in the  $y$  (axial) direction for the center temperature,

$$n = y_1 = 0.0508 \text{ m}, m = khy_1 = 0.830 \text{ W/m} \cdot \text{K} \cdot 4540 \text{ W/m}^2 \cdot \text{K} \cdot 0.0508 \text{ m} = 0.00360 \text{ X} = \alpha y_1^2 = (2.007 \times 10^{-7} \text{ m}^2/\text{s}) (2700 \text{ s}) (0.0508 \text{ m})^2 = 0.210$$

Using Fig. 14.3-6 for the center of a large plate (two parallel opposed planes),

$$Y_y = 0.80$$

Substituting into Eq. (14.3-12),

$$Y_{x,y} = (Y_x)(Y_y) = 0.13(0.80) = 0.104$$

Then,

$$T_1 - T_{x,y} = T_1 - T_0 = 115.6 - T_{x,y} = 115.6 - 294 = 0.104 T_{x,y} = 106.6^\circ\text{C}$$

This compares with  $104.4^\circ\text{C}$  obtained in Example 14.3-3 for only radial conduction.

### 14.3G Charts for Average Temperature in a Plate, Cylinder, and Sphere with Negligible Surface Resistance

If the surface resistance is negligible, the curves given in Fig. 14.3-13 will give the total fraction of unaccomplished change,  $E$ , for slabs, cylinders, or spheres for unsteady-state conduction. The value of  $E$  is

$$E = T_1 - T_{av} = T_1 - T_0 \quad (14.3-13)$$

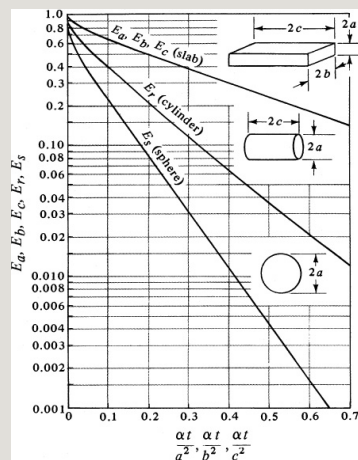


Figure 14.3-13. *Unsteady-state conduction and average temperatures for negligible surface resistance. From R. E. Treybal, Mass-Transfer Operations, 2nd ed. New York: McGraw-Hill Book Company, 1968. With permission.*

where  $T_0$  is the original uniform temperature,  $T_1$  is the temperature of the environment to which the solid is suddenly subjected, and  $T_{av}$  is the average temperature of the solid after  $t$  hours.

The values of  $E_a$ ,  $E_b$ , and  $E_c$  are each used for conduction between a pair of parallel faces, as in a plate. For example, for conduction in the  $a$  and  $b$  directions

in a rectangular bar,

$$E = E_a E_b \quad (14.3-14)$$

For conduction from all three sets of faces,

$$E = E_a E_b E_c \quad (14.3-15)$$

For conduction in a short cylinder  $2c$  long and radius  $a$ ,

$$E = E_c E_r \quad (14.3-16)$$

## **14.4 Numerical Finite-Difference Methods for Unsteady-State Conduction**

### **14.4A Unsteady-State Conduction in a Slab**

*1. Introduction.* As discussed in previous sections of this chapter, the partial differential equations for unsteady-state conduction in various

simple geometries can be solved analytically if the boundary conditions are constant at  $T = T_1$  with time. Also, in the solutions the initial profile of the temperature at  $t = 0$  is uniform at  $T = T_0$ . The unsteady-state charts used also have these same boundary conditions and initial condition. However, when the boundary conditions are not constant with time and/or the initial conditions are not constant with position, numerical methods must be used.

Numerical calculation methods for unsteady-state heat conduction are similar to numerical methods for steady state discussed in Section 13.5. The solid is subdivided into sections or slabs of equal length and a fictitious node is

placed at the center of each section. Then, a heat balance is made for each node. This method differs from the steady-state method in that we have heat accumulation in a node for unsteady-state conduction. The methods are well suited for a spreadsheet calculation.

*2. Equations for a slab.* The unsteady-state equation for conduction in the  $x$  direction in a slab is

$$\frac{\partial T}{\partial t} = \alpha \frac{\partial^2 T}{\partial x^2} \quad (14.1-10)$$

This equation can be set up for a numerical solution by expressing each partial derivative as an actual finite difference in  $\Delta T$ ,  $\Delta t$ , and  $\Delta x$ . However, an alternative method will be used to derive the final result by making a heat balance. Figure 14.4-1 shows a slab

centered at position  $n$ , represented by the shaded area. The slab has a width of  $\Delta x$  m and a cross-sectional area of  $A$  m<sup>2</sup>. The node at position  $n$  having a temperature of  $T_n$  is placed at the center of the shaded section; this node represents the total mass and heat capacity of the section or slab. Each node is imagined to be connected to the adjacent node by a fictitious, small conducting rod (see Fig. 4.15-3 for an example).

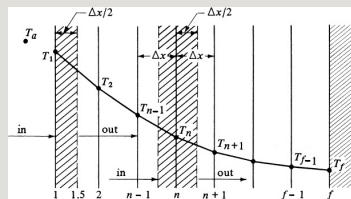


Figure 14.4-1. *Unsteady-state conduction in a slab.*

The figure shows the temperature profile at a given instant of time  $t$  s. Making a heat balance on this node or slab, the

rate of heat in – the rate of heat out = the rate of heat accumulation in  $\Delta t$  s:

$$[\rho \Delta x \frac{\partial T}{\partial t}]_{x=x_2} - [\rho \Delta x \frac{\partial T}{\partial t}]_{x=x_1} \approx [(\Delta x) \rho c_p \Delta T]_{t+\Delta t} - [(\Delta x) \rho c_p \Delta T]_t = kA \Delta x (T_{n-1} - T_n) - kA \Delta x (T_n - T_{n+1}) \quad (14.4-1)$$

where  $T_n$  is the temperature at point  $n$  at time  $t$  and  $T_{n+\Delta t}$  is the temperature at point  $n$  at time  $t + \Delta t$  later.

Rearranging and solving for  $T_{n+\Delta t}$ ,

$$T_{n+\Delta t} = \frac{1}{M} [T_{n+1} + (M-2)T_n + T_{n-1}] \quad (14.4-2)$$

where

$$M = \frac{2\alpha \Delta t}{(\Delta x)^2} = \frac{2(0.20\text{m})^2(2.00 \times 10^{-5}\text{m}^2\text{s})}{\Delta t} = 1000 \quad (14.4-3)$$

Note that in Eq. (14.4-2) the temperature  $T_{n+\Delta t}$  at position or node  $n$  and at a new



time  $t + \Delta t$  is calculated from the three points that are known at time  $t$ , the starting time. This is called the *explicit method*, because the temperature at a new time can be calculated explicitly from the temperatures at the previous time. In this method, the calculation proceeds directly from one time increment to the next until the final temperature distribution is calculated at the desired final time. Of course, the temperature distribution at the initial time and the boundary conditions must be known.

Once the value of  $\Delta x$  has been selected, then from Eq. (14.4-3) a value of  $M$  or the time increment  $\Delta t$  may be picked. For a given value of  $M$ , smaller values of  $\Delta x$  mean smaller values of  $\Delta t$ . The value of  $M$  must be as follows:

$$M \geq 2(14.4-4)$$

If  $M$  is less than 2, the second law of thermodynamics is violated. It also can be shown that for stability and convergence of the finite-difference solution,  $M$  must be  $\geq 2$ .

Stability means the errors in the solution do not grow exponentially as the solution proceeds but damp out.

Convergence means that the solution of the difference equation approaches the exact solution of the partial differential equation as  $\Delta t$  and  $\Delta x$  go to zero with  $M$  fixed. Using smaller sizes of  $\Delta t$  and  $\Delta x$  increases the accuracy in general but greatly increases the number of calculations required. Hence, a digital computer is often ideally suited for this type of calculation using a spreadsheet.

### *3. Simplified Schmidt method for a slab.*

If the value of  $M = 2$ , then a great simplification of Eq. (14.4-2) occurs, giving the Schmidt method:

$$T_{n,t+\Delta t} = T_{n-1,t} + T_{n+1,t} / 2 \quad (14.4-5)$$

This means that when a time  $\Delta t$  has elapsed, the new temperature at a given point  $n$  at  $t + \Delta t$  is the arithmetic average of the temperatures at the two adjacent nodes  $n + 1$  and  $n - 1$  at the original time  $t$ .

#### **14.4B Boundary Conditions for Numerical Method for a Slab**

*1. Convection at the boundary.* For the case where there is a finite convective resistance at the boundary and the temperature of the environment or fluid outside is suddenly changed to  $T_a$ , we can

derive the following for a slab.

Referring to Fig. 14.4-1, we make a heat balance on the outside half-element. The rate of heat in by convection – the rate of heat out by conduction = the rate of heat accumulations in  $\Delta t$  s:

$$hA(tT_a - tT_1) - kA\Delta x(tT_1 - tT_2) = (A\Delta x/2)\rho c_p \Delta t(tT_1.25 - tT_1.25) \quad (14.4-6)$$

where  $tT_1.25$  is the temperature at the midpoint of the  $0.5 \Delta x$  outside slab. As an approximation, the temperature  $T_1$  at the surface can be used to replace that of  $T_1.25$ . Rearranging,

$$T_1 t + \Delta t = \frac{1}{2} \left[ \frac{M}{N} T_a + \left( \frac{M}{N} - 2 \right) T_1 + 2 T_2 \right] \quad (14.4-7)$$

where

$$N = h\Delta x k \quad (14.4-8)$$

Note that the value of  $M$  must be such that

$$M \geq 2N + 2 \quad (14.4-9)$$

*2. Insulated boundary condition.* In the case for the boundary condition where the rear face is insulated, a heat balance is made on the rear  $1/2\Delta x$  slab just as on the front  $1/2\Delta x$  slab in Fig. 14.4-1. The resulting equation is the same as Eqs. (14.4-6) and (14.4-7), but  $h = 0$  or  $N = 0$  and  $T_{f-1} = T_{f+1}$  because of symmetry.

$$T_{f+1} = 1/M [(M-2)T_f + 2T_{f-1}] \quad (14.4-10)$$

*3. Alternative convective condition.* To use the equations above for a given problem, the same values of  $M$ ,  $\Delta x$  and

$\Delta t$  must be used. If  $N$  gets too large, so that  $M$  may be inconveniently too large, another form of Eq. (14.4-7) can be derived. By neglecting the heat accumulation in the front half-slab in Eq. (14.4-6),

$$T_{1,t+\Delta t} = \frac{N}{N+1} T_{t+\Delta t,a} + \frac{1}{N+1} T_{2,t} + \Delta t \quad (14.4-11)$$

Here, the value of  $M$  is not restricted by the  $N$  value. This approximation works fairly well when a large number of increments in  $\Delta x$  are used so that the amount of heat neglected is small compared to the total.

*4. Procedures for the use of initial boundary temperature.* When the temperature of the environment outside is suddenly changed to  $T_a$ , the following

## procedures should be used:

1. When  $M = 2$  and a hand calculation of a limited number of increments is used, a special procedure should be used in Eqs. (14.4-5) and (14.4-7) or (14.4-11). For the first time increment, one should use an average value for  $T_a$  of  $(T_a + T_1)/2$ , where  $T_1$  is the initial temperature at point 1. For all succeeding  $\Delta t$  values, the value of  $T_a$  should be used (D1, K1). This special procedure for determining the value of  $T_a$  to use for the first time increment increases the accuracy of the numerical method, especially after a few time intervals. If  $T_a$  varies with time  $t$ , a new value can be used for each  $t$  interval.
2. When  $M = 2$  and many time increments are used with a digital computer, this special procedure is not needed, and the same value of  $T_a$  is used for all time increments.
3. When  $M = 3$  or more and a hand calculation of a limited number of increments or a digital-computer calculation of many increments is used, only one value of  $T_a$  is used for all time increments. Note that when  $M = 3$  or more, many more calculations are needed compared to the case for  $M = 2$ . The most accurate results are obtained when  $M = 4$ , which is the preferred method, with slightly less accurate results for  $M = 3$  (D1, K1, K2).

### **EXAMPLE 14.4-1. Unsteady-State Conduction and the Schmidt Numerical Method**

A slab of material 1.00 m thick is at a uniform temperature of 100°C. The front surface is suddenly exposed to a constant environmental temperature of 0°C. The convective

resistance is zero ( $h = \infty$ ). The back surface of the slab is insulated. The thermal diffusivity is  $\alpha = 2.00 \times 10^{-5} \text{ m}^2/\text{s}$ . Using five slices, each 0.20 m thick, and the Schmidt numerical method with  $M = 2.0$ , calculate the temperature profile at  $t = 6000 \text{ s}$ . Use the special procedure for the first time increment.

**Solution:** Figure 14.4-2 shows the temperature profile at  $t = 0$  and the environmental temperature of  $T_a = 0^\circ\text{C}$  with five slices used. For the Schmidt method,  $M = 2$ . Substituting into Eq. (14.4-3) with  $\alpha = 2.00 \times 10^{-5}$  and  $\Delta x = 0.20$  and solving for  $\Delta t$ ,

$$M = (\Delta x)^2 \alpha \Delta t = (\Delta x)^2 \alpha \Delta t = (0.20 \text{ m})^2 (2.00 \times 10^{-5} \text{ m}^2/\text{s}) \Delta t$$

$$\Delta t = 1000 \text{ s} \quad (14.4-3)$$



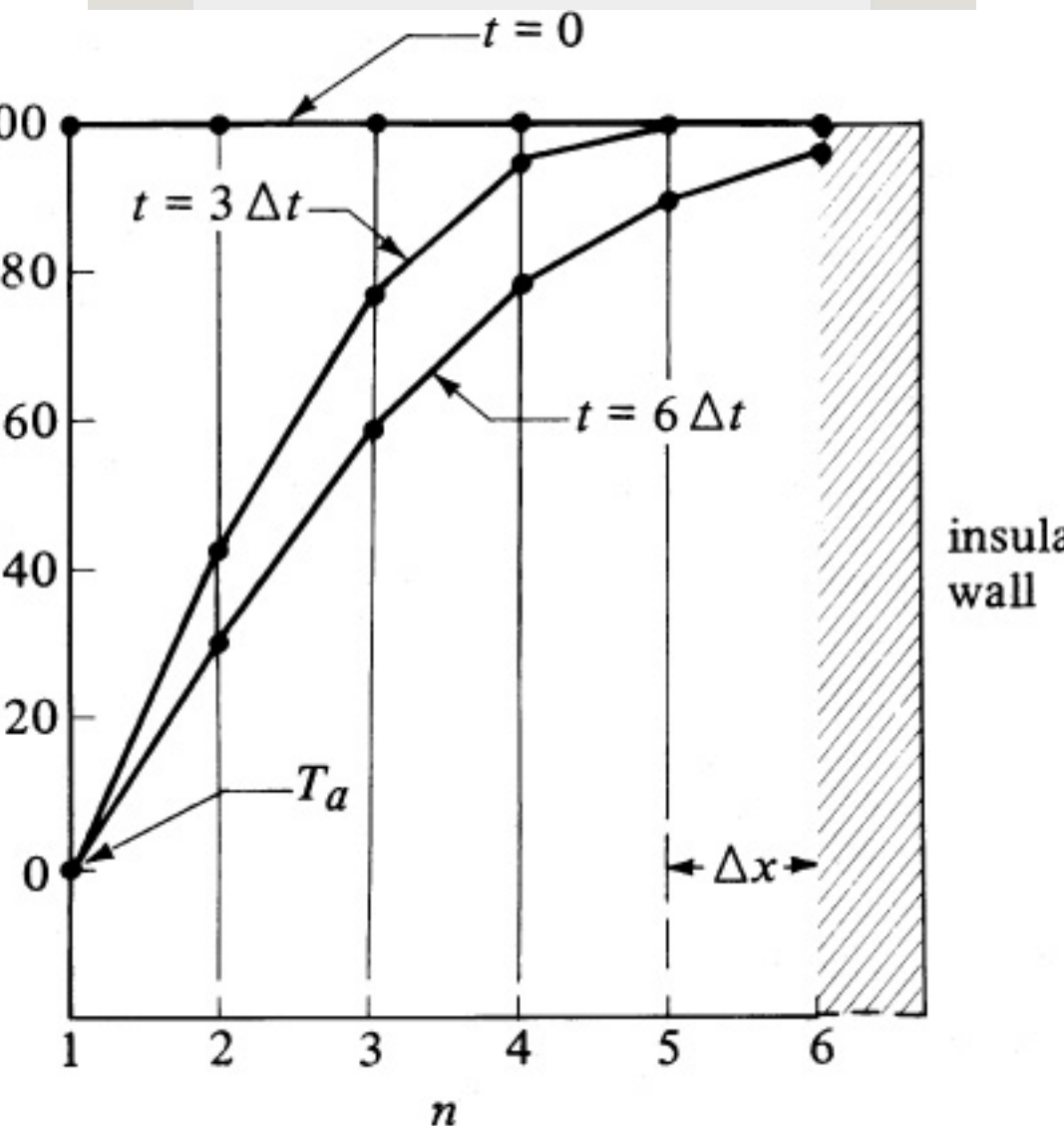


Figure 14.4-2. Temperature for numerical method, Example 14.4-1.

This means that  $(6000 \text{ s})/(1000 \text{ s/increment})$ , or six time increments, must be used to reach 6000 s.

For the front surface, where  $n = 1$ , the temperature  $T_a$  to use for the first  $\Delta t$  time increment, as stated previously, is

$$T_{a1} = T_a + T_{102} = T_{11n=1} \quad (14.4-12)$$

where  $T_1$  is the initial temperature at point 1. For the remaining time increments,

$$T_1 = T_{an=1} \quad (14.4-13)$$

To calculate the temperatures for all time increments for the slabs  $n = 2$  to 5, using Eq. (14.4-5),

$$T_{nt+\Delta t} = T_{n-1} + T_{n+1} \quad n=2,3,4,5 \quad (14.4-14)$$

For the insulated end for all time increments at  $n = 6$ , substituting  $M = 2$  and  $f = 6$  into Eq. (14.4-10),

$$T_{nt+\Delta t} = (2-2)tT_6 + 2tT_5 = tT_5 \quad (14.4-15)$$

For the first time increment of  $t + \Delta t$ , and calculating the temperature at  $n = 1$  by Eq. (14.4-12),

$$T_{0t+\Delta t} = T_a + 0T_1 = 0 + 100^\circ\text{C} = 50^\circ\text{C} = T_{a1}$$

For  $n = 2$ , using Eq. (14.4-14),

$$T_{3t+\Delta t} = T_{2t} + T_{4t} = 50^\circ\text{C} + 100^\circ\text{C} = 75^\circ\text{C}$$

Continuing for  $n = 3, 4, 5$ , we have

$$\begin{aligned} T_{3t+\Delta t} &= T_{2t} + T_{4t} = 100^\circ\text{C} + 100^\circ\text{C} = 100^\circ\text{C} \\ T_{4t+\Delta t} &= T_{3t} + T_{5t} = 100^\circ\text{C} + 100^\circ\text{C} = 100^\circ\text{C} \\ T_{5t+\Delta t} &= T_{4t} + T_{6t} = 100^\circ\text{C} + 100^\circ\text{C} = 100^\circ\text{C} \end{aligned}$$

For  $n = 6$ , using Eq. (14.4-15),

$$T_{6t+2\Delta t} = T_{5t} = 100^\circ\text{C}$$

For  $2\Delta t$ , using Eq. (14.4-13) for  $n = 1$ , and continuing for  $n = 2$  to 6, using Eqs. (14.4-14) and (14.4-15),

$$\begin{aligned} T_{1t+2\Delta t} &= T_a + 0T_1 = 0^\circ\text{C} \\ T_{2t+2\Delta t} &= T_{1t+\Delta t} + T_{3t+\Delta t} = 0^\circ\text{C} + 75^\circ\text{C} = 37.5^\circ\text{C} \\ T_{3t+2\Delta t} &= T_{2t+\Delta t} + T_{4t+\Delta t} = 37.5^\circ\text{C} + 100^\circ\text{C} = 68.75^\circ\text{C} \\ T_{4t+2\Delta t} &= T_{3t+\Delta t} + T_{5t+\Delta t} = 68.75^\circ\text{C} + 100^\circ\text{C} = 134.375^\circ\text{C} \\ T_{5t+2\Delta t} &= T_{4t+\Delta t} + T_{6t+\Delta t} = 134.375^\circ\text{C} + 100^\circ\text{C} = 234.375^\circ\text{C} \\ T_{6t+2\Delta t} &= T_{5t+\Delta t} + T_{6t+\Delta t} = 234.375^\circ\text{C} + 100^\circ\text{C} = 334.375^\circ\text{C} \end{aligned}$$

For  $3\Delta t$ ,

$$\begin{aligned} T_{1t+3\Delta t} &= 0^\circ\text{C} \\ T_{2t+3\Delta t} &= 37.5^\circ\text{C} \\ T_{3t+3\Delta t} &= 68.75^\circ\text{C} \\ T_{4t+3\Delta t} &= 134.375^\circ\text{C} \\ T_{5t+3\Delta t} &= 234.375^\circ\text{C} \\ T_{6t+3\Delta t} &= 334.375^\circ\text{C} \end{aligned}$$

$$+3\Delta t=100^{\circ}\text{C}+100^{\circ}\text{C}^2=100^{\circ}\text{C}T6t+3\Delta t=100^{\circ}\text{C}$$

For 4  $\Delta t$ ,

$$\begin{aligned} T1t+4\Delta t &= 0T2t+4\Delta t=0^{\circ}\text{C}+75^{\circ}\text{C}^2=37.5^{\circ}\text{C}T3t+4\Delta t=43.75^{\circ}\text{C} \\ +93.75^{\circ}\text{C}^2 &= 68.75^{\circ}\text{C}T4t+4\Delta t=75^{\circ}\text{C}+100^{\circ}\text{C}^2=87.5^{\circ}\text{C}T5t \\ +4\Delta t &= 93.75^{\circ}\text{C}+100^{\circ}\text{C}^2=96.88^{\circ}\text{C}T6t+4\Delta t=100^{\circ}\text{C} \end{aligned}$$

For 5  $t$ ,

$$\begin{aligned} T1t+5\Delta t &= 0T2t+5\Delta t=0^{\circ}\text{C}+68.75^{\circ}\text{C}^2=34.38^{\circ}\text{C}T3t \\ +5\Delta t &= 37.5^{\circ}\text{C}+87.5^{\circ}\text{C}^2=62.50^{\circ}\text{C}T4t \\ +5\Delta t &= 68.75^{\circ}\text{C}+96.88^{\circ}\text{C}^2=82.81^{\circ}\text{C}T5t \\ +5\Delta t &= 87.5^{\circ}\text{C}+100^{\circ}\text{C}^2=93.75^{\circ}\text{C}T6t+5\Delta t=96.88^{\circ}\text{C} \end{aligned}$$

For 6  $\Delta t$  (final time),

$$\begin{aligned} T1t+6\Delta t &= 0T2t+6\Delta t=0^{\circ}\text{C}+62.5^{\circ}\text{C}^2=31.25^{\circ}\text{C}T3t \\ +6\Delta t &= 34.38^{\circ}\text{C}+82.81^{\circ}\text{C}^2=58.59^{\circ}\text{C}T4t \\ +6\Delta t &= 62.50^{\circ}\text{C}+93.75^{\circ}\text{C}^2=78.13^{\circ}\text{C}T5t \\ +6\Delta t &= 87.81^{\circ}\text{C}+96.88^{\circ}\text{C}^2=89.84^{\circ}\text{C}T6t+6\Delta t=93.75^{\circ}\text{C} \end{aligned}$$

The temperature profiles for 3  $\Delta t$  increments and the final time of 6  $\Delta t$  increments are plotted in Fig. 14.4-2. This example shows how a hand calculation can be done. To increase the accuracy, more slab increments and more time increments are required. This, then, is ideally suited for computation using a spreadsheet with a computer.

#### **EXAMPLE 14.4-2. Unsteady-State Conduction Using a Digital Computer**

Repeat Example 14.4-1 using a digital computer. Use  $\Delta x = 0.05$  m. Write the spreadsheet program and compare the final temperatures with Example 14.4-1. Use the explicit method of Schmidt for  $M = 2$ . Although not needed for many time increments using the digital computer, use the special procedure for the value of  $T_a$  for the first time increment. Thus, a direct comparison can be made with Example 14.4-1 of the effect of the number of increments on the results.

**Solution:** The number of slabs to use is  $1.00 \text{ m}/(0.05 \text{ m/slab})$  or 20 slabs. Substituting into Eq. (14.4-3) with  $\alpha = 2.00 \times 10^{-5} \text{ m}^2/\text{s}$ ,  $\Delta x = 0.05 \text{ m}$ , and  $M = 2$ , and solving for  $\Delta t$ ,

$$M=2=(\Delta x)^2\alpha\Delta t=(0.05\text{m})^2(2.00\times10^{-5}\text{m}^2\text{s})\Delta t\Delta t=62.5\text{s}$$

Hence,  $(6000/62.5) = 96$  time increments should be used.  
The value of  $n$  goes from  $n = 1$  to 21.

Again, the equations to use for calculating the temperatures are Eqs. (14.4-12)–(14.4-15). However, the only differences are that in Eq. (14.4-14)  $n$  goes from 2 to 20, and in Eq. (14.4-15)  $n = 21$ , so that  $t+\Delta t T_{21} = t T_{20}$ .

Table 14.4-1. *Comparison of Results for Examples 14.4-1 and 14.4-2*

--

The spreadsheet for these equations is easily written and is left up to the reader. The results are tabulated in Table 14.4-1 for comparison with Example 14.4-1, where only five slices were used. The table shows that the results for five slices are reasonably close to those for 20 slices, with values in both cases deviating by 2% or less from each other.

As a rule-of-thumb guide for hand calculations, using a minimum of five slices and at least 8–10 time increments should give sufficient accuracy for most purposes. Only when very high accuracy is desired or several cases are to be solved is it desirable to solve the problem using a spreadsheet program.

**EXAMPLE 14.4-3. Unsteady-State Conduction with a**

### Convective Boundary Condition

Use the same conditions as Example 14.4-1, but a convective coefficient of  $h = 25.0 \text{ W/m}^2 \cdot \text{K}$  is now present at the surface. The thermal conductivity  $k = 10.0 \text{ W/m} \cdot \text{K}$ .

**Solution:** Equations (14.4-7) and (14.4-8) can be used for convection at the surface. From Eq. (14.4-8),  $N = h\Delta x/k = 25.0(0.20)/10.0 = 0.50$ . Then,  $2N + 2 = 2(0.50) + 2 = 3.0$ . However, by Eq. (14.4-9), the value of  $M$  must be equal to or greater than  $2N + 2$ . This means that a value of  $M = 2$  cannot be used. We will select the preferred method where  $M = 4.0$ . [Another, less accurate alternative is to use Eq. (14.4-11) for convection, and then the value of  $M$  is not restricted by the  $N$  value.]

Substituting into Eq. (14.4-3) and solving for  $\Delta t$ ,

$$M=4=(\Delta x)^2\alpha\Delta t=(0.20\text{m})^2(2.00\times 10^{-5}\text{m}^2/\text{s})\Delta t\Delta t=500\text{s}$$

Hence,  $6000/500 = 12$  time increments must be used.

For the first  $\Delta t$  time increment and for all time increments, the value of the environmental temperature  $T_a$  to use is  $T_a = 0^\circ\text{C}$  since  $M > 3$ . For convection at the node or point  $n = 1$ , we use Eq. (14.4-7), where  $M = 4$  and  $N = 0.50$ :

$$T_1 + \Delta t = 14[2(0.5)T_a + [4 - (2 \times 0.5 + 2)]T_1 + 2T_2] = 0.25T_a + 0.25T_1 + 0.50T_2 \quad (14.4-16)$$

For  $n = 2, 3, 4, 5$ , we use Eq. (14.4-2),

$$T_n + \Delta t = 14[tT_n + 1 + (4 - 2)tT_n + tT_{n-1}] \quad n=2,3,4,5 = 0.25tT_n + 1 + 0.50tT_n + 0.25tT_{n-1} \quad (14.4-17)$$

For  $n = 6$  (insulated boundary), we use Eq. (14.4-10) and  $f = 6$ .

$$T_6 + \Delta t = 14[(4 - 2)tT_6 + 2tT_5] = 0.50tT_6 + 0.50tT_5 \quad n=6 \quad (14.4-18)$$

For 1  $\Delta t$ , for the first time increment of  $t + \Delta t$ ,  $T_a = 0$ . Using Eq. (14.4-16) to calculate the temperature at node 1,

$$t_1 + \Delta t T_1 = 0.25(0) + 0.25(100^\circ\text{C}) + 0.50(100^\circ\text{C}) = 75^\circ\text{C}$$

For  $n = 2, 3, 4, 5$ , using Eq. (14.4-17),

$$T_2t$$

$$+\Delta t = 0.25tT_3 + 0.50tT_2 + 0.25tT_1 = 0.25(100^\circ\text{C}) + 0.50(100^\circ\text{C}) + 0.25(100^\circ\text{C}) = 100^\circ\text{C}$$

Also, in a similar calculation,  $T_3$ ,  $T_4$ , and  $T_5 = 100.0$ . For  $n = 6$ , using Eq. (14.4-18),  $T_6 = 100.0$ .

For 2  $\Delta t$ ,  $T_a = 0$ . Using Eq. (14.4-16),

$$t+2\Delta t T_1 = 0.25(0) + 0.25(75^\circ\text{C}) + 0.50(100^\circ\text{C}) = 68.75^\circ\text{C}$$

Using Eq. (14.4-17) for  $n = 2, 3, 4, 5$ ,

$$T_2t$$

$$+2\Delta t = 0.25(100^\circ\text{C}) + 0.50(100^\circ\text{C}) + 0.25(75^\circ\text{C}) = 93.75^\circ\text{C}$$

$$+2\Delta t = 0.25(100^\circ\text{C}) + 0.50(100^\circ\text{C}) + 0.25(100^\circ\text{C}) = 100^\circ\text{C}$$

Also,  $T_4$  and  $T_5 = 100.0$ . For  $n = 6$ , using Eq. (14.4-18),  $T_6 = 100.0$ .

For 3  $\Delta t$ ,  $T_a = 0$ . Using Eq. (14.4-16),

$$t+3\Delta t T_1 = 0.25(0) + 0.25(68.75^\circ\text{C}) + 0.50(93.75^\circ\text{C}) = 64.07^\circ\text{C}$$

Using Eq. (14.4-17) for  $n = 2, 3, 4, 5$ ,

$$T_2t$$

$$+3\Delta t = 0.25(100^\circ\text{C}) + 0.50(93.75^\circ\text{C}) + 0.25(68.75^\circ\text{C}) = 89.07^\circ\text{C}$$

$$+3\Delta t = 0.25(100^\circ\text{C}) + 0.50(100.0^\circ\text{C}) + 0.25(93.75^\circ\text{C}) = 98.44^\circ\text{C}$$

$$+3\Delta t = 0.25(100^\circ\text{C}) + 0.50(100.0^\circ\text{C}) + 0.25(100.0^\circ\text{C}) = 100^\circ\text{C}$$

Also,  $T_5 = 100^\circ\text{C}$  and  $T_6 = 100^\circ\text{C}$ .

In a similar manner, the calculations can be continued for the remaining time until a total of 12  $\Delta t$  increments have been used.

## 14.4C Other Numerical Methods for Unsteady-State Conduction

*1. Unsteady-state conduction in a cylinder.* In deriving the numerical equations for unsteady-state

conduction in a flat slab, the cross-sectional area was constant throughout. In a cylinder, it changes radially. To derive the equation for a cylinder, Fig. 14.4-3 is used, where the cylinder is divided into concentric hollow cylinders whose walls are  $\Delta x$  m thick. Assuming a cylinder 1 m long and making a heat balance on the slab at point  $n$ , the rate of heat in – rate of heat out = rate of heat accumulation:

$$\begin{aligned}
 &k[2\pi(n+1/2)\Delta x]\Delta x(tT-T_{n+1})- \\
 &k[2\pi(n-1/2)\Delta x]\Delta x(T_{n+1}-T_n)=2\pi n(\Delta x)^2\rho c_p\Delta t(T- \\
 &T_n)
 \end{aligned}
 \tag{14.4-19}$$

Rearranging, the final equation is

$$T_{n+1} = T_n + \frac{1}{2} \frac{\Delta x}{r_n} \frac{dT}{dr} \bigg|_{r=r_n} \Delta t$$

$$+1+(M-2)tT_n+2n-12ntT_{n-1}] \quad (14.4-20)$$

where  $M = (\Delta x)^2/(\alpha \Delta t)$  as before. Also, at the center where  $n = 0$ ,

$$T_0t+\Delta t=4MT_1t+M-4MT_1t \quad (14.4-21)$$

To use Equations (14.4-20) and (14.4-21),

$$M \geq 4 \quad (14.4-22)$$

Equations for convection at the outer surface of the cylinder have been derived (D1). If the heat capacity of the outer half-slab is neglected,

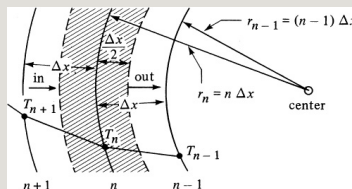


Figure 14.4-3. *Unsteady-state conduction in a cylinder.*



$$T_{n,t+\Delta t} = \frac{1}{2} T_{n-1,t} + \frac{1}{2} T_{n+1,t} + \frac{\alpha \Delta t}{\Delta x^2} (T_{n-1,t} - T_{n,t} + T_{n+1,t} - T_{n,t}) \quad (14.4-23)$$

where  $T_n$  is the temperature at the surface and  $T_{n-1}$  the temperature at a position in the solid  $\Delta x$  below the surface.

Equations for numerical methods for two-dimensional unsteady-state conduction have been derived and are available in a number of references (D1, K2).

*2. Unsteady-state conduction and implicit numerical method.* In some practical problems, the restrictions imposed on the value  $M \geq 2$  by stability requirements may prove inconvenient. Also, to minimize the

stability problems, implicit methods using different finite-difference formulas have been developed. An important one of these formulas is the Crank–Nicolson method, which will be considered here.

In deriving Eqs. (14.4-1) and (14.4-2), the rate at which heat entered the slab in Fig. 14.4-1 was taken to be the rate at time  $t$ :

$$\text{Rate of heat in at } t = kA\Delta A(tT_n - tT_{n-1}) \quad (14.4-24)$$

It was then assumed that this rate could be used during the whole interval from  $t$  to  $t + \Delta t$ . This is an approximation, however, since the rate changes during this  $\Delta t$  interval. A better value would be the average value of the rate at  $t$  and at  $t + \Delta t$ , or

average rate of heat in at  $t = kA\Delta A[(tT_n - 1 - tT_n) + (t + \Delta t T_n - 1 - t + \Delta t T_n)2]$

$$(14.4-25)$$

For the heat leaving, a similar type of average is used. The final equation is

$$T_{n+1}t + \Delta t - (2M+2)t + \Delta t T_{n+1} + T_{t+\Delta t}n - 1 = -tT_{n+1} + (2-2M)tT_n - tT_{n-1} \quad (14.4-26)$$

This means that now a new value of  $t + \Delta t T_n$  cannot be calculated only from values at time  $t$ , as in Eq. (14.4-2), but that all the new values of  $T$  at  $t + \Delta t$  at all points must be calculated simultaneously. To do this, an equation similar to Eq. (14.4-26) is written for each of the internal points. Each of these equations and the boundary equations are linear algebraic equations. These can

then be solved simultaneously by the standard methods, such as the Gauss–Seidel iteration technique, matrix inversion technique, and so on (G1, K1).

An important advantage of Eq. (14.4-26) is that the stability and convergence criteria are satisfied for all positive values of  $M$ . This means that  $M$  can have values less than 2.0. A disadvantage of the implicit method is the larger number of calculations needed for each time step. Explicit methods are simpler to use, but because of stability considerations, especially in complex situations, implicit methods are often preferred.

## **14.5 Chilling and Freezing of food and Biological Materials**

### **14.5A Introduction**

Unlike many inorganic and organic materials, which are relatively stable, food and other biological materials decay and deteriorate more or less rapidly with time at room temperature. This spoilage is due to a number of factors. Tissues of foods such as fruits and vegetables continue to undergo metabolic respiration after harvesting, and ripen and eventually spoil. Enzymes of the dead tissues of meats and fish remain active and induce oxidation and other deteriorating effects.

Microorganisms attack all types of foods by decomposing them so that spoilage occurs; chemical reactions also occur, such as the oxidation of fats.

At low temperatures, the growth rate of

microorganisms will be slowed if the temperature is below that which is optimum for growth. Enzyme activity and chemical reaction rates are also reduced at low temperatures. The rates of most chemical and biological reactions in the storage of chilled or frozen foods and biological materials are reduced by factors of 12 to 13 for each 10 K (10°C) drop in temperature.

Water plays an important role in these rates of deterioration, and it is present to a substantial percentage in most biological materials. To reach a temperature low enough for most of these rates to approximately cease, most of the water must be frozen. Materials such as food do not freeze at 0°C (32°F), as pure water does, but at a range of temperatures below 0°C.

However, because of some of the physical effects of ice crystals and other effects, such as concentrating of solutions, chilling of biological materials is often used for preservation instead of freezing.

Chilling of materials involves removing the sensible heat and heat of metabolism, and reducing the temperature, usually to a range of  $4.4^{\circ}\text{C}$  ( $40^{\circ}\text{F}$ ) to just above freezing.

Essentially no latent heat of freezing is involved. The materials can be stored for a week or so up to a few months, depending on the product stored and the gaseous atmosphere. Each material has its optimum chill storage temperature.

In the freezing of food and biological materials, the temperature is reduced so

that most of the water is frozen to ice. Depending on the final storage temperature, down to as low as  $-30^{\circ}\text{C}$ , the materials can be stored for up to a year or so. Often in the production of frozen foods, they are first treated by blanching or scalding to destroy enzymes.

#### **14.5B Chilling of Food and Biological Materials**

In the chilling of food and biological materials, the temperature of the materials is reduced to the desired chill storage temperature, which can be about  $-1.1^{\circ}\text{C}$  ( $30^{\circ}\text{F}$ ) to  $4.4^{\circ}\text{C}$  ( $40^{\circ}\text{F}$ ). For example, after slaughter, beef has a temperature of  $37.8^{\circ}\text{C}$  ( $100^{\circ}\text{F}$ ) to  $40^{\circ}\text{C}$  ( $104^{\circ}\text{F}$ ), and it is often cooled to about  $4.4^{\circ}\text{C}$  ( $40^{\circ}\text{F}$ ). Milk from cows must be chilled quickly to temperatures just above



freezing. Some fish fillets at the time of packing are at a temperature of  $7.2^{\circ}\text{C}$  ( $45^{\circ}\text{F}$ ) to  $10^{\circ}\text{C}$  ( $50^{\circ}\text{F}$ ) and are chilled to close to  $0^{\circ}\text{C}$ .

These rates of chilling or cooling are governed by the laws of unsteady-state heat conduction discussed in Sections 14.1 to 14.4. The heat is removed by convection at the surface of the material and by unsteady-state conduction in the material. The fluid outside the foodstuff or biological materials is used to remove this heat; in many cases, it is air. The air has previously been cooled by refrigeration to  $-1.1^{\circ}\text{C}$  to  $+4.4^{\circ}\text{C}$ , depending on the material and other conditions. The convective heat-transfer coefficients, which usually include radiation effects, can also be predicted by the methods discussed in Chapter 15;

for air, the coefficient varies from about 8.5 to 40  $\text{W/m}^2 \cdot \text{K}$  (1.5 to 7  $\text{btu/h} \cdot \text{ft}^2 \cdot ^\circ\text{F}$ ), depending primarily on air velocity.

In some cases, the fluid used for chilling is a liquid flowing over the surface, and the values of  $h$  can vary from about 280 to 1700  $\text{W/m}^2 \cdot \text{K}$  (50 – 300  $\text{btu/h} \cdot \text{ft}^2 \cdot ^\circ\text{F}$ ). In other cases, a contact or plate cooler is used, where chilled plates are in direct contact with the material. Then, the temperature of the surface of the material is usually assumed to be equal or close to that of the contact plates. Contact freezers are used for freezing biological materials.

Where the food is packaged in boxes or the material is tightly covered by a film of plastic, this additional resistance must be considered. One method for doing

this is to add the resistance of the package covering to that of the convective film:

$$R_T = R_P + R_C \quad (14.5-1)$$

where  $R_P$  is the resistance of covering,  $R_C$  the resistance of the outside convective film, and  $R_T$  the total resistance. Then, for each resistance,

$$R_C = 1/h_c A \quad (14.5-2)$$

$$R_P = \Delta x / k A \quad (14.5-3)$$

$$R_T = 1/h A \quad (14.5-4)$$

where  $h_c$  is the convective gas or liquid coefficient,  $A$  is the area,  $\Delta x$  is the thickness of the covering,  $k$  is the thermal conductivity of the covering, and  $h$  is the overall coefficient. The

overall coefficient  $h$  is the one to use in the unsteady-state charts. This assumes a negligible heat capacity of the covering, which is usually the case. Also, it assumes that the covering closely touches the food material so there is no resistance between the covering and the food.

The major sources of error in using the unsteady-state charts are inadequate data on the density, heat capacity, and thermal conductivity of the foods, and the prediction of the convective coefficient. Food materials are irregular anisotropic substances whose physical properties are often difficult to evaluate. Also, if evaporation of water occurs on chilling, latent heat losses can affect the accuracy of the results.

### EXAMPLE 14.5-1. Chilling Dressed Beef

Hodgson (H2) gives the physical properties of beef carcasses during chilling of  $\rho = 1073 \text{ kg/m}^3$ ,  $c_p = 3.48 \text{ kJ/kg} \cdot \text{K}$ , and  $k = 0.498 \text{ W/m} \cdot \text{K}$ . A large slab of beef 0.203 m thick and initially at a uniform temperature of  $37.8^\circ\text{C}$  is to be cooled so that the center temperature is  $10^\circ\text{C}$ . Chilled air at  $1.7^\circ\text{C}$  (assumed constant) with an  $h = 39.7 \text{ W/m}^2 \cdot \text{K}$  is used. Calculate the time needed.

**Solution:** The thermal diffusivity  $\alpha$  is

$$\alpha = \frac{k}{\rho c_p} = \frac{0.498 \text{ W/m} \cdot \text{K}}{1073 \text{ kg/m}^3 \cdot 3480 \text{ J/kg} \cdot \text{K}} = 1.334 \times 10^{-7} \text{ m}^2/\text{s}$$

Then, for the half-thickness  $x_1$  of the slab,

$$x_1 = 0.203/2 = 0.1015 \text{ m}$$

For the center of the slab,

$$n = x/x_1 = 0/x_1 = 0$$

Also,

$$m = \frac{hx_1}{k} = \frac{39.7 \text{ W/m}^2 \cdot \text{K} \cdot 0.1015 \text{ m}}{0.498 \text{ W/m} \cdot \text{K}} = 8.123$$
$$T_1 = 1.7 + 237.2 = 274.9 \text{ K}$$

$$T_0 = 37.8 + 273.2 = 311.0 \text{ K}$$
$$T = 10 + 273.2 = 283.2 \text{ K}$$
$$T_0 - T = 311.0 - 283.2 = 27.8$$
$$T_1 - T = 274.9 - 283.2 = -8.3$$
$$\frac{T_0 - T}{T_1 - T} = \frac{27.8}{-8.3} = -3.34$$

Using Fig. 14.3-6 for the center of a large flat plate,

$$X = 0.90 = \alpha t / x_1^2 = (1.334 \times 10^{-7}) (t) / (0.1015)^2$$

Solving,  $t = 6.95 \times 10^4 \text{ s}$  (19.3 h).

## 14.5C Freezing of Food and Biological Materials

*1. Introduction.* In the freezing of food and other biological materials, the removal of sensible heat in chilling occurs first and then the

removal of the latent heat of freezing. The latent heat of freezing water of 335 kJ/kg (144 btu/lbm) is a substantial portion of the total heat removed on freezing. Other slight effects, such as the heats of solution of salts and so on, may be present but are quite small. Actually, when materials such as meats are frozen to  $-29^{\circ}\text{C}$ , only about 90% of the water is frozen to ice, with the rest thought to be bound water (B1).

Riedel (R1) gives enthalpy–temperature–composition charts for the freezing of many different foods. These charts show that freezing does not occur at a given temperature but extends over a range of several degrees. As a consequence, there is no one freezing point with a single latent heat of

freezing.

Since the latent heat of freezing is present in the unsteady-state process of freezing, the standard unsteady-state conduction equations and charts given in this chapter cannot be used for prediction of freezing times. A full analytical solution of the rate of freezing of food and biological materials is very difficult because of the variation of physical properties with temperature, the amount of freezing that varies with temperature, and other factors. An approximate solution by Plank is often used.

*2. Approximate solution of Plank for freezing.* Plank (P2) has derived an approximate solution for the time of freezing that is often sufficient for

engineering purposes. The assumptions in the derivation are as follows: Initially, all the food is at the freezing temperature but is unfrozen. The thermal conductivity of the frozen part is constant. All the material freezes at the freezing point, with a constant latent heat. The heat transfer by conduction in the frozen layer occurs slowly enough that it is under pseudo-steady-state conditions.

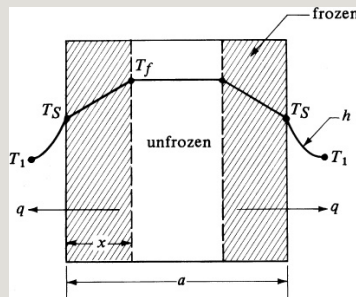


Figure 14.5-1. *Temperature profile during freezing.*

In Fig. 14.5-1, a slab of thickness  $a$  m is cooled from both sides by convection. At a given time  $t$  (sec), a thickness of  $x$



m of frozen layer has formed on both sides. The temperature of the environment is constant at  $T_1$  K and the freezing temperature is constant at  $T_f$ . An unfrozen layer in the center at  $T_f$  is present.

The heat leaving at time  $t$  is  $q$  W. Since we are at pseudo-steady state, at time  $t$ , the heat leaving by convection on the outside is

$$q = hA(T_s - T_1) \quad (14.5-5)$$

where  $A$  is the surface area. Also, the heat being conducted through the frozen layer of  $x$  thickness at steady state is

$$q = kAx(T_f - T_s) \quad (14.5-6)$$

where  $k$  is the thermal conductivity of the frozen material. In a given time  $dt$  s,

a layer  $dx$  thick of material freezes.

Then, multiplying  $A$  times  $dx$  times  $\rho$  gives the kg mass frozen. Multiplying this by the latent heat  $\lambda$  in J/kg and dividing by  $dt$ ,

$$q = A \, dx \, \rho \lambda \frac{dx}{dt} = A \rho \lambda dx \frac{dx}{dt} \quad (14.5-7)$$

where  $\rho$  is the density of the unfrozen material.

Next, to eliminate  $T_s$  from Eqs. (14.5-5) and (14.5-6), Eq. (14.5-5) is solved for  $T_s$  and substituted into Eq. (14.5-6), giving

$$q = (T_f - T_1) A x / k + 1/h \quad (14.5-8)$$

Equating Eq. (14.5-8) to (14.5-7),

$$(T_f - T_1) A x / k + 1/h = A \rho \lambda dx \frac{dx}{dt} \quad (14.5-9)$$

Rearranging and integrating between  $t = 0$  and  $x = 0$ , to  $t = t$  and  $x = a/2$ ,

$$(T_f - T_1) \int_0^t 0 \, dt = \lambda \rho \int_0^{a/2} (xk + 1h) dx \quad (14.5-10)$$

Integrating and solving for  $t$ ,

$$t = \lambda \rho (T_f - T_1) (a^2 h + a^2 8k) \quad (14.5-11)$$

To generalize the equation for other shapes,

$$t = \lambda \rho (T_f - T_1) (P a h + R a^2 k) \quad (14.5-12)$$

where  $a$  is the thickness of an infinite slab (as in Fig. 14.5-1), diameter of a sphere, diameter of a long cylinder, or smallest dimension of a rectangular block or brick. Also,

ere, 14 for infinite cylinder  $R=18$  for infinite slab, 124 fo

For a rectangular brick having dimensions  $a$  by  $\beta_1 a$  by  $\beta_2 a$ , where  $a$  is the shortest side, Ede (B1) has prepared a chart to determine the values of  $P$  and  $R$  to be used to calculate  $t$  in Eq. (14.5-12). Equation (14.5-11) can also be used for calculation of thawing times by replacing the  $k$  of the frozen material by the  $k$  of the thawed material.

**EXAMPLE 14.5-2. Freezing of Meat**

Slabs of meat 0.0635 m thick are to be frozen in an air-blast freezer at 244.3 K (−28.9°C). The meat is initially at the freezing temperature of 270.4 K (−2.8°C). The meat contains 75% moisture. The heat-transfer coefficient is  $h = 17.0 \text{ W/m}^2 \cdot \text{K}$ . The physical properties are  $\rho = 1057 \text{ kg/m}^3$  for the unfrozen meat and  $k = 1.038 \text{ W/m} \cdot \text{K}$  for the frozen meat. Calculate the freezing time.

**Solution:** Since the latent heat of fusion of water to ice is 335 kJ/kg (144 btu/lb<sub>m</sub>), for meat with 75% water,

$$\lambda = 0.75(335) = 251.2 \text{ kJ/kg}$$

The other given variables are  $a = 0.0635 \text{ m}$ ,  $T_f = 270.4 \text{ K}$ ,  $T_1 = 244.3 \text{ K}$ ,  $\rho = 1057 \text{ kg/m}^3$ ,  $h = 17.0 \text{ W/m}^2 \cdot \text{K}$ ,  $k = 1.038 \text{ W/m} \cdot \text{K}$ . Substituting into Eq. (14.6-11),

$$t = \lambda \rho T_f - T_1 (a^2 h$$

$$k) = (2.512 \times 1057 \text{ kg/m}^3) [1057 \text{ kg/m}^3 (270.4 \text{ K} - 244.3 \text{ K}) + (0.0635 \text{ m})^2 (17 \text{ W/m}^2 \cdot \text{K})] / [2.395 \times 10^4 \text{ s} (1.038 \text{ W/m} \cdot \text{K})] = 2.395 \times 10^4 \text{ s}$$

3. *Other methods for calculating freezing times.* Neumann (C1, C2) has derived a complicated equation for freezing in a slab. He assumes the following conditions: The surface temperature is the same as the environment, that is, no surface resistance. The temperature of freezing is constant. This method suffers from the limitation that a convection coefficient cannot be used at the surface, since it assumes no surface resistance. However, the method does include the effect of cooling from an original temperature, which may be above the freezing point.

Plank's equation does not make provision for an original temperature, which may be above the freezing point. An approximate method for calculating

the additional time necessary to cool from temperature  $T_0$  down to the freezing point  $T_f$  is as follows: Using the unsteady-state charts, calculate the time for the average temperature in the material to reach  $T_f$ , assuming that no freezing occurs and using the physical properties of the unfrozen material. If there is no surface resistance, Fig.

14.3-13 can be used directly for this. If a resistance is present, the temperature at several points in the material will have to be obtained from the unsteady-state charts and the average temperature calculated from these point temperatures. This may be partially trial and error, since the time is unknown and must be assumed. If the average temperature calculated is not at the freezing point, a new time must be assumed. This is an approximate method

since some material will actually freeze.

## **14.6 Differential Equation of Energy Change**

### **14.6A Introduction**

In Sections 8.1 and 8.2, we derived a differential equation of continuity and a differential equation of momentum transfer for a pure fluid. These equations were derived because overall mass, energy, and momentum balances made on a finite volume in the earlier parts of Chapter 4 did not tell us what goes on inside a control volume. In the overall balances performed, a new balance was made for each new system studied. However, it is often easier to start with the differential equations of continuity and momentum transfer in general form

and then simplify the equations by discarding unneeded terms for each specific problem.

In Chapter 13 on steady-state heat transfer and in this chapter on unsteady-state heat transfer, new overall energy balances were made on a finite control volume for each new situation. To progress further in our study of heat or energy transfer in flow and nonflow systems, we must use a differential volume to investigate in greater detail what goes on inside this volume. The balance will be made on a single phase and the boundary conditions at the phase boundary will be used for integration.

In the next section, we derive a general differential equation of energy change: the conservation-of-energy equation.



Then, this equation is modified for certain special cases that occur frequently. Finally, applications of the uses of these equations are given. Cases for both steady-state and unsteady-state energy transfer are studied using this conservation-of-energy equation, which is perfectly general and holds for steady- or unsteady-state conditions.

#### **14.6B Derivation of Differential Equation of Energy Change**

As in the derivation of the differential equation of momentum transfer, we write a balance on an element of volume of size  $\Delta x$ ,  $\Delta y$ ,  $\Delta z$ , which is stationary. We then write the law of conservation of energy, which is really the first law of thermodynamics for the fluid in this volume element at any time. The following is the same as Eq. (4.2-7)

for a control volume given in  
Section 4.7.

$$\begin{aligned} & \text{(rate of energy in)} - \\ & \text{(rate of energy out)} - \\ & \text{(rate of energy accumulation)} = \text{(rate of energy transfer from surroundings)} \\ & \quad (14.6-1) \end{aligned}$$

As in momentum transfer, the transfer of energy into and out of the volume element is by convection and molecular transport or conduction. There are two kinds of energy being transferred. The first is internal energy  $U$  in J/kg (btu/lbm) or any other set of units. This is the energy associated with random translational and internal motions of the molecules plus molecular interactions. The second is kinetic energy  $\rho v^2/2$ , which is the energy associated with the bulk fluid motion, where  $y$  is the local

fluid velocity, m/s (ft/s). Hence, the total energy per unit volume is  $(\rho U + \rho v^2/2)$ .

The rate of accumulation of energy in the volume element in  $m^3$  ( $ft^3$ ) is then

$$\Delta x \Delta y \Delta z \frac{\partial}{\partial t} (\rho U + \rho v^2/2) \quad (14.6-2)$$

The total energy entering by convection in the  $x$  direction at  $x$  minus that leaving at  $x + \Delta x$  is

$$\Delta y \Delta z [v_x (\rho U + \rho v^2/2)]_x - \Delta y \Delta z [v_x (\rho U + \rho v^2/2)]_{x+\Delta x} \quad (14.6-3)$$

Similar equations can be written for the  $y$  and  $z$  directions using velocities  $v_y$  and  $v_z$ , respectively.

The net rate of energy entering the element by conduction in the  $x$  direction is

$$\Delta y \Delta z [(q_x)_x - (q_x)_{x+\Delta x}] \quad (14.6-4)$$

Similar equations can be written for the  $y$  and  $z$  directions, where  $q_x$ ,  $q_y$ , and  $q_z$  are the components of the heat flux vector  $\mathbf{q}$ , which is in  $\text{W/m}^2$  ( $\text{btu/s} \cdot \text{ft}^2$ ) or any other convenient set of units.

The net work done by the system on its surroundings is the sum of the following three parts for the  $x$  direction. For the net work done against the gravitational force,

$$-\rho \Delta x \Delta y \Delta z (v_x g_x) \quad (14.6-5)$$

where  $g_x$  is gravitational force. The net work done against the static pressure  $p$  is

$$\Delta y \Delta z [(p v_x)_{x+\Delta x} - (p v_x)_x] \quad (14.6-6)$$

where  $p$  is  $\text{N/m}^2$  ( $\text{lbf/ft}^2$ ) or any other convenient set of units. For the net work against the viscous forces,

$$\Delta y \Delta z [(\tau_{xx} v_x + \tau_{xy} v_y + \tau_{xz} v_z)_x + \Delta x - (\tau_{xx} v_x + \tau_{xy} v_y + \tau_{xz} v_z)_x] (14.6-7)$$

In Section 8.2, these viscous forces are discussed in more detail.

Writing equations similar to (14.6-3)–(14.6-7) in all three directions; substituting these equations and Eq. (14.6-2) into (14.6-1); dividing by  $\Delta x$ ,  $\Delta y$ , and  $\Delta z$ ; and letting  $\Delta x$ ,  $\Delta y$ , and  $\Delta z$  approach zero, we obtain

$$\begin{aligned} \frac{\partial}{\partial t}(\rho U + \rho v^2) = & -[\frac{\partial}{\partial x}(\tau_{xx} v_x + \tau_{xy} v_y + \tau_{xz} v_z) + \rho v \frac{\partial v}{\partial x} + \rho v^2 \frac{\partial v}{\partial x} + \rho v^2 \frac{\partial v}{\partial y} + \rho v^2 \frac{\partial v}{\partial z}] \\ & -[\frac{\partial}{\partial y}(\tau_{xy} v_x + \tau_{yy} v_y + \tau_{yz} v_z) + \rho v \frac{\partial v}{\partial y} + \rho v^2 \frac{\partial v}{\partial x} + \rho v^2 \frac{\partial v}{\partial y} + \rho v^2 \frac{\partial v}{\partial z}] \\ & -[\frac{\partial}{\partial z}(\tau_{xz} v_x + \tau_{yz} v_y + \tau_{zz} v_z) + \rho v \frac{\partial v}{\partial z} + \rho v^2 \frac{\partial v}{\partial x} + \rho v^2 \frac{\partial v}{\partial y} + \rho v^2 \frac{\partial v}{\partial z}] \\ & + \rho(v_x g_x + v_y g_y + v_z g_z) - [\frac{\partial}{\partial x}(\rho v_x) + \frac{\partial}{\partial y}(\rho v_y) + \frac{\partial}{\partial z}(\rho v_z)] - \end{aligned}$$

$$\begin{aligned} & \partial \partial x (\tau_{xx} v_x + \tau_{xy} v_y \\ & + \tau_{xz} v_z) + \partial \partial y (\tau_{yx} v_x + \tau_{yy} v_y \\ & + \tau_{yz} v_z) + \partial \partial z (\tau_{zx} v_x + \tau_{zy} v_y + \tau_{zz} v_z) | \end{aligned}$$

For further details of this derivation, see (B2).

Equation (14.6-8) is the final equation of energy change relative to a stationary point. However, it is not in a convenient form. We first combine Eq. (14.6-8) with the equation of continuity, Eq. (8.1-23), with the equation of motion, Eq. (8.2-13), and express the internal energy in terms of fluid temperature  $T$  and heat capacity. Then, writing the resultant equation for a Newtonian fluid with constant thermal conductivity  $k$ , we obtain

$$\rho c_v D T / D t = k \nabla^2 T -$$

$$T(\partial p / \partial T)_r (\nabla \cdot \mathbf{v}) + \mu \phi \quad (14.6-9)$$

This equation utilizes Fourier's second law in three directions, where

$$k \nabla^2 T = k (\partial^2 T / \partial x^2 + \partial^2 T / \partial y^2 + \partial^2 T / \partial z^2) \quad (14.6-10)$$

The viscous-dissipation term  $\mu \phi$  is generally negligible except where extremely large velocity gradients exist. It will be omitted in the discussions to follow. Equation (14.6-9) is the equation of energy change for a Newtonian fluid with constant  $k$  in terms of the fluid temperature  $T$ .

#### **14.6C Special Cases of the Equation of Energy Change**

The following special forms of Eq. (14.6-9) for a Newtonian fluid with constant thermal conductivity are commonly encountered. First, Eq.

(14.6-9) will be written in rectangular coordinates without the  $\mu\phi$  term:

$$\rho c v (\partial T / \partial t + v_x \partial T / \partial x + v_y \partial T / \partial y + v_z \partial T / \partial z) = k (\partial^2 T / \partial x^2 + \partial^2 T / \partial y^2 + \partial^2 T / \partial z^2) - T (\partial p / \partial T)_p (\partial v_x / \partial x + \partial v_y / \partial y + \partial v_z / \partial z) \quad (14.6-11)$$

*1. Fluid at constant pressure.* The equations below can be used for constant-density fluids as well as for constant pressure.

$$\rho c_p D T / D t = k \nabla^2 T \quad (14.6-12)$$

In rectangular coordinates,

$$\rho c_p (\partial T / \partial t + v_x \partial T / \partial x + v_y \partial T / \partial y + v_z \partial T / \partial z) = k (\partial^2 T / \partial x^2 + \partial^2 T / \partial y^2 + \partial^2 T / \partial z^2) \quad (14.6-13)$$



In cylindrical coordinates,

$$\rho c_p (\partial T / \partial t + v_r \partial T / \partial r + v_\theta r \partial T / \partial \theta + v_z \partial T / \partial z) = k (\partial^2 T / \partial r^2 + 1/r \partial T / \partial r + 1/r^2 \partial^2 T / \partial \theta^2 + \partial^2 T / \partial z^2) \quad (14.6-14)$$

In spherical coordinates,

$$\rho c_p (\partial T / \partial t + v_r \partial T / \partial r + v_\theta r \partial T / \partial \theta + v_\phi r \sin \theta \partial T / \partial \phi) = k [ \partial^2 T / \partial r^2 + 1/r \partial T / \partial r + 1/r^2 \sin \theta \partial^2 T / \partial \theta^2 + \sin \theta \partial T / \partial \theta + 1/r^2 \sin^2 \theta \partial^2 T / \partial \phi^2 ] \quad (14.6-15)$$

For definitions of cylindrical and spherical coordinates, see Section 3.6. If the velocity  $v$  is zero,  $DT/Dt$  becomes  $\partial T / \partial t$ .

## 2. Fluid at constant density

$$\rho c_p DT/Dt = k \nabla^2 T \quad (14.6-16)$$

Note that this is identical to Eq. (14.7-12) for constant pressure.

3. *Solid*. Here, we consider  $\rho$  is constant and  $v = 0$ .

$$\rho c_p \frac{\partial T}{\partial t} = k \nabla^2 T \quad (14.6-17)$$

This is often referred to as *Fourier's second law* of heat conduction. This also holds for a fluid with zero velocity at constant pressure.

4. *Heat generation*. If there is heat generation in the fluid by electrical or chemical means, then  $q$ . can be added to the right side of Eq. (14.6-17)

$$\rho c_p \frac{\partial T}{\partial t} = k \nabla^2 T + q \quad (14.6-18)$$

where  $q$ . is the rate of heat generation in  $W/m^3$  (btu/h · ft<sup>3</sup>) or other suitable units.

Viscous dissipation is also a heat source, but its inclusion greatly complicates problem solving because the equations for energy and motion are then coupled.

*5. Other coordinate systems.* Fourier's second law of unsteady-state heat conduction can be written as follows:

For rectangular coordinates,

$$\frac{\partial T}{\partial t} = \frac{k}{\rho c_p} \nabla^2 T = \alpha (\frac{\partial^2 T}{\partial x^2} + \frac{\partial^2 T}{\partial y^2} + \frac{\partial^2 T}{\partial z^2}) \quad (14.6-19)$$

where  $\alpha = k/\rho c_p$ , thermal diffusivity in  $\text{m}^2/\text{s}$  ( $\text{ft}^2/\text{h}$ ).

For cylindrical coordinates,

$$\frac{\partial T}{\partial t} = \alpha (\frac{\partial^2 T}{\partial r^2} + \frac{1}{r} \frac{\partial T}{\partial r} + \frac{1}{r^2} \frac{\partial^2 T}{\partial \theta^2} + \frac{\partial^2 T}{\partial z^2}) \quad (14.6-20)$$

For spherical coordinates,

$$\frac{\partial T}{\partial r} + \frac{1}{r^2} \sin \theta \frac{\partial}{\partial \theta} \left( \sin \theta \frac{\partial T}{\partial \theta} \right) + \frac{1}{r^2 \sin^2 \theta} \frac{\partial^2 T}{\partial \phi^2} \quad (14.6-21)$$

## 14.7 Chapter Summary

Unsteady-state heat transfer is important because of the large number of heating and cooling problems that occur industrially. The equation for unsteady-state conduction with heat generation is:

$$\rho c_p \frac{\partial T}{\partial t} = \alpha (\frac{\partial^2 T}{\partial x^2} + \frac{\partial^2 T}{\partial y^2} + \frac{\partial^2 T}{\partial z^2}) + q \quad (14.1-9)$$

or

$$\rho c_p \frac{\partial T}{\partial t} = k \nabla^2 T + q \quad (14.6-18)$$

## Without Heat Generation

For rectangular coordinates,

$$\frac{\partial T}{\partial t} = \frac{k}{\rho c_p} \nabla^2 T = \alpha (\frac{\partial^2 T}{\partial x^2} + \frac{\partial^2 T}{\partial y^2} + \frac{\partial^2 T}{\partial z^2})$$

(14.6-19)

where  $\alpha = k/\rho c_p$ , thermal diffusivity in  $\text{m}^2/\text{s}$  ( $\text{ft}^2/\text{h}$ ).

For cylindrical coordinates,

$$\frac{\partial T}{\partial t} = \alpha (\frac{\partial^2 T}{\partial r^2} + \frac{1}{r} \frac{\partial T}{\partial r} + \frac{1}{r^2} \frac{\partial^2 T}{\partial \theta^2} + \frac{\partial^2 T}{\partial z^2})$$

(14.6-20)

For spherical coordinates,

$$\frac{\partial T}{\partial t} = \alpha [\frac{1}{r^2} \frac{\partial}{\partial r} (r^2 \frac{\partial T}{\partial r}) + \frac{1}{r^2 \sin \theta} \frac{\partial}{\partial \theta} (\sin \theta \frac{\partial T}{\partial \theta}) + \frac{1}{r^2 \sin^2 \theta} \frac{\partial^2 T}{\partial \phi^2}]$$

(14.6-21)

## Biot Number

When choosing the right solution method for unsteady heat transfer problems, it is important to find the controlling resistance (convection,

conduction or both) to heat transfer. The Biot number

$$NB_i = hx_c k \quad (14.2-4)$$

gives a direct indication of the relative importance of conduction and convection in determining the temperature history of a body being heated or cooled by convection at its surface.

Here  $hx_c k$  is called the Biot number  $NB_i$ , which is a dimensionless number, and  $x_c$  is a characteristic dimension of the body obtained from  $x_c = V/A$ .

For a sphere,

$$x_c = V/A = r \quad (14.2-5)$$

For a long cylinder,

$$x_c = \sqrt{V A / D} = r \sqrt{14.2-6}$$

For a long square rod,

$$x_c = \sqrt{V A / D} = (2x)^2 L^4 / (2x) L = x^2 (x = 1/2 \text{ thickness})$$

$$(14.2-7)$$

## Calculations Using the Biot Number as a Guide

1. With small Biot numbers ( $N_{Bi} < 0.1$ ), where the primary resistance to heat transfer is convection, the lumped capacity method can be used.

$$T - T_\infty = (T_0 - T_\infty) e^{-(hA/c_p V t)} \quad (14.2-3)$$

2. Large Biot numbers ( $N_{Bi} \gg 0.1$ ), where surface convective resistance is negligible compared to the internal resistance:

*Flat Plate of Thickness 2H:*

$$\frac{T - T_s}{T_0 - T_s} = \sum_{n=1}^{\infty} \frac{1}{n} \exp\left(-\frac{n^2 \pi^2 \alpha t}{4H^2}\right) \sin\left(\frac{n\pi x}{2H}\right) \quad n = 1, 3, 5, \dots \quad (14.3-6)$$

*Semi-infinite Solid:*

A) Use the following equation:

$$\frac{T - T_0}{T_1 - T_0} = 1 - Y = \operatorname{erfc} \frac{x}{\sqrt{2\alpha t}} \exp \left[ -\frac{h^2 x^2}{4\alpha t} \right] \quad (14.3-7)$$

B) Use Figure 14.3-3

3. Moderate Biot numbers ( $N_{Bi}$ ) where both internal and external resistances apply: convenient charts have been prepared:

A) Large flat plate (Figures 14.3-5 & 14.3-6)

B) Long cylinder (Figures 14.3-7 & 14.3-8)

C) Sphere (Figures 14.3-9 & 14.3-10)

## Numerical Finite-Difference Methods:

### *Equations for a Slab:*

A) Interior Node:

$$T_{n,t+\Delta t} = \frac{1}{M} [T_{n+1,t} + (M-2)T_{n,t} + T_{n-1,t}] \quad (14.4-2)$$

where

$$M = (\Delta x)^2 \alpha \Delta t \quad \text{and} \quad M \geq 2 \quad (14.4-3)$$



B) Convection at the Boundary:

$$T_{1,t+\Delta t} = \frac{1}{M+2} \left[ 2N T_a + (M-2N) T_{1,t} + 2T_{2,t} \right] \quad (14.4-7)$$

where

$$N = h \Delta x k \quad (14.4-8)$$

C) Insulated boundary condition:

$$T_{f,t+\Delta t} = \frac{1}{M-2} \left[ (M-2) T_{f,t} + 2T_{f-1,t} \right] \quad (14.4-10)$$

Equations for a cylinder and an implicit method (where  $M \geq 2$  is not feasible) are discussed in Section 14.5C.

## **Differential Equations of Energy Change**

Overall equation:

$$\rho c_v D T \frac{dT}{dt} = k \nabla^2 T - T(\partial p / \partial T)_r (\nabla \cdot \mathbf{v}) + \mu \phi \quad (14.6-9)$$

Fluid at constant density/pressure:

$$\rho c_p D T \frac{dT}{dt} = k \nabla^2 T \quad (14.6-12)$$

Heat generation:

$$\rho c_p D T \frac{dT}{dt} = k \nabla^2 T + q \quad (14.6-18)$$

## Problems

**14.2-1. *Temperature Response in Cooling a Wire.*** A small copper wire with a diameter of 0.792 mm and initially at 366.5 K is suddenly immersed in a liquid held constant at 311 K. The convection coefficient  $h = 85.2 \text{ W/m}^2 \cdot \text{K}$ . The physical properties can be assumed constant and are  $k = 374 \text{ W/m} \cdot \text{K}$ ,  $c_p = 0.389 \text{ kJ/kg} \cdot \text{K}$ , and  $\rho = 8890 \text{ kg/m}^3$ .

- Determine the time in seconds for the average temperature of the wire to drop to 338.8 K (one-half the initial temperature difference).
- Do the same but for  $h = 11.36 \text{ W/m}^2 \cdot \text{K}$ .
- For part (b), calculate the total amount of heat removed for a wire 1.0 m long.

**Ans.** (a)  $t = 5.66 \text{ s}$

**14.2-2. Quenching Lead Shot in a Bath.** Lead shot having an average diameter of 5.1 mm is at an initial temperature of 204.4°C. To quench the shot, it is added to a quenching oil bath held at 32.2°C and falls to the bottom. The time of fall is 15 s. Assuming an average convection coefficient of  $h = 199 \text{ W/m}^2 \cdot \text{K}$ , what will be the temperature of the shot after the fall? For lead,  $\rho = 11\,370 \text{ kg/m}^3$  and  $c_p = 0.138 \text{ kJ/kg} \cdot \text{K}$ .

**14.2-3. Unsteady-State Heating of a**

***Stirred Tank.*** A vessel is filled with  $0.0283 \text{ m}^3$  of water initially at  $288.8 \text{ K}$ . The vessel, which is well stirred, is suddenly immersed in a steam bath held at  $377.6 \text{ K}$ . The overall heat-transfer coefficient  $U$  between the steam and water is  $1136 \text{ W/m}^2 \cdot \text{K}$  and the area is  $0.372 \text{ m}^2$ . Neglecting the heat capacity of the walls and agitator, calculate the time in hours to heat the water to  $338.7 \text{ K}$ . [*Hint:* Since the water is well stirred, its temperature is uniform. Show that Eq. (6.2-3) holds by starting with Eq. (6.2-1).]

**14.3-1. *Temperature in a Refractory Lining.*** A combustion chamber has a 2-in.-thick refractory lining to protect the outer shell. To predict the thermal stresses at start-up, the temperature 0.2 in. below the surface is needed 1 min

after start-up. The following data are available: the initial temperature  $T_0 = 100^\circ\text{F}$ , the hot gas temperature  $T_1 = 3000^\circ\text{F}$ ,  $h = 40 \text{ btu/h} \cdot \text{ft}^2 \cdot ^\circ\text{F}$ ,  $k = 0.6 \text{ btu/h} \cdot \text{ft} \cdot ^\circ\text{F}$ , and  $\alpha = 0.020 \text{ ft}^2/\text{h}$ .

Calculate the temperature at a 0.2-in. depth and a 0.6-in. depth. Use Fig. 14.3-3 and justify its use by seeing if the lining acts as a semi-infinite solid during this 1-min period.

**Ans.** For  $x = 0.2 \text{ in.}$ ,  $(T - T_0)/(T_1 - T_0) = 0.28$  and  $T = 912^\circ\text{F}$  ( $489^\circ\text{C}$ ); for  $x = 0.6 \text{ in.}$ ,  $(T - T_0)/(T_1 - T_0) = 0.02$  and  $T = 158^\circ\text{F}$  ( $70^\circ\text{C}$ )

**14.3-2. Freezing Temperature in the Soil.** The average temperature of the soil to a considerable depth is approximately  $277.6 \text{ K}$  ( $40^\circ\text{F}$ ) during a winter day. If the outside air temperature suddenly

drops to 255.4 K (0°F) and stays there, how long will it take for a pipe 3.05 m (10 ft) below the surface to reach 273.2 K (32°F)? The convective coefficient is  $h = 8.52 \text{ W/m}^2 \cdot \text{K}$  ( $1.5 \text{ btu/h} \cdot \text{ft}^2 \cdot ^\circ\text{F}$ ). The soil's physical properties can be taken as  $5.16 \times 10^{-7} \text{ m}^2/\text{s}$  ( $0.02 \text{ ft}^2/\text{h}$ ) for the thermal diffusivity and  $1.384 \text{ W/m} \cdot \text{K}$  ( $0.8 \text{ btu/h} \cdot \text{ft} \cdot ^\circ\text{F}$ ) for the thermal conductivity. (*Note:* The solution is trial and error, since the unknown time appears twice in the graph for a semi-infinite solid.)

**14.3-3. Cooling a Slab of Aluminum.** A large piece of aluminum that can be considered a semi-infinite solid initially has a uniform temperature of 505.4 K. The surface is suddenly exposed to an environment at 338.8 K with a surface convection coefficient of  $455 \text{ W/m}^2 \cdot \text{K}$ .

Calculate the time in hours for the temperature to reach 388.8 K at a depth of 25.4 mm. The average physical properties are  $\alpha = 0.340 \text{ m}^2/\text{h}$  and  $k = 208 \text{ W/m} \cdot \text{K}$ .

**14.3-4. *Transient Heating of a Concrete Wall.*** A wall made of concrete 0.305 m thick is insulated on the rear side. The wall at a uniform temperature of 10°C (283.2 K) is exposed on the front side to a gas at 843°C (1116.2 K). The convection coefficient is  $28.4 \text{ W/m}^2 \cdot \text{K}$ , the thermal diffusivity is  $1.74 \times 10^{-3} \text{ m}^2/\text{h}$ , and the thermal conductivity is  $0.935 \text{ W/m} \cdot \text{K}$ .

- Calculate the time for the temperature at the insulated face to reach 232°C (505.2 K).
- Calculate the temperature at a point 0.152 m below the surface at this same time.

**Ans.** (a)  $\alpha t/x^2 = 0.25$ ,  $t = 13.4$  h

**14.3-5. *Cooking a Slab of Meat.*** A slab of meat 25.4 mm thick, originally at a uniform temperature of  $10^\circ\text{C}$ , is to be cooked from both sides until the center reaches  $121^\circ\text{C}$  in an oven at  $177^\circ\text{C}$ . The convection coefficient can be assumed constant at  $25.6 \text{ W/m}^2 \cdot \text{K}$ . Neglect any latent heat changes and calculate the time required. The thermal conductivity is  $0.69 \text{ W/m} \cdot \text{K}$  and the thermal diffusivity  $5.85 \times 10^{-4} \text{ m}^2/\text{h}$ . Use the Heisler chart.

**Ans.** 0.80 h (2880 s)

**14.3-6. *Unsteady-State Conduction in a Brick Wall.*** A flat brick wall 1.0 ft thick is the lining on one side of a furnace. If the wall is at a uniform temperature of



100°F and one side is suddenly exposed to a gas at 1100°F, calculate the time for the furnace wall at a point 0.5 ft from the surface to reach 500°F. The rear side of the wall is insulated. The convection coefficient is 2.6 btu/h · ft<sup>2</sup> · °F and the physical properties of the brick are  $k = 0.65$  btu/h · ft · °F and  $\alpha = 0.02$  ft<sup>2</sup>/h.

**14.3-7. Cooling a Steel Rod.** A long steel rod 0.305 m in diameter is initially at a temperature of 588 K. It is immersed in an oil bath maintained at 311 K. The surface convective coefficient is 125 W/m<sup>2</sup> · K. Calculate the temperature at the center of the rod after 1 h. The average physical properties of the steel are  $k = 38$  W/m · K and  $\alpha = 0.0381$  m<sup>2</sup>/h.

**Ans.**  $T = 391$  K

### **14.3-8. *Effect of Size on Heat-***

***Processing Meat.*** An autoclave held at  $121.1^{\circ}\text{C}$  is being used to process sausage meat 101.6 mm in diameter and 0.61 m long that is originally at  $21.1^{\circ}\text{C}$ . After 2 h, the temperature at the center is  $98.9^{\circ}\text{C}$ . If the diameter is increased to 139.7 mm, how long will it take for the center to reach  $98.9^{\circ}\text{C}$ ? The heat-transfer coefficient to the surface is  $h = 1100 \text{ W/m}^2 \cdot \text{K}$ , which is very large, so the surface resistance can be considered negligible. (Show this.) Neglect the heat transfer from the ends of the cylinder. The thermal conductivity  $k = 0.485 \text{ W/m} \cdot \text{K}$ .

**Ans. 3.78 h**

**14.3-9. *Temperature of Oranges on Trees During Freezing Weather.*** In

orange-growing areas, oranges freezing on the trees during cold nights is a serious economic concern. If the oranges are initially at a temperature of  $21.1^{\circ}\text{C}$ , calculate the center temperature of the orange if exposed to air at  $-3.9^{\circ}\text{C}$  for 6 h. The oranges are 102 mm in diameter and the convective coefficient is estimated as  $11.4 \text{ W/m}^2 \cdot \text{K}$ . The thermal conductivity  $k$  is  $0.431 \text{ W/m} \cdot \text{K}$  and  $\alpha$  is  $4.65 \times 10^{-4} \text{ m}^2/\text{h}$ . Neglect any latent heat effects.

$$\text{Ans. } (T_1 - T)/(T_1 - T_0) = 0.05, T = -2.65^{\circ}\text{C}$$

**14.3-10. *Hardening a Steel Sphere.*** To harden a steel sphere having a diameter of 50.8 mm, it is heated to 1033 K and then dunked into a large water bath at 300 K. Determine the time for the center

of the sphere to reach 366.5 K. The surface coefficient can be assumed as  $710 \text{ W/m}^2 \cdot \text{K}$ ,  $k = 45 \text{ W/m} \cdot \text{K}$ , and  $\alpha = 0.0325 \text{ m}^2/\text{h}$ .

**14.3-11. *Unsteady-State Conduction in a Short Cylinder.*** An aluminum cylinder is initially heated to a uniform temperature of  $204.4^\circ\text{C}$ . Then, it is plunged into a large bath held at  $93.3^\circ\text{C}$ , where  $h = 568 \text{ W/m}^2 \cdot \text{K}$ . The cylinder has a diameter of 50.8 mm and is 101.6 mm long. Calculate the center temperature after 60 s. The physical properties are  $\alpha = 9.44 \times 10^{-5} \text{ m}^2/\text{s}$  and  $k = 207.7 \text{ W/m} \cdot \text{K}$ .

**14.3-12. *Conduction in Three Dimensions in a Rectangular Block.*** A rectangular steel block 0.305 m by 0.457 m by 0.61 m is initially at  $315.6^\circ\text{C}$ . It is

suddenly immersed in an environment at  $93.3^{\circ}\text{C}$ . Determine the temperature at the center of the block after 1 h. The surface convection coefficient is  $34 \text{ W/m}^2 \cdot \text{K}$ . The physical properties are  $k = 38 \text{ W/m} \cdot \text{K}$  and  $\alpha = 0.0379 \text{ m}^2/\text{h}$ .

**14.4-1. *Schmidt Numerical Method for Unsteady-State Conduction.*** A material in the form of an infinite plate  $0.762 \text{ m}$  thick is at an initial uniform temperature of  $366.53 \text{ K}$ . The rear face of the plate is insulated. The front face is suddenly exposed to a temperature of  $533.2 \text{ K}$ . The convective resistance at this face can be assumed as zero. Calculate the temperature profile after  $0.875 \text{ h}$  using the Schmidt numerical method with  $M = 2$  and slabs  $0.1524 \text{ m}$  thick. The thermal diffusivity is  $0.0929 \text{ m}^2/\text{h}$ .

**Ans.**  $\Delta t = 0.125$  h, seven time increments needed

**14.4-2. *Unsteady-State Conduction with a Nonuniform Initial***

***Temperature Profile.*** Use the same conditions as in Problem 6.4-1 but with the following change: the initial temperature profile is not uniform but is 366.53 K at the front face and 422.1 K at the rear face with a linear variation between the two faces.

**14.4-3. *Unsteady-State Conduction***

***Using the Digital Computer.*** Repeat Problem 6.4-2 but use the computer and a spreadsheet. Use slabs 0.03048 m thick and  $M = 2.0$ . Calculate the temperature profile after 0.875 h.

**14.4-4. *Chilling Meat Using Numerical***

**Methods.** A slab of beef 45.7 mm thick and initially at a uniform temperature of 283 K is being chilled by a surface-contact cooler at 274.7 K on the front face. The rear face of the meat is insulated. Assume that the convection resistance at the front surface is zero. Using five slices and  $M = 2$ , calculate the temperature profile after 0.54 h. The thermal diffusivity is  $4.64 \times 10^{-4} \text{ m}^2/\text{h}$ .

**Ans.**  $\Delta t = 0.090 \text{ h}$ , six time increments

**14.4-5. Cooling Beef with Convective Resistance.** A large slab of beef is 45.7 mm thick and is at an initial uniform temperature of  $37.78^\circ\text{C}$ . It is being chilled at the front surface in a chilled air blast at  $-1.11^\circ\text{C}$  with a convective heat-transfer coefficient of  $h = 38.0 \text{ W}/\text{m}^2 \cdot \text{K}$ . The rear face of the meat is

insulated. The thermal conductivity of the beef is  $k = 0.498 \text{ W/m} \cdot \text{K}$  and  $\alpha = 4.64 \times 10^{-4} \text{ m}^2/\text{h}$ . Using a numerical method with five slices and  $M = 4.0$ , calculate the temperature profile after 0.27 h. [*Hint*: Since there is a convective resistance, the value of  $N$  must be calculated. Also, Eq. (6.4-7) should be used.]

**Ans.**  $17.16^\circ\text{C}$  ( $n = 1$ ),  $28.22^\circ\text{C}$  (2),  
 $34.48^\circ\text{C}$  (3),  $37.00^\circ\text{C}$  (4),  $37.67^\circ\text{C}$  (5),  
 $37.77^\circ\text{C}$  (6)

**14.4-6. Cooling Beef Using the Digital Computer.** Repeat Problem 6.4-5 using the digital computer. Use 20 slices and  $M = 4.0$ . Use a spreadsheet calculation.

**14.4-7. Convection and Unsteady-State Conduction.** For the conditions of



Example 6.4-3, continue the calculations for a total of 12 time increments. Plot the temperature profile.

#### **14.4-8. *Alternative Convective***

***Boundary Condition for Numerical Method.*** Repeat Example 6.4-3, but instead use the alternative boundary condition, Eq. (6.4-11). Also, use  $M = 4$ . Calculate the profile for the full 12 time increments.

**14.4-9. *Numerical Method for a Semi-infinite Solid and Convection.*** A semi-infinite solid initially at a uniform temperature of  $200^{\circ}\text{C}$  is cooled at its surface by convection. The cooling fluid at a constant temperature of  $100^{\circ}\text{C}$  has a convective coefficient of  $h = 250 \text{ W/m}^2 \cdot \text{K}$ . The physical properties of the solid are  $k = 20 \text{ W/m} \cdot \text{K}$  and  $\alpha = 4 \times 10^{-5} \text{ m}^2/$

s. Using a numerical method with  $\Delta x = 0.040$  m and  $M = 4.0$ , calculate the temperature profile after 50 s total time.

$$\text{Ans. } T_1 = 157.72, T_2 = 181.84, T_3 = 194.44, T_4 = 198.93, T_5 = 199.90^\circ\text{C}$$

**14.5-1. *Chilling a Slab of Beef.*** Repeat Example 14.5-1, where the slab of beef is cooled to  $10^\circ\text{C}$  at the center, but use air of  $0^\circ\text{C}$  at a lower value of  $h = 22.7$   $\text{W/m}^2 \cdot \text{K}$ .

$$\text{Ans. } (T_1 - T)/(T_1 - T_0) = 0.265, X = 0.92, t = 19.74 \text{ h}$$

**14.5-2. *Chilling Fish Fillets.*** Codfish fillets originally at  $10^\circ\text{C}$  are packed to a thickness of 102 mm. Ice is packed on both sides of the fillets and wet-strength paper separates the ice and fillets. The surface temperature of the fish can be

assumed as essentially  $0^{\circ}\text{C}$ . Calculate the time for the center of the fillets to reach  $2.22^{\circ}\text{C}$  and the temperature at this time at a distance of 25.4 mm from the surface. Also, plot temperature versus position for the slab. The physical properties are (B1)  $k = 0.571 \text{ W/m} \cdot \text{K}$ ,  $\rho = 1052 \text{ kg/m}^3$ , and  $c_p = 4.02 \text{ kJ/kg} \cdot \text{K}$ .

**14.5-3. Average Temperature in Chilling Fish.** Fish fillets having the same physical properties given in Problem 14.5-2 are originally at  $10^{\circ}\text{C}$ . They are packed to a thickness of 102 mm with ice on each side. Assuming that the surface temperature of the fillets is  $0^{\circ}\text{C}$ , calculate the time for the average temperature to reach  $1.39^{\circ}\text{C}$ . (*Note:* This is a case where the surface resistance is zero. Can Fig. 14.3-13 be used for this case?)

#### **14.5-4. *Time to Freeze a Slab of Meat.***

Repeat Example 14.5-2 using the same conditions except that a plate or contact freezer is used where the surface coefficient can be assumed as  $h = 142 \text{ W/m}^2 \cdot \text{K}$ .

**Ans.**  $t = 2.00 \text{ h}$

#### **14.5-5. *Freezing a Cylinder of Meat.***

A package of meat containing 75% moisture and in the form of a long cylinder 5 in. in diameter is to be frozen in an air-blast freezer at  $-25^\circ\text{F}$ . The meat is initially at the freezing temperature of  $27^\circ\text{F}$ . The heat-transfer coefficient is  $h = 3.5 \text{ btu/h} \cdot \text{ft}^2 \cdot ^\circ\text{F}$ . The physical properties are  $\rho = 64 \text{ lbm/ft}^3$  for the unfrozen meat and  $k = 0.60 \text{ btu/h} \cdot \text{ft} \cdot ^\circ\text{F}$  for the frozen meat. Calculate the freezing time.

**14.6-1. Heat Generation Using the Equation of Energy Change.** A plane wall with uniform internal heat generation of  $q$ . W/m<sup>3</sup> is insulated at four surfaces, with heat conduction only in the  $x$  direction. The wall has a thickness of  $2L$  m. The temperature at one wall at  $x = +L$  and at the other wall at  $x = -L$  is held constant at  $T_w$  K. Using the differential equation of energy change, Eq. (14.6-18), derive the equation for the final temperature profile.

$$\text{Ans. } T = \frac{q(L^2 - x^2)}{2k} + T_w$$

**14.6-2. Heat Transfer in a Solid Using the Equation of Energy Change.** A solid of thickness  $L$  is at a uniform temperature of  $T_0$  K. Suddenly, the front surface temperature of the solid at  $z = 0$

m is raised to  $T_1$  at  $t = 0$  and held there, and at  $z = L$  at the rear surface to  $T_2$  and held constant. Heat transfer occurs only in the  $z$  direction. For constant physical properties and using the differential equation of energy change, do as follows:

- Derive the partial differential equation and the boundary conditions (B.C.) for unsteady-state energy transfer.
- Do the same for steady state and integrate the final equation.

**Ans.** (a)  $\partial T / \partial t = \alpha \partial^2 T / \partial z^2$ ; B.C.(1):  $t = 0$ ,  $z = z$ ,  $T = T_0$ ; B.C.(2):  $t = t$ ,  $z = 0$ ,  $T = T_1$ ; B.C.(3):  $t = t$ ,  $z = L$ ,  $T = T_2$ ; (b)  $T = (T_2 - T_1)z/L + T_1$

### **14.6-3. Radial Temperature Profile**

***Using the Equation of Energy Change.***

Radial heat transfer is occurring by conduction through a long, hollow

cylinder of length  $L$  with the ends insulated.

- What is the final differential equation for steady-state conduction? Start with Fourier's second law in cylindrical coordinates, Eq. (14.6-20).
- Solve the equation for the temperature profile from part (a) for the boundary conditions given as follows:  $T = T_i$  for  $r = r_i$ ,  $T = T_o$  for  $r = r_o$ .
- Using part (b), derive an expression for the heat flow  $q$  in W.

**Ans.**  $T = T_i - (T_i - T_o) \frac{\ln(r/r_i)}{\ln(r_o/r_i)}$

#### 14.6-4. *Heat Conduction in a Sphere.*

Radial energy flow is occurring in a hollow sphere with an inside radius of  $r_i$  and an outside radius of  $r_o$ . At steady state, the inside surface temperature is constant at  $T_i$  and constant at  $T_o$  on the outside surface.

- Using the differential equation of energy change, solve the equation for the temperature profile.

- Using part (a), derive an expression for the heat flow in W.

### ***14.6-5. Variable Heat Generation and the Equation of Energy Change.***

A plane wall is insulated so that conduction occurs only in the  $x$  direction. The boundary conditions that apply at steady state are  $T = T_0$  at  $x = 0$  and  $T = T_L$  at  $x = L$ . Internal heat generation per unit volume is occurring and varies as  $q = q_0 e^{2\beta x/L}$ , where  $q_0$  and  $\beta$  are constants. Solve the general differential equation of energy change for the temperature profile.

### **References**

### **Notation**



# Chapter 15. Introduction to Convection

## 15.0 Chapter Objectives

On completion of this chapter, a student should be able to:

- Distinguish between the two main classifications of convective heat transfer, i.e., natural and forced convection
- Use the Buckingham method to determine the number of dimensionless parameters
- Derive equations that allow prediction of heat-transfer coefficients for a flat plate with laminar flow
- Calculate heat transfer coefficients for situations described in the chapter for forced convection; for example, calculating the heat-transfer coefficient for turbulent flow inside a pipe
- Calculate heat-transfer coefficients for situations described in the chapter for natural convection; for example, calculating the heat-transfer coefficient for a vertical wall

- Calculate heat-transfer coefficients when boiling or condensation is occurring
- Calculate heat-transfer coefficients for non-Newtonian fluids
- Calculate heat-transfer coefficients for unique situations like a scraped-surface heat exchanger

## **15.1 Introduction and Dimensional Analysis in Heat Transfer**

### **15.1A Introduction to Convection (Review)**

In most situations involving a liquid or a gas in heat transfer, convective heat transfer usually occurs as well as conduction. In most industrial processes where heat transfer is occurring, heat is being transferred from one fluid through a solid wall to a second fluid. In Fig. 15.1-1, heat is being transferred from the hot flowing fluid to the cold flowing fluid. The temperature profile is shown.

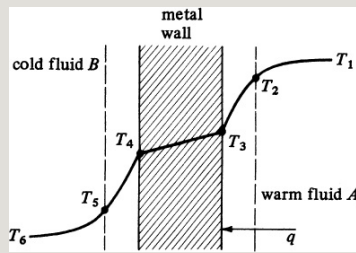


Figure 15.1-1. *Temperature profile for heat transfer by convection from one fluid to another.*

The velocity gradient, when the fluid is in turbulent flow, is very steep next to the wall in the thin viscous sublayer where turbulence is absent. Here, the heat transfer is mainly by conduction, with a large temperature difference of  $T_2 - T_3$  in the warm fluid. As we move farther away from the wall, we approach the turbulent region, where rapidly moving eddies tend to equalize the temperature. Hence, the temperature gradient is less and the difference  $T_1 - T_2$  is small. The average temperature of fluid A is slightly less than the peak value  $T_1$ . A similar explanation can be

given for the temperature profile in the cold fluid.

The convective coefficient for heat transfer through a fluid is given by

$$q=hA(T-T_w)(15.1-1)$$

where  $h$  is the convective coefficient in  $W/m^2 \cdot K$ ,  $A$  is the area in  $m^2$ ,  $T$  is the bulk or average temperature of the fluid in  $K$ ,  $T_w$  is the temperature of the wall in contact with the fluid in  $K$ , and  $q$  is the heat-transfer rate in  $W$ . In English units,  $q$  is in  $btu/h \cdot ft^2 \cdot ^\circ F$ ,  $A$  in  $ft^2$ , and  $T$  and  $T_w$  in  $^\circ F$ .

The type of fluid flow, whether laminar or turbulent, of the individual fluid has a great effect on the heat-transfer coefficient  $h$ , which is often called a *film coefficient*, since most of the resistance

to heat transfer is in a thin film close to the wall. The more turbulent the flow, the greater the heat-transfer coefficient.

There are two main classifications of convective heat transfer. The first is free or *natural convection*, where the motion of the fluid results from the density changes in heat transfer. The buoyant effect produces a natural circulation of the fluid, so it moves past the solid surface. In the second type, *forced convection*, the fluid is forced to flow by pressure differences, a pump, a fan, and so on.

Most of the correlations for predicting film coefficients  $h$  are semiempirical in nature and are affected by the physical properties of the fluid, the type and velocity of flow, the temperature

difference, and the geometry of the specific physical system. Some approximate values for convective coefficients were presented in Table 12.4-1. In the following correlations, either SI or English units can be used, since the equations are dimensionless.

To correlate these data for heat-transfer coefficients, dimensionless numbers such as the Reynolds and Prandtl numbers are used. The Prandtl number is the ratio of the shear component of diffusivity for momentum  $\mu/\rho$  to the diffusivity for heat  $k/\rho c_p$  and physically relates the relative thicknesses of the hydrodynamic layer and thermal boundary layer:

$$N_{Pr} = \mu/\rho k / \rho c_p = c_p \mu / k \quad (15.1-2)$$

Values of the  $N_{Pr}$  for gases are given in Appendix A.3 and range from about 0.5 to 1.0. Values for liquids range from about 2 to well over  $10^4$ . The dimensionless Nusselt number,  $N_{Nu}$ , is used to relate data for the heat-transfer coefficient  $h$  to the thermal conductivity  $k$  of the fluid and a characteristic dimension  $D$ :

$$N_{Nu} = hD/k \quad (15.1-3)$$

For example, for flow inside a pipe,  $D$  is the diameter.

### **15.1B Introduction to Dimensionless Groups**

As seen in many of the correlations for fluid flow and heat transfer, many dimensionless groups, such as the Reynolds number and Prandtl number, occur in these correlations.

Dimensional analysis is often used to group the variables in a given physical situation into dimensionless parameters or numbers that can be useful in experimentation and correlating data.

An important way of obtaining these dimensionless groups is to use dimensional analysis of differential equations as described in Chapter 4. Another useful method is the Buckingham method, in which the listing of the significant variables in the particular physical problem is done first. Then, we determine the number of dimensionless parameters into which the variables may be combined.

### **15.1C Buckingham Method**

*1. Heat transfer inside a pipe.* The



Buckingham theorem, discussed in Chapter 4, states that the function relationship among  $q$  quantities or variables whose units may be given in terms of  $u$  fundamental units or dimensions may be written as  $(q - u)$  dimensionless groups.

As an additional example to illustrate the use of this method, let us consider a fluid flowing in turbulent flow at velocity  $v$  inside a pipe of diameter  $D$  and undergoing heat transfer to the wall. We wish to predict the dimensionless groups relating the heat-transfer coefficient  $h$  to the variables  $D$ ,  $\rho$ ,  $\mu$ ,  $cp$ ,  $k$ , and  $v$ . The total number of variables is  $q = 7$ .

The fundamental units or dimensions are  $u = 4$  and are mass  $M$ , length  $L$ , time

$t$ , and temperature  $T$ . The units of the variables in terms of these fundamental units are as follows:

$$\begin{aligned} \mu &= \text{ML}^{-1}\text{T}^{-1} & D &= \text{L}^2\text{T}^{-1} & k &= \text{ML}^2\text{T}^{-2}\text{K}^{-1} \\ v &= \text{LT}^{-1} \end{aligned}$$

Hence, the number of dimensionless groups or  $\pi$ 's can be assumed to be  $7 - 4$ , or  $3$ . Then

$$\pi_1 = f(\pi_2, \pi_3) \quad (15.1-4)$$

We will choose the four variables  $D$ ,  $k$ ,  $\mu$ , and  $v$  to be common to all the dimensionless groups. Then, the three dimensionless groups are

$$\pi_1 = D a k b \mu c v d p \quad (15.1-5)$$

$$\pi_2 = D e k f \mu g v h c p \quad (15.1-6)$$

$$\pi_3 = D \rho \mu \kappa \nu \lambda h \quad (15.1-7)$$

For  $\pi_1$ , substituting the actual dimensions,

$$M^0 L^0 t^0 T^0 = 1 = L^a (M L^3 T)^b (M L T)^c (L T)^d (M L^3)^e \quad (15.1-8)$$

Summing for each exponent,

$$\begin{aligned} (L)^0 &= a + b - c + d - 3e \\ (M)^0 &= b + c + e \\ (t)^0 &= -3b - c - d \\ (T)^0 &= -b \end{aligned}$$

Solving these equations simultaneously,  $a = 1$ ,  $b = 0$ ,  $c = -1$ , and  $d = 1$ .

Substituting these values into Eq. (15.1-5),

$$\pi_1 = D \nu \rho \mu = N \text{Re} \quad (15.1-10)$$

Repeating for  $\pi_2$  and  $\pi_3$  and substituting

the actual dimensions,

$$\pi_2 = c_p \mu k = NPr \quad (15.1-11)$$

$$\pi_3 = h D k = NNu \quad (15.1-12)$$

Substituting  $\pi_1$ ,  $\pi_2$ , and  $\pi_3$  into Eq. (15.1-4) and rearranging,

$$h D k = f(D v \rho m, c_p \mu k) \quad (15.1-13)$$

This is in the form of the familiar equation for heat transfer inside pipes, Eq. (15.3-5).

This type of analysis is useful in empirical correlations of heat-transfer data. The importance of each dimensionless group, however, must be determined by experimentation (B1, M1).

2. *Natural convection heat transfer outside a vertical plane.* In the case of natural convection heat transfer from a vertical plane wall of length  $L$  to an adjacent fluid, different dimensionless groups should be expected as compared to forced convection inside a pipe, since velocity is not a variable. The buoyant force due to the difference in density between the cold and the heated fluid should be a factor. As seen in Eqs. (15.5-1) and (15.5-2), the buoyant force depends upon the variables  $\beta$ ,  $g$ ,  $\rho$ , and  $\Delta T$ . Hence, the list of variables to be considered and their fundamental units are as follows:

$$\begin{aligned} \rho &= M L^{-3} & \mu &= M L^{-1} t^{-1} & c_p &= L^2 t^{-1} T^{-1} & \beta &= 1/T & g &= L t^{-2} & \Delta T &= T & h &= M t^{-3} T k^{-1} & M &= M \end{aligned}$$

The number of variables is  $q = 9$ . Since  $u = 4$ , the number of dimensionless

groups or  $\pi$ 's is  $9 - 4$ , or  $5$ . Then  $\pi_1 = f(\pi_2, \pi_3, \pi_4, \pi_5)$ .

We will choose the four variables  $L$ ,  $\mu$ ,  $k$ , and  $g$  to be common to all the dimensionless groups:

$$\pi_2 = L \mu f k g h c p \quad \pi_3 = L \mu j k k g l \beta \quad \pi_4 = L m \mu n k o g p \Delta T \quad \pi_5 =$$

For  $\pi_1$ , substituting the dimensions,

$$1 = L^a (M L t)^b (M L^3 T)^c (L t^2)^d (M L^3) \quad (15.1-14)$$

Solving for the exponents as before,  $a=3/2$ ,  $b=-1$ ,  $c=0$ , and  $d=1/2$ . Then  $\pi_1$  becomes

$$\pi_1 = L^{3/2} \rho g^{1/2} m \quad (15.1-15)$$

Taking the square of both sides to eliminate fractional exponents,

$$\pi_1 = L^3 \rho^2 g \mu^2 \quad (15.1-16)$$

Repeating for the other  $\pi$  equations,

$$L^3 \rho^2 g \mu^2 \pi_2 = c \rho \mu k = N_{Pr} \quad \pi_3 = L \mu g \beta k \quad \pi_4 = k \Delta T L \mu g \quad \pi_5 = h L k =$$

Combining the dimensionless groups  $\pi_1$ ,  $\pi_3$ , and  $\pi_4$  as follows,

$$\pi_4 = L^3 \rho^2 g \mu^2 L \mu g \beta k k \Delta T L \mu g = L^3 \rho^2 g \beta \Delta T \mu^2 = N_{Gr} \quad (15.1-17)$$

Equation (15.1-17) is the Grashof group given in Eq. (15.5-4). Hence,

$$N_{Nu} = f(N_{Gr}, N_{Pr}) \quad (15.1-18)$$

## 15.2 Boundary-Layer Flow and Turbulence in Heat Transfer

### 15.2A Laminar Flow and Boundary-Layer Theory in Heat Transfer

In Section 11.1c, an exact solution was obtained for the velocity profile for isothermal laminar flow past a

flat plate. The solution of Blasius can be extended to include the convective heat-transfer problem for the same geometry and laminar flow. In Fig. 15.2-1, the thermal boundary layer is shown. The temperature of the fluid approaching the plate is  $T_{\infty}$  and that of the plate is  $T_s$  at the surface.

We start by writing the differential energy balance, Eq. (14.6-13):

$$\begin{aligned} \frac{\partial T}{\partial t} + v_x \frac{\partial T}{\partial x} + v_y \frac{\partial T}{\partial y} \\ + v_z \frac{\partial T}{\partial z} = k \rho c_p \left( \frac{\partial^2 T}{\partial x^2} + \frac{\partial^2 T}{\partial y^2} + \frac{\partial^2 T}{\partial z^2} \right) \end{aligned} \quad (15.2-1)$$

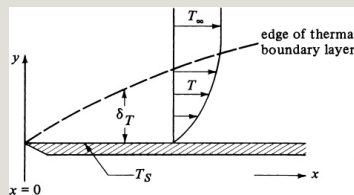


Figure 15.2-1. Laminar flow of fluid past a flat plate and thermal boundary layer.



If the flow is in the  $x$  and  $y$  directions,  $v_z = 0$ . At steady state,  $\partial T / \partial t = 0$ .

Conduction is neglected in the  $x$  and  $z$  directions, so  $\partial^2 T / \partial x^2 = \partial^2 T / \partial z^2 = 0$ .

Conduction occurs in the  $y$  direction.

The result is

$$v_x \frac{\partial T}{\partial x} + v_y \frac{\partial T}{\partial y} = k \rho c_p \frac{\partial^2 T}{\partial y^2} \quad (15.2-2)$$

The simplified momentum-balance equation used in the velocity boundary-layer derivation is very similar:

$$v_x \frac{\partial v_x}{\partial x} + v_y \frac{\partial v_x}{\partial y} = \mu \frac{\partial^2 v_x}{\partial y^2} \quad (11.1-5)$$

The continuity equation used previously is

$$\frac{\partial v_x}{\partial x} + \frac{\partial v_y}{\partial y} = 0 \quad (11.1-3)$$

Equations (11.1-5) and (11.1-3) were used by Blasius for solving the case for laminar boundary-layer flow. The boundary conditions used were

$$v_y = 0 \text{ at } y=0, \quad v_x = 1 \text{ at } y=\infty, \quad v_x = 1 \text{ at } x=0 \quad (15.2-2)$$

The similarity between Eqs. (11.1-5) and (15.2-2) is obvious. Hence, the Blasius solution can be applied if  $k/\rho c_p = \mu/\rho$ . This means the Prandtl number  $c_p \mu/k = 1$ . Also, the boundary conditions must be the same. This is done by replacing the temperature  $T$  in Eq. (15.2-2) by the dimensionless variable  $(T - T_s)/(T_\infty - T_s)$ . The boundary conditions become

$$\begin{aligned} v_x = v_y = (T - T_s)/(T_\infty - T_s) = 0 \text{ at } y=0 \\ v_x = v_y = (T - T_s)/(T_\infty - T_s) = 1 \text{ at } y=\infty \\ v_x = v_y = (T - T_s)/(T_\infty - T_s) = 1 \text{ at } x=0 \end{aligned}$$

$$T_s = 1 \text{ at } x=0 \quad (15.2-4)$$

We see that the equations and boundary conditions are identical for the temperature profile and the velocity profile. Hence, for any point  $x, y$  in the flow system, the dimensionless velocity variables  $v_x/v_\infty$  and  $(T - T_s)/(T_\infty - T_s)$  are equal. The velocity-profile solution is the same as the temperature-profile solution.

This means that the transfer of momentum and heat are directly analogous, and the boundary-layer thickness  $\delta$  for the velocity profile (hydrodynamic boundary layer) and the thermal boundary-layer thickness  $\delta_T$  are equal. This is important for gases, where the Prandtl numbers are close to 1.

By combining Eqs. (11.1-7) and (11.1-8), the velocity gradient at the surface is

$$(\partial v_x / \partial y)_{y=0} = 0.332 v_\infty x^{-1/2} N_{Re,x}^{1/2} \quad (15.2-5)$$

where  $N_{Re,x} = x v_\infty \rho / \mu$ . Also,

$$v_x v_\infty = T - T_s \quad (15.2-6)$$

Combining Eqs. (15.2-5) and (15.2-6),

$$\begin{aligned} (\partial T / \partial y)_{y=0} &= (T_\infty - T_s) \\ &\quad (0.332 x^{-1/2} N_{Re,x}^{1/2}) \quad (15.2-7) \end{aligned}$$

The convective equation can be related to the Fourier equation by the following, where  $q_y$  is in J/s or W (btu/h):

$$\begin{aligned} q_y A &= h x (T_s - T_\infty) = - \\ &\quad k (\partial T / \partial y)_{y=0} \quad (15.2-8) \end{aligned}$$

Combining Eqs. (15.2-7) and (15.2-8),

$$h_x k = N_{Nu,x} = 0.332 N_{Re,x}^{1/2} \quad (15.2-9)$$

where  $N_{Nu,x}$  is the dimensionless Nusselt number and  $h_x$  is the local heat-transfer coefficient at point  $x$  on the plate.

Pohlhausen (K1) was able to show that the relation between the hydrodynamic and thermal boundary layers for fluids with Prandtl number  $> 0.6$  gives approximately

$$\delta_T = N_{Pr}^{1/3} \delta \quad (15.2-10)$$

As a result, the equation for the local heat-transfer coefficient is

$$h_x = 0.332 k N_{Re,x}^{1/2} N_{Pr}^{1/3} \quad (15.2-11)$$

Also,

$$h_{xx}k = N \text{Nu}_{,x} = 0.332 \text{NRe}_{,x}^{1/2} \text{NPr}^{1/3} \quad (15.2-12)$$

The equation for the mean heat-transfer coefficient  $h$  from  $x = 0$  to  $x = L$  for a plate of width  $b$  and area  $bL$  is

$$\int_0^L h_x dx = \frac{1}{L} \int_0^L 0.332 k (\rho v \infty \mu)^{1/2} \text{NPr}^{1/3} x^{1/2} dx \quad (15.2-13)$$

Integrating,

$$h = 0.644 k L^{-1/2} \text{NRe}_{,L}^{1/2} \text{NPr}^{1/3} \quad (15.2-14)$$

$$hLk = N \text{Nu} = 0.644 \text{NRe}_{,L}^{1/2} \text{NPr}^{1/3} \quad (15.2-15)$$

As pointed out previously, this laminar boundary layer on smooth plates holds up to a Reynolds number of about  $5 \times 10^5$ . In using the results above, the fluid properties are usually evaluated at the film temperature  $T_f = (T_s + T_\infty)/2$ .

## 15.2B Approximate Integral Analysis of the Thermal Boundary Layer

As discussed in the analysis of the hydrodynamic boundary layer, the Blasius solution is accurate but limited in its scope. Other, more complex systems cannot be solved by this method. The approximate integral analysis used by von Kármán to calculate the hydrodynamic boundary layer was covered in Section 11.1. This approach can be used to analyze the thermal boundary layer.

This method will be outlined briefly. First, a control volume, as previously given in Fig. 11.3-1, is used to derive the final energy integral expression:

$$k_p v_p (\partial T / \partial y)_{y=0} = d/dx \int_0^{\delta_T} \rho v_x (T_\infty - T) dy \quad (15.2-16)$$

This equation is analogous to Eq. (11.3-1) combined with Eq. (11.3-4) for the momentum analysis, giving

$$\mu \rho (\partial v_x / \partial y)_{y=0} = \frac{d}{dx} \int_0^\infty \delta v_x (v_\infty - v_x) dy \quad (15.2-17)$$

Equation (15.2-16) can be solved if both a velocity profile and temperature profile are known. The assumed velocity profile used is Eq. (11.3-3):

$$v_x / v_\infty = \frac{3}{2} y \delta^{-1/2} (1 - \frac{1}{2} y \delta^{-1/2})^2 \quad (11.3-3)$$

The same form of temperature profile is assumed:

$$\frac{T - T_s}{T_\infty - T_s} = \frac{3}{2} y \delta_T^{-1/2} (1 - \frac{1}{2} y \delta_T^{-1/2})^2 \quad (15.2-18)$$

Substituting Eqs. (11.3-3) and (15.2-18) into the integral expression and solving,



$$NNu_x = 0.36 NRe_x^{1/2} NPr^{1/3} \quad (15.2-19)$$

This is only about 8% greater than the exact result in Eq. (15.2-11), which indicates that this approximate integral method can be used with confidence in cases where exact solutions cannot be obtained.

In a similar fashion, the integral momentum analysis method used for the turbulent hydrodynamic boundary layer in Chapter 11 can be used for the thermal boundary layer in turbulent flow. Again, the Blasius 1/7-power law is used for the temperature distribution. These results are quite similar to the experimental equations given in Section 15.4.

#### **15.2C Prandtl Mixing Length and Eddy Thermal Diffusivity**

1. *Eddy momentum diffusivity in turbulent flow.* In Section 11.2C, the total shear stress  $\tau_{yx}$  for turbulent flow was written as follows when the molecular and turbulent contributions are summed together:

$$\tau_{yx} = -\rho(\mu + \epsilon_t) \frac{dv_x}{dy} \quad (11.2-20)$$

The molecular momentum diffusivity  $\mu/\rho$  in  $m^2/s$  is a function only of the fluid molecular properties. However, the turbulent momentum eddy diffusivity  $\epsilon_t$  depends on the fluid motion. In Eq. (11.2-17), we related  $\epsilon_t$  to the Prandtl mixing length  $L$  as follows:

$$\epsilon_t = L^2 \left| \frac{dv_x}{dy} \right| \quad (11.2-17)$$

2. *Prandtl mixing length and eddy thermal diffusivity.* We can derive the eddy thermal diffusivity  $\alpha_t$  for turbulent

heat transfer in a similar manner, as follows. Eddies or clumps of fluid are transported a distance  $L$  in the  $y$  direction. At this point  $L$ , the clump of fluid differs in mean velocity from the adjacent fluid by the velocity  $v_x'$ , which is the fluctuating velocity component discussed in Section 11.2C. Energy is also transported the distance  $L$  with a velocity  $v_y'$  in the  $y$  direction together with the mass being transported. The instantaneous temperature of the fluid is  $T = T' + T^-$ , where  $T^-$  is the mean value and  $T'$  the deviation from the mean value. This fluctuating  $T'$  is similar to the fluctuating velocity  $v_x'$ . The mixing length is small enough that the temperature difference can be written as

$$T' = L \frac{dT^-}{dy} \quad (15.2-21)$$

The rate of energy transported per unit area is  $q_y/A$  and is equal to the mass flux in the  $y$  direction times the heat capacity times the temperature difference:

$$q_y A = -\rho c_p L \frac{dT}{dy} \quad (15.2-22)$$

In Section 11.2C, we assumed  $v_x' \cong v_y'$  and that

$$v_x' = v_y' = L |dv_x'/dy| \quad (15.2-23)$$

Substituting Eq. (15.2-23) into (15.2-22),

$$q_y A = -\rho c_p L^2 |dv_x'/dy| \frac{dT}{dy} \quad (15.2-24)$$

According to Eq. (11.2-17), the term  $L^2 |dv_x'/dy|$  is the momentum eddy diffusivity  $\epsilon_t$ . When this term is in the turbulent heat-transfer equation (15.2-24), it is called  $\alpha_t$ , eddy thermal

diffusivity. Then, Eq. (15.2-24) becomes

$$q_y A = -\rho c_p \alpha_t dT/dy \quad (15.2-25)$$

Combining this with the Fourier equation written in terms of the molecular thermal diffusivity  $\alpha$ ,

$$q_y A = -\rho c_p (\alpha + \alpha_t) dT/dy \quad (15.2-26)$$

*3. Similarities among momentum, heat, and mass transport.* Equation (15.2-26) is similar to Eq. (15.2-20) for total momentum transport. The eddy thermal diffusivity  $\alpha_t$  and the eddy momentum diffusivity  $\epsilon_t$  have been assumed equal in the derivations. Experimental data show that this equality is only approximate. An eddy mass diffusivity for mass transfer has been defined in a similar manner using the Prandtl mixing length theory and is assumed equal to  $\alpha_t$

and  $\varepsilon_t$ .

## 15.3 Forced Convection Heat Transfer Inside Pipes

### 15.3A Heat-Transfer Coefficient for Laminar Flow Inside a Pipe

Certainly, the most important convective heat-transfer process industrially is that of cooling or heating a fluid flowing inside a closed circular conduit or pipe. Different types of correlations for the convective coefficient are needed for laminar flow ( $N_{Re}$  below 2100), for fully turbulent flow ( $N_{Re}$  above 6000), and for the transition region ( $N_{Re}$  between 2100 and 6000).

For laminar flow of fluids inside horizontal tubes or pipes, the following equation of Sieder and Tate (S1) can be used for  $N_{Re} < 2100$ :

$$N_{Nu,a} = \frac{h_a D}{k} = 1.86 (N_{Re} N_{Pr} D/L)^{1/3} (\mu_b / \mu_w)^{0.14} \quad (15.3-1)$$

where  $D$  = pipe diameter in m,  $L$  = pipe length before mixing occurs in the pipe in m,  $\mu_b$  = fluid viscosity at bulk average temperature in  $\text{Pa} \cdot \text{s}$ ,  $\mu_w$  = viscosity at the wall temperature,  $c_p$  = heat capacity in  $\text{J/kg} \cdot \text{K}$ ,  $k$  = thermal conductivity in  $\text{W/m} \cdot \text{K}$ ,  $h_a$  = average heat-transfer coefficient in  $\text{W/m}^2 \cdot \text{K}$ , and  $N_{Nu}$  = dimensionless Nusselt number. All the physical properties are evaluated at the bulk fluid temperature except  $\mu_w$ . The Reynolds number is

$$N_{Re} = \frac{D v \rho}{\mu} \quad (15.3-2)$$

and the Prandtl number,

$$N_{Pr} = \frac{c_p \mu}{k} \quad (15.3-3)$$

This equation holds for  $(N_{Re} N_{Pr} D/L) >$

100. If used down to  $(N_{Re}N_{Pr}D/L) > 10$ , it still holds to  $\pm 20\%$  (B1). For  $(N_{Re}N_{Pr}D/L) > 100$ , another expression is available (P1).

In laminar flow, the average coefficient  $h_a$  depends strongly on heated length.

The average (arithmetic mean) temperature drop  $\Delta T_a$  is used in the equation to calculate the heat-transfer rate  $q$

$$q = h_a A \Delta T_a = h_a A (T_w - T_{bi}) + (T_w - T_{bo})^2 (15.3 - 4)$$

where  $T_w$  is the wall temperature in K,  $T_{bi}$  the inlet bulk fluid temperature, and  $T_{bo}$  the outlet bulk fluid temperature.

For large pipe diameters and large temperature differences  $\Delta T$  between pipe wall and bulk fluid, natural



convection effects can increase  $h$  (P1).  
Equations are also available for laminar flow in vertical tubes.

### **15.3B Heat-Transfer Coefficient for Turbulent Flow Inside a Pipe**

When the Reynolds number is above 6000, the flow is fully turbulent.

Since the rate of heat transfer is greater in the turbulent region, many industrial heat-transfer processes are in the turbulent region.

The following equation has been found to hold for tubes but is also used for pipes. It holds for a  $N_{Re} > 6000$ , a  $N_{Pr}$  between 0.7 and 16 000, and  $L/D > 60$ .

$$N_{Nu} = \frac{hL}{k} = 0.027 N_{Re}^{0.8} N_{Pr}^{1/3} (\mu_b/\mu_w)^{0.14} \quad (15.3-5)$$

where  $hL$  is the heat-transfer coefficient based on the log mean driving force

$\Delta T_{lm}$  (see Section 13.2B). The fluid properties except for  $\mu_w$  are evaluated at the mean bulk temperature. If the bulk fluid temperature varies from the inlet to the outlet of the pipe, the mean of the inlet and outlet temperatures is used. For an  $L/D < 60$ , where the entry is an abrupt contraction, an approximate correction is provided by multiplying the right-hand side of Eq. (15.3-5) by a correction factor given in Section 15.3E.

The use of Eq. (15.3-5) may be trial and error, since the value of  $hL$  must be known in order to evaluate  $T_w$  and, hence,  $\mu_w$  at the wall temperature. Also, if the mean bulk temperature increases or decreases in the tube length  $L$  because of heat transfer, the bulk temperature at length  $L$  must be estimated in order to have a mean bulk

temperature of the entrance and exit to use.

The heat-transfer coefficient for turbulent flow is somewhat greater for a pipe than for a smooth tube. This effect is much less than in fluid friction, and it is usually neglected in calculations.

Also, for liquid metals that have Prandtl numbers  $\ll 1$ , other correlations must be used to predict the heat-transfer coefficient (see Section 15.3F). For shapes of tubes other than circular, the equivalent diameter can be used, as discussed in Section 15.3D.

For air at 1 atm total pressure, the following simplified equation holds for turbulent flow in pipes:

$$h_L = 3.52 v^{0.8} D^{0.2} \text{ (SI)} \quad h_L = 0.5 v_s^{0.8} (D$$

## ')0.2(English)(15.3-6)

where  $D$  is in m,  $v$  in m/s, and  $h_L$  in  $W/m^2 \cdot K$  for SI units; and  $D'$  is in in.,  $v_s$  in ft/s, and  $h_L$  is in  $btu/h \cdot ft^2 \cdot ^\circ F$  for English units.

Water is often used in heat-transfer equipment. A simplified equation to use for a temperature range of  $T = 4 - 105^\circ C (40 - 220^\circ F)$  is

$$h_L = 429(1 + 0.0146T^\circ C)v^{0.8}D^{0.2} \quad (SI) \quad h_L = 150(1 + 0.011T^\circ F)v_s^{0.8}(D')^{0.2} \quad (English) \quad (15.3-7)$$

For organic liquids, a very simplified equation to use for approximations is as follows (P3):

$$h_L = 423v^{0.8}D^{0.2} \quad (SI) \quad h_L = 60v_s^{0.8}(D')^{0.2} \quad (English) \quad (15.3-8)$$

For flow inside helical coils and  $N_{Re}$

above  $10^4$ , the predicted film coefficient for straight pipes should be increased by the factor  $(1 + 3.5D/D_{\text{coil}})$ .

**EXAMPLE 15.3-1. Heating of Air in Turbulent Flow**

Air at 206.8 kPa and an average of 477.6 K is being heated as it flows through a tube of 25.4 mm inside diameter at a velocity of 7.62 m/s. The heating medium is 488.7 K steam condensing on the outside of the tube. Since the heat-transfer coefficient of condensing steam is several thousand  $\text{W/m}^2 \cdot \text{K}$  and the resistance of the metal wall is very small, it will be assumed that the surface wall temperature of the metal in contact with the air is 488.7 K. Calculate the heat-transfer coefficient for an  $L/D > 60$  and also the heat-transfer flux  $q/A$ .

**Solution:** From Appendix A.3, for physical properties of air at 477.6 K (204.4°C),  $\mu_b = 2.60 \times 10^{-5} \text{ Pa} \cdot \text{s}$ ,  $k = 0.03894 \text{ W/m} \cdot \text{K}$ ,  $\text{Pr} = 0.686$ . At 488.7 K (215.5°C),  $\mu_w = 2.65 \times 10^{-5} \text{ Pa} \cdot \text{s}$ .

$$\mu_b = 2.60 \times 10^{-5} \text{ Pa} \cdot \text{s} = 2.60 \times 10^{-5} \text{ kg/m} \cdot \text{s}$$

$$\dot{m} = \frac{P \cdot V}{R \cdot T} = \frac{206.8 \text{ kPa} \cdot 0.00254 \text{ m}^3}{8.314 \text{ J/mol} \cdot \text{K} \cdot 477.6 \text{ K}} = 1.509 \text{ kg/m}^3$$

The Reynolds number calculated at the bulk fluid temperature of 477.6 K is

$$\text{Re} = \frac{D \cdot v \cdot \rho}{\mu} = \frac{0.0254 \text{ m} \cdot 7.62 \text{ m/s} \cdot 1.509 \text{ kg/m}^3}{2.60 \times 10^{-5} \text{ kg/m} \cdot \text{s}} = 1.122 \times 10^4$$

Hence, the flow is turbulent and Eq. (15.3-5) will be used. Substituting into Eq. (15.3-5),

$$\frac{h}{\text{Pr}^{1/3}} = \frac{k}{D} \cdot 0.023 \cdot \text{Re}^{0.8} \cdot \left( \frac{\mu_b}{\mu_w} \right)^{0.14} \cdot \left( \frac{\mu_b}{\mu_w} \right)^{1/4} \cdot \left( \frac{\mu_b}{\mu_w} \right)^{1/4} \cdot \left( \frac{\mu_b}{\mu_w} \right)^{1/4}$$

$$\text{Solving, } h = 63.2 \text{ W/m}^2 \cdot \text{K} \quad (11.13 \text{ Btu/h} \cdot \text{ft}^2 \cdot ^\circ\text{F})$$

To solve for the flux  $q/A$ ,

$$q/A = h(T_w - T_b) = 63.2 \text{ W/m}^2 \cdot \text{K} (488.7 \text{ K} - 477.6 \text{ K}) = 701.1 \text{ W/m}^2 \quad (222.2 \text{ Btu/hr} \cdot \text{ft}^2)$$

### 15.3C Heat-Transfer Coefficient for Transition Flow Inside a Pipe

In the transition region for a  $N_{Re}$  between 2100 and 6000, the empirical equations are not well defined, just as in the case of fluid friction factors. No simple equation exists for accomplishing a smooth transition from heat transfer in laminar flow to that in turbulent flow, that is, a transition from Eq. (15.3-1) at a  $N_{Re} = 2100$  to Eq. (15.3-5) at a  $N_{Re} = 6000$ .

The plot in Fig. 15.3-1 represents an approximate relationship to use between the various heat-transfer parameters and the Reynolds number between 2100 and 6000. For below a  $N_{Re}$  of 2100, the curves represent Eq. (15.3-1), and above  $10^4$ , Eq. (15.3-5). The mean  $\Delta T_a$  of Eq. (15.3-4) should be used with the  $h_a$  in

Fig. 15.3-1.

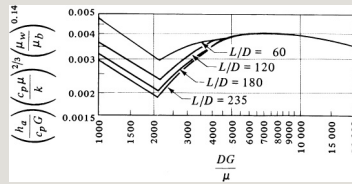


Figure 15.3-1. *Correlation of heat-transfer parameters for transition region for Reynolds numbers between 2100 and 6000. (From R. H. Perry and C. H. Chilton, Chemical Engineers' Handbook, 5th ed. New York: McGraw-Hill Book Company, 1973. With permission.)*

### 15.3D Heat-Transfer Coefficient for Noncircular Conduits

A heat-transfer system often used is one in which fluids flow at different temperatures in concentric pipes. The heat-transfer coefficient of the fluid in the annular space can be predicted by using the same equations as for circular pipes. However, the equivalent diameter defined in Section 5.1G must be used. For an annular space,  $D_{eq}$  is

the ID of the outer pipe  $D_1$  minus the OD of the inner pipe  $D_2$ . For other geometries, an equivalent diameter can also be used.

**EXAMPLE 15.3-2. Water Heated by Steam and Trial-and-Error Solution**

Water is flowing in a horizontal 1-in. Schedule 40 steel pipe at an average temperature of 65.6°C and a velocity of 2.44 m/s. It is being heated by condensing steam at 107.8°C on the outside of the pipe wall. The steam-side coefficient has been estimated as  $h_o = 10\,500 \text{ W/m}^2 \cdot \text{K}$ .

- Calculate the convective coefficient  $h_i$  for water inside the pipe.
- Calculate the overall coefficient  $U_i$  based on the inside surface area.
- Calculate the heat-transfer rate  $q$  for 0.305 m of pipe with the water at an average temperature of 65.6°C.

**Solution:** From Appendix A.5, the various dimensions are  $D_i = 0.0266 \text{ m}$  and  $D_o = 0.0334 \text{ m}$ . For water at a bulk average temperature of 65.6°C, from Appendix A.2,  $N_{Pr} = 2.72$ ,  $\rho = 0.980(1000) = 980 \text{ kg/m}^3$ ,  $k = 0.633 \text{ Wm} \cdot \text{K}$ , and  $\mu = 4.32 \times 10^{-4} \text{ Pa} \cdot \text{s} = 4.32 \times 10^{-4} \text{ kg/m} \cdot \text{s}$ .

The temperature of the inside metal wall is needed and will be assumed as about one-third the difference between 65.6 and 107.8, or 80°C =  $T_w$ , for the first trial. Hence,  $\mu_w$  at 80°C =  $3.56 \times 10^{-4} \text{ Pa} \cdot \text{s}$ .

First, the Reynolds number of the water is calculated at the bulk average temperature:

$$\text{NRe} = \frac{D_i \rho v}{\mu} = \frac{0.0266 \text{ m} (2.44 \text{ m/s})}{(980 \text{ kg/m}^3) (4.32 \times 10^{-4} \text{ kg/m} \cdot \text{s})} = 1.473 \times 10^5$$



Hence, the flow is turbulent. Using Eq. (15.3-5) and substituting known values,

$$7NRe^{0.8}Pr^{1/3}(\mu_b/\mu_w)^{0.14}h_L(0.0266m)^{0.663}Wm\cdot K=0.027(1.473\times 10^5)^{0.8}(2.72)^{13}[4.32\times 10^{-4}kgm\cdot s^{3.56}\times 10^{-4}$$

Solving,  $h_L = h_i = 13\,324\text{ W/m}^2 \cdot K$ .

For part (b), the various areas are as follows for 0.305-m pipe:

$$\begin{aligned}A_j &= \pi D_j L = \pi(0.0266m)(0.306m) = 0.0255m^2 \\ A_{lm} &= \pi D_o L - \pi D_i L \ln(\pi D_o L / \pi D_i L) = \pi(0.0334m)(0.305m) - \pi(0.0266m)(0.305m) \ln(\pi(0.0334m)(0.305m) / \pi(0.0266m)(0.305m)) \\ &= 0.029m^2 \\ A_o &= \pi D_o L = \pi(0.0334m)(0.305m) = 0.0320m^2\end{aligned}$$

The  $k$  for steel is  $45.0\text{ Wm}\cdot K$ . The resistances are

$$\begin{aligned}R_j &= 1/h_i A_i = 1/(13324\text{ Wm}^2\cdot K)(0.00255m^2) = 0.002943\text{ KW/Rm} \\ R_m &= 1/(2(0.0334m - 0.0266m)45\text{ Wm}\cdot K(0.029m^2)) = 0.002633\text{ KW/Ro} \\ R_o &= 1/h_o A_o = 1/(10500\text{ Wm}^2\cdot K)(0.032m^2) = 0.002976\text{ KW/R} \\ \Sigma R &= 0.002943\text{ KW} + 0.002633\text{ KW} + 0.002976\text{ KW} = 0.008552\text{ KW}\end{aligned}$$

The overall temperature difference is  $(107.8 - 65.6)^\circ C = 42.2^\circ C = 42.2\text{ K}$ .

The temperature drop across the water film is

$$\begin{aligned}\text{Temperature drop} &= R_i \Sigma R (42.2K) = (0.002943m^2/0.008552m^2)(42.2K) = 14.5K = 14.5^\circ C\end{aligned}$$

Hence,  $T_w = 65.6 + 14.5 = 80.1^\circ C$ . This is quite close to the original estimate of  $80^\circ C$ . The only physical property changing in the second estimate would be  $\mu_w$ . This would have a negligible effect on  $h_i$ , and a second trial is not necessary.

For part (b), the overall coefficient is, by Eq. (13.2-6),

$$\begin{aligned}q &= U_i A_i (T_o - T_i) = T_o - T_i \Sigma R U_j \\ U_j &= 1/A_i \Sigma R = 10.0255m^2/(0.008552KW) = 4586\text{ Wm}^2\cdot K\end{aligned}$$

For part (c), with the water at an average temperature of  $65.6^\circ C$ ,

$$\begin{aligned}T_o - T_i &= 107.8 - 65.6 = 42.2^\circ C = 42.2K \\ q &= U_j A_j (T_o - T_i) = 4586\text{ Wm}^2\cdot K(0.0255m^2)(42.2K) = 4935W\end{aligned}$$

### 15.3E Entrance-Region Effect on the Heat-Transfer Coefficient

Near the entrance of a pipe where the fluid is being heated, the temperature profile is not fully developed and the local coefficient  $h$  is greater than the fully developed heat-transfer coefficient  $h_L$  for turbulent flow. At the entrance itself, where no temperature gradient has been established, the value of  $h$  is infinite. The value of  $h$  drops rapidly and is approximately the same as  $h_L$  at  $L/D \cong 60$ , where  $L$  is the entrance length. These relations for turbulent flow inside a pipe where the entrance is an abrupt contraction are as follows:

$$h/h_L = 1 + (D/L)^2 \quad 0.2 < L/D < 20 \quad (15.3-9)$$

$$h/h_L = 1 + 6(D/L)^2 \quad 20 < L/D < 60 \quad (15.3-10)$$

where  $h$  is the average value for a tube

of finite length  $L$  and  $hL$  is the value for a very long tube.

### **15.3F Liquid-Metals Heat-Transfer Coefficient**

Liquid metals are sometimes used as heat-transfer fluids in cases where a fluid is needed over a wide temperature range at relatively low pressures. Liquid metals are often used in nuclear reactors and have high heat-transfer coefficients as well as a high heat capacity per unit volume. The high heat-transfer coefficients are due to the very high thermal conductivities and, hence, low Prandtl numbers. In liquid metals in pipes, heat transfer by conduction is very important in the entire turbulent core because of the high thermal conductivity and is often more important than the

convection effects.

For fully developed turbulent flow in tubes with uniform heat flux, the following equation can be used (L1):

$$Nu = hL/k = 0.625 N_{Pe}^{0.4} \quad (15.3-11)$$

where the Peclet number  $N_{Pe} = N_{Re} N_{Pr}$ . This holds for  $L/D > 60$  and  $N_{Pe}$  between 100 and  $10^4$ . For constant wall temperatures,

$$Nu = hL/k = 5.0 + 0.025 N_{Pe}^{0.8} \quad (15.3-12)$$

for  $L/D > 60$  and  $N_{Pe} > 100$ . All physical properties are evaluated at the average bulk temperature.

**EXAMPLE 15.3-3. Liquid-Metal Heat Transfer Inside a Tube**

A liquid metal flows at a rate of 4.00 kg/s through a tube having an inside diameter of 0.05 m. The liquid enters at 500 K and is heated to 505 K in the tube. The tube wall is

maintained at a temperature of 30 K above the fluid bulk temperature and constant heat flux is also maintained. Calculate the required tube length. The average physical properties are as follows:  $\mu = 7.1 \times 10^{-4} \text{ Pa} \cdot \text{s}$ ,  $\rho = 7400 \text{ kg/m}^3$ ,  $c_p = 120 \text{ J/kg} \cdot \text{K}$ ,  $k = 13 \text{ W/m} \cdot \text{K}$ .

**Solution:** The area is  $A = \pi D^2/4 = \pi(0.05)^2/4 = 1.963 \times 10^{-3} \text{ m}^2$ . Then,

$$u = m/\rho A c_s = 4 \text{ kg/s} / 7400 \text{ kg/m}^3 \cdot 1.963 \times 10^{-3} \text{ m}^2 = 0.275 \text{ m/s}.$$

The Reynolds number is

$$\text{Re} = D \rho u / \mu = 0.05 \text{ m} (7400 \text{ kg/m}^3) / (0.275 \text{ m/s}) 7.1 \times 10^{-4} \text{ kg} \cdot \text{s/m} = 1.435 \times 10^5$$

$$\text{Pr} = C_p \mu / k = 120 \text{ J/kg} \cdot \text{K} (7.1 \times 10^{-4} \text{ kg} \cdot \text{s/m}) / 13 \text{ W/m} \cdot \text{K} = 0.00655$$

Using Eq. (15.3-11), where  $\text{Nu}_e = \text{Re} \text{Pr} = (1.435 \times 10^5) (0.00655) = 939.93$

$$hL = kD(0.625) \text{Nu}_e^{0.4} = 13 \text{ W/m} \cdot \text{K} (0.05 \text{ m}) (939.93)^{0.4} = 2512 \text{ W/m}^2 \cdot \text{K}$$

Using a heat balance,

$$q = m c_p \Delta T = 4.0 \text{ kg/s} (120 \text{ J/kg} \cdot \text{K}) (505 \text{ K} - 500 \text{ K}) = 2400 \text{ W} \quad (15.3-13)$$

Substituting into Eq. (15.1-1),

$$qA = 2400 \text{ W} = hL(T_w - T) = 2512 \text{ W/m}^2 \cdot \text{K} (30 \text{ K}) = 75360 \text{ W/m}^2$$

Hence,  $A = 2400 \text{ W} / 75360 \text{ W/m}^2 = 3.185 \times 10^{-2} \text{ m}^2$ . Then,

$$A = 3.185 \times 10^{-2} \text{ m}^2 = \pi D L = \pi (0.05 \text{ m}) L$$

Solving,  $L = 0.203 \text{ m}$ .

## 15.4 Heat Transfer Outside Various Geometries in Forced Convection

### 15.4A Introduction

In many cases, a fluid is flowing

over completely immersed bodies such as spheres, tubes, plates, and so on, and heat transfer is occurring between the fluid and the solid only. Many of these shapes are of practical interest in process engineering. The sphere, cylinder, and flat plate are perhaps of greatest importance, with heat transfer between these surfaces and a moving fluid frequently encountered.

When heat transfer occurs during immersed flow, the flux is dependent on the geometry of the body, the position on the body (front, side, back, etc.), the proximity of other bodies, the flow rate, and the fluid properties. The heat-transfer coefficient varies over the body. The average heat-transfer coefficient is given in the empirical relationships to be

discussed in the following sections.

In general, the average heat-transfer coefficient on immersed bodies is given by

$$Nu = C Re^m Pr^{1/3} \quad (15.4-1)$$

where  $C$  and  $m$  are constants that depend on the various configurations. The fluid properties are evaluated at the film temperature  $T_f = (T_w + T_b)/2$ , where  $T_w$  is the surface or wall temperature and  $T_b$  the average bulk fluid temperature. The velocity in the  $Re$  is the undisturbed free stream velocity  $v$  of the fluid approaching the object.

#### **15.4B Flow Parallel to a Flat Plate**

When the fluid is flowing parallel to a flat plate and heat transfer is occurring between the whole plate of

length  $L$  m and the fluid, the  $N_{Nu}$  is as follows for a  $N_{Re,L}$  below  $3 \times 10^5$  in the laminar region and a  $N_{Pr} > 0.7$ :

$$N_{Nu} = 0.664 N_{Re,L}^{0.5} N_{Pr}^{1/3} \quad (15.4-2)$$

where  $N_{Re,L} = Lv\rho/\mu$  and  $N_{Nu} = hL/k$ .

For the completely turbulent region at a  $N_{Re,L}$  above  $3 \times 10^5$  (K1, K3) and  $N_{Pr} > 0.7$ ,

$$N_{Nu} = 0.0366 N_{Re,L}^{0.8} N_{Pr}^{1/3} \quad (15.4-3)$$

However, turbulence can start at a  $N_{Re,L}$  below  $3 \times 10^5$  if the plate is rough (K3), and then Eq. (15.4-3) will hold and give a  $N_{Nu}$  greater than that given by Eq. (15.4-2). For a  $N_{Re,L}$  below about  $2 \times 10^4$ , Eq. (15.4-2) gives the larger value of  $N_{Nu}$ .



### EXAMPLE 15.4-1. Cooling a Copper Fin

A smooth, flat, thin fin of copper extending out from a tube is 51 mm by 51 mm square. Its temperature is approximately uniform at 82.2°C. Cooling air at 15.6°C and 1 atm abs flows parallel to the fin at a velocity of 12.2 m/s.

- For laminar flow, calculate the heat-transfer coefficient,  $h$ .
- If the leading edge of the fin is rough so that all of the boundary layer or film next to the fin is completely turbulent, calculate  $h$ .

**Solution:** The fluid properties will be evaluated at the film temperature  $T_f = (T_w + T_b)/2$ :

$$T_f = T_w + T_b / 2 = 82.2 + 15.62 = 48.90^\circ\text{C} (322.1\text{K})$$

The physical properties of air at 48.9°C from Appendix A.3 are  $k = 0.0280 \text{ W/m} \cdot \text{K}$ ,  $\rho = 1.097 \text{ kg/m}^3$ ,  $\mu = 1.95 \times 10^{-5} \text{ Pa} \cdot \text{s}$ ,  $Pr = 0.704$ . The Reynolds number is, for  $L = 0.051 \text{ m}$ ,

$$N_{Re,L} = L v \rho / \mu = 0.051 \text{ m} (12.2 \text{ m/s}) / (1.097 \text{ kg/m}^3) 1.95 \times 10^{-5} \text{ kg} \cdot \text{m} / \text{s} = 3.49 \times 10^4$$

Substituting into Eq. (15.4-2),

$$N_{Nu} = h L / k = 0.664 N_{Re,L}^{1/2} Pr^{1/3} = 0.664 (3.49 \times 10^4)^{1/2} (0.704)^{1/3}$$

Solving,  $h = 60.7 \text{ W/m}^2 \cdot \text{K}$  (10.7 btu/h  $\cdot$  ft<sup>2</sup>  $\cdot$  °F).

For part (b), substituting into Eq. (15.4-3) and solving,  $h = 77.2 \text{ W/m}^2 \cdot \text{K}$  (13.6 btu/h  $\cdot$  ft<sup>2</sup>  $\cdot$  °F).

## 15.4C Cylinder with Axis Perpendicular to Flow

Often a cylinder containing a fluid inside is being heated or cooled by a fluid flowing perpendicular to its

axis. The equation for predicting the average heat-transfer coefficient of the outside of the cylinder for gases and liquids is Eq. (15.4-1) (K3, P3), with  $C$  and  $m$  as given in Table 15.4-1. The  $N_{Re} = Dv\rho/\mu$ , where  $D$  is the outside tube diameter and all physical properties are evaluated at the film temperature  $T_f$ . The velocity is the undisturbed free stream velocity approaching the cylinder.

Table 15.4-1. *Constants for Use in Eq. (15.4-1) for Heat Transfer to Cylinders with Axis Perpendicular to Flow ( $N_{Pr} > 0.6$ )*

#### 15.4D Flow Past a Single Sphere

When a single sphere is being heated or cooled by a fluid flowing past it,

the following equation can be used to predict the average heat-transfer coefficient for a  $N_{Re} = Dv\rho/\mu$  of 1 to 70 000 and a  $N_{Pr}$  of 0.6 to 400:

$$N_{Nu} = 2.0 + 0.60 N_{Re}^{0.5} N_{Pr}^{1/3} \quad (15.4-4)$$

The fluid properties are evaluated at the film temperature  $T_f$ . A somewhat more accurate correlation, which takes into account the effects of natural convection at these lower Reynolds numbers, is available for a  $N_{Re}$  range 1–17 000 from other sources (S2).

**EXAMPLE 15.4-2. Cooling of a Sphere**

Using the same conditions as Example 15.4-1, where air at 1 atm abs pressure and 15.6°C is flowing at a velocity of 12.2 m/s, predict the average heat-transfer coefficient for air flowing past a sphere having a diameter of 51 mm and an average surface temperature of 82.2°C. Compare this with the value of  $h = 77.2 \text{ W/m}^2 \cdot \text{K}$  for the flat plate in turbulent flow.

**Solution:** The physical properties at the average film temperature of 48.9°C are the same as for Example 15.4-1. The  $N_{Re}$  is

$$\begin{aligned} NRe &= Dv\rho\mu = 0.051\text{m}(12.2\text{ms}) \\ & (1.097\text{kgm}^3)1.95\times 10^{-5}\text{kgm}\cdot\text{s} = 3.49\times 10^4 \end{aligned}$$

Substituting into Eq. (15.4-4) for a sphere,

$$NNu = hDk = h(0.051\text{m})0.0280\text{Wm}\cdot\text{k} = 2.0 + 0.60NRe^{0.5}NP_r^{1/3} = 2.0 + (3.49\times 10^4)^{0.5}(0.704)^{1/3}$$

Solving,  $h = 56.1 \text{ W/m}^2 \cdot \text{K}$  ( $9.88 \text{ btu/h} \cdot \text{ft}^2 \cdot ^\circ\text{F}$ ). This value is somewhat smaller than the value of  $h = 77.2 \text{ W/m}^2 \cdot \text{K}$  ( $13.6 \text{ btu/h} \cdot \text{ft}^2 \cdot ^\circ\text{F}$ ) for a flat plate.

## 15.4E Flow Past Banks of Tubes or Cylinders

Many types of commercial heat exchangers are constructed with multiple rows of tubes, where the fluid flows at right angles to the bank of tubes. An example is a gas heater in which a hot fluid inside the tubes heats a gas passing over the outside of the tubes. Another example is a cold liquid stream inside the tubes being heated by a hot fluid on the outside.

Figure 15.4-1 shows the arrangement for banks of tubes in-line and banks of tubes staggered, where  $D$  is tube OD in

$m$  (ft),  $S_n$  is distance  $m$  (ft) between the centers of the tubes normal to the flow, and  $S_p$  is parallel to the flow. The open area to flow for in-line tubes is  $(S_n - D)$  and  $(S_p - D)$ ; for staggered tubes it is  $(S_n - D)$  and  $(S_p' - D)$ . Values of  $C$  and  $m$  to be used in Eq. (15.4-1) for a Reynolds-number range of 2000 to 40000 for heat transfer to banks of tubes containing more than 10 transverse rows in the direction of flow are given in Table 15.4-2. For less than 10 rows, Table 15.4-3 gives the correction factors.

For cases where  $S_n/D$  and  $S_p/D$  are not equal to each other, the reader should consult Grimison (G1) for more data. In baffled exchangers where there is normal leakage when all the fluid does not flow normally to the tubes, the average values of  $h$  obtained should be

multiplied by about 0.6 (P3). The Reynolds number is calculated using the minimum area open to flow for the velocity. All physical properties are evaluated at  $T_f$ .

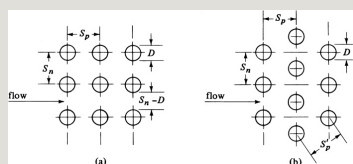


Figure 15.4-1. Nomenclature for banks of tubes in Table 15.4-2: (a) in-line tube rows, (b) staggered tube rows.

Table 15.4-2. Values of  $C$  and  $m$  to Be Used in Eq. (15.4-1) for Heat Transfer to Banks of Tubes Containing More Than 10 Transverse Rows

--	--

Source: E. D. Grimison, *Trans. ASME*, **59**, 583 (1937).

Table 15.4-3. Ratio of  $h$  for  $N$  Transverse Rows Deep to  $h$  for 10 Transverse Rows Deep (for Use with

## Table 15.4-2)

Source: W. M. Kays and R. K. Lo, *Stanford Univ. Tech. Rept. 15*, Navy Contract N6-ONR-251 T.O.6, 1952.

### **EXAMPLE 15.4-3. Heating Air by a Bank of Tubes**

Air at 15.6°C and 1 atm abs flows across a bank of tubes containing four transverse rows in the direction of flow and 10 rows normal to the flow at a velocity of 7.62 m/s as the air approaches the bank of tubes. The tube surfaces are maintained at 57.2°C. The outside diameter of the tubes is 25.4 mm and the tubes are in-line to the flow. The spacing  $S_n$  of the tubes normal to the flow is 38.1 mm and  $S_p$  is also 38.1 mm parallel to the flow. For a 0.305-m length of the tube bank, calculate the heat-transfer rate.

**Solution:** Referring to Fig. 15.4-1a,

$$S_n D = 38.1 \text{ mm} \quad 25.4 \text{ mm} = 1.5 \quad S_p D = 38.1 \text{ mm} \quad 25.4 \text{ mm} = 1.5$$

Since the air is heated in passing through the four transverse rows, an outlet bulk temperature of 21.1°C will be assumed. The average bulk temperature is then

$$T_b = 15.6 + 21.12 = 18.3^\circ\text{C}$$

The average film temperature is

$$T_f = T_w + T_b / 2 = 57.2 + 18.32 = 37.7^\circ\text{C}$$

From Appendix A.3, for air at 37.7°C,

$$k = 0.02700 \text{ W/m} \cdot \text{K} \quad \text{Pr} = 0.705 \quad c_p = 1.0048 \text{ kJ/kg} \cdot \text{K} \quad \rho = 1.137 \text{ kg/m}^3 \quad \mu = 1.90 \times 10^{-5} \text{ Pa} \cdot \text{s}$$

The ratio of the minimum-flow area to the total frontal area is  $(S_n - D)/S_n$ . The maximum velocity in the tube banks is then

$$v_{\max} = u S_n / (S_n - D) = 7.62 \text{ m/s} / (0.0381 \text{ m} - 0.0254 \text{ m})$$

$$(0.0381\text{m}-0.0254\text{m})=22.86\text{msNRe}=\text{Dum}\times\mu=0.0254\text{m}(22.86\text{ms}) \\ (1.137\text{kgm}^3)1.90\times10^{-5}\text{kgm}\cdot\text{s}=3.47\times10^4$$

For  $S_n/D = S_p/D = 1.5/1$ , the values of  $C$  and  $m$  from Table 15.4-2 are 0.278 and 0.620, respectively. Substituting into Eq. (15.4-1) and solving for  $h$ ,

$$h=k\text{DCNRemNPr}^{1/3}=[0.027\text{Wm}^{-1}\text{K}^{-1}(0.0254\text{m})]^{1/3} \\ (3.47\times10^4)^{1/3}(0.62)(0.705)^{1/3}=171.8\text{Wm}^{-2}\text{K}^{-1}$$

This  $h$  is for 10 rows. For only four rows in the transverse direction, the  $h$  must be multiplied by 0.90, as given in Table 15.4-3.

Since there are  $10 \times 4$  or 40 tubes, the total heat-transfer area per 0.305 m length is

$$A=40\pi DL=40\pi(0.0254\text{m})(0.305\text{m})=0.973\text{m}^2$$

The total heat-transfer rate  $q$  using an arithmetic average temperature difference between the wall and the bulk fluid is

$$q=hA(T_w-T_b)=(0.9\times171.8\text{Wm}^{-2}\text{K}^{-1})(0.973\text{m}^2) \\ (57.2^\circ\text{C}-15.3^\circ\text{C})=5852\text{W}$$

Next, a heat balance on the air is made to calculate its temperature rise  $\Delta T$  using the calculated  $q$ . First, the mass flow rate of air  $m$  must be calculated. The total frontal area of the tube-bank assembly of 10 rows of tubes each 0.305 m long is

$$A_t=10S_n(1.0)=10(0.0381\text{m})(0.305\text{m})=0.1162\text{m}^2$$

The density of the entering air at  $15.6^\circ\text{C}$  is  $\rho = 1.224 \text{ kg/m}^3$ . The mass flow rate  $m$  is

$$m=\rho A_t v=(1.224\text{kgm}^{-3})(0.1162\text{m}^2)(7.62\text{ms}^{-1})=1.084\text{kgs}$$

For the heat balance, the mean  $c_p$  of air at  $18.3^\circ\text{C}$  is  $1.0048 \text{ kJ/kg} \cdot \text{K}$ , and then

$$q=5852\text{W}=m c_p \Delta T=1.084\text{kgs}(1.0048\text{kJkg}^{-1}\text{K}^{-1})\Delta T$$

Solving,  $\Delta T = 5.37^\circ\text{C}$ .

Hence, the calculated outlet bulk gas temperature is  $15.6 + 5.37 = 20.97^\circ\text{C}$ , which is close to the assumed value of  $21.1^\circ\text{C}$ . If a second trial were to be made, the new average



## 15.4F Heat Transfer for Flow in Packed Beds

Correlations for heat-transfer coefficients for packed beds are useful in designing fixed-bed systems such as catalytic reactors, dryers for solids, and pebble-bed heat exchangers. In Section 6.2, the pressure drop in packed beds was considered and discussions of the geometry factors in these beds were given. For determining the rate of heat transfer in packed beds for a differential length  $dz$  in m,

$$dq = h(aSdz)(T_1 - T_2) \quad (15.4-5)$$

where  $a$  is the solid-particle surface area per unit volume of bed in  $m^{-1}$ ,  $S$  is the empty cross-sectional area of bed in  $m^2$ ,  $T_1$  is the bulk gas temperature in K, and

$T_2$  is the solid surface temperature.

For the heat transfer of gases in beds of spheres ( $G_2$ ,  $G_3$ ) and a Reynolds number range of 10–10 000,

$$\epsilon JH = \epsilon h c_p v' \rho (c_p \mu k)^{2/3} = 2.876 N_{Re} + 0.3023 N_{Re}^{0.35} \quad (15.4-6)$$

where  $v'$  is the superficial velocity based on the cross section of the empty container in m/s [see Eq. (6.2-6)],  $\epsilon$  is the void fraction,  $N_{Re} = D_p G' / \mu_f$ , and  $G' = v' \rho$  is the superficial mass velocity in  $\text{kg/m}^2 \cdot \text{s}$ . The subscript  $f$  indicates properties evaluated at the film temperature, with others at the bulk temperature. This correlation can also be used for a fluidized bed. An alternate equation to use in place of Eq. (15.4-6) for fixed and fluidized beds is Eq.

(21.3-36) for a Reynolds-number range of 10–4000. The term  $JH$  is called the Colburn  $J$  factor and is defined as in Eq. (15.4-6) in terms of  $h$ .

Equations for heat transfer to noncircular cylinders such as hexagons and so forth are given elsewhere (H1, J1, P3).

## **15.5 Natural Convection Heat Transfer**

### **15.5A Introduction**

Natural convection heat transfer occurs when a solid surface is in contact with a gas or liquid that is at a different temperature from the surface. Density differences in the fluid arising from the heating process provide the buoyancy force required to move the fluid. Free or natural

convection is observed as a result of the motion of the fluid. An example of heat transfer by natural convection is a hot radiator used for heating a room. Cold air encountering the radiator is heated and rises in natural convection because of buoyancy forces. The theoretical derivation of equations for natural convection heat-transfer coefficients requires the solution of motion and energy equations.

An important heat-transfer system occurring in process engineering is that in which heat is being transferred from a hot vertical plate to a gas or liquid adjacent to it by natural convection. The fluid is not moving by forced convection but only by natural or free convection. In Fig. 15.5-1, the vertical flat plate is

heated and the free convection boundary layer is formed. The velocity profile differs from that in a forced convection system in that the velocity at the wall is zero and also is zero at the other edge of the boundary layer, since the free stream velocity is zero for natural convection. The boundary layer initially is laminar, as shown, but at some distance from the leading edge, it starts to become turbulent. The wall temperature is  $T_w$  K and the bulk temperature  $T_b$ .

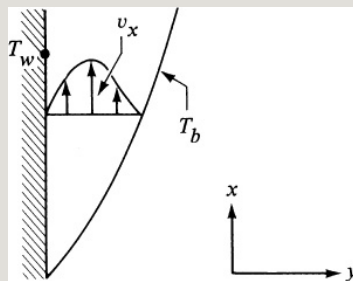


Figure 15.5-1. *Boundary-layer velocity profile for natural convection heat transfer from a heated vertical plate.*

## The differential momentum-balance

equation is written for the  $x$  and  $y$  directions for the control volume ( $dx \, dy \cdot 1$ ). The driving force is the buoyancy force in the gravitational field and is due to the density difference of the fluid. The momentum balance becomes

$$\rho(v_x \partial v_x / \partial x + v_y \partial v_x / \partial y) = g(\rho_b - \rho) + \mu \partial^2 v_x / \partial y^2 \quad (15.5-1)$$

where  $\rho_b$  is the density at the bulk temperature  $T_b$  and  $\rho$  the density at  $T$ . The density difference can be expressed in terms of the volumetric coefficient of expansion  $\beta$  and substituted back into Eq. (15.5-1):

$$\beta = (\rho_b - \rho) / \rho (T - T_b) \quad (15.5-2)$$

For gases,  $\beta = 1/T$ . The energy-balance equation can be expressed as follows:

$$\rho c_p (v_x \partial T / \partial x + v_y \partial T / \partial y) = k \partial^2 T / \partial y^2 \quad (15.5-3)$$

The solutions of these equations have been obtained by using integral methods of analysis discussed in Section 11.1B. Results have been obtained for a vertical plate, which is the simplest case and serves to introduce the dimensionless Grashof number discussed below. However, in other physical geometries the relations are too complex and empirical correlations have been obtained. These are discussed in the following sections.

### **15.5B Natural Convection from Various Geometries**

*1. Natural convection from vertical planes and cylinders.* For an isothermal vertical surface or plate with height  $L$  less than 1 m (P3), the

average natural convection heat-transfer coefficient can be expressed by the following general equation:

$$Nu = hL/k = a(L^3 \rho^2 g \beta \Delta T / \mu^2 c_p \mu / k)^m = a(N_{Gr} N_{Pr})^m \quad (15.5-4)$$

where  $a$  and  $m$  are constants from Table 15.5-1,  $N_{Gr}$  the Grashof number,  $\rho$  the density in  $\text{kg/m}^3$ ,  $\mu$  the viscosity in  $\text{kg/m} \cdot \text{s}$ ,  $\Delta T$  the positive temperature difference between the wall and bulk fluid or vice versa in K,  $k$  the thermal conductivity in  $\text{W/m} \cdot \text{K}$ ,  $c_p$  the heat capacity in  $\text{J/kg} \cdot \text{K}$ ,  $\beta$  the volumetric coefficient of expansion of the fluid in  $1/\text{K}$  [for gases  $\beta$  is  $1/(T_f \text{ K})$ ], and  $g$  is  $9.80665 \text{ m/s}^2$ . All the physical properties are evaluated at the film temperature  $T_f = (T_w + T_b)/2$ . In general, for a vertical cylinder with length  $L$  m, the same equations can be used as for a



vertical plate. In English units,  $\beta$  is  $1/(T_f$   
 $^{\circ}\text{F} + 460)$  in  $1/^{\circ}\text{R}$  and  $g$  is  $32.174 \times$   
 $(3600)^2 \text{ ft/h}^2$ .

Table 15.5-1. *Constants for Use with*  
*Eq. (15.5-4) for Natural Convection*

The Grashof number can be interpreted physically as a dimensionless number that represents the ratio of the buoyancy forces to the viscous forces in free convection and plays a role similar to that of the Reynolds number in forced convection.

**EXAMPLE 15.5-1. Natural Convection from the Vertical Wall of an Oven**

A heated vertical wall 1.0 ft (0.305 m) high of an oven for baking food with the surface at  $450^{\circ}\text{F}$  (505.4 K) is in contact with air at  $100^{\circ}\text{F}$  (311 K). Calculate the heat-transfer coefficient and the heat transfer/ft (0.305 m) width of wall. Note that heat transfer for radiation will not be considered. Use English and SI units.

**Solution:** The film temperature is

$$T_f = T_w + T_b/2 = 450 + 100/2 = 275^\circ\text{F} = 505.4 + 31/2 = 408.2 \text{ K}$$

The physical properties of air at  $275^\circ\text{F}$  are  $k = 0.0198 \text{ btu/h} \cdot \text{ft} \cdot ^\circ\text{F}$ ,  $0.0343 \text{ W/m} \cdot \text{K}$ ;  $\rho = 0.0541 \text{ lbm/ft}^3$ ,  $0.867 \text{ kg/m}^3$ ;  $N_{pr} = 0.690$ ;  $\mu = (0.0232 \text{ cp}) \times (2.4191) = 0.0562 \text{ lbm/ft} \cdot \text{h} = 2.32 \times 10^{-5} \text{ Pa} \cdot \text{s}$ ;  $\beta = 1/408.2 = 2.45 \times 10^{-3} \text{ K}^{-1}$ ;  $\beta = 1/(460 + 275) = 1.36 \times 10^{-3} \text{ }^\circ\text{R}^{-1}$ ;  $\Delta T = T_w - T_b = 450 - 100 = 350^\circ\text{F}$  (194.4 K). The Grashof number is, in SI units,

$$N_{Gr} = L^3 \rho^2 g \beta \Delta T / \mu^2 = (0.305 \text{ m})^3 (0.867 \text{ kg/m}^3)^2 (9.806 \text{ ms}^{-2}) / (2.45 \times 10^{-5} \text{ kg} \cdot \text{s}^{-1} \cdot \text{m}^{-1})^2 = 1.84 \times 10^8$$

The Grashof numbers calculated using English and SI units must, of course, be the same.

$$N_{Gr} N_{Pr} = (1.84 \times 10^8)(0.690) = 1.270 \times 10^8$$

Hence, from Table 15.5-1,  $a = 0.59$  and  $m = 14$  for use in Eq. (15.5-4). Solving for  $h$  in Eq. (15.5-4) and substituting known values,

$$h = k L a (N_{Gr} N_{Pr})^m = [0.0343 \text{ W/m} \cdot \text{K} (0.305 \text{ m})] (0.9) (1.270 \times 10^8)^{1/4} = 7.03 \text{ W/m}^2 \cdot \text{K} = 1.24 \text{ btu/h} \cdot \text{ft}^2 \cdot ^\circ\text{F}$$

For a 1-ft width of wall,  $A = 1 \times 1 = 1.0 \text{ ft}^2$  ( $0.305 \times 0.305 \text{ m}^2$ ). Then,

$$q = h A (T_w - T_b) = (1.24 \text{ btu/h} \cdot \text{ft}^2 \cdot ^\circ\text{F}) (1 \text{ ft}^2) (450^\circ\text{F} - 100^\circ\text{F}) = 433 \text{ btu/h}$$

$$q = h A (T_w - T_b) = (7.03 \text{ W/m}^2 \cdot \text{K}) (0.305 \text{ m} \times 0.305 \text{ m}) (194.4 \text{ K}) = 127.1 \text{ W}$$

A considerable amount of heat will also be lost by radiation. This will be considered in Chapter 17.

Simplified equations for the natural convection heat transfer from air to vertical planes and cylinders at 1 atm abs pressure are given in Table 15.5-2. In SI units, the equation for the range of

$N_{Gr}N_{Pr}$  of  $10^4$  to  $10^9$  is the one usually encountered, and this holds for  $(L^3\Delta T)$  values below about  $4.7 \text{ m}^3 \cdot \text{K}$  and film temperatures between 255 and 533 K. To correct the value of  $h$  to pressures other than 1 atm, the values of  $h$  in Table 15.5-2 can be multiplied by  $(p/101.32)^{1/2}$  for  $N_{Gr}N_{Pr}$  of  $10^4$  to  $10^9$ , and by  $(p/101.32)^{2/3}$  for  $N_{Gr}N_{Pr} > 10^9$ , where  $p$  = pressure in  $\text{kN/m}^2$ . In English units, the range of  $N_{Gr}N_{Pr}$  of  $10^4$  to  $10^9$  is encountered when  $(L^3\Delta T)$  is less than about  $300 \text{ ft}^3 \cdot ^\circ\text{F}$ . The value of  $h$  can be corrected to pressures other than 1.0 atm abs by multiplying the  $h$  at 1 atm by  $p^{1/2}$  for  $N_{Gr}N_{Pr}$  of  $10^4$  to  $10^9$ , and by  $p^{2/3}$  for  $N_{Gr}N_{Pr}$  above  $10^9$ , where  $p$  = atm abs pressure. Simplified equations are also given for water and organic liquids.

Table 15.5-2. *Simplified Equations for*

# Natural Convection from Various Surfaces

## **EXAMPLE 15.5-2. Natural Convection and the Simplified Equation**

Repeat Example 15.5-1 but use the simplified equation.

**Solution:** The film temperature of 408.2 K is in the range 255–533 K. Also,

$$L^3\Delta T = (0.305\text{m})^3(194.4\text{K}) = 5.5\text{m}^3\cdot\text{K}$$

This is slightly greater than the value of 4.7 given as the approximate maximum for use of the simplified equation. However, in Example 15.5-1 the value of  $Ng_r/N_{Pr}$  is below  $10^9$ , so the simplified equation from Table 15.5-2 will be used:

$$h = 1.37(\Delta T/L)^{1/4} = 1.37(194.4/0.305)^{1/4} = 6.88 \text{ W/m}^2\cdot\text{K} \quad (1.21 \text{ btu/h}\cdot\text{ft}^2\cdot^\circ\text{F})$$

The heat-transfer rate  $q$  is

$$q = hA(T_w - T_b) = (6.88 \text{ W/m}^2\cdot\text{K})(0.305\text{m} \times 0.305\text{m})(194.4\text{K}) = 124.4 \text{ W} \quad (424 \text{ btu/h})$$

This value is reasonably close to the value of 127.1 W for Example 15.5-1.

*2. Natural convection from horizontal cylinders.* For a horizontal cylinder with an outside diameter of  $D$  m, Eq. (15.5-4) is used with the constants given in Table

15.5-1. The diameter  $D$  is used for  $L$  in the equation. Simplified equations are given in Table 15.5-2. The usual case for pipes is for the  $NGrNPr$  range  $10^4$  to  $10^9$  (M1).

*3. Natural convection from horizontal plates.* For horizontal flat plates, Eq. (15.5-4) is also used with the constants given in Table 15.5-1 and the simplified equations in Table 15.5-2. The dimension  $L$  to be used is the length of a side of a square plate, the linear mean of the two dimensions for a rectangle, and 0.9 times the diameter of a circular disk.

*4. Natural convection in enclosed spaces.* Free convection in enclosed spaces occurs in a number of processing applications. One example is in an enclosed double-glazed window in

which two layers of glass are separated by a layer of air for energy conservation. The flow phenomena inside these enclosed spaces are complex, since a number of different types of flow patterns can occur. At low Grashof numbers, the heat transfer is mainly by conduction across the fluid layer. As the Grashof number is increased, different flow regimes are encountered.

The system for two vertical plates of height  $L$  m containing the fluid with a gap of  $\delta$  m is shown in Fig. 15.5-2, where the plate surfaces are at temperatures  $T_1$  and  $T_2$ . The Grashof number is defined as

$$N_{Gr,d} = \frac{\delta^3 \rho^2 g \beta (T_1 - T_2)}{\mu^2} \quad (15.5-5)$$

The Nusselt number is defined as

$$NNu_{\delta} = h\delta k \quad (15.5-6)$$

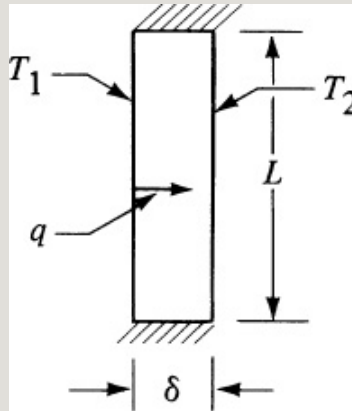


Figure 15.5-2. *Natural convection in enclosed vertical space.*

The heat flux is calculated from

$$qA = h(T_1 - T_2) \quad (15.5-7)$$

The physical properties are all evaluated at the mean temperature between the two plates.

For gases enclosed between vertical plates and  $(H_1, J_1, K_1, P_1)$ ,

$$NNu_{\delta} = h\delta k = 1.0(NGr_{\delta} NPr < 2 \times 10^3)$$

(15.5-8)

$$NNu_{\delta}=0.20(NGr_{\delta}NPr)^{1/4}(L/\delta)^{1/9}(6\times 10^3 < NGr_{\delta}NPr < 2\times 10^5)$$

(15.5-9)

$$NNu_{\delta}=0.073(NGr_{\delta}NPr)^{1/3}(L/\delta)^{1/9}(2\times 10^5 < NGr_{\delta}NPr < 2\times 10^7)$$

(15.5-10)

For liquids in vertical plates,

$$NNu_{\delta}=h\delta k=1.0(NGr_{\delta}NPr < 1\times 10^3)$$

(15.5-11)

$$NNu_{\delta}=0.28(NGr_{\delta}NPr)^{1/4}(L/\delta)^{1/4}(1\times 10^3 < NGr_{\delta}NPr < 1\times 10^7)$$

(15.5-12)

For gases or liquids in a vertical annulus, the same equations hold as for vertical plates.



For gases in horizontal plates with the lower plate hotter than the upper,

$$Nu_{\delta} = 0.21 (Gr_{\delta} Pr)^{1/4} (7 \times 10^3 < Gr_{\delta} Pr < 3 \times 10^5) \quad (15.5-13)$$

$$Nu_{\delta} = 0.061 (Gr_{\delta} Pr)^{1/3} (Gr_{\delta} Pr > 3 \times 10^5) \quad (15.5-14)$$

For liquids in horizontal plates with the lower plate hotter than the upper (G5),

$$Nu_d = 0.069 (Gr_d Pr)^{1/3} (1.5 \times 10^5 < Gr_d Pr < 1 \times 10^9) \quad (15.5-15)$$

**EXAMPLE 15.5-3. Natural Convection in an Enclosed Vertical Space**

Air at 1 atm abs pressure is enclosed between two vertical plates where  $L = 0.6$  m and  $\delta = 30$  mm. The plates are 0.4 m wide. The plate temperatures are  $T_1 = 394.3$  K and  $T_2 = 366.5$  K. Calculate the heat-transfer rate across the air gap.

**Solution:** The mean temperature between the plates is used to evaluate the physical properties:  $T_f = (T_1 + T_2)/2 = (394.3 + 366.5)/2 = 380.4$  K. Also,  $\delta = 30/1000 = 0.030$  m. From Appendix A.3,  $\rho = 0.9295$  kg/m<sup>3</sup>,  $\mu = 2.21 \times 10^{-5}$  Pa · s,  $k = 0.03219$  W/m · K,  $Pr = 0.693$ ,  $\beta = 1/T_f = 1/380.4 =$

$$2.639 \times 10^{-3} \text{K}^{-1}.$$

$$\begin{aligned} N_{Gr,d} &= (0.030 \text{m})^3 (0.9295 \text{kgm}^{-3})^2 (9.806 \text{ms}^{-2}) \\ &\quad (2.629 \times 10^{-3} \text{K}^{-1}) (394.3 \text{K} - 366.5 \text{K}) \\ &\quad (2.21 \times 10^{-5} \text{kgm}^{-1} \text{s})^2 = 3.423 \times 10^4 \end{aligned}$$

Also,  $N_{Gr,\delta} N_{Pr} = (3.423 \times 10^4) 0.693 = 2.372 \times 10^4$ . Using Eq. (15.5-9),

$$\begin{aligned} h &= k \delta (0.20) (N_{Gr,d} N_{Pr})^{1/4} (L/\delta)^{1/9} = 0.03219 (0.20) \\ &\quad (2.352 \times 10^4)^{1/4} / 40.030 (0.6/0.030)^{1/9} = 1.909 \text{W/m}^2 \text{K} \end{aligned}$$

The area  $A = (0.6 \times 0.4) = 0.24 \text{ m}^2$ . Substituting into Eq. (15.5-7),

$$\begin{aligned} q &= hA(T_1 - T_2) = (1.909 \text{Wm}^{-2} \text{K}) (0.24 \text{m}^2) \\ &\quad (394.3 \text{K} - 366.5 \text{K}) = 12.74 \text{W} \end{aligned}$$

*5. Natural convection from other shapes.* For spheres, blocks, and other types of enclosed air spaces, references elsewhere (H1, K1, M1, P1, P3) should be consulted. In some cases, when a fluid is forced over a heated surface at low velocity in the laminar region, combined forced convection plus natural convection heat transfer occurs. For further discussion of this, see (H1, K1, M1).

## 15.6 Boiling and Condensation

## 15.6A Boiling

*1. Mechanisms of boiling.* Heat transfer to a boiling liquid is very important in evaporation and distillation as well as in other kinds of chemical and biological processing, such as petroleum processing, control of the temperature of chemical reactions, evaporation of liquid foods, and so on. The boiling liquid is usually contained in a vessel with a heating surface of tubes or vertical or horizontal plates that supply the heat for boiling. The heating surfaces can be warmed electrically or by a hot or condensing fluid on the other side of the heated surface.

In boiling, the temperature of the liquid is the boiling point of this liquid at the

pressure in the equipment. The heated surface is, of course, at a temperature above the boiling point. Bubbles of vapor are generated at the heated surface and rise through the mass of liquid. The vapor accumulates in a vapor space above the liquid level and is withdrawn.

Boiling is a complex phenomenon. Suppose we consider a small heated horizontal tube or wire immersed in a vessel containing water boiling at 373.2 K (100°C). The heat flux is  $q/A$  W/m<sup>2</sup>;  $\Delta T = T_w - 373.2$  K, where  $T_w$  is the tube or wire wall temperature and  $h$  is the heat-transfer coefficient in W/m<sup>2</sup> · K. Starting with a low  $\Delta T$ , the  $q/A$  and  $h$  values are measured. This is repeated at higher values of  $\Delta T$  and the data obtained are plotted as  $q/A$  versus  $\Delta T$ , as shown in Fig. 15.6-1.

In the first region *A* of the plot in Fig. 15.6-1, at low temperature drops, the mechanism of boiling is essentially that of heat transfer to a liquid in natural convection. The variation of  $h$  with  $\Delta T_{0.25}$  is approximately the same as that for natural convection to horizontal plates or cylinders. The very few bubbles formed are released from the surface of the metal and rise without appreciably disturbing the normal natural convection.

In the region *B* of nucleate boiling for a  $\Delta T$  of about 5–25 K (9–45°F), the rate of bubble production increases so that the velocity of the liquid's circulation increases. The heat-transfer coefficient  $h$  increases rapidly and is proportional to  $\Delta T_2$  to  $\Delta T_3$  in this region.

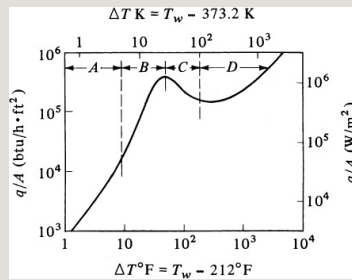


Figure 15.6-1. *Boiling mechanisms for water at atmospheric pressure, heat flux vs. temperature drop: (A) natural convection, (B) nucleate boiling, (C) transition boiling, (D) film boiling.*

In the region *C* of transition boiling, many bubbles are formed so quickly that they tend to coalesce and form a layer of insulating vapor. Increasing the  $\Delta T$  increases the thickness of this layer, and the heat flux and  $h$  drop as  $\Delta T$  is increased. In the region *D* of film boiling, bubbles detach themselves regularly and rise upward. At higher  $\Delta T$  values, radiation through the vapor layer next to the surface helps increase the  $q/A$  and  $h$ . Similar-shaped curves are obtained for other shapes of surfaces (M1).

The curve of  $h$  versus  $\Delta T$  has approximately the same shape as in Fig. 15.6-1. The values of  $h$  are quite large. At the beginning of region  $B$  in Fig. 15.6-1 for nucleate boiling,  $h$  has a value of about 5700–11 400 W/m<sup>2</sup> · K, or 1000–2000 btu/h · ft<sup>2</sup> · °F, and at the end of this region,  $h$  has a peak value of almost 57000 W/m<sup>2</sup> · K, or 10 000 btu/hr · ft<sup>2</sup> · °F. These values are quite high, and in most cases the percent resistance of the boiling film is only a few percent of the overall resistance to heat transfer.

The regions of commercial interest are the nucleate and film-boiling regions (P3). Nucleate boiling occurs in kettle-type and natural-circulation reboilers.

*2. Nucleate boiling.* In the nucleate-boiling region, the heat flux is affected

by  $\Delta T$ , pressure, the nature and geometry of the surface and system, and the physical properties of the vapor and liquid. Equations have been derived by Rohsenow et al. (P1) that apply to single tubes or flat surfaces and are quite complex.

Simplified empirical equations for estimating the boiling heat-transfer coefficients for water boiling on the outside of submerged surfaces at 1.0 atm abs pressure have been developed (J2).

For a horizontal surface (SI and English units),

$$h, \text{bm/h} \cdot \text{it}^2 \cdot ^\circ\text{F} = 151(\Delta T_{\text{of}})^{1/3} q/A, \\ \text{btu/h} \cdot \text{ft}^2, < 5000 h, \text{W/} \\ \text{m}^2 \cdot \text{K} = 1043(\Delta T_{\text{K}})^{1/3} q/A, \text{kW/}$$



$$m^2, < 16 (15.6-1)$$

$$h, \text{ btu/}$$

$$h \cdot \text{ft}^2 \cdot ^\circ\text{F} = 0.168(\Delta T \cdot ^\circ\text{F})^{3/5} q/A,$$

$$\text{btu/h} \cdot \text{ft}^2, < 75\,000 h, \text{ W/}$$

$$m^2 \cdot \text{K} = 5.56(\Delta T \text{ K})^{3/5} q/A, \text{ kW/}$$

$$m^2, < 240 (15.6-2)$$

For a vertical surface,

$$h, \text{ btu/h} \cdot \text{ft}^2 \cdot ^\circ\text{F} = 87(\Delta T \cdot ^\circ\text{F})^{1/7} q/A,$$

$$\text{btu/h} \cdot \text{ft}^2, < 10\,000 h, \text{ W/}$$

$$m^2 \cdot \text{K} = 537(\Delta T \text{ K})^{1/7} q/A, \text{ kW/}$$

$$m^2, < 3 (15.6-3)$$

$$h, \text{ btu/}$$

$$h \cdot \text{ft}^2 \cdot ^\circ\text{F} = 0.240(\Delta T \cdot ^\circ\text{F})^{3/4} q/A,$$

$$\text{btu/h} \cdot \text{ft}^2, < 20\,000 h, \text{ W/}$$

$$m^2 \cdot \text{K} = 7.95(\Delta T \text{ K})^{3/4} q/A, \text{ kW/}$$

$$m^2, < 63 (15.6-4)$$

where  $\Delta T = T_w - T_{\text{sat}}$  K or  $^\circ\text{F}$ .

If the pressure is  $p$  atm abs, the values of  $h$  at 1 atm given above are multiplied by  $(p/1)^{0.4}$ . Equations (15.6-1) and (15.6-3) are in the natural convection region.

For forced convection boiling inside tubes, the following simplified relation can be used (J3):

$$h = 2.55(\Delta T \text{ K})^{3/4} \text{ W/m}^2\cdot\text{K (SI)}$$

$$h = 0.077(\Delta T \text{ }^\circ\text{F})^{3/4} \text{ Btu/hr}\cdot\text{ft}^2\cdot\text{ }^\circ\text{F (English)}$$

(15.6-5)

where  $p$  in this case is in kPa (SI units) and psia (English units).

*3. Film boiling.* In the film-boiling region, the heat-transfer rate is low in view of the large temperature drop used, which is not utilized effectively. Film boiling has been subjected to considerable theoretical analysis.

Bromley (B3) gives the following equation to predict the heat-transfer coefficient in the film-boiling region on a horizontal tube:

$$h = 0.62[k_v^3 \rho_v (\rho_l - \rho_v) g (h_{fg} + 0.4 c_{pv} \Delta T) D \mu_v \Delta T]^{1/4} \quad (15.6-6)$$

where  $k_v$  is the thermal conductivity of the vapor in  $\text{W/m} \cdot \text{K}$ ,  $\rho_v$  is the density of the vapor in  $\text{kg/m}^3$ ,  $\rho_l$  is the density of the liquid in  $\text{kg/m}^3$ ,  $h_{fg}$  is the latent heat of vaporization in  $\text{J/kg}$ ,  $\Delta T = T_w - T_{\text{sat}}$ ,  $T_{\text{sat}}$ , the temperature of saturated vapor is in  $\text{K}$ ,  $D$  is the outside tube diameter in  $\text{m}$ ,  $\mu_v$  is the viscosity of the vapor in  $\text{Pa} \cdot \text{s}$ , and  $g$  is the acceleration of gravity in  $\text{m/s}^2$ . The physical properties of the vapor are evaluated at the film temperature of  $T_f = (T_w + T_{\text{sat}})/2$ , and  $h_{fg}$  at the saturation temperature. If the

temperature difference is quite high, some additional heat transfer occurs by radiation (H1).

**EXAMPLE 15.6-1. Rate of Heat Transfer in a Jacketed Kettle**

Water is being boiled at 1 atm abs pressure in a jacketed kettle with steam condensing in the jacket at 115.6°C. The inside diameter of the kettle is 0.656 m and the height is 0.984 m. The bottom is slightly curved but it will be assumed to be flat. Both the bottom and the sides up to a height of 0.656 m are jacketed. The kettle surface for heat transfer is 3.2-mm stainless steel with a  $k$  of 16.27 W/m · K. The condensing-steam coefficient  $h_i$  inside the jacket has been estimated as 10 200 W/m<sup>2</sup> · K. Predict the boiling heat-transfer coefficient  $h_o$  for the bottom surface of the kettle.

**Solution:** A diagram of the kettle is shown in Fig. 15.6-2. The simplified equations will be used for the boiling coefficient  $h_o$ . The solution is trial and error, since the inside metal surface temperature  $T_w$  is unknown. Assuming that  $T_w = 110^\circ\text{C}$ ,

$$\Delta T = T_w - T_{\text{sat}} = 110 - 100 = 10^\circ\text{C} = 10\text{K}$$

Substituting into Eq. (15.6-2),

$$h_o = 5.56(\Delta T) = 5.56(10)^3 = 5560 \text{ W/m}^2 \cdot \text{K} \quad qA = h\Delta T = 5560 \text{ W/m}^2 \cdot \text{K}(10\text{K}) = 55600 \text{ W/m}^2$$

To check the assumed  $T_w$ , the resistance  $R_i$  of the condensing steam,  $R_w$  of the metal wall, and  $R_o$  of the boiling liquid must be calculated. Assuming equal areas of the resistances for  $A = 1 \text{ m}^2$ , then by Eq. (13.2-2),

$$\begin{aligned} R_j &= 1/h_i A_i = 1/(10200 \text{ W/m}^2 \cdot \text{K}) \\ (1 \text{ m}^2) &= 9.80 \times 10^{-5} \text{ K/W} \\ R_w &= \Delta x/kA = (0.0030 \text{ m})/16.27 \text{ W/mK}(1 \text{ m}^2) = 19.66 \times 10^{-5} \text{ K/W} \\ R_o &= 1/h_o A_o = 1/(5560 \text{ W/m}^2 \cdot \text{K}) \\ (1 \text{ m}^2) &= 17.98 \times 10^{-5} \text{ K/W} \\ \Sigma R &= 9.80 \times 10^{-5} \text{ K/W} + 19.66 \times 10^{-5} \text{ K/W} \\ &\quad + 17.98 \times 10^{-5} \text{ K/W} = 47.44 \times 10^{-5} \text{ K/W} \end{aligned}$$

The temperature drop across the boiling film is then

$$\Delta T = R_o \Sigma R (115.6^\circ\text{C} - 100^\circ\text{C}) = 17.98 \times 10^{-5} \text{KW} / 4744 \times 10^{-5} \text{KW} (15.6^\circ\text{C}) = 5.9^\circ\text{C}$$

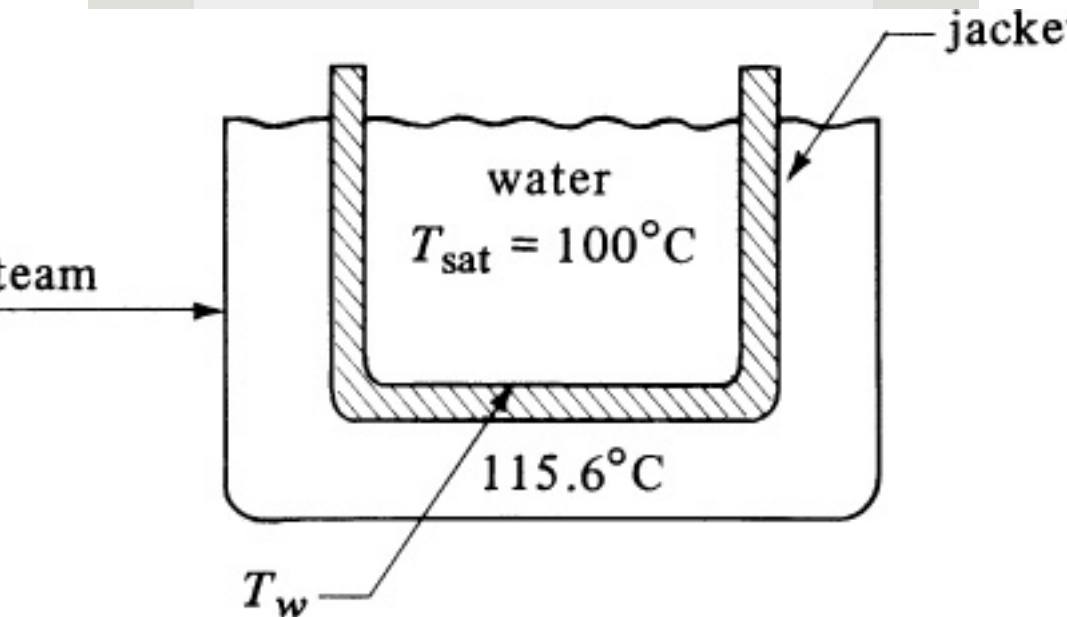


Figure 15.6-2. *Steam-jacketed kettle and boiling water for Example 15.6-1.*

Hence,  $T_w = 100 + 5.9 = 105.9^\circ\text{C}$ . This is lower than the assumed value of  $110^\circ\text{C}$ .

For the second trial,  $T_w = 108.3^\circ\text{C}$  will be used. Then,  $\Delta T = 108.3 - 100 = 8.3^\circ\text{C}$  and, from Eq. (15.6-2), the new  $h_o = 3180$ . Calculating the new  $R_o$   $31.44 \times 10^{-5}$ ,

$$\Delta T = 31.44 \times 10^{-5} \text{KW} / 60.90 \times 10^{-5} \text{KW} (15.6^\circ\text{C}) = 8.1^\circ\text{C}$$

and

$$T_w = 100 + 8.1 = 108.1^\circ\text{C}$$

This value is reasonably close to the assumed value of  $108.3^\circ\text{C}$ , so no further trials will be made.

## 15.6B Condensation

### *1. Mechanisms of condensation.*

Condensation of a vapor to a liquid and vaporization of a liquid to a vapor both involve a change of phase of a fluid with large heat-transfer coefficients. Condensation occurs when a saturated vapor such as steam comes in contact with a solid whose surface temperature is below the saturation temperature, to form a liquid such as water.

Normally, when a vapor condenses on a vertical or horizontal tube or other surface, a film of condensate is formed on the surface and flows over the surface by the action of gravity. It is this film of liquid between the surface and the vapor that forms the main resistance to heat transfer. This is called *film-type condensation*.

Another type of condensation, *dropwise condensation*, can occur where small drops are formed on the surface. These drops grow and coalesce, and the liquid flows from the surface. During this condensation, large areas of the tube are devoid of any liquid and are exposed directly to the vapor. Very high rates of heat transfer occur on these bare areas. The average coefficient can be as high as  $110\,000\text{ W/m}^2 \cdot \text{K}$  ( $20\,000\text{ btu/h} \cdot \text{ft}^2 \cdot ^\circ\text{F}$ ), which is five to 10 times larger than film-type coefficients. Film-condensation coefficients are normally much greater than those in forced convection and are on the order of magnitude of several thousand  $\text{W/m}^2 \cdot \text{K}$  or more.

Dropwise condensation occurs on contaminated surfaces and when

impurities are present. Film-type condensation is more dependable and more common. Hence, for normal design purposes, film-type condensation is assumed.

*2. Film-condensation coefficients for vertical surfaces.* Film-type condensation on a vertical wall or tube can be analyzed analytically by assuming laminar flow of the condensate film down the wall. The film thickness is zero at the top of the wall or tube and increases in thickness as it flows downward because of condensation. Nusselt (H1, W1) assumed that the heat transfer from the condensing vapor at  $T_{\text{sat}}$  K, through this liquid film and to the wall at  $T_w$  K was by conduction. Equating this heat transfer by conduction to that from



condensation of the vapor, a final expression can be obtained for the average heat-transfer coefficient over the whole surface.

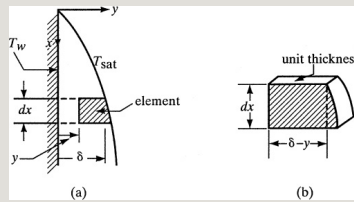


Figure 15.6-3. Film condensation on a vertical plate: (a) increase in film thickness with position, (b) balance on element of condensate.

In Fig. 15.6-3a, vapor at  $T_{sat}$  is condensing on a wall whose temperature is  $T_w$  K. The condensate is flowing downward in laminar flow. Assuming unit thickness, the mass of the element with liquid density  $\rho_l$  in Fig. 15.6-3b is  $(\delta - y)(dx \cdot 1)\rho_l$ . The downward force on this element is the gravitational force minus the buoyancy force, or  $(\delta - y)(dx) \times (\rho_l - \rho_v)g$  where  $\rho_u$  is the density of

the saturated vapor. This force is balanced by the viscous-shear force at the plane  $y$  of  $\mu l (dv/dy) (dx \cdot 1)$ .

Equating these forces,

$$(\delta - y)(\rho_l - \rho_v)g = \mu l (dv/dy)(dx) \quad (15.6-7)$$

Integrating and using the boundary condition that  $v = 0$  at  $y = 0$ ,

$$v = g(\rho_l - \rho_v) \mu l (\delta y - y^2/2) \quad (15.6-8)$$

The mass flow rate of film condensate at any point  $x$  for unit depth is

$$m = \int_0^\delta \rho_l v \, dy = \int_0^\delta \rho_l g (\rho_l - \rho_v) \mu l (\delta y - y^2/2) dy \quad (15.6-9)$$

Integrating,

$$m = \rho_l g (\rho_l - \rho_v) \delta^3 / 3 \mu l \quad (15.6-10)$$

At the wall, for area  $(dx \cdot 1)$  m<sup>2</sup>, the rate of heat transfer is as follows if a linear temperature distribution is assumed in the liquid between the wall and the vapor:

$$q_x = -k_l(dx \cdot 1) \frac{dT}{dy} \Big|_{y=0} = k_l dx (T_{\text{sat}} - T_w) \quad (15.6-11)$$

In a  $dx$  distance, the rate of heat transfer is  $q_x$ . Also, in this  $dx$  distance, the increase in mass from condensation is  $dm$ . Using Eq. (15.6-10),

$$dm = \frac{q_x}{h_{fg}} = \frac{k_l dx (T_{\text{sat}} - T_w)}{h_{fg}} \quad (15.6-12)$$

Making a heat balance for  $dx$  distance, the mass flow rate  $dm$  times the latent heat  $h_{fg}$  must equal the  $q_x$  from Eq. (15.6-11):

$$h_f g \rho l g (\rho_l - \rho_v) \delta^2 \frac{d\delta}{dx} = k_l (T_{\text{sat}} - T_w) \delta \quad (15.6-13)$$

Integrating, with  $\delta = 0$  at  $x = 0$  and  $\delta = \delta$  at  $x = x$ ,

$$\delta = \left[ \frac{4 \mu_l k_l x (T_{\text{sat}} - T_w) g h_f g \rho l (\rho_l - \rho_v)}{1} \right]^{1/4} \quad (15.6-14)$$

Using the local heat-transfer coefficient  $h_x$  at  $x$ , a heat balance gives

$$h_x (dx \cdot 1) (T_{\text{sat}} - T_w) = k_l (dx \cdot 1) (T_{\text{sat}} - T_w) \delta \quad (15.6-15)$$

This gives

$$h_x = k_l \delta \quad (15.6-16)$$

Combining Eqs. (15.6-14) and (15.6-16),

$$h_x = \left[ \rho_l (\rho_l - \rho_v) g h_{fg} k_l \frac{3}{4} \mu_l x (T_{\text{sat}} - T_w) \right]^{1/4} \quad (15.6-17)$$

By integrating over the total length  $L$ , the average value of  $h$  is obtained as follows:

$$h = \frac{1}{L} \int_0^L h_x dx = \frac{4}{3} h_x = L \quad (15.6-18)$$

$$h = 0.943 \left[ \rho_l (\rho_l - \rho_v) g h_{fg} k_l^3 \mu_l (T_{\text{sat}} - T_w) \right]^{1/4} \quad (15.6-19)$$

However, for laminar flow, experimental data are about 20% above Eq. (15.6-19).

Hence, the final recommended expression for vertical surfaces in laminar flow is (M1)

$$Nu = hD_k = 0.25 \left[ \rho_l (\rho_l - \rho_v) g h_{fg} D_k^3 \mu_l k_l \Delta T \right]^{1/4} \quad (15.6-20)$$

where  $\rho_l$  is the density of liquid in kg/m<sup>3</sup> and  $\rho_v$  that of the vapor,  $g$  is 9.8066 m/s<sup>2</sup>,  $L$  is the vertical height of the surface or tube in m,  $\mu_l$  is the viscosity of liquid in Pa · s,  $k_l$  is the liquid thermal conductivity in W/m · K,  $\Delta T = T_{\text{sat}} - T_w$  in K, and  $h_{fg}$  is the latent heat of condensation in J/kg at  $T_{\text{sat}}$ . All physical properties of the liquid except  $h_{fg}$  are evaluated at the film temperature  $T_f = (T_{\text{sat}} + T_w)/2$ . For long vertical surfaces, the flow at the bottom can be turbulent. The Reynolds number is defined as

$$\text{NRe} = 4m\pi D\mu_l = 4\Gamma\mu_l (\text{vertical tube, diameter } D) \quad (15.6-21)$$

$$\text{NRe} = 4mW\mu_l = 4\Gamma\mu_l (\text{vertical tube, width } W) \quad (15.6-22)$$

where  $m$  is total kg mass/s of condensate

at tube or plate bottom and  $\Gamma = m/\pi D$  or  $m/W$ . The  $N_{Re}$  should be below about 1800 for Eq. (15.6-20) to hold. The reader should note that some references define  $N_{Re}$  as  $\Gamma/\mu$ . Then this  $N_{Re}$  should be below 450.

For turbulent flow for  $N_{Re} > 1800$  (M1),

$$N_{Nu} = hL/k = 0.0077 (g \rho^{1/2} L^3 m^{1/2})^{1/3} (N_{Re})^{0.4} \quad (15.6-23)$$

Solution of this equation is by trial and error, since a value of  $N_{Re}$  must first be assumed in order to calculate  $h$ .

**EXAMPLE 15.6-2. Condensation on a Vertical Tube**

Steam saturated at 68.9 kPa (10 psia) is condensing on a vertical tube 0.305 m (1.0 ft) long having an OD of 0.0254 m (1.0 in.) and a surface temperature of 86.11°C (187°F). Calculate the average heat-transfer coefficient using English and SI units.

**Solution:** From Appendix A.2,

$$T_{sat} = T_{sat} = 193^\circ\text{F} (89.44^\circ\text{C})$$

$$T_w = 187^\circ\text{F} (86.11^\circ\text{C}) \quad T_f = T_w$$

$$+ T_{sat} = 187 + 193 = 190^\circ\text{F} (87.80^\circ\text{C})$$

$$\text{latent heat } h_{fg} = 1143.3 - 161.0 = 982.3 \text{ btu/lbm}$$

$$\begin{aligned}
 &= 2657.8 - 374.6 = 2283.2 \text{ kJ/kg} = 2.283 \times 10^6 \text{ J/kg} \\
 &\text{kgpl} = 10.01657 = 60.31 \text{ bm/ft}^3 = 60.3 (16.018) = 966.7 \text{ kg/m}^3 \\
 &\text{pu} = 140.95 = 0.02441 \text{ bm/it}^3 = 0.391 \text{ kg/m}^3 \\
 &\text{ul} = (0.324 \text{ cp}) (2.4191) = 0.7841 \text{ bm/it} \cdot \text{h} = 3.24 \times 10^{-4} \text{ Pa} \cdot \text{s} \\
 &\text{kl} = 0.390 \text{ btu/ft} \cdot \text{h} \cdot ^\circ\text{F} = (0.390) (1.7307) = 0.675 \text{ W/m} \cdot \text{K} \\
 &\text{L} = 1 \text{ ft} = 0.305 \text{ m} \quad \Delta T = T_{\text{M}} - T_{\text{w}} = 193 - 187 = 6^\circ\text{F} (3.33 \text{ K})
 \end{aligned}$$

Assuming a laminar film using Eq. (15.6-20) in English as well as SI units and neglecting  $\rho v$  as compared to  $\rho l$ .

$$\begin{aligned}
 \text{NNu} &= 1.13 (\text{pl}^2 \text{ghfgL}^3 \mu \text{kl} \Delta T)^{1/4} = 1.13 [(966.7 \text{ kg/m}^3)^2 (9.806 \text{ ms}^2) \\
 &\quad (2.283 \times 10^6 \text{ J/kg}) (0.305 \text{ m})^3 (3.24 \times 10^{-4} \text{ kg} \cdot \text{s/m}^2) (0.675 \text{ W/m} \cdot \text{K}) \\
 &\quad (3.33 \text{ K})] = 6040
 \end{aligned}$$

$$\text{NNu} = h \text{L} = h (0.305 \text{ m}) = 0.675 \text{ W/m} \cdot \text{K} = 6040$$

$$\text{Solving, } h = 13\,350 \text{ W/m}^2 \cdot \text{K} = 2350 \text{ btu/h} \cdot \text{ft}^2 \cdot ^\circ\text{F}.$$

Next, the  $\text{NRe}$  will be calculated to see if laminar flow occurs as assumed. To calculate the total heat transferred for a tube of area

$$\begin{aligned}
 A &= \pi D L = \pi (1/12) (1.0) = \pi/12 \text{ it}^2, A = \pi (0.0254)^2 \\
 (0.305 \text{ m})^2 q &= h A \Delta T \quad (15.6-24)
 \end{aligned}$$

However, this  $q$  must also equal that obtained by condensation of  $m \text{ lbm/h}$  or  $\text{kg/s}$ . Hence,

$$q = h A \Delta T = h \text{fgm} \quad (15.6-25)$$

Substituting the values given and solving for  $m$ ,

$$\begin{aligned}
 13550 \text{ W/m}^2 \cdot \text{K} (\pi) (0.0254 \text{ m}) (0.305 \text{ m}) \\
 (3.33 \text{ K}) &= (2.283 \times 10^6 \text{ m}^2 \text{s}^2) (m) \quad m = 4.74 \times 10^{-4} \text{ kgs} = 3.77 \text{ lbm/h}
 \end{aligned}$$

Substituting into Eq. (15.6-21),

$$\begin{aligned}
 \text{NRe} &= 4 m \pi D \mu = 4 (4.74 \times 10^{-4} \text{ kgs}) \pi (0.0254 \text{ m}) \\
 (324 \times 10^{-4} \text{ kgm} \cdot \text{s}) &= 73.5
 \end{aligned}$$

Hence, the flow is laminar as assumed.

### 3. Film-condensation coefficients outside horizontal cylinders. The



analysis of Nusselt can also be extended to the practical case of condensation outside a horizontal tube. For a single tube, the film starts out with zero thickness at the top of the tube and increases in thickness as it flows around to the bottom and then drips off. If there is a bank of horizontal tubes, the condensate from the top tube drips onto the one below; and so on.

For a vertical tier of  $N$  horizontal tubes placed one below the other with outside tube diameter  $D$  (M1),

$$Nu = hD/k_l = 0.725(\rho_l(\rho_l - \rho_v)ghfgD^3N\mu_l k_l \Delta T)^{1/4} \quad (15.6-26)$$

In most practical applications, the flow is in the laminar region and Eq. (15.6-26) holds (C3, M1).

## 15.7 Heat Transfer of Non-Newtonian Fluids

### 15.7A Introduction

Most of the studies on heat transfer with fluids have been done with Newtonian fluids. However, a wide variety of non-Newtonian fluids are encountered in the industrial chemical, biological, and food-processing industries. To design equipment to handle these fluids, the flow-property constants (rheological constants) must be available or must be measured experimentally.

Chapter 9 gave a detailed discussion of rheological constants for non-Newtonian fluids. Since many non-Newtonian fluids have high effective viscosities, they are often in laminar flow. Because the majority of non-Newtonian fluids are pseudoplastic

fluids, which can usually be represented by the power law, Eq. (9.1-2), the discussion will be concerned with such fluids. For other fluids, the reader is referred to Skelland (S3).

### 15.7B Heat Transfer Inside Tubes

*1. Laminar flow in tubes.* A large portion of the experimental investigations have been concerned with heat transfer of non-Newtonian fluids in laminar flow through cylindrical tubes. The physical properties that are needed for heat-transfer coefficients are density, heat capacity, thermal conductivity, and the rheological constants  $K'$  and  $n'$  or  $K$  and  $n$ .

In heat transfer in a fluid in laminar

flow, the mechanism is primarily one of conduction. However, for low flow rates and low viscosities, natural convection effects can be present. Since many non-Newtonian fluids are quite “viscous,” natural convection effects are reduced substantially. For laminar flow inside circular tubes of power-law fluids, the equation of Metzner and Gluck (M2) can be used with highly viscous, non-Newtonian fluids with negligible natural convection for horizontal or vertical tubes for the Graetz number  $NG_z > 20$  and  $n' > 0.10$ :

$$(NNu)_a = haDk = 1.75\delta^{1/3}(NG_z)^{1/3}(\gamma_b\gamma_w)^{0.14} \quad (15.7-1)$$

where

$$\delta = 3n' + 14n' \quad (15.7-2)$$

$$NG_z = n_k p k L = \pi^4 D \nu \rho \mu c p \mu k D L = \pi^4 N Re N Pr D L \quad (15.7-3)$$

The viscosity coefficients  $\gamma_b$  at temperature  $T_b$  and  $\gamma_w$  at  $T_w$  are defined as

$$\gamma_b \gamma_w = k_b'^{8n'-1} k_w'^{8n'-1} = k_b' k_b' \\ '= K_b K_w (15.7-4)$$

The nomenclature is as follows:  $k$  in  $\text{W}/\text{m} \cdot \text{K}$ ,  $c_p$  in  $\text{J}/\text{kg} \cdot \text{K}$ ,  $\rho$  in  $\text{kg}/\text{m}^3$ , flow rate  $m$  in  $\text{kg}/\text{s}$ , length of heated section of tube  $L$  in  $\text{m}$ , inside diameter  $D$  in  $\text{m}$ , the mean coefficient  $h_a$  in  $\text{W}/\text{m}^2 \cdot \text{K}$ , and  $K$  and  $n'$  rheological constants (see Section 3.5). The physical properties and  $K_b$  are all evaluated at the mean bulk temperature  $T_b$  and  $K_w$  at the average wall temperature  $T_w$ .

The value of the rheological constant  $n'$  or  $n$  has been found not to vary appreciably over wide temperature

ranges (S3). However, the rheological constant  $K'$  or  $K$  has been found to vary appreciably. A plot of  $\log K'$  versus  $1/T_{\text{abs}}$  (C1) or versus  $T^{\circ}\text{C}$  (S3) can often be approximated by a straight line.

Often, data for the temperature effect on  $K$  are not available. Since the ratio  $K_b/K_w$  is taken to the 0.14 power, this factor can sometimes be neglected without causing large errors. For a value of the ratio of 2:1, the error is only about 10%. A plot of  $\log$  viscosity versus  $1/T$  for Newtonian fluids is also often a straight line. The value of  $h_a$  obtained from Eq. (15.7-1) is the mean value to use over the tube length  $L$  with the arithmetic temperature difference  $\Delta T_a$ :

$$\Delta T_a = (T_w - T_{bi}) + (T_w - T_{bo})/2 \quad (15.7-5)$$

when  $T_w$  is the average wall temperature

for the whole tube and  $T_{bi}$  is the inlet bulk temperature and  $T_{bo}$  the outlet bulk temperature. The heat flux  $q$  is

$$q = h_a A \Delta T_a = h_a (\pi D L) \Delta T_a \quad (15.7-6)$$

**EXAMPLE 15.7-1. Heating a Non-Newtonian Fluid in Laminar Flow**

A non-Newtonian fluid flowing at a rate of  $7.56 \times 10^{-2}$  kg/s inside a 25.4-mm-ID tube is being heated by steam condensing outside the tube. The fluid enters the heating section of the tube, which is 1.524 m long, at a temperature of 37.8°C. The inside wall temperature  $T_w$  is constant at 93.3°C. The mean physical properties of the fluid are  $\rho = 1041$  kg/m<sup>3</sup>,  $c_{pm} = 2.093$  kJ/kg · K, and  $k = 1.212$  W/m · K. The fluid is a power-law fluid having the flow-property (rheological) constants  $n = n' = 0.40$ , which are approximately constant over the temperature range encountered, and  $K = 139.9$  N · s <sup>$n'$</sup> /m<sup>2</sup> at 37.8°C and 62.5 at 93.3°C. For this fluid, a plot of log  $K$  versus  $T^\circ\text{C}$  is approximately a straight line. Calculate the outlet bulk temperature of the fluid if it is in laminar flow.

**Solution:** The solution is trial and error, since the outlet bulk temperature  $T_{bo}$  of the fluid must be known in order to calculate  $h_a$  from Eq. (15.7-2). Assuming  $T_{bo} = 54.4^\circ\text{C}$  for the first trial, the mean bulk temperature  $T_b$  is  $(54.4 + 37.8)/2$ , or  $46.1^\circ\text{C}$ .

Plotting the two values of  $K$  given at 37.8 and 93.3°C as log  $K$  versus  $T^\circ\text{C}$ , and drawing a straight line through these two points, a value for  $K_b$  of 123.5 at  $T_b = 46.1^\circ\text{C}$  is read from the plot. At  $T_w = 93.3^\circ\text{C}$ ,  $K_w = 62.5$ .

Next,  $\delta$  is calculated using Eq. (15.7-2):

$$\delta = 3n' + 14n = 3(0.4) + 14(0.4) = 1.375$$

Substituting into Eq. (15.7-3),

$$NGz = mcpkL = (7.56 \times 10^{-2} \text{ kgs})(2.093 \times 10^3 \text{ J/kg} \cdot \text{K})(1.212 \text{ Wm} \cdot \text{K})(1.524 \text{ m}) = 85.7$$

From Eq. (15.7-4),

$$gbgw = KbKw = 123.562.5$$

Then, substituting into Eq. (15.7-1),

$$haDk = ha.$$

$$(1.212 \text{ Wm} \cdot \text{K}) = 1.75 \frac{1}{3} (NGz)^{1/3} (gbgw)^{0.14} = 1.75 (1.375)^{1/3} (85.7)^{1/3} (123.562.5)^{0.14} \quad (15.7-1)$$

Solving,  $h_a = 448.3 \text{ W/m}^2 \cdot \text{K}$ .

By a heat balance, the value of  $q$  in  $W$  is as follows:

$$q = mcpm(T_{bo} - T_{bi}) \quad (15.7-7)$$

This is equated to Eq. (15.7-6) to obtain

$$q = mcpm(T_{bo} - T_{bi}) = ha(\pi DL)\Delta T_a \quad (15.7-8)$$

The arithmetic mean temperature difference  $\Delta T_a$  by Eq. (15.7-5) is

$$\Delta T_a = \frac{(T_w - T_{bi}) + (T_w - T_{bo})}{2} = \frac{(93.3 - 37.8) + (93.3 - T_{bo})}{2} = 74.4 - 0.5T_{bo}$$

Substituting the known values in Eq. (15.7-8) and solving for  $T_{bo}$ ,

$$\begin{aligned} (7.56 \times 10^{-2})(2.093 \times 10^3) \\ (T_{bo} - 37.8) &= 448.3(\pi \times 0.0254 \times 1.524) \\ (74.4 - 0.5T_{bo})T_{bo} &= 54.1^\circ\text{C} \end{aligned}$$

This value of  $54.1^\circ\text{C}$  is close enough to the assumed value of  $54.5^\circ\text{C}$  that a second trial is not needed. Only the value of  $K_b$  would be affected. Known values can be substituted into Eq. (9.1-11) for the Reynolds number to show that it is less than 2100 and that the flow is laminar.

For less “viscous” non-Newtonian power-law fluids in laminar flow,



natural convection may affect the heat-transfer rates. Metzner and Gluck (M2) recommend use of an empirical correction to Eq. (15.7-1) for horizontal tubes.

*2. Turbulent flow in tubes.* For turbulent flow of power-law fluids through tubes. Clapp (C4) presents the following empirical equation for heat transfer:

$$N_{Nu} = hL/k = 0.0041(N_{Re,gen})^{0.99} [K'_{cp} K(8VD)^{n-1}]^{0.4} \quad (15.7-9)$$

where  $N_{Re,gen}$  is defined by Eq. (9.1-11) and  $hL$  is the heat-transfer coefficient based on the log mean temperature driving force. The fluid properties are evaluated at the bulk mean temperature. Metzner and Friend (M3) also give equations for turbulent heat transfer.

## **15.7C Natural Convection**

Acrivos (A1, S3) gives relationships for natural convection heat transfer to power-law fluids from various surface geometries such as spheres, cylinders, and plates.

## **15.8 Special Heat-Transfer Coefficients**

### **15.8A Heat Transfer in Agitated Vessels**

*1. Introduction.* Many chemical and biological processes are often carried out in agitated vessels. As discussed in Chapter 7, the liquids are generally agitated in cylindrical vessels with an impeller mounted on a shaft and driven by an electric motor. Typical agitators and vessel assemblies have been shown in Figs. 7.2-1 and 7.2-3. It is often necessary to cool or heat the contents of the vessel during agitation. This is

usually done by heat-transfer surfaces, which may be in the form of cooling or heating jackets in the wall of the vessel or coils of pipe immersed in the liquid.

*2. Vessel with heating jacket.* In Fig.

15.8-1a, a vessel with a cooling or heating jacket is shown. When heating, the fluid entering is often steam, which condenses inside the jacket and leaves at the bottom. The vessel is equipped with an agitator and, in most cases, with baffles (not shown).

Correlations for the heat-transfer coefficient from the agitated Newtonian liquid inside the vessel to the jacket walls of the vessel have the following form:

$$hD_{tk} = a(Da^2 N \rho \mu)^b (c_p \mu_k)^{1/3} (\mu_m w)^m \quad (15.8-1)$$

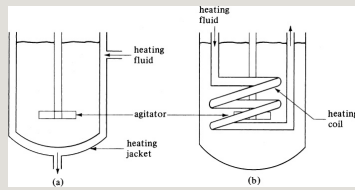


Figure 15.8-1. *Heat transfer in agitated vessels: (a) vessel with heating jacket, (b) vessel with heating coils.*

where  $h$  is the heat-transfer coefficient for the agitated liquid to the inner wall in  $\text{W}/\text{m}^2 \cdot \text{K}$ ,  $D_t$  is the inside diameter of the tank in m,  $k$  is thermal conductivity in  $\text{W}/\text{m} \cdot \text{K}$ ,  $D_a$  is the diameter of the agitator in m,  $N$  is rotational speed in revolutions per sec,  $\rho$  is fluid density in  $\text{kg}/\text{m}^3$ , and  $\mu$  is liquid viscosity in  $\text{Pa} \cdot \text{s}$ . All the liquid physical properties are evaluated at the bulk liquid temperature except  $\mu_w$ , which is evaluated at the wall temperature  $T_w$ . Listed below are some available correlations and the Reynolds-number range ( $\text{NRe}' = \text{Da}^2 \text{N} \rho / \mu$ ).

#### 1. Paddle agitator with no baffles (C5, U1)

$$a=0.36, b=2/3, m=0.21, NRe'=300 \text{ to } 3 \times 10^5$$

2. Flat-blade turbine agitator with no baffles (B4)

$$a=0.54, b=2/3, m=0.14, NRe'=30 \text{ to } 3 \times 10^5$$

3. Flat-blade turbine agitator with baffles (B4, B5)

$$a=0.74, b=2/3, m=0.14, NRe'=500 \text{ to } 3 \times 10^5$$

4. Anchor agitator with no baffles (U1)

$$a=1.0, b=1/2, m=0.18, NRe'=10 \text{ to } 300$$

$$a=0.36, b=2/3, m=0.18, NRe'=300 \text{ to } 4 \times 10^5$$

5. Helical-ribbon agitator with no baffles (G4)

$$a=0.633, b=1/2, m=0.18, NRe'=8 \text{ to } 8 \times 10^5$$

Some typical overall  $U$  values for jacketed vessels for various process applications are tabulated in Table 15.8-1.

Table 15.8-1. *Typical Overall Heat-Transfer Coefficients in Jacketed Vessels*

--	--

**EXAMPLE 15.8-1. Heat-Transfer Coefficient in Agitated Vessel with Jacket**

A jacketed 1.83-m-diameter agitated vessel with baffles is being used to heat a liquid that is at 300 K. The agitator is 0.61 m in diameter and is a flat-blade turbine rotating at 100 rpm. Hot water is in the heating jacket. The wall surface temperature is constant at 355.4 K. The liquid has the following bulk physical properties:  $\rho = 961 \text{ kg/m}^3$ ,  $c_p = 2500 \text{ J/kg} \cdot \text{K}$ ,  $k = 0.173 \text{ W/m} \cdot \text{K}$ , and  $\mu = 1.00 \text{ Pa} \cdot \text{s}$  at 300 K and  $0.084 \text{ Pa} \cdot \text{s}$  at 355.4 K. Calculate the heat-transfer coefficient to the wall of the jacket.

**Solution:** The following are given:

$$D_t = 1.83 \text{ m} \quad D_a = 0.61 \text{ m} \quad N = 100/60 \text{ rev/s}$$

$$\mu(300 \text{ K}) = 1.00 \text{ Pa} \cdot \text{s} = 1.00 \text{ kg/m} \cdot \text{s}$$

$$\mu_w(355.4 \text{ K}) = 0.084 \text{ Pa} \cdot \text{s} = 0.084 \text{ kg/m} \cdot \text{s}$$

First, calculating the Reynolds number at 300 K,

$$\text{NRe}' = \frac{D_a^2 N \rho \mu}{(0.61 \text{ m})^2 (1.667 \text{ rev/s}) (961 \text{ kg/m}^3) (1.00 \text{ kg/m} \cdot \text{s})} = 596$$

The Prandtl number is

$$\text{NPr} = \frac{c_p \mu}{k} = \frac{(2500 \text{ J/kg} \cdot \text{K}) (1.00 \text{ kg/m} \cdot \text{s})}{0.173 \text{ W/m} \cdot \text{K}} = 14450$$

Using Eq. (15.8-1) with  $a = 0.74$ ,  $b = a = 0.74$ ,  $b = 23$ , and  $m = 0.14$ ,

$$h D_t k = 0.74 (\text{NRe}')^{2/3} (\text{NPr})^{1/3} (\mu/\mu_w)^{0.14} \quad (15.8-1)$$

Substituting and solving for  $h$ ,

$$h(1.83 \text{ m}) (0.173 \text{ W/m} \cdot \text{K}) = 0.74 (596)^{2/3} (14450)^{1/3} [1 \text{ kg/m} \cdot \text{s} / 0.084 \text{ kg/m} \cdot \text{s}]^{0.14} \quad h = 170.6 \text{ W/m}^2 \cdot \text{K} \quad (30.0 \text{ Btu/h} \cdot \text{ft}^2 \cdot \text{°F})$$

A correlation to predict the heat-transfer coefficient of a power-law non-

Newtonian fluid in a jacketed vessel with a turbine agitator is also available elsewhere (C6).

*3. Vessel with heating coils.* In Fig. 15.8-1b, an agitated vessel with a helical heating or cooling coil is shown.

Correlations for the heat-transfer coefficient to the outside surface of the coils in agitated vessels are listed below for various types of agitators.

For a paddle agitator with no baffles (C5),

$$h_{Dk} = 0.87(Da^2 N \rho \mu)^{0.62} (c_p \mu k)^{1/3} (\mu \mu_w)^{0.14} \quad (15.8-2)$$

This holds for a Reynolds-number range of 300 to  $4 \times 10^5$ .

For a flat-blade turbine agitator with baffles, see (O1).

When the heating or cooling coil is in the form of vertical tube baffles with a flat-blade turbine, the following correlation can be used (D1):

$$=0.09(Da^2 N \rho \mu)^{0.65} (c_p \mu k)^{1/3} (Da Dt)^{1/3} (2nb)^0 (\mu/\mu_f)^0 (15$$

where  $D_o$  is the outside diameter of the coil tube in  $m$ ,  $nb$  is the number of vertical baffle tubes, and  $\mu_f$  is the viscosity at the mean film temperature.

Perry and Green (P3) give typical values of overall heat-transfer coefficients  $U$  for coils immersed in various liquids in agitated and nonagitated vessels.

### **15.8B Scraped-Surface Heat Exchangers**

Liquid–solid suspensions, viscous aqueous and organic solutions, and numerous food products, such as margarine and orange juice



concentrate, are often cooled or heated in a scraped-surface exchanger. This consists of a double-pipe heat exchanger with a jacketed cylinder containing steam or cooling liquid and an internal rotating shaft that is fitted with wiper blades, as shown in Fig. 15.8-2.

The viscous liquid product flows at low velocity through the central tube between the rotating shaft and the inner pipe. The rotating scrapers or wiper blades continually scrape the surface of liquid, preventing localized overheating and giving rapid heat transfer. In some cases, this device is also called a *votator heat exchanger*.

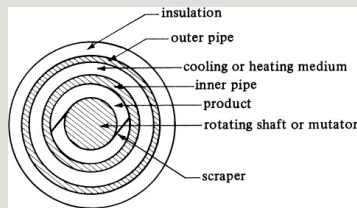


Figure 15.8-2. *Scraped-surface heat exchanger.*

Skelland et al. (S4) give the following equation to predict the inside heat-transfer coefficient for the votator:

$$hDk = \alpha (c_p \mu k)^b \left( \frac{D}{D_s} \right)^{1.0} \left( \frac{D}{N} \right)^{0.62} \left( \frac{D_s}{D} \right)^{0.55} (nB)^{0.53} \quad (15.8-4)$$

$$14\beta = 0.96 \text{ for viscous liquids } \alpha = 0.039 \beta = 0.70 \text{ for viscous liquids}$$

where  $D$  = diameter of the vessel in m,  
 $D_s$  = diameter of the rotating shaft in m,  
 $v$  = the axial flow velocity of liquid in m/s,  $N$  = the agitator speed in rev/s, and  $nB$  = the number of blades on the agitator. Data cover a region of axial flow velocities of 0.076 to 0.38 m/min

and rotational speeds of 100 to 750 rpm.

Typical overall heat-transfer coefficients in food applications are  $U = 1700 \text{ W/m}^2 \cdot \text{K}$  (300  $\text{btu/h} \cdot \text{ft}^2 \cdot \text{F}$ ) for cooling margarine with  $\text{NH}_3$ , 2270 (400) for heating applesauce with steam, 1420 (250) for chilling shortening with  $\text{NH}_3$ , and 2270 (400) for cooling cream with water (B6).

### **15.8C Extended Surface or Finned Exchangers**

*1. Introduction.* The use of fins or extended surfaces on the outside of a heat-exchanger pipe wall to give relatively high heat-transfer coefficients in the exchanger is quite common. An automobile radiator is such a device, where hot water passes inside through a bank of tubes and loses heat to the air. On the

outside of the tubes, extended surfaces receive heat from the tube walls and transmit it to the air by forced convection.

Two common types of fins attached to the outside of a tube wall are shown in Fig. 15.8-3. In Fig. 15.8-3a, there are a number of longitudinal fins spaced around the tube wall and the direction of gas flow is parallel to the axis of the tube. In Fig. 15.8-3b, the gas flows normally to the tubes containing many circular or transverse fins.

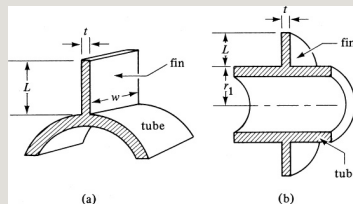


Figure 15.8-3. Two common types of fins on a section of circular tube: (a) longitudinal fin, (b) circular or transverse fin.

The qualitative effect of using extended surfaces can be shown approximately in Eq. (15.8-5) for a fluid inside a tube having a heat-transfer coefficient of  $h_i$  and an outside coefficient of  $h_o$ :

$$\frac{1}{U_i A_i} = \Sigma R \approx \frac{1}{h_i A_i} + R_{\text{metal}} + \frac{1}{h_o A_o} \quad (15.8-5)$$

The resistance  $R_{\text{metal}}$  of the wall can often be neglected. The presence of the fins on the outside increases  $A_o$  and hence reduces the resistance  $1/h_o A_o$  of the fluid on the outside of the tube. For example, if we have  $h_i$  for condensing steam, which is very large, and  $h_o$  for air outside the tube, which is quite small, increasing  $A_o$  greatly reduces  $1/h_o A_o$ . This, in turn, greatly reduces the total resistance, which increases the heat-transfer rate. If the positions of the two

fluids are reversed, with air inside and steam outside, little increase in heat transfer could be obtained by using fins.

Equation (15.8-5) is only an approximation, since the temperature on the outside surface of the bare tube is not the same as that at the end of the fin because of the added resistance to heat flow by conduction from the fin tip to the base of the fin. Hence, a unit area of fin surface is not as efficient as a unit area of bare tube surface at the base of the fin. A fin efficiency  $\eta_f$  has been mathematically derived for various geometries of fins.

*2. Derivation of the equation for fin efficiency.* We will consider a one-dimensional fin exposed to a surrounding fluid at temperature  $T_q$ , as

shown in Fig. 15.8-4. At the base of the fin, the temperature is  $T_0$  and at point  $x$  it is  $T_\infty$ . At steady state, the rate of heat conducted into the element at  $x$  is  $q_x|_x$  and is equal to the rate of heat conducted out plus the rate of heat lost by convection:

$$q_x|_x = q_x|_{x+\Delta x} + q_c$$

$$-kAdTdx|_x = -kAdTdx|_{x+\Delta x} + h(P\Delta x)(T - T_\infty) \quad (15.8-6)$$

Substituting Fourier's equation for conduction and the convection equation,

$$-kAdTdx|_x = -kAdTdx|_{x+\Delta x} + h(P\Delta x)(T - T_\infty) \quad (15.8-7)$$

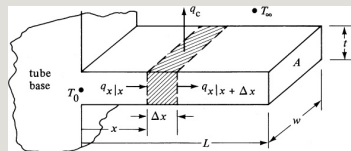


Figure 15.8-4. Heat balance for one-dimensional conduction and convection in a rectangular fin with a constant cross-sectional area.

where  $A$  is the cross-sectional area of the fin in  $\text{m}^2$ ,  $P$  is the perimeter of the fin in  $\text{m}$ , and  $(P \Delta x)$  is the area for convection. Rearranging Eq. (15.8-7), dividing by  $\Delta x$ , and letting  $\Delta x$  approach zero,

$$d^2T/dx^2 - hPkA(T - T_\infty) = 0 \quad (15.8-8)$$

Letting  $\theta = T - T_\infty$ , Eq. (15.8-8) becomes

$$d^2\theta/dx^2 - hPkA\theta = 0 \quad (15.8-9)$$

The first boundary condition is that  $\theta = \theta_0 = T_0 - T_\infty$  at  $x = 0$ . For the second boundary condition needed to integrate Eq. (15.8-9), several cases can be considered, depending upon the physical conditions at  $x = L$ . In the first case, the end of the fin is insulated and  $d\theta/dx = 0$  at  $x = L$ . In the second case, the fin loses



heat by convection from the tip surface, so that  $-k(dT/dx)_L = h(T_L = T_\infty)$ . The solution using the second case is quite involved and will not be considered here. Using the first case, where the tip is insulated, integration of Eq. (15.8-9) gives

$$\theta/\theta_0 = \cosh[m(L-x)]/\cosh mL \quad (15.8-10)$$

where  $m = (hP/kA)^{1/2}$ .

The heat lost by the fin is expressed as

$$q = -kA \left. \frac{dT}{dx} \right|_{x=0} \quad (15.8-11)$$

Differentiating Eq. (15.8-10) with respect to  $x$  and combining it with Eq. (15.8-11),

$$q = (hPkA)^{1/2} (\theta_0 - T_\infty) \tanh mL \quad (15.8-12)$$

In the actual fin, the temperature  $T$  in the fin decreases as the tip of the fin is approached. Hence, the rate of heat transfer per unit area decreases as the distance from the tube base is increased. To indicate this effectiveness of the fin in transferring heat, the fin efficiency  $\eta_f$  is defined as the ratio of the actual heat transferred from the fin to the heat transferred if the entire fin were at the base temperature  $T_0$ :

$$\eta_f = \frac{(hPkA)^{1/2}(T_0 - T_\infty) \tanh mL}{h(PL)(T_0 - T_\infty)} = \tanh mL / mL \quad (15.8-13)$$

where  $PL$  is the entire surface area of fin.

The expression for  $mL$  is

$$mL = (hPkA)^{1/2}L = [h(2w + 2t)k(wt)]^{1/2}L$$

$$1/2L(15.8-14)$$

For fins which are thin,  $2t$  is small compared to  $2w$ , and

$$mL = (2hkt)^{1/2}L(15.8-15)$$

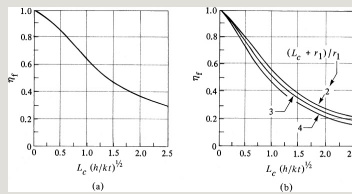


Figure 15.8-5. Fin efficiency  $\eta_f$  for various fins: (a) longitudinal or straight fins, (b) circular or transverse fins. (See Fig.15.8-3 for the dimensions of the fins.)

Equation (15.8-15) holds for a fin with an insulated tip. This equation can be modified to hold for the case where the fin loses heat from its tip. This can be done by extending the length of the fin by  $t/2$ , where the corrected length  $L_c$  to use in Eqs. (15.8-13)–(15.8-15) is

$$L_c = L + t/2 \quad (15.8-16)$$

The fin efficiency calculated from Eq. (15.8-13) for a longitudinal fin is shown in Fig. 15.8-5a. In Fig. 15.8-5b, the fin efficiency for a circular fin is presented. Note that the abscissa on the curves is  $L_c(h/kt)^{1/2}$  and not  $L_c(2h/kt)^{1/2}$  as in Eq. (15.8-15).

**EXAMPLE 15.8.-2. Fin Efficiency and Heat Loss from a Fin**

A circular aluminum fin, as shown in Fig. 15.8-3b ( $k = 222 \text{ W/m} \cdot \text{K}$ ), is attached to a copper tube having an outside radius of 0.04 m. The length of the fin is 0.04 m and the thickness is 2 mm. The outside wall or tube base is at 523.2 K and the external surrounding air at 343.2 K has a convective coefficient of  $30 \text{ W/m}^2 \cdot \text{K}$ . Calculate the fin efficiency and rate of heat loss from the fin.

**Solution:** The given data are  $T_0 = 523.2 \text{ K}$ ,  $T_\infty = 343.2 \text{ K}$ ,  $L = 0.04 \text{ m}$ ,  $r_1 = 0.04 \text{ m}$ ,  $t = 0.002 \text{ m}$ ,  $k = 222 \text{ W/m} \cdot \text{K}$ ,  $h = 30 \text{ W/m}^2 \cdot \text{K}$ .

By Eq. (15.8-16),  $L_c = L + t/2 = 0.040 + 0.002/2 = 0.041 \text{ m}$ . Then,

$$L_c(h/kt)^{1/2} = (0.041)[30 \cdot 222 / (0.002)]^{1/2} = 0.337$$

Also,  $(L_c + r_1)/r_1 = (0.041 + 0.040)/0.040 = 2.025$ . Using Fig. 15.8-5b,  $\eta_f = 0.89$ . The heat transfer from the fin itself is

$$q_f = \eta_f h A_f (T_0 - T_\infty) \quad (15.8-17)$$

where  $A_f$  is the outside surface area (annulus) of the fin and is given by the following for both sides of the fin:

$$A_f = 2\pi[(L_c + r_1)^2 - (r_1)^2] \text{ (circular fin)} \quad A_f = 2\pi(L_c \times w) \text{ (longitudinal fin)} \quad (15.8-18)$$

Hence,

$$A_f = 2\pi[(0.041\text{m} + 0.040\text{m})^2 - (0.040\text{m})^2] = 3.118 \times 10^{-2} \text{m}^2$$

Substituting into Eq. (15.8-17),

$$q_f = 0.89(30 \text{Wm}^{-2}\cdot\text{K})(3.118 \times 10^{-2} \text{m}^2) \\ (523.2\text{K} - 343.2\text{K}) = 149.9 \text{W}$$

*3. Overall heat-transfer coefficient for finned tubes.* Here, we consider the general case similar to Fig. 13.2-1b, where heat transfer occurs from a fluid inside a cylinder or tube, through the cylinder metal wall  $A$  of thickness  $\Delta x_A$ , and then to the fluid outside the tube, where the tube has fins on the outside. The heat is transferred through a series of resistances. The total heat  $q$  leaving the outside of the tube is the sum of heat loss by convection from the base of the bare tube  $q_t$  and the loss by convection from the fins,  $q_f$ :

$$q = q_t + q_f = h_o A_t (T_0 - T_\infty) + h_o A_f \eta_f (T_0 - T_\infty) \quad (15.8-19)$$

This can be written as a resistance since the paths are in parallel:

$$q = (h_o A_t + h_o A_f \eta_f) (T_0 - T_\infty) = \frac{T_0 - T_\infty}{1/h_o (A_t + A_f \eta_f)} = \frac{T_0 - T_\infty}{R} \quad (15.8-20)$$

where  $A_t$  is the area of the bare tube between the fins,  $A_f$  is the area of the fins, and  $h_o$  is the outside convective coefficient. The resistance in Eq. (13.2-10) can be substituted for the resistance  $(1/h_o A_o)$  in Eq. (13.2-5) for a bare tube to give the overall equation for a finned tube exchanger:

$$q = \frac{T_4 - T_1}{1/h_i A_i + \Delta x/kA + 1/h_o (A_t + A_f \eta_f)} = \frac{T_4 - T_1}{\sum R} \quad (15.8-21)$$

where  $T_4$  is the temperature of the fluid inside the tube and  $T_1$  is the outside fluid temperature. Writing Eq. (15.8-21) in the form of an overall heat-transfer coefficient  $U_i$  based on the inside area  $A_i$ ,  $q = U_i A_i (T_4 - T_1)$  and

$$U_i = \frac{1}{\frac{1}{h_i} + \frac{\Delta x}{k} \frac{A_i}{A_o} + \frac{1}{h_o} \frac{A_i}{A_o}} \quad (15.8-22)$$

The presence of fins on the outside of the tube changes the characteristics of the fluid flowing past the tube (either flowing parallel to the longitudinal finned tube or transverse to the circular finned tube). Hence, the correlations for fluid flow parallel to or transverse to bare tubes cannot be used to predict the outside convective coefficient  $h_o$ .

Correlations are available in the literature (K4, M1, P1, P3) for heat

transfer to various types of fins.

## 15.9 Chapter Summary

### Buckingham Method

Number of p groups =  $q - u$

Common solution for forced convection:

$N_{Nu} = \alpha N_{Re}^\beta N_{Pr}^\gamma$  where  $\alpha$ ,  $\beta$  and  $\gamma$  are constants

Common solution for Natural

convection:  $N_{Nu} = a(N_{Gr} N_{Pr})^m$  where  $a$  and  $m$  are constants

**Equations for Heat Transfer Coefficients  
(Additional Equations Found in Chapter Text)**

## Problems

**15.1-1. *Dimensional Analysis for Natural Convection.*** Repeat the dimensional analysis for natural



convection heat transfer to a vertical plate as given in Section 15.1.

However, do as follows:

- Carry out all the detailed steps solving for all the exponents in the  $\pi$ 's.
- Repeat, but in this case select the four variables  $L$ ,  $\mu$ ,  $c_p$ , and  $g$  to be common to all the dimensionless groups.

### **15.1-2. *Dimensional Analysis for***

### ***Unsteady-State Conduction.*** For

unsteady-state conduction in a solid, the following variables are involved:  $\rho$ ,  $c_p$ ,  $L$  (dimension of solid),  $t$ ,  $k$ , and  $z$  (location in solid). Determine the dimensionless groups relating the variables.

$$\text{Ans. } \pi_1 = k t \rho c_p L^2, \pi_2 = z/L$$

### **15.2-1. *Thermal and Hydrodynamic***

### ***Boundary Layer Thicknesses.*** Air at

294.3 K and 101.3 kPa with a free stream velocity of 12.2 m/s is flowing parallel to a smooth flat plate held at a surface temperature of 383 K. Do the following:

- At the critical  $N_{Re,L} = 5 \times 10^5$ , calculate the critical length  $x = L$  of the plate, the thickness  $\delta$  of the hydrodynamic boundary layer, and the thickness  $\delta T$  of the thermal boundary layer. Note that the Prandtl number is not 1.0.
- Calculate the average heat-transfer coefficient over the plate covered by the laminar boundary layer.

**15.2-2. Boundary-Layer Thicknesses and Heat Transfer.** Air at 37.8°C and 1 atm abs flows at a velocity of 3.05 m/s parallel to a flat plate held at 93.3°C. The plate is 1 m wide. Calculate the following at a position 0.61 m from the leading edge:

- The thermal boundary-layer thickness  $\delta T$  and the

hydrodynamic boundary-layer thickness  $\delta$ .

- Total heat transfer from the plate.

**15.3-1. *Heating Air by Condensing Steam.*** Air is flowing through a tube having an inside diameter of 38.1 mm at a velocity of 6.71 m/s, average temperature of 449.9 K, and pressure of 138 kPa. The inside wall temperature is held constant at 204.4°C (477.6 K) by steam condensing outside the tube wall. Calculate the heat-transfer coefficient for a long tube and the heat-transfer flux.

**Ans.**  $h = 39.38 \text{ W/m}^2 \cdot \text{K}$  (6.94 btu/h · ft<sup>2</sup> · °F)

**15.3-2. *Trial-and-Error Solution for Heating Water.*** Water is flowing inside a horizontal 1 1/4-in. Schedule 40 steel pipe at 37.8°C and a velocity of 1.52 m/

s. Steam at  $108.3^{\circ}\text{C}$  is condensing on the outside of the pipe wall and the steam coefficient is assumed constant at  $9100 \text{ W/m}^2 \cdot \text{K}$ .

- Calculate the convective coefficient  $h_i$  for the water. (Note that this is trial and error. A wall temperature on the inside must be assumed first.)
- Calculate the overall coefficient  $U_i$  based on the inside area and the heat-transfer flux  $q/A_i$  in  $\text{W/m}^2$ .

**15.3-3. *Laminar Flow and Heating of Oil.*** A hydrocarbon oil at  $175^{\circ}\text{F}$  enters a pipe having an inside diameter of  $0.0303 \text{ ft}$  and a length of  $15 \text{ ft}$ . The inside pipe surface temperature is constant at  $325^{\circ}\text{F}$ . The oil is to be heated to  $250^{\circ}\text{F}$  in the pipe. How many  $\text{lb}_\text{m}/\text{h}$  oil can be heated? (*Hint:* This solution is trial and error. One method is to assume a flow rate of, say,  $m = 75 \text{ lb mass/h}$ . Calculate the  $N_\text{Re}$  and the value of  $h_a$ . Then, make a heat balance to

solve for  $q$  in terms of  $m$ . Equate this  $q$  to the  $q$  from the equation  $q = h_a A \Delta T_a$ . Solve for  $m$ . This is the new  $m$  to use for the second trial.) The properties of the oil are  $c_{pm} = 0.50 \text{ btu/lb}_m \cdot ^\circ\text{F}$  and  $k_m = 0.083 \text{ btu/h} \cdot \text{ft} \cdot ^\circ\text{F}$ . The viscosity of the oil varies with temperature as follows:  $150^\circ\text{F}$ , 6.50 cp;  $200^\circ\text{F}$ , 5.05 cp;  $250^\circ\text{F}$ , 3.80 cp;  $300^\circ\text{F}$ , 2.82 cp;  $350^\circ\text{F}$ , 1.95 cp.

**Ans.**  $m = 84.2 \text{ lb}_m / \text{h}$  (38.2 kg/h)

**15.3-4. Heating Air by Condensing Steam.** Air at a pressure of 101.3 kPa and 288.8 K enters a tube having an inside diameter of 12.7 mm and a length of 1.52 m with a velocity of 24.4 m/s. Condensing steam on the outside of the tube maintains the inside wall temperature at 372.1 K. Calculate the convection coefficient of the air. (Note:

This solution is trial and error. First assume an outlet temperature of the air.)

**15.3-5. Heat Transfer with a Liquid Metal.** The liquid metal bismuth at a flow rate of 2.00 kg/s enters a tube having an inside diameter of 35 mm at 425°C and is heated to 430°C in the tube. The tube wall is maintained at a temperature of 25°C above the liquid bulk temperature. Calculate the tube length required. The physical properties are as follows (H1):  $k = 15.6 \text{ W/m} \cdot \text{K}$ ,  $c_p = 149 \text{ J/kg} \cdot \text{K}$ ,  $\mu = 1.34 \times 10^{-3} \text{ Pa} \cdot \text{s}$ .

**15.4-1. Heat Transfer from a Flat Plate.** Air at a pressure of 101.3 kPa and a temperature of 288.8 K is flowing over a thin, smooth, flat plate at 3.05 m/s. The plate length in the direction of flow is 0.305 m and its temperature is 333.2

K. Calculate the heat-transfer coefficient assuming laminar flow.

$$\text{Ans. } h = 12.35 \text{ W/m}^2 \cdot \text{K} \text{ (2.18 btu/h} \cdot \text{ft}^2 \cdot ^\circ\text{F)}$$

**15.4-2. Chilling Frozen Meat.** Cold air at  $-28.9^\circ\text{C}$  and 1 atm is recirculated at a velocity of 0.61 m/s over the exposed top flat surface of a piece of frozen meat. The sides and bottom of this rectangular slab of meat are insulated and the top surface is 254 mm by 254 mm square. If the surface of the meat is at  $-6.7^\circ\text{C}$ , predict the average heat-transfer coefficient to the surface. As an approximation, assume that either Eq. (15.4-2) or (15.4-3) can be used, depending on the  $N_{\text{Re,L}}$ .

$$\text{Ans. } h = 6.05 \text{ W/m}^2 \cdot \text{K}$$

### **15.4-3. *Heat Transfer to an Apple.***

Predict the heat-transfer coefficient for air being blown past an apple lying on a screen with large openings. The air velocity is 0.61 m/s at 101.32 kPa pressure and 316.5 K. The surface of the apple is at 277.6 K and its average diameter is 114 mm. Assume that it is a sphere.

### **15.4-4. *Heating Air by a Steam Heater.***

A total of 13,610 kg/h of air at 1 atm abs pressure and 15.6°C is to be heated by passing over a bank of tubes in which steam at 100°C is condensing. The tubes are 12.7 mm OD, 0.61 m long, and arranged in-line in a square pattern with  $S_p = S_n = 19.05$  mm. The bank of tubes contains six transverse rows in the direction of flow and 19 rows normal to the flow. Assume that the tube surface



temperature is constant at  $93.33^{\circ}\text{C}$ .  
Calculate the outlet air temperature.

**15.5-1. *Natural Convection from an Oven Wall.*** The oven wall in Example 15.5-1 is insulated so that the surface temperature is 366.5 K instead of 505.4 K. Calculate the natural convection heat-transfer coefficient and the heat-transfer rate per m of width. Use both Eq. (15.5-4) and the simplified equation. (*Note:* Radiation is being neglected in this calculation.) Use both SI and English units.

**15.5-2. *Losses by Natural Convection from a Cylinder.*** A vertical cylinder 76.2 mm in diameter and 121.9 mm high is maintained at 397.1 K at its surface. It loses heat by natural convection to air at 294.3 K. Heat is lost

from the cylindrical side and the flat circular end at the top. Calculate the heat loss, neglecting radiation losses. Use the simplified equations of Table 15.5-2 and those equations for the lowest range of  $N_{Gr} N_{Pr}$ . The equivalent  $L$  to use for the top flat surface is 0.9 times the diameter.

$$\text{Ans. } q = 26.0 \text{ W}$$

**15.5-3. *Heat Loss from a Horizontal Tube.*** A horizontal tube carrying hot water has a surface temperature of 355.4 K and an outside diameter of 25.4 mm. The tube is exposed to room air at 294.3 K. What is the natural convection heat loss for a 1-m length of pipe?

**15.5-4. *Natural Convection Cooling of an Orange.*** An orange 102 mm in

diameter having a surface temperature of  $21.1^{\circ}\text{C}$  is placed on an open shelf in a refrigerator held at  $4.4^{\circ}\text{C}$ . Calculate the heat loss by natural convection, neglecting radiation. As an approximation, the simplified equation for vertical planes can be used with  $L$  replaced by the radius of the sphere (M1). For a more accurate correlation, see (S2).

**15.5-5. *Natural Convection in an Enclosed Horizontal Space.*** Repeat Example 15.5-3, but for the case where the two plates are horizontal and the bottom plate is hotter than the upper plate. Compare the results.

**Ans.**  $q = 18.64 \text{ W}$

**15.5-6. *Natural Convection Heat Loss***

***in Double Window.*** A vertical double plate-glass window has an enclosed air-gap space of 10 mm. The window is 2.0 m high by 1.2 m wide. One window surface is at 25°C and the other at 10°C. Calculate the free convection heat-transfer rate through the air gap.

***15.5-7. Natural Convection Heat Loss for Water in Vertical Plates.*** Two vertical square metal plates having dimensions of  $0.40 \times 0.40$  m are separated by a gap of 12 mm and this enclosed space is filled with water. The average surface temperature of one plate is 65.6°C and the other plate is at 37.8°C. Calculate the heat-transfer rate through this gap.

***15.5-8. Heat Loss from a Furnace.*** Two horizontal metal plates having

dimensions of  $0.8 \times 1.0$  m comprise the top of a furnace and are separated by a distance of 15 mm. The lower plate is at  $400^{\circ}\text{C}$  and the upper at  $100^{\circ}\text{C}$ , and air at 1 atm abs is enclosed in the gap.

Calculate the heat-transfer rate between the plates.

**15.6-1. Boiling Coefficient in a Jacketed Kettle.** Predict the boiling heat-transfer coefficient for the vertical jacketed sides of the kettle given in Example 15.6-1. Then, using this coefficient for the sides and the coefficient from Example 15.6-1 for the bottom, predict the total heat transfer.

**Ans.**  $T_w = 107.65^{\circ}\text{C}$ ,  $\Delta T = 7.65$  K, and  $h$   
(vertical) =  $3560 \text{ W/m}^2 \cdot \text{K}$

**15.6-2. Boiling Coefficient on a**

**Horizontal Tube.** Predict the boiling heat-transfer coefficient for water under pressure boiling at  $250^{\circ}\text{F}$  for a horizontal surface of 116-in.-thick stainless steel having a  $k$  of  $9.4 \text{ btu/h} \cdot \text{ft} \cdot ^{\circ}\text{F}$ . The heating medium on the other side of this surface is a hot fluid at  $290^{\circ}\text{F}$  having an  $h$  of  $275 \text{ btu/h} \cdot \text{ft}^2 \cdot ^{\circ}\text{F}$ . Use the simplified equations. Be sure to correct this  $h$  value for the effect of pressure.

**15.6-3. Condensation on a Vertical Tube.** Repeat Example 15.6-2 but for a vertical tube 1.22 m (4.0 ft) high instead of 0.305 m (1.0 ft) high. Use SI and English units.

**Ans.**  $h = 9438 \text{ W/m}^2 \cdot \text{K}$ ,  $1663 \text{ btu/h} \cdot \text{ft}^2 \cdot ^{\circ}\text{F}$ ;  $N_{\text{Re}} = 207.2$  (laminar flow)

**15.6-4. *Condensation of Steam on Vertical Tubes.*** Steam at 1 atm abs pressure and  $100^{\circ}\text{C}$  is condensing on a bank of five vertical tubes, each 0.305 m high and having an OD of 25.4 mm. The tubes are arranged in a bundle and spaced far enough apart that they do not interfere with each other. The surface temperature of the tubes is  $97.78^{\circ}\text{C}$ . Calculate the average heat-transfer coefficient and the total kg condensate per hour.

**Ans.**  $h = 15\,240\text{ W/m}^2 \cdot \text{K}$

**15.6-5. *Condensation on a Bank of Horizontal Tubes.*** Steam at 1 atm abs pressure and  $100^{\circ}\text{C}$  is condensing on a horizontal tube bank with five layers of tubes ( $N = 5$ ) placed one below the other. Each layer has four tubes (total

tubes =  $4 \times 5 = 20$ ) and the OD of each tube is 19.1 mm. The tubes are each 0.61 m long and the tube surface temperature is  $97.78^{\circ}\text{C}$ . Calculate the average heat-transfer coefficient and the kg condensate per second for the whole condenser. Make a sketch of the tube bank.

**15.7-1. *Laminar Heat Transfer of a Power-Law Fluid.*** A non-Newtonian power-law fluid of banana purée flowing at a rate of  $300 \text{ lb}_\text{m}/\text{h}$  inside a 1.0-in.-ID tube is being heated by a hot fluid flowing outside the tube. The banana purée enters the heating section of the tube, which is 5 ft long, at a temperature of  $60^{\circ}\text{F}$ . The inside wall temperature is constant at  $180^{\circ}\text{F}$ . The fluid properties as given by Charm (C1) are  $\rho = 69.9 \text{ lb}_\text{m}/\text{ft}^3$ ,  $c_p = 0.875 \text{ btu}/\text{lb}_\text{m} \cdot ^{\circ}\text{F}$ , and  $k =$



0.320 btu/h · ft · °F. The fluid has the following rheological constants:  $n = n' = 0.458$ , which can be assumed constant, and  $K = 0.146 \text{ lbf} \cdot \text{sn} \cdot \text{ft}^2$  at 70°F and 0.0417 at 190°F. A plot of  $\log K$  versus  $T$  °F can be assumed to be a straight line. Calculate the outlet bulk temperature of the fluid in laminar flow.

**15.7-2. Heating a Power-Law Fluid in**

***Laminar Flow.*** A non-Newtonian power-law fluid having the same physical properties and rheological constants as the fluid in Example 15.7-1 is flowing in laminar flow at a rate of  $6.30 \times 10^{22} \text{ kg/s}$  inside a 25.4-mm-ID tube. It is being heated by a hot fluid outside the tube. The fluid enters the heating section of the tube at 26.7°C and leaves the heating section at an outlet bulk temperature of 46.1°C. The inside

wall temperature is constant at  $82.2^{\circ}\text{C}$ . Calculate the length of tube needed in m. (*Note:* In this case, the unknown tube length  $L$  appears in the equation for  $h_a$  and in the heat-balance equation.)

$$\text{Ans. } L = 1.722 \text{ m}$$

**15.8-1. Heat Transfer in a Jacketed Vessel with a Paddle Agitator.** A vessel with a paddle agitator and no baffles is used to heat a liquid at  $37.8^{\circ}\text{C}$ . A steam-heated jacket furnishes the heat. The vessel's inside diameter is 1.22 m; the agitator diameter is 0.406 m and it is rotating at 150 rpm. The wall surface temperature is  $93.3^{\circ}\text{C}$ . The physical properties of the liquid are  $\rho = 977 \text{ kg/m}^3$ ,  $c_p = 2.72 \text{ kJ/kg} \cdot \text{K}$ ,  $k = 0.346 \text{ W/m} \cdot \text{K}$ , and  $\mu = 0.100 \text{ kg/m} \cdot \text{s}$  at  $37.8^{\circ}\text{C}$  and  $7.5 \times 10^{-3}$  at  $93.3^{\circ}\text{C}$ . Calculate the heat-

transfer coefficient to the wall of the jacket.

### **15.8-2. *Heat Loss from Circular Fins.***

Use the data and conditions from Example 15.8-2 and calculate the fin efficiency and rate of heat loss from the following different fin materials:

- Carbon steel ( $k = 44 \text{ W/m} \cdot \text{K}$ ).
- Stainless steel ( $k = 17.9 \text{ W/m} \cdot \text{K}$ ).

**Ans.** (a)  $\eta_f = 0.66, q = 111.1 \text{ W}$

### **15.8-3. *Heat Loss from Longitudinal***

***Fin.*** A longitudinal aluminum fin, as shown in Fig. 15.8-3a ( $k = 230 \text{ W/m} \cdot \text{K}$ ), is attached to a copper tube having an outside radius of 0.04 m. The length of the fin is 0.080 m and the thickness is 3 mm. The tube base is held at 450 K and the external surrounding air at 300

K has a convective coefficient of  $25 \text{ W/m}^2 \cdot \text{K}$ . Calculate the fin efficiency and the heat loss from the fin per 1.0 m of length.

**15.8-4. Heat Transfer in a Finned Tube Exchanger.** Air at an average temperature of  $50^\circ\text{C}$  is being heated by flowing outside a steel tube ( $k = 45.1 \text{ W/m} \cdot \text{K}$ ) having an inside diameter of 35 mm and a wall thickness of 3 mm. The outside of the tube is covered with 16 longitudinal steel fins with a length  $L = 13 \text{ mm}$  and a thickness of  $t = 1.0 \text{ mm}$ . Condensing steam inside the tube at  $120^\circ\text{C}$  has a coefficient of  $7000 \text{ W/m}^2 \cdot \text{K}$ . The outside coefficient of the air has been estimated as  $30 \text{ W/m}^2 \cdot \text{K}$ . Neglecting fouling factors and using a tube 1.0 m long, calculate the overall heat-transfer coefficient  $U_i$  based on the

inside area  $A_i$ .

## References

## Notation

# Chapter 16. Heat Exchangers

## 16.0 Chapter Objectives

On completion of this chapter, a student should be able to:

- Describe the three common types of heat exchanges described in the chapter
- Calculate the log mean temperature difference ( $\Delta T_{lm}$ ) for counter/parallel flow heat exchangers
- Calculate the correction factor ( $F_T$ ) to account for the effect of multipass heat exchangers
- Define and calculate the heat exchanger effectiveness factor ( $\epsilon$ )
- Define what is meant by the terms *mixed* and *unmixed* as applied to a cross-flow-exchanger
- Calculate and define the effect that fouling has on the overall heat-transfer coefficient
- Perform a simple thermal design of a double-pipe heat exchanger

## 16.1 Types of Exchangers

*1. Introduction.* In the process industries, the transfer of heat between two fluids is generally done in heat exchangers. The most common type is one in which the hot and cold fluids do not come into direct contact with each other, but are separated by a tube wall or a flat or curved surface. The transfer of heat from the hot fluid to the wall or tube surface is accomplished by convection through the tube wall or plate by conduction, and then by convection to the cold fluid. In the preceding sections of this book we have discussed the calculation procedures for these various steps. Now, we will discuss some of the types of equipment used and overall thermal analyses of exchangers.

Complete, detailed design methods have been highly developed and will not be considered here.

2. *Double-pipe heat exchanger.* The simplest exchanger is the double-pipe or concentric-pipe exchanger. This is shown in Fig. 16.1-1, where one fluid flows inside one pipe and the other fluid flows in the annular space between the two pipes. The fluids can be in cocurrent or countercurrent flow. The exchanger can be made from a pair of single lengths of pipe with fittings at the ends or from a number of pairs of pipe interconnected in series. This type of exchanger is useful mainly for small flow rates.

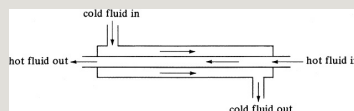


Figure 16.1-1. *Flow in a double-pipe heat exchanger.*



*3. Shell-and-tube exchanger.* If larger flows are involved, a shell-and-tube exchanger is used, which is the most important type of exchanger used in the process industries. In these exchangers, the flows are continuous. Many tubes in parallel are used, where one fluid flows inside these tubes. The tubes, arranged in a bundle, are enclosed in a single shell and the other fluid flows outside the tubes in the shell side. The simplest shell-and-tube exchanger is shown in Fig. 16.1-2a for one shell pass and one tube pass, or a 1–1 counterflow exchanger. The cold fluid enters and flows inside through all the tubes in parallel in one pass. The hot fluid enters at the other end and flows counterflow across the outside of the tubes. Cross-baffles are used so that the fluid is

forced to flow perpendicularly across the tube bank rather than parallel with it. The added turbulence generated by this cross-flow increases the shell-side heat-transfer coefficient.

In Fig. 16.1-2b, a 1–2 parallel–counterflow exchanger is shown. The liquid on the tube side flows in two passes, as shown, and the shell-side liquid flows in one pass. In the first pass of the tube side, the cold fluid is flowing counterflow to the hot shell-side fluid; in the second pass of the tube side, the cold fluid flows in parallel (cocurrent) with the hot fluid. Another type of exchanger has two shell-side passes and four tube passes. Sometimes, other combinations of number of passes are also used, with the 1–2 and 2–4 types being the most common.

4. *Cross-flow exchanger.* When a gas such as air is being heated or cooled, a common device used is the cross-flow heat exchanger shown in Fig. 16.1-3a. One of the fluids, which is a liquid, flows inside through the tubes, and the exterior gas flows across the tube bundle by forced or sometimes natural convection. The fluid inside the tubes is considered to be unmixed, since it is confined and cannot mix with any other stream. The gas flow outside the tubes is mixed, since it can move about freely between the tubes, and there will be a tendency for the gas temperature to equalize in the direction normal to the flow. For the unmixed fluid inside the tubes, there will be a temperature gradient both parallel and normal to the direction of flow.

A second type of cross-flow heat exchanger, shown in Fig. 16.1-3b, is typically used in air-conditioning and space-heating applications. In this type, the gas flows across a finned-tube bundle and is unmixed, since it is confined in separate flow channels between the fins as it passes over the tubes. The fluid in the tubes is unmixed.

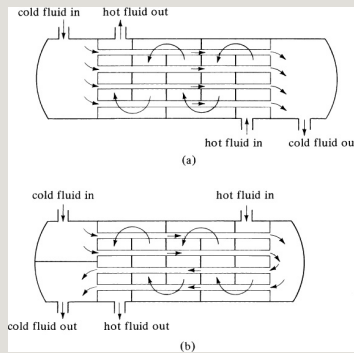


Figure 16.1-2. Shell-and-tube heat exchangers: (a) one shell pass and one tube pass (1-1 exchanger); (b) one shell pass and two tube passes (1-2 exchanger).

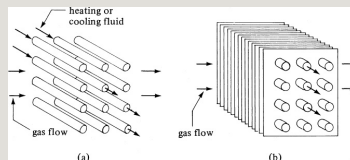


Figure 16.1-3. *Flow patterns of cross-flow heat exchangers: (a) one fluid mixed (gas) and one fluid unmixed; (b) both fluids unmixed.*

Discussions of other types of specialized heat-transfer equipment will be deferred to Section 15.8. The remainder of this section deals primarily with shell-and-tube and cross-flow heat exchangers.

## **16.2 Log-Mean-Temperature-Difference Correction Factors**

In Section 13.2B it was shown that when the hot and cold fluids in a heat exchanger are in true countercurrent flow or in cocurrent (parallel) flow, the log mean temperature difference should be used:

$$\Delta T_{lm} = \frac{\Delta T_2 - \Delta T_1}{\ln(\Delta T_2 / \Delta T_1)} \quad (16.2-1)$$

where  $\Delta T_2$  is the temperature difference at one end of the exchanger and  $\Delta T_1$  at the other end. This  $\Delta T_{1m}$  holds for a double-pipe heat exchanger and a 1–1 exchanger with one shell pass and one tube pass in parallel or counterflow.

In cases where a multiple-pass heat exchanger is involved, it is necessary to obtain a different expression for the mean temperature difference, depending on the arrangement of the shell and tube passes. Considering first the one-shell-pass, two-tube-pass exchanger in Fig. 16.1-2b, the cold fluid in the first tube pass is in counterflow with the hot fluid. In the second tube pass, the cold fluid is in parallel flow with the hot fluid. Hence, the log mean temperature difference, which applies either to parallel or to counterflow but not to a

mixture of both types (as in a 1–2 exchanger), cannot be used to calculate the true mean temperature drop without a correction.

The mathematical derivation of the equation for the proper mean temperature to use is quite complex. The usual procedure is to use a correction factor  $FT$  that is so defined that when it is multiplied by the  $\Delta T_{1m}$ , the product is the correct mean temperature drop  $\Delta T_m$  to use. In using the correction factors  $FT$ , it is immaterial whether the warmer fluid flows through the tubes or the shell (K1). The factor  $FT$  has been calculated (B1) for a 1–2 exchanger and is shown in Fig. 16.2-1a. Two dimensionless ratios are used as follows:

$$Z = \frac{T_{hi} - T_{ho}}{T_{co} - T_{ci}} \quad (16.2-2)$$

$$Y = T_{co} - T_{ci} / T_{hi} - T_{ci} \quad (16.2-3)$$

where  $T_{hi}$  = inlet temperature of hot fluid in K (°F),  $T_{ho}$  = outlet of hot fluid,  $T_{ci}$  inlet of cold fluid, and  $T_{co}$  = outlet of cold fluid.

In Fig. 16.2-1b, the factor  $F_T$  (B1) for a 2–4 exchanger is shown. In general, it is not recommended to use a heat exchanger for conditions under which  $F_T < 0.75$ . Another shell-and-tube arrangement should be used. Correction factors for two types of cross-flow exchanger are given in Fig. 16.2-2. Other types are available elsewhere (B1, P1).

Using the nomenclature of Eqs. (16.2-2) and (16.2-3), the  $\Delta T_{1m}$  of Eq. (16.2-1) can be written as



$$\Delta T_{lm} = (T_{hi} - T_{co}) - (T_{m} - T_{ci}) \left[ \frac{(T_{hi} - T_{co})}{(T_{ho} - T_{ci})} \right] \quad (16.2-4)$$

Then, the equation for an exchanger is

$$q = U_j A_j \Delta T_m = U_o A_o \Delta T_m \quad (16.2-5)$$

where

$$\Delta T_m = F T \Delta T_{lm} \quad (16.2-6)$$

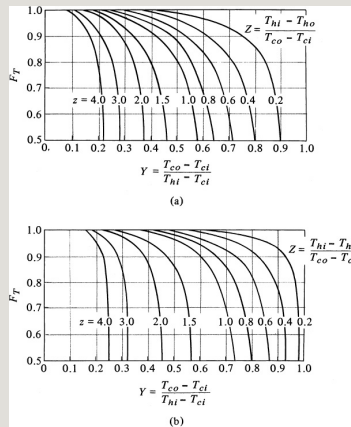


Figure 16.2-1. Correction factor  $F_T$  to log mean temperature difference: (a) 1–2 and 1–4 exchangers, (b) 2–4 exchangers. From R. A. Bowman, A. C. Mueller, and W. M. Nagle, Trans. A.S.M.E., **62**, 284, 285 (1940). With permission.

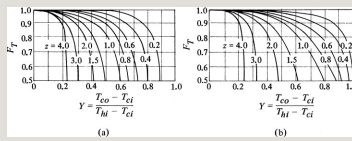


Figure 16.2-2. Correction factor  $F_T$  to log mean temperature difference for cross-flow exchangers [ $Z = (T_{hi} - T_{ho}) / (T_{co} - T_{ci})$ ] (a) single pass, shell fluid mixed, other fluid unmixed, (b) single pass, both fluids unmixed. From R. A. Bowman, A. C. Mueller, and W. M. Nagle, Trans. A.S.M.E., **62**, 288, 289 (1940). With permission.

### EXAMPLE 16.2-1. Temperature Correction Factor for a Heat Exchanger

A 1–2 heat exchanger containing one shell pass and two tube passes heats 2.52 kg/s of water from 21.1 to 54.4°C by using hot water under pressure entering at 115.6 and leaving at 48.9°C. The outside surface area of the tubes in the exchanger is  $A_o = 9.30 \text{ m}^2$ .

- Calculate the mean temperature difference  $\Delta T_m$  in the exchanger and the overall heat-transfer coefficient  $U_o$ .
- For the same temperatures but using a 2–4 exchanger, what would be the  $\Delta T_m$ ?

**Solution:** The temperatures are as follows:

$$T_{hi}=115.6^\circ\text{C} \quad T_{mi}=48.9^\circ\text{C} \quad T_{ci}=21.1^\circ\text{C} \quad T_{co}=54.4^\circ\text{C}$$

First making a heat balance on the cold water, assuming a  $c_{pm}$  of water of 4187 J/kg · K and  $T_{co} - T_{ci} = (54.4 - 21.1)^\circ\text{C} = 33.3^\circ\text{C} = 33.3 \text{ K}$ ,

$$q = \dot{m} c_{pm} (T_{co} - T_{ci}) = (2.52)(4187)(54.4 - 21.1) = 348200 \text{ W}$$

The log mean temperature difference using Eq. (16.2-4) is

$$\Delta T_{lm} = \frac{(115.6 - 54.4) - (48.9 - 21.1)}{\ln[(115.6 - 54.4) / (48.9 - 21.1)]} = 42.3^\circ\text{C} = 42.3 \text{ K}$$

Next, substituting into Eqs. (16.2-2) and (16.2-3),

$$Z = T_{hi} - T_{ho} T_{co} - T_{ci} = 115.6 - 48.954 \cdot 4 - 21.1 = 2.00 \quad (16.2-2)$$

$$Y = T_{co} - T_{ci} T_{hi} - T_{ci} = 54.4 - 21.1 \cdot 115.6 - 21.1 = 0.352 \quad (16.2-3)$$

From Fig. 16.2-1a,  $F_T = 0.74$ . Then, by Eq. (16.2-6),

$$\Delta T_m = F_T \Delta T_1 = 0.74(42.3) = 31.3^\circ\text{C} = 31.3\text{K} \quad (16.2-6)$$

Rearranging Eq. (16.2-5) to solve for  $U_o$  and substituting the known values, we have

$$U_o = \frac{q}{A_o \Delta T_m} = \frac{348200(9.30)}{(31.3)(211 \text{ bu/h} \cdot \text{ft}^2 \cdot ^\circ\text{F})} = 1196 \text{ W/m}^2 \cdot \text{K}$$

For part (b), using a 2–4 exchanger and Fig. 16.2-1b,  $F_T = 0.94$ . Then,

$$\Delta T_m = F_T \Delta T_1 = 0.94(42.3) = 39.8^\circ\text{C} = 39.8\text{K}$$

Hence, in this case the 2–4 exchanger utilizes more of the available temperature driving force.

## 16.3 Heat-Exchanger Effectiveness

*1. Introduction.* In the preceding section, the log mean temperature difference was used in the equation  $q = UA \Delta T_{lm}$  in the design of heat exchangers. This form is convenient when the inlet and outlet temperatures of the two fluids are known or can be determined by a heat balance. Then, the surface area

can be determined if  $U$  is known.

However, when the temperatures of the fluids leaving the exchanger are not known and a given exchanger is to be used, a tedious trial-and-error procedure is necessary. To solve these cases, a method called the heat-exchanger effectiveness  $\epsilon$  is used which does not involve any of the outlet temperatures.

The heat-exchanger effectiveness is defined as the ratio of the actual rate of heat transfer in a given exchanger to the maximum possible amount of heat transfer if an infinite heat-transfer area were available. The temperature profile for a counterflow heat exchanger is shown in Fig. 16.3-1.

## *2. Derivation of the effectiveness*

equation. The heat balance for the cold ( $C$ ) and hot ( $H$ ) fluids is

$$q = (m_{cp})_H (T_{Hi} - T_{Ho}) = (m_{cp})_C (T_{Co} - T_{Ci}) \quad (16.3-1)$$

Calling  $(m_{cp})_H = C_H$  and  $(m_{cp})_C = C_C$ , then in Fig. 16.3-1,  $C_H > C_C$ , and the cold fluid undergoes a greater temperature change than the hot fluid. Hence, we designate  $C_C$  as  $C_{\min}$  or minimum heat capacity. Then, if there is an infinite area available for heat transfer,  $T_{Co} = T_{Hi}$ . Then, the effectiveness  $\varepsilon$  is

$$\varepsilon = \frac{C_H (T_{Hi} - T_{Ho})}{C_C (T_{Hi} - T_{Ci})} = \frac{C_{\max} (T_{Hi} - T_{Ho})}{C_{\min} (T_{Hi} - T_{Ci})} \quad (16.3-2)$$

If the hot fluid is the minimum fluid,  $T_{Ho} = T_{Ci}$ , and

$$\varepsilon = \frac{C_{\min}(T_{\text{Co}} - T_{\text{Ci}})}{C_{\text{H}}(T_{\text{Hi}} - T_{\text{Ci}})} \quad (16.3-3)$$

In both equations, the denominators are the same and the numerator gives the actual heat transfer:

$$q = \varepsilon C_{\min}(T_{\text{Hi}} - T_{\text{Ci}}) \quad (16.3-4)$$

Note that Eq. (16.3-4) uses only inlet temperatures, which is an advantage when inlet temperatures are known and it is desired to predict the outlet temperatures for a given existing exchanger.

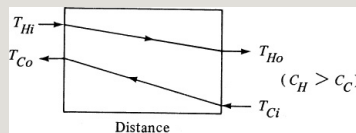


Figure 16.3-1. *Temperature profile for countercurrent heat exchanger.*

For the case of a single-pass counterflow exchanger, combining Eqs. (16.3-2) and (16.3-3),

$$\varepsilon = CH(T_{Hi} - T_{Ho})C_{min}(T_{Hi} - T_{Ci}) = CC(T_{Co} - T_{Ci})C_{min}(T_{Hi} - T_{Ci}) \quad (16.3-5)$$

We consider first the case when the cold fluid is the minimum fluid. Rewriting Eq. (13.2-20) using the present nomenclature,

$$q = CC(T_{Co} - T_{Ci}) = UA(T_{Ho} - T_o) - (T_{Hi} - T_{Co}) \ln[(T_{Ho} - T_{Ci}) / (T_{Hi} - T_{Co})] \quad (16.3-6)$$

Combining Eq. (16.3-1) with the left side of Eq. (16.3-5) and solving for  $T_{Hi}$ ,

$$T_{Hi} = T_{Ci} + 1/\varepsilon (T_{Co} - T_{Ci}) \quad (16.3-7)$$

Subtracting  $TC_o$  from both sides,

$$TH_i - TC_o = TC_i - TC_o + 1\epsilon(TC_o - TC_i) = (1\epsilon - 1)(TC_o - TC_i) \quad (16.3-8)$$

From Eq. (16.3-1) for  $C_{\min} = C_C$  and  $C_{\max} = C_H$ ,

$$TH_o = TH_i - C_{\min} C_{\max} (TC_o - TC_i) \quad (16.3-9)$$

This can be rearranged to give the following:

$$TH_o - TC_i = TH_i - TC_i - C_{\min} C_{\max} (TC_o - TC_i) \quad (16.3-10)$$

Substituting Eq. (16.3-7) into (16.3-10),

$$TH_o - TC_i = 1\epsilon(TC_o - TC_i) - C_{\min} C_{\max} (TC_o - TC_i) \quad (16.3-11)$$



Finally, substituting Eqs. (16.3-8) and (16.3-11) into (16.3-6), rearranging, taking the antilog of both sides, and solving for  $\epsilon$ ,

$$\epsilon = 1 - \exp[-UAC_{\min}(1 - C_{\min}C_{\max})] / [1 - C_{\min}C_{\max} \exp(-UAC_{\min}(1 - C_{\min}C_{\max}))] \quad (16.3-12)$$

We define NTU as the number of transfer units as follows:

$$NTU = UAC_{\min} \quad (16.3-13)$$

The same result would have been obtained if  $C_H = C_{\min}$ .

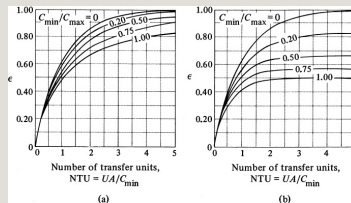


Figure 16.3-2. Heat-exchanger effectiveness  $\epsilon$ : (a) counterflow exchanger, (b) parallel flow exchanger.

For parallel flow we obtain

$$\epsilon = 1 - \exp[-C_{\min}(1 + C_{\min}C_{\max})] / 1 + C_{\min}C_{\max} \quad (16.3-14)$$

In Fig. 16.3-2, Eqs. (16.3-12) and (16.3-13) have been plotted in convenient graphical form. Additional charts are available for different shell-and-tube and cross-flow arrangements (K1).

**EXAMPLE 16.3-1. Effectiveness of a Heat Exchanger**

Water flowing at a rate of 0.667 kg/s enters a countercurrent heat exchanger at 308 K and is heated by an oil stream entering at 383 K at a rate of 2.85 kg/s ( $c_p = 1.89 \text{ kJ/kg} \cdot \text{K}$ ). The overall  $U = 300 \text{ W/m}^2 \cdot \text{K}$  and the area  $A = 15.0 \text{ m}^2$ . Calculate the heat-transfer rate and the exit-water temperature.

**Solution:** Assuming that the exit-water temperature is about 370 K, the  $c_p$  for water at an average temperature of  $(308 + 370)/2 = 339 \text{ K}$  is  $4.192 \text{ kJ/kg} \cdot \text{K}$  (Appendix A.2). Then,  $(mc_p)H = C_H = 2.85(1.89 \times 10^3) = 5387 \text{ W/K}$  and  $(mc_p)C = C_C = 0.667(4.192 \times 10^3) = 2796 \text{ W/K} = C_{\min}$ . Since  $C_C$  is the minimum,  $C_{\min}/C_{\max} = 2796/5387 = 0.519$ .

Using Eq. (16.3-13),  $\text{NTU} = UA/C_{\min} = 300(15.0)/2796 = 1.607$ . Using Fig. (16.3-2a) for a counterflow exchanger,  $\epsilon = 0.71$ . Substituting into Eq. (16.3-4),

$$q = \epsilon C_R (\text{THi} - \text{TCi}) = 0.71(2796)(383 - 308) = 148900 \text{ W}$$

Using Eq. (16.3-1),

$$q=148\,900=2796(T_{Co}-308)$$

Solving,  $T_{Co} = 361.3\text{ K}$ .

## 16.4 Fouling Factors and Typical Overall $U$ Values

In actual practice, heat-transfer surfaces do not remain clean. Dirt, soot, scale, and other deposits form on one or both sides of the tubes of an exchanger and on other heat-transfer surfaces. These deposits offer additional resistance to the flow of heat and reduce the overall heat-transfer coefficient  $U$ . In petroleum processes, coke and other substances can be deposited. Silting and deposits of mud and other materials can occur. Corrosion products that could constitute a serious resistance to heat transfer may form on the surfaces. Biological growth such as

algae can occur with cooling water and in the biological industries.

To avoid or lessen these fouling problems, chemical inhibitors are often added to minimize corrosion, salt deposition, and algae growth. Water velocities above 1 m/s are generally used to help reduce fouling. Large temperature differences may cause excessive deposition of solids on surfaces and should be avoided if possible.

The effect of such deposits and fouling is usually taken care of in design by adding a term for the resistance of the fouling on the inside and outside of the tube in Eq. (13.2-7) as follows:

$$U_j = \frac{1}{\frac{1}{h_i} + \frac{1}{h_{di}} + \frac{(r_o - r_i)A_i}{k_{AAA}}} \quad 1 \text{ m}$$

$$+A_i/A_{o,i}+A_i/A_{o,d}(16.4-1)$$

where  $h_{di}$  is the fouling coefficient for the inside and  $h_{do}$  the fouling coefficient for the outside of the tube in  $\text{W/m}^2 \cdot \text{K}$ . A similar expression can be written for  $U_o$  using Eq. (13.2-8).

Fouling coefficients recommended for use in designing heat-transfer equipment are available in many references (P2, N1). A short tabulation of some typical fouling coefficients is given in Table 16.4-1.

Table 16.4-1. *Typical Fouling Coefficients (P2, N1)*

Table 16.4-2. *Typical Values of Overall Heat-Transfer Coefficients in Shell-and-*

In order to perform preliminary estimates of sizes of shell-and-tube heat exchangers, typical values of overall heat-transfer coefficients are given in Table 16.4-2. These values should be useful as a check on the results of the design methods described in this chapter.

### **16.5 Double-Pipe Heat Exchanger**

In this section we will perform a thermal design of a double-pipe heat exchanger using the following example.

***EXAMPLE 16.5-1. Simplified Thermal Design of a Double-Pipe Heat Exchanger***

After fermentation, a mixture of ethanol and water is sent to a small distillation column. At the top of the distillation column, a 95% ethanol solution at 65°C is produced at a

flow rate of 3.5 kg/s. Your job is to design a double-pipe heat exchanger that will cool the 95% ethanol mixture to 40°C by using cooling water that is available at 10°C. Assume an outlet temperature of the cooling water of 55°C, and only use Schedule 40 pipe from **Appendix A.5**. Do not do viscosity corrections for heat transfer coefficients and the 95% ethanol solution will be pumped to the inside pipe.

*Step 1:* Complete the energy balance and calculate the amount of cooling water: Given an average heat capacity of the 95% ethanol solution of 2.6kJ/kg·K, then the heat lost by the 95% ethanol would be:

$$Q = mC_p\Delta T = (3.5 \text{ kgs})(2.6 \text{ kJ/kg}\cdot\text{K})(65^\circ\text{C} - 40^\circ\text{C}) = 227.5 \text{ kW}$$

Assuming that the system is adiabatic, then all the heat lost from the 95% ethanol solution will be gained by the cooling water. Thus, the mass flow rate of cooling water is equal to

$$m_{CW} = Q/C_p\Delta T = 227.5 \text{ kW} / (4.181 \text{ kJ/kg}\cdot\text{K}) \cdot (55^\circ\text{C} - 10^\circ\text{C}) = 1.209 \text{ kgs}$$

where the average heat capacity of the water is 4.181 kJ/kg·K, as shown in **Appendix A.2-5**.

*Step 2:* Calculate inner tube diameter and velocity:

Given an average density of the 95% ethanol solution of 816 kg/m<sup>3</sup> and estimating the inner tube velocity at 1 m/s to facilitate turbulence, the inner tube cross-sectional area and diameter are:

$$\begin{aligned} \text{Area} &= m_p \cdot v = 3.5 \text{ kgs} / (816 \text{ kg/m}^3) \\ (1 \text{ m/s}) &= 4.289 \times 10^{-3} \text{ m}^2 \\ \text{Diameter} &= D = \sqrt{4 \text{ACS} / \pi} = \sqrt{(4) / (4.289 \times 10^{-3} \text{ m}^2)} \pi = 0.074 \text{ m} = 74 \text{ mm} \end{aligned}$$

Looking at **Appendix A.5-1** and assuming that Schedule 40 pipe will suffice, the minimum nominal pipe size is 3 in. With this pipe choice, the inner diameter/area is 77.92 mm/4.769 × 10<sup>-3</sup> m<sup>2</sup>, which is slightly larger than the 74 mm/4.289 × 10<sup>-3</sup> m<sup>2</sup> required above, so we will have to calculate the true velocity given the pipe size chosen.

$$v = m_p / A_{cs} = 3.5 \text{ kgs} / (4.769 \times 10^{-3} \text{ m}^2) = 0.9 \text{ ms}$$

*Step 3:* Choose an outer tube diameter and calculate velocity:

Logically, the outer pipe must have a larger diameter than

the inside pipe. Looking at **Appendix A.5-1** and assuming that Schedule 40 pipe will suffice, the next largest pipe would be 3.5-in. Schedule 40 with an inside diameter of 90.12 mm and an outside diameter of 101.6 mm. However, this would only give a difference of around 1 mm between the outside diameter of the inside pipe to the inside diameter of the outside pipe (annulus). Thus, a better choice is 4.0-in. Schedule 40 with an inside diameter of 102.3 mm and an outside diameter of 114.3 mm. Therefore, the cross-sectional area available for flow in the annulus is

$$A_{csO} = \pi 4 (D_{iO} - D_o) = \pi 4 (102.3 \text{ mm} - 88.90 \text{ mm}) = 2.012 \times 10^{-3} \text{ m}^2$$

From this area and the calculated flowrate of the cooling water ( $\rho = 996 \text{ kg/m}^3$ ), the velocity of the water is

$$V_{cw} = m_{cw} / A_{csO} = 1.209 \text{ kg/s} / (2.012 \times 10^{-3} \text{ m}^2) = 0.603 \text{ m/s}$$

While the velocity is lower than 1 m/s, we will assume that we obtain turbulence, which enhances heat transfer.

*Step 4:* Calculate the inside heat-transfer coefficient from Eq. (15.3-5):

The viscosity and thermal conductivity of the 95% ethanol solution is  $9.72 \times 10^{-4} \text{ kg/(m} \cdot \text{s)}$  and  $0.175 \text{ W/(m} \cdot \text{K)}$  respectively, thus:

$$N_{Re,i} = D_{vp} \rho / \mu = (77.92 \text{ mm})(0.9 \text{ m/s}) / (9.72 \times 10^{-4} \text{ kg/m} \cdot \text{s}) = 58839$$

$$N_{Pr,i} = C_p \mu / k = (2.6 \text{ J/kg} \cdot \text{K})(9.72 \times 10^{-4} \text{ kg/m} \cdot \text{s}) / (0.175 \text{ W/m} \cdot \text{K}) = 14.441$$

*Step 5:* Calculate the outside heat transfer coefficient from Eq. (15.3-7):

Before using Eq. (15.3-7), we need to calculate the average cooling-water temperature and the equivalent diameter of the annular space.

$$T_{avg} = 100^\circ\text{C} + 55^\circ\text{C} / 2 = 32.5^\circ\text{C}$$

$$D_{eO} = 102.3 \text{ mm} - 88.9 \text{ mm} = 13.4 \text{ mm} = 0.0134 \text{ m}$$

Now, we can use the simplified equation for water to calculate the outside heat-transfer coefficient.



$$h_o = 1428[1 + 0.0146(\text{ToC})]v^{0.8} D^{0.2} = 1428[1 + 0.0146(32.5)](0.603)^{0.8}(0.0134)^{0.2} = 3348.4 \text{ W/m}^2\cdot\text{K}$$

*Step 6:* Calculate the outside overall heat-transfer coefficient ( $U_o$ ):

This is just the sum of the resistances. At this point, fouling coefficients (Table 16.4-1) could be added for completeness but this will be ignored for this example, along with the conduction through the Schedule 40 pipe. The heat transfer of interest in this design problem is the convection that occurs between the fluids. Due to sagging problems, we will limit the pipe length to 6 m and make bends in the pipe to get the necessary area needed for the design. In addition, we need to calculate the surface area where heat transfer occurs; this area is different from the cross-sectional area we needed to calculate for velocity.

$$L_p = 6 \text{ m} \quad A_o = \pi D O L_p = \pi(0.0889 \text{ m})(6 \text{ m}) = 1.676 \text{ m}^2 \quad A_j = \pi D_j L_p = \pi(0.07792 \text{ m})(6 \text{ m}) = 1.469 \text{ m}^2$$

Now, we can sum the resistances and calculate the overall heat-transfer coefficient.

$$R = 1/h_i \cdot A_i + 1/h_o \cdot A_o = 1/(966 \text{ W/m}^2\cdot\text{K})(1.469 \text{ m}^2) + 1/(3348.4 \text{ W/m}^2\cdot\text{K})(1.676 \text{ m}^2) = 8.83 \times 10^{-4} \text{ KW} \quad U_o = 1/R \cdot A_o = 1/(8.83 \times 10^{-4} \text{ KW})(1.676 \text{ m}^2) = 675.85 \text{ W/m}^2\cdot\text{K}$$

*Step 7:* Calculate the area needed for heat transfer and the number of bends needed:

Since we will design the exchanger in a counter-current fashion, we must calculate the log mean temperature difference.



Now, with the  $\Delta T_{lm}$  we will calculate the heat transfer area needed:

$$Q = (U_o A_o) \Delta T_{lm} \quad (U_o A_o) \Delta T_{lm} = Q \quad (675.9 \text{ W/m}^2\cdot\text{K}) \Delta T_{lm} = 227.5 \text{ kW} \quad \Delta T_{lm} = 227.5 \text{ kW} / (675.9 \text{ W/m}^2\cdot\text{K}) = 337.5 \text{ K}$$

Again, we are limited to 6-m-long pipe and thus we may not have enough area to satisfy the required area needed for heat transfer (18.49 m<sup>2</sup>), so we may need to bend the pipe.

The number of bends needed is equal to the total area needed for heat transfer divided by the surface area of one 6-m pipe at the chosen diameter:

$$N_{\text{bends}} = \frac{HEA}{A_o} = \frac{18.49 \text{ m}^2}{1.676 \text{ m}^2} = 11.03$$

Thus, we will need 11 bends to get the necessary area needed to accomplish the thermal design. As stated in the example heading, this is a simplified thermal design; there is much more to consider, such as pressure drop, before the true design can be accomplished.

## 16.6 Chapter Summary

### Three Common Types of Heat Exchangers

- Double pipe
- Shell and tube
- Cross-flow

### Log Mean Temperature Difference

$$\Delta T_{lm} = \frac{\Delta T_2 - \Delta T_1}{\ln(\Delta T_2 / \Delta T_1)} \quad (16.2-1)$$

### Correction Factor for Multipass Exchangers

$$q = U_j A_j \Delta T_m = U_o A_o \Delta T_m \quad (16.2-5)$$

where

$$\Delta T_m = F_T \Delta T_{1m} \quad (16.2-6)$$

$F_T$  will be obtained from Figures 16.2-1 and 16.2-2.

### Heat Exchanger Effectiveness

If the cold fluid is the minimum fluid,  $T_{Co} = T_{Hi}$ , then the effectiveness  $\varepsilon$  is

$$\varepsilon = \frac{C_H(T_{Hi} - T_{Ho})}{C_{\max}(T_{Hi} - T_{Ci})} = \frac{C_{\min}(T_{Hi} - T_{Co})}{C_{\min}(T_{Hi} - T_{Ci})} \quad (16.3-2)$$

If the hot fluid is the minimum fluid,  $T_{Ho} = T_{Ci}$ , and

$$\varepsilon = \frac{C_C(T_{Co} - T_{Ci})}{C_{\max}(T_{Hi} - T_{Ci})} = \frac{C_{\min}(T_{Ho} - T_{Ci})}{C_{\min}(T_{Hi} - T_{Ci})} \quad (16.3-3)$$

In both equations, the denominators are the same and the numerator gives the

actual heat transfer:

$$q = \epsilon C_{\min}(T_{Hi} - T_{Ci}) \quad (16.3-4)$$

### Fouling Factors and Overall U Values

$$U_j = \frac{1}{\frac{1}{h_i} + \frac{1}{h_{di}} + \frac{(r_o - r_i)A_i}{k_A} + \frac{1}{h_{do}} + \frac{A_i}{A_o h_o}} \quad (16.4-1)$$

## Problems

### 16.2-1. *Mean Temperature*

***Difference in an Exchanger.*** A 1–2 exchanger with one shell pass and two tube passes is used to heat a cold fluid from 37.8°C to 121.1°C by using a hot fluid entering at 315.6°C and leaving at 148.9°C. Calculate the  $\Delta T_{lm}$  and the mean temperature difference  $\Delta T_m$  in K.

**Ans.**  $\Delta T_{lm} = 148.9 \text{ K}$ ,  $\Delta T_m = 131.8 \text{ K}$

### 16.2-2. *Cooling Oil by Water in an*

**Exchanger.** Oil flowing at the rate of  $5.04 \text{ kg/s}$  ( $c_{pm} = 2.09 \text{ kJ/kg} \cdot \text{K}$ ) is cooled in a 1–2 heat exchanger from  $366.5 \text{ K}$  to  $344.3 \text{ K}$  by  $2.02 \text{ kg/s}$  of water entering at  $283.2 \text{ K}$ . The overall heat-transfer coefficient  $U_o$  is  $340 \text{ W/m}^2 \cdot \text{K}$ . Calculate the area required. (*Hint:* A heat balance must first be made to determine the outlet water temperature.)

**16.2-3. Heat Exchange Between Oil and Water.** Water is flowing at the rate of  $1.13 \text{ kg/s}$  in a 1–2 shell-and-tube heat exchanger, and is heated from  $45^\circ\text{C}$  to  $85^\circ\text{C}$  by an oil having a heat capacity of  $1.95 \text{ kJ/kg} \cdot \text{K}$ . The oil enters at  $120^\circ\text{C}$  and leaves at  $85^\circ\text{C}$ . Calculate the area of the exchanger if the overall heat-transfer coefficient is  $300 \text{ W/m}^2 \cdot \text{K}$ .

**16.3-1. Outlet Temperature and**

***Effectiveness of an Exchanger.*** Hot oil at a flow rate of 3.00 kg/s ( $c_p = 1.92 \text{ kJ/kg} \cdot \text{K}$ ) enters an existing counterflow exchanger at 400 K and is cooled by water entering at 325 K (under pressure) and flowing at a rate of 0.70 kg/s. The overall  $U = 350 \text{ W/m}^2 \cdot \text{K}$  and  $A = 12.9 \text{ m}^2$ . Calculate the heat-transfer rate and the exit oil temperature.

### References

### Notation

# Chapter 17. Introduction to Radiation Heat Transfer

## 17.0 Chapter Objectives

On completion of this chapter, a student should be able to:

- Calculate radiation heat transfer between black body surfaces
- Calculate radiation heat transfer between diffuse and grey surfaces
- Evaluate radiation view factors and use approximations given by Kirchhoff's law

## 17.1 Introduction to Radiation Heat-Transfer Concepts

### 17.1A Introduction and Basic Equation for Radiation

*1. Nature of radiant heat transfer.* In the preceding chapters of the book, we have studied conduction and

convection heat transfer. In conduction, heat is transferred from one part of a body to another, and the intervening material is heated. In convection, heat is transferred by the actual mixing of materials and by conduction. In radiant heat transfer, the medium through which the heat is transferred is usually not heated. Radiation heat transfer is the transfer of heat by electromagnetic radiation.

Thermal radiation is a form of electromagnetic radiation similar to X-rays, light waves, gamma rays, and so on, differing only in wavelength. It obeys the same laws as light: it travels in straight lines, can be transmitted through space and vacuum, and so on. It is an important mode of heat transfer and is especially important where large



temperature differences occur, as, for example, in a furnace with boiler tubes, in radiant dryers, or in an oven baking food. Radiation often occurs in combination with conduction and convection. An elementary discussion of radiant heat transfer will be given here, with a more advanced and comprehensive discussion being given in Section 17.4.

In an elementary sense, the mechanism of radiant heat transfer is composed of three distinct steps or phases:

1. The thermal energy of a hot source, such as the wall of a furnace at  $T_1$ , is converted into energy in the form of electromagnetic-radiation waves.
2. These waves travel through the intervening space in straight lines and strike a cold object at  $T_2$ , such as a furnace tube containing water to be heated.
3. The electromagnetic waves that strike the body are absorbed by the body and converted back to thermal

energy or heat.

*2. Absorptivity and black bodies.* When thermal radiation (such as light waves) falls upon a body, part is absorbed by the body in the form of heat, part is reflected back into space, and part may actually be transmitted through the body. For most cases in process engineering, bodies are opaque to transmission, so this will be neglected. Hence, for opaque bodies,

$$\alpha + \rho = 1.0 \quad (17.1-1)$$

where  $\alpha$  is absorptivity or fraction absorbed and  $\rho$  is reflectivity or fraction reflected.

A *black body* is defined as one that absorbs all radiant energy and reflects none. Hence,  $\rho = 0$  and  $\alpha = 1.0$  for a

black body. Actually, in practice there are no perfect black bodies, but a close approximation is a small hole in a hollow body, as shown in Fig. 17.1-1. The inside surface of the hollow body is blackened by charcoal. The radiation enters the hole and impinges on the rear wall; part is absorbed there and part is reflected in all directions. The reflected rays impinge again, part is absorbed, and the process continues. Hence, essentially all of the energy entering is absorbed and the area of the hole acts as a perfect black body. The surface of the inside walls is “rough” and rays are scattered in all directions, unlike a mirror, where they are reflected at a definite angle.

As stated previously, a black body absorbs all radiant energy falling on it

and reflects none. Such a black body also emits radiation, depending on its temperature, and does not reflect any. The ratio of the emissive power of a surface to that of a black body is called *emissivity*  $\epsilon$  and is 1.0 for a black body. Kirchhoff's law states that at the same temperature  $T_1$ ,  $\alpha_1$  and  $\epsilon_1$  of a given surface are the same, or

$$\alpha_1 = \epsilon_1 \quad (17.1-2)$$

Equation (17.1-2) holds for any black or nonblack solid surface.

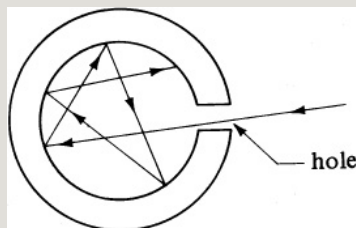


Figure 17.1-1. *Concept of a perfect black body.*

Table 17.1-1. *Total Emissivity,  $\epsilon$ , of*

## *Various Surfaces*

### *3. Radiation from a body and emissivity.*

The basic equation for heat transfer by radiation from a perfect black body with an emissivity  $\epsilon = 1.0$  is

$$q = A\sigma T^4 \quad (17.1-3)$$

where  $q$  is heat flow in W,  $A$  is  $m^2$  surface area of the body,  $\sigma$  is a constant  $5.676 \times 10^{-8} \text{ W/m}^2 \cdot \text{K}^4$  ( $0.1714 \times 10^{-8} \text{ btu/h} \cdot \text{ft}^2 \cdot ^\circ\text{R}^4$ ) and  $T$  is the temperature of the black body in K ( $^\circ\text{R}$ ).

For a body that is not a black body and has an emissivity  $\epsilon < 1.0$ , the emissive power is reduced by  $\epsilon$ , or

$$q = A\epsilon\sigma T^4 \quad (17.1-4)$$

Substances that have emissivities of less than 1.0 are called *gray bodies* when the emissivity is independent of the wavelength. All real materials have an emissivity  $\epsilon < 1$ .

Since the emissivity  $\epsilon$  and absorptivity  $\alpha$  of a body are equal at the same temperature, the emissivity, like absorptivity, is low for polished metal surfaces and high for oxidized metal surfaces. Typical values are given in Table 17.1-1 but do vary some with temperature. Most nonmetallic substances have high values. Additional data are tabulated in Appendix A.3.

#### **17.1B Radiation to a Small Object from Its Surroundings**

In the case of a small gray object of area  $A_1$  m<sup>2</sup> at temperature  $T_1$  in a large enclosure at a higher

temperature  $T_2$  there is a net radiation to the small object. The small body emits an amount of radiation to the enclosure given by Eq. (17.1-4) as  $A_1 \epsilon_1 \sigma T_1^4$ . The emissivity  $\epsilon_1$  of this body is taken at  $T_1$ . The small body also absorbs an amount of energy from its surroundings at  $T_2$  given by as  $A_1 \alpha_{12} \sigma T_2^4$ . The  $\alpha_{12}$  is the absorptivity of body 1 for radiation from the enclosure at  $T_2$ . The value of  $\alpha_{12}$  is approximately the same as the emissivity of this body at  $T_2$ . The net heat of absorption is then, by the Stefan–Boltzmann equation,

$$\begin{aligned}
 q &= A_1 \epsilon_1 \sigma T_1^4 - A_1 \alpha_{12} \sigma T_2^4 = A_1 \sigma (\epsilon_1 T_1^4 - \alpha_{12} T_2^4) \\
 &\quad (17.1-5)
 \end{aligned}$$

A further simplification of Eq. (17.1-5) is usually made for engineering purposes by using only one emissivity for the small body, at temperature  $T_2$ . Thus,

$$q = A_1 \epsilon \sigma (T_1^4 - T_2^4) \quad (17.1-6)$$

**EXAMPLE 17.1-1. Radiation to a Metal Tube**

A small, oxidized, horizontal metal tube with an OD of 0.0254 m (1 in.), 0.61 m (2 ft) long, and with a surface temperature at 588 K (600°F) is in a very large furnace enclosure with fire-brick walls and the surrounding air at 1088 K (1500°F). The emissivity of the metal tube is 0.60 at 1088 K and 0.46 at 588 K. Calculate the heat transfer to the tube by radiation using SI units.

**Solution:** Since the large-furnace surroundings are very large compared to the small enclosed tube, the surroundings, even if gray, when viewed from the position of the small body appear black, and Eq. (17.1-6) is applicable. Substituting given values into Eq. (17.1-6) with an  $\epsilon$  of 0.6 at 1088 K,

$$A_1 = \pi D L = \pi (0.0254 \text{ m}) (0.61 \text{ m}) = 0.049 \text{ m}^2 \quad q = A_1 \epsilon \sigma (T_1^4 - T_2^4) = (0.049 \text{ m}^2) (0.6) (5.676 \times 10^{-8} \text{ W m}^2 \cdot \text{K}^{-4}) = -2130 \text{ W}$$

Other examples of small objects in large enclosures occurring in the process industries are a loaf of bread in an oven



receiving radiation from the walls around it, a package of meat or food radiating heat to the walls of a freezing enclosure, a hot ingot of solid iron cooling and radiating heat in a large room, and a thermometer measuring the temperature in a large duct.

### **17.1C Effect of Radiation on the Temperature Measurement of a Gas**

When a temperature sensor or probe (thermometer, thermocouple, etc.) is used to measure the temperature of a gas flowing in an enclosure, significant errors can occur.

Radiation heat exchange will take place between the sensor and the wall and convection heat transfer between the sensor and the gas. The sensor will indicate a temperature between the true gas and wall surface temperatures. This is shown

in Fig. 17.1-2, where the wall temperature  $T_w$  is less than the true gas temperature  $T_g$ .

The equations for the heat transfer  $q_c$  by convection to the probe and radiation  $q_r$  from the probe to the wall are as follows for  $T_w < T_g$ :

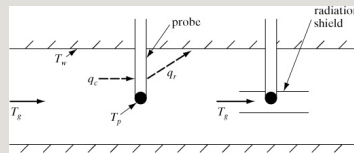


Figure 17.1-2. Temperature measurement of a gas showing radiation and convection heat transfer for a bare probe and a shielded probe.

$$q_c = hcA_p(T_g - T_p) = q_r = \epsilon A_p (5.676) \\ (T_p 100)^4 - (T_w 100)^4 \quad (17.7-7)$$

where  $A_p$  is the area of the tube in  $m^2$  and  $\epsilon$  is the emissivity of the probe.

**EXAMPLE 17.1-2. Effect of Radiation on Temperature Measurement in a Gas**

A thermocouple is measuring the temperature of hot air flowing in a pipe whose walls are at  $T_w = 400 \text{ K}$  ( $260^\circ\text{F}$ ). The true gas temperature  $T_g = 465 \text{ K}$  ( $377^\circ\text{F}$ ). Calculate the temperature  $T_p$  indicated by the thermocouple. The emissivity of the probe is assumed as  $\epsilon = 0.6$  and the convection heat-transfer coefficient  $h_c = 40 \text{ W/m}^2 \cdot \text{K}$ .

**Solution:** Substituting into Eq. (17.1-7) for convection,  $q_c$ , and for radiation,  $q_r$ ,

$$q_c = h_c A_p (T_g - T_p) = 40 A_p (465 - T_p) \quad q_r = 0.6 A_p (5.676) \left[ \left( \frac{T_p}{100} \right)^4 - \left( \frac{400}{100} \right)^4 \right]$$

Equating  $q_c = q_r$ , canceling out the term  $A_p$ , and solving,  $T_p = 451.4 \text{ K}$ . Hence, the thermocouple reading of  $T_p = 451.4 \text{ K}$  ( $352.5^\circ\text{F}$ ) is  $13.6 \text{ K}$  ( $24.5^\circ\text{F}$ ) lower than the true gas temperature of  $465 \text{ K}$  ( $377^\circ\text{F}$ ).

Probes with a radiation shield, as shown in Fig. 17.1-2, are often used to reduce radiation errors. The shield will have a temperature that is closer to the gas temperature than is the wall. Since the probe now radiates heat to a surface that is closer to the gas temperature, the radiation loss is less. It can be shown that with one shield, the radiation heat loss will be halved. Multiple shields can be used to further reduce the error. Using a polished surface on the probe to

reduce the emissivity lowers the radiation heat loss. This also reduces the measurement error.

## **17.2 Basic and Advanced Radiation Heat-Transfer Principles**

### **17.2A Introduction and Radiation Spectrum**

*1. Introduction.* This section will cover some basic principles together with some advanced topics on radiation. The exchange of radiation between two surfaces depends upon the size, shape, and relative orientation of these two surfaces and also upon their emissivities and absorptivities. In the cases to be considered, the surfaces are separated by nonabsorbing media such as air. When gases such as  $\text{CO}_2$  and  $\text{H}_2\text{O}$  vapor are present, some absorption by the gases occurs,

which is not considered until later in this section.

*2. Radiation spectrum and thermal radiation.* Energy can be transported in the form of electromagnetic waves, which travel at the speed of light.

Bodies may emit many forms of radiant energy, such as gamma rays, thermal energy, radio waves, and so on. In fact, there is a continuous spectrum of electromagnetic radiation. This electromagnetic spectrum is divided into a number of wavelength ranges, such as cosmic rays ( $\lambda < 10^{-13}$  m), gamma rays ( $\lambda = 10^{-13}$  to  $10^{-10}$  m), thermal radiation ( $\lambda = 10^{-7}$  to  $10^{-4}$  m), and so on. The electromagnetic radiation produced solely because of the temperature of the emitter is called thermal radiation and exists between the wavelengths of  $10^{-7}$

and  $10^{-4}$  m. This portion of the electromagnetic spectrum is of importance in radiant thermal heat transfer. Electromagnetic waves having wavelengths between  $3.8 \times 10^{-7}$  and  $7.6 \times 10^{-4}$  m, called *visible radiation*, can be detected by the human eye. This visible radiation lies within the thermal radiation range.

When different surfaces are heated to the same temperature, they do not all emit or absorb the same amount of thermal radiant energy. A body that absorbs and emits the maximum amount of energy at a given temperature is called a *black body*. A black body is a standard to which other bodies can be compared.

*3. Planck's law and emissive power.*

When a black body is heated to a temperature  $T$ , photons are emitted from the surface that have a definite distribution of energy. Planck's equation relates the monochromatic emissive power  $E_{B\lambda}$  in  $\text{W/m}^2$  at a temperature  $T$  in K and a wavelength in m:

$$E_{B\lambda} = 3.7418 \times 10^{-16} \lambda^{-5} [e^{1.4388 \times 10^{-2} \lambda T} - 1]^{-1} \quad (17.2-1)$$

A plot of Eq. (17.2-1) is given in Fig. 17.2-1 and shows that the energy given off increases with  $T$ . Also, for a given  $T$ , the emissive power reaches a maximum value at a wavelength that decreases as the temperature  $T$  increases. At a given temperature, the radiation emitted extends over a spectrum of wavelengths. The visible-light spectrum occurs in the low  $\lambda$  region. The sun has a temperature

of about 5800 K and the solar spectrum straddles this visible range.

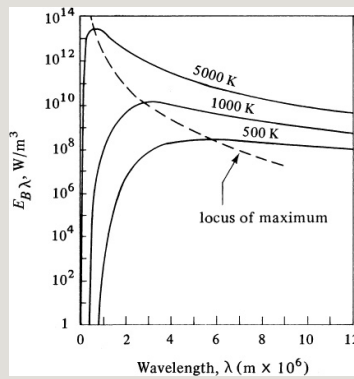


Figure 17.2-1. Spectral distribution of total energy emitted by a black body at various temperatures of the black body.

For a given temperature, the wavelength at which the black-body emissive power is a maximum can be determined by differentiating Eq. (17.2-1) with respect to  $\lambda$  at constant  $T$  and setting the result equal to zero. The result is as follows and is known as *Wien's displacement law*:

$$\lambda_{\max} T = 2.898 \times 10^{-3} \text{ m} \cdot \text{K} \quad (17.2-2)$$



The locus of the maximum values is shown in Fig. 17.2-1.

4. *Stefan–Boltzmann law*. The total emissive power is the total amount of radiation energy per unit area leaving a surface with temperature  $T$  over all wavelengths. For a black body, the total emissive power is given by the integral of Eq. (17.2-1) at a given  $T$  over all wavelengths, or the area under the curve in Fig. 17.2-1:

$$E_B = \int_0^\infty E_{B\lambda} d\lambda \quad (17.2-3)$$

This gives

$$E_B = \sigma T^4 \quad (17.2-4)$$

The result is the Stefan–Boltzmann law with  $\sigma = 5.676 \times 10^{-8} \text{ W/m}^2 \cdot \text{K}^4$ . The units of  $E_B$  are  $\text{W/m}^2$ .

5. *Emissivity and Kirchhoff's law.* An important property in radiation is the emissivity of a surface. The *emissivity*  $\epsilon$  of a surface is defined as the total emitted energy of the surface divided by the total emitted energy of a black body at the same temperature:

$$\epsilon = \frac{E}{E_B} = \frac{E}{\sigma T^4} \quad (17.2-5)$$

Since a black body emits the maximum amount of radiation,  $\epsilon$  is always 1.0.

We can derive a relationship between the absorptivity  $\alpha_1$  and emissivity  $\epsilon_1$  of a material by placing this material in an isothermal enclosure and allowing the body and enclosure to reach the same temperature at thermal equilibrium. If  $G$  is the irradiation on the body, the energy absorbed must equal the energy emitted:

$$\alpha_1 G = E_1 \quad (17.2-6)$$

If this body is removed and replaced by a black body of equal size, then at equilibrium,

$$\alpha_2 G = E_B \quad (17.2-7)$$

Dividing Eq. (17.2-6) by (17.2-7),

$$\alpha_1 \alpha_2 = E_1 E_B \quad (17.2-8)$$

However,  $\alpha_2 = 1.0$  for a black body.

Hence, since  $E_1/E_B = \epsilon_1$ ,

$$\alpha_1 = E_1 E_B = \epsilon_1 \quad (17.2-9)$$

This is Kirchhoff's law, which states that at thermal equilibrium  $\alpha = \epsilon$  of a body. When a body is not at equilibrium with its surroundings, the result is not valid.

6. *Concept of gray body.* A gray body is defined as a surface for which the monochromatic properties are constant over all wavelengths. For a gray surface,

$$\varepsilon_{\lambda} = \text{const.}, \alpha_{\lambda} = \text{const.}, (17.2-10)$$

Hence, the total absorptivity  $\alpha$  and the monochromatic absorptivity  $\alpha_{\lambda}$  of a gray surface are equal, as are  $\varepsilon$  and  $\varepsilon_{\lambda}$ :

$$\alpha = \alpha_1, \varepsilon = \varepsilon_1 (17.2-11)$$

Applying Kirchhoff's law to a gray body,  $\alpha_{\lambda} = \varepsilon_{\lambda}$  and

$$\alpha = \varepsilon (17.2-12)$$

As a result, the total absorptivity and emissivity are equal for a gray body even if the body is not in thermal equilibrium with its surroundings.

Gray bodies do not exist in practice; the concept of a gray body is an idealized one. The absorptivity of a surface actually varies with the wavelength of the incident radiation. Engineering calculations can often be based on the assumption of a gray body with reasonable accuracy. The  $\alpha$  is assumed constant even with a variation in  $\lambda$  of the incident radiation. Also, in actual systems, various surfaces may be at different temperatures. In these cases,  $\alpha$  for a surface is evaluated by determining the emissivity, not at the actual surface temperature but at the temperature of the source of the other radiating surface or emitter, since this is the temperature the absorbing surface would reach if the absorber and emitter were at thermal equilibrium. The temperature of the absorber has only a slight effect on the

absorptivity.

### **17.2B Derivation of View Factors in Radiation for Various Geometries**

*1. Introduction.* The concepts and definitions presented in Section 17.2A provide a sufficient foundation so that the net radiant exchange between surfaces can be determined. If two surfaces are arranged so that radiant energy can be exchanged, a net flow of energy will occur from the hotter surface to the colder surface. The size, shape, and orientation of two radiating surfaces or a system of surfaces are factors in determining the net heat-flow rate between them. To simplify the discussion, we assume that the surfaces are separated by a nonabsorbing medium such as air. This assumption is adequate for

many engineering applications.

However, in cases such as a furnace, the presence of  $\text{CO}_2$  and  $\text{H}_2\text{O}$  vapor makes such a simplification impossible because of their high absorptivities.

We will consider the simplest geometrical configuration first, that of radiation exchange between parallel, infinite planes. This assumption implies that there are no edge effects in the case of finite surfaces. First, we will consider the simplest case, in which the surfaces are black bodies, and then we will discuss more complicated geometries and gray bodies.

*2. View factor for parallel and infinite black planes.* If two parallel and infinite black planes at  $T_1$  and  $T_2$  are radiating

toward each other, plane 1 emits  $\sigma T_1^4$  radiation to plane 2, which is all absorbed. Also, plane 2 emits  $\sigma T_2^4$  radiation to plane 1, which is all absorbed. Then for plane 1, the net radiation is from plane 1 to 2,

$$q_{12} = A_1 \sigma (T_1^4 - T_2^4) \quad (17.2-13)$$

In this case, all the radiation from 1 to 2 is intercepted by 2; that is, the fraction of radiation leaving 1 that is intercepted by 2 is  $F_{12}$ , which is 1.0. The factor  $F_{12}$  is called the geometric view factor or simply the view factor. Hence,

$$q_{12} = F_{12} A_1 \sigma (T_1^4 - T_2^4) \quad (17.2-14)$$

where  $F_{12}$  is fraction of radiation leaving surface 1 in all directions, which is intercepted by surface 2. Also,



$$q_{21} = F_{21} A_2 \sigma (T_1^4 - T_2^4) \quad (17.2-15)$$

In the case of parallel plates,  $F_{12} = F_{21} = 1.0$  and the geometric factor is simply omitted.

*3. View factor for infinite parallel gray planes.* If both of the parallel plates  $A_1$  and  $A_2$  are gray, with emissivities and absorptivities of  $\epsilon_1 = \alpha_1$  and  $\epsilon_2 = \alpha_2$ , respectively, we can proceed as follows: Since each surface has an unobstructed view of the other, the view factor is 1.0. In unit time, surface  $A_1$  emits  $\epsilon_1 A_1 \sigma T_1^4$  radiation to  $A_2$ . Of this, the fraction  $\epsilon_2$  (where  $\alpha_2 = \epsilon_2$ ) is absorbed:

$$\text{absorbed by } A_2 = \epsilon_2 (\epsilon_1 A_1 \sigma T_1^4) \quad (17.2-16)$$

Also, the fraction  $(1 - \epsilon_2)$  or the amount  $(1 - \epsilon_2)(\epsilon_1 A_1 \sigma T_1^4)$  is reflected back to

$A_1$ . Of this amount,  $A_1$  reflects back to  $A_2$  a fraction  $(1 - \epsilon_1)$  or an amount  $(1 - \epsilon_1)(1 - \epsilon_2)(\epsilon_1 A_1 \sigma T_1^4)$ . The surface  $A_2$  absorbs the fraction  $\epsilon_2$ , or

$$\text{absorbed by } A_2 = \epsilon_2(1 - \epsilon_1)(1 - \epsilon_2)(\epsilon_1 A_1 \sigma T_1^4) \quad (17.2-17)$$

The amount reflected back to  $A_1$  from  $A_2$  is  $(1 - \epsilon_2)(1 - \epsilon_1)(1 - \epsilon_2)(\epsilon_1 A_1 \sigma T_1^4)$ . Then  $A_1$  absorbs  $\epsilon_1$  of this and reflects back to  $A_2$  an amount  $(1 - \epsilon_1)(1 - \epsilon_2)(1 - \epsilon_1)(1 - \epsilon_2) \times (\epsilon_1 A_1 \sigma T_1^4)$ . The surface  $A_2$  then absorbs

$$\text{absorbed by } A_2 = \epsilon_2(1 - \epsilon_1)(1 - \epsilon_2)(1 - \epsilon_1)(1 - \epsilon_2)(\epsilon_1 A_1 \sigma T_1^4) \quad (17.2-18)$$

This continues, and the total amount absorbed at  $A_2$  is the sum of Eqs. (17.2-16), (17.2-17), (17.2-18), and so on:

$$q_{1 \rightarrow 2} = A_1 \sigma T_1^4 [\epsilon_1 \epsilon_2 + \epsilon_1 \epsilon_2 (1 - \epsilon_1)(1 - \epsilon_2) + \epsilon_1 \epsilon_2 (1 - \epsilon_1)^2 (1 - \epsilon_2)^2 + \dots] \quad (17.2-19)$$

The result is a geometric series (M1):

$$q_{1 \rightarrow 2} = A_1 \sigma T_1^4 \epsilon_1 \epsilon_2 \frac{1 - (1 - \epsilon_1)(1 - \epsilon_2)}{\epsilon_1 + \epsilon_2 - 1} \quad (17.2-20)$$

Repeating the calculations above for the amount absorbed at  $A_1$  that comes from  $A_2$ ,

$$q_{2 \rightarrow 1} = A_1 \sigma T_2^4 \frac{1 - \epsilon_1 + \epsilon_1 \epsilon_2}{\epsilon_2 - 1} \quad (17.2-21)$$

The net radiation is the difference of Eqs. (17.2-20) and (17.2-21):

$$q_{12} = A_1 \sigma (T_1^4 - T_2^4) \frac{1 - \epsilon_1 + \epsilon_1 \epsilon_2}{\epsilon_2 - 1} \quad (17.2-22)$$

If  $\epsilon_1 = \epsilon_2 = 1.0$  for black bodies, Eq.

(17.2-22) becomes Eq. (17.2-13).

**EXAMPLE 17.2-1. Radiation Between Parallel Planes**

Two parallel gray planes that are very large have emissivities of  $\epsilon_1 = 0.8$  and  $\epsilon_2 = 0.7$ ; surface 1 is at  $1100^\circ\text{F}$  (866.5 K) and surface 2 is at  $600^\circ\text{F}$  (588.8 K). Use SI units for the following:

- What is the net radiation from 1 to 2?
- If the surfaces are both black, what is the net radiation?

**Solution:** For part (a), using Eq. (17.2-22) and substituting the known values,

$$q_{12A1} = \sigma(T_1^4 - T_2^4) \frac{1}{\frac{1}{\epsilon_1} + \frac{1}{\epsilon_2} - 1} = (5.676 \times 10^{-8} \text{ W m}^{-2} \cdot \text{K}^4) \frac{(866.5 \text{ K})^4 - (588.8 \text{ K})^4}{10.8 + 10.7 - 1} = 15010 \text{ W m}^{-2}$$

For black surfaces in part (b), using Eq. (17.2-13),

$$q_{12A1} = \sigma(T_1^4 - T_2^4) = (5.676 \times 10^{-8} \text{ W m}^{-2} \cdot \text{K}^4) [(866.5 \text{ K})^4 - (588.8 \text{ K})^4] = 25110 \text{ W m}^{-2}$$

Note the large reduction in radiation when surfaces with emissivities less than 1.0 are used.

Example 17.2-1 shows the large influence that emissivities less than 1.0 have on radiation. This fact is used to reduce radiation loss or gain from a surface by using planes as a radiation shield. For example, for two parallel surfaces of emissivity  $\epsilon$  at  $T_1$  and  $T_2$ , the

interchange is, by Eq. (17.2-22),

$$(q_{12})_0 A = \sigma (T_1^4 - T_2^4) 2\epsilon^{-1} \quad (17.2-23)$$

The subscript 0 indicates that there are no planes in between the two surfaces. Suppose that we now insert one or more radiation planes between the original surfaces. Then, it can be shown that

$$(q_{12})_N A = \frac{1}{N+1} \sigma (T_1^4 - T_2^4) 2\epsilon^{-1} \quad (17.2-24)$$

where  $N$  is the number of radiation planes or shields between the original surfaces. Hence, a great reduction in radiation heat loss is obtained by using these shields.

*4. Derivation of general equation for the view factor between black bodies.*

Suppose that we consider radiation

between two parallel black planes of finite size as shown in Fig. 17.2-2a. Since the planes are not infinite in size, some of the radiation from surface 1 does not strike surface 2, and vice versa. Hence, the net radiation interchange is less, since some is lost to the surroundings. The fraction of radiation leaving surface 1 in all directions, which is intercepted by surface 2, is called  $F_{12}$  and must be determined for each geometry by taking differential surface elements and integrating over the entire surface.

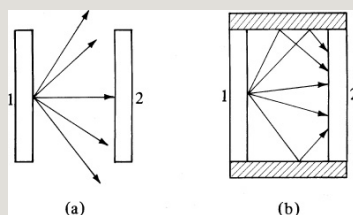


Figure 17.2-2. Radiation between two black surfaces: (a) two planes alone, (b) two planes connected by refractory reradiating walls.

Before we can derive a general relationship for the view factor between two finite bodies, we must consider and discuss two quantities, a solid angle and the intensity of radiation. A solid angle  $\omega$  is a dimensionless quantity that is a measure of an angle in solid geometry. In Fig. 17.2-3a, the differential solid angle  $d\omega_1$  is equal to the normal projection of  $dA_2$  divided by the square of the distance between the point  $P$  and area  $dA_2$ :

$$d\omega_1 = \frac{dA_2 \cos\theta_2}{r^2} \quad (17.2-25)$$

The units of a solid angle are steradian or sr. For a hemisphere, the number of sr subtended by this surface is  $2\pi$ .

The intensity of radiation for a black body,  $I_B$ , is the rate of radiation emitted

per unit area projected in a direction normal to the surface and per unit solid angle in a specified direction, as shown in Fig. 17.2-3b. The projection of  $dA$  on the line between centers is  $dA \cos \theta$ ,

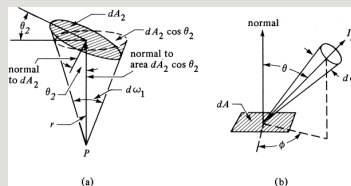


Figure 17.2-3. *Geometry for a solid angle and intensity of radiation: (a) solid-angle geometry, (b) intensity of radiation from emitting area  $dA$ .*

$$IB = dq dA \cos d\omega \quad (17.2-26)$$

where  $q$  is in W and  $IB$  is in  $W/m^2 \cdot sr$ . We assume that the black body is a diffuse surface that emits with equal intensity in all directions, that is,  $I = \text{constant}$ . The emissive power  $E_B$  that leaves a black-body plane surface is determined by integrating Eq. (17.2-26)



over all solid angles subtended by a hemisphere covering the surface. The final result is as follows [see references (H1, K1) for details]:

$$E_B = \pi I_B \quad (17.2-27)$$

where  $E_B$  is in  $\text{W/m}^2$ .

In order to determine the radiation heat-transfer rates between two black surfaces, we must determine the general case for the fraction of the total radiant heat that leaves a surface and arrives on a second surface. Using only black surfaces, we consider the case shown in Fig. 17.2-4, in which radiant energy is exchanged between area elements  $dA_1$  and  $dA_2$ . The line  $r$  is the distance between the areas, and the angles between this line and the normals to the

two surfaces are  $\theta_1$  and  $\theta_2$ . The rate of radiant energy that leaves  $dA_1$  in the direction given by the angle  $\theta_1$  is  $I_{B1} dA \cos \theta_1$ . The rate that leaves  $dA_1$  and arrives on  $dA_2$  is given by Eq. (17.2-28):

$$dq_{1 \rightarrow 2} = I_{B1} dA \cos \theta_1 d\omega_1 \quad (17.2-28)$$

where  $d\omega_1$  is the solid angle subtended by the area  $dA_2$  as seen from  $dA_1$ .

Combining Eqs. (17.2-25) and (17.2-28),

$$dq_{1 \rightarrow 2} = I_{B1} dA \cos \theta_1 \cos \theta_2 dA_2 / r^2 \quad (17.2-29)$$

From Eq. (17.2-27),  $I_{B1} = E_{B1} / \pi$ .

Substituting  $E_{B1} / \pi$  for  $I_{B1}$  into Eq. (17.2-29),

$$dq_{1 \rightarrow 2} = E_{B1} \cos \theta_1 \cos \theta_2 dA_1 dA_2 / \pi r^2 \quad (7.2-30)$$

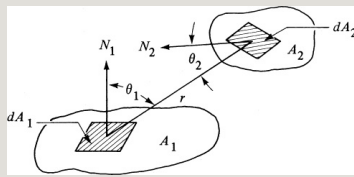


Figure 17.2-4. Area elements for radiation shape factor.

The energy leaving  $dA_2$  and arriving at  $dA_1$  is

$$dq_{2 \rightarrow 1} = E_{B2} \cos \theta_2 \cos \theta_1 dA_2 dA_1 / \pi r^2 \quad (17.2-31)$$

Substituting  $\sigma T_1^4$  for  $E_{B1}$  and  $\sigma T_2^4$  for  $E_{B2}$  from Eq. (17.2-4) and taking the difference of Eqs. (17.2-30) and (17.2-31) for the net heat flow,

$$dq_{12} = \sigma (T_1^4 - T_2^4) \cos \theta_1 \cos \theta_2 dA_1 dA_2 / \pi r^2 \quad (17.2-32)$$

Performing the double integrations over surfaces  $A_1$  and  $A_2$  will yield the total net heat flow between the finite areas:

$$q_{12} = \sigma(T_1^4 - T_2^4) \int_{A_1} \int_{A_2} \cos\theta_1 \cos\theta_2 dA_1 dA_2 / \pi r^2 \quad (17.2-33)$$

Equation (17.2-33) can also be written as

$$q_{12} = A_1 F_{12} \sigma(T_1^4 - T_2^4) = A_2 F_{21} \sigma(T_1^4 - T_2^4) \quad (17.2-34)$$

where  $F_{12}$  is a geometric shape factor or view factor and designates the fraction of the total radiation leaving  $A_1$  that strikes  $A_2$ , and  $F_{12}$  represents the fraction leaving  $A_2$  that strikes  $A_1$ . Also, the following relation exists:

$$A_1 F_{12} = A_2 F_{21} \quad (17.2-35)$$

that is valid for black surfaces and nonblack surfaces. The view factor  $F_{12}$  is then

$$A_1 \int A_2 \int A_1 \cos \theta_1 \cos \theta_2 dA_1 dA_2 \pi r^2 (17.2-36)$$

Values of the view factor can be calculated for a number of geometrical arrangements.

*5. View factors between black bodies for various geometries.* A number of basic relationships between view factors are given below.

The reciprocity relationship given by Eq. (17.2-35) is

$$A_1 F_{12} = A_2 F_{21} (17.2-35)$$

This relationship can be applied to any two surfaces  $i$  and  $j$ :

$$A_j F_{ij} = A_i F_{ji} (17.2-37)$$

If surface  $A_1$  can only see surface  $A_2$ ,

then  $F_{12} = 1.0$ .

If surface  $A_1$  sees a number of surfaces  $A_2, A_3, \dots$ , and all the surfaces form an enclosure, then the enclosure relationship is

$$F_{11} + F_{12} + F_{13} + \dots = 1.0 \quad (17.2-38)$$

If the surface  $A_1$  cannot see itself (surface is flat or convex),  $F_{11} = 0$ .

**EXAMPLE 17.2-2. View Factor from a Plane to a Hemisphere**

Determine the view factors between a plane  $A_1$  covered by a hemisphere  $A_2$ , as shown in Fig. 17.2-5.

**Solution:** Since surface  $A_1$  sees only  $A_2$ , the view factor  $F_{12} = 1.0$ . Using Eq. (17.2-35),

$$A_1 F_{12} = A_2 F_{21} \quad (17.2-35)$$

The area  $A_1 = \pi R_2^2$ ;  $A_2 = 2\pi R_2^2$ . Substituting into Eq. (17.2-35) and solving for  $F_{12}$ ,

$$F_{21} = F_{12} = \frac{A_1 A_2}{A_2^2} = (1.0) \frac{\pi R_2^2}{2\pi R_2^2} = 0.5$$

Using Eq. (17.2-38) for surface  $A_1$ ,  $F_{11} = 1.0 - F_{12} = 1.0 - 0.5 = 0.5$ . Also, writing Eq. (17.2-38) for surface  $A_2$ ,

$$F_{22} + F_{21} = 1.0 \quad (17.2-39)$$

Solving for  $F_{22}$ ,  $F_{22} = 1.0 - F_{21} = 1.0 - 1/2 = 1/2$ .

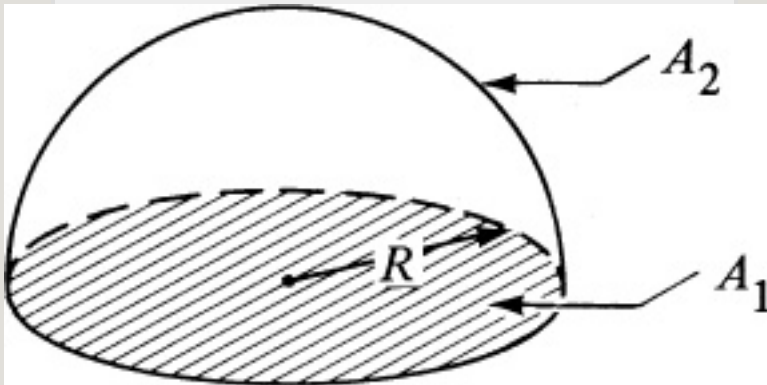


Figure 17.2-5. Radiant exchange between a flat surface and a hemisphere for Example 17.2-2.

### EXAMPLE 17.2-3. Radiation Between Parallel Disks

In Fig. 17.2-6, a small disk of area  $A_1$  is parallel to a large disk of area  $A_2$ , with  $A_1$  centered directly below  $A_2$ . The distance between the centers of the disks is  $R$  and the radius of  $A_2$  is  $a$ . Determine the view factor for radiant heat transfer from  $A_1$  to  $A_2$ .

**Solution:** The differential area for  $A_2$  is taken as the circular ring of radius  $x$  so that  $dA_2 = 2\pi x dx$ . The angle  $\theta_1 = \theta_2$ . Using Eq. (17.2-36),

$$F_{12} = \frac{1}{A_1} \int \frac{A_2}{A_1} \cos \theta_1 \cos \theta_2 dA_1 dA_2 \pi r^2 \quad (17.2-36)$$

In this case, the area  $A_1$  is very small compared to  $A_2$ , so  $dA_1$  can be integrated to  $A_1$  and the other terms inside the integral can be assumed constant. From the geometry shown,  $r = (R^2 + x^2)^{1/2}$ ,  $\cos \theta_1 = R/(R^2 + x^2)^{1/2}$ . Making these substitutions into the equation for  $F_{12}$ ,

$$F_{12} = \int_0^a \frac{a^2 R^2 x dx}{(R^2 + x^2)^2}$$

Integrating,

$$F_{12} = \frac{a^2 R^2}{R^2 + a^2}$$

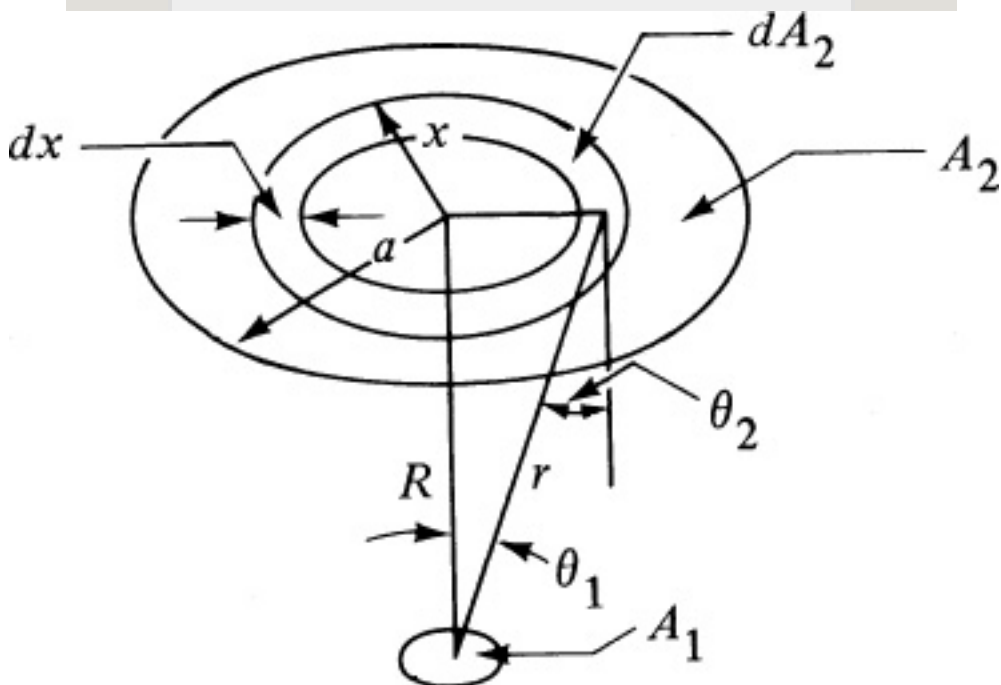


Figure 17.2-6. View factor for radiation from a small element to a parallel disk for Example 17.2-3.

The integration of Eq. (17.2-36) has been performed for numerous geometrical configurations and values of  $F_{12}$  tabulated. Then,

$$q_{12} = A_1 F_{12} \sigma (T_1^4 - T_2^4) = A_2 F_{21} \sigma (T_1^4 - T_2^4) \quad (17.2-34)$$

where  $F_{12}$  is the fraction of the radiation leaving  $A_1$  that is intercepted by  $A_2$  and  $F_{21}$  is the fraction reaching  $A_1$  from  $A_2$ . Since the flux from 1 to 2 must equal that from 2 to 1, Eq. (17.2-34) becomes Eq. (17.2-35) as given previously:

$$A_1 F_{12} = A_2 F_{21} \quad (17.2-35)$$

Hence, one selects the surface whose view factor can be determined most easily. For example, the view factor  $F_{12}$  for a small surface  $A_1$  completely enclosed by a large surface  $A_2$  is 1.0, since all the radiation leaving  $A_1$  is intercepted by  $A_2$ . In Fig. 17.2-7 the view factors  $F_{12}$  between parallel planes are given, and in Fig. 17.2-8 the view factors for adjacent perpendicular rectangles. View



factors for other geometries are given elsewhere (H1, K1, P1, W1).

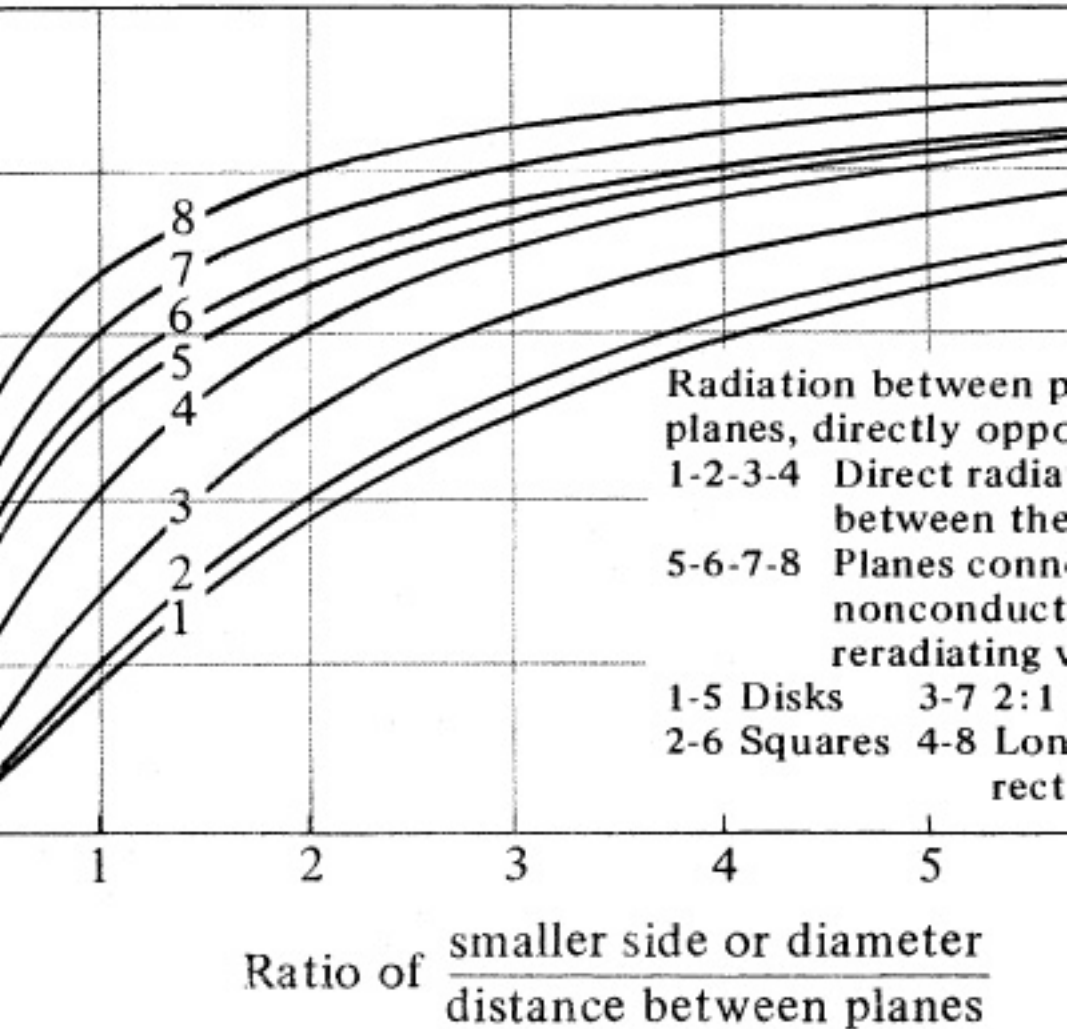


Figure 17.2-7. View factor between parallel planes directly opposed. From W. H. McAdams, Heat Transmission, 3rd ed. New York: McGraw-Hill Book Company, 1954. With permission.

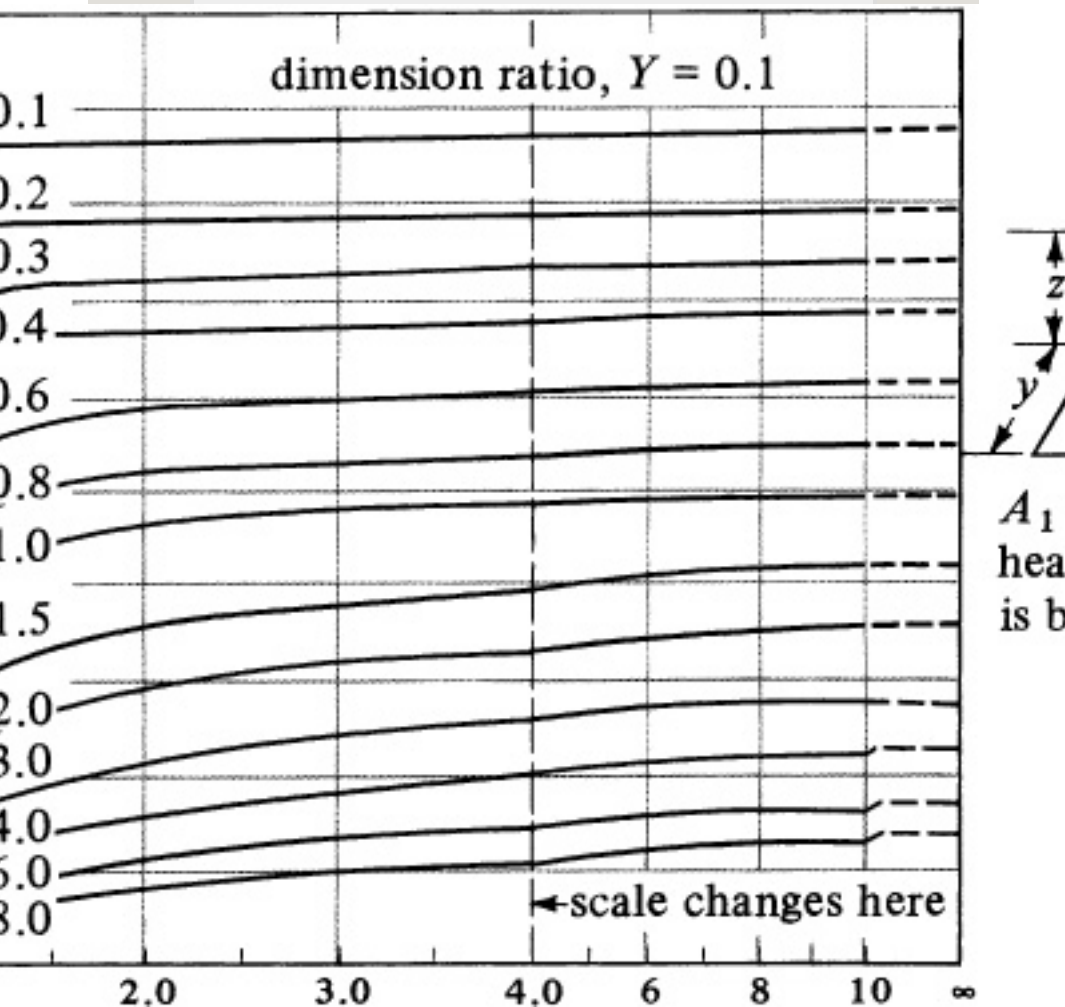


Figure 17.2-8. View factor for adjacent perpendicular rectangles. From H. C. Hottel, Mech. Eng., 52, 699 (1930).

### 17.2C View Factors When Surfaces Are Connected by Reradiating Walls

If the two black-body surfaces  $A_1$  and  $A_2$  are connected by

nonconducting (refractory) but reradiating walls, as in Fig. 17.2-2b, a larger fraction of the radiation from surface 1 is intercepted by 2. This view factor is called  $F_{12}$ . The case of two surfaces connected by the walls of an enclosure such as a furnace is a common example of this. The general equation for this case, assuming a uniform refractory temperature, has been derived (M1) for two radiant sources  $A_1$  and  $A_2$  that are not concave, so they do not see themselves:

$$F_{12} = \frac{A_2}{A_1 + A_2} \left( 1 - \frac{A_1}{A_2} F_{12} \right) \quad (17.2-40)$$

Also, as before,

$$A_1 F_{12} = A_1 F_{21} \quad (17.2-41)$$

$$q_{12} = F_{12} A_1 \sigma (T_1^4 - T_2^4) \quad (17.2-42)$$

The factor  $F_{12}$  for parallel planes is given in Fig. 17.2-7; for other geometries, it can be calculated from Eq. (17.2-36). For view factors  $F_{12}$  and  $F_{21}$  for parallel tubes adjacent to a wall, as in a furnace as well as for variation in refractory wall temperature, refer to (M1) and (P1). If there are no reradiating walls,

$$F_{12} = F_{21} \quad (17.2-43)$$

### 17.2D View Factors and Gray Bodies

A general and more practical case, which is the same as for Eq. (17.2-40) but with the surfaces  $A_1$  and  $A_2$  being gray with emissivities  $\epsilon_1$  and  $\epsilon_2$ , will be considered.

Nonconducting reradiating walls are present as before. Since the two surfaces are now gray, there will be some reflection of radiation, which will decrease the net radiant exchange between the surfaces below that for black surfaces. The final equations for this case are

$$q_{12} = f_{12} A_1 \sigma (T_1^4 - T_2^4) \quad (17.2-44)$$

$$\mathcal{F}_{12} = F_{12} + \frac{A_1 A_2 (1 - \epsilon_2)}{A_1 + A_2 (1 - \epsilon_1)} \quad (17.2-45)$$

where  $\mathcal{F}_{12}$  is the new view factor for two gray surfaces  $A_1$  and  $A_2$  that cannot see themselves and are connected by reradiating walls. If no refractory walls are present,  $F_{12}$  is used in place of  $F_{12}^-$  in Eq. (17.2-41). Again,

$$A_1 \mathcal{F}_{12} = A_2 \mathcal{F}_{21} \quad (17.2-46)$$

**EXAMPLE 17.2-4. Radiation Between Infinite Parallel Gray Planes**

Derive Eq. (17.2-22) by starting with the general equation for radiation between two gray bodies  $A_1$  and  $A_2$  that are infinite parallel planes having emissivities  $\epsilon_1$  and  $\epsilon_2$ , respectively.

**Solution:** Since there are no reradiating walls, by Eq. (17.2-43)  $F_{12}$  becomes  $F_{12}$ . Also, since all the radiation from surface 1 is intercepted by surface 2,  $F_{12} = 1.0$ . Substituting into Eq. (17.2-45), noting that  $A_1/A_2 = 1.0$ ,

$$\mathcal{F} = 11F_{12} + A_1A_2(1\epsilon_2 - 1) + (1\epsilon_1 - 1) = 11 + 1(1\epsilon_2 - 1) + (1\epsilon_1 - 1) = 11\epsilon_1 + 1\epsilon_2 - 1$$

Then, using Eq. (17.2-44),

$$q_{12} = \mathcal{F} 12 A_1 \sigma (T_1^4 - T_2^4) = A_1 \sigma (T_1^4 - T_2^4) 11\epsilon_1 + 1\epsilon_2 - 1$$

This is identical to Eq. (17.2-22).

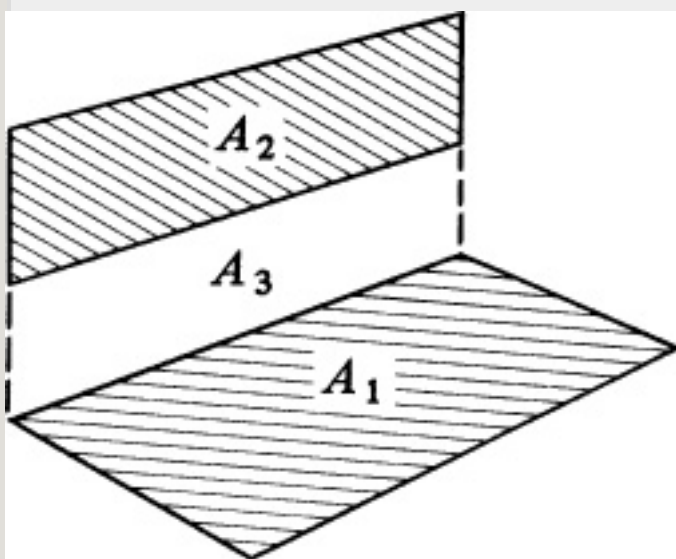


Figure 17.2-9. Configuration for Example 17.2-5.

**EXAMPLE 17.2-5. Complex View Factor for**

### **Perpendicular Rectangles**

Find the view factor  $F_{12}$  for the configuration shown in Fig. 17.2-9 of the rectangle with area  $A_2$  displaced from the common edge of rectangle  $A_1$  and perpendicular to  $A_1$ . The temperature of  $A_1$  is  $T_1$  and that of  $A_2$  and  $A_3$  is  $T_2$ .

**Solution:** The area  $A_3$  is a fictitious area between areas  $A_2$  and  $A_1$ . Designate the area  $A_2$  plus  $A_3$  as  $A_{(23)}$ . The view factor  $F_{1(23)}$  for areas  $A_1$  and  $A_{(23)}$  can be obtained from Fig. 17.2-8 for adjacent perpendicular rectangles. Also,  $F_{13}$  can be obtained from Fig. 17.2-8. The radiation interchange between  $A_1$  and  $A_{(23)}$  is equal to that intercepted by  $A_2$  and by  $A_3$ :

$$A_1 F_{1(23)} \sigma (T_1^4 - T_2^4) = A_1 F_{12} \sigma (T_1^4 - T_2^4) + A_1 F_{13} (T_1^4 - T_2^4) \quad (17.2-47)$$

Hence,

$$A_1 F_{1(23)} = A_1 F_{12} + A_1 F_{13} \quad (17.2-48)$$

Solving for  $F_{12}$ ,

$$F_{12} = F_{1(23)} - F_{13} \quad (17.2-49)$$

Methods similar to those used in this example can be employed to find the shape factors for a general orientation of two rectangles in perpendicular planes or parallel rectangles ( $H_1$ ,  $K_1$ ).

#### **EXAMPLE 17.2-6. Radiation to a Small Package**

A small, cold package having an area  $A_1$  and emissivity  $\epsilon_1$  is at temperature  $T_1$ . It is placed in a warm room with the walls at  $T_2$  and an emissivity of  $\epsilon_2$ . Using Eq. (17.2-45),

derive the view factor for this and the equation for the radiation heat transfer.

**Solution:** For the small surface  $A_1$  completely enclosed by the enclosure  $A_2$ ,  $F_{12} = F_{21}$  by Eq. (17.2-43), since there are no reradiating (refractory) walls. Also,  $F_{12} = 1.0$ , since all the radiation from  $A_1$  is intercepted by the enclosure  $A_2$  because  $A_1$  does not have any concave surfaces and cannot “see” itself. Since  $A_2$  is very large compared to  $A_1$ ,  $A_1/A_2 = 0$ . Substituting into Eq. (17.2-45),

$$\mathcal{F}_{12} = 1 + F_{12} + A_1/A_2(1/\epsilon_2 - 1) + (1/\epsilon_1 - 1) = 1 + 0 + (1/\epsilon_2 - 1) + (1/\epsilon_1 - 1) = \epsilon_1$$

Substituting into Eq. (17.2-44),

$$q_{12} = \mathcal{F}_{12} A_1 \sigma (T_1^4 - T_2^4) = \epsilon_1 A_1 \sigma (T_1^4 - T_2^4)$$

This is the same as Eq. (17.2-6) derived previously.

For solving complicated radiation problems involving more than four or five heat-transfer surfaces, matrix methods have been developed and are discussed in detail elsewhere (H1, K1).

## 17.2E Radiation in Absorbing Gases

*1. Introduction to absorbing gases in radiation.* As discussed in this section, solids and liquids emit radiation over a continuous spectrum. However, most gases that



are monatomic or diatomic, such as He, Ar, H<sub>2</sub>, O<sub>2</sub>, and N<sub>2</sub>, are virtually transparent to thermal radiation; that is, they emit practically no radiation and do not absorb radiation. Gases with a dipole moment and higher polyatomic gases emit significant amounts of radiation and also absorb radiant energy within the same bands in which they emit radiation. These gases include CO<sub>2</sub>, H<sub>2</sub>O, CO, SO<sub>2</sub>, NH<sub>3</sub>, and organic vapors.

For a particular gas, the width of the absorption or emission bands depends on the pressure and also the temperature. If an absorbing gas is heated, it radiates energy to the cooler surroundings. The net radiation heat-transfer rate between surfaces is decreased in these cases because the gas

absorbs some of the radiant energy being transported between the surfaces.

2. *Absorption of radiation by a gas.* The absorption of radiation in a gas layer can be described analytically, since the absorption by a given gas depends on the number of molecules in the path of radiation. Increasing the partial pressure of the absorbing gas or the path length increases the amount of absorption. We define  $I_{\lambda 0}$  as the intensity of radiation at a particular wavelength before it enters the gas, and  $I_{\lambda L}$  as the intensity at the same wavelength after having traveled a distance of  $L$  in the gas. If the beam impinges on a gas layer of thickness  $dL$ , the decrease in intensity,  $dI_{\lambda}$ , is proportional to  $I_{\lambda}$  and  $dL$ :

$$dI_{\lambda} = -\alpha I_{\lambda} dL \quad (17.2-50)$$

where  $I_\lambda$  is in W/m<sup>2</sup>. Integrating,

$$I_L = I_\lambda e^{-\alpha_\lambda L} \quad (17.2-51)$$

The constant  $\alpha_\lambda$  depends on the particular gas, its partial pressure, and the wavelength of radiation. This equation is called Beer's law. Gases frequently absorb only in narrow-wavelength bands.

*3. Characteristic mean beam length of an absorbing gas.* The calculation methods for gas radiation are quite complicated. For the purpose of engineering calculations, Hottel (M1) has presented approximate methods for calculating radiation and absorption when gases such as CO<sub>2</sub> and water vapor are present. Thick layers of a gas absorb more energy than do thin layers.

Hence, in addition to specifying the pressure and temperature of a gas, we must specify a characteristic length (mean beam length) of a gas mass to determine the emissivity and absorptivity of a gas. The mean beam length  $L$  depends on the specific geometry.

For a black differential receiving surface area  $dA$  located in the center of the base of a hemisphere of radius  $L$  containing a radiating gas, the mean beam length is  $L$ . The mean beam length has been evaluated for various geometries, as presented in Table 17.2-1. For other shapes,  $L$  can be approximated by

$$L=3.6VA(17.2-52)$$

where  $V$  is volume of the gas in  $m^3$ ,  $A$  is

surface area of the enclosure in  $m^2$ , and  $L$  is in m.

Table 17.2-1. *Mean Beam Length for Gas Radiation to Entire Enclosure Surface ( $M1, R2, P1$ )*

4. *Emissivity, absorptivity, and radiation of a gas.* Gas emissivities have been correlated and Fig. 17.2-10 gives the gas emissivity  $\epsilon_G$  of  $CO_2$  at a total pressure of the system of 1.0 atm abs. The  $p_G$  is the partial pressure of  $CO_2$  in atm and  $L$  is the mean beam length in m. The emissivity  $\epsilon_G$  is defined as the ratio of the rate of energy transfer from the hemispherical body of gas to a surface element at the midpoint divided by the rate of energy transfer from a black hemisphere surface of radius  $L$  and

temperature  $T_G$  to the same element.

The rate of radiation emitted from the gas is  $\sigma \epsilon_G T_1^4$  in W/m<sup>2</sup> of receiving surface element, where  $\epsilon_G$  is evaluated at  $T_G$ . If the surface element at the midpoint at  $T_1$  is radiating heat back to the gas, the absorption rate of the gas will be  $\sigma \alpha_G T_1^4$ , where  $\alpha_G$  is the absorptivity of the gas for black-body radiation from the surface at  $T_1$ . The  $\alpha_G$  of CO<sub>2</sub> is determined from Fig. 17.2-10 at  $T_1$ , but instead of the parameter  $p_{GL}$ , the parameter  $p_{GL}(T_1/T_G)$  is used. The resulting value from the chart is then multiplied by  $(T_G/T_1)^{0.65}$  to give  $\alpha_G$ . The net rate of radiant transfer between a gas at  $T_G$  and a black surface of finite area  $A_1$  at  $T_1$  is then

$$q = \sigma A (\epsilon_G T_G^4 - \alpha_G T_1^4) \quad (17.2-53)$$

When the total pressure is not 1.0 atm, a correction chart is available to correct the emissivity of CO<sub>2</sub>. Charts are also available for water vapor (H<sub>1</sub>, K<sub>1</sub>, M<sub>1</sub>). When both CO<sub>2</sub> and H<sub>2</sub>O are present the total radiation is reduced somewhat, since each gas is somewhat opaque to radiation from the other gas. Charts for these interactions are also available (H<sub>1</sub>, K<sub>1</sub>, M<sub>1</sub>, P<sub>1</sub>).

**EXAMPLE 17.2-7. Gas Radiation to a Furnace Enclosure**

A furnace is in the form of a cube 0.3 m on an interior side, and these interior walls can be approximated as black surfaces. The gas inside at 1.0 atm total pressure and 1100 K contains 10 mol % CO<sub>2</sub> and the rest is O<sub>2</sub> and N<sub>2</sub>. The small amount of water vapor present will be neglected. The walls of the furnace are maintained at 600 K by external cooling. Calculate the total heat transfer to the walls neglecting heat transfer by convection.

**Solution:** From Table 17.2-1, the mean beam length for radiation to a cube face is  $L = 0.60D = 0.60(0.30) = 0.180$  m. The partial pressure of CO<sub>2</sub> is  $p_G = 0.10(100) = 0.10$  atm. Then,  $p_GL = 0.10(0.180) = 0.0180$  atm · m. From Fig. 17.2-10,  $\epsilon_G = 0.064$  at  $T_G = 1100$  K.

To obtain  $\alpha_G$ , we evaluate  $\alpha_G$  at  $T_1 = 600$  K and  $p_GL(T_1/T_G) = (0.0180)(600/1100) = 0.00982$  atm · m. From Fig. 17.2-10, the uncorrected value of  $\alpha_G = 0.048$ . Multiplying this by the correction factor  $(T_G/T_1)^{0.65}$ , the final correction

value is

$$\alpha_G = 0.048(1100/600)0.65 = 0.0712$$

Substituting into Eq. (17.2-53),

$$\begin{aligned} q &= \sigma A (\epsilon_G T_G^4 - \alpha_G T_1^4) = (5.676 \times 10^{-8} \text{ W m}^2 \cdot \text{K}^4) | \\ &0.064(1100 \text{ K})^4 - 0.0712(600 \text{ K})^4 | \\ &= 4.795 \times 10^3 \text{ W m}^2 = 4.795 \text{ kW m}^2 \end{aligned}$$

For six sides,  $A = 6(0.3 \times 0.3) = 0.540 \text{ m}^2$ . Then,

$$q = 4.795(0.540) = 2.589 \text{ kW}$$

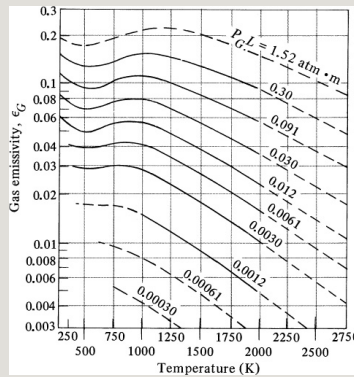


Figure 17.2-10. Total emissivity of the gas carbon dioxide at a total pressure of 1.0 atm. From W. H. McAdams, *Heat Transmission*, 3rd ed. New York: McGraw-Hill Book Company, 1954. With permission.

For the case where the walls of the enclosure are not black, some of the radiation striking the walls is reflected back to the other walls and into the gas. As an approximation when the



emissivity of the walls is greater than 0.7, an effective emissivity  $\epsilon'$  can be used:

$$\epsilon' = \epsilon + 1.02(17.2-54)$$

where  $\epsilon$  is the actual emissivity of the enclosure walls. Then Eq. (9.4-53) is modified to give the following (M1):

$$q = \sigma A \epsilon' (\epsilon_G T_G^4 - \alpha_G T_1^4) \quad (17.2-55)$$

Other approximate methods are available for gases containing suspended luminous flames, clouds of nonblack particles, refractory walls and absorbing gases present, and so on (M1, P1).

## 17.3 Chapter Summary

### Radiation from a Perfect Black Body

$$q = A \sigma T^4 \quad (17.1-3)$$

**Radiation from a Non-black/gray Body Surface ( $0 < \epsilon < 1$ )**

$$q = A\epsilon\sigma T^4 \quad (17.1-4)$$

**Radiation to a Small Object from Its Surroundings**

$$q = A_1\epsilon\sigma(T_1^4 - T_2^4) \quad (17.1-6)$$

**Net Radiation for Infinite Parallel Gray Planes**

$$q_{12} = A_1\sigma(T_1^4 - T_2^4) \frac{1}{\frac{1}{\epsilon_1} + \frac{1}{\epsilon_2} - 1} \quad (17.2-22)$$

**View Factors (Geometric Shape Factor Corrections)**

$$F_{12} = \frac{1}{A_1} \int_{A_1} \int_{A_2} \cos\theta_1 \cos\theta_2 dA_1 dA_2 / \pi r^2 \quad (17.2-36)$$

## **Problems**

**17.1-1. *Radiation to a Tube from a Large Enclosure.*** Repeat Example 17.1-1, but use the slightly more accurate Eq. (17.1-5) with two different emissivities.

$$\text{Ans. } q = -2171 \text{ W } (-7410 \text{ btu/h})$$

**17.1-2. *Baking a Loaf of Bread in an Oven.*** A loaf of bread having a surface temperature of 373 K is being baked in an oven whose walls and the air inside are at 477.4 K. The bread moves continuously through the large oven on an open chain-belt conveyor. The emissivity of the bread is estimated as 0.85, and the loaf can be assumed to be a rectangular solid 114.3 mm high  $\times$  114.3 mm wide  $\times$  330 mm long. Calculate the radiation heat-transfer rate to the bread, assuming that it is small compared to the oven and neglecting natural convection heat transfer.

**Ans.**  $q = 278.4 \text{ W (950 btu/h)}$

**17.1-3. *Radiation and Convection from a Steam Pipe.*** A horizontal, oxidized steel pipe carrying steam and having an

OD of 0.1683 m has a surface temperature of 374.9 K and is exposed to air at 297.1 K in a large enclosure. Calculate the heat loss for 0.305 m of pipe from natural convection plus radiation. For the steel pipe, use an  $\epsilon$  of 0.79.

**Ans.**  $q = 163.3 \text{ W (557 btu/h)}$

**17.1-4. Radiation and Convection to a Loaf of Bread.** Calculate the total heat-transfer rate to the loaf of bread in Problem 17.1-2, including the radiation plus natural convection heat transfer. For radiation, first calculate a value of  $h_r$ . For natural convection, use the simplified equations for the lower  $NG_rNP_r$  range. For the four vertical sides, the equation for vertical planes can be used with an  $L$  of 114.3 mm. For the top

surface, use the equation for a cooled plate facing upward, and for the bottom, a cooled plate facing downward. The characteristic  $L$  for a horizontal rectangular plate is the linear mean of the two dimensions.

**17.1-5. *Heat Loss from a Pipe.*** A bare stainless-steel tube having an outside diameter of 76.2 mm and an  $\epsilon$  of 0.55 is placed horizontally in air at 294.2 K. The pipe surface temperature is 366.4 K. Calculate the value of  $h_c + h_r$  for convection plus radiation and the heat loss for 3 m of pipe.

**17.2-1. *Radiation Shielding.*** Two very large and parallel planes each have an emissivity of 0.7. Surface 1 is at 866.5 K and surface 2 is at 588.8 K. Use SI and English units.

- What is the net radiation loss of surface 1?
- To reduce this loss, two additional radiation shields also having an emissivity of 0.7 are placed between the original surfaces. What is the new radiation loss?

**Ans.** (a) 13 565 W/m<sup>2</sup>, 4304 btu/h · ft<sup>2</sup>;

(b) 4521 W/m<sup>2</sup>, 1435 btu/h · ft<sup>2</sup>

### **17.2-2. *Radiation from a Craft in***

***Space.*** A space satellite in the shape of a sphere is traveling in outer space, where its surface temperature is held at 283.2 K. The sphere “sees” only outer space, which can be considered as a black body with a temperature of 0 K. The polished surface of the sphere has an emissivity of 0.1. Calculate the heat loss per m<sup>2</sup> by radiation.

**Ans.**  $q_{12}/A_1 = 36.5 \text{ W/m}^2$

### **17.2-3. *Radiation and the Complex***

**View Factor.** Find the view factor  $F_{12}$  for the configuration shown in Fig.

P17.2-3. The areas  $A_4$  and  $A_3$  are fictitious areas (C1). The area  $A_2 + A_4$  is called  $A_{(24)}$  and  $A_1 + A_3$  is called  $A_{(13)}$ . Areas  $A_{(24)}$  and  $A_{(13)}$  are perpendicular to each other. [*Hint:* Follow the methods in Example 17.2-5. First, write an equation similar to Eq. (17.2-48) that relates the interchange between  $A_3$  and  $A_{(24)}$ . Then, relate the interchange between  $A_{(13)}$  and  $A_{(24)}$ . Finally, relate  $A_{(13)}$  and  $A_4$ .]

$$\text{Ans. } A_1 F_{12} = A_{(13)} F_{(13)(24)} + A_3 F_{34} - A_3 F_{3(24)} - A_{(13)} F_{(13)4}$$

**17.2-4. Radiation Between Parallel Surfaces.** Two parallel surfaces, each  $1.83 \times 1.83$  m square, are spaced 0.91 m apart. The surface temperature of  $A_1$  is

811 K and that of  $A_2$  is 533 K. Both are black surfaces.

- Calculate the radiant heat transfer between the two surfaces.
- Do the same as for part (a), but for the case where the two surfaces are connected by nonconducting reradiating walls.
- Repeat part (b), but where  $A_1$  has an emissivity of 0.8 and  $A_2$  an emissivity of 0.7.

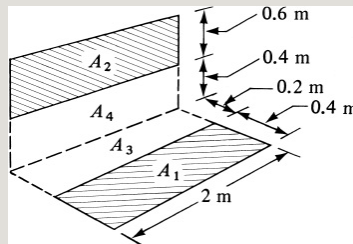


Figure P17.2-3. *Geometric configuration for Problem 17.2-3.*

**17.2-5. Radiation Between Adjacent Perpendicular Plates.** Two adjacent rectangles are perpendicular to each other. The first rectangle is  $1.52 \times 2.44$  m and the second  $1.83 \times 2.44$  m, with the 2.44-m side common to both. The



temperature of the first surface is 699 K and that of the second is 478 K. Both surfaces are black. Calculate the radiant heat transfer between the two surfaces.

**17.2-6. View Factor for Complex Geometry.** Using the dimensions given in Fig. P17.2-3, calculate the individual view factors and also  $F_{12}$ .

**17.2-7. Radiation from a Surface to the Sky.** A plane surface having an area of  $1.0 \text{ m}^2$  is insulated on the bottom side and is placed on the ground and exposed to the atmosphere at night. The upper surface is exposed to air at 290 K, and the convective heat-transfer coefficient from the air to the plane is  $12 \text{ W/m}^2 \cdot \text{K}$ . The plane radiates to the clear sky. The effective radiation temperature of the sky can be assumed as 80 K. If the plane

is a black body, calculate the temperature of the plane at equilibrium.

$$\text{Ans. } T = 266.5 \text{ K} = -6.7^\circ\text{C}$$

**17.2-8. Radiation and Heating of Planes.** Two plane disks, each 1.25 m in diameter, are parallel and directly opposite each other. They are separated by a distance of 0.5 m. Disk 1 is heated by electrical resistance to 833.3 K. Both disks are insulated on all faces except the two faces directly opposite each other. Assume that the surroundings emit no radiation and that the disks are in space. Calculate the temperature of disk 2 at steady state and also the electrical energy input to disk 1. (*Hint:* The fraction of heat lost from area number 1 to space is  $1 - F_{12}$ .)

**Ans.**  $F_{12} = 0.45$ ,  $T_2 = 682.5 \text{ K}$

**17.2-9. Radiation by Disks to Each Other and to Their Surroundings.** Two disks, each 2.0 m in diameter, are parallel and directly opposite each other, and are separated by a distance of 2.0 m. Disk 1 is held at 1000 K by electric heating and disk 2 at 400 K by cooling water in a jacket at the rear of the disk. The disks radiate only to each other and to the surrounding space at 300 K. Calculate the electric heat input and also the heat removed by the cooling water.

**17.2-10. View Factor by Integration.** A small black disk is vertical, with an area of 0.002 m<sup>2</sup>, and radiates to a vertical black plane surface that is 0.03 m wide and 2.0 m high, and is opposite and parallel to the small disk. The disk

source is 2.0 m away from the vertical plane and placed opposite the bottom of the plane. Determine  $F_{12}$  by integration of the view-factor equation.

$$\text{Ans. } F_{12} = 0.00307$$

### **17.2-11. Gas Radiation to a Gray**

**Enclosure.** Repeat Example 17.2-7 but with the following changes:

- The interior walls are not black surfaces but gray surfaces with an emissivity of 0.75.
- The conditions are the same as part (a) with gray walls, but in addition, heat is transferred by natural convection to the interior walls. Assume an average convective coefficient of  $8.0 \text{ W/m}^2 \cdot \text{K}$ .

$$\text{Ans. (b) } q(\text{convection} + \text{radiation}) = 4.426 \text{ W}$$

**17.2-12. Gas Radiation and Convection to a Stack.** A furnace discharges hot flue

gas at 1000 K and 1 atm abs pressure containing 5% CO<sub>2</sub> into a stack having an inside diameter of 0.50 m. The inside walls of the refractory lining are at 900 K and the emissivity of the lining is 0.75. The convective heat-transfer coefficient of the gas has been estimated as 10Wm<sup>2</sup>·K. Calculate the rate of heat transfer  $q/A$  from the gas by radiation plus convection.

### References

### Notation

# **Chapter 18. Introduction to Mass Transfer**

## **18.0 Chapter Objectives**

On completion of this chapter, a student should be able to:

- Use both the American and SI units when solving mass-transfer problems
- Explain the basics of Fick's law and similarity to other rate-transfer processes
- Be able to predict binary diffusion coefficients for both gases and liquids
- Explain the physical significance of a mass-transfer coefficient
- Solve simple problems involving molecular diffusion, convection, and chemical reaction

## **18.1 Introduction to Mass Transfer and Diffusion**

### **18.1A Similarity of Mass, Heat, and Momentum Transfer Processes**

*1. Introduction.* In Chapter 1, we noted that the various separation processes have certain basic principles that can be classified into three fundamental transfer (or “transport”) processes: momentum transfer, heat transfer, and mass transfer. The fundamental process of *momentum transfer* occurs in such operations as fluid flow, mixing, sedimentation, and filtration. Heat transfer occurs in conductive and convective transfer of heat, evaporation, distillation, and drying.

The third fundamental transfer process, *mass transfer*, occurs in distillation, absorption, drying, liquid–liquid extraction, adsorption, ion exchange, crystallization, and membrane processes. When mass is being

transferred from one distinct phase to another, or through a single phase, the basic mechanisms are the same whether the phase is a gas, liquid, or solid. This was also shown for heat transfer, where the transfer of heat by conduction followed Fourier's law in a gas, solid, or liquid.

*2. General molecular transport equation.* All three of the molecular transport processes—momentum, heat, and mass—are characterized by the same general type of equation,

rate of a transfer process = driving force / resistance

This can be written as follows for molecular diffusion of the property momentum, heat, or mass:

$$J_z = -\delta d \Gamma dz$$



### *3. Molecular diffusion equations for momentum, heat, and mass transfer.*

Newton's equation for momentum transfer for constant density can be written as follows:

$$\tau_{zx} = -\mu \frac{dv_x}{dz} \quad (18.1-1)$$

where  $\tau_{zx}$  is momentum transferred/ $s \cdot m^2$ ,  $\mu/\rho$  is kinematic viscosity in  $m^2/s$ ,  $z$  is distance in  $m$ , and  $v_x$  is momentum/ $m^3$ , where the momentum has units of  $kg \cdot m/s$ .

Fourier's law for heat conduction can be written as follows for constant  $\rho$  and  $c_p$ :

$$q_z/A = -\alpha \frac{d(\rho c_p T)}{dz} \quad (18.1-2)$$

where  $q_z/A$  is heat flux in  $W/m^2$ ,  $\alpha$  is the thermal diffusivity in  $m^2/s$ , and  $\rho c_p T$  is  $J/m^3$ .

The equation for molecular diffusion of mass is Fick's law and is also similar to Eq. (18.1-2). It is written as follows for constant total concentration in a fluid:

$$J_{Az}^* = -D_{AB} \frac{dc_A}{dz} \quad (18.1-3)$$

where  $J_{Az}^*$  is the molar flux of component  $A$  in the  $z$  direction due to molecular diffusion in  $\text{kg mol } A/s \cdot m^2$ ,  $D_{AB}$  is the molecular diffusivity of the molecule  $A$  in  $B$  in  $m^2/s$ ,  $c_A$  is the concentration of  $A$  in  $\text{kg mol}/m^3$ , and  $z$  is the distance of diffusion in  $m$ . In cgs units,  $J_{Az}^*$  is  $\text{g mol } A/s \cdot cm^2$ ,  $D_{AB}$  is  $cm^2/s$ , and  $c_A$  is  $\text{g mol } A/cm^3$ . In English units,  $J_{Az}^*$  is  $\text{lb mol}/h \cdot ft^2$ ,  $D_{AB}$  is  $ft^2/h$ , and  $c_A$  is  $\text{lb mol}/ft^3$ .

The similarity of Eqs. (18.1-1), (18.1-2), and (18.1-3) for momentum, heat, and

mass transfer should be obvious. All the fluxes on the left-hand side of the three equations have as units transfer of a quantity of momentum, heat, or mass per unit time per unit area. The transport properties  $\mu/\rho$ ,  $\alpha$  and  $D_{AB}$  all have units of  $\text{m}^2/\text{s}$ , and the concentrations are represented as momentum/ $\text{m}^3$ ,  $\text{J}/\text{m}^3$ , or  $\text{kg mol}/\text{m}^3$ .

*4. Turbulent diffusion equations for momentum, heat, and mass transfer.* In Section 15.2C, equations were given showing the similarities among momentum, heat, and mass transfer in turbulent transfer. For turbulent momentum transfer and constant density,

$$\tau_{zx} = -(\mu_r + \epsilon_t) d(v_x \rho) dz \quad (18.1-4)$$

For turbulent heat transfer for constant  $\rho$  and  $c_p$ ,

$$q_z A = -(\alpha + \alpha_t) d(\rho c_p T) dz \quad (18.1-5)$$

For turbulent mass transfer for constant  $c$ ,

$$J_A z^* = -(D_{AB} + \epsilon M) d c_A dz \quad (18.1-6)$$

In these equations,  $\epsilon_t$  is the turbulent or eddy momentum diffusivity in  $m^2/s$ ,  $\alpha_t$  is the turbulent or eddy thermal diffusivity in  $m^2/s$ , and  $\epsilon M$  is the turbulent or eddy mass diffusivity in  $m^2/s$ . Again, these equations are quite similar to each other. Many of the theoretical equations and empirical correlations for turbulent transport to various geometries are also quite similar.

### 18.1B Examples of Mass-Transfer Processes

Mass transfer is important in many areas of science and engineering. It occurs when a component in a mixture migrates in the same phase or from phase to phase because of a difference in concentration between two points. Many familiar phenomena involve mass transfer. Liquid in an open pail of water evaporates into still air because of the difference in concentration of water vapor at the water's surface and the surrounding air. There is a "driving force" from the surface to the air. A piece of sugar added to a cup of coffee eventually dissolves by itself and diffuses to the surrounding solution. When newly cut and moist green timber is exposed to the atmosphere, the wood will dry partially when water in the timber

diffuses through the wood to the surface and then to the atmosphere. In a fermentation process, nutrients and oxygen dissolved in the solution diffuse to the microorganisms. In a catalytic reaction, the reactants diffuse from the surrounding medium to the catalyst surface where reaction occurs.

Many purification processes involve mass transfer. In uranium processing, a uranium salt in solution is extracted by an organic solvent. Distillation to separate alcohol from water involves mass transfer. Removal of  $\text{SO}_2$  from flue gas is done by absorption in a basic liquid solution.

We can treat mass transfer in a manner somewhat similar to that used in heat

transfer with Fourier's law of conduction. However, an important difference is that in molecular mass transfer, one or more of the components of the medium is moving. In heat transfer by conduction, the medium is usually stationary and only energy in the form of heat is being transported. This introduces some differences between heat and mass transfer that will be discussed in this chapter.

### **18.1C Fick's Law for Molecular Diffusion**

Molecular diffusion or molecular transport can be defined as the transfer or movement of individual molecules through a fluid by means of the random, individual movements of the molecules. We can imagine the molecules traveling only in straight lines and changing

direction by bouncing off other molecules after collision. Since the molecules travel in a random path, molecular diffusion is often called a *random-walk process*.

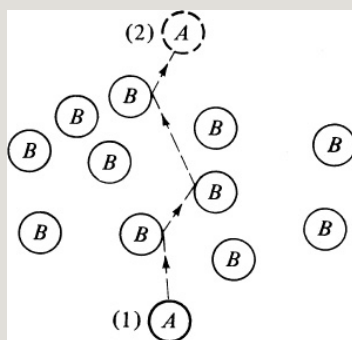


Figure 18.1-1. *Schematic diagram of molecular diffusion process.*

In Fig. 18.1-1, the *molecular diffusion process* is shown schematically. A random path that molecule *A* might take in diffusing through *B* molecules from point (1) to (2) is shown. If there are a greater number of *A* molecules near point (1) than at (2), then, since molecules diffuse randomly in both



directions, more A molecules will diffuse from (1) to (2) than from (2) to (1). The net diffusion of A is from high- to low-concentration regions.

As another example, a drop of blue liquid dye is added to a cup of water. The dye molecules will diffuse slowly by molecular diffusion to all parts of the water. To increase this rate of mixing of the dye, the liquid can be mechanically agitated by a spoon and *convective mass transfer* will occur. The two modes of heat transfer, conduction and convective heat transfer, are analogous to molecular diffusion and convective mass transfer.

First, we will consider the diffusion of molecules when the whole bulk fluid is not moving but is stationary. Diffusion of the molecules is due to a

concentration gradient. The general Fick's law equation can be written as follows for a binary mixture of  $A$  and  $B$ :

$$J_{Az}^* = -cD_{AB} \frac{dx_A}{dz} \quad (18.1-7)$$

where  $c$  is total concentration of  $A$  and  $B$  in  $\text{kg mol } A + B/\text{m}^3$ , and  $x_A$  is the mole fraction of  $A$  in the mixture of  $A$  and  $B$ . If  $c$  is constant, then, since  $c_A = cx_A$ ,

$$cdx_A = d(cx_A) = dc_A \quad (18.1-8)$$

Substituting into Eq. (18.1-7), we obtain Eq. (18.1-3) for constant total concentration:

$$J_{Az}^* = -D_{AB} \frac{dc_A}{dz} \quad (18.1-3)$$

This equation is the one more commonly used in many molecular diffusion processes. If  $c$  varies some, an

average value is often used with Eq. (18.1-3).

**EXAMPLE 18.1-1. Molecular Diffusion of Helium in Nitrogen**

A mixture of He and N<sub>2</sub> gas is contained in a pipe at 298 K and 1 atm total pressure that is constant throughout. At one end of the pipe at point 1, the partial pressure  $p_{A1}$  of He is 0.60 atm and at the other end it is 0.2 m (20 cm)  $p_{A2} = 0.20$  atm. Calculate the flux of He at steady state if  $D_{AB}$  of the He–N<sub>2</sub> mixture is  $0.687 \times 10^{-4} \text{ m}^2/\text{s}$  ( $0.687 \text{ cm}^2/\text{s}$ ). Use SI and cgs units.

**Solution:** Since total pressure  $P$  is constant, then  $c$  is constant, where  $c$  is as follows for a gas according to the perfect gas law:

$$PV = nRT \quad (18.1-9)$$

$$nV = PRT = c \quad (18.1-10)$$

where  $n$  is kg mol A plus B,  $V$  is volume in  $\text{m}^3$ ,  $T$  is temperature in K,  $R$  is  $8314.3 \text{ m}^3 \cdot \text{Pa}/\text{kgmol} \cdot \text{K}$  or  $R$  is  $82.057 \times 10^{-3} \text{ m}^3 \cdot \text{atm}/\text{kgmol} \cdot \text{K}$ , and  $c$  is kg mol A plus B/ $\text{m}^3$ . In cgs units,  $R$  is  $82.057 \text{ cm}^3 \cdot \text{atm}/\text{gmol} \cdot \text{K}$ .

For steady state, the flux  $J_{Az}^*$  in Eq. (18.1-3) is constant. Also,  $D_{AB}$  for a gas is constant. Rearranging Eq. (18.1-3) and integrating,

$$J_{Az}^* \int_{z_1}^{z_2} dz = -D_{AB} \int_{c_{A1}}^{c_{A2}} dc \quad J_{Az}^* = D_{AB} (c_{A1} - c_{A2}) \int_{z_1}^{z_2} dz$$

Also, from the perfect gas law,  $p_A V = n_A R T$ , and

$$c_{A1} = p_{A1} / RT = n_{A1} / V \quad (18.1-12)$$

Substituting Eq. (18.1-12) into (18.1-11),

$$J_{Az}^* = D_{AB} (p_{A1} - p_{A2}) / RT (z_2 - z_1) \quad (18.1-13)$$

This is the final equation to use, which is in a form easily used for gases. Partial pressures are  $p_{A1} = 0.6 \text{ atm} = 0.6 \times 1.01325 \times 10^5 = 6.08 \times 10^4 \text{ Pa}$  and  $p_{A2} = 0.2 \text{ atm} = 0.2 \times 1.01325 \times 10^5 = 2.027 \times 10^4 \text{ Pa}$ . Then, using SI units,

$$JA^* = \frac{(0.687 \times 10^{-4} \text{ m})(6.08 \times 10^4 \text{ Pa} - 2.027 \times 10^4 \text{ Pa})}{(8314.3 \text{ J kmol}^{-1} \text{ K}^{-1})(298 \text{ K})}$$

$$(0.2 \text{ m} - 0 \text{ m})JA^* = 5.63 \times 10^{-6} \text{ kg mol}^{-1} (\text{A}) \text{ m}^2 \text{ s}^{-1}$$

If pressures in atm are used with SI units,

$$JA^* = \frac{(0.687 \times 10^{-4} \text{ m})(0.60 \text{ atm} - 0.20 \text{ atm})}{(82.06 \text{ J kmol}^{-1} \text{ K}^{-1})(298 \text{ K})}$$

$$(0.2 \text{ m} - 0 \text{ m})JA^* = 5.63 \times 10^{-6} \text{ kg mol}^{-1} (\text{A}) \text{ m}^2 \text{ s}^{-1}$$

For cgs units, substituting into Eq. (18.1-13),

$$JA^* = \frac{(0.687 \text{ cm})(0.60 \text{ atm} - 0.20 \text{ atm})(82.06 \text{ J kmol}^{-1} \text{ K}^{-1})}{(298 \text{ K})(20 \text{ m} - 0 \text{ m})} = 5.63 \times 10^{-6} \text{ kg mol}^{-1} (\text{A}) \text{ cm}^2 \text{ s}^{-1}$$

Other driving forces (besides concentration differences) for diffusion also occur because of temperature, pressure, electrical potential, and other gradients. Details are given elsewhere (B3).

### 18.1D General Case for Diffusion of Gases A and B plus Convection

Up to now, we have considered Fick's law for diffusion in a stationary fluid; that is, there has

been no net movement or convective flow of the entire phase of the binary mixture  $A$  and  $B$ . The diffusion flux  $J_A^*$  occurred because of the concentration gradient. The rate at which moles of  $A$  passed a fixed point to the right, which will be taken as a positive flux, is  $J_A^* \text{ kg mol } A/s \cdot m^2$ . This flux can be converted to a velocity of diffusion of  $A$  to the right by

$$J_A^*(\text{kg mol } A/s \cdot m^2) = v_{Ad} C_A (\text{m}^3 \cdot \text{kg mol } A/m^3) \quad (18.1-14)$$

where  $v_{Ad}$  is the diffusion velocity of  $A$  in  $\text{m/s}$ .

Now let us consider what happens when the whole fluid is moving in bulk or convective flow to the right. The molar

average velocity of the whole fluid relative to a stationary point is  $v_M$  m/s. Component A is still diffusing to the right, but now its diffusion velocity  $v_{Ad}$  is measured relative to the moving fluid. To a stationary observer, A is moving faster than the bulk of the phase, since its diffusion velocity  $v_{Ad}$  is added to that of the bulk phase  $v_M$ . Expressed mathematically, the velocity of A relative to the stationary point is the sum of the diffusion velocity and the average or convective velocity:

$$v_A = v_{Ad} + v_M \quad (18.1-15)$$

where  $v_A$  is the velocity of A relative to a stationary point. Expressed pictorially,

$$v_A \rightarrow v_{Ad} \quad v_M \rightarrow$$

Multiplying Eq. (18.1-15) by  $c_A$ ,

$$c_A v_A = c_A v_{Ad} + c_A v_M \quad (18.1-16)$$

Each of the three terms represents a flux. The first term,  $c_A v_A$ , can be represented by the flux  $N_A$  kg mol  $A/s \cdot m^2$ . This is the total flux of  $A$  relative to the stationary point. The second term is  $J_A^*$ , the diffusion flux relative to the moving fluid. The third term is the convective flux of  $A$  relative to the stationary point. Hence, Eq. (18.1-16) becomes

$$N_A = J_A^* + c_A v_M \quad (18.1-17)$$

Let  $N$  be the total convective flux of the whole stream relative to the stationary point. Then,

$$N = c v_M = N_A + N_B \quad (18.1-18)$$

Or, solving for  $v_M$ ,

$$vM = N_A + N_B c \quad (18.1-19)$$

Substituting Eq. (18.1-19) into Eq. (18.1-17),

$$N_A = J_A^* + c A c (N_A + N_B) \quad (18.1-20)$$

Since  $J_A^*$  is Fick's law, Eq. (18.1-7) is

$$N_A = -c D_{AB} \frac{dx_A}{dz} + c A c (N_A + N_B) \quad (18.1-21)$$

Equation (18.1-21) is the final general equation to use for diffusion plus convection when the flux  $N_A$  is used, which is relative to a stationary point. A similar equation can be written for  $N_B$ .

$$N_B = -c D_{BA} \frac{dx_B}{dz} + c B c (N_A + N_B) \quad (18.1-22)$$

To solve Eq. (18.1-21) or (18.1-22), the



relation between the flux  $N_A$  and  $N_B$  must be known. Equations (18.1-21) and (18.1-22) hold for diffusion in a gas, liquid, or solid.

For equimolar counterdiffusion,  $N_A = -N_B$  and the convective term in Eq. (18.1-21) becomes zero. Then,  $N_A = J_A^* = -N_B = -J_B^*$ .

## 18.2 Diffusion Coefficient

### 18.2A Diffusion Coefficients for Gases

*1. Experimental determination of diffusion coefficients.* A number of different experimental methods have been used to determine the molecular diffusivity for binary gas mixtures. Several of the important methods are described here. One method is to evaporate a pure liquid in a narrow tube with a gas passed

over the top, as shown in Fig.

19.1-2a. The fall in liquid level is measured with time and the diffusivity calculated from Eq. (19.1-17).

In another method, two pure gases having equal pressures are placed in separate sections of a long tube separated by a partition. The partition is slowly removed and diffusion proceeds. After a given time, the partition is reinserted and the gas in each section analyzed. The diffusivities of the vapor of solids such as naphthalene, iodine, and benzoic acid in a gas have been obtained by measuring the rate of evaporation of a sphere. Equation (19.1-23) can be used.

A method often used is the two-bulb

method (N1). The apparatus consists of two glass bulbs with volumes  $V_1$  and  $V_2$  m<sup>3</sup> connected by a capillary of cross-sectional area  $A$  m<sup>2</sup> and length  $L$ , whose volume is small compared to  $V_1$  and  $V_2$ , as shown in Fig. 18.2-1. Pure gas  $A$  is added to  $V_1$  and pure  $B$  to  $V_2$  at the same pressures. The valve is opened, diffusion proceeds for a given time, and then the valve is closed and the mixed contents of each chamber are sampled separately.

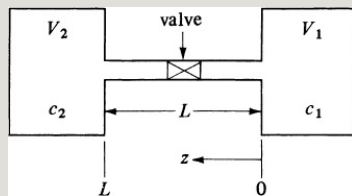


Figure 18.2-1. *Diffusivity measurement of gases by the two-bulb method.*

The equations can be derived by neglecting the capillary volume and assuming each bulb is always of a

uniform concentration. Assuming quasi-steady-state diffusion in the capillary,

$$J_A^* = -DAB \frac{dc}{dz} = -DAB(c_2 - c_1)L \quad (18.2-1)$$

where  $c_2$  is the concentration of A in  $V_2$  at time  $t$  and  $c_1$  in  $V_1$ . The rate of diffusion of A going to  $V_2$  is equal to the rate of accumulation in  $V_2$ :

$$J_A^* = -DAB(c_2 - c_1)AL = V_2 \frac{dc_2}{dt} \quad (18.2-2)$$

The average value  $c_{av}$  at equilibrium can be calculated by a material balance from the starting compositions  $c_{10}$  and  $c_{20}$  at  $t = 0$ :

$$(V_1 + V_2)c_{av} = V_1c_{10} + V_2c_{20} \quad (18.2-3)$$

A similar balance at time  $t$  gives

$$(V_1 + V_2)c_{av} = V_1c_{10} + V_2c_{20} \quad (18.2-4)$$

Substituting  $c_1$  from Eq. (18.2-4) into Eq. (18.2-2), rearranging, and integrating between  $t = 0$  and  $t = t$ , the final equation is

$$c_{av} - c_2 c_{av} - c_{20} = \exp[-D_{AB}(V_1 + V_2)(L/A)(V_2/V_1)t] \quad (18.2-5)$$

If  $c_2$  is obtained by sampling at  $t$ ,  $D_{AB}$  can be calculated.

*2. Experimental diffusivity data.* Some typical data are given in Table 18.2-1. Other data are tabulated in Perry and Green (P1) and Reid et al. (R1). The values range from about  $0.05 \times 10^{-4} \text{ m}^2/\text{s}$ , where a large molecule is present, to about  $1.0 \times 10^{-4} \text{ m}^2/\text{s}$ , where  $\text{H}_2$  is present at room temperatures. The relation between diffusivity in  $\text{m}^2/\text{s}$  and

ft<sup>2</sup>/h is  $1 \text{ m}^2/\text{s} = 3.875 \times 10^4 \text{ ft}^2/\text{h}$ .

### *3. Prediction of diffusivity for gases.*

The diffusivity of a binary gas mixture in the dilute gas region, that is, at low pressures near atmospheric, can be predicted using the kinetic theory of gases. The gas is assumed to consist of rigid spherical particles that are completely elastic on collision with another molecule, which implies that momentum is conserved.

Table 18.2-1. *Diffusion Coefficients of Gases at 101.32 kPa Pressure*



In a simplified treatment, it is assumed that there are no attractive or repulsive forces between the molecules. The derivation uses the mean free path  $\lambda$ ,

which is the average distance that a molecule has traveled between collisions. The final equation is

$$D_{AB} = \frac{1}{3} \bar{u} \lambda \quad (18.2-6)$$

where  $\bar{u}$  is the average velocity of the molecules. The final equation obtained after substituting expressions for  $\bar{u}$  and  $\lambda$  into Eq. (18.2-6) is approximately correct, since it correctly predicts  $D_{AB}$  proportional to  $1/\text{pressure}$  and approximately predicts the temperature effect.

A more accurate and rigorous treatment must consider the intermolecular forces of attraction and repulsion between molecules as well as the different sizes of molecules  $A$  and  $B$ . Chapman and Enskog (H3) solved the Boltzmann

equation, which uses a distribution function instead of the mean free path  $\lambda$ . To solve the equation, a relation between the attractive and repulsive forces between a given pair of molecules must be used. For a pair of nonpolar molecules, a reasonable approximation to the forces is the Lennard–Jones function.

The final relation for predicting the diffusivity of a binary gas pair of  $A$  and  $B$  molecules is

$$D_{AB} = 1.8583 \times 10^{-7} \frac{T^{3/2}}{P \sigma_{AB}^2 \Omega_{D,AB}} \left( \frac{1}{M_A} + \frac{1}{M_B} \right)^{1/2} \quad (18.2-7)$$

where  $D_{AB}$  is the diffusivity in  $\text{m}^2/\text{s}$ ,  $T$  is the temperature in K,  $M_A$  is the molecular weight of  $A$  in kg mass/kg mol,  $M_B$  is the molecular weight of  $B$ ,



and  $P$  is the absolute pressure in atm.

The term  $\sigma_{AB}$  is an “average collision diameter” ( $\sigma_{AB} = \frac{\sigma_A + \sigma_B}{2}$ ) and  $\Omega_{D,AB}$  is a collision integral based on the Lennard–Jones potential. Values of  $\sigma_A$  and  $\sigma_B$  can be found in Appendix A.6.1 and  $\Omega_{D,AB}$  can be obtained from a number of sources (B3, G2, H3, R1) or from the following equation.

$$5610 + 0.1930 \exp(0.47635 T^*) + 1.03587 \exp(1.52996 T^*) + (18.2 - 8)$$

where  $T^* = kT/\epsilon_{AB}$  and  $\epsilon_{ABk} = \epsilon_A k \epsilon_B k$

Values for  $\epsilon_A k$  and  $\epsilon_B k$  can also be found in Appendix A.6.1.

The collision integral  $\Omega_{D,AB}$  is a ratio that gives the deviation of a gas with interactions as compared to a gas of

rigid, elastic spheres. This value would be 1.0 for a gas with no interactions. Equation (18.2-7) predicts diffusivities with an average deviation of about 8% up to about 1000 K (R1). For a polar–nonpolar gas mixture, Eq. (18.2-7) can be used if the correct force constant is used for the polar gas ( $M_1$ ,  $M_2$ ). For polar–polar gas pairs, the potential-energy function commonly used is the *Stockmayer potential* ( $M_2$ ).

The effect of concentration of  $A$  in  $B$  in Eq. (18.2-7) is not included. However, for real gases with interactions, the maximum effect of concentration on diffusivity is about 4% (G2). In most cases, the effect is considerably less, and hence it is usually neglected.

Equation (18.2-7) is relatively

complicated to use, and often some of the constants such as  $\sigma_{AB}$  are not available or are difficult to estimate. Hence, the semiempirical method of Fuller et al. (F1), which is much more convenient to use, is often preferred. The equation was obtained by correlating many recent data and it uses atomic volumes from Table 18.2-2, which are summed for each gas molecule. The equation is

*Table 18.2-2. Atomic Diffusion Volumes for Use with the Fuller, Schettler, and Giddings Method\**



\*Parentheses indicate that the value listed is based on only a few data points.

*Source:* Reprinted with permission from E. N. Fuller, P. D. Schettler, and J. C. Giddings, *Ind. Eng. Chem.*, **58**, 19 (1966). American Chemical Society.

$$D_{AB} = 1.00 \times 10^{-7} T^{1.75} (1/M_A + 1/M_B)^{1/2} P [(\sum v_A)^{1/3} + (\sum v_B)^{1/3}]^2 \quad (18.2-9)$$

where  $\sum v_A$  = the sum of structural volume increments, Table 18.2-2, and  $D_{AB}$  = m<sup>2</sup>/s. This method can be used for mixtures of nonpolar gases or for a polar–nonpolar mixture. However, its accuracy is not quite as good as that of Eq. (18.2-7).

Equation 18.2-9 shows that  $D_{AB}$  is proportional to  $1/P$  and to  $T^{1.75}$ . If an experimental value of  $D_{AB}$  is available at a given  $T$  and  $P$ , and it is desired to have a value of  $D_{AB}$  at another  $T$  and  $P$ , one should correct the experimental value to the new  $T$  and  $P$  by means of the relationship  $D_{AB} \propto T^{1.75}/P$ .

4. *Schmidt number of gases.* The

*Schmidt number* of a gas mixture of dilute  $A$  in  $B$  is dimensionless and is defined as

$$N_{Sc} = \mu \rho D_{AB} \quad (18.2-10)$$

where  $\mu$  is viscosity of the gas mixture, which is viscosity of  $B$  for a dilute mixture in  $\text{Pa} \cdot \text{s}$  or  $\text{kg/m} \cdot \text{s}$ ,  $D_{AB}$  is diffusivity in  $\text{m}^2/\text{s}$ , and  $\rho$  is the density of the mixture in  $\text{kg/m}^3$ . For a gas, the Schmidt number can be assumed independent of temperature over moderate ranges and independent of pressure up to about 10 atm or  $10 \times 10^5$  Pa.

The Schmidt number is the dimensionless ratio of the molecular momentum diffusivity  $\mu/\rho$  to the molecular mass diffusivity  $D_{AB}$ . Values

of the Schmidt number for gases range from about 0.5 to 2. For liquids, Schmidt numbers range from about 100 to over 10 000 for viscous liquids.

**EXAMPLE 18.2-1. Estimation of Diffusivity of a Gas Mixture**

Normal butanol (*A*) is diffusing through air (*B*) at 1 atm abs. Using the Fuller et al. method, estimate the diffusivity  $D_{AB}$  for the following temperatures and compare with the experimental data:

- For 0°C
- For 25.9°C
- For 0°C and 2.0 atm abs

**Solution:** For part (a),  $P = 1.00$  atm,  $T = 273 + 0 = 273$  K,  $M_A$  (butanol) = 74.1, and  $M_B$  (air) = 29. From Table 18.2-2,

$$\sum v_A = 4(16.5) + 10(1.98) + 1(5.48) = 91.28. \quad \sum v_B = 20.1 \text{ (air)}$$

Substituting into Eq. (18.2-9),

$$D_{AB} = 1.0 \times 10^{-7} (273)^{1/4} (1/74.1 + 1/29)^{1/4} (91.28)^{1/3} + (20.1)^{1/3} = 7.73 \times 10^{-6} \text{ m}^2/\text{s}$$

This value deviates by +10% from the experimental value of  $7.03 \times 10^{-6} \text{ m}^2/\text{s}$  from Table 18.2-1.

For part (b),  $T = 273 + 25.9 = 298.9$ . Substituting into Eq. (18.2-9),  $D_{AB} = 9.05 \times 10^{-6} \text{ m}^2/\text{s}$ . This value deviates by +4% from the experimental value of  $8.70 \times 10^{-6} \text{ m}^2/\text{s}$ .

For part (c), the total pressure  $P = 2.0$  atm. Using the value predicted in part (a) and correcting for pressure,

$$D_{AB} = 7.73 \times 10^{-6} (1.0/2.0) = 3.865 \times 10^{-6} \text{ m}^2/\text{s}$$

## 18.2B Diffusion Coefficients for Liquids

*1. Experimental determination of diffusivities.* Several different methods are used to determine diffusion coefficients experimentally in liquids. In one method, unsteady-state diffusion in a long capillary tube is carried out and the diffusivity determined from the concentration profile. If the solute  $A$  is diffusing in  $B$ , the diffusion coefficient determined is  $D_{AB}$ . Also, the value of diffusivity is often very dependent upon the concentration of the diffusing solute  $A$ . For liquids, unlike gases, the diffusivity  $D_{AB}$  does not equal  $D_{BA}$ .

In a fairly common method, a relatively dilute solution and a slightly more concentrated solution are placed in

chambers on opposite sides of a porous membrane of sintered glass, as shown in Fig. 18.2-2. Molecular diffusion takes place through the narrow passageways of the pores in the sintered glass while the two compartments are stirred. The effective diffusion length is  $\tau\delta$ , where the tortuosity  $\tau > 1$  is a constant and corrects for the fact that the path is actually greater than  $\delta$  cm. In this method, discussed by Bidstrup and Geankoplis (B4), the effective diffusion length is obtained by calibrating with a solute such as KCl having a known diffusivity.

To derive the equation, quasi-steady-state diffusion in the membrane is assumed:

$$N_A = \epsilon D_{AB} = c - c' \tau \delta \quad (18.2-11)$$



where  $c$  is the concentration in the lower chamber at a time  $t$ ,  $c'$  is the concentration in the upper chamber, and  $\epsilon$  is the fraction of area of the glass open to diffusion. Making a balance on solute  $A$  in the upper chamber, where the rate in = rate out + rate of accumulation, making a similar balance on the lower chamber, using volume  $V = V'$ , and combining and integrating, the final equation is

$$\ln(c_0 - c_0'c - c') = 2\epsilon A \tau \delta V D A B t \quad (18.2-12)$$

where  $2\epsilon A / \tau \delta V$  is a cell constant that can be determined using a solute of known diffusivity, such as KCl. The values  $c_0$  and  $c_0'$  are initial concentrations, and  $c$  and  $c'$  are final concentrations.

## *2. Experimental liquid diffusivity data.*

Experimental diffusivity data for binary mixtures in the liquid phase are given in Table 18.2-3. All the data are for dilute solutions of the diffusing solute in the solvent. In liquids, the diffusivities often vary quite markedly with concentration. Hence, the values in Table 18.2-3 should be used with some caution when outside the dilute range. Additional data are given in (P1). Values for biological solutes in solution are given in the next section. As noted in the table, the diffusivity values are quite small and in the range of about  $0.5 \times 10^{-9}$  to  $5 \times 10^{-9}$  m<sup>2</sup>/s for relatively nonviscous liquids. Diffusivities in gases are larger by a factor of  $10^4$ – $10^5$ .

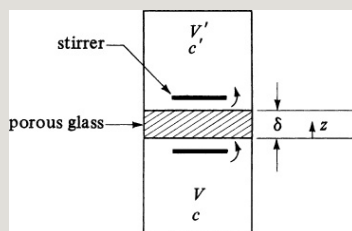


Figure 18.2-2. *Diffusion cell for determination of diffusivity in a liquid.*

## Table 18.2-3. *Diffusion Coefficients for Dilute Liquid Solutions*

### 18.2C Prediction of Diffusivities in Liquids

The equations for predicting diffusivities of dilute solutes in liquids are by necessity semiempirical, since the theory for diffusion in liquids is not well established as yet. The Stokes–Einstein equation, one of the first theories, was derived for a very large spherical molecule ( $A$ ) diffusing in a liquid solvent ( $B$ ) of small molecules. Stokes’ law was used to describe the drag on the moving solute molecule. Then, the equation

was modified by assuming that all molecules are alike and arranged in a cubic lattice, and by expressing the molecular radius in terms of the molar volume (W5),

$$D_{AB} = 9.96 \times 10^{-16} T \mu V_A^{1/3} \quad (18.2-13)$$

where  $D_{AB}$  is diffusivity in  $\text{m}^2/\text{s}$ ,  $T$  is temperature in K,  $\mu$  is viscosity of solution in  $\text{Pa} \cdot \text{s}$  or  $\text{kg}/\text{m} \cdot \text{s}$ , and  $V_A$  is the solute molar volume at its normal boiling point in  $\text{m}^3/\text{kg mol}$ . This equation applies very well to extremely large unhydrated and sphere-like solute molecules of about 1000 molecular weight or greater (R1), or in cases where the  $V_A$  is above about  $0.500 \text{ m}^3/\text{kg mol}$  (W5) in aqueous solution.

For smaller solute molar volumes, Eq.

(18.2-12) does not hold. Several other theoretical derivations have been attempted, but the equations do not predict diffusivities very accurately. Hence, a number of semitheoretical expressions have been developed (R1). The Wilke–Chang (T3, W5) correlation can be used for most general purposes where the solute (*A*) is dilute in the solvent (*B*):

$$D_{AB} = 1.173 \times 10^{-16} (\phi M_B)^{1/2} T \mu_B^{-1} V_A^{0.6} \quad (18.2-14)$$

where  $M_B$  is the molecular weight of solvent *B*,  $\mu_B$  is the viscosity of *B* in Pa · s or kg/m · s,  $V_A$  is the solute molar volume at the boiling point (L2), which can be obtained from Table 18.2-4, and  $\phi$  is an “association parameter” of the solvent, where  $\phi$  is 2.6 for water, 1.9 for methanol, 1.5 for ethanol, 1.0 for

benzene, 1.0 for ether, 1.0 for heptane, and 1.0 for other unassociated solvents. When values of  $V_A$  are above  $0.500 \text{ m}^3/\text{kg mol}$  ( $500 \text{ cm}^3/\text{g mol}$ ), Eq. (18.2-13) should be used.

When water is the solute, values from Eq. (18.2-14) should be multiplied by a factor of 1/2.3 (R1). Equation (18.2-14) predicts diffusivities with a mean deviation of 10–15% for aqueous solutions and about 25% in nonaqueous solutions. Outside the range 278–313 K, the equation should be used with caution. For water as the diffusing solute, an equation by Reddy and Doraiswamy is preferred (R2). Skelland (S5) summarizes the correlations available for binary systems. Geankoplis (G2) discusses and gives an equation to predict diffusion in a ternary system,

where a dilute solute  $A$  is diffusing in a mixture of  $B$  and  $C$  solvents. This case is often approximated in industrial processes.

**EXAMPLE 18.2-2. Prediction of Liquid Diffusivity**

Predict the diffusion coefficient of acetone ( $\text{CH}_3\text{COCH}_3$ ) in water at  $25^\circ$  and  $50^\circ\text{C}$  using the Wilke–Chang equation. The experimental value is  $1.28 \times 10^{-9} \text{ m}^2/\text{s}$  at  $25^\circ\text{C}$  (298 K).

**Solution:** From Appendix A.2, the viscosity of water at  $25.0^\circ\text{C}$  is  $\mu_B = 0.8937 \times 10^{-3} \text{ Pa} \cdot \text{s}$  and at  $50^\circ\text{C}$ ,  $0.5494 \times 10^{-3}$ . From Table 18.2-4 for  $\text{CH}_3\text{COCH}_3$  with 3 carbons + 6 hydrogens + 1 oxygen,

$$V_A = 3(0.0148) + 6(0.0037) + 1(0.0074) = 0.0740 \text{ m}^3/\text{kg mol}$$

For water, the association parameter  $\phi = 2.6$  and  $M_B = 18.02 \text{ kg mass/kg mol}$ . For  $25^\circ\text{C}$ ,  $T = 298 \text{ K}$ . Substituting into Eq. (18.2-14),

$$\begin{aligned} D_{AB} &= (1.173 \times 10^{-16}) \\ (\phi M_B)^{1/2} T \mu_B V_A^{0.6} &= (1.173 \times 10^{-16}) (2.6 \times 18.02)^{1/2} (298) \\ &\quad (0.8937 \times 10^{-3}) (0.0740)^{0.6} = 1.277 \times 10^{-9} \text{ m}^2/\text{s} \end{aligned}$$

For  $50^\circ\text{C}$  or  $T = 323 \text{ K}$ ,

$$\begin{aligned} D_{AB} &= (1.173 \times 10^{-16}) (2.6 \times 18.02)^{1/2} (323) (0.5494 \times 10^{-3}) \\ &\quad (0.0740)^{0.6} = 2.251 \times 10^{-9} \text{ m}^2/\text{s} \end{aligned}$$

Table 18.2-4. *Atomic and Molar Volumes at the Normal Boiling Point*

## **18.2D Prediction of Diffusivities of Electrolytes in Liquids**

Electrolytes in aqueous solution such as KCl dissociate into cations and anions. Each ion diffuses at a different rate. If the solution is to remain electrically neutral at each point (assuming the absence of any applied electric-potential field), the cations and anions diffuse effectively as one component, and the ions have the same net motion or flux. Hence, the average diffusivity of the electrolyte KCl is a combination of the diffusion coefficients of the two ions. Its value is in between the diffusivity values for the two ions.

The well-known Nernst–Haskell equation for dilute, single-salt solutions



can be used at 25°C to predict the overall diffusivity  $D_{AB}$  of the salt  $A$  in the solvent  $B$  (R1):

$$D_{AB}^{\circ} = 8.928 \times 10^{-10} T (1/n_{++} + 1/n_{--}) (1/\lambda_{++} + 1/\lambda_{--}) \quad (18.2-15)$$

where  $D_{AB}^{\circ}$  is in  $\text{cm}^2/\text{s}$ ,  $n_{+}$  is the valence of the cation,  $n_{-}$  is the valence of the anion, and  $\lambda_{+}$  and  $\lambda_{-}$  are the limiting ionic conductances in very dilute solutions in  $(\text{A}/\text{cm}^2)(\text{V}/\text{cm})(\text{g equiv.}/\text{cm}^2)$ . Values of the conductances are given in Table 18.2-5 at 25°C. The value of  $T = 298.2$  in Eq. (18.2-15) when using values of  $\lambda_{+}$  and  $\lambda_{-}$  given in Table 18.2-5 at 25°C.

The diffusion coefficient of an individual ion  $i$  at 25°C can be calculated from

$$D_j = 2.662 \times 10^{-7} \lambda_{\text{ini}} (18.2-16)$$

Then, Eq. (18.2-15) becomes

$$DAB_o = \frac{n_1 + n_2 n_2 / D_1 + n_1 / D_2}{(18.2-17)}$$

To correct  $DAB_o$  for temperature, first calculate  $DAB_o$  at  $25^\circ\text{C}$  from Eq. (18.2-15) using the  $\lambda_+$  and  $\lambda_-$  values given in Table 18.2-5 at  $25^\circ\text{C}$ . Then, multiply this  $DAB_o$  at  $25^\circ\text{C}$  by  $T / (344 \mu W)$ , where  $\mu W$  is the viscosity of water in cp at the new  $T$  (R1).

Table 18.2-5. *Limiting Ionic Conductances in Water at  $25^\circ\text{C}$  (R4)*

**EXAMPLE 18.2-3. Diffusivities of Electrolytes**

Predict the diffusion coefficients of dilute electrolytes for the following cases:

- For KCl at 25°C, predict  $D_{AB}$  and compare with the value in Table 18.2-3.
- Predict the value for KCl at 18.5°C. The experimental value is  $1.7 \times 10^{-5} \text{ cm}^2/\text{s}$  (S9).
- For  $\text{CaCl}_2$  predict  $D_{AB}$  at 25°C. Compare with the experimental value of  $1.32 \times 10^{-5} \text{ cm}^2/\text{s}$  (C10). Also predict  $D_i$  of the ion  $\text{Ca}^{2+}$  and of  $\text{Cl}^-$  and use Eq. (18.2-16).

**Solution:** For part (a) from Table 18.2-5,  $\lambda_+(\text{K}^+) = 73.5$  and  $\lambda_-(\text{Cl}^-) = 76.3$ . Substituting into Eq. (18.2-15),

$$D_{AB} = 8.928 \times 10^{-10} (298) \left( \frac{1}{1} + \frac{1}{1} \left( \frac{1}{73.5} + \frac{1}{76.3} \right) \right) = 1.993 \times 10^{-5} \text{ cm}^2/\text{s}$$

The experimental value in Table 18.2-3 is  $1.87 \times 10^{-5} \text{ cm}^2/\text{s}$ , which is reasonably close considering that this value is not at infinite dilution.

For part (b), the correction factor for temperature is  $T/(334 \mu_w)$ . For  $T = 273.2 + 18.5 = 291.7 \text{ K}$  from Table A.2-4,  $\mu_w = 1.042 \text{ cp}$ . Then,  $T/(334 \mu_w) = 291.7/(334 \times 1.042) = 0.8382$ . Correcting the value of  $D_{AB}$  at 25°C to 18.5°C, ionic conductances in  $(\text{A}/\text{cm}^2)(\text{V}/\text{cm})(\text{g equiv.}/\text{cm}^2)$

$$D_{AB}(185^\circ\text{C}) = 0.8382 D_{AB}(25^\circ\text{C}) = 0.8382 (1.993 \times 10^{-5}) = 1.671 \times 10^{-5} \text{ cm}^2/\text{s}$$

This compares with the experimental value of  $1.7 \times 10^{-5} \text{ cm}^2/\text{s}$ .

For part (c), for  $\text{CaCl}_2$ , from Table 18.2-5,  $\lambda_+(\text{Ca}^{2+}/2) = 59.5$ ,  $\lambda_-(\text{Cl}^-) = 76.3$ ,  $n_+ = 2$ , and  $n_- = 1$ . Again, using Eq. (18.2-15),

$$D_{AB} = 8.928 \times 10^{-10} (298) \left( \frac{1}{2} + \frac{1}{1} \left( \frac{1}{59.5} + \frac{1}{76.3} \right) \right) = 1.335 \times 10^{-5} \text{ cm}^2/\text{s}$$

This compares well with the experimental value of  $1.32 \times 10^{-5}$  (C10).

To calculate the individual ion diffusivities at 25°C using Eq. (18.2-16),

$$D_{\text{Ca}^{2+}} = 2.662 \times 10^{-7} \lambda_+ n_+ = 2.662 \times 10^{-7} (59.5)^2 = 0.792 \times 10^{-5} \text{ cm}^2/\text{s}$$

$$D_{\text{Cl}^-} = 2.662 \times 10^{-7} \lambda_- n_- = 2.662 \times 10^{-7} (76.3)$$

$$n = 2.662 \times 10^{-7} (76.3)^2 = 2.031 \times 10^{-5} \text{ cm}^2/\text{s}$$

Substituting into Eq. (18.2-17) for 25°C,

$$D_{AB} = \frac{n_{++}n_{-}/D_{++} + n_{+}/D_{-}}{(2.031 \times 10^{-5})} = \frac{2 + 11/(0.792 \times 10^{-5})}{1.335 \times 10^{-5}} = 1.335 \times 10^{-5} \text{ cm}^2/\text{s}$$

Hence, one can see that the diffusivity of the salt is in between that of the two ions.

## 18.2E Diffusion of Biological Solutes in Liquids

*1. Introduction.* The diffusion of small solute molecules and especially macromolecules (*e.g.*, proteins) in aqueous solutions are important in the processing and storing of biological systems and in the life processes of microorganisms, animals, and plants. Food processing is an important area where diffusion plays a significant role. In the drying of liquid solutions of fruit juice, coffee, and tea, water and frequently volatile flavor or aroma constituents are removed. These constituents

diffuse through the liquid during evaporation.

In fermentation processes, nutrients, sugars, oxygen, and so on diffuse to the microorganisms, and waste products and, at times, enzymes diffuse away. In the kidney dialysis machine various waste products diffuse through the blood solution to a membrane and then pass through the membrane to an aqueous solution.

Macromolecules in solution that have molecular weights of tens of thousands or more were often called *colloids*, but now we know they generally form true solutions. The diffusion behavior of protein macromolecules in solution is affected by their large sizes and shapes, which can be random coils, rods, or

globules (spheres or ellipsoids). Also, interactions of the large molecules with the small solvent and/or solute molecules affect the diffusion of the macromolecules as well as the small solute molecules.

In addition to the Fickian diffusion to be discussed here, mediated transport often occurs in biological systems where chemical interactions occur. This latter type of transport will not be discussed here.

*2. Interaction and “binding” in diffusion.* Protein macromolecules are very large compared to small solute molecules such as urea, KCl, and sodium caprylate, and often have a number of sites for interaction or “binding” of the solute or ligand

molecules. An example is the binding of oxygen to hemoglobin in the blood.

Human serum albumin protein binds most of the free fatty acids in the blood and increases their apparent solubility.

Bovine serum albumin, which is in milk, binds 23 mol sodium caprylate/mol albumin when the albumin concentration is 30 kg/m<sup>3</sup> solution and the sodium caprylate is about 0.05 molar (G6). Hence, Fickian-type diffusion of macromolecules and small solute molecules can be greatly affected by the presence of both types of molecules even in dilute solutions.

*3. Experimental methods for determining diffusivity.* Methods for determining the diffusivity of biological solutes are similar to those discussed previously in Section 18.2, with some

modifications. In the diaphragm diffusion cell shown in Fig. 18.2-2, the chamber is made of Lucite® or Teflon® instead of glass, since protein molecules bind to glass. Also, the porous membrane through which the molecular diffusion occurs is composed of cellulose acetate or other polymers (G5, G6, K1).

*4. Experimental data for biological solutes.* Most of the experimental data in the literature on protein diffusivities have been extrapolated to zero concentration since the diffusivity is often a function of concentration. A tabulation of the diffusivities of a few proteins and also of small solutes often present in biological systems is given in Table 18.2-6.



The diffusion coefficients for the large protein molecules are on the order of magnitude of  $5 \times 10^{-11} \text{ m}^2/\text{s}$  compared to the values of about  $1 \times 10^{-9} \text{ m}^2/\text{s}$  for the small solutes in Table 18.2-6. This means macromolecules diffuse at a rate about 20 times as slow as small solute molecules for the same concentration differences.

When the concentration of macromolecules such as proteins increases, the diffusion coefficient would be expected to decrease, since the diffusivity of small solute molecules decreases with increasing concentration. However, experimental data (G4, C7) show that the diffusivity of macromolecules such as proteins decreases in some cases and increases in others as protein concentration

increases. Surface charges on the molecules appear to play a role in these phenomena.

When small solutes such as urea, KCl, and sodium caprylate, which are often present with protein macromolecules in solution, diffuse through these protein solutions, the diffusivity decreases with increasing polymer concentration (C7, G5, G6, N3). Experimental data for the diffusivity of the solute sodium caprylate ( $A$ ) diffusing through bovine serum albumin ( $P$ ) solution show that the diffusivity  $D_{AP}$  of  $A$  through  $P$  is markedly reduced as the protein ( $P$ ) concentration is increased (G5, G6). A large part of the reduction is due to the binding of  $A$  to  $P$  so that there is less free  $A$  to diffuse. The rest is due to blockage by the large molecules.

Table 18.2-6. *Diffusion Coefficients for Dilute Biological Solutes in Aqueous Solution*

5. *Prediction of diffusivities for biological solutes.* For predicting the diffusivity of small solutes alone in aqueous solution with molecular weights less than about 1000, or solute molar volumes less than about 0.500 m<sup>3</sup>/kg mol, Eq. (18.2-14) should be used. For larger solutes, the equations to be used are not as accurate. As an approximation, the Stokes–Einstein equation (18.2-13) can be used:

$$D_{AB} = 9.96 \times 10^{-16} T \mu V_A^{1/3} \quad (18.2-13)$$

Probably a better approximate equation to use is the semiempirical equation of

Polson (P3), which is recommended for a molecular weight above 1000. A modification of his equation to take into account different temperatures is as follows for dilute aqueous solutions:

$$D_{AB} = 9.40 \times 10^{-15} T \mu (M_A)^{1/3} \quad (18.2-18)$$

where  $M_A$  is the molecular weight of the large molecule A. When the shape of the molecule deviates greatly from a sphere, this equation should be used with caution.

**EXAMPLE 18.2-4. Prediction of Diffusivity of Albumin**

Predict the diffusivity of bovine serum albumin at 298 K in water as a dilute solution using the modified Polson equation (18.2-18) and compare with the experimental value in Table 18.2-6.

**Solution:** The molecular weight of bovine serum albumin (A) from Table 18.2-6 is  $M_A = 67\,500$  kg/kg mol. The viscosity of water at 25°C is  $0.8937 \times 10^{-3}$  Pa · s and  $T = 298$  K. Substituting into Eq. (18.2-18),

$$D_{AB} = 9.40 \times 10^{-15} T \mu (M_A)^{1/3} = (9.40 \times 10^{-15}) 298 (0.8937 \times 10^{-3}) (67500)^{1/3} = 7.70 \times 10^{-11} \text{ m}^2/\text{s}$$

This value is 11% higher than the experimental value of  $6.81 \times 10^{-11}$  m<sup>2</sup>/s.

6. *Prediction of diffusivity of small solutes in protein solution.* When a small solute ( $A$ ) diffuses through a macromolecule ( $P$ ) protein solution, Eq. (18.2-14) cannot be used to predict the small solute because of blockage to diffusion by the large molecules. The data needed to predict these effects are the diffusivity  $D_{AB}$  of solute  $A$  in water alone, the water of hydration on the protein, and an obstruction factor. A semitheoretical equation that can be used to approximate the diffusivity  $D_{AP}$  of  $A$  in globular-type protein  $P$  solutions is as follows, where only the blockage effect is considered (C8, G5, G6) and no binding is present:

$$D_{AP} = D_{AB}(1 - 1.81 \times 10^{-3} c_p) \quad (18.2-19)$$

where  $c_p = \text{kg P/m}^3$ . Then, the diffusion equation is

$$N_A = D A P (c_{A1} - c_{A2}) / (z_2 - z_1)$$

where  $c_{A1}$  is concentration of A in  $\text{kg mol A/m}^3$ .

*7. Prediction of diffusivity with binding present.* When A is in a protein solution P and binds to P, the diffusion flux of A is equal to the flux of unbound solute A in the solution plus the flux of the protein–solute complex. Methods for predicting this flux are available (G5, G6) when binding data have been experimentally obtained. The equation used is

$$DAP = \frac{[DAB(1 - 1.81 \times 10^{-3} c_p) (\% \text{Free A} 100) + DP(\% \text{Bound A} 100)]}{(18.2 - 21)}$$

where  $D_P$  is the diffusivity of the protein alone in the solution,  $\text{m}^2/\text{s}$ , and free  $A$  is that  $A$  not bound to the protein, which is determined from the experimental binding coefficient. Then, Eq. (18.2-20) is used to calculate the flux, where  $c_A$  is the total concentration of  $A$  in the solution.

## **18.3 Convective Mass Transfer**

### **18.3A Convective Mass-Transfer Coefficient**

When a fluid is flowing outside a solid surface in forced convection motion, we can express the rate of convective mass transfer from the surface to the fluid, or vice versa, by the following equation:

$$N_A = k_c(c_{L1} - c_{Li}) \quad (18.3-1)$$

where  $k_c$  is a mass-transfer coefficient in

m/s,  $c_{L1}$  is the bulk fluid concentration in kg mol A/m<sup>3</sup>, and  $c_{Li}$  is the concentration in the fluid next to the surface of the solid. This mass-transfer coefficient is very similar to the heat-transfer coefficient  $h$  and is a function of the system geometry, fluid properties, and flow velocity. In Chapter 21, we consider convective mass transfer in detail.

## **18.4 Molecular Diffusion Plus Convection and Chemical Reaction**

### **18.4A Different Types of Fluxes and Fick's Law**

In Section 18.1D, the flux  $J_A^*$  was defined as the molar flux of A in kg mol A/s · m<sup>2</sup> relative to the molar average velocity  $v_M$  of the whole or bulk stream. Also,  $N_A$  was defined as the molar flux of A relative to stationary coordinates. Fluxes and

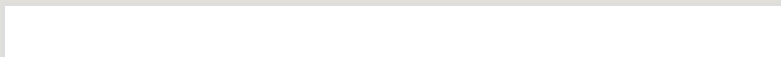


velocities can also be defined in other ways. Table 18.4-1 lists the different types of fluxes and velocities often used in binary systems.

The velocity  $v$  is the mass average velocity of the stream relative to stationary coordinates and can be obtained by actually weighing the flow for a timed increment. It is related to the velocity  $v_A$  and  $v_B$  by

$$v = w_A v_A + w_B v_B = \frac{\rho_A}{\rho} v_A + \frac{\rho_B}{\rho} v_B \quad (18.4-1)$$

Table 18.4-1. *Different Types of Fluxes and Velocities in Binary Systems*



where  $w_A$  is  $\rho_A/\rho$ , the weight fraction of

$A$ ;  $w_B$  is the weight fraction of  $B$ ; and  $v_A$  is the velocity of  $A$  relative to stationary coordinates in m/s. The molar average velocity  $v_M$  in m/s is relative to stationary coordinates:

$$v_M = x_A v_A + x_B v_B = c_A v_A + c_B v_B \quad (18.4-2)$$

The molar diffusion flux relative to the molar average velocity  $v_M$  defined previously is

$$J_A^* = c_A (v_A - v_M) \quad (18.4-3)$$

The molar diffusion flux  $J_A$  relative to the mass average velocity  $v$  is

$$J_A = c_A (v_A - v) \quad (18.4-4)$$

As given previously, Fick's law from Table 18.4-1 is relative to  $v_M$ :

$$J_A^* = -cD_{AB} \frac{dx_A}{dz} \quad (18.4-5)$$

Fick's law can also be defined in terms of a mass flux relative to  $y$  as given in Table 18.4-1:

$$i_A = -\rho D_{AB} \frac{dw_A}{dz} \quad (18.4-6)$$

**EXAMPLE 18.4-1. Proof of the Mass Flux Equation**

Table 18.4-1 gives the following relation:

$$i_A + i_B = 0 \quad (18.4-7)$$

Prove this relationship using the definitions of the fluxes in terms of velocities.

**Solution:** From Table 18.4-1, substituting  $\rho_A(u_A - u)$  for  $j_A$  and  $\rho_B(u_B - u)$  for  $j_B$ , and rearranging,

$$\rho_A v_A - \rho_A v + \rho_B v_B - \rho_B v = 0 \quad (18.4-8)$$

$$\rho_A v_A + \rho_B v_B - v(\rho_A + \rho_B) = 0 \quad (18.4-9)$$

Substituting Eq. (18.4-1) for  $u$  and  $p$  for  $\rho_A + \rho_B$ , the identity is proved.

## 18.4B Equation of Continuity for a Binary Mixture

A general equation can be derived for a binary mixture of  $A$  and  $B$  for

diffusion and convection that also includes the terms for unsteady-state diffusion and chemical reaction. We shall make a mass balance on component  $A$  on an element  $\Delta x \Delta y \Delta z$  fixed in space, as shown in Fig. 18.4-1. The general mass balance on  $A$  is

$$(\text{rate of mass } A \text{ in}) - (\text{rate of mass } A \text{ out}) + (\text{rate of generation of mass } A) = \text{rate of accumulation of mass } A \quad (18.4-10)$$

The rate of mass  $A$  entering in the direction relative to stationary coordinates is  $(n_{Ax}|_x) \Delta y \Delta z$  kg  $A$ /s, and leaving is  $(n_{Ax}|_x) \Delta y \Delta z$ . Similar terms can be written for the  $y$  and  $z$  directions. The rate of chemical production of  $A$  is  $r_A$  kg  $A$  generated/s  $\cdot$  m<sup>3</sup> volume, and the total rate generated is  $r_A(\Delta x \Delta y \Delta z)$  kg

$A/s$ . The rate of accumulation of  $A$  is  $(\partial \rho_A / \partial t) \Delta x \Delta y \Delta z$ . Substituting into Eq. (18.4-10) and letting  $\Delta x \Delta y \Delta z$  approach zero,

$$\frac{\partial \rho_A}{\partial t} + (\frac{\partial n_{Ax}}{\partial x} + \frac{\partial n_{Ay}}{\partial y} + \frac{\partial n_{Az}}{\partial z}) = r_A \quad (18.4-11)$$

In vector notation,

$$\frac{\partial \rho_A}{\partial t} + (\nabla \cdot \mathbf{n}_A) = r_A \quad (18.4-12)$$

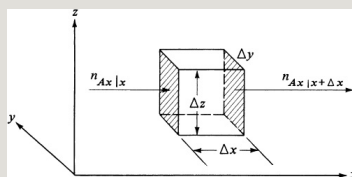


Figure 18.4-1. Mass balance for  $A$  in a binary mixture.

Dividing both sides of Eq. (18.4-11) by  $M_A$ ,

$$\frac{\partial c_A}{\partial t} + (\frac{\partial N_{Ax}}{\partial x} + \frac{\partial N_{Ay}}{\partial y} + \frac{\partial N_{Az}}{\partial z}) = R_A \quad (18.4-13)$$

where  $R_A$  is  $\text{kg mol } A \text{ generated/s} \cdot \text{m}^3$ .  
 Substituting  $N_A$  and Fick's law from  
 Table 18.4-1,

$$N_A = -cD_{AB} \frac{dx_A}{dz} + c_A v_M \quad (18.4-14)$$

and writing the equation for all three  
 directions, Eq. (18.4-13) becomes

$$\frac{\partial c_A}{\partial t} + (\nabla \cdot c_A \mathbf{v}_M) - (\nabla \cdot c D_{AB} \nabla x_A) = R_A \quad (18.4-15)$$

This is the final general equation.

#### 18.4C Special Cases of the Equation of Continuity

##### 1. Equation for constant $c$ and $D_{AB}$ .

In diffusion with gases, the total pressure  $P$  is often constant. Then, since  $c = P/RT$ ,  $c$  is constant for constant temperature  $T$ . Starting with the general equation (18.4-15) and

substituting  $\nabla x_A = \nabla c_A/c$ , we obtain

$$\frac{\partial c_A}{\partial t} + c_A(\nabla \cdot \mathbf{v}_M) + (\mathbf{v}_M \cdot \nabla c_A) - D_{AB} \nabla^2 c_A = R_A \quad (18.4-16)$$

## 2. *Equimolar counterdiffusion for gases.*

For the special case of equimolar counterdiffusion of gases at constant pressure and no reaction,  $c = \text{constant}$ ,  $\mathbf{v}_M = 0$ ,  $D_{AB} = \text{constant}$ ,  $R_A = 0$ , and Eq. (18.4-15) becomes

$$\frac{\partial c_A}{\partial t} = D_{AB}(\frac{\partial^2 c_A}{\partial x^2} + \frac{\partial^2 c_A}{\partial y^2} + \frac{\partial^2 c_A}{\partial z^2}) \quad (18.4-17)$$

This equation is also used for unsteady-state diffusion of a dilute solute  $A$  in a solid or a liquid when  $D_{AB}$  is constant.

## 3. *Equation for constant $\rho$ and $D_{AB}$ (liquids).*

In dilute liquid solutions, the mass density  $\rho$  and  $D_{AB}$  can often be

considered constant. Starting with Eq. (18.4-12), we substitute  $n_A = -\rho D_{AB} \nabla w_A + \rho A v$  from Table 18.4-1 into this equation. Then, using the fact that for constant  $\rho$ ,  $\nabla w_A = \nabla \rho_A / \rho$  and also that  $(\nabla \cdot v) = 0$ , substituting these into the resulting equation, and dividing both sides by  $M_A$ , we obtain

$$\frac{\partial c_A}{\partial t} + (v \cdot \nabla) c_A - D_{AB} \nabla^2 c_A = R_A \quad (18.4-18)$$

## 18.5 Chapter Summary

### Fick's Law of Diffusion

$$J_{Az}^* = -D_{AB} \frac{dc_A}{dz} \quad (18.1-3)$$

### Prediction of Diffusion Coefficients for Gasses

#### Chapman–Enskog Equation

$$D_{AB} = 1.8583 \times 10^{-7} T^{3/2} P \sigma_{AB}^2 \Omega_{D,AB} (1/M_A + 1/M_B)^{1/2} \quad (18.2-7)$$



## Fuller Method

$$D_{AB} = 1.00 \times 10^{-7} T^{1.75} \left( \frac{1}{M_A} + \frac{1}{M_B} \right)^{1/2} P \left[ (\sum v_A)^{1/3} + (\sum v_B)^{1/3} \right]^2 \quad (18.2-9)$$

## Prediction of Diffusion Coefficients for Liquids

### Stokes-Einstein

$$D_{AB} = 9.96 \times 10^{-16} T \mu_B V_A^{1/3} \quad (18.2-13)$$

### Wilke-Chang

$$D_{AB} = 1.173 \times 10^{-16} (\phi_B M_B)^{1/2} T \mu_B V_A^{0.6} \quad (18.2-14)$$

## General Equation for Molecular Diffusion, Convection, and Chemical Reaction

$$\frac{\partial c_A}{\partial t} + (\nabla \cdot c_A \mathbf{v}_M) - (\nabla \cdot D_{AB} \nabla x_A) = R_A \quad (18.4-15)$$

## Problems

### 18.1-1. *Diffusion of Methane*

*Through Helium.* A gas of CH<sub>4</sub> and

He is contained in a tube at 101.32 kPa pressure and 298 K. At one point, the partial pressure of methane is  $p_{A1} = 60.79 \text{ kPa}$ , and at a point 0.02 m distance away,  $p_{A2} = 20.26 \text{ kPa}$ . If the total pressure is constant throughout the tube, calculate the flux of  $\text{CH}_4$  (methane) at steady state for equimolar counterdiffusion.

$$\text{Ans. } J_{Az}^* = 5.52 \times 10^{-5} \text{ kg mol A/s} \cdot \text{m}^2 (5.52 \times 10^{-6} \text{ g mol A/s} \cdot \text{cm}^2)$$

**18.1-2. Diffusion of  $\text{CO}_2$  in a Binary Gas Mixture.** The gas  $\text{CO}_2$  is diffusing at steady state through a tube 0.20 m long having a diameter of 0.01 m and containing  $\text{N}_2$  at 298 K. The total pressure is constant at 101.32 kPa. The partial pressure of  $\text{CO}_2$  is 456 mmHg at one end and 76 mmHg at the other end.

The diffusivity  $D_{AB}$  is  $1.67 \times 10^{-5} \text{ m}^2/\text{s}$  at 298 K. Calculate the flux of  $\text{CO}_2$  in cgs and SI units for equimolar counterdiffusion.

**18.2-1. *Estimation of Diffusivity of a Binary Gas.*** For a mixture of ethanol ( $\text{CH}_3\text{CH}_2\text{OH}$ ) vapor and methane ( $\text{CH}_4$ ), predict the diffusivity using the method of Fuller et al. (F1)

- At  $1.0132 \times 10^5 \text{ Pa}$  and 298 and 373 K
- At  $2.0265 \times 10^5 \text{ Pa}$  and 298 K

**Ans.** (a)  $D_{AB} = 1.43 \times 10^{-5} \text{ m}^2/\text{s}$  (298 K)

**18.2-2. *Diffusion Flux and Effect of Temperature and Pressure.*** Equimolar counterdiffusion is occurring at steady state in a tube 0.11 m long containing  $\text{N}_2$  and  $\text{CO}$  gases at a total pressure of 1.0 atm abs. The partial pressure of  $\text{N}_2$

is 80 mmHg at one end and 10 mm at the other end. Predict the  $D_{AB}$  by the method of Fuller et al. (F1)

- Calculate the flux in  $\text{kg mol/s} \cdot \text{m}^2$  at 298 K for  $\text{N}_2$ .
- Repeat at 473 K. Does the flux increase?
- Repeat at 298 K, but for a total pressure of 3.0 atm abs. The partial pressure of  $\text{N}_2$  remains at 80 and 10 mmHg, as in part (a). Does the flux change?

**Ans.** (a)  $D_{AB} = 2.05 \times 10^{-5} \text{ m}^2/\text{s}$ ,  $N_A = 7.02 \times 10^{-7} \text{ kg mol/s} \cdot \text{m}^2$ ; (b)  $N_A = 9.92 \times 10^{-7} \text{ kg mol/s} \cdot \text{m}^2$ ; (c)  $N_A = 2.34 \times 10^{-7} \text{ kg mol/s} \cdot \text{m}^2$

### 18.2-3. *Estimation of Liquid*

**Diffusivity.** It is desired to predict the diffusion coefficient of dilute acetic acid ( $\text{CH}_3\text{COOH}$ ) in water at 282.9 K and at 298 K using the Wilke–Chang method. Compare the predicted values with the experimental values in Table 18.2-3.

**Ans.**  $D_{AB} = 0.897 \times 10^{-9} \text{ m}^2/\text{s}$  (282.9 K),

$$D_{AB} = 1.396 \times 10^{-9} \text{ m}^2/\text{s} \text{ (288 K)}$$

**18.2-4. Estimation of Diffusivity of Methanol in  $\text{H}_2\text{O}$ .** The diffusivity of dilute methanol in water has been determined experimentally to be  $1.26 \times 10^{-9} \text{ m}^2/\text{s}$  at 288 K.

- Estimate the diffusivity at 293 K using the Wilke–Chang equation.
- Estimate the diffusivity at 293 K by correcting the experimental value at 288 K to 293 K. (*Hint:* Do this by using the relationship  $D_{AB} \propto T/\mu_B$ .)

**18.2-5. Estimation of Diffusivity of Electrolyte  $\text{NaOH}$ .** Dilute  $\text{NaOH}$  is diffusing in an aqueous solution. Do as follows:

- Estimate the diffusivity of  $\text{NaOH}$  at  $25^\circ\text{C}$ . Also, calculate the diffusivity of the individual ions  $\text{Na}^+$  and  $\text{OH}^-$ .
- Estimate the diffusivity of  $\text{NaOH}$  at  $15^\circ\text{C}$ .

**Ans.** (a)  $D_{ABO} = 2.128 \times 10^{-5} \text{ cm}^2/\text{s}$ ;

(b)  $D_{ABO} = 1.609 \times 10^{-5} \text{ cm}^2/\text{s}$

**18.2-6. *Estimation of Diffusivity of  $\text{LaCl}_3$  and Temperature Effect.***

Estimate the diffusion coefficient of the salt  $\text{LaCl}_3$  in a dilute aqueous solution at  $25^\circ\text{C}$  and at  $35^\circ\text{C}$ . Also, calculate the diffusion coefficient for the ions  $\text{La}^{3+}$  and  $\text{Cl}^-$  at  $25^\circ\text{C}$ . What percent increase in rate of diffusion will occur in going from 25 to  $35^\circ\text{C}$  if the same dilute concentration difference is present at both temperatures?

**Ans.**  $D_{ABO}(35^\circ\text{C}) = 1.649 \times 10^{-5} \text{ cm}^2/\text{s}$

**18.2-7. *Prediction of Diffusivity of Enzyme Urease in Solution.*** Predict the diffusivity of the enzyme urease in a dilute solution in water at 298 K using

the modified Polson equation and compare the result with the experimental value in Table 18.2-6.

**Ans.** Predicted  $D_{AB} = 3.995 \times 10^{-11} \text{ m}^2/\text{s}$

**18.2-8. *Diffusion of Sucrose in Gelatin.***

A layer of gelatin in water 5 mm thick and containing 5.1 wt % gelatin at 293 K separates two solutions of sucrose. The concentration of sucrose in the solution at one surface of the gelatin is constant at 2.0 g sucrose/100 mL solution, and 0.2 g/100 mL at the other surface. Calculate the flux of sucrose in kg sucrose/s · m<sup>2</sup> through the gel at steady state.

**18.2-9. *Diffusivity of Oxygen in Protein***

**Solution.** Oxygen is diffusing through a solution of bovine serum albumin

(BSA) at 298 K. Oxygen has been shown not to bind to BSA. Predict the diffusivity  $D_{AP}$  of oxygen in a protein solution containing 11 g protein/100 mL solution. (*Note:* See Table 18.2-3 for the diffusivity of  $O_2$  in water.)

**Ans.**  $D_{AP} = 1.930 \times 10^{-9} \text{ m}^2/\text{s}$

**18.2-10. Diffusion of Uric Acid in Protein Solution and Binding.** Uric acid ( $A$ ) at  $37^\circ\text{C}$  is diffusing in an aqueous solution of proteins ( $P$ ) containing 8.2 g protein/100 mL solution. Uric acid binds to the proteins, and over the range of concentrations present, 1.0 g mol of acid binds to the proteins for every 3.0 g mol of total acid present in the solution. The diffusivity  $D_{AB}$  of uric acid in water is  $1.21 \times 10^{-5} \text{ cm}^2/\text{s}$  and  $D_P = 0.091 \times 10^{-5} \text{ cm}^2/\text{s}$ .



- Assuming no binding, predict the ratio  $D_{AP}/D_{AB}$  due only to blockage effects.
- Assuming blockage plus binding effects, predict the ratio  $D_{AP}/D_{AB}$ . Compare this with the experimental value for  $D_{AP}/D_{AB}$  of 0.616 (C8).
- Predict the flux in g uric acid/s · cm<sup>2</sup> for a concentration of acid of 0.05 g/L at point (1) and 0 g/L at point (2) a distance 1.5 μm away.

**Ans. (c)**  $N_A = 2.392 \times 10^{-6} \text{ g/s} \cdot \text{cm}^2$

**18.4-1. *Sum of Molar Fluxes.*** Prove the following equation using definitions in Table 18.4-1:

$$N_A + N_B = c v_M$$

**18.4-2. *Different Forms of Fick's Law.*** Using Eq. (1), prove Eq. (2):

$$j_A = -D_{AB} \frac{dw_A}{dz} \quad (1)$$

$$j_A = -D_{AB} \frac{dx_A}{dz} \quad (2)$$

(*Hint:* First relate  $w_A$  to  $x_A$ . Then, differentiate this equation to relate  $dw_A$  and  $dx_A$ . Finally, use  $M = x_A M_A + x_B M_B$  to simplify.)

### 18.4-3. *Other Forms of Fick's Law.*

Show that the following form of Fick's law is valid:

$$c(v_A - v_B) = -c D_{AB} x_A x_B dx_A/dz$$

(*Hint:* Start with  $N_A = J_A^* + c_A v_M$ .

Substitute the expression for  $J_A^*$  from Table 18.4-1 and simplify.)

**18.4-4. *Different Forms of Equation of Continuity.*** Starting with Eq. (18.4-12),

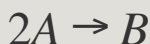
$$\partial \rho_A / \partial t + (\nabla \cdot n_A) = r_A \quad (18.4-12)$$

convert this to the following for constant  $\rho$ :

$$\partial \rho_A \partial t + (\mathbf{v} \cdot \nabla \rho_A) - (\nabla \cdot D_{AB} \nabla \rho_A) = r_A \quad (1)$$

[*Hint:* From Table 18.4-1, substitute  $\mathbf{n}_A = \mathbf{j}_A + \rho_A \mathbf{v}$  into Eq. (18.4-12). Note that  $(\nabla \cdot \mathbf{v}) = 0$  for constant  $\rho$ . Then, substitute Fick's law in terms of  $\mathbf{j}_A$ .]

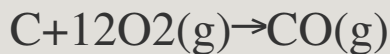
**18.4-5. Diffusion and Reaction at a Surface.** Gas  $A$  is diffusing from a gas stream at point 1 to a catalyst surface at point 2 and reacts instantaneously and irreversibly as follows:



Gas  $B$  diffuses back to the gas stream. Derive the final equation for  $N_A$  at constant pressure  $P$  and steady state in terms of partial pressures.

$$\text{Ans. } N_A = \frac{2D_{AB}P}{RT} (z_2 - z_1) \ln \frac{1 - p_{A2}/2P}{1 - p_{A1}/2P}$$

**18.4-6. Diffusion and Chemical Reaction of Molten Iron in Process Metallurgy.** In a steelmaking process using molten pig iron that contains carbon, a spray of molten iron particles containing 4.0 wt % carbon falls through a pure-oxygen atmosphere. The carbon diffuses through the molten iron to the surface of the drop, where it is assumed that it reacts instantly at the surface because of the high temperature, as follows, according to a first-order reaction:



Calculate the maximum drop size allowable so that the final drop after a 2.0-s fall contains an average of 0.1 wt % carbon. Assume that the mass-transfer rate of gases at the surface is

very great, so there is no outside resistance. Assume no internal circulation of the liquid. Hence, the decarburization rate is controlled by the rate of diffusion of carbon to the surface of the droplet. The diffusivity of carbon in iron is  $7.5 \times 10^{-9} \text{ m}^2/\text{s}$  (S7). (*Hint: Can Fig. 14.3-9 be used for this case?*)

**Ans.** radius = 0.217 mm

**18.4-7. Effect of Slow Reaction Rate on Diffusion.** Gas A diffuses from point 1 to a catalyst surface at point 2, where it reacts as follows:  $2A \rightarrow B$ . Gas B diffuses back a distance  $\delta$  to point 1.

- Derive the equation for  $N_A$  for a very fast reaction using mole fraction units  $x_{A1}$ , and so on.
- For  $D_{AB} = 0.2 \times 10^{-4} \text{ m}^2/\text{s}$ ,  $x_{A1} = 0.97$ ,  $P = 101.21 \text{ kPa}$ ,  $\delta = 1.30 \text{ mm}$ , and  $T = 298 \text{ K}$ , solve for  $N_A$ .
- Do the same as in part (a) but for a slow first-order

reaction where  $k_1'$  is the reaction velocity constant.

- Calculate  $N_A$  and  $x_{A2}$  for part (c) where  $k_1'=0.52 \times 10^{-2}$  m/s.

**Ans.** (b)  $N_A = 8.35 \times 10^{-4}$  kg mol/s · m<sup>2</sup>

## References

## Notation

# Chapter 19. Steady-State Mass Transfer

## 19.0 Chapter Objectives

On completion of this chapter, a student should be able to:

- Calculate diffusion fluxes for the two classic cases: (a) equimolar counterdiffusion and (b) a diffusing through stagnant, nondiffusing B
- Calculate diffusion fluxes through a varying cross-sectional area
- Calculate diffusion fluxes for a multicomponent system of gases
- Calculate diffusion fluxes for diffusion in solids by using the additional concepts of solubility, permeability, tortuosity, and void fraction
- Calculate the Knudsen number for a gas and determine the appropriate diffusion coefficient
- Calculate the diffusion fluxes in situations where both diffusion and chemical reaction occur

- Use the numerical methods to solve two-dimensional steady-state conduction problems

## 19.1 Molecular Diffusion in Gases

### 19.1A Equimolar Counterdiffusion in Gases

In the application of mass transfer to industrial applications, there are two classic cases. The first being “equimolar counterdiffusion” and the second “a diffusing through stagnant, nondiffusing B. Equimolar is especially important in the discussion of distillation, whereas stagnant B is valuable for absorption. In Fig. 19.1-1, a diagram is given of two gases  $A$  and  $B$  at constant total pressure  $P$  in two large chambers connected by a tube where molecular diffusion at steady state is occurring. Stirring in each chamber keeps the concentrations in the



chamber uniform. The partial pressures  $p_{A1} > p_{A2}$  and  $p_{B2} > p_{B1}$ . Molecules of  $A$  diffuse to the right and molecules of  $B$  to the left. Since the total pressure  $P$  is constant throughout, the net moles of  $A$  diffusing to the right must equal the net moles of  $B$  diffusing to the left. If this is not so, the total pressure would not remain constant. This means that

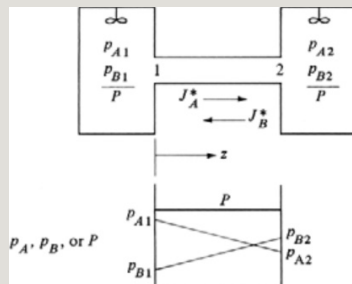


Figure 19.1-1. *Equimolar counterdiffusion of gases A and B.*

$$J_{Az} = -J_{Bz} \quad (19.1-1)$$

The subscript  $z$  is often dropped when

the direction is obvious. Writing Fick's law for  $B$  for constant  $c$ ,

$$J_B^* = -D_B A \frac{dc_B}{dz} \quad (19.1-2)$$

Now, since  $P = p_A + p_B = \text{constant}$ , then

$$c = c_A + c_B \quad (19.1-3)$$

Differentiating both sides,

$$dc_A = -dc_B \quad (19.1-4)$$

Equating Eq. (18.1-3) to (19.1-2),

$$J_A^* = -D_{AB} \frac{dc_A}{dz} = -J_B^* = -(-)D_B A \frac{dc_B}{dz} \quad (19.1-5)$$

Substituting Eq. (19.1-4) into (19.1-5) and canceling like terms,

$$D_{AB} = D_{BA} \quad (19.1-6)$$

This shows that for a binary gas mixture of  $A$  and  $B$ , the diffusivity coefficient  $D_{AB}$  for  $A$  diffusing into  $B$  is the same as  $D_{BA}$  for  $B$  diffusing into  $A$ .

**EXAMPLE 19.1-1. Equimolar Counterdiffusion**

Ammonia gas ( $A$ ) is diffusing through a uniform tube 0.10 m long containing  $N_2$  gas ( $B$ ) at  $1.0132 \times 10^5$  Pa pressure and 298 K. The diagram is similar to Fig. 19.1-1. At point 1,  $p_{A1} = 1.013 \times 10^4$  Pa and at point 2,  $p_{A2} = 0.507 \times 10^4$  Pa. The diffusivity  $D_{AB} = 0.230 \times 10^{-4}$  m<sup>2</sup>/s.

- Calculate the flux  $J_A^*$  at steady state.
- Repeat for  $J_B^*$ .

**Solution:** Equation (18.1-13) can be used, where  $P = 1.0132 \times 10^5$  Pa,  $z_2 - z_1 = 0.10$  m, and  $T = 298$  K. Substituting into Eq. (18.1-13) for part (a),

$$J_A^* = D_{AB}(p_{A1} - p_{A2})RT(z_2 - z_1) = (0.23 \text{ m}^2 \text{ s}) \\ (1.013 \times 10^4 \text{ Pa} - 0.507 \times 10^4 \text{ Pa})(8314 \text{ m}^3 \text{ Pa} \text{ kmol}^{-1} \text{ K})(298 \text{ K}) \\ (0.1 \text{ m} - 0 \text{ m}) J_A^* = 4.70 \times 10^{-7} \text{ kmol(A) m}^2 \text{ s}^{-1}$$

Rewriting Eq. (18.1-13) for component  $B$  for part (b), and noting that  $p_{B1} = P - p_{A1} = 1.0132 \times 10^5 - 1.013 \times 10^4 = 9.119 \times 10^4$  Pa and  $p_{B2} = P - p_{A2} = 1.0132 \times 10^5 - 0.507 \times 10^4 = 9.625 \times 10^4$  Pa,

$$J_B^* = D_{AB}(p_{B1} - p_{B2})RT(z_2 - z_1) = (0.23 \text{ m}^2 \text{ s}) \\ (9.119 \times 10^4 \text{ Pa} - 9.625 \times 10^4 \text{ Pa})(8314 \text{ m}^3 \text{ Pa} \text{ kmol}^{-1} \text{ K})(298 \text{ K}) \\ (0.1 \text{ m} - 0 \text{ m}) J_B^* = -4.70 \times 10^{-7} \text{ kmol(A) m}^2 \text{ s}^{-1}$$

The negative value for  $J_B^*$  means the flux goes from point 2 to point 1.

## 19.1B Special Case for $A$ Diffusing Through Stagnant, Nondiffusing $B$

The case of diffusion of  $A$  through stagnant or nondiffusing  $B$  at steady state often occurs. In this case, one boundary at the end of the diffusion path is impermeable to component  $B$ , so it cannot pass through. One example, shown in Fig. 19.1-2a, is in the evaporation of a pure liquid such as benzene ( $A$ ) at the bottom of a narrow tube, where a large amount of inert or nondiffusing air ( $B$ ) is passed over the top. The benzene vapor ( $A$ ) diffuses through the air ( $B$ ) in the tube. The boundary at the liquid surface at point 1 is impermeable to air, since air is insoluble in benzene liquid. Hence, air ( $B$ ) cannot diffuse into or away from the surface. At point 2, the partial pressure  $p_{A2} = 0$ , since a large volume of air is passing by.

Another example, shown in Fig.

19.1-2b, occurs in the absorption of  $\text{NH}_3$  (A) vapor, which is in air (B) by water.

The water surface is impermeable to the air, since air is only very slightly soluble in water. Thus, since B cannot diffuse,  $N_B = 0$ .

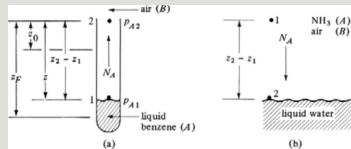


Figure 19.1-2. Diffusion of A through stagnant, nondiffusing B: (a) benzene evaporating into air, (b) ammonia in air being absorbed into water.

To derive the case for A diffusing in stagnant, nondiffusing B,  $N_B = 0$  is substituted into the general Eq. (18.1-21):

$$N_A = -cD_{AB} \frac{dx_A}{dz} + c_A v_A (N_A + 0) \quad (19.1-7)$$

The convective flux of A is  $(c_A/c)(N_A + 0)$ . Keeping the total pressure  $P$  constant, and substituting  $c = P/RT$ ,  $p_A = x_A P$ , and  $c_A/c = p_A/P$  into Eq. (19.1-7),

$$N_A = -DABRT dp_A/dz + p_A N_A \quad (19.1-8)$$

Rearranging and integrating,

$$N_A(1 - p_A/P) = -DABRT dp_A/dz \quad (19.1-9)$$

$$N_A \int_{z_1}^{z_2} dz = -\frac{DABRT}{P(1 - p_{A1}/P)} \int_{p_{A1}}^{p_{A2}} \frac{dp_A}{p_A} \quad (19.1-10)$$

$$N_A = \frac{DABP}{RT(z_2 - z_1)} \ln \frac{P - p_{A2}}{P - p_{A1}} \quad (19.1-11)$$

Equation (19.1-11) is the final equation to be used to calculate the flux of A. However, it is often written in another

form. A log mean value of the inert  $B$  is defined as follows: since  $P = p_{A1} + p_{B1} = p_{A2} + p_{B2}$ ,  $p_{B1} = P - p_{A1}$ , and  $p_{B2} = P - p_{A2}$ ,

$$PBM = p_{B2} - p_{B1} \ln(p_{B2}/p_{B1}) = p_{A1} - p_{A2} \ln[(P - p_{A2})/(P - p_{A1})] \quad (19.1-12)$$

Substituting Eq. (19.1-12) into (19.1-11),

$$N_A = DABPRT(z_2 - z_1)p_{BM}(p_{A1} - p_{A2}) \quad (19.1-13)$$

**EXAMPLE 19.1-2. Diffusion of Water Through Stagnant, Nondiffusing Air**

Water in the bottom of a narrow metal tube is held at a constant temperature of 293 K. The total pressure of air (assumed dry) is  $1.01325 \times 10^5$  Pa (1.0 atm) and the temperature is 293 K (20°C). Water evaporates and diffuses through the air in the tube, and the diffusion path  $z_2 - z_1$  is 0.1524 m (0.5 ft) long. The diagram is similar to Fig. 19.1-2a. Calculate the rate of evaporation at steady state in  $\text{kg mol/s} \cdot \text{m}^2$ . The diffusivity of water vapor at 293 K and 1 atm pressure is  $0.250 \times 10^{-4} \text{ m}^2/\text{s}$ . Assume that the system is isothermal.

**Solution:** From Appendix A.2, the vapor pressure of water at 20°C is 17.54 mm, or  $p_{A1} = 17.54/760 = 0.0231$  atm =  $0.0231(1.01325 \times 10^5) = 2.341 \times 10^3$  Pa,  $p_{A2} = 0$  (pure air).

Since the temperature is 20°C (68°F),  $T = 460 + 68 = 528^\circ\text{R} = 293\text{ K}$ . To calculate the value of  $p_{BM}$  from Eq. (19.1-12),

$$\begin{aligned} p_{B1} &= P - p_{A1} = 1.00 - 0.0231 = 0.9769\text{ atm} \\ p_{B2} &= P - p_{A2} = 1.00 - 0 = 1.00\text{ atm} \\ p_{BM} &= p_{B2} - p_{B1} \ln(p_{B2}/p_{B1}) = 1.00 - 0.9769 \ln(1.00/0.9769) = 0.988\text{ atm} = 1.001 \times 10^5\text{ Pa} \end{aligned}$$

Since  $p_{B1}$  is close to  $p_{B2}$ , the linear mean  $(p_{B1} + p_{B2})/2$  could be used and would be very close to  $p_{BM}$ .

Substituting into Eq. (19.1-13) with  $z_2 - z_1 = 0.5\text{ ft}$  (0.1524 m),

$$\begin{aligned} N_A &= DABPRT(z_2 - z_1)p_{BM}(p_{A1} - p_{A2}) / NA = (0.250\text{ m}^2\text{s}) \\ &\quad (1.01325 \times 10^5\text{ Pa})(8314\text{ m}^3\text{Pa/kgmole}\cdot\text{K})(293\text{ K})(0.1524\text{ m}) \\ &\quad (1.001 \times 10^5\text{ Pa})(2.341 \times 10^3\text{ Pa} - 0\text{ Pa}) \\ NA &= 1.595 \times 10^{-7}\text{ kgmole/m}^2\cdot\text{s} \end{aligned}$$

A more basic solution eliminating  $p_{BM}$  is shown below (Eq. 19.1-11).

$$\begin{aligned} NA &= DABPRT(z_2 - z_1) \ln(P - p_{A2} / P - p_{A1}) / NA = (0.250\text{ m}^2\text{s}) \\ &\quad (1.01325 \times 10^5\text{ Pa})(8314\text{ m}^3\text{Pa/kgmole}\cdot\text{K})(293\text{ K}) \\ &\quad (0.1524\text{ m}) \ln(1.01325 \times 10^5\text{ Pa} - 0\text{ Pa} / 1.01325 \times 10^5\text{ Pa} - 2.341 \times 10^3\text{ Pa}) \\ NA &= 1.595 \times 10^{-7}\text{ kgmole/m}^2\cdot\text{s} \end{aligned}$$

### **EXAMPLE 19.1-3. Diffusion in a Tube with Change in Path Length**

Diffusion of water vapor in a narrow tube is occurring as in Example 19.1-2 under the same conditions as Example 19.1-2. However, as shown in Fig. 19.1-2a, at a given time  $t$ , the level is  $z$  m from the top. As diffusion proceeds, the level drops slowly. Derive the equation for the time  $t_F$  for the level to drop from a starting point of  $z_0$  m at  $t = 0$  to  $z_F$  at  $t = t_F$  s, as shown.

**Solution:** We assume a pseudo-steady-state condition since the level drops very slowly. As time progresses, the path length  $z$  increases. At any time  $t$ , Eq. (19.1-13) holds, but the path length is  $z$  and Eq. (19.1-13) becomes as follows, where  $N_A$  and  $z$  are now variables:

$$N_A = DABPRTz p_{BM}(p_{A1} - p_{A2}) \quad (19.1-14)$$



Assuming a cross-sectional area of  $1 \text{ m}^2$ , the level drops  $dz$  m in  $dt$  s, and  $\rho_A (dz \cdot 1)/M_A$  is the kg mol of A that have left and diffused. Then,

$$N_A \cdot 1 = \rho_A (dz \cdot 1) M_A dt \quad (19.1-15)$$

Equating Eq. (19.1-15) to (19.1-14), rearranging, and integrating between the limits of  $z = z_0$  when  $t = 0$  and  $z = z_F$  when  $t = t_F$ ,

$$\rho_A M_A \int_{z_0}^{z_F} dz = DABP(p_{A1} - p_{A2}) RT p_{BM} \int_0^{t_F} dt \quad (19.1-16)$$

Solving for  $t_F$ ,

$$t_F = \rho_A (z_F^2 - z_0^2) RT p_{BM} / 2 DABP (p_{A1} - p_{A2}) \quad (19.1-17)$$

The method shown in Example 19.1-3 has been used to experimentally determine the diffusivity  $D_{AB}$ . In this experiment, the starting path length  $z_0$  is measured at  $t = 0$  together with the final  $z_F$  at  $t_F$ . Then, Eq. (19.1-17) is used to calculate  $D_{AB}$ .

### 19.1C Diffusion Through a Varying Cross-Sectional Area

So far, in the cases at steady state we have considered  $N_A$  and  $J_A^*$  as constants in the integrations. In these

cases, the cross-sectional area  $A$  m<sup>2</sup> through which the diffusion occurs has been constant with varying distance  $z$ . In some situations, the area  $A$  may vary. Then, it is convenient to define  $N_A$  as

$$N_A = N^A A \quad (19.1-18)$$

where  $N^A$  is kg moles of  $A$  diffusing per second or kg mol/s. At steady state,  $N^A$  will be constant but not  $A$  for a varying area.

*1. Diffusion from a sphere.* To illustrate the use of Eq. (19.1-18), the important case of diffusion to or from a sphere in a gas will be considered. This situation appears often, in such cases as the evaporation of a drop of liquid, the evaporation of a ball of naphthalene,

and the diffusion of nutrients to a sphere-like microorganism in a liquid. Figure 19.1-3a shows a sphere of fixed radius  $r_1$  m in an infinite gas medium. Component (A) at partial pressure  $p_{A1}$  at the surface is diffusing into the surrounding stagnant medium (B), where  $p_{A2} = 0$  at some large distance away. Steady-state diffusion will be assumed.

The flux  $N_A$  can be represented by Eq. (19.1-18), where  $A$  is the cross-sectional area  $4\pi r^2$  at point  $r$  distance from the center of the sphere. Also,  $N_A$  is a constant at steady state:

$$N_A = N_A \cdot 4\pi r^2 \quad (19.1-19)$$

Since this is a case of A diffusing through stagnant, nondiffusing B, Eq.

(19.1-9) will be used in its differential form and  $N_A$  will be equated to Eq. (19.1-19), giving

$$N_A = N^{-} A 4 \pi r^2 = -DABRT dp_A (1 - p_A/P) dr \quad (19.1-20)$$

Note that  $dr$  was substituted for  $dz$ . Rearranging and integrating between  $r_1$  and some point  $r_2$  a large distance away,

$$N^{-} A 4 \pi \int_{r_1}^{r_2} r^2 dr = -DABRT \int_{p_A1}^{p_A2} dp_A (1 - p_A/P) \quad (19.1-21)$$

$$N^{-} A 4 \pi (1/2 r_1^2 - 1/2 r_2^2) = DABPRT \ln \frac{P - p_A2}{P - p_A1} \quad (19.1-22)$$

Since  $r_2 \gg r_1$ ,  $1/r_2 \cong 0$ . Substituting  $p_{BM}$  from Eq. (19.1-12) into Eq. (19.1-22),

$$N_A 4\pi r^2 = N_A 1 = D_{AB} P r_1 P_{A1} - p_{A2} p_{BM} \quad (19.1-23)$$

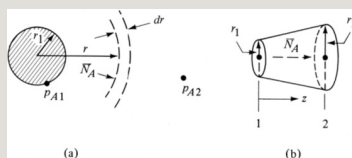


Figure 19.1-3. *Diffusion through a varying cross-sectional area: (a) from a sphere to a surrounding medium, (b) through a circular conduit that is tapered uniformly.*

This equation can be simplified further. If  $p_{A1}$  is small compared to  $P$  (a dilute gas phase),  $p_{BM} \cong P$ . Also, setting  $2r_1 = D_1$ , diameter, and  $c_{A1} = p_{A1}/RT$ , we obtain

$$N_{A1} = 2D_{AB} D_1 (c_{A1} - c_{A2}) \quad (19.1-24)$$

This equation can also be used for liquids, where  $D_{AB}$  is the diffusivity of  $A$  in the liquid.

A sphere of naphthalene having a radius of 2.0 mm is suspended in a large volume of still air at 318 K and  $1.01325 \times 10^5$  Pa (1 atm). The surface temperature of the naphthalene can be assumed to be at 318 K and its vapor pressure at 318 K is 0.555 mmHg. The  $D_{AB}$  of naphthalene in air at 318 K is  $6.92 \times 10^{-6}$  m<sup>2</sup>/s. Calculate the rate of evaporation of naphthalene from the surface.

**Solution:** The flow diagram is similar to Fig. 19.1-3a.  $D_{AB} = 6.92 \times 10^{-6}$  m<sup>2</sup>/s,  $p_{A1} = (0.555/760)(1.01325 \times 10^5) = 74.0$  Pa,  $p_{A2} = 0$ ,  $r_1 = 2/1000$  m,  $R = 8314$  m<sup>3</sup> · Pa/kg mol · K,  $p_{B1} = P - p_{A1} = 1.01325 \times 10^5 - 74.0 = 1.01251 \times 10^5$  Pa, and  $p_{B2} = P - p_{A2} = 1.01325 \times 10^5 - 0$ . Since the values of  $p_{B1}$  and  $p_{B2}$  are close to each other,

$$PBM = p_{B1} + p_{B2} = (1.0125 + 1.01325) \times 10^5 = 1.0129 \times 10^5 \text{ Pa}$$

Substituting into Eq. (19.1-23),

$$\begin{aligned} NA &= D_{AB} P (p_{A1} - p_{A2}) / R r_1 p_{BM} NA = (6.92 \times 10^{-6} \text{ m}^2/\text{s}) \\ & (1.01325 \times 10^5 \text{ Pa}) (74.0 \text{ Pa} - 0 \text{ Pa}) / (8314 \text{ m}^3/\text{kg mol} \cdot \text{K}) \\ & (318 \text{ K}) (2/1000 \text{ m}) \\ (1.0129 \times 10^5 \text{ Pa}) NA &= 9.68 \times 10^{-8} \text{ kg mol/m}^2 \cdot \text{s} \end{aligned}$$

If the sphere in Fig. 19.1-3a is evaporating, the radius  $r$  of the sphere decreases slowly with time. The equation for the time it takes for the sphere to evaporate completely can be derived by assuming pseudo-steady state and by equating the diffusion flux equation (19.1-23), where  $r$  is now a variable, to the moles of solid A evaporated per  $dt$  time and per unit area

as calculated from a material balance (see Problem 19.1-9 for this case). The material-balance method is similar to Example 19.1-3. The final equation is

$$t_F = \frac{\rho_A r_1^2}{2D} \ln \left( \frac{p_{A1} - p_{A2}}{p_{A1} - p_{A2}^*} \right) \quad (19.1-25)$$

where  $r_1$  is the original sphere radius,  $\rho_A$  the density of the sphere, and  $M_A$  the molecular weight.

*2. Diffusion through a conduit of a nonuniform cross-sectional area.* In Fig. 19.1-3b, component A is diffusion at steady state through a circular conduit that is tapered uniformly, as shown. At point 1 the radius is  $r_1$  and at point 2 it is  $r_2$ . At position  $z$  in the conduit, for A diffusing through stagnant, nondiffusing B,

$$N_A = N_A \pi r^2 = -DABRT dp_A (1 - p_A/P) dz \quad (19.1-26)$$

Using the geometry shown, the variable radius  $r$  can be related to position  $z$  in the path as follows:

$$r = (r_2^2 - r_1^2 z^2 - z^2)z + r_1^2 \quad (19.1-27)$$

This value of  $r$  is then substituted into Eq. (19.1-26) to eliminate  $r$  and the equation integrated:

$$N_A \pi \int_{z_1}^{z_2} dz [(r_2^2 - r_1^2 z^2 - z^2)z + r_1^2]^2 = -DABRT \int_{p_{A1}}^{p_{A2}} dp_A (1 - p_A/P) \quad (19.1-28)$$

A case similar to this is given in Problem 19.1-10.

### 19.1D Multicomponent Diffusion of Gases

The equations derived so far have



been for a binary system of  $A$  and  $B$ , which is probably the most important and most useful one.

However, multicomponent diffusion sometimes occurs where three or more components,  $A, B, C, \dots$ , are present. The simplest case is for diffusion of  $A$  in a gas through a stagnant, nondiffusing mixture of  $B, C, D, \dots$  at constant total pressure.

Hence,  $N_B = 0, N_C = 0, \dots$ . The final equation derived using the Stefan–Maxwell method (G1) for steady-state diffusion is

$$N_A = D_{Am} P R T (z_2 - z_1) p_{iM} (p_{A1} - p_{A2}) \quad (19.1-29)$$

where  $p_{iM}$  is the log mean of  $p_{i1} = P - p_{A1}$  and  $p_{i2} = P - p_{A2}$ . Also,

$$D_{Am} = 1x_B'/D_{AB} + x_C'/D_{AC} + (19.1-30)$$

where  $x_B' = \text{mol B/mol inerts} = x_B/(1 - x_A)$ ,  $x_C' = x_{Cl}/(1 - x_A)$ , ....

**EXAMPLE 19.1-5. Diffusion of A Through Nondiffusing B and C**

At 298 K and 1 atm total pressure, methane (A) is diffusing at steady state through nondiffusing argon (B) and helium (C). At  $z_1 = 0$ , the partial pressures in atm are  $p_{A1} = 0.4$ ,  $p_{B1} = 0.4$ , and  $p_{C1} = 0.2$ , and at  $z_2 = 0.005$  m,  $p_{A2} = 0.1$ ,  $p_{B2} = 0.6$ , and  $p_{C2} = 0.3$ . The binary diffusivities from Table 18.2-1 are  $D_{AB} = 2.02 \times 10^{-5} \text{ m}^2/\text{s}$ ,  $D_{AC} = 6.75 \times 10^{-5} \text{ m}^2/\text{s}$ , and  $D_{BC} = 7.29 \times 10^{-5} \text{ m}^2/\text{s}$ . Calculate  $N_A$ .

**Solution:** At point 1,  $x_B' = x_{B1}/(1 - x_{A1}) = 0.4/(1 - 0.4) = 0.667$ . At point 2,  $x_B' = 0.6/(1 - 0.1) = 0.667$ . The value  $x_B'$  is constant throughout the path. Also,  $x_C' = x_{C1}/(1 - x_{A1}) = 0.2/(1 - 0.4) = 0.333$ .

Substituting into Eq. (19.1-30),

$$D_{Am} = 1x_B'/D_{AB} + x_C'/D_{AC} = 10.667/2.02 \times 10^{-5} \text{ m}^2/\text{s} + 0.333/6.75 \times 10^{-5} \text{ m}^2/\text{s} = 2.635 \times 10^{-5} \text{ m}^2/\text{s}$$

For calculating  $p_{iM}$ ,  $p_{i1} = P - p_{A1} = 1.0 - 0.4 = 0.6$  atm,  $p_{i2} = P - p_{A2} = 1.0 - 0.1 = 0.90$ . Then,

$$p_{iM} = p_{i2} - p_{i1} \ln(p_{i2}/p_{i1}) = 0.90 \ln(0.90/0.60) = -0.740 \text{ atm} = -7.496 \times 10^4 \text{ Pa}$$

$$p_{A1} = 0.4(1.01325 \times 10^5) = 4.053 \times 10^4 \text{ Pa}$$

$$p_{A2} = 0.1(1.01325 \times 10^5) = 1.013 \times 10^4 \text{ Pa}$$

Substituting into Eq. (19.1-29),

$$N_A = D_{Am} P (p_{A1} - p_{A2}) / RT (z_2 - z_1) p_{iM} N_A = (2.635 \times 10^{-5} \text{ m}^2/\text{s}) (1.01325 \times 10^5 \text{ Pa}) (4.053 \times 10^4 \text{ Pa} - 1.013 \times 10^4 \text{ Pa}) (8314 \text{ m}^3 \text{ Pa} / \text{kgmole} \cdot \text{K}) (298 \text{ K}) (0.005 \text{ m} - 0 \text{ m}) (7.496 \times 10^4 \text{ Pa})$$

$$N_A = 8.74 \times 10^{-5} \text{ kgmole/m}^2 \cdot \text{s}$$

A number of analytical solutions have been obtained for other cases, such as for equimolar diffusion of three components, diffusion of components *A* and *B* through stagnant *C*, and the general case of two or more components diffusing in a multicomponent mixture. These are discussed in detail with examples by Geankoplis (G1); the reader is referred there for further details.

## 19.2 Molecular Diffusion in Liquids

### 19.2A Introduction

Diffusion of solutes in liquids is very important in many industrial processes, especially in such separation operations as liquid–liquid extraction or solvent extraction, gas absorption, and distillation. Diffusion in liquids also occurs in many situations in nature, such as oxygenation of rivers and lakes by the air and diffusion of salts in blood.

It should be apparent that the rate of molecular diffusion in liquids is

considerably slower than in gases. The molecules in a liquid are very close together compared to a gas. Hence, the molecules of the diffusing solute  $A$  will collide with molecules of liquid  $B$  more often and diffuse more slowly than in gases. In general, the diffusion coefficient in a gas will be on the order of magnitude of about  $10^5$  times greater than in a liquid. However, the flux in a gas is not that much greater, being only about 100 times faster, since the concentrations in liquids are considerably higher than in gases.

### **19.2B Equations for Diffusion in Liquids**

Since the molecules in a liquid are packed together much more closely than in gases, the density and the resistance to diffusion in a liquid are much greater. Also, because of this

closer spacing of the molecules, the attractive forces between molecules play an important role in diffusion. Since the kinetic theory of liquids is only partially developed, we write the equations for diffusion in liquids similar to those for gases.

In diffusion in liquids, an important difference from diffusion in gases is that the diffusivities are often quite dependent on the concentration of the diffusing components.

*1. Equimolar counterdiffusion.* Starting with the general equation (18.1-21), we can obtain for equimolar counterdiffusion, where  $N_A = -N_B$ , an equation similar to Eq. (18.1-11) for gases at steady state:

$$N_A = D_{AB} \frac{(c_{A1} - c_{A2})}{z_2 - z_1} \quad (19.2-1)$$

where  $N_A$  is the flux of  $A$  in  $\text{kg mol } A/\text{s} \cdot \text{m}^2$ ,  $D_{AB}$  is the diffusivity of  $A$  in  $B$  in  $\text{m}^2/\text{s}$ ,  $c_{A1}$  is the concentration of  $A$  in  $\text{kg mol } A/\text{m}^3$  at point 1,  $x_{A1}$  is the mole fraction of  $A$  at point 1, and  $c_{av}$  is defined by

$$c_{av} = (\rho M)_{av} = (\rho_1 M_1 + \rho_2 M_2)/2 \quad (19.2-2)$$

where  $c_{av}$  is the average total concentration of  $A + B$  in  $\text{kg mol}/\text{m}^3$ ,  $M_1$  is the average molecular weight of the solution at point 1 in  $\text{kg mass}/\text{kg mol}$ , and  $\rho_1$  is the average density of the solution in  $\text{kg}/\text{m}^3$  at point 1.

Equation (19.2-1) uses the average value of  $D_{AB}$ , which may vary some with concentration, and the average value of

$c$ , which may also vary with concentration. Usually, the linear average of  $c$  is used, as in Eq. (19.2-2). The case of equimolar counterdiffusion in Eq. (19.2-1) only occurs very infrequently in liquids.

*2. Diffusion of A through nondiffusing B.* The most important case of diffusion in liquids is that where solute  $A$  is diffusing and solvent  $B$  is stagnant or nondiffusing. An example is a dilute solution of propionic acid ( $A$ ) in a water ( $B$ ) solution being contacted with toluene. Only the propionic acid ( $A$ ) diffuses through the water phase, to the boundary, and then into the toluene phase. The toluene–water interface is a barrier to diffusion of  $B$  and  $N_B = 0$ . Such cases often occur in industry (T1). If Eq. (19.1-13) is rewritten in terms of

concentrations by substituting  $c_{av} = P/RT$ ,  $c_{A1} = p_{A1}/RT$ , and  $x_{BM} = p_{BM}/P$ , we obtain the equation for liquids at steady state:

$$N_A = DAB c_{av} (z_2 - z_1) x_{BM} (x_{A1} - x_{A2}) \quad (19.2-3)$$

where

$$x_{BM} = x_{B2} - x_{B1} \ln(x_{B2}/x_{B1}) \quad (19.2-4)$$

Note that  $x_{A1} + x_{B1} = x_{A2} + x_{B2} = 1.0$ . For dilute solutions,  $x_{BM}$  is close to 1.0 and  $c$  is essentially constant. Then, Eq. (19.2-3) simplifies to

$$N_A = DAB (c_{A1} - c_{A2}) (z_2 - z_1) \quad (19.2-5)$$

**EXAMPLE 19.2-1. Diffusion of Ethanol (A) Through Water (B)**

An ethanol (A)–water (B) solution in the form of a stagnant film 2.0 mm thick at 293 K is in contact at one surface with an organic solvent in which ethanol is soluble and water is



insoluble. Hence,  $N_B = 0$ . At point 1, the concentration of ethanol is 16.8 wt % and the solution density is  $\rho_1 = 972.8$  kg/m<sup>3</sup>. At point 2, the concentration of ethanol is 6.8 wt % and  $\rho_2 = 988.1$  kg/m<sup>3</sup> (P1). The diffusivity of ethanol is  $0.740 \times 10^{-9}$  m<sup>2</sup>/s (T1). Calculate the steady-state flux  $N_A$ .

**Solution:** The diffusivity is  $D_{AB} = 0.740 \times 10^{-9}$  m<sup>2</sup>/s. The molecular weights of A and B are  $M_A = 46.05$  and  $M_B = 18.02$ . For a wt % of 6.8, the mole fraction of ethanol (A) is as follows when using 100 kg of solution:

$$x_{A2} = 6.8/46.056.8/46.05 + 93.2/18.02 = 0.14770.1477 + 5.17 = 0.0277$$

Then,  $x_{B2} = 1 - 0.0277 = 0.9723$ . Calculating  $x_{A1}$  in a similar manner,  $x_{A1} = 0.0732$  and  $x_{B1} = 1 - 0.0732 = 0.9268$ . To calculate the molecular weight  $M_2$  at point 2,

$$M_2 = 100 \text{ kg} (0.1477 + 5.17) \text{ kg mol} = 18.75 \text{ kg/kg mol}$$

Similarly,  $M_1 = 20.07$ . From Eq. (19.2-2),

$$c_{av} = \rho_1 / (M_1 + \rho_2 M_2) = 972.8 / (20.07 + 988.1 / 18.752) = 50.6 \text{ kg mol/m}^3$$

To calculate  $x_{BM}$  from Eq. (19.2-4), we can use the linear mean since  $x_{B1}$  and  $x_{B2}$  are close to each other:

$$x_{BM} = x_{B1} + x_{B2} = 0.9268 + 0.97232 = 0.949$$

Substituting into Eq. (19.2-3) and solving,

$$N_A = D_{AB} c_{av} (x_{A1} - x_{A2}) (z_2 - z_1) x_{BM} N_A = (0.740 \times 10^{-9} \text{ m}^2 \text{ s}) (50.6 \text{ kg mol/m}^3) (0.0732 - 0.0277) (2/1000 \text{ m}) (0.949) N_A = 8.99 \times 10^{-7} \text{ kg mole/m}^2 \text{ s}$$

## 19.3 Molecular Diffusion in Solids

### 19.3A Introduction and Types of Diffusion in Solids

Even though rates of diffusion of gases, liquids, and solids in solids

are generally slower than rates in liquids and gases, mass transfer in solids is quite important in chemical and biological processing. Some examples are leaching of foods, such as soybeans, and of metal ores; drying of timber, salts, and foods; diffusion and catalytic reaction in solid catalysts; separation of fluids by membranes; diffusion of gases through polymer films used in packaging; and treating of metals at high temperatures by gases.

We can broadly classify transport in solids into two types of diffusion: diffusion that can be considered to follow Fick's law and does not depend primarily on the actual structure of the solid, and diffusion in porous solids where the actual structure and void

channels are important. These two broad types of diffusion will be considered.

### **19.3B Diffusion in Solids Following Fick's Law**

*1. Derivation of equations.* This type of diffusion in solids does not depend on the actual structure of the solid. The diffusion occurs when the fluid or solute diffusing is actually dissolved in the solid to form a more or less homogeneous solution—for example, in leaching, where the solid contains a large amount of water and a solute is diffusing through this solution, or in the diffusion of zinc through copper, where solid solutions are present. Also, the diffusion of nitrogen or hydrogen through rubber, or in some cases diffusion of water in foodstuffs, can be classified here, since equations of

similar type can be used.

Generally, simplified equations are used. Using the general equation (18.1-21) for binary diffusion,

$$N_A = -cD_{AB} \frac{dx_A}{dz} + cA_c(N_A + N_B) \quad (18.1-21)$$

the bulk-flow term,  $(c_A/c)(N_A + N_B)$ , even if present, is usually small, since  $c_A/c$  or  $x_A$  is quite small. Hence, it is neglected. Also,  $c$  is assumed constant, giving the following equation for diffusion in solids

$$N_A = -D_{AB} \frac{dc_A}{dz} \quad (19.3-1)$$

where  $D_{AB}$  is diffusivity in  $\text{m}^2/\text{s}$  of  $A$  through  $B$  and is usually assumed constant, independent of pressure for solids. Note that  $D_{AB} \neq D_{BA}$  in solids.

Integration of Eq. (19.3-1) for a solid slab at steady state gives

$$N_A = D_{AB}(c_{A1} - c_{A2}) \frac{z_2 - z_1}{L} \quad (19.3-2)$$

For the case of diffusion radially through a cylinder wall of inner radius  $r_1$  and outer  $r_2$ , and length  $L$ ,

$$N_A 2\pi r L = -D_{AB} \frac{dc_A}{dr} \quad (19.3-3)$$

$$N_A = D_{AB}(c_{A1} - c_{A2}) \frac{2\pi L \ln(r_2/r_1)}{L} \quad (19.3-4)$$

This case is similar to conduction heat transfer radially through a hollow cylinder, as shown in Fig. 13.1-3.

As stated above, the diffusion coefficient  $D_{AB}$  in the solid is not dependent upon the pressure of the gas or liquid on the outside of the solid. For example, if  $\text{CO}_2$

gas is outside a slab of rubber and is diffusing through the rubber,  $D_{AB}$  would be independent of  $p_A$ , the partial pressure of  $\text{CO}_2$  at the surface. The solubility of  $\text{CO}_2$  in the solid, however, is directly proportional to  $p_A$ . This is similar to the case of the solubility of  $\text{O}_2$  in water being directly proportional to the partial pressure of  $\text{O}_2$  in the air by Henry's law.

The solubility of a solute gas (A) in a solid is usually expressed as  $S$  in  $\text{m}^3$  solute (at STP of  $0^\circ\text{C}$  and 1 atm) per  $\text{m}^3$  solid per atm partial pressure of (A).

Also,  $S = \text{cm}^3 (\text{STP})/\text{atm} \cdot \text{cm}^3 \text{ solid}$  in the cgs system. To convert this to  $c_A$  concentration in the solid in  $\text{kg mol A}/\text{m}^3$  using SI units,

$$c_A = S m^3(\text{STP}) /$$

$$c_A = \frac{p_A}{S} = \frac{p_A}{0.051 \text{ m}^3 (\text{at STP of } 0^\circ\text{C and } 1 \text{ atm}) / \text{m}^3 \text{ solid} \cdot \text{atm}} \quad (19.3-5)$$

Using cgs units,

$$c_A = \frac{p_A}{S} = \frac{p_A}{0.051 \text{ g mol}^{-1} \text{ cm}^3 \text{ solid}} \quad (19.3-6)$$

**EXAMPLE 19.3-1. Diffusion of  $\text{H}_2$  Through a Neoprene Membrane**

The gas hydrogen at  $17^\circ\text{C}$  and  $0.010 \text{ atm}$  partial pressure is diffusing through a membrane of vulcanized neoprene rubber  $0.5 \text{ mm}$  thick. The pressure of  $\text{H}_2$  on the other side of the neoprene is zero. Calculate the steady-state flux, assuming that the only resistance to diffusion is in the membrane. The solubility  $S$  of  $\text{H}_2$  gas in neoprene at  $17^\circ\text{C}$  is  $0.051 \text{ m}^3 (\text{at STP of } 0^\circ\text{C and } 1 \text{ atm}) / \text{m}^3 \text{ solid} \cdot \text{atm}$ , and the diffusivity  $D_{AB}$  is  $1.03 \times 10^{-10} \text{ m}^2/\text{s}$  at  $17^\circ\text{C}$ .

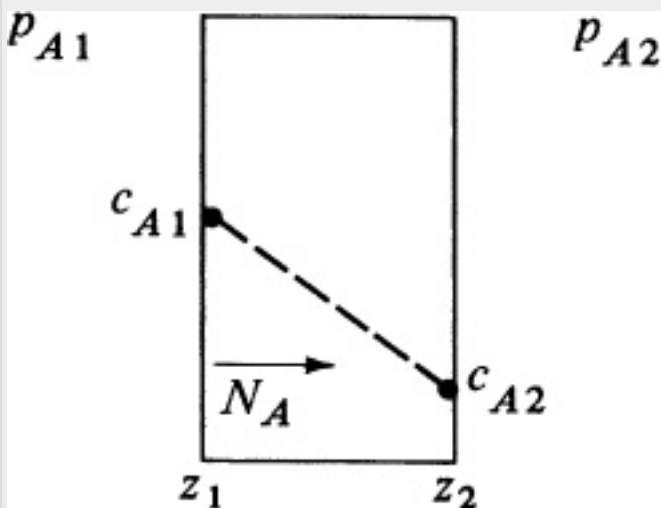


Figure 19.3-1. Concentrations for Example 19.3-1.

**Solution:** A sketch showing the concentration is shown in Fig. 19.3-1. The equilibrium concentration  $c_{A1}$  at the inside surface of the rubber is, from Eq. (19.3-5),

$$c_{A1} = S_{22} p_{A1} = 0.051 (0.010) 22.414 = 2.28 \times 10^{-5} \text{ kmole (H}_2\text{) m}^3 \text{ (solid)}$$

Since  $p_{A2}$  at the other side is 0,  $c_{A2} = 0$ . Substituting into Eq. (19.3-2) and solving,

$$\begin{aligned} N_A &= DAB(c_{A1} - c_{A2}) \frac{z_2 - z_1}{z} = (1.03 \times 10^{-10} \text{ m}^2 \text{ s}) \\ &\quad (2.28 \times 10^{-5} \text{ kmol m}^{-3} - 0 \text{ kmol m}^{-3}) \\ (0.0005 \text{ m} - 0 \text{ m}) N_A &= 4.69 \times 10^{-12} \text{ kmol (H}_2\text{) m}^2 \text{ s} \end{aligned}$$

*2. Permeability equations for diffusion in solids.* In many cases, the experimental data for diffusion of gases in solids are not given as diffusivities and solubilities but as permeabilities,  $P_M$ , in  $\text{m}^3$  of solute gas  $A$  at STP ( $0^\circ\text{C}$  and 1 atm press), diffusing per second per  $\text{m}^2$  cross-sectional area, through a solid 1 m thick under a pressure difference of 1 atm pressure. This can be related to Fick's equation (19.3-2) as follows:

$$N_A = DAB(c_{A1} - c_{A2}) \frac{z_2 - z_1}{z} \quad (19.3-2)$$



From Eq. (19.3-5),

$$c_{A2} = S p_{A2} / 22.414 \quad (19.3-7)$$

Substituting Eq. (19.3-7) into (19.3-2),

$$N_A = DAB S (p_{A1} - p_{A2}) / 22.414 (z_2 - z_1) = P_M (p_{A1} - p_{A2}) / 22.414 (z_2 - z_1) \text{ kg mol/s} \cdot \text{m}^2 \quad (19.3-8)$$

where the permeability  $P_M$  is

$$P_M = DAB S \text{m}^3(\text{STP}) / (\text{s} \cdot \text{m}^2 \text{C.S.} \cdot \text{atm}) / \text{m} \quad (19.3-9)$$

Permeability ( $P_M$ ) is also given in the literature in several other sets of units. For the cgs system, the permeability is given as  $\text{cm}^3(\text{STP}) / (\text{s} \cdot \text{cm}^2 \text{C.S. atm/cm})$ . In some cases in the literature, the permeability is given as  $\text{cm}^3(\text{STP}) / (\text{s} \cdot \text{cm}^2 \text{C.S.} \cdot \text{cm Hg/cm thickness})$ . These

are related as follows:

$$\frac{p_A - p_B}{p_A} \cdot \frac{V}{V_0} \cdot \frac{M}{M_0} \cdot \frac{t}{t_0} = \frac{p_A - p_B}{p_A} \cdot \frac{V}{V_0} \cdot \frac{M}{M_0} \cdot \frac{t}{t_0} = 104 \text{ cm}^3(\text{STP}) \cdot \text{cm} \cdot \text{cm}^2 \cdot \text{atm} (19.3-8)$$

$$\frac{p_A - p_B}{p_A} \cdot \frac{V}{V_0} \cdot \frac{M}{M_0} \cdot \frac{t}{t_0} = 1.316 \times 10^2 \text{ cm}^3(\text{STP}) \cdot \text{cm} \cdot \text{cm}^2 \cdot \text{atm} (19.3-9)$$

When there are several solids 1, 2, 3, ..., in series and  $L_1, L_2, \dots$  represent the thickness of each, then Eq. (19.3-8) becomes

$$\frac{p_A - p_B}{p_A} = \frac{L_1}{P M_1} + \frac{L_2}{P M_2} + \dots (19.3-12)$$

where  $p_A - p_B$  is the overall partial pressure difference.

### *3. Experimental diffusivities, solubilities, and permeabilities.*

Accurate prediction of diffusivities in solids is generally not possible because of the lack of knowledge of the theory

of the solid state. Hence, experimental values are needed. Some experimental data for diffusivities, solubilities, and permeabilities are given in Table 19.3-1 for gases diffusing in solids and solids diffusing in solids.

For the simple gases such as He, H<sub>2</sub>, O<sub>2</sub>, N<sub>2</sub>, and CO<sub>2</sub>, with gas pressures up to 1 or 2 atm, the solubility in solids such as polymers and glasses generally follows Henry's law and Eq. (19.3-5) holds.

Also, for these gases the diffusivity and permeability are independent of concentration, and hence pressure. For the effect of temperature  $T$  in K, the  $\ln PM$  is approximately a linear function of  $1/T$ . Also, the diffusion of one gas, say H<sub>2</sub>, is approximately independent of the other gases present, such as O<sub>2</sub> and N<sub>2</sub>.

For metals such as Ni, Cd, and Pt, where gases such as H<sub>2</sub> and O<sub>2</sub> are diffusing, it has been found experimentally that the flux is approximately proportional to (pA<sub>1</sub>-pA<sub>2</sub>), so Eq. (19.3-8) does not hold (B1). When water is diffusing through polymers, unlike the simple gases,  $P_M$  may depend somewhat on the relative pressure difference (C1, B1). Further data are available in monographs by Crank and Park (C1) and Barrer (B1).

**EXAMPLE 19.3-2. Diffusion Through a Packaging Film Using Permeability**

A polyethylene film 0.00015 m (0.15 mm) thick is being considered for use in packaging a pharmaceutical product at 30°C. If the partial pressure of O<sub>2</sub> outside the package is 0.21 atm and inside it is 0.01 atm, calculate the diffusion flux of O<sub>2</sub> at steady state. Use permeability data from Table 19.3-1. Assume that the resistances to diffusion both outside and inside the film are negligible compared to the resistance of the film.

**Solution:** From Table 19.3-1,  $P_M = 4.17(10^{-12})$  m<sup>3</sup> solute (STP)/(s · m<sup>2</sup> · atm/m). Substituting into Eq. (19.3-8),

$$N_A = \frac{P_M(pA_1 - pA_2)}{z_2 - z_1} = \frac{(4.17 \times 10^{-12} \text{ m}^3 \text{ s}^{-1} \text{ m}^{-2} \text{ atm}^{-1}) (0.21 \text{ atm} - 0.01 \text{ atm})}{(0.00015 \text{ m} - 0 \text{ m})} = 2.480 \times 10^{-10} \text{ kg mol m}^{-2} \text{ s}^{-1}$$

Note that a film made of nylon has a much smaller value of permeability  $P_M$  for  $O_2$  and would make a more suitable barrier.

## Table 19.3-1. *Diffusivities and Permeabilities in Solids*

4. *Membrane separation processes.* In Chapters 24 and 25, a detailed discussion is given of the various membrane separation processes for gas separation by membranes, dialysis, reverse osmosis, ultrafiltration, and microfiltration.

### **19.3C Diffusion in Porous Solids That Depends on Structure**

1. *Diffusion of liquids in porous solids.* In Section 19.3B, we used Fick's law and treated the solid as a uniform homogeneous-like material with an experimental diffusivity

$D_{AB}$ . In this section, we are concerned with porous solids that have pores or interconnected voids in the solid that affect the diffusion. A cross section of a typical porous solid is shown in Fig. 19.3-2.

For the situation where the voids are filled completely with liquid water, the concentration of salt in water at boundary 1 is  $c_{A1}$  and at point 2 is  $c_{A2}$ . The salt, in diffusing through the water in the void volume, takes a tortuous path that is unknown and greater than  $(z_2 - z_1)$  by a factor  $\tau$ , called *tortuosity*. Diffusion does not occur in the inert solid. For a dilute solution using Eq. (19.2-5) for diffusion of salt in water at steady state,

$$N_A = \epsilon D_{AB} (c_{A1} - c_{A2}) \tau (z_2 - z_1)$$

where  $\epsilon$  is the open void fraction,  $D_{AB}$  is the diffusivity of salt in water, and  $\tau$  is a factor that corrects for the path longer than  $(z_2 - z_1)$ . For inert-type solids,  $\tau$  can vary from about 1.5 to 5. The terms are often combined into an effective diffusivity:

$$D_{Aeff} = \epsilon \tau D_{AB} \text{ m}^2/\text{s} \quad (19.3-14)$$

**EXAMPLE 19.3-3. Diffusion of KCl in Porous Silica**

A sintered solid of silica 2.0 mm thick is porous, with a void fraction  $\epsilon$  of 0.30 and a tortuosity  $\tau$  of 4.0. The pores are filled with water at 298 K. At one face, the concentration of KCl is held at 0.10 g mol/liter, and fresh water flows rapidly past the other face. Neglecting any other resistance but that in the porous solid, calculate the diffusion of KCl at steady state.

**Solution:** The diffusivity of KCl in water from Table 18.2-3 is  $D_{AB} = 1.87 \times 10^{-9} \text{ m}^2/\text{s}$ . Also,  $c_{A1} = 0.10/1000 = 1.0 \times 10^{-4} \text{ g mol/cm}^3 = 0.10 \text{ kg mol/m}^3$ , and  $c_{A2} = 0$ . Substituting into Eq. (19.3-13),

$$N_A = \epsilon D_{AB} (c_{A1} - c_{A2}) \tau (z_2 - z_1) = 0.30 (1.870 \times 10^{-9} \text{ m}^2/\text{s}) (0.10 \text{ kg mol/m}^3 - 0 \text{ kg mol/m}^3) 4.0 (0.002 \text{ m}) = 7.01 \times 10^{-9} \text{ kg mol/m}^2 \cdot \text{s}$$

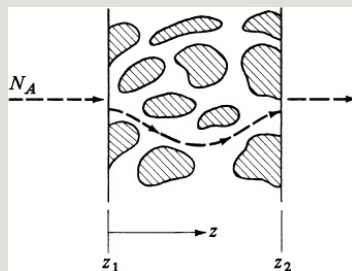


Figure 19.3-2. Sketch of a typical porous solid.

2. *Diffusion of gases in porous solids.* If the voids shown in Fig. 19.3-2 are filled with gases, then a somewhat similar situation exists. If the pores are very large so that diffusion occurs only by Fickian-type diffusion, then Eq. (19.3-13) becomes, for gases,

$$N_A = \epsilon D_{AB} (c_{A1} - c_{A2}) \tau (z_2 - z_1) = \epsilon D_{AB} (p_{A1} - p_{A2}) \tau RT (z_2 - z_1) \quad (19.3-15)$$

Again, the value of the tortuosity must be determined experimentally. Diffusion is assumed to occur only through the



voids or pores and not through the actual solid particles.

A correlation of tortuosity versus the void fraction of various unconsolidated porous media, such as beds of glass spheres, sand, salt, talc, and so on (S1), gives the following approximate values of  $\tau$  for different values of  $\varepsilon$ ;  $\varepsilon = 0.2$ ,  $\tau = 2.0$ ;  $\varepsilon = 0.4$ ,  $\tau = 1.75$ ;  $\varepsilon = 0.6$ ,  $\tau = 1.65$ .

When the pores are quite small in size and on the order of magnitude of the mean free path of the gas, other types of diffusion occur, which are discussed in Section 19.4.

## **19.4 Diffusion of Gases in Porous Solids and Capillaries**

### **19.4A Introduction**

In Section 19.3C, diffusion in porous

solids that depends on structure was discussed for liquids and gases. For gases, it was assumed that the pores were very large and Fickian-type diffusion occurred. However, the pores are often small in diameter and the mechanism of diffusion is basically changed.

Diffusion of gases in small pores frequently occurs in heterogeneous catalysis where gases diffuse through very small pores to react on the surface of the catalyst. In the freeze-drying of foods such as turkey meat, gaseous  $H_2O$  diffuses through the very fine pores of the meat's structure.

Since the pores or capillaries of porous solids are often small, the diffusion of gases may depend upon the diameter of

the pores. We first define a mean free path  $\lambda$ , which is the average distance a gas molecule travels before it collides with another gas molecule:

$$\lambda = 3.2 \mu P R T^2 \pi M (19.4 - 1)$$

where  $\lambda$  is in m,  $\mu$  is viscosity in  $\text{Pa} \cdot \text{s}$ ,  $P$  is pressure in  $\text{N/m}^2$ ,  $T$  is temperature in K,  $M$  = molecular weight in  $\text{kg/kg mol}$ , and  $R = 8.3143 \times 10^3 \text{N} \cdot \text{m/kg mol} \cdot \text{K}$ . Note that low pressures give large values of  $\lambda$ . For liquids, since  $\lambda$  is so small, diffusion follows Fick's law.

In the next sections, we shall consider what happens to the basic mechanisms of diffusion in gases as the relative value of the mean free path compared to the pore diameter varies. The total pressure  $P$  in the system will be constant, but

partial pressures of  $A$  and  $B$  may be different.

#### 19.4B Knudsen Diffusion of Gases

In Fig. 19.4-1a, a gas molecule  $A$  at partial pressure  $p_{A1}$  at the entrance to a capillary is diffusing through the capillary having a diameter  $d$  m. The total pressure  $P$  is constant throughout. The mean free path  $\lambda$  is large compared to the diameter  $d$ . As a result, the molecule collides with the wall and molecule-wall collisions are important. This type of diffusion is called *Knudsen diffusion*.

The Knudsen diffusivity is independent of pressure  $P$  and is calculated from

$$D_{KA} = \frac{1}{3} \bar{c} \lambda_A \quad (19.4-2)$$

where  $D_{KA}$  is diffusivity in  $\text{m}^2/\text{s}$ ,  $\bar{c}$  is

average pore radius in m, and  $\bar{v}_A$  is the average molecular velocity for component  $A$  in m/s. Using the kinetic theory of gases to evaluate  $\bar{v}_A$  the final equation for  $D_{KA}$  is

$$D_{KA} = 97.0 \bar{r}^{-1/2} (T M_A)^{1/2} \quad (19.4-3)$$

where  $M_A$  is molecular weight of  $A$  in kg/kg mol and  $T$  is temperature in K.

**EXAMPLE 19.4-1. Knudsen Diffusivity of Hydrogen**

A  $H_2$  ( $A$ )— $C_2H_6$  ( $B$ ) gas mixture is diffusing in a pore of a nickel catalyst used for hydrogenation at  $1.01325 \times 10^5$  Pa pressure and 373 K. The pore radius is 60 Å (angstrom). Calculate the Knudsen diffusivity  $D_{KA}$  of  $H_2$ .

**Solution:** Substituting into Eq. (19.4-3) for  $\bar{r} = 6.0 \times 10^{-9}$  m,  $M_A = 2.016$ , and  $T = 373$  K,

$$D_{KA} = 97.0 \bar{r}^{-1/2} (T M_A)^{1/2} = 97.0 (6.0 \times 10^{-9})^{-1/2} (373 \times 2.016)^{1/2} = 7.92 \times 10^{-6} \text{ m}^2/\text{s}$$

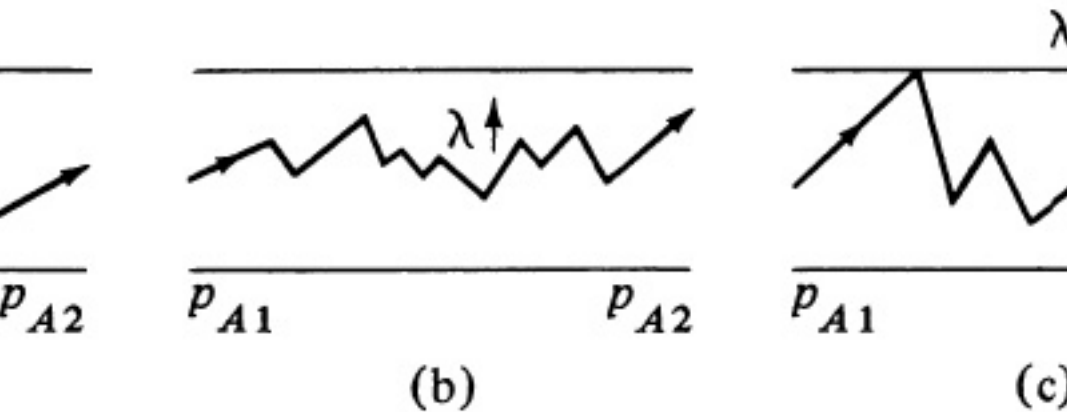


Figure 19.4-1. Types of diffusion of gases in small capillary tubes: (a) Knudsen gas diffusion, (b) molecular or Fick's gas diffusion, (c) transition gas diffusion.

The flux equation for Knudsen diffusion in a pore is

$$N_A = -DK_A \frac{dp_A}{dz} \quad (19.4-4)$$

Integrating between  $z_1 = 0$ ,  $p_A = p_{A1}$  and  $z_2 = L$ ,  $p_A = p_{A2}$ ,

$$N_A = DK_A \frac{p_{A1} - p_{A2}}{L} \quad (19.4-5)$$

The diffusion of  $A$  for Knudsen diffusion is completely independent of  $B$ , since  $A$  collides with the walls of the pore and not with  $B$ . A similar equation can be written for component  $B$ .

When the Knudsen number  $N_{Kn}$  defined as

$$N_{Kn} = \frac{L}{\lambda} \quad (19.4-6)$$

is  $\geq 10$ , the diffusion is primarily Knudsen and Eq. (19.4-5) predicts the flux to within about a 10% error. As  $N_{Kn}$  gets larger, this error decreases, since the diffusion approaches the Knudsen type.

## 19.4C Molecular Diffusion of Gases

As shown in Fig. 19.4-1b, when the mean free path  $\lambda$  is small compared to the pore diameter  $d$  or where  $N_{Kn} \leq 1/100$ , molecule–molecule collisions predominate and molecule–wall collisions are few. Ordinary molecular or Fickian diffusion holds and Fick’s law predicts the diffusion to within about 10%. The error diminishes as  $N_{Kn}$  gets smaller since the diffusion more closely approaches the Fickian type.

The equation for molecular diffusion given in previous sections is

$$N_A = -DABPRT \frac{dx_A}{dz} + x_A(N_A + N_B) \quad (19.4-7)$$

A flux ratio factor  $\alpha$  can be defined as

$$\alpha = 1 + \text{NBNA}(19.4-8)$$

Combining Eqs. (19.4-7) and (19.4-8) and integrating for a path length of  $L$  cm,

$$N_A = D_{AB} P \alpha R T L \ln \frac{1 - \alpha x_A}{1 - \alpha x_{A1}} \quad (19.4-9)$$

If the diffusion is equimolar,  $N_A = -N_B$ , and Eq. (19.4-7) becomes Fick's law. The molecular diffusivity  $D_{AB}$  is inversely proportional to the total pressure  $P$ .

#### 19.4D Transition-Region Diffusion of Gases

As shown in Fig. 19.4-1c, when the mean free path  $\lambda$  and pore diameter are intermediate in size between the two limits given for Knudsen and molecular diffusion, transition-type diffusion occurs, where molecule—



molecule and molecule–wall collisions are important in diffusion.

The transition-region diffusion equation can be derived by adding the momentum loss due to molecule–wall collisions in Eq. (19.4-4) and that is due to molecule–molecule collisions in Eq. (19.4-7) on a slice of capillary. No chemical reactions are occurring. The final differential equation is (G1)

$$N_A = -D_{NA} P R T \frac{dx_A}{dz} \quad (19.4-10)$$

where

$$D_{NA} = \frac{1}{\frac{1}{D_{AB}} + \frac{1}{D_{KA}}} \quad (19.4-11)$$

This transition region diffusivity  $D_{NA}$  depends slightly on concentration  $x_A$ .

Integrating Eq. (19.4-10),

$$N_A = D_{AB} P \alpha_{RTL} \ln \frac{1 - \alpha x_A^2 + D_{AB}/DK_A}{1 - \alpha x_A + D_{AB}/DK_A} \quad (19.4-12)$$

This equation has been shown experimentally to be valid over the entire transition region ( $R_1$ ). It reduces to the Knudsen equation at low pressures and to the molecular diffusion equation at high pressures. An equation similar to Eq. (19.4-12) can also be written for component  $B$ .

The term  $D_{AB}/DK_A$  is proportional to  $1/P$ . Hence, as the total pressure  $P$  increases, the term  $D_{AB}/DK_A$  becomes very small and  $N_A$  in Eq. (19.4-12) becomes independent of total pressure, since  $D_{AB}P$  is independent of  $P$ . At low total pressures, Eq. (19.4-12) becomes

the Knudsen diffusion equation (19.4-5), and the flux  $N_A$  becomes directly proportional to  $P$  for constant  $x_{A1}$  and  $x_{A2}$ .

In Fig. 19.4-2, this is illustrated for a fixed capillary diameter where the flux increases as total pressure increases and then levels off at high pressure. The relative position of the curve depends, of course, on the capillary diameter and the molecular and Knudsen diffusivities. Using only a smaller diameter,  $D_{KA}$  would be smaller and the Knudsen flux line would be parallel to the existing line at low pressures. At high pressures, the flux line would asymptotically approach the existing horizontal line, since molecular diffusion is independent of capillary diameter.

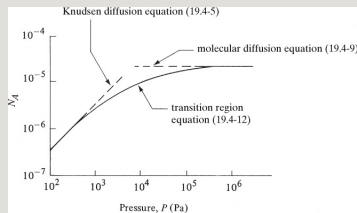


Figure 19.4-2. *Effect of total pressure  $P$  on the diffusion flux  $N_A$  in the transition region.*

If  $A$  is diffusing in a catalytic pore and reacts at the surface at the pore's end so that  $A \rightarrow B$ , then at steady state, equimolar counterdiffusion occurs, or  $N_A = -N_B$ . Then, from Eq. (19.3-8),  $\alpha = 1 - 1 = 0$ . The effective diffusivity  $D_{NA}$  from Eq. (19.4-11) becomes

$$D_{NA}' = \frac{1}{D_{AB}} + \frac{1}{D_{KA}} \quad (19.4-13)$$

The diffusivity is then independent of concentration and is constant.

Integration of Eq. (19.4-10) then gives

$$N_A = D_{NA}' \frac{P}{R T L} (x_{A1} - x_{A2}) = D_{NA}' \frac{P}{R T L} (p_{A1} - p_{A2}) \quad (19.4-14)$$

This simplified diffusivity  $D_{NA}'$  is often used in diffusion in porous catalysts even when equimolar counterdiffusion is not occurring. It greatly simplifies the equations for diffusion and reaction to use this simplified diffusivity.

An alternative simplified diffusivity can be obtained by using an average value of  $x_A$  in Eq. (19.4-11) to give

$$D_{NA}'' = 1(1 - \alpha x_{Aav}) / D_{AB} + 1 / D_{KA} \quad (19.4-15)$$

where  $x_{Aav} = (x_{A1} + x_{A2})/2$ . This diffusivity is more accurate than  $D_{NA}'$ . Integration of Eq. (19.4-10) gives

$$N_A = D_{NA}'' P_{RTL} (x_{A1} - x_{A2}) = D_{NA}' P_{RTL} (p_{A1} - p_{A2}) \quad (19.4-16)$$

#### 19.4E Flux Ratios for Diffusion of Gases in Capillaries

1. *Diffusion in an open system.* If diffusion in porous solids or channels with no chemical reaction is occurring where the total pressure  $P$  remains constant, then for an open binary counterdiffusing system, the ratio of  $N_A/N_B$  is constant in all of the three diffusion regimes and is (G1)

$$N_B/N_A = -M_A/M_B \quad (19.4-17)$$

Hence,

$$\alpha = 1 - M_A/M_B \quad (19.4-18)$$

In this case, gas flows past the two open ends of the system. However, when chemical reaction occurs, stoichiometry determines the ratio  $N_B/N_A$ , and not Eq. (19.4-17).

2. *Diffusion in a closed system.* When molecular diffusion is occurring in a closed system, shown in Fig. 19.1-1, at constant total pressure  $P$ , equimolar counterdiffusion occurs.

**EXAMPLE 19.4-2. Transition-Region Diffusion of He and N<sub>2</sub>**

A gas mixture at a total pressure of 0.10 atm abs and 298 K is composed of N<sub>2</sub> (A) and He (B). The mixture is diffusing through an open capillary 0.010 m long having a diameter of  $5 \times 10^{-6}$  m. The mole fraction of N<sub>2</sub> at one end is  $x_{A1} = 0.8$  and at the other end is  $x_{A2} = 0.2$ . The molecular diffusivity  $D_{AB}$  is  $6.98 \times 10^{-5}$  m<sup>2</sup>/s at 1 atm, which is an average value determined by several investigators.

- Calculate the flux  $N_A$  at steady state.
- Use the approximate equations (19.4-14) and (19.4-16) for this case.

**Solution:** The given values are  $T = 273 + 25 = 298$  K,  $r = 5 \times 10^{-6}/2 = 2.5 \times 10^{-6}$  m,  $L = 0.01$  m,  $P = 0.1(1.01325 \times 10^5) = 1.013 \times 10^4$  Pa,  $x_{A1} = 0.8$ ,  $x_{A2} = 0.2$ ,  $D_{AB} = 6.98 \times 10^{-5}$  m<sup>2</sup>/s at 1 atm. Other values needed are  $M_A = 28.02$  kg/kg mol,  $M_B = 4.003$ .

The molecular diffusivity at 0.1 atm is  $D_{AB} = 6.98 \times 10^{-5}/0.1 = 6.98 \times 10^{-4}$  m<sup>2</sup>/s. Substituting into Eq. (19.4-3) for the Knudsen diffusivity,

$$D_{KA} = 97.0(2.5 \times 10^{-6})298/28.02 = 7.91 \times 10^{-4} \text{ m}^2/\text{s}$$

From Eq. (19.4-17),

$$N_B N_A = -M_A M_B = -28.02(4.003) = -2.645$$

From Eq. (19.4-8),

$$a=1+NBNA=1-2.645=-1.645$$

Substituting into Eq. (19.4-12) for part (a),

$$NA=(6.98 \times 10^{-4} \text{ m}^2 \text{ s})(1.013 \times 10^4 \text{ Pa})(-1.645) \\ (8314 \text{ m}^3 \text{ Pa} \cdot \text{kg} \cdot \text{mol}^{-1} \cdot \text{K})(298 \text{ K}) \\ (0.01 \text{ m}) \ln 1 + 1.645(0.2) + 6.98/7.911 + 1.645(0.8) + 6.98/7.91 NA = 6.40 \times 10^{-5} \text{ kg} \cdot \text{mol}^{-2} \cdot \text{s}$$

For part (b), the approximate equation (19.4-13) is used:

$$DNA' = 1/DAB + 1/DKA = 1/6.98 \times 10^{-4} \text{ m}^2 \text{ s} \\ + 1/7.91 \times 10^{-4} \text{ m}^2 \text{ s} DNA' = 3.708 \times 10^{-4} \text{ m}^2 \text{ s}$$

Substituting into Eq. (19.4-14), the approximate flux is

$$NA = -DNA' PRTL(xA1 - xA2) = (3.708 \times 10^{-4} \text{ m}^2 \text{ s}) \\ (1.013 \times 10^4 \text{ Pa})(8314 \text{ m}^3 \cdot \text{Pa} \cdot \text{kg} \cdot \text{mol}^{-1} \cdot \text{K})(298 \text{ K})(0.01 \text{ m}) \\ (0.8 - 0.2) NA = 9.10 \times 10^{-5} \text{ kg} \cdot \text{mol}^{-2} \cdot \text{s}$$

Hence, the calculated flux is approximately 40% high when using the approximation of equimolar counterdiffusion ( $\alpha = 0$ ).

The more accurate approximate equation (19.4-15) is used next. The average concentration is  $x_{Aav} = (xA1 + xA2)/2 = (0.8 + 0.2)/2 = 0.50$ .

$$DNA'' = 1/(1 - \alpha x_{Aav})/DAB + 1/DKADNA'' = 1/(1 + 1.654 \times 0.5)/ \\ (6.98 \times 10^{-4} \text{ m}^2 \text{ s}) + 1/(7.91 \times 10^{-4} \text{ m}^2 \text{ s}) DNA'' = 2.581 \times 10^{-4} \text{ m}^2 \text{ s}$$

Substituting into Eq. (19.4-16),

$$NA = -DNA'' PRTL(xA1 - xA2) = (2.581 \times 10^{-4} \text{ m}^2 \text{ s}) \\ (1.013 \times 10^4 \text{ Pa})(8314 \text{ m}^3 \cdot \text{Pa} \cdot \text{kg} \cdot \text{mol}^{-1} \cdot \text{K})(298 \text{ K})(0.01 \text{ m}) \\ (0.8 - 0.2) NA = 6.33 \times 10^{-5} \text{ kg} \cdot \text{mol}^{-2} \cdot \text{s}$$

In this case, the flux is only -1.1% low.

## 19.4F Diffusion of Gases in Porous Solids

In actual diffusion in porous solids, the pores are not straight and cylindrical but irregular. Hence, the



equations for diffusion in pores must be modified somewhat for actual porous solids. The problem is further complicated by the fact that the pore diameters vary and the Knudsen diffusivity is a function of pore diameter.

As a result of these complications, investigators often measure effective diffusivities  $D_{A \text{ eff}}$  in porous media, where

$$N_A = D_{A \text{ eff}} P R T L (x_{A1} - x_{A2}) \quad (19.4-19)$$

If a tortuosity factor  $\tau$  is used to correct the length  $L$  in Eq. (19.4-16), and the right-hand side is multiplied by the void fraction  $\epsilon$ , Eq. (19.4-16) becomes

$$N_A = \epsilon D_{A \text{ eff}} \tau P R T L (x_{A1} - x_{A2})$$

(19.4-20)

Comparing Eqs. (19.4-19) and (19.4-20),

$$D_{Aeff} = \epsilon D_{NA} \tau \quad (19.4-21)$$

In some cases, investigators measure  $D_{Aeff}$  but use  $D_{NA}'$  instead of the more accurate  $D_{NA}$  in Eq. (19.4-21).

Experimental data (G2, S2, S3) show that  $\tau$  varies from about 1.5 to over 10. A reasonable range for many commercial porous solids is about 2–6 (S2). If the porous solid consists of a bidispersed system of micropores and macropores instead of a monodispersed pore system, the above approach should be modified (C2, S3).

Discussions and references for diffusion

in porous inorganic-type solids, organic solids, and freeze-dried foods such as meat and fruit are given elsewhere (S2, S3).

Another type of diffusion that may occur is surface diffusion. When a molecular layer of adsorption occurs on the solid, the molecules can migrate on the surface. Details are given elsewhere (S2, S3).

### **19.5 Diffusion in Biological Gels**

Gels can be looked upon as semisolid materials that are “porous.” They are composed of macromolecules that are usually in dilute aqueous solution with the gel comprising a few wt % of the water solution. The “pores” or open spaces in the gel structure are filled with

water. The rates of diffusion of small solutes in the gels are somewhat less than in aqueous solution. The main effect of the gel structure is to increase the path length for diffusion, assuming no electrical-type effects (S4).

Recent studies by electron microscopy (L1) have shown that the macromolecules of the gel agarose (a major constituent of agar) exist as long and relatively straight threads. This suggests a gel structure of loosely interwoven, extensively hydrogen-bonded polysaccharide macromolecules.

Some typical gels are agarose, agar, and gelatin. A number of organic polymers exist as gels in various types of solutions. To measure the diffusivity of

solutes in gels, unsteady-state methods are used. In one method, the gel is melted and poured into a narrow tube open at one end. After solidification, the tube is placed in an agitated bath containing the solute for diffusion. The solute leaves the solution at the gel boundary and diffuses through the gel itself. After a period of time, the amount of solute diffusing in the gel is determined to give the diffusion coefficient of the solute in the gel.

A few typical values of diffusivities of some solutes in various gels are given in Table 19.5-1. In some cases, the diffusivity of the solute in pure water is given so that the decrease in diffusivity due to the gel can be seen. For example, from Table 19.5-1 at 278 K, urea in water has a diffusivity of  $0.880 \times 10^{-}$

$9\text{m}^2/\text{s}$ , and in 2.9 wt % gelatin, it has a value of  $0.640 \times 10^{-9}\text{m}^2/\text{s}$ , a decrease of 27%.

Table 19.5-1. *Typical Diffusivities of Solutes in Dilute Biological Gels in Aqueous Solution*

In both agar and gelatin, the diffusivity of a given solute decreases more or less linearly with an increase in wt % gel. However, extrapolation to 0% gel gives a value smaller than that shown for pure water. It should be noted that in different preparations or batches of the same type of gel, the diffusivities can vary by as much as 10 to 20%.

**EXAMPLE 19.5-1. Diffusion of Urea in Agar**

A tube or bridge of a gel solution of 1.05 wt % agar in water at 278 K is 0.04 m long and connects two agitated solutions

of urea in water. The urea concentration in the first solution is 0.2 g mol urea per liter solution and it is 0 in the other. Calculate the flux of urea in kg mol/s · m<sup>2</sup> at steady state.

**Solution:** From Table 19.5-1 for the solute urea at 278 K,  $D_{AB} = 0.727 \times 10^{-9} \text{ m}^2/\text{s}$ . For urea diffusing through stagnant water in the gel, Eq. (19.2-3) can be used. However, since the value of  $x_{A1}$  is less than about 0.01, the solution is quite dilute and  $x_{BM} \approx 1.00$ . Hence, Eq. (19.2-5) can be used. The concentrations are  $c_{A1} = 0.20/1000 = 0.0002 \text{ g mol/cm}^3 = 0.20 \text{ kg mol/m}^3$  and  $c_{A2} = 0$ . Substituting into Eq. (19.2-5),

$$N_A = D_{AB}(c_{A1} - c_{A2})/z = (0.727 \times 10^{-9} \text{ m}^2/\text{s}) \\ (0.20 \text{ kg mol/m}^3 - 0 \text{ kg mol/m}^3) / (0.40 \text{ m} - 0 \text{ m}) = 3.63 \times 10^{-9} \text{ kg mol/m}^2 \cdot \text{s}$$

## 19.6 Special Cases of the General Diffusion Equation at Steady State

### 19.6A Special Cases of the General Diffusion Equation at Steady State

*1. Introduction and physical conditions at the boundaries.* The general equation for diffusion and convection of a binary mixture in one direction with no chemical reaction has been given previously:

$$N_A = -cD_{AB} \frac{dx_A}{dz} + c_A c (N_A + N_B) \quad (18.1-21)$$

To integrate this equation at steady state, it is necessary to specify the boundary conditions at  $z_1$  and  $z_2$ . In many mass-transfer problems, the molar ratio  $N_A/N_B$  is determined by the physical conditions occurring at the two boundaries.

As an example, one boundary of the diffusion path may be impermeable to species  $B$  because  $B$  is insoluble in the phase at this boundary. Diffusion of ammonia ( $A$ ) and nitrogen ( $B$ ) through a gas phase to a water phase at the boundary is such a case, since nitrogen is essentially insoluble in water. Hence,  $N_B = 0$ , since at steady state  $N_B$  must have the same value at all points in the path of  $z_2 - z_1$ . In some cases, a heat balance in the adjacent phase at the boundary can determine the flux ratios.



For example, if component  $A$  condenses at a boundary and releases its latent heat to component  $B$ , which vaporizes and diffuses back, the ratios of the latent heats determine the flux ratio.

In another example, the boundary concentration can be fixed by having a large volume of a phase flowing rapidly by with a given concentration  $x_{A1}$ . In some cases, the concentration  $x_{A1}$  may be set by an equilibrium condition, whereby  $x_{A1}$  is in equilibrium with some fixed composition at the boundary. Chemical reactions can also influence the rates of diffusion and the boundary conditions.

*2. Equimolar counterdiffusion.* For the special case of equimolar counterdiffusion, where  $N_A = -N_B$ , Eq.

(18.1-21) becomes, as shown previously, for steady state and constant  $c$ ,

$$N_A = J_A^* = -c D_{AB} \frac{dx_A}{dz} = D_{AB} (c_{A1} - c_{A2}) \frac{z_2 - z_1}{L} \quad (19.6-1)$$

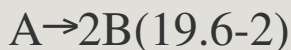
3. *Diffusion of A through stagnant, nondiffusing B.* For gas A diffusing through stagnant nondiffusing gas B,  $N_B = 0$ , and integration of Eq. (18.1-21) gives Eq. (19.1-13):

$$N_A = D_{AB} \frac{P}{RT} \frac{(p_{A1} - p_{A2})}{(z_2 - z_1)} \ln \frac{p_B (p_{A1} - p_{A2})}{p_{A1} (p_B - p_{A2})} \quad (19.1-13)$$

Several other more complicated cases of integration of Eq. (18.1-21) are considered next.

4. *Diffusion and chemical reaction at a boundary.* Often in catalytic reactions,

where  $A$  and  $B$  are diffusing to and from a catalyst surface, the relation between the fluxes  $N_A$  and  $N_B$  at steady state is controlled by the stoichiometry of a reaction at a boundary. An example is gas  $A$  diffusing from the bulk gas phase to the catalyst surface, where it reacts instantaneously and irreversibly in a heterogeneous reaction as follows:



Gas  $B$  then diffuses back, as shown in Fig. 19.6-1.

At steady state, 1 mol of  $A$  diffuses to the catalyst for every 2 mol of  $B$  diffusing away, or  $N_B = -2N_A$ . The negative sign indicates that the fluxes are in opposite directions. Rewriting Eq. (18.1-21) in terms of mole fractions,

$$N_A = -cD_{AB} \frac{dx_A}{dz} + x_A(N_A + N_B) \quad (19.6-3)$$

Next, substituting  $N_B = -2N_A$  into Eq. (19.6-3),

$$N_A = -cD_{AB} \frac{dx_A}{dz} + x_A(N_A - 2N_A) \quad (19.6-4)$$

Rearranging and integrating with constant  $c$  ( $P = \text{constant}$ ), we obtain the following:

**1. *Instantaneous surface reaction.***

$$N_A \int_{z_1=0}^{z_2=\delta} dz = -cD_{AB} \int_{x_{A1}}^{x_{A2}} \frac{dx_A}{1+x_A} \quad (19.6-5)$$

$$N_A = cD_{AB} \delta \ln \frac{1+x_{A1}}{1+x_{A2}} \quad (19.6-6)$$

Since the reaction is instantaneous,  $x_{A2} = 0$ , because no A can exist next to the

catalyst surface. Equation (19.6-6) describes the overall rate of the process of diffusion plus instantaneous chemical reaction.

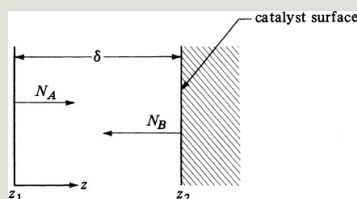


Figure 19.6-1. Diffusion of A and heterogeneous reaction at a surface.

**2. Slow surface reaction.** If the heterogeneous reaction at the surface is not instantaneous but slow for the reaction  $A \rightarrow 2B$ , and the reaction is first order,

$$N_A z = \delta = k_1' c_A = k_1' c_{xA} \quad (19.6-7)$$

where  $k_1'$  is the first-order heterogeneous reaction velocity constant in m/s. Equation (19.6-6) still holds for

this case, but the boundary condition  $x_{A2}$  at  $z = \delta$  is obtained by solving for  $x_A$  in Eq. (19.6-7),

$$x_A = x_{A2} = N_{Az} \delta / k_1' c = N_A k_1' / (19.6-8)$$

For steady state,  $N_{Az} = \delta = N_A$ .

Substituting Eq. (19.6-8) into (19.6-6),

$$N_A = c D_{AB} \delta \ln \frac{1 + x_{A1}}{1 + N_A / k_1'} \quad (19.6-9)$$

The rate in Eq. (19.6-9) is less than in Eq. (19.6-7), since the denominator in the latter equation is  $1 + x_{A2} = 1 + 0$  and in the former is  $1 + N_A / k_1'$ .

**EXAMPLE 19.6-1. Diffusion and Chemical Reaction at a Boundary**

Pure gas *A* diffuses from point 1 at a partial pressure of 101.32 kPa to point 2 at a distance 2.00 mm away. At point 2, it undergoes a chemical reaction at the catalyst surface and  $A \rightarrow 2B$ . Component *B* diffuses back at steady state. The total pressure is  $P = 101.32$  kPa. The temperature is 300 K and  $D_{AB} = 0.15 \times 10^{-4} \text{ m}^2/\text{s}$ .

- For instantaneous rate of reaction, calculate  $x_{A2}$  and  $N_A$ .
- For a slow reaction where  $k_1' = 5.63 \times 10^3 \text{ m/s}$ , calculate  $x_{A2}$  and  $N_A$ .

**Solution:** For part (a),  $p_{A2} = x_{A2} = 0$  since no  $A$  can exist next to the catalyst surface. Since  $N_B = -2N_A$ , Eq. (19.6-6) will be used as follows:  $\delta = 2.00 \times 10^{-3} \text{ m}$ ,  $T = 300 \text{ K}$ ,  $c = P/RT = 101.32 \times 10^3 / (8314 \times 300) = 4.062 \times 10^{-2} \text{ kg mol/m}^3$ ,  $x_{A1} = p_{A1}/P = 101.32 \times 10^3 / 101.32 \times 10^3 = 1.00$ .

$$N_A = c D A B \delta \ln 1 + x_{A1} + x_{A2} = (4.062 \times 10^{-2} \text{ kg mol/m}^3) (0.15 \times 10^{-4} \text{ m}^2 \text{s}) 2.00 \times 10^{-3} \text{ m} \ln 1 + 1.001 + 0 N_A = 2.112 \times 10^{-4} \text{ kg mol/m}^2 \text{s}$$

For part (b), from Eq. (19.6-8),  $x_{A2} = N_A / k_1' C = N_A / (5.63 \times 10^{-3} \times 4.062 \times 10^{-2})$ . Substituting into Eq. (19.6-9),

$$N_A = (4.062 \times 10^{-2} \text{ kg mol/m}^3) (0.15 \times 10^{-4} \text{ m}^2 \text{s}) 2.00 \times 10^{-3} \text{ m} \ln 1 + 1.001 + N_A / (5.63 \times 10^{-3} \text{ m} \times 4.062 \times 10^{-2} \text{ kg mol/m}^3)$$

Solving by trial and error,  $N_A = 1.004 \times 10^{-4} \text{ kg mol A/s} \cdot \text{m}^2$ . Then,  $x_{A2} = (1.004 \times 10^{-4}) / (5.63 \times 10^{-3} \times 4.062 \times 10^{-2}) = 0.4390$ .

In part (a) of Example 19.6-1, even though the rate of reaction is instantaneous, the flux  $N_A$  is diffusion-controlled. As the reaction rate slows, the flux  $N_A$  is also decreased.

*5. Diffusion and homogeneous reaction in a phase.* Equation (19.6-6) was derived for the case of chemical reaction of  $A$  at the boundary on a catalyst surface. In some cases, component  $A$  undergoes an irreversible chemical reaction in the homogeneous phase  $B$

while diffusing, as follows:  $A \rightarrow C$ .

Assume that component  $A$  is very dilute in phase  $B$ , which can be a gas or a liquid. Then, at steady state the equation for diffusion of  $A$  is as follows, where the bulk-flow term is dropped:

$$N_A z = -D_A B \frac{dc_A}{dz} + 0 \quad (19.6-10)$$

Writing a material balance on  $A$  shown in Fig. 19.6-2 for the  $\Delta z$  element for steady state,

$$+(\text{rate of generation of } A) = (\text{rate of } A \text{ out}) + (\text{rate of accumulation}) \quad (19.6-11)$$

The first-order reaction rate of  $A$  per  $\text{m}^3$  volume is

$$\text{rate of generation} = k_1' c_A \quad (19.6-12)$$

where  $k'$  is the reaction velocity constant



in s-1. Substituting into Eq. (19.6-11) for a cross-sectional area of 1 m<sup>2</sup> with the rate of accumulation being 0 at steady state,

$$N_A z|_z(1) - k' c_A(1)(\Delta z) = N_A z|_z + \Delta z(1) + 0 \quad (19.6-13)$$

Next, we divide through by  $\Delta z$  and let  $\Delta z$  approach zero:

$$-dN_A/dz = k' c_A \quad (19.6-14)$$

Substituting Eq. (19.6-10) into (19.6-14),

$$d^2 c_A / dz^2 = k' D_A B c_A \quad (19.6-15)$$

The boundary conditions are  $c_A = c_{A1}$  for  $z = 0$  and  $c_A = c_{A2}$  for  $z = L$ . Solving,

$$c_A = c_{A2} \sinh(k' D_A B z) + c_{A1} \sinh[k$$

$$D_{AB}(L-z) \left| \sinh(k'D_{AB}L) \right| (19.6-16)$$

This equation can be used at steady state to calculate  $c_A$  at any  $z$  and can be used for reactions in gases, liquids, or even solids where the solute  $A$  is dilute.

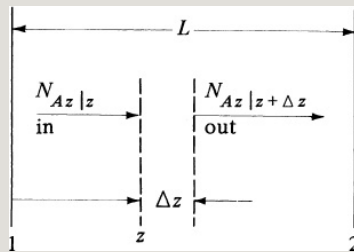


Figure 19.6-2. *Homogeneous chemical reaction and diffusion in a fluid.*

As an alternative derivation of Eq. (19.6-15), we can use Eq. (18.4-18) for constant  $\rho$  and  $D_{AB}$ :

$$\frac{\partial c_A}{\partial t} + (v \cdot \nabla c_A) - D_{AB} \nabla^2 c_A = R_A \quad (18.4-18)$$

We set the first term  $\partial c_A / \partial t = 0$  for

steady state. Since we are assuming dilute solutions and neglecting the bulk flow term,  $v = 0$ , we make the second term in Eq. (18.4-17) zero. For first-order reaction of  $A$  where  $A$  disappears,  $R_A = -k' c_A$  kg mol  $A$  generated/s  $\cdot$  m<sup>3</sup>. Writing the diffusion term  $-D_{AB}\nabla^2 c_A$  for the  $z$  direction only, we obtain

$$D_{AB} \frac{d^2 c_A}{dz^2} = k' c_A \quad (19.6-17)$$

which is, of course, identical to Eq. (19.6-15).

## 19.7 Numerical Methods for Steady-State Molecular Diffusion in two Dimensions

### 19.7A Derivation of Equations for Numerical Methods

*1. Derivation of methods for steady state.* In Fig. 19.7-1, a two-dimensional solid shown with unit

thickness is divided into squares. The numerical methods for steady-state molecular diffusion are very similar to those for steady-state heat conduction discussed in Section 13.5. Hence, only a brief summary will be given here. The solid inside of a square is imagined to be concentrated at the center of the square at  $c_{n,m}$  and is called a “node,” which is connected to adjacent nodes by connecting rods through which the mass diffuses.

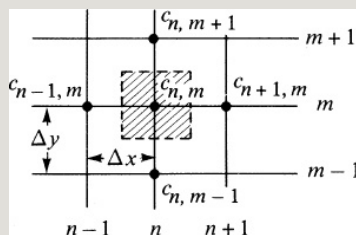


Figure 19.7-1. Concentrations and spacing of nodes for two-dimensional steady-state molecular diffusion.

A total mass balance is made at steady

state by stating that the sum of the molecular diffusion to the shaded area for unit thickness must equal zero:

$$DAB\Delta y\Delta x(c_{n-1,m}-c_{n,m})+DAB\Delta y\Delta x(c_{n+1,m}-c_{n,m})+DAB\Delta x\Delta y(c_{n,m}+1-c_{n,m})+DAB\Delta x\Delta y(c_{n,m}+1-c_{n,m})=0 \quad (19.7-1)$$

where  $c_{n,m}$  is the concentration of A at node  $n,m$  in kg mol A/m<sup>3</sup>. Setting  $\Delta x = \Delta y$ , and rearranging,

$$c_{n,m+1}+c_{n,m-1}+c_{n+1,m}+c_{n-1,m}-4c_{n,m}=0 \quad (19.7-2)$$

*2. Iteration method of numerical solution.* In order to solve Eq. (19.7-2), a separate equation is written for each unknown point giving  $N$  linear algebraic equations for  $N$  unknown points. For a

hand calculation using a modest number of nodes, the iteration method can be used to solve the equations, where the right-hand side of Eq. (19.7-2) is set equal to a residual  $N^{-n,m}$ :

$$c_{n,m+1} + c_{n,m-1} + c_{n+1,m} + c_{n-1,m} - 4c_{n,m} = N^{-n,m} \quad (19.7-3)$$

Setting the equation equal to zero,  $N^{-n,m} = 0$  for steady state and  $c_{n,m}$  is calculated by

$$c_{n,m} = \frac{c_{n,m+1} + c_{n,m-1} + c_{n+1,m} + c_{n-1,m}}{4} \quad (19.7-4)$$

Equations (19.7-3) and (19.7-4) are the final equations to be used to calculate all the concentrations at steady state.

Example 13.5-1 for steady-state heat conduction illustrates the detailed steps

for the iteration method, which are identical to those for steady-state diffusion.

Once the concentrations have been calculated, the flux can be calculated for each element as follows. Referring to Fig. 19.7-1, the flux for the node or element  $c_{n,m}$  to  $c_{n,m-1}$  is ( $\Delta x = \Delta y$ )

$$N = ADAB\Delta y(c_{n,m} - c_{n,m-1}) = [(\Delta x) \\ (1)]DAB\Delta y(c_{n,m} - c_{n,m-1}) \\ (19.7-5) N = N = DAB(c_{n,m} - c_{n,m-1})$$

where the area  $A$  is  $\Delta x$  times 1 m deep and  $N$  is kg mol  $A/s$ . Equations are written for the other appropriate elements and the sum of the fluxes calculated. This numerical method is well suited for use with a computer spreadsheet.

## 19.7B Equations for Special Boundary Conditions for Numerical Method

### 1. Equations for boundary

*conditions.* When one of the nodal points  $c_{n,m}$  is at a boundary where convective mass transfer is occurring to a constant concentration  $c_q$  in the bulk fluid shown in Fig. 19.7-2a, a different equation must be derived. Making a mass balance on the node  $n, m$ , where mass in = mass out at steady state,

$$\begin{aligned} & DAB\Delta y\Delta x(c_{n-1,m}- \\ & c_{n,m}) + DAB\Delta x^2\Delta y(c_{n,m+1}- \\ & c_{n,m}) + DAB\Delta x^2\Delta y(c_{n,m-1}- \\ & c_{n,m}) = k_c\Delta y(c_{n,m}-c_\infty) \end{aligned} \quad (19.7-6)$$

where  $k_c$  is the convective mass-transfer coefficient in m/s defined by Eq. (18.3-1).



Setting  $\Delta x = \Delta y$ , rearranging, and setting the resultant equation equal to  $N_{n,m}^-$ , the residual, the following results:

1. For convection at a boundary (Fig. 19.7-2a),

$$k_c \Delta x D_{AB} C_{\infty} + \frac{1}{2} (C_{n-1,m} + C_{n,m} + 1 + C_{n,m-1}) - C_{n,m} (k_c \Delta x D_{AB} + 2) = N_{n,m}^- \quad (19.7-7)$$

This equation is similar to Eq. (13.5-16) for heat conduction and convection, with  $k_c \Delta x / D_{AB}$  being used in place of  $h \Delta x / k$ . Similarly, Eqs. (19.7-8)–(19.7-10) have been derived for the other boundary conditions shown in Fig. 19.7-2.

2. For an insulated boundary (Fig. 19.7-2b),

$$12(c_{n,m} + 1 + c_{n,m-1}) + c_{n-1,m} - 2c_{n,m} = N_{n,m}^- \quad (19.7-8)$$

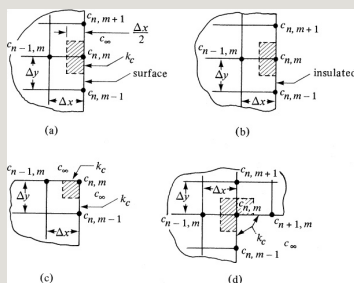


Figure 19.7-2. Different boundary conditions for steady-state diffusion: (a) convection at a boundary, (b) insulated boundary, (c) exterior corner with convective boundary, (d) interior corner with convective boundary.

**3.** For an exterior corner with convection at the boundary (Fig. 19.7-2c),

$$k_c \Delta x D A B c_{\infty} + 12(c_{n-1,m} + c_{n,m-1}) - c_{n,m}(k_c \Delta x D A B + 1) = N_{n,m}^- \quad (19.7-9)$$

**4.** For an interior corner with convection at the boundary (Fig. 19.7-2d),

$$k_c \Delta x D A B c_{\infty} + c_{n-1,m} + c_{n,m}$$

$$+1+12(c_{n+1,m}+c_{n,m-1})-c_{n,m}(k_c \Delta x D_{AB}+3)=N_{n,m}^{-}(19.7-10)$$

2. *Boundary conditions with a distribution coefficient.* When Eq. (19.7-7) was derived, the distribution coefficient  $K$  between the liquid and the solid at the surface interface was 1.0. The distribution coefficient, as shown in Fig. 19.7-3, is defined as

$$K=c_{n,m}L/c_{n,m}(19.7-11)$$

where  $c_{n,m}L$  is the concentration in the liquid adjacent to the surface and  $c_{n,m}$  is the concentration in the solid adjacent to the surface. Then, in deriving Eq. (19.7-6), the right-hand side  $k_c \Delta y(c_{n,m} - c_{\infty})$  becomes

$$k_c \Delta y(c_{n,m}L - c_{\infty})(19.7-12)$$

where  $c_{\infty}$  is the concentration in the bulk fluid. Substituting  $Kc_{n,m}$  for  $c_{n,m}L$  from Eq. (19.7-11) into Eq. (19.7-12) and multiplying and dividing by  $K$ ,

$$Kk_c \Delta y (Kc_{n,m} - c_{\infty}) = Kk_c \Delta y (c_{n,m} - c_{\infty}) \quad (19.7-13)$$

Hence, whenever  $k_c$  appears as in Eq. (19.7-7),  $Kk_c$  should be substituted, and when  $c_{\infty}$  appears,  $c_{\infty}/K$  should be used. Then, Eq. (19.7-7) becomes as follows:

1. For convection at a boundary (Fig. 19.7-2a),

$$(Kk_c \Delta x D_{AB}) c_{\infty} + \frac{1}{2} (c_{n-1,m} + c_{n,m+1} + c_{n,m-1}) - c_{n,m} (Kk_c \Delta x D_{AB} + 2) = N_{n,m}^- \quad (19.7-14)$$

Equations (19.7-9) and (19.7-10) can be rewritten in a similar manner as follows:

2. For an exterior corner with convection at the boundary (Fig. 19.7-2c),

$$(Kk_c\Delta x DAB)c_\infty + K + \frac{1}{2}(c_{n-1,m} + c_{n,m-1}) - c_{n,m}(Kk_c\Delta x DAB + 1) = N_{n,m}^- \quad (19.7-15)$$

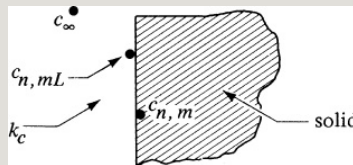


Figure 19.7-3. *Interface concentrations for convective mass transfer at a solid surface and an equilibrium distribution coefficient  $K = c_{n,mL}/c_{n,m}$ .*

3. For an interior corner with convection at the boundary (Fig. 19.7-2d),

$$(Kk_c\Delta x DAB)c_\infty + K + c_{n-1,m} + c_{n,m} + 1 + \frac{1}{2}(c_{n+1,m} + c_{n,m-1}) - c_{n,m}(Kk_c\Delta x DAB + 3) = N_{n,m}^- \quad (19.7-16)$$

### EXAMPLE 19.7-1. Numerical Method for Convection and Steady-State Diffusion

For the two-dimensional hollow solid chamber shown in Fig. 19.7-4, determine the concentrations at the nodes as shown at steady state. At the inside surfaces, the concentrations remain constant at  $6.00 \times 10^{-3} \text{ kg mol/m}^3$ . At the outside surfaces, the convection coefficient  $k_c = 2 \times 10^{-7} \text{ m/s}$  and  $c_\infty = 2.00 \times 10^{-3} \text{ kg mol/m}^3$ . The diffusivity in the solid is  $D_{AB} = 1.0 \times 10^{-9} \text{ m}^2/\text{s}$ . The grid size is  $\Delta x = \Delta y = 0.005 \text{ m}$ . Also, determine the diffusion rates per 1.0 m depth. The distribution coefficient  $K = 1.0$ .

**Solution:** To simplify the calculations, all the concentrations will be multiplied by  $10^3$ . Since the chamber is symmetrical, we do the calculations on the 18 shaded portion shown. The fixed known values are  $c_{1,3} = 6.00$ ,  $c_{1,4} = 6.00$ , and  $c_\infty = 2.00$ . Because of symmetry,  $c_{1,2} = c_{2,3}$ ,  $c_{2,5} = c_{2,3}$ ,  $c_{2,1} = c_{3,2}$ , and  $c_{3,3} = c_{3,5}$ . To speed up the calculations, we will make estimates of the unknown concentrations as follows:  $c_{2,2} = 3.80$ ,  $c_{2,3} = 4.20$ ,  $c_{2,4} = 4.40$ ,  $c_{3,1} = 2.50$ ,  $c_{3,2} = 2.70$ ,  $c_{3,3} = 3.00$ , and  $c_{3,4} = 3.20$ .

For the interior points  $c_{2,2}$ ,  $c_{2,3}$ , and  $c_{2,4}$ , we use Eqs. (19.7-3) and (19.7-4); for the corner convection point  $c_{3,1}$ , we use Eq. (19.7-9); and for the other convection points  $c_{3,2}$ ,  $c_{3,3}$ ,  $c_{3,4}$ , we use Eq. (19.7-7). The term  $k_c \Delta x / D_{AB} = (2 \times 10^{-7})(0.005) / (1.0 \times 10^{-9}) = 1.00$ .

*First approximation.* Starting with  $c_{2,2}$ , we use Eq. (19.7-3) and calculate the residual  $N_{2,2}$ :

$$c_{1,2} + c_{3,2} + c_{2,1} + c_{2,3} - 4c_{2,2} = N_{2,2} = 2.40 + 2.70 + 2.70 + 4.20 - 4(3.80) = -1.40$$

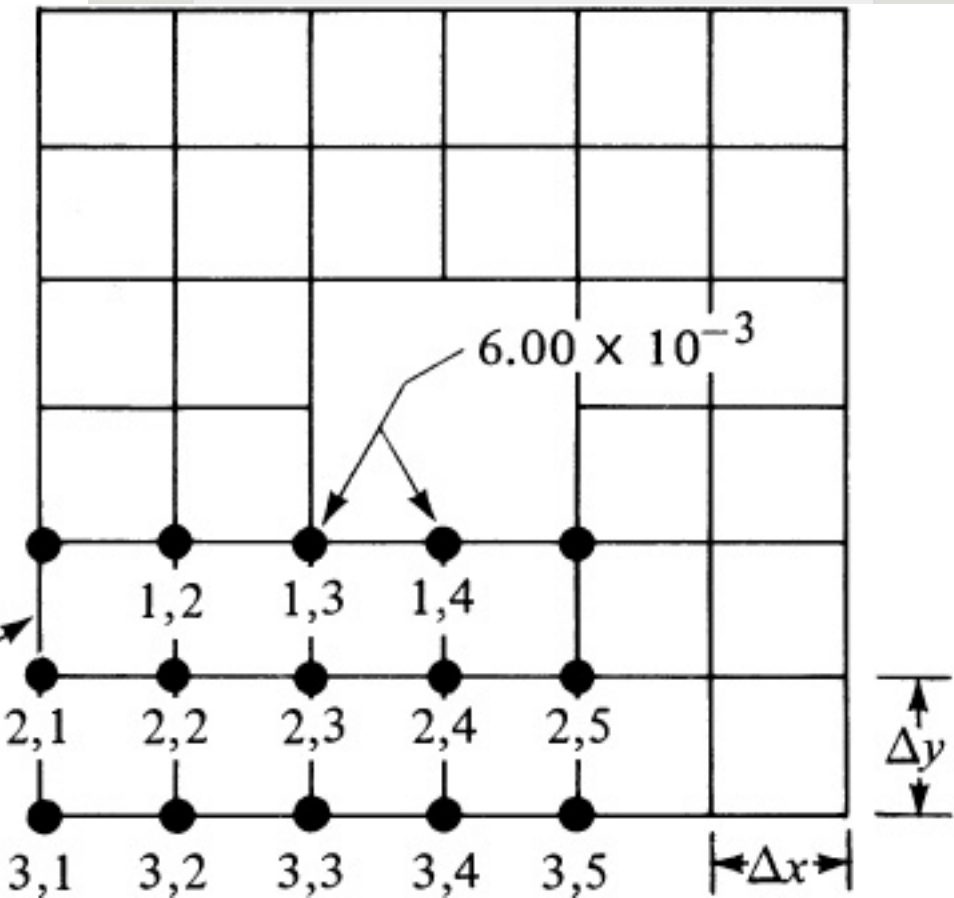


Figure 19.7-4. Concentrations for a hollow chamber for Example 19.7-1.

Hence,  $c_{2,2}$  is not at steady state. Next, we set  $N_{2,2}$  equal to zero and calculate a new value of  $c_{2,2}$  from Eq. (19.7-4):

$$c_{2,2} = c_{1,2} + c_{3,2} + c_{2,1} + c_{2,3} = 4.20 + 2.70 + 2.70 + 4.20 = 3.45$$

This new value of  $c_{2,2}$  replaces the old value.

For  $c_{2,3}$ ,

$$4 + c_{1,3} + c_{3,3} - 4c_{2,3} = N_{2,3} = 3.45 + 4.40 + 6.00 + 3.00 - 4(4.20) = 0.05$$

For  $c_{2,4}$ ,

$$5 + c_{1,4} + c_{3,4} - 4c_{2,4} = N_{2,4} = 4.21 + 4.21 + 6.00 + 3.20 - 4(4.40) = 0.02$$

For  $c_{3,1}$ , we use Eq. (19.7-9):

$$(1.0)c_{\infty} + 12(c_{2,1} + c_{3,2}) - (1.0 + 1)c_{3,1} = N^3, 1(1.0)2.00 + 12(2.70 + 2.70) - 2.0(2.50) = -0.30$$

Setting Eq. (19.7-9) equal to zero and solving for  $c_{3,1}$ ,

$$(1.0)2.00 + 12(2.70 + 2.70) - (2.0)c_{3,1} = 0 \quad c_{3,1} = 2.35$$

For  $c_{3,2}$ , we use Eq. (19.7-7):

$$(1.0)c_{\infty} + 12(2 \times c_{2,2} + c_{3,1} + c_{3,3}) - (1.0 + 2)c_{3,2} = N^3, 2(1.0)2.00 + 12(2 \times 3.45 + 2.35 + 3.00) - (3.0)2.70 = 0.03(1.0)2.00 + 12(2 \times 3.45 + 2.35 + 3.00) - (3.0)c_{3,2} = 0 \quad c_{3,2} = 2.71$$

For  $c_{3,3}$ ,

$$(1.0)c_{\infty} + 12(2 \times c_{2,3} + c_{3,2} + c_{3,4}) - (3.0)c_{3,3} = N^3, 3(1.0)2.00 + 12(2 \times 4.21 + 2.71 + 3.20) - (3.0)3.00 = 0.17(1.0)2.00 + 12(2 \times 4.21 + 2.71 + 3.20) - (3.0)c_{3,3} = 0 \quad c_{3,3} = 3.06$$

For  $c_{3,4}$ ,

$$(1.0)c_{\infty} + 12(2 \times c_{2,4} + c_{3,3} + c_{3,5}) - (3.0)c_{3,4} = N^3, 4(1.0)2.00 + 12(2 \times 4.41 + 3.06 + 3.06) - 3.0(3.20) = -0.13(1.0)2.00 + 12(2 \times 4.41 + 3.06 + 3.06) - (3.0)c_{3,4} = 0 \quad c_{3,4} = 3.16$$

Having completed one sweep across the grid map, we can perform a second approximation using the new values calculated, starting with  $c_{2,2}$  or any other node. We continue until all the residuals are as small as desired. The final values after three approximations are  $c_{2,2} = 3.47$ ,  $c_{2,3} = 4.24$ ,  $c_{2,4} = 4.41$ ,  $c_{3,1} = 2.36$ ,  $c_{3,2} = 2.72$ ,  $c_{3,3} = 3.06$ , and  $c_{3,4} = 3.16$ .

To calculate the diffusion rates, we first calculate the total convective diffusion rate, leaving the bottom surface at nodes  $c_{3,1}$ ,  $c_{3,2}$ ,  $c_{3,3}$ , and  $c_{3,4}$  for 1.0 m depth:

$$N = k_c(\Delta x \cdot 1)[c_{3,1} - c_{\infty} + (c_{3,2} - c_{\infty}) + (c_{3,3} - c_{\infty}) + c_{3,4} - c_{\infty}] \\ (2 \times 10^{-7})(0.005 \times 1) \\ [2.36 - 2.00 + (2.72 - 2.00) + (3.06 - 2.00) + 3.16 - 2.2] \times 10^{-3} N = 2.540 \times 10^{-12} \text{ kgmols}$$

Note that the first and fourth paths include only one-half of a surface. Next, we calculate the total diffusion rate in the solid entering the top surface inside, using an equation



similar to Eq. (19.7-5):

$$N = DAB(\Delta x \cdot 1) \Delta y [(c_{1,3} - c_{2,3}) + c_{1,4} - c_{2,4}] (1.0 \times 10^{-9}) \\ (0.005 \times 1) 0.005 [(6.00 - 4.24) + 6.00 - 4.412] \times 10^{-3} N = 2.55 \times 10^{-12} \text{ kgmols}$$

At steady state, the diffusion rate leaving by convection should equal that entering by diffusion. These results indicate a reasonable check. Using smaller grids would give even more accuracy. Note that the results for the diffusion rate should be multiplied by 8.0 for the whole chamber.

## 19.8 Chapter Summary

### Fick's Law of Diffusion

$$J_{Az} = -DABdcAdz \quad (18.1-3)$$

### Two Classic Cases of Diffusion with Gases

Equimolar counterdiffusion:

$$N_A = J_{Az} = DAB(p_{A1} - p_{A2})RT(z_2 - z_1) \\ (18.1-13)$$

A diffusing through stagnant,  
nondiffusing B:

$$N_A = DABPRT(z_2 - z_1) \ln \frac{P - p_{A2}}{P - p_{A1}} \quad (19.1-11)$$

## Two Classic Cases of Diffusion with Liquids

Equimolar counterdiffusion:

$$N_A = D_{AB}(c_{A1} - c_{A2})z_2 - z_1 \quad (19.3-2)$$

A diffusing through stagnant,  
nondiffusing B:

$$N_A = D_{AB}c_{avg}(z_2 - z_1) \ln \frac{1 - x_{A2}}{1 - x_{A1}}$$

Diffusion fluxes through a varying  
cross-sectional area (sphere):

$$N_A 4\pi(r_1 - r_2) = \frac{D_{AB}P}{RT} \ln \frac{p_{A2}P - p_{A1}}{p_{A1}P - p_{A2}} \quad (19.1-22)$$

## Multicomponent Diffusion Coefficients for Gases

$$D_{Am} = \frac{x_B'}{D_{AB}} + \frac{x_C'}{D_{AC}} + \dots \quad (19.1-30)$$

where  $x_B' = \text{mol B/mol inerts} = x_B/(1 - x_A)$ ,  $x_C' = x_C/(1 - x_A)$ , ...

## Permeability Equations for Diffusion in Solids

$$N_A = D_{AB} S (p_{A1} - p_{A2}) \frac{22.414 (z_2 - z_1)}{PM (p_{A1} - p_{A2})} \frac{1}{22.414 (z_2 - z_1)} \text{ kg mol/s} \cdot \text{m}^2 \quad (19.3-8)$$

## Diffusion of Liquids and Gases in Porous Solids

$$N_A = \epsilon D_{AB} (c_{A1} - c_{A2}) \tau (z_2 - z_1) = \epsilon D_{AB} (p_{A1} - p_{A2}) \frac{\tau}{RT} (z_2 - z_1) \quad (19.3-15)$$

## Knudsen Diffusion of Gases (Diffusion in Small Pores)

Where the Knudsen number  $N_{Kn}$  defined as

$$N_{Kn} = \lambda / 2r \quad (19.4-6)$$

If it is  $\geq 10/1$ , the diffusion is primarily Knudsen.

$$D_{KA} = 97.0 r \sqrt{T} \quad (19.4-3)$$

where  $M_A$  is the molecular weight of A in kg/kg mol and  $T$  is the temperature in K.

### Transition Diffusion of Gases (Diffusion in Small Pores)

Where  $10 > N_{Kn} > 0.01$ , the diffusion coefficient is:

$$D_{NA} = \frac{1}{\frac{1}{D_{AB}} + \frac{1}{D_{KA}}} \quad (19.4-11)$$

### Diffusion and Chemical Reaction at a Boundary

Instantaneous surface reaction:

$$N_A = c D_{AB} \delta \ln \frac{1+x_A}{1+x_{A2}} \quad (19.6-6)$$

Slow surface reaction:

$$N_A = c D_{AB} \delta \ln \frac{1+x_A}{1+x_{A2} + N_A/k_c} \quad (19.6-9)$$

### Problems

**19.1-1. *Equimolar Counterdiffusion of a Binary Gas Mixture.*** Helium and nitrogen gas are contained in a conduit 5 mm in diameter and 0.1 m long at 298 K with a uniform constant pressure of 1.0 atm abs. The partial pressure of He at one end of the tube is 0.060 atm and at the other end it is 0.020 atm. The diffusivity can be obtained from Table 18.2-1. Calculate the following for steady-state equimolar counterdiffusion:

- Flux of He in  $\text{kg mol/s} \cdot \text{m}^2$  and  $\text{g mol/s} \cdot \text{cm}^2$
- Flux of  $\text{N}_2$
- Partial pressure of He at a point 0.05 m from either end

**19.1-2. *Equimolar Counterdiffusion of  $\text{NH}_3$  and  $\text{N}_2$  at Steady State.*** Ammonia gas (A) and nitrogen gas (B) are diffusing in counterdiffusion through a

straight glass tube 2.0 ft (0.610 m) long with an inside diameter of 0.080 ft (24.4 mm) at 298 K and 101.32 kPa. Both ends of the tube are connected to large mixed chambers at 101.32 kPa. The partial pressure of  $\text{NH}_3$  is constant at 20.0 kPa in one chamber and at 6.666 kPa in the other. The diffusivity at 298 K and 101.32 kPa is  $2.30 \times 10^{-5} \text{ m}^2/\text{s}$ .

- Calculate the diffusion of  $\text{NH}_3$  in lb mol/h and kg mol/s.
- Calculate the diffusion of  $\text{N}_2$ .
- Calculate the partial pressures at a point 1.0 ft (0.305 m) in the tube and plot  $p_A$ ,  $p_B$ , and  $P$  versus distance  $z$ .

**Ans.** (a) Diffusion of  $\text{NH}_3 = 7.52 \times 10^{-7}$  lb mol A/h,  $9.48 \times 10^{-11}$  kg mol A/s; (c)  $p_A = 1.333 \times 10^4$  Pa

### ***19.1-3. Diffusion of A Through Stagnant B and Effect of a Type of***

**Boundary on Flux.** Ammonia gas is diffusing through  $N_2$  under steady-state conditions with  $N_2$  nondiffusing since it is insoluble in one boundary. The total pressure is  $1.013 \times 10^5$  Pa and the temperature is 298 K. The partial pressure of  $NH_3$  at one point is  $1.333 \times 10^4$  Pa, and at the other point 20 mm away it is  $6.666 \times 10^3$  Pa. The  $D_{AB}$  for the mixture at  $1.013 \times 10^5$  Pa and 298 K is  $2.30 \times 10^{-5} m^2/s$ .

- Calculate the flux of  $NH_3$  in  $kg \text{ mol/s} \cdot m^2$ .
- Do the same as (a) but assume that  $N_2$  also diffuses; that is, both boundaries are permeable to both gases and the flux is equimolar counterdiffusion. In which case is the flux greater?

**Ans.** (a)  $N_A = 3.44 \times 10^{-6} \text{ kg mol/s} \cdot m^2$

**19.1-4. Diffusion of Methane Through Nondiffusing Helium.** Methane gas is diffusing in a straight tube 0.1 m long

containing helium at 298 K and a total pressure of  $1.01325 \times 10^5$  Pa. The partial pressure of  $\text{CH}_4$  is  $1.400 \times 10^4$  Pa at one end and  $1.333 \times 10^3$  Pa at the other end. Helium is insoluble in one boundary, and hence is nondiffusing or stagnant. The diffusivity is given in Table 18.2-1. Calculate the flux of methane in  $\text{kg mol/s} \cdot \text{m}^2$  at steady state.

**19.1-5. *Mass Transfer from a Naphthalene Sphere to Air.*** Mass transfer is occurring from a naphthalene sphere having a radius of 10 mm. The sphere is in a large volume of still air at  $52.6^\circ\text{C}$  and 1 atm abs pressure. The vapor pressure of naphthalene at  $52.6^\circ\text{C}$  is 1.0 mmHg. The diffusivity of naphthalene in air at  $0^\circ\text{C}$  is  $5.16 \times 10^{-6} \text{m}^2/\text{s}$ . Calculate the rate of evaporation of naphthalene from the surface in kg



mol/s · m<sup>2</sup>. [*Note*: The diffusivity can be corrected for temperature using the temperature-correction factor from the Fuller et al. (F1) equation (18.2-8).]

**19.1-6. *Estimation of Diffusivity of a Binary Gas.*** For a mixture of ethanol (CH<sub>3</sub>CH<sub>2</sub>OH) vapor and methane (CH<sub>4</sub>), predict the diffusivity using the method of Fuller et al. (F1)

- At  $1.0132 \times 10^5$  Pa and 298 and 373 K
- At  $2.0265 \times 10^5$  Pa and 298 K

**Ans.** (a)  $D_{AB} = 1.43 \times 10^{-5} \text{ m}^2/\text{s}$  (298K)

**19.1-7. *Diffusion Flux and Effect of Temperature and Pressure.*** Equimolar counterdiffusion is occurring at steady state in a tube 0.11 m long containing N<sub>2</sub> and CO gases at a total pressure of 1.0 atm abs. The partial pressure of N<sub>2</sub>

is 80 mmHg at one end and 10 mm at the other end. Predict the  $D_{AB}$  by the method of Fuller et al.

- Calculate the flux in  $\text{kg mol/s} \cdot \text{m}^2$  at 298 K for  $\text{N}_2$ .
- Repeat at 473 K. Does the flux increase?
- Repeat at 298 K but for a total pressure of 3.0 atm abs. The partial pressure of  $\text{N}_2$  remains at 80 and 10 mmHg, as in part (a). Does the flux change?

**Ans.** (a)  $D_{AB} = 2.05 \times 10^{-5} \text{m}^2/\text{s}$ ,  $N_A = 7.02 \times 10^{-7} \text{ kg mol/s} \cdot \text{m}^2$ ; (b)  $N_A = 0.92 \times 10^{-7} \text{ kg mol/s} \cdot \text{m}^2$ ; (c)  $N_A = 2.34 \times 10^{-7} \text{ kg mol/s} \cdot \text{m}^2$

**19.1-8. *Evaporation Losses of Water in an Irrigation Ditch.*** Water at  $25^\circ\text{C}$  is flowing in a covered irrigation ditch below ground. Every 100 ft, there is a vent line with a 1.0 in. inside diameter and it is 1.0 ft long to the outside atmosphere at  $25^\circ\text{C}$ . There are 10 vents

in the 1000-ft ditch. The outside air can be assumed to be dry. Calculate the total evaporation loss of water in  $\text{lb}_m/\text{d}$ .

Assume that the partial pressure of water vapor at the surface of the water is the vapor pressure, 23.76 mmHg at  $25^\circ\text{C}$ . Use the diffusivity from Table 18.2-1.

**19.1-9. *Time Necessary to Completely Evaporate a Sphere.*** A drop of liquid toluene is kept at a uniform temperature of  $25.9^\circ\text{C}$  and is suspended in air by a fine wire. The initial radius  $r_1 = 2.00$  mm. The vapor pressure of toluene at  $25.9^\circ\text{C}$  is  $P_{A1} = 3.84 \text{ kPa}$  and the density of liquid toluene is  $866 \text{ kg}/\text{m}^3$ .

- Derive Eq. (19.1-25) to predict the time  $t_F$  for the drop to evaporate completely in a large volume of still air. Show all steps.
- Calculate the time in seconds for complete

evaporation.

**Ans.** (b)  $t_F = 1388s$

**19.1-10. Diffusion in a Nonuniform Cross-Sectional Area.** The gas ammonia ( $A$ ) is diffusing at steady state through  $N_2$  ( $B$ ) by equimolar counterdiffusion in a conduit 1.22 m long at  $25^\circ\text{C}$  and a total pressure of 101.32 kPa abs. The partial pressure of ammonia at the left end is 25.33 kPa and at the right end 5.066 kPa. The cross section of the conduit is in the shape of an equilateral triangle, the length of each side of the triangle being 0.0610 m at the left end and tapering uniformly to 0.0305 m at the right end. Calculate the molar flux of ammonia. The diffusivity is  $D_{AB} = 0.230 \times 10^{-4}\text{m}^2/\text{s}$ .

**19.1-11. Sum of Molar Fluxes.** Prove

the following equation using the definitions in Table 18.4-1:

$$N_A + N_B = c v_M$$

**19.1-12. *Proof of Derived Relation.***

Using the definitions from Table 18.4-1, prove the following:

$$j_A = n_A - w_A(n_A + n_B)$$

**19.1-13. *Different Forms of Fick's Law.*** Using Eq. (1), prove Eq. (2):

$$j_A = -\rho D_{AB} dw_A/dz \quad (1)$$

$$j_A = -c^2 \rho M_A M_B D_{AB} dx_A/dz \quad (2)$$

(*Hint:* First relate  $w_A$  to  $x_A$ . Then, differentiate this equation to relate  $dw_A$  and  $dx_A$ . Finally, use  $M = x_A M_A + x_B M_B$  to simplify.)

### 19.1-14. *Other Form of Fick's Law.*

Show that the following form of Fick's law is valid:

$$c(v_A - v_B) = -c D_{AB} \frac{dx_A}{dx} \frac{dz}{dz}$$

(*Hint:* Start with  $N_A = J_A^* + c_A v_M$ .

Substitute the expression for  $J_A^*$  from Table 18.4-1 and simplify.)

**19.1-15. *Different Form of the Equation of Continuity.*** Starting with Eq. (18.4-12),

$$\frac{\partial \rho_A}{\partial t} + (\nabla \cdot \mathbf{n}_A) = r_A \quad (18.4-12)$$

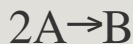
convert this to the following for constant  $\rho$ :

$$\frac{\partial \rho_A}{\partial t} + (v \cdot \nabla \rho_A) - (\nabla \cdot D_{AB} \nabla \rho_A) = r_A \quad (1)$$

[*Hint:* From Table 18.4-1, substitute  $\mathbf{n}_A$

$= \mathbf{j}_A + \rho_A \mathbf{v}$  into Eq. (18.4-12). Note that  $(\nabla \cdot \mathbf{v}) = 0$  for constant  $\rho$ . Then, substitute Fick's law in terms of  $\mathbf{j}_A$ .]

**19.1-16. *Diffusion and Reaction at a Surface.*** Gas  $A$  is diffusing from a gas stream at point 1 to a catalyst surface at point 2 and reacts instantaneously and irreversibly as follows:



Gas  $B$  diffuses back to the gas stream. Derive the final equation for  $N_A$  at constant pressure  $P$  and steady state in terms of partial pressures.

$$\text{Ans. } N_A = \frac{2D_{AB}P}{RT(z_2 - z_1)} \ln \frac{1 - p_{A2}/2P}{1 - p_{A1}/2P}$$

**19.1-17. *Unsteady-State Diffusion and Reaction.*** Solute  $A$  is diffusing at

unsteady state into a semi-infinite medium of pure  $B$  and undergoes a first-order reaction with  $B$ . Solute  $A$  is dilute. Calculate the concentration  $c_A$  at points  $z = 0, 4$ , and  $10$  mm from the surface for  $t = 1 \times 10^5$  s. Physical property data are  $D_{AB} = 1 \times 10^{-9} \text{ m}^2/\text{s}$ ,  $k' = 1 \times 10^{-4} \text{ s}^{-1}$ ,  $c_{A0} = 1.0 \text{ kg mol/m}^3$ . Also calculate the kg mol absorbed/ $\text{m}^2$ .

**19.1-18. Multicomponent Diffusion.** At a total pressure of  $202.6 \text{ kPa}$  and  $358 \text{ K}$ , ammonia gas ( $A$ ) is diffusing at steady state through an inert, nondiffusing mixture of nitrogen ( $B$ ) and hydrogen ( $C$ ). The mole fractions at  $z_1 = 0$  are  $x_{A1} = 0.8$ ,  $x_{B1} = 0.15$ , and  $x_{C1} = 0.05$ ; and at  $z_2 = 4.0 \text{ mm}$ ,  $x_{A2} = 0.2$ ,  $x_{B2} = 0.6$ , and  $x_{C2} = 0.2$ . The diffusivities at  $358 \text{ K}$  and  $101.3 \text{ kPa}$  are  $D_{AB} = 3.28 \times 10^{-5} \text{ m}^2/\text{s}$  and  $D_{AC} = 1.093 \times 10^{-4} \text{ m}^2/\text{s}$ . Calculate



the flux of ammonia.

$$\text{Ans. } N_A = 4.69 \times 10^{-4} \text{ kg mol A/s} \cdot \text{m}^2$$

**19.1-19. Diffusion in Liquid Metals and Variable Diffusivity.** The diffusion of tin (A) in liquid lead (B) at 510°C was carried out by using a 10.0-mm-long capillary tube and maintaining the mole fraction of tin at  $x_{A1}$  at the left end and  $x_{A2}$  at the right end of the tube. In the range of concentrations of  $0.2 \leq x_A \leq 0.4$ , the diffusivity of tin in lead has been found to be a linear function of  $x_A$  (S4):

$$D_{AB} = A + Bx_A$$

where  $A$  and  $B$  are constants and  $D_{AB}$  is in  $\text{m}^2/\text{s}$ .

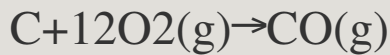
- Assuming the molar density to be constant at  $c = c_A$

+  $c_B = c_{av}$ , derive the final integrated equation for the flux  $N_A$ , assuming steady state and that A diffuses through stagnant B.

- For this experiment,  $A = 4.8 \times 10^{-9}$ ,  $B = -6.5 \times 10^{-9}$ ,  $c_{av} = 50 \text{ kg mol/m}^3$ ,  $x_{A1} = 0.4$ , and  $x_{A2} = 0.2$ . Calculate  $N_A$ .

**Ans.** (b)  $N_A = 4.055 \times 10^{-6} \text{ kg mol A/s} \cdot \text{m}^2$

**19.1-20. Diffusion and Chemical Reaction of Molten Iron in Process Metallurgy.** In a steelmaking process using molten pig iron containing carbon, a spray of molten iron particles containing 4.0 wt % carbon falls through a pure-oxygen atmosphere. The carbon diffuses through the molten iron to the surface of the drop, where it is assumed that it reacts instantly at the surface because of the high temperature, as follows, according to a first-order reaction:



Calculate the maximum drop size allowable so that the final drop after a 2.0-s fall contains an average of 0.1 wt % carbon. Assume that the mass-transfer rate of gases at the surface is very great, so there is no outside resistance. Assume no internal circulation of the liquid. Hence, the decarburization rate is controlled by the rate of diffusion of carbon to the surface of the droplet. The diffusivity of carbon in iron is  $7.5 \times 10^{-9} \text{ m}^2/\text{s}$  (S7). (*Hint: Can Fig. 14.3-13 be used for this case?*)

**Ans.** radius = 0.217 mm

**19.1-21. *Effect of a Slow Reaction Rate on Diffusion.*** Gas A diffuses from point 1 to a catalyst surface at point 2, where

it reacts as follows:  $2A \rightarrow B$ . Gas  $B$  diffuses back a distance  $\delta$  to point 1.

- Derive the equation for  $N_A$  for a very fast reaction using mole fraction units  $x_{A1}$ , and so on.
- For  $D_{AB} = 0.2 \times 10^{-4} \text{ m}^2/\text{s}$ ,  $x_{A1} = 0.97$ ,  $P = 101.32 \text{ kPa}$ ,  $\delta = 1.30 \text{ mm}$ , and  $T = 298 \text{ K}$ , solve for  $N_A$ .
- Do the same as in part (a) but for a slow first-order reaction where  $k_1'$  is the reaction velocity constant.
- Calculate  $N_A$  and  $x_{A2}$  for part (c) where  $k_1' = 0.53 \times 10^{-2} \text{ m/s}$ .

**Ans.** (b)  $N_A = 8.35 \times 10^{-4} \text{ kg mol/s} \cdot \text{m}^2$

**19.1-22. Diffusion and Heterogeneous Reaction on a Surface.** In a tube of radius  $R$  m filled with a liquid, dilute component  $A$  is diffusing in the nonflowing liquid phase represented by

$$N_A = -D_{AB} \frac{dc_A}{dz}$$

where  $z$  is distance along the tube axis.

The inside wall of the tube exerts a catalytic effect and decomposes A so that the heterogeneous rate of decomposition on the wall in kg mol A/s is equal to  $k_c A A_w$ , where  $k$  is a first-order constant and  $A_w$  is the wall area in m<sup>2</sup>. Neglect any radial gradients (this means a uniform radial concentration).

Derive the differential equation for unsteady state for diffusion and reaction for this system. [*Hint*: First make a mass balance for A for a  $\Delta z$  length of tube as follows: rate of input (diffusion) + rate of generation (heterogeneous) = rate of output (diffusion) + rate of accumulation.]

$$\text{Ans. } \partial c_A \partial t = D_{AB} \partial^2 c_A \partial z^2 - 2k_r c_A$$

### 19.2-1. *Diffusion of A Through*

***Stagnant B in a Liquid.*** The solute HCl (A) is diffusing through a thin film of water (B) 2.0 mm thick at 283 K. The concentration of HCl at point 1 at one boundary of the film is 12.0 wt % HCl (density  $\rho_1 = 1060.7 \text{ kg/m}^3$ ), and at the other boundary at point 2 it is 6.0 wt % HCl ( $\rho_2 = 1030.3 \text{ kg/m}^3$ ). The diffusion coefficient of HCl in water is  $2.5 \times 10^{-9} \text{ m}^2/\text{s}$ . Assuming steady state and one boundary impermeable to water, calculate the flux of HCl in  $\text{kg mol/s} \cdot \text{m}^2$ .

**Ans.**  $N_A = 2.372 \times 10^{-6} \text{ kg mol/s} \cdot \text{m}^2$

***19.2-2. Diffusion of Ammonia in an Aqueous Solution.*** An ammonia (A)–water (B) solution at 278 K and 4.0 mm thick is in contact at one surface with an organic liquid at this interface. The

concentration of ammonia in the organic phase is held constant and is such that the equilibrium concentration of ammonia in the water at this surface is 2.0 wt % ammonia (density of aqueous solution 991.7 kg/m<sup>3</sup>) and the concentration of ammonia in water at the other end of the film 4.0 mm away is 10 wt % (density 961.7 kg/m<sup>3</sup>). Water and the organic are insoluble in each other. The diffusion coefficient of NH<sub>3</sub> in water is  $1.24 \times 10^{-9}$  m<sup>2</sup>/s.

- At steady state, calculate the flux  $N_A$  in kg mol/s · m<sup>2</sup>.
- Calculate the flux  $N_B$ . Explain.

### **19.2-3. Estimation of Liquid**

**Diffusivity.** It is desired to predict the diffusion coefficient of dilute acetic acid (CH<sub>3</sub>COOH) in water at 282.9 K and at 298 K using the Wilke–Chang method.

Compare the predicted values with the experimental values in Table 18.2-3.

**Ans.**  $D_{AB} = 0.897 \times 10^{-9} \text{ m}^2/\text{s}$  (282.9 K),  
 $D_{AB} = 1.396 \times 10^{-9} \text{ m}^2/\text{s}$  (288 K)

**19.2-4. Estimation of Diffusivity of Methanol in  $\text{H}_2\text{O}$ .** The diffusivity of dilute methanol in water has been determined experimentally to be  $1.26 \times 10^{-9} \text{ m}^2/\text{s}$  at 288 K.

- Estimate the diffusivity at 293 K using the Wilke–Chang equation.
- Estimate the diffusivity at 293 K by correcting the experimental value at 288 K to 293 K. (*Hint:* Do this by using the relationship  $D_{AB} \propto T/\mu_B$ .)

**19.2-5. Estimation of Diffusivity of Electrolyte  $\text{NaOH}$ .** Dilute  $\text{NaOH}$  is diffusing in an aqueous solution. Do as follows:



- Estimate the diffusivity of NaOH at 25°C. Also, calculate the diffusivity of the individual ions Na<sup>+</sup> and OH<sup>-</sup>.
- Estimate the diffusivity of NaOH at 15°C.

**Ans.** (a)  $D_{ABO} = 2.128 \times 10^{-5} \text{ cm}^2/\text{s}$ ;

(b)  $D_{ABO} = 1.609 \times 10^{-5} \text{ cm}^2/\text{s}$

### ***19.2.6. Estimation of Diffusivity of LaCl<sub>3</sub> and Temperature Effect.***

Estimate the diffusion coefficient of the salt LaCl<sub>3</sub> in dilute aqueous solution at 25°C and at 35°C. Also, calculate the diffusion coefficient for the ions La<sup>3+</sup> and Cl<sup>-</sup> at 25°C. What percent increase in rate of diffusion will occur in going from 25 to 35°C if the same dilute concentration difference is present at both temperatures?

**Ans.**  $D_{ABO}(35^\circ\text{C}) = 1.649 \times 10^{-5} \text{ cm}^2/\text{s}$

### ***19.3-1. Diffusion of CO<sub>2</sub> Through***

**Rubber.** A flat plug 30 mm thick having an area of  $4.0 \times 10^{-4} \text{ m}^2$  and made of vulcanized rubber is used for closing an opening in a container. The gas  $\text{CO}_2$  at  $25^\circ\text{C}$  and 2.0 atm pressure is inside the container. Calculate the total leakage or diffusion of  $\text{CO}_2$  through the plug to the outside in  $\text{kg mol CO}_2/\text{s}$  at steady state. Assume that the partial pressure of  $\text{CO}_2$  outside is zero. From Barrer (B1), the solubility of the  $\text{CO}_2$  gas is  $0.90 \text{ m}^3 \text{ gas}$  (at STP of  $0^\circ\text{C}$  and 1 atm) per  $\text{m}^3 \text{ rubber}$  per atm pressure of  $\text{CO}_2$ . The diffusivity is  $0.11 \times 10^{-9} \text{ m}^2/\text{s}$ .

**Ans.**  $1.178 \times 10^{-13} \text{ kg mol CO}_2/\text{s}$

**19.3-2. Leakage of Hydrogen Through Neoprene Rubber.** Pure hydrogen gas at 2.0 atm abs pressure and  $27^\circ\text{C}$  is flowing past a vulcanized neoprene

rubber slab 5 mm thick. Using the data from Table 19.3-1, calculate the diffusion flux in  $\text{kg mol/s} \cdot \text{m}^2$  at steady state. Assume no resistance to diffusion outside the slab and zero partial pressure of  $\text{H}_2$  on the outside.

**19.3-3. Relation between Diffusivity and Permeability.** The gas hydrogen is diffusing through a sheet of vulcanized rubber 20 mm thick at  $25^\circ\text{C}$ . The partial pressure of  $\text{H}_2$  is 1.5 atm inside and 0 outside. Using the data from Table 19.3-1, calculate the following:

- The diffusivity  $D_{AB}$  from the permeability  $P_M$  and solubility  $S$ , and compare with the value in Table 19.3-1.
- The flux  $N_A$  of  $\text{H}_2$  at steady state.

**Ans.** (b)  $N_A = 1.144 \times 10^{-10} \text{ kg mol/s} \cdot \text{m}^2$

**19.3-4. *Loss from a Tube of Neoprene.***

Hydrogen gas at 2.0 atm and 27°C is flowing in a neoprene tube 3.0 mm inside diameter and 11 mm outside diameter. Calculate the leakage of  $H_2$  through a tube 1.0 m long in kg mol  $H_2/s$  at steady state.

**19.3-5. *Diffusion Through Membranes***

***in Series.*** Nitrogen gas at 2.0 atm and 30°C is diffusing through a membrane of nylon 1.0 mm thick and polyethylene 8.0 mm thick in series. The partial pressure at the other side of the two films is 0 atm. Assuming no other resistances, calculate the flux  $NA$  at steady state.

**19.3-6. *Diffusion of  $CO_2$  in a Packed***

***Bed of Sand.*** It is desired to calculate the rate of diffusion of  $CO_2$  gas in air at

steady state through a loosely packed bed of sand at 276 K and a total pressure of  $1.013 \times 10^5$  Pa. The bed depth is 1.25 m and the void fraction  $\epsilon$  is 0.30. The partial pressure of  $\text{CO}_2$  is  $2.026 \times 10^3$  Pa at the top of the bed and 0 Pa at the bottom. Use a  $\tau$  of 1.87.

**Ans.**  $N_A = 1.609 \times 10^{-9} \text{ kg mol CO}_2/\text{s} \cdot \text{m}^2$

### ***19.3-7. Packaging to Keep Food Moist.***

Cellophane is being used to keep food moist at 38°C. Calculate the loss of water vapor in g/d at steady state for a wrapping 0.10 mm thick and an area of 0.200 m<sup>2</sup> when the vapor pressure of water vapor inside is 10 mmHg and the air outside contains water vapor at a pressure of 5 mmHg. Use the larger permeability in Table 19.3-1.

**Ans.** 0.1663 g H<sub>2</sub>O/day.

**19.3-8. *Loss of Helium and***

***Permeability.*** A window of SiO<sub>2</sub> 2.0 mm thick and  $1.0 \times 10^{-4} \text{ m}^2$  in area is used to view the contents of a metal vessel at 20°C. Helium gas at 202.6 kPa is contained in the vessel. To be conservative, use  $D_{AB} = 5.5 \times 10^{-14} \text{ m}^2/\text{s}$  from Table 19.3-1.

- Calculate the loss of He in kg mol/h at steady state.
- Calculate the permeability  $P_M$ .

**Ans.** (a) Loss =  $8.833 \times 10^{-15} \text{ kg mol He/h}$

**19.4-1. *Knudsen Diffusivities.*** A

mixture of He (A) and Ar (B) is diffusing at  $1.013 \times 10^5 \text{ Pa}$  total pressure and 298 K through a capillary having a radius of 100 Å.

- Calculate the Knudsen diffusivity of He (A).
- Calculate the Knudsen diffusivity of Ar (B).
- Compare with the molecular diffusivity  $D_{AB}$ .

**Ans.** (a)  $D_{KA} = 8.37 \times 10^{-6} \text{ m}^2/\text{s}$ ; (c)  $D_{AB}$   
 $= 7.29 \times 10^{-5} \text{ m}^2/\text{s}$

**19.4-2. Transition-Region Diffusion.** A mixture of He (A) and Ar (B) at 298 K is diffusing through an open capillary 15 mm long with a radius of  $1000 \text{ \AA}$ . The total pressure is  $1.013 \times 10^5 \text{ Pa}$ . The molecular diffusivity  $D_{AB}$  at  $1.013 \times 10^5 \text{ Pa}$  is  $7.29 \times 10^{-5} \text{ m}^2/\text{s}$ .

- Calculate the Knudsen diffusivity of He (A).
- Predict the flux  $N_A$  using Eq. (19.4-18) and Eq. (19.4-12) if  $x_{A1} = 0.8$  and  $x_{A2} = 0.2$ . Assume steady state.
- Predict the flux  $N_A$  using the approximate Eqs. (19.4-14) and (19.4-16).

**19.4-3. Diffusion in a Pore in the**

**Transition Region.** Pure  $\text{H}_2$  gas ( $A$ ) at one end of a noncatalytic pore of radius  $50 \text{ \AA}$  and length  $1.0 \text{ mm}$  ( $x_{A1} = 1.0$ ) is diffusing through this pore with pure  $\text{C}_2\text{H}_6$  gas ( $B$ ) at the other end at  $x_{A2} = 0$ . The total pressure is constant at  $1013.2 \text{ kPa}$ . The predicted molecular diffusivity of  $\text{H}_2 - \text{C}_2\text{H}_6$  is  $8.60 \times 10^{-5} \text{ m}^2/\text{s}$  at  $101.32 \text{ kPa}$  and  $373 \text{ K}$ . Calculate the Knudsen diffusivity of  $\text{H}_2$  and flux  $N_A$  of  $\text{H}_2$  in the mixture at  $373 \text{ K}$  and steady state.

$$\text{Ans. } D_{KA} = 6.60 \times 10^{-6} \text{ m}^2/\text{s}, N_A = 1.472 \times 10^{-3} \text{ kg mol A/s} \cdot \text{m}^2$$

**19.4-4. Transition-Region Diffusion in a Capillary.** A mixture of nitrogen gas ( $A$ ) and helium ( $B$ ) at  $298 \text{ K}$  is diffusing through a capillary  $0.10 \text{ m}$  long in an open system with a diameter of  $10 \text{ }\mu\text{m}$ .



The mole fractions are constant at  $x_{A1} = 1.0$  and  $x_{A2} = 0$ . See Example 19.4-2 for physical properties.

- Calculate the Knudsen diffusivity  $D_{KA}$  and  $D_{KB}$  at the total pressures of 0.001, 0.1, and 10.0 atm.
- Calculate the flux  $N_A$  at steady state at these pressures.
- Plot  $N_A$  versus  $P$  on log–log paper. What are the limiting lines at lower pressures and very high pressures? Calculate and plot these lines.

**19.5-1. *Prediction of Diffusivity of an Enzyme Urease in Solution.*** Predict the diffusivity of the enzyme urease in a dilute solution in water at 298 K using the modified Polson equation and compare the result with the experimental value in Table 19.5-1.

**Ans.** Predicted  $D_{AB} = 3.995 \times 10^{-11} \text{ m}^2/\text{s}$

**19.5-2. *Diffusion of Sucrose in Gelatin.***

A layer of gelatin in water 5 mm thick and containing 5.1 wt % gelatin at 293 K separates two solutions of sucrose. The concentration of sucrose in the solution at one surface of the gelatin is constant at 2.0 g sucrose/100 mL solution, and 0.2 g/100 mL at the other surface. Calculate the flux of sucrose in kg sucrose/s · m<sup>2</sup> through the gel at steady state.

**19.5-3. Diffusivity of Oxygen in a Protein Solution.** Oxygen is diffusing through a solution of bovine serum albumin (BSA) at 298 K. Oxygen has been shown not to bind to BSA. Predict the diffusivity *D*<sub>AB</sub> of oxygen in a protein solution containing 11 g protein/100 mL solution. (Note: See Table 18.2-3 for the diffusivity of O<sub>2</sub> in water.)

$$\text{Ans. } D_{AP} = 1.930 \times 10^{-9} \text{ m}^2/\text{s}$$

**19.5-4. Diffusion of Uric Acid in a Protein Solution and Binding.** Uric acid (A) at 37°C is diffusing in an aqueous solution of proteins (P) containing 8.2 g protein/100 mL solution. Uric acid binds to the proteins, and over the range of concentrations present, 1.0 g mol of acid binds to the proteins for every 3.0 g mol of total acid present in the solution. The diffusivity  $D_{AB}$  of uric acid in water is  $1.21 \times 10^{-5} \text{ cm}^2/\text{s}$  and  $D_P = 0.091 \times 10^{-5} \text{ cm}^2/\text{s}$ .

- Assuming no binding, predict the ratio  $D_{AP}/D_{AB}$  due only to blockage effects.
- Assuming blockage plus binding effects, predict the ratio  $D_{AP}/D_{AB}$ . Compare this with the experimental value for  $D_{AP}/D_{AB}$  of 0.616.
- Predict the flux in g uric acid/s · cm<sup>2</sup> for a concentration of acid of 0.05 g/L at point (1) and 0 g/L at point (2) a distance 1.5 μm away.

**Ans.** (c)  $N_A = 2.392 \times 10^{-6} \text{g/s} \cdot \text{cm}^2$

**19.7-1. Numerical Method for Steady-State Diffusion.** Using the results from Example 19.7-1, calculate the total diffusion rate in the solid using the bottom nodes and paths of  $c_{2,2}$  to  $c_{3,2}$ ,  $c_{2,3}$  to  $c_{3,3}$ , and so on. Compare with the other diffusion rates in Example 19.7-1.

**Ans.**  $N = 2.555 \times 10^{-12} \text{kg mol/s}$

**19.7-2. Numerical Method for Steady-State Diffusion with a Distribution Coefficient.** Use the conditions given in Example 19.7-1, except that the distribution coefficient defined by Eq. (19.7-11) between the concentration in the liquid adjacent to the external surface and the concentration in the solid adjacent to the external surface is

$K = 1.2$ . Calculate the steady-state concentrations and the diffusion rates.

**19.7-3. Spreadsheet Solution for Steady-State Diffusion.** Use the conditions given in Example 19.7-1, but instead of using  $\Delta x = 0.005$  m, use  $\Delta x = \Delta y = 0.001$  m. The overall dimensions of the hollow chamber remain as in Example 19.7-1; the only difference is that more nodes will be used. Write the spreadsheet program and solve for the steady-state concentrations using the numerical method. Also, calculate the diffusion rates and compare with Example 19.7-1.

**19.7-4. Numerical Method with Fixed Surface Concentrations.** Steady-state diffusion is occurring in a two-dimensional solid, as shown in Fig.

19.7-4. The grid  $\Delta x = \Delta y = 0.010$  m.  
The diffusivity  $D_{AB} = 2.00 \times 10^{-9} \text{ m}^2/\text{s}$ .  
At the inside of the chamber, the surface concentration is held constant at  $2.00 \times 10^{-3} \text{ kg mol/m}^3$ . At the outside surfaces, the concentration is constant at  $8.00 \times 10^{-3}$ . Calculate the steady-state concentrations and the diffusion rates per m of depth.

### References

### Notation

# Chapter 20. Unsteady-State Mass Transfer

## 20.0 Chapter Objectives

On completion of this chapter, a student should be able to:

- Derive the equation for unsteady-state mass transfer with and without chemical reaction
- Use the Fourier series solution for unsteady-state diffusion in a flat plate with negligible surface resistance
- Use convenient charts to help solve unsteady-state problems, where both internal and external resistances apply
- Apply numerical, finite-difference methods for unsteady-state conduction problems
- Derive the differential equation of energy change

## 20.1 Unsteady-State Diffusion

### 20.1A Derivation of a Basic Equation

In Chapters 18 and 19, we considered various mass-transfer systems where the concentration or partial pressure at any point and the diffusion flux were constant with time, hence at steady state. Before steady state can be reached, time must elapse after the mass-transfer process is initiated for the unsteady-state conditions to disappear.

A general property balance for unsteady-state molecular diffusion was made for the properties momentum, heat, and mass. For no generation present, this was

$$\frac{\partial \Gamma}{\partial t} = D \frac{\partial^2 \Gamma}{\partial z^2}$$

In Section 14.1, an unsteady-state equation for heat conduction was



derived,

$$\frac{\partial T}{\partial t} = \alpha \frac{\partial^2 T}{\partial x^2} \quad (14.1-10)$$

The derivation of the unsteady-state diffusion equation in one direction for mass transfer is similar to that performed for heat transfer in obtaining Eq. (14.1-10). We refer to Fig. 20.1-1, where mass is diffusing in the  $x$  direction in a cube composed of a solid, stagnant gas, or stagnant liquid and having dimensions  $\Delta x$ ,  $\Delta y$ ,  $\Delta z$ . For diffusion in the  $x$  direction, we write

$$N_{Ax} = -D_{AB} \frac{\partial c_A}{\partial x} \quad (20.1-1)$$

The term  $\partial c_A / \partial x$  means the partial of  $c_A$  with respect to  $x$  or the rate of change of  $c_A$  with  $x$  when the other variable, time  $t$ , is kept constant.

Next, we make a mass balance on component A in terms of moles for no generation:

$$\text{rate of input} = \text{rate of output} + \text{rate of accumulation} \quad (20.1-2)$$

The rate of input and rate of output in kg mol A/s are

$$\text{rate of input} = N_A x|_x = -D_{AB} \partial c_A \partial x|_x \quad (20.1-3)$$

$$\text{rate of output} = N_A x|_{x+\Delta x} = -D_{AB} \partial c_A \partial x|_{x+\Delta x} \quad (20.1-4)$$

The rate of accumulation is as follows for the volume  $\Delta x \Delta y \Delta z$  m<sup>3</sup>:

$$\text{rate of accumulation} = (\Delta x \Delta y \Delta z) \partial c_A \partial t \quad (20.1-5)$$

Substituting Eqs. (20.1-3), (20.1-4), and (20.1-5) into (20.1-2) and dividing by

$\Delta x \Delta y \Delta z,$

$$-D_{AB} \frac{\partial c_A}{\partial x} \bigg|_x - \frac{\partial c_A}{\partial x} \bigg|_{x+\Delta x} \Delta x \Delta y \Delta z = \frac{\partial c_A}{\partial t} \Delta x \Delta y \Delta z \quad (20.1-6)$$

Letting  $\Delta x$  approach zero,

$$\frac{\partial c_A}{\partial t} = D_{AB} \frac{\partial^2 c_A}{\partial x^2} \quad (20.1-7)$$

The equation above holds for a constant diffusivity  $D_{AB}$ . If  $D_{AB}$  is a variable,

$$\frac{\partial c_A}{\partial t} = \frac{\partial}{\partial x} \left( D_{AB} \frac{\partial c_A}{\partial x} \right) \quad (20.1-8)$$

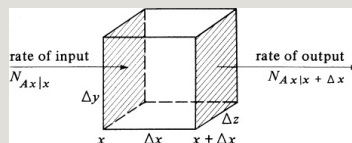


Figure 20.1-1. *Unsteady-state diffusion in one direction.*

Equation (20.1-7) relates the concentration  $c_A$  with position  $x$  and time  $t$ . For diffusion in all three directions, a similar derivation gives

$$\frac{\partial c_A}{\partial t} = D_{AB} \left( \frac{\partial^2 c_A}{\partial x^2} + \frac{\partial^2 c_A}{\partial y^2} + \frac{\partial^2 c_A}{\partial z^2} \right) \quad (20.1-9)$$

In the remainder of this section, the solutions of Eqs. (20.1-7) and (20.1-9) will be considered. Note the mathematical similarity between the equation for heat conduction, Eq. 14.1-10, and Eq. (20.1-7) for diffusion. Because of this similarity, the mathematical methods used for solution of the unsteady-state heat-conduction equation can be used for unsteady-state mass transfer. This is discussed more fully in Sections 20.1B, 20.1C, and 20.3.

$$\frac{\partial T}{\partial t} = \alpha \frac{\partial^2 T}{\partial x^2} \quad (14.1-10)$$

### **20.1B Diffusion in a Flat Plate with Negligible Surface Resistance**

To illustrate an analytical method of

solving Eq. (20.1-7), we will derive the solution for unsteady-state diffusion in the  $x$  direction for a plate of thickness  $2x_1$ , as shown in Fig. 20.1-2. For diffusion in one direction,

$$\partial c_A / \partial t = D_{AB} \partial^2 c_A / \partial x^2 \quad (20.1-7)$$

Dropping the subscripts  $A$  and  $B$  for convenience,

$$\partial c / \partial t = D \partial^2 c / \partial x^2 \quad (20.1-10)$$

The initial profile of the concentration in the plate at  $t = 0$  is uniform at  $c = c_0$  for all  $x$  values, as shown in Fig. 20.1-2. At time  $t = 0$ , the concentration of the fluid in the environment outside is suddenly changed to  $c_1$ . For a very high mass-transfer coefficient outside the surface, resistance will be negligible and the

concentration at the surface will be equal to that in the fluid, which is  $c_1$ .

The initial and boundary conditions are

$$c = c_0 \text{ at } t = 0, x = 0, Y = c_1 - c_0 = 0 \text{ at } t = 0, x = 2x_1, Y = c_1 - c_0 = 0$$

Redefining the concentration so it goes between 0 and 1,

$$Y = \frac{c - c_0}{c_1 - c_0} \quad (20.1-12)$$

$$\frac{\partial Y}{\partial t} = D \frac{\partial^2 Y}{\partial x^2} \quad (20.1-13)$$

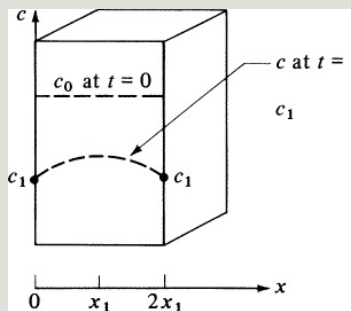


Figure 20.1-2. Unsteady-state diffusion in a flat plate with negligible surface resistance.

The solution of Eq. (20.1-13) is an

infinite Fourier series and is identical to the solution of Eq. (14.1-10) for heat transfer:

$$-12\pi^2 X^4) \sin 1\pi x^2 x_1 + 13 \exp(-32\pi^2 X^4) \sin 3\pi x^2 x_1 + 15 \exp(-64\pi^2 X^4) \sin 5\pi x^2 x_1 + \dots \quad (20.1-14)$$

where

$$X = \sqrt{\alpha t} \quad \text{and} \quad x_1 = x/L$$

The solution of equations similar to Eq. (20.1-14) is time-consuming; convenient charts for various geometries are available and will be discussed in the next section.

### 20.1C Unsteady-State Diffusion in Various Geometries

*1. Convection and boundary conditions at the surface.* In Fig. 20.1-2, there was no convective resistance at the surface. However,

in many cases when a fluid is outside the solid, convective mass transfer is occurring at the surface. A convective mass-transfer coefficient  $k_c$ , similar to a convective heat-transfer coefficient, is defined as follows:

$$N_A = k_c(c_{L1} - c_{Li}) \quad (20.1-15)$$

where  $k_c$  is a mass-transfer coefficient in m/s,  $c_{L1}$  is the bulk fluid concentration in kg mol  $A/m^3$ , and  $c_{Li}$  is the concentration in the fluid just adjacent to the surface of the solid. The coefficient  $k_c$  is an empirical coefficient and will be discussed more fully in Section 21.1.

In Fig. 20.1-3a, the case where a mass-transfer coefficient is present at the boundary is shown. The concentration



drop across the fluid is  $c_{L1} - c_{Li}$ . The concentration in the solid  $c_i$  at the surface is in equilibrium with  $c_{Li}$ .

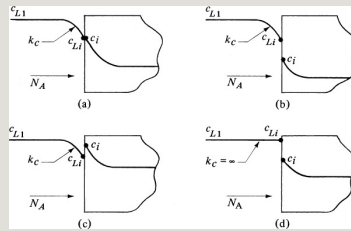


Figure 20.1-3. *Interface conditions for convective mass transfer and an equilibrium distribution coefficient  $K = c_{Li}/c_i$ : (a)  $K = 1$ , (b)  $K > 1$ , (c)  $K < 1$ , (d)  $K > 1$ , and  $k_c = \infty$ .*

In Fig. 20.1-3a the concentration  $c_{Li}$  in the liquid adjacent to the solid and  $c_i$  in the solid at the surface are in equilibrium and are equal. However, unlike heat transfer, where the temperatures are equal, the concentrations here are in equilibrium and are related by

$$K = c_{Li}/c_i \quad (20.1-16)$$

where  $K$  is the equilibrium distribution coefficient (similar to Henry's law coefficient for a gas and liquid). The value of  $K$  in Fig. 20.1-3a is 1.0.

In Fig. 20.1-3b the distribution coefficient  $K > 1$  and  $c_{Li} > c_i$ , even though they are in equilibrium. Other cases are shown in Fig. 20.1-3c and d. This was also discussed in Section 19.7B.

*2. Relation between mass- and heat-transfer parameters.* In order to use the unsteady-state heat-conduction charts in Chapter 14 for solving unsteady-state diffusion problems, the dimensionless variables or parameters for heat transfer must be related to those for mass transfer. In Table 20.1-1 the relations between these variables are tabulated.

For  $K \neq 1.0$ , whenever  $k_c$  appears, it is given as  $Kk_c$ , and whenever  $c_1$  appears, it is given as  $c_1/K$ .

*3. Charts for diffusion in various geometries.* The various heat-transfer charts for unsteady-state conduction can be used for unsteady-state diffusion and are as follows:

1. Semi-infinite solid, Fig. 14.3-3.
2. Flat plate, Figs. 14.3-5 and 14.3-6.
3. Long cylinder, Figs. 14.3-7 and 14.3-8.
4. Sphere, Figs. 14.3-9 and 14.3-10.
5. Average concentrations, zero convective resistance, Fig. 14.3-13.

Table 20.1-1. *Relation between Mass- and Heat-Transfer Parameters for Unsteady-State Diffusion\**



\*  $x$  is the distance from the center of the slab, cylinder, or sphere; for a semi-infinite slab,  $x$  is the distance from the surface,  $c_0$  is the original uniform concentration in the solid,  $c_1$  the concentration in the fluid outside the slab, and  $c$  the concentration in the solid at position  $x$  and time  $t$ .

**EXAMPLE 20.1-1. Unsteady-State Diffusion in a Slab of Agar Gel**

A solid slab of 5.15 wt % agar gel at 278 K is 10.16 mm thick and contains a uniform concentration of urea of 0.1 kg mol/m<sup>3</sup>. Diffusion is only in the  $x$  direction through two parallel flat surfaces 10.16 mm apart. The slab is suddenly immersed in pure turbulent water, so the surface resistance can be assumed to be negligible; that is, the convective coefficient  $k_c$  is very large. The diffusivity of urea in the agar from Table 19.5-1 is  $4.72 \times 10^{-10}$  m<sup>2</sup>/s.

- Calculate the concentration at the midpoint of the slab (5.08 mm from the surface) and 2.54 mm from the surface after 10 h.
- If the thickness of the slab is halved, what would be the midpoint concentration in 10 h?

**Solution:** For part (a),  $c_0 = 0.10$  kg mol/m<sup>3</sup>,  $c_1 = 0$  for pure water, and  $c$  = concentration at distance  $x$  from center line and time  $t$  s. The equilibrium-distribution coefficient  $K$  in Eq. (20.1-16) can be assumed to be 1.0, since the water in the aqueous solution in the gel and outside should be very similar in properties. From Table 20.1-1,

$$Y = \frac{c_1 - c}{c_1 - c_0} = \frac{0 - c}{0.10 - 0} = -10c$$

Also,  $x_1 = 10.16/(1000 \times 2) = 5.08 \times 10^{-3}$  m (half-slab thickness),  $x = 0$  (center), and  $X = DABt/x_1^2 = (4.72 \times 10^{-10}) / (10 \times 3600) / (5.08 \times 10^{-3})^2 = 0.658$ . The relative position  $n = x/x_1 = 0/5.08 \times 10^{-3} = 0$ , and relative resistance  $m = DAB/Kk_{cx_1} = 0$  since  $k_c$  is very large (zero resistance).

From Fig. 14.3-5 for  $X = 0.658$ ,  $m = 0$ , and  $n = 0$ ,

$$Y = 0.275 = 0 - c_0 - 0.10$$

Solving,  $c = 0.0275$  kg mol/m<sup>3</sup> for  $x = 0$ .

For the point 2.54 mm from the surface or 2.54 mm from the center,  $x = 2.54/1000 = 2.54 \times 10^{-3}$  m,  $X = 0.658$ ,  $m = 0$ ,  $n = x/x_1 = 2.54 \times 10^{-3} / 5.08 \times 10^{-3} = 0.5$ . Then, from Fig. 14.3-5,  $Y = 0.172$ . Solving,  $c = 0.0172$  kg mol/m<sup>3</sup>.

For part (b) and half the thickness,  $X = 0.658/(0.5)^2 = 2.632$ ,  $n = 0$ , and  $m = 0$ . Hence,  $Y = 0.0020$  and  $c = 2.0 \times 10^{-4}$  kg mol/m<sup>3</sup>.

### **EXAMPLE 20.1-2. Unsteady-State Diffusion in a Semi-infinite Slab**

A very thick slab has a uniform concentration of solute A of  $c_0 = 1.0 \times 10^{-2}$  kg mol A/m<sup>3</sup>. Suddenly, the front face of the slab is exposed to a flowing fluid having a concentration  $c_1 = 0.10$  kg mol A/m<sup>3</sup> and a convective coefficient  $k_c = 2 \times 10^{-7}$  m/s. The equilibrium distribution coefficient  $K = c_{Li}/c_i = 2.0$ . Assuming that the slab is a semi-infinite solid, calculate the concentration in the solid at the surface ( $x = 0$ ) and  $x = 0.01$  m from the surface after  $t = 3 \times 10^4$  s. The diffusivity in the solid is  $DAB = 4 \times 10^{-9}$  m<sup>2</sup>/s.

**Solution:** To use Fig. 14.3-3, use Table 20.1-1.

$$Kk_c DAB t = 2.0(2 \times 10^{-7} \text{ m/s}) 4 \times 10^{-9} \text{ m}^2/\text{s} (3 \times 10^4 \text{ s}) = 1.095$$

For  $x = 0.01$  m from the surface in the solid,

$$x^2 DAB t = 0.001 \text{ m}^2 (4 \times 10^{-9} \text{ m}^2/\text{s}) (3 \times 10^4 \text{ s}) = 0.457$$

From the chart,  $1 - Y = 0.26$ . Then, substituting into the equation for  $(1 - Y)$  from Table 20.1-1 and solving,

$$1 - Y = c - c_0 \frac{1}{K - c_0} = c - \frac{(1 \times 10^{-2} \text{ kgmole/m}^3)}{(10 \times 10^{-2} \text{ kgmole/m}^3 / 2) - (1 \times 10^{-2} \text{ kgmole/m}^3)} = 0.26c = 2.04 \times 10^{-2} \text{ kgmole/m}^3 \quad (\text{for } x = 0.01 \text{ m})$$

For  $x = 0 \text{ m}$  (i.e., at the surface of the solid),

$$x^2 \frac{\partial^2 A}{\partial t} = 0$$

From the chart,  $1 - Y = 0.62$ . Solving,  $c = 3.48 \times 10^{-2}$ . This value is the same as  $c_i$ , as shown in Fig. 20.1-3b. To calculate the concentration  $c_{Li}$  in the liquid at the interface,

$$c_{Li} = K c_i = 2.0 (3.48 \times 10^{-2} \text{ kgmole/m}^3) = 6.96 \times 10^{-2} \text{ kgmole/m}^3$$

A plot of these values will be similar to Fig. 20.1-3b.

*4. Unsteady-state diffusion in more than one direction.* In Section 14.3F, a method was given for unsteady-state heat conduction, in which the one-dimensional solutions were combined to yield solutions for several-dimensional systems. The same method can be used for unsteady-state diffusion in more than one direction. Rewriting Eq. (14.3-11) for diffusion in a rectangular block in the  $x$ ,  $y$ , and  $z$  directions,

$$Y_{x,y,z} = (Y_x)(Y_y)(Y_z) = \frac{c - c_0}{c_1 - c_0} \frac{1}{K - c_0} \quad (20.1-17)$$

where  $c_{x,y,z}$  is the concentration at the point  $x, y, z$  from the center of the block. The value of  $Y_x$  for the two parallel faces is obtained from Fig. 14.3-5 or 14.3-6 for a flat plate in the  $x$  direction. The values of  $Y_y$  and  $Y_z$  are similarly obtained from the same charts. For a short cylinder, an equation similar to Eq. (14.3-12) is used, and for average concentrations, equations similar to Eqs. (14.3-14), (14.3-15), and (14.3-16) are used.

## **20.2 Unsteady-State Diffusion and Reaction in a Semi-Infinite Medium**

### **20.2A Unsteady-State Diffusion and Reaction in a Semi-Infinite Medium**

We now consider a case where dilute  $A$  is absorbed at the surface of a solid or stagnant fluid phase and then unsteady-state diffusion and reaction occur in the phase. The fluid or solid

phase  $B$  is considered semi-infinite. At the surface, where  $z = 0$ , the concentration of  $c_A$  is kept constant at  $c_{A0}$ . The dilute solute  $A$  reacts by a first-order mechanism



and the rate of generation is  $-k'c_A$ . The same diagram as in Fig. 19.6-2 holds. Using Eq. (19.6-13) but substituting  $(\partial c_A / \partial t)(\Delta z)$  (1) for the rate of accumulation,

$$N_{Az}|_z(1) - k'c_A(1)(\Delta z) = N_{Az}|_z + \Delta z(1) + (\partial c_A / \partial t)(\Delta z)(1) \quad (20.2-2)$$

This becomes

$$\partial c_A / \partial t = D_{AB} \partial^2 c_A / \partial z^2 - k'c_A \quad (20.2-3)$$

The initial and boundary conditions are



$$c_A = 0 \text{ for } z > 0, c_A = c_{A0} \text{ for } z = 0, c_A = 0 \text{ for } t > 0, z = \infty, c_A = 0 \text{ for } t > 0 \quad (20.2-2)$$

The solution by Danckwerts (D1) is

$$c_A - c_{A0} = \frac{1}{2} \exp\left(-\frac{z^2}{4DABt}\right) \operatorname{erfc}\left(\frac{z}{2\sqrt{DABt}} - \frac{k't}{\sqrt{DABt}}\right) + \frac{1}{2} \exp\left(-\frac{z^2}{4DABt}\right) \operatorname{erfc}\left(\frac{z}{2\sqrt{DABt}} + \frac{k't}{\sqrt{DABt}}\right) \quad (20.2-5)$$

The total amount  $Q$  of  $A$  absorbed up to time  $t$  is

$$Q = c_{A0} DAB / k' \left[ \left( \frac{k't}{\sqrt{DABt}} + \frac{1}{2} \right) \operatorname{erfc}\left(\frac{k't}{\sqrt{DABt}} + \frac{1}{2}\right) + \frac{k't}{\sqrt{DABt}} \right] \quad (20.2-6)$$

where  $Q$  is kg mol  $A$  absorbed/m<sup>2</sup>.

Many actual cases are approximated by this case. The equation is useful where absorption occurs at the surface of a stagnant fluid or a solid and unsteady-state diffusion and reaction occur in the solid or fluid. The results can be used to measure the diffusivity of a gas in a

solution, to determine the reaction-rate constants  $k'$  of dissolved gases, and to determine the solubilities of gases in liquids with which they react. Details are given in (D2).

**EXAMPLE 20.2-1. Reaction and Unsteady-State Diffusion**

Pure CO<sub>2</sub> gas at 101.32 kPa pressure is absorbed into a dilute alkaline buffer solution containing a catalyst. The dilute, absorbed solute CO<sub>2</sub> undergoes a first-order reaction, with  $k' = 35 \text{ s}^{-1}$  and  $D_{AB} = 1.5 \times 10^{-9} \text{ m}^2/\text{s}$ . The solubility of CO<sub>2</sub> is  $2.961 \times 10^{-7} \text{ kgmol/m}^3 \cdot \text{Pa}$  (D2). The surface is exposed to the gas for 0.010 s. Calculate the kg mol CO<sub>2</sub> absorbed/m<sup>2</sup> surface.

**Solution:** For use in Eq. (20.2-6),  $kt = 35(0.01) = 0.350$ . Also,  $c_{A0} = 2.961 \times 10^{-7} \text{ (kg mol/m}^3 \cdot \text{Pa)}(101.32 \times 10^3 \text{ Pa)} = 3.00 \times 10^{-2} \text{ kg mol SO}_2/\text{m}^3$ .

$$Q = (3.00 \times 10^{-2}) \sqrt{1.5 \times 10^{-9} / 35} [(0.35 + 12) \operatorname{erfc} 0.35 + 0.35 / \pi e^{-0.35}] Q = 1.458 \times 10^{-7} \text{ kgmol/m}^2$$

## 20.3 Numerical Methods for Unsteady-State Molecular Diffusion

### 20.3A Introduction

Unsteady-state diffusion often occurs in inorganic, organic, and biological solid materials. If the boundary

conditions are constant with time, if they are the same on all sides or surfaces of the solid, and if the initial concentration profile is uniform throughout the solid, the methods described in Section 20.1 can be used. However, these conditions are not always fulfilled, in which case numerical methods must be used.

### **20.3B Unsteady-State Numerical Methods for Diffusion**

*1. Derivation for unsteady state for a slab.* For unsteady-state diffusion in one direction, Eq. (20.1-9) becomes

$$\partial c_A / \partial t = D_{AB} \partial^2 c_A / \partial x^2 \quad (20.3-1)$$

Since this equation is identical mathematically to the unsteady-state heat-conduction Eq. (14.1-10),

$$\frac{\partial T}{\partial t} = \alpha \frac{\partial^2 T}{\partial x^2} \quad (14.1-10)$$

identical mathematical methods can be used for solving both diffusion and conduction numerically.

Figure 20.3-1 shows a slab of width  $\Delta x$  centered at point  $n$ , represented by the shaded area. Making a mole balance of  $A$  on this slab at the time  $t$  when the rate in – rate out = rate of accumulation in  $\Delta t$  s,

$$DAB A \Delta x (c_{n-1} - c_n) - DAB A \Delta x (c_n - c_{n+1}) = (A \Delta x) \frac{dc_n}{dt} \Delta t \quad (20.3-2)$$

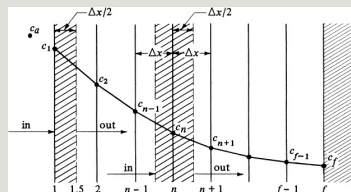


Figure 20.3-1. *Unsteady-state diffusion in a slab.*

where  $A$  is cross-sectional area and  $t + \Delta t C_n$  is concentration at point  $n$  one  $\Delta t$  later. Rearranging,

$$c_{n,t+\Delta t} = \frac{1}{M} [c_{n+1,t} + (M-2)c_{n,t} + c_{n-1,t}] \quad (20.3-3)$$

where  $M$  is a constant.

$$M = (\Delta x)^2 D A B \Delta t \quad (20.3-4)$$

As in heat conduction,  $M \geq 2$ .

In using Eq. (20.3-3), the concentration  $c_n$  at position  $n$  and the new time  $t + \Delta t$  is calculated explicitly from the known three points at  $t$ . In this calculation method, starting with the known concentrations at  $t = 0$ , the calculations proceed directly from one time increment to the next until the final time is reached.

## 2. *Simplified Schmidt method for a slab.*

If the value of  $M = 2$ , a simplification of Eq. (20.3-3) occurs, giving the Schmidt method:

$$c_{n+1} = c_n + \frac{1}{2} \Delta t (2c_n - c_{n-1}) \quad (20.3-5)$$

### **20.3C Boundary Conditions for Numerical Methods for a Slab**

*1. Convection at a boundary.* For the case where convection occurs outside in the fluid and the concentration of the fluid outside is suddenly changed to  $c_a$ , we can make a mass balance on the outside half-slab in Fig. 20.3-1. Following the methods used for heat transfer to derive Eq. (14.4-7), we write rate of mass entering by convection – rate of mass leaving by diffusion = rate of mass accumulation in  $\Delta t$  hours:

$$k_c A (c - c_1) - DAB A \Delta x (c - c_2) = (A \Delta x / 2) \Delta t (c - c_1) \quad (20.3-6)$$

where  $c_{1.25}$  is the concentration at the midpoint of the  $0.5 \Delta x$  outside slab. As an approximation, using  $c_1$  for  $c_{1.25}$  and rearranging Eq. (20.3-6),

$$c_t + \Delta t = 1/M [2N t_c a + [M - (2N + 2)] t_{c1} + 2 t_{c2}] \quad (20.3-7)$$

$$N = k_c \Delta x DAB \quad (20.3-8)$$

where  $k_c$  is the convective mass-transfer coefficient in m/s. Again, note that  $M \geq (2N + 2)$ .

*2. Insulated boundary condition.* For the insulated boundary at  $f$  in Fig. 20.3-1, setting  $k_c = 0$  ( $N = 0$ ) in Eq. (20.3-7), we obtain

$$c_{ft} + \Delta t = \frac{1}{M} [(M-2)c_{cf} + 2c_{cf} - 1] \quad (20.3-9)$$

3. *Alternative convective equation at the boundary.* Another form of Eq. (20.3-7) to use if  $N$  gets too large can be obtained by neglecting the accumulation in the front half-slab of Eq. (20.3-6) to give

$$c_{1t} + \Delta t = \frac{N}{N+1} c_{0t} + \Delta t + \frac{1}{N+1} c_{2t} + \Delta t \quad (20.3-10)$$

The value of  $M$  is not restricted by the  $N$  value in this equation. When a large number of increments in  $\Delta x$  are used, the amount of mass neglected is small compared to the total.

4. *Procedure for use of initial boundary concentration.* For the first time increment, we should use an average value for  $c_a$  of  $(c_a + c_{c1})/2$ , where  $c_{c1}$  is



the initial concentration at point 1. For succeeding times, the full value of  $c_a$  should be used. This special procedure for the value of  $c_a$  increases the accuracy of the numerical method, especially after a few time intervals.

In Section 14.4B, concerning numerical methods for heat-transfer, a detailed discussion is given on the best value of  $M$  to use in Eq. (20.3-3). The most accurate results are obtained for  $M = 4$ .

*5. Boundary conditions with distribution coefficient.* Equations for boundary conditions in Eqs. (20.3-7) and (20.3-10) were derived for the distribution coefficient  $K$  given in Eq. (20.3-7) being 1.0. When  $K$  is not 1.0, as in the boundary conditions for steady state,  $Kk_c$  should be substituted for  $k_c$  in

Eq. (20.3-8) to become as follows (see also Sections 19.7B and 20.1C):

$$N = K k c \Delta x D_{AB} (20.3-11)$$

Also, in Eqs. (20.3-7) and (20.3-10), the term  $c_a/K$  should be substituted for  $c_a$ .

Other cases, such as for diffusion between dissimilar slabs in series, resistance between slabs in series, and so on, are covered in detail in (G1), with actual numerical examples being given. In reference (G1), the implicit numerical method is discussed.

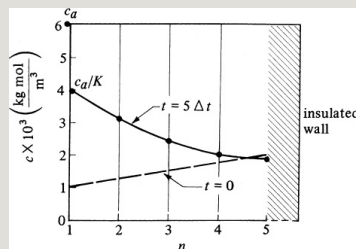
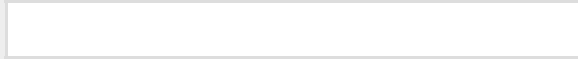


Figure 20.3-2. Concentrations for numerical method for unsteady-state diffusion, Example 20.3-1.

**EXAMPLE 20.3-1. Numerical Solution for Unsteady-State Diffusion with a Distribution Coefficient**

A slab of material 0.004 m thick has an initial concentration profile of solute A as follows, where  $x$  is distance in m from the exposed surface:



The diffusivity  $D_{AB} = 1.0 \times 10^{-9} \text{ m}^2/\text{s}$ . Suddenly, the top surface is exposed to a fluid having a constant concentration  $c_a = 6 \times 10^{-3} \text{ kg mol A/m}^3$ . The distribution coefficient  $K = c_a/c_n = 1.50$ . The rear surface is insulated, so that unsteady-state diffusion is occurring only in the  $x$  direction. Calculate the concentration profile after 2500s. The convective mass-transfer coefficient  $k_c$  can be assumed as infinite. Use  $\Delta x = 0.001 \text{ m}$  and  $M = 2.0$ .

**Solution:** Figure 20.3-2 shows the initial concentration profile for four slices and  $c_a = 6 \times 10^{-3}$ . Since  $M = 2$ , substituting into Eq. (20.3-4) with  $\Delta x = 0.001 \text{ m}$  and solving for  $\Delta t$ ,

$$M=2=(\Delta x)^2 D_{AB} \Delta t = (0.001 \text{ m})^2 (1 \times 10^{-9} \text{ m}^2/\text{s}) \Delta t \Delta t = 500 \text{ s}$$

Hence, 2500 s/(500 s/increment) or five time increments are needed.

For the front surface, where  $n = 1$ , the concentration to use for the first time increment, as stated previously, is

$$c_1 = c_a / K = 0.004 \text{ (20.3-12)}$$

where  $c_1$  is the initial concentration at  $n = 1$ . For the remaining time increments,

$$c_1 = c_a K (n=1) \text{ (20.3-13)}$$

To calculate the concentrations for all time increments for slabs  $n = 2, 3, 4$ , using Eq. (20.3-5) for  $M = 2$ ,

$$c_{n+1} = c_n - 1 + c_n + 1 \text{ (20.3-14)}$$

For the insulated end at  $n = 5$ , substituting  $M = 2$  and  $f = n = 5$  into Eq. (20.3-9),

$$c5t+\Delta t=(2-2)ct5+2ct42=ct4(n=5)(20.3-15)$$

For  $1 \Delta t$  or  $t + 1 \Delta t$ , the first time increment, calculating the concentration for  $n = 1$  by Eq. (20.3-12),

$$c1t+\Delta t=ca/K+0c12=6 \times 10^{-3}/1.5+1 \times 10^{-32}=2.5 \times 10^{-3}$$

For  $n = 2, 3$ , and  $4$ , using Eq. (20.3-14),

$$\begin{aligned} c2t+\Delta t &= c_{n-1}t + c_{n-1}t2 = c1t \\ +c3t2 &= 2.5 \times 10^{-3} + 1.5 \times 10^{-322 \times 10^{-3}} c3t + \Delta t = c2t \\ +c4t2 &= 2.5 \times 10^{-3} + 1.75 \times 10^{-32} = 1.5 \times 10^{-3} c4t + \Delta t = c3t \\ +c5t2 &= 1.5 \times 10^{-3} + 2.0 \times 10^{-32} = 1.75 \times 10^{-3} \end{aligned}$$

For  $n = 5$ , using Eq. (20.3-15),

$$c5t+\Delta t=c4t=1.75 \times 10^{-3}$$

For  $2\Delta t$ , using Eq. (20.3-13) for  $n = 1$ , using Eq. (20.3-14) for  $n = 2 - 4$ , and using Eq. (20.3-15) for  $n = 5$ ,

$$\begin{aligned} &c1t \\ +2\Delta t &= caK = 6 \times 10^{-3}/1.5 = 4.0 \times 10^{-3} \quad (\text{constant for rest of time}) c2t \\ +2\Delta t &= c1t + \Delta t + c3t + \Delta t2 = 4 \times 10^{-3} + 1.5 \times 10^{-32} = 2.75 \times 10^{-3} c3t \\ &+2\Delta t = c2t + \Delta t + c4t \\ +\Delta t2 &= 2 \times 10^{-3} + 1.75 \times 10^{-32} = 1.875 \times 10^{-3} c4t + 2\Delta t = c3t + \Delta t \\ +c5t + \Delta t2 &= 1.5 \times 10^{-3} + 1.75 \times 10^{-32} = 1.625 \times 10^{-3} c5t \\ +2\Delta t &= c4t = 1.75 \times 10^{-3} t + \Delta t \end{aligned}$$

For  $3\Delta t$ ,

$$\begin{aligned} c1t+3\Delta t &= 4 \times 10^{-3} c2t \\ +3\Delta t &= 4 \times 10^{-3} + 1.875 \times 10^{-32} = 2.938 \times 10^{-3} c3t \\ +3\Delta t &= 2.75 \times 10^{-3} + 1.625 \times 10^{-32} = 2.188 \times 10^{-3} c4t \\ +3\Delta t &= 1.875 \times 10^{-3} + 1.75 \times 10^{-32} = 1.813 \times 10^{-3} c5t \\ +3\Delta t &= 1.625 \times 10^{-3} \end{aligned}$$

For  $4\Delta t$ ,

$$\begin{aligned} c1t+4\Delta t &= 4 \times 10^{-3} c2t \\ +4\Delta t &= 4 \times 10^{-3} + 2.188 \times 10^{-32} = 3.094 \times 10^{-3} c3t \\ +4\Delta t &= 2.938 \times 10^{-3} + 1.813 \times 10^{-322.376 \times 10^{-3}} c4t \\ +4\Delta t &= 2.188 \times 10^{-3} + 1.625 \times 10^{-32} = 1.906 \times 10^{-3} c5t \\ +4\Delta t &= 1.813 \times 10^{-3} \end{aligned}$$

For  $5\Delta t$ ,

$$c1t+5\Delta t=4 \times 10^{-3} c2t$$

$$\begin{aligned}
 +5\Delta t &= 4 \times 10^{-3} + 2.376 \times 10^{-3} = 3.188 \times 10^{-3} c_3 t \\
 +5\Delta t &= 3.094 \times 10^{-3} + 1.906 \times 10^{-3} = 2.500 \times 10^{-3} c_4 t \\
 +5\Delta t &= 2.376 \times 10^{-3} + 1.813 \times 10^{-3} = 2.095 \times 10^{-3} c_5 t \\
 +5\Delta t &= 1.906 \times 10^{-3}
 \end{aligned}$$

The final concentration profile is plotted in Fig. 20.3-2. To increase the accuracy, more slab increments and time increments are needed. This type of calculation is suitable for use with a computer spreadsheet.

## 20.4 Chapter Summary

The equation for unsteady-state mass transfer without chemical reaction is:

$$\partial c_A / \partial t = D_{AB} \partial^2 c_A / \partial x^2 \quad (20.1-7)$$

The equation for unsteady-state diffusion in a flat plate with negligible surface resistance is:

$$\begin{aligned}
 &Y \\
 &-12\pi^2 X^4) \sin 1\pi x^2 x^1 + 13 \exp(32\pi^2 X^4) \sin 3\pi x^2 x^1 + 15 \exp( \\
 &(20.1-14)
 \end{aligned}$$

Charts for diffusion in various geometries. The various heat-transfer

charts for unsteady-state conduction can be used for unsteady-state diffusion and are as follows:

1. Semi-infinite solid, Fig. 14.3-3.
2. Flat plate, Figs. 14.3-5 and 14.3-6.
3. Long cylinder, Figs. 14.3-7 and 14.3-8.
4. Sphere, Figs. 14.3-9 and 14.3-10.
5. Average concentrations, zero convective resistance, Fig. 14.3-13.

## Numerical Finite-Difference Methods

### *Equations for a Slab:*

A) Interior node:

$$c_{n,t+\Delta t} = \frac{1}{M} [c_{n+1,t} + (M-2)c_{n,t} + c_{n-1,t}] \quad (20.3-3)$$

$$\text{where } M = (\Delta x)^2 D_{AB} \Delta t \quad (20.3-4)$$

B) Convection at the boundary:

$$c_1 t + \Delta t = \frac{1}{M} [2Nc_a + [M - (2N + 2)]t c_1 + 2t c_2] \quad (20.3-7)$$

$$\text{where } N = k_c \Delta x D A B \quad (20.3-8)$$

C) Insulated boundary condition:

$$c_f = \frac{1}{M} [(M - 2)t c_f + 2t c_f - 1] t + \Delta t$$

## Problems

**20.1-1. *Unsteady-State Diffusion in a Thick Slab.*** Repeat Example

20.1-2 but use a distribution coefficient  $K = 0.50$  instead of 2.0.

Plot the data.

**Ans.**  $c = c_i = 5.75 \times 10^{-2} (x = 0), c = 2.78 \times 10^{-2} (x = 0.01 \text{ m}), c_{Li} = 2.87 \times 10^{-2} \text{ kg mol/m}^3$

**20.1-2. *Plot of Concentration Profile in Unsteady-State Diffusion.*** Using the

same conditions as in Example 20.1-2, calculate the concentration at the points  $x = 0, 0.005, 0.01, 0.015$ , and  $0.02$  m from the surface. Also calculate  $c_{Li}$  in the liquid at the interface. Plot the concentrations in a manner similar to Fig. 20.1-3b, showing interface concentrations.

**20.1-3. *Unsteady-State Diffusion in Several Directions.*** Use the same conditions as in Example 20.1-1 except that the solid is a rectangular block 10.16 mm thick in the  $x$  direction, 7.62 mm thick in the  $y$  direction, and 10.16 mm thick in the  $z$  direction, and diffusion occurs at all six faces. Calculate the concentration at the midpoint after 10 h.

$$\text{Ans. } c = 6.20 \times 10^{-4} \text{ kg mol/m}^3$$



**20.1-4. *Drying of Moist Clay.*** A very thick slab of clay has an initial moisture content of  $c_0 = 14 \text{ wt } \%$ . Air is passed over the top surface to dry the clay. Assume a relative resistance of the gas at the surface of zero. The equilibrium moisture content at the surface is constant at  $c_1 = 3.0 \text{ wt } \%$ . The diffusion of the moisture in the clay can be approximated by a diffusivity of  $D_{AB} = 1.29 \times 10^{-8} \text{ m}^2/\text{s}$ . After 1.0 h of drying, calculate the concentration of water at points 0.005, 0.01, and 0.02 m below the surface. Assume that the clay is a semi-infinite solid and that the  $Y$  value can be represented using concentrations of wt % rather than  $\text{kg mol}/\text{m}^3$ . Plot the values versus  $x$ .

**20.1-5. *Unsteady-State Diffusion in a Cylinder of Agar Gel.*** A wet cylinder of

agar gel at 278 K containing a uniform concentration of urea of  $0.1 \text{ kg mol/m}^3$  has a diameter of 30.48 mm and is 38.1 mm long with flat, parallel ends. The diffusivity is  $4.72 \times 10^{-10} \text{ m}^2/\text{s}$ .

Calculate the concentration at the midpoint of the cylinder after 100 h for the following cases if the cylinder is suddenly immersed in turbulent pure water:

- For radial diffusion only.
- Diffusion occurs radially and axially.

**20.1-6. *Drying of Wood.*** A flat slab of Douglas fir wood 50.8 mm thick and containing 30 wt % moisture is being dried from both sides (neglecting ends and edges). The equilibrium moisture content at the surface of the wood due to the drying air blown over it is held at 5 wt % moisture. The drying can be

assumed to be represented by a diffusivity of  $3.72 \times 10^{-6} \text{ m}^2/\text{h}$ .

Calculate the time for the center to reach 10% moisture.

**20.2-1. *Unsteady-State Diffusion and Reaction.*** Solute *A* is diffusing at unsteady state into a semi-infinite medium of pure *B* and undergoes a first-order reaction with *B*. Solute *A* is dilute. Calculate the concentration  $c_A$  at points  $z = 0, 4$ , and  $10 \text{ mm}$  from the surface for  $t = 1 \times 10^5 \text{ s}$ . Physical property data are  $D_{AB} = 1 \times 10^{-9} \text{ m}^2/\text{s}$ ,  $k' = 1 \times 10^{-4} \text{ s}^{-1}$ ,  $c_{A0} = 1.0 \text{ kg mol/m}^3$ . Also calculate the  $\text{kg mol absorbed/m}^2$ .

**20.3-1. *Numerical Method for Unsteady-State Diffusion.*** A solid slab  $0.01 \text{ m}$  thick has an initial uniform concentration of solute *A* of  $1.00 \text{ kg}$

mol/m<sup>3</sup>. The diffusivity of A in the solid is  $D_{AB} = 1.0 \times 10^{-10}$  m<sup>2</sup>/s. All surfaces of the slab are insulated except the top surface. The surface concentration is suddenly dropped to zero concentration and held there. Unsteady-state diffusion occurs in the one  $x$  direction with the rear surface insulated. Using a numerical method, determine the concentrations after  $12 \times 10^4$  s. Use  $\Delta x = 0.002$  m and  $M = 2.0$ . The value of  $K$  is 1.0.

**Ans.**

$c_1=0$  (front surface,  $x=0$  m )  $c_2=0.3125$  kg mol/0.008 m)  $c_6=0.9375$ (insulated surface,  $x=0.01$  m)

### **20.3-2. Digital Computer and**

**Unsteady-State Diffusion.** Using the conditions of Problem 20.3-1, solve that problem by digital computer. Use  $\Delta x =$

0.0005 m. Write the spreadsheet program and plot the final concentrations. Use the explicit method,  $M = 2$ .

**20.3-3. Numerical Method and Different Boundary Condition.** Use the same conditions as for Example 20.3-1, but in this case the rear surface is not insulated. At time  $t = 0$ , the concentration at the rear surface is also suddenly changed to  $c_5 = 0$  and held there. Calculate the concentration profile after 2500 s. Plot the initial and final concentration profiles and compare with the final profile of Example 20.3-1.

### References

### Notations



# Chapter 21. Convective Mass Transfer

## 21.0 Chapter Objectives

On completion of this chapter, a student should be able to:

- Distinguish between the mass-transfer coefficients for the two classic cases: (a) equimolar counterdiffusion and (b) adiffusing through stagnant, nondiffusing B
- Recognize the analogies among mass, heat, and momentum transfer
- Use the Buckingham method to determine the number of dimensionless parameters
- Derive equations that allow prediction of heat-transfer coefficients for a flat plate with laminar flow
- Calculate mass-transfer coefficients for situations described in the chapter; for example, calculating the mass transfer coefficient for flow inside a pipe
- Explain the differences between the four basic models for mass-transfer coefficients

## 21.1 Convective Mass Transfer

### 21.1A Introduction to Convective Mass Transfer

In the previous sections, we have emphasized molecular diffusion in stagnant fluids or fluids in laminar flow. In many cases, the rate of diffusion is slow and more rapid transfer is desired. To do this, the fluid velocity is increased until turbulent mass transfer occurs.

To have a fluid in convective flow usually requires the fluid to be flowing past another immiscible fluid or a solid surface. An example is a fluid flowing in a pipe, where part of the pipe wall is made by a slightly dissolving solid material such as benzoic acid. The benzoic acid dissolves and is transported perpendicularly to the main stream from



the wall. When a fluid is in turbulent flow and is flowing past a surface, the actual velocity of small particles of fluid cannot be described clearly as in laminar flow. In laminar flow, the fluid flows in streamlines and its behavior can usually be described mathematically. However, in turbulent motion, there are no streamlines; instead, there are large eddies or “chunks” of fluid moving rapidly in seemingly random fashion.

When a solute  $A$  is dissolving from a solid surface, there is a high concentration of this solute in the fluid at the surface, and its concentration, in general, decreases as the distance from the wall increases. However, minute samples of fluid adjacent to each other do not always have concentrations close to each other. This occurs because

eddies having solute in them move rapidly from one part of the fluid to another, transferring relatively large amounts of solute. This turbulent diffusion or eddy transfer is quite fast in comparison to molecular transfer.

Three regions of mass transfer can be visualized. In the first, which is adjacent to the surface, a thin, viscous sublayer film is present. Most of the mass transfer occurs by molecular diffusion, since few or no eddies are present. A large concentration drop occurs across this film as a result of the slow diffusion rate.

The transition or buffer region is adjacent to the first region. Some eddies are present, and the mass transfer is the sum of turbulent and molecular

diffusion. There is a gradual transition in this region from the transfer by mainly molecular diffusion at one end to mainly turbulent at the other end.

In the *turbulent region* adjacent to the buffer region, most of the transfer is by turbulent diffusion, with a small amount by molecular diffusion. The concentration decrease is very small here since the eddies tend to keep the fluid concentration uniform. A more detailed discussion of these three regions is given in Chapter 11.

A typical plot for the mass transfer of a dissolving solid from a surface to a turbulent fluid in a conduit is given in Fig. 21.1-1. The concentration drop from  $c_{A1}$  adjacent to the surface is very abrupt close to the surface and then

levels off. This curve is very similar to the shapes found for heat and momentum transfer. The average or mixed concentration  $c_A^-$  is shown and is slightly greater than the minimum  $c_{A2}$ .

### 21.1B Types of Mass-Transfer Coefficients

*1. Definition of mass-transfer coefficient.* Since our understanding of turbulent flow is incomplete, we attempt to write the equations for turbulent diffusion in a manner similar to that for molecular diffusion. For turbulent mass transfer for constant  $c$ , Eq. (18.1-6), is written as

$$J_A^* = -(D_{AB} + \epsilon_M) \frac{dc_A}{dz} \quad (21.1-1)$$

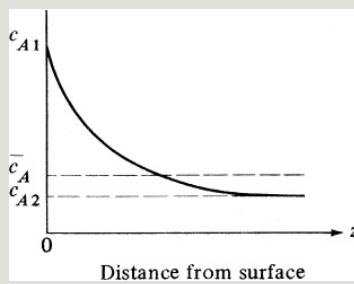


Figure 21.1-1. Concentration profile in turbulent mass transfer from a surface to a fluid.

where  $D_{AB}$  is the molecular diffusivity in  $\text{m}^2/\text{s}$  and  $\epsilon_M$  the mass eddy diffusivity in  $\text{m}^2/\text{s}$ . The value of  $\epsilon_M$  is variable and is near zero at the interface or surface, and increases as the distance from the wall increases. We therefore use an average value  $\bar{\epsilon}_M$  since the variation of  $\epsilon_M$  is not generally known. Integrating Eq. (21.1-1) between points 1 and 2,

$$J_A^* D_{AB} + \bar{\epsilon}_M z_2 - z_1 (c_{A1} - c_{A2}) \quad (21.1-2)$$

The flux  $J_A^*$  is based on the surface area  $A_1$  since the cross-sectional area

may vary. The value of  $z_2 - z_1$ , the distance of the path, is often not known. Hence, Eq. (21.1-2) is simplified and is written using a convective mass-transfer coefficient  $k_c'$

$$J_A^* = k_c'(c_{A1} - c_{A2}) \quad (21.1-3)$$

where  $J_A^*$  is the flux of A from the surface  $A_1$  relative to the whole bulk phase,  $k_c'$  is  $(D_{AB} + \epsilon^{-1}M)/(z_2 - z_1)$ , an experimental mass-transfer coefficient in  $\text{kg mol/s} \cdot \text{m}^2 \cdot (\text{kg mol/m}^3)$  or simplified as  $\text{m/s}$ , and  $c_{A2}$  is the concentration at point 2 in  $\text{kg mol A/m}^3$  or, more usually, the average bulk concentration  $\bar{c}_A$ . This definition of a convective mass-transfer coefficient  $k_c'$  is quite similar to the convective heat-transfer coefficient  $h$ .

2. *Mass-transfer coefficient for equimolar counterdiffusion.* Generally, we are interested in  $N_A$ , the flux of A relative to stationary coordinates. We can start with the following equation, which is similar to that for molecular diffusion with the term  $\epsilon M$  added:

$$N_A = -c(D_{AB} + \epsilon M) \frac{dx_A}{dz} + x_A(N_A + N_B) \quad (21.1-4)$$

For the case of equimolar counterdiffusion, where  $N_A = -N_B$ , and integrating at steady state, calling  $k_c' = (D_{AB} + \epsilon M)/(z_2 - z_1)$ ,

$$N_A = k_c'(c_{A1} - c_{A2}) \quad (21.1-5)$$

Equation (21.1-5) is the defining equation for the mass-transfer coefficient. However, we often define the concentration in terms of mole

fraction if a liquid or gas, or in terms of partial pressure if a gas. Hence, we can define the mass-transfer coefficient in several ways. If  $y_A$  is mole fraction in a gas phase and  $x_A$  in a liquid phase, then Eq. (21.1-5) can be written as follows for equimolar counterdiffusion:

$$\text{Gases: } N_A = k_c'(c_{A1} - c_{A2}) = k_G'(p_{A1} - p_{A2}) = k_y'(y_{A1} - y_{A2}) \quad (21.1-6)$$

$$\text{Liquids: } N_A = k_c'(c_{A1} - c_{A2}) = k_L'(c_{A1} - c_{A2}) = k_x'(x_{A1} - x_{A2}) \quad (21.1-7)$$

All of these mass-transfer coefficients can be related to each other. For example, using Eq. (21.1-6) and substituting  $y_{A1} = c_{A1}/c$  and  $y_{A2} = c_{A2}/c$  into the equation,

$$N_A = k_c'(c_{A1} - c_{A2}) = k_y'(y_{A1} - y_{A2}) = k_y'(c_{A1}/c - c_{A2}/c) = k_y'c(c_{A1} - c_{A2})$$



$$c_A^2)(21.1-8)$$

Hence,

$$k_c' = k_y' c \quad (21.1-9)$$

These relations among mass-transfer coefficients, together with the various flux equations, are given in Table 21.1-1.

Table 21.1-1. *Flux Equations and Mass-Transfer Coefficients*

--	--

3. *Mass-transfer coefficient for A diffusing through stagnant, nondiffusing B.* For A diffusing through stagnant, nondiffusing B, where  $N_B = 0$ , Eq. (21.1-4) gives for steady state

$$N_A = k_c$$

$$x_{BM}(c_{A1} - c_{A2}) = k_c(c_{A1} - c_{A2})N_A = k_x$$

$$x_{BM}(x_{A1} - x_{A2}) = k_x(x_{A1} - x_{A2})$$

$$(21.1-10)$$

where the  $x_{BM}$  and its counterpart  $y_{BM}$  are similar to Eq. (19.1-12) and  $k_c$  is the mass-transfer coefficient for  $A$  diffusing through stagnant  $B$ . Also,

$$x_{BM} = x_{B2} - x_{B1} \ln(x_{B2}/$$

$$x_{B1}) \quad y_{BM} = y_{B2} - y_{B1} \ln(y_{B2}/y_{B1})$$

$$(21.1-11)$$

Rewriting Eq. (21.1-10) using other units,

$$(\text{Gases}): N_A = k_c(c_{A1} -$$

$$c_{A2}) = k_G(p_{A1} - p_{A2}) = k_y(y_{A1} - y_{A2})$$

$$(21.1-12)$$

$$(\text{Liquids}): N_A = k_c(c_{A1} -$$

$$c_{A2}) = k_L(c_{A1} - c_{A2}) = k_x(x_{A1} - x_{A2}) \quad (21.1-13)$$

Again, all the mass-transfer coefficients can be related to each other and are given in Table 21.1-1. For example, setting Eq. (21.1-10) equal to (21.1-13),

$$N_A = k_c' x_B M(c_{A1} - c_{A2}) = k_x(x_{A1} - x_{A2}) = k_x(c_{A1}c - c_{A2}c) \quad (21.1-14)$$

Hence,

$$k_c' x_B M = k_x c \quad (21.1-15)$$

**EXAMPLE 21.1-1. Vaporizing A and Convective Mass Transfer**

A large volume of pure gas *B* at 2 atm pressure is flowing over a surface from which pure *A* is vaporizing. The liquid *A* completely wets the surface, which is a blotting paper. Hence, the partial pressure of *A* at the surface is the vapor pressure of *A* at 298 K, which is 0.20 atm. The  $k_y'$  has been estimated to be  $6.78 \times 10^{-5} \text{ kg mol/s} \cdot \text{m}^2 \cdot \text{mol frac}$ . Calculate  $N_A$ , the vaporization rate, and also the value of  $k_y$  and  $k_G$ .

**Solution:** This is the case of *A* diffusing through *B*, where the flux of *B* normal to the surface is zero, since *B* is not soluble in liquid *A*.  $p_{A1} = 0.20 \text{ atm}$  and  $p_{A2} = 0$  in the pure

gas *B*. Also,  $y_{A1} = p_{A1}/P = 0.20/2.0 = 0.10$  and  $y_{A2} = 0$ . We can use Eq. (21.1-12) with mole fractions:

$$N_A = k_y(y_{A1} - y_{A2}) \quad (21.1-12)$$

However, we have a value for  $k_y'$  which is related to  $k_y$  from Table 21.1-1 by

$$k_y y_{BM} = k_y' \quad (21.1-16)$$

The term  $y_{BM}$  is similar to  $x_{BM}$  and is, from Eq. (21.1-11),

$$y_{BM} = y_{B2} - y_{B1} \ln(y_{B2}/y_{B1}) / y_{B1} = 1 - y_{A1} = 1 - 0.10 = 0.90 \quad y_{B2} = 1 - y_{A2} = 1 - 0 = 1.0 \quad (21.1-11)$$

Substituting into Eq. (21.1-11),

$$y_{BM} = 1.0 - 0.90 \ln(1.0/0.90) = 0.95$$

Then, from Eq. (21.1-16),

$$k_y = k_y' y_{BM} = 6.78 \times 10^{-5} \text{ kg mol}^{-1} \text{ m}^{-2} \text{ s}^{-1} \text{ mole}^{-1} \times 0.95 = 7.138 \times 10^{-5} \text{ kg mol}^{-1} \text{ m}^{-2} \text{ s}^{-1} \text{ mole}^{-1}$$

Also, from Table 21.1-1,

$$k_{GyBMP} = k_y y_{BM} \quad (21.1-17)$$

Hence, solving for  $k_G$  and substituting knowns,

$$k_G = k_y P = 7.138 \times 10^{-5} \text{ kg mol}^{-1} \text{ m}^{-2} \text{ s}^{-1} \text{ mole}^{-1} \times 1.01325 \times 10^5 \text{ Pa} = 3.522 \times 10^{-10} \text{ kg mol}^{-1} \text{ m}^{-2} \text{ s}^{-1} \text{ Pa}^{-1} \quad k_G = k_y P = 7.138 \times 10^{-5} \text{ kg mol}^{-1} \text{ m}^{-2} \text{ s}^{-1} \text{ mole}^{-1} \times 1.01325 \times 10^5 \text{ Pa} = 3.522 \times 10^{-10} \text{ kg mol}^{-1} \text{ m}^{-2} \text{ s}^{-1} \text{ Pa}^{-1}$$

For the flux, using Eq. (21.1-12),

$$N_A = k_y(y_{A1} - y_{A2}) = 7.138 \times 10^{-5} \text{ kg mol}^{-1} \text{ m}^{-2} \text{ s}^{-1} (0.1 - 0) = 7.138 \times 10^{-6} \text{ kg mol}^{-1} \text{ m}^{-2} \text{ s}^{-1}$$

Also,

$$p_{A1} = 0.20 \text{ atm} = 0.20(1.01325 \times 10^5) = 2.026 \times 10^4 \text{ Pa}$$

Using Eq. (21.1-12) again,

$$N_A = k_G(p_{A1} - p_{A2}) = 3.552 \times 10^{-10} \text{ kg mol}^{-1} \text{ m}^{-2} \text{ s}^{-1} \text{ Pa}^{-1} (2.026 \times 10^4 \text{ Pa} - 0) \quad N_A = 7.138 \times 10^{-6} \text{ kg mol}^{-1} \text{ m}^{-2} \text{ s}^{-1} \quad N_A = k_G(p_{A1} - p_{A2}) = 3.552 \times 10^{-10} \text{ kg mol}^{-1} \text{ m}^{-2} \text{ s}^{-1} \text{ Pa}^{-1} (2.026 \times 10^4 \text{ Pa} - 0) \quad N_A = 7.138 \times 10^{-6} \text{ kg mol}^{-1} \text{ m}^{-2} \text{ s}^{-1}$$

$$pA_2 = 3.569 \times 10^{-5} \text{ kg mol}^{-1} \cdot \text{atm} (0.2 \text{ atm} - 0) N_A = 7.138 \times 10^{-6} \text{ kg mol}^{-1} \cdot \text{m}^2$$

Note that in this case, since the concentrations were dilute,  $y_{BM}$  is close to 1.0 and  $k_y$  and  $k_y'$  differ very little.

### 21.1C Mass-Transfer Coefficients for the General Case of A and B Diffusing and Convective Flow Using Film Theory

Equation (21.1-4) can be integrated assuming a simplified film theory where the mass transfer is assumed to occur through a thin film next to the wall of thickness  $\delta_f$  and by molecular diffusion. Then, the experimental value of  $k_c'$  for dilute solutions is used to determine the film thickness  $\delta_f$ :

$$k_c' = D_{AB} / \delta_f \quad (21.1-18)$$

Rewriting Eq. (21.1-4),

$$N_A = c D_{AB} \frac{dx}{dz} + x_A (N_B + N_B) \quad (21.1-19)$$

The convective term is  $x_A(N_A + N_B)$ .

Rearranging and integrating,

$$1/c_D A B \int_{z=0}^z -\delta f = - \int_{x_A1}^{x_A2} dx_A N_A - x_A (N_A + N_B) \quad (21.1-20)$$

$$N_A = N_A N_A + N_B k c' \ln [N_A / (N_A + N_B) - x_A2 N_A / (N_A + N_B) - x_A1] \quad (21.1-21)$$

For  $N_B = 0$ , Eq. (21.1-21) reduces to Eq. (21.1-10).

### **21.1D Mass-Transfer Coefficients under High Flux Conditions**

The final Eq. (21.1-21) is a result of assuming the film theory where molecular diffusion occurs across the film  $\delta_f$ . This assumes that this film thickness is unaffected by high fluxes and bulk or convective flow

(diffusion-induced convection). As a result, other definitions of the mass-transfer coefficient that include this effect of diffusion-induced convection have been derived. One common method by Bird et al. (B1) and Skelland (S8) is given as follows for the case of  $A$  diffusing through stagnant, nondiffusing  $B$  where diffusion-induced convection is present.

Rewriting Eq. (21.1-19) for the flux  $N_A$  at the surface  $z = 0$  where  $x_A = x_{A1}$ ,

$$N_A = -cD_{AB} \left( \frac{dx_A}{dz} \right)_{z=0} + x_{A1} (N_A + 0) \quad (21.1-22)$$

Note that the convective term is defined in terms of  $x_{A1}$  and not the average value.

Defining a mass-transfer coefficient in terms of the diffusion flux,

$$-cD_{AB}(dx_A/dz)_{z=0} = k_{c0}c(x_{A1} - x_{A2}) \quad (21.1-23)$$

Substituting Eq. (21.1-23) into (21.1-22) and solving for  $N_A$ ,

$$N_A = k_{c0}c(x_{A1} - x_{A2}) / (1 - x_{A1}) \quad (21.1-24)$$

At low concentrations and fluxes,  $k_{c0}$  approaches  $k_c'$  for no bulk flow, or  $N_A = k_c'(x_{A1} - x_{A2})$ .

In general, a coefficient  $k_c$  may be defined without regard to convective flow:

$$N_A = k_{cc}(x_{A1} - x_{A2}) \quad (21.1-25)$$

Combining Eqs. (21.1-24) and



(21.1-25),

$$k_{c0} = (1 - x_{A1})k_c \quad (21.1-26)$$

The relationship between  $k_{c0}$  or  $k_c$  for high flux and  $k_c'$  for low flux will be considered. These corrections or relationships will be derived using the film theory for the transfer of  $A$  by molecular diffusion and convective flow, with  $B$  being stagnant and nondiffusing. This has been done previously and is obtained by setting  $N_B = 0$  in Eq. (21.1-21) to obtain the following, which is identical to Eq. (21.1-10):

$$N_A = k_c' x_{BM}(c_{A1} - c_{A2}) = k_c(c_{A1} - c_{A2}) \quad (21.1-27)$$

Hence, for the film theory,

$$k_c k_c' = 1 + x_B M = k_x k_x' \quad (21.1-28)$$

Combining Eqs. (21.1-26) and (21.1-28),

$$k_c k_c' = 1 + x_A M = k_x k_x' \quad (21.1-29)$$

For this film theory, Eqs. (21.1-28) and (21.1-29) are independent of the Schmidt number. These correction factors predicted by the film theory give results that are reasonably close to those using more complex theories—the penetration theory and boundary layer theory—that are discussed later in Section 21.5C. An advantage of this simple film theory is that it is quite useful in solving complex systems.

**EXAMPLE 21.1-2. High-Flux Correction Factors**

Toluene A is evaporating from a wetted porous slab by having inert pure air at 1 atm flowing parallel to the flat surface. At a certain point, the mass-transfer coefficient  $k_x'$  for very low fluxes has been estimated as 0.20 lb mol/hr ·

ft<sup>2</sup>. The gas composition at the interface at this point is  $x_{A1} = 0.65$ . Calculate the flux  $N_A$  and the ratios  $k_c/k_c'$  or  $k_x/k_x'$  and  $k_{c0}/k_c'$  or  $k_{x0}/k_x'$  to correct for high flux.

**Solution:** For the flux  $N_A$ , using Eq. (21.1-11),

$$x_{BM} = x_{B2} - x_{B1} \ln(x_{B2}/x_{B1}) = 1.00 - 0.35 \ln(1.00/0.35) = 0.619$$

Using Eq. (21.1-10) in terms of  $k_x'$  where  $k_c'c = k_x'$

$$N_A = k_x' x_{BM} (x_{A1} - x_{A2}) = 0.20 \text{ lbmol/hr-ft}^2 \cdot 0.619 (0.65 - 0) = 0.210 \text{ lbmol/hr-ft}^2$$

Using Eq. (21.1-28),

$$k_c k_c' = k_x k_x' = 1 x_{BM} = 10.619 = 1.616$$

Then,  $k_x = 1.616 k_x' = 1.616 (0.20 \text{ lbmol/hr-ft}^2) = 0.323 \text{ lbmol/hr-ft}^2$ .

Using Eq. (21.1-29),

$$k_{c0} k_c = k_{x0} k_x = 1 - x_{A1} x_{BM} = 1 - 0.650 \cdot 0.619 = 0.565$$

and  $k_{x0} = 0.565 (0.200) = 0.113 \text{ lb mol/hr} \cdot \text{ft}^2$ .

## 21.1E Methods for Experimentally Determining Mass-Transfer Coefficients

Many different experimental methods have been employed to obtain mass-transfer coefficients. In determining the mass-transfer coefficient to a sphere, Steele and Geankoplis (S3) used a solid sphere of benzoic acid held rigidly by a rear support in a pipe. Before the run, the

sphere was weighed. After flow of the fluid for a timed interval, the sphere was removed, dried, and weighed again to give the amount of mass transferred, which was small compared to the weight of the sphere. From the mass transferred and the area of the sphere, the flux  $N_A$  was calculated. Then, the driving force ( $c_{AS} - 0$ ) was used to calculate  $k_L$ , where  $c_{AS}$  is the solubility and the water contained no benzoic acid.

Another method used is to flow gases over various geometries that are wet with evaporating liquids. For mass transfer from a flat plate, a porous blotter wet with the liquid serves as the plate.

If the solution is quite dilute, then the

mass-transfer coefficient measured is  $k_c \cong k_c'$  and the dilute low-flux coefficient  $k_c'$  or  $k_x'$  is experimentally obtained.

## **21.2 Dimensional Analysis in Mass Transfer**

### **21.2A Introduction**

The use of dimensional analysis enables us to predict the various dimensional groups that are very helpful in correlating experimental mass-transfer data. As we saw for fluid flow and heat transfer, the Reynolds number, Prandtl number, Grashof number, and Nusselt number are often used in correlating experimental data. The Buckingham theorem discussed in Section 15.1C states that the functional relationship among  $q$  quantities or variables

whose units may be given in terms of  $u$  fundamental units or dimensions may be written as  $(q - u)$  dimensionless groups.

### **21.2B Dimensional Analysis for Convective Mass Transfer**

We consider a case of convective mass transfer where a fluid is flowing by forced convection in a pipe and mass transfer is occurring from the wall to the fluid. The fluid flows at a velocity  $v$  inside a pipe of diameter  $D$ , and we wish to relate the mass-transfer coefficient  $k_c'$  to the variables  $D$ ,  $\rho$ ,  $\mu$ ,  $v$ , and  $D_{AB}$ . The total number of variables is  $q = 6$ . The fundamental units or dimensions are  $u = 3$  and are mass  $M$ , length  $L$ , and time  $t$ . The units of the variables are

$$k c$$

$$'=L t \rho =M L^3 \mu =M L t v =L t D A B =L^2 t D =L$$

The number of dimensionless groups of  $\pi$ 's are then  $6 - 3$ , or  $3$ . Then,

$$\pi_1 = f(\pi_2, \pi_3) \quad (21.2-1)$$

We choose the variables  $DAB$ ,  $\rho$ , and  $D$  to be the variables common to all the dimensionless groups, which are

$$\pi_1 = D A B a \rho^b D^c k c' \quad (21.2-2)$$

$$\pi_2 = D A B d \rho e D^f v \quad (21.2-3)$$

$$\pi_3 = D A B g \rho h D^j \mu \quad (21.2-4)$$

For  $\pi_1$ , we substitute the actual dimensions as follows:

$$1 = (L^2 t)^a (M L^3)^b (L)^c (L t)^d \quad (21.2-5)$$

Summing for each exponent,

$$(L)^0 = 2a - 3b + c + 1 \quad (M)^0 = b \quad (t)^0 = a - 1 \quad (21.2-6)$$

Solving these equation simultaneously,  $a = -1$ ,  $b = 0$ ,  $c = 1$ . Substituting these values into Eq. (21.2-2),

$$\pi_1 = k c' D D A B = N S h \quad (21.2-7)$$

Repeating for  $\pi_2$  and  $\pi_3$ ,

$$\pi_2 = v D D A B \quad (21.2-8)$$

$$\pi_3 = \mu \rho D A B = N S c \quad (21.2-9)$$

If we divide  $\pi_2$  by  $\pi_3$  we obtain the Reynolds number:

$$\frac{\pi_2}{\pi_3} = \frac{v D A B}{(\mu \rho D A B)} = \frac{D v \rho}{\mu} = N R c \quad (21.2-10)$$



Hence, substituting into Eq. (21.2-1),

$$N_{Sh}=f(N_{Re},N_{Sc}) \quad (21.2-11)$$

## **21.3 Mass-Transfer Coefficients for Various Geometries**

### **21.3A Dimensionless Numbers Used to Correlate Data**

The experimental data for mass-transfer coefficients obtained using various kinds of fluids, different velocities, and different geometries are correlated using dimensionless numbers similar to those for heat and momentum transfer. Methods of dimensional analysis are discussed in Sections 15.1 and 21.2.

The most important dimensionless number is the Reynolds number  $N_{Re}$ , which indicates degree of turbulence:

$$N_{Re} = L v \rho \mu \quad (21.3-1)$$

where  $L$  is diameter  $D_p$  is for a sphere, diameter  $D$  is for a pipe, or length  $L$  is for a flat plate. The velocity  $v$  is the mass average velocity in a pipe. In a packed bed, the superficial velocity  $v'$  in the empty cross section is often used, or sometimes  $v = v'/\epsilon$  is used, where  $v$  is the interstitial velocity and  $\epsilon$  is the void fraction of a bed.

The *Schmidt number* is

$$N_{Sc} = \mu \rho D_A B \quad (21.3-2)$$

The viscosity  $\mu$  and density  $\rho$  used are for the actual flowing mixture of solute  $A$  and fluid  $B$ . If the mixture is dilute, properties of the pure fluid  $B$  can be used. The Prandtl number  $c_p \mu / k$  for heat transfer is analogous to the Schmidt

number for mass transfer. The Schmidt number is the ratio of the shear component for diffusivity  $\mu/\rho$  to the diffusivity for mass transfer  $D_{AB}$ ; it physically relates the relative thickness of the hydrodynamic layer and mass-transfer boundary layer.

The *Sherwood number*, which is dimensionless, is

$$N_{Sh} = kc'LD_{AB} = kcy_BMLD_{AB} = kx'cLD_{AB} = \dots (21.3-3)$$

Other substitutions from Table 21.1-1 can be made for  $kc'$  in Eq. (21.3-3).

The *Stanton number* occurs often and is

$$N_{St} = kc'v = ky'GM = kG'PGM = \dots (21.3-4)$$

Again, substitution for  $kc'$  can be made:

$$G_M = v\rho/M_{av} = vC.$$

The mass-transfer coefficient is often correlated as a dimensionless  $JD$  factor, which is related to  $kc'$  and  $N_{Sh}$  as follows:

$$JD = kc'v/(N_{Sc})^{2/3} = kG_M/(N_{Sc})^{2/3} = N_{Sh}/(N_{Re}N_{Sc})^{1/3} \quad (21.3-5)$$

For heat transfer, a dimensionless  $JH$  factor is as follows:

$$JH = hcpG/(N_{Pr})^{2/3} \quad (21.3-6)$$

### **21.3B Analogies among Mass, Heat, and Momentum Transfer**

*1. Introduction.* In molecular transport of momentum, heat, or mass, there are many similarities,

which were pointed out in Chapters 2–15. The molecular diffusion equations of Newton for momentum, Fourier for heat, and Fick for mass are very similar, and we can say that we have analogies among these three molecular transport processes. There are also similarities in turbulent transport, as discussed in Sections 15.2C and 18.1A, where the flux equations were written using the turbulent eddy momentum diffusivity  $\epsilon_t$ , the turbulent eddy thermal diffusivity  $\alpha_t$ , and the turbulent eddy mass diffusivity  $\epsilon_M$ . However, these similarities are not as well defined mathematically or physically and are more difficult to relate to each other.

A great deal of effort in the literature has

been devoted to developing analogies among these three transport processes for turbulent transfer so as to allow prediction of one from any of the others. We discuss several next.

*2. Reynolds analogy.* Reynolds was the first to note similarities in transport processes and relate turbulent momentum and heat transfer. Since then, mass transfer has also been related to momentum and heat transfer. We derive this analogy from Eqs. (18.1-4)–(18.1-6) for turbulent transport. For fluid flow in a pipe, for heat transfer from the fluid to the wall, Eq. (18.1-5) becomes as follows, where  $z$  is distance from the wall:

$$q_A = -\rho c_p (\alpha + \alpha_t) dT/dz \quad (21.3-7)$$

For momentum transfer, Eq. (18.1-4) becomes

$$\tau = -\rho(\mu\rho + \epsilon_t)dv/dz \quad (21.3-8)$$

Next, we assume that  $\alpha$  and  $\mu/\rho$  are negligible and that  $\alpha_t = \epsilon_t$ . Then, dividing Eq. (21.3-7) by (21.3-8),

$$(\tau q/A) c_p dT = dv \quad (21.3-9)$$

If we assume that heat flux  $q/A$  in a turbulent system is analogous to momentum flux  $\tau$ , the ratio  $\tau/(q/A)$  must be constant for all radial positions. We now integrate between conditions at the wall where  $T = T_i$  and  $v = 0$  to some point in the fluid where  $T$  is the same as the bulk  $T$ , and assume that the velocity at this point is the same as  $v_{av}$ , the bulk velocity. Also,  $q/A$  is understood to be the flux at the wall, as is the shear at the

wall, written as  $\tau_s$ . Hence,

$$\tau_q/A_{cp}(T-T_i)=v_{av}-0 \quad (21.3-10)$$

Also, substituting  $q/A = h(T - T_i)$  and  $\tau_s = f v_{av}^2 \rho / 2$  from into Eq. (21.3-10),

$$f/2 = h_{cp} v_{av} \rho = h_{cp} G \quad (21.3-11)$$

In a similar manner, using Eq. (18.1-6) for  $J_A^*$  and  $J_A^* = k_c'(c_{A1} - c_{A2})$ , we can relate this to Eq. (21.3-8) for momentum transfer. Then, the complete Reynolds analogy is

$$f/2 = h_{cp} G = k_c' v_{av} \quad (21.3-12)$$

Experimental data for gas streams agree approximately with Eq. (21.3-12) if the Schmidt and Prandtl numbers are near 1.0 and only skin friction is present in flow past a flat plate or inside a pipe.



When liquids are present and/or form drag is present, the analogy is not valid.

*3. Other analogies.* The Reynolds analogy assumes that the turbulent diffusivities  $\epsilon_t$ ,  $\alpha_t$ , and  $\epsilon_M$  are all equal and that the molecular diffusivities  $\mu/\rho$ ,  $\alpha$ , and  $D_{AB}$  are negligible compared to the turbulent diffusivities. When the Prandtl number  $(\mu/\rho)/\alpha$  is 1.0, then  $\mu/\rho = \alpha$ ; also, for  $N_{Sc} = 1.0$ ,  $\mu/\rho = D_{AB}$ . Then,  $(\mu/\rho + \epsilon_t) = (\alpha + \alpha_t) = (D_{AB} + \epsilon_M)$  and the Reynolds analogy can be obtained with the molecular terms present. However, the analogy breaks down when the viscous sublayer becomes important, since the eddy diffusivities diminish to zero and the molecular diffusivities become important.

Prandtl modified the Reynolds analogy

by writing the regular molecular diffusion equation for the viscous sublayer and a Reynolds analogy equation for the turbulent core region. Then, since these processes are in series, these equations were combined to produce an overall equation (G1). The results again are poor for fluids where the Prandtl and Schmidt numbers differ from 1.0.

Von Kármán further modified the Prandtl analogy by considering the buffer region in addition to the viscous sublayer and the turbulent core. These three regions are shown in the universal velocity profile in Fig. 11.2-2. Again, an equation is written for molecular diffusion in the viscous sublayer using only the molecular diffusivity and a Reynolds analogy equation for the

turbulent core. Both the molecular and eddy diffusivity are used in an equation for the buffer layer, where the velocity in this layer is used to obtain an equation for the eddy diffusivity. These three equations are then combined to give the von Kármán analogy. Since then, numerous other analogies have appeared (P1, S4).

*4. Chilton and Colburn J-factor analogy.* The most successful and most widely used analogy is the Chilton and Colburn *J*-factor analogy (C2). This analogy is based on experimental data for gases and liquids in both the laminar and turbulent flow regions and is written as follows:

$$f_2 = J_H = h_{cp} G (N_{Pr})^{2/3} = J_D = k_c \\ \nu_{av} (N_{Pr})^{2/3} \quad (21.3-13)$$

Although this is an equation based on experimental data for both laminar and turbulent flow, it can be shown to satisfy the exact solution derived from laminar flow over a flat plate in Section 15.2.

Equation (21.3-13) has been shown to be quite useful in correlating momentum, heat, and mass-transfer data. It permits the prediction of an unknown transfer coefficient when one of the other coefficients is known. In momentum transfer, the friction factor is obtained for the total drag or friction loss, which includes form drag or momentum losses due to blunt objects as well as skin friction. For flow past a flat plate or in a pipe, where no form drag is present,  $f/2 = J_H = J_D$ . When form drag is present, as in flow in packed beds or past other blunt objects,

$f/2$  is greater than  $J_H$  or  $J_D$ , and  $J_H \cong J_D$ .

### 21.3C Derivation of Mass-Transfer Coefficients in Laminar Flow

*1. Introduction.* When a fluid is flowing in laminar flow and mass transfer by molecular diffusion is occurring, the equations are very similar to those for heat transfer by conduction in laminar flow. The phenomena of heat and mass transfer are not always completely analogous, since in mass transfer several components may be diffusing. Also, the flux of mass perpendicular to the direction of the flow must be small so as not to distort the laminar velocity profile.

In theory, it is not necessary to have experimental mass-transfer coefficients for laminar flow, since the equations for

momentum transfer and diffusion can be solved. However, in many actual cases, it is difficult to describe mathematically the laminar flow for certain geometries, such as flow past a cylinder or in a packed bed. Hence, experimental mass-transfer coefficients are often obtained and correlated. A simplified theoretical derivation will be given for two cases of laminar flow.

*2. Mass transfer in laminar flow in a tube.* We consider the case of mass transfer from a tube wall to a fluid inside in laminar flow, where, for example, the wall is made of solid benzoic acid that is dissolving in water. This is similar to heat transfer from a wall to the flowing fluid where natural convection is negligible. For fully developed flow, the parabolic velocity derived as Eqs.

(4.1-18) and (4.1-20) is

$$v_x = v_{\max} [1 - (r/R)^2] = 2v_{\text{av}} [1 - (r/R)^2] \quad (21.3-14)$$

where  $v_x$  is the velocity in the  $x$  direction at the distance  $r$  from the center. For steady-state diffusion in a cylinder, a mass balance can be made on a differential element where the rate in by convection plus diffusion equals the rate out radially by diffusion to give

$$v_x \partial c_A / \partial x = D_{AB} (1/r \partial c_A / \partial r + \partial^2 c_A / \partial r^2 + \partial^2 c_A / \partial x^2) \quad (21.3-15)$$

Then,  $\partial^2 c_A / \partial x^2 = 0$  if the diffusion in the  $x$  direction is negligible compared to that by convection. Combining Eqs. (21.3-14) and (21.3-15), the final solution (S1) is a complex series similar to the Graetz solution for heat transfer

and a parabolic velocity profile.

If it is assumed that the velocity profile is flat, as in rodlike flow, the solution is more easily obtained (S1). A third solution, called the approximate *Leveque solution*, has been obtained, where there is a linear velocity profile near the wall and the solute diffuses only a short distance from the wall into the fluid. This is similar to the parabolic-velocity-profile solution at high flow rates. Experimental design equations are presented in Section 21.3D for this case.

*3. Diffusion in a laminar falling film.* In Section 4.4, we derived the equation for the velocity profile in a falling film shown in Fig. 21.3-1a. We will consider mass transfer of solute A into a laminar falling film, which is important in



wetted-wall columns, in developing theories to explain mass transfer in stagnant pockets of fluids, and in turbulent mass transfer. The solute  $A$  in the gas is absorbed at the interface and then diffuses a distance into the liquid so that it has not penetrated the whole distance  $x = \delta$  at the wall. At steady state, the inlet concentration  $c_A = 0$ . The concentration profile of  $c_A$  at a point  $z$  distance from the inlet is shown in Fig. 21.3-1a.

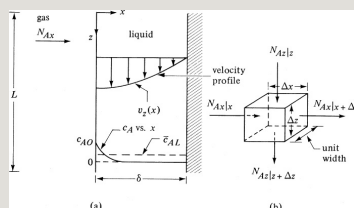


Figure 21.3-1. *Diffusion of solute A in a laminar falling film: (a) velocity profile and concentration profile, (b) small element for mass balance.*

A mass balance will be made on the element shown in Fig. 21.3-1b. For

steady state, rate of input = rate of output:

$$N_{Ax}|_x(1\Delta z) + N_{Az}|_z(1\Delta x) = N_{Ax}|_{x+\Delta x}(1\Delta z) + N_{Az}|_{z+\Delta z}(1\Delta x) \quad (21.3-16)$$

For a dilute solution, the diffusion equation for  $A$  in the  $x$  direction is

$$N_{Ax} = -DAB \partial c_A / \partial x + \text{zero convection} \quad (21.3-17)$$

For the  $z$  direction, the diffusion is negligible:

$$N_{Az} = 0 + c_A v_z \quad (21.3-18)$$

Dividing Eq. (21.3-16) by  $\Delta x \Delta z$ , letting  $\Delta x$  and  $\Delta z$  approach zero, and substituting Eqs. (21.3-17) and (21.3-18) into the result, we obtain

$$v_z \frac{\partial c_A}{\partial z} = DAB \frac{\partial^2 c_A}{\partial x^2} \quad (21.3-19)$$

From Eqs. (4.4-24) and (4.4-25), the velocity profile is parabolic and is  $v_z = v_{z \max} [1 - (x/\delta_2)^2]$ . Also,  $v_{z \max} = 3/2 v_{z \text{ av}}$ . If the solute has penetrated only a short distance into the fluid, that is, short contact times of  $t = z^2 / v_{\max}$ , then the  $A$  that has diffused has been carried along at the velocity  $v_{z \max}$ , or  $v_{\max}$  if the subscript  $z$  is dropped. Then, Eq. (21.3-19) becomes

$$\frac{\partial c_A}{\partial (z/v_{\max})} = DAB \frac{\partial^2 c_A}{\partial x^2} \quad (21.3-20)$$

Using the boundary conditions of  $c_A = 0$  at  $z = 0$ ,  $c_A = c_{A0}$  at  $x = 0$ , and  $c_A = 0$  at  $x = \infty$ , we can integrate Eq. (21.3-20) to obtain

$$c_A/c_{A0} = \text{erfc}(x \sqrt{4DABz/v_{\max}})$$

(20.3-21)

where  $\text{erf } y$  is the error function and  $\text{erfc } y = 1 - \text{erf } y$ . Values of  $\text{erf } y$  are standard tabulated functions.

To determine the local molar flux at the surface  $x = 0$  at position  $z$  from the top entrance, we write (B1)

$$N_{Ax}(z)|_{x=0} = -D_{AB} \left. \frac{\partial c_A}{\partial x} \right|_{x=0} = c_{A0} D_{AB} \nu_{\max} \pi z \quad (21.3-22)$$

The total moles of  $A$  transferred per second to the liquid over the entire length  $z = 0$  to  $z = L$ , where the vertical surface is unit width, is

$$N_{A(L \cdot 1)} = (1) \int_0^L (N_{Ax})|_{x=0} dz = (L \cdot 1) c_{A0} D_{AB} \nu_{\max} \pi \int_0^L z dz = (L \cdot 1) c_{A0} D_{AB} \nu_{\max} \pi \left( \frac{1}{2} L^2 \right)$$

The term  $L/\nu_{\max}$  is  $t_L$ , the time of

exposure of the liquid to the solute  $A$  in the gas. This means the rate of mass transfer is proportional to  $D_{AB}^{0.5}$  and  $1/tL^{0.5}$ . This is the basis for the penetration theory in turbulent mass transfer where pockets of liquid are exposed to unsteady-state diffusion (penetration) for short contact times.

### **21.3D Mass Transfer for Flow Inside Pipes**

*1. Mass transfer for laminar flow inside pipes.* When a liquid or gas is flowing inside a pipe and the Reynolds number  $Dv\rho/\mu$  is below 2100, laminar flow occurs.

Experimental data obtained for mass transfer from the walls for gases ( $G_2$ ,  $L_1$ ) are plotted in Fig. 21.3-2 for values of  $W/D_{AB}pL$  less than about 70. The ordinate is  $(c_A - c_{A0})/(c_{Ai} - c_{A0})$ , where  $c_A$  is the exit

concentration,  $c_{A0}$  is the inlet concentration, and  $c_{Ai}$  is the concentration at the interface between the wall and the gas. The dimensionless abscissa is  $W/D_{AB}\rho L$  or  $N_{Re}N_{Sc}(D/L)(\pi/4)$ , where  $W$  is the flow in kg/s and  $L$  is the length of the mass-transfer section in m. Since the experimental data follow the rodlike plot, that line should be used. The velocity profile is assumed fully developed to parabolic form at the entrance.

For liquids that have small values of  $D_{AB}$ , data follow the parabolic flow line, which is as follows for  $W/D_{AB}\rho L$  over 400:

$$c_A - c_{A0} = c_{Ai} - c_{A0} \left( 1 - \frac{2}{3} \left( \frac{W}{D_{AB}\rho L} \right)^{-2/3} \right) \quad (21.3-24)$$

2. *Mass transfer for turbulent flow inside pipes.* For turbulent flow when  $Du\rho/\mu > 2100$  for gases or liquids flowing inside a pipe,

$$NSh = kc$$

$$B = kcpBMPDDAB = 0.023(Du\rho\mu)^{0.83}(\mu\rho DAB)^{0.33} \quad (21.3-25)$$

The equation holds for  $N_{Sc}$  of 0.6 to 3000 (G2, L1). Note that the  $N_{Sc}$  for gases is in the range 0.5–3 and for liquids is above 100 in general.

Equation (21.3-25) for mass transfer and Eq. (15.3-5) for heat transfer inside a pipe are similar to each other.

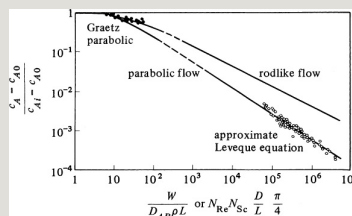


Figure 21.3-2. Data for diffusion in a fluid in streamline flow inside a pipe: filled circles, vaporization data of Gilliland and Sherwood (G2); open circles, dissolving-solids data of Linton and Sherwood (L1). W. H. Linton and T. K. Sherwood, Chem. Eng. Progr., **46**,

*3. Mass transfer for flow inside wetted-wall towers.* When a gas is flowing inside the core of a wetted-wall tower, the same correlations that are used for mass transfer of a gas in laminar or turbulent flow in a pipe are applicable. This means that Eqs. (21.3-24) and (21.3-25) can be used to predict mass transfer for the gas. For the mass transfer in the liquid film flowing down the wetted-wall tower, Eqs. (21.3-22) and (21.3-23) can be used for Reynolds numbers of  $4 \leq Re$  as defined by Eq. (4.4-29) up to about 1200, and the theoretically predicted values should be multiplied by about 1.5 because of ripples and other factors. These equations hold for short contact times or Reynolds numbers above about 100



(S1).

**EXAMPLE 21.3-1. Mass Transfer Inside a Tube**

A tube is coated on the inside with naphthalene and has an inside diameter of 20 mm and a length of 1.10 m. Air at 318 K and an average pressure of 101.3 kPa flows through this pipe at a velocity of 0.80 m/s. Assuming that the absolute pressure remains essentially constant, calculate the concentration of naphthalene in the exit air. Use the physical properties given in Example 19.1-4.

**Solution:** From Example 19.1-4,  $D_{AB} = 6.92 \times 10^{-6} \text{ m}^2/\text{s}$  and the vapor pressure  $p_{Ai} = 74.0 \text{ Pa}$  or  $c_{Ai} = p_{Ai}/RT = 74.0/(8314.3 \times 318) = 2.799 \times 10^{-5} \text{ kg mol/m}^3$ . For air, from Appendix A.3,  $\mu = 1.932 \times 10^{-5} \text{ Pa} \cdot \text{s}$ ,  $\rho = 1.114 \text{ kg/m}^3$ . The Schmidt number is

$$\text{N}_{\text{Sc}} = \mu \rho D_{AB} = 1.932 \times 10^{-5} \text{ Pa} \cdot \text{s} (1.114 \text{ kg/m}^3) (6.92 \times 10^{-6} \text{ m}^2/\text{s}) = 2.506$$

The Reynolds number is

$$\text{N}_{\text{Re}} = D v \rho \mu = (0.020 \text{ m}) (0.80 \text{ m/s}) (1.114 \text{ kg/m}^3) 1.932 \times 10^{-5} \text{ Pa} \cdot \text{s} = 922.6$$

Hence, the flow is laminar. Then,

$$\text{N}_{\text{Re}} \text{N}_{\text{Sc}} \text{DL} \pi^4 = 922.6 (2.506) 0.020 1.10 \pi^4 = 33.02$$

Using Fig. 21.3-2 and the rodlike flow line,  $(c_A - c_{A0})/(c_{Ai} - c_{A0}) = 0.55$ . Also,  $c_{A0}$  (inlet) = 0. Then,  $(c_A - 0)/(2.799 \times 10^{-5} - 0) = 0.55$ . Solving,  $c_A$  (exit concentration) =  $1.539 \times 10^{-5} \text{ kg mol/m}^3$ .

## 21.3E Mass Transfer for Flow Outside Solid Surfaces

*1. Mass transfer in flow parallel to flat plates. The mass transfer and*

vaporization of liquids from a plate or flat surface to a flowing stream is of interest in the drying of inorganic and biological materials, in the evaporation of solvents from paints, for plates in wind tunnels, and in flow channels in chemical process equipment.

When the fluid flows past a plate in a free stream in an open space, the boundary layer is not fully developed. For gases or evaporation of liquids in the gas phase and for the laminar region of  $N_{Re,L} = Lv\rho/\mu$  less than 15000, the data can be represented within  $\pm 25\%$  by the equation (S4)

$$JD = 0.664 N_{Re,L}^{-0.5} \quad (21.3-26)$$

Writing Eq. (21.3-26) in terms of the

Sherwood number  $N_{Sh}$ ,

$kc$

$$N_{Sh} = 0.664 N_{Re,L}^{1/2} Pr^{1/3} \quad (21.3-27)$$

where  $L$  is the length of plate in the direction of flow. Also,  $J_D = J_H = f/2$  for this geometry. For gases and  $N_{Re,L}$  of 15000–300000, the data are represented within  $\pm 30\%$  by  $J_D = J_H = f/2$  as

$$J_D = 0.036 N_{Re,L}^{-0.2} \quad (21.3-28)$$

Experimental data for liquids are correlated within about  $\pm 40\%$  by the following for a  $N_{Re,L}$  of 600–50000 (L2):

$$J_D = 0.99 N_{Re,L}^{-0.5} \quad (21.3-29)$$

**EXAMPLE 21.3-2. Mass Transfer from a Flat Plate**

A large volume of pure water at 26.1°C is flowing parallel to a flat plate of solid benzoic acid, where  $L = 0.244$  m in the

direction of flow. The water velocity is 0.061 m/s. The solubility of benzoic acid in water is 0.02948 kg mol/m<sup>3</sup>. The diffusivity of benzoic acid is 1.245 × 10<sup>-9</sup> m<sup>2</sup>/s. Calculate the mass-transfer coefficient  $k_L$  and the flux  $N_A$ .

**Solution:** Since the solution is quite dilute, the physical properties of water at 26.1°C from Appendix A.2 can be used:

$$\mu = 8.71 \times 10^{-4} \text{ Pa} \cdot \text{s} = 996 \text{ kg/m}^3 \text{ DAB} = 1.245 \times 10^{-9} \text{ m}^2/\text{s}$$

The Schmidt number is

$$\text{N}_{\text{Sc}} = \mu \rho \text{DAB} = 8.71 \times 10^{-4} \text{ Pa} \cdot \text{s} (996 \text{ kg/m}^3) / (1.245 \times 10^{-9} \text{ m}^2/\text{s}) = 702$$

The Reynolds number is

$$\text{N}_{\text{Re}} = L u \rho \mu = (0.244 \text{ m}) (0.061 \text{ m/s}) (996 \text{ kg/m}^3) / 8.71 \times 10^{-4} \text{ Pa} \cdot \text{s} = 1.700 \times 10^4$$

Using Eq. (21.3-29),

$$\text{JD} = 0.99 \text{N}_{\text{Re}}^{1/2} \text{N}_{\text{Sc}}^{-1/3} = 0.99 (1.700 \times 10^4)^{1/2} (702)^{-1/3} = 0.00758$$

The definition of  $\text{JD}$  from Eq. (21.3-5) is

$$\text{JD} = k' c' u (\text{N}_{\text{Sc}})^{2/3} \quad (21.3-5)$$

Solving for  $k'$ ,  $k' = \text{JD} u (\text{N}_{\text{Sc}})^{-2/3}$ . Substituting known values and solving,

$$k' = 0.00758 (0.061 \text{ m/s}) (702)^{-2/3} = 5.85 \times 10^{-6} \text{ m/s}$$

In this case, diffusion is for  $A$  through nondiffusing  $B$ , so  $k_c$  in Eq. (21.1-10) should be used:

$$N_A = k' x_{\text{BM}} (c_{A1} - c_{A2}) = k_c (c_{A1} - c_{A2}) \quad (21.1-10)$$

Since the solution is very dilute,  $x_{\text{BM}} \approx 1.0$  and  $k' \approx k_c$ . Also,  $c_{A1} = 2.948 \times 10^{-2} \text{ kg mol/m}^3$  (solubility) and  $c_{A2} = 0$  (large volume of fresh water). Substituting into Eq. (21.1-10),

$$N_A = k_c (c_{A1} - c_{A2}) = (5.85 \times 10^{-6} \text{ m/s}) (2.948 \times 10^{-2} \text{ kg mol/m}^3 - 0) = 1.726 \times 10^{-7} \text{ kg mol/m}^2 \cdot \text{s}$$

2. *Mass transfer for flow past single spheres.* For flow past single spheres and for very low  $N_{Re} = D_p v \rho / \mu$ , where  $v$  is the average velocity in the empty test section before the sphere, the Sherwood number, which is  $kc'D_p/D_{AB}$ , should approach a value of 2.0. This can be shown from Eq. (19.1-24), which was derived for a stagnant medium.

Rewriting Eq. (19.1-24) as follows, where  $D_p$  is the sphere diameter,

$$N_A = 2D_{AB}D_p(c_{A1} - c_{A2}) = k_c(c_{A1} - c_{A2}) \quad (21.3-30)$$

The mass-transfer coefficient  $k_c$ , which is  $kc'$  for a dilute solution, is then

$$kc' = 2D_{AB}/D_p \quad (21.3-31)$$

Rearranging,

$$k_c' D_p / DAB = NSh = 2.0(21.3-32)$$

Of course, natural convection effects could increase  $k_c'$ .

For gases, for a Schmidt number range of 0.6–2.7 and a Reynolds number range of 1–48000, a modified equation (G1) can be used:

$$NSh = 2 + 0.552 NRe^{0.53} NSc^{1/3} (21.3-33)$$

This equation also holds for heat transfer, where the Prandtl number replaces the Schmidt number and the Nusselt number  $hD_p/k$  replaces the Sherwood number.

For liquids (G3) and a Reynolds number range of 2 to about 2000, the following can be used:

$$N_{Sh}=2+0.95N_{Re}^{0.5}N_{Sc}^{1/3} \quad (21.3-34)$$

For liquids and a Reynolds number of 2000–17000, the following can be used (S5):

$$N_{Sh}=0.347N_{Re}^{0.62}N_{Sc}^{1/3} \quad (21.3-35)$$

**EXAMPLE 21.3-3. Mass Transfer from a Sphere**

Calculate the value of the mass-transfer coefficient and the flux for mass transfer from a sphere of naphthalene to air at 45°C and 1 atm abs flowing at a velocity of 0.305 m/s. The diameter of the sphere is 25.4 mm. The diffusivity of naphthalene in air at 45°C is  $6.92 \times 10^{-6} \text{ m}^2/\text{s}$  and the vapor pressure of solid naphthalene is 0.555 mmHg. Use English and SI units.

**Solution:** In English units,  $D_{AB} = 6.92 \times 10^{-6} (3.875 \times 10^4) = 0.2682 \text{ ft}^2/\text{hr}$ . The diameter  $D_p = 0.0254 \text{ m} = 0.0254(3.2808) = 0.0833 \text{ ft}$ . From Appendix A.3, the physical properties of air will be used, since the concentration of naphthalene is low:

$$\rho = 1.113 \text{ kg/m}^3 = 1.113 \text{ kg/m}^3 (1 \text{ lbm/ft}^3 / 16.0185 \text{ kg/m}^3) = 0.0695 \text{ lbm/ft}^3$$

$$\mu = 1.13 \times 10^{-5} \text{ Pa}\cdot\text{s} = 1.13 \times 10^{-5} \text{ Pa}\cdot\text{s} (1 \text{ lbm/ft}\cdot\text{hr} / 3600 \text{ s}) = 0.0467 \text{ lbm/ft}\cdot\text{hr}$$

The Schmidt number is

$$N_{Sc} = \frac{\mu}{\rho D_{AB}} = \frac{0.0467 \text{ lbm/ft}\cdot\text{hr} (0.0695 \text{ lbm/ft}^3)}{(0.2682 \text{ ft}^2/\text{hr})} = 2.505$$

$$N_{Sc} = \frac{\mu}{\rho D_{AB}} = \frac{1.93 \times 10^{-5} \text{ Pa}\cdot\text{s} (1.113 \text{ kg/m}^3)}{(6.92 \times 10^{-6} \text{ m}^2/\text{s})} = 2.505$$

The Reynolds number is

$$N_{Re} = \frac{D_p \rho u}{\mu} = \frac{(0.0833 \text{ ft}) (3600 \text{ ft/s}) (0.0695 \text{ lbm/ft}^3)}{0.0467 \text{ lbm/ft}\cdot\text{hr}} = 446$$

$$N_{Re} = \frac{D_p \rho u}{\mu} = \frac{(0.0254 \text{ m}) (0.3048 \text{ m/s}) (1.113 \text{ kg/m}^3)}{1.93 \times 10^{-5} \text{ Pa}\cdot\text{s}} = 446$$

Equation (21.3-33) for gases will be used:

$$NSh=2+0.552(NRe)^{0.53}(NSc)^{1/3}=2+0.552(446)^{0.53}(2.505)^{1/3}=21.0$$

From Eq. (21.3-3),

$$NSh=kc'LDAB=kc'DpDAB$$

Substituting the knowns and solving,

$$21=kc'0.0833ft0.2682ft^2hrkc'=67.6ft^3hr^21=kc'0.0254m6.92\times10^{-6}m^2skc'=5.72\times10^{-3}ms$$

From Table 21.1-1,

$$kc'c=kc'PRT=kG'P$$

Hence, for  $T = 45 + 273 = 318 \text{ K} = 318(1.8) = 574^\circ\text{R}$ ,

$$kG'=kc'RT=67.6ft^3hr(0.7302ft^3\text{-atmlbmol}\cdot^\circ\text{R})(574^\circ\text{R})=0.1616\text{lbmolhr}\cdot\text{ft}^2\text{-atmkG}'=5.72\times10^{-3}ms(8314.34m^3\text{-Pakgmol}\cdot\text{K})(318\text{K})=2.163\times10^{-9}\text{kgmols}\cdot\text{m}^2\cdot\text{Pa}$$

Since the gas is very dilute,  $y_{BM} \approx 1.0$  and  $kG' \approx kG$ .

Substituting into Eq. (21.1-12) for  $A$  diffusing through stagnant  $B$  and noting that  $p_{A1} = 0.555/760 = 7.303 \times 10^{-4} \text{ atm} = 74.0 \text{ Pa}$  and  $p_{A2} = 0$  (pure air),

$$NA=kG(p_{A1}-p_{A2})=0.1616\text{lbmolhr}\cdot\text{ft}^2\text{-atm}(7.303\times10^{-4}\text{ atm}-0\text{atm})=1.180\times10^{-4}\text{lbmolhr}\cdot\text{ft}^2NA=2.163\times10^{-9}\text{kgmols}\cdot\text{m}^2\cdot\text{Pa}(74\text{Pa}-0\text{Pa})=1.599\times10^{-7}\text{kgmols}\cdot\text{m}^2$$

The area of the sphere is

$$A=\pi Dp^2=\pi(0.0833ft)^2=2.18\times10^{-2}ft^2A=2.18\times10^{-2}ft^2(1m^3.2808ft)^2=2.025\times10^{-3}m^2$$

$$\text{Total amount evaporated} = NA = (1.18 \times 10^{-4} \text{ lbmol/hr} \cdot \text{ft}^2)(2.18 \times 10^{-2} \text{ ft}^2) = 2.572 \times 10^{-6} \text{ lbmol/hr} = (1.599 \times 10^{-4} \text{ kgmol/s} \cdot \text{m}^2)(2.025 \times 10^{-3} \text{ m}^2) = 3.238 \times 10^{-10} \text{ kg mol/s}$$

*3. Mass transfer to packed beds.* Mass transfer to and from packed beds occurs often in processing operations, including



drying operations, adsorption or desorption of gases or liquids by solid particles such as charcoal, and mass transfer of gases and liquids to catalyst particles. By using a packed bed, a large amount of mass-transfer area can be contained in a relatively small volume.

The void fraction in a bed is  $\epsilon$   $m^3$  volume void space divided by the  $m^3$  total volume of void space plus solid. The values range from 0.3 to 0.5 in general. Because of flow channeling, nonuniform packing, and so forth, accurate experimental data are difficult to obtain and data from different investigators can deviate considerably.

For a Reynolds number range of 10–10000 for gases in a packed bed of spheres ( $D_4$ ), the recommended

correlation with an average deviation of about  $\pm 20\%$  and a maximum of about  $\pm 50\%$  is

$$JD = JH = 0.4548 \epsilon N_{Re}^{-0.4069} \quad (21.3-36)$$

It has been shown (G4, G5) that  $JD$  and  $JH$  are approximately equal. The Reynolds number is defined as  $N_{Re} = D_p v' \rho / \mu$ , where  $D_p$  is the diameter of the spheres and  $v'$  is the superficial mass average velocity in the empty tube without packing. For Eqs. (21.3-36)–(21.3-39) and Eqs. (21.3-5)–(21.3-6),  $v'$  is used.

For mass transfer of liquids in packed beds, the correlations of Wilson and Geankoplis (W1) should be used. For a Reynolds number  $D_p v' \rho / \mu$  range of 0.0016–55 and a Schmidt number range

of 165–70000, the equation to use is

$$JD = 1.09 \epsilon N Re^{-2/3} \quad (21.3-37)$$

For liquids and a Reynolds number range of 55–1500 and a Schmidt number range of 165–10 690,

$$JD = 0.250 \epsilon N Re^{-0.31} \quad (21.3-38)$$

Or, as an alternate, Eq. (21.3-36) can be used for liquids for a Reynolds number range of 10–1500.

For fluidized beds of spheres, Eq. (21.3-36) can be used for gases and liquids and a Reynolds number range of 10–4000. For liquids in a fluidized bed and a Reynolds number range of 1–10 (D4),

$$\epsilon JD = 1.1068 N Re^{-0.72} \quad (21.3-39)$$

If packed beds of solids other than spheres are used, approximate correction factors can be used with Eqs. (21.3-36)–(21.3-38) for spheres. This is done, for example, for a given nonspherical particle as follows: The particle diameter to use in the equations for predicting  $JD$  is the diameter of a sphere with the same surface area as the given solid particle. The flux to these particles in the bed is then calculated using the area of the given particles. An alternative approximate procedure is given in (G6).

#### *4. Calculation method for packed beds.*

To calculate the total flux in a packed bed,  $JD$  is first obtained and then  $k_c$  in m/s from the  $JD$ . Then, knowing the total volume  $V_b$  m<sup>3</sup> of the bed (void plus solids), the total external surface area  $A$

$m_2$  of the solids for mass transfer is calculated using Eqs. (21.3-40) and (21.3-41):

$$a = 6(1 - \epsilon) D_p \quad (21.3-40)$$

where  $a$  is the  $m_2$  surface area/ $m^3$  total volume of bed when the solids are spheres, and

$$A = a V_b \quad (21.3-42)$$

To calculate the mass-transfer rate, the log mean driving force at the inlet and outlet of the bed should be used:

$$N_A A = A k_c (c_{Ai} - c_{A1}) - (c_{Ai} - c_{A2}) \ln \frac{c_{Ai} - c_{A1}}{c_{Ai} - c_{A2}} \quad (21.3-42)$$

where the final term is the log mean driving force:  $c_{Ai}$  is the concentration at the surface of the solid, in  $\text{kg mol}/m^3$ ;

$c_{A1}$  is the inlet bulk fluid concentration; and  $c_{A2}$  is the outlet. The material-balance equation on the bulk stream is

$$N_{AA} = V(c_{A2} - c_{A1}) \quad (21.3-43)$$

where  $V$  is the volumetric flow rate of fluid entering in  $\text{m}^3/\text{s}$ . Equations (21.3-42) and (21.3-43) must both be satisfied. The use of these two equations is similar to the use of the log mean temperature difference and heat balance in heat exchangers. These two equations can also be used for a fluid flowing in a pipe or past a flat plate, where  $A$  is the pipe wall area or plate area.

**EXAMPLE 21.3-4. Mass Transfer of a Liquid in a Packed Bed**

Pure water at  $26.1^\circ\text{C}$  flows at the rate of  $5.514 \times 10^{-7} \text{ m}^3/\text{s}$  through a packed bed of benzoic-acid spheres having a diameter of 6.375 mm. The total surface area of the spheres in the bed is  $0.01198 \text{ m}^2$  and the void fraction is 0.436. The tower diameter is 0.0667 m. The solubility of benzoic acid in water is  $2.948 \times 10^{-2} \text{ kg mol}/\text{m}^3$ .

- Predict the mass-transfer coefficient  $k_c$ . Compare with the experimental value of  $4.665 \times 10^{-6}$  m/s by Wilson and Geankoplis (W1).
- Using the experimental value of  $k_c$ , predict the outlet concentration of benzoic acid in the water.

**Solution:** Since the solution is dilute, the physical properties of water will be used at 26.1°C from Appendix A.2. At 26.1°C,  $\mu = 0.8718 \times 10^{-3}$  Pa · s,  $\rho = 996.7$  kg/m<sup>3</sup>. At 25.0°C,  $\mu = 0.8940 \times 10^{-3}$  Pa · s, and from Table 18.2-3,  $D_{AB} = 1.21 \times 10^{-9}$  m<sup>2</sup>/s. To correct  $D_{AB}$  to 26.1°C using Eq. (18.2-13),  $D_{AB} \propto T/\mu$  Hence,

$$D_{AB}(26.1^\circ\text{C}) = (1.21 \times 10^{-9} \text{ m}^2/\text{s})(299.1 \text{ K}/298 \text{ K}) \\ (0.8940 \times 10^{-3} \text{ Pa} \cdot \text{s} / 0.8718 \times 10^{-3} \text{ Pa} \cdot \text{s}) = 1.254 \times 10^{-9} \text{ m}^2/\text{s}$$

The tower cross-sectional area =  $(\pi/4)(0.0667 \text{ m})^2 = 3.494 \times 10^{-3} \text{ m}^2$ . Then  $u' = (5.514 \times 10^{-7} \text{ m}^3/\text{s}) / (3.494 \times 10^{-3} \text{ m}^2) = 1.578 \times 10^{-4} \text{ m/s}$ . Then,

$$N_{Sc} = \mu \rho D_{AB} = 0.8718 \times 10^{-3} \text{ Pa} \cdot \text{s} (996.7 \text{ kg/m}^3) \\ (1.254 \times 10^{-9} \text{ m}^2/\text{s}) = 702.6$$

The Reynolds number is

$$N_{Re} = D \rho u' \mu = (0.0667 \text{ m})(1.578 \times 10^{-4} \text{ m/s}) \\ (996.7 \text{ kg/m}^3) / 0.8718 \times 10^{-3} \text{ Pa} \cdot \text{s} = 1.150$$

Using Eq. (21.3-37) and assuming  $k_c = k'_c$  for dilute solutions,

$$J_D = 1.09 \eta N_{Re}^{-2/3} = 1.090.436(1.150)^{-2/3} = 2.277$$

Then, using Eq. (21.3-5) and solving,

$$J_D = k'_c u' (N_{Sc})^{2/3} \quad 2.277 = k'_c (1.578 \times 10^{-4} \text{ m/s}) (702.6)^{2/3}$$

The predicted  $k'_c = 4.447 \times 10^{-6}$ . This compares with the experimental value of  $4.665 \times 10^{-6}$  m/s.

For part (b), using Eqs. (21.3-42) and (21.3-43),

$$A k_c = (c_{Ai} - c_{A1}) - (c_{Ai} - c_{A2}) \ln \frac{c_{Ai} - c_{A1}}{c_{Ai} - c_{A2}} \\ - c_{A2} = V (c_{A2} - c_{A1}) \quad (21.344)$$

The values to substitute into Eq. (21.3-44) are  $c_{Ai} = 2.948 \times 10^{-2}$ ,  $c_{A1} = 0$ ,  $A = 0.01198$ ,  $V = 5.514 \times 10^{-7}$ .

$$\begin{aligned} &0.01198(4.665 \times 10^{-6}) \\ &(c_{A2}-0) \ln 2.948 \times 10^{-2} - 0.948 \times 10^{-2} - c_{A2} = (5.514 \times 10^{-17}) \\ &(c_{A2}-0) \end{aligned}$$

Solving,  $c_{A2} = 2.842 \times 10^{-3} \text{ kg mol/m}^3$ .

*5. Mass transfer for flow past single cylinders.* Experimental data have been obtained for mass transfer from single cylinders when the flow is perpendicular to the cylinder. The cylinders are long and mass transfer to the ends of a cylinder is not considered. For the Schmidt number range of 0.6 to 2.6 for gases and 1000 to 3000 for liquids, and a Reynolds number range of 50 to 50000, data from many references (B3, L1, M1, S4, V1) have been plotted, and the correlation to use is as follows:

$$JD = 0.600(NRe)^{-0.487} (21.3-45)$$

The data scatter considerably by up to  $\pm 30\%$  This correlation can also be used



for heat transfer, with  $JD = JH$ .

*6. Mass transfer for liquid metals.* In recent years, several correlations for mass-transfer coefficients of liquid metals have appeared in the literature. It has been found (G1) that with moderate safety factors, the correlations for nonliquid metals mass transfer may be used for liquid metals mass transfer. Care must be taken to ensure that the solid surface is wetted. Also, if the solid is an alloy, there may exist a resistance to diffusion in the solid phase.

## **21.4 Mass Transfer to Suspensions of Small Particles**

### **21.4A Introduction**

Mass transfer from or to small suspended particles in an agitated solution occurs in a number of

process applications. In liquid-phase hydrogenation, hydrogen diffuses from gas bubbles, through an organic liquid, and then to small suspended catalyst particles. In fermentation, oxygen diffuses from small gas bubbles, through the aqueous medium, and then to small suspended microorganisms.

For a liquid–solid dispersion, increased agitation over and above that necessary to freely suspend very small particles has a minimal effect on the mass-transfer coefficient  $k_L$  to the particle (B2). When the particles in a mixing vessel are just completely suspended, turbulence forces balance those due to gravity, and the mass-transfer rates are the same as for particles freely moving under gravity. With very small particles

of, say, a few  $\mu\text{m}$  or so, which is the size of many microorganisms in fermentations and some catalyst particles, their size is smaller than eddies, which are about  $100\ \mu\text{m}$  or so in size. Hence, increased agitation will have little effect on mass transfer except at very high agitation.

For a gas–liquid–solid dispersion, such as in fermentation, the same principles hold. However, increased agitation increases the number of gas bubbles and hence the interfacial area. The mass-transfer coefficients from the gas bubble to the liquid and from the liquid to the solid are relatively unaffected.

#### **21.4B Equations for Mass Transfer to Small Particles**

*1. Mass transfer to small particles < 0.6 mm.* Equations for predicting

mass transfer to small particles in suspension have been developed which cover three size ranges of particles. The equation for particles,  $< 0.6 \text{ mm}$  ( $600 \text{ }\mu\text{m}$ ) is discussed first.

The following equation has been shown to hold for predicting mass-transfer coefficients from small gas bubbles such as oxygen or air to the liquid phase or from the liquid phase to the surface of small catalyst particles, microorganisms, other solids, or liquid drops (B2, C3):

$$k_L' = 2D_{AB}D_p + 0.31N \text{Sc}^{-2/3}(\Delta\rho\mu_c g p c^2)^{1/3} (21.4 - 1)$$

where  $D_{AB}$  is the diffusivity of the solute A in solution in  $\text{m}^2/\text{s}$ ,  $D_p$  is the diameter of the gas bubble or the solid particle in m,  $\mu_c$  is the viscosity of the solution in

kg/ms,  $g = 9.80665 \text{ m/s}^2$ ,  $\Delta\rho = (\rho_c - \rho_p)$  or  $(\rho_p - \rho_c)$ ,  $\rho_c$  is the density of the continuous phase in kg/m<sup>3</sup>, and  $\rho_p$  is the density of the gas or solid particle. The value of  $\Delta\rho$  is always positive.

The first term on the right in Eq. (21.4-1) is the molecular diffusion term, and the second term is that due to free fall or the rise of the sphere due to gravitational forces. This equation has been experimentally checked for dispersions of low-density solids in agitated dispersions and for small gas bubbles in agitated systems.

**EXAMPLE 21.4-1. Mass Transfer from Air Bubbles in Fermentation**

Calculate the maximum rate of absorption of O<sub>2</sub> in a fermenter from air bubbles at 1 atm abs pressure and having diameters of 100  $\mu\text{m}$  at 37°C into water having a zero concentration of dissolved O<sub>2</sub>. The solubility of O<sub>2</sub> from air in water at 37°C is  $2.26 \times 10^{-7} \text{ g mol O}_2/\text{cm}^3 \text{ liquid}$  or  $2.26 \times 10^{-4} \text{ kg mol O}_2/\text{m}^3$ . The diffusivity of O<sub>2</sub> in water at 37°C is  $3.25 \times 10^{-9} \text{ m}^2/\text{s}$ . Agitation is used to produce the air bubbles.

**Solution:** The mass-transfer resistance inside the gas bubble to the outside interface of the bubble can be neglected since it is negligible (B2). Hence, the mass-transfer coefficient  $k_L'$  outside the bubble is needed. The given data are

$$D_P = 100 \mu\text{m} = 1 \times 10^{-4} \text{m} \quad D_{AB} = 3.25 \times 10^{-9} \text{m}^2/\text{s}$$

At  $37^\circ\text{C}$ ,

$$\begin{aligned} \mu &= 6.947 \times 10^{-4} \text{Pa}\cdot\text{s} = 6.947 \times 10^{-4} \text{kgm}\cdot\text{s}/\text{spc}(\text{water}) = 994 \text{kgm}^3, \rho(\text{air}) = 1.13 \text{kgm}^3 \\ N_{Sc} &= \mu c_p c D_{AB} = 6.947 \times 10^{-4} \text{Pa}\cdot\text{s} (9.25 \times 10^{-9} \text{m}^2/\text{s}) = 215 \\ N_{Sc} &= (215)^{2/3} = 35.9 \\ \Delta\rho &= \rho - \rho_p = 994 \text{kg}/\text{m}^3 - 1.13 \text{kg}/\text{m}^3 = 993 \text{kg}/\text{m}^3 \end{aligned}$$

Substituting into Eq. (21.4-1),

$$\begin{aligned} k_L' &= 2D_{AB}D_P + 0.31N_{Sc}^{-2/3}(\Delta\rho\mu c_p c)^{1/3}k_L \\ &= 2(3.25 \times 10^{-9} \text{m}^2/\text{s})(1 \times 10^{-4} \text{m}) + 0.31359[(993 \text{kgm}^3) \\ &\quad (6.947 \times 10^{-4} \text{kgm}\cdot\text{s})(9.806 \text{ms}^2)(994 \text{kgm}^3)]^{1/3}k_L \\ &= 6.50 \times 10^{-5} \text{m}/\text{s} + 16.40 \times 10^{-5} \text{m}/\text{s} = 2.290 \times 10^{-4} \text{m}/\text{s} \end{aligned}$$

The flux is as follows, assuming  $k_L = k_L'$  for dilute solutions:

$$\begin{aligned} N_A &= k_L(c_{A1} - c_{A2}) = 2.290 \times 10^{-4} \text{m}/\text{s} (2.290 \times 10^{-4} \text{kg}/\text{m}^3 - 0) \\ N_A &= 5.18 \times 10^{-8} \text{kgmol}(\text{O}_2)/\text{s}\cdot\text{m}^2 \end{aligned}$$

Knowing the total number of bubbles and their area, the maximum possible rate of transfer of  $\text{O}_2$  to the fermentation liquid can be calculated.

In Example 21.4-1,  $k_L$  was small. For mass transfer of  $\text{O}_2$  in a solution to a microorganism with  $D_P \cong 1 \mu\text{m}$ , the term  $2D_{AB}/D_P$  would be 100 times larger. Note that at large diameters, the second term in Eq. (21.4-1) becomes small and the mass-transfer coefficient  $k_L$  becomes

essentially independent of size  $D_p$ . In agitated vessels with gas introduced below the agitator in aqueous solutions, or when liquids are aerated with sintered plates, the gas bubbles are often in the size range covered by Eq. (21.4-1) (B2, C3, T1).

In aerated mixing vessels, the mass-transfer coefficients are essentially independent of the power input.

However, as the power is increased, the bubble size decreases and the mass-transfer coefficient continues to follow Eq. (21.4-1). The dispersions include those in which the solid particles are just completely suspended in mixing vessels. Increase in agitation intensity above the level needed for complete suspension of these small particles results in only a small increase in  $k_L$  (C3).

Equation (21.4-1) has also been shown to apply to heat transfer and can be written as follows (B2, C3):

$$Nu = hD_p/k = 2.0 + 0.31 N_{Pr}^{1/3} (D_p^3 \rho_c \Delta \rho / \mu_c^2)^{1/3} \quad (21.4-2)$$

*2. Mass transfer to large gas bubbles > 2.5 mm.* For large gas bubbles or liquid drops > 2.5 mm, the mass-transfer coefficient can be predicted by

$$k_L$$

$$k_L' = 0.42 N_{Sc}^{-0.5} (\Delta \rho \mu_c g / \rho_c^2)^{1/3} \quad (21.4-3)$$

Large gas bubbles are produced when pure liquids are aerated in mixing vessels and sieve-plate columns (C1). In this case, the mass-transfer coefficient  $k_L'$  or  $k_L$  is independent of the bubble size and is constant for a given set of physical properties. For the same physical properties, the large-bubble Eq.



(21.4-3) gives values of  $k_L$  about three to four times larger than Eq. (21.4-1) for small particles. Again, Eq. (21.4-3) shows that the  $k_L$  is essentially independent of agitation intensity in an agitated vessel and gas velocity in a sieve-tray tower.

*3. Mass transfer to particles in the transition region.* For mass transfer in the transition region between small and large bubbles in the size range 0.6–2.5 mm, the mass-transfer coefficient can be approximated by assuming that it increases linearly with bubble diameter (B2, C3).

*4. Mass transfer to particles in highly turbulent mixers.* In the preceding three regions, the density difference between phases is sufficiently large to cause the

force of gravity to primarily determine the mass-transfer coefficient. This also includes solids just completely suspended in mixing vessels. When agitation power is increased beyond that needed for the suspension of solid or liquid particles and the turbulence forces become larger than the gravitational forces, Eq. (21.4-1) is not followed, and Eq. (21.4-4) should be used where small increases in  $k_L'$  are observed (B2, C3):

$$k_L' N Sc^{2/3} = 0.13 \left( \frac{P}{V} \right) \mu_c \rho_c^{1/4} \quad (21.4-4)$$

where  $P/V$  is power input per unit volume as defined in Section 7.2. The data deviate substantially by up to 60% from this correlation. In the case of gas-liquid dispersions, it is quite impractical for agitation systems to exceed

gravitational forces.

The experimental data are complicated by the fact that very small particles are easily suspended, and if their size is on the order of the smallest eddies, the mass-transfer coefficient will remain constant until a large increase in power input is added above that required for suspension.

## **21.5 Models for Mass-Transfer Coefficients**

### **21.5A Laminar Flow and Boundary-Layer Theory in Mass Transfer**

Previously, an exact solution was obtained for the hydrodynamic boundary layer for isothermal laminar flow past a plate, and in Section 15.2A an extension of the Blasius solution was also used to derive an expression for convective

heat transfer. In an analogous manner, we use the Blasius solution for convective mass transfer for the same geometry and laminar flow. In Fig. 21.5-1, the concentration boundary layer is shown, where the concentration of the fluid approaching the plate is  $c_{A\infty}$  and  $c_{AS}$  in the fluid adjacent to the surface.

We start by using the differential mass balance, Eq. (18.4-17), and simplifying it for steady state where  $\partial c_A / \partial t = 0$ ;  $R_A = 0$ ; flow is only in the  $x$  and  $y$  directions, so  $v_z = 0$ ; and neglecting diffusion in the  $x$  and  $z$  directions to give

$$v_x \frac{\partial c_A}{\partial x} + v_y \frac{\partial c_A}{\partial y} = D_{AB} \frac{\partial^2 c_A}{\partial y^2} \quad (21.5-1)$$

The momentum boundary-layer

equation is very similar:

$$u \frac{\partial u}{\partial x} + v \frac{\partial u}{\partial y} = \nu \frac{\partial^2 u}{\partial y^2} \quad (11.1-5)$$

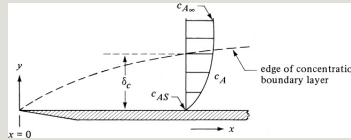


Figure 21.5-1. *Laminar flow of fluid past a flat plate and concentration boundary layer.*

The thermal boundary-layer equation is also similar:

$$u \frac{\partial T}{\partial x} + v \frac{\partial T}{\partial y} = \alpha \frac{\partial^2 T}{\partial y^2} \quad (15.2-2)$$

The continuity equation used previously is

$$\frac{\partial u}{\partial x} + \frac{\partial v}{\partial y} = 0 \quad (11.1-3)$$

The dimensionless concentration

boundary conditions are

$$\begin{aligned} v_x v_\infty &= T - T_S \quad T_\infty - T_S = c_A - c_{AS} \quad c_{A\infty} - c_{AS} = 0 \text{ at } y=0 \\ v_x v_\infty &= T - T_S \quad T_\infty - T_S = c_A - c_{AS} \quad c_{A\infty} - c_{AS} = 1 \text{ at } y=\infty \end{aligned} \quad (21.5-2)$$

The similarity among the three differential equations (21.5-1), (11.1-5), and (15.2-2) is obvious, as is the similarity among the three sets of boundary conditions in Eq. (21.5-2). In Section 15.2A, the Blasius solution was applied to convective heat transfer when  $(\mu/\rho)/\alpha = N_{Pr} = 1.0$ . We use the same type of solution for laminar convective mass transfer when  $(\mu/\rho)/D_{AB} = N_{Sc} = 1.0$ .

The velocity gradient at the surface was derived previously:

$$(\partial v_x \partial y)_{y=0} = 0.332 v_\infty x N_{Re,x}^{1/2} \quad (15.2-5)$$

where  $N_{Re,x} = x v_\infty \rho / \mu$ . Also, from Eq. (21.5-2),

$$v_x v_\infty = c_A - c_A S c_A \infty - c_A S \quad (21.5-3)$$

Differentiating Eq. (21.5-3) and combining the result with Eq. (15.2-5),

$$\begin{aligned} (\partial c_A \partial y)_{y=0} &= (c_A \infty - c_A S) \\ &= (0.332 x N_{Re,x}^{1/2}) \quad (21.5-4) \end{aligned}$$

The convective mass-transfer equation can be written as follows and related to Fick's equation for dilute solutions:

$$\begin{aligned} N_A y &= k c' (c_A S - c_A \infty) = - \\ D_{AB} (\partial c_A \partial y)_{y=0} \quad (21.5-5) \end{aligned}$$

Combining Eqs. (21.5-4) and (21.5-5),

$$k_c$$

$$Sh_x = 0.332 Re_x^{1/2} Sc^{1/3} \quad (21.5-6)$$

This relationship is restricted to gases with a  $Sc = 1.0$ .

The relationship between the thickness  $\delta$  of the hydrodynamic and  $\delta_c$  of the concentration boundary layers where the Schmidt number is not 1.0 is

$$\delta/\delta_c = Sc^{1/3} \quad (21.5-7)$$

As a result, the equation for the local convective mass-transfer coefficient is

$$k_c$$

$$Sh_x = 0.332 Re_x^{1/2} Sc^{1/3} \quad (21.5-8)$$

We can obtain the equation for the mean mass-transfer coefficient  $k_c'$  from  $x = 0$  to  $x = L$  for a plate of width  $b$  by



integrating as follows:

$$k_c' = b b L \int_0^L k_c' dx \quad (21.5-9)$$

The result is

$$k_c' L D A B = N S h = 0.664 N R e, L^{1/2} N S c^{1/3}$$

This is similar to the heat-transfer equation for a flat plate, Eq. (15.2-15), and also agrees with the experimental mass-transfer equation (21.3-27) for a flat plate.

In Chapter 11, an approximate integral analysis was performed for the laminar hydrodynamic and the turbulent hydrodynamic boundary layers. This was also done in Section 15.2 for the thermal boundary layer. An approximate integral analysis can also be done in

exactly the same manner for the laminar and turbulent concentration boundary layers.

### **21.5B Prandtl Mixing Length and Turbulent Eddy Mass Diffusivity**

In many applications, the flow in mass transfer is turbulent and not laminar. The turbulent flow of a fluid is quite complex as the fluid undergoes a series of random eddy movements throughout the turbulent core. When mass transfer is occurring, we refer to this as eddy mass diffusion. In Sections 11.2C and 15.2, we derived equations for turbulent eddy thermal diffusivity and momentum diffusivity using the Prandtl mixing length theory.

In a similar manner, we can derive a relation for the turbulent eddy mass

diffusivity,  $\epsilon_M$ . Eddies are transported a distance  $L$ , called the Prandtl mixing length, in the  $y$  direction. At this point  $L$ , the fluid eddy differs in velocity from the adjacent fluid by the velocity  $v_x'$ , which is the fluctuating velocity component given in Section 11.2. The instantaneous rate of mass transfer of  $A$  at a velocity  $v_y'$  for a distance  $L$  in the  $y$  direction is

$$J_{Ay} = c_A' v_A' (21.5-11)$$

where  $c_A'$  is the instantaneous fluctuating concentration. The instantaneous concentration of the fluid is  $c_A = \bar{c}_A + c_A'$ , where  $\bar{c}_A$  is the mean value and  $c_A'$  the deviation from the mean value. The mixing length  $L$  is small enough that the concentration difference is

$$cA' = Ldc^-A dy \quad (21.5-12)$$

The rate of mass transported per unit area is  $JAy^*$ . Combining Eqs. (21.5-11) and (21.5-12),

$$JAy^* = -v_y' Ldc^-A dy \quad (21.5-13)$$

From Eq. (15.2-23),

$$v_y' = v_x' = L|dv^-x dy| \quad (21.5-14)$$

Substituting Eq. (21.5-14) into (21.5-13),

$$JAy^* = -L^2|dv^-x dy| |dc^-A dy| \quad (21.5-15)$$

The term  $L^2|dyx/dy|$  is called the turbulent eddy mass diffusivity  $\epsilon_M$ . Combining Eq. (21.5-15) with the diffusion equation in terms of  $D_{AB}$ , the total flux is

$$J_A y^* = -(D_{AB} + \epsilon M) dc_A dy \quad (21.5-16)$$

The similarities between Eq. (21.5-16) for mass transfer and heat and momentum transfer have been pointed out in detail in Section 18.1A.

### **21.5C Models for Mass-Transfer Coefficients**

*1. Introduction.* For many years, mass-transfer coefficients, which were based primarily on empirical correlations, have been used in the design of process equipment. A better understanding of the mechanisms of turbulence is needed before we can give a theoretical explanation of convective mass-transfer coefficients. Several theories of convective mass transfer, such as the eddy diffusivity theory, have been presented in this chapter. In the

following sections, we briefly present some of these theories and discuss how they can be used to extend empirical correlations.

*2. Film mass-transfer theory.* The film theory, which is the simplest and most elementary theory, assumes the presence of a fictitious laminar film next to the boundary. This film, where only molecular diffusion is assumed to be occurring, has the same resistance to mass transfer as actually exists in the viscous, transition, and turbulent core regions. Then, the actual mass-transfer coefficient  $k_c'$  is related to this film thickness  $\delta_f$  by

$$J A^* = k_c' (c_{A1} - c_{A2}) = D_{AB} \delta_f (c_{A1} - c_{A2}) \quad (21.517)$$

$$k_c' = D_{AB} \delta f \quad (21.5-18)$$

The mass-transfer coefficient is proportional to  $D_{AB}^{1/2}$ . However, since we have shown that in Eq. (21.3-13)  $J_D$  is proportional to  $(\mu/\rho D_{AB})^{2/3}$ , then  $k_c' \propto D_{AB}^{2/3}$ . Hence, the film theory is not correct. The great advantage of the film theory is its simplicity when it can be used in complex situations such as penetration theory and boundary-layer theory, described below.

*3. Penetration theory.* The penetration theory derived by Higbie and modified by Danckwerts (D3) was derived for diffusion or penetration into a laminar falling film for short contact times in Eq. (21.3-23) and is as follows:

$$k_c' = 4 D_{AB} \pi t L \quad (21.5-19)$$

where  $t_L$  is the time of penetration of the solute in seconds. This was extended by Danckwerts. He modified this for turbulent mass transfer and postulated that a fluid eddy has a uniform concentration in the turbulent core and is swept to the surface and undergoes unsteady-state diffusion. Then, the eddy is swept away to the eddy core and other eddies are swept to the surface and stay for a random amount of time. A mean surface renewal factor  $s$  in  $s^{-1}$  is defined as follows:

$$k_c' = DABs \quad (21.5-20)$$

The mass-transfer coefficient  $k_c'$  is proportional to  $DAB$ . In some systems, such as where liquid flows over packing and semistagnant pockets occur where the surface is being renewed, the



results approximately follow Eq. (21.5-20). The value of  $s$  must be obtained experimentally. Others (D3, T2) have derived more complex combination film-surface renewal theories that predict a gradual change of the exponent on  $D_{AB}$  from 0.5 to 1.0, depending on turbulence and other factors. Penetration theories have been used in cases where diffusion and chemical reaction are occurring (D3).

*4. Boundary-layer theory.* The boundary-layer theory has been discussed in detail in Section 21.5 and is useful in predicting and correlating data for fluids flowing past solid surfaces. For laminar flow and turbulent flow the mass-transfer coefficient  $k_c' \propto D_{AB}^{2/3}$ . This has been experimentally verified for many cases.

## 21.6 Chapter Summary

### Types of Mass-Transfer Coefficients

- Equimolar counterdiffusion:

$$\text{Gases: } N_A = k_c'(c_{A1} - c_{A2}) = k_G'(p_{A1} - p_{A2}) = k_y'(y_{A1} - y_{A2}) \quad (21.1-6)$$

$$\text{Liquids: } N_A = k_c'(c_{A1} - c_{A2}) = k_L'(c_{A1} - c_{A2}) = k_x'(x_{A1} - x_{A2}) \quad (21.1-7)$$

- For A diffusing through stagnant, nondiffusing B, where  $N_B = 0$ , Eq. (21.1-4) gives for steady state

$$N_A = k_c' x_{BM}(c_{A1} - c_{A2}) = k_c(c_{A1} - c_{A2}) N_A = k_x' x_{BM}(x_{A1} - x_{A2}) = k_x(x_{A1} - x_{A2}) \quad (21.1-10)$$

where the  $x_{BM}$  and its counterpart  $y_{BM}$  are similar to Eq. (19.1-12) and  $k_c$  is the mass-transfer coefficient for A diffusing through stagnant B. Also,

$$x_{BM} = x_{B2} - x_{B1} \ln(x_{B2}/x_{B1}) \quad y_{BM} = y_{B2} - y_{B1} \ln(y_{B2}/y_{B1}) \quad (21.1-11)$$

Rewriting Eq. (21.1-10) using other units,

$$\begin{aligned} \text{(Gases): } N_A &= k_c(c_{A1} - c_{A2}) = k_G(p_{A1} - p_{A2}) = k_y(y_{A1} - y_{A2}) \\ &\quad (21.1-12) \end{aligned}$$

$$\begin{aligned} \text{(Liquides): } N_A &= k_c(c_{A1} - c_{A2}) = k_L(c_{A1} - c_{A2}) = k_x(x_{A1} - x_{A2}) \\ &\quad (21.1-13) \end{aligned}$$

### Dimensional Analysis for Mass Transfer

$$N_{Sh} = f(N_{Rc}, N_{Sc}) \quad (21.2-11)$$

### Prediction of Mass-Transfer Coefficients



### Models for Mass-Transfer Coefficients

- *Film mass-transfer theory.*

$$J_A^* = k_c'(c_{A1} - c_{A2}) = D_{AB} \delta f(c_{A1} - c_{A2}) \quad (21.5-17)$$

$$k_c' = D_{AB} \delta f \quad (21.5-18)$$

- *Penetration theory.*

$$k_c' = 4DAB\pi L(21.5-19)$$

$$k_c' = DABs(21.5-20)$$

- *Boundary-layer theory.*

$$k_c'LDAB = NSh = 0.664NRe^{1/2}NSc^{1/3}(21.5-10)$$

## Problems

**21.1-1. Flux and Conversion of Mass-Transfer Coefficient.** A value of  $k_G$  was experimentally determined to be  $1.08 \text{ lb mol/h} \cdot \text{ft}^2 \cdot \text{atm}$  for  $A$  diffusing through stagnant  $B$ . For the same flow and concentrations, it is desired to predict  $k_G'$  and the flux of  $A$  for equimolar counterdiffusion.

The partial pressures are  $p_{A1} = 0.20 \text{ atm}$ ,  $p_{A2} = 0.05 \text{ atm}$ , and  $P = 1.0 \text{ atm}$  abs total. Use English and SI units.

**Ans.**  $k_G' = 0.943 \text{ lb mol/h} \cdot \text{ft}^2 \cdot \text{atm}$ ,  
 $1.262 \times 10^{-8} \text{ kg mol/s} \cdot \text{m}^2 \cdot \text{Pa}$ ,  $N_A =$   
 $0.1414 \text{ lb mol A/h} \cdot \text{ft}^2$ ,  $1.918 \times 10^{-4} \text{ kg}$

**21.1-2. Conversion of Mass-Transfer Coefficients.** Prove or show the following relationships, starting with the flux equations:

- Convert  $k_c'$  to  $k_y$  and  $k_G$ .
- Convert  $k_L$  to  $k_x$  and  $k_x'$ .
- Convert  $k_G$  to  $k_y$  and  $k_c$ .

**21.1-3. Absorption of H<sub>2</sub>S by Water.** In a wetted-wall tower an air–H<sub>2</sub>S mixture is flowing by a film of water that is flowing as a thin film down a vertical plate. The H<sub>2</sub>S is being absorbed from the air to the water at a total pressure of 1.50 atm abs and 30°C. A value for  $k_c'$  of  $9.567 \times 10^{-4}$  m/s has been predicted for the gas-phase mass-transfer coefficient. At a given point, the mole fraction of H<sub>2</sub>S in the liquid at the

liquid–gas interface is  $2.0(10^{-5})$  and  $p_A$  of  $H_2S$  in the gas is 0.05 atm. The Henry's law equilibrium relation is  $p_A(\text{atm}) = 609x_A$  (mole fraction in liquid). Calculate the rate of absorption of  $H_2S$ . (*Hint*: Call point 1 the interface and point 2 the gas phase. Then, calculate  $p_{A1}$  from Henry's law and the given  $x_A$ . The value of  $p_{A2}$  is 0.05 atm.)

**Ans.**  $N_A = -1.485 \times 10^{-6} \text{ kg mol/s} \cdot \text{m}^2$

**21.1-4. *Effect of High Flux on Mass-Transfer Coefficients.*** Using the data from Example 21.1-2, also calculate the flux ratios  $k_{x0}/k_{x'}$  for  $x_{A1} = 0.20$  and  $x_{A1} = 0.01$ . Tabulate these ratios for the three values of  $x_{A1}$  and plot the ratio versus  $x_{A1}$ .

**21.2-1. *Dimensional Analysis in Mass***

**Transfer.** A fluid is flowing in a vertical pipe and mass transfer is occurring from the pipe wall to the fluid. Relate the convective mass-transfer coefficient  $k_c'$  to the variables  $D$ ,  $\rho$ ,  $\mu$ ,  $v$ ,  $D_{AB}$ ,  $g$ , and  $\Delta\rho$ , where  $D$  is pipe diameter,  $L$  is pipe length, and  $\Delta\rho$  is the density difference.

**Ans.**  $k_c'$

$$k_c' = f(g, L, \rho, \Delta\rho, \mu, D, v, D_{AB})$$

**21.3-1. Mass Transfer from a Flat Plate to a Liquid.** Using the data and physical properties of Example 21.3-2, calculate the flux for a water velocity of 0.152 m/s and a plate length of  $L = 0.137$  m. Do not assume that  $x_{BM} = 1.0$  but actually calculate its value.

**21.3-2. Mass Transfer from a Pipe Wall.** Pure water at 26.1°C is flowing at

a velocity of 0.0305 m/s in a tube having an inside diameter of 6.35 mm. The tube is 1.829 m long, with the last 1.22 m having the walls coated with benzoic acid. Assuming that the velocity profile is fully developed, calculate the average concentration of benzoic acid at the outlet. Use the physical property data from Example 21.3-2. [*Hint*: First, calculate the Reynolds number  $Dv\rho/\mu$ . Then, calculate  $N_{Re}N_{Sc}(D/L)(\pi/4)$ , which is the same as  $W/DAB\rho L$ .]

**Ans.**  $(c_A - c_{A0})/(c_{Ai} - c_{A0}) = 0.0744$ ,  $c_A = 2.193 \times 10^{-3} \text{ kg mol/m}^3$

**21.3-3. Mass-Transfer Coefficient for Various Geometries.** It is desired to estimate the mass-transfer coefficient  $k_G$  in  $\text{kg mol/s} \cdot \text{m}^2 \cdot \text{Pa}$  for water vapor in air at 338.6 K and 101.32 kPa flowing in



a large duct past solids of different geometries. The velocity in the duct is 3.66 m/s. The water vapor concentration in the air is small, so the physical properties of air can be used. Water vapor is being transferred to the solids. Do this for the following geometries:

- A single 25.4-mm-diameter sphere.
- A packed bed of 25.4-mm spheres with  $\epsilon = 0.35$ .

**Ans.** (a)  $k_G = 1.984 \times 10^{-8} \text{ kg mol/s} \cdot \text{m}^2$   
 $\text{Pa (1.482 lb mol/h} \cdot \text{ft}^2 \text{ atm)}$

**21.3-4. Mass Transfer to Definite Shapes.** Estimate the value of the mass-transfer coefficient in a stream of air at 325.6 K flowing in a duct past the following shapes made of solid naphthalene. The velocity of the air is 1.524 m/s at 325.6 K and 202.6 kPa. The  $D_{AB}$  of naphthalene in air is  $5.16 \times$

10<sup>-6</sup> m<sup>2</sup>/s at 273 K and 101.3 kPa.

- For air flowing parallel to a flat plate 0.152 m in length
- For air flowing past a single sphere 12.7 mm in diameter

**21.3-5. Mass Transfer to Packed Bed and Driving Force.** Pure water at 26.1°C is flowing at a rate of 0.0701 ft<sup>3</sup>/h through a packed bed of 0.251-in. benzoic-acid spheres having a total surface area of 0.129 ft<sup>2</sup>. The solubility of benzoic acid in water is 0.00184 lb mol benzoic acid/ft<sup>3</sup> solution. The outlet concentration  $c_{A2}$  is  $1.80 \times 10^{-4}$  lb mol/ft<sup>3</sup>. Calculate the mass-transfer coefficient  $k_c$ .

**21.3-6. Mass Transfer in Liquid Metals.** Mercury at 26.5°C is flowing through a packed bed of lead spheres

having a diameter of 2.096 mm with a void fraction of 0.499. The superficial velocity is 0.02198 m/s. The solubility of lead in mercury is 1.721 wt %, the Schmidt number is 124.1, the viscosity of the solution is  $1.577 \times 10^{-3} \text{ Pa} \cdot \text{s}$ , and the density is 13 530 kg/m<sup>3</sup>.

- Predict the value of  $J_D$ . Use Eq. (21.3-38) if applicable. Compare with the experimental value of  $J_D = 0.076$  (D2).
- Predict the value of  $k_c$  for the case of  $A$  diffusing through nondiffusing  $B$ .

**Ans.** (a)  $J_D = 0.0784$ ; (b)  $k_c = 6.986 \times 10^{-5} \text{ m/s}$

**21.3-7. Mass Transfer from a Pipe and Log Mean Driving Force.** Use the same physical conditions as in Problem 21.3-2, but the velocity in the pipe is now 3.05 m/s. Do as follows:

- Predict the mass-transfer coefficient  $kc'$ . (Is this turbulent flow?)
- Calculate the average benzoic acid concentration at the outlet. [*Note:* In this case, Eqs. (21.3-42) and (21.3-43) must be used with the log mean driving force, where  $A$  is the surface area of the pipe.]
- Calculate the total kg mol of benzoic acid dissolved per second.

**21.3-8. *Derivation of Relation between  $JD$  and  $N_{Sh}$*** . Equation (21.3-3) defines the Sherwood number and Eq. (21.3-5) defines the  $JD$  factor. Derive the relation between  $N_{Sh}$  and  $JD$  in terms of  $N_{Re}$  and  $N_{Sc}$ .

$$\text{Ans. } N_{Sh} = JD N_{Re} N_{Sc}^{1/3}$$

**21.3-9. *Driving Force to Use in Mass Transfer***. Derive Eq. (21.3-42) for the log mean driving force to use for a fluid flowing in a packed bed or in a tube. (*Hint:* Start by making a mass balance

and a diffusion-rate balance over a differential area  $dA$  as follows:

$$N_A dA = k_c (c_{Ai} - c_A)dA = V dc_A$$

where  $V = m^3/s$  flow rate. Assume dilute solutions.)

**21.4-1. *Maximum Oxygen Uptake of a Microorganism.*** Calculate the maximum possible rate of oxygen uptake at  $37^\circ\text{C}$  of a microorganism having a diameter of  $23\ \mu\text{m}$  suspended in an agitated aqueous solution. It is assumed that the surrounding liquid is saturated with  $\text{O}_2$  from air at 1 atm abs pressure. It will be assumed that the microorganism can utilize the oxygen much faster than it can diffuse to it. The microorganism has a density very close to that of water. Use physical-property

data from Example 21.4-1. (*Hint:* Since the oxygen is consumed faster than it is supplied, the concentration  $c_{A2}$  at the surface is zero. The concentration  $c_{A1}$  in the solution is at saturation.)

**Ans.**  $k_c = 9.75 \times 10^{-3} \text{ m/s}$ ,  $N_A = 2.20 \times 10^{-6} \text{ kg mol O}_2 / \text{s} \cdot \text{m}^2$

### **21.4-2. Mass Transfer of O<sub>2</sub> in**

**Fermentation Process.** A total of 5.0 g of wet microorganisms having a density of 1100 kg/m<sup>3</sup> and a diameter of 0.667  $\mu\text{m}$  are added to 0.100 L of aqueous solution at 37°C in a shaker flask for a fermentation. Air can enter through a porous stopper. Use physical property data from Example 21.4-1.

- Calculate the maximum rate possible for mass transfer of oxygen in kg mol O<sub>2</sub>/s to the surface of the microorganism, assuming that the solution is saturated with air at 101.32 kPa abs pressure.

- By material balances on other nutrients, the actual utilization of  $O_2$  by the microorganism is  $6.30 \times 10^{-6} \text{ kg mol } O_2/\text{s}$ . What would be the actual concentration of  $O_2$  in the solution as percent saturation during the fermentation?

**Ans.** (a)  $kL' = 9.82 \times 10^{-3} \text{ m/s}$ ,  $N_{AA} = 9.07 \times 10^{-5} \text{ kg mol } O_2 / \text{s}$ ; (b) 6.95% saturation

**21.5-1. Mass Transfer and Turbulence Models.** Pure water at a velocity of 0.11 m/s is flowing at  $26.1^\circ\text{C}$  past a flat plate of solid benzoic acid where  $L = 0.40 \text{ m}$ . Do as follows:

- Assuming dilute solutions, calculate the mass-transfer coefficient  $k_c$ . Use physical-property data from Example 21.3-2.
- Using the film model, calculate the equivalent film thickness.
- Using the penetration model, calculate the time of penetration.
- Calculate the mean surface renewal factor using the modified penetration model.

**Ans.** (b)  $\delta f = 0.2031 \text{ mm}$ ; (d)  $s = 3.019$   
 $\times 10^{-2} \text{ s}^{-1}$

## References

## Notation



## **Part 2: Separation Process Principles**

# Chapter 22. Absorption and Stripping

## 22.0 Chapter Objectives

On completion of this chapter, a student should be able to:

- Calculate the degrees of freedom for a system in equilibrium
- Calculate flows and composition in single and multiple equilibrium contact stages by using both an equilibrium relationship and a material balance
- Use analytical and graphical techniques to calculate the number of stages needed for either an absorber or stripper
- Calculate rates of mass transfer across fluid–fluid interfaces using two-film theory
- Estimate tray efficiency from correlations of mass-transfer coefficients using two-film theory
- State the differences between loading point and flooding point in a packed column
- Estimate the pressure drop across a trayed and packed

column

- Estimate column diameter
- Compare the three different types of trays based on efficiency and design
- Calculate, for a packed column, the height equivalent to a theoretical plate/stage; then, explain its difference from the height of a transfer unit
- Calculate, for a packed column, the number of theoretical plates/stages; then, explain its difference from the number of transfer units

## **22.1 Equilibrium and Mass Transfer Between Phases**

### **22.1A Phase Rule and Equilibrium**

In order to predict the concentration of a solute in each of two phases in equilibrium, experimental equilibrium data must be available.

If the two phases are not in equilibrium, the rate of mass transfer is proportional to the driving force, which is the departure from

equilibrium. In all cases involving equilibria, two phases are involved, such as gas–liquid or liquid–liquid. The important variables affecting the equilibrium of a solute are temperature, pressure, and concentration.

The equilibrium between two phases in a given situation is restricted by the phase rule:

$$F=C-P+2 \quad (22.1-1)$$

where  $P$  is the number of phases at equilibrium,  $C$  is the number of total components in the two phases when no chemical reactions are occurring, and  $F$  is the number of variants or degrees of freedom of the system. For example, for the gas–liquid system of  $\text{CO}_2$ –air–water,

there are two phases and three components (considering air as one inert component). Then, by Eq. (22.1-1),

$$F = C - P + 2 = 3 - 2 + 2 = 3$$

This means that there are 3 degrees of freedom. If the total pressure and temperature are set, only one variable is left that can be set arbitrarily. If the mole fraction composition  $x_A$  of  $\text{CO}_2$  (A) in the liquid phase is set, the mole fraction composition  $y_A$  or pressure  $p_A$  in the gas phase is automatically determined.

The phase rule does not tell us the partial pressure  $p_A$  in equilibrium with the selected  $x_A$ . The value of  $p_A$  must be determined experimentally. The two phases can, of course, be gas–liquid,

liquid–solid, and so on. For example, the equilibrium distribution of acetic acid between a water phase and an isopropyl ether phase has been determined experimentally for various conditions.

### **22.1B Gas–Liquid Equilibrium**

*1. Gas–liquid equilibrium data.* To illustrate how to obtain experimental gas–liquid equilibrium data, the system  $\text{SO}_2$ –air–water will be considered. An amount of gaseous  $\text{SO}_2$ , air, and water is put in a closed container and shaken repeatedly at a given temperature until equilibrium is reached. Samples of the gas and liquid are analyzed to determine the partial pressure  $p_A$  in atm of  $\text{SO}_2$  (A) in the gas and mole fraction  $x_A$  in the liquid. Figure 22.1-1 shows a plot of

data from Appendix A.3 of the partial pressure  $p_A$  of  $\text{SO}_2$  in the vapor in equilibrium with the mole fraction  $x_A$  of  $\text{SO}_2$  in the liquid at 293 K (20°C).

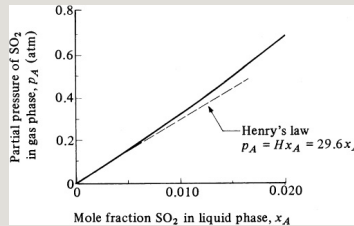


Figure 22.1-1. *Equilibrium plot for  $\text{SO}_2$ –water system at 293 K (20°C).*

2. *Henry's law.* Often, the equilibrium relation between  $p_A$  in the gas phase and  $x_A$  can be expressed by a straight-line Henry's law equation at low concentrations:

$$p_A = H x_A \quad (22.1-2)$$

where  $H$  is the Henry's law constant in

atm/mole fraction for the given system. If both sides of Eq. (22.1-2) are divided by total pressure  $P$  in atm,

$$y_A = H' x_A \quad (22.1-3)$$

where  $H'$  is the Henry's law constant in mole frac gas/mole frac liquid and is equal to  $H/P$ . Note that  $H'$  depends on total pressure, whereas  $H$  does not.

In Fig. 22.1-1, the data follow Henry's law up to a concentration  $x_A$  of about 0.005, where  $H = 29.6$  atm/mol frac. In general, up to a total pressure of about  $5 \times 10^5$  Pa (5 atm) the value of  $H$  is independent of  $P$ . Data for some common gases with water are given in Appendix A.3.

**EXAMPLE 22.1-1. Dissolved Oxygen Concentration in Water**



What will be the concentration of oxygen dissolved in water at 298 K when the solution is in equilibrium with air at 1 atm total pressure? The Henry's law constant is  $4.38 \times 10^4$  atm/mol fraction.

**Solution:** The partial pressure  $p_A$  of oxygen (A) in air is 0.21 atm. Using Eq. (22.1-2),

$$0.21 = Hx_A = 4.38 \times 10^4 x_A$$

Solving,  $x_A = 4.80 \times 10^{-6}$  mol fraction. This means that  $4.80 \times 10^{-6}$  mol  $O_2$  is dissolved in 1.0 mol water plus oxygen, or 0.000853 part  $O_2$ /100 parts water.

### 22.1C Single-Stage Equilibrium Contact

In many operations of the chemical and other process industries, the transfer of mass from one phase to another occurs, usually accompanied by a separation of the mixture's components, since one component will be transferred to a larger extent than will another component.

A single-stage process can be defined as one in which two different phases are brought into intimate contact with each other and then are separated. During the

time of contact, intimate mixing occurs and the various components diffuse and redistribute themselves between the two phases. If mixing time is long enough, the components are essentially at equilibrium in the two phases after separation and the process is considered a single equilibrium stage.

A single equilibrium stage can be represented as shown in Fig. 22.1-2. The two entering phases of known amounts and compositions,  $L_0$  and  $V_2$ , enter the stage; mixing and equilibration occur; and the two exit streams,  $L_1$  and  $V_1$ , leave in equilibrium with each other. Making a total mass balance,

$$L_0 + V_2 = L_1 + V_1 = M \quad (22.1-4)$$

where  $L$  is kg (lb<sub>m</sub>),  $V$  is kg, and  $M$  is

total kg.

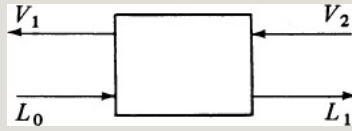


Figure 22.1-2. *Single-stage equilibrium process.*

Assuming that three components,  $A$ ,  $B$ , and  $C$ , are present in the streams and making a balance on  $A$  and  $C$ ,

$$L_0 x_{A0} + V_2 y_{A2} = L_1 x_{A1} + V_1 y_{A1} = M x_{AM} \quad (22.1-5)$$

$$L_0 x_{C0} + V_2 y_{C2} = L_1 x_{C1} + V_1 y_{C1} = M x_{CM} \quad (22.1-6)$$

An equation for  $B$  is not needed since  $x_A + x_B + x_C = 1.0$ . The mass fraction of  $A$  in the  $L$  stream is  $x_A$  and it is  $y_A$  in the  $V$  stream. The mass fraction of  $A$  in the  $M$  stream is  $x_{AM}$ .

To solve the three equations, the equilibrium relations between the

components must be known. In Section 22.1D, this will be done for a gas–liquid system and in Chapter 26 for a vapor–liquid system. Note that Eqs. (22.1-4)–(22.1-6) can also be written using mole units, with  $L$  and  $V$  having units of moles, and  $x_A$  and  $y_A$  having units of mole fraction.

#### **22.1D Single-Stage Equilibrium Contact for a Gas–Liquid System**

In the usual gas-liquid system, the solute  $A$  is in the gas phase  $V$ , along with inert air  $B$ , and in the liquid phase  $L$ , along with inert water  $C$ . Assuming that air is essentially insoluble in the water phase and that water does not vaporize to the gas phase, the gas phase is a binary  $A$ – $B$  and the liquid phase is a binary  $A$ – $C$ . Using moles and mole fraction units, Eq. (22.1-4) holds for a single-stage

process for the total material balance. Since component  $A$  is the only component that redistributes between the two phases, a balance on  $A$  can be written as follows:

$$L'(x_{A01}-x_{A0})+V'(y_{A21}-y_{A2})=L'(x_{A11}-x_{A1})+V'(y_{A11}-y_{A1}) \quad (22.1-7)$$

where  $L'$  is moles inert water  $C$  and  $V'$  is moles inert air  $B$ . Both  $L'$  and  $V'$  are constant and usually known.

To solve Eq. (22.1-7), the relation between  $y_{A1}$  and  $x_{A1}$  in equilibrium is given by Henry's law:

$$y_{A1}=H'x_{A1} \quad (22.1-8)$$

If the solution is not dilute, equilibrium data in the form of a plot of  $p_A$  or  $y_A$  versus  $x_A$  must be available, as in Fig.

## 22.1-1.

### **EXAMPLE 22.1-2. Equilibrium Stage Contact for CO<sub>2</sub>–Air–Water**

A gas mixture at 1.0 atm pressure abs containing air and CO<sub>2</sub> in a single-stage mixer is in continuous contact with pure water at 293 K. The two exit streams of gas and liquid reach equilibrium. The inlet gas flow rate is 100 kg mol/h, with a mole fraction of CO<sub>2</sub> of  $y_{A2} = 0.20$ . The liquid flow rate entering is 300 kg mol water/h. Calculate the amounts and compositions of the two outlet phases. Assume that water does not vaporize to the gas phase.

**Solution:** The flow diagram is the same as given in Fig. 22.1-2. The inert water flow is  $L' = L_0 = 300$  kg mol/h. The inert air flow  $V'$  is obtained from Eq. (22.1-9):

$$V' = V(1 - y_A) \quad (22.1-9)$$

Hence, the inert air flow is  $V' = V_2(1 - y_{A2}) = 100(1 - 0.20) = 80$  kg mol/h. Substituting into Eq. (22.1-7) to make a balance on CO<sub>2</sub> (A),

$$300(0.01 - 0) + 80(0.20 - 0.20) = 300(x_{A1} - x_{A1}) + 80(y_{A1} - y_{A1}) \quad (22.1-10)$$

At 293 K, the Henry's law constant from Appendix A.3 is  $H = 0.142 \times 10^4$  atm/mol frac. Then,  $H' = H/P = 0.142 \times 10^4/1.0 = 0.142 \times 10^4$  mol frac gas/mol frac liquid. Substituting into Eq. (22.1-8),

$$y_{A1} = 0.142 \times 10^4 x_{A1} \quad (22.1-11)$$

Substituting Eq. (22.1-11) into (22.1-10) and solving,  $x_{A1} = 1.41 \times 10^{-4}$  and  $y_{A1} = 0.20$ . To calculate the total flow rates leaving,

$$L_1 = L' + x_{A1} = 300 + 1.41 \times 10^{-4} \times 300 = 300 \text{ kg mol/h} \\ V_1 = V' + y_{A1} = 80 + 0.20 = 100 \text{ kg mol/h}$$

In this case, since the liquid solution is so dilute,  $L_0 \cong L_1$ .

## 22.1E Countercurrent Multiple-Contact Stages

### *1. Derivation of a general equation.*

In Section 22.1C, we used single-stage contact to transfer the solute  $A$  between the  $V$  and  $L$  phases. In order to transfer more solute from, say, the  $V_1$  stream, the single-stage contact can be repeated by again contacting the  $V_1$  stream leaving the first stage with fresh  $L_0$ . This can be repeated using multiple stages. However, this is a waste of the  $L_0$  stream and gives a dilute product in the outlet  $L_1$  streams. To conserve use of the  $L_0$  stream and to get a more concentrated product, countercurrent multiple-stage contacting is generally used. This is somewhat similar to countercurrent heat transfer in a heat exchanger, where the outlet heated stream more closely

approaches the temperature of the inlet hot stream.

The process flow diagram for a countercurrent stage process is shown in Fig. 22.1-3. The inlet  $L$  stream is  $L_0$  and the inlet  $V$  stream is  $V_{N+1}$  instead of  $V_2$  as for a single-stage in Fig. 22.1-2. The outlet product streams are  $V_1$  and  $L_N$  and the total number of stages is  $N$ . The component  $A$  is being exchanged between the  $V$  and  $L$  streams. The  $V$  stream is composed mainly of component  $B$  and the  $L$  stream of component  $C$ . Components  $B$  and  $C$  may or may not be somewhat miscible in each other. The two-phase system can be gas–liquid, vapor–liquid, liquid–liquid, or other.

Making a total overall balance on all



stages,

$$L_0 + V_{N+1} = L_N + V_1 = M \quad (22.1-12)$$

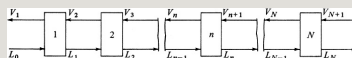


Figure 22.1-3. Countercurrent multiple-stage process.

where  $V_{N+1}$  is mol/h entering,  $L_N$  is mol/h leaving the process, and  $M$  is the total flow. Note in Fig. 22.1-3 that any two streams leaving a stage are in equilibrium with each other. For example, in stage  $n$ ,  $V_n$  and  $L_n$  are in equilibrium. For an overall component balance on  $A$ ,  $B$ , or  $C$ ,

$$L_0 x_0 + V_{N+1} y_{N+1} = L_N x_N + V_1 y_1 = M x_M \quad (22.1-13)$$

where  $x$  and  $y$  are mole fractions. Flows in kg/h (lb<sub>m</sub>/h) and mass fraction can

also be used in these equations.

Making a total balance over the first  $n$  stages,

$$L_0 + V_{N+1} = L_N + V_1 \quad (22.1-14)$$

Making a component balance over the first  $n$  stages,

$$L_0 x_0 + V_{n+1} y_{n+1} = L_n x_n + V_1 y_1 \quad (22.1-15)$$

Solving for  $y_{n+1}$  in Eq. (22.1-15),

$$y_{n+1} = \frac{L_n x_n V_{n+1} + v_1 y_1 - L_0 x_0 V_n}{V_{n+1}} \quad (22.1-16)$$

This is an important material-balance equation, often called an *operating line*. It relates the concentration  $y_{n+1}$  in the  $V$  stream with  $x_n$  in the  $L$  stream passing it.

The terms  $V_1$ ,  $y_1$ ,  $L_0$ , and  $x_0$  are constant and are usually known or can be determined from Eqs. (22.1-12)–(22.1-15).

*2. Countercurrent contact with immiscible streams.* An important case in which the solute  $A$  is being transferred occurs when the solvent stream  $V$  contains components  $A$  and  $B$  with no  $C$ , and the solvent stream  $L$  contains  $A$  and  $C$  with no  $B$ . The two streams  $L$  and  $V$  are immiscible in each other, with only  $A$  being transferred. When Eq. (22.1-16) is plotted on an  $x$ - $y$  plot ( $x_A$  and  $y_A$  of component  $A$ ) such as Fig. 22.1-4, it is often curved, since the slope  $L_n/V_{n+1}$  of the operating line varies if the  $L$  and  $V$  streams vary from stage to stage.

In Fig. 22.1-4, the equilibrium line that relates the compositions of two streams leaving a stage in equilibrium with each other is plotted. To determine the number of ideal stages required to bring about a given separation or reduction of the concentration of A from  $y_{N+1}$  to  $y_1$ , the calculation is often done graphically. Starting at stage 1,  $y_1$  and  $x_0$  are on the operating line, Eq. (22.1-16), plotted in the figure. The vapor  $y_1$  leaving is in equilibrium with the leaving  $x_1$  and both compositions are on the equilibrium line. Then  $y_2$  and  $x_1$  are on the operating line and  $y_2$  is in equilibrium with  $x_2$ , and so on. Each stage is represented by a step drawn on Fig. 22.1-4. The steps are continued on the graph until  $y_{N+1}$  is reached. Alternatively, we can start at  $y_{N+1}$  and draw the steps going to  $y_1$ .

If the streams  $L$  and  $V$  are dilute in component  $A$ , the streams are approximately constant and the slope  $L_n/V_{n+1}$  of Eq. (22.1-16) is nearly constant. Hence, the operating line is essentially a straight line on an  $x$ - $y$  plot. In distillation, where only components  $A$  and  $B$  are present, Eq. (22.1-16) also holds for the operating line; this will be covered in Chapter 26. Cases where  $A$ ,  $B$ , and  $C$  are appreciably soluble in each other often occur in liquid–liquid extraction and will be discussed in Chapter 27.

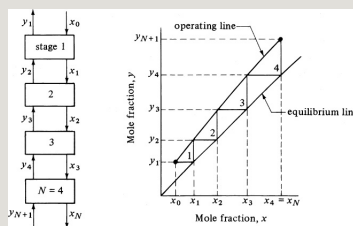


Figure 22.1-4. Number of stages in a countercurrent multiple-stage contact process.

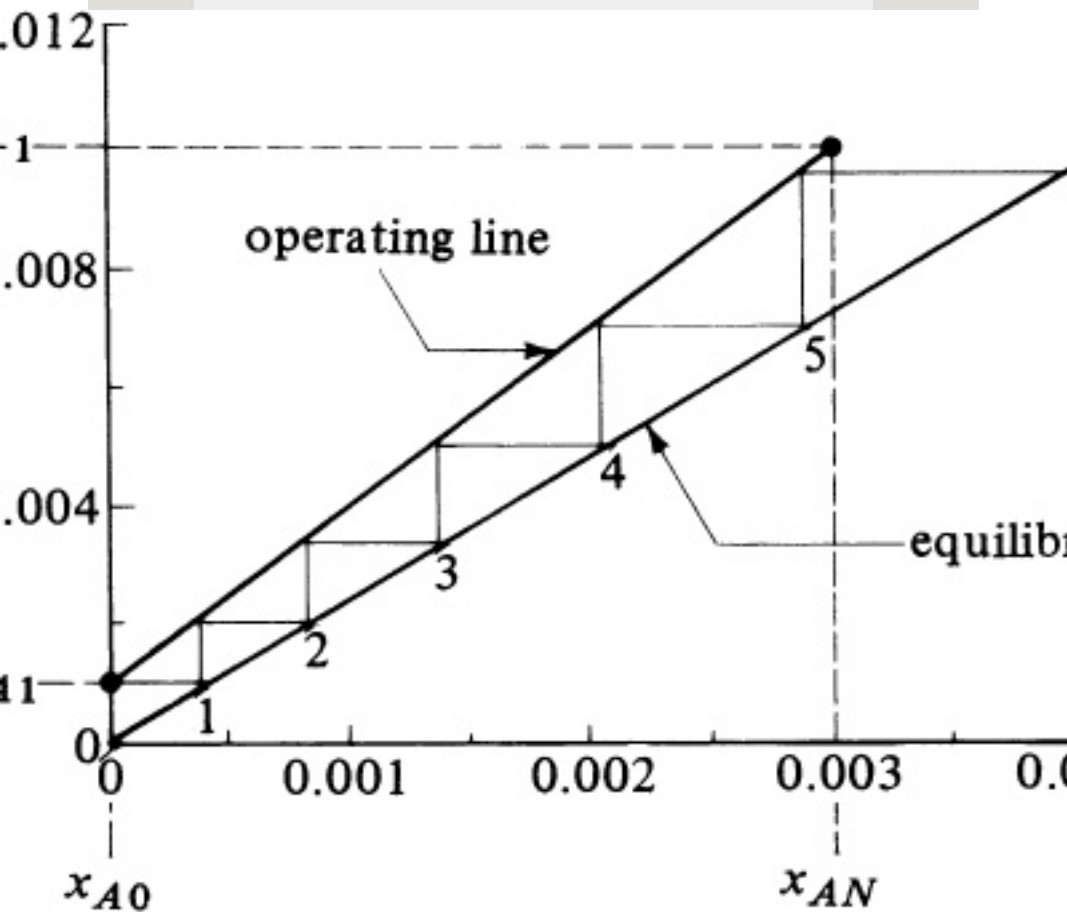
**EXAMPLE 22.1-3. Absorption of Acetone in a Countercurrent Stage Tower**

It is desired to absorb 90% of the acetone in a gas containing 1.0 mol % acetone in air in a countercurrent stage tower. The total inlet gas flow to the tower is 30.0 kg mol/h, and the total inlet pure water flow to be used to absorb the acetone is 90 kg mol H<sub>2</sub>O/h. The process is to operate isothermally at 300 K and a total pressure of 101.3 kPa. The equilibrium relation for the acetone (A) in the gas–liquid is  $y_A = 2.53x_A$ . Determine the number of theoretical stages required for this separation.

**Solution:** The process flow diagram is similar to Fig. 22.1-4. Given values are  $y_{A,N+1} = 0.01$ ,  $x_{A,0} = 0$ ,  $V_{N+1} = 30.0$  kg mol/h, and  $L_0 = 90.0$  kg mol/h. Making an acetone material balance,

$$\begin{aligned} \text{amount of entering acetone} &= y_{A,N+1}V_N \\ +1 &= 0.01(30.0) = 0.30 \text{ kg mol/h entering air} \\ &= (1 - y_{A,N+1})V_{N+1} = (1 - 0.01)(30.0) = 29.7 \text{ kg mol/h} \\ \text{acetone leaving in } V_1 &= 0.10(0.30) = 0.030 \text{ kg mol/h} \\ \text{acetone leaving in } L_N &= 0.90(0.30) = 0.27 \text{ kg mol/h} \\ hV_1 &= 29.7 + 0.03 + 29.73 \text{ kg mol air + acetone/h} \\ h y_{A,1} &= 0.030 + 29.73 = 0.00101 L_N = 90.0 + 0.27 = 90.27 \text{ kg mol water + acetone/h} \\ h x_{A,N} &= 0.2790.27 = 0.00300 \end{aligned}$$

Since the flow of liquid varies only slightly from  $L_0 = 90.0$  at the inlet to  $L_N = 90.27$  at the outlet and  $V$  from 30.0 to 29.73, the slope  $L_N/V_{N+1}$  of the operating line in Eq. (22.1-16) is essentially constant. This line is plotted in Fig. 22.1-5 together with the equilibrium relation  $y_A = 2.53x_A$ . Starting at point  $y_{A,1}$ ,  $x_{A,0}$ , the stages are drawn as shown. About 5.2 theoretical stages are required.



Mole fraction acetone in water,  $x_A$

Figure 22.1-5. Theoretical stages for countercurrent absorption in Example 22.1-3.

### 22.1F Analytical Equations for Countercurrent Stage Contact

When the flow rates  $V$  and  $L$  in a countercurrent process are essentially constant, the operating-

line equation (22.1-16) becomes straight. If the equilibrium line is also a straight line over the concentration range, simplified analytical expressions can be derived for the number of equilibrium stages in a countercurrent stage process.

Referring again to Fig. 22.1-3, Eq. (22.1-17) is an overall component balance on component A:

$$L_0x_0 + V_{N+1}y_{N+1} = L_Nx_N + V_1y_1 \quad (22.1-17)$$

Rearranging,

$$L_Nx_N - V_{N+1}y_{N+1} = L_0x_0 - V_1y_1 \quad (22.1-18)$$

Making a component balance for A on the first  $n$  stages,



$$L_0x_0 + V_{n+1}y_{n+1} = L_nx_n + V_1y_1 \quad (22.1-19)$$

Rearranging,

$$L_0x_0 - V_1y_1 = L_nx_n - V_{n+1}y_{n+1} \quad (22.1-20)$$

Equating Eq. (22.1-18) to Eq. (22.1-20),

$$L_nx_n - V_{n+1}y_{n+1} = L_Nx_N - V_{N+1}y_{N+1} \quad (22.1-21)$$

Since the molar flows are constant,  $L_n = L_N = \text{constant} = L$  and  $V_{n+1} = V_{N+1} = \text{constant} = V$ . Then Eq. (22.1-21) becomes

$$L(x_n - x_N) = V(y_{n+1} - y_{N+1}) \quad (22.1-22)$$

Since  $y_{n+1}$  and  $x_{n+1}$  are in equilibrium and the equilibrium line is straight,  $y_{n+1}$

$= mx_{n+1}$ . Also,  $y_{N+1} = mx_{N+1}$ .

Substituting  $mx_{n+1}$  for  $y_{n+1}$  and calling  $A = L/mV$ , Eq. (21.1-22) becomes

$$x_{n+1} - Ax_n = y_{N+1}/m - Ax_N \quad (22.1-23)$$

where  $A$  is an absorption factor and is constant.

All factors on the right-hand side of Eq. (22.1-23) are constant. This equation is a linear first-order difference equation and can be solved by the calculus of finite-difference methods (G1, M1). The final derived equations are as follows.

For transfer of solute  $A$  from phase  $L$  to  $V$  (stripping),

$$x_0 - x_N x_0 - (y_{N+1}/m) = (1/A)^{N+1} - (1/A) \\ (1/A)^{N+1} - 1 \quad (22.1-24)$$

$$N = \ln \left| x_0 - (y_{N+1}/m)x_N - (y_{N+1}/m)(1 - A) + A \right| \ln(1/A) \quad (22.1-25)$$

When  $A = 1$ ,

$$N = x_0 - x_N x_N - (y_{N+1}/m) \quad (22.1-26)$$

For transfer of solute  $A$  from phase  $V$  to  $L$  (absorption),

$$y_{N+1} - y_1 y_{N+1} - m x_0 = A N + 1 - A A N + 1 - 1 \quad (22.1-27)$$

$$N = \ln \left| y_{N+1} - r m_0 y_1 - r m_0 (1 - 1/A) + 1/A \right| \ln A \quad (22.1-28)$$

When  $A = 1$ ,

$$N = y_{N+1} - y_1 y_1 - r m_0 \quad (22.1-29)$$

The term  $A$  is often called the *absorption factor* and  $S$  the *stripping*

*factor*, where  $S = 1/A$ . These equations can be used with any consistent set of units such as mass flow and mass fraction or molar flow and mole fraction. Such series of equations are often called *Kremser equations* and are convenient to use.

If the equilibrium line is not straight but curved somewhat, the slope will vary and, hence,  $m$  and  $A = L/mV$  will vary. For absorption (referring to Fig. 22.1-4) at the concentrated end, the slope  $m_N$  or tangent of the equilibrium line at the concentrations  $y_N, x_N$  leaving this bottom stage  $N$  is used. This  $m_N$  is at point  $x_N$  on the equilibrium line. For the top or dilute end at stage 1 of the tower, the slope of the equilibrium line  $m_1$  at the concentrations  $y_1, x_1$  leaving this stage is employed. This  $m_1$  is at point  $y_1$

on the equilibrium line. Then,  $A_N = L_N / m_N V_{N+1}$  and  $A_1 = L_0 / m_1 V_1$ . The geometric average is used, where  $A = A_N A_1$  (P1, T3). Also, the dilute  $m_1$  is used in Eqs. (22.1-27)–(22.1-29).

For stripping at the top or concentrated stage, the slope  $m_1$  or tangent to the equilibrium line at the concentrations  $y_1$ ,  $x_1$  leaving this stage is used. This  $m_1$  is at point  $y_1$  on the equilibrium line. At the bottom stage or dilute end of the tower, the slope  $m_N$  of the equilibrium line at the points  $y_N$ ,  $x_N$  is used. This  $m_N$  is at  $x_N$  on the equilibrium line. Then,  $A_N = L_N / m_N V_{N+1}$ ,  $A_1 = L_0 / m_1 V_1$ , and  $A = A_N A_1$ . Again, the dilute  $m_N$  is used in Eqs. (22.1-24)–(22.1-26). Sometimes only the values of  $A$  and  $m$  at the dilute end are used since more of the stages are in this region.

**EXAMPLE 22.1-4. Number of Stages by Analytical Equation**

Repeat Example 22.1-3 but use the Kremser analytical equations for countercurrent stage processes.

**Solution:** At one end of the process at stage 1,  $V_1 = 29.73$  kg mol/h,  $y_{A1} = 0.00101$ ,  $L_0 = 90.0$ , and  $x_{A0} = 0$ . Also, the equilibrium relation is  $y_A = 2.53x_A$ , where  $m = 2.53$ . Then,

$$A_1 = LmV = L_0mV_1 = 90.0(2.53)(29.73) = 1.20$$

At stage  $N$ ,  $V_{N+1} = 30.0$ ,  $y_{AN+1} = 0.01$ ,  $L_N = 90.27$ , and  $x_{AN} = 0.00300$ .

$$A_N = L_NmV_{N+1} = 90.27(2.53)(30.0) = 1.19$$

The geometric average  $A = A_1A_N = 1.20 \times 1.19 = 1.195$ .

The acetone solute is transferred from the  $V$  to the  $L$  phase (absorption). Substituting into Eq. (22.1-28),

$$N = \ln[0.01 - 2.53(0)0.00101 - 2.53(0)(1 - 1.195) + 1.195] / \ln(1.195) = 5.04 \text{ stages}$$

This compares closely with the 5.2 stages obtained using the graphical method.

## 22.1G Introduction and Equilibrium Relations

*1. Introduction to interphase mass transfer.* In Chapter 20, we considered mass transfer from a fluid phase to another phase, which was most often a solid phase. The solute  $A$  was usually transferred from the fluid phase by convective mass

transfer and through the solid by diffusion. In this section, we will consider the mass transfer of solute A from one fluid phase by convection and then through a second fluid phase by convection. For example, the solute may diffuse through a gas phase and then diffuse through and be absorbed in an adjacent and immiscible liquid phase. This occurs in the case of absorption of ammonia from air by water.

The two phases are in direct contact with each other, such as in a packed, tray, or spray-type tower, and the interfacial area between the phases is usually not well defined. In two-phase mass transfer, a concentration gradient will exist in each phase, causing mass

transfer to occur. At the interface between the two fluid phases, equilibrium exists in most cases.

*2. Equilibrium relations.* Even when mass transfer is occurring, equilibrium relations are important to determine concentration profiles for predicting rates of mass transfer. In Section 22.1, the equilibrium relation in a gas–liquid system and Henry’s law were discussed. In Section 20.1C, a discussion covered equilibrium distribution coefficients between two phases. These equilibrium relations will be used in a discussion of mass transfer between phases in this section.

### **22.1H Concentration Profiles in Interphase Mass Transfer**

In the majority of mass-transfer systems, two phases, which are



essentially immiscible in each other, are present together with an interface between these two phases. Assuming solute  $A$  is diffusing from the bulk gas phase  $G$  to the liquid phase  $L$ , it must pass through phase  $G$ , through the interface, and then into phase  $L$  in series. A concentration gradient must exist to cause this mass transfer through the resistances in each phase, as shown in Fig. 22.1-6. The average or bulk concentration of  $A$  in the gas phase in mole fraction units is  $y_{AG}$ , where  $y_{AG} = p_A/P$ , and in the bulk liquid phase in mole fraction units it is  $x_{AL}$ .

The concentration in the bulk gas phase  $y_{AG}$  decreases to  $y_{Ai}$  at the interface. The liquid concentration starts at  $x_{Ai}$  at the interface and falls to  $x_{AL}$ . At the

interface, since there would be no resistance to transfer across this interface,  $y_{Ai}$  and  $x_{Ai}$  are in equilibrium and are related by the equilibrium distribution relation

$$y_{Ai}=f(x_{Ai}) \quad (22.1-30)$$

where  $y_{Ai}$  is a function of  $x_{Ai}$ . They are related by an equilibrium plot such as Fig. 22.1-7. If the system follows Henry's law,  $y_{AP}$  or  $p_A$  and  $x_A$  are related by Eq. (22.1-2) at the interface.

Experimentally, the resistance at the interface has been shown to be negligible for most cases of mass transfer where chemical reactions do not occur, such as absorption of common gases from air to water and extraction of organic solutes from one phase to

another. However, there are some exceptions. Certain surface-active compounds may concentrate at the interface and cause an “interfacial resistance” that slows down the diffusion of solute molecules. Theories for predicting when interfacial resistance may occur are often obscure and unreliable.

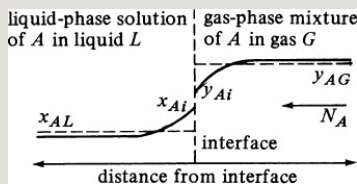


Figure 22.1-6. Concentration profile of solute A diffusing through two phases.

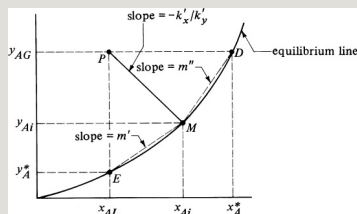


Figure 22.1-7. Concentration driving forces and interface concentrations in interphase mass transfer (equimolar counterdiffusion).

## 22.11 Mass Transfer Using Film Mass-Transfer Coefficients and Interface Concentrations

1. *Equimolar counterdiffusion.* For equimolar counterdiffusion, the concentrations of Fig. 22.1-6 can be plotted on an  $x$ - $y$  diagram as in Fig. 22.1-7. Point  $P$  represents the bulk phase compositions  $x_{AG}$  and  $x_{AL}$  of the two phases and point  $M$  the interface concentrations  $y_{Ai}$  and  $x_{Ai}$ . For  $A$  diffusing from the gas to liquid and  $B$  in equimolar counterdiffusion from liquid to gas,

$$N_A = k_y'(y_{AG} - y_{Ai}) = k_x'(x_{Ai} - x_{AL}) \quad (22.1-31)$$

where  $k_y'$  is the gas-phase mass-transfer coefficient in  $\text{kg mol/s} \cdot \text{m}^2 \cdot \text{mol frac}$  ( $\text{g mol/s} \cdot \text{cm}^2 \cdot \text{mol frac}$ ,  $\text{lb mol/h} \cdot \text{ft}^2 \cdot \text{mol frac}$ ), and  $k_x'$  is the liquid-phase mass-transfer coefficient in  $\text{kg mol/s} \cdot$

$\text{m}^2 \cdot \text{mol frac} (\text{g mol/s} \cdot \text{cm}^2 \cdot \text{mol frac},$   
 $\text{lb mol/h} \cdot \text{ft}^2 \cdot \text{mol frac}).$  Rearranging  
 Eq. (22.1-31),

$$-k_x'ky' = y_{AG} - y_{Ai}x_{AL} - x_{Ai} \quad (22.1-32)$$

The driving force in the gas phase is  $(y_{AG} - y_{Ai})$  and in the liquid phase it is  $(x_{Ai} - x_{AL})$ . The slope of the line  $PM$  is  $-k_x'/k_y'$ . This means that if the two film coefficients  $k_x'$  and  $k_y'$  are known, the interface compositions can be determined by drawing line  $PM$  with a slope  $-k_x'/k_y'$  intersecting the equilibrium line.

The bulk-phase concentrations  $y_{AG}$  and  $x_{AL}$  can be determined by simply sampling the mixed bulk gas phase and sampling the mixed bulk liquid phase. The interface concentrations are

determined by Eq. (22.1-29).

2. *Diffusion of A through stagnant or nondiffusing B.* For the common case of A diffusing through a stagnant gas phase and then through a stagnant liquid phase, the concentrations are shown in Fig. 22.1-8, where  $P$  again represents bulk-phase compositions and  $M$  represents interface compositions. The equations for A diffusing through a stagnant gas and then through a stagnant liquid are

$$N_A = k_y'(y_{AG} - y_{Ai}) = k_x'(x_{Ai} - x_{AL}) \quad (22.1-31)$$

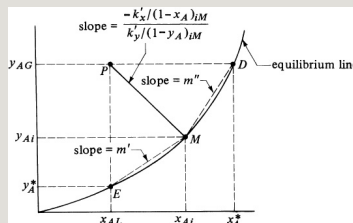


Figure 22.1-8. Concentration driving forces and interface concentrations in interphase mass transfer (A diffusing through

*stagnant B*).

Now,

$$k_y = k_y' (1 - y_A)_{iM} \quad k_x = k_x' (1 - x_A)_{iM} \quad (22.1-34)$$

where

$$(1 - y_A)_{iM} = (1 - y_{Ai}) - (1 - y_{AG}) \ln[(1 - y_{Ai}) / (1 - y_{AG})] \quad (22.1-35)$$

$$(1 - x_A)_{iM} = (1 - x_{AL}) - (1 - x_{Ai}) \ln[(1 - x_{AL}) / (1 - x_{Ai})] \quad (22.1-36)$$

Then,

$$N_A = k_y' (1 - y_A)_{iM} (y_{AG} - y_{Ai}) = k_x' (1 - x_A)_{iM} (x_{Ai} - x_{AL}) \quad (22.1-37)$$

Note that  $(1 - y_A)_{iM}$  is the same as  $y_{BM}$  of Eq. (21.1-11) but is written for the

interface, and  $(1 - x_A)iM$  is the same as  $x_{BM}$  of Eq. (21.1-11). Using Eq. (22.1-37) and rearranging,

$$-kx'/(1-x_A)iMky'/(1-y_A)iM=yAG-yAix_{AL}-x_{Ai}(22.1-38)$$

The slope of the line  $PM$  in Fig. 22.1-8 to obtain the interface compositions is given by the left-hand side of Eq. (22.1-38). This differs from the slope of Eq. (22.1-32) for equimolar counterdiffusion by the terms  $(1 - y_A)iM$  and  $(1 - x_A)iM$ . When  $A$  is diffusing through stagnant  $B$  and the solutions are dilute,  $(1 - y_A)iM$  and  $(1 - x_A)iM$  are close to 1.

A trial-and-error method is needed to use Eq. (22.1-38) to get the slope, since the left-hand side contains the terms  $y_{Ai}$



and  $x_{Ai}$  that are being sought. For the first trial,  $(1 - y_A)iM$  and  $(1 - x_A)iM$  are assumed to be 1.0, and Eq. (22.1-38) is used to get the slope and  $y_{Ai}$  and  $x_{Ai}$  values. Then, for the second trial, these values of  $y_{Ai}$  and  $x_{Ai}$  are used to calculate a new slope to get new values of  $y_{Ai}$  and  $x_{Ai}$ . This is repeated until the interface compositions do not change. Three trials are usually sufficient.

**EXAMPLE 22.1-5. Interface Compositions in Interphase Mass Transfer**

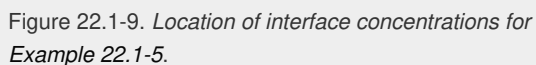
The solute  $A$  is being absorbed from a gas mixture of  $A$  and  $B$  in a wetted-wall tower with the liquid flowing as a film downward along the wall. At a certain point in the tower, the bulk gas concentration  $y_{AG} = 0.380$  mol fraction and the bulk liquid concentration is  $x_{AL} = 0.100$ . The tower is operating at 298 K and  $1.013 \times 10^5$  Pa, and the equilibrium data are as follows:

--

The solute  $A$  diffuses through stagnant  $B$  in the gas phase and then through a nondiffusing liquid.

Using correlations for dilute solutions in wetted-wall towers, the film mass-transfer coefficient for  $A$  in the gas phase is predicted as  $k_y = 1.465 \times 10^{-3}$  kg mol A/s  $\cdot$  m<sup>2</sup>  $\cdot$  mol frac (1.08 lb mol/h  $\cdot$  ft<sup>2</sup>  $\cdot$  mol frac), and for the liquid phase as  $k_x = 1.967 \times 10^{-3}$  kg mol A/s  $\cdot$  m<sup>2</sup>  $\cdot$  mol frac (1.45 lb mol/h  $\cdot$  ft<sup>2</sup>

**Solution:** Since the correlations are for dilute solutions,  $(1 - y_A)_{iM}$  and  $(1 - x_A)_{iM}$  are approximately 1.0 and the coefficients are the same as  $ky'$  and  $kx'$ . The equilibrium data are plotted in Fig. 22.1-9. Point  $P$  is plotted at  $y_{AG} = 0.380$  and  $x_{AL} = 0.100$ . For the first trial,  $(1 - y_A)_{iM}$  and  $(1 - x_A)_{iM}$  are assumed as 1.0, and the slope of line  $PM$  is, from Eq. (22.1-38),



$$-kx'/(1-xA)iMky'/(1-yA)iM = -1.967 \times 10^{-3} / 1.01465 \times 10^{-3} / 1.0 = -1.342$$

A line through point  $P$  with a slope of  $-1.342$  is plotted in Fig. 22.1-9 intersecting the equilibrium line at  $M_1$ , where  $y_{Ai} = 0.183$  and  $x_{Ai} = 0.247$ .

For the second trial, we use  $y_{Ai}$  and  $x_{Ai}$  from the first trial to calculate the new slope. Substituting into Eqs. (22.1-35) and (22.1-36),

$$(1-yA)iM = (1-yAi) - (1-yAG) \ln[(1-yAi)/(1-yAG)] = (1-0.183) - (1-0.380) \ln[(1-0.183)/(1-0.380)] = 0.715$$

$$(1-xA)iM = (1-xAL) - (1-xAi) \ln[(1-xAL)/(1-xAi)] = (1-0.100) - (1-0.247) \ln[(1-0.100)/(1-0.247)] = 0.825$$

Substituting into Eq. (22.1-38) to obtain the new slope,

$$-kx'/(1-xA)iMky'/(1-yA)iM = -1.967 \times 10^{-3} / 0.8251.465 \times 10^{-3} / 0.715 = -1.163$$

A line through point  $P$  with a slope of  $-1.163$  is plotted and intersects the equilibrium line at  $M$ , where  $y_{Ai} = 0.197$  and  $x_{Ai} = 0.257$ .

Using these new values for the third trial, the following values are calculated:

$$(1-yA)iM = (1-0.197) - (1-0.380) \ln[(1-0.197)/(1-0.380)] = 0.709$$

$$(1-xA)iM = (1-0.100) - (1-0.257) \ln[(1-0.100)/(1-0.257)] = 0.820$$

$$-kx'/(1-xA)iMky'/(1-yA)iM = -1.967 \times 10^{-3} / 0.8201.465 \times 10^{-3} / 0.709 = -1.160$$

This slope of  $-1.160$  is essentially the same as the slope of  $-1.163$  for the second trial. Hence, the final values are  $y_{Ai} = 0.197$  and  $x_{Ai} = 0.257$  and are shown as point  $M$ .

To calculate the flux, Eq. (22.1-37) is used:

$$NA = ky'(1-yA)iM(yAG - yAi) = 1.465 \times 10^{-3} \cdot 0.709(0.380 - 0.197) = 3.78 \times 10^{-4} \text{ kg mol/s} \cdot \text{m}^2$$

$$NA = 1.080 \cdot 0.709(0.380 - 0.197) = 0.27851 \text{ b mol/h} \cdot \text{it}^2$$

$$NA = kx'(1-xA)iM(xAi - xAL) = 1.967 \times 10^{-3} \cdot 0.820(0.257 - 0.100) = 3.78 \times 10^{-4} \text{ kg mol/s} \cdot \text{m}^2$$

Note that the flux  $N_A$  through each phase is the same as in the other phase, which should be the case at steady state.

## 22.1J Overall Mass-Transfer Coefficients and Driving Forces

*1. Introduction.* Film or single-phase mass-transfer coefficients  $ky'$  and  $kx'$  or  $k_y$  and  $k_x$  are often difficult to measure experimentally, except in certain experiments designed so that the concentration difference across one phase is small and can be neglected. As a result, overall mass-transfer coefficients  $K'y$  and  $Kx'$  are measured based on the gas phase or liquid phase. This method is used in heat transfer, where overall heat-transfer coefficients are measured based on inside or outside areas instead of film coefficients.

The overall mass transfer  $ky'$  is defined as

$$N_A = K_y'(y_{AG} - y_A^*)(22.1-39)$$

where  $k_y'$  is based on the overall gas-phase driving force in  $\text{kg mol/s} \cdot \text{m}^2 \cdot \text{mol frac}$ , and  $y_A^*$  is the value that would be in equilibrium with  $x_{AL}$ , as shown in Fig. 22.1-7. Also,  $K_x'$  is defined as

$$N_A = K_x'(x_A^* - x_{AL})(22.1-40)$$

where  $K_x'$  is based on the overall liquid-phase driving force in  $\text{kg mol/s} \cdot \text{m}^2 \cdot \text{mol frac}$  and  $x_A^*$  is the value that would be in equilibrium with  $y_{AG}$ .

*2. Equimolar counterdiffusion and/or diffusion in dilute solutions.* Equation (22.1-31) holds for equimolar counterdiffusion, or, when the solutions are dilute, Eqs. (22.1-37) and (22.1-31) are identical:

$$N_A = k y' (y_{AG} - y_{Ai}) = k x' (x_{Ai} - x_{AL})$$

(22.1-31)

From Fig. 22.1-7,

$$y_{AG} - y_{A^*} = (y_{AG} - y_{Ai}) + (y_{Ai} - y_{A^*})$$

(22.1-41)

Between the points  $E$  and  $M$ , the slope  $m'$  can be given as

$$m' = \frac{y_{Ai} - y_{A^*}}{x_{Ai} - x_{AL}} \quad (22.1-42)$$

Solving Eq. (22.1-42) for  $(y_{Ai} - y_{A^*})$  and substituting into Eq. (22.1-41),

$$y_{AG} - y_{A^*} = (y_{AG} - y_{Ai}) + m' (x_{Ai} - x_{AL})$$

(22.1-43)

Then, on substituting Eqs. (22.1-39) and (22.1-31) into (22.1-43) and canceling out  $N_A$ ,

$$1K_y' = 1k_y' + m'k_x' \quad (22.1-44)$$

The left-hand side of Eq. (22.1-44) is the total resistance based on the overall gas driving force and equals the gas film resistance  $1/k_y'$  plus the liquid film resistance  $m'/k_x'$ .

In a similar manner, from Fig. 22.1-7,

$$x_A^* - x_{AL} = (x_A^* - x_{Ai}) + (x_{Ai} - x_{AL}) \quad (22.1-45)$$

$$m'' = y_{AG} - y_{Ai} x_A^* - x_{Ai} \quad (22.1-46)$$

Proceeding as before,

$$1K_x' = 1m''k_y' + 1k_x' \quad (22.1-47)$$

Several special cases of Eqs. (22.1-44) and (22.1-47) will now be discussed. The numerical values of  $k_x'$  and  $k_y'$  are

roughly similar. The values of the slopes  $m'$  and  $m_0$  are very important. If  $m'$  is quite small, so that the equilibrium curve in Fig. 22.1-7 is almost horizontal, a small value of  $y_A$  in the gas will give a large value of  $x_A$  in equilibrium in the liquid. The gas solute  $A$  is then very soluble in the liquid phase, and hence the term  $m'/k'_x$  in Eq. (22.1-44) is very small. Then,

$$1/K_y' \cong 1/k_y' \quad (22.1-48)$$

and the major resistance is in the gas phase, or the “gas phase is controlling.” The point  $M$  has moved down very close to  $E$ , so that

$$y_{AG} - y_A^* \cong y_{AG} - y_{Ai} \quad (22.1-49)$$

Similarly, when  $m''$  is very large, the solute  $A$  is very insoluble in the liquid,



$1/(m''k'_y)$  becomes small, and

$$1Kx' \cong 1kx' \quad (22.1-50)$$

The “liquid phase is controlling” and  $x_{Ai} \cong x_A^*$ . Systems for absorption of oxygen or CO<sub>2</sub> from air by water are similar to Eq. (22.1-50).

*3. Diffusion of A through stagnant or nondiffusing B.* For the case of A diffusing through nondiffusing B, Eqs. (22.1-37) and (22.1-43) hold and Fig. 22.1-8 is used:

$$N_A = ky'(1-y_A)_i M(y_{AG} - y_{Ai}) = kx'(1-x_A)_i M(x_{Ai} - x_{AL}) \quad (22.1-37)$$

$$y_{AG} - y_A^* = (y_{AG} - y_{Ai}) + m'(x_{Ai} - x_{AL}) \quad (22.1-43)$$

We must, however, define the equations

for the flux using overall coefficients as follows:

$$N_A = [K_y'(1-y_A)^*M](y_{AG} - y_A^*) = [K_x'(1-x_A)^*M](x_A^* - x_{AL}) \quad (22.1-51)$$

The bracketed terms are often written as follows:

$$K_y = K_y'(1-y_A)^*M \quad K_x = K_x'(1-x_A)^*M \quad (22.1-52)$$

where  $K_y$  is the overall gas mass-transfer coefficient for  $A$  diffusing through stagnant  $B$  and  $K_x$  is the overall liquid mass-transfer coefficient. These two coefficients are concentration-dependent. Substituting Eqs. (22.1-37) and (22.1-51) into (22.1-43), we obtain

$$1/K_y'/(1-y_A)^*M = 1/k_y'/(1-y_A)^i M + m$$

$$k'_{x'}/(1-x_A) iM \quad (22.1-53)$$

where

$$(1-y_A)^* M = (1-y_A^*) - (1-y_{AG}) \ln \left| \frac{(1-y_A^*)}{(1-y_{AG})} \right| \quad (22.1-54)$$

Similarly, for  $K_{x'}$ ,

$$1 K_{x'}/(1-x_A)^* M = 1 m'' k_{y'}/(1-y_A) iM + 1 k_{x'}/(1-x_A) iM \quad (22.1-55)$$

where

$$(1-x_A)^* M = (1-x_{AL}) - (1-x_A^*) \ln \left[ \frac{(1-x_{AL})}{(1-x_A^*)} \right] \quad (22.1-56)$$

It should be noted that the relations derived here also hold for any two-phase system, where  $y$  stands for one phase and  $x$  for the other phase. For example, for the extraction of the solute acetic

acid ( $A$ ) from water ( $y$  phase) by isopropyl ether ( $x$  phase), the same relations will hold.

**EXAMPLE 22.1-6. Overall Mass-Transfer Coefficients from Film Coefficients**

Using the same data as in Example 22.1-5, calculate the overall mass-transfer coefficient  $K_y'$ , the flux, and the percent resistance in the gas and liquid films. Do this for the case of  $A$  diffusing through stagnant  $B$ .

**Solution:** From Fig. 22.1-9,  $y_A^* = 0.052$ , which is in equilibrium with the bulk liquid  $x_{AL} = 0.10$ . Also,  $y_{AG} = 0.380$ . The slope of chord  $m$  between  $E$  and  $M$  from Eq. (22.1-42) is, for  $y_{Ai} = 0.197$  and  $x_{Ai} = 0.257$ ,

$$m' = y_{Ai} - y_A^* x_{Ai} - x_{AL} = 0.197 - 0.052(0.257) - 0.100 = 0.923$$

From Example 22.1-5,

$$k_y'(1 - y_A)_i M = 1.465 \times 10^{-3} / 0.709 \quad k_x'(1 - x_A)_i M = 1.967 \times 10^{-3} / 0.820$$

Using Eq. (22.1-54),

$$(1 - y_A)^* M = (1 - y_A^*) - (1 - y_{AG}) \ln[(1 - y_A^*) / (1 - y_{AG})] = (1 - 0.052) - (1 - 0.380) \ln[(1 - 0.052) / (1 - 0.380)] = 0.733$$

Then, using Eq. (21.1-53),

$$\frac{1}{K_y'} = \frac{1}{k_y'(1 - y_A)_i M} + \frac{1}{m' k_x'(1 - x_A)_i M} = \frac{1}{1.465 \times 10^{-3} / 0.709} + \frac{1}{0.923 \times 1.967 \times 10^{-3} / 0.820} = \frac{1}{484.0 + 384.8} = \frac{1}{868.8}$$

Solving,  $K_y' = 8.90 \times 10^{-4}$ . The percent resistance in the gas film is  $(484.0 / 868.8)100 = 55.7\%$  and in the liquid film 44.3%. The flux is as follows, using Eq. (22.1-51):

$$N_A = [K_y'(1 - y_A)^* M](y_{AG} - y_A^*) = 8.90 \times 10^{-4} \times 0.773(0.380 - 0.052) = 3.78 \times 10^{-4} \text{ kg mol/s} \cdot \text{m}^2$$

This, of course, is the same flux value as was calculated in Example 22.1-5 using the film equations.

4. *Discussion of overall coefficients.* If the two-phase system is such that the major resistance is in the gas phase, as in Eq. (22.1-48), then to increase the overall rate of mass transfer, efforts should be centered on increasing the gas-phase turbulence, not the liquid-phase turbulence. For a two-phase system where the liquid film resistance is controlling, turbulence should be increased in this phase to increase rates of mass transfer.

To design mass-transfer equipment, the overall mass-transfer coefficient is synthesized from the individual film coefficients, as discussed in this section.

Generally, when the major resistance to mass transfer is in the gas phase, the overall mass transfer coefficient  $K_y'$  or

the film coefficient  $k_y'$  is used. An example would be absorption of ammonia from air to water. When the major resistance is in the liquid phase, as in absorption of oxygen from air by water,  $K_x'$  or  $k_x'$  is used.

## **22.2 Introduction to Absorption**

### **22.2A Absorption**

Absorption is a mass-transfer process in which a vapor solute  $A$  in a gas mixture is absorbed by means of a liquid in which the solute is more or less soluble. The gas mixture consists mainly of an inert gas and the solute. The liquid also is primarily immiscible in the gas phase; that is, its vaporization into the gas phase is relatively slight. A typical example is absorption of the solute ammonia from an air–

ammonia mixture by water.

Subsequently, the solute is recovered from the solution by distillation. In the reverse process of desorption or stripping, the same principles and equations hold.

Equilibrium relations for gas–liquid systems in absorption were discussed in Section 22.1, and such data are needed for design of absorption towers. Some data are tabulated in Appendix A.3.

Other, more extensive data are available in Perry and Green (P1, P2).

## **22.2B Equipment for Absorption and Distillation**

*1. Various types of tray (plate) towers for absorption and distillation.* In order to efficiently bring the vapor and liquid into contact in absorption and distillation,

tray towers of the following types are often used.

1. *Sieve tray*. The sieve tray shown in Fig. 22.2-1a is very common. Essentially, the same tray is used in distillation and gas absorption. In the sieve tray, vapor bubbles up through simple holes in the tray through the flowing liquid. Hole sizes range from 3 to 12 mm in diameter, with 5 mm a common size. The vapor area of the holes varies between 5 to 15% of the tray area. The liquid is held on the tray surface and prevented from flowing down through the holes by the kinetic energy of the gas or vapor. The depth of liquid on the tray is maintained by an overflow, outlet weir. The overflow liquid flows into the downspout to the next tray below.
2. *Valve tray*. A modification of the sieve tray is the valve tray shown in Fig. 22.2-1b. This consists of an opening in the tray and a lift-valve cover with guides to keep the cover properly positioned over the opening. This provides a variable open area that is varied by the vapor flow inhibiting leakage of liquid down the opening at low vapor rates. Hence, this type of tray can operate over a greater range of flow rates than can the sieve tray, with a cost of only about 20% more than a sieve tray. The valve tray is being increasingly used today (S5).

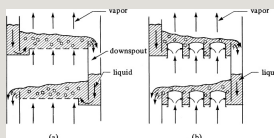




Figure 22.2-1. Tray contacting devices: (a) detail of sieve-tray tower, (b) detail of valve-tray tower.

**3. Bubble-cap tray.** Bubble-cap trays have been used for over 100 years, but since 1950 they have been generally superseded by sieve-type or valve trays because of their cost, which is almost double that of sieve-type trays. In the bubble tray, the vapor or gas rises through the opening in the tray into the bubble caps. Then, the gas flows through slots in the periphery of each cap and bubbles upward through the flowing liquid. Details and design procedures for many of these and other types of trays are given elsewhere (B2, P2, T1). Efficiencies for the different types of trays are discussed in Section 22.6.

**2. Structured packing for absorption and distillation.** Structured packing has become competitive with conventional tray towers, especially in tower revamps where increased capacity and/or efficiency is desired (K1, L2). The thin corrugated-metal sheets are formed in a triangular cross-section. The vapor flow goes upward through the triangular channels, which are set at a  $45^\circ$  angle with the vertical. The sheets are

arranged so the liquid flows downward in the opposite direction and spreads over the surfaces, as in a wetted-wall tower.

The open void fraction typically varies from 0.91 to 0.96 and the specific surface area from 165 to 330 m<sup>2</sup>/m<sup>3</sup> volume (50 to 100 ft<sup>2</sup>/ft<sup>3</sup>). In many cases, the packing sheet contains perforations or holes about 2–4 mm ID spaced 0.5–1.5 cm apart to help wet both the upper and lower sides of the sheet.

*3. Packed towers for absorption and distillation.* Packed towers are used for continuous countercurrent contacting of gas and liquid in absorption as well as for vapor–liquid contacting in distillation. The tower in Fig. 22.2-2

consists of a cylindrical column containing a gas inlet and distributing space at the bottom, a liquid inlet and distributing device at the top, a gas outlet at the top, a liquid outlet at the bottom, and a packing or filling in the tower. The gas enters the distributing space below the packed section and rises upward through the openings or interstices in the packing and contacts the descending liquid flowing through the same openings. A large area of intimate contact between the liquid and gas is provided by the packing.

*4. Types of random packing for absorption and distillation.* Many different types of tower packings have been developed and a number are used quite often. Common types of packing that are dumped at random in the tower

are shown in Fig. 22.2-3. Such packings and other commercial packings are available in sizes of 3 mm to about 75 mm. Most of the tower packings are made of materials such as clay, porcelain, metal, or plastic. High void spaces of 65–95% are characteristic of good packings. The packings permit relatively large volumes of liquid to pass countercurrently to the gas flow through the openings with relatively low pressure drops for the gas. These same types of packings are also used in vapor–liquid separation processes of distillation.

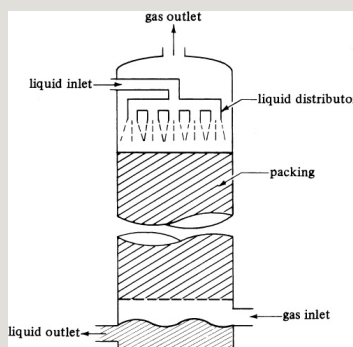


Figure 22.2-2. *Packed tower flows and characteristics for absorption.*

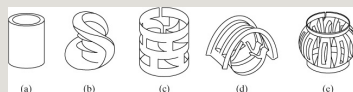


Figure 22.2-3. *Typical random or dumped tower packings: (a) Raschig ring; (b) Berl saddle; (c) Pall ring; (d) Intalox metal, IMTP; (e) Jaeger Metal Tri-Pack.*

Ceramic Raschig rings and Berl saddles shown in Figs. 22.2-3a and b are older types of random packing and are seldom used now (K1). Pall rings (second-generation packing), shown in Fig. 22.2-3c, are made of plastic or metal; they are much more efficient and are still used now. They have porosities or void spaces of 0.90–0.96 and areas of 100–200 m<sup>2</sup>/m<sup>3</sup> (30–60 ft<sup>2</sup>/ft<sup>3</sup>). The latest or third-generation packings are the Intalox metal type, shown in Fig. 22.2-3d, which is a combination of the Berl saddle and the Pall ring, and the

Metal Tri-Pack, shown in Fig. 22.2-3e, which is a Pall ring with a spherical shape. Porosities range from 0.95 to 0.98. Many other types of new packings are available. These third-generation packings are only slightly more efficient than the Pall rings.

Stacked packings having sizes of 75 mm or so and larger are also used. The packing is stacked vertically, with open channels running uninterruptedly through the bed. The advantage of the lower pressure drop of the gas is offset in part by the poorer gas–liquid contact in stacked packings. Typical stacked packings are wood grids, drip-point grids, and spiral partition rings among others.

### **22.3 Pressure Drop and Flooding in Packed Towers**

In a given packed tower with a given type and size of packing, and with a definite flow of liquid, there is an upper limit to the rate of gas flow, called the *flooding velocity*. Above this gas velocity, the tower cannot operate. At low gas velocities, the liquid flows downward through the packing, essentially uninfluenced by the upward gas flow. As the gas flow rate is increased at low gas velocities, the pressure drop is proportional to the flow rate to the 1.8 power. At a gas flow rate called the *loading point*, the gas starts to hinder the liquid downflow, and local accumulations or pools of liquid start to appear in the packing. The pressure drop of the gas starts to rise at a faster rate. As the gas flow rate is increased, the liquid holdup or

accumulation increases. At the flooding point, the liquid can no longer flow down through the packing and is blown out with the gas.

In an actual, operating tower, the gas velocity is well below flooding. The optimum economic gas velocity is about one-half or more of the flooding velocity. It depends upon a balance of economic factors including equipment cost, pressure drop, and processing variables. Pressure drop in the packing is an important consideration in the design of a tower and is covered in detail below.

### *1. Pressure drop in random packings.*

Empirical correlations for various random packings based on experimental



data are used to predict the pressure drop in the gas flow. The original correlation by Eckert (K1) correlated the gas and liquid flow rates and properties with pressure drop. The latest version has been replotted by Strigle (K1, S4) and is shown in Fig. 22.3-1. The line for  $\Delta P = 2.0$  in. H<sub>2</sub>O/ft has been extrapolated. The ordinate (capacity parameter) is  $v_G [\rho_G / (\rho_L - \rho_G)]^{0.5} F_p^{0.5} \nu^{0.05}$  and the abscissa (flow parameter) is  $(G_L / G_G) (\rho_G / \rho_L)^{0.5}$ , where  $y_G$  is superficial gas velocity in ft/s,  $\rho_G$  is gas density in lb<sub>m</sub>/ft<sup>3</sup>,  $y_G = G_G / \rho_G$ ,  $\rho_L$  is liquid density in lb<sub>m</sub>/ft<sup>3</sup>,  $F_p$  is a packing factor in ft<sup>-1</sup>,  $\nu$  is kinematic viscosity  $\mu_L / (\rho_L / 62.4)$  in centstokes,  $\mu_L$  is liquid viscosity in cp,  $G_L$  is liquid mass velocity in lb<sub>m</sub>/(s · ft<sup>2</sup>), and  $G_G$  is gas mass velocity in lb<sub>m</sub>/(s · ft<sup>2</sup>). Note that this capacity parameter is not

dimensionless and that only these units should be used. This correlation predicts pressure drops to an accuracy of  $\pm 11\%$  (L2).

The packing factor  $F_p$  is almost inversely proportional to packing size. This packing factor  $F_p$  is determined empirically for each size and type of packing, and some data are given in Table 22.3-1. A very extensive list of values of  $F_p$  is given by Kister (K1).

## *2. Pressure drop in structured packings.*

An empirical correlation for structured packings is given in Fig. 22.3-2 by Kister and Gill (K1). They modified the Eckert correlation for random packings to better fit only the structured-packing data. An extrapolated line for  $\Delta P = 0.05$  in. H<sub>2</sub>O/ft and for  $\Delta P = 2.0$  a line has

been added. The packing factors  $F_p$  to be used for structured packing are those given in Table 22.3-1 and references (K1, L2, P2). The units on the ordinate and abscissa of Fig. 22.3-2 are the same as those for Fig. 22.3-1.

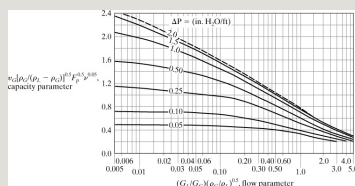


Figure 22.3-1. Pressure-drop correlation for random packings by Strigle. Data from R. F. Strigle, Jr., *Random Packings and Packed Towers*, © 1987, Houston: Gulf Publishing Company.

*3. Flooding pressure drop in packed and structured packings.* It is important for proper design to be able to predict the flooding pressure drop in towers and, hence, the limiting flow rates at flooding. Figures 22.3-1 and 22.3-2 do not predict flooding conditions. Kister and Gill (K2) have developed an

empirical equation to predict the limiting pressure drop at flooding. This equation is

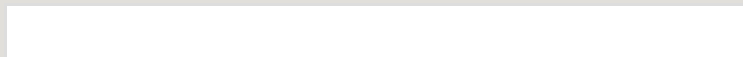
$$\Delta P_{\text{flood}} = 0.115 F_p^{0.7} (22.3-1)$$

where  $\Delta P_{\text{flood}}$  is in in. H<sub>2</sub>O/ft height of packing and  $F_p$  is the packing factor in ft<sup>-1</sup> given in Table 22.3-1 for random or structured packing. To convert from English to SI units, 1.00 in. H<sub>2</sub>O/ft height = 83.33 mm H<sub>2</sub>O/m height of packing. This can be used for packing factors from 9 up to 60. It predicts all of the data for flooding within  $\pm 15\%$  and most for  $\pm 10\%$ . At a packing factor of 60 or higher, Eq. (22.3-1) should not be used; instead, the pressure drop at flooding can be taken as 2.00 in. H<sub>2</sub>O/ft (166.7 mm H<sub>2</sub>O/m).

The following procedure can be used to determine the limiting flow rates and the tower diameter:

1. First, a suitable random packing or structured packing is selected, giving an  $F_p$  value.
2. A suitable liquid-to-gas ratio  $GL/GG$  is selected along with the total gas flow rate.
3. The pressure drop at flooding is calculated using Eq. (22.3-1), or if  $F_p$  is 60 or over, the  $DP_{flooding}$  is taken as 2.0 in./ft packing height.
4. Then, the flow parameter is calculated and, using the pressure drop at flooding and either Fig. 22.3-1 or 22.3-2, the capacity parameter is read off the plot.
5. Using the capacity parameter, the value of  $GG$  is obtained, which is the maximum value at flooding.

Table 22.3-1. *Packing Factors for Random and Structured Packing*



Data from Ref. (K1, L2, P2, S4). The relative mass-transfer coefficient,  $f_p$ , is discussed in Section 22.8B.

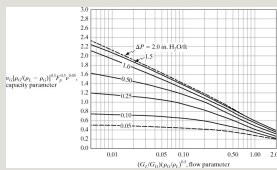


Figure 22.3-2. *Pressure-drop correlation for structured packings by Kister and Gill (K2). From H. Z. Kister, Distillation Design, New York: McGraw-Hill Book Company, 1992. With permission.*

6. Using a suitable % of the flooding value of  $GG$  for design, a new  $GG$  and  $GL$  are obtained. The pressure drop can also be obtained from Figure 22.3-1 or 22.3-2.
7. Knowing the total gas flow rate and  $GG$ , the tower cross-sectional area and ID can be calculated.

*4. Approximate design factors to use.* In using random packing, the ratio of tower diameter to packing size should be 10/1 or greater. This is to ensure good liquid and gas distribution. For every 3 m (10 ft) height of packing, a liquid redistribution should be used to prevent the channeling of liquid to the sides. Random-packed towers are generally used only for diameters of 1.0 m (3.3 ft)

or less. Tray towers less than 0.6 m (2 ft) in diameter are usually not used because of cleaning and access problems.

The start of loading in packed towers is usually at about 65–70% of the flooding velocity (L2). For absorption, the tower should be designed using about 50–70% of the gas flooding velocity, with the high value used at high flow parameters. For atmospheric-pressure distillation, values of 70–80% can be used (S5). For distillation and structured packing, 80% of flooding is often used in design (L1). For tray towers, see Chapter 26.

**EXAMPLE 22.3-1. Pressure Drop and Tower Diameter for Ammonia Absorption**

Ammonia is being absorbed in a tower using pure water at 25°C and 1.0 atm abs pressure. The feed rate is 1440 lbm/h (653.2 kg/h) and contains 3.0 mol % ammonia in air. The process design specifies a liquid-to-gas mass flow rate ratio  $G_L/G_G$  of 2/1 and the use of 1-in. metal Pall rings.

- Calculate the pressure drop in the packing and gas mass velocity at flooding. Using 50% of the flooding velocity, calculate the pressure drop, gas and liquid flows, and tower diameter.
- Repeat (a) above but use Mellapak 250Y structured packing.

**Solution:** The gas and liquid flows in the bottom of the tower are the largest, so the tower will be sized for these flows. Assume that approximately all of the ammonia is absorbed. The gas average mol wt is  $28.97(0.97) + 17.0(0.03) = 28.61$ . The weight fraction of ammonia is  $0.03(17)/(28.61) = 0.01783$ .

$$\rho_G = (492460 + 77)(28.64)(359) = 0.073091 \text{ lbm/ft}^3$$

Assuming the water is dilute, from Appendix A.2-4, the water viscosity  $\mu = 0.8937$  cp. From A.2-3, the water density is  $0.99708 \text{ gm/cm}^3$ . Then,  $\rho_L = 0.99708(62.43) = 62.25 \text{ lbm/ft}^3$ . Also,  $\nu = \mu/\rho = 0.8937/0.99708 = 0.8963$  centistokes.

From Table 22.3-1, for 1-in. Pall rings,  $F_p = 56 \text{ ft}^{-1}$ . Using Eq. 22.3-1,  $\Delta P_{\text{flood}} = 0.115 F_p 0.7 = 0.115(56)0.7 = 1.925 \text{ in. H}_2\text{O/ft}$  packing height. The flow parameter for Fig. 22.3-1 is

$$(GL/GG)(\rho_G/\rho_L)^{0.5} = (2.0)(0.07309/62.25)^{0.5} = 0.06853$$

Using Fig. 22.3-1, for a flow parameter of 0.06853 (abscissa) and a pressure drop of 1.925 in./ft at flooding, a capacity parameter (ordinate) of 1.7 is read off the plot. Then, substituting into the capacity parameter equation and solving for  $u_G$ ,

$$1.7 = u_G [\rho_G (\rho_L - \rho_G)]^{0.5} F_p 0.5 u^{0.05} = u_G [0.07309(62.25 - 0.07309)]^{0.5} (56)^{0.5} (0.8963)^{0.05}$$

$u_G = 6.663 \text{ ft/s}$ . Then  $G_G = u_G \rho_G = 6.663(0.07309) = 0.4870 \text{ lbm/(s} \cdot \text{ft}^2)$  at flooding. Using 50% of the flooding velocity for design,  $G_G = 0.5(0.4870) = 0.2435 \text{ lbm/(s} \cdot \text{ft}^2)$  [ $1.189 \text{ kg/(s} \cdot \text{m}^2)$ ]. Also, the liquid flow rate  $G_L = 2.0(0.2435) = 0.4870 \text{ lbm/(s} \cdot \text{ft}^2)$  [ $2.378 \text{ kg/(s} \cdot \text{m}^2)$ ].

To calculate the tower pressure drop at 50% of flooding,  $G_G = 0.2435$  and  $G_L = 0.4870$ , and the new capacity parameter is  $0.5(1.7) = 0.85$ . Using this value of 0.85 and the same flow parameter, 0.06853, a value of 0.18 in.



water/ft is obtained from Fig. 22.3-1.

The tower cross-sectional area =  $(1440/3600 \text{ lb}_m/\text{s})$   
 $(1/0.2435 \text{ lb}_m/(\text{s} \cdot \text{ft}^2)) = 1.6427 \text{ ft}^2 = (\pi/4)D^2$ . Solving,  $D =$   
 $1.446 \text{ ft}$  (0.441 m). The amount of ammonia in the outlet  
water, assuming all of the ammonia is absorbed, is  
 $0.01783(1440) = 25.68 \text{ lb}$ . Since the liquid flow rate is 2  
times the gas flow rate, the total liquid flow rate is  $2.0(1440)$   
 $= 2880 \text{ lb}_m/\text{hr}$ . Hence, the flow rate of the pure inlet water is  
 $2880 - 25.68 = 2858.3 \text{ lb}_m/\text{s}$ .

For part (b), using Mellapak 250Y,  $F_p = 20$  from Table  
22.3-1. The  $\Delta p_{\text{flood}} = 0.115 F_p^{0.7} = 0.115(20)^{0.7} = 0.936 \text{ in.}$   
water/ft. The flow parameter of 0.06853 is the same. Using  
Fig. 22.3-2, a capacity parameter = 1.38 at flooding is  
obtained. Then,

$$1.38 = GG \rho_G [p_G \rho_L - p_G]^{0.5} F_p^{0.5} u^{0.05} = (GG)(0.07309) \\ [0.07309(62.25 - 0.07309)]^{0.5} (20)^{0.5} (0.8963)^{0.05}$$

Solving,  $GG = 0.6615 \text{ lb}_m/(\text{h} \cdot \text{ft}^2)$ . For 50% flood,  $GG =$   
 $0.5(0.6615) = 0.3308 \text{ lb}_m/(\text{s} \cdot \text{ft}^2)$  [ $1.615 \text{ kg}/(\text{s} \cdot \text{m}^2)$ ]. Also,  
the liquid flow rate is  $GL = 2(0.3308) = 0.6616 \text{ lb}_m/(\text{s} \cdot \text{ft}^2)$   
[ $3.230 \text{ kg}/(\text{s} \cdot \text{m}^2)$ ]. The new capacity parameter is  $0.5(1.38)$   
 $= 0.69$ . (See Fig. 22.3-3.) Using this and Fig. 22.3-2, a  
pressure drop of 0.11 in. water/ft is obtained.

The tower's cross-sectional area =  $(1440/3600)(1/0.3308) =$   
 $1.209 \text{ ft}^2 = (\pi/4)D^2$ . Solving,  $D = 1.241 \text{ ft}$  (0.3784 m). Note  
that the tower with structured packing uses about 25% less  
cross-sectional area.

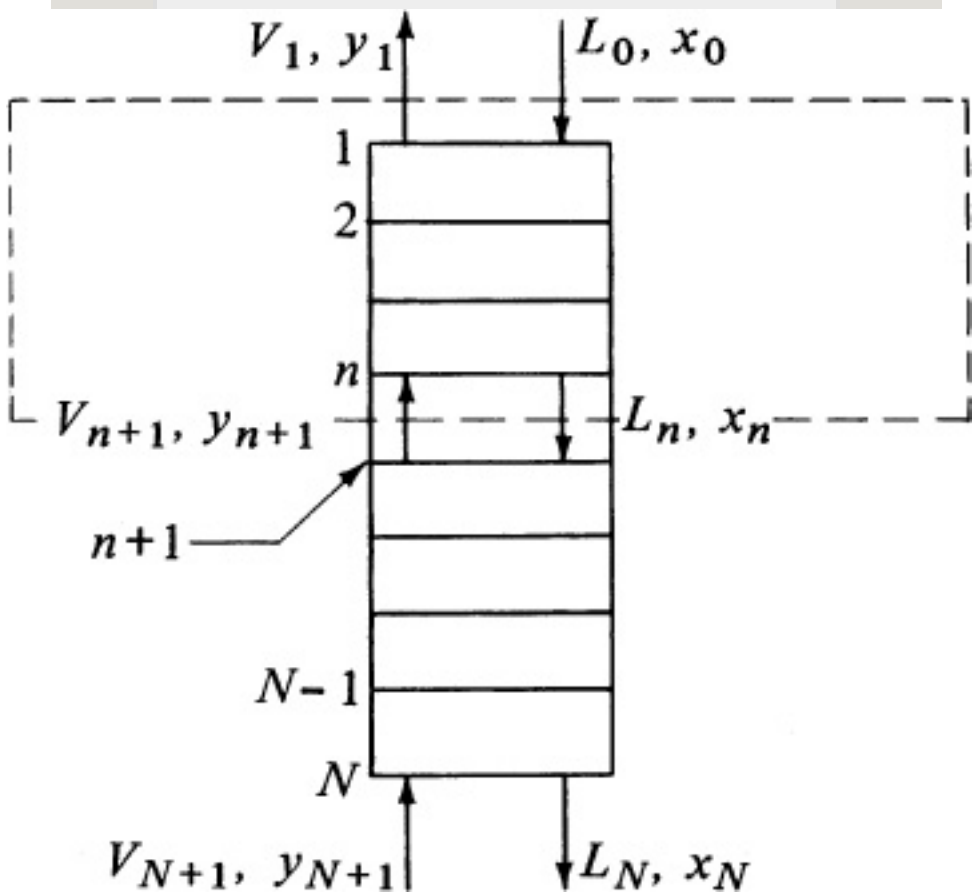


Figure 22.3-3. Material balance in an absorption tray tower.

## 22.4 Design of Plate Absorption Towers

*1. Operating-line derivation.* A plate (tray) absorption tower has the same process flow diagram as the countercurrent multiple-stage

process in Fig. 22.1-3 and is shown as a vertical tray tower in Fig.

22.3-3. In the case of solute  $A$  diffusing through a stagnant gas ( $B$ ) and then into a stagnant fluid, as in the absorption of acetone ( $A$ ) from air ( $B$ ) by water, the moles of inert or stagnant air and inert water remain constant throughout the entire tower. If the rates are  $V'$  kg mol inert air/s and  $L'$  kg mol inert solvent water/s or in kg mol inert/s  $\cdot$  m<sup>2</sup> units (lb mol inert/h  $\cdot$  ft<sup>2</sup>), an overall material balance on component  $A$  in Fig. 22.3-3 is

$$L'(x_0 - x_N) + V'(y_{N+1} - y_1) = L'(x_{N+1} - x_N) + V'(y_1 - y_{N+1}) \quad (22.4-1)$$

A balance around the dashed-line box gives

$$L'(x_0 - x_N) + V'(y_{N+1} - y_1) = L$$

$$(x_N - x_0) + V'(y_1 - y_{N+1}) \quad (22.4-2)$$

where  $x$  is the mole fraction  $A$  in the liquid,  $y$  the mole fraction of  $A$  in the gas,  $L_n$  the total moles liquid/s, and  $V_{n+1}$  the total moles gas/s. The total flows/s of liquid and gas vary throughout the tower.

Equation (22.4-2) is the material balance or operating line for the absorption tower and is similar to Eq. (22.1-16) for a countercurrent-stage process, except that the inert streams  $L'$  and  $V'$  are used instead of the total flow rates  $L$  and  $V$ . Equation (22.4-2) relates the concentration  $y_{n+1}$  in the gas stream with  $x_n$  in the liquid stream passing it. The terms  $V'$ ,  $L'$ ,  $x_0$ , and  $y_1$  are constant and are usually known or can be

determined.

*2. Graphical determination of the number of trays.* A plot of the operating-line equation (22.4-2) as  $y$  versus  $x$  will give a curved line. If  $x$  and  $y$  are very dilute, the denominators  $1 - x$  and  $1 - y$  will be close to 1.0, and the line will be approximately straight, with a slope  $\cong L/V$ . The number of theoretical trays is determined by simply stepping off the number of trays, as done in Fig. 22.1-4 for a countercurrent multiple-stage process.

**EXAMPLE 22.4-1. Absorption of  $\text{SO}_2$  in a Tray Tower**

A tray tower is to be designed to absorb  $\text{SO}_2$  from an air stream by using pure water at 293 K (68°F). The entering gas contains 20 mol %  $\text{SO}_2$  and that leaving contains 2 mol % at a total pressure of 101.3 kPa. The inert air flow rate is 150 kg air/h  $\cdot$  m<sup>2</sup>, and the entering water flow rate is 6000 kg water/h  $\cdot$  m<sup>2</sup>. Assuming an overall tray efficiency of 25%, how many theoretical trays and actual trays are needed? Assume that the tower operates at 293 K (20°C).

**Solution:** First, calculating the molar flow rates,

$$V' = 15029 = 5.18 \text{ kg mol inert air/h} \cdot \text{m}^2\text{L}$$

$$'=600018.0=333 \text{ kg mol inert water/h}\cdot\text{m}^2$$

Referring to Fig. 22.3-3,  $y_{N+1} = 0.20$ ,  $y_1 = 0.02$ , and  $x_0 = 0$ .

Substituting into Eq. (22.4-1) and solving for  $x_N$ ,

$$333(0.1-0)+5.18(0.201-0.20)=333(x_{N1}-x_N)+5.18(0.021-0.02)x_N=0.00355$$

Substituting into Eq. (22.4-2), using  $V'$  and  $L'$  as  $\text{kg mol/h} \cdot \text{m}^2$  instead of  $\text{kg mol/s} \cdot \text{m}^2$ ,

$$\begin{aligned} &333(0.1-0)+5.18(y_{N+1}-y_N) \\ &+1)=333(x_{N1}-x_N)+5.18(0.021-0.02) \end{aligned}$$

In order to plot the operating line, several intermediate points will be calculated. Setting  $y_{n+1} = 0.07$  and substituting into the operating equation,

$$0+5.18(0.071-0.07)=333(x_{N1}-x_N)+5.18(0.021-0.02)$$

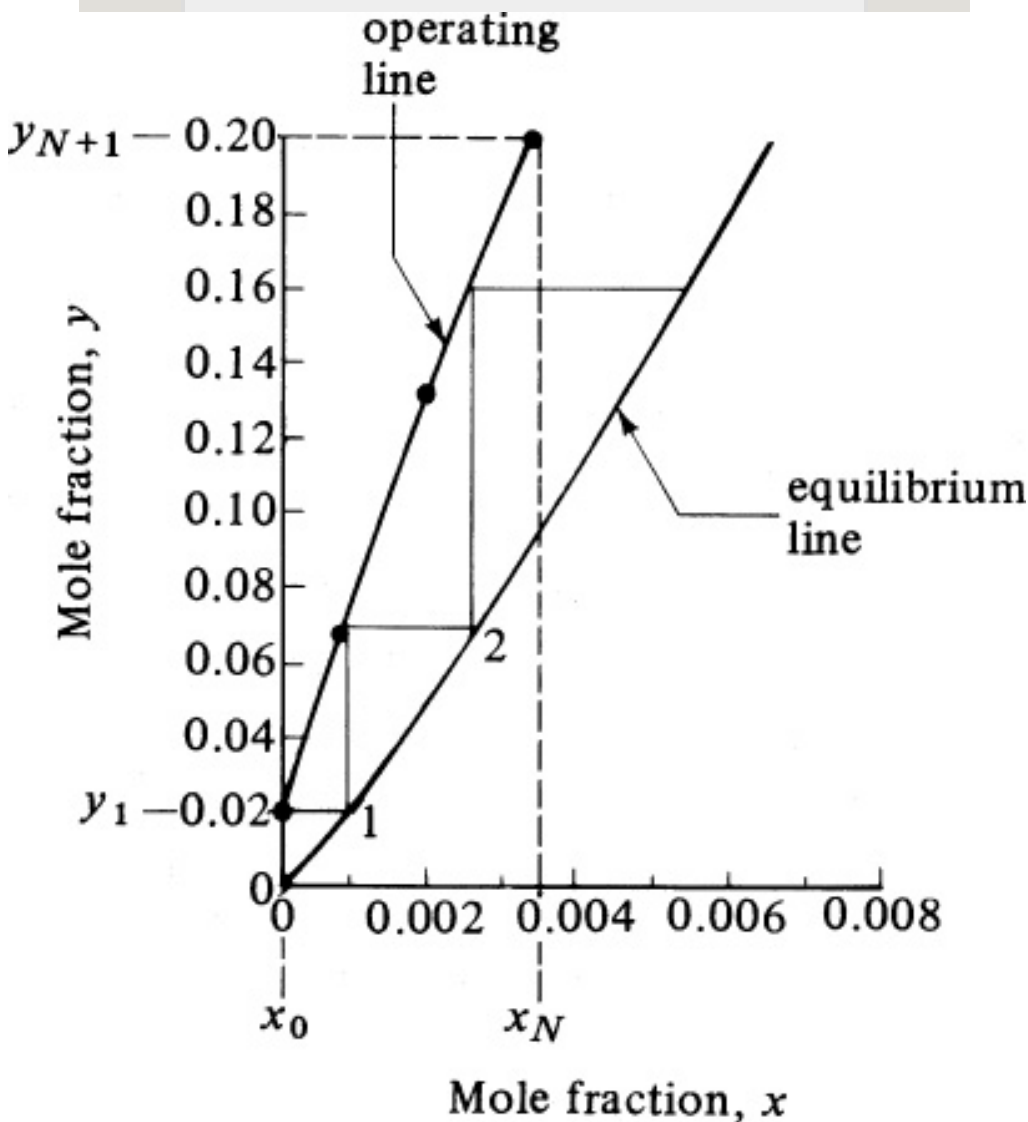


Figure 22.5-1. Theoretical number of trays for absorption of  $\text{SO}_2$  in Example 22.4-1.

Hence,  $x_n = 0.000855$ . To calculate another intermediate point, we set  $y_{n+1} = 0.13$ , and  $x_n$  is calculated as 0.00201. The two end points and the two intermediate points on the operating line are plotted in Fig. 22.5-1, as are the equilibrium data from Appendix A.3. The operating line is somewhat curved.

The number of theoretical trays is determined by stepping off the steps to give 2.4 theoretical trays. The actual number of trays is  $2.4/0.25 = 9.6$  trays.

## 22.5 Design of Packed Towers for Absorption

### 22.5A Introduction to Design of Packed Towers for Absorption

*1. Operating-line derivation.* For the case of solute  $A$  diffusing through a stagnant gas and then into a stagnant fluid, an overall material balance on component  $A$  in Fig. 22.5-2 (note the notation change in Fig. 22.5-2 with inlets  $y_1$  and  $x_2$ ) for a packed tower is

$$L'(x_{21}-x_2)+V'(y_{11}-y_1)=L'(x_{11}-x_1)+V'(y_{21}-y_2) \quad (22.5-1)$$

where  $L'$  is kg mol inert liquid/s or kg mol inert liquid/s  $\cdot$  m<sup>2</sup>,  $V'$  is kg mol inert gas/s or kg mol inert gas/s  $\cdot$  m<sup>2</sup>, and  $y_1$



and  $x_1$  are mole fractions  $A$  in gas and liquid, respectively. The flows  $L'$  and  $V'$  are constant throughout the tower, but the total flows  $L$  and  $V$  are not constant.

A balance around the dashed-line box in Fig. 22.5-2 gives the operating-line equation:

$$L'(x_1 - x) + V'(y_1 - y) = L'(x_{11} - x_1) + V'(y_1 - y) \quad (22.5-2)$$

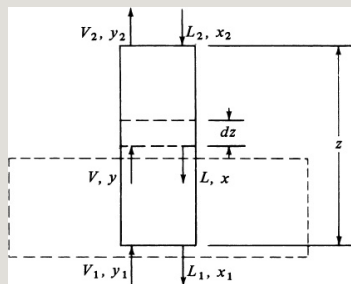


Figure 22.5-2. *Material balance for a countercurrent packed absorption tower.*

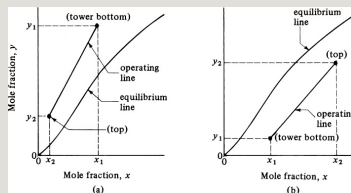


Figure 22.5-3. Location of operating lines: (a) for absorption of A from V to L stream, (b) for stripping of A from L to V stream.

This equation, when plotted on  $yx$  coordinates, will give a curved line, as shown in Fig. 22.5-3a. Equation (22.5-2) can also be written in terms of partial pressure  $p_1$  of A, where  $y_1/(1 - y_1) = p_1/(P - p_1)$ , and so on. If  $x$  and  $y$  are very dilute,  $(1 - x)$  and  $(1 - y)$  can be taken as 1.0 and Eq. (22.5-2) becomes

$$L'x + V'y_1 \cong L'x_1 + V'y \quad (22.5-3)$$

This has a slope  $L'/V'$  and the operating line is essentially straight.

When the solute is being transferred from the  $L$  to the  $V$  stream, the process is called *stripping*. The operating line is below the equilibrium line, as shown in Fig. 22.5-3b.

2. *Limiting and optimum  $L'/V'$  ratios.* In the absorption process, the inlet gas flow  $V_1$  (Fig. 22.5-2) and its composition  $y_1$  are generally set. The exit concentration  $y_2$  is also usually set by the designer, and the concentration  $x_2$  of the entering liquid is often fixed by process requirements. Hence, the amount of the entering liquid flow  $L_2$  or  $L'$  is open to choice.

In Fig. 22.5-4a, the flow  $V_1$  and the concentrations  $y_2$ ,  $x_2$ , and  $y_1$  are set. When the operating line has a minimum slope and touches the equilibrium line at point  $P$ , the liquid flow  $L'$  is a minimum at  $L'_{\min}$ . The value of  $x_1$  is a maximum at  $x_{1\max}$  when  $L'$  is a minimum. At point  $P$ , the driving forces  $y - y^*$ ,  $y - y_i$ ,  $x^* - x$ , and  $x_i - x$  are all zero. To solve for  $L'_{\min}$  the values  $y_1$  and  $x_{1\max}$  are

substituted into the operating-line equation. In some cases, if the equilibrium line is curved concavely downward, the minimum value of  $L$  is reached by the operating line becoming tangent to the equilibrium line instead of intersecting it.

The choice of the optimum  $L'/V'$  ratio to use in the design depends on an economic balance. In absorption, too high a value requires a large liquid flow and hence a large-diameter tower. The cost of recovering the solute from the liquid by distillation will be high. A small liquid flow results in a high tower, which is also costly. As an approximation, the optimum liquid flow rate for absorption can be taken as 1.2–1.5 times the limiting rate  $L'_{min}$  with 1.5 usually used (S6).

For stripping or transfer of solute from  $L$  to  $V$ , where the operating line has a maximum slope and touches the equilibrium line at point  $P$  in Fig.

22.5-4b, then the gas flow is at the minimum  $V'_{min}$ . The value of  $y_2$  is at a maximum at  $y_{2max}$ . As in absorption, the optimum gas flow rate is taken at about 1.5 times  $V'_{min}$ . In liquid extraction, covered later in Chapter 27, the same conditions for stripping hold for extracting solute from feed liquid  $L$  to solvent  $V$ .

*3. Analytical equations for a theoretical number of steps or trays.* Analytical equations to calculate the number of theoretical trays  $N$  in an absorption tower are the same as Eqs. (22.5-25) and (22.5-28) for calculating the number of stages in countercurrent stage processes.

These are as follows. (Note that the notation refers to Fig. 22.5-2 and not Fig. 22.5-4.)

For transfer of the solute from phase  $V$  to phase  $L$  (absorption),

$$N = \ln[(y_1 - mx_2)(y_2 - mx_1)(1 - 1/A) + 1/A] \ln A \quad (22.5-4)$$

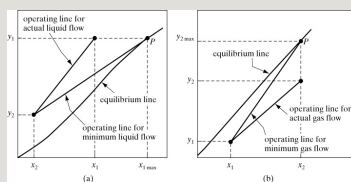


Figure 22.5-4. Operating line for limiting conditions: (a) absorption, (b) stripping.

For transfer of the solute from phase  $L$  to phase  $V$  (stripping),

$$N = \ln[(x_2 - y_1/m)(x_1 - y_1/m)(1 - A) + A] \ln(1/A) \quad (22.5-5)$$

where  $A = L/mV$ .

If the equilibrium line and/or operating line is slightly curved,  $m$  and  $A = L/mV$  will vary. For absorption (referring to Fig. 22.5-2), at the bottom concentrated end tray, the slope  $m_1$  or tangent at the point  $x_1$  on the equilibrium line is used. At the dilute top tray, the slope  $m_2$  of the equilibrium line at point  $y_2$  is used. Then,  $A_1 = L_1/m_1V_1$ ,  $A_2 = L_2/m_2V_2$ , and  $A=A_1A_2$ . Also, the dilute  $m_2$  is used in Eq. (22.5-4). For stripping, at the top or concentrated stage, the slope  $m_2$  or tangent at point  $y_2$  on the equilibrium line is used. At the bottom or dilute end, the slope  $m_1$  at point  $x_1$  on the equilibrium line is used. Then,  $A_1 = L_1/m_1V_1$ ,  $A_2 = L_2/m_2V_2$ , and  $A=A_1A_2$ . Again, the dilute  $m_1$  is used in Eq. (22.5-5).

**EXAMPLE 22.5-1. Minimum Liquid Flow Rate and Analytical Determination of Number of Trays**

A tray tower is absorbing ethyl alcohol from an inert gas stream using pure water at 303 K and 101.3 kPa. The inlet gas stream flow rate is 100.0 kg mol/h and it contains 2.2 mol % alcohol. It is desired to recover 90% of the alcohol. The equilibrium relationship is  $y = mx = 0.68x$  for this dilute stream. Using 1.5 times the minimum liquid flow rate, determine the number of trays needed. Do this graphically and also using the analytical equations.

**Solution:** The given data are  $y_1 = 0.022$ ,  $x_2 = 0$ ,  $V_1 = 100.0$  kg mol/h, and  $m = 0.68$ . Then,  $V' = V_1(1 - y_1) = 100.0(1 - 0.022) = 97.8$  kg mol inert/h. Moles alcohol/h in  $V_1$  are  $100 - 97.8 = 2.20$ . Removing 90%, moles/h in outlet gas  $V_2 = 0.10(2.20) = 0.220$ .  $V_2 = V' + 0.220 = 97.8 + 0.22 = 98.02$ .  $y_2 = 0.22/98.02 = 0.002244$ . The equilibrium line is plotted in Fig. 22.5-5 along with  $y_2$ ,  $x_2$ , and  $y_1$ . The operating line for minimum liquid flow  $L_{\min}$  is drawn from  $y_2$ ,  $x_2$  to point  $P$ , touching the equilibrium line where  $x_{1\max} = y_1/m = 0.022/0.68 = 0.03235$ . Substituting into the operating-line equation (22.5-1) and solving for  $L_{\min}$ ,

$$\begin{aligned} L'(x_{21}-x_2)+V'(y_{11}-y_1) &= L'(x_{11}-x_1)+V'(y_{21}-y_2)L_{\min} \\ (0.032351-0)+97.8(0.0221-0.022) &= L_{\min} \\ (0.032351-0.03235)+97.8(0.0022441-0.002244) &= 0 \end{aligned}$$

$L'_{\min} = 59.24$  kg mol/h. Using 1.5  $L'_{\min}$ ,  $L' = 1.5(59.24) = 88.86$ . Using  $L' = 88.86$  in Eq. (22.5-1) and solving for the outlet concentration,  $x_1 = 0.02180$ . The operating line is plotted as a straight line through the points  $y_2$ ,  $x_2$  and  $y_1$ ,  $x_1$  in Fig. 22.5-5. An intermediate point is calculated by setting  $y = 0.012$  in Eq. (22.5-2) and solving for  $x = 0.01078$ . Plotting this point shows that the operating line is very linear. This occurs because the solutions are dilute.



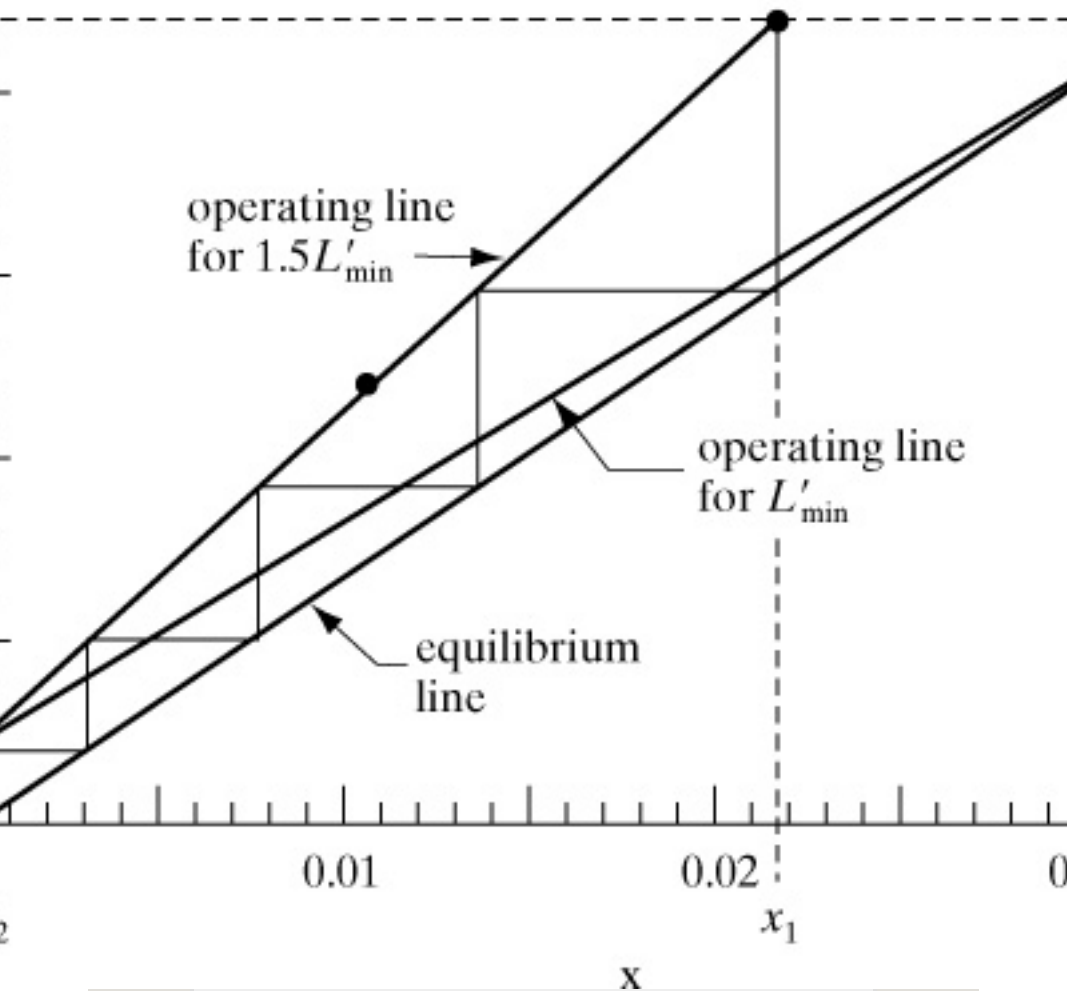


Figure 22.5-5. Operating line for minimum and actual liquid flow in Example 25.5-1.

The number of theoretical trays obtained by stepping them off is 4.0 trays. The total flow rates are  $V_1 = 100.0$ ,  $V_2 = V/(1 - y_2) = 97.8/(1 - 0.002244) = 98.02$ ,  $L_2 = L' = 88.86$ , and  $L_1 = L'/(1 - x_1) = 88.86/(1 - 0.02180) = 90.84$ . To calculate the number of trays analytically,  $A_1 = L_1/mV_1 = 90.84/(0.68)(100) = 1.336$ ,  $A_2 = L_2/mV_2 = 88.86/(0.68)(98.02) = 1.333$ . Using the geometric average,  $A = 1.335$ . Using Eq. (22.5-4),

$$N = \frac{1}{\ln A} \ln \left[ \frac{(y_1 - mx_2)(y_2 - mx_1)(1 - 1/A) + 1}{(y_1 - mx_1)(y_2 - mx_2)(1 - 1/A) + 1} \right]$$

$$A = 1.335 \ln \left[ \frac{(0.022 - 0.002244 - 0)(1 - 1/1.335) + 1}{1.335} \right]$$

$N = 4.04$  theoretical steps, which agrees closely with the 4.0 steps obtained graphically.

*4. Film and overall mass-transfer coefficients in packed towers.* It is very difficult to measure experimentally the interfacial area  $A$   $m^2$  between phases  $L$  and  $V$ . It is also difficult to measure the film coefficients  $k_x'$  and  $k_y'$  and the overall coefficients  $K_x'$  and  $K_y'$ .

Usually, experimental measurements in a packed tower yield a volumetric mass-transfer coefficient that combines the interfacial area and mass-transfer coefficient.

Defining  $a$  as interfacial area in  $m^2$  per  $m^3$  volume of packed section, the volume of packing in a height  $dz$  m (Fig. 22.5-2) is  $S dz$ , and

$$dA = aSdz \quad (22.5-6)$$

where  $S$  is m<sup>2</sup> cross-sectional area of tower. The volumetric film and overall mass-transfer coefficients are then defined as

$$k_y' a = k_g \text{ mols} \cdot \text{m}^3 \text{ packing} \cdot \text{mol frac} x$$

$$'a = k_g \text{ mols} \cdot \text{m}^3 \text{ packing} \cdot \text{mol frac}(\text{SI}) k_y$$

$$'a = k_g \text{ mols} \cdot \text{m}^3 \text{ packing} \cdot \text{mol frac} x$$

$$'a = k_g \text{ mols} \cdot \text{m}^3 \text{ packing} \cdot \text{mol frac}(\text{SI}) k_y$$

$$'a = \text{lb mol} \cdot \text{h} \cdot \text{ft}^3 \text{ packing} \cdot \text{mol frac} x$$

$$'a = \text{lb mol} \cdot \text{h} \cdot \text{ft}^3 \text{ packing} \cdot \text{mol frac}(\text{English})$$

*5. Design method for packed towers using mass-transfer coefficients.* For absorption of  $A$  from stagnant  $B$ , the operating-line equation (22.5-2) holds. For the differential height of tower  $dz$  in Fig. 22.5-2, the moles of  $A$  leaving  $V$  equal the moles entering  $L$ :

$$d(Vy) = d(Lx) \quad (22.5-7)$$

where  $V = \text{kg mol total gas/s}$ ,  $L = \text{kg mol total liquid/s}$ , and  $d(Vy) = d(Lx) = \text{kg mol } A \text{ transferred/s in height } dz \text{ m}$ . The kg mol  $A$  transferred/s from Eq. (22.5-7) must equal the kg mol  $A$  transferred/s from the mass-transfer equation for  $N_A$ . Equation (22.1-37) gives the flux  $N_A$  using the gas-film and liquid-film coefficients:

$$N_A = k_y'(1 - y_A)_i M (y_{AG} - y_{Ai}) = k_x'(1 - x_A)_i M (x_{Ai} - x_{AL}) \quad (22.1-37)$$

where  $(1 - y_A)_i M$  and  $(1 - x_A)_i M$  are defined by Eqs. (22.1-35) and (22.1-36). Multiplying the left-hand side of Eq. (22.1-37) by  $dA$  and the two right-side terms by  $aS \, dz$  from Eq. (22.5-6),

$$N_A dA = k_y' a (1 - y_A)_i M (y_{AG} - y_{Ai}) S dz = k_x' a (1 - x_A)_i M (x_{Ai} -$$

$$x_{AL})Sdz(22.5-8)$$

where  $N_A dA = \text{kg mol } A \text{ transferred/s in height } dz \text{ m (lb mol/h)}$ .

Equating Eq. (22.5-7) to Eq. (22.5-8) and using  $y_{AG}$  for the bulk gas phase and  $x_{AL}$  for the bulk liquid phase,

$$d(Vy_{AG}) = ky'_a(1 - y_A)iM(y_{AG} - y_{Ai})Sdz(22.5-9)$$

$$d(Lx_{AL}) = kx'_a(1 - x_A)iM(x_{Ai} - x_{AL})Sdz(22.5-10)$$

Since  $V' = V(1 - y_{AG})$  or  $V = V'/(1 - y_{AG})$ ,

$$\begin{aligned} d(Vy_{AG}) &= d(V'(1 - y_{AG})y_{AG}) = V' \\ &\quad d(y_{AG}1 - y_{AG}) = V'dy_{AG}(1 - y_{AG}) \end{aligned} (22.5-11)$$

Substituting  $V$  for  $V/(1 - y_{AG})$  in Eq. (22.5-11) and then equating Eq. (22.5-11) to (22.5-9),

$$V dy_{AG} (1 - y_{AG}) = k_y' a (1 - y_A) i_M (y_{AG} - y_{Ai}) S dz \quad (22.5-12)$$

Repeating for Eq. (22.5-10), since  $L = L/(1 - x_{AL})$ ,

$$L dx_{AL} (1 - x_{AL}) = k_x' a (1 - x_A) i_M (x_{Ai} - x_{AL}) S dz \quad (22.5-13)$$

Dropping the subscripts  $A$ ,  $G$ , and  $L$ , and integrating, the final equations are as follows using film coefficients:

$$\int_0^1 dz = z = \int_{y_2}^{y_1} \frac{V dy}{k_y' a S (1 - y) i_M (1 - y) (y - y_i)} \quad (22.5-14)$$

$$\int_0^1 dz = z = \int_{x_2}^{x_1} \frac{L dx}{k_x' a S (1 - x) i_M (1 - x) (x_i - x)} \quad (22.5-15)$$

In a similar manner, the final equations can be derived using overall coefficients:

$$z = \int_{y^*}^1 y^2 y_1 V dy K y' a S (1-y)^* M (1-y) (y - y^*) \quad (22.5-16)$$

$$z = \int_{x^*}^1 x^2 x_1 L dx K x' a S (1-x)^* M (1-x) (x^* - x) \quad (22.5-17)$$

In the general case, the equilibrium and the operating lines are usually curved, and  $k'_x a$ ,  $k'_{ya}$ ,  $K'_{xa}$ , and  $K'_{xa}$  vary somewhat with total gas and liquid flows. Then, Eqs. (22.5-14)–(22.5-17) must be integrated numerically or graphically. The methods for doing this for concentrated mixtures will be discussed in Section 22.7. Methods for dilute gases will be considered below.

## Towers

Since a considerable percentage of the absorption processes include absorption of a dilute gas  $A$ , these cases will be considered using a simplified design procedure.

The concentrations can be considered dilute for engineering design purposes when the mole fractions  $y$  and  $x$  in the gas and liquid streams are less than about 0.10, that is, 10%. The flows will vary by less than 10% and the mass-transfer coefficients by considerably less than this. As a result, the average values of the flows  $V$  and  $L$  and the mass-transfer coefficients at the top and bottom of the tower can be taken outside the integral. Likewise, the terms  $(1 - y)iM/(1 - y)$ ,  $(1 - y)*M/(1 - y)$ ,  $(1 - x)iM/(1 - x)$ , and  $(1 - x)*M/(1 - x)$  can be



taken outside and average values at the top and bottom of the tower used. (Often these terms are close to 1.0 and can be dropped out entirely.) Then, Eqs. (22.5-14)–(22.5-17) become

$$z = [Vky'aS(1-y)^i M^{1-y}]_{av} \int y^2 y^1 dy - y_i \quad (22.5-18)$$

$$z = [Lkx'aS(1-x)^i M^{1-x}]_{av} \int x^2 x^1 dx - x_i \quad (22.5-19)$$

$$z = [VKy'aS(1-y)^* M^{1-y}]_{av} \int y^2 y^1 dy - y^* \quad (22.5-20)$$

$$z = [LKx'aS(1-x)^* M^{1-x}]_{av} \int x^2 x^1 dx - x^* \quad (22.5-21)$$

Since the solutions are dilute, the operating line will be essentially straight. Assuming the equilibrium line is approximately straight over the range

of concentrations used,  $(y - y_i)$  varies linearly with  $y$  and also with  $x$ :

$$y - y_j = ky + b \quad (22.5-22)$$

where  $k$  and  $b$  are constants. Therefore, the integral of Eq. (22.5-18) can be integrated to give the following:

$$\int_{y_2}^{y_1} \frac{y \, dy}{(y - y_i)^M} = \frac{y_1 - y_2}{(y - y_i)^{M-1}} \quad (22.5-23)$$

where  $(y - y_i)^M$  is the log mean driving force:

$$(y - y_j)^M = \frac{(y_1 - y_{i1}) - (y_2 - y_{i2}) \ln \left| \frac{y_1 - y_{i1}}{y_2 - y_{i2}} \right|}{M} \quad (22.5-24)$$

Similarly, Eq. (22.5-20) gives

$$(y - y^*)^M = \frac{(y_1 - y_{1}^*) - (y_2 - y_{2}^*) \ln \left| \frac{y_1 - y_{1}^*}{y_2 - y_{2}^*} \right|}{M} \quad (22.5-25)$$

If the term  $(1 - y)iM/(1 - y)$  is considered 1.0, then by substituting Eq. (22.5-23) into (22.5-18) and doing the same for Eqs. (22.5-19)–(22.5-21), the final results are as follows:

$$VS(y_1 - y_2) = k_y' a z (y - y_j) M \quad (22.5-26)$$

$$LS(x_1 - x_2) = k_x' a z (x_j - x) M \quad (22.5-27)$$

$$VS(y_1 - y_2) = K_y' a z (y - y^*) M \quad (22.5-28)$$

$$LS(x_1 - x_2) = K_x' a z (x^* - x) M \quad (22.5-29)$$

where the left-hand side is the kg mol absorbed/s · m<sup>2</sup> (lb mol/h · ft<sup>2</sup>) by material balance and the right-hand side is the rate equation for mass transfer.

The value of  $V$  is the average  $(V_1 + V_2)/2$  and of  $L$  is  $(L_1 + L_2)/2$ .

Equations (22.5-26)–(22.5-29) can be

used in slightly different ways. The general steps to follow are discussed below and shown in Fig. 22.5-6.

1. The operating-line equation (22.5-2) is plotted as a straight line, as in Fig. 22.5-6. Calculate  $V_1$ ,  $V_2$ , and  $V_{av} = (V_1 + V_2)/2$ ; also calculate  $L_1$ ,  $L_2$ , and  $L_{av} = (L_1 + L_2)/2$ .
2. Average experimental values of the film coefficients  $k'_y a$  and  $k'_x a$  are available or may be obtained from empirical correlations. The interface compositions  $y_{i1}$  and  $x_{i1}$  at point  $y_1$ ,  $x_1$  in the tower are determined by plotting line  $P_1 M_1$ , whose slope is calculated by Eq. (22.5-30):

$$\text{slope} = -k_x' a / (1 - x)_{iM} k_y' a / (1 - y)_{iM} = -k_x a / k_y a (22.5-30)$$

$$\text{slope} \cong -k_x' a / (1 - x_1) k_y' a / (1 - y_1) (22.5-31)$$

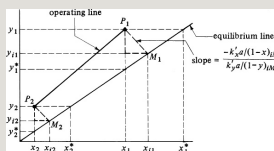


Figure 22.5-6. Operating-line and interface compositions in a packed tower for the absorption of dilute gases.

If terms  $(1 - x)_{iM}$  and  $(1 - y)_{iM}$  are used, the procedure is trial and error, as in Example 22.1-5. However, since the solutions are dilute, the terms  $(1 - x_1)$  and  $(1 - y_1)$  can be used in Eq. (22.5-31) without trial and error and with only a small error in slope. If the coefficients  $k_y a$  and  $k_x a$  are

available for the approximate concentration range, they can be used, since they include the terms  $(1 - x)_{iM}$  and  $(1 - y)_{iM}$ . For line  $P_2M_2$  at the other end of the tower, values of  $y_{i2}$  and  $x_{i2}$  are determined using Eq. (22.5-30) or (22.5-31), as well as  $y_2$  and  $x_2$ .

3. If the overall coefficient  $K_y'a$  is being used,  $y_1^*$  and  $y_2^*$  are determined as shown in Fig. 22.5-6. If  $K_x'a$  is used,  $x_1^*$  and  $y_1^*$  are obtained.
4. Calculate the log mean driving force  $(y - y_i)M$  by Eq. (22.5-24) if  $k_y'a$  is used. For  $K_y'a$ ,  $(y - y^*)M$  is calculated by Eq. (22.5-25). Using the liquid coefficients, the appropriate driving forces are calculated.
5. Calculate the column height  $z$  m by substituting into the appropriate form of Eqs. (22.5-26)–(22.5-29).

**EXAMPLE 22.5-2. Absorption of Acetone in a Packed Tower**

Acetone is being absorbed by water in a packed tower having a cross-sectional area of  $0.186 \text{ m}^2$  at  $293 \text{ K}$  and  $101.32 \text{ kPa}$  (1 atm). The inlet air contains 2.6 mol % acetone and the outlet contains 0.5%. The gas flow is  $13.65 \text{ kg mol inert air/h}$  ( $30.1 \text{ lb mol/h}$ ). The pure-water inlet flow is  $45.36 \text{ kg mol water/h}$  ( $100 \text{ lb mol/h}$ ). Film coefficients for the given flows in the tower are  $k_y'a = 3.78 \times 10^{-2} \text{ kg mol/s} \cdot \text{m}^3 \cdot \text{mol frac}$  ( $8.50 \text{ lb mol/h} \cdot \text{ft}^3 \cdot \text{mol frac}$ ) and  $k_x'a = 6.16 \times 10^{-2} \text{ kg mol/s} \cdot \text{m}^3 \cdot \text{mol frac}$  ( $13.85 \text{ lb mol/h} \cdot \text{ft}^3 \cdot \text{mol frac}$ ). Equilibrium data are given in Appendix A.3.

- Calculate the tower height using  $k_y'a$ .
- Repeat, using  $k_x'a$ .
- Calculate  $K_y'a$  and the tower height.

**Solution:** From Appendix A.3 for acetone–water and  $x_A = 0.0333$  mol frac,  $p_A = 30/760 = 0.0395$  atm or  $y_A = 0.0395$  mol frac. Hence, the equilibrium line is  $y_A = mx_A$  or  $0.0395 = m(0.0333)$ . Then,  $y = 1.186x$ . This equilibrium line is plotted in Fig. 22.5-7. The given data are  $L' = 45.36$  kg mol/h,  $V' = 13.65$  kg mol/h,  $y_1 = 0.026$ ,  $y_2 = 0.005$ , and  $x_2 = 0$ .

Substituting into Eq. (22.5-1) for an overall material balance using flow rates as kg mol/h instead of kg mol/s,

$$45.36(0.1-0) + 13.65(0.0261-0.026) = 45.36(x_1-0) + 13.65(0.0051-0.005)x_1 = 0.00648$$

The points  $y_1, x_1$  and  $y_2, x_2$  are plotted in Fig. 22.5-7 and a straight line is drawn for the operating line.

Using Eq. (22.5-31), the approximate slope at  $y_1, x_1$  is

$$\text{slope} \cong -\frac{Kx'_A/(1-x_1)Ky'_A/(1-y_1)}{(1-0.00648)} = \frac{-6.16 \times 10^{-2}}{37.78 \times 10^{-2}/(1-0.026)} = -1.60$$

Plotting this line through  $y_1, x_1$ , the line intersects the equilibrium line at  $y_{11} = 0.0154$  and  $x_{11} = 0.0130$ . Also,  $y_1^* = 0.0077$ . Using Eq. (22.5-30) to calculate a more accurate slope, the preliminary values of  $y_{11}$  and  $x_{11}$  will be used in the trial-and-error solution. Substituting into Eq. (22.1-35),

$$(1-y_1) \ln \frac{(1-y_{11})}{(1-y_1)} - (1-y_{11}) \ln \left[ \frac{(1-y_{11})}{(1-y_1)} \right] = (1-0.0154) \ln \frac{(1-0.025)}{(1-0.0154)} - (1-0.025) \ln \left[ \frac{(1-0.0154)}{(1-0.020)} \right] = 0.979$$

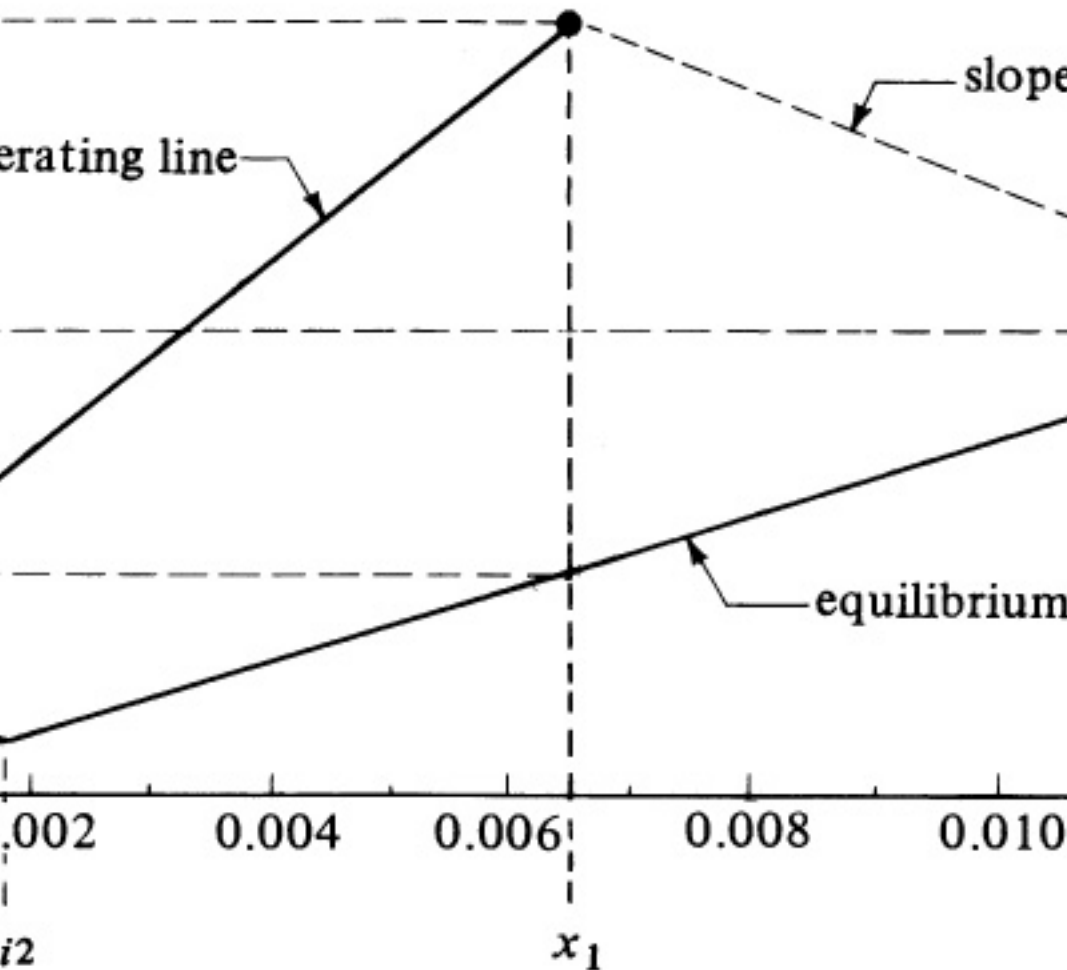


Figure 22.5-7. Location of interface compositions for Example 22.5-2.

Using Eq. (22.1-36),

$$(1-x)_i M = (1-x_1) - (1-x_1) \ln \left[ \frac{(1-x_1)}{(1-x_{i1})} \right] = (1-0.00648) - (1-0.0130) \ln \left[ \frac{(1-0.00648)}{(1-0.0130)} \right] = 0.993$$

Substituting into Eq. (22.5-30),

$$\text{slope} = -kx'a / (1-x)_i M k_y'a / (1-y)_i M = 6.16 \times 10^{-2} / 0.9933.78 \times 10^{-2} / 0.929 = -1.61$$

Hence, the approximate slope and interface values are accurate enough.

For the slope at point  $y_2, x_2$ ,

$$\text{slope} \equiv -k_x' a / (1-x_2) k_y' a / (1-y_2) = -6.16 \times 10^{-2} / (1-0) 3.78 \times 10^{-2} / (1-0.005) = -1.62$$

The slope changes little in the tower. Plotting this line,  $y_2 = 0.0020$ ,  $x_2 = 0.0018$ , and  $y_2^* = 0$ .

Substituting into Eq. (22.5-24),

$$(y-y_2)M = (y_1-y_{i1}) - (y_2-y_{i2}) \ln[(y_1-y_{i1})/(y_2-y_{i2})] = (0.026-0.0154) - (0.005-0.0020) \ln[(0.026-0.0154)/(0.005-0.0020)] = 0.00602$$

To calculate the total molar flow rates in kg mol/s,

$$\begin{aligned} V_1 &= V'1 - y_1 = 13.65/36001 - 0.026 = 3.893 \times 10^{-3} \text{ kg mol/s} \\ V_2 &= V'1 - y_2 = 13.65/36001 - 0.005 = 3.811 \times 10^{-3} \text{ kg mol/s} \\ sV_{av} &= V_1 + V_2 = 3.893 \times 10^{-3} + 3.811 \times 10^{-3} = 7.704 \times 10^{-3} \text{ kg mol/s} \\ sL &\approx L_1 \approx L_2 \approx L_{av} = 45.363600 = 1.260 \times 10^{-2} \text{ kg mol/s} \end{aligned}$$

For part (a), substituting into Eq. (22.5-26) and solving,

$$V_{av} S(y_1 - y_2) = k_y' a z (y - y_2) M \quad 3.852 \times 10^{-3} 0.186 (0.0260 - 0.005) = (3.78 \times 10^{-2}) z (0.00602) z = 1.911 \text{ m} (6.27 \text{ ft})$$

For part (b), using an equation similar to Eq. (22.5-24),

$$\begin{aligned} (x_j - x)M &= (x_{i1} - x_1) - (x_{i2} - x_2) \ln[(x_{i1} - x_1)/(x_{i2} - x_2)] \\ &= (0.0130 - 0.00648) - (0.0018 - 0) \ln[(0.0130 - 0.00648)/(0.0018 - 0)] = 0.00368 \end{aligned}$$

Substituting into Eq. (22.5-27) and solving,

$$1.260 \times 10^{-2} 0.186 (0.00648 - 0) = (36.16 \times 10^{-2}) z (0.00368) z = 1.936 \text{ m}$$

This agrees with part (a) quite closely.

For part (c), substituting into Eq. (22.1-54) for point  $y_1, x_1$ ,

$$\begin{aligned} (1-y)^* M &= (1-y_1^*) - (1-y_1) \ln[(1-y_1^*)/(1-y_1)] = (1-0.0077) - \\ &= (1-0.026) \ln[(1-0.0077)/(1-0.026)] = 0.983 \end{aligned}$$

The overall mass-transfer coefficient  $K_y' a$  at point  $y_1, x_1$  is calculated by substituting into Eq. (22.1-53):

$$1 K_y' a / (1-y)^* M = 1 k_y' a / (1-y) + M / m' k_x' a / (1-x) \quad 1 M_1 K_y$$



$$a/0.983=13.78 \times 10^{-2}/0.979+1.1866.16 \times 10^{-2}/0.993K_y$$

$$a=2.183 \times 10^{-2} \text{ kg mol/s} \cdot \text{m}^3 \cdot \text{mol frac}$$

Substituting into Eq. (22.5-25),

$$(y-y^*)M=(y_1-y_1^*)-(y_2-y_2^*)\ln[(y_1-y_1^*)/(y_2-y_2^*)]=(0.0260-0.0077)-(0.0050-0)\ln[(0.0260-0.0077)/(0.0050-0)]=0.01025$$

Finally, substituting into Eq. (22.5-28),

$$3.852 \times 10^{-3} \cdot 0.186(0.0260-0.0050)=(2.183 \times 10^{-2})z(0.01025)z=1.944 \text{ m}$$

This is in agreement with parts (a) and (b).

## 22.5C Design of Packed Towers Using Transfer Units

### *1. Design for concentrated solutions.*

Another and in some ways more useful design method for packed towers is the use of the transfer-unit concept. For the most common case of  $A$  diffusing through stagnant and nondiffusing  $B$ , Eqs. (22.5-14)–(22.5-17) can be rewritten as

$$z=HG \int_{y_2}^{y_1} \frac{y_1(1-y)}{y(y_1-y)} dy = HGNG \quad (22.5-32)$$

$$z=HL \int_{x_2}^{x_1} \frac{x_1(1-x)}{x(x_1-x)} dx = (x_i -$$

$$x)=HLNL(22.5-33)$$

$$z=HOG \int y^2 y^1 (1-y)^* M dy (1-y)(y-y^*)=HOGNOG(22.5-34)$$

$$z=HOL \int x^2 x^1 (1-x)^* M dx (1-x)(x^*-x)=HOLNOL(22.5-35)$$

where

$$HG=Vky'aS=Vky^a(1-y)iMS(22.5-36)$$

$$HL=Lkx'aS=Lkx^a(1-x)iMS(22.5-37)$$

$$HOG=VKy'aS=VKy^a(1-y)^*MS(22.5-38)$$

$$HOL=LKx'aS=LKx^a(1-x)^*MS(22.5-39)$$

where  $(1 - y)i_M$  is defined by Eq.

$(22.1-35)$ ,  $(1 - x)_{iM}$  by Eq. (22.1-36),  $(1 - y)^*_{M}$  by Eq. (22.1-54), and  $(1 - x)^*_{M}$  by Eq. (22.1-56). The units of  $H$  are in m (ft).  $HG$  is the height of a transfer unit based on the gas film. The values of the heights of transfer units are more constant than the mass-transfer coefficients. For example,  $ky'a$  is often proportional to  $V^{0.7}$ , so then  $HG \propto V^{1.0}/V^{0.7} \propto V^{0.3}$ . The average values of the mass-transfer coefficients,  $(1 - y)_{iM}$ ,  $(1 - y)^*_{M}$ ,  $(1 - x)_{iM}$ , and  $(1 - x)^*_{M}$ , must be used in Eqs. (22.5-36)–(22.5-39).

The integrals on the right side of Eqs. (22.5-32)–(22.5-35) are the number of transfer units  $N_G$ ,  $N_L$ ,  $NOG$ , and  $NOL$ , respectively. The height of the packed tower is then

$$z = H_G N_G = H_L N_L = H_{OG} N_{OG} = H_{OL} N_{OL} \quad (22.5-40)$$

These equations are basically no different from those using mass-transfer coefficients. One still needs  $k_y'a$  and  $k_x'a$  to determine interface concentrations. Disregarding  $(1 - y)_{iM}/(1 - y)$ , which is near 1.0 in Eq. (22.5-32), the greater the amount of absorption  $(y_1 - y_2)$  or the smaller the driving force  $(y - y_i)$ , the larger the number of transfer units  $NG$  and the taller the tower.

*2. Design for dilute solutions.* When the solutions are dilute, with concentrations below 10%, the terms  $(1 - y)_{iM}/(1 - y)$ ,  $(1 - x)_{iM}/(1 - x)$ ,  $(1 - y)^*_{M}/(1 - y)$ , and  $(1 - x)^*_{M}/(1 - x)$  in Eqs. (22.5-32)–(22.5-35) can be taken outside the integral and average values used. Since these are quite close to 1.0, they can be dropped out. The equations then become

$$z=HGNG=HG \int y_2 y_1 dy y - y_i \quad (22.5-41)$$

$$z=HLNL=HL \int x_2 x_1 dx x_i - x \quad (22.5-42)$$

$$z=HOGNOG=HOG \int y_2 y_1 dy y - y^* \quad (22.5-43)$$

$$z=HOLNOL=HOL \int x_2 x_1 dx x^* - x \quad (22.5-44)$$

If both the operating and equilibrium lines are straight and dilute, the integrals in Eqs. (22.5-41)–(22.5-44) can be integrated, giving the number of transfer units:

$$NG = y_1 - y_2 (y - y_i) M \quad (22.5-45)$$

$$NL = x_1 - x_2 (x_i - x) M \quad (22.5-46)$$

$$NOG=(y_1-y_2)(y-y^*)M \quad (22.5-47)$$

$$NOL=(x_1-x_2)(x^*-x)M \quad (22.5-48)$$

where  $(y - y_i)_M$  is defined in Eq. (22.5-24) and  $(y - y^*)_M$  in (22.5-25).

When the major resistance to mass transfer is in the gas phase, as in absorption of acetone from air by water, the overall number of transfer units based on the gas phase  $NOG$  or the film  $NG$  should be used. When the major resistance is in the liquid phase, as in absorption of  $O_2$  by water or stripping of a slightly soluble solute from water,  $NOL$  or  $NL$  should be employed. This was also discussed in detail in Section 22.1J. Often, the film coefficients are not available and then it is more convenient to use  $NOG$  or  $NOL$ .

By combining the operating line with the integrals in Eqs. (22.5-43) and (22.5-44), using the equilibrium-line equation  $y = mx$ , and letting  $A = L/mV$ , different forms of the equations for absorption with *NOG* and for stripping with *NOL* are obtained:

$$\text{NOG} = \frac{1}{A} \ln \left[ \frac{(1 - 1/A)(y_1 - mx_2)}{(1 - 1/A)(y_1 - mx_1)} + 1/A \right] \quad (22.5-49)$$

$$\text{NOL} = \frac{1}{A} \ln \left[ \frac{(1 - A)(x_2 - y_1/m)}{(1 - A)(x_2 - y_1/m) + A} \right] \quad (22.5-50)$$

The values of  $m$  and  $A$  to use in the equations above when operating and/or equilibrium lines are slightly curved are discussed in detail in Section 22.5 for use with Eqs. (22.5-4) and (22.5-5).

When the operating and equilibrium lines are straight and not parallel, the

number of overall gas-transfer units  $NOG$  for absorption in Eq. (22.5-49) is related to the number of theoretical trays or stages  $N$  in Eq. (22.5-4) by

$$NOG = N \ln A (1 - 1/A) \quad (22.5-51)$$

The height of a theoretical tray or stage, HETP, in m is related to  $HOG$  by

$$HETP = HOG \ln(1/A) (1 - A) / A \quad (22.5-52)$$

A detailed discussion of HETP is given in Section 22.6A. Note that if the operating and equilibrium lines are parallel ( $A = 1.0$ ), then  $HOG = HETP$  and  $NOG = N$ . Equations (22.5-4) and (22.5-5) can be used to analytically calculate  $N$ , the number of theoretical steps.



**EXAMPLE 22.5-3. Use of Transfer Units and Analytical Equations for a Packed Tower**

Repeat Example 22.5-2 using transfer units and height of a transfer unit as follows:

- Use  $H_G$  and  $N_G$  to calculate tower height.
- Use  $H_{OG}$  and  $N_{OG}$  to calculate tower height.
- Use Eq. (22.5-49) to calculate  $N_{OG}$  and tower height.
- Using the analytical equations, calculate HETP from Eq. (22.5-52), the number of theoretical steps  $N$  from Eq. (22.5-4), and the tower height.

**Solution:** From Example 22.5-2,  $ky'a = 3.78 \times 10^{-2} \text{ kg mol/s} \cdot \text{m}^2 \cdot \text{mol frac}$ ,  $Ky'a = 2.183 \times 10^{-2} \text{ kg mol/s} \cdot \text{m}^2 \cdot \text{mol frac}$ , average  $V = 3.852 \times 10^{-3} \text{ kg mol/s}$ , and  $S = 0.186 \text{ m}^2$ .

For part (a), from Eq. (22.5-36),

$$HG = Vky'aS = 3.852 \times 10^{-3} (3.78 \times 10^{-2}) (0.186) = 0.548 \text{ m}$$

From Eq. (22.5-24) in Example 22.5-2,  $(y - y_i)_{iM} = 0.00602$ . Also,  $y_1 = 0.026$  and  $y_2 = 0.005$ . Then, using Eq. (22.5-45),

$$NG = y_1 - y_2 (y - y_i)_{iM} = 0.026 - 0.005 (0.00602) = 3.488 \text{ transfer units}$$

Substituting in Eq. (22.5-41),

$$z = HGNG = (0.548)(3.488) = 1.911 \text{ m (6.27 ft)}$$

For part (b), using Eq. (22.5-38),

$$HOG = VKy'aS = 3.852 \times 10^{-3} (2.183 \times 10^{-2}) (0.186) = 0.949 \text{ m}$$

From Eq. (22.5-25) in Example 22.5-2,  $(y - y^*)_{iM} = 0.01025$ . Then, using Eq. (22.5-47),

$$NOG = (y_1 - y_2) (y - y^*)_{iM} = (0.026 - 0.005) (0.01025) = 2.049 \text{ transfer units}$$

From Eq. (22.5-43),

$$z = HOGNOG = (0.949)(2.049) = 1.945 \text{ m (6.38 ft)}$$

Note that the number of transfer units  $NOG = 2.049$  is not the same as  $NG = 3.488$ .

For part (c), from Example 22.5-2,  $m = 1.186$ , and the average  $V = 3.852 \times 10^{-3}$ ,  $L = 1.260 \times 10^{-2}$ ,  $y_1 = 0.026$ ,  $y_2 = 0.005$ , and  $x_2 = 0$ .

Then,  $A = L/mV = 1.260 \times 10^{-2} / (1.186 \times 3.852 \times 10^{-3}) = 2.758$ . Substituting into Eq. (22.5-49),

$$NOG = \frac{1}{1 - 1/2.758} \ln \left[ \frac{(1 - 1/2.758)(0.026 - 1.186 \times 0.005 - 1.186 \times 0) + 1/2.758}{1 - 1/2.758} \right] = 2.043 \text{ transfer units}$$

This compares closely with the value of 2.049 in part (b). Also,  $z = HOG/NOG = (0.949)/(2.043) = 1.939 \text{ m}$ .

For part (d), to calculate HETP, Eq. (22.5-52) is used:

$$HETP = HOG \ln(1/A) / (1 - 1/A) = (0.949) \ln(1/2.758) / (1 - 1/2.758) = 1.510 \text{ m}$$

Using Eq. (22.5-4) to calculate  $N$ ,

$$N = \frac{1}{1 - 1/2.758} \ln \left[ \frac{(y_1 - mx_2)(y_2 - mx_2)(1 - 1/A) + 1/A}{(y_1 - mx_2)(y_2 - mx_2)(1 - 1/A) + 1/A} \right] = 1.283 \text{ theoretical steps}$$

This compares with a value of 1.35 steps obtained graphically in Figure 22.5-7:

$$z = N(HETP) = 1.283(1.510 \text{ m}) = 1.938 \text{ m}$$

In order to relate  $HOG$  to the film coefficients  $H_G$  and  $H_L$ , Eq. (22.1-53) is rewritten for dilute solutions:

$$1/K_y a = 1/k_y a + m k_x a \quad (22.5-53)$$

Then, substituting  $H_G = V/k_y a S$ ,  $H_L = L/k_x a S$ , and  $HOG = V/K_y a S$  into Eq. (22.5-53) and canceling like terms,

$$HOG = H_G + (mV/L) H_L \quad (22.5-54)$$

Similarly, using Eq. (22.1-55),

$$HOL = H_L + (L/mV) H_G \quad (22.5-55)$$

Note that often in the literature, the terms  $H_y$ ,  $H_x$ ,  $H_{Oy}$ , and

$HO_x$  are used instead of  $HG$ ,  $HL$ ,  $HOG$ , and  $HOL$ ; they are identical to each other.

## 22.6 Efficiency of Random-Packed and Structured Packed Towers

### 22.6A Calculating the Efficiency of Random-Packed and Structured Packed Towers

In tray towers, a theoretical tray is defined as a tray in which equilibrium is attained between the gas or vapor leaving and the liquid leaving the tray. In random-packed or structured packed towers, the same approach is used, where the HETP in m (ft) is defined as the height of the packed column necessary to give a separation equal to one theoretical plate. The design of mass-transfer towers requires an evaluation of the number of theoretical stages or transfer units. Hence, the height of packing  $H$  in m

(ft) required to perform a given separation is

$$H=n(\text{HETP})(22.6-1)$$

where  $n$  is the number of theoretical stages needed. Using the number-of-transfer-units method, the height  $H$  is

$$H=\text{HOGNOG}(22.6-2)$$

where  $\text{HOG}$  is the overall height of a transfer unit in m (ft) and  $\text{NOG}$  is the number of transfer units.

The HETP and overall height of a transfer unit  $\text{HOG}$  can be related by the following equation, which is the same as Eq. (22.5-52):

$$\text{HETP}=\text{HOG}\ln[m/(L/V)]m/(L/V)-1(22.6-3)$$

where  $m$  is the slope of the equilibrium line in mole fraction units and  $L$  and  $V$  are molar flow rates. If the operating line and equilibrium line are parallel, then  $HETP = HOG$ . In distillation, the operating and equilibrium lines diverge below the feed point and converge above, so that the average  $mV/L$  is about 1.0 and  $HETP \cong HTU$  for distillation. This is usually not true for absorption or stripping towers. Although the HETP concept lacks a sound theoretical basis, unlike the mass-transfer and  $HOG$  concepts, it is simple and easy to use in computer equilibrium stage-to-stage calculations in distillation and is widely used to estimate packing height (S3). It is especially useful in multicomponent systems.

For a tray tower, the HETP can be

defined as

$$\text{HETP} = T E_0 \quad (22.6-4)$$

where  $E_0$  is the overall tray efficiency and  $T$  is the tray spacing, which varies from about 0.3 m for a 0.5-m-diameter tower and 0.6 m for a 1.0-m-diameter tower, to about 0.8 m (2.6 ft) for much larger towers over 4 m in diameter.

#### **22.6B Estimation of Efficiencies of Tray and Packed Towers**

In order to design the number of trays or packing heights needed, efficiencies must be obtained.

*1. Efficiency of tray towers.* For estimating the overall tray efficiency of bubble-tray towers for distillation, the O'Connell (O1) correlation can be used (K2) with about a  $\pm 10\%$  error. The

following equation for these data from Lockett (L1) can be used for sieve and valve trays as well, but predictions will be slightly conservative:

$$E_0 = 0.492(\mu_L \alpha)^{-0.245} (22.6 - 5)$$

where  $E_0$  is fraction efficiency,  $\alpha$  is relative volatility of the two key components at the average tower temperature, and  $\mu_L$  is the molar average viscosity in cp of the liquid feed at the average tower temperature of the top and the bottom. Most typical efficiencies are between 40 and 80%.

To estimate the overall tray efficiency for absorption towers, the O'Connell correlation (O1) can be used. This correlation is represented by the the following equation (S3):

$$\log E_0 = 1.597 - 0.199 \log(mML\mu_L / \rho_L) - 0.0896 [\log(mML\mu_L / \rho_L)]^2 (22.6 - 6)$$

where  $E_0$  is overall average % tray efficiency,  $ML$  is the average molecular weight of the liquid,  $m$  is the slope of the equilibrium line in mole fraction units,  $\rho_L$  is the liquid density in lb<sub>m</sub>/ft<sup>3</sup>, and  $\mu_L$  is molar average liquid viscosity in cp at the average tower temperature.

The average deviation of the data is  $\pm 16.3\%$  and the maximum is 157%.

This can be used for bubble-cap, sieve, and valve-type trays. Note that these tray efficiencies are quite low and in the range of 1% to 50%, with typical values of 10 to 30%.

## 2. *Efficiency of random-packed towers.*

For estimates for random packing, Eq.



(22.6-7) can be used to determine the HETP for second- and third-generation packings only (S2):

$$\text{HETP} = 0.0180 d_p \text{ (SI)} \quad \text{HETP} = 1.5 d_p \text{ (English)} \\ (22.6-7)$$

where HETP is in m and  $d_p$  is packing diameter in mm. In English units, HETP is in ft and  $d_p$  is in in. Also, for small-diameter towers, where the tower diameter  $D$  is less than 0.60 m (2 ft),  $\text{HETP} = D$ , but not less than 0.3 m (1 ft).

For vacuum service (S3),

$$\text{HETP} = 0.0180 d_p \\ + 0.15 \text{ (SI)} \quad \text{HETP} = 1.5 d_p \\ + 0.50 \text{ (English)} \quad (22.6-8)$$

The equations above are useful for low-

viscosity liquids. For absorption with high-viscosity liquids, the values of HETP are much greater, with values of 1.5 to 1.8 m (5 to 6 ft).

*3. Efficiency of structured packing in towers.* For approximate estimates of the efficiency of structured packings at low to moderate pressure with low viscosity liquids (K4),

$$\text{HETP} = 100/a + 0.10(\text{SI}) \quad \text{HETP} = 100/a + 0.33(\text{English}) \quad (22.6-9)$$

where HETP is in m and  $a$  is surface area in  $\text{m}^2/\text{m}^3$ . In English units, HETP is in ft and  $a$  in  $\text{ft}^2/\text{ft}^3$ . The value added of 0.10 m gives the estimate a conservative bias (K1). Values of HETP range from about 0.3 to 0.6 m (1.0 to 2.0 ft). For wire mesh (gauze), structured-packing

values range from 0.1 to 0.3 m (0.3 to 1.0 ft).

**EXAMPLE 22.6-1. Estimation of Tray and Packing Efficiencies and Tower Height**

A liquid mixture of benzene–toluene is to be distilled in a fractionating tower at 101.3 kPa pressure. The feed of 100 kg mol/h is liquid, containing 45 mol % benzene and 55 mol % toluene, and enters at 327.6 K (130°F). A distillate containing 95 mol % benzene and 5 mol % toluene and a bottoms containing 10 mol % benzene and 90 mol % toluene are to be obtained. The reflux ratio is 4:1. The average heat capacity of the feed is 159 kJ/kg mol · K (38 btu/lb mol · °F) and the average latent heat 32 099 kJ/kg mol (13 800 btu/lb mol). The number of theoretical steps needed is calculated as 7.6. The feed composition  $x_F = 0.45$ ,  $x_D = 0.95$ , and  $x_W = 0.10$ . Do as follows:

- Using valve trays, calculate the overall efficiency  $E_o$  and the tower height. Assume a tray spacing  $T$  of 0.6 m.
- Using 2-in. metal Pall rings, calculate the HETP and the tower height.
- Using Flexipac No. 2 structured packing, calculate the tower height.

**Solution:** For part (a), from Fig. 26.1-1 at 1 atm abs and  $x_W = 0.10$ , the boiling temperature is 106.5°C. At the top, for  $x_D = 0.95$ , the dew point is 82.3°C. The average is  $(106.5 + 82.3)/2$  or 94.4°C.

Using Table A.3-12 and Fig. A.3-4 at 94.4°C, the viscosity of benzene is 0.26 cp, and of toluene, 0.295 cp. The molar average viscosity is  $\mu_L = 0.45(0.26) + 0.55(0.295) = 0.279$  cp.

From Table 26.1-1, the vapor pressure of benzene  $P_A$  at 94.4°C is 153.3 kPa, and for toluene,  $P_B = 62.2$  kPa. Hence, the average relative volatility  $\alpha = 153.3/62.2 = 2.465$ .

Using Eq. (22.6-5),  $E_0 = 0.492(\mu L \alpha)^{-0.245} = 0.492(0.279 \times 2.465)^{-0.245} = 0.539$ . Using Eq. (22.6-4),  $HETP = T/E_0 = 0.6/0.539 = 1.113$  m/theoretical steps. The number of tray theoretical steps =  $7.6 - 1$  step for the reboiler, or 6.6 steps. Hence, tower tray height  $H = 1.113(6.6) = 7.35$  m.

For part (b), for 2-in. (25.4 × 2 mm) Pall rings, Eq. (22.6-7) gives

$$HETP = 0.0180d_p = 0.0180(25.4 \times 2) = 0.914 \text{ m}$$

For 6.6 theoretical steps, tower height  $H = 0.914(6.6) = 6.03$  m.

For part (c), for Flexipac No. 2 structured packing and using Table 22.3-1,  $a = 223$  m/m<sup>2</sup>. From Eq. (22.6-9),

$$HETP = 100/a + 0.10 = 100/223 + 0.10 = 0.548 \text{ m}$$

Tower height  $H = 0.548(6.6) = 3.617$  m

## 22.7 Absorption of Concentrated Mixtures in Packed Towers

In Section 22.5B, simplified design methods were given for absorption of dilute gases in packed towers when the mole fractions in the gas and liquid streams were less than about 10%. Straight operating lines and approximately straight equilibrium lines are obtained. In concentrated gas mixtures, the

operating line and usually the equilibrium line will be substantially curved and  $k_x$ 's and  $k_y$ 's may vary with total flows. Then, the design equations (22.5-14)–(22.5-17) must be integrated graphically or numerically:

$$\int_0^z dz = z = \int_{y_2}^{y_1} \frac{V dy}{k_y' a S (1-y) i M (1-y) (y-y_i)} \quad (22.5-14)$$

$$\int_0^z dz = z = \int_{x_2}^{x_1} \frac{L dx}{k_x' a S (1-x) i M (1-x) (x_i-x)} \quad (22.5-15)$$

$$\int_0^z dz = z = \int_{y_2}^{y_1} \frac{V dy}{K_y' a S (1-y)^* M (1-y) (y-y^*)} \quad (22.5-16)$$

$$\int_0^z dz = z = \int_{x_2}^{x_1} \frac{L dx}{K_x' a S (1-x)^* M (1-x) (y-x^*)} \quad (22.5-17)$$

The detailed general steps to follow are:

1. The operating-line equation (22.5-2) and the equilibrium line are plotted.
2. The values of the film coefficients  $ky'a$  and  $kx'a$  are obtained from empirical equations. These two film coefficients are functions of  $G_{yn}$ , kg total gas/s · m<sup>2</sup>, and  $G_{xm}$ , kg total liquid/s · m<sup>2</sup>, where  $n$  and  $m$  are in the range 0.2–0.8. Using the operating-line-equation values, total  $V$  and  $L$  are calculated for different values of  $y$  and  $x$  in the tower and converted to  $G_y$  and  $G_x$ . Then, values of  $ky'a$  and  $kx'a$  are calculated. If the variation between  $ky'a$  or  $kx'a$  at the top and bottom of the tower is small, an average value can be used.
3. Starting with the tower bottom at point  $P_1(y_1, x_1)$ , the interface compositions  $y_{i1}$ ,  $x_{i1}$  are determined by plotting a line  $P_1M_1$  with a slope calculated by Eq. (22.5-30). This line intersects the equilibrium line at the interface concentrations at point  $M_1$ :

$$\text{slope} = -kx'a/(1-x)_{iM} = -ky'a/(1-y)_{iM} \quad (22.5-30)$$

where  $(1-y)_{iM}$  and  $(1-x)_{iM}$  are determined from Eqs. (22.1-35) and (22.1-36), respectively. This is trial and error. As a first trial,  $(1-x_1)$  can be used for  $(1-x)_{iM}$  and  $(1-y_1)$  for  $(1-y)_{iM}$ . The values of  $y_{i1}$  and  $x_{i1}$  determined in the first trial are used in Eq. (22.5-30) for the second trial.

4. At point  $P_2(y_2, x_2)$ , determine a new slope using Eq. (22.5-30) and repeating step 3. Do this for several intermediate points in the tower. This slope may vary

throughout the tower.

5. Using the values of  $y_i$  and  $x_i$ , calculate the values of  $f(y)$  as follows:

$$f(y) = Vky'aS(1-y)iM(1-y)(y-y_i) \quad (22.7-1)$$

Then, numerically or graphically integrate Eq. (22.5-14) between  $y_2$  and  $y_1$  to obtain the tower height. If  $k'x_a$  or other coefficients are used, the appropriate functions indicated in Eqs. (22.5-15)–(22.5-17) are used. If the stream is quite dilute,  $(1 - y)iM$  or  $(1 - x)iM$  can be assumed to be 1.0.

**EXAMPLE 22.7-1. Design of an Absorption Tower with a Concentrated Gas Mixture**

A tower packed with 25.4-mm ceramic rings is to be designed to absorb  $\text{SO}_2$  from air by using pure water at 293 K and  $1.013 \times 10^5$  Pa abs pressure. The entering gas contains 20 mol %  $\text{SO}_2$  and that leaving contains 2 mol %. The inert air flow is  $6.53 \times 10^{-4}$  kg mol air/s and the inert water flow is  $4.20 \times 10^{-2}$  kg mol water/s. The tower cross-sectional area is 0.0929 m<sup>2</sup>. For dilute  $\text{SO}_2$ , the film mass-transfer coefficients at 293 K are, for 25.4-mm (1-in.) rings ( $W_1$ ),

$$ky'a = 0.0594 \text{ Gy} \quad 0.7 \text{ Gy} \quad 0.25 \text{ kx'a} = 0.152 \text{ Gx} \quad 0.82$$

where  $ky'a$  is kg mol/s · m<sup>3</sup> · mol frac,  $kx'a$  is kg mol/s · m<sup>3</sup> · mol frac, and  $G_x$  and  $G_y$  are kg total liquid or gas,

respectively, per sec per m<sup>2</sup> tower cross section. Calculate the tower height.

**Solution:** The given data are  $V = 6.53 \times 10^{-4}$  kg mol air/s (5.18 lb mol/h),  $L' = 4.20 \times 10^{-2}$  kg mol/s (333 lb mol/h),  $y_1 = 0.20$ ,  $y_2 = 0.02$ , and  $x_2 = 0$ .

Substituting into the overall material-balance equation (22.5-1),

$$L'(x_2 - x_1) + V(y_1 - y_2) = L'(x_1 - x_2) + V(y_2 - y_1)$$

$$(y_1 - y_2)4.20 \times 10^{-2} + 6.53 \times 10^{-4}(0.21 - 0.2) = 4.20 \times 10^{-2}(x_1 - x_2) + 6.53 \times 10^{-4}(0.021 - 0.02)$$

Solving,  $x_1 = 0.00355$ . The operating line Eq. (22.5-2) is

$$4.20 \times 10^{-2}(x_1 - x) + 6.53 \times 10^{-4}(0.21 - 0.2) = 4.20 \times 10^{-2}(0.003551 - 0.00355) + 6.53 \times 10^{-4}(y_1 - y)$$

Setting  $y = 0.04$  in the operating-line equation above and solving for  $x$ ,  $x = 0.000332$ . Selecting other values of  $y$  and solving for  $x$ , points on the operating line were calculated as shown in Table 22.7-1 and plotted in Fig. 22.7-1 together with the equilibrium data from Appendix A.3.

The total molar flow  $V$  is calculated from  $V' = V/(1 - y)$ . At  $y = 0.20$ ,  $V = 6.53 \times 10^{-4}/(1 - 0.2) = 8.16 \times 10^{-4}$ . Other values are calculated and tabulated in Table 22.7-1. The total mass flow  $G_y$  in kg/s · m<sup>2</sup> is equal to the mass flow of air plus SO<sub>2</sub> divided by the cross-sectional area:

Table 22.7-1. *Calculated Data for Example 22.7-1*

--



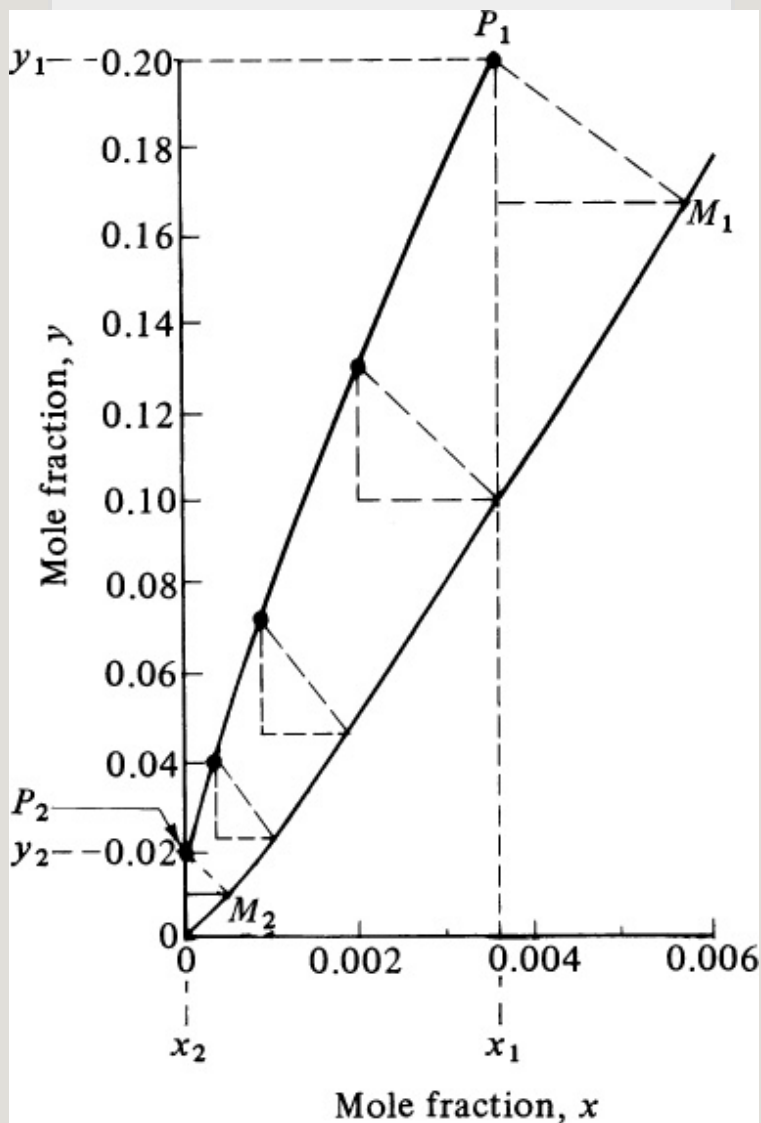


Figure 22.7-1. Operating line and interface compositions for Example 22.7-1.

$$Gy = 6.53 \times 10^{-4}(29) \text{ kg air/s} + 6.53 \times 10^{-4}(y_1 - y) \\ (64.1) \text{ kg SO}_2/\text{s} \cdot 0.929 \text{ m}^2$$

Setting  $y = 0.20$ ,

$$Gy = 6.53 \times 10^{-4}(29) + 6.53 \times 10^{-4}(0.21 - 0.2)64.1 \cdot 0.929 = 0.3164 \text{ kg/} \\ \text{s} \cdot \text{m}^2$$

Similarly,  $G_y$  is calculated for all points and tabulated. For the liquid flow,  $L = L'/(1 - x)$ . Also, for the total liquid mass flow rate,

$$G_x = 4.20 \times 10^{-2}(18) + 4.20 \times 10^{-2}(x_1 - x)64.10.929$$

Calculated values of  $L$  and  $G_x$  for various values of  $x$  are tabulated in Table 22.7-1.

To calculate values of  $kx'a$ , for  $x = 0$ ,  $G_x = 8.138$  and

$$kx'a = 0.152G_x 0.82 = 0.152(8.138)0.82 = 0.848 \text{ kg mol/} \\ \text{s m}^3\text{-mol frac}$$

The rest of these values are calculated and given in Table 22.7-1. For the value of  $ky'a$ , for  $y = 0.02$ ,  $G_y = 0.2130$ ,  $G_x = 8.138$ , and

$$ky'a = 0.0594G_y 0.7G_x 0.25 = 0.0594(0.2130)0.7(8.138)0.25 = 0.03398 \text{ kg mol/} \\ \text{s m}^3\text{-mol frac}$$

This and other calculated values of  $ky'a$  are tabulated. Note that these values vary considerably in the tower.

Next, the interface compositions  $y_i$  and  $x_i$  must be determined for the given  $y$  and  $x$  values on the operating line. For the point  $y_1 = 0.20$  and  $x_1 = 0.00355$ , we make a preliminary estimate of  $(1 - y)_i M \cong 1 - y \cong 1 - 0.20 \cong 0.80$ , together with the estimate of  $(1 - x)_i M \cong 1 - x \cong 1 - 0.00355 \cong 0.996$ . The slope of the line  $P_1 M_1$  by Eq. (22.5-30) is approximately

$$\text{slope} = kx'a / ((1 - x)_i M k_y'a (1 - y)_i M) = -0.857 / ((0.996)0.04496 / (0.80)) = -15.3$$

Plotting this on Fig. 22.7-1,  $y_i = 0.1688$  and  $x_i = 0.00566$ . Using these values for the second trial in Eqs. (22.1-35) and (22.1-36),

$$(1 - y)_i M = (1 - 0.1688) - (1 - 0.20) \ln[(1 - 0.1688) / (1 - 0.20)] = 0.816 \\ (1 - x)_i M = (1 - 0.00355) - (1 - 0.00566) \ln[(1 - 0.00355) / (1 - 0.00566)] = 0.995$$

The new slope by Eq. (22.5-30) is  $(-0.857 / 0.995) / (0.04496 / 0.816) = -15.6$ . Plotting,  $y_i = 0.1685$  and  $x_i = 0.00565$ . This is shown as point  $M_1$ . This calculation is repeated until point  $y_2$ ,  $x_2$  is reached. The slope of Eq.

(22.5-30) increases markedly in going up the tower, being – 24.6 at the top of the tower. The values of  $y_i$  and  $x_i$  are given in Table 22.7-1.

In order to integrate Eq. (22.5-14), values of  $(1 - y)$ ,  $(1 - y)^{1/M}$ , and  $(y - y_i)$  are needed and are tabulated in Table 22.7-1. Then, for  $y = 0.20$ ,  $f(y)$  is calculated from Eq. (22.7-1):

$$f(y) = Vky'aS(1-y)^{1/M}(1-y)(y - y_1) = 8.16 \times 10^{-4} \times 0.04496(0.0929)^{0.816}(0.800)(0.0315) = 6.33$$

This is repeated for other values of  $y$  from  $y_2$  to  $y_1$ . Then, the function  $f(y)$  is used to numerically integrate Eq. (22.5-14), giving  $z = 1.588$  m.

## 22.8 Estimation of Mass-Transfer Coefficients for Packed Towers

### 22.8A Experimental Determination of Film Coefficients

The individual film mass-transfer coefficients  $k_y'a$  and  $k_x'a$  depend generally upon Schmidt number, gas and liquid mass velocities, and the size and shape of the packing. The interactions among these factors are quite complex. Hence, the correlations for mass-transfer coefficients are highly empirical. The

reliability of these correlations is not too satisfactory. Deviations of up to 25% are not uncommon. A major difficulty arises because it is an overall coefficient or resistance that is measured experimentally, which represents the two film resistances in series. To obtain the single-phase film coefficient, the experiment must be arranged so that the other film resistance is negligible or can be approximately calculated.

To measure the liquid film mass-transfer coefficient  $k_x'a$ , a system for absorption or desorption of very insoluble gases such as  $O_2$  or  $CO_2$  in water is used. The experiment gives  $K_x'a$ , which equals  $k_x'a$  (which can give  $HL$ ), since the gas-phase resistance is negligible.

To measure the gas-phase film coefficient  $k_y'a$ , we desire to use a system such that the solute is very soluble in the liquid and the liquid-phase resistance is negligible. Most such systems, for example,  $\text{NH}_3$ –air–water, have a liquid-phase resistance of about 10%. By subtracting this known liquid-phase resistance (obtained by correcting  $k_x'a$  data for absorption of  $\text{CO}_2$  or  $\text{O}_2$  to  $\text{NH}_3$  data for  $k_x'a$ ) from the overall resistance in Eq. (22.1-53), we obtain the coefficient  $k_y'a$  or  $HG$ . Details of these systems are discussed elsewhere (G1, S1, S2).

### 22.8B Correlations for Film Coefficients

Correlations for experimental coefficients can be expressed in terms of  $HL$  and  $HG$  or  $k_x'a$  and  $k_y'a$ , which are related by Eqs. (22.5-36)

and (22.5-37). For the first generation of packings, such as Raschig rings and Berl saddles, extensive correlations are available (T1). However, comprehensive data on the individual coefficients  $HL$  and  $HG$  for the newer packings, which have higher mass-transfer coefficients and capacity, are not generally available. These newer packings are more commonly used today.

However, as an alternative method for comparing the performance of different types and sizes of these newer random packings, the system  $\text{CO}_2$ –air–NaOH solution is often used (P2, S4). Air containing 1.0 mole  $\text{CO}_2$  at  $24^\circ\text{C}$  ( $75^\circ\text{F}$ ) is absorbed in a packed tower using 1.0 N (4 wt %) NaOH solution (E2, E3, P2,

S4). An overall coefficient  $KGa$  is measured.

In this system, the liquid film is controlling but the gas film resistance is not negligible. The fast chemical reaction between NaOH and CO<sub>2</sub> takes place close to the interface, which gives a steeper concentration gradient for CO<sub>2</sub> in the water film. Hence, the value of  $KGa$  is much larger than for absorption of CO<sub>2</sub> in water. Because of this, these experimental values are not used to predict the absorption for other systems in towers.

These experimental results, however, can be used to compare the performances of various packings. To do this, the ratio  $f_p$  of  $KGa$  for a given packing to that for 112-in. Raschig rings

at a liquid velocity  $G_x$  of 5000 lb<sub>m</sub>/h · ft<sup>2</sup> (6.782 kg/s · m<sup>2</sup>) and  $G_y$  of 1000 lb<sub>m</sub>/h · ft<sup>2</sup> (1.356 kg/s · m<sup>2</sup>) is obtained; these are given in Table 22.3-1. The  $f_p$  value is a relative ratio of the total interfacial areas, since the reaction of CO<sub>2</sub> in NaOH solution takes place in the relatively static holdup pools and in the dynamic holdup. Some  $f_p$  data have been obtained at  $G_y = 500$  lb<sub>m</sub>/h · ft<sup>2</sup> instead of 1000 (E3). Eckert et al. (E2) showed that there is no effect of  $G_y$  in the range of 200–1000 lb<sub>m</sub>/h · ft<sup>2</sup> on the overall  $KGa$ . This is expected where the liquid film resistance controls (S1). Values of  $f_p$  for various investigators agree within ±10% or less.

### **22.8C Predicting Mass-Transfer Film Coefficients**

For estimating the performance  $HL(H_x)$  and  $HG(H_y)$  of a new



packing, the values of  $f_p$  can be used to correct the experimental  $H_x$  values for oxygen absorption or desorption and the  $H_y$  value for  $\text{NH}_3$  absorption with 112-in. Raschig rings. These values must also be corrected for Schmidt number, liquid viscosity, and flow rates.

*1. Gas film coefficient  $H_y$ .* Using the  $\text{NH}_3$  absorption data corrected for the liquid film resistance of approximately 10%,  $H_G$  has been found to vary as  $G_y$  to an exponent between 0.3 and 0.4 (S1, T1) for values of  $G_y$  up to about 700  $\text{lb}_m/\text{h} \cdot \text{ft}^2$  ( $0.949 \text{ kg}/\text{s} \cdot \text{m}^2$ ). A value of 0.35 is used. For liquid flows of  $G_x$  from 500 to 5000  $\text{lb}_m/\text{h} \cdot \text{ft}^2$  ( $0.678\text{--}6.782 \text{ kg}/\text{s} \cdot \text{m}^2$ ),  $H_y$  varies as  $G_x^{-0.4}\text{--}G_x^{-0.6}$ , with the value of  $G_x^{-0.5}$  used. Also, the value of  $H_y$  has been found to be

proportional to  $N_{Sc}^{0.5}$  of the gas phase. A value for  $H_y$  of 0.74 ft (0.226 m) is obtained from the correlation for 112-in. Raschig rings for the  $NH_3$  system (S1) corrected for the small liquid film resistance of 10% at  $G_x = 5000 \text{ lb}_m/\text{h} \cdot \text{ft}^2$  ( $6.782 \text{ kg/s} \cdot \text{m}^2$ ) and  $G_y = 500 \text{ lb}_m/\text{h} \cdot \text{ft}^2$  ( $0.678 \text{ kg/s} \cdot \text{m}^2$ ). The value of  $G_y = 500$  will be used instead of 1000, since there is no effect of  $G_y$  on  $f_p$  in this range. For the  $NH_3$  system,  $N_{Sc} = 0.66$  at  $25^\circ\text{C}$ . Then, for estimation of  $H_G$  for a new solute system and packing and flow rates of  $G_x$  and  $G_y$  using SI units,

$$H_G = H_y = (0.226 f_p) (N_{Sc}^{0.660})^{0.5} (G_x 6.782)^{-0.5} (G_y 0.678)^{0.35} (22.8)^{-1}$$

where  $f_p$  for the new packing is given in Table 22.3-1 and  $H_G$  is in m.

2. *Liquid film coefficient  $H_x$* . For gas flow rates up to loading or about 50% of the flooding velocity, the effect of  $G_y$  on  $H_x$  is small and can be neglected (S1). Using the oxygen desorption data,  $H_x$  is proportional to the liquid  $N_{Sc}^{0.5}$ . The  $N_{Sc} = 372$  at  $25^\circ\text{C}$  for  $\text{O}_2$  in water and the viscosity  $\mu$  is  $0.8937 \times 10^{-3} \text{ kg/m} \cdot \text{s}$ . Data for different packings show that  $H_x$  is proportional to  $(G_x/\mu)$  to the 0.22–0.35 exponent, with an average of  $(G_x/\mu)^{0.3}$ . A value of  $H_x = 1.17 \text{ ft (0.357 m)}$ , where  $G_x = 5000 \text{ lb}_m/\text{h} \cdot \text{ft}^2$  is obtained from the correlation (S1) for the  $\text{O}_2$  system and 12-in. Raschig rings. Then, to predict  $H_x$  for a new solute system and packing at velocities of  $G_x$  and  $G_y$  using SI units,

$$HL=H_x=(0.357\text{fp})(N_{Sc}372)^{0.5}(G_x/\mu^{6.782/0.8937\times10^{-3}})^{0.3}(22.8-2)$$

These equations can be used for values of  $G_y$  up to almost 1000 lb<sub>m</sub>/h · ft<sup>2</sup> and  $G_x$  up to 5000 and remain below loading.

**EXAMPLE 22.8-1. Prediction of Film Coefficients for CO<sub>2</sub> Absorption**

Predict  $H_G$ ,  $H_L$ , and  $H_{OL}$  for absorption of CO<sub>2</sub> from air by water in a dilute solution in a packed tower with 12-in. metal Pall rings at 303 K (30°C) and 101.32 kPa pressure. The flow rates are  $G_x = 4.069$  kg/s · m<sup>2</sup> (3000 lb<sub>m</sub>/h · ft<sup>2</sup>) and  $G_y = 0.5424$  kg/s · m<sup>2</sup> (400 lb<sub>m</sub>/h · ft<sup>2</sup>).

**Solution:** From Appendix A.3-18, for CO<sub>2</sub> at 1 atm,  $p_A = 1.86 \times 10^{-3}$  atm. Hence,  $y_A = p_A/1.0 = 1.86 \times 10^{-3}$  (mole fraction units). Also, from Appendix A.3-3 for air at 303 K,  $\mu = 1.866 \times 10^{-5}$  kg/m · s and the density  $\rho = 1.166$  kg/m<sup>3</sup>. The diffusivity for CO<sub>2</sub> at 276.2 K from Table 18.2-1 is  $0.142 \times 10^{-4}$  m<sup>2</sup>/s. Correcting this to 303 K by Eq. (18.2-8),  $D_{AB} = 0.142 \times 10^{-4} (303/276.2)^{1.75} = 0.1670 \times 10^{-4}$  m<sup>2</sup>/s. Hence,

$$N_{Sc} = \mu \rho D = 1.866 \times 10^{-5} (1.166) (0.1670 \times 10^{-4}) = 0.958$$

From Table 22.3-1, the relative mass-transfer coefficient for 12-in. metal Pall rings compared to that for 12-in. Raschig rings is  $f_p = 1.34$ . Substituting into Eq. (22.8-1),

$$H_G = (0.2261.34) (0.9580.660) 0.5 (4.0696.782) - 0.5 (0.54240.678) 0.35 = 0.2426 \text{ m} (0.796 \text{ ft})$$

From Appendix A.2-4, the viscosity of water at 303 K is  $0.8007 \times 10^{-3}$  kg/m · s and the density  $\rho = 995.68$  kg/m<sup>3</sup>. At 298 K the viscosity of water is  $0.8937 \times 10^{-3}$  kg/s · m.

From Table 18.2-3, the  $D_{AB}$  of CO<sub>2</sub> in water is  $2.00 \times 10^{-9}$  m<sup>2</sup>/s at 25°C. Using Eq. (18.2-13) to correct it to 303 K,  $D_{AB} = (0.8937 \times 10^{-3} / 0.8007 \times 10^{-3}) (303/298) (2.00 \times 10^{-9}) = 2.270 \times 10^{-9}$  m<sup>2</sup>/s. Then,

$$N_{Sc} = \mu p DAB = 0.8007 \times 10^{-3} (995.68) (2.270 \times 10^{-9}) = 354.3$$

Substituting into Eq. (22.8-2),

$$\begin{aligned} HL &= (0.357fp)(N_{Sc}^{0.372})^{0.5} (G_x / \mu)^{0.782 / 0.8937 \times 10^{-3}} \\ 0.3HL &= (0.3571.34) (354.3372)^{0.5} (4.069 / 0.8007 \times 10^{-3} - 36.782 / 0.8937 \times 10^{-3})^{0.3} = 0.2306 \text{ m} \quad (0.759 \text{ ft}) \end{aligned}$$

To calculate the value of  $H_{OL}$ , the molar flow rates are calculated, where for dilute air,  $V = G_y/MW = 0.5424/28.97 = 0.01872 \text{ kg mol/s} \cdot \text{m}^2$ , and for water,  $L = G_x/MW = 4.069/18.0 = 0.2261 \text{ kg mol/s} \cdot \text{m}^2$ . Substituting into Eq. (22.5-55),

$$H_{OL} = H_{Ox} = HL + (L/mV)HG = 0.2306 + [(0.2261)/(1.86 \times 10^3 \times 0.01872)]0.2426 = 0.2306 + 0.001575 = 0.2322 \text{ m}$$

The percent resistance in the gas film is  $0.001575(100)/0.2322 = 0.68\%$ . This shows that for a very insoluble gas, even though  $H_G$  is similar in value to  $H_L$ , the large value of  $m$  causes the gas-phase resistance to be very small. Hence,  $H_{OL} \approx H_L$ . For a soluble gas like  $\text{NH}_3$ , where  $m = 1.20$  at 303 K compared to  $1.86 \times 10^3$  for  $\text{CO}_2$ , the percent resistance in the gas film would be about 90% (see Problem 22.8-1). The different gas and liquid Schmidt numbers for  $\text{NH}_3$  would have only a small effect on the results.

## 22.9 Heat Effects and Temperature Variations in Absorption

### 22.9A Heat Effects in Absorption

The temperature in an absorption tower can vary from the top to the bottom of the tower when the inlet gas contains a relatively high concentration of solute. Solute

absorption by the liquid yields a heat of solution that raises the liquid temperature. Also, if evaporation of the solvent to the gas phase occurs, the liquid temperature is cooled. The curvature of the equilibrium line depends upon the absorption of the solute, the heat-transfer rate between phases, and the evaporation or condensation of the liquid solvent.

Calculated temperature profiles may also have a maximum in the tower. This can occur when the entering gas temperature is considerably below the exit solvent temperature and/or the volatile solvent evaporates. Solvent evaporation cools the liquid near the tower bottom and a temperature maximum occurs. Detailed, rigorous heat and mass-balance equations are

needed for mass transfer of the solute, mass transfer of the solvent, heat transfer between the gas and liquid, and enthalpy balances. Equations and examples are given by Sherwood et al. (S1), Stockar and Wilke (S7), and Treybal (T2). Note that in actual towers, intercoolers are often used to keep the towers isothermal.

### **22.9B Simplified Design Method**

A simplified adiabatic design method is sometimes used when the entering gas contains solvent vapor and/or solvent evaporation occurs. Heat of solution of the solute is also included in the design. Then, using an overall enthalpy balance, the exit liquid temperature is calculated. This rise in liquid temperature can then be used to adjust the equilibrium-line

curvature. First, an overall enthalpy balance is made that includes sensible heat for inlet and outlet gas temperatures, heat of solution of the solute, heat of vaporization of the solvent, and sensible heat for the inlet and the unknown outlet liquid temperature. This outlet temperature is then obtained.

The equilibrium line for the top entering liquid temperature is plotted, with the given slope at the dilute concentration. Next, an equilibrium line at this higher outlet liquid temperature is plotted. The outlet concentration  $x_1$  is then located on this equilibrium line. Then, assuming a linear liquid temperature profile, the temperature of point  $x$ , which is halfway between the top and bottom concentrations, is obtained. This  $x$  value



is then located on the equilibrium line for this new temperature. The final curved equilibrium line is plotted with the slope at the dilute end, through the  $x$  at the halfway point, and finally through the  $x_I$  point. This method is illustrated in Example 22.9-1.

**EXAMPLE 22.9-1. Heat Balance for a Nonisothermal Absorption Tower**

The gas feed at 20°C and 1 atm to a packed absorption tower contains 6.0 mol % of NH<sub>3</sub> (on a dry basis) in air. The inlet gas is saturated with water vapor. The absorbing pure liquid water enters at 25°C. The outlet gas contains 0.5% of NH<sub>3</sub> on a dry basis; it is assumed to be saturated with water vapor and leaves at 25°C. For a feed of 100 g mol dry gas, 190 g mol of pure water are to be used for absorption. The heat of solution for 1.0 g mol NH<sub>3</sub> gas absorbed in water is  $\Delta H = -8310$  cal/g mol (S1). Equilibrium data (P1) are as follows for this system, where  $y = mx$ :

\*Interpolated

**Solution:** For the inlet gas, where  $y_1 = 0.06$ , the moles  $\text{NH}_3 = 0.06(100) = 6.0$  and moles air  $= 0.94(100) = 94.0$ . For the outlet gas, where  $y_2 = 0.005$ , the moles air  $= 94.0$  and moles  $\text{NH}_3 = 94.0 [0.005/(1 - 0.005)] = 0.472$ . The total is 94.472 moles. The moles  $\text{NH}_3$  absorbed  $= 6.0 - 0.472 = 5.528$ . The outlet  $x_1 = (5.528)/(190 + 5.528) = 0.0283$ . From Appendix A.2-9, the latent heat of water at  $25^\circ\text{C}$  is  $(2442.3 \text{ J/g})/(1/4.184 \text{ J/cal})(18.02 \text{ g/g mol}) = 10519 \text{ cal/g mol}$ . The vapor pressure of water at  $20^\circ\text{C} = 2.346 \text{ kPa}$  and at  $25^\circ\text{C}$ ,

3.169 kPa.

The moles  $\text{H}_2\text{O}$  in the inlet gas at  $20^\circ\text{C} = (100.0)(2.346)/(101.325 - 2.346) = 2.370$  moles vapor. In the outlet gas moles  $\text{H}_2\text{O}$  vapor  $= (94.472)(3.169)/(101.325 - 3.169) = 3.050$  moles vapor. The moles of  $\text{H}_2\text{O}$  vaporized  $= 3.050 - 2.370 = 0.680$ .

An enthalpy balance is made for ammonia gas and air in and liquid water at  $25^\circ\text{C}$ . For air, from Appendix A.3-3,  $c_p = (1.0048 \text{ J/g} \cdot \text{K})(1/4.184 \text{ J/cal})(28.972 \text{ g/g mol}) = 6.957 \text{ cal/g mol} \cdot \text{K}$ . For water vapor, from Fig. A.3-1 in the Appendix,  $c_p = 8.0 \text{ cal/g mol} \cdot \text{K}$ , and for  $\text{NH}_3$  gas,  $c_p = 8.58 \text{ cal/g mol} \cdot \text{K}$ . The sensible heat for the entering gas at  $20^\circ\text{C}$  is as follows. For air, the sensible heat  $q = 94(6.957)(20 - 25) = -3270 \text{ cal}$ . For water vapor,  $q = (2.370)(8.0)(20 - 25) = 295 \text{ cal}$ . For  $\text{NH}_3$  gas,  $q = (6.00)(8.58)(20 - 25) = -257 \text{ cal}$ . The total sensible heat is  $-3270 - 95 - 257 = -3622 \text{ cal}$ . The latent heat of water vapor entering  $q = 2.370(10\,519) = 24\,930 \text{ cal}$ . The sensible heat of the entering liquid at  $25^\circ\text{C}$  is 0.

For the exit gas at  $25^\circ\text{C}$ , the sensible heat  $= 0$ . The latent heat of the water vapor  $= 3.050(10\,519) = 32\,083 \text{ cal}$ . The heat of solution of  $\text{NH}_3$  absorption  $= 5.528(-8310) = 245\,938 \text{ cal}$ . From Appendix A.2-11, assuming dilute liquid water,  $c_p = (1.000 \text{ cal/g} \cdot \text{K})(18.02 \text{ g/g mol}) = 18.02 \text{ cal/g mol} \cdot \text{K}$ . The total g moles of outlet liquid  $= 190 + 5.528 - 0.68 = 194.85$ . The sensible heat  $q$  of the outlet liquid  $= (194.85)(18.02)(T_1 - 25) = 3511(T_1 - 25) \text{ cal}$ , where  $T_1$  is the unknown outlet temperature in  $^\circ\text{C}$ . Equating the heat in to the heat out,

$$-3622 + 24930 = 0 + 32083 - 45938 = 3511(T_1 - 25)$$

Solving,  $(T_1 - 25) = 10.02^\circ\text{C}$ , which is the temperature increase of the outlet liquid. The outlet  $T_1 = 35.02^\circ\text{C}$  or  $35^\circ\text{C}$ .

In Fig. 22.9-1, a straight operating line is plotted since the solution is dilute. The equilibrium line for  $25^\circ\text{C}$  is also shown with a slope  $m = 1.005$  at the top of the tower. At the tower bottom, at  $35^\circ\text{C}$ , the exit  $x_1 = 0.0283$ . The equilibrium line at  $35^\circ\text{C}$  is shown. The point  $x_1$  is located on this  $35^\circ\text{C}$  line and on the curved equilibrium line for the tower. The assumed linear temperature profile is also shown. Selecting a value of  $x = (0 + 0.0283)/2 = 0.0142$  with a temperature of

(35 + 25)/2 or 30°C, the point  $x_1 = 0.0412$  is plotted on the 30°C equilibrium line. The final curved equilibrium line is plotted with a slope at the origin of 1.005 at 25°C, through the point  $x = 0.0142$  on the 30°C equilibrium line, and then through the point  $x_1 = 0.0283$  on the 35°C equilibrium line. Since the equilibrium line is curved, the number of overall transfer units  $No_y$  can be obtained by numerical or graphical integration as before using Eq. (22.5-43).

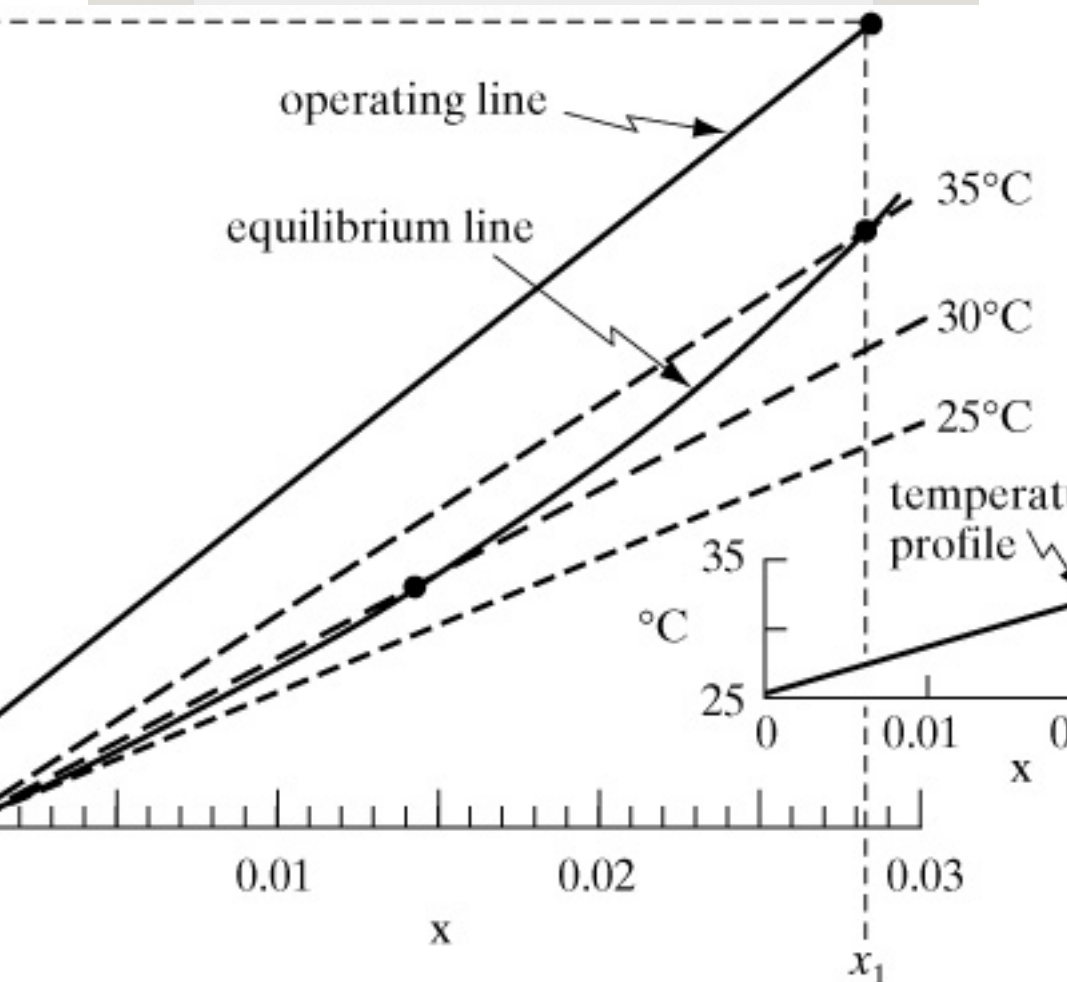


Figure 22.9-1. Operating line and curved equilibrium line for Example 22.9-1. The calculated linear temperature profile is also shown.

## 22.10 Chapter Summary

The equilibrium between two phases in a given situation is restricted by the phase rule:

$$F=C-P+2(22.1-1)$$

*Henry's law:*

$$p_A = H x_A(22.1-2)$$

If both sides of Eq. (22.1-2) are divided by total pressure  $P$  in atm,

$$y_A = H' x_A(22.1-3)$$

### Operating Line

$$y_{n+1} = L_n x_n V_{n+1} + v_1 y_1 - L_0 x_0 V_n + 1(22.1-16)$$

### Kremser Equations

For transfer of solute  $A$  from phase  $L$  to  $V$  (stripping),

$$N = \ln \left[ \frac{x_0 - (y_{N+1}/m)x_N - (y_{N+1}/m)(1-A)}{A} \right] \ln(1/A) \quad (22.1-25)$$

For transfer of solute  $A$  from phase  $V$  to  $L$  (absorption),

$$N = \ln \left[ \frac{y_{N+1} - mx_0}{y_1 - mx_0(1-A) + 1A} \right] \ln A \quad (22.1-28)$$

### **Equimolar Counterdiffusion**

$$N_A = k_y'(y_{AG} - y_{Ai}) = k_x'(x_{Ai} - x_{AL}) \quad (22.1-31)$$

### **Diffusion of A Through Stagnant or Nondiffusing B**

$$N_A = k_y(y_{AG} - y_{Ai}) = k_x(x_{Ai} - x_{AL}) \quad (22.1-33)$$

Now,

$$k_y = k_y' (1 - y_A) \quad k_x = k_x' (1 - x_A) \quad (22.1-34)$$

The overall mass transfer  $K_y'$  for equimolar counterdiffusion is defined as

$$N_A = K_y' (y_{AG} - y_A^*) \quad (22.1-39)$$

where

$$\frac{1}{K_y'} = \frac{1}{k_y'} + m' \frac{1}{k_x'} \quad (22.1-44)$$

or

$$N_A = K_x' (x_A^* - x_{AL}) \quad (22.1-40)$$

where

$$\frac{1}{K_x'} = \frac{1}{m''} \frac{1}{k_y'} + \frac{1}{k_x'} \quad (22.1-47)$$

**Design for Tower Height for Dilute**

## Solution ( $z$ = Height)

$$z = H_G N_G = H_G \int_{y_i}^{y_2} \frac{1}{y} dy \quad (22.5-41)$$

$$z = H_L N_L = H_L \int_{x_i}^{x_2} \frac{1}{x} dx \quad (22.5-42)$$

$$z = H_G N_G = H_G \int_{y^*}^{y_2} \frac{1}{y} dy \quad (22.5-43)$$

$$z = H_L N_L = H_L \int_{x^*}^{x_2} \frac{1}{x} dx \quad (22.5-44)$$

## Problems

**22.1-1. *Equilibrium and Henry's Law Constant.*** The partial pressure of  $\text{CO}_2$  in air is  $1.333 \times 10^{-4}$  Pa and the total pressure is  $1.133 \times 10^{-5}$  Pa. The gas phase is in equilibrium with a water solution at 303 K. What is the value of  $x_A$  for  $\text{CO}_2$  in

equilibrium in the solution? (See Appendix A.3 for the Henry's law constant.)

**Ans.**  $x_A = 7.07 \times 10^{-5}$  mol frac  $\text{CO}_2$

**22.1-2. Gas Solubility in an Aqueous**

**Solution.** At 303 K, the concentration of  $\text{CO}_2$  in water is  $0.90 \times 10^{-4}$  kg  $\text{CO}_2$ /kg water. Using the Henry's law constant from Appendix A.3, what partial pressure of  $\text{CO}_2$  must be kept in the gas to prevent the  $\text{CO}_2$  from vaporizing from the aqueous solution?

**Ans.**  $p_A = 6.93 \times 10^3$  Pa (0.0684 atm)

**22.1-3. Phase Rule for a Gas-Liquid**

**System.** For the system  $\text{SO}_2$ –air–water, the total pressure is set at 1 atm abs and the partial pressure of  $\text{SO}_2$  in the vapor is set at 0.20 atm. Calculate the number



of degrees of freedom,  $F$ . What variables are unspecified and hence can be arbitrarily set?

**22.1-4. *Equilibrium Stage Contact for Gas–Liquid System.*** A gas mixture at  $2.026 \times 10^5$  Pa total pressure containing air and  $\text{SO}_2$  is brought into contact in a single-stage equilibrium mixer with pure water at 293 K. The partial pressure of  $\text{SO}_2$  in the original gas is  $1.52 \times 10^4$  Pa. The inlet gas contains 5.70 total kg mol and the inlet water 2.20 total kg mol. The exit gas and liquid leaving are in equilibrium. Calculate the amounts and compositions of the outlet phases. Use equilibrium data from Fig. 22.2-1.

**Ans.**  $x_{A1} = 0.00495$ ,  $y_{A1} = 0.0733$ ,  $L_1 = 2.211$  kg mol,  $V_1 = 5.69$  kg mol

**22.1-5. Absorption in a Countercurrent Stage Tower.** Repeat Example 22.1-3 using the same conditions but with the following change. Use a pure water flow to the tower of 108 kg mol H<sub>2</sub>O/h, that is, 20% above the 90 used in Example 22.1-3. Determine the number of stages required graphically. Repeat, using the analytical Kremser equation.

**22.1-6. Stripping Taint from Cream by Steam.** Countercurrent stage stripping is to be used to remove a taint from cream. The taint is present in the original cream to the stripper at a concentration of 20 parts per million (ppm). For every 100 kg of cream entering per unit time, 50 kg of steam will be used for stripping. It is desired to reduce the concentration of the taint in the cream to 1 ppm. The equilibrium

relation between the taint in the steam vapor and the liquid cream is  $y_A = 10 x_A$ , where  $y_A$  is ppm of taint in the steam and  $x_A$  ppm in the cream (E1).

Determine the number of theoretical stages needed. [*Hint*: In this case, for stripping from the liquid ( $L$ ) stream to the vapor ( $V$ ) stream, the operating line will be below the equilibrium line on the  $y_A - x_A$  diagram. It is assumed that none of the steam condenses in the stripping. Use ppm in the material balances.]

**Ans.** Number stages = 1.85 (stepping down starting from the concentrated end)

### ***22.1-7. Overall Mass-Transfer Coefficient from Film Coefficients.***

Using the same data as in Example 22.1-5, calculate the overall mass-

transfer coefficients  $K_x'$ , the flux, and the percent resistance in the gas film.

**Ans.**  $K_x'$  mol/s  $\cdot$  m<sup>2</sup>  $\cdot$  mol frac,  $K_x = 1.519 \times 10^{-3}$ ,  $N_A = 3.78 \times 10^{-4}$  kg mol/s  $\cdot$  m<sup>2</sup>, 36.7% resistance

### ***22.1-8. Interface Concentrations and Overall Mass-Transfer Coefficients.***

Use the same equilibrium data and film coefficients  $k_y'$  and  $k_x'$  as in Example 22.1-5. However, use bulk concentrations of  $y_{AG} = 0.25$  and  $x_{AL} = 0.05$ . Calculate the following:

- Interface concentrations  $y_{Ai}$  and  $x_{Ai}$  and flux  $N_A$
- Overall mass-transfer coefficients  $K_y'$  and  $K_y$  and flux  $N_A$
- Overall mass-transfer coefficient  $K_x'$  and flux  $N_A$

### ***22.5-1. Amount of Absorption in a Tray Tower.*** An existing tower contains

the equivalent of 3.0 theoretical trays and is being used to absorb  $\text{SO}_2$  from air by pure water at 293 K and  $1.013 \times 10^5$  Pa. The entering gas contains 20 mol %  $\text{SO}_2$  and the inlet air flow rate is  $150 \text{ kg inert air/h} \cdot \text{m}^2$ . The entering water rate is  $6000 \text{ kg/h} \cdot \text{m}^2$ . Calculate the outlet composition of the gas. (*Hint: This is a trial-and-error solution. Assume an outlet gas composition of, say,  $y_1 = 0.01$ . Plot the operating line and determine the number of theoretical trays needed. If this number is not 3.0 trays, assume another value of  $y_1$ , and so on.*)

**Ans.**  $y_1 = 0.009$

**22.5-2. Analytical Method for Number of Trays in Absorption.** Use the analytical equations in Section 22.4 for

countercurrent tray contact to calculate the number of theoretical trays needed for Example 22.5-1 using 1.3 Lmin'.

**22.5-3. Absorption of Ammonia in a Tray Tower.** A tray tower is to be used to remove 99% of the ammonia from an entering air stream containing 6 mol % ammonia at 293 K and  $1.013 \times 10^5$  Pa. The entering pure-water flow rate is 188 kg H<sub>2</sub>O/h · m<sup>2</sup> and the inert air flow is 128 kg air/h · m<sup>2</sup>. Calculate the number of theoretical trays needed. Use equilibrium data from Appendix A.3. For the dilute end of the tower, plot an expanded diagram to step off the number of trays more accurately.

**Ans.**  $y_1 = 0.000639$  (exit),  $x_N = 0.0260$  (exit), 3.8 theoretical trays

**22.5-4. Minimum Liquid Flow in a Packed Tower.** The gas stream from a chemical reactor contains 25 mol % ammonia and the rest are inert gases. The total flow is 181.4 kg mol/h to an absorption tower at 303 K and  $1.013 \times 10^5$  Pa pressure, where water containing 0.005 mol frac ammonia is the scrubbing liquid. The outlet gas concentration is to be 2.0 mol % ammonia. What is the minimum flow  $L_{min}$ ? Using 1.5 times the minimum, plot the equilibrium and operating lines.

**Ans.**  $L_{min} = 262.6 \text{ kg mol/h}$

**22.5-5. Steam Stripping and Number of Trays.** A relatively nonvolatile hydrocarbon oil contains 4.0 mol % propane and is being stripped by direct superheated steam in a stripping tray

tower to reduce the propane content to 0.2%. The temperature is held constant at 422 K by internal heating in the tower at  $2.026 \times 10^5$  Pa pressure. A total of 11.42 kg mol of direct steam is used for 300 kg mol of total entering liquid. The vapor–liquid equilibria can be represented by  $y = 25x$ , where  $y$  is mole fraction propane in the steam and  $x$  is mole fraction propane in the oil. Steam can be considered as an inert gas and will not condense. Plot the operating and equilibrium lines and determine the number of theoretical trays needed.

**Ans.** 5.6 theoretical trays (stepping down from the tower top)

**22.5-6. Absorption of Ammonia in a Packed Tower.** A gas stream contains 4.0 mol %  $\text{NH}_3$  and its ammonia content



is reduced to 0.5 mol % in a packed absorption tower at 293 K and  $1.013 \times 10^5$  Pa. The inlet pure-water flow is 68.0 kg mol/h and the total inlet gas flow is 57.8 kg mol/h. The tower diameter is 0.747 m. The film mass-transfer coefficients are  $k_y'a = 0.0739$  kg mol/s  $\cdot$  m<sup>3</sup>  $\cdot$  mol frac and  $k_x'a$  mol/s  $\cdot$  m<sup>3</sup>  $\cdot$  mol frac. Using the design methods for dilute gas mixtures, do as follows:

- Calculate the tower height using  $k_y'a$ .
- Calculate the tower height using  $K_y'a$ .

**Ans.** (a)  $z = 2.362$  m (7.75 ft)

**22.5-7. Tower Height Using an Overall Mass-Transfer Coefficient.** Repeat Example 22.5-2, using the overall liquid mass-transfer coefficient  $K_x'a$  to calculate the tower height.

**22.5-8. Experimental Overall Mass-Transfer Coefficient.** In a tower 0.254 m in diameter that is absorbing acetone from air at 293 K and 101.32 kPa using pure water, the following experimental data were obtained. The height of 25.4-mm Raschig rings = 4.88 m,  $V' = 3.30$  kg mol air/h,  $y_1 = 0.01053$  mol frac acetone,  $y_2 = 0.00072$ ,  $L' = 9.03$  kg mol water/h, and  $x_1 = 0.00363$  mol frac acetone. Calculate the experimental value of  $K_y a$ .

**22.5-9. Conversion to Transfer-Unit Coefficients from Mass-Transfer Coefficients.** Experimental data on absorption of dilute acetone in air by water at 80°F and 1 atm abs pressure in a packed tower with 25.4-mm Raschig rings were obtained. The inert gas flow was 95 lb<sub>m</sub> air/h · ft<sup>2</sup> and the pure-water

flow was  $987 \text{ lb}_m/\text{h} \cdot \text{ft}^2$ . The experimental coefficients are  $kGa = 4.03 \text{ lb mol/h} \cdot \text{ft}^3 \cdot \text{atm}$  and  $kLa = 16.6 \text{ lb mol/h} \cdot \text{ft}^3 \cdot \text{lb mol/h} \cdot \text{ft}^3$ . The equilibrium data can be expressed by  $c_A = 1.37 p_A$ , where  $c_A = \text{lb mol/ft}^3$  and  $p_A = \text{atm}$  partial pressure of acetone.

- Calculate the film height of transfer units  $H_G$  and  $H_L$ .
- Calculate  $H_{OG}$ .

**Ans.** (b)  $H_{OG} = 0.957 \text{ ft (0.292 m)}$

### **22.5-10. Height of Tower Using**

**Transfer Units.** Repeat Example 22.5-2 but use transfer units and calculate  $H_L$ ,  $N_L$ , and tower height.

### **22.5-11. Experimental Value of HOG.**

Using the experimental data given in Problem 22.5-8, calculate the number of

transfer units  $NOG$  and the experimental value of  $HOG$ .

$$\text{Ans. } HOG = 1.265 \text{ m}$$

### **22.5-12. Pressure Drop and Tower**

**Diameter.** Use the same conditions as in Example 22.3-1 but with the following changes. The gas feed rate is 2000 lb<sub>m</sub>/h and the design ratio of  $GL/GG$  is 2.2/1. Using 60% of flooding and 1 in. Intalox packing, calculate the pressure drop, gas and liquid flows, and tower diameter.

$$\text{Ans. } \Delta p = 0.250 \text{ in. water/ft packing, } D = 1.452 \text{ ft (0.4425 m)}$$

### **22.5-13. Minimum Liquid Flow Rate in**

**Absorption.** Using the data from Example 22.5-1, calculate the number of trays graphically and analytically for an operating flow rate of 1.3 times the

minimum liquid flow rate.

**Ans.**  $N = 5.34$  steps (analytical)

**22.5-14. *Experimental Height of a Transfer Unit and Analytical***

**Equations.** A packed tower 4.0 m tall is used to absorb ethyl alcohol from an inert gas by 90 kg mol/h of pure water at 303 K and 101.3 kPa. The total gas stream flow rate of 100 kg mol/h contains 2.0 mol % alcohol and the exit concentration is 0.20 mol %. The equilibrium relation is  $y = mx = 0.68 x$  for this dilute stream. Using the analytical equations, calculate the number of theoretical trays  $N$ , the number of transfer units  $NOG$ ,  $HOG$ , and HETP.

**Ans.**  $HOG = 0.860$  m (2.823 ft),  $N =$

**22.6-1. Murphree Efficiency and Actual Number of Trays.** For the distillation of heptane and ethyl benzene in Problem 26.4-2, the Murphree tray efficiency is estimated as 0.55.

Determine the actual number of trays needed by stepping off the trays using the tray efficiency of 0.55. Also, calculate the overall tray efficiency  $E_0$ .

**22.6-2. Packing and Tray Efficiencies for an Absorption Tower.** An absorber in a petroleum refinery uses a lean oil to absorb butane from a natural gas stream. The composition of the key component butane in the gas phase is related to its composition in the liquid phase at equilibrium by  $y = mx = 0.7 x$ . At the tower bottom, where the flows are

largest,  $\rho_L = 57.9 \text{ lb}_m/\text{ft}^3$  ( $927 \text{ kg}/\text{m}^3$ ). At the average tower temperature,  $\mu_L = 1.4 \text{ cp}$  and the average molecular weight of the liquid is  $M_L = 245$ . Estimate the efficiency for a valve-tray tower and the HETP for Norton Intalox 2T structured packing.

### **22.6-3. Estimation of the Tower**

#### **Diameter of a Sieve Tray. A**

distillation sieve-tray tower is being used to distill a hydrocarbon feed. The vapor flow rate at the tower bottom is 21 000 kg/hr and the liquid flow rate is 19 500 kg/hr. The density of the liquid  $\rho_L = 673 \text{ kg}/\text{m}^3$  and  $\rho_V = 3.68 \text{ kg}/\text{m}^3$ . Assume a tray spacing of 24 in. (0.610 m).

Calculate the tower diameter assuming the tower operates at 80% of flooding.

Assume  $\sigma = 22.5 \text{ dyn}/\text{cm}$ .

**Ans.**  $K_V = 0.35$ ,  $D = 1.372 \text{ m}$  (4.50 ft)

**22.7-1. Liquid Film Coefficients and Design of an  $\text{SO}_2$  Tower.** Using the data for Example 22.7-1, calculate the height of the tower using Eq. (22.5-15), which is based on the liquid film mass-transfer coefficient  $k_x'a$ . (*Note:* The interface values  $x_i$  have already been obtained.)

**Ans.**  $z = 1.586 \text{ m}$

**22.7-2. Design of an  $\text{SO}_2$  Tower Using Overall Coefficients.** Using the data for Example 22.7-1, calculate the tower height using the overall mass-transfer coefficient  $K_y'a$ . [*Hint:* Calculate  $K_y'a$  at the top of the tower and at the bottom of the tower from the film coefficients. Then, use a linear average of the two values for the design. Obtain the values



of  $y^*$  from the operating- and equilibrium-line plot. Numerically or graphically integrate Eq. (22.5-16), keeping  $K_y'a$  outside the integral.]

### ***22.7-3. Height of a Packed Tower***

***Using Transfer Units.*** For Example 22.7-1, calculate the tower height using the  $HG$  and the number of transfer units  $NG$ . [*Hint: Calculate  $HG$  at the tower top using Eq. (22.5-36) and at the tower bottom. Use the linear average value for  $HG$ . Calculate the number of transfer units  $NG$  by numerical or graphical integration of the integral of Eq. (22.5-32). Then, calculate the tower height.*]

**Ans.**  $HG = 0.2036$  m (average value)

### ***22.7-4. Design of Absorption Tower***

**Using Transfer Units.** The gas  $\text{SO}_2$  is being scrubbed from a gas mixture by pure water at 303 K and  $1.013 \times 10^5$  Pa. The inlet gas contains 6.00 mol %  $\text{SO}_2$  and the outlet 0.3 mol %  $\text{SO}_2$ . The tower cross-sectional area of packing is  $0.426 \text{ m}^2$ . The inlet gas flow is  $13.65 \text{ kg mol inert air/h}$  and the inlet water flow is  $984 \text{ kg mol inert water/h}$ . The mass-transfer coefficients are  $HL = 0.436 \text{ m}$  and  $kGa = 6.06 \times 10^7 \text{ kg mol/s} \cdot \text{m}^3 \cdot \text{Pa}$ , and are to be assumed constant in the tower for the given concentration range. Use equilibrium data from Appendix A.3. By numerical or graphical integration, determine  $NG$ . Calculate the tower height. (*Note:* The equilibrium line is markedly curved, so numerical or graphical integration is necessary even for this dilute mixture.)

**Ans.**  $N_G = 8.47$  transfer units,  $z = 1.311$  m

**22.8-1. Correction of Film Coefficients for  $\text{NH}_3$  Absorption.** Use the same system and conditions given in Example 22.8-1, except that  $\text{NH}_3$  is being absorbed instead of  $\text{CO}_2$ . The flow rates are the same. Predict  $H_G$ ,  $H_L$ ,  $H_{OG}$ , and percent resistance in the liquid phase.

**Ans.**  $H_{OG} = 0.2244$  m, % resistance = 9.4%

**22.8-2. Prediction of Film Coefficients for Acetone Absorption.** Predict  $H_G$ ,  $H_L$ , and  $H_{OG}$  for absorption of acetone from air by water in a dilute aqueous solution using 2-in. Intalox metal IMTP packing at  $20^\circ\text{C}$  and 1 atm abs pressure. The flow rates are  $G_x = 3.391 \text{ kg/s} \cdot \text{m}^2$

(2500 lb<sub>m</sub>/h · ft<sup>2</sup>) and  $G_y = 0.678 \text{ kg/s} \cdot \text{m}^2$  (500 lb<sub>m</sub>/h · ft<sup>2</sup>). Use equilibrium data from Appendix A.3-21 and the diffusivity for acetone in water from Table 18.2-3. The diffusivity of acetone in air at 1 atm abs is  $0.109 \times 10^{-4} \text{ m}^2/\text{s}$  at 0°C (P1).

**Ans.**  $H_G = 0.3416 \text{ m}$ ,  $H_{OG} = 0.3921 \text{ m}$

### **22.9-1. *Nonisothermal Absorption***

**Tower.** Use the same operating conditions as in Example 22.9-1 for absorption of NH<sub>3</sub> except for the following change. The inlet gas temperature is 15°C and it is saturated with water vapor. Calculate the outlet water temperature  $T_1$  and the overall number of transfer units  $N_{Oy}$  by numerical or graphical integration.

**Ans.**  $T_1 = 32.05^{\circ}\text{C}$

### References

### Notation

# Chapter 23. Humidification Processes

## 23.0 Chapter Objectives

On completion of this chapter, a student should be able to:

- Calculate properties of ideal gas mixtures and determine the properties of dry air–water vapor mixtures
- Plot processes on a psychrometric chart and analyze processes involving dry air–water vapor mixtures to perform energy and mass balances for the processes
- Calculate and distinguish the four types of humidity described in the chapter
- Calculate the dew point of an air–water mixture
- Explain the significance of the wet bulb temperature and how it can be used to estimate humidity
- Use the rate equations for heat and mass transfer to plot both the operating and equilibrium line
- Use analytical and graphical techniques to calculate the height of the water-cooling tower for a given heat load

## 23.1 Vapor Pressure of Water and Humidity

### 23.1A Vapor Pressure of Water

*1. Introduction.* In a number of the separation processes and transport processes, it is necessary to make calculations involving the properties of mixtures of water vapor and air. These calculations involve knowledge of the concentration of water vapor in air under various conditions of temperature and pressure, the thermal properties of these mixtures, and the changes occurring when these mixtures are brought into contact with water or with wet solids in drying.

*Humidification* involves the transfer of water from the liquid phase into a gaseous mixture of air and water vapor.

*Dehumidification* involves the reverse transfer, whereby water vapor is transferred from the vapor state to the liquid state. Humidification and dehumidification can also refer to vapor mixtures of materials such as benzene, but most practical applications occur with water. To better understand humidity, it is first necessary to discuss the vapor pressure of water.

*2. Vapor pressure of water and physical states.* Pure water can exist in three different physical states: solid ice, liquid, and vapor. The physical state in which it exists depends on the pressure and temperature.

Figure 23.1-1 illustrates the various physical states of water and the pressure–temperature relationships at



equilibrium. In Fig. 23.1-1, the regions of the solid, liquid, and vapor states are shown. Along the line  $AB$ , the liquid and vapor phases coexist. Along line  $AC$ , the ice and liquid phases coexist. Along line  $AD$ , the ice and vapor phases coexist. If ice at point (1) is heated at constant pressure, the temperature rises and the physical condition is represented as moving horizontally. As the horizontal line crosses  $AC$ , the solid melts and, on crossing  $AB$ , the liquid vaporizes. Moving from point (3) to (4), ice sublimates (vaporizes) to a vapor without becoming a liquid.

Liquid and vapor coexist in equilibrium along the line  $AB$ , which is the vapor-pressure line for water. Boiling occurs when the vapor pressure of the water is equal to the total pressure above the

water's surface. For example, at  $100^{\circ}\text{C}$  ( $212^{\circ}\text{F}$ ) the vapor pressure of water is 101.3 kPa (1.0 atm), and therefore it will boil at 1 atm pressure. At  $65.6^{\circ}\text{C}$  ( $150^{\circ}\text{F}$ ), from the steam tables in Appendix A.2, the vapor pressure of water is 25.7 kPa (3.72 psia). Hence, at 25.7 kPa and  $65.6^{\circ}\text{C}$ , water will boil.

If a pan of water is held at  $65.6^{\circ}\text{C}$  in a room at 101.3 kPa abs pressure, the vapor pressure of water will again be 25.7 kPa. This illustrates an important property of the vapor pressure of water, which is not influenced by the presence of an inert gas such as air; that is, the vapor pressure of water is essentially independent of the total pressure of the system.

### **23.1B Humidity and a Humidity Chart**

1. *Definition of humidity.* The humidity  $H$  of an air–water vapor mixture is defined as the kg of water vapor contained in 1 kg of dry air. The humidity so defined depends only on the partial pressure  $p_A$  of water vapor in the air and on the total pressure  $P$  (assumed throughout this chapter to be 101.325 kPa, 1.0 atm abs, or 760 mmHg). Using the molecular weight of water ( $A$ ) as 18.02 and of air as 28.97, the humidity  $H$  in kg H<sub>2</sub>O/kg dry air, or in English units as lb H<sub>2</sub>O/lb dry air, is as follows:

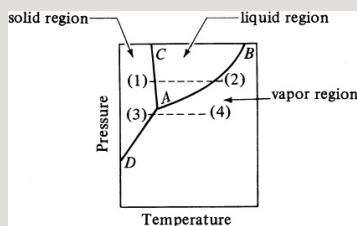


Figure 23.1-1. *Phase diagram for water.*

$$\frac{H \text{ kg H}_2\text{O}}{\text{kg dry air}} = \frac{p_A}{p - p_A} \times \frac{18.02 \text{ kg H}_2\text{O}}{\text{kg mol air}} \times \frac{128.97 \text{ kg H}_2\text{O}}{\text{kg mol H}_2\text{O}} \times \frac{1}{23.1 - 1}$$

$$H = 18.02 \times 28.97 \times \frac{p_A}{p - p_A} \times \frac{1}{22}$$

Saturated air is air in which the water vapor is in equilibrium with liquid water at the given conditions of pressure and temperature. In this mixture, the partial pressure of the water vapor in the air–water mixture is equal to the vapor pressure  $p_{AS}$  of pure water at the given temperature. Hence, the saturation humidity  $H_s$  is

$$H_s = 18.02 \times 28.97 \times \frac{p_{AS}}{p - p_{AS}} \times \frac{1}{22} \quad (23.1-2)$$

**2. Percentage humidity.** The percentage humidity  $HP$  is defined as 100 times the actual humidity  $H$  of the air divided by the humidity  $H_s$  if the air was saturated

at the same temperature and pressure:

$$HP=100HHS(23.1-3)$$

3. *Percentage relative humidity.* The amount of saturation of an air–water vapor mixture is also given as percentage relative humidity  $HR$  using partial pressures:

$$HR=100pApAS(23.1-4)$$

Note that  $HR \neq HP$ , since  $HP$  expressed in partial pressures by combining Eqs. (23.1-1), (23.1-2), and (23.1-3) is

$$HP=100HHS=(100)18.0228.97pAP-pA/18.0228.97pASP-pAS=pApASP-pASP-pA(100)(23.1-5)$$

This, of course, is not the same as Eq. (23.1-4).

**EXAMPLE 23.1-1. Humidity from Vapor-Pressure Data**

The air in a room is at 26.7°C (80°F) and a pressure of 101.325 kPa and contains water vapor with a partial pressure  $p_A = 2.76$  kPa. Calculate the following:

- Humidity,  $H$
- Saturation humidity,  $H_s$ , and percentage humidity,  $H_P$
- Percentage relative humidity,  $H_R$

**Solution:** From the steam tables at 26.7°C, the vapor pressure of water is  $p_{AS} = 3.50$  kPa (0.507 psia) also,  $p_A = 2.76$  kPa and  $P = 101.3$  kPa (14.7 psia). For part (a), using Eq. (23.1-1),

$$H = 18.0228.97 \frac{p_A}{P - p_A} = 18.02(2.76)28.97(101.3 - 2.76) = 0.01742 \text{ kg H}_2\text{O/kg air}$$

For part (b), using Eq. (23.1-2), the saturation humidity is

$$H_s = 18.0228.97 \frac{p_{AS}}{P - p_{AS}} = 18.02(3.50)28.97(101.3 - 3.50) = 0.02226 \text{ kg H}_2\text{O/kg air}$$

The percentage humidity, from Eq. (23.1-3), is

$$H_P = 100 \frac{H}{H_s} = 100(0.01742)0.02226 = 78.3\%$$

For part (c), from Eq. (23.1-4), the percentage relative humidity is

$$H_R = 100 \frac{p_A}{p_{AS}} = 100(2.76)3.50 = 78.9\%$$

*4. Dew point of an air–water vapor mixture.* The temperature at which a given mixture of air and water vapor would be saturated is called the *dew-point temperature* or simply the *dew*

*point.* For example, at  $26.7^{\circ}\text{C}$  ( $80^{\circ}\text{F}$ ), the saturation vapor pressure of water is  $p_{AS} = 3.50 \text{ kPa}$  ( $0.507 \text{ psia}$ ). Hence, the dew point of a mixture containing water vapor having a partial pressure of  $3.50 \text{ kPa}$  is  $26.7^{\circ}\text{C}$ . If an air–water vapor mixture is at  $37.8^{\circ}\text{C}$  (often called the dry bulb temperature, since this is the actual temperature a dry thermometer bulb would indicate in this mixture) and it contains water vapor of  $p_A = 3.50 \text{ kPa}$ , the mixture would not be saturated. On cooling to  $26.7^{\circ}\text{C}$ , the air would be saturated, that is, at the dew point. On further cooling, some water vapor would condense, since the partial pressure cannot be greater than the saturation vapor pressure.

*5. Humid heat of an air–water vapor mixture.* The humid heat  $c_s$  is the

amount of heat in J (or kJ) required to raise the temperature of 1 kg of dry air plus the water vapor present by 1 K or 1°C. The heat capacity of air and water vapor can be assumed constant over the temperature ranges usually encountered at 1.005 kJ/kg dry air · K and 1.88 kJ/kg water vapor · K, respectively. Hence, for SI and English units,

$$c_s \text{ kJ/} \\ \text{kg dry air} \cdot \text{K} = 1.005 + 1.88H \text{ (SI)} \\ c_s \text{ btu/} \\ \text{lbm dry air} \cdot ^\circ\text{F} = 0.24 + 0.45H \text{ (English)} \\ (23.1-6)$$

[In some cases,  $c_s$  will be given as  $(1.005 + 1.88H)10^3 \text{ J/kg} \cdot \text{K}$ .]

*6. Humid volume of an air–water vapor mixture.* The humid volume  $v_H$  is the total volume in m<sup>3</sup> of 1 kg of dry air



plus the vapor it contains at 101.325 kPa (1.0 atm) abs pressure and the given gas temperature. Using the ideal gas law,

$$v_H = \frac{m_H}{\rho_H}$$

$$\begin{aligned} & \frac{1}{2} \frac{dH}{dT} = \frac{1}{2} \left( \frac{dH}{dT} \right)_{\text{air}} + \frac{1}{2} \left( \frac{dH}{dT} \right)_{\text{vapor}} \\ & \text{air} = 359492 T^\circ R (128.97 + 118.02 H) = (0.0252 + 0.405 H) T^\circ R \end{aligned}$$

For a saturated air–water vapor mixture,  $H = H_s$ , and  $v_H$  is the saturated volume.

*7. Total enthalpy of an air–water vapor mixture.* The total enthalpy of 1 kg of air plus its water vapor is  $H_y$  J/kg or kJ/kg dry air. If  $T_0$  is the datum temperature chosen for both components, the total enthalpy is the sensible heat of the air–water vapor mixture plus the latent heat  $\lambda_0$  in J/kg or kJ/kg water vapor of the water vapor at  $T_0$ . Note that  $(T - T_0)^\circ\text{C} = (T - T_0)$  K and that this enthalpy is

referred to liquid water.

$$H_y \text{ kJ/kg dry air} = c_s(T - T_0) + H\lambda_0 = (1.005 + 1.88H)(T - T_0) \\ \text{C}) + H\lambda_0 \quad H_y \text{ Btu/lbm dry air} = (0.24 + 0.45H)(T - T_0) \\ \text{F}) + H\lambda_0 \quad (23.1-8)$$

If the total enthalpy is referred to a base temperature  $T_0$  of  $0^\circ\text{C}$  ( $32^\circ\text{F}$ ), the equation for  $H_y$  becomes

$$H_y \text{ kJ/kg dry air} = (1.005 + 1.88H)(T - 0) + 2501.4H \text{ (SI)} \\ H_y \text{ Btu/lbm dry air} = (0.24 + 0.45H)(T - 32) + 1075.4H \text{ (English)} \quad (23.-9)$$

*8. Humidity chart of air–water vapor mixtures.* A convenient chart of the properties of air–water vapor mixtures at 1.0 atm abs pressure is the humidity chart in Fig. 23.1-2. In this figure, the

humidity  $H$  is plotted versus the actual temperature of the air–water vapor mixture (dry bulb temperature).

The curve marked 100% running upward to the right gives the saturation humidity  $H_s$  as a function of temperature. In Example 23.1-1, for  $26.7^\circ\text{C}$ ,  $H_s$  was calculated as 0.02226 kg  $\text{H}_2\text{O}/\text{kg}$  air. Plotting this point for  $26.7^\circ\text{C}$  ( $80^\circ\text{F}$ ) and  $H_s = 0.02226$  on Fig. 23.1-2, it falls on the 100% saturated line.

Any point below the saturation line represents unsaturated air–water vapor mixtures. The curved lines below the 100% saturation line and running upward to the right represent unsaturated mixtures of definite percentage humidity  $H_p$ . Going

downward vertically from the saturation line at a given temperature, the line between 100% saturation and zero humidity  $H$  (the bottom horizontal line) is divided evenly into 10 increments of 10% each.

All the percentage humidity lines  $H_p$  mentioned and the saturation humidity line  $H_s$  can be calculated from the data for vapor pressure of water.

**EXAMPLE 23.1-2. Use of the Humidity Chart**

Air entering a dryer has a temperature (dry bulb temperature) of 60°C (140°F) and a dew point of 26.7°C (80°F). Using the humidity chart, determine the actual humidity  $H$ , percentage humidity  $H_p$ , humid heat  $c_s$ , and humid volume  $v_H$  in SI and English units.

**Solution:** The dew point of 26.7°C is the temperature at which the given mixture is at 100% saturation. Starting at 26.7°C (Fig. 23.1-2), and drawing a vertical line until it intersects the line for 100% humidity, a humidity of  $H = 0.0225$  kg H<sub>2</sub>O/kg dry air is read off the plot. This is the actual humidity of the air at 60°C. Stated in another way, if air at 60°C and having a humidity  $H = 0.0225$  is cooled, its dew point will be 26.7°C. In English units,  $H = 0.0225$  lb H<sub>2</sub>O/lb dry air.

Locating this point where  $H = 0.0225$  and  $t = 60^\circ\text{C}$  on the chart, the percentage humidity  $H_p$  is found to be 14% by

linear interpolation vertically between the 10 and 20% lines.

The humid heat for  $H = 0.0225$  is, from Eq. (23.1-6),

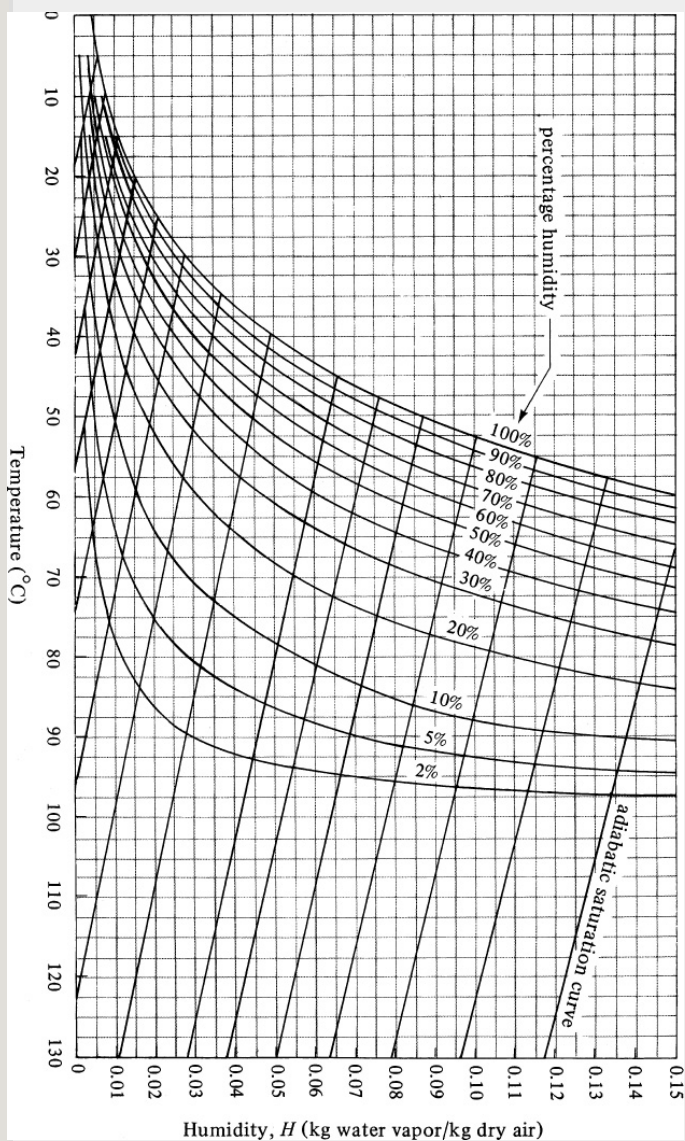


Figure 23.1-2. Humidity chart for mixtures of air and water vapor at a total pressure of 101.325 kPa (760 mmHg). From R. E. Treybal, *Mass-Transfer Operations*, 3rd ed. New York: McGraw-Hill Book Company, 1980. With permission.

$$\begin{aligned}cs &= 1.005 + 1.88(0.0225) = 1.047 \text{ kJ/} \\ &\text{kg dry air} \cdot K \text{ or } 1.047 \times 103 \text{ J/} \\ \text{kg} \cdot Kcs &= 0.24 + 0.45(0.0225) = 0.250 \text{ btu/} \\ &\text{lbm dry air} \cdot ^\circ\text{F (English)}\end{aligned}$$

The humid volume at 60°C (140°F), from Eq. (23.1-7), is

$$u_H = (2.83 \times 10^{-3} + 4.56 \times 10^{-3} \times 0.0225)(60 + 273) = 0.977 \text{ m}^3/\text{kg dry air}$$

In English units,

$$u_H = (0.0252 + 0.0405 \times 0.0225)(460 + 140) = 15.67 \text{ ft}^3/\text{lbm dry air}$$

### 23.1C Adiabatic Saturation Temperatures

Consider the process shown in Fig. 23.1-3, where the entering gas of an air–water vapor mixture is contacted with a spray of liquid water. The gas exits, having a different humidity and temperature and the process is adiabatic. The water is recirculated, with some makeup water added.

The temperature of the water being recirculated reaches a steady-state temperature called the *adiabatic saturation temperature*,  $T_s$ . If the

entering gas at temperature  $T$  having a humidity of  $H$  is not saturated,  $T_s$  will be lower than  $T$ . If the contact between the entering gas and the spray of droplets is enough to bring the gas and liquid to equilibrium, the exiting air is saturated at  $T_s$ , having a humidity  $H_s$ .

Writing an enthalpy balance (heat balance) over the process, a datum of  $T_s$  is used. The enthalpy of the makeup  $H_2O$  is then zero. This means that the total enthalpy of the entering gas mixture = enthalpy of the exiting gas mixture, or, using Eq. (23.1-8),

$$c_s(T - T_s) + H\lambda_s = c_s(T_s - T_s) + H_s\lambda_s \quad (23.1-10)$$

Or, rearranging, and using Eq. (23.1-6) for  $c_s$ ,

$$H - H_s T - T_s = -c S \lambda S = 1.005 + 1.88 H \lambda S (\text{SI})$$

$$H - H_s T - T_s = 0.24 + 0.45 H \lambda S (\text{English})$$

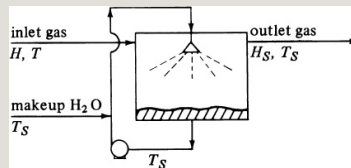


Figure 23.1-3. *Adiabatic air–water vapor saturator.*

Equation (23.1-11) is the equation of an adiabatic humidification curve when plotted on Fig. 23.1-2, which passes through the points  $H_s$  and  $T_s$  on the 100% saturation curve, as well as other points of  $H$  and  $T$ . These series of lines, running upward to the left, are called *adiabatic humidification lines* or *adiabatic saturation lines*. Since  $cs$  contains the term  $H$ , the adiabatic lines are not quite straight when plotted on the humidity chart.



If a given gas mixture at  $T_1$  and  $H_1$  is contacted for a sufficiently long time in an adiabatic saturator, it will leave saturated at  $HS_1$  and  $TS_1$ . The values of  $HS_1$  and  $TS_1$  are determined by following the adiabatic saturation line going through point  $T_1H_1$  until it intersects the 100% saturation line. If contact is not sufficient, the exiting mixture will be at a percentage saturation less than 100% but on the same line.

**EXAMPLE 23.1-3. Adiabatic Saturation of Air**

An air stream at 87.8°C having a humidity  $H = 0.030$  kg H<sub>2</sub>O/kg dry air is contacted with water in an adiabatic saturator. It is cooled and humidified to 90% saturation.

- What are the final values of  $H$  and  $T$ ?
- For 100% saturation, what would be the values of  $H$  and  $T$ ?

**Solution:** For part (a), the point  $H = 0.030$  and  $T = 87.8^\circ\text{C}$  is located on the humidity chart. The adiabatic saturation curve through this point is followed upward to the left until it intersects the 90% line at 42.5°C and  $H = 0.0500$  kg H<sub>2</sub>O/kg dry air.

For part (b), the same line is followed to 100% saturation, where  $T = 40.5^\circ\text{C}$  and  $H = 0.0505$  kg H<sub>2</sub>O/kg dry air.

### 23.1D Wet Bulb Temperature

The adiabatic saturation temperature is the steady-state temperature attained when a large amount of water is contacted by the entering gas. The *wet bulb temperature* is the steady-state nonequilibrium temperature reached when a small amount of water is contacted under adiabatic conditions by a continuous stream of gas. Since the amount of liquid is small, the temperature and humidity of the gas are not changed, contrary to the case of adiabatic saturation, where the temperature and humidity of the gas are changed.

The method used to measure the wet bulb temperature is illustrated in Fig. 23.1-4, where a thermometer is covered by a wick or cloth. The wick is kept wet

by water and is immersed in a flowing stream of air–water vapor having a temperature of  $T$  (dry bulb temperature) and humidity  $H$ . At steady state, water is evaporating to the gas stream. The wick and water are cooled to  $T_w$  and stay at this constant temperature. The latent heat of evaporation is exactly balanced by the convective heat flowing from the gas stream at  $T$  to the wick at a lower temperature  $T_w$ .

A heat balance on the wick can be made. The datum temperature is taken at  $T_w$ . The amount of heat lost by vaporization, neglecting the small sensible heat change of the vaporized liquid and radiation, is

$$q = M A N \lambda_w A (23.1 - 12)$$

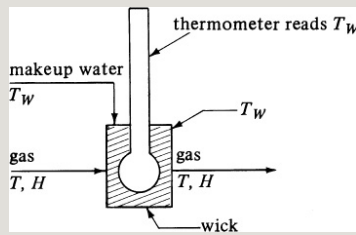


Figure 23.1-4. *Measurement of wet bulb temperature.*

where  $q$  is kW (kJ/s),  $MA$  is the molecular weight of water,  $N_A$  is kg mol H<sub>2</sub>O evaporating/ s · m<sup>2</sup>,  $A$  is surface area m<sup>2</sup>, and  $\lambda W$  is the latent heat of vaporization at  $T_w$  in kJ/kg H<sub>2</sub>O. In English units,  $q$  is btu/h,  $N_A$  is lb mol/h · ft<sup>2</sup>, and  $\lambda W$  is btu/lb<sub>m</sub> H<sub>2</sub>O. The flux  $N_A$  is

$$N_A = k_y' x_{BM} (y_W - y) = k_y (y_W - y) \quad (23.1-13)$$

where  $k_y'$  is the mass-transfer coefficient in kg mol/s · m<sup>2</sup> · mol frac,  $x_{BM}$  is the log mean inert mole fraction of the air,  $y_W$  is the mole fraction of

water vapor in the gas at the surface, and  $y$  is the mole fraction in the gas. For a dilute mixture,  $x_{BM} \cong 1.0$  and  $k'_y \cong k_y$ . The relation between  $H$  and  $y$  is

$$y = \frac{H}{M_A} \frac{1}{M_B + H/M_A} \quad (23.1-14)$$

where  $M_B$  is the molecular weight of air and  $M_A$  is the molecular weight of  $H_2O$ . Since  $H$  is small, as an approximation,

$$y \cong \frac{H}{M_B} \frac{1}{M_A} \quad (23.1-15)$$

Substituting Eq. (23.1-15) into (23.1-13) and then substituting the resultant into Eq. (23.1-12),

$$q = M_B k_y \lambda W (H_w - H)_A \quad (23.1-16)$$

The rate of convective heat transfer from the gas stream at  $T$  to the wick at  $T_w$  is

$$q=h(T-T_W)A \quad (23.1-17)$$

where  $h$  is the heat-transfer coefficient in  $kW/m^2 \cdot K$  ( $btu/h \cdot ft^2 \cdot ^\circ F$ ).

Equating Eq. (23.1-16) to Eq. (23.1-17) and rearranging,

$$H-H_W T-T_W = -h/M B k_y 1 W \quad (23.1-18)$$

Experimental data on the value of  $h/M B k_y$ , called the *psychrometric ratio*, show that for water vapor–air mixtures, the value is approximately 0.96–1.005. Since this value is close to the value of  $c_s$  in Eq. (23.1-11), approximately 1.005, Eqs. (23.1-18) and (23.1-11) are almost the same. This means that the adiabatic saturation lines can also be used for wet bulb lines with reasonable accuracy. (Note that this is only true for water vapor and not for other vapors,

such as benzene.) Hence, the wet bulb determination is often used to measure the humidity of an air–water vapor mixture.

**EXAMPLE 23.1-4. Wet Bulb Temperature and Humidity**

A water vapor–air mixture having a dry bulb temperature of  $T = 60^\circ\text{C}$  is passed over a wet bulb, as shown in Fig. 23.1-4, and the wet bulb temperature obtained is  $T_w = 29.5^\circ\text{C}$ . What is the humidity of the mixture?

**Solution:** The wet bulb temperature of  $29.5^\circ\text{C}$  can be assumed to be the same as the adiabatic saturation temperature  $T_s$ , as discussed. Following the adiabatic saturation curve of  $29.5^\circ\text{C}$  until it reaches the dry bulb temperature of  $60^\circ\text{C}$ , the humidity is  $H = 0.0135 \text{ kg H}_2\text{O/kg dry air}$ .

## 23.2 Introduction and Types of Equipment for Humidification

*1. Introduction to gas–liquid contactors.* When a relatively warm liquid is brought into direct contact with a gas that is unsaturated, some of the liquid is vaporized. The liquid temperature will drop mainly because of the latent heat of

evaporation. This direct contact of a gas with a pure liquid occurs most often in contacting air with water. This is done for the following purposes: humidifying air for control of the moisture content of air in drying or air conditioning; dehumidifying air, where cold water condenses some water vapor from warm air; and water cooling, where evaporation of water to the air cools warm water.

In Section 23.1, the fundamentals of humidity and adiabatic humidification were discussed. In this section, the performance and design of continuous air–water contactors is considered. The emphasis is on water cooling, since this is the most important type of process in the process industries. There are many



cases in industry in which warm water is discharged from heat exchangers and condensers when it would be more economical to cool and reuse it than to discard it.

*2. Towers for water cooling.* In a typical water-cooling tower, warm water flows countercurrently to an air stream.

Typically, the warm water enters the top of a packed tower and cascades down through the packing, exiting at the bottom. Air enters at the bottom of the tower and flows upward through the descending water. The tower packing often consists of slats of plastic or of a packed bed. The water is distributed by troughs and overflows to cascade over slat gratings or packing that provides large interfacial areas of contact, in the form of droplets and films of water,

between the water and air. The flow of air upward through the tower can be induced by the buoyancy of the warm air in the tower (natural draft) or by the action of a fan. Detailed descriptions of towers are given in other texts (B1, T1).

The water cannot be cooled below the wet bulb temperature. The driving force for the evaporation of the water is approximately the vapor pressure of the water less the vapor pressure it would have at the wet bulb temperature. The water can be cooled only to the wet bulb temperature and, in practice, it is cooled to about 3 K or more above this. Only a small amount of water is lost by evaporation in cooling water. Since the latent heat of vaporization of water is about 2300 kJ/kg, a typical change of about 8 K in water temperature

corresponds to an evaporation loss of about 1.5%. Hence, the total flow of water is usually assumed to be constant in calculations of tower size.

In humidification and dehumidification, intimate contact between the gas phase and liquid phase is needed for large rates of mass transfer and heat transfer. The gas-phase resistance controls the rate of transfer. Spray or packed towers are used to give large interfacial areas and to promote turbulence in the gas phase.

## **23.3 Theory and Calculations for Cooling-Water Towers**

### **23.3A Theory and Calculations for Cooling-Water Towers**

*1. Temperature and concentration profiles at an interface.* In Fig. 23.3-1, the temperature profile and

concentration profile in terms of humidity are shown at the water–gas interface. Water vapor diffuses from the interface to the bulk gas phase with a driving force in the gas phase of  $(H_i - H_G)$  kg H<sub>2</sub>O/kg dry air.

There is no driving force for mass transfer in the liquid phase, since water is a pure liquid. The temperature driving force is  $T_L - T_i$  in the liquid phase and  $T_i - T_G$  K or °C in the gas phase. Sensible heat flows from the bulk liquid to the interface in the liquid. Sensible heat also flows from the interface to the gas phase. Latent heat also leaves the interface in the water vapor, diffusing to the gas phase. The sensible heat flow from the liquid to the interface equals the sensible heat flow in the gas plus the latent heat

flow in the gas.

The conditions in Fig. 23.3-1 occur at the upper part of the cooling tower. In the lower part of the cooling tower, the temperature of the bulk water is higher than the wet bulb temperature of the air but may be below the dry bulb temperature. Then, the direction of the sensible heat flow in Fig. 23.3-1 is reversed.

*2. Rate equations for heat and mass transfer.* We shall consider a packed water-cooling tower with air flowing upward and water countercurrently downward in the tower. The total interfacial area between the air and water phases is unknown, since the surface area of the packing is not equal to the interfacial area between the water

droplets and the air. Hence, we define a quantity  $a$ , defined as  $m_2$  of interfacial area per  $m_3$  volume of packed section, or  $m_2/m_3$ . This is combined with the gas-phase mass-transfer coefficient  $k_G$  in  $\text{kg mol/s} \cdot m_2 \cdot \text{Pa}$  or  $\text{kg mol/s} \cdot m_2 \cdot \text{atm}$  to give a volumetric coefficient  $k_G a$  in  $\text{kg mol/s} \cdot m_3 \text{ volume} \cdot \text{Pa}$  or  $\text{kg mol/s} \cdot m_3 \cdot \text{atm}$  ( $\text{lb mol/h} \cdot \text{ft}^3 \cdot \text{atm}$ ).

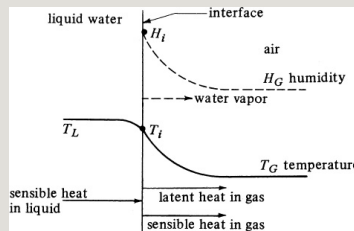


Figure 23.3-1. *Temperature and concentration profiles in upper part of cooling-water tower.*

The process is carried out adiabatically; the various streams and conditions are shown in Fig. 23.3-2, where

$$L = \text{water flow, kg water/s} \cdot m^2 (\text{lbm/}$$

2)  $T_L$  = temperature of water, °C or K (°F)  
 $G$  = dry air flow,  $\text{s} \cdot \text{m}^2 (\text{lbm}/$   
 $G$  = temperature of air, °C or K (°F)  
 $H$  = humidity of air, kg  
 kg dry air (lb water/

lb dry air)  
 $H_y$  = enthalph of air-  
 water vapor mixture, J/kg dry air (btu/  
 lb)  $m$  dry air

The enthalpy  $H_y$  as given in Eq. (23.1-8)  
 is

$$H_y = c_s(T - T_0) + H\lambda_0 = (1.005 + 1.88H)103(T - 0) + 2.501 \times 10^6 H \text{ (SI)}$$

$$H_y = c_s(T - T_0) + H\lambda_0 = (1.005 + 1.88H)103(T - 0) + 2.501 \times 10^6 H \text{ (English)} \quad (23.1-8)$$

The base temperature selected is 0°C or 273 K (32°F). Note that  $(T - T_0)^\circ\text{C} = (T - T_0)\text{K}$ .

Making a total heat balance for the

dashed-line box shown in Fig. 23.3-2, an operating line is obtained:

$$G(H_y - H_{y1}) = Lc_L(T_L - T_{L1}) \quad (23.3-1)$$

This assumes that  $L$  is essentially constant, since only a small amount is evaporated. The heat capacity  $c_L$  of the liquid is assumed constant at  $4.187 \times 10^3 \text{ J/kg} \cdot \text{K}$  ( $1.00 \text{ btu/lbm} \cdot ^\circ\text{F}$ ). When plotted on a chart of  $H_y$  versus  $T_L$ , Eq. (23.3-1) is a straight line with a slope of  $Lc_L/G$ . Making an overall heat balance over both ends of the tower,



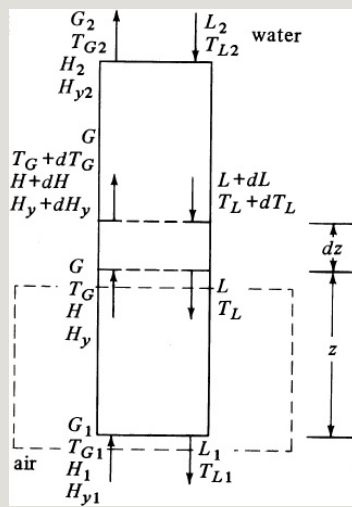


Figure 23.3-2. Continuous countercurrent adiabatic water cooling.

$$G(H_{y2}-H_{y1})=L_cL(T_{L2}-T_{L1}) \quad (23.3-2)$$

Again, making a heat balance for the  $dz$  column height and neglecting sensible-heat terms compared to the latent heat,

$$L_c L dT_L = G dH_y \quad (23.3-3)$$

The total sensible heat transfer from the bulk liquid to the interface is (refer to Fig. 23.3-1)

$$L_c L_d T_L = G d H_y = h L_a dz (T_L - T_i) \quad (23.3-4)$$

where  $h_{La}$  is the liquid-phase volumetric heat-transfer coefficient in  $\text{W/m}^3 \cdot \text{K}$  ( $\text{btu/h} \cdot \text{ft}^3 \cdot ^\circ\text{F}$ ) and  $T_i$  is the interface temperature.

For adiabatic mass transfer, the rate of heat transfer due to the latent heat in the water vapor being transferred can be obtained from Eq. (23.1-16) by rearranging and using a volumetric basis:

$$q_{\lambda} A = M_B k_G A P \lambda_0 (H_i - H_G) dz \quad (23.3-5)$$

where  $q_{\lambda}/A$  is in  $\text{W/m}^2$  ( $\text{btu/h} \cdot \text{ft}^2$ ),  $M_B$  = molecular weight of air,  $k_G A$  is a volumetric mass-transfer coefficient in the gas in  $\text{kg mol/s} \cdot \text{m}^3 \cdot \text{Pa}$ ,  $P$  = atm pressure in Pa,  $\lambda_0$  is the latent heat of

water in J/kg water,  $H_i$  is the humidity of the gas at the interface in kg water/kg dry air, and  $H_G$  is the humidity of the gas in the bulk gas phase in kg water/kg dry air. The rate of sensible heat transfer in the gas is

$$q_s A = h_G a (T_i - T_G) dz \quad (23.3-6)$$

where  $q_s/A$  is in W/m<sup>2</sup> and  $h_G a$  is a volumetric heat-transfer coefficient in the gas in W/m<sup>3</sup> · K.

Now, from Fig. 23.3-1, Eq. (23.3-4) must equal the sum of Eqs. (23.3-5) and (23.3-6):

$$\begin{aligned} G dH_y = & MBk_G a P \lambda_0 (H_i - H_G) dz \\ & + h_G a (T_i - T_G) dz \end{aligned} \quad (23.3-7)$$

Equation (23.1-18) states that

$$hGaMBkya \cong cS(23.3-8)$$

Substituting  $PkGa$  for  $kya$ ,

$$hGaMBPkGa \cong cS(23.3-9)$$

Substituting Eq. (23.3-9) into Eq. (23.3-7) and rearranging,

$$GdHy = MBkGaPdZ[(cSTi + \lambda_0 Hi) - (cSTG + \lambda_0 HG)](23.3-10)$$

Adding and subtracting  $cST_0$  inside the brackets,

$$GdHy = MBkGaPdZ\{cs(Ti - T_0) + Hi\lambda_0 - [cs(TG - T_0) + HG\lambda_0]\}(23.3-11)$$

The terms inside the braces are  $(Hy_i - Hy)$ , and Eq. (23.3-11) becomes

$$GdHy = MBkGaPdZ(Hy_i - Hy)$$

(23.3-12)

Integrating, the final equation to use for calculating the tower height is

$$\int_0^Z dz = \frac{G}{K_G a} \int_{H_{y1}}^{H_{yi}} \frac{dH_y}{H_{yi} - H_y} \quad (23.3-13)$$

If Eq. (23.3-4) is equated to Eq. (23.3-12) and the result rearranged,

$$-h_L a K_G a M B P = H_{yi} - H_{yTi} - T_L \quad (23.3-14)$$

### **23.3B Design of Water-Cooling Tower Using Film Mass-Transfer Coefficients**

The tower design is done using the following steps:

1. The enthalpy of saturated air  $H_{yi}$  is plotted versus  $T_i$  on an  $H$ -versus- $T$  plot as shown in Fig. 23.3-3. This enthalpy is calculated by means of Eq. (23.1-8) using the saturation humidity from the humidity chart for a given temperature, with  $0^\circ\text{C}$  (273 K) as a base temperature. Calculated

values are tabulated in Table 23.3-1.

2. Knowing the entering air conditions  $T_{G1}$  and  $H_1$ , the enthalpy of this air  $H_{y1}$  is calculated from Eq. (23.1-8). The point  $H_{y1}$  and  $T_{L1}$  (desired exiting water temperature) is plotted in Fig. 23.3-3 as one point on the operating line. The operating line is plotted with a slope  $LcL/G$  and ends at point  $T_{L2}$ , which is the entering water temperature. This gives  $H_{y2}$ . Alternatively,  $H_{y2}$  can be calculated from Eq. (23.3-2).
3. Knowing  $hLa$  and  $kGa$ , lines with a slope of  $-hLa/kGaMBP$  are plotted as shown in Fig. 23.3 3. From Eq. (23.3-14), point  $P$  represents  $H_y$  and  $T_L$  on the operating line, and point  $M$  represents  $H_{yi}$  and  $T_i$ , the interface conditions. Hence, line  $MS$  or  $H_{yi} - H_y$  represents the driving force in Eq. (23.3-13).
4. The driving force  $H_{yi} - H_y$  is computed for various values of  $T_L$  between  $T_{L1}$  and  $T_{L2}$ . Then, the function  $1/(H_{yi} - H_y)$  is integrated from  $H_{y1}$  to  $H_{y2}$  by numerical or graphical integration to obtain the value of the integral in Eq. (23.3-13). Finally, the height  $z$  is calculated from Eq. (23.3-13).

Table 23.3-1. *Enthalpies of Saturated Air–Water Vapor Mixtures (0°C Base Temperature)*

--

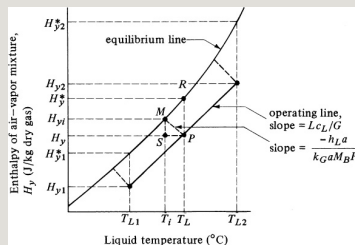


Figure 23.3-3. *Temperature enthalpy diagram and operating line for water-cooling tower.*

### 23.3C Design of Water-Cooling Tower Using Overall Mass-Transfer Coefficients

Often, only an overall mass-transfer coefficient  $KGa$  in  $\text{kg mol/s} \cdot \text{m}^3 \cdot \text{Pa}$  or  $\text{kg mol/s} \cdot \text{m}^3 \cdot \text{atm}$  is available, and Eq. (23.3-13) becomes

$$z = \frac{G}{M_B k_G a P} \int_{H_{y1}}^{H_{y2}} \frac{dH_y}{H_y - H_y^*} \quad (23.3-15)$$

The value of  $H_y^*$  is determined by going vertically from the value of  $H_y$  at point  $P$  up to the equilibrium line to give  $H_y^*$  at point  $R$ , as shown in Fig. 23.3-3. In many cases, the experimental film coefficients  $kGa$  and  $hLa$  are not

available. The few experimental data available indicate that  $hLa$  is quite large; the slope of the lines  $-hLa/(kGaMBP)$  in Eq. (23.3-14) would be very large and the value of  $H_{yi}$  would approach that of  $H_y^*$  in Fig. 23.3-3.

The tower design using the overall mass-transfer coefficient is done using the following steps:

1. The enthalpy–temperature data from Table 23.3-1 are plotted as shown in Fig. 23.3-3.
2. The operating line is calculated as in steps 1 and 2 for the film coefficients and plotted in Fig. 23.3-3.
3. In Fig. 23.3-3, point  $P$  represents  $H_y$  and  $T_L$  on the operating line and point  $R$  represents  $H_y^*$  on the equilibrium line. Hence, the vertical line  $RP$  or  $H_y^* - H_y$  represents the driving force in Eq. (23.3-15).
4. The driving force  $H_y^* - H_y$  is computed for various values of  $T_L$  between  $T_{L1}$  and  $T_{L2}$ . Then, the function  $1/(H_y^* - H_y)$  is integrated from  $H_{y1}$  to  $H_{y2}$  by numerical or graphical methods to obtain the value of the integral in Eq. (23.3-15). Finally, the height  $z$  is obtained from Eq.



(23.3-15).

If experimental cooling data from an actual run in a cooling tower with known height  $z$  are available, then, using Eq. (23.3-15), the experimental value of  $KGa$  can be obtained.

**EXAMPLE 23.3-1. Design of Water-Cooling Tower Using Film Coefficients**

A packed countercurrent water-cooling tower using a gas flow rate of  $G = 1.356 \text{ kg dry air/s} \cdot \text{m}^2$  and a water flow rate of  $L = 1.356 \text{ kg water/s} \cdot \text{m}^2$  is to cool the water from  $T_{L2} = 43.3^\circ\text{C}$  ( $110^\circ\text{F}$ ) to  $T_{L1} = 29.4^\circ\text{C}$  ( $85^\circ\text{F}$ ). The entering air at  $29.4^\circ\text{C}$  has a wet bulb temperature of  $23.9^\circ\text{C}$ . The mass-transfer coefficient  $kGa$  is estimated as  $1.207 \times 10^{-7} \text{ kg mol/s} \cdot \text{m}^3 \cdot \text{Pa}$  and  $hLa/kGaMBP$  as  $4.187 \times 10^4 \text{ J/kg} \cdot \text{K}$  ( $10.0 \text{ btu/lbm} \cdot ^\circ\text{F}$ ). Calculate the height of packed tower  $z$ . The tower operates at a pressure of  $1.013 \times 10^5 \text{ Pa}$ .

**Solution:** Following the steps outlined, the enthalpies from the saturated air–water vapor mixtures from Table 23.3-1 are plotted in Fig. 23.3-4. The inlet air at  $T_{G1} = 29.4^\circ\text{C}$  has a wet bulb temperature of  $23.9^\circ\text{C}$ . The humidity from the humidity chart is  $H_1 = 0.0165 \text{ kg H}_2\text{O/kg dry air}$ . Substituting into Eq. (23.1-8) and noting that  $(29.4 - 0)^\circ\text{C} = (29.4 - 0) \text{ K}$ ,

$$Hy_1 = (1.005 + 1.88 \times 0.0165)103(29.4 - 0) + 0.501 \times 106(0.0165) = 7.17 \times 10^3 \text{ J/kg}$$

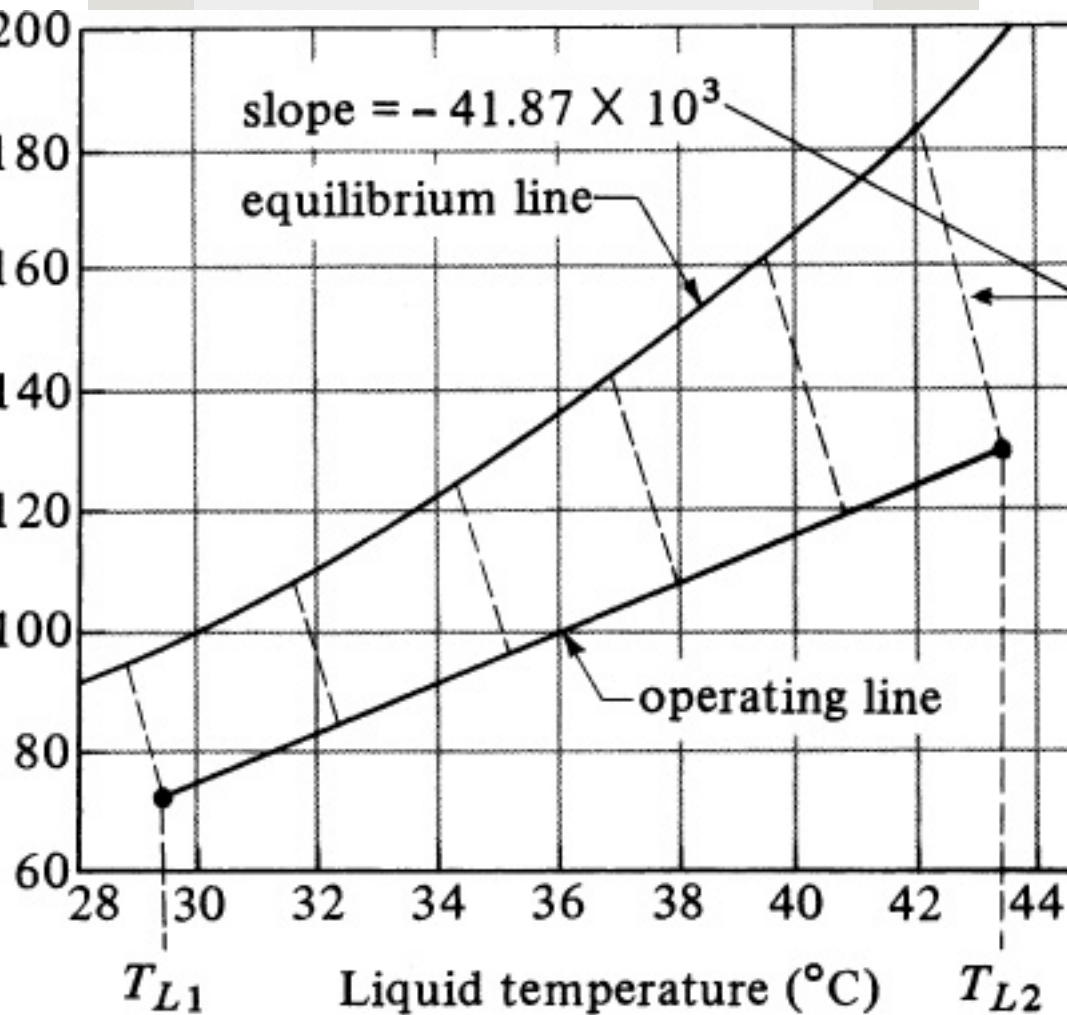


Figure 23.3-4. Graphical solution of Example 23.3-1.

Table 23.3-2. Enthalpy Values for Solution to Example 23.3-1  
(Enthalpy in J/kg Dry Air)

--

The point  $H_{y1} = 71.7 \times 10^3$  and  $T_{L1} = 29.4^\circ\text{C}$  is plotted. Then, substituting into Eq. (23.3-2) and solving,

$$1.356(H_{y2} - 71.7 \times 10^3) = 1.356(4.187 \times 10^3)(43.3 - 29.4)$$

$H_{y2} = 129.9 \times 10^3$  J/kg dry air (55.8 btu/lbm). The point  $H_{y2}$

$= 129.9 \times 10^3$  and  $T_{L2} = 43.3^\circ\text{C}$  is also plotted, giving the operating line. Lines with slope  $-hLa/kGaMBP = -41.87 \times 10^3 \text{ J/kg} \cdot \text{K}$  are plotted, giving  $H_{yi}$  and  $H_y$  values, which are tabulated in Table 23.3-2 along with derived values as shown. Values of the function  $1/(H_{yi} - H_y)$  are used with numerical integration between the values  $H_{y1} = 71.7 \times 10^3$  to  $H_{y2} = 129.9 \times 10^3$  to obtain the integral

$$\int_{H_{y1}}^{H_{y2}} \frac{dH_y}{H_{yi} - H_y} = 1.82$$

Substituting into Eq. (23.3-13),

$$z = \frac{GMBkGaP}{(1.013 \times 10^5)(1.82)} = 1.35629(1.207 \times 10^{-7}) = 6.98 \text{ m}(22.9 \text{ ft})$$

### 23.3D Minimum Value of Air Flow

Often, the air flow  $G$  is not fixed but must be set for the design of the cooling tower. As shown in Fig. 23.3-5, for a minimum value of  $G$ , the operating line  $MN$  is drawn through the point  $H_{y1}$  and  $T_{L1}$  with a slope that touches the equilibrium line at  $T_{L2}$ , point  $N$ . If the equilibrium line is quite curved, line  $MN$  could become tangent to the equilibrium line at a point farther down the equilibrium line than point  $N$ . For the actual tower, a value of  $G$

greater than  $G_{\min}$  must be used.

Often, a value of  $G$  equal to 1.3 to 1.5 times  $G_{\min}$  is used.

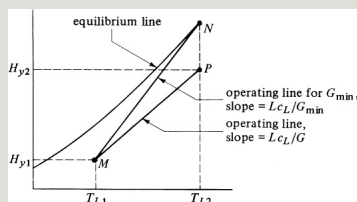


Figure 23.3-5. Operating-line construction for minimum gas flow.

### 23.3E Design of Water-Cooling Tower Using the Height of a Transfer Unit

Frequently, another form of the film mass-transfer coefficient is used in Eq. (23.3-13):

$$z = HG \int_{H_{y1}}^{H_{y2}} \frac{dH_y}{H_y - H^*} \quad (23.3-16)$$

$$HG = \frac{G M B k_G a P}{k_L} \quad (23.3-17)$$

where  $HG$  is the height of a gas enthalpy transfer unit in m, and the integral term

is called the number of transfer units. The term  $HG$  is often used since it is less dependent upon flow rates than  $kGa$ .

In many cases, yet another form of the overall mass-transfer coefficient  $KGa$  in  $\text{kg mol/s} \cdot \text{m}^3 \cdot \text{Pa}$  or  $\text{kg mol/s} \cdot \text{m}^3 \cdot \text{atm}$  is used, and Eq. (23.3-15) becomes

$$z = \frac{G}{K_G a P} \int_{H_y}^{H_y^*} \frac{dH_y}{H_y^* - H_y} \quad (23.3-18)$$

where  $HOG$  is the height of an overall gas enthalpy transfer unit in m. The value of  $H_y^*$  is determined by going vertically from the value of  $H_y$  up to the equilibrium line, as shown in Fig.

23.3-3. This method should be used only when the equilibrium line is almost straight over the range used. However,

the *HOG* is often used even if the equilibrium line is somewhat curved because of the lack of film mass-transfer-coefficient data.

### **23.3F Temperature and Humidity of an Air Stream in a Tower**

The procedures outlined above do not yield any information on the changes in temperature and humidity of the air–water vapor stream through the tower. If this information is of interest, a graphical method by Mickley (M1) is available. The equation used for the graphical method is derived by first setting Eq. (23.3-6) equal to  $GcsdT_G$  and then combining it with Eqs. (23.3-12) and (23.3-9) to yield Eq. (23.3-19):

$$dH_y dT_G = H_{yi} - H_{yT_i} - T_G \quad (23.3-19)$$

### **23.3G Dehumidification Tower**

For the cooling or humidification tower discussed above, the operating line lies below the equilibrium line, and water is cooled and air humidified. In a dehumidification tower, cool water is used to reduce the humidity and temperature of the air that enters. In this case, the operating line is above the equilibrium line. Similar calculation methods are used (T1).

### **23.4 Chapter Summary**

#### **Humidity**

$$H=18.0228.97p_{AP}-p_A(23.1-1)$$

#### **Saturation Humidity**

$$H_s=18.0228.97p_{ASP}-p_{AS}(23.1-2)$$

#### **Percentage Humidity**

$$HP=100HHS(23.1-3)$$

### Percentage Relative Humidity

$$HR=100pApAS(23.1-4)$$

### Total Enthalpy

$$\begin{aligned} H_y \text{ kJ/kg dry air} &= (1.005 + 1.88H) \\ & (T^\circ\text{C} - 0) + 2501.4H \text{ (SI)} \\ H_y \text{ btu/lbm dry air} &= (0.24 + 0.45H)(T^\circ\text{F} \\ & - 32) + 1075.4H \text{ (English)} \end{aligned}$$

### Design of Water-Cooling Tower Using Overall Mass-Transfer Coefficients

$$z = GMBkGaP \int_{H_y1}^{H_y2} \frac{dH_y}{H_y - H_y^*} \quad (23.3-15)$$

## Problems

### 23.1-1. *Humidity from Vapor Pressure.*

The air in a room is at 37.8°C and a total pressure of 101.3 kPa abs containing water vapor with a partial pressure  $p_A = 3.59 \text{ kPa}$ . Calculate:



- Humidity
- Saturation humidity and percentage humidity
- Percentage relative humidity

### **23.1-2. *Percentage and Relative***

***Humidity.*** The air in a room has a humidity  $H$  of 0.021 kg H<sub>2</sub>O/kg dry air at 32.2°C and 101.3 kPa abs pressure. Calculate:

- Percentage humidity  $HP$
- Percentage relative humidity  $HR$

**Ans.** (a)  $HP = 67.5\%$ ; (b)  $HR = 68.6\%$

**23.1-3. *Use of the Humidity Chart.*** The air entering a dryer has a temperature of 65.6°C (150°F) and a dew point of 15.6°C (60°F). Using the humidity chart, determine the actual humidity and percentage humidity. Calculate the humid volume of this mixture and also

calculate  $c_s$  using SI and English units.

**Ans.**  $H = 0.0113 \text{ kg H}_2\text{O/kg dry air}$ ,  $HP = 5.3\%$ ,  $c_s = 1.026 \text{ kJ/kg} \cdot \text{K}$  ( $0.245 \text{ btu/lbm} \cdot ^\circ\text{F}$ ),  $vH = 0.976 \text{ m}^3 \text{ air} + \text{water vapor/kg dry air}$

**23.1-4. *Properties of Air to a Dryer.*** An air–water vapor mixture going to a drying process has a dry bulb temperature of  $57.2^\circ\text{C}$  and a humidity of  $0.030 \text{ kg H}_2\text{O/kg dry air}$ . Using the humidity chart and appropriate equations, determine the percentage humidity, saturation humidity at  $57.2^\circ\text{C}$ , dew point, humid heat, and humid volume.

**23.1-5. *Adiabatic Saturation***

***Temperature.*** Air at  $82.2^\circ\text{C}$  having a humidity  $H = 0.0655 \text{ kg H}_2\text{O/kg dry air}$

is contacted with water in an adiabatic saturator. It exits at 80% saturation.

- What are the final values of  $H$  and  $T^{\circ}\text{C}$ ?
- For 100% saturation, what would be the values of  $H$  and  $T$ ?

**Ans.** (a)  $H = 0.079 \text{ kg H}_2\text{O/kg dry air}$ ,  $T = 52.8^{\circ}\text{C}$

**23.1-6. *Adiabatic Saturation of Air.*** Air having a temperature of  $76.7^{\circ}\text{C}$  and a dew-point temperature of  $40.6^{\circ}\text{C}$  enters an adiabatic saturator. It exits the saturator 90% saturated. What are the final values of  $H$  and  $T^{\circ}\text{C}$ ?

**23.1-7. *Humidity from Wet and Dry Bulb Temperatures.*** An air–water vapor mixture has a dry bulb temperature of  $65.6^{\circ}\text{C}$  and a wet bulb temperature of  $32.2^{\circ}\text{C}$ . What is the humidity of the

mixture?

**Ans.**  $H = 0.0175 \text{ kg H}_2\text{O/kg dry air}$

### **23.1-8. Humidity and Wet Bulb**

**Temperature.** The humidity of an air–water vapor mixture is  $H = 0.030 \text{ kg H}_2\text{O/kg dry air}$ . The dry bulb temperature of the mixture is  $60^\circ\text{C}$ . What is the wet bulb temperature?

**23.1-9. Dehumidification of Air.** Air having a dry bulb temperature of  $37.8^\circ\text{C}$  and a wet bulb temperature of  $26.7^\circ\text{C}$  is to be dried by first cooling to  $15.6^\circ\text{C}$  to condense water vapor and then heating to  $23.9^\circ\text{C}$ .

- Calculate the initial humidity and percentage humidity.
- Calculate the final humidity and percentage humidity. [*Hint:* Locate the initial point on the humidity chart. Then, go horizontally (cooling) to

the 100% saturation line. Follow this line to 15.6°C. Then, go horizontally to the right to 23.9°C.]

**Ans.** (b)  $H = 0.0115 \text{ kg H}_2\text{O/kg dry air}$ ,  
 $HP = 60\%$

**23.1-10. Cooling and Dehumidifying Air.** Air entering an adiabatic cooling chamber has a temperature of 32.2°C and a percentage humidity of 65%. It is cooled by a cold water spray and saturated with water vapor in the chamber. After leaving, it is heated to 23.9°C. The final air has a percentage humidity of 40%.

- What is the initial humidity of the air?
- What is the final humidity after heating?

**23.3-1. Countercurrent Water-Cooling Tower.** A forced-draft countercurrent water-cooling tower is to cool water

from 43.3 to 26.7°C. The air enters the bottom of the tower at 23.9°C with a wet bulb temperature of 21.1°C. The value of  $HG$  for the flow conditions is  $HG = 0.533$  m. The heat-transfer resistance in the liquid phase will be neglected; that is,  $h_L$  is very large. Hence, values of  $H^*_{*y}$  should be used. Calculate the tower height needed if 1.5 times the minimum air rate is used.

**23.3-2. Minimum Gas Rate and Height of a Water-Cooling Tower.** It is planned to cool water from 110°F to 85°F in a packed countercurrent water-cooling tower using entering air at 85°F with a wet bulb temperature of 75°F. The water flow is 2000 lb<sub>m</sub>/h · ft<sup>2</sup> and the air flow is 1400 lb<sub>m</sub> air/h · ft<sup>2</sup>. The overall mass-transfer coefficient is  $KGa = 6.90$  lb mol/h · ft<sup>3</sup> · atm.

- Calculate the minimum air rate that can be used.
- Calculate the tower height needed if the air flow of  $1400 \text{ lb}_m \text{ air/h} \cdot \text{ft}^2$  is used.

**Ans.** (a)  $G_{\min} = 935 \text{ lb}_m \text{ air/h} \cdot \text{ft}^2$  ( $4241 \text{ kg air/h} \cdot \text{m}^2$ ); (b)  $z = 21.8 \text{ ft}$  ( $6.64 \text{ m}$ )

### **23.3-3. *Design of a Water-Cooling***

***Tower.*** Recalculate Example 23.3-1, but calculate the minimum air rate and use 1.75 times the minimum air rate.

### **23.3-4. *Effect of Changing Air***

***Conditions on a Cooling Tower.*** For the cooling tower in Example 23.3-1, to what temperature will the water be cooled if the entering air enters at  $29.4^\circ\text{C}$  but the wet bulb temperature is  $26.7^\circ\text{C}$ ? The same gas and liquid flow rates are used. The water enters at  $43.3^\circ\text{C}$ , as before. (*Hint:* In this case,  $T_{L1}$  is the unknown. The tower height is

the same as in Example 23.3-1. The slope of the operating line is as before. The solution is trial and error. Assume a value of  $T_{L1}$  that is greater than  $29.4^{\circ}\text{C}$ . Do numerical or graphical integration to see if the same height is obtained.)

### References

### Notation



# **Chapter 24. Filtration and Membrane Separation Processes (Liquid–Liquid or Solid–Liquid Phase)**

## **24.0 Chapter Objectives**

On completion of this chapter, a student should be able to:

- Describe the five most common types of dead-end filtration equipment
- Describe the use of filter media and aids, and the usefulness of washing
- Use mathematical-models–based flow through packed beds to predict required filter areas
- Analyze filtration data to calculate cake and membrane resistances
- Calculate filtration and washing times
- Distinguish effects on membrane mass transfer due to permeability, selectivity, concentration polarization, and fouling

- Distinguish among microfiltration, ultrafiltration, nanofiltration, and reverse osmosis in terms of average pore size and unique role in purification
- Differentiate between concentration polarization and membrane fouling
- Calculate mass-transfer rates for microfiltration, ultrafiltration, nanofiltration, and reverse osmosis
- Calculate osmotic pressure

## **24.1 Introduction to Dead-End Filtration**

### **24.1A Introduction**

In filtration, suspended solid particles in a fluid of liquid or gas are physically or mechanically removed by using a porous medium that retains the particles as a separate phase or cake and passes the clear filtrate. Commercial filtrations cover a very wide range of applications. The fluid can be a gas or a liquid. The suspended solid particles can be

very fine (in the micrometer range) or much larger, very rigid or plastic particles, spherical or very irregular in shape, and aggregates of particles or individual particles. The valuable product may be the clear filtrate from the filtration or the solid cake. In some cases, complete removal of the solid particles is required; in other cases, only partial removal is necessary.

The feed or slurry solution may carry a heavy load of solid particles or a very small amount. When the concentration is very low, the filters can operate for extremely long periods of time before the filter needs cleaning. Because of the wide diversity of filtration problems, a multitude of filter types has been developed.

Industrial filtration equipment differs from laboratory filtration equipment only in the amount of material handled and in the necessity for low-cost operation. A typical laboratory filtration apparatus is shown in Fig. 24.1-1, which is similar to a Büchner funnel. The liquid is made to flow through the filter cloth or paper by a vacuum on the exit end. The slurry consists of the liquid and the suspended particles. The passage of the particles is blocked by the small openings in the pores of the filter cloth. A support with relatively large holes is used to hold the filter cloth. The solid particles build up in the form of a porous filter cake as the filtration proceeds. This cake itself also acts as a filter for the suspended particles. As the cake builds up, resistance to flow also increases.

In Sections 24.1 and 24.2, the ordinary type of filtration will be considered, where a pressure difference is used to force the liquid through the filter cloth and the filter cake that builds up.

In Section 30.4E, centrifugal filtration will be discussed, where centrifugal force is used instead of a pressure difference. In many filtration applications, ordinary filters and centrifugal filters are often competitive and either type can be used.

#### **24.1B Types of Filtration Equipment**

*1. Classification of filters.* There are a number of ways to classify types of filtration equipment; unfortunately, it is not possible to devise a single classification scheme that includes all types of filters. In one

classification, filters are categorized according to whether the desired product is the filter cake or the clarified filtrate or outlet liquid. In either case, the slurry can have a relatively large percentage of solids so that a cake is formed, or it may have just a trace of suspended particles.

Filters can also be classified by operating cycle. Filters can be operated as batch, where the cake is removed after a run, or they may be continuous, where the cake is constantly removed. In another classification, filters can be of the gravity type, where the liquid simply flows by means of a hydrostatic head, or pressure or vacuum can be used to increase the flow rates. An important method of classification depends upon

the mechanical arrangement of the filter media. The filter cloth can be in a series arrangement as flat plates in an enclosure, as individual leaves dipped in the slurry, or on rotating-type rolls in the slurry. In the following sections, only the most important types of filters will be described. For more details, see references (B1, P1).

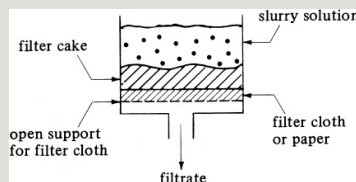


Figure 24.1-1. *Simple laboratory filtration apparatus.*

**2. Bed filters.** The simplest type of filter is the bed filter shown schematically in Fig. 24.1-2. This type is useful mainly in cases where relatively small amounts of solids are to be removed from large amounts of water in clarifying the

liquid. Often, the bottom layer is composed of coarse pieces of gravel resting on a perforated or slotted plate. Above the gravel is fine sand, which acts as the actual filter medium. Water is introduced at the top onto a baffle that spreads the water out. The clarified liquid is drawn out at the bottom.

The filtration continues until the precipitate of filtered particles has clogged the sand so that the flow rate drops. Then, the flow is stopped and water is introduced in the reverse direction so that it flows upward, backwashing the bed and carrying the precipitated solid away. This apparatus can only be used on precipitates that do not adhere strongly to the sand and can be easily removed by backwashing. Open-tank filters are used in filtering



municipal water supplies.

*3. Plate-and-frame filter presses.* One of the important types of filters is the plate-and-frame filter press, which is shown diagrammatically in Fig. 24.1-3a. These filters consist of plates and frames assembled alternately with a filter cloth over each side of the plates. The plates have channels cut in them so that clear filtrate liquid can drain down along each plate. The feed slurry is pumped into the press and flows through the duct into each of the open frames so that slurry fills the frames. The filtrate flows through the filter cloth and the solids build up as a cake on the frame side of the cloth. The filtrate flows between the filter cloth and the face of the plate through the channels to the outlet.

The filtration proceeds until the frames are completely filled with solids. In Fig. 24.1-3a, all the discharge outlets go to a common header. In many cases, the filter press will have a separate discharge for each frame. Then, visual inspection can be made to see if the filtrate is running clear. If it is running cloudy because of a break in the filter cloth or other factors, it can be shut off separately. When the frames are completely full, the frames and plates are separated and the cake removed. The filter is then reassembled and the cycle is repeated.

If the cake is to be washed, it is left in the plates and through-washing is performed, as shown in Fig. 24.1-3b. In this press, a separate channel is provided for the wash-water inlet. The wash

water enters the inlet, which has ports opening behind the filter cloths at every other plate of the filter press. The wash water then flows through the filter cloth, through the entire cake (not half the cake as in filtration), through the filter cloth at the other side of the frames, and out the discharge channel. It should be noted that there are two kinds of plates in Fig. 24.1-3b: those having ducts to admit wash water behind the filter cloth; these plates alternate with plates without such ducts.

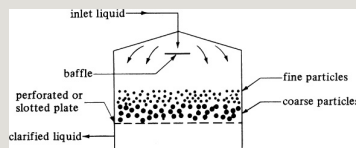


Figure 24.1-2. *Bed filter of solid particles.*

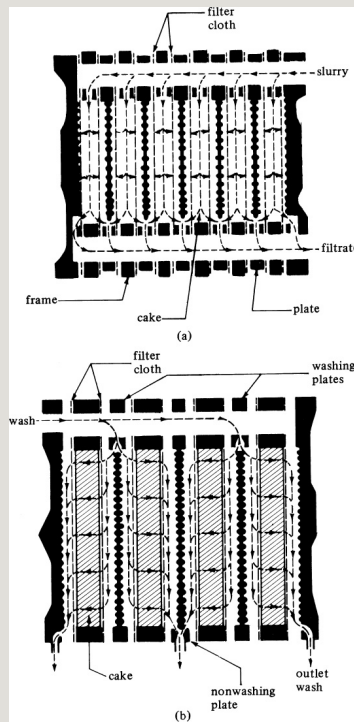


Figure 24.1-3. *Diagrams of plate-and-frame filter presses: (a) filtration of slurry with closed delivery, (b) through washing in a press with open delivery.*

The plate-and-frame presses suffer from the disadvantages common to batch processes. The cost of labor for removing the cakes and reassembling plus the cost of fixed charges for downtime can be an appreciable part of the total operating cost. Some newer types of plate-and-frame presses have

duplicate sets of frames mounted on a rotating shaft. Half of the frames are in use while the others are being cleaned, saving downtime and labor costs. Other advances in automation have been applied to these types of filters.

Filter presses are used in batch processes but cannot be employed for high-throughput processes. They are simple to operate, very versatile and flexible in operation, and can be used at high pressures, when necessary, if viscous solutions are being used or the filter cake has a high resistance.

*4. Leaf filters.* The filter press is useful for many purposes but is not economical for handling large quantities of sludge or for efficient washing with a small amount of wash water. The wash water

often channels in the cake and large volumes of wash water may be needed. The leaf filter shown in Fig. 24.1-4 was developed for larger volumes of slurry and more efficient washing. Each leaf is a hollow wire framework covered by a sack of filter cloth.

A number of these leaves are hung in parallel in a closed tank. The slurry enters the tank and is forced under pressure through the filter cloth, where the cake deposits on the outside of the leaf. The filtrate flows inside the hollow framework and out a header. The wash liquid follows the same path as the slurry. Hence, the washing is more efficient than the through-washing in plate-and-frame filter presses. To remove the cake, the shell is opened. Sometimes air is blown in the reverse

direction into the leaves to help in dislodging the cake. If the solids are not wanted, water jets can be used to simply wash away the cakes without opening the filter.

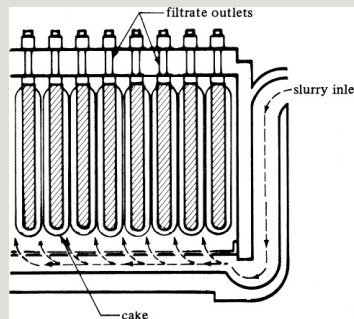


Figure 24.1-4. *Leaf filter.*

Leaf filters also suffer from the disadvantages of batch operation. They can be automated for the filtering, washing, and cleaning cycle. However, they are still cyclical and are used for batch processes and relatively modest throughput processes.

5. *Continuous rotary filters.* Plate-and-frame filters suffer from the disadvantages common to all batch processes and cannot be used for large-capacity processes. A number of continuous-type filters are available, as discussed below.

*(a) Continuous rotary vacuum-drum filter.* This filter, shown in Fig. 24.1-5, filters, washes, and discharges the cake in a continuous, repeating sequence. The drum is covered with a suitable filtering medium. The drum rotates and an automatic valve in the center serves to activate the filtering, drying, washing, and cake-discharge functions in the cycle. The filtrate leaves through the axle of the filter.

The automatic valve provides separate



outlets for the filtrate and the wash liquid. Also, if needed, a connection for compressed-air blowback just before discharge can be used to help in cake removal by the knife scraper. The maximum pressure differential for the vacuum filter is only 1 atm. Hence, this type is not suitable for viscous liquids or for liquids that must be enclosed. If the drum is enclosed in a shell, pressures above atmospheric can be used; however, the cost of a pressure-type filter is about two times that of a vacuum-type rotary-drum filter (P2).

Modern, high-capacity processes use continuous filters. The important advantages are that the filters are continuous and automatic, and labor costs are relatively low. However, the capital cost is relatively high.

*(b) Continuous rotary disk filter.* This filter consists of concentric vertical disks mounted on a horizontal rotating shaft. The filter operates on the same principle as the vacuum-type rotary-drum filter. Each disk is hollow and covered with a filter cloth and is partly submerged in the slurry. The cake is washed, dried, and scraped off when the disk is in the upper half of its rotation. Washing is less efficient than with the rotating-drum type.

*(c) Continuous rotary horizontal filter.* This type is a vacuum filter with the rotating annular filtering surface divided into sectors. As the horizontal filter rotates, it successively receives slurry, is washed, dried, and the cake is then scraped off. The washing efficiency is better than with the rotary-disk filter.

This filter is widely used in ore-extraction processes, pulp washing, and other large-capacity processes.

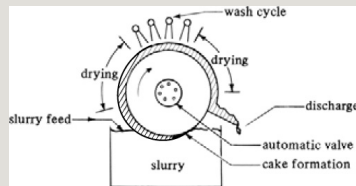


Figure 24.1-5. *Schematic of continuous rotary vacuum-drum filter.*

### 24.1C Filter Media and Filter Aids

*1. Filter media.* The filter medium for industrial filtration must fulfill a number of requirements. First and foremost, it must remove the solids to be filtered from the slurry and give a clear filtrate. Also, the pores should not become plugged so that the rate of filtration becomes too slow. The filter medium must allow the filter cake to be removed easily and cleanly. Obviously, it must have

sufficient strength so as not to tear and it must be chemically resistant to the solutions used.

Some widely used filter media are twill or duckweave heavy cloth, other types of woven heavy cloth, woolen cloth, glass cloth, paper, felted pads of cellulose, metal cloth, nylon cloth, dacron cloth, and other synthetic cloths. The ragged fibers of natural materials are more effective in removing fine particles than are smooth plastic or metal fibers. Sometimes the filtrate may come through somewhat cloudy at first before the first layers of particles, which help filter the subsequent slurry, are deposited. This filtrate can be recycled for refiltration.

2. *Filter aids.* Certain filter aids may be

used to aid filtration. These are often incompressible diatomaceous earth or kieselguhr, which is composed primarily of silica. Also used are wood cellulose and other inert porous solids.

These filter aids can be used in a number of ways. They can be used as a precoat before the slurry is filtered. This will prevent gelatinous-type solids from plugging the filter medium and also give a clearer filtrate. They can also be added to the slurry before filtration. This increases the porosity of the cake and reduces the cake's resistance during filtration. In a rotary filter, the filter aid may be applied as a precoat; subsequently, thin slices of this layer are sliced off with the cake.

The use of filter aids is usually limited

to cases where the cake is discarded or where the precipitate can be separated chemically from the filter aid.

## 24.2 Basic Theory of Filtration

### 24.2A Introduction to the Basic Theory of Filtration

*1. Pressure drop of fluid through a filter cake.* Figure 24.2-1 is a cross section through a filter cake and filter medium at a definite time  $t$  s from the start of the flow of filtrate. At this time, the thickness of the cake is  $L$  m (ft). The filter cross-sectional area is  $A$  m<sup>2</sup> (ft<sup>2</sup>), and the linear velocity of the filtrate in the  $L$  direction is  $v$  m/s (ft/s) based on the filter area  $A$  m<sup>2</sup>.

The flow of the filtrate through the packed bed of cake can be described by

an equation similar to Poiseuille's law, assuming laminar flow occurs in the filter channels. In Chapter 5, Eq. (5.1-2), the Poiseuille's equation for laminar flow in a straight tube was given, which can be written as

-

$$\Delta p L = 32 \mu v D^2 (SI) - \Delta p L = 32 \mu v g_c D^2 (\text{English}) \quad (24.2.1)$$

where  $\Delta p$  is pressure drop in  $\text{N/m}^2$  ( $\text{lbf/ft}^2$ ),  $v$  is open-tube velocity in  $\text{m/s}$  ( $\text{ft/s}$ ),  $D$  is diameter in  $\text{m}$  ( $\text{ft}$ ),  $L$  is length in  $\text{m}$  ( $\text{ft}$ ),  $\mu$  is viscosity in  $\text{Pa} \cdot \text{s}$  or  $\text{kg/m} \cdot \text{s}$  ( $\text{lbm/ft} \cdot \text{s}$ ), and  $g_c$  is  $34.174 \text{ lbm} \cdot \text{ft/lbf} \cdot \text{s}^2$ .

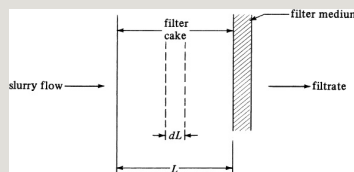


Figure 24.2-1. *Cross section through a filter cake.*

For laminar flow in a packed bed of particles, the *Carman–Kozeny relation*, which is similar to Eq. (24.2-1) and to the Blake–Kozeny equation (6.2-12), has been shown to apply to filtration:

$$-\Delta p_c L = k_1 \mu v (1 - \epsilon)^2 S_0^2 \epsilon^3 \quad (24.2-2)$$

where  $k_1$  is a constant and equals 4.17 for random particles of definite size and shape,  $\mu$  is viscosity of filtrate in  $\text{Pa} \cdot \text{s}$  ( $\text{lb}_m/\text{ft} \cdot \text{s}$ ),  $v$  is linear velocity based on filter area in  $\text{m/s}$  ( $\text{ft/s}$ ),  $\epsilon$  is void fraction or porosity of cake,  $L$  is thickness of cake in  $\text{m}$  ( $\text{ft}$ ),  $S_0$  is specific surface area of particle in  $\text{m}^2$  ( $\text{ft}^2$ ) of particle area per  $\text{m}^3$  ( $\text{ft}^3$ ) volume of solid particle, and  $\Delta p_c$  is pressure drop in the cake in  $\text{N/m}^2$  ( $\text{lb}_f/\text{ft}^2$ ). For English units, the right-



hand side of Eq. (24.2-2) is divided by  $g_c$ . The linear velocity is based on the empty cross-sectional area and is

$$v = dV/dtA \quad (24.2-3)$$

where  $A$  is filter area in  $m^2$  ( $ft^2$ ) and  $V$  is total  $m^3$  ( $ft^3$ ) of filtrate collected up to time  $t$  s. The cake thickness  $L$  may be related to the volume of filtrate  $V$  by a material balance. If  $c_s$  is  $kg$  solids/ $m^3$  ( $lb_m/ft^3$ ) of filtrate, a material balance gives

$$LA(1-\epsilon)\rho_p = c_s(V + \epsilon LA) \quad (24.2-4)$$

where  $\rho_p$  is density of solid particles in the cake in  $kg/m^3$  ( $lb_m/ft^3$ ) solid. The final term of Eq. (24.2-4) is the volume of filtrate held in the cake. This is usually small and will be neglected.

Substituting Eq. (24.2-3) into (24.2-2) and using Eq. (24.2-4) to eliminate  $L$ , we obtain the final equation as

$$\frac{dV}{A dt} = -\Delta p \frac{k_1(1-\epsilon)S_0^2 \rho_p \epsilon^3 \mu c}{\Delta p c \alpha \mu c S V A} \quad (24.2-5)$$

where  $\alpha$  is the specific cake resistance in  $\text{m/kg}(\text{ft/lb}_m)$ , defined as

$$\alpha = \frac{k_1(1-\epsilon)S_0^2 \rho_p \epsilon^3}{\Delta p} \quad (24.2-6)$$

For the filter-medium resistance, we can write, by analogy with Eq. (24.2-5),

$$\frac{dV}{A dt} = -\Delta p f \mu R_m \quad (24.2-7)$$

where  $R_m$  is the resistance of the filter medium to filtrate flow in  $\text{m}^{-1}(\text{ft}^{-1})$  and  $\Delta p_f$  is the pressure drop. When  $R_m$  is treated as an empirical constant, it

includes the resistance to flow of the piping leads to and from the filter and the filter-medium resistance.

Since the resistances of the cake and the filter medium are in series, Eqs. (24.2-5) and (24.2-7) can be combined and become

$$dVA dt = -\Delta p \mu (\alpha_c S V A + R_m) \quad (24.2-8)$$

where  $\Delta p = \Delta p_c + \Delta p_f$ . Sometimes, Eq. (24.2-8) is modified as follows:

$$dVA dt = -\Delta p \mu \alpha_c S A (V + V_e) \quad (24.2-9)$$

where  $V_e$  is a volume of filtrate necessary to build up a fictitious filter cake whose resistance is equal to  $R_m$ .

The volume of filtrate  $V$  can also be related to  $W$ , the kg of accumulated dry

cake solids, as follows:

$$W = cS V = \rho c x (1 - m c x) V \quad (24.2-10)$$

where  $c_x$  is mass fraction of solids in the slurry,  $m$  is mass ratio of wet cake to dry cake, and  $\rho$  is density of filtrate in  $\text{kg/m}^3$  ( $\text{lb}_m/\text{ft}^3$ ).

*2. Specific cake resistance.* From Eq. (24.2-6), we see that the specific cake resistance is a function of void fraction  $\epsilon$  and  $S_0$ . It is also a function of pressure, since pressure can affect  $\epsilon$ . By conducting constant-pressure experiments at various pressure drops, the variation of  $\alpha$  with  $\Delta p$  can be determined.

Alternatively, compression–permeability experiments can be performed. A filter cake at a low

pressure drop and atm pressure is built up by gravity filtering in a cylinder with a porous bottom. A piston is loaded on top and the cake compressed to a given pressure. Then, filtrate is fed to the cake and  $\alpha$  is determined by a differential form of Eq. (24.2-9). This is then repeated for other compression pressures (G1).

If  $\alpha$  is independent of  $-\Delta p$ , the sludge is incompressible. Usually,  $\alpha$  increases with  $-\Delta p$ , since most cakes are somewhat compressible. An empirical equation often used is

$$\alpha = \alpha_0 (-\Delta p)^s \quad (24.2-11)$$

where  $\alpha_0$  and  $s$  are empirical constants. The compressibility constant  $s$  is zero for incompressible sludges or cakes. The

constant  $s$  usually falls between 0.1 to 0.8. Sometimes the following equation is used:

$$\alpha = \alpha_0' [1 + \beta(-\Delta p)s'] \quad (24.2-12)$$

where  $\alpha_0'$ ,  $\beta$ , and  $s'$  are empirical constants. Experimental data for various sludges are given by Grace (G1).

The data obtained from filtration experiments often do not have a high degree of reproducibility. The state of agglomeration of the particles in the slurry can vary and have an effect on the specific cake resistance.

#### **24.2B Filtration Equations for Constant-Pressure Filtration**

*1. Basic equations for filtration rate in a batch process.* Often, a filtration is done under conditions of constant

pressure. Equation (24.2-8) can be inverted and rearranged to give

$$dt dV = \mu \alpha c s A^2 (-\Delta p) V + \mu A (-\Delta p) R_m = K_p V + B \quad (24.2-13)$$

where  $K_p$  is in  $s/m^6$  ( $s/ft^6$ ) and  $B$  in  $s/m^3$  ( $s/ft^3$ ):

$$K_p = \mu \alpha c s A^2 (-\Delta p) \\ (SI) K_p = \mu \alpha c s A^2 (-\Delta p) g_c (\text{English}) \quad (24.2-14)$$

$$B = \mu R_m A (-\Delta p) \\ (SI) B = \mu R_m A (-\Delta p) g_c (\text{English}) \quad (24.2-15)$$

For constant pressure, constant  $\alpha$ , and incompressible cake,  $V$  and  $t$  are the only variables in Eq. (24.2-13).

Integrating to obtain the time of filtration in  $t$  s,

$$\int_0^t \frac{dt}{V} = \int_0^V \frac{dV}{K_p V^2 + B} \quad (24.2-16)$$

$$t = K_p \frac{V^2}{2} + BV \quad (24.2-17)$$

Dividing by  $V$

$$\frac{t}{V} = K_p \frac{V}{2} + B \quad (24.2-18)$$

where  $V$  is total volume of filtrate in  $\text{m}^3$  ( $\text{ft}^3$ ) collected to  $t$  s.

To evaluate Eq. (24.2-17), it is necessary to know  $\alpha$  and  $R_m$ . This can be done by using Eq. (24.2-18). Data for  $V$  collected at different times  $t$  are obtained. Then, the experimental data are plotted as  $t/V$  versus  $V$ , as in Fig. 24.2-2. Often, the first point on the graph does not fall on the line and is omitted. The slope of the line is  $K_p/2$  and the intercept  $B$ . Then, using Eqs. (24.2-14) and (24.2-15), values of  $\alpha$  and



$R_m$  can be determined.

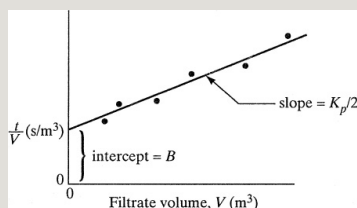


Figure 24.2-2. *Determination of constants in a constant-pressure filtration run.*

**EXAMPLE 24.2-1. Evaluation of Filtration Constants for Constant-Pressure Filtration**

Data for the laboratory filtration of  $\text{CaCO}_3$  slurry in water at 298.2 K (25°C) are reported as follows at a constant pressure ( $-\Delta p$ ) of 338 kN/m<sup>2</sup> (7060 lb<sub>f</sub>/ft<sup>2</sup>); see (R1, R2, M1). The filter area of the plate-and-frame press was  $A = 0.0439 \text{ m}^2$  (0.473 ft<sup>2</sup>) and the slurry concentration was  $c_s = 23.47 \text{ kg/m}^3$  (1.465 lb<sub>m</sub>/ft<sup>3</sup>). Calculate the constants  $\alpha$  and  $R_m$  from the experimental data given, where  $t$  is time in s and  $V$  is filtrate volume collected in m<sup>3</sup>.

**Solution:** First, the data are calculated as  $t/V$  and tabulated in Table 24.2-1. The data are plotted as  $t/V$  versus  $V$  in Fig. 24.2-3, the intercept is determined as  $B = 6400 \text{ s/m}^3$  (181 s/ft<sup>3</sup>), and the slope as  $K_p/2 = 3.00 \times 10^6 \text{ s/m}^6$ . Hence,  $K_p = 6.00 \times 10^6 \text{ s/m}^6$  (4820 s/ft<sup>6</sup>).

At 298.2 K, the viscosity of water is  $8.937 \times 10^{-4} \text{ Pa} \cdot \text{s}$  ·  $8.937 \times 10^{-4} \text{ kg/m} \cdot \text{s}$ . Substituting known values into Eq. (24.2-14) and solving,

$$K_p = 6.00 \times 10^6 = \mu \alpha c_s A^2 (-\Delta p) = (8.937 \times 10^{-4}) (\alpha) (23.47) (0.0439)^2 (338 \times 10^3) \alpha = 1.863 \times 10^{11} \text{ m/kg} \quad (2.77 \times 10^{11} \text{ ft/lbm})$$

Table 24.2-1. *Values of  $t/V$  for Example 24.2-1 ( $t = \text{s}$ ,  $V =$*

$m^3$ )

$\frac{t}{V} \times 10^{-3}$   
(s/m<sup>3</sup>)

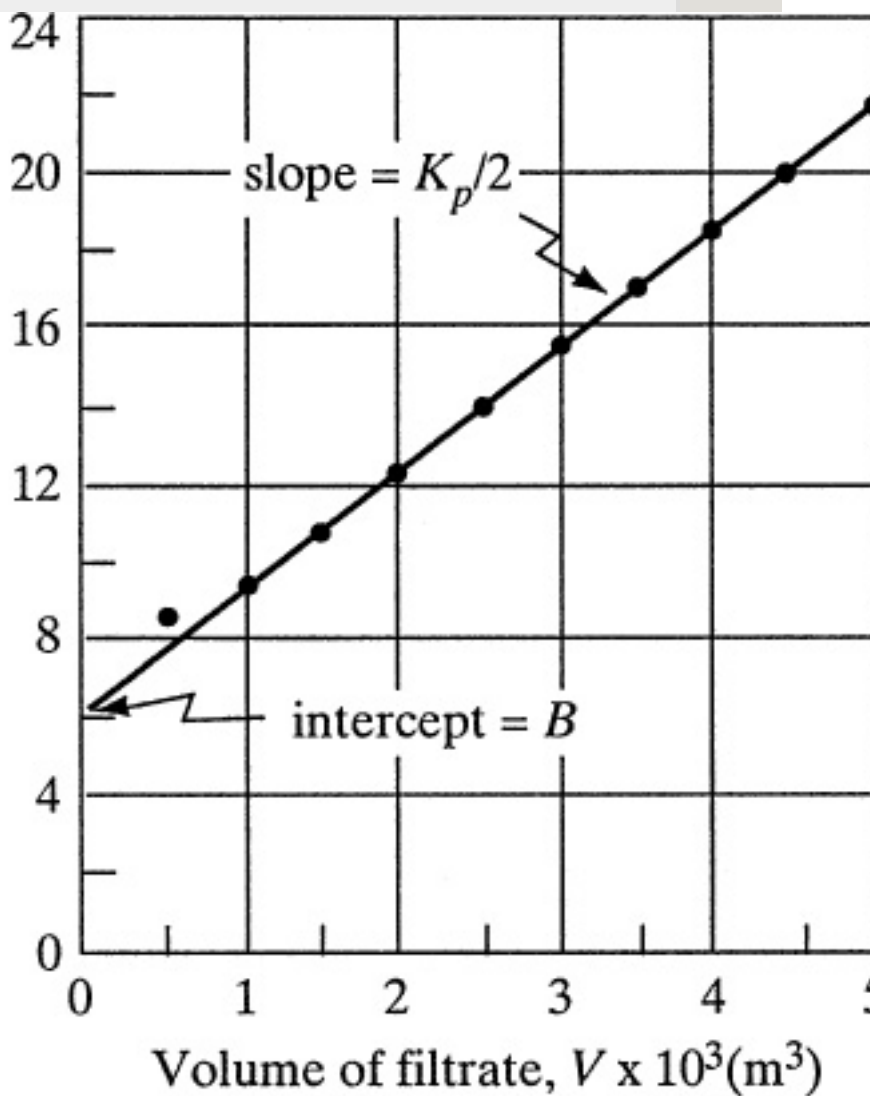


Figure 24.2-3. Determination of constants for Example 24.2-1.

Substituting into Eq. (24.2-15) and solving,

$$B=6400=\mu R_m A(-\Delta p)=(8.937 \times 10^{-4}) \\ (R_m)0.0439(338 \times 103) R_m=10.63 \times 1010 \text{ m}^{-1}(3.24 \times 1010) \text{ ft} \\ -1$$

#### **EXAMPLE 24.2-2. Time Required to Perform a Filtration**

The same slurry used in Example 24.2-1 is to be filtered in a plate-and-frame press having 20 frames and 0.873 m<sup>2</sup> (9.4 ft<sup>2</sup>) area per frame. The same pressure will be used in constant-pressure filtration. Assuming the same filter-cake properties and filter cloth, calculate the time to recover 3.37 m<sup>3</sup> (119 ft<sup>3</sup>) filtrate.

**Solution:** In Example 24.2-1, the area  $A = 0.0439 \text{ m}^2$ ,  $K_p = 6.00 \times 10^6 \text{ s/m}^6$ , and  $B = 6400 \text{ s/m}^3$ . Since the  $\alpha$  and  $R_m$  will be the same as before,  $K_p$  can be corrected. From Eq. (14.2-14),  $K_p$  is proportional to  $1/A^2$ . The new area is  $A = 0.873(20) = 17.46 \text{ m}^2$  (188 ft<sup>2</sup>). The new  $K_p$  is

$$K_p=6.00 \times 10^6 (0.0439/17.46)^2=37.93 \text{ s/m}^6 (0.03042 \text{ s/ft}^6)$$

The new  $B$  is proportional to  $1/A$  from Eq. (24.2-15):

$$B=(6400)0.0439/17.46=16.10 \text{ s/m}^3 (0.456 \text{ s/ft}^3)$$

Substituting into Eq. (24.2-17),

$$t=K_p 2V^2+BV=37.932(3.37)^2+(16.10)(3.37)=269.7 \text{ s}$$

Using English units,

$$t=K_p 2V^2+BV=0.030422(119)^2+(0.456)(119)=269.7 \text{ s}$$

*2. Equations for washing filter cakes and total cycle time.* Washing a cake after the filtration cycle has been completed takes place by displacement of the filtrate and by diffusion. The

amount of wash liquid should be sufficient to give the desired washing effect. To calculate washing rates, it is assumed that the conditions during washing are the same as those that existed at the end of the filtration. It is assumed that the cake structure is not affected when wash liquid replaces the slurry liquid in the cake.

In filters where the wash liquid follows a flow path similar to that during filtration, as in leaf filters, the final filtering rate gives the predicted washing rate. For constant-pressure filtration, using the same pressure in washing as in filtering, the final filtering rate is the reciprocal of Eq. (24.2-13):

$$(dV/dt)_f = 1/K_p V_f + B \quad (24.2-19)$$

where  $(dV/dt)_f$  = rate of washing in  $m^3/s$  ( $ft^3/s$ ) and  $V_f$  is the total volume of filtrate for the entire period at the end of filtration in  $m^3$  ( $ft^3$ ).

For plate-and-frame filter presses, the wash liquid travels through a cake twice as thick and an area only half as large as in filtering, so the predicted washing rate is one-fourth of the final filtration rate:

$$(dV/dt)_f = 1/4 (dV/dt)_f + B \quad (24.2-20)$$

In actual experience, the washing rate may be less than predicted because of cake consolidation, channeling, and the formation of cracks. Washing rates in a small plate-and-frame filter were found to be from 70 to 92% of that predicted (M1).

After washing is completed, additional time is needed to remove the cake, clean the filter, and reassemble the filter. The total filter-cycle time is the sum of the filtration time, plus the washing time, plus the cleaning time.

**EXAMPLE 24.2-3. Rate of Washing and Total Filter-Cycle Time**

At the end of the filtration cycle in Example 24.2-2, a total filtrate volume of  $3.37 \text{ m}^3$  is collected in a total time of 269.7 s. The cake is to be washed by through-washing in the plate-and-frame press using a volume of wash water equal to 10% of the filtrate volume. Calculate the time of washing and the total filter-cycle time if cleaning the filter takes 20 min.

**Solution:** For this filter, Eq. (24.2-20) holds. Substituting  $K_p = 37.93 \text{ s/m}^6$ ,  $B = 16.10 \text{ s/m}^3$ , and  $V_f = 3.37 \text{ m}^3$ , the washing rate is as follows:

$$(dV/dt)_f = 141(37.93)(3.37) + 16.10 = 1.737 \times 10^{-3} \text{ m}^3/\text{s} \quad (0.0613 \text{ it}^3/\text{s})$$

The time of washing is then as follows for  $0.10(3.37)$ , or  $0.337 \text{ m}^3$  of wash water:

$$t = 0.337 \text{ m}^3 / 1.737 \times 10^{-3} \text{ m}^3/\text{s} = 194.0 \text{ s}$$

The total filtration cycle is

$$269.760 + 194.060 + 20 = 27.73 \text{ min}$$

### 3. Equations for continuous filtration. In

a filter that is continuous in operation, such as a rotary-drum vacuum type, the feed, filtrate, and cake move at steady, continuous rates. In a rotary drum the pressure drop is held constant for the filtration. The cake formation involves a continual change in conditions. In continuous filtration, the resistance of the filter medium is generally negligible compared with the cake resistance. So in Eq. (24.2-13),  $B = 0$ .

Integrating Eq. (24.2-13), with  $B = 0$ ,

$$\int_0^t dt = K_p \int_0^V \frac{dV}{V^2} \quad (24.2-21)$$

$$t = K_p V \quad (24.2-22)$$

where  $t$  is the time required for formation of the cake. In a rotary-drum filter, the filter time  $t$  is less than the total cycle time  $t_c$  by

$$t = f \tau_c \quad (24.2-23)$$

where  $f$  is the fraction of the cycle used for cake formation. In the rotary drum,  $f$  is the fraction submergence of the drum surface in the slurry.

Next, substituting Eq. (24.2-14) and Eq. (24.2-23) into (24.2-22) and rearranging,

$$\text{flow rate} = V A t c = [2f(-\Delta p) t c \mu \alpha c s]^{1/2} \quad (24.2-24)$$

If the specific cake resistance varies with pressure, the constants in Eq. (24.2-11) are needed to predict the value of  $\alpha$  to be used in Eq. (24.2-24).

Experimental verification of Eq. (24.2-24) shows that the flow rate varies inversely with the square root of the viscosity and the cycle time ( $N_1$ ).



When short cycle times are used in continuous filtration and/or the filter medium resistance is relatively large, the filter resistance term  $B$  must be included, and Eq. (24.2-13) becomes

$$t = \frac{V}{A} \left( \frac{K}{v} + \frac{B}{v^2} \right) \quad (24.2-25)$$

Then, Eq. (24.2-25) becomes

$$\text{flow rate} = \frac{V}{A} \frac{1}{t} = \frac{R_m}{t} + \frac{[R_m^2 / (t^2 + 2cS\alpha(-\Delta p)f / (\mu t))]^{1/2}}{2\alpha cS} \quad (24.2-26)$$

**EXAMPLE 24.2-4. Filtration in a Continuous Rotary-Drum Filter**

A rotary-vacuum-drum filter having a 33% submergence of the drum in the slurry is to be used to filter a  $\text{CaCO}_3$  slurry as given in Example 24.2-1 using a pressure drop of 67.0 kPa. The solids concentration in the slurry is  $c_x = 0.191$  kg solid/kg slurry and the filter cake is such that the kg wet cake/kg dry cake =  $m = 2.0$ . The density and viscosity of the filtrate can be assumed to be those of water at 298.2 K. Calculate the filter area needed to filter 0.778 kg slurry/s. The filter-cycle time is 250 s. The specific cake resistance can be represented by  $\alpha = (4.37 \times 10^9)(-\Delta p)^{0.3}$ , where  $-\Delta p$  is in Pa and  $\alpha$  is in  $\text{m/kg}$ .

**Solution:** From Appendix A.2 for water,  $\rho = 996.9$   $\text{kg/m}^3$ ,  $\mu = 0.8937 \times 10^{-3}$  Pa  $\cdot$  s. From Eq. (24.2-10),

$$cs = pcx1 - mcx = 996.9(0.191)1 - (2.0)(0.191) = 308.1 \text{ kg solids/} \\ \text{m}^3 \text{ filtrate}$$

Solving for  $\alpha$ ,  $\alpha = (4.37 \times 10^9) (67.0 \times 10^3)^{0.3} = 1.225 \times 10^{11}$  m/kg. To calculate the flow rate of the filtrate,

$$V_{tc} = 0.778(cx)/(cs) = (0.778 \text{ kg slurry}) \\ (0.191 \text{ kg solid/kg slurry}) / \sin(1308.1 \text{ kg solid/} \\ \text{m}^3 \text{ filtrate}) = 4.823 \times 10^{-4} \text{ m}^3 \text{ filtrate/s}$$

Substituting into Eq. (24.2-24), neglecting and setting  $B = 0$ , and solving,

$$V_{tc} = 4.823 \times 10^{-4} A = [2(0.33)(67.0 \times 10^3)250(0.8937 \times 10^{-3}) \\ (1.225 \times 10^{11})(308.1)]^{1/2}$$

Hence,  $A = 6.60 \text{ m}^2$ .

## 24.2C Filtration Equations for Constant-Rate Filtration

In some cases, filtration runs are made under conditions of constant rate rather than constant pressure. This occurs if the slurry is fed to the filter by a positive-displacement pump. Equation (24.2-8) can be rearranged to give the following for a constant rate ( $dV/dt$ ) m<sup>3</sup>/s:

$$\frac{dV}{dt} = \frac{\mu \alpha c_s A^2 (-\Delta p) V + \mu A (-\Delta p) R_m}{K_p V + B} \quad (24.2-27)$$

where

$$KV = (\mu \alpha c s A^2 dV/dt)$$

$$(SI) KV = (\mu \alpha c s A^2 g dV/dt) \text{ (English)} \\ (24.2-28)$$

$$C = (\mu R_m A dV/dt)$$

$$(SI) C = (\mu R_m A g dV/dt) \text{ (English)}$$

$KV$  is in  $N/m^5$  ( $lbf/ft^5$ ) and  $C$  is in  $N/m^2$  ( $lbf/ft^2$ ).

Assuming that the cake is incompressible,  $KV$  and  $C$  are constants characteristic of the slurry, cake, rate of filtrate flow, and so on. Hence, a plot of pressure,  $-\Delta p$ , versus the total volume of filtrate collected,  $V$ , gives a straight line for a constant rate  $dV/dt$ . The slope of the line is  $KV$  and the intercept is  $C$ . The pressure increases as the cake thickness increases and the volume of

filtrate collected increases.

The equations can also be rearranged in terms of  $-\Delta p$  and time  $t$  as variables. At any moment during the filtration, the total volume  $V$  is related to the rate and total time  $t$  as follows:

$$V = t \frac{dV}{dt} \quad (24.2-30)$$

Substituting Eq. (24.2-30) into Eq. (24.2-27),

$$\begin{aligned} -\Delta p = & [\mu \alpha c S A^2 \left( \frac{dV}{dt} \right)^2] t \\ & + (\mu R_m A \frac{dV}{dt}) \quad (24.2-31) \end{aligned}$$

For the case where the specific cake resistance  $\alpha$  is not constant but varies as in Eq. (24.2-11), this can be substituted for  $\alpha$  in Eq. (24.2-27) to obtain a final equation.

## 24.3 Membrane Separations

### 24.3A Introduction

Separations by the use of membranes are becoming increasingly important in the process industries. In this relatively new separation process, the membrane acts as a semipermeable barrier and separation occurs by the membrane controlling the rate of movement of various molecules between two liquid phases, two gas phases, or a liquid and a gas phase. The two fluid phases are usually miscible and the membrane barrier prevents actual, ordinary hydrodynamic flow. A classification of the main types of membrane separation follows.

### 24.3B Classification of Membrane Processes

*1. Gas diffusion in a porous solid. In*

this type of separation, a gas phase is present on both sides of the membrane, which is a microporous solid. The rates of molecular diffusion of the various gas molecules depend on the pore sizes and the molecular weights. This type of diffusion in the molecular, transition, and Knudsen regions was discussed in detail in Section 19.4.

*2. Liquid permeation or dialysis.* In this case, because of concentration differences, the small solutes in one liquid phase diffuse readily through a porous membrane to the second liquid (or vapor) phase. Passage of large molecules through the membrane is more difficult. This membrane process has been applied in chemical processing separations such as the separation of

$\text{H}_2\text{SO}_4$  from nickel and copper sulfates in aqueous solutions, food processing, and artificial kidneys, and will be covered in detail in Section 24.8. In electrodialysis, separation of ions occurs by imposing an emf difference across the membrane.

*3. Gas permeation in a membrane.* The membrane in this process is usually a polymer such as rubber, polyamide, and so on, and is not a porous solid. The solute gas first dissolves in the membrane and then diffuses in the solid to the other gas phase. This was discussed in detail in Section 19.3 for solutes following Fick's law and will be considered again, for the case where resistances are present, in Section 25.1A. In Chapter 25, different process flow patterns are considered. Examples

of membrane separations are helium being separated from natural gas and nitrogen from air. Separation of a gas mixture occurs because each type of molecule diffuses at a different rate through the membrane.

*4. Reverse osmosis.* A membrane, which impedes the passage of a low-molecular-weight solute, is placed between a solute–solvent solution and a pure solvent. The solvent diffuses into the solution by osmosis. In reverse osmosis, a reverse pressure difference is imposed that causes the flow of solvent to reverse, as in the desalination of seawater. This process is also used to separate other low-molecular-weight solutes, such as salts, sugars, and simple acids from a solvent (usually water). This process will be covered in detail in



## Section 24.7.

*5. Ultrafiltration membrane process.* In this process, pressure is used to obtain a separation of molecules by means of a semipermeable polymeric membrane (M2). The membrane discriminates on the basis of molecular size, shape, or chemical structure and separates relatively high-molecular-weight solutes such as proteins, polymers, colloidal materials such as minerals, and so on. The osmotic pressure is usually negligible because of the high molecular weights. This will be covered in Section 24.6.

*6. Microfiltration membrane process.* In microfiltration, a pressure-driven flow through the membrane is used to separate micron-size particles from

fluids. The particles are usually larger than those in ultrafiltration. Examples are separation of bacteria, paint pigment, yeast cells, and so on from solutions. This process will be covered in Section 24.5.

*7. Gel permeation chromatography.* The porous gel retards diffusion of the high-molecular-weight solutes. The driving force is concentration. This process is quite useful in analyzing complex chemical solutions and in the purification of very specialized and/or valuable components.

## **24.4 Microfiltration Membrane Processes**

### **24.4A Introduction**

In microfiltration, pressure-driven flow through a membrane is used to

separate micron-size particles from fluids. The size range of particles ranges from  $0.02\ \mu\text{m}$  to  $10\ \mu\text{m}$  (H2). This microfiltration separates particles from solutions. The particles are usually larger than the solutes in reverse osmosis and ultrafiltration. Hence, osmotic pressure is negligible. At the very low end of the size range, very large soluble macromolecules are retained. Bacteria and other microorganisms (P2) are also retained on these membranes. Other particles in this size range are paint pigments, yeast cells, suspended matter such as cells from fermentation broth, particles in beer pasteurization, and so on. The dividing line between ultrafiltration and microfiltration is not very distinct.

The pore sizes of the membranes and the permeate flux are typically larger than for reverse osmosis and ultrafiltration. Usually, the pressure drop used across the membranes varies from 1 psi to 50 psi (H<sub>2</sub>). The types of membranes are extremely varied and can be ceramics, polymers, and so on.

Many different geometries of membranes are used. These include spiral-wound, plate-and-frame, hollow fiber, and cartridge filters with pleated membranes, among others. Disposable cartridges are also used.

#### **24.4B Models for Microfiltration**

*1. Dead-end microfiltration flow model.* In many laboratory batch filtrations, the batch process is run in a dead-end flow, with the membrane

replacing the conventional filter paper. The particles build up with time as a cake and the clarified permeate is forced through the membrane, as shown in Fig. 24.4-1a. The permeate flux equation is (H2)

$$N_w = \Delta P / \mu (R_m + R_c) \quad (24.4-1)$$

where  $N_w$  is the solvent flux in  $\text{kg}/(\text{s} \cdot \text{m}^2)$ ,  $\Delta P$  is the pressure difference in Pa,  $\mu$  is viscosity of the solvent in  $\text{Pa} \cdot \text{s}$ ,  $R_m$  is the membrane resistance in  $\text{m}^2/\text{kg}$ , and  $R_c$  is the cake resistance in  $\text{m}^2/\text{kg}$ , which increases with time due to cake buildup.

Eq. (24.4-1) is similar to Eq. (24.2-8) for ordinary filtration discussed in Section 24.2 of this text. Solutions to this equation are also given there.

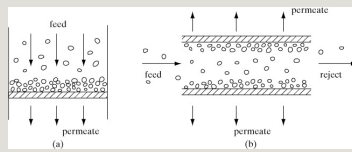


Figure 24.4-1. *Process flow for microfiltration: (a) dead-end flow, (b) cross-flow.*

## 2. *Cross-flow microfiltration flow model.*

In the cross-flow model shown in Fig. 24.4-1b, the operation is similar to that for reverse osmosis and ultrafiltration because the flow of bulk solution is parallel to the membrane surface and not through it (H2). The permeate flow through the membrane carries particles to the surface, where they form a thin layer. A relatively high flow rate tangential to the surface sweeps the deposited particles toward the filter exit, depositing a relatively thin cake layer. This thin cake layer is similar to the gel layer formed in ultrafiltration. This cross-flow is effective in controlling

concentration polarization and cake buildup, allowing relatively high fluxes to be maintained.

This concentration-polarization model for convection of particles to the cake layer is balanced by particle diffusion by Brownian diffusion away from the cake surface. This model is similar to the flux equation (24.6-3) for ultrafiltration. Other models are also given elsewhere (H2).

## **24.5 Ultrafiltration Membrane Processes**

### **24.5A Introduction**

Ultrafiltration is a membrane process that is quite similar to reverse osmosis. It is a pressure-driven process where the solvent and, when present, small solute molecules pass

through the membrane and are collected as a permeate. Larger solute molecules do not pass through the membrane and are recovered in a concentrated solution. The solutes or molecules to be separated generally have molecular weights greater than 500 and up to 1000000 or more, such as macromolecules of proteins, polymers, and starches, as well as colloidal dispersions of clays, latex particles, and microorganisms.

Unlike reverse osmosis, ultrafiltration membranes are too porous to be used for desalting. The rejection  $R$ , often called retention, is also given by Eq. (24.6-7), which is defined for reverse osmosis. Ultrafiltration is also used to separate a mixture of different-molecular-weight proteins. The molecular-weight cut-off



of the membrane is defined as the molecular weight of globular proteins, which are 90% retained by the membrane. A rule of thumb is that the molecular mass must differ by a factor of 10 for a good separation (P2).

Ultrafiltration is used in many different processes at the present time. Some of these are separation of oil–water emulsions, concentration of latex particles, processing of blood and plasma, fractionation or separation of proteins, recovery of whey proteins in cheese manufacturing, removal of bacteria and other particles to sterilize wine, and clarification of fruit juices.

Membranes for ultrafiltration are, in general, similar to those for reverse osmosis and are commonly asymmetric

and more porous. The membrane consists of a very thin, dense skin supported by a relatively porous layer for strength. Membranes are made from aromatic polyamides, cellulose acetate, cellulose nitrate, polycarbonate, polyimides, polysulfone, and so forth (M3, P3, R3).

#### **24.5B Types of Equipment for Ultrafiltration**

The equipment for ultrafiltration is similar to that used for reverse osmosis and gas separation processes, described in Sections 24.6F and 25.1C. The tubular-type unit is less prone to fouling and more easily cleaned than any of the other three types; however, this type is relatively costly.

Flat sheet membranes in a plate-and-

frame unit offer the greatest versatility but at the highest capital cost (P3).

Membranes can easily be cleaned or replaced by disassembly of the unit.

Spiral-wound modules provide relatively low costs per unit membrane area. These units are more prone to fouling than tubular units but are more resistant to fouling than hollow-fiber units. Hollow-fiber modules are the least resistant to fouling as compared to the other three types. However, the hollow-fiber configuration has the highest ratio of membrane area per unit volume.

Cross-flow filtration is the most common type of model used (P2).

Spiral-wound flat sheets are used most of all, followed by hollow-fiber units.

Batch processes are also quite common.

Stirred tanks with a membrane that

approximate cross-flow operation are also used (R3).

#### **24.5C Flux Equations for Ultrafiltration**

The flux equation for diffusion of a solvent through the membrane is:

$$N_w = A_w(\Delta P - \Delta \pi) \quad (24.5-1)$$

In ultrafiltration, the membrane does not allow passage of the solute, which is generally a macromolecule. The concentration in moles/liter of the large solute molecules is usually small.

Hence, the osmotic pressure is very low and can be neglected. Then, Eq. (24.7-2) becomes

$$N_w = A_w(\Delta P) \quad (24.5-2)$$

Ultrafiltration units operate at about 5–100 psi pressure drop, compared to 400–

2000 for reverse osmosis. For low-pressure drops of, say, 5–10 psi and dilute solutions of up to 1 wt % or so, Eq. (24.5-1) predicts the performance reasonably well for well-stirred systems.

Since the solute is rejected by the membrane, it accumulates and starts to build up at the surface of the membrane. As pressure drop is increased and/or concentration of the solute is increased, concentration polarization occurs, which is much more severe than in reverse osmosis. This is shown in Fig. 24.5-1a, where  $c_1$  is the concentration of the solute in the bulk solution, kg solute/m<sup>3</sup>,  $c_s$  is the concentration of the solute at the surface of the membrane, and  $c_p$  is the concentration in the permeate.

As the pressure drop increases, this

increases the solvent flux  $N_w$  to and through the membrane. This results in a higher convective transport of the solute to the membrane; that is, the solvent carries with it more solute. The concentration  $c_s$  increases and gives a larger back molecular diffusion of solute from the membrane to the bulk solution. At steady state, the convective flux equals the diffusion flux:

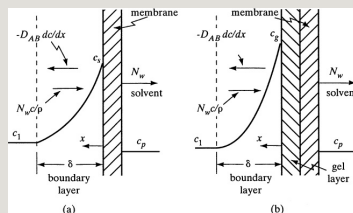


Figure 24.5-1. Concentration polarization in ultrafiltration: (a) concentration profile before gel formation, (b) concentration profile with a gel layer formed at membrane surface.

$$N_w c/p = -D_{AB} dc/dx \quad (24.5-3)$$

where  $N_w c/p = [\text{kg solvent}/(\text{s} \cdot \text{m}^2)](\text{kg solute}/\text{m}^3)/(\text{kg solvent}/\text{m}^3) = \text{kg solute}/\text{s}$

·  $m_2$ ;  $D_{AB}$  is diffusivity of solute in solvent,  $m^2/s$ ; and  $x$  is distance,  $m$ .

Integrating this equation between the limits of  $x = 0$  and  $c = c_s$  and  $x = \delta$  and  $c = c_1$ ,

$$N_w \rho = (D_{AB} \delta) \ln(c_s - c_p) - (D_{AB} \delta) \ln(c_1 - c_p) = k_c \ln(c_s - c_p) - k_c \ln(c_1 - c_p) \quad (24.5-4)$$

where  $k_c$  is the mass-transfer coefficient,  $m/s$ . Further increases in pressure drop increase the value of  $c_s$  to a limiting concentration, at which the accumulated solute forms a semisolid gel where  $c_s = c_g$ , as shown in Fig. 24.5-1b. For the usual case of almost-complete solute retention (P2),  $c_p = 0$  and Eq. (24.5-4) becomes

$$N_w \rho = k_c \ln(c_s / c_1) \quad (24.5-5)$$

Additional increases in pressure drop do

not change  $c_g$  and the membrane is said to be “gel polarized.” Then, Eq. (24.5-4) becomes (P1, P3, R3)

$$N_w p = k c \ln(c_g/c_1) \quad (24.5-6)$$

With increases in pressure drop, the gel layer increases in thickness, causing the solvent flux to decrease because of the added gel-layer resistance. Finally, the net flux of solute by convective transfer becomes equal to the back diffusion of solute into the bulk solution because of the polarized concentration gradient, as given by Eq. (24.5-6).

The added gel-layer resistance next to the membrane causes an increased resistance to solvent flux, as given by

$$N_w = \Delta P / (A_w + R_g) \quad (24.5-7)$$



where  $1/A_w$  is the membrane resistance and  $R_g$  is the variable gel-layer resistance,  $(\text{s} \cdot \text{m}^2 \cdot \text{atm})/\text{kg}$  solvent. The solvent flux in this gel-polarized regime is independent of pressure difference and is determined by Eq. (24.5-6) for back diffusion. Experimental data confirm the use of Eq. (24.5-6) for a large number of macromolecular solutions, such as proteins and so forth as well as colloidal suspensions, such as latex particles and so forth (P1, P3).

#### **24.5D Effects of Processing Variables in Ultrafiltration**

A plot of typical experimental data for flux versus pressure difference is shown in Fig. 24.5-2 (H1, P3). At low pressure differences and/or low solute concentrations, the data typically follow Eq. (24.5-1). For a given bulk concentration,  $c_1$ , the flux

approaches a constant value at high pressure differences, as shown in Eq. (24.5-6). Also, more-dilute protein concentrations give higher flux rates, as expected from Eq. (24.5-6). Most commercial applications are flux-limited by concentration polarization and operate in the region where the flux is approximately independent of pressure difference (R3).

Using experimental data, a plot of  $N_w/\rho$  versus  $\ln c_1$  is a straight line with a negative slope of  $k_c$ , the mass-transfer coefficient, as shown by Eq. (24.5-6). These plots also give the value of  $c_g$ , the gel concentration. Data (P1) show that the gel concentration for many macromolecular solutions is about 25 wt %, with a range of 5 to 50%. For colloidal dispersions, it is about 65 wt

%, with a range of 50 to 75%.

The concentration-polarization effects for hollow fibers are often quite small, due to the low solvent flux. Hence, Eq. (24.5-1) describes the flux. In order to increase the ultrafiltration solvent flux, cross-flow of fluid past the membrane can be used to sweep away part of the polarized layer, thereby increasing  $k_c$  in Eq. (24.5-6). Higher velocities and other methods are used to increase turbulence and hence  $k_c$ . In most cases, the solvent flux is too small to operate in a single-pass mode. It is necessary to recirculate the feed past the membrane, with recirculation rates of 10/1 to 100/1 often used.

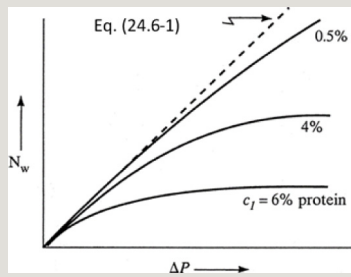


Figure 24.5-2. *Effect of pressure difference on solvent flux.*

Methods for predicting the mass-transfer coefficient  $k_c$  in Eq. (24.5-6) are given by others (P1, P3) for known geometries such as channels and so forth.

Predictions of flux in known geometries using these methods and experimental values of  $c_g$  in Eq. (24.5-6) in the gel polarization regime compare with experimental values for macromolecular solutions within about 25–30%.

However, for colloidal dispersions the experimental flux is higher than the theoretical by factors of 20–30 for laminar flow and 8–10 for turbulent flow. Hence, Eq. (24.5-6) is not useful

for predicting the solvent flux accurately. Generally, for design of commercial units, it is necessary to obtain experimental data on single modules.

## **24.6 Reverse-Osmosis Membrane Processes**

### **24.6A Introduction**

*1. Introduction.* To be useful for the separation of different species, a membrane must allow passage of certain molecules and exclude or greatly restrict the passage of others. In osmosis, a spontaneous transport of solvent occurs from a dilute solute or salt solution to a concentrated solute or salt solution across a semipermeable membrane that allows passage of the solvent but impedes passage of the salt solutes.

In Fig. 24.6-1a, the solvent water normally flows through the semipermeable membrane to the salt solution. The levels of both liquids are the same, as shown. The solvent flow can be reduced by exerting a pressure on the salt-solution side and membrane, as shown in Fig. 24.6-1b, until at a certain pressure, called the osmotic pressure  $\pi$  of the salt solution, equilibrium is reached and the amount of the solvent passing in opposite directions is equal. The chemical potentials of the solvent on both sides of the membrane are equal. The properties of the solution determine only the value of the osmotic pressure, not the membrane, provided that it is truly semipermeable. To reverse the flow of the water so that it flows from the

salt solution to the fresh solvent, as in Fig. 24.6-1c, the pressure is increased above the osmotic pressure on the solution side.

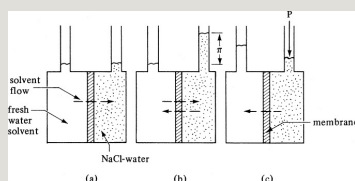


Figure 24.6-1. *Osmosis and reverse osmosis: (a) osmosis, (b) osmotic equilibrium, (c) reverse osmosis.*

This phenomenon, called *reverse osmosis*, is used in a number of processes. An important commercial use is in the desalination of seawater or brackish water to produce fresh water. Unlike distillation and freezing processes used to remove solvents, reverse osmosis can operate at ambient temperature without phase change. This process is quite useful for the processing of thermally and chemically unstable

products. Applications include concentration of fruit juices and milk, recovery of protein and sugar from cheese whey, and concentration of enzymes.

## *2. Osmotic pressure of solutions.*

Experimental data show that the osmotic pressure  $\pi$  of a solution is proportional to the concentration of the solute and temperature  $T$ . Van't Hoff originally showed that the relationship is similar to that for pressure of an ideal gas. For example, for dilute water solutions,

$$\pi = n V_m R T \quad (24.6-1)$$

where  $n$  is the number of kg mol of solute,  $V_m$  is the volume of pure solvent water in m<sup>3</sup> associated with  $n$  kg mol of solute,  $R$  is the gas law constant 82.057



$\times 10^{-3} \text{ m}^3 \cdot \text{atm/kg mol} \cdot \text{K}$ , and  $T$  is temperature in K. If a solute exists as two or more ions in solution,  $n$  represents the total number of ions. For more concentrated solutions, Eq. (24.6-1) is modified using the osmotic coefficient  $\phi$ , which is the ratio of the actual osmotic pressure  $\pi$  to the ideal  $\pi$  calculated from the equation. For very dilute solutions,  $\phi$  has a value of unity and usually decreases as concentration increases. In Table 24.6-1, some experimental values of  $\pi$  are given for NaCl solutions, sucrose solutions, and seawater solutions (S1, S3).

**EXAMPLE 24.6-1. Calculation of the Osmotic Pressure of a Salt Solution**

Calculate the osmotic pressure of a solution containing 0.10 g mol NaCl/1000 g H<sub>2</sub>O at 25°C.

**Solution:** From Table A.2-3, the density of water = 997.0 kg/m<sup>3</sup>. Then,  $n = 2 \times 0.10 \times 10^{-3} \text{ 2.00} \times 10^{-4} \text{ kg mol}$  (NaCl gives two ions). Also, the volume of the pure solvent water  $V_m = 1.00 \text{ kg}/(997.0 \text{ kg/m}^3)$ . Substituting into Eq. (24.6-1),

$$\pi = nV_mRT = 2.00 \times 10^{-4} (82.057 \times 10^{-3}) \\ (298.15) 1.000 / 997.04.88 \text{ atm}$$

This compares with the experimental value in Table 24.6-1 of 4.56 atm.

*3. Types of membranes for reverse osmosis.* One of the more important membranes for reverse-osmosis desalination and many other reverse-osmosis processes is the cellulose–cetate membrane. The asymmetric membrane is made as a composite film in which a thin, dense layer about 0.1–10  $\mu\text{m}$  thick of extremely fine pores is supported on a much thicker (50–125  $\mu\text{m}$ ) layer of microporous sponge with little resistance to permeation. The thin, dense layer has the ability to block the passage of quite small solute molecules. In desalination, the membrane rejects the salt solute and allows the solvent water to pass through. Solutes that are most effectively excluded by the

cellulose–acetate membrane are the salts NaCl, NaBr, CaCl<sub>2</sub>, and Na<sub>2</sub>SO<sub>4</sub>; sucrose; and tetraalkyl ammonium salts. The main limitations of the cellulose–acetate membrane are that for the most part it can only be used in aqueous solutions and that it must be used below about 60°C.

Table 24.6-1. *Osmotic Pressure of Various Aqueous Solutions at 25°C (P1, S1, S3)*

--

\*Value for standard seawater.

Another important membrane useful for seawater, wastewater, nickel-plating rinse solutions, and other solutes is the synthetic aromatic polyamide membrane “Permasep,” made in the form of very

fine, hollow fibers (L1, P4). When used industrially, this type of membrane withstands continued operation at pH values of 10 to 11 (S2). Many other anisotropic membranes have also been synthesized from synthetic polymers, some of which can be used in organic solvents, at higher temperatures, and at high or low pH (M3, R3).

#### **24.6B Flux Equations for Reverse Osmosis**

*1. Basic models for membrane processes.* There are two basic types of mass-transport mechanisms that can take place in membranes. In the first basic type, using tight membranes, which are capable of retaining solutes of about  $10 \text{ \AA}$  in size or less, diffusion-type transport mainly occurs. Both the solute and the solvent migrate by molecular or

Fickian diffusion in the polymer, driven by concentration gradients set up in the membrane by the applied pressure difference. In the second basic type, using loose, microporous membranes that retain particles larger than  $10 \text{ \AA}$ , a sieve-type mechanism occurs, where the solvent moves through the micropores in an essentially viscous flow and the solute molecules small enough to pass through the pores are carried by convection with the solvent. For details of this second type of mechanism, see (M3, W1).

*2. Diffusion-type model.* For diffusion-type membranes, the steady-state equations governing the transport of solvent and solute are, to a first approximation, as follows (M3, M4).

For the diffusion of the solvent through the membrane, as shown in Fig. 24.6-2,

$$N_w = P_w L_m (\Delta P - \Delta \pi) = A_w (\Delta P - \Delta \pi) \quad (24.6-2)$$

$$A_w = P_w L_m \quad (24.6-3)$$

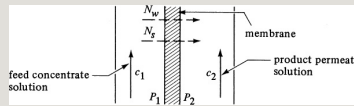


Figure 24.6-2. Concentrations and fluxes in a reverse-osmosis process.

where  $N_w$  is the solvent (water) flux in  $\text{kg/s} \cdot \text{m}^2$ ;  $P_w$  is the solvent membrane permeability,  $\text{kg solvent/s} \cdot \text{m} \cdot \text{atm}$ ;  $L_m$  is the membrane thickness,  $\text{m}$ ;  $A_w$  is the solvent permeability constant,  $\text{kg solvent/s} \cdot \text{m}^2 \cdot \text{atm}$ ;  $\Delta P = P_1 - P_2$  (hydrostatic pressure difference with  $P_1$  pressure exerted on feed and  $P_2$  on product solution),  $\text{atm}$ ; and  $\Delta \pi = \pi_1 - \pi_2$

(osmotic pressure of feed solution – osmotic pressure of product solution), atm. Note that subscript 1 is the feed or upstream side of the membrane and 2 is the product or downstream side of the membrane.

For the diffusion of the solute through the membrane, an approximation for the flux of the solute is (C1, M5)

$$N_s = D_s K_s L_m (c_1 - c_2) = A_s (c_1 - c_2) \quad (24.6-4)$$

$$A_s = D_s K_s L_m \quad (24.6-5)$$

where  $N_s$  is the solute (salt) flux in kg solute/s · m<sup>2</sup>;  $D_s$  is the diffusivity of solute in membrane, m<sup>2</sup>/s;  $K_s = c_m/c$  (distribution coefficient), concentration of solute in the membrane/concentration of solute in solution;  $A_s$  is the solute

permeability constant, m/s;  $c_1$  is the solute concentration in upstream or feed (concentrate) solution, kg solute/m<sup>3</sup>; and  $c_2$  is the solute concentration in downstream or product (permeate) solution, kg solute/m<sup>3</sup>. The distribution coefficient  $K_s$  is approximately constant over the membrane.

Making a material balance at steady state for the solute, the solute diffusing through the membrane must equal the amount of solute leaving in the downstream or product (permeate) solution:

$$N_s = N_w c_2 \quad (24.6-6)$$

where  $c_2$  is the concentration of solute in stream 2 (permeate), kg solute/m<sup>3</sup>. If the stream 2 is dilute in solute,  $c_2$  is



approximately the density of the solvent. In reverse osmosis, the solute rejection  $R$  is defined as the ratio concentration difference across the membrane divided by the bulk concentration on the feed or concentrate side (fraction of solute remaining in the feed stream):

$$R = \frac{c_1 - c_2}{c_1} = 1 - \frac{c_2}{c_1} \quad (24.6-7)$$

This can be related to the flux equations as follows, by first substituting Eqs. (24.6-2) and (24.6-4) into Eq. (24.6-6) to eliminate  $N_w$  and  $N_s$  in Eq. (24.6-6). Then, solving for  $c_2/c_1$  and substituting this result into Eq. (24.6-7),

$$R = \frac{B(\Delta P - \Delta \pi)}{1 + B(\Delta P - \Delta \pi)} \quad (24.6-8)$$

$$B = \frac{P_w D_s K_{scw}}{A_w A_{scw}} \quad (24.6-9)$$

where  $B$  is in  $\text{atm}^{-1}$ . Note that  $B$  is

composed of the various physical properties  $P_w$ ,  $D_s$ , and  $K_s$  of the membrane, and must be determined experimentally for each membrane. Usually, it is the product  $D_s K_s$  that is determined, not the values of  $D_s$  and  $K_s$  separately. Also, many of the data reported in the literature give values of  $(P_w/L_m)$  or  $A_w$  in  $\text{kg solvent/s} \cdot \text{m}^2 \cdot \text{atm}$  and  $(D_s K_s/L_m)$  or  $A_s$  in  $\text{m/s}$  and not separate values of  $L_m$ ,  $P_w$ , and so on.

**EXAMPLE 24.6-2. Experimental Determination of Membrane Permeability**

Experiments at 25°C were performed to determine the permeabilities of a cellulose–acetate membrane (A1, W1). The laboratory test section shown in Fig. 24.6-3 has membrane area  $A = 2.00 \times 10^{-3} \text{ m}^2$ . The inlet feed solution concentration of NaCl is  $c_1 = 10.0 \text{ kg NaCl/m}^3 \text{ solution}$  (10.0 g NaCl/L,  $\rho_1 = 1004 \text{ kg solution/m}^3$ ). The water recovery is assumed low so that the concentration  $c_1$  in the entering feed solution flowing past the membrane and the concentration of the exit feed solution are essentially equal. The product solution contains  $c_2 = 0.39 \text{ kg NaCl/m}^3 \text{ solution}$  ( $\rho_2 = 997 \text{ kg solution/m}^3$ ) and its measured flow rate is  $1.92 \times 10^{-8} \text{ m}^3 \text{ solution/s}$ . A pressure differential of 5514 kPa (54.42 atm) is used. Calculate the permeability constants of the membrane and the solute rejection  $R$ .

**Solution:** Since  $c_2$  is very low (dilute solution), the value of  $c_w$  can be assumed as the density of water (Table 24.6-1),

or  $c_{w2} = 997 \text{ kg solvent/m}^3$ . To convert the product flow rate to water flux,  $N_w$ , using an area of  $2.00 \times 10^{-3} \text{ m}^2$ ,

$$N_w = (1.92 \times 10^{-8} \text{ m}^3/\text{s})(997 \text{ kg solvent/m}^3) / (2.00 \times 10^{-3} \text{ m}^2) = 9.57 \times 10^{-3} \text{ kg solvent/s}\cdot\text{m}^2$$

Substituting into Eq. (24.6-6),

$$N_s = N_w c_{w2} c_{w2} = (9.57 \times 10^{-3})(0.39)997 = 3.774 \times 10^{-6} \text{ kg solute NaCl/s}\cdot\text{m}^2$$

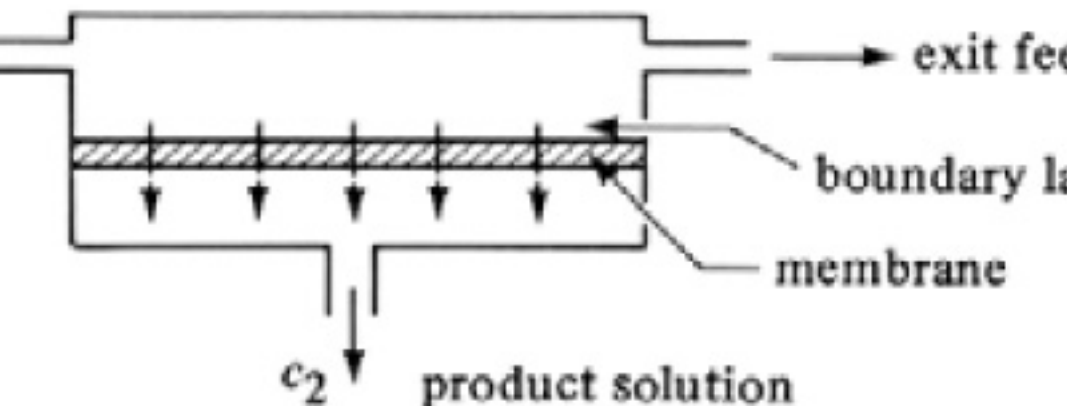


Figure 24.6-3. Process flow diagram of experimental reverse-osmosis laboratory unit.

To determine the osmotic pressures from Table 24.6-1, the concentrations are converted as follows: For  $c_1$ , 10 kg NaCl is in 1004 kg solution/ $\text{m}^3$  ( $\rho_1 = 1004$ ). Then,  $1004 - 10 = 994 \text{ kg H}_2\text{O}$  in  $1 \text{ m}^3$  solution. Hence, in the feed solution, where the molecular weight of NaCl = 58.45,  $(10.00 \times 1000)/(994 \times 58.45) = 0.1721 \text{ g mol NaCl/kg H}_2\text{O}$ . From Table 24.6-1,  $\pi_1 = 7.80 \text{ atm}$  by linear interpolation. Substituting into Eq. (24.6-1), the predicted  $\pi_1 = 8.39 \text{ atm}$ , which is higher than the experimental value. For the product solution,  $997 - 0.39 = 996.6 \text{ kg H}_2\text{O}$ . Hence,  $(0.39 \times 1000)/(996.6 \times 58.45) = 0.00670 \text{ g mol NaCl/kg H}_2\text{O}$ . From Table 24.6-1,  $\pi_2 = 0.32 \text{ atm}$ . Then,  $\Delta\pi = \pi_1 - \pi_2 = 7.80 - 0.32 = 7.48 \text{ atm}$  and  $\Delta P = 54.42 \text{ atm}$ .

Substituting into Eq. (24.6-2),

$$N_w = 9.57 \times 10^{-3} = P_w L_m (\Delta P - \Delta \pi) = P_w L_m (54.42 - 7.48)$$

Solving,  $(P_w/L_m) = A_w = 2.039 \times 10^{-4}$  kg solvent/s  $\cdot$  m<sup>2</sup>  $\cdot$  atm. Substituting into Eq. (24.6-4),

$$N_s = 3.744 \times 10^{-6} = D_s K_s L_m (c_1 - c_2) = D_s K_s L_m (10.00 - 0.39)$$

Solving,  $(D_s K_s/L_m) = A_s = 3.896 \times 10^{-7}$  m/s.

To calculate the solute rejection  $R$  by substituting into Eq. (24.6-7),

$$R = c_1 - c_2 c_1 = 10.00 - 0.39 / 10.00 = 0.961$$

Also, substituting into Eq. (24.6-9) and then Eq. (24.6-8),

$$\begin{aligned} B &= P_w/L_m (D_s K_s/ \\ L_m) c_w^2 &= 2.039 \times 10^{-4} (3.896 \times 10^{-7}) / 997 = 0.5249 \text{ atm} \\ -1R &= B(\Delta P - \Delta \pi) / 1 + B(\Delta P \\ -\Delta \pi) &= 0.5249(54.42 - 7.48) / 1 + 0.5249(54.42 - 7.48) = 0.961 \end{aligned}$$

## 24.6C Effects of Operating Variables

In many commercial units, operating pressures in reverse osmosis range from about 1035 up to 10 350 kPa (150 up to 1500 psi). Comparison of Eq. (24.6-2) for solvent flux with Eq. (24.6-4) for solute flux shows that the solvent flux  $N_w$  depends only on the net pressure difference, while the solute flux  $N_s$  depends only on the concentration difference. Hence, as

the feed pressure is increased, solvent or water flow through the membrane increases and the solute flow remains approximately constant, giving a lower solute concentration in the product solution.

At a constant applied pressure, increasing the feed solute concentration increases the product solute concentration. This is caused by the increase in the feed osmotic pressure, since as more solvent is extracted from the feed solution (as water recovery increases), the solute concentration becomes higher and the water flux decreases. Also, the amount of solute present in the product solution increases because of the higher feed concentration.

If a reverse-osmosis unit has a large membrane area (as in a commercial unit), and the path between the feed inlet and outlet is long, the outlet feed concentration can be considerably higher than the inlet feed  $c_1$ . Then, the salt flux will be greater at the outlet feed as compared to the inlet (K2). Many manufacturers use the feed solute or salt concentration average between inlet and outlet to calculate the solute or salt rejection  $R$  in Eq. (24.6-7).

**EXAMPLE 24.6-3. Prediction of Performance in a Reverse-Osmosis Unit**

A reverse-osmosis membrane to be used at 25°C for a NaCl feed solution containing 2.5 g NaCl/L (2.5 kg NaCl/m<sup>3</sup>,  $\rho = 999 \text{ kg/m}^3$ ) has a water permeability constant  $A_w = 4.81 \times 10^{-4} \text{ kg/s} \cdot \text{m}^2 \cdot \text{atm}$  and a solute (NaCl) permeability constant  $A_s = 4.42 \times 10^{-7} \text{ m/s}$  (A1). Calculate the water flux and solute flux through the membrane using  $\Delta P = 27.20 \text{ atm}$  and the solute rejection  $R$ . Also, calculate  $c_2$  of the product solution.

**Solution:** In the feed solution,  $c_1 = 2.5 \text{ kg NaCl/m}^3$  and  $\rho_1 = 999 \text{ kg solution/m}^3$ . Hence, for the feed,  $999 - 2.5 = 996.5 \text{ kg H}_2\text{O}$  in  $1.0 \text{ m}^3$  solution; also, for the feed,  $(2.50 \times 1000)/(996.5 \times 58.45) = 0.04292 \text{ g mol NaCl/kg H}_2\text{O}$ . From Table 24.6-1,  $\pi_1 = 1.97 \text{ atm}$ . Since the product solution  $c_2$  is unknown, a value of  $c_2 = 0.1 \text{ kg NaCl/m}^3$  will be

assumed. Also, since this is quite dilute,  $\rho_2 = 997 \text{ kg solution/m}^3$  and  $C_{w2} = 997 \text{ kg solvent/m}^3$ . Then, for the product solution,  $(0.10 \times 1000)/(996.9 \times 58.45) = 0.00172 \text{ g mol NaCl/kg H}_2\text{O}$  and  $\pi_2 = 0.08 \text{ atm}$ . Also,  $\Delta\pi = \pi_1 - \pi_2 = 1.97 - 0.08 = 1.89 \text{ atm}$ .

Substituting into Eq. (24.6-2),

$$N_w = A_w(\Delta P - \Delta\pi) = 4.81 \times 10^{-4} (27.20 - 1.89) = 1.217 \times 10^{-2} \text{ kg H}_2\text{O/s}\cdot\text{m}^2$$

For calculation of  $R$ , substituting first into Eq. (24.6-9),

$$B = A_w A_{sc} w_2 = 4.81 \times 10^{-4} \times 44.42 \times 10^{-7} \times 997 = 1.092 \text{ atm}\cdot\text{m}^{-1}$$

Next, substituting into Eq. (24.6-8),

$$R = B(\Delta P - \Delta\pi) + B(\Delta P - \Delta\pi) = 1.092(27.20 - 1.89) + 1.092(27.20 - 1.89) = 0.965$$

Using this value of  $R$  in Eq. (24.6-7),

$$R = 0.965 = c_1 - c_2 \quad c_1 = 2.50 - c_2 \quad 2.50 - c_2 = 0.965$$

Solving,  $c_2 = 0.0875 \text{ kg NaCl/m}^3$  for the product solution. This is close enough to the assumed value of  $c_2 = 0.10$  that  $\pi_2$  will not change significantly on a second trial. Hence, the final value of  $c_2$  is  $0.0875 \text{ kg NaCl/m}^3$  ( $0.0875 \text{ g NaCl/L}$ ).

Substituting into Eq. (24.6-4),

$$N_s = A_s(c_1 - c_2) = 4.42 \times 10^{-7} (2.50 - 0.0875) = 1.066 \times 10^{-6} \text{ kg NaCl/s}\cdot\text{m}^2$$

## 24.6D Concentration Polarization in Reverse-Osmosis Diffusion Model

In desalination, localized concentrations of solute build up at the point where the solvent leaves the solution and enters the

membrane. The solute accumulates in a relatively stable boundary layer (Fig. 24.6-3) next to the membrane. Concentration polarization,  $\beta$ , is defined as the ratio of the salt concentration at the membrane surface to the salt concentration in the bulk feed stream  $c_1$ .

Concentration polarization causes the water flux to decrease, since the osmotic pressure  $\pi_1$  increases as the boundary layer concentration increases and the overall driving force ( $\Delta P - \Delta \pi$ ) decreases. Also, the solute flux increases, since the solute concentration increases at the boundary. Hence, the  $\Delta P$  must often be increased to compensate, which results in higher power costs (K2).

The effect of the concentration



polarization  $\beta$  can be included approximately by modifying the value of  $\Delta\pi$  in Eqs. (24.6-2) and (24.6-8) as follows (P3):

$$\Delta\pi = \beta\pi_1 - \pi_2 \quad (24.6-10)$$

It is assumed that the osmotic pressure  $\pi_1$  is directly proportional to the concentration, which is approximately correct. Also, Eq. (24.6-4) can be modified as

$$N_s = A_s(\beta c_1 - c_2) \quad (24.6-11)$$

The usual concentration polarization ratio is 1.2 to 2.0; that is, the concentration in the boundary layer is 1.2–2.0 times  $c_1$  in the bulk feed solution. This ratio is often difficult to predict. In desalination of seawater, using values of about 1000 psia =  $\Delta P$ ,

$\pi_1$  can be large. Increasing this  $\pi_1$  by a factor of 1.2–2.0 can appreciably reduce the solvent flux. For brackish waters containing 2–10 g/L and using  $\Delta P$  values of 17–55 atm abs, the value of  $\pi_1$  is low and concentration polarization is not important.

The boundary layer can be reduced by increasing the turbulence using higher feed-solution velocities. However, this extra flow results in a smaller ratio of product solution to feed. Also, screens can be put in the path to induce turbulence. Equations for predicting the mass-transfer coefficient to the surface and, hence, the concentration polarization, are given for specific geometries such as flow past plates, inside tubes, outside tubes, and so on (H2, N2). Then, equations for the flux of

water can be used with these mass-transfer coefficients in a manner similar to that for ultrafiltration given in Section 24.5.

#### **24.6E Permeability Constants for Reverse-Osmosis Membranes**

Permeability constants for membranes must be determined experimentally for the particular type of membrane to be used. For cellulose–acetate membranes, typical water permeability constants  $A_w$  range from about  $1 \times 10^{-4}$  to  $5 \times 10^{-4}$  kg solvent/s  $\cdot$  m<sup>2</sup>  $\cdot$  atm (A1, M4, W1). Values for other types of membranes can differ widely. Generally, the water permeability constant for a particular membrane does not depend upon the solute present. For the solute permeability constants  $A_s$  of cellulose–acetate

membranes, some relative typical values are as follows, assuming a value of  $A_s = 4 \times 10^{-7}$  m/s for NaCl:  $1.6 \times 10^{-7}$  m/s ( $\text{BaCl}_2$ ),  $2.2 \times 10^{-7}$  ( $\text{MgCl}_2$ ),  $2.4 \times 10^{-7}$  ( $\text{CaCl}_2$ ),  $4.0 \times 10^{-7}$  ( $\text{Na}_2\text{SO}_4$ ),  $6.0 \times 10^{-7}$  (KCl), and  $6.0 \times 10^{-7}$  ( $\text{NH}_4\text{Cl}$ ) (A1).

#### **24.6F Types of Equipment for Reverse Osmosis**

The equipment for reverse osmosis is quite similar to that for gas permeation membrane processes described in Section 25.1C. In the plate-and-frame-type unit, thin plastic support plates with thin grooves are covered on both sides with membranes, as in a filter press. Pressurized feed solution flows between the closely spaced membranes (L1). Solvent permeates the membrane and flows in the

grooves to an outlet. In the tubular-type unit, membranes in the form of tubes are inserted inside porous-tube casings, which serve as a pressure vessel. These tubes are then arranged in bundles like a heat exchanger.

In the spiral-wound unit, a planar membrane is used and a flat, porous support material is sandwiched between the membranes. Then, the membranes, support, and a mesh feed-side spacer are wrapped in a spiral around a tube. In the hollow-fiber unit, fibers of 100–200  $\mu\text{m}$  diameter with walls about 25  $\mu\text{m}$  thick are arranged in a bundle similar to a heat exchanger (L1, R3).

#### **24.6G Complete-Mixing Model for Reverse Osmosis**

The process flow diagram for the complete-mixing model is shown in

Fig. 24.6-4. The model is a simplified one for use with low concentrations of salt at about 1% or so, such as occur in brackish waters. Also, a relatively low recovery of solvent occurs and the effects of concentration polarization are small. Since the concentration of the permeate is very low, the permeate side acts as though it were completely mixed.

For the overall material balance for dilute solutions,

$$q_f = q_1 + q_2 \quad (24.6-12)$$

where  $q_f$  is volumetric flow rate of feed, m<sup>3</sup>/s;  $q_2$  is flow rate of permeate, m<sup>3</sup>/s; and  $q_1$  is flow rate of residue or exit, m<sup>3</sup>/s. Making a solute balance,

$$c_f q_f = c_1 q_1 + c_2 q_2 \quad (24.6-13)$$

Defining the cut or fraction of solvent recovered as  $\theta = q_2/q_f$ , Eq. (24.7-13) becomes

$$c_f = (1-\theta)c_1 + \theta c_2 \quad (24.6-14)$$

The equations previously derived for the fluxes and rejection are useful in this case and are as follows:

$$N_w = A_2(\Delta P - \Delta \pi) \quad (24.6-2)$$

$$N_s = A_s(c_1 - c_2) \quad (24.6-4)$$

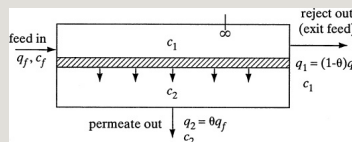


Figure 24.6-4. *Process flow for complete-mixing model for reverse osmosis.*

$$R = \frac{c_1 - c_2}{c_1} \quad (24.6-7)$$

$$R = B(\Delta P - \Delta \pi) / 1 + B(\Delta P - \Delta \pi) \quad (24.6-8)$$

When the cut or fraction recovered,  $\theta$ , is specified, the solution is trial and error. Since the permeate and reject concentrations  $c_1$  and  $c_2$  are unknown, a value of  $c_2$  is assumed. Then,  $c_1$  is calculated from Eq. (24.6-14). Next,  $N_w$  is obtained from Eq. (24.6-2) and  $c_2$  from Eqs. (24.6-7) and (24.6-8). If the calculated value of  $c_2$  does not equal the assumed value, the procedure is repeated.

When concentration-polarization effects are present, an estimated value of  $\beta$  can be used to make an approximate correction for these effects. This is used in Eq. (24.6-10) to obtain a value of  $\Delta \pi$  for use in Eqs. (24.6-2) and (24.6-8). Also, Eq. (24.6-11) will replace Eq.



(24.6-4). A more detailed analysis of this complete mixing model is given by others (H1, K1), in which the mass-transfer coefficient in the concentration-polarization boundary layer is used.

The cross-flow model for reverse osmosis is similar to that for gas separation by membranes, which will be discussed in Section 25.4. Because of the small solute concentration, the permeate side acts as if completely mixed. Hence, even if the module is designed for countercurrent or cocurrent flow, the cross-flow model is valid. This is discussed in detail elsewhere (H1).

## **24.7 Dialysis**

### **24.7A Series Resistances in Membrane Processes**

In membrane processes with liquids,

the solute molecules must first be transported or diffused through the liquid film of the first liquid phase on one side of the solid membrane, then through the membrane itself, and finally through the film of the second liquid phase. This is shown in Fig. 24.7-1a, where  $c_1$  is the bulk liquid-phase concentration of the diffusing solute  $A$  in  $\text{kg mol } A/\text{m}^3$ ,  $c_{1i}$  is the concentration of  $A$  in the fluid just adjacent to the solid, and  $c_{1iS}$  is the concentration of  $A$  in the solid at the surface and is in equilibrium with  $C_{1i}$ . The mass-transfer coefficients are  $k_{c1}$  and  $k_{c2}$  in  $\text{m/s}$ . The equilibrium distribution coefficient  $K'$  is defined as

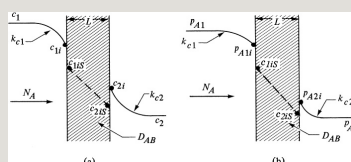


Figure 24.7-1. *Concentration profiles for membrane processes: (a) two liquid films and a solid, (b) two gas films and a solid.*

$$K' = \frac{c_1}{c_2} = \frac{L}{l_1 + l_2} = \frac{c_1 l_1}{c_2 l_2} \quad (24.7-1)$$

Note that  $K'$  is the inverse of  $K$  defined in Eq. (20.1-16).

The flux equations through each phase are all equal to each other at steady state and are as follows:

$$N_A = k_{c1}(c_1 - c_{1i}) = \frac{DAB}{L}(c_{1i} - c_{2i}) = k_{c2}(c_{2i} - c_2) \quad (24.7-2)$$

Substituting  $c_{1i} = K' c_{2i}$  and  $c_{2i} = K' c_{1i}$  into Eq. (24.7-2),

$$N_A = k_{c1}(c_1 - c_{1i}) = \frac{DAB}{L} K' (c_{1i} - c_{2i}) = \frac{DAB}{L} K' (c_{1i} - c_{1i}) = 0$$

$$(24.7-3)$$

$$P_M = D_{AB} K' L \quad (24.7-4)$$

where  $p_M$  is the permeance in the solid in m/s,  $L$  is the thickness in m, and  $D_{AB}$  is the diffusivity of A in the solid in m<sup>2</sup>/s. Note that the permeance  $p_M$  in Eq. (24.7-4) is different from the permeability  $p_M$  defined in Eq. (19.3-9). Also, the value of  $p_M$  is inversely proportional to the thickness  $L$ . Instead of determining  $D_{AB}$  and  $K'$  in two separate experiments, it is more convenient to determine  $p_M$  in one separate diffusion experiment. Solving each of the parts of Eq. (24.7-3) for the concentration difference,

$$\begin{aligned} c_1 - c_{1i} &= N_A k_{c1} (c_{1i} - c_2) = N_A p_M c_2 (c_1 - c_2) \\ c_2 &= N_A k_{c2} \quad (24.7-5) \end{aligned}$$

Adding the equations, the internal

concentrations  $c_{1i}$  and  $c_{2i}$  drop out, and the final equation is

$$N_A = \frac{c_1 - c_2}{\frac{1}{k_{c1}} + \frac{L}{D_{AB}} + \frac{1}{k_{c2}}} \quad (24.7-6)$$

In some cases, the resistances in the two liquid films are quite small compared to the membrane resistance, which controls the permeation rate.

**EXAMPLE 24.7-1. Membrane Diffusion and Liquid Film Resistances**

A liquid containing dilute solute  $A$  at a concentration  $c_1 = 3 \times 10^{-2}$  kg mol/m<sup>3</sup> is flowing rapidly past a membrane of thickness  $L = 3.0 \times 10^{-5}$  m. The distribution coefficient  $K' = 1.5$  and  $D_{AB} = 7.0 \times 10^{-11}$  m<sup>2</sup>/s in the membrane. The solute diffuses through the membrane, and its concentration on the other side is  $c_2 = 0.50 \times 10^{-2}$  kg mol/m<sup>3</sup>. The mass-transfer coefficient  $k_{c1}$  is large and can be considered as infinite, and  $k_{c2} = 2.02 \times 10^{-5}$  m/s.

- Derive the equation to calculate the steady-state flux  $N_A$  and make a sketch.
- Calculate the flux and the concentrations at the membrane interfaces.

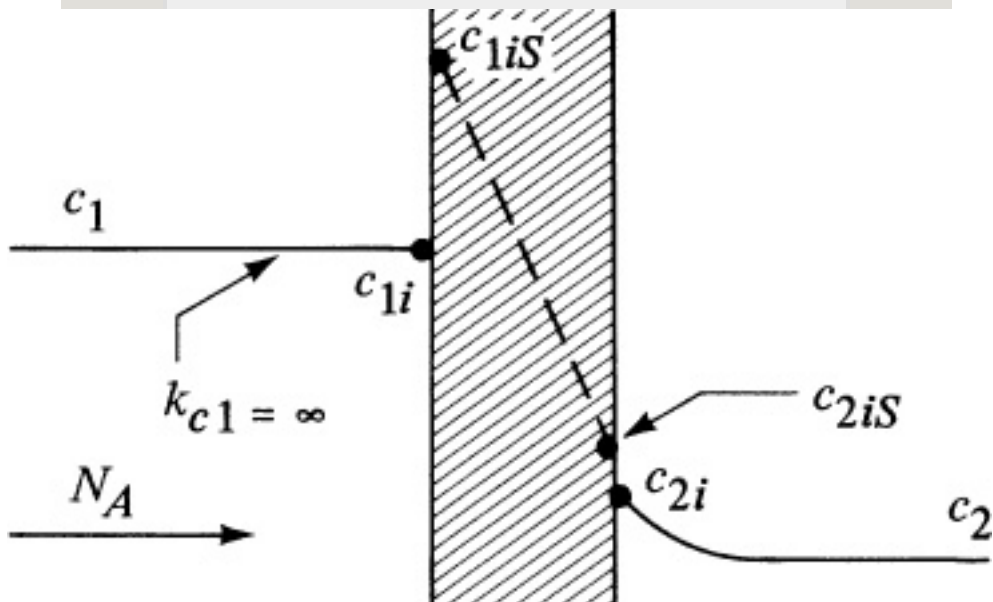


Figure 24.7-2. Concentrations for Example 24.7-1.

**Solution:** For part (a), the sketch is shown in Fig. 24.7-2. Note that the concentration profile on the left side is flat ( $k_{c1} = \infty$ ) and  $c_1 = c_{1i}$ . The derivation is the same as for Eq. (24.7-6), but  $1/k_{c1} = 0$  to give

$$N_A = c_1 - c_{2i} / pM + 1/k_{c2} \quad (24.7-7)$$

For part (b), to calculate the flux using Eqs. (24.7-4) and (24.7-7),

$$\begin{aligned} pM &= DABK'L = 7.0 \times 10^{-11} (1.5) 3.0 \times 10^{-5} = 3.5 \times 10^{-6} \text{ m} \\ sN_A &= c_1 - c_{2i} / pM + 1/ \\ k_{c2} &= 3.0 \times 10^{-2} / 3.5 \times 10^{-6} + 1/2.02 \times 10^{-5} = 7.458 \times 10^{-8} \text{ kg mol/} \\ &\quad \text{s} \cdot \text{m}^2 \end{aligned}$$

To calculate  $c_{2i}$ ,

$$N_A = 7.458 \times 10^{-8} = k_{c2}(c_{2i} - c_2) = 2.02 \times 10^{-5}(c_{2i} - 0.5 \times 10^{-2})$$

Solving,  $c_{2i} = 0.869 \times 10^{-2} \text{ kg mol/m}^3$ . Also, using Eq. (24.7-1),

$$K' = 1.5 = c_{2iS} c_{2i} = c_{2iS} 0.869 \times 10^{-2}$$

Solving,  $c_{2iS} = 1.304 \times 10^{-2} \text{ kg mol/m}^3$ .

## 24.7B Dialysis Processes

Dialysis uses a semipermeable membrane to separate species by virtue of their different diffusion rates in the membrane. The feed solution or dialyzate, which contains the solutes to be separated, flows on one side of the membrane and the solvent or diffusate stream flows on the other side. Some solvent may also diffuse across the membrane in the opposite direction, which reduces performance by diluting the dialyzate.

In practice, dialysis is used to separate species that differ appreciably in size and thus have a reasonably large difference in diffusion rates. Solute fluxes depend on the concentration gradient in the membrane. Hence,

dialysis is characterized by low flux rates in comparison to other membrane processes, such as reverse osmosis and ultrafiltration, which depend on applied pressure.

In general, dialysis is used with aqueous solutions on both sides of the membrane. The film resistances can be appreciable compared to the membrane resistance. Applications include recovery of sodium hydroxide in cellulose processing, recovery of acids from metallurgical liquors, removal of products from a culture solution in fermentation, desalting of cheese whey solids, and reduction of the alcohol content of beer. Many small-scale applications occur in the pharmaceutical industry.

#### **24.7C Types of Equipment for Dialysis**



Various geometrical configurations are used in liquid membrane processes. A common one is similar to a filter press, where the membrane is a flat plate. Vertical solid membranes are placed in between alternating liquor and solvent feed frames, with the liquor to be dialyzed being fed to the bottom and the solvent to the top of these frames. The dialyzate and the diffusate are removed through channels located at the top and bottom of the frames, respectively. The most important type consists of many small tubes or very fine hollow fibers arranged in a bundle, like a heat exchanger. This type of unit has a very high ratio of membrane area to the volume of the unit.

#### **24.7D Hemodialysis in an Artificial Kidney**

An important example of the liquid permeation process is dialysis with an artificial kidney in the biomedical field. In this application for purifying human blood, the principal solutes removed are the small solutes urea, uric acid, creatinine, phosphates, and excess amounts of chloride. A typical membrane used is cellophane about 0.025 mm thick, which allows small solutes to diffuse but retains the large proteins in the blood. During the hemodialysis, blood is passed on one side of the membrane while an aqueous dialyzing fluid flows on the other side. Solutes such as urea, uric acid, NaCl, and so on, which have elevated concentrations in the blood, diffuse across the membrane to the dialyzing aqueous solution, which contains certain

concentrations of solutes such as potassium salts, and so on, to ensure that concentrations in the blood do not drop below certain levels. In one configuration, the membranes are stacked in the form of a multilayered sandwich, with blood flowing past one side of the membrane and dialyzing fluid past the other side. The hollow fiber type is used quite often.

**EXAMPLE 24.7-2. Dialysis to Remove Urea from Blood**

Calculate the flux and the rate of removal of urea at steady state in g/h from blood in a cuprophane (cellophane) membrane dialyzer at 37°C. The membrane is 0.025 mm thick and has an area of 2.0 m<sup>2</sup>. The mass-transfer coefficient on the blood side is estimated as  $k_{c1} = 1.25 \times 10^{-5}$  m/s and that on the aqueous side is  $3.33 \times 10^{-5}$  m/s. The permeance of the membrane is  $8.73 \times 10^{-6}$  m/s (B2). The concentration of urea in the blood is 0.02 g urea/100 mL and that in the dialyzing fluid will be assumed as 0.

**Solution:** The concentration  $c_1 = 0.02/100 = 2.0 \times 10^{-4}$  g/mL = 200 g/m<sup>3</sup> and  $c_2 = 0$ . Substituting into Eq. (24.7-6),

$$N_A = \frac{c_1 - c_2}{\frac{1}{k_{c1}} + \frac{L}{D} + \frac{1}{k_{c2}}} = \frac{200 - 0}{\frac{1}{1.25 \times 10^{-5}} + \frac{0.025}{8.73 \times 10^{-6}} + \frac{1}{3.33 \times 10^{-5}}} = 8.91 \times 10^{-4} \text{ g/s} \cdot \text{m}^2$$

For a time of 1 h and an area of 2.0 m<sup>2</sup>,

$$\text{rate of removal} = 8.91 \times 10^{-4} (3600) (2.0) = 6.42 \text{ g urea/h}$$

## 24.8 Chapter Summary

### *Dead-End Filtration*

#### **Types of Dead End Filters**

1. Bed filters
2. Plate-and-frame filter presses
3. Leaf filters
4. Continuous rotary filters

#### **Filtration Equations for Constant-Pressure Filtration**

$$\frac{dV}{dt} = \frac{\mu \alpha c s A^2 (-\Delta p)}{V + \mu A (-\Delta p) R_m} = \frac{K_p V}{V + B} \quad (24.2-13)$$

where

$$t = \frac{K_p}{2} V^2 + B V \quad (24.2-17)$$

Dividing by  $V$

$$tV = K_p V^2 + B \quad (24.2-18)$$

### **Filtration Equations for Constant-Rate Filtration**

$$-\Delta p = (\mu \alpha c_s A^2 dV/dt) V + (\mu R_m A dV/dt) = K V V + C \quad (24.2-27)$$

### ***Cross-Flow Filtration***

#### **Flux Equation for Ultrafiltration**

$$N_w p = k c \ln(c/s/c_1) \quad (24.5-4)$$

#### **Flux Equation for Reverse Osmosis**

$$N_w = P_w L_m (\Delta P - \Delta \pi) = A_w (\Delta P - \Delta \pi) \quad (24.6-2)$$

#### **Flux Equation for Dialysis**

$$N_A = c_1 - c_2 / (k c_1 + 1/p_M + 1/k c_2) \quad (24.7-6)$$

## **Problems**

### **24.2-1. *Constant-Pressure Filtration and Filtration Constants.***

Data for the filtration of  $\text{CaCO}_3$  slurry in water at 298.2 K (25°C) are reported as follows ( $R_1$ ,  $R_2$ ,  $M_1$ ) at a constant pressure ( $-\Delta p$ ) of 46.2 kN/m<sup>2</sup> (6.70 psia). The area of the plate-and-frame press was 0.0439 m<sup>2</sup> (0.473 ft<sup>2</sup>) and the slurry concentration was 23.47 kg solid/m<sup>3</sup> filtrate. Calculate the constants  $\alpha$  and  $R_m$ . Data are given as  $t$  = time in s and  $V$  = volume of filtrate collected in m<sup>3</sup>.

**Ans.**  $\alpha = 1.106 \times 10^{11} \text{ m/kg}$  ( $1.65 \times 10^{11} \text{ ft/lbm}$ ),  $R_m = 6.40 \times 10^{10} \text{ m}^{-1}$  ( $1.95 \times 10^{10} \text{ ft}^{-1}$ )

### **24.2-2. Filtration Constants for**

**Constant-Pressure Filtration.** Data for constant-pressure filtration at 194.4 kN/

$m_2$  are reported for the same slurry and press as in Problem 24.2-1 as follows, where  $t$  is in s and  $V$  in  $m^3$ :

Calculate the constants  $\alpha$  and  $R_m$ .

$$\text{Ans. } \alpha = 1.61 \times 10^{11} \text{ m/kg}$$

### **24.2-3. *Compressibility of Filter Cake.***

Use the data for specific cake resistance  $\alpha$  from Example 24.2-1 and Problems 24.2-1 and 24.2-2 and determine the compressibility constant  $s$  in Eq. (24.2-11). Plot  $\ln \alpha$  versus  $\ln(-\Delta p)$  and determine the slope  $s$ .

**24.2-4. *Prediction of Filtration Time and Washing Time.*** The slurry used in Problem 24.2-1 is to be filtered in a plate-and-frame press having 30 frames

and  $0.873 \text{ m}^2$  area per frame. The same pressure,  $46.2 \text{ kN/m}^2$ , will be used in constant-pressure filtration. Assume the same filter-cake properties and filter cloth, and calculate the time to recover  $2.26 \text{ m}^3$  of filtrate. At the end, using through-washing and  $0.283 \text{ m}^3$  of wash water, calculate the time of washing and the total filter-cycle time if cleaning the press takes 30 min.

**24.2-5. Constants in Constant-Pressure Filtration.** McMillen and Webber (M2), using a filter press with an area of  $0.0929 \text{ m}^2$ , performed constant-pressure filtration at  $34.5 \text{ kPa}$  of a  $13.9 \text{ wt } \%$   $\text{CaCO}_3$  solids-in-water slurry at  $300 \text{ K}$ . The mass ratio of wet cake to dry cake was  $1.59$ . The dry-cake density was  $1017 \text{ kg/m}^3$ . The data obtained are as follows, where  $W = \text{kg filtrate}$  and  $t =$



time in s:

Calculate the values of  $\alpha$  and  $R_m$ .

**24.2-6. *Constant-Pressure Filtration and Washing in a Leaf Filter.*** An experimental filter press having an area of  $0.0414 \text{ m}^2$  ( $R_1$ ) is used to filter an aqueous  $\text{BaCO}_3$  slurry at a constant pressure of  $267 \text{ kPa}$ . The filtration equation obtained was

$$tV = 10.25 \times 10^6 V + 3.4 \times 10^3$$

where  $t$  is in s and  $V$  in  $\text{m}^3$ .

- If the same slurry and conditions are used in a leaf press having an area of  $6.97 \text{ m}^2$ , how long will it take to obtain  $1.00 \text{ m}^3$  of filtrate?
- After filtration, the cake is to be washed with  $0.100 \text{ m}^3$  of water. Calculate the time of washing.

**Ans.** (a)  $t = 381.8 \text{ s}$

**24.2-7. Constant-Rate Filtration of Incompressible Cake.** The filtration equation for filtration at a constant pressure of 38.7 psia (266.8 kPa) is

$$tV = 6.10 \times 10^{-5} V + 0.01$$

where  $t$  is in s,  $-\Delta p$  in psia, and  $V$  in liters. The specific resistance of the cake is independent of pressure. If the filtration is run at a constant rate of 10 liters/s, how long will it take to reach 50 psia?

**24.2-8. Effect of Filter-Medium Resistance on a Continuous Rotary-Drum Filter.** Repeat Example 24.2-4 for the continuous rotary-drum vacuum filter but do not neglect the constant  $R_m$ , which is the filter-medium resistance to

flow. Compare with the results of Example 24.2-4.

$$\text{Ans. } A = 7.78 \text{ m}^2$$

**24.2-9. *Throughput in a Continuous Rotary-Drum Filter.*** A rotary-drum filter having an area of  $2.20 \text{ m}^2$  is to be used to filter the  $\text{CaCO}_3$  slurry given in Example 24.2-4. The drum has a 28% submergence and the filter-cycle time is 300 s. A pressure drop of  $62.0 \text{ kN/m}^2$  is to be used. Calculate the slurry feed rate in  $\text{kg slurry/s}$  for the following cases:

- Neglect the filter-medium resistance.
- Do not neglect the value of  $B$ .

**24.5-1. *Flux for Ultrafiltration.*** A solution containing 0.9 wt % protein is to undergo ultrafiltration using a pressure difference of 5 psi. The

membrane permeability is  $A_w = 1.37 \times 10^{-2} \text{ kg/s} \cdot \text{m}^2 \cdot \text{atm}$ . Assuming no effects of polarization, predict the flux in  $\text{kg/s} \cdot \text{m}^2$  and in units of  $\text{gal/ft}^2 \cdot \text{day}$ , which are often used in industry.

**Ans.**  $9.88 \text{ gal/ft}^2 \cdot \text{day}$

**24.5-2. Time for Ultrafiltration Using Recirculation.** It is desired to use ultrafiltration for 800 kg of a solution containing 0.05 wt % of a protein to obtain a solution of 1.10 wt %. The feed is recirculated past the membrane with a surface area of  $9.90 \text{ m}^2$ . The permeability of the membrane is  $A_w = 2.50 \times 10^{-2} \text{ kg/s} \cdot \text{m}^2 \cdot \text{atm}$ . Neglecting the effects of concentration polarization, if any, calculate the final amount of solution and the time to achieve this, using a pressure difference of 0.50 atm.

**24.6-1. *Osmotic Pressure of Salt and Sugar Solutions.*** Calculate the osmotic pressure of the following solutions at 25°C and compare with the experimental values:

- Solution of 0.50 g mol NaCl/kg H<sub>2</sub>O. (See Table 24.6-1 for the experimental value.)
- Solution of 1.0 g sucrose/kg H<sub>2</sub>O. (Experimental value = 0.0714 atm.)
- Solution of 1.0 g MgCl<sub>2</sub>/kg H<sub>2</sub>O. (Experimental value = 0.660 atm.)

**Ans.** (a)  $\pi = 24.39$  atm; (b)  $\pi = 0.0713$  atm; (c)  $\pi = 0.768$  atm

**24.6-2. *Determination of Permeability Constants for Reverse Osmosis.*** A cellulose–acetate membrane with an area of  $4.0 \times 10^{-3}$  m<sup>2</sup> is used at 25°C to determine the perme ability constants for reverse osmosis of a feed salt solution containing 12.0 kg NaCl/m<sup>3</sup> ( $\rho$

= 1005.5 kg/m<sup>3</sup>). The product solution has a concentration of 0.468 kg NaCl/m<sup>3</sup> ( $\rho = 997.3 \text{ kg/m}^3$ ). The measured product flow rate is  $3.84 \times 10^{-8} \text{ m}^3/\text{s}$  and the pressure difference used is 56.0 atm. Calculate the permeability constants and the solute rejection  $R$ .

**Ans.**  $A_w = 2.013 \times 10^{-4} \text{ kg solvent/s} \cdot \text{m}^2 \cdot \text{atm}$ ,  $R = 0.961$

### **24.6-3. Performance of a Laboratory**

**Reverse-Osmosis Unit.** A feed solution

at 25°C contains 3500 mg NaCl/L ( $\rho = 999.5 \text{ kg/m}^3$ ). The permeability constant

$A_w = 3.50 \times 10^{-4} \text{ kg solvent/s} \cdot \text{m}^2 \cdot \text{atm}$

and  $A_s = 2.50 \times 10^{-7} \text{ m/s}$ . Using a  $\Delta P =$

35.50 atm, calculate the fluxes, solute rejection  $R$ , and product solution

concentration in mg NaCl/L. Repeat, but

using a feed solution of 3500 mg BaCl<sub>2</sub>/

L. Use the same value of  $A_w$ , but  $A_s = 1.00 \times 10^{-7}$  m/s (A1).

**24.6-4. *Effect of Pressure on the Performance of a Reverse-Osmosis Unit.*** Using the same conditions and permeability constants as in Example 24.6-3, calculate the fluxes, solute rejection  $R$ , and product concentration  $c_2$  for  $\Delta P$  pressures of 17.20, 27.20, and 37.20 atm. (*Note:* The values for 27.20 atm have already been calculated.) Plot the fluxes,  $R$ , and  $c_2$ , versus the pressure.

**24.6-5. *Effect of Concentration Polarization on Reverse Osmosis.*** Repeat Example 24.6-3 but use a concentration polarization of 1.5. (*Note:* The flux equations and the solute rejection  $R$  should be calculated using

this new value of  $c_1$ .)

$$\text{Ans. } N_w = 1.171 \times 10^{-2} \text{ kg solvent/s} \cdot \text{m}^2, c_2 = 0.1361 \text{ kg NaCl/m}^3$$

### ***24.6-6. Performance of a Complete-Mixing Model for Reverse Osmosis.***

Use the same feed conditions and pressures given in Example 24.6-3.

Assume that the cut or fraction recovered of the solvent water will be 0.10 instead of the very low water recovery assumed in Example 24.6-3.

Hence, the concentrations of the entering feed solution and the exit feed will not be the same. The flow rate  $q_2$  of the permeate water solution is 100 gal/h. Calculate  $c_1$  and  $c_2$  in kg NaCl/m<sup>3</sup> and the membrane area in m<sup>2</sup>.

$$\text{Ans. } c_1 = 2.767 \text{ kg/m}^3, c_2 = 0.0973 \text{ kg/}$$



$$m_3, \text{ area} = 8.68 \text{ m}^2$$

### ***24.7-1. Diffusion Through Liquids and***

***a Membrane.*** A membrane process is

being designed to recover solute A from

a dilute solution where  $c_1 = 2.0 \times 10^{-2}$

kg mol A/m<sup>3</sup> by dialysis through a

membrane to a solution where  $c_2 = 0.3 \times$

$10^{-2}$ . The membrane thickness is  $1.59 \times$

$10^{-5}$  m, the distribution coefficient  $K' =$

0.75,  $D_{AB} = 3.5 \times 10^{-11}$  m<sup>2</sup>/s in the

membrane, the mass-transfer coefficient

in the dilute solution is  $k_{c1} = 3.5 \times 10^{-2}$

m/s, and  $k_{c2} = 2.1 \times 10^{-5}$ .

- Calculate the individual resistances, total resistance, and total percent resistance of the two films.
- Calculate the flux at steady state and the total area in m<sup>2</sup> for a transfer of 0.01 kg mol solute/h.
- Increasing the velocity of both liquid phases flowing past the surface of the membrane will increase the mass-transfer coefficients, which are

approximately proportional to  $v^{0.6}$ , where  $v$  is velocity. If the velocities are doubled, calculate the total percent resistance of the two films and the percent increase in flux.

**Ans.** (a) Total resistance =  $6.823 \times 10^{-5}$  s/m, 11.17% resistance; (b)  $N_A = 2.492 \times 10^{-8}$  kg mol A/s  $\cdot$  m<sup>2</sup>, area = 111.5 m<sup>2</sup>

**24.7-2. Suitability of a Membrane for Hemodialysis.** Experiments are being conducted to determine the suitability of a cellophane membrane 0.029 mm thick for use in an artificial-kidney device. In an experiment at 37°C using NaCl as the diffusing solute, the membrane separates two components containing stirred aqueous solutions of NaCl, where  $c_1 = 1.0 \times 10^{-4}$  g mol/cm<sup>3</sup> (100 g mol/m<sup>3</sup>) and  $c_2 = 5.0 \times 10^{-7}$ . The mass-transfer coefficients on either side of the membrane have been estimated as  $k_{c1} = k_{c2} = 5.24 \times 10^{-5}$  m/s. Experimental data

obtained gave a flux  $N_A = 8.11 \times 10^{-4}$  g mol NaCl/s · m<sup>2</sup> at pseudo-steady-state conditions.

- Calculate the permeability  $p_M$  in m/s and  $D_{AB} K'$  in m<sup>2</sup>/s.
- Calculate the percent resistance to diffusion in the liquid films.

## References

## Notation

# Chapter 25. Gaseous Membrane Systems

## 25.0 Chapter Objectives

On completion of this chapter, a student should be able to:

- Describe, in membrane processes with two gas phases, the three resistances associated with the flux through a membrane
- Explain the differences between a symmetric and an asymmetric membrane
- Describe the three common types of equipment used for gas-permeation membrane processes
- Describe the four ideal flow patterns in a membrane separator and, for each respective model, solve numerically for the membrane area.

## 25.1 Gas Permeation

### 25.1A Series Resistances in Membrane Processes

In membrane processes with two gas phases and a solid membrane, similar equations can be written for the case illustrated in, Fig. 24.7-1b. The equilibrium relation between the solid and gas phases is given by

$$H = S \frac{22.414}{c} = \frac{c_1}{S_1} = \frac{c_2}{S_2} \quad (25.1-1)$$

where  $S$  is the solubility of  $A$  in  $\text{m}^3$  (STP)/ $\text{atm} \cdot \text{m}^3$  solid, as shown in Eq. (19.3-5), and  $H$  is the equilibrium relation in  $\text{kg mol}/\text{m}^3 \cdot \text{atm}$ . This is similar to Henry's law. The flux equations in each phase are as follows:

$$\begin{aligned} N_A &= k_{c1} \frac{1}{RT} (p_{A1} - p_{A1i}) = D_{AB} L (c_1 S - c_2 S) \quad (25.1-2) \\ &= D_{AB} S L (22.414) (p_{A1i} - p_{A2i}) \quad (25.1-3) \end{aligned}$$

$$=kc_2RT(p_{A2i}-p_{A2})(25.1-4)$$

The permeability  $P_M$  given previously is

$$P_M = DAB S m^3(STP) \cdot ms \cdot m^2 C.S. \cdot atm (19.3-9)$$

The permeability  $P_M$  is given in kg mol units by dividing Eq. (19.3-9) by 22.414 m<sup>3</sup>/kg mol:

$$mol \cdot ms \cdot m^2 C.S. \cdot atm = 122.414 m^3(STP) \cdot ms \cdot m^2 C.S. \cdot atm (20.1-9)$$

Then, the flux  $N_A$  through the membrane given by Eq. (25.1-3) becomes

$$N_A = P_M L (p_{A1i} - p_{A2i}) (25.1-6)$$

Eliminating the interfacial concentrations as before,

$$N_A = (p_{A1} - p_{A2}) \frac{1}{(k_{c1}/RT) + 1/(P_M/L) + 1/(k_{c2}/RT)} (25.1-7)$$

In the case where pure A ( $p_{A1}$ ) is on the left side of the membrane, there is no diffusional resistance in the gas phase, and  $k_{c1}$  can be considered to be infinite. Note that  $k_{G1} = k_{c1}/RT$ .

An example of gas permeation in a membrane is the use of a polymeric membrane as an oxygenator for a heart–lung machine to oxygenate blood. In this biomedical application, pure O<sub>2</sub> gas is on one side of a thin membrane and blood is on the other side. Oxygen diffuses through the membrane into the blood and CO<sub>2</sub> diffuses in the reverse direction into the gas stream.

### **25.1B Types of Membranes and Permeabilities for Separation of Gases**

*1. Types of dense-phase symmetric membranes.* Early membranes were limited in their use because of low

selectivities in separating two gases and quite low permeation fluxes.

This low-flux problem was due to the fact that the membranes had to be relatively thick (1 mil or 1/1000 of an inch or greater) in order to avoid tiny holes, which reduced the separation by allowing viscous or Knudsen flow of the feed.

Development of silicone polymers (1-mil thickness) increased the permeability by factors of 10–20 or so. These are called dense-phase symmetric membranes.

## *2. Types of asymmetric membranes.*

Newer asymmetric membranes include a very thin but dense skin on one side of the membrane supported by a porous substructure (R1). The dense skin has a thickness of about 1000Å and the



porous support thickness is about 25–100  $\mu$  m. The flux increase of these membranes is thousands of times higher than the 1-mil-thick original membranes. Some typical materials currently used for asymmetric membranes are a composite of polysulfone coated with silicone rubber, cellulose acetate and modified cellulose acetates, aromatic polyamides or aromatic polyimides, and silicone–polycarbonate copolymer on a porous support.

*3. Permeability of membranes.* The permeability  $P_M$  in Eqs. (19.3-9) and (25.1-6) is defined as  $D_{ABS}$  in  $\text{m}^3$  (STP)/ $\text{s m}^2 \text{ C.S.} \cdot \text{atm/m}$ . Since mixtures of gases are often present,  $P_A'$  for gas  $A$  and  $P_B'$  for gas  $B$  will be used instead of  $P_M$ . The different sets of units used and

their conversion factors are given in Table 25.1-1. Sometimes, units are given in terms of Barrers, as also defined in Table 25.1-1.

The accurate prediction of permeabilities of gases in membranes is generally not possible, and experimental values are needed. Experimental data for common gases in some typical dense-phase membranes are given in Table 25.1-2. Note that there are wide differences among the permeabilities of various gases in a given membrane. Silicone rubber exhibits very high permeabilities for the gases in the table.

Table 25.1-1. *Conversion Factors for Permeability  $PA'$  and Permeance  $PA'/t$*

--

## Table 25.1-2. *Permeabilities of Various Gases in Dense-Phase Symmetric Membranes*

For the effect of temperature  $T$  in K,  $\ln PA'$  is approximately a linear function of  $1/T$  and increases with  $T$ . However, operation at high temperatures can often degrade the membranes. When a mixture of gases is present, reductions in permeability of an individual component of up to 10% or so can often occur. In a few cases, much larger reductions have been observed (R1). Hence, when using a mixture of gases, experimental data should be obtained to determine if there is any interaction between the gases. The presence of water vapor can have similar effects on the permeabilities and can also possibly

damage the membranes.

*4. Permeance of membranes.* In many cases, especially in asymmetric membranes, the thickness  $t$  is not measured and only experimental values of permeance  $PA'/t$  are given.

Conversion factors are also given in Table 25.1-1.

#### **25.1C Types of Equipment for Gas-Permeation Membrane Processes**

*1. Flat membranes.* Flat membranes are mainly used in experiments to characterize the permeability of the membrane. The modules are easy to fabricate and use, and the areas of the membranes are well defined. In some cases, modules are stacked together like a multilayer sandwich or plate-and-frame filter press. The major drawback of this type is the

very small membrane area per unit of separator volume. Small commercial flat membranes are used for producing oxygen-enriched air for individual medical applications.

*2. Spiral-wound membranes.* This configuration retains the simplicity of fabricating flat membranes while markedly increasing the membrane area per unit of separator volume up to 100 ft<sup>2</sup> /ft<sup>3</sup> (328 m<sup>2</sup> /m<sup>3</sup>) and decreasing pressure drops (R1). The assembly consists of a sandwich of four sheets wrapped around a central core of a perforated collecting tube. The four sheets consist of a top sheet of an open separator grid for the feed channel, a membrane, a porous felt backing for the permeate channel, and another membrane, as shown in Fig. 25.1-1. The

spiral-wound element is 100–200 mm in diameter and is about 1–1.5 m long in the axial direction. The flat sheets before rolling are about 1–1.5 m by about 2–2.5 m. The space between the membranes (open grid for feed) is about 1 mm and the thickness of the porous backing (for permeate) is about 0.2 mm.

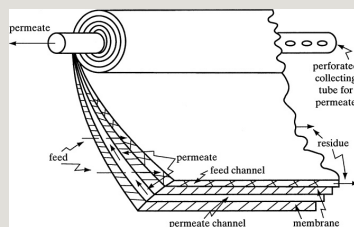


Figure 25.1-1. *Spiral-wound elements and assembly.* From R. I. Berry, *Chem. Eng.*, 88 (July 13), 63 (1981). With permission.

The whole spiral-wound element is located inside a metal shell. The feed gas enters at the left end of the shell, enters the feed channel, and flows through this channel in the axial direction of the spiral to the right end of

the assembly (Fig. 25.1-1). Then the exit residue gas leaves the shell at this point. The feed stream, which is in the feed channel, permeates perpendicularly through the membrane. This permeate then flows through the permeate channel in a direction perpendicular to the feed stream toward the perforated collecting tube, where it leaves the apparatus at one end. This is illustrated in Fig. 25.1-2, where the local gas-flow paths are shown for a small element of the assembly.

*3. Hollow-fiber membranes.* The membranes are in the shape of very-small-diameter hollow fibers. The inside diameter of the fibers is in the range of 100–500  $\mu\text{m}$  and the outside diameter is 200–1000  $\mu\text{m}$ , with the length up to 3–5 m. The module resembles a shell-and-

tube heat exchanger. Thousands of fine tubes are bound together at each end into a tube sheet that is surrounded by a metal shell having a diameter of 0.1–0.2 m, so that the membrane area per unit volume is up to 10000 m<sup>2</sup> /m<sup>3</sup> as in Fig. 25.1-3. A typical large industrial permeator has fibers of 200  $\mu$  m ID and 400  $\mu$  m OD in a shell 6 in. in diameter and 10 ft long (P5).

Typically, the high-pressure feed enters the shell side at one end and leaves at the other end. The hollow fibers are closed at one end of the tube bundles. The permeate gas inside the fibers flows countercurrently to the shell-side flow and is collected in a chamber where the open ends of the fibers terminate. Then, the permeate exits the device.



In some lower-pressure operations, such as for separation of air to produce nitrogen, the feed enters inside the tubes (P5).

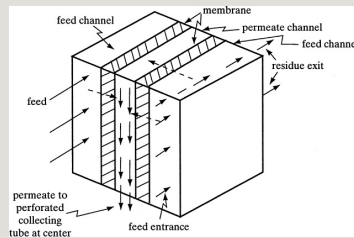


Figure 25.1-2. *Local gas-flow paths for a spiral-wound separator.*

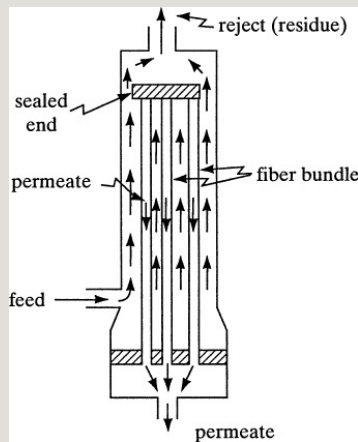


Figure 25.1-3. *Hollow-fiber separator assembly.*

## 25.1D Introduction to Types of Flow in Gas Permeation

## *1. Types of flow and diffusion*

*gradients.* In a membrane process, high-pressure feed gas is supplied to one side of the membrane and permeates normal to the membrane. The permeate leaves in a direction normal to the membrane, accumulating on the low-pressure side. Because of the very high diffusion coefficient in gases, concentration gradients in the gas phase in the direction normal to the surface of the membrane are quite small. Hence, gas film resistances compared to the membrane resistance can be neglected. This means that the concentration in the gas phase in a direction perpendicular to the membrane is essentially uniform, whether or not the gas stream is flowing parallel to

the surface.

If the gas stream is flowing parallel to the membrane in essentially plug flow, a concentration gradient occurs in this direction. Hence, several cases can occur in the operation of a membrane module. The permeate side of the membrane can be operated so that the phase is completely mixed (uniform concentration) or so that the phase is in plug flow. The high-pressure feed side can also be completely mixed or in plug flow. Countercurrent or cocurrent flow can be used when both sides are in plug flow. Hence, separate theoretical models must be derived for these different types of operation, as discussed in Sections 25.2–25.6.

## *2. Assumptions used and ideal flow*

*patterns*. In deriving theoretical models for gas separation by membranes, isothermal conditions and negligible pressure drop in the feed stream and permeate stream are generally assumed. It is also assumed that the effects of total pressure and/or composition of the gas are negligible and that the permeability of each component is constant (i.e., no interactions between different components).

Since there are a number of idealized flow patterns, the important types are summarized in Fig. 25.1-4. In Fig. 25.1-4a, complete mixing is assumed for the feed chamber and the permeate chamber. Similar to a continuous-stirred tank, the reject or residue and the product or permeate compositions are equal to their respective uniform

compositions in the chambers.

An ideal cross-flow pattern is given in Fig. 25.1-4b, where the feed stream is in plug flow and the permeate flows in a normal direction away from the membrane without mixing. Since the feed composition varies along its flow path, the local permeate concentration also varies along the membrane path.

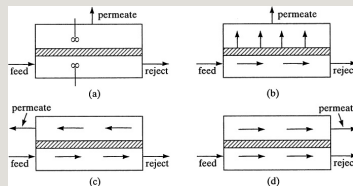


Figure 25.1-4. *Ideal flow patterns in a membrane separator for gases: (a) complete mixing, (b) cross-flow, (c) countercurrent flow, (d) cocurrent flow.*

In Fig. 25.1-4c, both the feed stream and permeate stream are in plug flow countercurrent to each other. The composition of each stream varies along

its flow path. Cocurrent flow of the feed and permeate streams is shown in Fig. 25.1-4d.

## **25.2 Complete-Mixing Model for Gas Separation by Membranes**

### **25.2A Basic Equations Used**

In Fig. 25.2-1, a detailed process flow diagram is shown for complete mixing. When a separator element is operated at a low recovery (i.e., where the permeate flow rate is a small fraction of the entering feed rate), there is a minimal change in composition. Then, the results derived using the complete-mixing model provide reasonable estimates of permeate purity. This case was derived by Weller and Steiner (W2).

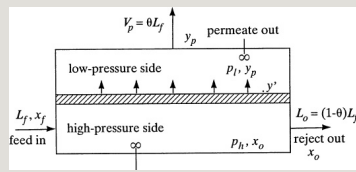


Figure 25.2-1. Process flow for complete mixing case.

Using nomenclature similar to that for distillation (P5), using the feed and nonpermeate flow rate as  $L$  and composition  $x$  mole fraction and the permeate flow rate as  $V$  and composition  $y$ .

The overall material balance (Fig. 25.2-1) is as follows:

$$L_f = L_o + V_p \quad (25.2-1)$$

where  $L_f$  is total feed flow rate in  $\text{cm}^3$  (STP)/s;  $L_o$  is outlet reject flow rate,  $\text{cm}^3$  (STP)/s; and  $V_p$  is outlet permeate flow rate,  $\text{cm}^3$  (STP)/s. The cut or fraction of feed permeated,  $\theta$ , is given as

$$\theta = V_p L_f (25.2-2)$$

The rate of diffusion or permeation of species  $A$  (in a binary of  $A$  and  $B$ ) is given below by an equation similar to Eq. (25.1-6) but using  $\text{cm}^3$  (STP)/s as rate of permeation rather than flux in  $\text{kg mol/s} \cdot \text{cm}^2$ :

$$V_A A_m = V_p p A_m = (P_A' t) (p_h - p_l) x_o \quad (25.2-3)$$

where  $P_A'$  is permeability of  $A$  in the membrane,  $\text{cm}^3$  (STP)  $\cdot \text{cm}/(\text{s} \cdot \text{cm}^2 \cdot \text{cm Hg})$ ;  $V_A$  is flow rate of  $A$  in permeate,  $\text{cm}^3$  (STP)/s;  $A_m$  is membrane area,  $\text{cm}^2$ ;  $t$  is membrane thickness, cm;  $p_h$  is total pressure in the high-pressure (feed) side, cm Hg;  $p_l$  is total pressure in the low-pressure or permeate side, cm Hg;  $x_o$  is mole fraction of  $A$  in reject side;  $x_f$  is



mole fraction of  $A$  in feed; and  $y_p$  is mole fraction of  $A$  in the permeate. Note that  $p_{hx_o}$  is the partial pressure of  $A$  in the reject gas phase and  $p_{ly_p}$  is the partial pressure in the permeate side. A similar equation can be written for component  $B$ :

$$V_B A_m = V_p (1 - y_p) A_m = (P_B' t) [p_h (1 - x_o) - p_l (1 - y_p)] \quad (25.2-4)$$

where  $P'_B$  is permeability of  $B$ ,  $\text{cm}^3 (\text{STP}) \cdot \text{cm} / (\text{s} \cdot \text{cm}^2 \cdot \text{cm Hg})$ . The ideal separation factor  $\alpha^*$  is

$$\alpha^* = P_A' / P_B' \quad (25.2-5)$$

Dividing Eq. (25.2-3) by (25.2-4),

$$y_p (1 - y_p) = \alpha^* [x_o - (p_l / p_h) y_p] (1 - x_o) - (p_l / p_h) (1 - y_p) \quad (25.2-6)$$

This equation relates the reject concentration  $x_o$  to the permeate concentration  $y_p$ . The concentration in the bulk or reject gas phase is  $x_o$ . The permeate concentration  $y_p$  in the bulk gas phase is the same as the gas concentration  $y'$  on the lower-pressure side immediately adjacent to the dense-phase membrane or on the low-pressure side of the dense skin layer of the asymmetric membrane, which is called the interface or local concentration.

Equation (25.2-6) is a quadratic equation and its solution is

$$y_p = \frac{-b \pm \sqrt{b^2 - 4ac}}{2a} \quad (25.2-7)$$

where

$$\alpha = 1 - \alpha^*, b = -1 + \alpha^* + 1/r + \alpha^* - 1, c = -\alpha^* \alpha^*, r = p_l/p_h$$

Making an overall material balance on component A,

$$L_f x_f = L_o x_o + V_p y_p \quad (25.2-8)$$

Dividing by  $L_f$  and solving for the outlet reject composition,

$$x_o = x_f - \theta y_p (1 - \theta) \quad \text{or} \quad y_p = \frac{x_f - x_o}{\theta(1 - \theta)} \quad (25.2-9)$$

Substituting  $V_p = \theta L_f$  from Eq. (25.2-2) into Eq. (25.2-3) and solving for the membrane area,  $A_m$ ,

$$A_m = \theta L_f y_p (P A' / t) (p_h x_o - p_l y_p) \quad (25.2-10)$$

### **25.2B Solution of Equations for Design of a Complete-Mixing Case**

For design of a system, there are seven variables in the complete-

mixing model (H1),  $x_f$ ,  $x_o$ ,  $y_p$ ,  $\theta$ ,  $\alpha^*$ ,  $p_l/p_h$ , and  $A_m$ , four of which are independent variables. Two commonly occurring cases are considered here.

*Case 1.* This is the simplest case, where  $x_f$ ,  $x_o$ ,  $\alpha^*$ , and  $p_l/p_h$  are given and  $y_p$ ,  $\theta$ , and  $A_m$  are to be determined by solution of the equations. By use of the quadratic equation, Eq. (25.2-7) is solved for the permeate composition  $y_p$  in terms of  $x_o$ . Hence, to solve this case,  $y_p$  is first calculated using Eq. (25.2-7). Then, the fraction of feed permeated,  $\theta$ , is calculated using Eq. (25.2-9) and the membrane area,  $A_m$ , is calculated using Eq. (25.2-10).

**EXAMPLE 25.2-1. Design of a Membrane Unit for Complete Mixing**

A membrane is to be used to separate a gaseous mixture of A and B whose feed flow rate is  $L_f = 1 \times 10^4 \text{ cm}^3 \text{ (STP)/s}$

and feed composition of A is  $x_f = 0.50$  mole fraction. The desired composition of the reject is  $x_o = 0.25$ . The membrane thickness  $t = 2.54 \times 10^{-3}$  cm, the pressure on the feed side is  $p_h = 80$  cm Hg, and on the permeate side it is  $p_l = 20$  cm Hg. The permeabilities are  $PA' = 5 \times 10^{-10}$  cm<sup>3</sup> (STP) · cm/(s · cm<sup>2</sup> · cm Hg) and  $P_B = 5 \times 10^{-10}$ . Assuming the complete-mixing model, calculate the permeate composition,  $y_p$ , the fraction permeated,  $\theta$ , and the membrane area,  $A_m$ .

**Solution:** Substituting into Eq. (25.2-5),

$$\alpha^* = PA'PB' = 50 \times 10^{-10} / (5 \times 10^{-10}) = 10$$

Using Eq. (25.2-7),

$$r = p_l/p_h = 20/80 = 0.25 \quad a = 1 - \alpha^* = 1 - 10 = -9 \quad b = -1 + \alpha^* + 1r + \alpha^* r(\alpha^* - 1)$$

$$= -1 + 10 + 10.25 + 0.250.25(10 - 1) = 22.0 \quad c = -\alpha^* r \text{ or } = -100.25(0.25) = -10 \quad y_p = -b + b^2 - 4ac / 2a = -22.0 + (22.0)^2 - 4(-9)(-10) / 2(-9) = 0.604$$

Using the material-balance equation (25.2-9),

$$x_o = x_f - \theta y_p (1 - \theta); 0.25 = 0.50 - \theta(0.604)(1 - \theta)$$

Solving,  $\theta = 0.706$ . Also, using Eq. (25.2-10),

$$A_m = \theta L_f y_p (PA'/t)(p_h x_o - p_l y_p) = 0.706(1 \times 10^4)(0.604) [50 \times 10^{-10} / (2.54 \times 10^{-3})] (80 \times 0.25 - 20 \times 0.604) = 2.735 \times 10^8 \text{ cm}^2 (2.735 \times 10^4 \text{ m}^2)$$

**Case 2.** In this case,  $x_f$ ,  $\theta$ ,  $\alpha^*$ , and  $p_l/p_h$  are given and  $y_p$ ,  $x_o$ , and  $A_m$  are to be determined. Equation (25.2-7) cannot be solved for  $y_p$  since  $x_o$  is unknown. Hence,  $x_o$  from Eq. (25.2-9) is substituted into Eq. (25.2-7) and the

resulting equation solved for  $y_p$  using the quadratic equation, to give

$$y_p = \frac{-b_1 + b_1^2 - 4a_1c_1}{2a_1} \quad (25.2-11)$$

where

$$\begin{aligned} a_1 &= \theta + p_1 p_h - p_1 p_h \theta - \alpha^* \theta - \alpha^* p_1 p_h \\ + \alpha^* p_1 p_h \theta & b_1 = 1 - \theta - x_f - p_1 p_h + p_1 p_h \theta + \alpha^* \theta \\ + \alpha^* p_1 p_h - \alpha^* p_1 p_h \theta & + \alpha^* x_f c_1 = -\alpha^* x_f \end{aligned}$$

After solving for  $y_p$ , the value of  $x_o$  is calculated from Eq. (25.2-9) and  $A_m$  from Eq. (25.2-10).

**EXAMPLE 25.2-2. Membrane Design for the Separation of Air**

It is desired to determine the membrane area needed to separate an air stream using a membrane 1 mil thick with an oxygen permeability of  $P_A = 500 \times 10^{-10} \text{ cm}^3 (\text{STP}) \cdot \text{cm}/(\text{s} \cdot \text{cm}^2 \cdot \text{cm Hg})$ . An  $\alpha^* = 10$  for oxygen permeability divided by nitrogen permeability ( $S_2$ ) will be used. The feed rate is  $L_f = 1 \times 10^6 \text{ cm}^3 (\text{STP})/\text{s}$  and the fraction cut  $\theta = 0.20$ . The pressures selected for use are  $p_h = 190 \text{ cm Hg}$  and  $p_l = 19 \text{ cm Hg}$ . Again, assuming the complete-mixing model, calculate the permeate composition, the reject composition, and the area.

**Solution:** Using Eq. (25.2-11) for a feed composition of  $x_f =$

0.209,

$$\begin{aligned}
 a1 &= \theta + p1ph - p1ph\theta\alpha^*\theta - \alpha^*p1ph \\
 + \alpha^*p1ph\theta &= 0.2 + 19190 - 19190(0.2) - 10(0.2) - 10(19)190 + 10(19190) \\
 (0.2) &= -2.52 \\
 b1 &= 1 - \theta - xf - p1ph + p1ph\theta + \alpha^*\theta + \alpha^*p1ph - \alpha^*p1ph\theta \\
 + \alpha^*xf &= 1 - 0.2 - 0.209 - 19190 + 19190(0.2) + 10(0.2) + 10(19190) - 10(19190) \\
 (0.2) &+ 10(0.209) = 5.401 \\
 c1 &= -\alpha^*xf = -10(0.209) = -2.09 \\
 yp &= -b1 + b12 - 4a1c12a1 = -5.401 + (5.401)^2 - 4(-2.52) \\
 &(-2.09)^2 - (2.52) = 0.5067
 \end{aligned}$$

Substituting into Eq. (25.2-9),

$$x_o = x_f - \theta y_p(1 - \theta) = 0.209 - 0.2(0.5067)(1 - 0.2) = 0.1346$$

Finally, using Eq. (25.2-10) to find the area,

$$\begin{aligned}
 A_m &= \theta L f_p (PA/t)(ph_{x_o} - ph_{y_p}) = 0.2(1 \times 10^6)(0.5067) \\
 &[500 \times 10 - 10 / (2.54 \times 10^{-3})] \\
 &(190 \times 0.1346 - 19 \times 0.5067) = 3.228 \times 10^8 \text{ cm}^2
 \end{aligned}$$

## 25.2C Minimum Concentration of Reject Stream

If all of the feed is permeated, then  $\theta = 1$  and the feed composition  $x_f = y_p$ . For all values of  $\theta < 1$ , the permeate composition  $y_p > x_f$  (H1).

Substituting the value  $y_f = x_p$  into Eq. (25.2-7) and solving, the minimum reject composition  $x_{oM}$  for a given  $x_f$  value is obtained as

$$x_{oM} = x_f [1 + (\alpha^* - 1)plph(1 - x_f)]\alpha^*(1 -$$

$$x_f) + x_f(25.2-12)$$

Hence, a feed of  $x_f$  concentration cannot be stripped lower than a value of  $x_{oM}$  even with an infinitely large membrane area for a completely mixed system. To strip beyond this limiting value, a cascade-type system could be used. However, a single unit that is not completely mixed but is designed for plug flow could also be used.

**EXAMPLE 25.2-3. Effect of Feed Composition on Minimum Reject Concentration**

Calculate the minimum reject concentration for Example 25.2-1 where the feed concentration is  $x_f = 0.50$ . Also, what is the effect of raising the feed purity to  $x_f = 0.65$ ?

**Solution:** Substituting  $x_f = 0.50$  into Eq. (25.2-12),

$$x_{oM} = x_f [1 + (\alpha^* - 1) \text{plph}(1 - x_f)] \alpha^* (1 - x_f) + x_f = 0.50 [1 + (10 - 1) (2080)(1 - 0.50)] 10(1 - 0.50) + 0.50 = 0.1932$$

For  $x_f = 0.65$ ,

$$x_{oM} = 0.65 [1 + (10 - 1)(2080)(1 - 0.65)] 10(1 - 0.65) + 0.65 = 0.2780$$

## 25.3 Complete-Mixing Model for



## Multicomponent Mixtures

### 25.3A Derivation of Equations

When multicomponent mixtures are present, the iteration method of Stern et al. (S1) is quite useful. This method will be derived for a ternary mixture of components  $A$ ,  $B$ , and  $C$ . The process flow diagram is the same as Fig. 25.2-1, where the feed composition  $x_f$  is  $x_{fA}$ ,  $x_{fB}$ , and  $x_{fC}$ .

The known values are

$x_{fA}, x_{fB}, x_{fC}; L_f; \theta; p_h, p_l; P_A', P_B', P_C'$ ; and  $t$

The unknown values to be determined are

$y_{pA}, y_{pB}, y_{pC}; x_{oA}, x_{oB}, x_{oC}; V_p$  or  $L_o$ ; and  $A_m$

These eight unknowns can be obtained

by solving a set of eight simultaneous equations using an iteration method. Three rate-of-permeation equations similar to Eq. (25.2-3) are as follows for components  $A$ ,  $B$ , and  $C$ :

$$V_{pypA} = P_A' t_{Am} (p_{xoA} - p_{ypA}) \quad (25.3-1)$$

$$V_{pypB} = P_B' t_{Am} (p_{xoB} - p_{ypB}) \quad (25.3-2)$$

$$V_{pypC} = P_C' t_{Am} (p_{xoC} - p_{ypC}) \quad (25.3-3)$$

The three material-balance equations similar to Eq. (25.2-9) are written for components  $A$ ,  $B$ , and  $C$ :

$$x_{oA} = 1 - \theta x_{fA} - \theta_1 - \theta_{ypA} \quad (25.3-4)$$

$$x_{oB} = 1 - \theta x_{fB} - \theta_1 - \theta_{ypB} \quad (25.3-5)$$

$$x_{oC} = 1 - \theta x_{fC} - \theta y_{pC} \quad (25.3-6)$$

Also, two final equations can be written as

$$\sum n_{ypn} = y_{pA} + y_{pB} + y_{pC} = 1.0 \quad (25.3-7)$$

$$\sum n_{xon} = x_{oA} + x_{oB} + x_{oC} = 1.0 \quad (25.3-8)$$

Substituting  $x_{oA}$  from Eq. (25.3-4) into Eq. (25.3-1) and solving for  $A_m$ ,

$$A_m = V_p y_{pA} t P_A' [P_h^{1-\theta} (x_{fA} - \theta y_{pA}) - \theta y_{pA}] \quad (25.3-9)$$

For component  $B$ , Eq. (25.3-5) is substituted into Eq. (25.3-2), giving

$$A_m = V_p y_{pB} t P_B' [P_h^{1-\theta} (x_{fB} - \theta y_{pB}) - \theta y_{pB}] \quad (25.3-10)$$

Rearranging Eq. (25.3-10) and solving

for  $y_{pB}$ ,

$$y_{pB} = \frac{p_h x_{fB} / (1 - \theta) V_{pt} / (P_B' A_m) + \theta p_h / (1 - \theta) + p_l}{(25.3-11)}$$

In a similar manner, Eq. (25.3-12) is derived for  $y_{pC}$ :

$$y_{pC} = \frac{p_h x_{fC} / (1 - \theta) V_{pt} / (P_C' A_m) + \theta p_h / (1 - \theta) + p_l}{(25.3-12)}$$

### **25.3B Iteration Solution Procedure for Multicomponent Mixtures**

The following iteration or trial-and-error procedure can be used to solve the equations above:

1. A value of  $y_{pA}$  is assumed where  $y_{pA} > x_{fA}$ .
2. Using Eq. (25.2-2) and the known value of  $\theta$ ,  $V_p$  is calculated.
3. The membrane area is calculated from Eq. (25.3-9).
4. The values of  $y_{pB}$  and  $y_{pC}$  are calculated from Eqs. (25.3-11) and (25.3-12).

5. The sum  $\sum y_{pn}$  is calculated from Eq. (25.3-7). If this sum is not equal to 1.0, steps 1 through 5 are repeated until the sum is 1.0.
6. Finally,  $x_{oA}$ ,  $x_{oB}$ , and  $x_{oC}$  are calculated from Eqs. (25.3-4), (25.3-5), and (25.3-6).

**EXAMPLE 25.3-1. Design of Membrane Unit for Multicomponent Mixture**

A multicomponent gaseous mixture having a composition of  $x_{IA} = 0.25$ ,  $x_{IB} = 0.55$ , and  $x_{IC} = 0.20$  is to be separated by a membrane with a thickness of  $2.54 \times 10^{-3}$  cm using the complete-mixing model. The feed flow rate is  $1.0 \times 10^4$  cm<sup>3</sup> (STP)/s and the permeabilities are  $P_A = 200 \times 10^{-10}$  cm<sup>3</sup> (STP) · cm/(s · cm<sup>2</sup> · cm Hg),  $P_B = 50 \times 10^{-10}$ , and  $P_C = 25 \times 10^{-10}$ . The pressure on the feed side is 300 cm Hg and 30 cm Hg on the permeate side. The fraction permeated will be 0.25. Calculate the permeate composition, reject composition, and membrane area using the complete-mixing model.

**Solution:** Following the iteration procedure, a value of  $y_{pA} = 0.50$  is assumed. Substituting into Eq. (25.2-2) for step 2,

$$V_p = \theta L f = 0.25 \times 1.0 \times 10^4 = 0.25 \times 10^4 \text{ cm}^3 (\text{STP})/\text{s}$$

Using Eq. (25.3-9), the membrane area for step 3 is

$$\begin{aligned} A_m &= V_p y_{pA} P_A [\phi_{h1} - \theta(x_{fA} - \theta y_{pA}) - \phi_{lpA}] = 0.25 \times 10^4 (0.50) \\ &\quad (2.54 \times 10^{-3}) 200 \times 10^{-10} / \\ &= [3001 - 0.25(0.25 - 0.25 \times 0.50) - 30(0.50)] 4.536 \times 10^6 \text{ cm}^2 \end{aligned}$$

Following step 4, the values  $y_{pB}$  and  $y_{pC}$  are calculated using Eqs. (25.3-11) and (25.3-12):

$$\begin{aligned} y_{pB} &= \phi_{hB} f_B / (1 - \theta) V_{pt} / (P_B A_m) + \theta \phi_{hB} / (1 - \theta) + \phi_{lpB} = 300 \times 0.55 / \\ &\quad (1 - 0.25) 0.25 \times 10^4 \times 2.54 \times 10^{-3} / \\ &\quad (50 \times 10^{-10} \times 4.536 \times 10^6) + 0.25 \times 300 / \\ (1 - 0.25) + 30 &= 0.5366 y_{pC} = \phi_{hC} f_C / (1 - \theta) V_{pt} / (P_C A_m) + \theta \phi_{hC} / \\ (1 - \theta) + \phi_{lpC} &= 300 \times 0.20 / (1 - 0.25) 0.25 \times 10^4 \times 2.54 \times 10^{-3} / \\ (25 \times 10^{-10} \times 4.536 \times 10^6) &+ 0.25 \times 300 / (1 - 0.25) + 30 = 0.1159 \end{aligned}$$

Substituting into Eq. (25.3-7),

$$\Sigma n_{ypn} = y_{pA} + y_{pB} + y_{pC} = 0.5000 + 0.5366 + 0.1159 = 1.1525$$

For the second iteration, assuming that  $y_{pA} = 0.45$ , the following values are calculated:

$$A_m = 3.546 \times 10^6 \text{ cm}^2, y_{pB} = 0.4410, y_{pC} = 0.0922, \Sigma n_{ypn} = 0.9832$$

The final iteration values are  $A_m = 3.536 \times 10^6 \text{ cm}^2$ ;  $y_{pA} = 0.4555$ ,  $y_{pB} = 0.4502$ ; and  $y_{pC} = 0.0943$ . Substituting into Eqs. (25.3-4), (25.3-5), and (25.3-6),

$$x_{oA} = 11 - \theta x_{fA} - \theta 1 -$$

$$\theta y_{pA} = 11 - 0.25(0.25) - 0.251 - 0.25(0.4555) = 0.1815, x_{oB} = 11 - \theta x_{fB} - \theta 1 -$$

$$\theta y_{pB} = 11 - 0.25(0.55) - 0.251 - 0.25(0.4502) = 0.5833, x_{oC} = 11 - \theta x_{fC} - \theta 1 - \theta y_{pC} = 11 - 0.25(0.20) - 0.251 - 0.25(0.0943) = 0.2352$$

## 25.4 Cross-Flow Model for Gas Separation by Membranes

### 25.4A Derivation of the Basic Equations

A detailed flow diagram for the cross-flow model derived by Weller and Steiner (W1, W2) is shown in Fig. 25.4-1. In this case, the longitudinal velocity of the high-pressure or reject stream is large enough that this gas stream is in plug flow and flows parallel to the membrane. On the low-pressure side, the permeate stream is almost

pulled into vacuum, so that the flow is essentially perpendicular to the membrane.

This model assumes no mixing in the permeate side as well as no mixing on the high-pressure side. Hence, the permeate composition at any point along the membrane is determined by the relative permeation rates of the feed components at that point. This cross-flow pattern approximates that in an actual spiral-wound membrane separator (Fig. 25.1-1) with a high-flux asymmetric membrane resting on a porous felt support (P1, R1).

Referring to Fig. 25.4-1, the local permeation rate over a differential membrane area  $dA_m$  at any point in the stage is

$$y dV = P A' t [p_h x - p_l y] dA_m \quad (25.4-1)$$

$$(1-y) dV = P B' t [p_h (1-x) - p_l (1-y)] dA_m \quad (25.4-2)$$

where  $dL = dV$  and is the total flow rate permeating through the area  $dA_m$ .

Dividing Eq. (25.4-1) by (25.4-2) gives

$$y_{1-y} = \alpha^* [x - (p_l/p_h)y] (1-x) - (p_l/p_h)(1-y) \quad (25.4-3)$$

This equation relates the permeate composition  $y$  to the reject composition  $x$  at a point along the path. It is similar to Eq. (25.2-6) for complete mixing.

Hwang and Kammermeyer (H1) give a computer program for the solution of the above system of differential equations by numerical methods.

Weller and Steiner (W1, W2) used some



ingenious transformations and were able to obtain an analytical solution to the three equations as follows:

$$(1-\theta^*)(1-x)(1-xf)=(uf-E/Du-E/D)R(uf-\alpha^*+Fu-\alpha^*+F)S(uf-Fu-F)T \quad (25.4-4)$$

where

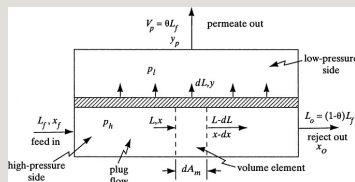


Figure 25.4-1. *Process flow diagram for cross-flow model.*

$$\begin{aligned} \theta^* &= 1 - LLf_i = x_1 - x_u = -Di + (D^2i_2 + 2Ei \\ &+ F_2)0.5D = 0.5[(1 - \alpha^*)p_l p_h + \alpha^*]E = \alpha^*2 - \\ DFF &= -0.5[(1 - \\ \alpha^*)p_l p_h - 1]R &= 12D - 1S = \alpha^*(D - 1) + F(2D - 1) \\ (\alpha^*/2 - F)T &= 11 - D - (E1F) \end{aligned}$$

The term  $uf$  is the value of  $u$  at  $i = i_f = xf/$

$(1 - x_f)$ . The value of  $\theta^*$  is the fraction permeated up to the value of  $x$  in Fig. 25.4-1. At the outlet where  $x = x_o$ , the value of  $\theta^*$  is equal to  $\theta$ , the total fraction permeated. The composition of the exit permeate stream is  $y_p$  and is calculated from the overall material balance, Eq. (25.2-9).

The total membrane area was obtained by Weller and Steiner (W1, W2) using some additional transformations of Eqs. (25.4-1)–(25.4-3) to give

$$A_m = t L f_{ph} P B' \int_{i_o}^{i_f} \frac{(1 - \theta^*)(1 - x) d(i_f - i)}{(1 + i - p) \ln(1 + f_i)} \quad (25.4-5)$$

where

$$f_i = (D_i - F) + (D^2 i^2 + 2 E_i + F^2)^{0.5}$$

Values of  $\theta^*$  in the integral can be

obtained from Eq. (25.4-4). The integral can be calculated numerically. The term  $i_f$  is the value of  $i$  at the feed  $x_f$ , and  $i_o$  is the value of  $i$  at the outlet  $x_o$ . A shortcut approximation of the area without using a numerical integration, available from Weller and Steiner (W1), has a maximum error of about 20%.

#### **25.4B Procedure for Design of Cross-Flow Case**

In the design for the complete-mixing model, there are seven variables and two of the most common cases were discussed in Section 25.2B. Similarly, for the cross-flow model these same common cases occur.

*Case 1.* The values of  $x_f$ ,  $x_o$ ,  $\alpha^*$ , and  $p_l / p_h$  are given and  $y_p$ ,  $\theta$  and  $A_m$  are to be determined. The value of  $\theta^*$  or  $\theta$  can be

calculated directly from Eq. (25.4-4) since all other values in this equation are known. Then,  $y_p$  is calculated from Eq. (25.2-9). To calculate the area  $A_m$ , a series of values of  $x$  less than the feed  $x_f$  and greater than the reject outlet  $x_o$  are substituted into Eq. (25.4-4) to give a series of  $\theta^*$  values. These values are then used to numerically or graphically integrate Eq. (25.4-5) to obtain the area  $A_m$ .

*Case 2.* In this case, the values of  $x_f$ ,  $\theta$ ,  $\alpha^*$ , and  $p_l/p_h$  are given and  $y_p$ ,  $x_o$ , and  $A_m$  are to be determined. This is trial and error, where values of  $x_o$  are substituted into Eq. (25.4-4) to solve the equation. The membrane area is calculated as in Case 1.

- Calculate  $y_p$ ,  $x_o$ , and  $A_m$ .
- Compare the results with Example 25.2-2.

$$\begin{aligned} i &= if = xf1 - xf = 0.2091 - 0.209 = 0.2642i = 0.16421 - 0.1642 = 0.1965D = 0.5[(1 - \alpha^*)plph \\ &+ \alpha^*] = 0.5[(1 - 10)19190 + 10] = 4.550F = -0.5[(1 - \alpha^*)plph \\ &- 1] = \\ &- 0.5[(1 - 10)19190 - 1] = 0.950E = \alpha^*2 - DF = 102 - 4.550(0.950) = 0.6775R = 12D \\ &- 1 = 12(4.550) - 1 = 0.12346S = \alpha^*(D - 1) + F(2D - 1) \\ &(\alpha^*/2 - F) = 10(4.550 - 1) + 0.950(2 \times 4.550 - 1) \\ &(10/2 - 0.950) = 1.1111T = 11 - D - (E/ \\ &F) = 11 - 4.550 - 0.6775/0.950 = -0.2346uf = -Di \\ &+ (D2i2 + 2Ei + F2)0.5 = -(4.550) \\ &(0.2642) + [(4.550)2(0.2642)2 + 2(0.6775) \\ &(0.2642) + (0.950)2]0.5 = 0.4427u = -(4.550) \\ &(0.1965) + [(4.550)2(0.1965)2 + 2(0.6775) \\ &(0.1965) + (0.950)2]0.5 = 0.5089(1 - \theta^*)(1 - x) \\ &(1 - xf) = (1 - \theta^*)(1 - 0.1642) \end{aligned}$$

Using the material-balance equation (25.2-9) to calculate  $y_p$ ,

$$y_p = x_f - x_o(1 - \theta) = 0.209 - 0.1190(1 - 0.2000) = 0.5690$$

To calculate  $y_p$  at  $\theta^* = 0$ , Eqs. (25.4-3) and (25.2-17) must be used, giving  $y_p = 0.6550$ .

To solve for the area, Eq. (25.4-5) can be written as

$$A_m = t L f_{PB} \int_{i_o}^{i_i} \frac{F_i}{(1 - \theta^*)(1 - x)(f_i - i)} [1 + i - \text{PlPh}(1 + f_i)] di = t L f_{PB} \int_{i_o}^{i_i} F_i di \quad (25.4-6)$$

where the function  $F_i$  is defined as above. Values of  $F_i$  will be calculated for different values of  $i$  in order to integrate the equation. For  $\theta^* = 0.200$ ,  $x_o = 0.119$ , and from Eq. (25.4-4),

$$i_o = x_o(1 - x) = 0.119(1 - 0.119) = 0.1351$$

From Eq. (25.4-5),

$$\begin{aligned} F_i &= (D_i - F) + (D_i^2 + 2E_i \\ &+ F^2)0.5 = (4.55 \times 0.1351 - 0.950) + [(4.55)^2(0.1351)^2] \\ &+ 2(0.6775)(0.1351) + (0.95)^2]0.508744 \end{aligned}$$

Using the definition of  $F_i$  from Eq. (25.4-6),

$$\begin{aligned} F_i &= (0 - \theta^*)(1 - x)(f_i - i) [1 + i - \text{plph}(1 + f_i)] = (1 - 0.200)(1 - 0.119) \\ &(0.8744 - 0.1351) [1 + 0.1351 - 1.9190(1 + 0.8744)] = 1.1520 \end{aligned}$$

Other values of  $F_i$  are calculated for the remaining values of  $\theta^*$  and are tabulated in Table 25.4-1. The integral of Eq. (25.4-6) is obtained by using the values from Table 25.4-1 and numerically integrating  $F_i$  versus  $i$  to give an area of 0.1082. Finally, substituting into Eq. (25.4-6),

$$A_m = t L f_{PB} \int_{i_o}^{i_i} F_i di = 2.54 \times 10^{-3} (1 \times 106) 190 (50 \times 10^{-10}) / 10 (0.1082) = 2.893 \times 10^8 \text{ cm}^2$$

For part (b), from Example 25.2-2,  $y_p = 0.5067$  and  $A_m = 3.228 \times 10^8 \text{ cm}^2$ . Hence, the cross-flow model yields a higher  $y_p$  of 0.5690, compared to 0.5067 for the complete-mixing model. Also, the area for the cross-flow model is 10% less than for the complete-mixing model.

## 25.5 Derivation of Equations for Countercurrent and Cocurrent Flow for Gas Separation by Membranes

### 25.5A Concentration Gradients in Membranes

*1. Dense-phase membrane.* In gas separation using a dense-phase symmetrical polymer membrane, the solute diffuses through the high-pressure-side gas film to the membrane surface. Then, it dissolves in the membrane. At the interface, equilibrium occurs. The solute then diffuses through the solid membrane and finally diffuses through the gas film. The gas film resistances are quite small and can be neglected (N1). In Fig. 25.5-1a, the concentration profiles are shown. The concentration  $y$  in the flowing bulk gas phase is the same as  $y$  at the interface of the dense polymer and

depends on the flow pattern of the permeate phase.

2. *Asymmetric membrane.* As shown in Fig. 25.5-1b, the membrane includes a very thin, dense polymer membrane that is about 0.1 to 1  $\mu\text{ m}$  thick (M1, P5) and a very thick porous layer 50–200  $\mu\text{ m}$  thick. A typical hollow-fiber membrane for air separation has an ID of 95  $\mu\text{ m}$  and an OD of 135  $\mu\text{ m}$ , with a wall thickness of 20  $\mu\text{ m}$ .

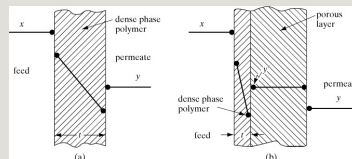


Figure 25.5-1. *Concentration profiles in membranes. (a) dense-phase symmetrical membranes, (b) asymmetric membrane.*

The concentration gradient in the thin, dense polymer phase is similar to that for the symmetrical membrane.



However, the concentration  $y$  of component  $A$  in the bulk permeate gas phase is not the same as  $y'$  at the surface of the thin, dense polymer layer. The concentration  $y$  of the bulk gas permeate stream depends on the flow pattern and material balances. Also, the value of  $y$  can be greater or less than  $y'$ .

The porous layer is so open that there is assumed to be little or no resistance to the flow and  $y'$  is constant along this path. Hence, it is assumed that there is no penetration or mixing of the bulk gas phase  $y$  inside the porous layer.

#### **25.5B Derivation of Equations for Countercurrent Flow in Dense-Phase Symmetric Membranes**

A flow diagram for this countercurrent-flow model is given in Fig. 25.5-2, where both streams

are in plug flow. The derivation follows that given by others (B1, N1, P2, W3).

Making a total material balance,

$$L_f = L_o + V_p \quad (25.5-1)$$

where  $L_f$  is total feed flow rate,  $\text{cm}^3$  (STP)/s,  $L_o$  is outlet nonpermeate (reject) flow rate,  $\text{cm}^3$  (STP)/s, and  $V_p$  is outlet permeate flow rate,  $\text{cm}^3$  (STP)/s. The permeation rates of A and in B in a binary mixture are similar to Eqs. (25.2-3) and (25.2-4):

$$V_A/A_m = V_y/A_m = (P_A'/t)(p_{hx} - p_{ly}) \quad (25.5-2)$$

$$V_B/A_m = V(1-y)/A_m = (P_B'/t)[p_h(1-x) - p_l(1-y)] \quad (25.5-3)$$

where  $PA'$  is the permeability of  $A$ ,  $\text{cm}^3 (\text{STP}) \cdot \text{cm}/(\text{s} \cdot \text{cm}^2 \cdot \text{cm Hg})$ ;  $V_A$  is the flow rate of  $A$  in permeate,  $\text{cm}^3 (\text{STP})/\text{s}$ ;  $A_m$  is the membrane area,  $\text{cm}^2$ ;  $p_h$  is the total pressure in the high-pressure side,  $\text{cm Hg}$ ; and  $p_l$  is the total pressure in the low-pressure side,  $\text{cm Hg}$ .

The flux of  $A$  out of the element with area  $dA_m$  is

$$dL_A = y dL = (PA'/t)[p_h x - p_l y] dA_m \quad (25.5-4)$$

The flux of  $B$  is

$$dL_B = (1-y) dL = (PB'/t)[p_h(1-x) - p_l(1-y)] dA_m \quad (25.5-5)$$

Making a total balance on the reject stream for area  $dA_m$ ,

$$L=L-dL+dLA+dLB(25.5-6)$$

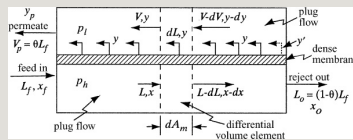


Figure 25.5-2. Flow diagram for the countercurrent-flow model with a dense-phase symmetric membrane.

This gives

$$dL=dLA+dLB(25.5-7)$$

Making a balance on A for area  $dA_m$ ,

$$Lx=(L-dL)(x-dx)+dLA(25.5-8)$$

Rearranging,

$$dLA=L dx+x dL(25.5-9)$$

Substituting Eq. (25.5-7) into (25.5-9),

$$Ldx=(1-x)dLA-xdLB(25.5-10)$$

Making a total balance on the permeate stream for area  $dA_m$ ,

$$V = V - dV + dLA + dLB \quad (25.5-11)$$

This gives

$$dV = dLA + dLB \quad (25.5-12)$$

Making a balance on  $A$  for area  $dA_m$ ,

$$Vy = (V - dV)(y - dy) + dLA \quad (25.5-13)$$

Rearranging,

$$dLA = Vdy + ydV \quad (25.5-14)$$

Substituting Eq. (25.5-12) into (25.5-14),

$$Vdy = (1 - y)dLA - ydLB \quad (25.5-15)$$

To eliminate the variables  $L$  and  $V$ , an

overall balance is made for the area  $dA_m$  and the reject outlet stream:

$$L=L_o+V(25.5-16)$$

$$Lx=L_o x_o+Vy(25.5-17)$$

To eliminate  $V$ ,  $V$  from Eq. (25.5-16) is substituted into (25.5-17) and solved for  $L$ :

$$L=L_o(x_o-y)/(x-y)(25.5-18)$$

To eliminate  $L$ ,  $L$  from Eq. (25.5-16) is substituted into (25.5-17) and solved for  $V$ :

$$V=L_o(x_o-x)/(x-y)(25.5-19)$$

Substituting Eq. (25.5-18) into (25.5-10),

$$L_o(x_o-y)dx(x-y)=(1-x)dL_{A-x}dL_B(25.5-20)$$

Substituting Eqs. (25.5-4) and (25.5-5) into Eq. (25.5-20),

$$L_o(x_o-y)dx(x-y)=(1-x)[(P_A'/t)(p_h x - p_l y)]dA_{m-x}[(P_B'/t)(p_h(1-x) - p_l(1-y))]dA_m(25.5-21)$$

Rearranging,

$$L_o(P_B'/t)p_h dx dA_m = -(x - y)(y - x_o) \{ (1-x)\alpha^*(x - ry) - x[(1-x) - r(1-y)] \} (25.5-22)$$

where  $r = p_l/p_h$  and  $\alpha^* = (P_A'/t)/(P_B'/t)$ .

In a similar manner, substituting Eq. (25.5-19) into (25.5-15),

$$L_o(x_o-x)dy(x-y)=(1-y)dL_{A-y}dL_B(25.5-23)$$

Again, substituting Eqs. (25.5-4) and (25.5-5) into Eq. (25.5-23) and rearranging,

$$L_o(PB/t)phdx dA_m = -(x-y)(x-x_o)\{(1-y)\alpha^*(x-ry)-y[(1-x)-r(1-y)]\} \quad (25.5-24)$$

Dividing Eq. (25.5-24) by (25.5-22),

$$dy/dx = (y-x_o)(x-x_o)\{(1-y)\alpha^*(x-ry)-y[(1-x)-r(1-y)]\} \{[(1-x)\alpha^*(x-ry)-x[(1-x)-r(1-y)]]\} \quad (25.5-25)$$

Inverting Eq. (25.5-22),

$$dA_m/dx = -L_o[(y-x_o)/(x-y)](PB'/t)ph\{(1-y)\alpha^*(x-ry)-x[(1-x)-r(1-y)]\} \quad (25.5-26)$$

### 25.5C Solution of Countercurrent Flow Equations in Dense-Phase Symmetric Membranes

At the outlet of the residue stream of



composition  $x_o$ , the permeates  $y'$  and  $x_o$  are related by Eq. (25.2-6), repeated here as Eq. (25.5-27), where  $y_p = y'$ :

$$y'_1 - y_1' = \alpha^* [x_1 - (p_l/p_h)y_1'] (1 - x_1) - (p_l/p_h)(1 - y')$$

(25.5-27)

The solution to this quadratic equation is given as Eq. (25.2-7).

In order to solve Eqs. (25.5-25) and (25.5-26), the following procedure can be used, where  $x_o$  is known or set:

1. Using Eq. (25.5-27), the value of  $y'$  is calculated for  $x = x_o$ .
2. To integrate Eq. (25.5-25), the value of  $(dy/dx)$  at  $x = x_o$  must be calculated. However, this value is indeterminate since the denominator is zero. Using L'Hopital's rule (N1, P4, R1), the numerator is differentiated with respect to  $x$  and the denominator with respect to  $x$ , and the value of  $y$  is set as  $y'$  to give

$$(dy/dx)_{x=x_0} = (y' - x_0)[\alpha^* - (\alpha^* - 1)y'] / \{ \alpha^*(1 - x_0)(x_0 - ry') - x_0[(1 - x_0) - r(1 - y')] - (y' - x_0)[(\alpha^* - 1)(2ry' - x_0 - r) - 1] \}$$

(25.5-28)

3. Starting at the residual end at  $x_0$ , Eq. (25.5-25) is integrated numerically to give the  $y$ -versus- $x$  relationship and  $y_p$  (P2, R1).
4. The relationship of  $y$  versus  $x$  is substituted into Eq. (25.5-26), which is integrated from  $x_f$  to  $x_0$  to obtain the area  $A_m$ .
5. Substituting into the material-balance Eqs. (25.2-8) and (25.2-2), the cut or fraction of feed permeated,  $\theta$ , is calculated (N1, R1, W3).
6. If  $\theta$  is set and  $x_0$  is unknown, the solution is trial and error. The value of  $x_0$  is assumed and the integration of Eq. (25.5-25) is performed to obtain  $y_p$ . Then,  $x_0$  is calculated from Eq. (25.2-9). This is repeated until the assumed and calculated values of  $x_0$  agree.

### 25.5D Derivation of Equations for Countercurrent Flow in Asymmetric Membranes

The flow diagram for this countercurrent-flow model is shown in Fig. 25.5-3, where both streams are in plug flow. The permeate  $y'$  leaving the membrane differs from

the symmetric-membrane case and is not the same as the bulk-phase concentration  $y$  at this point. This is also shown in Fig. 25.5-1b.

The flux of  $A$  out of the element with area  $dA_m$  is

$$dL_A = y dL = (P A' / t) (p_{hx} - p_{hy}) dA_m \quad (25.5-29)$$

where  $y'$  is given by Eq. (25.5-30), which is similar to Eqs. (25.5-27) and (25.2-6):

$$y' = \frac{1 - y}{1 - y'} = \alpha^* [x - (p_l / p_h) y'] (1 - x) - (p_l / p_h) (1 - y') \quad (25.5-30)$$

The flux of  $B$  is

$$dL_B = (1 - y) dL = (P B' / t) [(p_h (1 - x) - p_l (1 - y'))] dA_m \quad (25.5-31)$$

Equations (25.5-29) and (25.5-31) differ from Eqs. (25.5-4) and (25.5-5) for the symmetric membrane in that  $y'$  is used instead of  $y$  in the terms for concentration difference.

The rest of the derivation is identical to that for the dense-phase symmetric membrane (N1, R1). The final equations are

$$L_o(PB'/t)phdx dA_m = -(x-y)(y-x_o)\{(1-x)\alpha^*(x-ry')-x[(1-x)-r(1-y)]\} \quad (25.5-32)$$

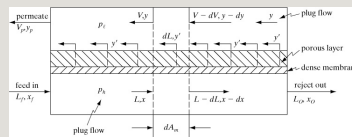


Figure 25.5-3. Flow diagram for countercurrent flow with an asymmetric membrane.

$$dx dy = (y-x_o)(x-x_o)\{(1-y)\alpha^*(x-ry')-y[(1-x)-r(1-y')]\}\{(1-x)\alpha^*(x-ry)-x[(1-x)-r(1-y')]\} \quad (25.5-33)$$

Inverting Eq. (25.5-32),

$$\frac{dA}{dx} = -L_o(PB'/t) \left[ \frac{(y-x_o)}{(x-y)} \right] \{ (1-x)\alpha^*(x-ry') - x[(1-x)-r(1-y')] \}$$

(25.5-34)

Equations (25.5-27) for  $y'$  and (25.5-28) for  $(dy/dx)$  at  $x = x_o$  for symmetric membranes are also applicable here for asymmetric membranes. The method of solution for the equations above is similar to that for symmetric membranes.

#### **25.5E Derivation of Equations for Cocurrent Flow in Asymmetric Membranes**

For cocurrent flow, the cocurrent model is shown in Fig. 25.5-4. The derivation uses Eqs. (25.5-29)–(25.5-31) as before. Proceeding in a manner similar to the countercurrent case, the final equations are (N1, P2,

R1):

$$dy/dx = (y - x_f)(x - x_f) \{ (1 - y) \alpha^* (x - ry') - y[(1 - x) - r(1 - y')] \} \{ (1 - x) \alpha^* (x - ry) - x[(1 - x) - r(1 - y')] \} \quad (25.5-35)$$

$$dA_m/dx = Lf(PB'/t) [(y - x_f)/(x - y)] \{ (1 - x) \alpha^* (x - ry') - x[(1 - x) - r(1 - y')] \} \quad (25.5-36)$$

The method of solution is similar to that for countercurrent flow. Integration of Eq. (25.5-35) is started at the feed inlet, where  $y'$  is determined by using  $x_f$  instead of  $x_o$  in Eq. (25.5-27). Then, using Eq. (25.5-28) with  $x_f$  instead of  $x_o$ ,  $(dy/dx)$  at  $x = x_f$  is calculated. This is then used to integrate Eq. (25.5-35) starting at the feed end, where  $x = x_f$ . Finally, Eq. (25.5-36) is integrated to obtain  $A_m$ .

## 25.5F Effects of Processing Variables on Gas Separation

*1. Effects of pressure ratio and separation factor on recovery.* Using the Weller-Steiner equation (25.2-6) for the complete-mixing model, the effects of pressure ratio,  $p_h / p_l$ , and separation factor,  $\alpha^*$ , on permeate purity can be determined for a fixed feed composition. Figure 25.5-5 is a plot of this equation for a feed concentration of 30% (S3). For symmetric and asymmetric membranes, this equation can be expected to provide estimates of product purity and trends for conditions of low to modest recovery in all types of models, including complete-mixing, cross-flow, and countercurrent.

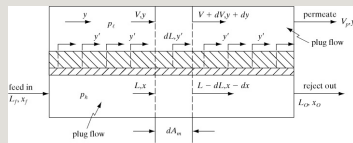


Figure 25.5-4. Flow diagram for cocurrent flow with an asymmetric membrane.

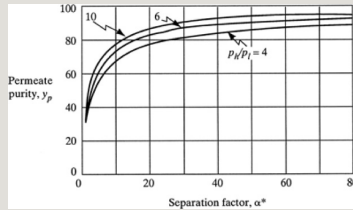


Figure 25.5-5. Effects of separation factor and pressure ratio on permeate purity. (Feed  $x_f = 0.30$ .) Data from “Membranes Separate Gases Selectively,” by D. J. Stookey, C. J. Patton, and G. L. Malcolm, Chem. Eng. Progr., **82**(11), 36, ©1986, American Institute of Chemical Engineers.

Figure 25.5-5 shows that above an  $\alpha^*$  of 20, the product purity is not greatly affected. Also, above a pressure ratio of about 6, this ratio has a diminishing effect on product purity.

If liquids are present in the gas separation process, a liquid film can increase the membrane resistance



markedly. Liquids can also damage the membrane by chemical action or by swelling or softening. If water vapor is present in the gas streams, the dew point may be reached in the residue product and liquid may condense. Condensation of hydrocarbons must also be avoided.

## *2. Effects of process flow patterns on separation in symmetric membranes.*

Detailed parametric studies have been done by various investigators (P2, P3, W3) for binary systems. They compared the four flow patterns of complete mixing, cross-flow, cocurrent, and countercurrent flow. In Fig. 25.5-6 (W3), the permeate concentration is shown plotted versus stage cut,  $\theta$ , for a feed of air ( $x_f = 0.209$  for oxygen) with  $\alpha^* = 10$  and  $p_h / p_l = 5$ . It is shown that, as expected, the countercurrent flow

pattern gives the best separation. The other patterns—cross-flow, cocurrent, and complete mixing—give lower separations in descending order. Note that when the stage cut  $\theta = 0$ , all flow patterns are equivalent to the complete mixing model and give the same permeate composition. Also, at  $\theta = 1.00$ , all patterns again give the same value of  $y_p = 0.209$ , which is also the feed composition.

The required membrane areas for the same process conditions and air feed versus stage cut were also determined (W3). The areas for all four types of flow pattern were shown to be within about 10% of each other. The countercurrent and cross-flow patterns give the lowest area required.

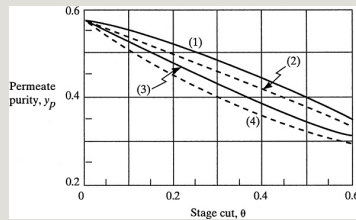


Figure 25.5-6. *Effect of flow pattern in symmetric membranes. Operating conditions for air are as follows:  $x_f = 0.209$ ,  $a^* = 10$ ,  $p_H/p_L = 380 \text{ cm Hg} / 76 \text{ cm Hg} = 5$ .  $PA' = 500 \times 10^{-10} \text{ cm}^3 (\text{STP}) \cdot \text{cm} / \text{s} \cdot \text{cm}^2 \cdot \text{cm Hg}$ . (1) countercurrent flow, (2) cross-flow, (3) cocurrent flow, (4) complete mixing (W3). Reprinted from W. P. Walawender and S. A. Stern, Sep. Sci., 7, 553 (1972). Reprinted by permission of Taylor & Francis Ltd.*

### 3. *Effects of process flow patterns on separation in asymmetric membranes.*

Calculations using the mathematical models for asymmetric membranes give virtually identical performances for cocurrent and countercurrent flow (G1, P1, P4). The porous support prevents mixing of the bulk permeate concentration and the skin surface concentration  $y'$  as shown in Fig. 25.5-1b. Hence, the direction of the bulk flow permeate stream has no effect.

Experimental tests using helium recovery from natural gas (P1, P4), nitrogen recovery from air (G1), and helium from nitrogen (G1) show that the experimental data and the model predictions agree quite well.

#### *4. Effect of pressure drop on separations in asymmetric membranes.*

In hollow-fiber membranes (N1), an appreciable pressure drop can occur for flow inside long tubes or for tubes with very small inside diameters. In the shell side, the pressure drop is generally very small and is neglected. Pressure drop in the tubes is always detrimental to the separation. For feed inside the tubes, the actual average feed pressure will be less than the inlet feed pressure. If the permeate flow is inside the tubes, then the actual average permeate pressure

will be higher than the permeate outlet pressure. In both of these cases, the driving force for permeation is reduced and less separation occurs.

To reduce these pressure effects, where the stage cut  $\theta$  is small, giving a low permeate flow rate, it is preferable to have the large feed flow rate in the shell, where the pressure drop is small. For a high stage cut, the feed should be inside the tubes, where most of the feed permeates into the shell.

Using the model equations, the pressure drop inside the tubes can be accounted for by using the Hagen–Poisuille equation (4.4-11) for laminar flow:

$$\Delta p(z_2 - z_1) = 32\mu v D^2 \quad (4.4-11)$$

where  $z_2 - z_1$  is total length. Writing this

for a differential length  $dz$  cm and a  $dp_h$  in Pascals,

$$dp_h dz = -32 \mu v D^2 (25.5-37)$$

Converting the feed flow rate  $L$  cm<sup>3</sup>/s at  $T_s$  and  $p_s$  (STP) to the actual velocity  $v$  at  $T$  and  $p_h$ ,

$$dp_h dz = -128 \mu \pi D^4 N_T (L T T_s p_s p_h) \quad (25.5-38)$$

where  $N_T$  is the number of tubes in parallel. The average viscosity  $\mu$  can be approximated by using the average mole fraction of the feed and the residual outlet. The average  $\mu$  is then the sum of the mole fractions of each component times the viscosity of the pure gases.

The final equation is (G1, N1, P1):

$$dp_h^2 dz = -256 \mu L T_p S \pi D^4 N_T T_s (25.5-39)$$

The area  $A_m$  can be related to  $z$  by  $dA_m = \pi DNT dz$ . This then relates  $dA_m$  to  $dph$ .

In integrating the model equations, a constant (uniform)  $p_h$  is first assumed (G1, P1, P5). This gives the relation between  $y$  and  $x$  and  $A_m$ . Then, using the material-balance equation (25.5-18) between  $L$  and  $y$  and  $x$ , Eq. (25.5-39) is used to generate a new pressure profile. This process is then repeated.

## **25.6 Derivation of Finite-Difference Numerical Method for Asymmetric Membranes**

### **25.6A Countercurrent Flow**

The flow diagram for the numerical method is shown in Fig. 25.6-1.

Using the method derived by McCabe et al. (M1) and taking an area  $\Delta A_m$ , the mass balances on both streams can be written as

$$\Delta V = L_{in} - L_{out} \quad (25.6-1)$$

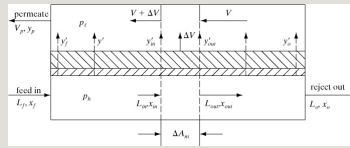


Figure 25.6-1. Flow diagram for countercurrent flow with an asymmetric membrane using the finite-difference method.

The value of  $y_{in}'$  can be calculated from Eq. (25.5-37) using  $x_{in}$  for  $x$  and  $y_{in}'$  for  $y'$ . Also,  $y_{out}'$  can be calculated similarly from  $x_{out}$ . Then, writing a balance on  $A$ ,

$$\Delta V y_{av}' = L_{in} x_{in} - L_{out} x_{out} \quad (25.6-2)$$

where  $y_{av}' = (y_{in}' + y_{out}')/2$ . Substituting  $L_{out}$  from Eq. (25.6-1) into (25.6-2),

$$\Delta V = L_{in} (x_{in} - x_{out}) (y_{av}' - x_{out}) \quad (25.6-3)$$

Equations (25.5-27), (25.6-2), and



(25.6-3) can be solved numerically starting at the feed  $x_f = x_{in}$  to determine the permeate  $\Delta V$  and  $y_{av}'$  for each  $\Delta A_m$ , and increments of  $x$  to  $x_o$  at the outlet reject. Usually 10 or so increments of  $x$  from  $x_f$  to  $x_o$  are sufficient.

Then, to obtain the values of  $V$  and the bulk composition  $y$  as a function of  $x$ , the calculation is started at  $x_o$ . Using Eqs. (25.6-4) and (25.6-5), the increments of  $\Delta V$  are added to get  $V$ , and  $y$  is calculated for each  $\Delta A_m$  increment up to  $x_f$  at the feed inlet:

$$V = \sum \Delta V \quad (25.6-4)$$

$$y = \sum y_{av}' \Delta V / V \quad (25.6-5)$$

For cocurrent or parallel flow, the only difference is in calculating  $V$ . Starting at  $x_f$  inlet and using Eqs. (25.6-4) and

(25.6-5), the increments of  $\Delta V$  are added to get  $V$  up to  $x_o$ .

To calculate the area for countercurrent or cocurrent flow, rewriting Eq. (25.5-4),

$$\Delta V y_{av'} \Delta A_m = \Delta V A \Delta A_m = (P' A / t) p h (x - r y')_{av} \quad (25.6-6)$$

where  $r = p l / p h$ . The average driving force is

$$(x - r y')_{av} = [(x_{in} - y_{in}') + (x_{out} - y_{out}')] / 2 \quad (25.6-7)$$

Solving for  $\Delta A_m$ ,

$$\Delta A_m = \Delta V y_{av'} (P A' l t) p h (x - r y')_{av} \quad (25.6-8)$$

Starting at  $x_f$ ,  $\Delta A_m$  is calculated for each

increment to obtain  $\Sigma \Delta A_m$  versus  $x$ .

### 25.6B Short-Cut Numerical Method

Making an approximate material balance to obtain a  $y_{av}'$  or  $y_p$  for the total area from  $y_f'$  to  $y_o'$  (M1),

$$y_p = y_{av}' = (y_f' + y_o')/2 \quad (25.6-9)$$

An overall and component material balance gives

$$L_f = L_o + V_p \quad (25.6-10)$$

$$L_f x_f = L_o x_o + V_p y_p \quad (25.6-11)$$

Substituting Eq. (25.6-10) into Eq. (25.6-11),

$$L_f x_f = (L_f - V_p) x_o + V_p y_p \quad (25.6-12)$$

Equation (25.6-12) can be solved for  $V_p$

and Eq. (25.6-10) solved for  $L_o$ .

To calculate the approximate area for countercurrent or cocurrent flow, Eq. (25.6-8) is rewritten for the total area  $A_m$ :

$$A_m = V_p y_{av}' (P A' / t) \ln \frac{(x - r y')}{(x_o - r y_o')} \quad (25.6-13)$$

where  $(x - r y')_{lm}$  is the ln mean of  $(x_f - r y_f')$  and  $(x_o - r y_o')$ . Since plots of  $x$  and  $y'$  versus  $A_m$  are approximately straight lines, this approximate area is within about 15% of the  $A_m$  calculated by the finite-difference method.

**EXAMPLE 25.6-1. Air Separation Using an Asymmetric Membrane for Countercurrent Flow**

It is desired to design a hollow-fiber asymmetric membrane for air separation to produce a residue that contains 97.0%  $N_2$  using countercurrent flow. The dense polymer layer is inside the tubes and the feed is in the tubes. Experimental values for commercial membranes give separation factors  $\alpha^*$  of  $O_2/N_2$  between 3 and 7 ( $H_2$ ), with a typical value of 5.0 ( $G_1$ ). Permeance values of  $PA'/t$  are given ( $H_2$ ) of  $5 \times$

$10^{-6}$  to  $250 \times 10^{-6} \text{ cm}^3 \text{ (STP)/(s} \cdot \text{cm}^2 \cdot \text{cm Hg)}$  with a typical value of  $20 \times 10^{-6} \text{ (G1)}$ . The typical values will be used. The feed or tube side pressure is 103.4 kPa abs and the shell side or permeate is 103.4 kPa. The feed rate of air is  $10.0 \text{ m}^3 \text{ (STP)/h}$ .

- Using the finite-difference method, calculate the permeate composition, the fraction  $\theta$  of feed permeated, and the residue and permeate flows. Assume negligible pressure drop in the tubes. Calculate the composition  $y$  of the permeate as a function of the residue composition  $x$ .
- Calculate the membrane area needed.
- Using the short-cut procedure, calculate the permeate composition,  $\theta$ , flows, and membrane area.
- Repeat (a) for cocurrent flow. Plot  $x$ ,  $y$ , and  $y'$  for countercurrent and cocurrent flow versus area.

**Solution:** For part (a),  $L_f = 10.0 \text{ m}^3 \text{ (STP)/h}$ ,  $x_f = 0.209$ ,  $x_o = 0.03$ ,  $p_h = 1034 \text{ kPa}$ ,  $p_l = 103.4 \text{ kPa}$ ,  $PA'/t = 20 \times 10^{-6} \text{ cm}^3 \text{ (STP)/(s} \cdot \text{cm}^2 \cdot \text{cm Hg)}$ ,  $\alpha^* = 5.0$ . Using Table 25.1-1,

$$PA'/t = (20 \times 10^{-6})(7.501 \times 10^{-6}) = 1.500 \times 10^{-10} \text{ m}^3 \text{ (STP)/} \\ (\text{s} \cdot \text{m}^2 \cdot \text{Pa}) \quad r = p_l/p_h = 103.4/1034 = 0.10$$

Starting at the feed inlet (Fig. 25.6-2), where  $x_f = 0.209$ , using an area  $\Delta A_m$ , going from  $x_f = x_1 = 0.209$  to  $x_2 = 0.190$ , and using Eq. (25.5-27) to calculate  $y'$ ,

$$y'_1 - y'_2 = \alpha^* x_1 - (p_l/p_h) y'_1 [1 - x_1] - (p_l/p_h) (1 - y'_1) \quad (25.5-27)$$

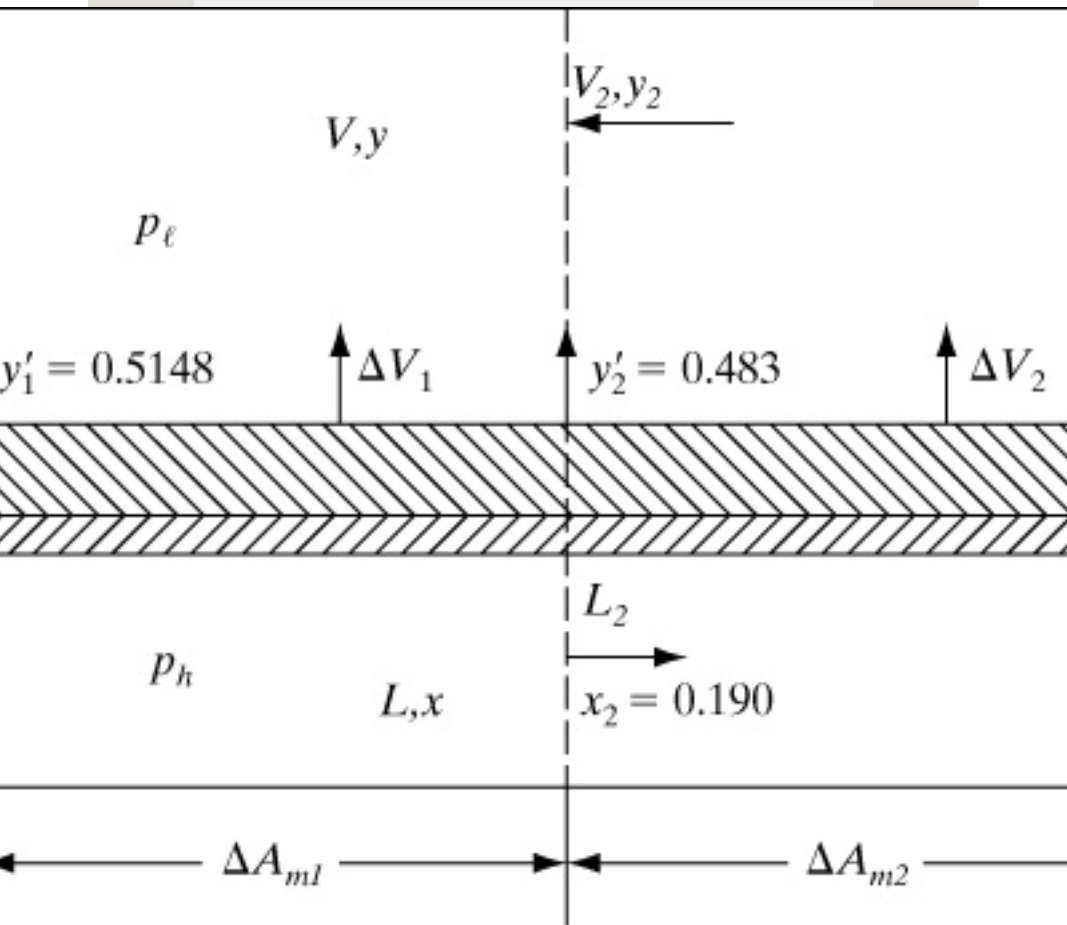


Figure 25.6-2. Finite-difference elements for countercurrent flow in Example 25.6-1.

The solution to this is given by the quadratic equation (25.2-7):

$$y' = \frac{-b \pm \sqrt{b^2 - 4ac}}{2a} \quad (25.2-7)$$

where  $a = 1 - \alpha^*$ ,  $b = -1 + \alpha^* + 1/r + x/r(\alpha^* - 1)$ , and  $c = -a^*x/r$ . Substituting and solving for  $y_1'$  where  $x_1 = 0.209$ ,

$$\begin{aligned} a &= 1 - 5 = -4.0 \\ b &= -1 + 5.0 + 10.1 + x_1(5 - 1)0.1 = 14.0 + 40x_1 = 14.0 + 40(0.209) = 22.36 \\ c &= -a^*x_1/r = -50.10 = -50x_1 = -50(0.209) = -10.45 \\ y_1' &= \frac{-22.36 \pm \sqrt{(22.36)^2 - 4(-4.0)(-10.45)}}{2(-4.0)} = 0.5148 \end{aligned}$$

Again, for  $x_2 = 0.190$ ,  $y_2' = 0.4830$  is obtained from Eq.

(25.5-27).

Then,  $y_{av}' = (y_1' + y_2')/2 = (0.5148 + 0.4830)/2 = 0.4989$ .

Substituting into Eq. (25.6-3),

$$\Delta V_1 = L_1(x_1 - x_2)(y_{av}' - x_2) = 10.0 \cdot (0.209 - 0.190) \cdot (0.4989 - 0.190) = 0.6151 \text{ m}^3/\text{h}$$

Then, by Eq. (25.6-1),

$$L_2 = L_1 - \Delta V_1 = 10.0 - 0.6151 = 9.3849 \text{ m}^3/\text{h}$$

$$y_{av}' = 0.4989 \cdot (0.6151) = 0.3069$$

For the second increment for  $\Delta A_{m2}$  in Fig. 25.6-2, solving for  $y_3'$  with  $x_3 = 0.170$ ,

$$a = -4.0, b = 14.0 + 40(0.170) = 20.8, c = -50(0.170) = -8.5$$

Using Eq. (25.2-7),  $y_3' = 0.4471$ . Then,  $y_{av}' = (y_2' + y_3')/2 = (0.4830 + 0.4471)/2 = 0.4651$

$$\Delta V_2 = L_2(x_2 - x_3)(y_{av}' - x_3) = 9.3849(0.190 - 0.170) \cdot (0.4651 - 0.170) = 0.6360 \text{ m}^3/\text{h}$$

Also,

$$L_3 = L_2 - \Delta V_2 = 9.3849 - 0.6360 = 8.7489 \text{ m}^3/\text{h}$$

$$y_{av}' = 0.4651(0.6360) = 0.2958$$

This is continued, and for the eighth increment,  $x_8 = 0.07$ ,  $x_9 = 0.050$ ,  $y_8' = 0.2198$ ,  $y_9' = 0.1629$ ,  $y_{av}' = 0.1914$ ,  $\Delta V_8 = 0.7757$ , and  $L_9 = 4.7088$ . For the final or ninth increment,  $x_{10} = x_o = 0.030$ ,  $x_9 = 0.050$ ,  $y_9' = 0.1629$ ,  $y_{10}' = 0.1014$ ,  $y_{av}' = 0.1322$ ,  $\Delta V_9 = 0.9215$ , and  $L_{10} = L_o = 3.7873 \text{ m}^3/\text{h}$ . The permeate flow rate  $V_p = L_f - L_o = 10.00 - 3.7873 = 6.2127 \text{ m}^3/\text{h}$ . The stage cut  $\theta = 6.2127/10.00 = 0.6213$ .

To calculate the bulk composition  $y$  as a function of  $x$  for countercurrent flow, it is necessary to start at  $x_o$ . Using Eq. (25.6-4),

$$V_9 = \Sigma \Delta V = V_{10} + V_9 = 0 + 0.9215 = 0.9215$$

For calculation of  $y_9$  using Eq. (25.6-5),

$$y_9 = \Sigma y_{av}' V_9 = 0.1322(0.9215) = 0.1218$$

For the eighth plus ninth increments,

This calculation is continued up to the feed entrance. Values of  $y$ ,  $x$ , and  $y'$  are given in Table 25.6-1.

$$V = \Sigma \Delta V = 0 + \Delta V_1 = 0 + 0.6151 = 0.6151 \text{ y1} = \Sigma y_{av}$$

$$\Delta V V = 0.4989(0.6151)0.6151 = 0.306906151 = 0.4989$$
$$V = \sum \Delta V = V_1 + \Delta V_2 = 0.6151 + 0.6360 = 1.2511 \text{ y}^2 = 0.3069 + 0.4651(0.6360)1.2511 = 0.4817$$
$$x_1 - ry_1' = 0.209 - 0.10(0.5148) = 0.15752 \quad x_2 - ry_2' = 0.190 - 0.10(0.4830) = 0.14170$$

$$-ry')_{av} = (0.15752 + 0.14170)/2 = 0.1496$$
$$\Delta A_{m1} = (0.6151)(1/3600)(0.4989)(1500 \times 10^{-10})(1034 \times 103) \\ (01496) = 3.674 \text{ m}^2$$
$$\begin{aligned} x_2 - ry_2' &= 0.14170x_3 - ry_3' = 0.170 - 0.10(0.4471) = 0.12529(x_3 \\ &- ry_3')_{av} = (0.14170 + 0.12529)/2 = 0.13350 \Delta Am_2 = (0.6360) \\ &(1/3600)(0.4651)(1500 \times 10^{-10})(1034 \times 103) \\ &\quad (0.13350) = 3.968 \text{ m}_2 \end{aligned}$$



This is continued, and the results are given in Table 25.6-1. The final total area is 45.94 m<sup>2</sup>.

For part (c), using the shortcut procedure, Eq. (25.6-9) gives the value of  $y_p$ :

$$y_p = y_{av'} = (y_f' + y_0')/2 = (0.5148 + 0.1014)/2 = 0.3081$$

This value of 0.3081 compares to 0.3181 for the numerical method. Making a component balance in Eq. (25.6-12),

$$L_f x_f = (L_f - V_p) x_o + V_p y_p \quad 10.0(0.209) = (10.0 - V_p)0.03 + V_p(0.3081)$$

Solving,  $V_p = 6.437$  and  $L_o = (10.00 - 6.437) = 3.563$ . This gives a stage cut  $\theta = 6.437/10.00 = 0.6437$ , as compared with 0.6213 for the numerical method. To calculate the area, the driving forces are

$$\begin{aligned} x_f - y_f' &= 0.209 - 0.10(0.5148) = 0.15752 \\ x_o - y_o' &= 0.030 - 0.10(0.1014) = 0.01986 \\ \ln m &= (0.15752 + 0.01986) \ln(0.15752/0.01986) = 0.06648 \end{aligned}$$

The area from Eq. (25.6-13) is

$$A_m = 6.437(1/3600)(0.3081)(1500 \times 10 - 10)(1034 \times 103) (0.06648) = 53.43 \text{ m}^2$$

This value of 53.43 is about 16% greater than the numerical method. A plot of these data for the numerical method is given in Fig. 25.6-3.

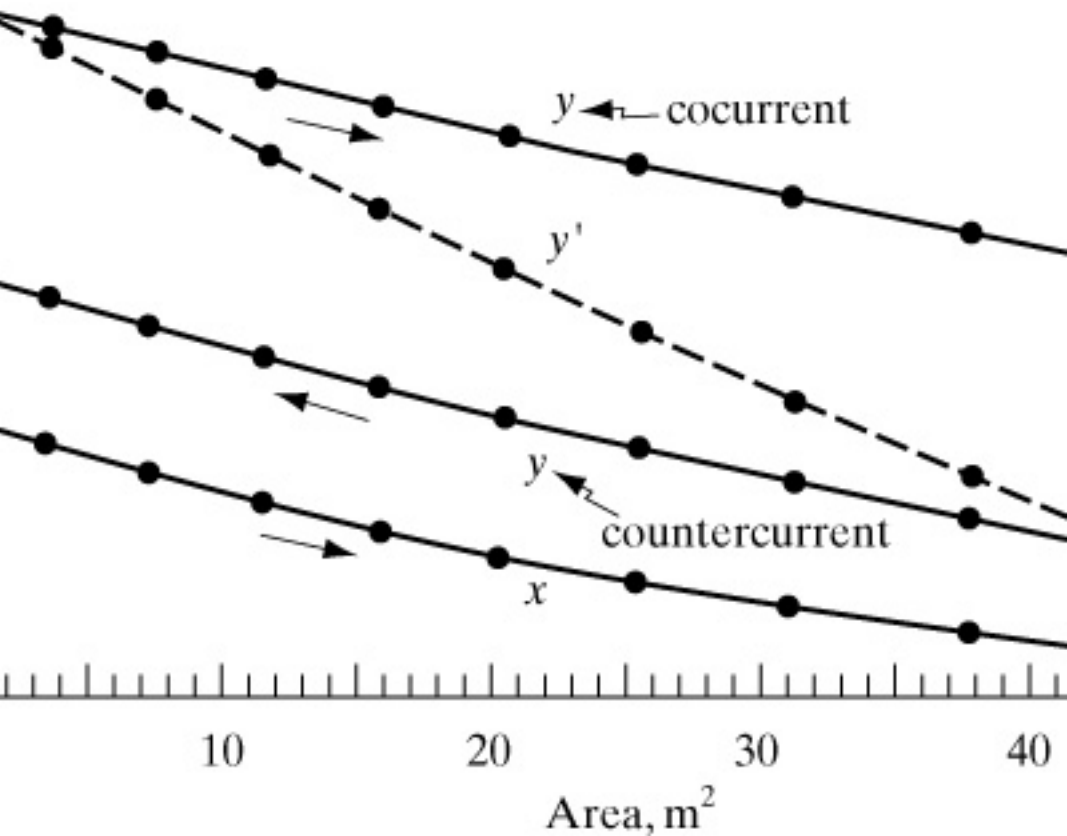


Figure 25.6-3. Plot of composition versus area for the numerical method in Example 25.6-1.

### 25.6C Use of a Spreadsheet for the Finite-Difference Numerical Method

The numerical method can easily be adapted so that a spreadsheet can be used to solve the problem for

asymmetric membranes. Using Excel® or other programs, basic formulas can be entered into cells.

Output data from a spreadsheet are given in Table 25.6-2 for Example 25.6-1. Input data for the calculations are, briefly, as follows: In cells D3–D10, known values are entered. In cell D11, the equation for  $r = p_l/p_h$  is given by the formula  $\$D\$8/\$D\$7$ .

Row 13 is used to keep track of the indexes used in this part of the calculation. Row 14 gives the input values of  $x_1$ ,  $x_2$ , and so on. In rows 15–18, the values of  $a$ ,  $b$ ,  $c$ , and  $y'$  are calculated using Eqs. (25.2-7) and (25.5-27). For example, in cell B18, the formula entered is  $=(-B16+\text{SQRT}(B16*B16-$

$4 \cdot B15 \cdot B17) / (2 \cdot B15)$ . In row 19,  $y_{av}' = (y_1' + y_2') / 2$ . In row 20,  $\Delta V$  is calculated from Eq. (25.6-3). The formula in cell C20 is  $=B21 \cdot (B14 - C14) / (C19 - C14)$  and in D20 it is  $=C21 \cdot (C14 - D14) / (D19 - D14)$ . In row 21,  $L$  is calculated from Eq. (25.6-1), where  $L_2 = L_1 - \Delta V_1$  by using the formula in cell C21, which is  $=(C2 - B21)$ , for C22,  $=(D20 - B21)$ , and so on.

Row 23 is a new set of indexes for countercurrent flow. To calculate  $V$  in row 24 using Eq. (25.6-4), where  $V = \Sigma \Delta V$ , and starting at the outlet  $x_o$ , the formula in cell K24 is  $=K20$ , in J24,  $=J20 + K24$ , and so on. For row 25, to calculate  $\Sigma y_{av}' \Delta V$ , the formula in cell K25 is  $=K19 \cdot K20$ , in J25,  $J19 \cdot J20 + K25$ , and so on. For the bulk permeate composition,  $y$  is calculated in row 26

from Eq. (25.6-5), where  $y = \Sigma y_{av'} \Delta V / V$ .  
In cell B26, the formula is =B25/B24.

Rows 28–32 are optional and are used to check the mass balances for the inlet and outlet streams. In cell B29, the mass in is =\$D\$4; the mass out in B30 is =B24+K21. Similarly, cell B31 is =\$D\$4\*\$D\$5 and B32 is =B24\*B26+K21\*K14.

For cocurrent flow, starting at  $x_f$ , Eq. (25.6-4), where  $V = \Sigma \Delta V$ , is calculated in row 35. In row 36,  $\Sigma y_{av'} \Delta V$  is calculated using the formula in cell C36 of =19\*C20, in D36, =D19\*D20+C36, and so on. Then, Eq. (25.6-5) is used to calculate the bulk composition  $y$  from  $\Sigma y_{av'} \Delta V / V$  in row 37.

To calculate the areas, in row 41 (=  $x -$

$ry'_{av}$  is calculated for each increment, using Eq. (25.6-7). The formula in cell B41 is  $=((B14-\$D\$11*B18)+(C14-\$D\$11*C18))/2$ . In cell B42, the conversion of  $V$  m<sup>3</sup>/h to m<sup>3</sup>/s and kPa to Pa is performed using  $=(\$D\$9*\$D\$7*1000*3600)$ . In row 43, using Eq. (25.6-8) to calculate  $\Delta A_m$ , the formula in cell B43 is  $C19*C20/(\$B\$42*B41)$ . In row 44, all of the  $\Delta A_m$  values in row 43 are added to get the total  $A_m$  using  $=SUM(B43:J43)$ .

## 25.6D Calculation of Pressure-Drop Effects on Permeation

*1. Estimation of the number of tubes and length.* In order to calculate the pressure drop inside the hollow-fiber tubes, the dimensions, number of tubes, and area  $A_m$  of the membrane must be known. The following procedure can be employed. The

shortcut procedure is first used with Eqs. (25.6-9)–(25.6-13). This gives  $L_f$ ,  $L_o$ ,  $V_p$ ,  $y_{av}'$ , and  $A_m$ . Then, the average flow rate in the tubes is calculated from the equation  $L_{av} = (L_f + L_o)/2$ .

The number of tubes in parallel  $NT$  must be estimated from typical laboratory or commercial data. For example, for air with a flow rate of 3 m<sup>3</sup>/h,  $3.8 \times 10^4$  fibers ( $NT$ ) are used with an ID of 95  $\mu\text{m}$ , and a length  $(z_2 - z_1)$  of 48.26 cm. For a flow rate  $L_f$  of 10.0 m<sup>3</sup>/hr in Example 25.6-1 and to keep a similar and reasonable velocity in the tubes, the  $NT$  needed will be directly proportional to the inlet  $L_f$ . Then, knowing the  $A_m$ , an estimated total length  $(z_2 - z_1)$  of the tubes can be calculated from Eq. (25.6-14):

Table 25.6-2. *Output from a Spreadsheet for the Finite-Difference Method for Example 25.6-1*



$$A_m = \pi D N T (z_2 - z_1) \quad (25.6-14)$$

2. *Finite-difference method to include the effect of pressure drop.* For the finite-difference numerical method, Eq. (25.6-14) can be rewritten as

$$\Delta A_m = \pi D N T (\Delta z) \quad (25.6-15)$$

Also, Eq. (25.5-38) can be rewritten for a finite increment of  $\Delta z$  length:

$$\Delta p h \Delta z = -128 \mu \pi D^4 N T (L T T S p s p h a v) \quad (25.6-16)$$

The following steps, which may require



several iterations, can be used in the finite-difference numerical method to include the effect of pressure drop in the tubes:

1. For the first increment shown in Fig. 25.6-2, a constant inlet pressure  $p_{h1}$  ( $p_h$ ) is used for  $p_{hav}$  to calculate  $y_1'$  and  $y_2'$   $\Delta V_1$ ,  $L_2$ , and  $\Delta A_{m1}$  from Eqs. (25.5-27), (25.6-1), (25.6-3), (25.6-7), and (25.6-8).
2. The value of  $NT$  is obtained from typical data as discussed above in subsection 1, above. Using Eq. (25.6-15), the incremental length  $\Delta z$  is obtained.
3. Using  $L_{av} = (L_1 + L_2)/2$  and the inlet  $p_{h1}$  for  $p_{hav}$ , the  $\Delta p_h$  for the first increment is calculated from Eq. (25.6-16).
4. For the second iteration, the new  $p_{h\ av}$  to use is calculated from  $p_{hav} = p_{h1} - \Delta p_h/2$ . A new value of the outlet  $p_{h2} = p_{h1} - \Delta p_h$  is used to recalculate a new  $y_2'$  from Eq. (25.5-27). The value of  $y_1'$  remains the same. Then, by repeating steps 1 through 4, a new value of  $\Delta p_h$  is obtained. Usually only three or so iterations are needed to obtain a constant value of  $\Delta p_h$ ,  $p_{hav}$ , and  $\Delta A_{m1}$ . Using a spreadsheet as in Ex. 25.6-1, this procedure can be repeated for each finite section.

### *3. Determination of the effect of pressure drop using the shortcut*

*method.* The values of  $L_{av}$ ,  $NT$ ,  $A_m$ , and overall length ( $z_2 - z_1$ ) are obtained from the shortcut calculation in subsection 1, above. The shortcut value of the overall pressure drop ( $p_h - p_{ho}$ ) can be obtained from Eq. (25.6-16) using  $p_h$  at the inlet as  $p_{h\ av}$  and the overall length ( $z_2 - z_1$ ). Then, for a second and final iteration, the new and corrected pressures  $p_{h\ av} = p_h - \Delta p_h / 2$  and  $p_{ho} = p_h - \Delta p_h$  are used in Eqs. (25.5-27) and (25.6-9)–(25.6-13) to recalculate  $y_o'$ ,  $y_{av}'$ ,  $V_p$ , and  $A_m$  again. This recalculated  $A_m$  will include an approximate effect of pressure drop in the tubes.

## 25.7 Chapter Summary

### Series Resistances in a Membrane Process

$$N_A = (p_{A1} - p_{A2}) \left[ \frac{1}{(k_c / RT)} + \frac{1}{(P_M / L)} + \frac{1}{(k_c / RT)} \right] \quad (25.1-7)$$

## Three Common Types of Equipment for a Gas Permeation Process

1. Flat membrane
2. Spiral-wound membrane
3. Hollow-fiber membrane

## Four Ideal Flow Patterns in a Membrane Separator and Their Associated Membrane Area Equation:

1. Complete-Mixing Model:

$$A_m = \theta L f_{yp} (P A' / t) (p_{hx} - p_{ly}) \quad (25.2-10)$$

2. Cross-Flow Model:

$$A_m = t L f_{ph} P B' \int_{i_o}^{i_f} (1 - \theta^*) (1 - x) d i (f_i - i) [1 + i - p l_{ph} (1 + f_i)] \quad (25.4-5)$$

where

$$f_i = (D_i - F) + (D_i^2 + 2E_i + F^2)^{0.5}$$

3. Countercurrent Model:

$$dA_m dx = -L_o [(y - x_o) / (x - y)] (P B' / t) p_h \{ (1 - y) \alpha^* (x - r y) - x [ (1 - x) - r (1 - y) ] \} \text{ (Symmetric membrane)} \quad (25.5-26)$$

$$dA_m dx = -L_o [(y - x_o) / (x - y)] (P B' / t) p_h \{ (1 - y) \alpha^* (x - r y') - x [ (1 - x) - r (1 - y') ] \} \text{ (Asymmetric membrane)} \quad (25.5-34)$$

#### 4. Cocurrent Model:

$$dA_{mdx} = Lf[(y - xf)/(x - y)](PB'/t) \ln \left\{ \frac{(1 - x)\alpha^*(x - ry') - x}{(1 - x) - r(1 - y')} \right\} \quad (25.5-36)$$

## Problems

**25.1-1. Gas-Permeation Membrane for Oxygenation.** To determine the suitability of silicone rubber for use as a membrane for a heart–lung machine to oxygenate blood, an experimental value of the permeability at 30°C of oxygen was obtained, where  $P_M = 6.50 \times 10^{-7} \text{ cm}^3 \text{ O}_2 \text{ (STP)/(s} \cdot \text{cm}^2 \cdot \text{cm Hg/mm)}$ .

- Predict the maximum flux of  $\text{O}_2$  in  $\text{kg mol/s} \cdot \text{m}^2$  with an  $\text{O}_2$  pressure of 700 mmHg on one side of the membrane and an equivalent pressure in the blood film side of 50 mm. The membrane is 0.165 mm thick. Since the gas film is pure oxygen, the gas film resistance is zero. Neglect the blood film resistance in this case.
- Assuming a maximum requirement for an adult of 300  $\text{cm}^3 \text{ O}_2 \text{ (STP)}$  per minute, calculate the membrane surface area required in  $\text{m}^2$ . (*Note:* The actual area needed should be considerably larger

since the blood film resistance, which must be determined by experiment, can be appreciable.)

**Ans. (b)  $1.953 \text{ m}^2$**

**25.2-1. *Derivation of the Equation for Permeate Concentration.*** Derive Eq.

(25.2-11) for Case 2 for complete mixing. Note that  $x_o$  from Eq. (25.2-9) must first be substituted into Eq. (25.2-6) before multiplying out the equation and solving for  $y_p$ .

**25.2-2. *Use of the Complete-Mixing Model for Membrane Design.*** A

membrane having a thickness of  $2 \times 10^{-3} \text{ cm}$ , permeability  $PA' = 400 \times 10^{-10} \text{ cm}^3 (\text{STP}) \cdot \text{cm}/(\text{s} \cdot \text{cm}^2 \cdot \text{cm Hg})$ , and  $\alpha^* = 10$  is to be used to separate a gas mixture of *A* and *B*. The feed flow rate is  $L_f = 2 \times 10^{-3} \text{ cm}^3 (\text{STP})/\text{s}$  and its composition is  $x_f = 0.413$ . The feed-side

pressure is 80 cm Hg and the permeate-side pressure is 20 cm Hg. The reject composition is to be  $x_o = 0.30$ . Using the complete-mixing model, calculate the permeate composition, fraction of feed permeated, and membrane area.

**Ans.**  $y_p = 0.678$

**25.2-3. Design Using the Complete-Mixing Model.** A gaseous feed stream having a composition  $x_f = 0.50$  and a flow rate of  $2 \times 10^{-3} \text{ cm}^3 \text{ (STP)/s}$  is to be separated in a membrane unit. The feed-side pressure is 40 cm Hg and the permeate is 10 cm Hg. The membrane has a thickness of  $1.5 \times 10^{-3} \text{ cm}$ , permeability  $PA' = 40 \times 10^{-10} \text{ cm}^3 \text{ (STP)} \times \text{cm}/(\text{s} \cdot \text{cm}^2 \cdot \text{cm Hg})$ , and  $\alpha^* = 10$ . The fraction of feed permeated is 0.529.

- Use the complete-mixing model to calculate the permeate composition, reject composition, and membrane area.
- Calculate the minimum reject concentration.
- If the feed composition is increased to  $x_f = 0.60$ , what is this new minimum reject concentration?

**Ans.** (a)  $A_m = 5.153 \times 10^7 \text{ cm}^2$  (c)  $x_{oM} = 0.2478$

**25.2-4. *Effect of Permeabilities on a Minimum Reject Concentration.*** For the conditions of Problem 25.2-2,  $x_f = 0.413$ ,  $\alpha^* = 10$ ,  $p_l = 20 \text{ cm Hg}$ ,  $p_h = 80 \text{ cm Hg}$ , and  $x_o = 0.30$ . Calculate the minimum reject concentration for the following cases:

- Calculate  $x_{oM}$  for the given conditions.
- Calculate the effect on  $x_{oM}$  if the permeability of  $B$  increases so that  $\alpha^*$  decreases to 5.
- Calculate the limiting value of  $x_{oM}$  when  $\alpha^*$  is lowered to its minimum value of 1.0. Make a plot of

$x_{oM}$  versus  $\alpha^*$  for these three cases.

**25.2-5. Minimum Reject Concentration and Pressure Effect.** For Example 25.2-2 for separation of air, do as follows:

- Calculate the minimum reject concentration.
- If the pressure on the feed side is reduced by one-half, calculate the effect on  $x_{oM}$ .

**Ans.** (b)  $x_{oM} = 0.0624$

**25.3-1. Separation of Multicomponent Gas Mixtures.** Using the same feed composition and flow rate, pressures, and membrane as in Example 25.3-1, do the following, using the complete-mixing model:

- Calculate the permeate composition, reject composition, and membrane area for a fraction permeated of 0.50 instead of 0.25.
- Repeat part (a) but for  $\theta = 0.90$ .



- Make a plot of permeate composition  $y_{pA}$  versus  $\theta$  and also of area  $A_m$  versus  $\theta$  using the calculated values for  $\theta = 0.25, 0.50$ , and  $0.90$ .

**25.3-2. Separation of Helium from Natural Gas.** A typical composition of a natural gas (S1) is 0.5% He (A), 17.0% N<sub>2</sub> (B), 76.5% CH<sub>4</sub> (C), and 6.0% higher hydrocarbons (D). The membrane proposed to separate helium has a thickness of  $2.54 \times 10^{-3}$  cm, and the permeabilities are  $P'_A = 60 \times 10^{-10}$  cm<sup>3</sup> (STP) · cm/(s · cm<sup>2</sup> · cm Hg),  $P'_B = 3.0 \times 10^{-10}$  and  $P'_C = 1.5 \times 10^{-10}$ . It is assumed that the higher hydrocarbons are essentially nonpermeable ( $P'_D \cong 0$ ). The feed flow rate is  $2.0 \times 10^5$  cm<sup>3</sup> (STP)/s. The feed pressure  $p_h = 500$  cm Hg and the permeate pressure  $p_l = 20$  cm Hg.

- For a fraction permeated of 0.2, calculate the permeate composition, reject composition, and membrane area using the complete mixing model.

- Use the permeate from part (a) as feed to a completely mixed second stage. The pressure  $p_h = 500$  cm Hg and  $p_l = 20$  cm. For a fraction permeated of 0.20, calculate the permeate composition and membrane area.

**25.4-1. Design Using the Cross-Flow Model for a Membrane.** Use the same conditions for the separation of an air stream as given in Example 25.4-1. The given values are  $x_f = 0.209$ ,  $\alpha^* = 10$ ,  $p_h = 190$  cm Hg,  $p_l = 19$  cm Hg,  $L_f = 1 \times 10^6$  cm<sup>3</sup> (STP)/s,  $PA' = 500 \times 10^{-10}$  cm<sup>3</sup> (STP) · cm/(s · cm<sup>2</sup> · cm Hg), and  $t = 2.54 \times 10^{-3}$  cm. Do as follows using the cross-flow model:

- Calculate  $y_p$ ,  $x_o$ , and  $A_m$  for  $\theta = 0.40$ .
- Calculate  $y_p$  and  $x_o$  for  $\theta = 0$ .

**Ans.** (a)  $y_p = 0.452$ ,  $x_o = 0.0303$ ,  $A_m = 6.94 \times 10^8$  cm<sup>2</sup> (S6); (b)  $y_p = 0.655$ ,  $x_o = 0.209$

### ***25.5-1. Equations for the Cocurrent and Countercurrent Flow Models.***

Derive the equations for the following cases:

- For cocurrent flow, show the detailed steps for deriving Eqs. (25.5-35) and (25.5-36).
- For countercurrent flow, show the detailed steps in obtaining Eq. (25.5-22) from (25.5-4) and (25.5-5). Also, show the detailed steps to derive Eq. (25.5-24).

***25.5-2. Design Using the Countercurrent-Flow Model for a Membrane.*** Use the same conditions as given in Example 25.4-1 for the separation of an air stream. The given values are  $x_f = 0.209$ ,  $\alpha^* = 10$ ,  $p_h = 190$  cm Hg,  $p_l = 19$  cm Hg,  $L_f = 1 \times 10^6$  cm<sup>3</sup> (STP)/s,  $PA' = 500 \times 10^{-10}$  cm<sup>3</sup> (STP) · cm/(s · cm<sup>2</sup> · cm Hg), and  $t = 2.54 \times 10^{-3}$  cm. Using the countercurrent-flow model, calculate  $y_p$ ,  $x_o$ , and  $A_m$  for  $\theta =$

0.40. (*Note:* This problem involves a trial-and-error procedure along with the numerical solution of two differential equations.)

### ***25.6-1. Effect of Pressure Drop on Asymmetric Membrane Calculations.***

Using the same conditions as in Example 25.6-1, do as follows:

- Use the shortcut method to calculate the overall pressure drop  $\Delta p_h$  using Eq. (25.6-16) over the entire length. Use typical data for air given in Section 25.D to calculate  $NT$ , fiber length  $z_2 - z_1$ , and so forth. Assume  $T = 25^\circ + 273$  K and  $p_h = 1034$  kPa,  $T_s = 273$  K,  $p_s = 101.325$  kPa.
- With the above values of  $p_h$ , use the shortcut method in a second iteration to recalculate  $A_m$ . (Be sure to correct for  $P_{ho}$  at  $x_o$  and  $y_o'$ ).
- Calculate the pressure drop if the number of tubes  $NT$  in part (a) is reduced by 50%.

**Ans.** (a)  $NT = 1.267 \times 10^5$ ,  $(z_2 - z_1) = 1.413$  m,  $\Delta p_h = 20.74$  kPa; (b)  $A_m =$

$$54.10 \text{ m}^2; \text{ (c) } \Delta p_h = 82.96 \text{ kPa}$$

**25.6-2. Spreadsheet Calculation for an Asymmetric Membrane.** Using the conditions for Example 25.6-1, write the detailed spreadsheet and calculate the results. Compare these results with those in Table 25.6-2.

**25.6-3. Comparison of Experimental and Predicted Spreadsheet Results in a Pilot-Unit Asymmetric Membrane.** A pilot-size membrane used to separate air in order to obtain nitrogen has the following dimensions with the feed inside the tubes: total  $N_T = 3.8 \times 10^4$  fibers, ID =  $95 \mu\text{m}$ , OD =  $135 \mu\text{m}$ , length of fibers = 19 in. An experimental run gave the following results. Feed rate  $L_f = 1.086 \text{ m}^3/\text{h}$ ,  $L_o = 0.654 \text{ m}^3/\text{h}$ ,  $V_p = 0.450 \text{ m}^3/\text{h}$ ,  $x_o =$

0.067 mole fraction oxygen,  $y_p = 0.413$ ,  $p_h = 703.81$  kPa,  $p_l = 98.10$  kPa, and  $T = 25^\circ\text{C}$ . The permeances determined previously are  $(P' \text{ O}_2 / t) = 1.50 \times 10^{-10} \text{ m}^3 (\text{STP})/(\text{s} \cdot \text{m}^2 \cdot \text{Pa})$ ,  $(P' \text{ N}_2 / t) = 2.47 \times 10^{-10}$ . Flow is counter current. Do as follows:

- Predict the pressure drop in the tubes using the shortcut method.
- Using a spreadsheet, predict the performance of this run and compare these results with the experimental values. Note that this is trial and error, since the area is fixed but the value of  $x_o$  is not. First, assume a value of  $x_o$ . Then, divide the difference between  $x_f = 0.209$  and  $x_o$  into nine equal parts and perform the spreadsheet calculation. If the calculated and actual areas do not agree, assume another value of  $x_o$ , and so forth. Neglect pressure drop.

**Ans.** (a)  $\Delta p_h = 4.455$  kPa; (b)  $x_o = 0.079$ ,  $V_p = 0.442 \text{ m}^3/\text{hr}$ ,  $y_p = 0.398$

## References

## Notation

# Chapter 26. Distillation

## 26.0 Chapter Objectives

On completion of this chapter, a student should be able to:

- Plot an  $x$ ,  $y$  diagram using Raoult's law
- Distinguish between a minimum and a maximum boiling azeotrope
- Describe the three common types of column internals used in a distillation tower
- Describe the concept of constant molal overflow
- Describe the differences between batch and fractional distillation
- Use the McCabe–Thiele method to solve a variety of binary distillation problems
- Describe and calculate the three types of tray efficiencies discussed in the chapter
- Calculate column diameter and heights



- Use shortcut methods for multicomponent distillation to calculate number of stages and optimal feed stage

## 26.1 Equilibrium Relations Between Phases

### 26.1A Phase Rule and Raoult's Law

As in the gas–liquid systems, the equilibrium in vapor–liquid systems is restricted by the phase rule, Eq. (22.1-1). As an example, we shall use the ammonia–water, vapor–liquid system. For two components and two phases,  $F$  from Eq. (22.1-1) is 2 degrees of freedom. The four variables are temperature, pressure, and the composition  $y_A$  of  $\text{NH}_3$  in the vapor phase, and  $x_A$  in the liquid phase. The composition of water ( $B$ ) is fixed if  $y_A$  or  $x_A$  is specified, since  $y_A + y_B = 1.0$  and  $x_A + x_B = 1.0$ . If the pressure is fixed, only one more variable can be set. If we set the

liquid composition, the temperature and vapor composition are automatically set.

An ideal law, *Raoult's law*, can be defined for vapor–liquid phases in equilibrium:

$$p_A = P_A x_A \quad (26.1-1)$$

where  $p_A$  is the partial pressure of component  $A$  in the vapor in Pa (atm),  $P_A$  is the vapor pressure of pure  $A$  in Pa (atm), and  $x_A$  is the mole fraction of  $A$  in the liquid. This law holds only for ideal solutions, such as benzene–toluene, hexane–heptane, and methyl alcohol–ethyl alcohol, which are usually substances very similar to each other. Many systems that are ideal or nonideal solutions follow Henry's law in dilute

solutions.

### 26.1B Boiling-Point Diagrams and $x$ - $y$ Plots

Often, the vapor–liquid equilibrium relations for a binary mixture of  $A$  and  $B$  are given as a boiling-point diagram, shown in Fig. 26.1-1 for the system benzene ( $A$ )–toluene ( $B$ ) at a total pressure of 101.32 kPa. The upper line is the saturated vapor line (the *dew-point line*) and the lower line is the saturated liquid line (the *bubble-point line*). The two-phase region is in the region between these two lines.

In Fig. 26.1-1, if we start with a cold liquid mixture of  $x_{A1} = 0.318$  and heat the mixture, it will start to boil at  $98^{\circ}\text{C}$  (371.2 K) and the composition of the first vapor in equilibrium is  $y_{A1} = 0.532$ .

As we continue boiling, the composition  $x_A$  will move to the left since  $y_A$  is richer in A.

The system benzene–toluene follows Raoult’s law, so the boiling-point diagram can be calculated from the pure vapor-pressure data in Table 26.1-1 and the following equations:

$$p_A + p_B = P \quad (26.1-2)$$

$$P x_A + P_B (1 - x_A) = P \quad (26.1-3)$$

$$y_A = p_A / P = P_A x_A / P \quad (26.1-4)$$

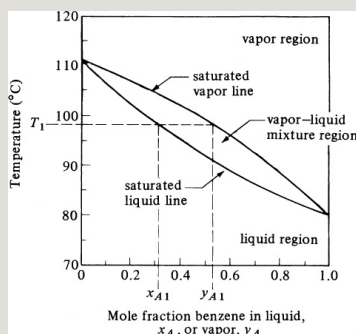


Figure 26.1-1. Boiling-point diagram for benzene (A)–toluene (B)

at 101.325 kPa (1 atm) total pressure.

## Table 26.1-1. *Vapor-Pressure and Equilibrium-Mole-Fraction Data for Benzene–Toluene System*

### **EXAMPLE 26.1-1. Use of Raoult's Law for Boiling-Point Diagram**

Calculate the vapor and liquid compositions in equilibrium at 95°C (368.2 K) for benzene–toluene using the vapor pressure from Table 26.1-1 at 101.32 kPa.

**Solution:** At 95°C from Table 26.1-1 for benzene,  $P_A = 155.7$  kPa and  $P_B = 63.3$  kPa. Substituting into Eq. (26.1-3) and solving,

$$155.7(x_A) + 63.3(1 - x_A) = 101.32 \text{ kPa (760 mmHg)}$$

Hence,  $x_A = 0.411$  and  $x_B = 1 - x_A = 1 - 0.411 = 0.589$ . Substituting into Eq. (26.1-4),

$$y_A = P_A x_A / P = 155.7(0.411) / 101.32 = 0.632$$

A common method of plotting the equilibrium data is shown in Fig. 26.1-2, where  $y_A$  is plotted versus  $x_A$  for the benzene–toluene system. The 45° line is given to show that  $y_A$  is richer in

component A than is  $x_A$ .

The boiling-point diagram in Fig. 26.1-1 is typical of an ideal system following Raoult's law. Nonideal systems differ considerably. In Fig. 26.1-3a, the boiling-point diagram is shown for a maximum-boiling azeotrope. The maximum temperature  $T_{\max}$  corresponds to a concentration  $x_{Az}$  and  $x_{Az} = y_{Az}$  at this point. The plot of  $y_A$  versus  $x_A$  would show the curve crossing the  $45^\circ$  line at this point. Acetone–chloroform is an example of such a system. In Fig. 26.1-3b, a minimum-boiling azeotrope is shown with  $y_{Az} = x_{Az}$  at  $T_{\min}$ . Ethanol–water is such a system.

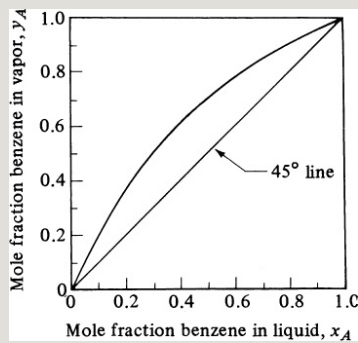


Figure 26.1-2. *Equilibrium diagram for system benzene (A)–toluene (B) at 101.32 kPa (1 atm).*

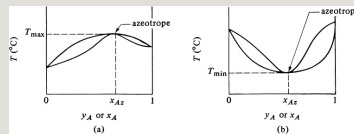


Figure 26.1-3. *Equilibrium boiling-point diagrams: (a) maximum-boiling azeotrope, (b) minimum-boiling azeotrope.*

## 26.2 Single and Multiple Equilibrium Contact Stages

### 26.2A Equipment for Distillation

*1. Various types of tray (plate) towers for absorption and distillation.* In order to efficiently bring the vapor and liquid into contact in absorption and distillation, tray towers of the following types

are often used:

1. *Sieve tray.* The sieve tray shown in Fig. 26.2-1a is very common. Essentially the same tray is used in distillation and gas absorption. In the sieve tray, vapor bubbles up through simple holes in the tray through the flowing liquid. Hole sizes range from 3 to 12 mm in diameter, with 5 mm a common size. The vapor area of the holes varies between 5 to 15% of the tray area. The liquid is held on the tray surface and is prevented from flowing down through the holes by the kinetic energy of the gas or vapor. The depth of liquid on the tray is maintained by an overflow outlet weir. The overflow liquid flows into the downspout to the next tray below.

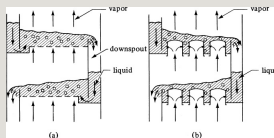


Figure 26.2-1. Tray contacting devices: (a) detail of sieve-tray tower, (b) detail of valve-tray tower.

2. *Valve tray.* A modification of the sieve tray is the valve tray shown in Fig. 26.2-1b. This consists of an opening in the tray and a lift-valve cover with guides to keep the cover properly positioned over the opening. This provides a variable open area that is varied by the vapor flow inhibiting leakage of liquid down the opening at low vapor rates. Hence, this type of tray can operate over a greater range of flow rates than can the sieve tray, with a



cost of only about 20% more than a sieve tray. The valve tray is being increasingly used today (S2).

3. *Bubble-cap tray.* Bubble-cap trays have been used for over 100 years, but since 1950 they have been generally superseded by sieve-type or valve trays because of their cost, which is almost double that of sieve-type trays. In the bubble tray, the vapor or gas rises through the opening in the tray into the bubble caps. Then, the gas flows through slots in the periphery of each cap and bubbles upward through the flowing liquid. Details and design procedures for many of these and other types of trays are given elsewhere (B2, P2, T1). Efficiencies for the different types of trays are discussed in Section 26.5.

2. *Structured packing for absorption and distillation.* Structured packing has become competitive with conventional tray towers, especially in tower revamps where increased capacity and/or efficiency is desired (K1, L1). In typical corrugated-sheet packing, the thin corrugated-metal sheets are formed in a triangular cross section. The vapor flow goes upward through the triangular channels, which are set at a  $45^\circ$  angle

with the vertical. The sheets are arranged so the liquid flows downward in the opposite direction and spreads over the surfaces, as in a wetted-wall tower.

The open void fraction typically varies from 0.91 to 0.96 and the specific surface area from 165 to 330 m<sup>2</sup>/m<sup>3</sup> volume (50 to 100 ft<sup>2</sup>/ft<sup>3</sup>). In many cases, the packing sheet contains perforations or holes about 2–4 mm ID spaced 0.5–1.5 cm apart to help wet both the upper and lower sides of the sheet.

*3. Packed towers for absorption and distillation.* Packed towers are used for continuous countercurrent contacting of gas and liquid in absorption as well as for vapor–liquid contacting in

distillation. The tower in Fig. 26.2-2 consists of a cylindrical column containing a gas inlet and distributing space at the bottom, a liquid inlet and distributing device at the top, a gas outlet at the top, a liquid outlet at the bottom, and a packing or filling in the tower. The gas enters the distributing space below the packed section and rises upward through the openings or interstices in the packing and contacts the descending liquid flowing through the same openings. A large area of intimate contact between the liquid and gas is provided by the packing.

*4. Types of random packing for absorption and distillation.* Many different types of tower packings have been developed and a number are used quite often. Common types of packing

that are dumped at random in the tower are shown in Fig. 26.2-3. Such packings and other commercial packings are available in sizes of 3 mm to about 75 mm. Most of the tower packings are made of materials such as clay, porcelain, metal, or plastic. High void spaces of 65–95% are characteristic of good packings. The packings permit relatively large volumes of liquid to pass countercurrent to the gas flow through the openings with relatively low pressure drops for the gas. These same types of packings are also used in vapor–liquid separation processes of distillation.

Ceramic Raschig rings and Berl saddles shown in Figs. 26.2-3a and b are older types of random packing and are seldom used now (K1). Pall rings (second-

generation packing) shown in Fig. 26.2-3c, are made of plastic or metal; they are much more efficient and are still currently used. They have porosities or void spaces of 0.90–0.96 and areas of 100–200 m<sup>2</sup>/m<sup>3</sup> (30–60 ft<sup>2</sup>/ft<sup>3</sup>). The latest or third-generation packings are the Intalox metal type, shown in Fig. 26.2-3d, which is a combination of the Berl saddle and the Pall ring, and the Jaeger Metal Tri-Pack, shown in Fig. 26.2-3e, which is a Pall ring with a spherical shape. Porosities range from 0.95 to 0.98. Many other types of new packings are available. These third-generation packings are only slightly more efficient than the Pall rings.

Stacked packings having sizes of 75 mm or so and larger are also used. The packing is stacked vertically, with open

channels running uninterrupted through the bed. The advantage of the lower pressure drop of the gas is offset in part by the poorer gas–liquid contact in stacked packings. Typical stacked packings are wood grids, drip-point grids, spiral partition rings, and others.

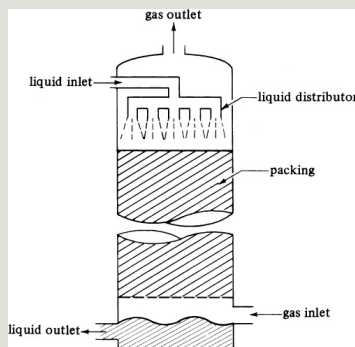


Figure 26.2-2. *Packed tower flows and characteristics for absorption.*

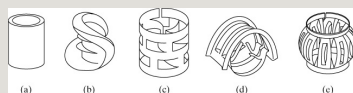


Figure 26.2-3. *Typical random or dumped tower packings: (a) Raschig ring; (b) Berl saddle; (c) Pall ring; (d) Intalox metal, IMTP; (e) Jaeger Metal Tri-Pack.*

## 26.2B Single-Stage Equilibrium Contact for Vapor–Liquid System

If a vapor–liquid system is being considered, where the stream  $V_2$  is a vapor and  $L_0$  is a liquid, and the two streams are brought into contact in a single equilibrium stage that is quite similar to Fig. 22.1-2, the boiling point or the  $x$ - $y$  equilibrium diagram must be used, because an equilibrium relation similar to Henry's law is not available. Since we are considering only two components,  $A$  and  $B$ , only Eqs. (22.1-4) and (22.1-5) are used for the material balances. If sensible heat effects are small and the latent heats of both compounds are the same, then when 1 mol of  $A$  condenses, 1 mol of  $B$  must vaporize. Hence, the total moles of vapor  $V_2$  entering will equal  $V_1$  leaving. Also, moles  $L_0 = L_1$ . This case is called one of

*constant molal overflow.* An example is the benzene–toluene system.

**EXAMPLE 26.2-1. Equilibrium Contact of Vapor–Liquid Mixture**

A vapor at the dew point and 101.32 kPa containing a mole fraction of 0.40 benzene (*A*) and 0.60 toluene (*B*) and 100 kg mol total is brought into contact with 110 kg mol of a liquid at the boiling point containing a mole fraction of 0.30 benzene and 0.70 toluene. The two streams are contacted in a single stage, and the outlet streams leave in equilibrium with each other. Assume constant molal overflow. Calculate the amounts and compositions of the exit streams.

**Solution:** The process flow diagram is the same as in Fig. 22.1-2. The given values are  $V_2 = 100$  kg mol,  $y_{A2} = 0.40$ ,  $L_0 = 110$  Kg mol, and  $x_{A0} = 0.30$ . For constant molal overflow,  $V_2 = V_1$  and  $L_0 = L_1$ . Substituting into Eq. (22.1-5) to make a material balance on component *A*,

$$L_0 x_{A0} + V_2 y_{A2} = L_1 x_{A1} + V_1 y_{A1} \quad (22.1-5)$$

$$110(0.30) + 100(0.40) = 110x_{A1} + 100y_{A1} \quad (26.2-1)$$

To solve Eq. (26.2-1), the equilibrium relation between  $y_{A1}$  and  $x_{A1}$  in Fig. 26.1-1 must be used. This is by trial and error, since an analytical expression is not available that relates  $y_A$  and  $x_A$ .

First, we assume that  $x_{A1} = 0.20$  and substitute into Eq. (26.2-1) to solve for  $y_{A1}$ :

$$110(0.30) + 100(0.40) = 110(0.20) + 100y_{A1}$$

Solving,  $y_{A1} = 0.51$ . The equilibrium relations for benzene–toluene are plotted in Fig. 26.2-4. It is evident that  $y_{A1} = 0.51$  and  $x_{A1} = 0.20$  do not fall on the curve. This point is plotted on the graph. Next, assuming that  $x_{A1} = 0.40$  and



solving,  $y_{A1} = 0.29$ . This point is also plotted in Fig. 26.2-4. Assuming that  $x_{A1} = 0.30$ ,  $y_{A1} = 0.40$ . A straight line is drawn between these three points that represents Eq. (26.2-1). At the intersection of this line with the equilibrium curve,  $y_{A1} = 0.455$  and  $x_{A1} = 0.25$ , which agree with Eq. (26.2-1).

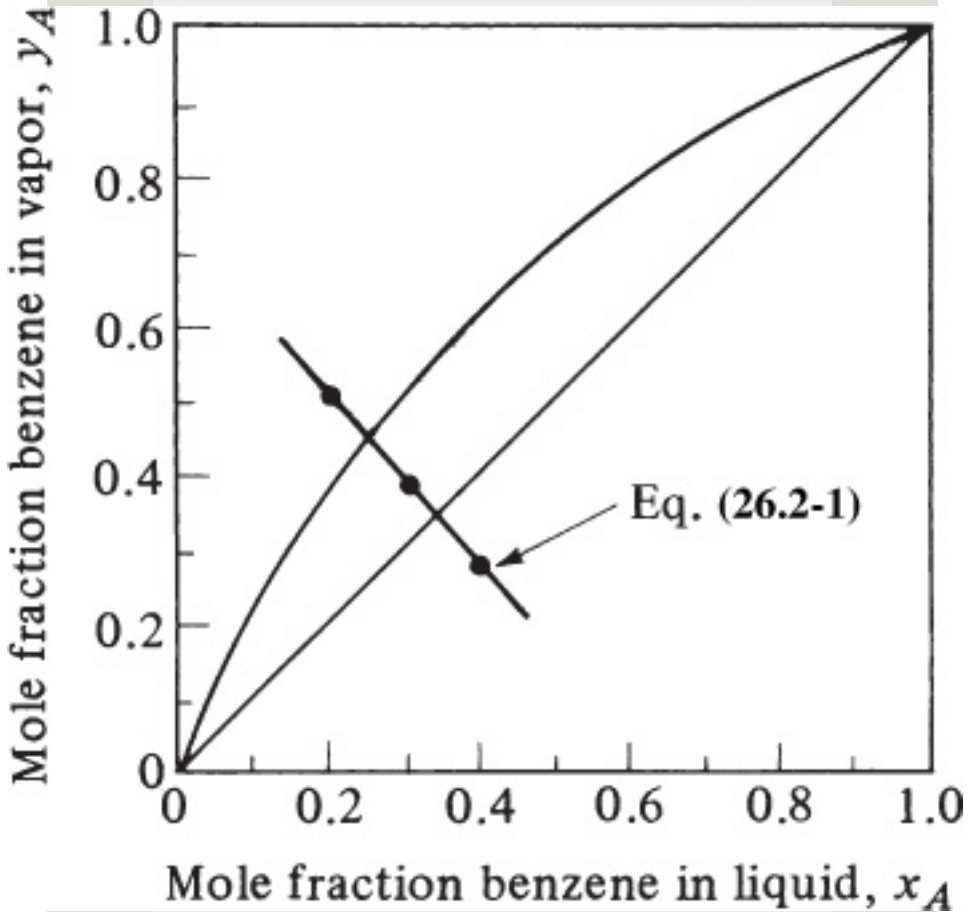


Figure 26.2-4. Solution to Example 26.2-1.

## 26.3 Simple Distillation Methods

### 26.3A Introduction

The separation process known as distillation is a method for separating the various components of a liquid solution that depends upon the distribution of these components between a vapor phase and a liquid phase. All components are present in both phases. The vapor phase is created from the liquid phase by vaporization at the boiling point.

The basic requirement for the separation of components by distillation is that the composition of the vapor be different from the composition of the liquid with which it is in equilibrium at the boiling point of the liquid. Distillation is concerned with solutions where all components are appreciably volatile, such as ammonia–water or ethanol–water solutions, where both components

will be in the vapor phase. By contrast, in evaporation of a solution of salt and water, for example, the water is vaporized but the salt is not. The process of absorption differs from distillation in that one of the components in absorption is essentially insoluble in the liquid phase. An example is absorption of ammonia from air by water, where air is insoluble in the water–ammonia solution.

### **26.3B Relative Volatility of Vapor–Liquid Systems**

In Fig. 26.1-2, in the equilibrium diagram for a binary mixture of  $A$  and  $B$ , the greater the distance between the equilibrium line and the  $45^\circ$  line, the greater the difference between the vapor composition  $y_A$  and liquid composition  $x_A$ . Hence, the separation is more easily made.

A numerical measure of this separation is the relative volatility  $\alpha_{AB}$ . This is defined as the ratio of the concentration of  $A$  in the vapor to the concentration of  $A$  in the liquid divided by the ratio of the concentration of  $B$  in the vapor to the concentration of  $B$  in the liquid:

$$\alpha_{AB} = \frac{y_A/x_A}{y_B/x_B} = \frac{y_A/x_A(1-y_A)}{(1-x_A)} \quad (26.3-1)$$

where  $\alpha_{AB}$  is the relative volatility of  $A$  with respect to  $B$  in the binary system.

If the system obeys Raoult's law, as does the benzene–toluene system,

$$y_A = P_A x_A \quad y_B = P_B x_B \quad (26.3-2)$$

Substituting Eq. (26.3-2) into (26.3-1) for an ideal system,

$$\alpha_{AB} = P_{APB} / (26.3-3)$$

Equation (26.3-1) can be rearranged to give

$$y_A = \alpha x_A / (1 + (\alpha - 1)x_A) \quad (26.3-4)$$

where  $\alpha = \alpha_{AB}$ . When the value of  $\alpha$  is above 1.0, a separation is possible. The value of  $\alpha$  may change as concentration changes. When binary systems follow Raoult's law, the relative volatility often varies only slightly over a large concentration range at constant total pressure.

**EXAMPLE 26.3-1. Relative Volatility for Benzene–Toluene System**

Using the data from Table 26.1-1, calculate the relative volatility for the benzene–toluene system at 85°C (358.2 K) and 105°C (378.2 K).

**Solution:** At 85°C, substituting into Eq. (26.3-3) for a system following Raoult's law,

$$\alpha = P_{APB} / 116.946.0 = 2.54$$

Similarly at 105°C,

$$\alpha=204.286.0=2.38$$

The variation in  $\alpha$  is about 7%.

## 26.3C Equilibrium or Flash Distillation

### *1. Introduction to distillation methods.*

Distillation can be carried out by either of two main methods in practice. The first method of distillation involves the production of a vapor by boiling the liquid mixture to be separated in a single stage and recovering and condensing the vapors. No liquid is allowed to return to the single-stage still to contact the rising vapors. The second method of distillation involves the return of a portion of the condensate to the still. The vapors rise through a series of stages or trays, and part of the condensate flows downward through the series of stages or trays countercurrent to the vapors. This second method is called *fractional distillation*, *distillation*

*with reflux, or rectification.*

There are three important types of distillation that occur in a single stage or still and that do not involve rectification. The first of these is equilibrium or flash distillation, the second is simple batch or differential distillation, and the third is simple steam distillation.

*2. Equilibrium or flash distillation.* In *equilibrium or flash distillation*, which occurs in a single stage, a liquid mixture is partially vaporized. The vapor is allowed to come to equilibrium with the liquid, and the vapor and liquid phases are then separated. This can be done batchwise or continuously.

In Fig. 26.3-1, a binary mixture of components *A* and *B* flowing at the rate

of  $F$  mol/h into a heater is partially vaporized. Then, the mixture reaches equilibrium and is separated. The composition of  $F$  is  $x_F$  mole fraction of  $A$ . A total material balance on component  $A$  is as follows:

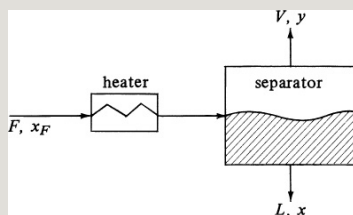


Figure 26.3-1. *Equilibrium or flash distillation.*

$$F x_F = V y + L x \quad (26.3-5)$$

Since  $L = F - V$ , Eq. (26.3-5) becomes

$$F x_F = V y + (F - V) x \quad (26.3-6)$$

Usually, the moles per hour of feed  $F$ , moles per hour of vapor  $V$ , and moles per hour of  $L$  are known or set. Hence,



there are two unknowns  $x$  and  $y$  in Eq. (26.3-6). The other relationship needed in order to solve Eq. (26.3-6) is the equilibrium line. A convenient method to use is to plot Eq. (26.3-6) on the  $x$ - $y$  equilibrium diagram. The intersection of the equation and the equilibrium line is the desired solution. This is similar to Example 26.2-1 and shown in Fig. 26.2-4.

### 26.3D Simple Batch or Differential Distillation

In *simple batch* or *differential distillation*, liquid is first charged to a heated kettle. The liquid charge is boiled slowly and the vapors are withdrawn as rapidly as they form to a condenser, where the condensed vapor (distillate) is collected. The first portion of vapor condensed will be richest in the more volatile

component  $A$ . As vaporization proceeds, the vaporized product becomes leaner in  $A$ .

In Fig. 26.3-2, a simple still is shown. Originally, a charge of  $L_1$  moles of components  $A$  and  $B$  with a composition of  $x_1$  mole fraction of  $A$  is placed in the still. At any given time, there are  $L$  moles of liquid left in the still with composition  $x$ , and the composition of the vapor leaving in equilibrium is  $y$ . A differential amount  $dL$  is vaporized.

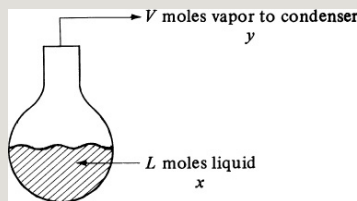


Figure 26.3-2. Simple batch or differential distillation.

The composition in the still pot changes with time. In deriving the equation for

this process, we assume that a small amount of  $dL$  is vaporized. The composition of the liquid changes from  $x$  to  $x-dx$  and the amount of liquid from  $L$  to  $L-dL$ . A material balance on  $A$  can be made, where the original amount = the amount left in the liquid + the amount of vapor:

$$xL = (x-dx)(L-dL) + ydL \quad (26.3-7)$$

Multiplying out the right side,

$$xL = xL - xdL - Ldx + dx dL + ydL \quad (26.3-8)$$

Neglecting the term  $dx dL$  and rearranging,

$$dLL = dx y - x \quad (26.3-9)$$

Integrating,

$$\int_{L_2}^{L_1} \frac{L_1}{L} dL = \ln \frac{L_1}{L_2} = \int_{x_2}^{x_1} \frac{x_2}{x} dx - x \quad (26.3-10)$$

where  $L_1$  is the original moles charged,  $L_2$  is the moles left in the still,  $x_1$  is the original composition, and  $x_2$  is the final composition of liquid.

The equilibrium curve gives the relationship between  $y$  and  $x$ . The integration of Eq. (26.3-10) can be done by calculating values of  $f(x) = 1/(y - x)$  and numerically or graphically integrating Eq. (26.3-10) between  $x_1$  and  $x_2$ . Equation (26.3-10) is known as the *Rayleigh equation*. The average composition of total material distilled,  $y_{av}$ , can be obtained by material balance:

$$L_1 x_1 = L_2 x_2 + (L_1 - L_2) y_{av} \quad (26.3-11)$$

A mixture of 100 mol containing 50 mol % *n*-pentane and 50 mol % *n*-heptane is distilled under differential conditions at 101.3 kPa until 40 mol are distilled. What is the average composition of the total vapor distilled and the composition of the liquid left? The equilibrium data are as follows, where *x* and *y* are mole fractions of *n*-pentane:

--

**Solution:** The given values to be used in Eq. (26.3-10) are  $L_1 = 100$  mol,  $x_1 = 0.50$ ,  $L_2 = 60$  mol, and  $V$  (moles distilled) = 40 mol. Substituting into Eq. (26.3-10),

$$\ln 100/60 = 0.510 = \int_{x_2}^{x_1} \frac{dx}{x(1-x)} \quad (26.3-12)$$

The unknown is  $x_2$ , the composition of the liquid  $L_2$  at the end of the differential distillation. To solve this by numerical integration, equilibrium values of *y* versus *x* are plotted so values of *y* can be obtained from this curve at small intervals of *x*. Alternatively, instead of plotting, the equilibrium data can be fitted to a polynomial function. For  $x = 0.594$ , the equilibrium value of  $y = 0.925$ . Then,  $f(x) = 1/(y - x) = 1/(0.925 - 0.594) = 3.02$ . Other values of  $f(y)$  are similarly calculated.

The numerical integration of Eq. (26.3-10) is performed from  $x_1 = 0.5$  to  $x_2$  such that the integral = 0.510 by Eq. (26.3-12) in Fig. 26.3-3. Hence,  $x_2 = 0.277$ . Substituting into Eq. (26.3-11) and solving for the average composition of the 40 mol distilled,

$$100(0.50) = 60(0.277) + 40(y_{av}) \quad y_{av} = 0.835$$

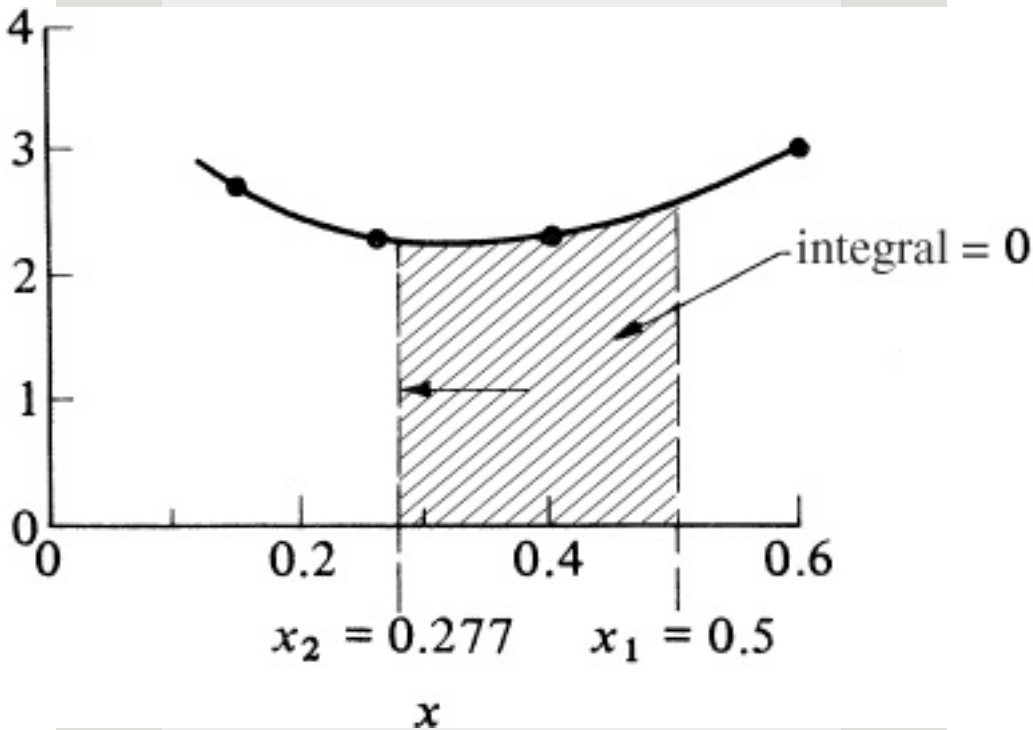


Figure 26.3-3. Numerical integration for Example 26.3-2.

### 26.3E Simple Steam Distillation

At atmospheric pressure high-boiling, liquids cannot be purified by distillation, since the components of the liquid may decompose at the high temperatures required. Often, the high-boiling substances are essentially insoluble in water, so a

separation at lower temperatures can be obtained by *simple steam distillation*. This method is often used to separate a high-boiling component from small amounts of nonvolatile impurities.

If a layer of liquid water (*A*) and an immiscible high-boiling component (*B*) such as a hydrocarbon are boiled at 101.3 kPa abs pressure, then, by the phase rule, Eq. (22.1-1), for three phases and two components,

$$F = 2 - 3 + 2 = 1 \text{ degree of freedom}$$

Hence, if the total pressure is fixed, the system is fixed. Since there are two liquid phases, each will exert its own vapor pressure at the prevailing temperature and cannot be influenced by

the presence of the other. When the sum of the separate vapor pressures equals the total pressure, the mixture boils and

$$P_A + P_B = P \quad (26.3-13)$$

where  $P_A$  is vapor pressure of pure water  $A$  and  $P_B$  is vapor pressure of pure  $B$ . Then, the vapor composition is

$$y_A = \frac{P_A}{P} \quad y_B = \frac{P_B}{P} \quad (26.3-14)$$

As long as the two liquid phases are present, the mixture will boil at the same temperature, giving a vapor of constant composition  $y_A$ . The temperature is found by using the vapor-pressure curves for pure  $A$  and pure  $B$ .

Note that by steam distillation, as long as liquid water is present, the high-boiling component  $B$  vaporizes at a



temperature well below its normal boiling point without using a vacuum. The vapors of water ( $A$ ) and high-boiling component ( $B$ ) are usually condensed in a condenser and the resulting two immiscible liquid phases separated. This method has the disadvantage that large amounts of heat must be used to evaporate the water simultaneously with the high-boiling compound.

The ratio moles of  $B$  distilled to moles of  $A$  distilled is

$$n_{B/A} = P_{B/A}(26.3-15)$$

Steam distillation is sometimes used in the food industry for the removal of volatile taints and flavors from edible fats and oils. In many cases, vacuum

distillation is used instead of steam distillation to purify high-boiling materials. The total pressure is quite low so that the vapor pressure of the system reaches the total pressure at relatively low temperatures.

Van Winkle (V1) derives equations for steam distillation where an appreciable amount of a nonvolatile component is present with the high-boiling component. This involves a three-component system. He also considers other cases for binary batch, continuous, and multicomponent batch steam distillation.

## **26.4 Binary Distillation with Reflux Using the McCabe–Thiele and Lewis Methods**

### **26.4A Introduction to Distillation with Reflux**

From a simplified point of view,

rectification (fractionation) or stage distillation with reflux can be considered to be a process in which a series of flash-vaporization stages are arranged in a series in such a manner that the vapor and liquid products from each stage flow countercurrently to each other. The liquid in a stage is conducted or flows to the stage below and the vapor from a stage flows upward to the stage above. Hence, in each stage, a vapor stream  $V$  and a liquid stream  $L$  enter, are mixed and equilibrated, and a vapor and a liquid stream leave in equilibrium. This process flow diagram was shown in Fig. 22.1-2 for a single stage and an example was given in Example 26.2-1 for a benzene–toluene mixture.

For the countercurrent contact with multiple stages in Fig. 22.1-3, the material-balance or operating-line equation (22.1-16) was derived, which relates the concentrations of the vapor and liquid streams passing each other in each stage. In a distillation column, the stages (referred to as *sieve plates* or *trays*) in a distillation tower are arranged vertically, as shown schematically in Fig. 26.4-1.

In Fig. 26.4-1, the feed enters the column somewhere in the middle of the column. If the feed is liquid, it flows down to a sieve tray or stage. Vapor enters the tray and bubbles through the liquid on this tray as the entering liquid flows across. The vapor and liquid leaving the tray are essentially in equilibrium. The vapor continues up to

the next tray or stage, where it is again contacted with a downflowing liquid. In this case, the concentration of the more volatile component (the lower-boiling component A) is being increased in the vapor from each stage going upward and decreased in the liquid from each stage going downward. The final vapor product coming overhead is condensed in a condenser and a portion of the liquid product (distillate) is removed, which contains a high concentration of A. The remaining liquid from the condenser is returned (refluxed) as a liquid to the top tray.

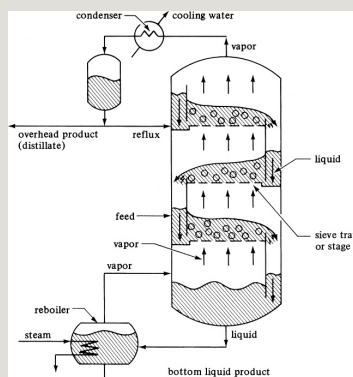


Figure 26.4-1. *Process flow of a fractionating tower containing sieve trays.*

The liquid leaving the bottom tray enters a reboiler, where it is partially vaporized, and the remaining liquid, which is lean in *A* or rich in *B*, is withdrawn as liquid product. The vapor from the reboiler is sent back to the bottom stage or tray. Only three trays are shown in the tower of Fig. 26.4-1. In most cases, the number of trays is much greater. In the sieve tray, the vapor enters through an opening and bubbles up through the liquid to provide intimate contact between the liquid and vapor on the tray. In a theoretical tray, the vapor and liquid leaving are in equilibrium. The reboiler can be considered as a theoretical stage or tray.

#### **26.4B McCabe–Thiele Method of Calculation for the Number of Theoretical Stages**

*1. Introduction and assumptions.* A mathematical–graphical method for determining the number of theoretical trays or stages needed for a given separation of a binary mixture of  $A$  and  $B$  has been developed by McCabe and Thiele. The method uses material balances around certain parts of the tower, which give operating lines somewhat similar to Eq. (22.1-16) and the  $x$ - $y$  equilibrium curve for the system.

The main assumption made in the McCabe–Thiele method is that there must be equimolar overflow through the tower between the feed inlet and the top tray, and the feed inlet and bottom tray. This is shown in Fig. 26.4-2, where liquid and vapor streams enter a tray, are equilibrated, and leave. A total material

balance gives

$$V_{n+1} + L_{n-1} = V_n + L_n \quad (26.4-1)$$

A component balance on A gives

$$V_{n+1}y_{n+1} + L_{n-1}x_{n-1} = V_ny_n + L_nx_n \quad (26.4-2)$$

where  $V_{n+1}$  is mol/h of vapor from tray  $n + 1$ ,  $L_n$  is mol/h liquid from tray  $n$ ,  $y_{n+1}$  is mole fraction of A in  $V_{n+1}$ , and so on. The compositions  $y_n$  and  $x_n$  are in equilibrium and the temperature of the tray  $n$  is  $T_n$ . If  $T_n$  is taken as a datum, it can be shown by a heat balance that the sensible heat differences in the four streams are quite small if heats of solution are negligible. Hence, only the latent heats in streams  $V_{n+1}$  and  $V_n$  are important. Since molar latent heats for chemically similar compounds are



almost the same,  $V_{n+1} = V_n$  and  $L_n = L_{n-1}$ . Therefore, we have constant molal overflow in the tower.

2. *Equations for an enriching section.* In Fig. 26.4-3, a continuous-distillation column is shown, with feed being introduced to the column at an intermediate point and an overhead distillate product and a bottoms product being withdrawn. The upper part of the tower above the feed entrance is called the *enriching section*, since the entering feed of binary components  $A$  and  $B$  is enriched in this section, so that the distillate is richer in  $A$  than the feed. The tower is at steady state.

An overall material balance around the entire column in Fig. 26.4-3 states that the entering feed of  $F$  mol/h must equal

the distillate  $D$  in mol/h plus the bottoms  $W$  in mol/h:

$$F=D+W \quad (26.4-3)$$

A total material balance on component  $A$  gives

$$F x_F = D x_D + W x_W \quad (26.4-4)$$

In Fig. 26.4-4a, the distillation-tower section above the feed, the enriching section, is shown schematically. The vapor from the top tray having a composition  $y_1$  passes to the condenser, where it is condensed so that the resulting liquid is at the boiling point. The reflux stream  $L$  mol/h and distillate  $D$  mol/h have the same composition, so  $y_1 = x_D$ . Since equimolal overflow is assumed,  $L_1 = L_2 = L_n$  and  $V_1 = V_2 = V_n = V_{n+1}$ .

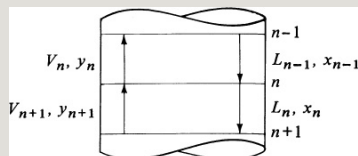


Figure 26.4-2. Vapor and liquid flows entering and leaving a tray.

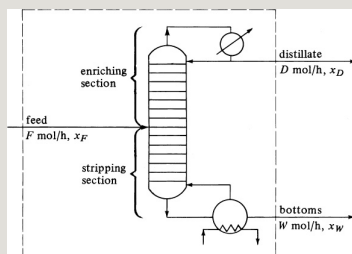


Figure 26.4-3. Distillation column showing material-balance sections for McCabe–Thiele method.

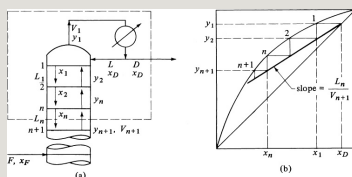


Figure 26.4-4. Material balance and operating line for enriching section: (a) schematic of tower, (b) operating and equilibrium lines.

Making a total material balance over the dashed-line section in Fig. 26.4-4a,

$$V_{n+1} = L_n + D \quad (26.4-5)$$

$$V_{n+1}y_{n+1} = L_n x_n + D x_D \quad (26.4-6)$$

Solving for  $y_{n+1}$ , the enriching-section operating line is

$$y_{n+1} = \frac{L_n}{V_{n+1}} x_n + \frac{D}{V_{n+1}} x_D \quad (26.4-7)$$

Since  $V_{n+1} = L_n + D$ ,  $L_n/V_{n+1} = R/(R + 1)$  and Eq. (26.4-7) becomes

$$y_{n+1} = \frac{R}{R+1} x_n + \frac{x_D}{R+1} \quad (26.4-8)$$

where  $R = L_n/D = \text{reflux ratio} = \text{constant}$ . Equation (26.4-7) is a straight line on a plot of vapor composition versus liquid composition. It relates the compositions of two streams passing each other and is plotted in Fig. 26.4-4b. The slope is  $L_n/V_{n+1}$  or  $R/(R + 1)$ , as given in Eq. (26.4-8). It intersects the  $y = x$  line (45° diagonal line) at  $x = x_D$ .

The intercept of the operating line at  $x = 0$  is  $y = x_D/(R + 1)$ .

The theoretical stages are determined by starting at  $x_D$  and stepping off the first plate to  $x_1$ . Then,  $y_2$  is the composition of the vapor passing the liquid  $x_1$ . In a similar manner, the other theoretical trays are stepped off down the tower in the enriching section to the feed tray.

### *3. Equations for a stripping section.*

Making a total material balance over the dashed-line section in Fig. 26.4-5a for the stripping section of the tower below the feed entrance,

$$V_{m+1} = L_m + W \quad (26.4-9)$$

Making a balance on component A,

$$V_{m+1}y_{m+1} = L_mx_m + Wx_W \quad (26.4-10)$$

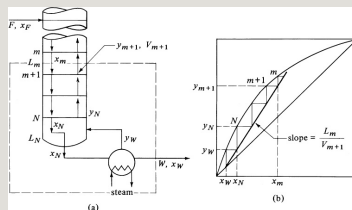


Figure 26.4-5. Material balance and operating line for a stripping section: (a) schematic of tower, (b) operating and equilibrium lines.

Solving for  $y_{m+1}$ , the stripping-section operating line is

$$y_{m+1} = L_m V_{m+1} x_m + W x_W V_m + 1 \quad (26.4-11)$$

Again, since equimolal flow is assumed,  $L_m = L_N = \text{constant}$  and  $V_{m+1} = V_N = \text{constant}$ . Equation (26.4-11) is a straight line when plotted as  $y$  versus  $x$  in Fig. 26.4-5b, with a slope of  $L_m/V_{m+1}$ . It intersects the  $y = x$  line at  $x = x_W$ . The intercept at  $x = 0$  is  $y = -W x_W / V_{m+1}$ .

Again, the theoretical stages for the

stripping section are determined by starting at  $x_W$ , going up to  $y_W$ , and then across to the operating line, and so on.

*4. Effect of feed conditions.* The condition of the feed stream  $F$  entering the tower determines the relation between the vapor  $V_m$  in the stripping section and  $V_n$  in the enriching section, as well as between  $L_m$  and  $L_n$ . If the feed is part liquid and part vapor, the vapor will add to  $V_m$  to give  $V_n$ .

For convenience, we represent the condition of the feed by the quantity  $q$ , which is defined as

mol of feed at entering conditions / mol of vapor

If the feed enters at its boiling point, the numerator of Eq. (26.4-12) is the same as the denominator, and  $q = 1.0$ .

Equation (26.4-12) can also be written in terms of enthalpies:

$$q = \frac{H_V - H_F}{H_V - H_L} \quad (26.4-13)$$

where  $H_V$  is the enthalpy of the feed at the dew point,  $H_L$  is the enthalpy of the feed at the boiling point (bubble point), and  $H_F$  is the enthalpy of the feed at its entrance conditions. If the feed enters as vapor at the dew point,  $q = 0$ . For cold liquid feed  $q > 1.0$ , for superheated vapor  $q < 0$ , and for the feed being part liquid and part vapor,  $q$  is the fraction of feed that is liquid.

We can also look at  $q$  as the number of moles of saturated liquid produced on the feed plate by each mole of feed added to the tower. In Fig. 26.4-6, a diagram shows the relationship between



flows above and below the feed  
entrance. From the definition of  $q$ , the  
following equations hold:

$$L_m = L_n + qF \quad (26.4-14)$$

$$V_n = V_m + (1-q)F \quad (26.4-15)$$

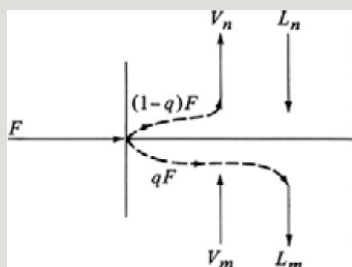


Figure 26.4-6. Relationship between flows above and below the feed entrance.

The point of intersection of the  
enriching and the stripping operating-  
line equations on an  $x$ - $y$  plot can be  
derived as follows. Rewriting Eqs.  
(26.4-6) and (26.4-10) without the tray  
subscripts:

$$V_{ny} = L_{nx} + D_x D \quad (26.4-16)$$

$$V_{my} = L_{mx} - W_x W \quad (26.4-17)$$

where the  $y$  and  $x$  values are the point of intersection of the two operating lines.

Subtracting Eq. (26.4-16) from (26.4-17),

$$(V_m - V_n)y = (L_m - L_n)x - (D_x D + W_x W) \quad (26.4-18)$$

Substituting Eqs. (26.4-4), (26.4-14), and (26.4-15) into Eq. (26.4-18) and rearranging,

$$y = q_{q-1}x - x_{Fq-1} \quad (26.4-19)$$

This equation is the  $q$ -line equation and is the locus of the intersection of the two operating lines. Setting  $y = x$  in Eq. (26.4-19), the intersection of the  $q$ -line

equation with the  $45^\circ$  line is  $y = x = x_F$ , where  $x_F$  is the overall composition of the feed.

In Fig. 26.4-7, the  $q$  line is plotted for various feed conditions given below the figure. The slope of the  $q$  line is  $q/(q - 1)$ . For example, for the liquid below the boiling point,  $q > 1$  and the slope is  $> 1.0$ , as shown. The enriching and operating lines are plotted for the case of a feed of part liquid and part vapor, and the two lines intersect on the  $q$  line. A convenient way to locate the stripping operating line is to first plot the enriching operating line and the  $q$  line. Then, draw the stripping line between the intersection of the  $q$  line and enriching operating line, and the point  $y = x = x_W$ .

5. *Location of the feed tray in a tower and number of trays.* To determine the number of theoretical trays needed in a tower, the stripping and operating lines are drawn to intersect on the  $q$  line, as shown in Fig. 26.4-8. Starting at the top at  $x_D$ , the trays are stepped off. For trays 2 and 3, the steps can go to the enriching operating line, as shown in Fig. 26.4-8a. At step 4, the step goes to the stripping line. A total of about 4.6 theoretical steps are needed. The feed enters on tray 4.

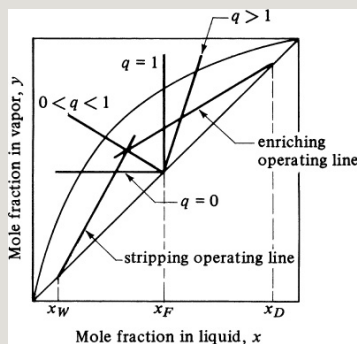


Figure 26.4-7. Location of the  $q$  line for various feed conditions: liquid below boiling point ( $q > 1$ ), liquid at boiling point ( $q = 1$ ), liquid + vapor ( $0 < q < 1$ ), saturated vapor ( $q = 0$ ).

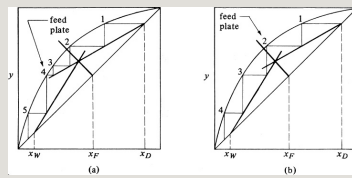


Figure 26.4-8. Method of stepping off the number of theoretical trays and location of the feed plate: (a) improper location of feed on tray 4, (b) proper location of feed on tray 2 to give minimum number of steps.

For the correct method, the shift is made on step 2 to the stripping line, as shown in Fig. 26.4-8b. A total of only about 3.7 steps are needed, with the feed on tray 2. To keep the number of trays to a minimum, the shift from the enriching to the stripping operating line should be made at the first opportunity after passing the operating-line intersection.

In Fig. 26.4-8b, the feed is part liquid and part vapor, since  $0 < q < 1$ . Hence, in adding the feed to tray 2, the vapor portion of the feed is separated and added beneath plate 2, and the liquid

added to the liquid from above entering tray 2. If the feed is all liquid, it should be added to the liquid flowing to tray 2 from the tray above. If the feed is all vapor, it should be added below tray 2 and join the vapor rising from the plate below.

Since a reboiler is considered a theoretical step, when the vapor  $y_W$  is in equilibrium with  $x_W$ , as in Fig. 26.4-5b, the number of theoretical trays in a tower is equal to the number of theoretical steps minus one.

**EXAMPLE 26.4-1. Rectification of a Benzene–Toluene Mixture**

A liquid mixture of benzene–toluene is to be distilled in a fractionating tower at 101.3 kPa pressure. The feed of 100 kg mol/h is liquid, containing 45 mol % benzene and 55 mol % toluene, and enters at 327.6 K (130°F). A distillate containing 95 mol % benzene and 5 mol % toluene and a bottoms containing 10 mol % benzene and 90 mol % toluene are to be obtained. The reflux ratio is 4:1. The average heat capacity of the feed is 159 kJ/kg mol · K (38 btu/lb mol · °F) and the average latent heat 32099 kJ/kg mol (13 800 btu/lb mol). Equilibrium data for this system are given in Table 26.1-1 and Fig. 26.1-1. Calculate the kg

moles per hour distillate, kg moles per hour bottoms, and the number of theoretical trays needed.

**Solution:** The given data are  $F = 100$  kg mol/h,  $x_F = 0.45$ ,  $x_D = 0.95$ ,  $x_W = 0.10$ , and  $R = L_n/D = 4$ . For the overall material balance substituting into Eq. (26.4-3),

$$F=D+W100=D+W(26.4-3)$$

Substituting into Eq. (26.4-4) and solving for  $D$  and  $W$ ,

$$\begin{aligned} Fx_F &= Dx_D + Wx_W 100(0.45) = D(0.95) + (100-D) \\ (0.10)D &= 41.2 \text{ kg mol/h} \quad W = 58.8 \text{ kg mol/h} \end{aligned} (26.4-4)$$

For the enriching operating line, using Eq. (26.4-8),

$$y_{n+1} = RR + 1x_n + x_{DR} + 1 = 44 + 1x_n + 0.954 + 1 = 0.800x_n + 0.190$$

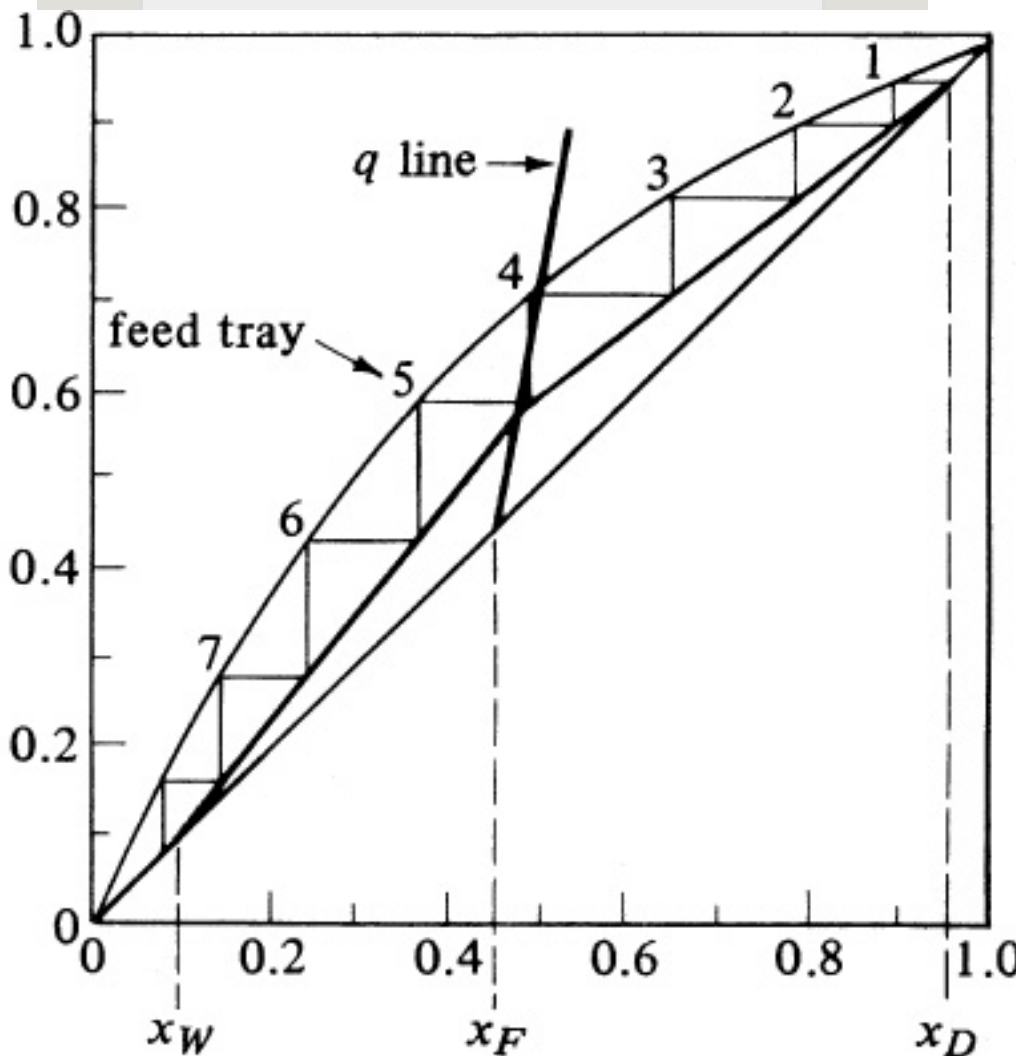
The equilibrium data from Table 26.1-1 and the enriching operating line above are plotted in Fig. 26.4-9.

Next, the value of  $q$  is calculated. From the boiling-point diagram, Fig. 26.1-1, for  $x_F = 0.45$ , the boiling point of the feed is 93.5°C or 366.7 K (200.3°F). From Eq. (26.4-13),

$$q = HV - HFHV - HL(26.4-13)$$

The value of  $Hv - H_L$  = latent heat = 32099 kJ/kg mol. The numerator of Eq. (26.4-13) is

$$HV - HF = (HV - H_L) + (H_L - HF)(26.4-20)$$



**Mole fraction in liquid,  $x$**

Figure 26.4-9. McCabe–Thiele diagram for distillation of benzene–toluene for Example 26.4-1.

Also,

$$HL-HF=cpL(TB-TF)(26.4-21)$$

where the heat capacity of the liquid feed  $cpL = 159 \text{ kJ/kg mol} \cdot \text{K}$ ,  $TB = 366.7 \text{ K}$  (boiling point of feed), and  $TF = 327.6 \text{ K}$  (inlet feed temperature). Substituting Eqs. (26.4-20) and



(26.4-21) into (26.4-13),

$$q=(HV-HL)+cpL(TB-TF)HV-HL \quad (26.4-22)$$

Substituting the known values into Eq. (26.4-22),

$$q=32099+159(366.7-327.6)32099=1.195(\text{SI}) \quad q=13800+38(200.3-130)13800=1.195(\text{English})$$

From Eq. (26.4-19), the slope of the  $q$  line is

$$qq-1=1.195/1.195-1=6.12$$

The  $q$  line is plotted in Fig. 26.4-9 starting at the point  $y = x_F = 0.45$  with a slope of 6.12.

The stripping operating line is drawn connecting the point  $y = x = x_W = 0.10$ , with the intersection of the  $q$  line and the enriching operating line. Starting at the point  $y = x = x_D$ , the theoretical steps are drawn in, as shown in Fig. 26.4-9. The number of theoretical steps is 7.6, or 7.6 steps minus a reboiler, which gives 6.6 theoretical trays. The feed is introduced on tray 5 from the top.

## 26.4C Total and Minimum Reflux Ratio for McCabe–Thiele Method

*1. Total reflux.* In distillation of a binary mixture  $A$  and  $B$ , the feed conditions, distillate composition, and bottoms composition are usually specified and the number of theoretical trays are to be calculated. However, the number of theoretical trays needed depends upon the operating lines. To fix the operating

lines, the reflux ratio  $R = L_n/D$  at the top of the column must be set.

One of the limiting values of reflux ratio is that of total reflux, or  $R = \infty$ . Since  $R = L_n/D$  and, by Eq. (26.4-5),

$$V_{n+1} = L_n + D \quad (26.4-5)$$

then  $L_n$  is very large, as is the vapor flow  $V_n$ . This means that the slope  $R/(R + 1)$  of the enriching operating line becomes 1.0 and the operating lines of both sections of the column coincide with the  $45^\circ$  diagonal line, as shown in Fig. 26.4-10.

The number of theoretical trays required is obtained as before by stepping off the trays from the distillate to the bottoms. This gives the minimum number of trays that can possibly be used to obtain the

given separation. In actual practice, this condition can be realized by returning all the overhead condensed vapor  $V_1$  from the top of the tower back to the tower as reflux, that is, total reflux. Also, all the liquid in the bottoms is reboiled. Hence, all the products distillate and bottoms are reduced to zero flow, as is the fresh feed to the tower.

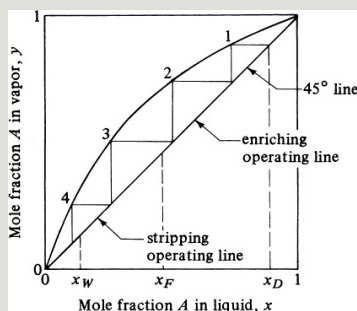


Figure 26.4-10. Total reflux and minimum number of trays by the McCabe–Thiele method.

This condition of total reflux can also be interpreted as requiring infinite sizes of condenser, reboiler, and tower diameter

for a given feed rate.

If the relative volatility  $\alpha$  of the binary mixture is approximately constant, the following analytical expression by Fenske can be used to calculate the minimum number of theoretical steps  $N_m$  when a total condenser is used:

$$N_m = \frac{\log(x_{D1} - x_{W1} / x_{D2} - x_{W2})}{\log \alpha_{av}} \quad (26.4-23)$$

For small variations in  $\alpha$ ,  $\alpha_{av} = (\alpha_1 \alpha_W)^{1/2}$ , where  $\alpha_1$  is the relative volatility of the overhead vapor and  $\alpha_W$  is the relative volatility of the bottoms liquid.

*2. Minimum reflux ratio.* The minimum reflux ratio can be defined as the reflux ratio  $R_m$  that will require an infinite number of trays for the given desired

separation of  $x_D$  and  $x_W$ . This corresponds to the minimum vapor flow in the tower, and hence the minimum reboiler and condenser sizes. This case is shown in Fig. 26.4-11. If  $R$  is decreased, the slope of the enriching operating line  $R/(R + 1)$  is decreased, and the intersection of this operating line and the stripping line with the  $q$  line moves farther from the  $45^\circ$  line and closer to the equilibrium line. As a result, the number of steps required to give a fixed  $x_D$  and  $x_W$  increases. When the two operating lines touch the equilibrium line, a “pinch point” at  $y'$  and  $x'$  occurs, where the number of steps required becomes infinite. The slope of the enriching operating line is as follows from Fig. 26.4-11, since the line passes through the points  $x'$ ,  $y'$ , and  $x_D(y = x_D)$ :

$$R_m R_{m+1} = x_D - y' x_D - x \quad (26.4-24)$$

In some cases, where the equilibrium line has an inflection in it, as shown in Fig. 26.4-12, the operating line at minimum reflux will be tangent to the equilibrium line.

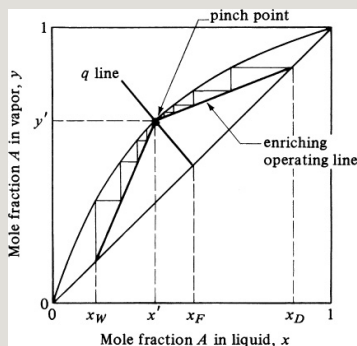


Figure 26.4-11. Minimum reflux ratio and infinite number of trays by the McCabe–Thiele method.

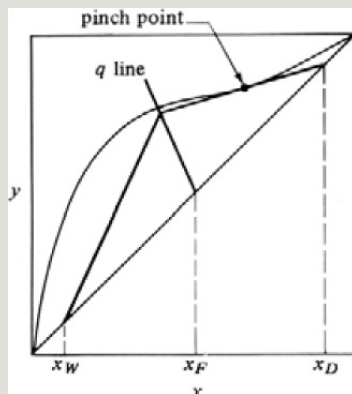


Figure 26.4-12. *Minimum reflux ratio and infinite number of trays when the operating line is tangent to the equilibrium line.*

### *3. Operating and optimum reflux ratio.*

For the case of total reflux, the number of plates is a minimum, but the tower diameter is infinite. This corresponds to an infinite cost of tower as well as steam and cooling water. This is one limit in the tower operation. Also, for minimum reflux, the number of trays is infinite, which again gives an infinite cost. These are the two limits in operation of the tower.

The actual operating reflux ratio to use lies between these two limits. To select the proper value of  $R$  requires a complete economic balance on the fixed costs of the tower and the operating costs. The optimum reflux ratio to use for lowest total cost per year is between

the minimum  $R_m$  and total reflux. This has been shown for many cases to be at an operating reflux ratio between  $1.2 R_m$  and  $1.5 R_m$ .

**EXAMPLE 26.4-2. Minimum Reflux Ratio and Total Reflux in Rectification**

For the rectification in Example 26.4-1, where a benzene–toluene feed is being distilled to give a distillate composition of  $x_D = 0.95$  and a bottoms composition of  $x_W = 0.10$ , calculate the following:

- Minimum reflux ratio  $R_m$
- Minimum number of theoretical plates at total reflux

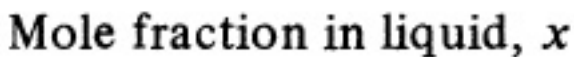
**Solution:** For part (a), the equilibrium line is plotted in Fig. 26.4-13 and the  $q$ -line equation is also shown for  $x_F = 0.45$ . Using the same  $x_D$  and  $x_W$  as in Example 26.4-1, the enriching operating line for minimum reflux is plotted as a dashed line and intersects the equilibrium line at the same point at which the  $q$  line intersects. Reading off the values of  $x = 0.49$  and  $y = 0.702$  substituting into Eq. (26.4-24), and solving for  $R_m$ ,

$$R_m R_m + 1 = x_D - y^* x_D - x = 0.95 - 0.702(0.95 - 0.49)$$

Hence, the minimum reflux ratio  $R_m = 1.17$ .

For the case of total reflux in part (b), the theoretical steps are drawn as shown in Fig. 26.4-13. The minimum number of theoretical steps is 5.8, which gives 4.8 theoretical trays plus a reboiler.





### 26.4D Special Cases for Rectification Using the McCabe–Thiele Method

*1. Stripping-column distillation.* In

some cases, the feed to be distilled is not supplied to an intermediate point in a column but is added to the top of the stripping column, as shown in Fig. 26.4-14a. The feed is usually a saturated liquid at the boiling point, and the overhead product  $VD$  is the vapor rising from the top plate, which goes to a condenser with no reflux or liquid returned to the tower.

The bottoms product  $W$  usually has a high concentration of the less volatile component  $B$ . Hence, the column operates as a stripping tower, with the vapor removing the more volatile  $A$  from the liquid as it flows downward. Assuming constant molar flow rates, a material balance of the more volatile component  $A$  around the dashed line in Fig. 26.4-14a gives, on rearrangement,

$$y_{m+1} = L_m V_{m+1} x_m - W x_W V_{m+1} + 1 \quad (26.4-25)$$

This stripping-line equation is the same as the stripping-line equation for a complete tower given as Eq. (26.4-11). It intersects the  $y = x$  line at  $x = x_W$ , and the slope is constant at  $L_m/V_{m+1}$ .

If the feed is saturated liquid, then  $L_m = F$ . If the feed is cold liquid below the boiling point, the  $q$  line should be used and  $q > 1$ :

$$L_m = qF \quad (26.4-26)$$

In Fig. 26.4-14, the stripping operating-line equation (26.4-25) is plotted and the  $q$  line, Eq. (26.4-19), is also shown for  $q = 1.0$ . Starting at  $x_F$ , the steps are drawn down the tower.

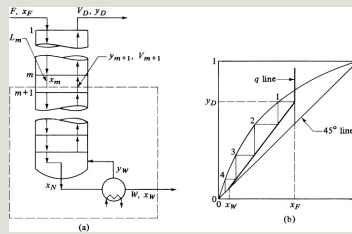


Figure 26.4-14. *Material balance and operating line for stripping tower: (a) flows in tower, (b) operating and equilibrium line.*

### EXAMPLE 26.4-3. Number of Trays in a Stripping Tower

A liquid feed at the boiling point of 400 kg mol/h containing 70 mol % benzene (*A*) and 30 mol % toluene (*B*) is fed to a stripping tower at 101.3 kPa pressure. The bottoms product flow is to be 60 kg mol/h containing only 10 mol % *A* and the rest *B*. Calculate the kg mol/h overhead vapor, its composition, and the number of theoretical steps required.

**Solution:** Referring to Fig. 26.4-14a, the known values are  $F = 400$  kg mol/h,  $x_F = 0.70$ ,  $W = 60$  kg mol/h, and  $x_W = 0.10$ . The equilibrium data from Table 26.1-1 are plotted in Fig. 26.4-15. Making an overall material balance,

$$F = W + VD \quad 400 = 60 + VD$$

Solving,  $VD = 340$  kg mol/h. Making a component *A* balance and solving,

$$F x_F = W x_W + V D y_D \quad 400(0.70) = 60(0.10) + 340(y_D) \quad y_D = 0.806$$

For a saturated liquid, the  $q$  line is vertical and is plotted in Fig. 26.4-15. The operating line is plotted through the point  $y = x_W = 0.10$  and the intersection of  $y_D = 0.806$  with the  $q$  line. Alternatively, Eq. (26.4-25) can be used, with a slope of  $L_m/V_{m+1} = 400/340$ . Stepping off the trays from the top, 5.3 theoretical steps or 4.3 theoretical trays plus a reboiler are needed.

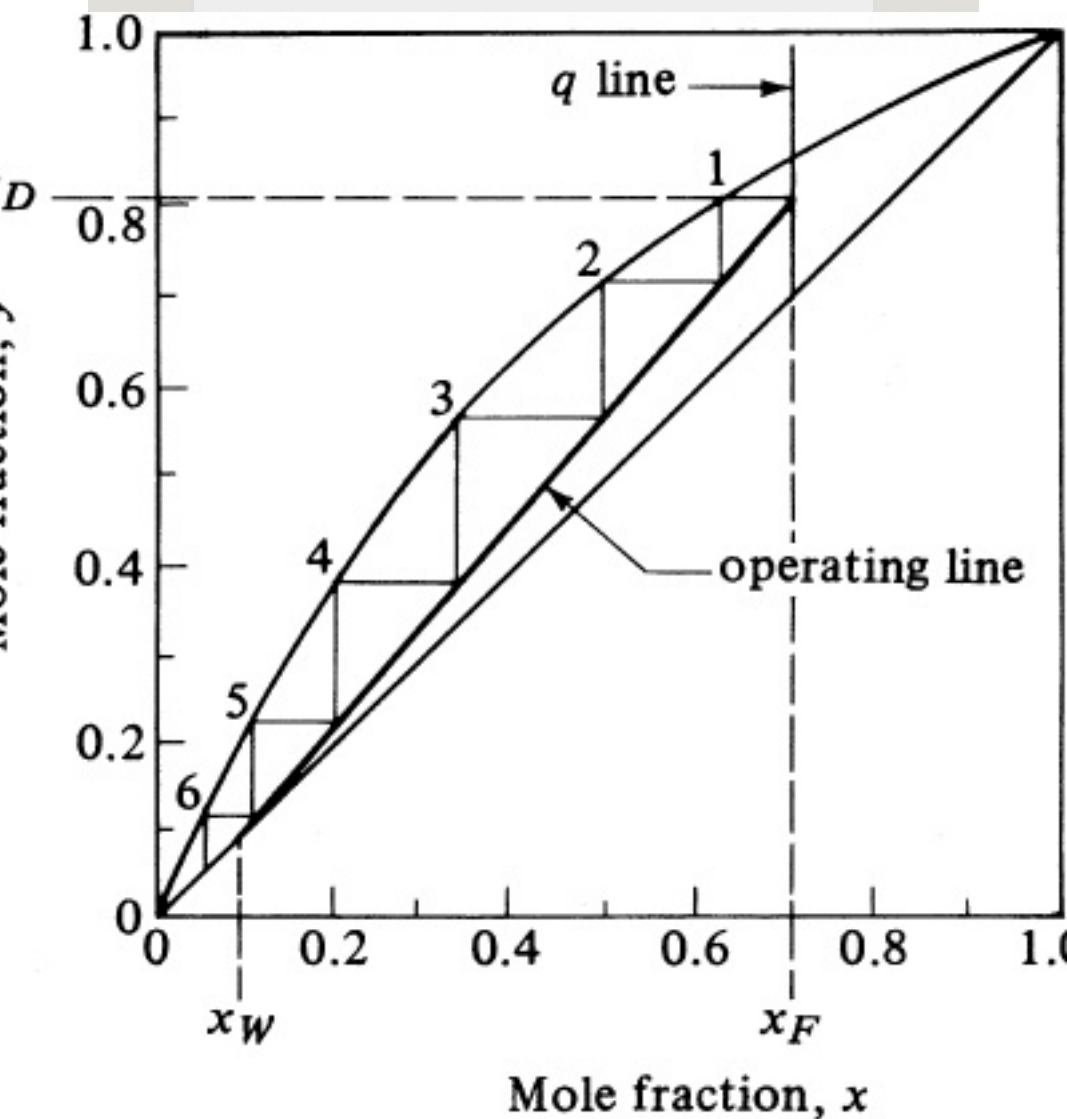


Figure 26.4-15. Stripping tower for Example 26.4-3.

## 2. Enriching-column distillation.

Enriching towers are also used at times, where the feed enters the bottom of the

tower as a vapor. The overhead distillate is produced in the same manner as in a complete fractionating tower and is usually quite rich in the more volatile component  $A$ . The liquid bottoms are usually comparable to the feed in composition, being slightly leaner in component  $A$ . If the feed is saturated vapor, the vapor in the tower  $V_n = F$ . The enriching-line equation (26.4-7) holds, as does the  $q$ -line equation (26.4-19).

3. Rectification with direct steam injection. Generally, the heat to a distillation tower is applied to one side of a heat exchanger (reboiler) and the steam does not come into direct contact with the boiling solution, as shown in Fig. 26.4-5. However, when an aqueous solution of more volatile  $A$  and water  $B$

is being distilled, the heat required may be provided by the use of open steam injected directly at the bottom of the tower. The reboiler exchanger is then not needed.

The steam is injected as small bubbles into the liquid in the tower bottom, as shown in Fig. 26.4-16a. The vapor leaving the liquid is then in equilibrium with the liquid if sufficient contact is obtained. Making an overall balance on the tower and a balance on A,

$$F+S=D+W \quad (26.4-27)$$

$$F x_F + S y_S = D x_D + W x_W \quad (26.4-28)$$

where  $S$  = mol/h of steam and  $y_S = 0$  = mole fraction of A in steam. The enriching operating-line equation is the same as for indirect steam.

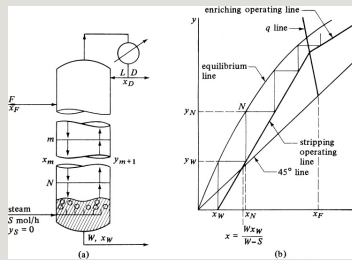


Figure 26.4-16. Use of direct steam injection: (a) schematic of tower, (b) operating and equilibrium lines.

For the stripping-line equation, an overall balance and a balance on component A are as follows:

$$L_{m+1} + S = V_{m+1} + W \quad (26.4-29)$$

$$L_{m+1}x_{m+1} + S(0) = V_{m+1}y_m + 1 + Wx_W \quad (26.4-30)$$

Solving for  $y_{m+1}$  in Eq. (26.4-30),

$$y_{m+1} = \frac{L_{m+1}x_{m+1} - Wx_W}{V_{m+1} + 1} \quad (26.4-31)$$

For saturated steam entering,  $S = V_{m+1}$



and hence, by Eq. (26.4-29),  $L_m = W$ . Substituting into Eq. (26.4-31), the stripping operating line is

$$y_{m+1} = W s_{xm} - W S x_W \quad (26.4-32)$$

When  $y = 0$ ,  $x = x_W$ . Hence, the stripping line passes through the point  $y = 0$ ,  $x = x_W$ , as shown in Fig. 26.4-16b, and is continued to the  $x$  axis. Also, for the intersection of the stripping line with the  $45^\circ$  line, when  $y = x$  in Eq. (26.4-32),  $x = W x_W / (W - S)$ .

For a given reflux ratio and overhead distillate composition, the use of open steam rather than closed requires an extra fraction of a stage, since the bottom step starts below the  $y = x$  line (Fig. 26.4-16b). The advantage of open steam lies in simpler construction of the

heater, which is a sparger.

#### *4. Rectification tower with side stream.*

In certain situations, intermediate product or side streams are removed from sections of the tower between the distillate and the bottoms. The side stream may be vapor or liquid and may be removed at a point above the feed entrance or below, depending on the composition desired.

The flows for a column with a liquid side stream removed above the feed inlet are shown in Fig. 26.4-17. The top enriching operating line above the liquid side stream and the stripping operating line below the feed are found in the usual way. The equation for the  $q$  line is also unaffected by the side stream and is found as before. The liquid side stream

alters the liquid rate below it, and hence the material balance or operating line in the middle portion between the feed and liquid side stream plates as well.

Making a total material balance on the top portion of the tower, as shown in the dashed-line box in Fig. 26.4-17,

$$V_{S+1} = L_S + O + D \quad (26.4-33)$$

where  $O$  is mol/h saturated liquid removed as a side stream. Since the liquid side stream is saturated,

$$L_n = L_S + O \quad (26.4-34)$$

$$V_{S+1} = V_{n+1} \quad (26.4-35)$$

Making a balance on the most volatile component,

$$VS+1yS+1=LSxS$$

$$+OxoDxD(26.4-36)$$

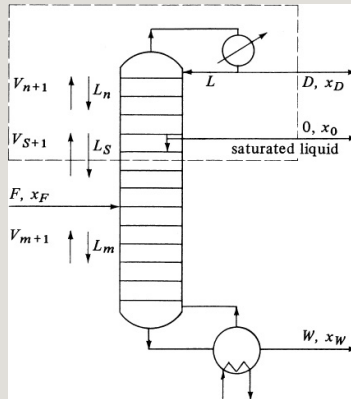


Figure 26.4-17. Process flow for a rectification tower with a liquid side stream.

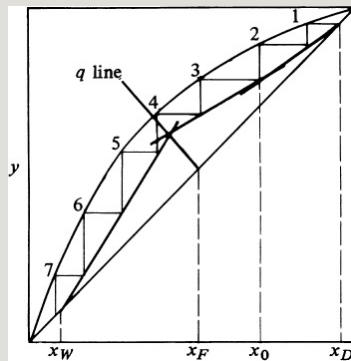


Figure 26.4-18. McCabe–Thiele plot for a tower with a liquid side stream above the feed.

Solving for  $y_{S+1}$ , the operating line for the region between the side stream and

the feed is

$$y_{S+1} = L_S V_{S+1} + x_S - O_{xO} + D x_D V_S + 1 \quad (26.4-37)$$

The slope of this line is  $L_S/V_{S+1}$ . The line can be located as shown in Fig. 26.4-18 by the  $q$  line, which determines the intersection of the stripping line and Eq. (26.4-37), or it may be fixed by the specification of  $x_O$ , the side-stream composition. The step on the McCabe–Thiele diagram must be at the intersection of the two operating lines at  $x_O$  in an actual tower. If this does not occur, the reflux ratio can be altered slightly to change the steps.

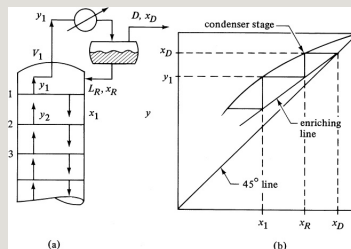


Figure 26.4-19. *Partial condenser where the vapor and liquid leave in equilibrium: (a) process flow diagram, (b) McCabe–Thiele plot.*

*5. Partial condensers.* In a few cases, it may be desired that the overhead distillate product be removed as a vapor instead of a liquid. This can also occur when the low boiling point of the distillate makes complete condensation difficult. The liquid condensate in a partial condenser is returned to the tower as reflux and the vapor removed as product, as shown in Fig. 26.4-19.

If the time of contact between the vapor product and the liquid is sufficient, the partial condenser is a theoretical stage. Then, the composition  $x_R$  of the liquid reflux is in equilibrium with the vapor composition  $y_D$ , where  $y_D = x_D$ . If the cooling in the condenser is rapid and the vapor and liquid do not reach

equilibrium, only a partial stage separation is obtained.

## **26.5 Tray Efficiencies**

### **26.5A Tray Efficiencies**

In all the previous discussions of theoretical trays or stages in distillation, we assumed that the vapor leaving a tray was in equilibrium with the liquid leaving. However, if the time of contact and the degree of mixing on the tray are insufficient, the streams will not be in equilibrium. As a result, the efficiency of the stage or tray will not be 100%. This means that we must use more actual trays for a given separation than the theoretical number of trays determined by calculation. The discussions in this section apply to both absorption and

distillation tray towers.

Three types of tray or plate efficiency are used: *overall tray efficiency  $E_o$* , *Murphree tray efficiency  $E_M$* , and *point or local tray efficiency  $E_{MP}$*  (sometimes called *Murphree point efficiency*). These will be considered individually.

#### **26.5B Types of Tray Efficiencies**

*1. Overall tray efficiency.* The *overall tray or plate efficiency  $E_o$*  concerns the entire tower and is simple to use, but it is the least fundamental. It is defined as the ratio of the number of theoretical or ideal trays needed in an entire tower to the number of actual trays used:

$$E_o = \frac{\text{number of ideal trays}}{\text{number of actual trays}} \quad (26.5-1)$$

For example, if eight theoretical steps



are needed and the overall efficiency is 60%, the number of theoretical trays is eight minus a reboiler, or seven trays. The actual number of trays is  $7/0.60$ , or 11.7 trays.

*2. Murphree tray efficiency.* The *Murphree tray efficiency*  $EM$  is defined as follows:

$$EM = \frac{y_n - y_{n+1}}{y_n^* - y_{n+1}} \quad (26.5-2)$$

where  $y_n$  is the average actual concentration of the mixed vapor leaving the tray  $n$  as shown in Fig. 26.5-1,  $y_{n+1}$  is the average actual concentration of the mixed vapor entering tray  $n$ , and  $y_n^*$  is the concentration of the vapor that would be in equilibrium with the liquid of concentration  $x_n$  leaving the tray to the

downcomer.

The liquid entering the tray has a concentration of  $x_{n-1}$ ; as it travels across the tray, its concentration drops to  $x_n$  at the outlet. Hence, there is a concentration gradient in the liquid as it flows across the tray. The vapor entering the tray comes in contact with liquid of different concentrations, and the outlet vapor will not be uniform in concentration.

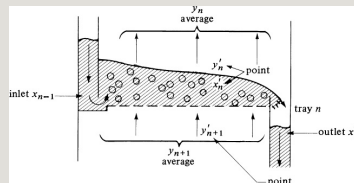


Figure 26.5-1. Vapor and liquid compositions on a sieve tray and tray efficiency.

*3. Point efficiency.* The *point* or *local efficiency*  $EMP$  on a tray is defined as

$$EMP = y_n' - y_{n+1}' / y_n^* - y_{n+1}' \quad (26.5-3)$$

where  $y_n'$  is the concentration of the vapor at a specific point in plate  $n$  as shown in Fig. 26.5-1,  $y_{n+1}'$  is the concentration of the vapor entering the plate  $n$  at the same point, and  $y_n^*$  is the concentration of the vapor that would be in equilibrium with  $x_n'$  at the same point. Since  $y_n'$  cannot be greater than  $y_n^*$ , the local efficiency cannot be greater than 1.00 or 100%.

In small-diameter towers, the vapor flow sufficiently agitates the liquid so that it is uniform on the tray. Then, the concentration of the liquid leaving is the same as that on the tray. Then,  $y_n' = y_n$ ,  $y_{n+1}' = y_{n+1}$ , and  $y_n'^* = y_n^*$ . The point efficiency then equals the Murphree tray efficiency, or  $E_M = EMP$ .

In large-diameter columns, incomplete mixing of the liquid occurs on the trays. Some vapor will contact the entering liquid  $x_{n-1}$ , which is richer in component  $A$  than  $x_n$ . This will give a richer vapor at this point than at the exit point, where  $x_n$  leaves. Hence, the tray efficiency  $E_M$  will be greater than the point efficiency  $E_{MP}$ . The value of  $E_M$  can be related to  $E_{MP}$  by integration of  $E_{MP}$  over the entire tray.

### **26.5C Relationship Between Tray Efficiencies**

The relationship between  $E_{MP}$  and  $E_M$  can be derived mathematically if the amount of liquid mixing is specified together with the amount of vapor mixing. Derivations for three different sets of assumptions are given by Robinson and Gilliland (R1). However, experimental data

are usually needed to obtain amounts of mixing. Semitheoretical methods for predicting  $EMP$  and  $EM$  are summarized in detail by Van Winkle (V1).

When the Murphree tray efficiency  $EM$  is known or can be predicted, the overall tray efficiency  $E_o$  can be related to  $EM$  by several methods. In the first method, an analytical expression is as follows when the slope  $m$  of the equilibrium line is constant as well as the slope  $L/V$  of the operating line:

$$E_o = \frac{\log[1 + EM(mV/L - 1)]}{\log(mV/L)}$$

(26.5-4)

If the equilibrium and operating lines of the tower are not straight, a graphical method employing the McCabe–Thiele

diagram can be used to determine the actual number of trays when the Murphree tray efficiency is known. In Fig. 26.5-2, a diagram is given for an actual plate as compared with an ideal plate. The triangle  $acd$  represents an ideal plate and the smaller triangle  $abe$  the actual plate. For the case shown, the Murphree efficiency  $EM = 0.60 = ba/ca$ . The dashed line going through point  $b$  is drawn so that  $ba/ca$  for each tray is 0.60. The trays are stepped off using this efficiency, and the total number of steps gives the actual number of trays needed. The reboiler is considered to be one theoretical tray, so the true equilibrium curve is used for this tray, as shown. In Fig. 26.5-2, 6.0 actual trays plus a reboiler are obtained.

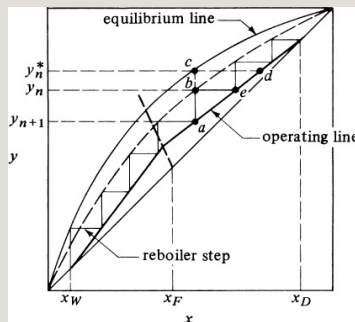


Figure 26.5-2. Use of the Murphree plate efficiency to determine the actual number of trays.

## 26.6 Flooding Velocity and Diameter of Tray Towers Plus Simple Calculations for Reboiler and Condenser Duties

### 26.6A Flooding Velocity and Diameter of Tray Towers

In tray towers, the maximum vapor velocity can be limited either by entrainment of small liquid droplets or by the liquid-handling capacity of the tray downcomer, whereby the liquid in the downcomer backs up to the next tray. The general basis for design uses the allowable-vapor-velocity concept. The equation by

Fair (F1) for estimating the maximum allowable vapor velocity for sieve, bubble-cap, or valve trays is

$$v_{\max} = K_v (\sigma / 20)^{0.2} \rho_L - \rho_V / \rho_V (26.6 - 1)$$

where  $v_{\max}$  is the allowable vapor velocity in ft/s based on the total cross-sectional area minus the area of one downcomer,  $\sigma$  is the surface tension of the liquid in dyn/cm (mN/m), and  $\rho_L$  and  $\rho_V$  are liquid and gas densities, kg/m<sup>3</sup> or lb<sub>m</sub>/ft<sup>3</sup>. The value of  $K_v$  in ft/s is obtained from Fig. 26.6-1, where  $L$  and  $V$  are total flow rates in kg/h or lb<sub>m</sub>/h. As a rule-of-thumb, the value of  $K_v$  should be multiplied by a factor of 0.91 to account for the downspout area of 9% of the tray (T2).



Equation (26.6-1) holds for nonfoaming systems. For many absorbers, the  $K_\sigma$  should be multiplied by 0.90 or so to account for foaming (S3). For the final design, the  $v_{\max}$  above should be multiplied by 0.80 to be 20% below flooding. For organic liquids, a typical value of  $\sigma$  is about 20–25 dyn/cm. For water with a surface tension of about 72 dyn/cm, the flooding velocity is larger by a factor of about  $(72/22.5)^{0.20}$ , or 1.26/1.

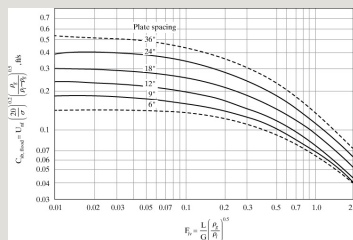


Figure 26.6-1. Estimation of  $K_v$  value for allowable vapor velocity. From Fair, J. R., *Petro/Chem. Eng.*, **33**(10), 45 (1961). Reprinted with permission from *Petroleum Refiner*, 37 (4), 153 (1958), copyright 1958, Gulf Pub. Co..

#### EXAMPLE 26.6-1. Tray Diameter of a Valve-Tray

### Absorption Tower

A valve-tray absorption tower is being used to absorb and recover ethyl alcohol vapor in air by pure water. The tower operates at 30°C and a pressure of 110 kPa abs. The entering gas contains 2.0 mol % ethyl alcohol in water, and 95% of the alcohol is recovered in the outlet water. The inlet pure aqueous flow is 186 kg mol/h and the inlet gas flow is 211.7 kg mol/h. Calculate the required tower diameter. A tray spacing of 0.610 m (2.0 ft) will be assumed. Use a factor of 0.95 for possible foaming.

**Solution:** The molecular weight of the entering air at the tower bottom where the flow rates are the greatest is

$$M=0.98(29.0)+0.02(46.1)=29.34\text{kg/kg mol}$$

The density of the vapor is

$$\rho V=29.34\text{kg/kg mol}(22.414\text{m}^3/\text{kg mol})(273.2)(110) \\ (273.2+30)(101.325)=1.280\text{kg/m}^3$$

The mass flow rate of the gas is  $V = 211.7(29.34) = 6211$  kg/h. Moles ethyl alcohol absorbed =  $0.95(0.02)(211.7) = 4.02$ . The outlet aqueous flow rate  $L = 186.0 + 4.02 = 190.02$  kg mol/h. The liquid mass flow rate is

$$L=186.0(18)+4.02(46.1)=3533\text{ kg/h}$$

The outlet water density, assuming a dilute solution at 30°C from Appendix A.2-3, is  $\rho L = 0.995(1000) = 995$  kg/m<sup>3</sup>. Then,

$$LV(\rho V \rho V)^{0.5}=(3533)(6211)(1.280995)^{0.5}=0.02040$$

Using Fig. 26.6-1 for a 24-in. tray spacing,  $K_u = 0.385$  ft/s. Substituting into Eq. (26.6-1) and using a surface tension of 70 (slightly less than water),

$$u_{\max}=0.385(7020)^{0.2995}-1.2801.280=13.78\text{ ft/s}$$

Multiplying the above by 0.91 to account for downspout area, by 0.95 for foaming, and by 0.80 for 80% of flooding,

$$u_{\text{design}}=13.78(0.91)(0.95)(0.80)=9.531\text{ ft/s or }2.905\text{ m/s}$$

The tower cross-section equals

$$(6211\text{kg/h})(3600\text{s/h})/(1.28\text{kg/m}^3)(2.905\text{ft/s})=0.464\text{m}^2$$

Solving for the diameter,  $\pi D^2/4 = 0.464$ . Then,  $D = 0.7686$  m (2.522 ft).

## 26.6B Condenser and Reboiler Duties Using the McCabe–Thiele Method

When dealing with saturated liquid feeds, reboiler and condenser duties are essentially equal. When dealing with a total condenser, the condenser duty can be calculated from the following equation:

$$q_c = D(R+1)\Delta H_{vap} \quad (26.6-2)$$

where  $\Delta H_{vap}$  is the average molar heat of vaporization at the top of the column. For a partial condenser:

$$q_c = D(R)\Delta H_{vap} \quad (26.6-3)$$

For a partial reboiler:

$$q_R = B V_m H_{vap}' \quad (26.6-4)$$

where  $\Delta H_{\text{vap}}'$  is the average molar heat of vaporization at the bottom of the column, and  $V_n = V_m + (1 - q)F$ .

## **26.7 Fractional Distillation Using the Enthalpy–Concentration Method**

### **26.7A Enthalpy–Concentration Data**

*1. Introduction.* In Section 26.4B, the McCabe–Thiele method was used to calculate the number of theoretical steps or trays needed for a given separation of a binary mixture of  $A$  and  $B$  by rectification or fractional distillation. The main assumptions in the method are that the latent heats are equal, sensible heat differences are negligible, and constant molal overflow occurs in each section of the distillation tower. In this section, we will consider fractional distillation using

enthalpy–concentration data where the molal overflow rates are not necessarily constant. The analysis will be made using enthalpy as well as material balances.

*2. Enthalpy–concentration data.* An enthalpy–concentration diagram for a binary vapor–liquid mixture of *A* and *B* takes into account latent heats, heats of solution or mixing, and sensible heats of the components of the mixture. The following data are needed to construct such a diagram at a constant pressure: (1) heat capacity of the liquid as a function of temperature, composition, and pressure; (2) heat of the solution as a function of temperature and composition; (3) latent heats of vaporization as a function of composition and pressure or

temperature; and (4) boiling point as a function of pressure, composition, and temperature.

The diagram at a given constant pressure is based on arbitrary reference states of liquid and temperature, such as 273 K (32°F). The saturated liquid line in enthalpy  $h$  kJ/kg (btu/lbm) or kJ/kg mol is calculated by

$$h = x_A c_{pA}(T - T_0) + (1 - x_A) c_{pB}(T - T_0) + \Delta H_{sol}(26.7 - 1)$$

where  $x_A$  is wt or mole fraction  $A$ ,  $T$  is boiling point of the mixture in K (°F) or °C,  $T_0$  is reference temperature, K,  $c_{pA}$  is the liquid heat capacity of the component  $A$  in kJ/kg · K (btu/lbm · °F) or kJ/kg mol · K,  $c_{pB}$  is heat capacity of  $B$ , and  $\Delta H_{sol}$  is heat of solution at  $T_0$  in

kJ/kg (btu/lbm) or kJ/kg mol. If heat is evolved on mixing, the  $\Delta H_{\text{sol}}$  will be a negative value in Eq. (26.7-1). Often, the heats of solution are small, as in hydrocarbon mixtures, and are neglected.

The saturated vapor enthalpy line of  $H$  kJ/kg (btu/lbm) or kJ/kg mol of a vapor composition  $y_A$  is calculated by

$$H = y_A[\lambda_A + c_{pyA}(T - T_0)] + (1 - y_A)[\lambda_B + c_{pyB}(T - T_0)] \quad (26.7-2)$$

where  $c_{pyA}$  is the vapor heat capacity for  $A$  and  $c_{pyB}$  for  $B$ . The latent heats  $\lambda_A$  and  $\lambda_B$  are the values at the reference temperature  $T_0$ . Generally, the latent heat is given as  $\lambda_{Ab}$  at the normal boiling point  $T_{bA}$  of the pure component  $A$  and  $\lambda_{Bb}$  for  $B$ . Then, to correct this to

the reference temperature  $T_0$  for use in Eq. (26.7-2),

$$\lambda_A = c_{pA}(T_{bA} - T_0) + \lambda_{Ab} - c_{pyA}(T_{bA} - T_0) \quad (26.7-3)$$

$$\lambda_B = c_{pB}(T_{bB} - T_0) + \lambda_{Bb} - c_{pyB}(T_{bB} - T_0) \quad (26.7-4)$$

In Eq. (26.7-3), the pure liquid is heated from  $T_0$  to  $T_{bA}$ , vaporized at  $T_{bA}$ , and then cooled as a vapor to  $T_0$ . Similarly, Eq. (26.7-4) also holds for  $\lambda_B$ . For convenience, the reference temperature  $T_0$  is often taken as equal to the boiling point of the lower-boiling component A. This means  $\lambda_A = \lambda_{Ab}$ . Hence, only  $\lambda_{Bb}$  must be corrected to  $\lambda_B$ .

**EXAMPLE 26.7-1. Enthalpy–Concentration Plot for Benzene–Toluene**

Prepare an enthalpy–concentration plot for benzene–toluene at 1 atm pressure. Equilibrium data are given in Table 26.1-1 and Figs. 26.1-1 and 26.1-2. Physical property



data are given in Table 26.7-1.

**Solution:** A reference temperature of  $T_0 = 80.1^\circ\text{C}$  will be used for convenience so that the liquid enthalpy of pure benzene ( $x_A = 1.0$ ) at the boiling point will be zero. For the first point, we will select pure toluene ( $x_A = 0$ ). For liquid toluene at the boiling point of  $110.6^\circ\text{C}$ , using Eq. (26.7-1) with zero heat of solution and data from Table 26.7-1,

Table 26.7-1. *Physical Property Data for Benzene and Toluene*

--	--

$$h = x_A c_{pA}(T - 80.1) + (1 - x_A) c_{pB}(T - 80.1) + 0 \quad (26.7-5)$$

$$h = 0 + (1 - 0)(167.5)(110.6 - 80.1) = 5109 \text{ kJ/kg mol}$$

For the saturated vapor enthalpy line, Eq. (26.7-2) is used. However, we must first calculate  $\lambda_B$  at the reference temperature  $T_0 = 80.1^\circ\text{C}$ , using Eq. (26.7-4):

$$\lambda_B = c_{pB}(T_b - T_0) + \lambda_{Bb} - c_{pB}(T_b - T_0)$$

$$(26.7-4) = 167.5(110.6 - 80.1) + 33330 - 138.2(110.6 - 80.1) = 34224 \text{ kJ/kg mol}$$

To calculate  $H$ , Eq. (26.7-2) is used, and  $y_A = 0$ :

$$H = y_A[\lambda_A + c_{pA}(T - T_0)] + (1 - y_A)[\lambda_B + c_{pB}(T - T_0)]$$

$$(26.7-2) = 0 + (1 - 0)[34224 + 138.2(110.6 - 80.1)] = 38439 \text{ kJ/kg mol}$$

For pure benzene,  $x_A = 1.0$  and  $y_A = 1.0$ . Using Eq. (26.7-5), since  $T = T_0 = 80.1$ ,  $h = 0$ . For the saturated vapor enthalpy, using Eq. (26.7-2) and  $T = 80.1$ ,

$$H = 1.0[30820 + 96.3(80.1 - 80.1)] + 0 = 30820$$

Selecting  $x_A = 0.50$ , the boiling point  $T_b = 92^\circ\text{C}$  and the temperature of saturated vapor for  $y_A = 0.50$  is  $98.8^\circ\text{C}$  from Fig. 26.1-1. Using Eq. (26.7-5) for the saturated liquid enthalpy at the boiling point,

$$h = 0.5(138.2)(92 - 80.1) + (1 - 0.5)(167.5)(92 - 80.1) = 1820$$

Using Eq. (26.7-2) for  $y_A = 0.5$ , the saturated vapor enthalpy at  $98.8^\circ\text{C}$  is

$$H = 0.5[30820 + 96.3(98.8 - 80.1)] + (1 - 0.5)[34224 + 138.2(98.8 - 80.1)] = 34716$$

Selecting  $x_A = 0.30$  and  $y_A = 0.30$ ,  $h = 2920$  and  $H = 36268$ . Also, for  $x_A = 0.80$  and  $y_A = 0.80$ ,  $h = 562$  and  $H = 32380$ . These values are tabulated in Table 26.7-2 and plotted in Fig. 26.7-1.

Some properties of the enthalpy–concentration plot are as follows: The region in between the saturated vapor line and the saturated liquid line is the two-phase liquid–vapor region. From Table 26.1-1, for  $x_A = 0.411$ , the vapor in equilibrium is  $y_A = 0.632$ . These two points are plotted in Fig. 26.7-1; this tie line represents the enthalpies and compositions of the liquid and vapor phases in equilibrium. Other tie lines can be drawn in a similar manner. The region below the  $h$ -versus- $x_A$  line represents liquid below the boiling point.

Table 26.7-2. *Enthalpy–Concentration*

# Data for Benzene–Toluene Mixtures at 101.325 kPa (1 atm) Total Pressure

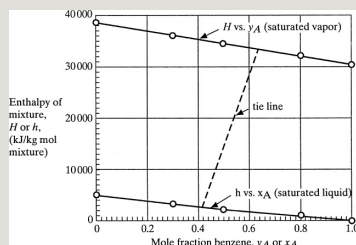


Figure 26.7-1. Enthalpy-concentration plot for benzene–toluene mixture at 1.0 atm abs.

## 26.7B Distillation in the Enriching Section of a Tower

To analyze the enriching section of a fractionating tower using enthalpy–concentration data, we make an overall and a component balance in Fig. 26.7-2:

$$V_{n+1} = L_n + D \quad (26.7-6)$$

$$V_{n+1}y_{n+1} = L_nx_n + Dx_D \quad (26.7-7)$$

Equation (26.7-7) can be rearranged to give the enriching-section operating line:

$$y_{n+1} = L_n V_{n+1} x_n + D x_D V_n + 1 \quad (26.7-8)$$

This is the same as Eq. (26.4-7) for the McCabe–Thiele method, but now the liquid and vapor flow rates  $V_{n+1}$  and  $L_n$  may vary throughout the tower, and Eq. (26.7-8) will not be a straight line on an  $x$ - $y$  plot.

Making an enthalpy balance,

$$V_{n+1} H_{n+1} = L_n h_n + D h_D + q_c \quad (26.7-9)$$

where  $q_c$  is the condenser duty, kJ/h or kW (btu/h). An enthalpy balance can be made just around the condenser:

$$q_c = V_1 H_1 - L_h D - D h D \quad (26.7-10)$$

By combining Eqs. (26.7-9) and (26.7-10) to eliminate  $q_c$ , an alternative form is obtained:

$$V_{n+1} H_{n+1} = L_n h_n + V_1 H_1 - L_h D \quad (26.7-11)$$

Substituting the value of  $L_n$  from Eq. (26.7-6) into (26.7-11),

$$V_{n+1} H_{n+1} = (V_{n+1} - D) h_n + V_1 H_1 - L_h D \quad (26.7-12)$$

Equations (26.7-8) and (26.7-12) are the final working equations for the enriching section.

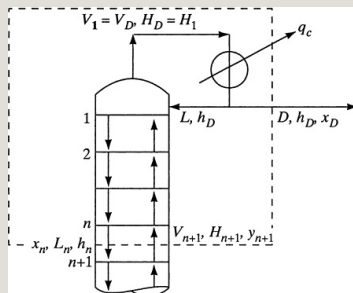


Figure 26.7-2. *Enriching section of a distillation tower.*

In order to plot the operating line Eq. (26.7-8), the terms  $V_{n+1}$  and  $L_n$  must be determined from Eq. (26.7-12). If the reflux ratio is set,  $V_1$  and  $L$  are known. The values  $H_1$  and  $h_D$  can be determined by means of Eqs. (26.7-1) and (26.7-2) or from an enthalpy–concentration plot. If a value of  $x_n$  is selected, it is a trial-and-error solution to obtain  $H_{n+1}$ , since  $y_{n+1}$  is not known. The steps to follow are given below:

1. Select a value of  $x_n$ . Assume  $V_{n+1} = V_1 = L + D$  and  $L_n = L$ . Then, using these values in Eq. (26.7-8), calculate an approximate value for  $y_{n+1}$ . This assumes a straight operating line.

2. Using this  $y_{n+1}$ , obtain  $H_{n+1}$ , and obtain  $h_n$  using  $x_n$ .  
Substitute these values into Eq. (26.7-12) and solve for  $V_{n+1}$ . Obtain  $L_n$  from Eq. (26.7-6).
3. Substitute into Eq. (26.7-8) and solve for  $y_{n+1}$ .
4. If the calculated value of  $y_{n+1}$  does not equal the assumed value of  $y_{n+1}$ , repeat steps 2–3. Generally, a second trial is not needed. Assume another value of  $x_n$  and repeat steps 1–4.
5. Plot the curved operating line for the enriching section.  
Generally, only a few values for the flows  $L_n$  and  $V_{n+1}$  are needed to determine the operating line, which is slightly curved.

### 26.7C Distillation in the Stripping Section of a Tower

To analyze the stripping section of a distillation tower, an overall and a component material balance are made on Fig. 26.4-5a:

$$L_m = W + V_{m+1} \quad (26.7-13)$$

$$L_m x_m = W x_W + V_{m+1} y_{m+1} \quad (26.7-14)$$

$$y_{m+1} = \frac{L_m}{V_{m+1}} x_m + \frac{W}{V_{m+1}} x_W$$

$$+1(26.7-15)$$

Making an enthalpy balance with  $q_R$  kJ/h or kW(btu/h) entering the reboiler in Fig. 26.4-5a, and substituting  $(V_{m+1} + W)$  for  $L_m$  from Eq. (26.7-13),

$$V_{m+1}H_{m+1} = (V_{m+1} + W)h_m + q_R - W h_W \quad (26.7-16)$$

Making an overall enthalpy balance in Fig. 26.4-3,

$$q_R = D h_D + W h_W + q_c - F h_F \quad (26.7-17)$$

The final working equations to use are Eqs. (26.7-15)–(26.7-17).

Using a method similar to that for the enriching section to solve the equations, select a value of  $y_{m+1}$  and calculate an approximate value for  $x_m$  from Eq.



(26.7-15), assuming constant molal overflow. Then, calculate  $V_{m+1}$  and  $L_m$  from Eqs. (26.7-16) and (26.7-13). Finally, use Eq. (26.7-15) to determine  $x_m$ . Compare this calculated value of  $x_m$  with the assumed value.

**EXAMPLE 26.7-2. Distillation Using the Enthalpy–Concentration Method**

A liquid mixture of benzene–toluene is being distilled under the same conditions as in Example 26.4-1, except that a reflux ratio of 1.5 times the minimum reflux ratio is to be used. The value  $R_m = 1.17$  from Example 26.4-2 will be used. Use enthalpy balances to calculate the flow rates of the liquid and vapor at various points in the tower, and plot the curved operating lines. Determine the number of theoretical stages needed.

**Solution:** The given data are as follows:  $F = 100$  kg mol/h,  $x_F = 0.45$ ,  $x_D = 0.95$ ,  $x_W = 0.10$ ,  $R = 1.5R_m = 1.5(1.17) = 1.755$ ,  $D = 41.2$  kg mol/h,  $W = 58.8$  kg mol/h. The feed enters at  $54.4^\circ\text{C}$  and  $q = 1.195$ . The flows at the top of the tower are calculated as follows:

$$LD = 1.755; L = 1.755(41.2) = 72.3; V_1 = L + D = 72.3 + 41.2 = 113.5$$

From Fig. 26.1-1, the saturation temperature at the top of the tower for  $y_1 = x_D = 0.95$  is  $82.3^\circ\text{C}$ . Using Eq. (26.7-2),

$$H_1 = 0.95[30820 + 96.3(82.3 - 80.1)] + (1 - 0.95)[34224 + 138.2(82.3 - 80.1)] = 31206$$

This value of 31 206 could also have been obtained from the enthalpy–concentration plot, Fig. 26.7-1. The boiling point of the distillate  $D$  is obtained from Fig. 26.1-1 and is  $81.1^\circ\text{C}$ . Using Eq. (26.7-5),

$$h_D = 0.95(138.2)(81.1 - 80.1) + (1 - 0.95)(167.5)(81.1 - 80.1) = 139$$

Again, this value could have been obtained from Fig. 26.7-1.

Following the procedure outlined for the enriching section for step 1, a value of  $x_n = 0.55$  is selected. Assuming a straight operating line for Eq. (26.7-8), an approximate value of  $y_{n+1}$  is obtained:

$$y_{n+1} = 72.3113.5x_n + 41.2113.5(0.95) = 0.637(x_n) + 0.345 = 0.637(0.55) + 0.345 = 0.695$$

Starting with step 2 and using Fig. 26.7-1, for  $x_n = 0.55$ ,  $h_n = 1590$ , and for  $y_{n+1} = 0.695$ ,  $H_{n+1} = 33\,240$ . Substituting into Eq. (26.7-12) and solving,

$$V_{n+1}(33240) = (V_{n+1} - 41.2)1590 + 113.5(31206) - 72.3(139)V_n + 1 = 109.5$$

Using Eq. (26.7-6),

$$109.5 = L_n + 41.2 \text{ or } L_n = 68.3$$

For step 3, substituting into Eq. (26.7-8),

$$y_{n+1} = 68.3109.5(0.55) + 41.2109.5(0.95) = 0.700$$

This calculated value of  $y_{n+1} = 0.700$  is sufficiently close to the approximate value of 0.695 that no further trials are needed.

Selecting another value for  $x_n = 0.70$  and, using Eq. (26.7-8), an approximate value of  $y_{n+1}$  is calculated:

$$y_{n+1} = 72.3113.5(0.70) + 41.2113.5(0.95) = 0.791$$

Using Fig. 26.7-1 for  $x_n = 0.70$ ,  $h_n = 1000$ , and for  $y_{n+1} = 0.791$ ,  $H_{n+1} = 32\,500$ . Substituting into Eq. (26.7-12) and solving,

$$V_{n+1}(32500) = (V_{n+1} - 41.2)1000 + 113.5(31206) - 72.3(139)V_n + 1 = 110.8$$

Using Eq. (26.7-6),

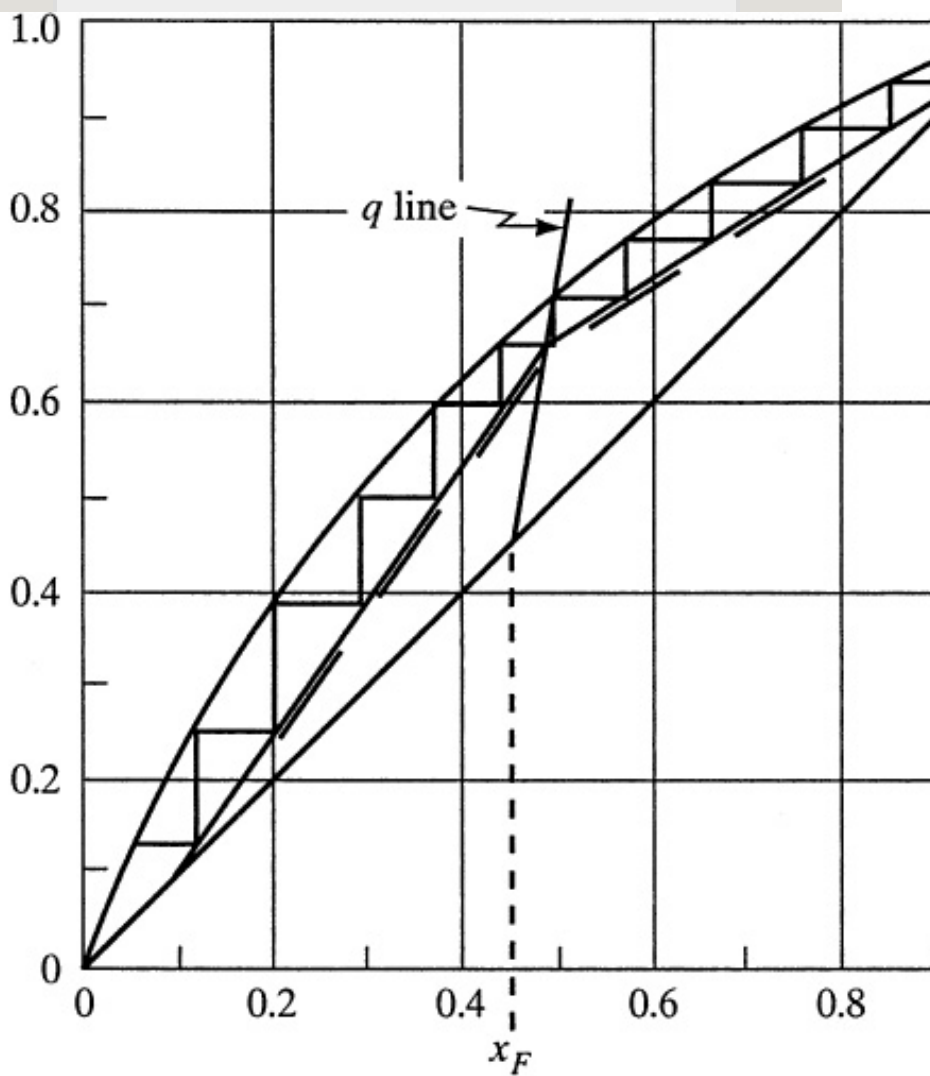
$$L_n = 110.8 - 41.2 = 69.6$$

Substituting into Eq. (26.7-8),

$$y_{n+1} = 69.6110.8(0.70) + 41.2110.8(0.95) = 0.793$$

In Fig. 26.7-3, the points for the curved operating line in the enriching section are plotted. This line is approximately straight and is very slightly above that for constant molal overflow.

action  
or,  $y$



Mole fraction in liquid,  $x$

Figure 26.7-3. Plot of curved operating lines using enthalpy-concentration method for Example 26.7-2. Solid lines are for enthalpy-concentration method and dashed lines are for constant molal overflow.

Using Eq. (26.7-10), the condenser duty is calculated:

$$q_c = 113.5(31\,206) - 72.3(139) - 41.2(139) = 3526\,100 \text{ kJ/h}$$

To obtain the reboiler duty  $q_R$ , values for  $h_W$  and  $h_F$  are needed. Using Fig. 26.7-1 for  $x_W = 0.10$ ,  $h_W = 4350$ . The feed is at 54.5°C. Using Eq. (26.7-5),

$$h_F = 0.45(138.2)(54.5 - 80.1) + (1 - 0.45)(167.5)(54.5 - 80.1) = -3929$$

Using Eq. (26.7-17),

$$q_R = 41.2(139) + 58.8(4350) + 3526100 - 100(-3929) = 4180500 \text{ kJ/h}$$

Using Fig. 26.4-5 and making a material balance below the bottom tray and around the reboiler,

$$L_N = W + V_W \quad (26.7-18)$$

Rewriting Eq. (26.7-16) for this bottom section,

$$V_W h_W = (V_W + W)h_N + q_R - W h_W \quad (26.7-19)$$

From the equilibrium diagram, Fig. 26.1-2, for  $x_W = 0.10$ ,  $y_W = 0.207$ , which is the vapor composition leaving the reboiler.

For equimolal overflow in the stripping section, using Eqs. (26.4-14) and (26.4-15),

$$L_m = L_n + qF = 72.3 + 1.195(100) = 191.8 \quad (26.4-14)$$

$$V_{m+1} = V_{n+1} - (1-q)F = 113.5 - (1 - 1.195)100 = 133.0 \quad (26.4-15)$$

Selecting  $y_{m+1} = y_W = 0.207$ , and using Eq. (26.7-15), an approximate value of  $x_m = x_N$  is obtained:

$$y_{m+1} = L_m V_{m+1} x_m - W x_W V_m + 10.207 = 191.8(133.0)(x_N) - 58.8(133.0)(0.10) \quad (26.7-15)$$

Solving,  $x_N = 0.174$ . From Fig. (26.7-1), for  $x_N = 0.174$ ,  $h_N = 3800$ , and for  $y_W = 0.207$ ,  $H_W = 37\,000$ . Substituting into Eq. (26.7-19),

$$VW(37000)=(VW+58.8)(3800)+4180500-58.8(4350)$$

Solving,  $VW = 125.0$ . Using Eq. (26.7-18),  $LN = 183.8$ .

Substituting into Eq. (26.7-15) and solving for  $xN$ ,

$$0.207=183.8125.0(xN)-58.8125.0(0.10)xN=0.173$$

This value of 0.173 is quite close to the approximate value of 0.174.

Assuming a value of  $y_{m+1} = 0.55$  and using Eq. (26.7-15), an approximate value of  $x_m$  is obtained:

$$y_{m+1}=0.55=191.8133.0(x_m)-58.8133.0(0.10)x_m=0.412$$

From Fig. (26.7-1), for  $x_m = 0.412$ ,  $h_m = 2300$ , and for  $y_{m+1} = 0.55$ ,  $H_m = 34400$ . Substituting into Eq. (26.7-16),

$$V_{m+1}(34400)=(V_{m+1}+58.8)(2300)+4180500-58.8(4350)$$

Solving,  $V_{m+1} = 126.5$ . Using Eq. (26.7-13),

$$L_m=W+V_{m+1}=58.8+126.5=185.3$$

Substituting into Eq. (26.7-15) and solving for  $x_m$ ,

$$y_{m+1}=0.55=185.3126.5x_m-58.8126.5(0.1)x_m=0.407$$

This value of 0.407 is sufficiently close to the approximate value of 0.412 that no further trials are needed. The two points calculated for the stripping section are plotted in Fig. 26.7-3. This stripping line is also approximately straight and is very slightly above the operating line for constant molal overflow.

Using the operating line for the enthalpy balance method, the number of theoretical steps is 10.4. Using the equimolal method, 9.9 steps are obtained. This difference would be larger if the reflux ratio of 1.5 times  $R_m$  were decreased to, say, 1.2 or 1.3. At larger reflux ratios, this difference in number of steps would be less.

Note that in Example 26.7-2, in the stripping section the vapor flow

increases slightly from 125.0 to 126.5 in going from the reboiler to near the feed tray. These values are lower than the value of 133.0 obtained assuming equimolal overflow. Similar conclusions hold for the enriching section. The enthalpy–concentration method is useful in calculating the internal vapor and liquid flows at any point in the column. These data are then used in sizing the trays. Also, calculations of  $q_c$  and  $q_R$  are used in designing the condenser and reboiler. This method is very applicable to design using a computer solution for binary and multicomponent mixtures to make tray-to-tray mass and enthalpy balances for the whole tower. The more restrictive Ponchon–Savarit graphical method for only binary mixtures is available (K3, T2).

## 26.8 Distillation of Multicomponent Mixtures

### 26.8A Introduction to Multicomponent Distillation

Many industrial distillation processes involve the separation of more than two components. The general principles of design for multicomponent distillation towers are the same in many respects as those described for binary systems. There is one mass balance for each component in the multicomponent mixture. Enthalpy or heat balances are made that are similar to those for the binary case. Equilibrium data are used to calculate boiling points and dew points. The concepts of minimum reflux and total reflux as limiting cases are also used.

- 1. Number of distillation towers needed.*

In binary distillation, one tower was used to separate the two components  $A$  and  $B$  into relatively pure components, with  $A$  in the overhead and  $B$  in the bottoms. However, in a multicomponent mixture of  $n$  components,  $n - 1$  fractionators will be required for separation. For example, for a three-component system of components  $A$ ,  $B$ , and  $C$ , where  $A$  is the most volatile and  $C$  the least volatile, two columns will be needed, as shown in Fig. 26.8-1. The feed of  $A$ ,  $B$ , and  $C$  is distilled in column 1, and  $A$  and  $B$  are removed in the overhead, and  $C$  is removed in the bottoms. Since the separation in this column is between  $B$  and  $C$ , the bottoms containing  $C$  will contain a small amount of  $B$  and often a negligible amount of  $A$  (often called the trace component). The amount of the trace



component  $A$  in the bottoms can usually be neglected if the relative volatilities are reasonably large. In column 2, the feed of  $A$  and  $B$  is distilled, with  $A$  in the distillate containing a small amount of component  $B$  and a much smaller amount of  $C$ . The bottoms containing  $B$  will also be contaminated with a small amount of  $C$  and  $A$ . Alternately, column 1 could be used to remove  $A$  overhead, with  $B$  plus  $C$  being fed to column 2 for separation of  $B$  and  $C$ .

*2. Design calculation methods.* In multicomponent distillation, as in binary, ideal stages or trays are assumed in the stage-to-stage calculations. Using equilibrium data, equilibrium calculations are used to obtain the boiling point and equilibrium vapor composition from a given liquid

composition or the dew point, and liquid composition from a given vapor composition. Material balances and heat balances similar to those described in Section 26.7 are then used to calculate the flows to and from the adjacent stages. These stage-to-stage design calculations involve trial-and-error calculations, and high-speed digital computers are generally used to provide rigorous solutions.

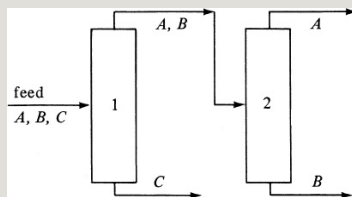


Figure 26.8-1. *Separation of a ternary system of A, B, and C.*

In a design, the conditions of the feed are generally known or specified (temperature, pressure, composition, flow rate). Then, in most cases, the

calculation procedure follows either of two general methods. In the first method, the desired separation or split between two of the components is specified and the number of theoretical trays is calculated for a selected reflux ratio. It is clear that with more than two components in the feed, the complete compositions of the distillate and bottoms are not then known, and trial-and-error procedures must be used. In the second method, the number of stages in the enriching section and stripping section, and the reflux ratio are specified or assumed, and the separation of the components is calculated using assumed liquid and vapor flows and temperatures for the first trial. This approach is often preferred for computer calculations (H2, P1). In the trial-and-error procedures, the design method of Thiele and Geddes

( $P_1$ ,  $S_1$ ,  $T_1$ ), which is reliable, is often used to calculate the resulting distillate and bottoms compositions together with tray temperatures and compositions.

Various combinations and variations of the rigorous calculation methods above are available in the literature ( $H_2$ ,  $P_1$ ,  $S_1$ ) and will not be considered further.

The variables in the design of a distillation column are all interrelated, and there are only a certain number of these that may be fixed in the design. For a more detailed discussion of the specification of these variables, see Kwauk ( $K_2$ ).

*3. Shortcut calculation methods.* In the remainder of this chapter, shortcut calculation methods for the approximate solution of multicomponent distillation

are considered. These methods are quite useful for rapidly studying a large number of cases to help orient the designer, determine approximate optimum conditions, or provide information for a cost estimate. Before discussing these methods, equilibrium relationships and calculation methods of bubble point, dew point, and flash vaporization for multicomponent systems will be covered.

### **26.8B Equilibrium Data in Multicomponent Distillation**

For multicomponent systems that can be considered ideal, Raoult's law can be used to determine the composition of the vapor in equilibrium with the liquid. For example, for a system composed of four components,  $A$ ,  $B$ ,  $C$ , and  $D$ ,

$$p_A = P A x_A, p_B = P B x_B, p_C = P C x_C, p_D = P D x_D \quad (26.8-1)$$

$$p_A P = P A P x_A, y_B = P B P x_B, y_C = P C P x_C, y_D = P D P x_D \quad (26.8-2)$$

In hydrocarbon systems, because of nonidealities, the equilibrium data are often represented by

$$y_A = K_A x_A, y_B = K_B x_B, y_C = K_C x_C, y_D = K_D x_D \quad (26.8-3)$$

where  $K_A$  is the vapor–liquid equilibrium constant or distribution coefficient for component A. These  $K$  values for light hydrocarbon systems (methane to decane) have been determined semiempirically and each  $K$  is a function of temperature and pressure. Convenient  $K$  factor charts are available from Depriester (D1) and Hadden and Grayson (H1). For light hydrocarbon systems,  $K$  is generally assumed not to be a function of

composition, which is sufficiently accurate for most engineering calculations. Note that for an ideal system,  $K_A = P_A/P$ , and so on. As an example, data for the hydrocarbons *n*-butane, *n*-pentane, *n*-hexane, and *n*-heptane are plotted in Fig. 26.8-2 at 405.3 kPa (4.0 atm) absolute (D1, H1).

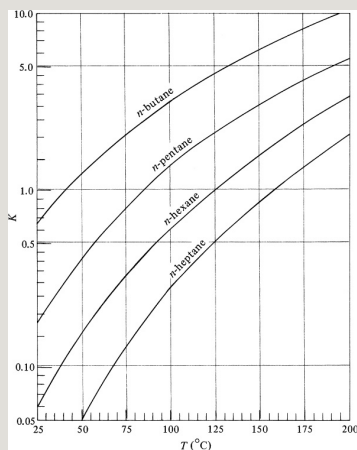


Figure 26.8-2. *Equilibrium  $K$  values for light hydrocarbon systems at 405.3 kPa (4.0 atm) absolute.*

The relative volatility  $\alpha_i$  for each individual component in a multicomponent mixture can be defined

in a manner similar to that for a binary mixture. If component  $C$  in a mixture of  $A$ ,  $B$ ,  $C$ , and  $D$  is selected as the base component,

$$\alpha_A = K_A/K_C, \alpha_B = K_B/K_C, \alpha_C = K_C/K_C = 1.0, \alpha_D = K_D/K_C$$

The values of  $K_i$  will be a stronger function of temperature than the  $\alpha_i$  values, since the  $K_i$  lines in Fig. 26.8-2 all increase with temperature in a similar manner.

### 26.8C Boiling Point, Dew Point, and Flash Distillation

*1. Boiling point.* At a specified pressure, the boiling point or bubble point of a given multicomponent mixture must satisfy the relation  $\sum y_i = 1.0$ . For a mixture of  $A$ ,  $B$ ,  $C$ , and  $D$ , with  $C$  as the base component,



$$\sum y_i = \sum K_i x_i = K_C \sum \alpha_i x_i = 1.0 \quad (26.8-5)$$

The calculation is a trial-and-error process, as follows: First a temperature is assumed and the values of  $\alpha_i$  are calculated from the values of  $K_i$  at this temperature. Then, the value of  $K_C$  is calculated from  $K_C = 1.0 / \sum \alpha_i x_i$ . The temperature corresponding to the calculated value of  $K_C = 1.0 / \sum \alpha_i x_i$ . The temperature corresponding to the calculated value of  $K_C$  is compared to the assumed temperature. If the values differ, the calculated temperature is used for the next iteration. After the final temperature is known, the vapor composition is calculated from

$$y_j = \alpha_j x_j \sum (\alpha_i x_i) \quad (26.8-6)$$

2. *Dew point.* For the dew-point

calculation, which is also trial and error,

$$\sum x_i = \sum (y_i K_i) = (1/K_C) \sum (y_i \alpha_i) = 1.0 \quad (26.8-7)$$

The value of  $K_C$  is calculated from  $K_C = 1.0 / \sum \alpha_i x_i$ . After the final temperature is known, the liquid composition is calculated from

$$x_i = y_i / \alpha_i \sum (y_i / \alpha_i) \quad (26.8-8)$$

**EXAMPLE 26.8-1. Boiling Point of a Multicomponent Liquid**

A liquid feed to a distillation tower at 405.3 kPa abs is fed to a distillation tower. The composition in mole fractions is as follows: *n*-butane ( $x_A = 0.40$ ), *n*-pentane ( $x_B = 0.25$ ), *n*-hexane ( $x_C = 0.20$ ), *n*-heptane ( $x_D = 0.15$ ). Calculate the boiling point and the vapor in equilibrium with the liquid.

**Solution:** First, a temperature of 65°C is assumed and the values of  $K$  obtained from Fig. 26.8-2. Using component  $C$  (*n*-hexane) as the base component, the following values are calculated using Eq. (26.8-5) for the first trial:

The calculated value of  $K_C$  is 0.2745, which corresponds to 69°C, Fig. 26.8-2. Using 69°C for trial 2, a temperature of 70°C is obtained. Using 70°C for trial 3, the calculations shown give a final calculated value of 70°C, which is the bubble point. Values of  $y_i$  are calculated from Eq. (26.8-6).

3. *Flash distillation of multicomponent mixture.* For flash distillation, the process flow diagram is shown in Fig. 26.3-1. Defining  $f = V/F$  as the fraction of the feed vaporized and  $(1 - f) = L/F$  as the fraction of the feed remaining as liquid, and making a component  $i$  balance as in Eq. (26.3-6), the following is obtained:

$$y_i = f - 1 f x_i + x_i F f \quad (26.8-9)$$

where  $y_i$  is the composition of  $i$  in the vapor in equilibrium with  $x_i$  in the liquid after vaporization. For equilibrium,  $y_i = K_i x_i = K C \alpha_i x_i$ , where  $\alpha_i = K_i / K_C$ . Then, Eq. (26.8-9) becomes

$$y_i = K C \alpha_i x_i = f - 1 f x_i + x_i F f \quad (26.8-10)$$

Solving for  $x_i$  and summing for all components,

$$\sum x_i = \sum x_i F_f (K C \alpha_i - 1) + 1 = 1.0 \quad (26.8-11)$$

This is solved by trial and error by first assuming a temperature if the fraction  $f$  vaporized has been set. When the  $\sum x_i$  values add up to 1.0, the proper temperature has been chosen. The composition of the vapor  $y_i$  can be obtained from  $y_i = K C \alpha_i x_i$  or by a material balance.

#### **26.8D Key Components in Multicomponent Distillation**

Fractionation of a multicomponent mixture in a distillation tower will allow separation only between two components. For a mixture of  $A$ ,  $B$ ,  $C$ ,  $D$ , and so on, a separation in one tower can only be made between  $A$  and  $B$ , or  $B$  and  $C$ , and so on. The components separated are called the *light key*, which is the more volatile

(identified by the subscript  $L$ ), and the *heavy key* (the subscript  $H$ ). The components more volatile than the light key are called *light components* and will be present in the bottoms in small amounts. The components less volatile than the heavy key are called *heavy components* and will be present in the distillate in small amounts. The two key components are present in significant amounts in both the distillate and the bottoms.

#### **26.8E Total Reflux for Multicomponent Distillation**

##### *1. Minimum stages for total reflux.*

Just as in binary distillation, the minimum number of theoretical stages or steps,  $N_m$ , can be determined for multicomponent distillation for total reflux. The Fenske equation (26.4-23) also

applies to any two components in a multicomponent system. When applied to the heavy key  $H$  and the light key  $L$ , it becomes

$$N_m = \log[(x_{LDD}/x_{HDD})(x_{HWW}/x_{LWW})] \log(\alpha_{L,av}) \quad (26.8-12)$$

where  $x_{LD}$  is mole fraction of the light key in the distillate,  $x_{LW}$  is mole fraction in bottoms,  $x_{HD}$  is mole fraction of the heavy key in distillate, and  $x_{HW}$  is mole fraction in the bottoms. The average value of  $\alpha_L$  of the light key is calculated from  $\alpha_{LD}$  at the top temperature (dew point) of the tower and  $\alpha_{LW}$  at the bottoms temperature:

$$\alpha_{L,av} = \alpha_{LD} \alpha_{LW} \quad (26.8-13)$$

Note that the distillate dew-point and bottoms boiling-point estimation is

partially trial and error, since the distribution of the other components in the distillate and bottoms is not known and can affect these values.

*2. Distribution of other components.* To determine the distribution or concentration of other components in the distillate and bottoms at total reflux, Eq. (26.8-12) can be rearranged and written for any other component  $i$  as follows:

$$x_i^D = \frac{(\alpha_i, \text{av}) N_m x_i^W}{H_D + x_i^W} \quad (26.8-14)$$

These concentrations of the other components determined at total reflux can be used as approximations with finite and minimum reflux ratios. More accurate methods for finite and minimum reflux are available elsewhere

(H2, S1, V1).

**EXAMPLE 26.8-2. Calculation of Top and Bottom Temperatures and Total Reflux**

The liquid feed of 100 mol/h at the boiling point given in Example 26.8-1 is fed to a distillation tower at 405.3 kPa and is to be fractionated so that 90% of the *n*-pentane (*B*) is recovered in the distillate and 90% of the *n*-hexane (*C*) is recovered in the bottoms. Calculate the following:

- Moles per hour and composition of distillate and bottoms
- Top temperature (dew point) of distillate and boiling point of bottoms
- Minimum stages for total reflux and distribution of other components in the distillate and bottoms

**Solution:** For part (a), material balances are made for each component, with component *n*-pentane (*B*) being the light key (*L*) and *n*-hexane (*C*) the heavy key (*H*). For the overall balance,

$$F=D+W(26.8-15)$$

For component *B*, the light key,

$$x_B F F = 0.25(100) = 25.0 = y_B D D + x_B W W (26.8-16)$$

Since 90% of *B* is in the distillate,  $y_B D D = (0.90)(25) = 22.5$ . Hence,  $x_B W W = 2.5$ . For component *C*, the heavy key,

$$x_C F F = 0.20(100) = 20.0 = y_C D D + x_C W W (26.8-17)$$

Also, 90% of *C* is in the bottoms and  $x_C W W = 0.90(20) = 18.0$ . Then,  $y_C D D = 2.0$ . For the first trial, it is assumed that no component *D* (heavier than the heavy key *C*) is in the distillate and no light *A* is in the bottoms. Hence, moles *A* in distillate =  $y_A D D = 0.40(100) = 40.0$ . Also, moles *D* in bottoms =  $x_D W W = 0.15(100) = 15.0$ . These values are tabulated below.



For the dew point of the distillate (top temperature) in part (b), a value of 67°C will be estimated for the first trial. The  $K$  values are read from Fig. 26.8-2 and the  $\alpha$  values calculated. Using Eqs. (26.8-7) and (26.8-8), the following values are calculated:

The calculated value of  $K_C$  is 0.2627, which corresponds very closely to 67°C, the final temperature of the dew point.

For the bubble point of the bottoms, a temperature of 135°C is assumed for trial 1 and Eqs. (26.8-5) and (26.8-6) are used for the calculations. A second trial using 132°C gives the final temperature as shown below:

The calculated value of  $K_C$  is 1.144, which is close to the value at 132°C.

For part (c), the proper  $\alpha$  values of the light key  $L$  ( $n$ -pentane) to use in Eq. (26.8-13) are as follows:

$$2.50(t=67^\circ\text{C at the column top})\alpha_L W = 2.04(t=132^\circ\text{C at the column bottom})\alpha_L, \text{av} = \alpha_L D \alpha_L W = 2.50(2.04) = 2.258(26.8-13)$$

Substituting into Eq. (26.8-12),

$$N_m = \log[(0.349 \times 64.5 / 0.031 \times 64.5) (0.507 \times 35.5 / 0.070 \times 35.5)] \log(2258) = 5.404 \text{ theoretical stages (4.404 theoretical trays)}$$

The distribution or compositions of the other components can be calculated using Eq. (26.8-14). For component  $A$ , the average  $\alpha$  value to use is

$$\alpha_{AD} \alpha_{AW} = 6.73 \times 4.348 = 5.409 \times \alpha_{DD} \times \alpha_{WW} = (\alpha_A, \text{av}) N_m \times H_{DD} \times H_{WW} = (5.409) 5.404 \times 0.031(64.5) 0.507(355) = 1017(26.8-14)$$

Making an overall balance on  $A$ ,

$$x_{AFF} = 40.0 = x_{ADD} + x_{AWW} \quad (26.8-18)$$

Substituting  $x_{ADD} = 1017 x_{AWW}$  from Eq. (26.8-14) into

(26.8-18) and solving,

$$x_{AWW}=0.039, x_{ADD}=39.961$$

For the distribution of component  $D$ ,

$$\alpha_{D,av}=0.385 \times 0.530=0.452.$$

$$x_{DDD}x_{DWW}=(\alpha_{D,av})N_m x_{HDD}x_{HWW}=(0.452)5.404(0.031)(645)(0.507)(355)=0.001521x_{DFF}=15.0=x_{DDD}+x_{DWW}$$

Solving,  $x_{DDD} = 0.023$ ,  $x_{DWW} = 14.977$ .

The revised distillate and bottoms compositions are as follows:

--

Hence, the number of moles of  $D$  in the distillate is quite small, as is the number of moles of  $A$  in the bottoms.

Using the new distillate composition, a recalculation of the dew point, assuming  $67^\circ\text{C}$ , gives a calculated value of  $K_c = 0.2637$ . This is very close to that of 0.2627 obtained when the trace amount of  $D$  in the distillate was assumed as zero. Hence, the dew point is  $67^\circ\text{C}$ . Repeating the bubble-point calculation for the bottoms, assuming  $132^\circ\text{C}$ , a calculated value of  $K_c = 1.138$ , which is close to the value at  $132^\circ\text{C}$ . Hence, the bubble point remains at  $132^\circ\text{C}$ . If either the bubble- or dew-point temperatures had changed, the new values would then be used in a recalculation of  $N_m$ .

## 26.8F Shortcut Method for the Minimum Reflux Ratio for Multicomponent Distillation

As in the case of binary distillation, the minimum reflux ratio  $R_m$  is the reflux ratio that will require an infinite number of trays for the given

separation of the key components.

For binary distillation, only one “pinch point” occurs where the number of steps becomes infinite, and that is usually at the feed tray. For multicomponent distillation, two pinch points or zones of constant composition occur: one in the section above the feed plate and another below the feed tray. The rigorous plate-by-plate stepwise procedure for calculating  $R_m$  is trial and error, and can be extremely tedious for hand calculations.

Underwood’s shortcut method for calculating  $R_m$  (U1, U2) uses constant average  $\alpha$  values and assumes constant flows in both sections of the tower. This method provides a reasonably accurate value. The two equations to be solved in

order to determine the minimum reflux ratio are

$$1-q = \sum \alpha_i x_i F \alpha_i^{-\theta} \quad (26.8-19)$$

$$R_{m+1} = \sum \alpha_i x_i D \alpha_i^{-\theta} \quad (26.8-20)$$

The values of  $x_i D$  for each component in the distillate in Eq. (26.8-20) are supposed to be the values at the minimum reflux. However, as an approximation, the values obtained using the Fenske total reflux equation are used. Since each  $\alpha_i$  may vary with temperature, the average value of  $\alpha_i$  to use in the preceding equations is approximated by using  $\alpha_i$  at the average temperature of the top and bottom of the tower. Some (P1, S1) have used the average  $\alpha$  that is used in the Fenske equation or the  $\alpha$  at the entering feed

temperature. To solve for  $R_m$ , the value of  $\theta$  in Eq. (26.8-19) is first obtained by trial and error. This value of  $\theta$  lies between the  $\alpha$  value of the light key and the  $\alpha$  value of the heavy key, which is 1.0. Using this value of  $\theta$  in Eq. (26.8-20), the value of  $R_m$  is obtained directly. When distributed components appear between the key components, modified methods described by others (S1, T2, V1) can be used.

### **26.8G Shortcut Method for Number of Stages at Operating Reflux Ratio**

*1. Number of stages at operating reflux ratio.* The determination of the minimum number of stages for total reflux presented in Section 26.8E and the minimum reflux ratio presented in Section 26.8F are useful for setting the allowable ranges for the number of stages and flow

conditions. These ranges are helpful in selecting the particular operating conditions for a design calculation. The relatively complex rigorous procedures for doing a stage-by-stage calculation at any operating reflux ratio have been discussed in Section 26.8A.

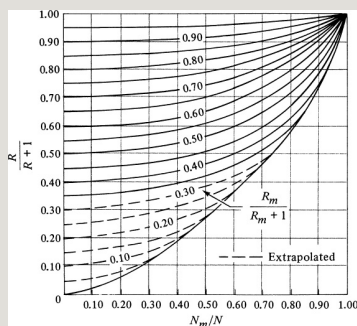


Figure 26.8-3. *Erbar–Maddox correlation between reflux ratio and number of stages (RM based on Underwood method). From J. H. Erbar and R. N. Maddox, Petrol. Refiner, **40**(5), 183 (1961).*

An important shortcut method for determining the theoretical number of stages required for an operating reflux ratio  $R$  is the empirical correlation of

Erbar and Maddox (E1) given in Fig. 26.8-3. This correlation is somewhat similar to a correlation by Gilliland (G1) and should be considered as an approximate method. In Fig. 26.8-3, the operating reflux ratio  $R$  (for flow rates at the column top) is correlated with the minimum  $R_m$  obtained using the Underwood method, the minimum number of stages  $N_m$  obtained by the Fenske method, and the number of stages  $N$  at the operating  $R$ .

## *2. Estimate of feed-plate location.*

Kirkbride (K1) has devised an approximate method to estimate the number of theoretical stages above and below the feed that can be used to estimate the feed-stage location. This empirical relation is as follows:

$$\log N_e N_s = 0.206 \log[(x_{HF} x_{LF}) W D (x_{LW} x_{HD})^2] \quad (26.8-21)$$

where  $N_e$  is the number of theoretical stages above the feed plate and  $N_s$  is the number of theoretical stages below the feed plate.

**EXAMPLE 26.8-3. Minimum Reflux Ratio and the Number of Stages at the Operating Reflux Ratio**

Using the conditions and results given in Example 26.8-2, calculate the following:

- Minimum reflux ratio using the Underwood method
- Number of theoretical stages at an operating reflux ratio  $R$  of  $1.5R_m$  using the Erbar–Maddox correlation
- Location of feed tray using the Kirkbride method

**Solution:** For part (a), the temperature to use for determining the values of  $\alpha_i$  is the average between the top of 67°C and the bottom of 132°C (from Example 26.8-2), and it is  $(67 + 132)/2$ , or 99.5°C. The  $K_i$  values obtained from Fig. 26.8-2 and the  $\alpha_i$  values, and distillate and feed compositions to use in Eqs. (26.8-19) and (26.8-20) are as follows:

--	--	--	--	--	--

Substituting into Eq. (26.8-19) with  $q = 1.0$  for feed at the boiling point,



$$1-q=1-1=0=5.20(0.40)5.20-\theta+2.30(0.25)2.30-\theta \\ +1.00(0.20)1.00-\theta+0.467(0.15)0.467-\theta(26.8-22)$$

This is trial and error, so a value of  $\theta = 1.210$  will be used for the first trial ( $\theta$  must be between 2.30 and 1.00). This and other trials are shown below:

The final value of  $\theta = 1.2096$  is substituted into Eq. (26.8-20) to solve for  $R_m$ :

$$R_m$$

$$+1=5.20(0.6197)5.20-1.2096+2.30(0.3489)2.30-1.2096+1.00(0.031)1.00-1.2096+0.467(0.0004)0.467-1.2096$$

Solving,  $R_m = 0.395$ .

For part (b), the following values are calculated:  $R = 1.5R_m = 1.5(0.395) = 0.593$ ,  $R/(R + 1) = 0.593/(0.593 + 1.0) = 0.3723$ ,  $R_m/(R_m + 1) = 0.395/(0.395 + 1.0) = 0.2832$ . From Fig. 26.8-3,  $N_m/N = 0.49$ . Hence,  $N_m/N = 0.49 = 5.40/N$ . Solving,  $N = 11.0$  theoretical stages in the tower. This gives  $11.0 - 1.0$  (reboiler), or 10.0 theoretical trays.

For the location of the feed tray in part (c), using Eq. (26.8-21),

$$\log N_e N_s = 0.206 \log [(0.200/25)^{35.51664} (4.84/0.0704)^{0.0310}] = 0.07344$$

Hence,  $N_e/N_s = 1.184$ . Also,  $N_e + N_s = 1.184 N_s + N_s = N = 11.0$  stages.

Solving,  $N_s = 5.0$  and  $N_e = 6.0$ . This means that the feed tray is 6.0 trays from the top.

## 26.9 Chapter Summary

### Raoult's Law

$$p_A = P A x_A \quad (26.1-1)$$

$$p_A + p_B = P \quad (26.1-2)$$

$$P_A x_A + P_B (1 - x_A) = P \quad (26.1-3)$$

$$y_A = p_A / P = P_A x_A / P \quad (26.1-4)$$

## Column Internals

### *Three Common Tray Types*

1. Sieve tray
2. Valve tray
3. Bubble-cap tray

## Structured Packing

## Random Packing

## Material Balance Batch Distillation

$$\int_{L_2}^{L_1} \frac{dL}{L} = \ln \frac{L_1}{L_2} = \int_{x_2}^{x_1} \frac{dx}{x} \quad (26.3-10)$$

## McCabe–Thiele Method

$$F=D+W(26.4-3)$$

A total material balance on component A gives

$$F x_F = D x_D + W x_W(26.4-4)$$

*Operating-line enriching section:*

$$y_{n+1} = R x_n + x_D R + 1(26.4-8)$$

*Operating-line stripping section:*

$$y_{m+1} = L x_m + W x_W V_{m+1} + 1(26.4-11)$$

*q line:*

1 mol of feed at entering conditions mol latent heat of vapor

If the feed enters at its boiling point, the numerator of Eq. (26.4-12) is the same

as the denominator, and  $q = 1.0$ .

Equation (26.4-12) can also be written in terms of enthalpies:

$$q = \frac{H_V - H_F}{H_V - H_L} \quad (26.4-13)$$

$$y = \frac{q}{q-1} x - \frac{x_F}{q-1} \quad (26.4-19)$$

### Tray Efficiencies

#### 1. Overall tray efficiency.

$$E_o = \frac{\text{number of ideal trays}}{\text{number of actual trays}} \quad (26.5-1)$$

2. *Murphree tray efficiency.* The Murphree tray efficiency  $E_M$  is defined as follows:

$$E_M = \frac{y_n - y_{n+1}}{y_n^* - y_{n+1}} \quad (26.5-2)$$

3. *Point efficiency.* The *point* or *local efficiency*  $E_{MP}$  on a tray is defined as

$$EMP = y_{n+1}' - y_{n+1} + y_{n+1}' - y_{n+1}^* \quad (26.5-3)$$

### Maximum Allowable Vapor Velocity

$$v_{\max} = K_v (\sigma/20)^{0.2} \rho_L - \rho_v \rho_v \quad (26.6-1)$$

### Condenser duty

*Total condenser:*

$$q_c = D(R+1)\Delta H_{\text{vap}} \quad (26.6-2)$$

*Partial condenser:*

$$q_c = D(R)\Delta H_{\text{vap}} \quad (26.6-3)$$

### Reboiler Duty

*Partial reboiler:*

$$q_R = B V_m H_{\text{vap}}' \quad (26.6-4)$$

### Multicomponent Distillation

*Fenske equation:*

$$N_m = \log[(x_{LDD}/x_{HDD})(x_{HWW}/x_{LWW})] \log(\alpha_{L,av}) \quad (26.8-12)$$

*Distribution of other components:*

$$x_{iDD}x_{iWW} = (\alpha_i, av) N_m x_{HDD} x_{HWW} \quad (26.8-14)$$

*Underwood equations:*

$$1 - q = \sum \alpha_i x_i F \alpha_i^{-\theta} \quad (26.8-19)$$

$$R_{m+1} = \sum \alpha_i x_i D \alpha_i^{-\theta} \quad (26.8-20)$$

where  $R_{actual} = 1.5 R_m$

Actual stages are found using Fig. 26.8-3 and the feed-plate location is found from the following equation.

*Estimate of feed-plate location/  
Kirkbride (K1) equation:*

$$\log N_e N_s = 0.206 \log[(x_H F x_L F) W D (x_L W x_H D)^2] \\ (26.8-21)$$

## Problems

### 26.1-1. *Phase Rule for a Vapor*

**System.** For the system  $\text{NH}_3$ –water and only a vapor phase present, calculate the number of degrees of freedom. What variables can be fixed?

**Ans.**  $F = 3$  degrees of freedom;  
variables  $T$ ,  $P$ ,  $y_A$

### 26.1-2. *Boiling Point and Raoult's*

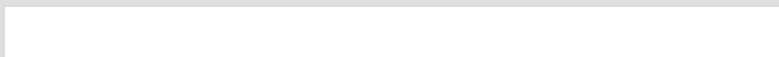
**Law.** For a benzene–toluene system, do as follows, using the data from Table 26.1-1:

- At 378.2 K, calculate  $y_A$  and  $x_A$  using Raoult's law.
- If a mixture has a composition of  $x_A = 0.40$  and is

at 358.2 K and 101.32 kPa pressure, will it boil? If not, at what temperature will it boil and what will be the composition of the vapor that comes off first?

### **26.1-3. *Boiling-Point-Diagram***

**Calculation.** The vapor-pressure data are given below for a hexane–octane system:



- Using Raoult's law, calculate and plot the  $x$ - $y$  data at a total pressure of 101.32 kPa.
- Plot the boiling-point diagram.

**26.2-1. *Single-Stage Contact of a Vapor–Liquid System.*** A mixture of 100 mol containing 60 mol %  $n$ -pentane and 40 mol %  $n$ -heptane is vaporized at 101.32 kPa abs pressure until 40 mol of vapor and 60 mol of liquid in equilibrium with each other are produced. This occurs in a single-stage



system and the vapor and liquid are kept in contact with each other until vaporization is complete. The equilibrium data are given in Example 26.3-2. Calculate the composition of the vapor and the liquid.

**26.3-1. *Relative Volatility of a Binary System.*** Using the equilibrium data for the *n*-pentane–*n*-heptane system given in Example 26.3-2, calculate the relative volatility for each concentration and plot  $\alpha$  versus the liquid composition  $x_A$ .

**26.3-2. *Comparison of Differential and Flash Distillation.*** A mixture of 100 kg mol that contains 60 mol % *n*-pentane (A) and 40 mol % *n*-heptane (B) is vaporized at 101.32 kPa pressure under differential conditions until 40 kg mol are distilled. Use equilibrium data from

## Example 26.3-2.

- What is the average composition of the total vapor distilled and the composition of the remaining liquid?
- If this same vaporization is done in an equilibrium or flash distillation and 40 kg mol are distilled, what is the composition of the vapor distilled and of the remaining liquid?

**Ans.** (a)  $x_2 = 0.405$ ,  $y_{av} = 0.892$ ; (b)  $x_2 = 0.430$ ,  $y_2 = 0.854$

**26.3-3. Differential Distillation of Benzene–Toluene.** A mixture containing 70 mol % benzene and 30 mol % toluene is distilled under differential conditions at 101.32 kPa (1 atm). A total of one-third of the moles in the feed is vaporized. Calculate the average composition of the distillate and the composition of the remaining liquid. Use equilibrium data from Table 26.1-1.

### **26.3-4. *Steam Distillation of***

***Ethylaniline.*** A mixture contains 100 kg of  $\text{H}_2\text{O}$  and 100 kg of ethylaniline (mol wt = 121.1 kg/kg mol), which is immiscible with water. A very slight amount of a nonvolatile impurity is dissolved in the organic. To purify the ethylaniline, it is steam-distilled by bubbling saturated steam into the mixture at a total pressure of 101.32 kPa (1 atm). Determine the boiling point of the mixture and the composition of the vapor. The vapor pressure of each of the pure compounds is as follows ( $T_1$ ):

### **26.3-5. *Steam Distillation of Benzene.***

A mixture of 50 g mol of liquid benzene and 50 g mol of water is boiling at 101.32 kPa pressure. Liquid benzene is immiscible in water. Determine the

boiling point of the mixture and the composition of the vapor. Which component will first be removed completely from the still? Vapor-pressure data for the pure components are as follows:

**26.4-1. *Distillation Using the McCabe–Thiele Method.*** A rectification column is fed 100 kg mol/h of a mixture of 50 mol % benzene and 50 mol % toluene at 101.32 kPa abs pressure. The feed is liquid at the boiling point. The distillate is to contain 90 mol % benzene and the bottoms 10 mol % benzene. The reflux ratio is 4.52:1. Calculate the kg mol/h distillate, kg mol/h bottoms, and the number of theoretical trays needed using the McCabe–Thiele method.

**Ans.**  $D = 50 \text{ kg mol/h}$ ,  $W = 50 \text{ kg mol/h}$ ,  
4.9 theoretical trays plus reboiler

**26.4-2. Rectification of a Heptane–Ethyl Benzene Mixture.** A saturated liquid feed of  $200 \text{ mol/h}$  at the boiling point containing  $42 \text{ mol } \%$  heptane and  $58\%$  ethyl benzene is to be fractionated at  $101.32 \text{ kPa abs}$  to give a distillate containing  $97 \text{ mol } \%$  heptane and a bottoms containing  $1.1 \text{ mol } \%$  heptane. The reflux ratio used is  $2.5:1$ . Calculate the  $\text{mol/h}$  distillate,  $\text{mol/h}$  bottoms, theoretical number of trays, and the feed tray number. Equilibrium data are given below at  $101.32 \text{ kPa abs}$  pressure for the mole fraction  $n$ -heptane  $H$  and  $y_H$ :

**Ans.**  $D = 85.3 \text{ mol/h}$ ,  $W = 114.7 \text{ mol/h}$ ,  
 $9.5 \text{ trays} + \text{reboiler}$ , feed on tray 6 from

**26.4-3. Graphical Solution for a Minimum Reflux Ratio and Total Reflux.** For the rectification given in Problem 26.4-1, where an equimolar liquid feed of benzene and toluene is being distilled to give a distillate of composition  $x_D = 0.90$  and a bottoms of composition  $x_W = 0.10$ , calculate the following using graphical methods:

- Minimum reflux ratio  $R_m$
- Minimum number of theoretical plates at total reflux

**Ans.** (a)  $R_m = 0.91$ ; (b) 4.0 theoretical trays plus a reboiler

**26.4-4. Minimum Number of Theoretical Plates and Minimum Reflux Ratio.** Determine the minimum

reflux ratio  $R_m$  and the minimum number of theoretical plates at total reflux for the rectification of a mixture of heptane and ethyl benzene as given in Problem 26.4-2. Do this by using the graphical methods of McCabe–Thiele.

**26.4-5. Rectification Using a Partially Vaporized Feed.** A total feed of 200 mol/h having an overall composition of 42 mol % heptane and 58 mol % ethyl benzene is to be fractionated at 101.3 kPa pressure to give a distillate containing 97 mol % heptane and a bottoms containing 1.1 mol % heptane. The feed enters the tower partially vaporized so that 40 mol % is liquid and 60 mol % is vapor. Equilibrium data are given in Problem 26.4-2. Calculate the following:

- Moles per hour distillate and bottoms.

- Minimum reflux ratio  $R_m$ .
- Minimum steps and theoretical trays at total reflux.
- Theoretical number of trays required for an operating reflux ratio of 2.5:1. Compare with the results of Problem 26.4-2, which uses a saturated liquid feed.

### **26.4-6. *Distillation Using a Vapor***

**Feed.** Repeat Problem 26.4-1 but use a feed that is saturated vapor at the dew point. Calculate the following:

- Minimum reflux ratio  $R_m$
- Minimum number of theoretical plates at total reflux
- Theoretical number of trays at an operating reflux ratio of  $1.5(R_m)$

### **26.4-7. *Enriching Tower for Benzene–***

**Toluene.** An enriching tower is fed 100 kg mol/h of a saturated vapor feed containing 40 mol % benzene (A) and 60 mol % toluene (B) at 101.32 kPa abs.



The distillate is to contain 90 mol % benzene. The reflux ratio is set at 4.0:1. Calculate the kg mol/h distillate  $D$  and bottoms  $W$ , and their compositions. Also, calculate the number of theoretical plates required.

**Ans.**  $D = 20$  kg mol/h,  $W = 80$  kg mol/h,  
 $x_W = 0.275$

**26.4-8. Stripping Tower.** A liquid mixture containing 10 mol %  $n$ -heptane and 90 mol %  $n$ -octane is fed at its boiling point to the top of a stripping tower at 101.32 kPa abs. The bottoms are to contain 98 mol %  $n$ -octane. For every 3 mol of feed, 2 mol of vapor is withdrawn as product. Calculate the composition of the vapor and the number of theoretical plates required. The equilibrium data below are given as

mole fraction *n*-heptane.

**26.4-9. Stripping Tower and Direct Steam Injection.** A liquid feed at the boiling point contains 3.3 mol % ethanol and 96.7 mol % water and enters the top tray of a stripping tower. Saturated steam is injected directly into the liquid in the bottom of the tower. The overhead vapor that is withdrawn contains 99% of the alcohol in the feed. Assume equimolar overflow for this problem. Equilibrium data for mole fraction of alcohol are as follows at 101.32 kPa abs pressure (1 atm abs):

- For an infinite number of theoretical steps, calculate the minimum moles of steam needed per mole of feed. (*Note:* Be sure to plot the *q* line.)

- Using twice the minimum moles of steam, calculate the number of theoretical steps needed, the composition of the overhead vapor, and the bottoms composition.

**Ans.** (a) 0.121 mol steam/mol feed; (b) 5.0 theoretical steps,  $x_D = 0.135$ ,  $x_W = 0.00033$

**26.5-1. Murphree Efficiency and the Actual Number of Trays.** For the distillation of heptane and ethyl benzene in Problem 26.4-2, the Murphree tray efficiency is estimated as 0.55.

Determine the actual number of trays needed by stepping off the trays using the tray efficiency of 0.55. Also, calculate the overall tray efficiency  $E_o$ .

**26.5-2. Packing and Tray Efficiencies for an Absorption Tower.** An absorber in a petroleum refinery uses a lean oil to absorb butane from a natural gas stream.

The composition of the key component butane in the gas phase is related to its composition in the liquid phase at equilibrium by  $y = mx = 0.7x$ . At the tower's bottom, where the flows are largest,  $\rho_L = 57.9 \text{ lb}_m/\text{ft}^3$  ( $927 \text{ kg}/\text{m}^3$ ). At the average tower temperature,  $\mu_L = 1.4 \text{ cp}$  and the average molecular weight of the liquid is  $M_L = 245$ . Estimate the efficiency for a valve-tray tower and the HETP for Norton Intalox 2T structured packing.

### **26.6-1. Estimation of the Tower**

**Diameter of a Sieve Tray.** A distillation sieve-tray tower is being used to distill a hydrocarbon feed. The vapor flow rate at the tower's bottom is  $21\,000 \text{ kg}/\text{hr}$  and the liquid flow rate is  $19\,500 \text{ kg}/\text{hr}$ . The density of the liquid  $\rho_L = 673 \text{ kg}/\text{m}^3$  and  $\rho_V = 3.68 \text{ kg}/\text{m}^3$ . Assume a tray

spacing of 24 in. (0.610 m). Calculate the tower diameter assuming the tower operates at 80% of flooding. Assume  $\sigma = 22.5$  dyn/cm.

**Ans.**  $K_v = 0.35$ ,  $D = 1.372$  m (4.50 ft)

**26.7-1. Use of the Enthalpy–**

**Concentration Method to Distill an**

**Ethanol–Water Solution.** A mixture of

50 wt % ethanol and 50 wt % water that

is saturated liquid at the boiling point is

to be distilled at 101.3 kPa pressure to

give a distillate containing 85 wt %

ethanol and a bottoms containing 3 wt

% ethanol. The feed rate is 453.6 kg/h

and a reflux ratio of 1.5 is to be used.

Use equilibrium and enthalpy data from

Appendix A.3. Note that the data are

given in wt fraction and kJ/kg. Use these

consistent units in plotting the enthalpy–

concentration data and equilibrium data.

Do as follows:

- Calculate the amount of distillate and bottoms.
- Calculate the number of theoretical trays needed.
- Calculate the condenser and reboiler loads.

**Ans.** (a)  $D = 260.0$  kg/h,  $W = 193.6$  kg/h

(b) 3.9 trays plus a reboiler (c)  $q_c = 698$   
 $750$  kJ/h,  $q_R = 704\ 770$  kJ/h

**26.7-2. Distillation of an Ethanol–Water Solution Using the Enthalpy–Concentration Method.** Repeat Problem 26.7-1 but use a reflux ratio of 2.0 instead of 1.5.

**Ans.** 3.6 theoretical trays plus reboiler

**26.7-3. Minimum Reflux and the Theoretical Number of Trays.** A feed of ethanol–water containing 60 wt %

ethanol is to be distilled at 101.32 kPa pressure to give a distillate containing 85 wt % ethanol and a bottoms containing 2 wt % ethanol. The feed rate is 10000 kg/h and its enthalpy is 116.3 kJ/kg (50 btu/lb<sub>m</sub>). Use consistent units of kg/h, weight fraction, and kJ/kg.

- Calculate the amount of distillate and bottoms.
- Determine the minimum reflux ratio using enthalpy–concentration data from Appendix A.3.
- Using 2.0 times the minimum reflux ratio, determine the theoretical number of trays needed.
- Calculate the condenser and reboiler heat loads.
- Determine the minimum number of theoretical plates at total reflux.

**Ans.** (b)  $R_m = 0.373$  (c) 4.4 theoretical trays plus reboiler (d)  $q_c = 3634$  kW,  $q_R = 4096$  kW (e) 2.8 theoretical trays plus reboiler

**26.7-4. Distillation of Benzene–Toluene Feed Using the Enthalpy–Concentration Method.** A liquid feed of 100 kg mol/h of benzene–toluene at the boiling point contains 55 mol % benzene and 45 mol % toluene. It is being distilled at 101.32 kPa pressure to give a distillate with  $x_D = 0.98$  and bottoms of  $x_W = 0.04$ . Using a reflux ratio of 1.3 times the minimum and the enthalpy-concentration method, do as follows:

- Determine the theoretical number of trays needed.
- Calculate the condenser and reboiler heat loads.
- Determine the minimum number of theoretical trays at total reflux.

**26.7-5. Use of an Enthalpy–Concentration Plot.** For the benzene–toluene system, do as follows:



- Plot the enthalpy–concentration data using values from Table 26.7-2. For a value of  $x = 0.60 = y$ , calculate the saturated liquid enthalpy  $h$  and the saturated vapor enthalpy  $H$ , and plot these data on the graph.
- A mixture contains 60 mol of benzene and 40 mol of toluene. This mixture is heated so that 30 mol of vapor are produced. The mixture is in equilibrium. Determine the enthalpy of this overall mixture and plot this point on the enthalpy–concentration diagram.

**26.8-1. *Flash Vaporization of a Multicomponent Feed.*** For the feed to the distillation tower of Example 26.8-1, calculate the following:

- The dew point of the feed and the composition of the liquid in equilibrium. (*Note:* The boiling point of 70°C has already been calculated.)
- The temperature and composition of both phases when 40% of the feed is vaporized in a flash distillation.

**Ans.** (a) 107°C,  $x_A = 0.114$ ,  $x_B = 0.158$ ,  $x_C = 0.281$ ,  $x_D = 0.447$ ; (b) 82°C,  $x_A = 0.260$ ,  $x_B = 0.254$ ,  $x_C = 0.262$ ,  $x_D =$

$$0.224; y_A = 0.610, y_B = 0.244, y_C = 0.107, y_D = 0.039$$

**26.8-2. Boiling Point, Dew Point, and Flash Vaporization.** The composition of a liquid feed in mole fraction is as follows: *n*-butane ( $x_A = 0.35$ ), *n*-pentane ( $x_B = 0.20$ ), *n*-hexane ( $x_C = 0.25$ ), *n*-heptane ( $x_D = 0.20$ ). At a pressure of 405.3 kPa, calculate the following;

- Boiling point and composition of the vapor in equilibrium
- Dew point and composition of the liquid in equilibrium
- Temperature and composition of both phases when 60% of the feed is vaporized in a flash distillation.

**26.8-3. Vaporization of Multicomponent Alcohol Mixture.** The vapor-pressure data are given below for the following alcohols:

The composition of a liquid alcohol mixture to be fed to a distillation tower at 101.32 kPa is as follows: methyl alcohol ( $x_A = 0.30$ ), ethyl alcohol ( $x_B = 0.20$ ) *n*-propyl alcohol ( $x_C = 0.15$ ), and *n*-butyl alcohol ( $x_D = 0.35$ ). Calculate the following, assuming that the mixture follows Raoult's law:

- Boiling point and composition of vapor in equilibrium
- Dew point and composition of liquid in equilibrium
- Temperature and composition of both phases when 40% of the feed is vaporized in a flash distillation

**Ans.** (a)  $83^\circ\text{C}$ ,  $y_A = 0.589$ ,  $y_B = 0.241$ ,  $y_C = 0.084$ ,  $y_D = 0.086$ ; (b)  $100^\circ\text{C}$ ,  $x_A = 0.088$ ,  $x_B = 0.089$ ,  $x_C = 0.136$ ,  $x_D = 0.687$

**26.8-4. Total Reflux, Minimum Reflux, and Number of Stages.** The following feed of 100 mol/h at the boiling point and 405.3 kPa pressure is fed to a fractionating tower: *n*-butane ( $x_A = 0.40$ ), *n*-pentane ( $x_B = 0.25$ ), *n*-hexane ( $x_C = 0.20$ ), and *n*-heptane ( $x_D = 0.15$ ). This feed is distilled so that 95% of the *n*-pentane is recovered in the distillate and 95% of the *n*-hexane in the bottoms. Calculate the following:

- Moles per hour and composition of distillate and bottoms.
- Top and bottom temperature of tower.
- Minimum stages for total reflux and distribution of other components (trace components) in the distillate and bottoms, that is, moles and mole fractions. [Also correct the compositions and moles in part (a) for the traces.]
- Minimum reflux ratio using the Underwood method.
- Number of theoretical stages at an operating reflux

ratio of 1.3 times the minimum using the Erbar–Maddox correlation.

- Location of the feed tray using the Kirkbride method.

**Ans.** (a)  $D = 64.75$  mol/h,  $x_{AD} = 0.6178$ ,  $x_{BD} = 0.3668$ ,  $x_{CD} = 0.0154$ ,  $x_{DD} = 0$ ;  $W = 35.25$  mol/h,  $x_{AW} = 0$ ,  $x_{BW} = 0.0355$ ,  $x_{CW} = 0.5390$ ,  $x_{DW} = 0.4255$ ; (b) top,  $66^{\circ}\text{C}$ ; bottom,  $134^{\circ}\text{C}$ ; (c)  $N_m = 7.14$  stages; trace compositions,  $x_{AW} = 1.2 \times 10^{-4}$ ,  $x_{DD} = 4.0 \times 10^{-5}$ ; (d)  $R_m = 0.504$ ; (e)  $N = 16.8$  stages; (f)  $N_e = 9.1$  stages,  $N_s = 7.7$  stages, feed 9.1 stages from top

### **26.8-5. *Shortcut Design of a***

#### ***Multicomponent Distillation Tower.*** A

feed of part liquid and part vapor ( $q = 0.30$ ) at 405.4 kPa is fed at the rate of 1000 mol/h to a distillation tower. The overall composition of the feed is  $n$ -butane ( $x_A = 0.35$ ),  $n$ -pentane ( $x_B =$

0.30), *n*-hexane ( $x_C = 0.20$ ), and *n*-heptane ( $x_D = 0.15$ ). The feed is distilled so that 97% of the *n*-pentane is recovered in the distillate and 85% of the *n*-hexane is recovered in the bottoms. Calculate the following:

- Amount and composition of products, and top and bottom tower temperatures
- Number of stages at total reflux and distribution of other components in the products
- Minimum reflux ratio, number of stages at  $1.2R_m$ , and feed-tray location

### **26.8-6. *Distillation of a***

#### ***Multicomponent Alcohol Mixture.***

A feed of 30 mol % methanol (A), 20% ethanol (B), 15% *n*-propanol (C), and 35% *n*-butanol (D) is distilled at 101.32 kPa abs pressure to give a distillate composition containing 95.0 mol % methanol and a residue composition

containing 5.0% methanol and the other components as calculated. The feed is below the boiling point, so that  $q = 1.1$ . The operating reflux ratio is 3.0. Assume that Raoult's law applies and use vapor-pressure data from Problem 26.8-3. Calculate the following:

- Composition and amounts of distillate and bottoms for a feed of 100 mol/h.
- Top and bottom temperatures and number of stages at total reflux. (Also, calculate the distribution of the other components.)
- Minimum reflux ratio, number of stages at  $R = 3.00$ , and feed-tray location.

**Ans.** (a)  $D = 27.778$  mol/h,  $x_{AD} = 0.95$ ,  $x_{BD} = 0.05$ ,  $x_{CD} = 0$ ,  $x_{DD} = 0$ ;  $W = 72.222$  mol/h,  $x_{AW} = 0.0500$ ,  $x_{BW} = 0.2577$ ,  $x_{CW} = 0.2077$ ,  $x_{DW} = 0.4846$ ; (b)  $65.5^{\circ}\text{C}$  top temperature,  $94.3^{\circ}\text{C}$  bottom,  $N_m = 9.21$  stages,  $x_{CD} = 3.04 \times 10^{-5}$ ,  $x_{DD} = 8.79 \times 10^{-7}$  (trace compositions);

(c)  $R_m = 2.20$ ,  $N = 16.2$  stages,  $N_s = 7.6$ ,  
 $N_e = 8.6$ , feed on stage 8.6 from top

### ***26.8-7. Shortcut Design Method for a Distillation of Ternary Mixture.***

A liquid feed at its bubble point is to be distilled in a tray tower to produce the distillate and bottoms as follows: Feed,  $x_{AF} = 0.047$ ,  $x_{BF} = 0.072$ ,  $x_{CF} = 0.881$ ; distillate,  $x_{AD} = 0.1260$ ,  $x_{BD} = 0.1913$ ,  $x_{CD} = 0.6827$ ; bottoms,  $x_{AW} = 0$ ,  $x_{BW} = 0.001$ ,  $x_{CW} = 0.999$ . Average  $\alpha$  values to use are  $\alpha_A = 4.19$ ,  $\alpha_B = 1.58$ ,  $\alpha_C = 1.00$ .

- For a feed rate of 100 mol/h, calculate  $D$  and  $W$ , the number of stages at total reflux, and the distribution (concentration) of A in the bottoms.
- Calculate  $R_m$  and the number of stages at  $1.25R_m$ .

## **References**

## **Notation**





# Chapter 27. Liquid–Liquid Extraction

## 27.0 Chapter Objectives

On completion of this chapter, a student should be able to:

- List some reasons to choose liquid–liquid extraction over other separation techniques like distillation
- Distinguish between the raffinate and extract layers
- Calculate the amounts and compositions in both phases of a single-stage equilibrium extraction process using the lever-arm rule
- Calculate flooding velocities for packed towers using Figure 27.3-3
- Determine the size of multicompartment extraction columns

## 27.1 Introduction to Liquid–Liquid Extraction

### 27.1A Introduction to Extraction Processes

In order to separate one or more of the components in a mixture, the mixture is brought into contact with another phase. The two-phase pair can be gas–liquid, which was discussed in Chapters 22 and 23; vapor–liquid, which was covered in Chapter 26; liquid–liquid; or fluid–solid. In this section, *liquid–liquid extraction separation processes* are considered first. Alternative terms for the same process are *liquid extraction* or *solvent extraction*.

In distillation, the liquid is partially vaporized to create another phase, which is a vapor. The separation of the components depends on the relative vapor pressures of the substances. The vapor and liquid phases are similar chemically. In liquid–liquid extraction,

the two phases are chemically quite different, which leads to a separation of the components according to physical and chemical properties.

Solvent extraction can sometimes be used as an alternative to separation by distillation or evaporation. For example, acetic acid can be removed from water by distillation or by solvent extraction using an organic solvent. The resulting organic solvent–acetic acid solution is then distilled. Choice of distillation or solvent extraction would depend on relative costs (C1). In another example, high-molecular-weight fatty acids can be separated from vegetable oils by extraction with liquid propane or by high-vacuum distillation, which is more expensive.

In the pharmaceutical industry, products such as penicillin occur in fermentation mixtures that are quite complex, and liquid extraction can be used to separate the penicillin. Many metal separations are being done commercially by extraction of aqueous solutions, such as copper–iron, uranium–vanadium, and tantalum–columbium.

### **27.1B Equilibrium Relations in Extraction**

*1. Phase rule.* Generally in a liquid–liquid system, we have three components,  $A$ ,  $B$ , and  $C$ , and two phases in equilibrium. Substituting into the phase rule, Eq. (22.1-1), the number of degrees of freedom is 3. The variables are temperature, pressure, and four concentrations. The four concentrations occur because only two of the three mass-

fraction concentrations in a phase can be specified. The third must make the total mass fractions equal to 1.0:  $x_A + x_B + x_C = 1.0$ . If pressure and temperature are set, which is the usual case, then, at equilibrium, setting one concentration in either phase fixes the system.

*2. Triangular coordinates and equilibrium data.* Equilateral triangular coordinates are often used to represent the equilibrium data for a three-component system, since there are three axes. This is shown in Fig. 27.1-1. Each of the three corners represents a pure component,  $A$ ,  $B$ , or  $C$ . The point  $M$  represents a mixture of  $A$ ,  $B$ , and  $C$ . The perpendicular distance from the point  $M$  to the base  $AB$  represents the mass fraction  $x_C$  of  $C$  in the mixture at  $M$ , the

distance to base  $CB$  represents the mass fraction  $x_A$  of  $A$ , and the distance to base  $AC$  represents the mass fraction  $x_B$  of  $B$ . Thus,

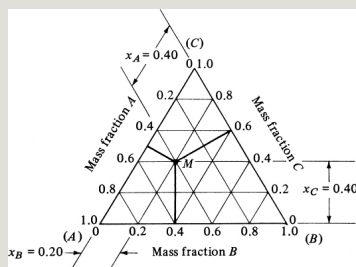


Figure 27.1-1. *Coordinates for a triangular diagram.*

$$x_A + x_B + x_C = 0.40 + 0.20 + 0.40 = 1.0 \quad (27.1-1)$$

A common phase diagram in which a pair of components  $A$  and  $B$  are partially miscible is shown in Fig. 27.1-2.

Typical examples are methyl isobutyl ketone ( $A$ )–water ( $B$ )–acetone ( $C$ ), water ( $A$ )–chloroform ( $B$ )–acetone ( $C$ ), and benzene ( $A$ )–water ( $B$ )–acetic acid ( $C$ ).

Referring to Fig. 27.1-2, liquid  $C$  dissolves completely in  $A$  or in  $B$ . Liquid  $A$  is only slightly soluble in  $B$  and  $B$  is only slightly soluble in  $A$ . The two-phase region is included inside below the curved envelope. An original mixture of composition  $M$  will separate into two phases  $a$  and  $b$  that are on the equilibrium tie line through point  $M$ . Other tie lines are also shown. The two phases are identical at point  $P$ , the *Plait point*.

*3. Equilibrium data on rectangular coordinates.* Since triangular diagrams have some disadvantages due to the special coordinates, a more useful method of plotting the three-component data is to use rectangular coordinates. This is shown in Fig. 27.1-3 for the system acetic acid ( $A$ )–water ( $B$ )–



isopropyl ether solvent (*C*). Data for this system are from Appendix A.3. The solvent pair *B* and *C* are partially miscible. The concentration of component *C* is plotted on the vertical axis and that of *A* on the horizontal axis. The concentration of component *B* is obtained by difference from Eqs. (27.1-2) or (27.1-3):

$$x_B = 1.0 - x_A - x_C \quad (27.1-2)$$

$$y_B = 1.0 - y_A - y_C \quad (27.1-3)$$

The two-phase region in Fig. 27.1-3 is inside the envelope and the one-phase region is outside. A tie line *gi* is shown connecting the water-rich layer *i*, called the *raffinate layer*, and the ether-rich solvent layer *g*, called the *extract layer*. The raffinate composition is designated

by  $x$  and the extract by  $y$ . Hence, the mass fraction of  $C$  is designated as  $y_C$  in the extract layer and as  $x_C$  in the raffinate layer. To construct the tie line  $gi$  using the equilibrium  $y_A - x_A$  plot below the phase diagram, vertical lines to  $g$  and  $i$  are drawn.

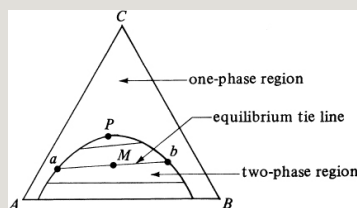


Figure 27.1-2. Liquid–liquid phase diagram where components  $A$  and  $B$  are partially miscible.

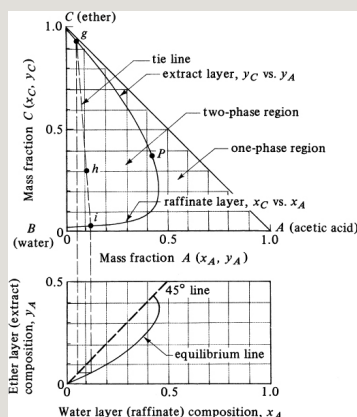


Figure 27.1-3. Acetic acid ( $A$ )–water ( $B$ )–isopropyl ether ( $C$ )

**EXAMPLE 27.1-1. Material Balance for Equilibrium Layers**

An original mixture weighing 100 kg and containing 30 kg of isopropyl ether (*C*), 10 kg of acetic acid (*A*), and 60 kg water (*B*) is equilibrated and the equilibrium phases separated. What are the compositions of the two equilibrium phases?

**Solution:** The composition of the original mixture is  $x_C = 0.30$ ,  $x_A = 0.10$ , and  $x_B = 0.60$ . This composition of  $x_C = 0.30$  and  $x_A = 0.10$  is plotted as point *h* on Fig. 27.1-3. The tie line *gi* is drawn through point *h* by trial and error. The composition of the extract (ether) layer at *g* is  $y_A = 0.04$ ,  $y_C = 0.94$ , and  $y_B = 1.00 - 0.04 - 0.94 = 0.02$  mass fraction. The raffinate (water)-layer composition at *i* is  $x_A = 0.12$ ,  $x_C = 0.02$ , and  $x_B = 1.00 - 0.12 - 0.02 = 0.86$ .

Another common type of phase diagram is shown in Fig. 27.1-4, where the solvent pairs *B* and *C* and *A* and *C* are partially miscible. Examples are the system styrene (*A*)–ethylbenzene (*B*)–diethylene glycol (*C*) and the system chlorobenzene (*A*)–methyl ethyl ketone (*B*)–water (*C*).

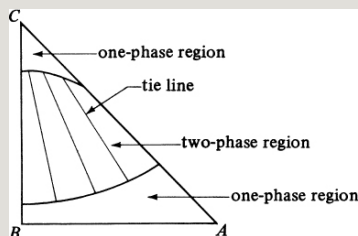


Figure 27.1-4. Phase diagram where the solvent pairs B–C and A–C are partially miscible.

## 27.2 Single-Stage Equilibrium Extraction

### 27.2A Single-Stage Equilibrium Extraction

*1. Derivation of lever-arm rule for graphical addition.* This will be derived for use with the rectangular extraction-phase-diagram charts. In Fig. 27.2-1a, two streams,  $L$  kg and  $V$  kg, containing components  $A$ ,  $B$ , and  $C$ , are mixed (added) to give a resulting mixture stream  $M$  kg total mass. Writing an overall mass balance and a balance on  $A$ ,

$$V+L=M(27.2-1)$$

$$V y_A + L x_A = M x_{AM} \quad (27.2-2)$$

where  $x_{AM}$  is the mass fraction of A in the  $M$  stream. Writing a balance for component C,

$$V y_C + L x_C = M x_{CM} \quad (27.2-3)$$

Combining Eqs. (27.2-1) and (27.2-2),

$$L V = y_A - x_{AM} x_{AM} - x_A \quad (27.2-4)$$

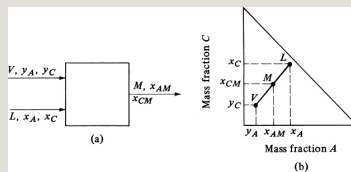


Figure 27.2-1. Graphical addition and lever-arm rule: (a) process flow, (b) graphical addition.

Combining Eqs. (27.2-1) and (27.2-3),

$$L V = y_C - x_{CM} x_{CM} - x_C \quad (27.2-5)$$

Equating Eqs. (27.2-4) and (27.2-5) and

rearranging,

$$x_C - x_{CM}x_A - x_{AM} = x_{CM} - y_Cx_{AM} - y_A \quad (27.2-6)$$

This shows that points  $L$ ,  $M$ , and  $V$  must lie on a straight line. By using the properties of similar right triangles,

$$L(\text{kg})V(\text{kg}) = VM^-LM^- \quad (27.2-7)$$

This is the lever-arm rule, which states that  $\text{kg } L / \text{kg } V$  is equal to the length of line  $VM^-$  / length of line  $LM^-$ . Also,

$$L(\text{kg})M(\text{kg}) = VMLV^- \quad (27.2-8)$$

These same equations also hold for  $\text{kg mol}$  and  $\text{mol frac}$ ,  $\text{lb}_m$ , and so on.

**EXAMPLE 27.2-1. Amounts of Phases in Solvent Extraction**

The compositions of the two equilibrium layers in Example

27.1-1 are for the extract layer ( $V$ ),  $y_A = 0.04$ ,  $y_B = 0.02$ , and  $y_C = 0.94$ , and for the raffinate layer ( $L$ ),  $x_A = 0.12$ ,  $x_B = 0.86$ , and  $x_C = 0.02$ . The original mixture contained 100 kg and  $x_{AM} = 0.10$ . Determine the amounts of  $V$  and  $L$ .

**Solution:** Substituting into Eq. (27.2-1),

$$V + L = M = 100$$

Substituting into Eq. (27.2-2), where  $M = 100$  kg and  $x_{AM} = 0.10$ ,

$$V(0.04) + L(0.12) = 100(0.10)$$

Solving the two equations simultaneously,  $L = 75.0$  and  $V = 25.0$ . Alternatively, using the lever-arm rule, the distance  $hg$  in Fig. 27.1-3 is measured as 4.2 units and  $gi$  as 5.8 units. Then, by Eq. (27.2-8),

$$LM = L100 = hgi = 4.25.8$$

Solving,  $L = 72.5$  kg and  $V = 27.5$  kg, which is in reasonably close agreement with the material-balance method.

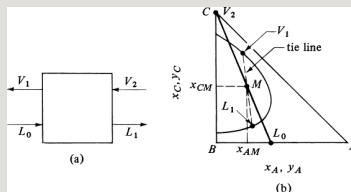


Figure 27.2-2. *Single-stage equilibrium liquid–liquid extraction: (a) process flow diagram, (b) plot on phase diagram.*

## 2. Single-stage equilibrium extraction.

We now study the separation of  $A$  from a mixture of  $A$  and  $B$  by a solvent  $C$  in a

single equilibrium stage. The process is shown in Fig. 27.2-2a, where the solvent, as stream  $V_2$ , enters together with the stream  $L_0$ . The streams are mixed and equilibrated and the exit streams  $L_1$  and  $V_1$  leave in equilibrium with each other.

The equations for this process are the same as those given in Section 22.1 for a single equilibrium stage, where  $y$  represents the composition of the  $V$  streams and  $x$  the  $L$  streams:

$$L_0 + V_2 = L_1 + V_1 = M \quad (27.2-9)$$

$$L_0 y_{A2} + V_2 y_{A2} = L_1 x_{A1} + V_1 y_{A1} = M x_{AM} \quad (27.2-10)$$

$$L_0 y_{C2} + V_2 y_{C2} = L_1 x_{C1} + V_1 y_{C1} = M x_{CM} \quad (27.2-11)$$

Since  $x_A + x_B + x_C = 1.0$ , an equation for  $B$  is not needed. To solve the three



equations, the equilibrium-phase diagram in Fig. 27.2-2b is used. Since the amounts and compositions of  $L_0$  and  $V_2$  are known, we can calculate the values of  $M$ ,  $x_{AM}$ , and  $x_{CM}$  from Eqs. (27.2-9)–(27.2-11). The points  $L_0$ ,  $V_2$ , and  $M$  can be plotted as shown in Fig. 27.2-2b. Then, using trial and error, a tie line is drawn through point  $M$ , which locates the compositions of  $L_1$  and  $V_1$ . The amounts of  $L_1$  and  $V_1$  can be determined by substitution into Eqs. (27.2-9)–(27.2-11) or by using the lever-arm rule.

## **27.3 Types of Equipment and Design for Liquid–Liquid Extraction**

### **27.3A Introduction and Equipment Types**

As in the separation processes of absorption and distillation, the two phases in liquid–liquid extraction must

be brought into intimate contact with a high degree of turbulence in order to obtain high mass-transfer rates. After this contact of the two phases, they must be separated. In both absorption and distillation, this separation is rapid and easy because of the large difference in density between the gas or vapor phase and the liquid phase. In solvent extraction, the density difference between the two phases is not large and separation is more difficult.

There are two main classes of solvent-extraction equipment: vessels in which mechanical agitation is provided for mixing, and vessels in which the mixing is done by the flow of the fluids themselves. The extraction equipment can be operated batchwise or continuously as in absorption and in

distillation.

### **27.3B Mixer–Settlers for Extraction**

To provide efficient mass transfer, a mechanical mixer is often used to provide intimate contact between the two liquid phases. One phase is usually dispersed into the other in the form of small droplets. Sufficient time of contact should be provided for the extraction to take place.

Small droplets produce large interfacial areas and faster extraction. However, the droplets must not be so small that the subsequent settling time in the settler is too large.

The design and power requirements for baffled agitators or mixers have been discussed in detail in Section 7.2. In Fig.

27.3-1a, a typical mixer–settler is shown, where the mixer or agitator is entirely separate from the settler. The feed of aqueous phase and organic phase are blended in the mixer, and then the mixed phases are separated in the settler. In Fig. 27.3-1b, a combined mixer–settler is shown, which is sometimes used in the extraction of uranium salts or copper salts from aqueous solutions. Both types of mixer–settlers can be used in series for countercurrent or multiple-stage extraction. Typical stage efficiencies for a mixer–settler are 75–100%.

### **27.3C Spray Extraction Towers**

Packed and spray-tower extractors provide differential contact, where mixing and settling proceed continuously and simultaneously

(C2). In the plate-type towers or mixer–settler contactors, the extraction and settling proceeds in discrete stages. In Fig. 27.3-2, the heavy liquid enters at the top of the spray tower, fills the tower as the continuous phase, and flows out through the bottom. The light liquid enters through a nozzle distributor at the bottom, which disperses or sprays the droplets upward. The light liquid coalesces at the top and flows out. In some cases, the heavy liquid is sprayed downward into a rising, light continuous phase.

The spray tower has a very large axial dispersion (back-mixing) in the continuous phase. Hence, only one or two stages are usually present in such a tower. Typical performance parameters

for a spray tower are given in Table 27.3-1. Despite its very low cost, this type of tower is rarely used. It can be used when a rapid, irreversible chemical reaction occurs, as in neutralization of waste acids (W1).

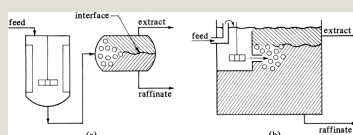


Figure 27.3-1. Typical mixer-settlers for extraction: (a) separate mixer-settler, (b) combined mixer-settler.

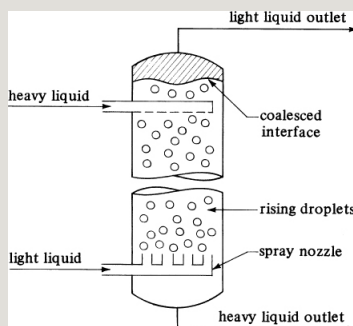


Figure 27.3-2. Spray-type extraction tower.

## 27.3D Packed Extraction Towers

A more effective type of tower is

made by packing the column with random packing such as Raschig rings, Berl saddles, Pall rings, and so on, which cause the droplets to coalesce and redisperse at frequent intervals throughout the tower. The axial mixing is reduced considerably. A packed tower is more efficient than a spray tower, but back-mixing still occurs and the HETS (height equivalent to a theoretical stage) is generally greater than for the pulsed and mechanically agitated towers discussed later in Sections 27.3F and G.

Packed towers are used where only a few stages are needed (S2) and generally with low-interfacial-tension systems of about 10 dyn/cm or so (W1). When using random packings, it is

preferable to choose a material that is preferentially wetted by the continuous phase. For example, stoneware Raschig rings or Berl saddles are used for water as the continuous phase and carbon rings or saddles for toluene as the continuous phase (T1). Packed towers more often use random packing and use structured packing less often. Some typical performance values for packed towers are given in Table 27.3-1.

The few data available for structured packing have similar HETS values as packed or sieve-tray towers but give higher capacities (H1). The structured packings used for extraction are similar to those used for distillation.

In packed absorption towers, flooding occurs when the gas velocity is



increased until the liquid cannot flow downward and is carried up by the gas out of the tower. In packed liquid-extraction towers, flooding occurs when increasing the dispersed or continuous flow rates causes both phases to leave at the outlet of the continuous phase.

A *flooding correlation* is given in Fig. 27.3-3, where  $V_C$  and  $V_D$  are superficial velocities of continuous and dispersed phases in ft/h,  $\rho_C$  and  $\rho_D$  are densities of continuous and dispersed phases in  $\text{lb}_m/\text{ft}^3$ ,  $\Delta\rho$  is  $|\rho_C - \rho_D|$ ,  $\mu_C$  is viscosity of continuous phase in  $\text{lb}_m/\text{ft} \cdot \text{h}$ ,  $a$  is specific surface area of packing in  $\text{ft}^2/\text{ft}^3$  (Table 22.3-1),  $\epsilon$  is void fraction of packed section (Table 22.3-1), and  $\sigma$  is interfacial tension between phases in  $\text{lb}_m/\text{h}^2$ . For simplicity, calculations will assume  $k_1 = 1$ . (Note:  $1.0 \text{ dyn/cm} = 28$

572 lb<sub>m</sub>/h<sub>2</sub>.) It is recommended that the design flow rates be set at 50% of flooding due to uncertainties in the correlation.

### Table 27.3-1. *Typical Performance for Several Types of Commercial Extraction Towers*

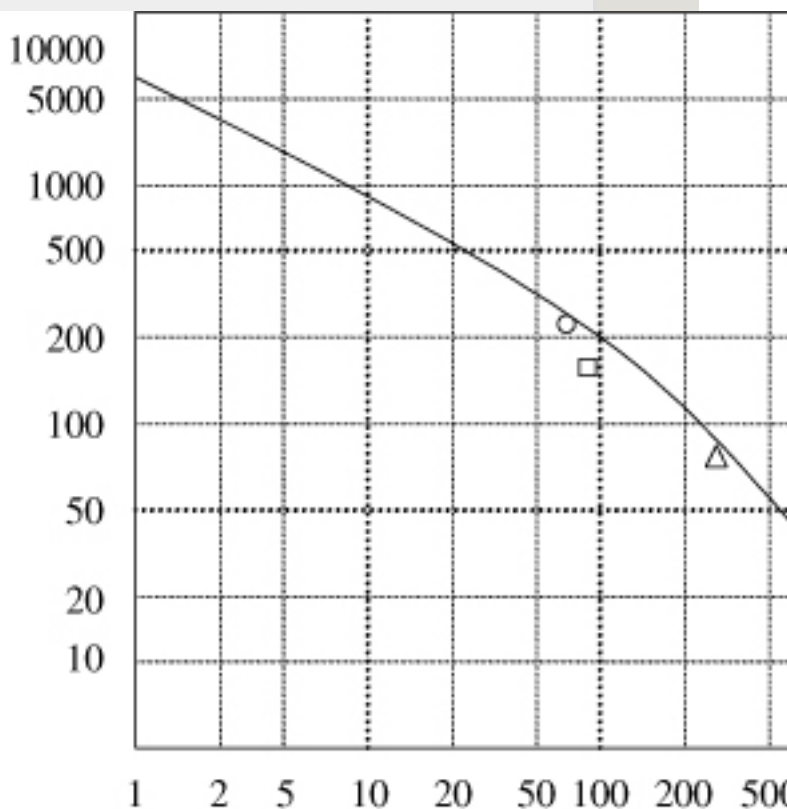
\*Throughput for diameter  $D_1 = 7.6$  cm. For larger towers of  $D_2$  diameter see Eq. (27.3-3).

#### **EXAMPLE 27.3.1. Prediction of Flooding and Packed-Tower Diameter**

Toluene as the dispersed phase is being used to extract diethylamine from a dilute water solution in a packed tower of 1-in. Pall rings at 26.7°C. The flow rate of toluene  $V = 84$  ft<sup>3</sup>/h and of water solution  $L = 56$  ft<sup>3</sup>/h. The physical properties of the dilute solutions are: for the aqueous continuous phase (C),  $\rho_C = 62.2$  lb<sub>m</sub>/ft<sup>3</sup>,  $\mu_C = 0.860$  cp =  $0.860(2.4191) = 2.080$  lb<sub>m</sub>/ft · h; for the dispersed phase,  $\rho_D = 54.0$  lb<sub>m</sub>/ft<sup>3</sup>. The interfacial tension  $\sigma = 25$  dyn/cm (T1). Do as follows:

- Predict the flooding velocity.
- Using 50% of flooding, determine the tower diameter.
- If the separation requires 5.0 theoretical stages, calculate the tower height.

$$2 \left( \frac{\mu_C}{\Delta \rho} \right) \left( \frac{a}{\varepsilon} \right)^{1.5}$$



$$\frac{(V_C^{0.5} + k_1 V_D^{0.5})^2 \rho_C}{a \mu_C}$$

Figure 27.3-3. Flooding correlation for packed extraction towers. From Claudia Irina Koncsag and Alina Barbulescu (2011). "Liquid-Liquid Extraction with and without a Chemical Reaction," Mass Transfer in Multiphase Systems and its Applications, Prof. Mohamed El-Amin (Ed.), ISBN: 978-953-307-215-9, InTech, available from: <http://www.intechopen.com/books/mass-transfer-in-multiphasesystems-and-its-applications/liquid-liquid-extraction-with-and-without-a-chemical-reaction>.

**Solution:** For part (a), from Table 22.3-1 for 1-in. Pall rings, the surface area  $a = 63 \text{ ft}^2/\text{ft}^3$ , assume  $k_1 = 1$ , and  $\varepsilon = 0.94$  void fraction. Also,  $\sigma = (25 \text{ dyn/cm})(28 \text{ 572 lb}_m/\text{h}^2)/(\text{dyn/cm})$

= 714 300 lbm/h<sup>2</sup>. Then, for the ordinate in Fig. 27.3-3,

$$\begin{aligned} & (\sigma C) 0.2 (\mu C \Delta p) \\ (a \varepsilon) 1.5 &= (71430062.2) 0.2 (2.08062.2 - 54.0) \\ & (630.94) 1.5 = 902.8 \end{aligned}$$

From Fig. 27.3-3, the abscissa value is 170. Hence,

$$170 = (VC0.5 + k_1 VD0.5) 2 \rho C \mu C = (VC0.5 + VD0.5) 2 (62.2) (63) (2.080)$$

Solving,  $(VC0.5 + VD0.5) = 18.92$ . Also, since  $VD/VC = V/L = 84/56 = 1.5$ , the final result gives  $VD = 108.45$  ft/h and  $VC = 72.30$  ft/h for the flooding velocity.

For part (b), using 50% of flooding,  $VD = 54.2$ ,  $VC = 36.15$  ft/h, and  $VC + VD = 90.35$  ft/h =  $90.35/3.2808 = 27.54$  m/h. This is still in the typical range given for packed towers in Table 27.3-1 of 12–30 m/h.

The tower cross-sectional area =  $L/VC = (56 \text{ ft}^3/\text{h})/(36.15 \text{ ft/h}) = 1.549 \text{ ft}^2$ . Then,  $\pi D^2/4 = 1.549$  and  $D = 1.404 \text{ ft}$  (0.428 m).

For part (c), use the average HETS for packed towers from Table 27.3-1 of  $(0.4 + 1.5)/2$ , or 0.95 m (3.117 ft). Then, the tower height is (HETS ft/stage) (number of stages) or  $3.117(5.0) = 15.58 \text{ ft}$  (4.75 m). Adding about 2 ft to the top and bottom for inlet nozzles and settling zones, the total height =  $15.58 + 2 + 2 = 19.58 \text{ ft}$  (5.97 m).

To use Fig. 27.3-3, the value of the interfacial tension  $\sigma$  is needed. This is a very important variable for extraction and can vary from about 5 to 50 dyn/cm. The interfacial tension between immiscible phases that must be settled must be sufficiently high for rapid

coalescence. Also, high values of  $\sigma$  mean that often extra energy or agitation must be used in the tower for dispersion of one phase in the other. However, too low a value may result in too-slow coalescence or stable emulsions.

To estimate the *interfacial tension* of a two-phase system when experimental data are not available, Eq. (27.3-1) can be used for type-one ternary systems, with an average deviation of about  $\pm 15\%$  (T1):

$$\sigma = -7.34 \ln [x_{AB} + x_{BA} + (x_{CA} + x_{CB})/2] - 4.90 \quad (27.3-1)$$

where  $\sigma$  is the interfacial tension in dyn/cm,  $x_{AB}$  is the mole fraction of solvent *A* in the saturated solvent-rich *B* layer,  $x_{BA}$  is the mole fraction of *B* in the saturated

solvent-rich A layer,  $x_{CA}$  is the mole fraction of the distributed solute C in A, and  $x_{CB}$  is the mole fraction of solute C in B. This equation holds only for a range of values for  $[x_{AB} + x_{BA} + (x_{CA} + x_{CB})/2]$  between 0.0004 and 0.30. A value of 1.0 indicates complete solution of the phases at the plait point. The range of  $\sigma$  values is 4–52.5 dyn/cm.

**EXAMPLE 27.3-2. Estimation of Interfacial Tension**

Equilibrium data for the system water (*A*)–acetic acid (*C*)–methylisobutyl ketone (MIBK) (*B*) are as follows in wt %, where the acetic acid concentration is dilute (P1):

Estimate the interfacial tension for the data point containing some acetic acid.

**Solution:** The molecular weight for  $A$  is 18.02, for  $B$  is 100.16, and for  $C$  is 60.05. Converting 1.7 wt % ( $B$ ) to mole fraction  $x_{BA}$  in the ( $A$ )-rich layer,

$$XBA=1.7/100.1695.46/18.02+2.85/60.05+1.7/100.16=0.003163$$

Also, 2.85 wt % (C) in the (A)-rich layer becomes  $x_{CA} = 0.00885$ . Similarly, 2.80 wt % (C) becomes  $x_{AB} = 0.1365$ , and 1.87 wt % (C) becomes  $x_{CB} = 0.02736$ .

Substituting into Eq. (27.3-1),

$$\sigma = -7.34 \ln[0.1365 + 0.003163 + (0.00885 + 0.02736)/2] - 4.90 = 8.65$$

dyn/cm

For the binary liquid system, water (A)–MIBK (B), the calculated mole fractions are  $x_{BA} = 0.002825$  and  $x_{AB} = 0.1074$ . Then, using Eq. (27.3-1),  $\sigma = 11.49$  dyn/cm.

### 27.3E Perforated-Plate (Sieve-Tray) Extraction Towers

Perforated plates or sieve trays are also used for dispersion of liquid drops and coalescence on each tray, as shown in Fig. 27.3-4. This is similar to the sieve trays described in Fig. 22.2-1a for distillation and absorption. The downcomers carry the heavier continuous liquid phase from one tray to the next. The light dispersed phase coalesces below the tray, jets up to the tray above, and then coalesces on the tray above. Overflow weirs are not used on down-comers (S2).

The holes in the tray are 0.32–0.64 cm

in diameter, and the % of open tray area is 15–25% of the column cross-sectional area. Tray spacings of 10–25 cm are used.

The following equation can be used to estimate the fractional tray efficiency  $E_o$  in a tray tower (P1):

$$E_o = 0.352 T^{0.5} \sigma d_o^{0.35} (VD/VC)^{0.42} (27.3 - 2)$$

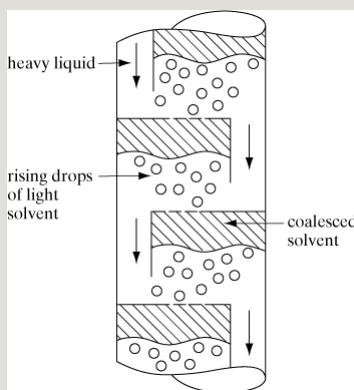


Figure 27.3-4. *Perforated-plate or sieve-tray extraction tower.*

where  $\sigma$  is interfacial tension in dyn/cm,  $T$  is tray spacing in ft,  $d_o$  is hole



diameter in ft, and  $V_D$  and  $V_C$  are superficial velocities in ft/s. For systems with high interfacial tensions, heights of transfer units are relatively high and stage efficiencies low.

Some typical operating conditions in tray towers are given in Table 27.3-1. To scale-up towers from small to larger sizes, the same sum of superficial velocities  $V_C + V_D$  should be used (S2). A throughput design value of about 50% of flooding also should be used for all types of extraction towers.

**EXAMPLE 27.3-3. Tray Efficiency for Perforated-Plate Tower**

Acetic acid is being extracted from water by the solvent methylisobutyl ketone in a perforated-plate tower at 25°C. The flow rate of the continuous aqueous phase is 120 ft<sup>3</sup>/h and that of the dispersed solvent phase is 240 ft<sup>3</sup>/h. The interfacial tension is 9.1 dyn/cm. The tray spacing is 1.0 ft and the hole size on the tray is 0.25 in. Estimate the fraction tray efficiency  $E_o$ .

**Solution:**  $V_D/V_C = 240/120$ ,  $\sigma = 9.1$  dyn/cm,  $T = 1.0$  ft, and  $d_o = 0.25/12 = 0.02083$  ft. Substituting into Eq. (27.3-2),

## 27.3F Pulsed Packed and Sieve-Tray Towers

There are many types of towers that are mechanically agitated to increase the mass-transfer efficiency and/or the throughput. An ordinary packed tower or one with special sieve plates can be pulsed by applying a rapid reciprocating motion of relatively short amplitude to the liquid contents. A reciprocating plunger pump, bellows pump, or high-pressure air pulse is externally connected to the space containing the continuous fluid so that the entire contents of the tower move up or down. Continuous inlet flows of continuous and dispersed phases enter and exit the tower.

1. *Pulsed packed towers.* Pulsing packed towers reduces the HETS considerably, by about a factor of 2 or so. Pulsing is also useful in handling liquids with high interfacial tensions, up to 30–40 dyn/cm (W1). Typical values for HETS of 0.15–0.3 m are given in Table 27.3-1. Since pulsing is uniform across the cross section, scale-up of tower size can be accomplished by using the same value of  $VD + VC$  (W1).

2. *Pulsed sieve-tray towers.* Typical amplitudes used are from 0.6 to 2.5 cm and frequencies from 100 to 250 cycles/min (P1). Typical hole size is 0.32 cm diameter, with 20–25% free space on the tray and 5.1 cm (2 in.) tray spacing. The trays occupy the entire cross section of the tower and there are no downspouts. During upward pulsing, the

light liquid is forced through the holes and droplets rise to the tray above.

During downward pulsing, the heavy liquid behaves in a similar manner.

Typical operating values are given in Table 27.3-1. Pulsing the tower markedly reduces the HETS.

### **27.3G Mechanically Agitated Extraction Towers**

There are many types of mechanically agitated towers, two of the most important of which are the Scheibel tower shown in Fig.

27.3-5a and the Karr tower shown in Fig. 27.3-5b.

*1. Scheibel tower.* In the Scheibel tower, a series of rotating turbine agitators form dispersions that coalesce in passing through the knitted mesh. The mixture then passes through the outer

settling zone. The tower thus operates as a series of mixer–settler extraction units.

The tower operates with high efficiencies, as shown in Table 27.3-1.

In scaling up from a total combined flow rate  $Q_1$  for both phases in  $\text{m}^3/\text{s}$  to  $Q_2$ , the diameter  $D_2$  is approximately related to  $D_1$  by (L1, S1)

$$D_2/D_1 = (Q_2/Q_1)^{0.4} \quad (27.3-3)$$

Also, in scaling up from diameter  $D_1$  to  $D_2$ , the HETS varies as follows:

$$(HETS)_2/(HETS)_1 = (D_2/D_1)^{0.5} \quad (27.3-4)$$

Equations for scale-up of the column internals are available (L1, S4).

*2. Karr reciprocating-plate tower.* As

shown in Fig. 27.3-5b for the Karr column, the perforated trays are moved up and down to increase agitation and to pulse the liquids. This results in a more uniform drop-size distribution because the shear forces are more uniform over the tower cross section (K1, P1).

Typical parameters are an amplitude of plate movement of 2.5 cm (1 in.), 100–150 strokes/min, and plate spacing of 5–15 cm. Trays contain holes 1.4 cm in diameter and open space of 50–60% (W1). Scale-up procedures for the Karr column are relatively accurate. In scaling up a small tower with diameter  $D_1$  to a larger size  $D_2$ , the total throughput per unit area ( $V_C + V_D$ ), plate spacing, and amplitude are kept constant. Then, the HETS in m and the strokes per minute (SPM) are scaled up

by (K1, P1)

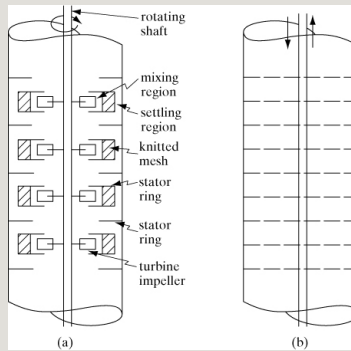


Figure 27.3-5. Mechanically agitated extraction towers: (a) Scheibel rotating-agitator tower, (b) Karr reciprocating-plate tower.

$$\frac{(HETS2)}{(HETS1)} = \left(\frac{D2}{D1}\right)^{0.38} \quad (27.3-5)$$

$$\frac{(SPM2)}{(SPM1)} = \left(\frac{D1}{D2}\right)^{0.14} \quad (27.3-6)$$

Typical performance values are given in Table 27.3-1.

## 27.4 Continuous Multistage Countercurrent Extraction

### 27.4A Introduction

In Section 27.2, single-stage equilibrium contact was used to transfer solute  $A$  from one liquid to another liquid phase. To transfer more solute, single-stage contact can be repeated by bringing the exit  $L_1$  stream into contact with fresh solvent  $V_2$ , as shown in Fig. 27.2-2. In this way, a greater percentage removal of solute  $A$  is obtained. However, this is not only wasteful of the solvent stream but also gives a dilute product of  $A$  in the outlet solvent extract streams. In order to use less solvent and to obtain a more concentrated exit extract stream, countercurrent multistage contacting is often employed.

Many of the fundamental equations for countercurrent gas absorption and



rectification are the same as or similar to those used in countercurrent extraction. Because of the frequently high solubility of the two liquid phases in each other, the equilibrium relationships in extraction are more complicated than in absorption and distillation.

#### **27.4B Continuous Multistage Countercurrent Extraction**

*1. Countercurrent process and overall balance.* The process flow for this extraction process is the same as given previously in Fig. 22.1-3 and is shown in Fig. 27.4-1. The feed stream containing the solute *A* to be extracted enters at one end of the process and the solvent stream enters at the other end. The extract and raffinate streams flow countercurrently from stage to stage, and the final products are the extract

stream  $V_1$  leaving stage 1 and the raffinate stream  $L_N$  leaving stage  $N$ .

Making an overall balance on all  $N$  stages,

$$L_0 + V_{N+1} = L_N + V_1 = M \quad (27.4-1)$$

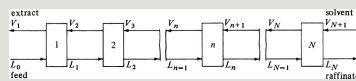


Figure 27.4-1. *Countercurrent-multistage-extraction-process flow diagram.*

where  $M$  represents total kg/h (lb<sub>m</sub>/h) and is a constant,  $L_0$  is the inlet feed flow rate in kg/h,  $V_{N+1}$  is the inlet solvent flow rate in kg/h,  $V_1$  is the exit extract stream, and  $L_N$  is the exit raffinate stream. Making an overall component balance on component C,

$$L_0 x_{C0} + V_{N+1} y_{CN+1} = L_N x_{CN} + V_1 y_{C1} = M x_{CM} \quad (27.4-2)$$

Combining Eqs. (27.4-1) and (27.4-2) and rearranging,

$$x_{CM} = L_0 x_{C0} + V_{N+1} y_{CN} + 1 L_0 + V_N + 1 = L_N x_{CN} + V_1 y_{C1} \quad L_N + V_1 \quad (27.4-3)$$

A similar balance on component A gives

$$x_{AM} = L_0 x_{A0} + V_{N+1} y_{AN} + 1 L_0 + V_N + 1 = L_N x_{AN} + V_1 y_{A1} \quad L_N + V_1 \quad (27.4-4)$$

Equations (27.4-3) and (27.4-4) can be used to calculate the coordinates of point  $M$  on the phase diagram, which ties together the two entering streams  $L_0$  and  $V_{N+1}$ , and the two exit streams  $V_1$  and  $L_N$ . Usually, the flows and compositions of  $L_0$  and  $V_{N+1}$  are known and the desired exit composition  $x_{AN}$  is set. If we plot points  $L_0$ ,  $V_{N+1}$ , and  $M$  as in Fig. 27.4-2, a straight line must connect these three points. Then,  $L_N$ ,  $M$ ,

and  $V_1$  must lie on one line. Moreover,  $L_N$  and  $V_1$  must also lie on the phase envelope, as shown. These balances also hold for  $\text{lb}_m$  and mass fraction,  $\text{kg mol}$  and mol fractions, and so on.

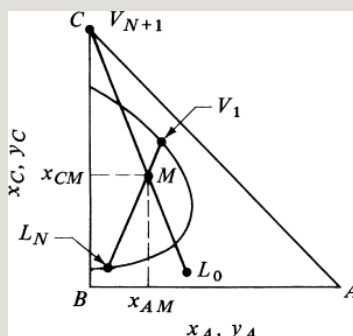


Figure 27.4-2. Use of the mixture point  $M$  for overall material balance in countercurrent solvent extraction.

#### EXAMPLE 27.4-1. Material Balance for Countercurrent Stage Process

Pure solvent isopropyl ether at the rate of  $V_{N+1} = 600 \text{ kg/h}$  is being used to extract an aqueous solution of  $L_0 = 200 \text{ kg/h}$  containing 30 wt % acetic acid ( $A$ ) by countercurrent multistage extraction. The desired exit acetic acid concentration in the aqueous phase is 4%. Calculate the compositions and amounts of the ether extract  $V_1$  and the aqueous raffinate  $L_N$ . Use equilibrium data from Appendix A.3.

**Solution:** The given values are  $V_{N+1} = 600$ ,  $y_{AN+1} = 0$ ,  $y_{CN+1} = 1.0$ ,  $L_0 = 200$ ,  $x_{A0} = 0.30$ ,  $x_{B0} = 0.70$ ,  $x_{C0} = 0$ , and  $x_{AN} = 0.04$ . In Fig. 27.4-3,  $V_{N+1}$  and  $L_0$  are plotted. Also, since  $L_N$  is on the phase boundary, it can be plotted at  $x_{AN} =$

0.04. For the mixture point  $M$ , substituting into Eqs. (27.4-3) and (27.4-4),

$$x_{CM} = L_0 x_{C0} + V_N + 1 y_{CN} + 1 L_0 + V_N + 1 = 200(0) + 600(1.0)200 + 600 = 0.75 \quad (27.4-3)$$

$$X_{AM} = L_0 x_{A0} + V_N + 1 y_{AN} + 1 L_0 + V_N + 1 = 200(0.30) + 600(0)200 + 600 = 0.075 \quad (27.4-4)$$

Using these coordinates, the point  $M$  is plotted in Fig. 27.4-3. We locate  $V_1$  by drawing a line from  $L_N$  through  $M$  and extending it until it intersects the phase boundary. This gives  $y_{A1} = 0.08$  and  $y_{C1} = 0.90$ . For  $L_N$ , a value of  $x_{CN} = 0.017$  is obtained. By substituting into Eqs. (27.4-1) and (27.4-2), and solving,  $L_N = 136 \text{ kg/h}$  and  $V_1 = 664 \text{ kg/h}$ .

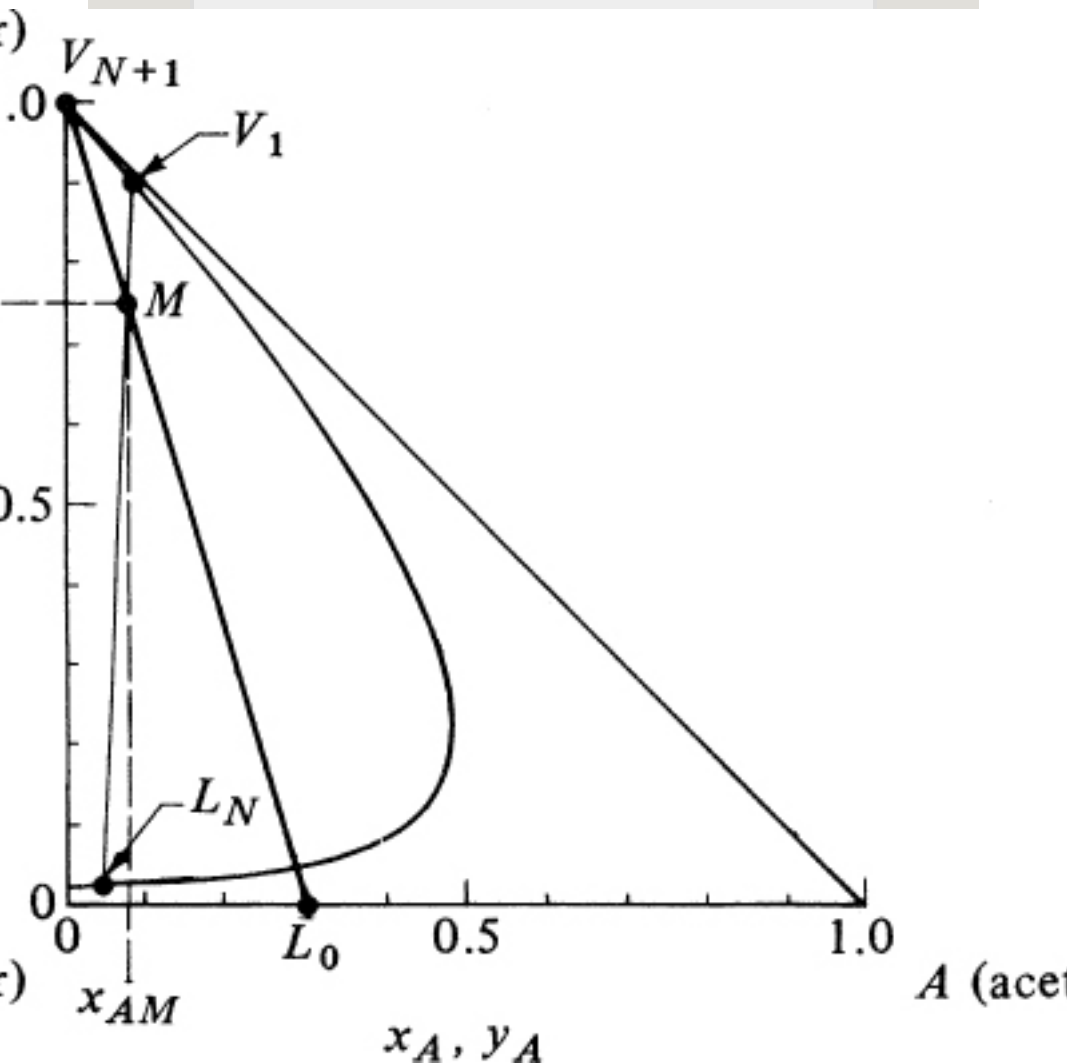


Figure 27.4-3. Method to perform overall material balance for Example 27.4-1.

2. *Stage-to-stage calculations for countercurrent extraction.* The next step after an overall balance has been made is to go stage by stage to determine the

concentrations at each stage and the total number of stages  $N$  needed to reach  $L_N$  in Fig. 27.4-1.

Making a total balance on stage 1,

$$L_0 + V_2 = L_1 + V_1 \quad (27.4-5)$$

Making a similar balance on stage  $n$ ,

$$L_{n-1} + V_{n+1} = L_n + V_n \quad (27.4-6)$$

Rearranging Eq. (27.4-5) to obtain the difference  $\Delta$  in flows,

$$L_0 - V_1 = L_1 - V_2 = \Delta \quad (27.4-7)$$

This value of  $\Delta$  in kg/h is constant, and for all stages,

$$\begin{aligned} \Delta = L_0 - V_1 = L_n - V_{n+1} = L_N - V_N \\ + 1 = \end{aligned} \quad (27.4-8)$$

This also holds for a balance on component  $A$ ,  $B$ , or  $C$ :

$$Lx_{\Delta} = L_0x_0 - V_1y_1 = L_nx_n - V_{n+1}y_{n+1} = L_Nx_N - V_{N+1}y_{N+1} \quad (27.4-9)$$

Combining Eqs. (27.4-8) and (27.4-9) and solving for  $x_{\Delta}$ ,

$$\Delta x_{\Delta} = L_0x_0 - V_1y_1 - L_0 - V_1 = L_nx_n - V_{n+1}y_{n+1} - L_n - V_{n+1} = L_Nx_N - V_{N+1}y_{N+1} - L_N - V_{N+1} \quad (27.4.10)$$

where  $x_{\Delta}$  is the  $x$  coordinate of point  $\Delta$ .

Equations (27.4-7) and (27.4-8) can be written as

$$L_0 = \Delta + V_1 \quad L_n = \Delta + V_{n+1} \quad L_N = \Delta + V_{N+1} \quad (27.4-11)$$

From Eq. (27.4-11), we see that  $L_0$  is on



a line through  $\Delta$  and  $V_1$ ,  $L_n$  is on a line through  $\Delta$  and  $V_{n+1}$ , and so on. This means  $\Delta$  is a point common to all streams passing each other, such as  $L_0$  and  $V_1$ ,  $L_n$  and  $V_{n+1}$ ,  $L_N$  and  $V_{N+1}$ , and so on. The coordinates for locating this  $\Delta$  operating point are given for  $x_{C\Delta}$  and  $x_{A\Delta}$  in Eq. (27.4-10). Since the end points  $V_{N+1}$ ,  $L_N$  or  $V_1$ , and  $L_0$  are known,  $x_\Delta$  can be calculated and point  $\Delta$  located. Alternatively, the  $\Delta$  point is located graphically in Fig. 27.4-4 as the intersection of lines  $L_0V_1$  and  $L_NV_{N+1}$ .

In order to step off the number of stages using Eq. (27.4-11), we start at  $L_0$  and draw the line  $L_0\Delta$ , which locates  $V_1$  on the phase boundary. Next, a tie line through  $V_1$  locates  $L_1$ , which is in equilibrium with  $V_1$ . Then, line  $L_1\Delta$  is drawn giving  $V_2$ . The tie line  $V_2L_2$  is

then drawn. This stepwise procedure is repeated until the desired raffinate composition  $L_N$  is reached. The number of stages  $N$  required to perform the extraction is thus obtained.

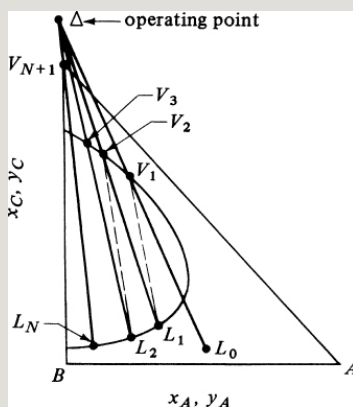


Figure 27.4-4. Operating point  $\Delta$  and the number of theoretical stages needed for countercurrent extraction.

#### **EXAMPLE 27.4-2. Number of Stages in Countercurrent Extraction**

Pure isopropyl ether of 450 kg/h is being used to extract an aqueous solution of 150 kg/h with 30 wt % acetic acid (A) by countercurrent multistage extraction. The exit acid concentration in the aqueous phase is 10 wt %. Calculate the number of stages required.

**Solution:** The known values are  $V_{N+1} = 450$ ,  $y_{AN+1} = 0$ ,  $y_{CN+1} = 1.0$ ,  $L_0 = 150$ ,  $x_{A0} = 0.30$ ,  $x_{B0} = 0.70$ ,  $x_{C0} = 0$ ,  $x_{AN} = 0.10$ . The points  $V_{N+1}$ ,  $L_0$ , and  $L_N$  are plotted in Fig. 27.4-5. For the mixture point  $M$ , substituting into Eqs. (27.4-3) and (27.4-4),  $x_{CM} = 0.75$  and  $x_{AM} = 0.075$ . The point  $M$  is

plotted and  $V_1$  is located at the intersection of line  $L_{NM}$  with the phase boundary to give  $y_{A1} = 0.072$  and  $y_{C1} = 0.895$ . (This construction is not shown. See Example 27.4-1 for construction of lines.)

The lines  $L_0V_1$  and  $L_NV_{N+1}$  are drawn and the intersection is the operating point  $\Delta$  as shown. Alternatively, the coordinates of  $\Delta$  can be calculated from Eq. (27.4-10) to locate point  $\Delta$ . Starting at  $L_0$  we draw line  $L_0\Delta$ , which locates  $V_1$ . Then, a tie line through  $V_1$  locates  $L_1$  in equilibrium with  $V_1$ . (The tie-line data are obtained from an enlarged plot such as the bottom of Fig. 27.4-3.) Line  $L_1\Delta$  is drawn next to locate  $V_2$ . A tie line through  $V_2$  gives  $L_2$ . A line  $L_2\Delta$  gives  $V_3$ . A final tie line gives  $L_3$ , which has gone beyond the desired  $L_N$ . Hence, about 2.5 theoretical stages are needed.

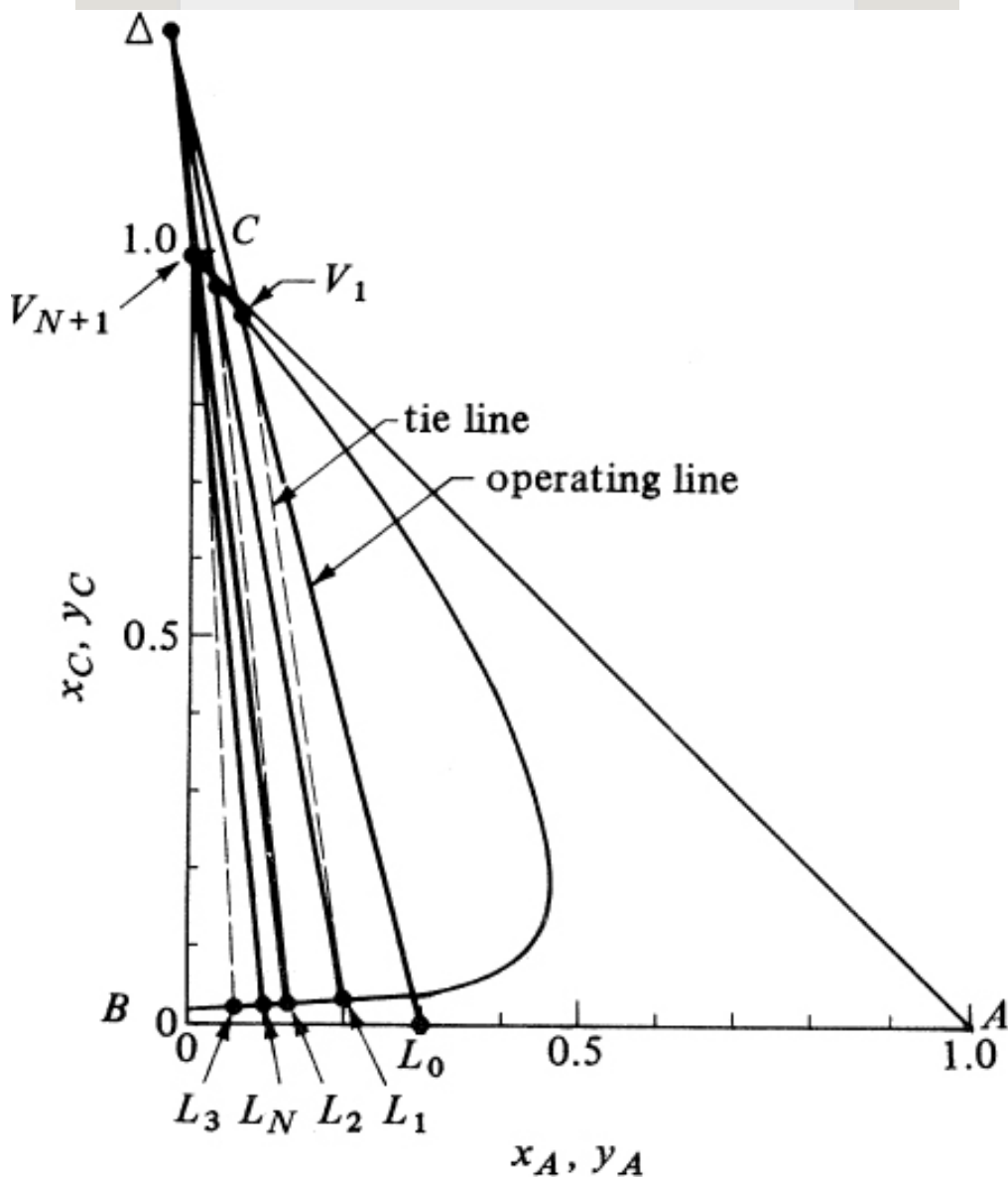


Figure 27.4-5. Graphical solution for countercurrent extraction in Example 27.4-2.

3. *Minimum solvent rate.* If a solvent rate  $V_{N+1}$  is selected at too low a value,

a limiting case will be reached with a line through  $\Delta$  and a tie line being the same. Then, an infinite number of stages will be needed to reach the desired separation. The minimum amount of solvent has been reached. For actual operation, a greater amount of solvent must be used.

The procedure for obtaining this minimum is as follows: A tie line is drawn through point  $L_0$  (Fig. 27.4-4) to intersect the extension of line  $LN V_{N+1}$ . Other tie lines to the left of this tie line are drawn, including one through  $L_N$  to intersect the line  $LN V_{N+1}$ . The intersection of a tie line on line  $LN V_{N+1}$ , which is nearest to  $V_{N+1}$ , represents the  $\Delta_{\min}$  point for minimum solvent. The actual position of  $\Delta$  used must be closer to  $V_{N+1}$  than  $\Delta_{\min}$  for a finite number of

stages. This means that more solvent must be used. Usually, the tie line through  $L_0$  represents the  $\Delta_{\min}$ .

#### **27.4C Countercurrent-Stage Extraction with Immiscible Liquids**

If the solvent stream  $V_{N+1}$  contains components  $A$  and  $C$  and the feed stream  $L_0$  contains  $A$  and  $B$ , and if components  $B$  and  $C$  are relatively immiscible in each other, the stage calculations may be made more easily. The solute  $A$  is relatively dilute and is being transferred from  $L_0$  to  $V_{N+1}$ .

Referring to Fig. 27.4-1 and making an overall balance for  $A$  over the whole system and then over the first  $n$  stages,

$$L'(x_{01}-x_0)+V'(y_{N+11}-y_{N+1})=L'(x_{N1}-x_N)+V'(y_{11}-y_1) \quad (27.4-12)$$

$$L'(x_{01}-x_0)+V'(y_{n+11}-y_{n+1})=L'x_{n1}-x_n+V'(y_{11}-y_1) \quad (27.4-13)$$

where  $L' = \text{kg inert } B/h$ ,  $V' = \text{kg inert } C/h$ ,  $y = \text{mass fraction } A \text{ in } V \text{ stream}$ , and  $x = \text{mass fraction } A \text{ in } L \text{ stream}$ . Thus, Eq. (27.4-13) is an operating-line equation whose slope  $\cong L'/V'$ . If  $y$  and  $x$  are quite dilute, the line will be straight when plotted on an  $x$ - $y$  diagram.

The number of stages are stepped off as shown previously in Fig. 22.1-5 for cases of distillation and absorption.

If the equilibrium line is relatively dilute, then, since the operating line is essentially straight, the analytical Eqs. (22.1-24)–(22.1-29) given in Section 22.1F can be used to calculate the number of stages.

**EXAMPLE 27.4-3. Extraction of Nicotine with Immiscible Liquids**

An inlet water solution of 100 kg/h containing 0.010 wt fraction nicotine (*A*) in water is stripped with a kerosene stream of 200 kg/h containing 0.0005 wt fraction nicotine in a countercurrent-stage tower. The water and kerosene are essentially immiscible in each other. It is desired to reduce the concentration of the exit water to 0.0010 wt fraction nicotine. Determine the theoretical number of stages needed. The equilibrium data are as follows (C4), with *x* the weight fraction of nicotine in the water solution and *y* in the kerosene:



- Plot the equilibrium data and graphically determine the number of theoretical steps.
- Use the Kremser equation (22.1-24) and calculate the number of theoretical steps.

**Solution:** The given values are  $L_0 = 100$  kg/h,  $x_0 = 0.010$ ,  $V_{N+1} = 200$  kg/h,  $y_{N+1} = 0.0005$ , and  $x_N = 0.0010$ . The inert streams are

$$\begin{aligned} L' &= L(1-x) = L_0(1-x_0) = 100(1-0.010) = 99.00 \text{ kg water/h} \\ V' &= V(1-y) = V_{N+1}(1-y_{N+1}) \\ &= 200(1-0.0005) = 199.9 \text{ kg kerosene/h} \end{aligned}$$

Making an overall balance on *A* using Eq. (27.4-12) and solving,  $y_1 = 0.00498$ . These points on the operating line are plotted in Fig. 27.4-6.

Since the operating-line equation is for dilute solutions, a straight line is drawn. The equilibrium data are plotted and the line is slightly curved.

For part (a), the number of stages are stepped off, giving  $N = 4.5$  theoretical stages.



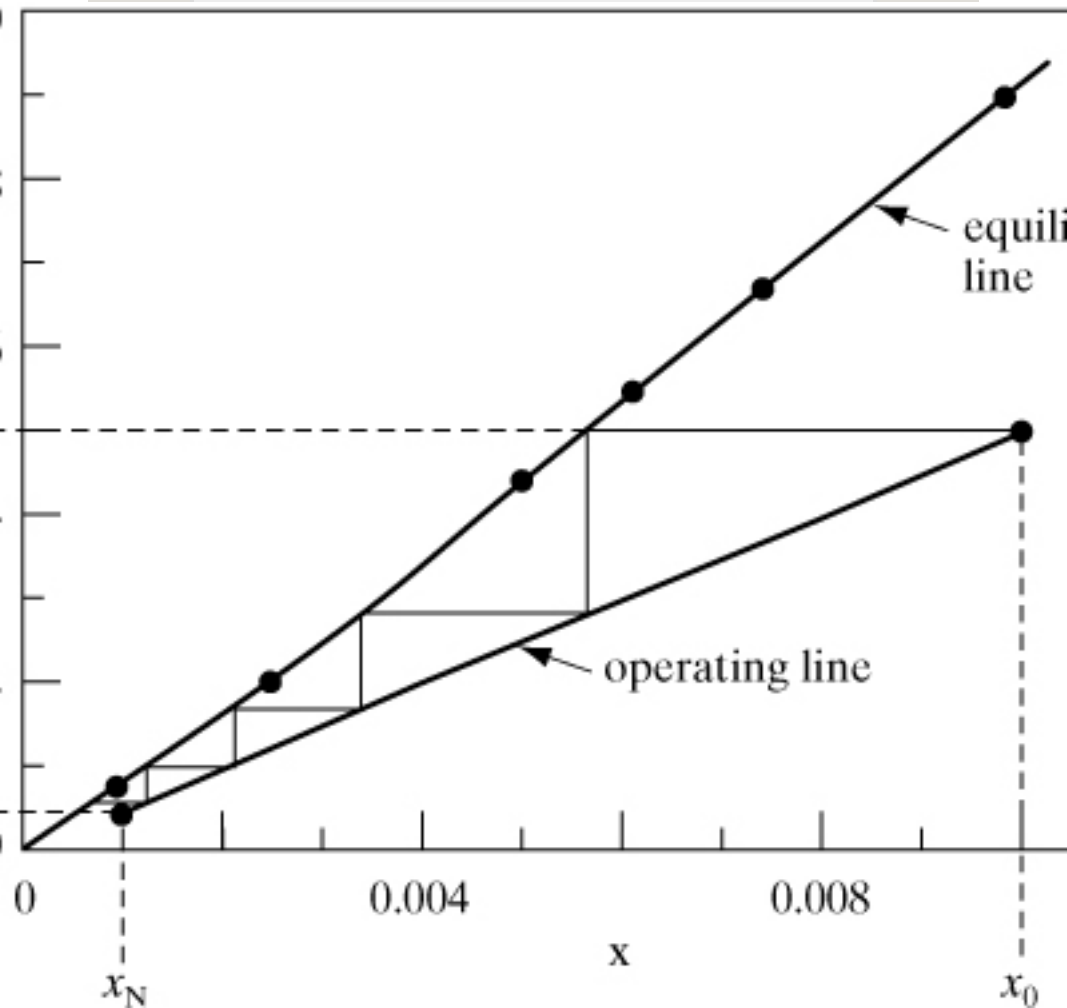


Figure 27.4-6. Solution for extraction with immiscible liquids in Example 27.4-3.

For part (b), to calculate the total flow rates  $L_N$  and  $V_1$ , the following equations can be solved:

$$\begin{aligned} L' &= 99.0 = L_N(1 - x_N) = L_N(1 - 0.0010), L_N = 99.10 \text{ kg/hV} \\ ' &= 199.9 = V_1(1 - y_1) = V_1(1 - 0.00497), V_1 = 200.9 \text{ kg/h} \end{aligned}$$

Also,  $L_0 = 100$  and  $V_{N+1} = 200 \text{ kg/h}$ . To use Eq. (22.1-24), the slope of the equilibrium curve must be calculated at the top and bottom of the tower, since the line is not straight. At the top on the equilibrium curve, at the point  $y_1 = 0.00498$ , the tangent or slope at this point is determined to be  $m_1 =$

0.91. At the bottom or dilute end, at  $x_N = 0.0010$  on the equilibrium curve, the line is straight, and  $m_2$  can be calculated from the equilibrium data as  $m_2 = 0.000806/0.001010 = 0.798$ . Then  $A_1 = L/(mV) = L_0/(m_1 V_1) = 100/(0.91 \times 200.9) = 0.547$ . Also,  $A_2 = LN/(m_2 V_{N+1}) = 99.1/(0.798 \times 200) = 0.621$ . The average value of  $A = 0.547 \times 0.621 = 0.583$ .

Substituting into Eq. (22.1-25) using  $m = m_2 = 0.798$ ,

$$N = \ln[x_0 - (y_N + 1/m)x_N - (y_N + 1/m)(1-A) + A] \ln(1/A) = \ln[0.010 - 0.0005/0.798 - 0.0005/0.798(1 - 0.583) + 0.583] / \ln(1/0.583)$$

$N = 4.45$  theoretical stages. This compares closely with the graphical-method result of 4.5 theoretical stages.

## 27.4D Design of Towers for Extraction

*1. Operating-line equation for relatively immiscible liquids.* In this case, as shown in Fig. 27.4-7a, the liquid feed stream  $L$  and the solvent stream  $V$  are relatively immiscible in each other and solute  $A$  is relatively dilute in both streams. The outlet feed stream is commonly called the raffinate and the outlet solvent stream the extract. For the countercurrent extraction of  $A$  from the feed stream  $L$  to the solvent

stream  $V$ , an overall material balance around the dashed-line box gives the following operating line equation:

$$L'(x_1 - x) + V'(y_1 - y) = L'(x_2 - x_1) + V'(y_2 - y) \quad (27.4-14)$$

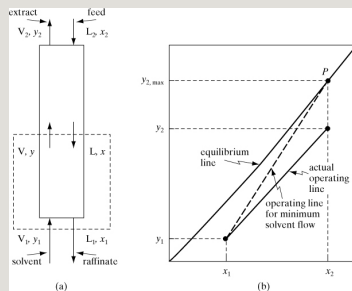


Figure 27.4-7. Extraction-tower flows: (a) process flow and material balance for a countercurrent extraction tower, (b) operating line for minimum solvent flow for a tower and the actual operating line.

where  $L' = \text{kg feed } B/\text{h}$ ,  $V' = \text{kg solvent}/\text{h}$ ,  $y = \text{mass fraction } A \text{ in solvent } V$  stream, and  $x = \text{mass fraction } A \text{ in feed } L$  stream.

This operating-line equation will be

slightly curved when plotted on an  $x$ - $y$  diagram as in Fig. 27.4-7b. Note that units of mole fraction and molar flow rates can also be used. The number of theoretical steps are stepped off as previously shown in Fig. 27.4-6. If the two liquid solvent and feed streams are immiscible in each other,  $L'$  and  $V'$  are constant.

*2. Limiting solvent flows and optimum  $L/V$  ratios.* In an extraction process, the inlet feed flow  $L_2$  and its composition  $x_2$  are usually set. The exit concentration  $x_1$  in the raffinate ( $L_1$  stream) is often set by the designer. The inlet concentration  $y_1$  of the solvent ( $V_1$  stream) is generally fixed by process requirements in regenerating the solvent for recycle back to the tower. Hence, the amount of the entering solvent flow  $V_1$  or  $V'$  is open to

choice.

In Fig. 27.4-7b, the concentrations  $x_1$ ,  $x_2$ , and  $y_1$  are set. When the operating line has a maximum slope and touches the equilibrium line at point  $P$ , then the solvent flow is at a minimum at  $V_{\min}'$ . The value of  $y_2$  is at a maximum of  $y_{2,\max}$ . As in absorption and stripping, the optimum flow rate is taken as 1.2–1.5 times  $V_{\min}'$ , with 1.5 normally used (S4). Note that if the equilibrium line is curved and highly concave upward, then, for the minimum value  $V_{\min}'$ , the operating line is tangent to the equilibrium line instead of intersecting it. The optimum is then taken as 1.2–1.5 times  $V_{\min}'$ .

*3. Analytical equations for number of trays.* The analytical equation to

calculate the number of theoretical trays  $N$  for extraction is the same as Eq. (22.5-5) for stripping in gas–liquid separations and is given as

$$N = \ln \left| \frac{(x_2 - y_1/m)(x_1 - y_1/m)(1 - A) + A}{\ln(1/A)} \right| \quad (27.4-15)$$

where  $A = L/mV$ . The value of  $A$  may vary in the tower if the operating and equilibrium lines are curved somewhat. Referring to Fig. 27.4-7b, at the concentrated top of the tower, the slope  $m_2$  or tangent at point  $y_2$  on the equilibrium line is used. At the bottom or dilute end, the slope  $m_1$  at point  $x_1$  on the equilibrium line is used. Then,  $A_1 = L_1/m_1V_1$ ,  $A_2 = L_2/m_2V_2$ , and  $A = A_1A_2$ . Also, the dilute  $m_1$  is used in Eq. (27.4-15). A useful equation is Eq. (27.4-16), which allows one to calculate

the performance of an existing tower when the number of theoretical steps  $N$  are known:

$$\frac{x_2 - x_1}{x_2 - y_1/m} = \left(\frac{1}{A}\right)^{N+1} - \left(\frac{1}{A}\right) \left(\frac{1}{A}\right)^{N+1-1} \quad (27.4-16)$$

#### **27.4E Design of Packed Towers for Extraction Using Mass-Transfer Coefficients**

The use of mass-transfer coefficients in extraction is similar to their use for stripping in absorption. The equations for dilute solutions and essentially immiscible solvents using overall coefficients are essentially identical to those for stripping with dilute solutions as given previously in Section 22.5C as Eqs. (22.5-43) and (22.5-44). For extraction,

$$z = \frac{H}{L} \ln \frac{N}{O} = \frac{H}{L} \int_{x_1}^{x_2} \frac{dx}{x - x^*} \quad (27.4-17)$$

$$HOL=LKx'aS(27.4-18)$$

If both the operating and equilibrium lines are straight and dilute, the integral in Eq. (27.4-17) can be integrated to give

$$NOL=(x_1-x_2)(x^*-x)M(27.4-19)$$

where

$$(x^*-x)M=(x_1^*-x_1)-(x_2^*-x_2)\ln[(x_1^*-x_1)/(x_2^*-x_2)](27.4-20)$$

In terms of the  $V$  phase,

$$NOV=(y_1-y_2)(y-y^*)M(27.4-21)$$

where  $(y - y^*)M$  is defined in Eq. (22.5-25). The value of the overall number of transfer units  $NOL$  can also be determined using Eq. (22.5-50) as



$$NOL = \frac{1}{A} \ln \left[ \frac{(1-A)(x_2 - y_1/m)}{(1-A)(x_1 - y_1/m) + A} \right] \quad (27.4-22)$$

**EXAMPLE 27.4-4. Extraction of Acetone from Water with Trichloroethane in a Tower**

An inlet water solution of 800 kg/h containing 12.0 wt % acetone is extracted with the solvent trichloroethane containing 0.5 wt % acetone in a countercurrent tray tower at 25°C. The solvents water and trichloroethane are essentially immiscible in each other up to a concentration of acetone in water of 27 wt %. The exit concentration in the water (raffinate) stream is set at 1.0 wt % acetone. The equilibrium data are as follows (T2), where  $x$  is the weight fraction of acetone in the water solution and  $y$  in the trichloroethane solution:

--	--

- Determine the minimum solvent rate needed.
- Using 1.3 times the minimum rate, graphically determine the number of theoretical steps needed.
- Calculate the number of steps using the analytical equation.
- Using a packed tower, the height of a transfer unit  $H_{OL}$  is estimated to be 1.2 m. Calculate the number of transfer units  $N_{OL}$  and the tower height.

**Solution:** For part (a), the given values are  $L_2 = 800$  kg/h,  $x_2 = 0.12$ ,  $x_1 = 0.01$ ,  $y_1 = 0.005$ . The inlet stream is

$$L' = L_2(1 - x_2) = 800(1 - 0.12) = 704.0 \text{ kg water/h}$$

The equilibrium data are plotted in Fig. 27.4-8, and the line is curved somewhat. The operating line for minimum solvent flow is plotted from point  $x_1, y_1$  to point  $P$ , where  $x_2 = 0.12$  on the equilibrium line and  $y_{2,\max} = 0.184$ .

Rewriting Eq. (27.4-14) for an overall balance, and substituting the known values,

$$L'(x_2 - x_1) + V'(y_1 - y_2) = L'(x_1 - x_2) + V'(y_2 - y_1) \\ 704(0.121 - 0.0051) + V(0.0051 - 0.005) = 704(0.011 - 0.01) + V(0.1841 - 0.184)$$

Solving,  $V = V_{min} = 403.2$  kg solvent/h. Setting  $x = 0.07$  in Eq. (27.4-14) and solving,  $y = 1062$ . Repeating this for several other  $x$  values, these points on the operating line are plotted in Fig. 27.4-8. This operating line for minimum solvent flow (dashed line) is slightly curved and does not intersect or become tangent to the equilibrium line at any point other than  $P$ .

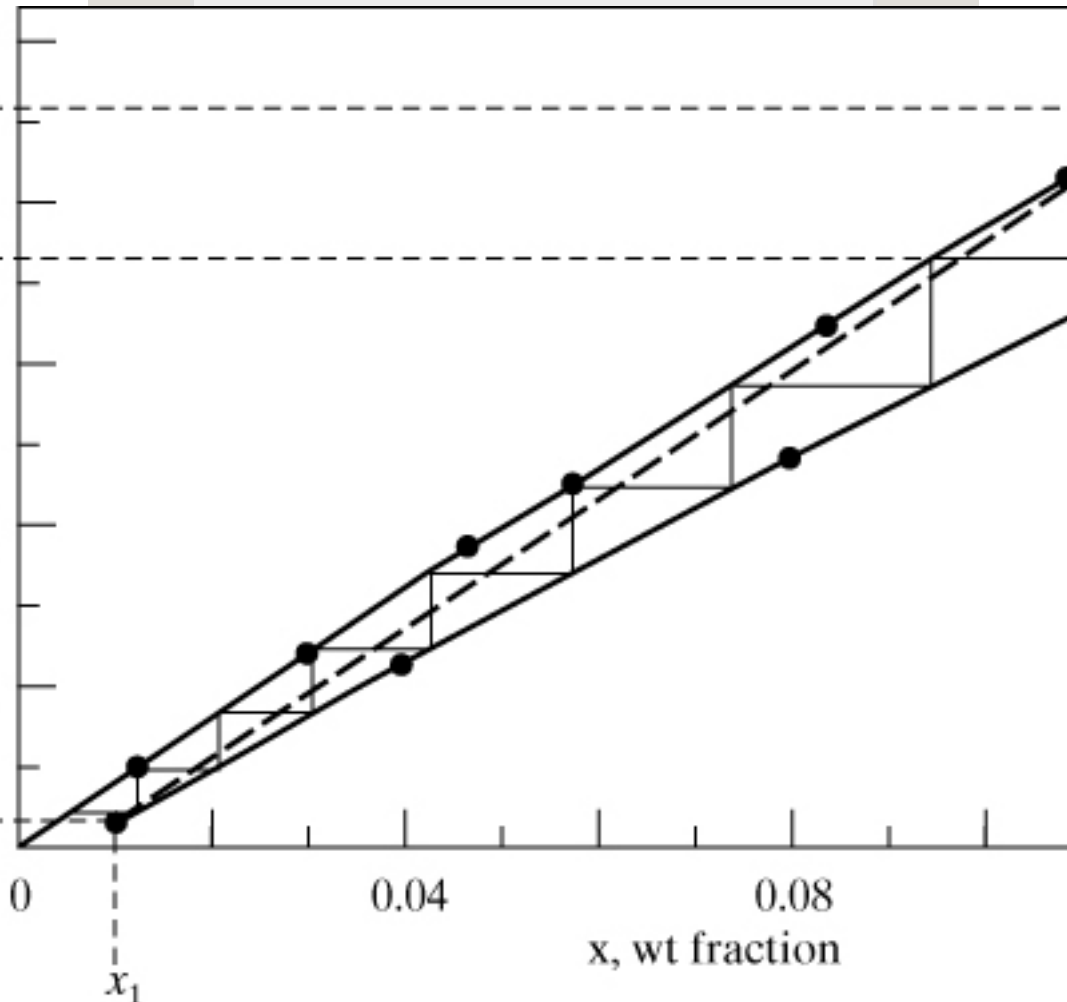


Figure 27.4-8. *Operating and equilibrium lines for Example 27.4-4.*

For part V'=1.3Vmin'=1.3(403.2)=524.2 kg solvent/h.  
Substituting into the operating-line equation (27.4-14) and solving for y<sub>2</sub>,

$$L'(x_2 - x_1) + V'(y_1 - y_2) = L'(x_1 - x_0) + V'(y_2 - y_1) \\ 704(0.121 - 0.011) + 524.2(0.0051 - 0.005) = 704(0.011 - 0.01) + 524.2(y_2 - 0.0051)$$

Then, y<sub>2</sub> = 0.1486. As before, calculating several points on the operating line, which is curved, for x = 0.04, y = 0.0453; for x = 0.08, y = 0.0977. Plotting these points shows a curved operating line. Stepping off the trays, a total of 7.4 steps are obtained.

For part (c), the total flows are first calculated as

$$L_1 = L' - x_1 = 7041 - 0.01 = 711.1, V_1 = V' - y_1 = 524.21 - 0.005 = 526.8 \\ L_2 = 800, V_2 = V' - y_2 = 524.21 - 0.1486 = 615.7$$

The value of m<sub>2</sub> is the slope or tangent at point y<sub>2</sub> on the equilibrium line, which gives m<sub>2</sub> = 1.49. The value of m<sub>1</sub> at point x<sub>1</sub> at the dilute end on the equilibrium line is, from the first set of equilibrium data points, equal to y/x = 0.0196/0.0120 = 1.633 = m<sub>1</sub>. Then,

$$A_1 = L_1 m_1 V_1 = 711.11 \cdot 1.633(526.8) = 0.827 A_2 = L_2 m_2 V_2 = 8001.49(615.7) = 0.872 A = A_1 A_2 = 0.827(0.872) = 0.849$$

Using Eq. (27.4-15),

$$N = \ln \left[ \frac{x_2 - (y_1/m)}{x_1 - (y_1/m)} \right] \frac{1}{1-A} + A \ln \left( \frac{1}{A} \right) = \ln \left[ \frac{0.12 - 0.0005/1.633}{0.01 - 0.0005/1.633} \right] \frac{1}{1-0.849} + 0.849 \ln(1/0.849)$$

Then, N = 7.46 theoretical steps. This agrees closely with the graphical value of 7.4.

For part (d), Eq. (27.4-19) will not be used, because the operating and equilibrium lines are slightly curved. Using Eq. (27.4-22),

$$NOL = \frac{1}{1-A} \ln \left[ \frac{(1-A)(x_2 - y_1/m)}{x_1 - y_1/m} \right] + A = \frac{1}{1-0.849} \ln \left[ \frac{(1-0.849)(0.12 - 0.005/1.633)}{0.01 - 0.005/1.633} \right] + 0.849$$

$$(0.12-0.005/1.633001-0.005/1.633)+0.849]$$

Solving,  $N_{OL} = 8.09$  transfer units. Then,  $z = H_{OL}N_{OL} = 1.2(8.09) = 9.71$  m.

## 27.5 Chapter Summary

### Lever-Arm Rule

$$L(\text{kg})M(\text{kg})=V_M L V^-(27.2-8)$$

These same equations also hold for kg mol and mol frac, lb<sub>m</sub>, and so on.

### Sieve-Tray Efficiency

$$E_o=0.352T^{0.5}\sigma d_o^{0.35}(V_D/VC)^{0.42}(27.3-2)$$

### Scheibel Tower Scale-Up

$$D_2 D_1=(Q_2 Q_1)^{0.4}(27.3-3)$$

Also, in scaling up from diameter  $D_1$  to  $D_2$ , the HETS varies as follows:

$$(\text{HETS})_2/(\text{HETS})_1=(D_2/$$

$$D1)0.5(27.3-4)$$

Equations for scale-up of the column internals are available (L1, S4).

### **Multistage Countercurrent Extraction**

$$x_{CM} = \frac{L_0 x_{C0} + V_{N+1} y_{CN} + 1 L_0 + V_{N+1}}{200 + 600} = \frac{200(0) + 600(1.0)}{200 + 600} = 0.75 \quad (27.4-3)$$

$$X_{AM} = \frac{L_0 x_{A0} + V_{N+1} y_{AN} + 1 L_0 + V_{N+1}}{200 + 600} = \frac{200(0.30) + 600(0)}{200 + 600} = 0.075 \quad (27.4-4)$$

### *Operating Line*

$$L'(x_1 - x) + V'(y_1 - y) = L'(x_1 - x_1) + V'(y_1 - y) \quad (27.4-14)$$

where  $L'$  = kg feed  $B$ /h,  $V'$  = kg solvent/h,  $y$  = mass fraction  $A$  in solvent  $V$  stream, and  $x$  = mass fraction  $A$  in feed  $L$  stream.

## *Analytical Equations for Number of Trays*

$$N = \frac{\ln[(x_2 - y_1/m)(x_1 - y_1/m)(1 - A) + A]}{\ln(1/A)} \quad (27.4-15)$$

where  $A = L/mV$ .

## *Height of a Packed Tower*

$$z = \text{HOL} \text{NOL} = \text{HOL} \int_{x_2}^{x_1} \frac{dx}{x - x^*} \quad (27.4-17)$$

$$\text{HOL} = L K_x' a S \quad (27.4-18)$$

$\text{NOL}$  can also be determined using Eq. (22.5-50) as

$$\text{NOL} = \frac{1}{1 - A} \ln \left[ \frac{(1 - A)(x_2 - y_1/m)}{(x_1 - y_1/m) + A} \right] \quad (27.4-22)$$

## **Problems**

**27.1-1. *Composition of Two Liquid Phases in Equilibrium.*** An original mixture weighing 200 kg and containing 50 kg of isopropyl ether, 20 kg of acetic acid, and 130 kg of water is equilibrated in a mixer–settler and the phases are separated. Determine the amounts and compositions of the raffinate and extract layers. Use equilibrium data from Appendix A.3.

**27.1-1. *Single-Stage Extraction.*** A single-stage extraction is performed in which 400 kg of a solution containing 35 wt % acetic acid in water is contacted with 400 kg of pure isopropyl ether. Calculate the amounts and compositions of the extract and raffinate layers. Solve for the amounts both algebraically and by the lever-arm rule. What percent of

the acetic acid is removed? Use equilibrium data from Appendix A.3.

**Ans.**  $L_1 = 358$  kg,  $x_{B1} = 0.715$ ,  $x_{C1} = 0.03$ ,  $V_1 = 442$  kg,  $y_{A1} = 0.11$ ,  $y_{C1} = 0.86$ , 34.7% removed.

**27.2-2. Single-Stage Extraction with Unknown Composition.** A feed mixture weighing 200 kg of unknown composition containing water, acetic acid, and isopropyl ether is contacted in a single stage with 280 kg of a mixture containing 40 wt % acetic acid, 10 wt % water, and 50 wt % isopropyl ether. The resulting raffinate layer weighs 320 kg and contains 29.5 wt % acetic acid, 66.5 wt % water, and 4.0 wt % isopropyl ether. Determine the original composition of the feed mixture and the composition of the resulting extract



layer. Use equilibrium data from Appendix A.3.

$$\text{Ans. } x_{A0} = 0.032, x_{B0} = 0.948, y_{A1} = 0.15$$

**27.2-3. Extraction of Acetone in a Single Stage.** A mixture weighing 1000 kg contains 23.5 wt % acetone and 76.5 wt % water, and is to be extracted by 500 kg methylisobutyl ketone in a single-stage extraction. Determine the amounts and compositions of the extract and raffinate phases. Use equilibrium data from Appendix A.3.

**27.3-1. Flooding Velocity and Tower Diameter.** Using the same flow rates for each stream and feed conditions as in Ex. 27.3-1, with 1-in. Pall rings, design a tower for 50% of flooding with the

aqueous phase dispersed instead of the toluene phase. Compare results.

**Ans.** Diameter = 1.274 ft

**27.3-2. Interfacial Tension in an Extraction System.** Equilibrium data for the system water (*A*)–acetic acid (*C*)–isopropyl ether (*B*) are given in Appendix A.3-24. Using the data in dilute solution, where the wt fraction of acetic acid in the water-rich phase is 0.69%, calculate the interfacial tension.

**Ans.**  $\sigma = 20.28 \text{ dyn/cm}$

**27.3-3. Perforated-Plate Tray Efficiency.** An organic solvent is extracting an acid from a water solution in a perforated plate tower. The dispersed organic solvent flow rate is 600 ft<sup>3</sup>/h and the continuous aqueous

flow rate is 400 ft<sup>3</sup>/h. The interfacial tension is 15 dyn/cm and the tray spacing is 1.1 ft. The hole size is 0.40 cm. Estimate the tray efficiency. What happens if the solvent flow rate is reduced to 400 ft<sup>3</sup>/h?

**Ans.**  $E_o = 0.133$  (solvent 600 ft<sup>3</sup>/h)

**27.4-1. Multiple-Stage Extraction with Fresh Solvent in Each Stage.** Pure water is to be used to extract acetic acid from 400 kg of a feed solution containing 25 wt % acetic acid in isopropyl ether. Use equilibrium data from Appendix A.3.

- If 400 kg of water is used, calculate the percent recovery in the water solution in a one-stage process.
- If a multiple three-stage system is used and 133.3 kg fresh water is used in each stage, calculate the overall percent recovery of the acid in the total

outlet water. (*Hint:* First, calculate the outlet extract and raffinate streams for the first stage using 400 kg of feed solution and 133 kg of water. For the second stage, 133 kg of water contacts the outlet organic phase from the first stage. For the third stage, 133.3 kg of water contacts the outlet organic phase from the second stage, and so on.)

### ***27.4-2. Overall Balance in***

***Countercurrent Stage Extraction.*** An aqueous feed of 200 kg/h containing 25 wt % acetic acid is being extracted by pure isopropyl ether at the rate of 600 kg/h in a countercurrent multistage system. The exit acid concentration in the aqueous phase is to contain 3.0 wt % acetic acid. Calculate the compositions and amounts of the exit extract and raffinate streams. Use equilibrium data from Appendix A.3.

### ***27.4-3. Minimum Solvent and***

***Countercurrent Extraction of Acetone.***

An aqueous feed solution of 1000 kg/h

containing 23.5 wt % acetone and 76.5 wt % water is being extracted in a countercurrent multistage extraction system using pure methylisobutyl ketone solvent at 298–299 K. The outlet water raffinate will contain 2.5 wt % acetone. Use equilibrium data from Appendix A.3.

- Calculate the minimum solvent that can be used. [Hint: In this case, the tie line through the feed  $L_0$  represents the condition for minimum solvent flow rate. This gives  $V_{1\min}$ . Then, draw lines  $LN_{V_{1\min}}$  and  $L_0V_{N+1}$  to give the mixture point  $M_{\min}$  and the coordinate  $x_{AM\min}$ . Using Eq. (27.4-4), solve for  $V_{N+1\min}$ , the minimum value of the solvent flow rate  $V_{N+1}$ .]
- Using a solvent flow rate of 1.5 times the minimum, calculate the number of theoretical stages.

**27.4-4. Countercurrent Extraction of Acetic Acid and Minimum Solvent.** An aqueous feed solution of 1000 kg/h of acetic acid–water solution contains 30.0

wt % acetic acid and is to be extracted in a countercurrent multistage process with pure isopropyl ether to reduce the acid concentration to 2.0 wt % acid in the final raffinate. Use equilibrium data from Appendix A.3.

- Calculate the minimum solvent flow rate that can be used. (*Hint:* See Problem 27.4-3 for the method to use.)
- If 2500 kg/h of ether solvent is used, determine the number of theoretical stages required. (*Note:* It may be necessary to replot on an expanded scale the concentrations at the dilute end.)

**Ans.** (a) Minimum solvent flow rate  $V_{N+1} = 1630$  kg/h; (b) 7.5 stages

**27.4-5. Number of Stages in Countercurrent Extraction.** Repeat Example 27.4-2 but use an exit acid concentration in the aqueous phase of 4.0 wt %.

### **27.4-6. Extraction with Immiscible**

**Solvents.** A water solution of 1000 kg/h containing 1.5 wt % nicotine in water is stripped with a kerosene stream of 2000 kg/h containing 0.05 wt % nicotine in a countercurrent stage tower. The exit water is to contain only 10% of the original nicotine, that is, 90% is removed. Use equilibrium data from Example 27.4-3. Calculate the number of theoretical stages needed.

**Ans.** 3.7 stages

### **27.4-7. Numbers of Transfer Units for**

**the Extraction of Nicotine.** Using the data from Example 27.4-3 for nicotine extraction, replot the equilibrium and operating lines. For this system using a packed tower, the height of a transfer unit has been estimated as  $H_{OL} = 1.1$  m.

Calculate the number of transfer units by two different methods and compare the values. Also, calculate the tower height.

**Ans.**  $NOL = 5.76$  transfer units (Eq. 12.7-22),  $z = 6.34$  m

**27.4-8. Minimum Solvent Rate with Immiscible Solvents.** Determine the minimum solvent kerosene rate to perform the desired extraction in Example 27.4-3. Using 1.50 times this minimum rate, determine the number of theoretical stages needed graphically as well as by using the analytical equation.

**Ans.**  $V' = 153.8$  kg/h,  $N = 6.86$   
analytically

**27.4-9. Stripping Nicotine from Kerosene.** A kerosene flow of 100 kg/h



contains 1.4 wt % nicotine and is to be stripped with pure water in a countercurrent multistage tower. It is desired to remove 90% of the nicotine. Using a water rate of 1.50 times the minimum, determine the number of theoretical stages required. (Use the equilibrium data from Example 27.4-3.)

**27.4-10. *Extraction of Acetone from Water and the Number of Transfer Units.*** Repeat Example 27.4-4 for the extraction of acetone from water using 1.5 times the minimum solvent flow rate. Do as follows:

- Graphically determine the number of theoretical steps needed.
- Calculate the number of steps using the analytical equation.
- For a packed tower with this system, the height of the transfer unit *HOL* has been estimated as 0.9 m.

Calculate the number of transfer units  $NOL$  and the tower height.

**Ans.** (b)  $N = 5.34$  steps analytically; (c)  
 $NOL = 6.21$  transfer units

**27.4-11.** Predicting Extraction for an Existing Tower with a Given Number of Steps. An existing tower contains 5.0 theoretical steps. It is desired to predict its performance under the following conditions using the system water–acetone–trichloroethane given in Example 27.4-4: An inlet water stream of 1000 kg/h containing 8.0 wt % acetone is extracted with 750 kg/h trichloroethane containing 1.0 wt % acetone in this countercurrent tower at 25°C. Determine the outlet concentration  $x_1$  in the water solution and in the trichloroethane solution using an analytical equation. Also, plot the

equilibrium and operating lines, and step off 5.0 steps. Assume dilute solutions.

**Ans.**  $x_1 = 0.01205$ ,  $y_2 = 0.0932$

### References

### Notation

# **Chapter 28. Adsorption and Ion Exchange**

## **28.0 Chapter Objectives**

On completion of this chapter, a student should be able to:

- Outline the steps that make up a typical adsorption process
- Compare three types of isotherms given in the text that are used for correlating adsorption-equilibria data
- Explain the concept of the width of the mass-transfer zone and break point
- Calculate from experimental data the total bed height needed for fixed-bed adsorption
- Recognize that the techniques used in ion exchange so closely resemble those used in adsorption that, for the majority of engineering purposes, ion exchange can be considered as a special case of adsorption

## **28.1 Introduction to Adsorption Processes**

## 28.1A Introduction

In adsorption processes, one or more components of a gas or liquid stream are adsorbed on the surface of a solid adsorbent and a separation is accomplished. In commercial processes, the adsorbent is usually in the form of small particles in a fixed bed. The fluid is passed through the bed and the solid particles adsorb components from the fluid. When the bed is almost saturated, the flow in this bed is stopped and the bed is regenerated thermally or by other methods so that desorption occurs. The adsorbed material (adsorbate) is thereby recovered and the solid adsorbent is ready for another cycle of adsorption.

Applications of liquid-phase adsorption

include removal of organic compounds from water or organic solutions, colored impurities from organics, and various fermentation products from fermentor effluents. Separations include paraffins from aromatics and fructose from glucose using zeolites.

Applications of gas-phase adsorption include the removal of water from hydrocarbon gases, sulfur compounds from natural gas, solvents from air and other gases, and odors from air.

### **28.1B Physical Properties of Adsorbents**

Many adsorbents have been developed for a wide range of separations. Typically, the adsorbents are in the form of small pellets, beads, or granules ranging from about 0.1 mm to 12 mm in size,

with the larger particles being used in packed beds. A particle of adsorbent has a very porous structure, with many fine pores and pore volumes up to 50% of total particle volume. The adsorption often occurs as a monolayer on the surface of the fine pores, although several layers sometimes occur. Physical adsorption, or van der Waals adsorption, usually occurs between the adsorbed molecules and the solid internal pore surface, and it is readily reversible.

The overall adsorption process consists of a series of steps. When the fluid is flowing past the particle in a fixed bed, the solute first diffuses from the bulk fluid to the gross exterior surface of the particle. Then, the solute diffuses inside

the pore to the surface of the pore.

Finally, the solute is adsorbed on the surface. Hence, the overall adsorption process is a series of steps.

There are a number of commercial adsorbents and some of the main examples are described below. All are characterized by very large pore surface areas of 100 to over 2000 m<sup>2</sup>/g.

1. *Activated carbon.* This is a microcrystalline material made by thermal decomposition of wood, vegetable shells, coal, and so on, and has surface areas of 300 to 1200 m<sup>2</sup>/g with average pore diameters of 10 to 60 Å. Organics are generally adsorbed by activated carbon.
2. *Silica gel.* This adsorbent is made by the acid treatment of a sodium silicate solution that is then dried. It has a surface area of 600 to 800 m<sup>2</sup>/g and average pore diameters of 20 to 50 Å. It is primarily used to dehydrate gases and liquids, and to fractionate hydrocarbons.
3. *Activated alumina.* To prepare this material, hydrated aluminum oxide is activated by heating to drive off the water. It is used mainly to dry gases and liquids. Surface areas range from 200 to 500 m<sup>2</sup>/g, with average pore



diameters of 20 to 140 Å.

4. *Molecular sieve zeolites.* These zeolites are porous crystalline aluminosilicates that form an open crystal lattice containing precisely uniform pores, which makes it different from other types of adsorbents that have a range of pore sizes. Different zeolites have pore sizes from about 3 to 10 Å. Zeolites are used for drying, separation of hydrocarbons, mixtures, and many other applications.
5. *Synthetic polymers or resins.* These are made by polymerizing two major types of monomers. Those made from aromatics such as styrene and divinylbenzene are used to adsorb nonpolar organics from aqueous solutions. Those made from acrylic esters are used with more-polar solutes in aqueous solutions.

### **28.1C Equilibrium Relations for Adsorbents**

The equilibrium between the concentration of a solute in the fluid phase and its concentration on the solid somewhat resembles the equilibrium solubility of a gas in a liquid. Data are plotted as adsorption isotherms, as shown in Fig. 28.1-1. The concentration in the solid phase is expressed as  $q$ , kg adsorbate

(solute)/kg adsorbent (solid), and in the fluid phase (gas or liquid) as  $c$ , kg adsorbate/m<sup>3</sup> fluid.

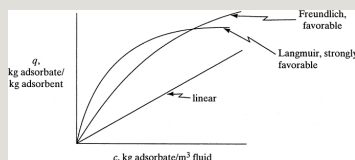


Figure 28.1-1. *Some common types of adsorption isotherms.*

Data that follow a linear law can be expressed by an equation similar to Henry's law:

$$q = Kc \quad (28.1-1)$$

where  $K$  is a constant determined experimentally, m<sup>3</sup>/kg adsorbent. This linear isotherm is not common, but in the dilute region it can be used to approximate data for many systems.

The Freundlich isotherm equation,

which is empirical, often approximates data for many physical adsorption systems and is particularly useful for liquids:

$$q = Kc^n \quad (28.1-2)$$

where  $K$  and  $n$  are constants and must be determined experimentally. If a log–log plot is made for  $q$  versus  $c$ , the slope is the dimensionless exponent  $n$ . The dimensions of  $K$  depend on the value of  $n$ . This equation is sometimes used to correlate data for hydrocarbon gases on activated carbon.

The Langmuir isotherm equation has a theoretical basis and is given by the following, where  $q_o$  and  $K$  are empirical constants:

$$q = \frac{q_o K c}{1 + K c} \quad (28.1-3)$$

where  $q_0$  is kg adsorbate/kg solid and  $K$  is kg/m<sup>3</sup>. The equation was derived assuming that there are only a fixed number of active sites available for adsorption, that only a monolayer is formed, and that the adsorption is reversible and reaches an equilibrium condition. By plotting  $1/q$  versus  $1/c$ , the slope is  $K/q_0$  and the intercept is  $1/q_0$ .

Almost all adsorption systems show that as temperature is increased, the amount adsorbed by the adsorbent decreases strongly. This is useful since adsorption is normally at room temperatures and desorption can be attained by raising the temperature.

**EXAMPLE 28.1-1. Adsorption Isotherm for Phenol in Wastewater**

Batch tests were performed in the laboratory using solutions of phenol in water and particles of granular

activated carbon (R1). The equilibrium data at room temperature are shown in Table 28.1-1. Determine the isotherm that fits the data.

**Solution:** Plotting the data as  $1/q$  versus  $1/c$ , the results are not a straight line and do not follow the Langmuir isotherm equation (28.1-3). A plot of  $\log q$  versus  $\log c$  in Fig. 28.1-2 gives a straight line and, hence, follows the Freundlich isotherm equation (28.1-2). The slope  $n$  is 0.229 and the constant  $K$  is 0.199, to give

$$q = 0.199c^{0.229}$$

Table 28.1-1. *Equilibrium Data for Example 28.1-1 (R1)*

--	--

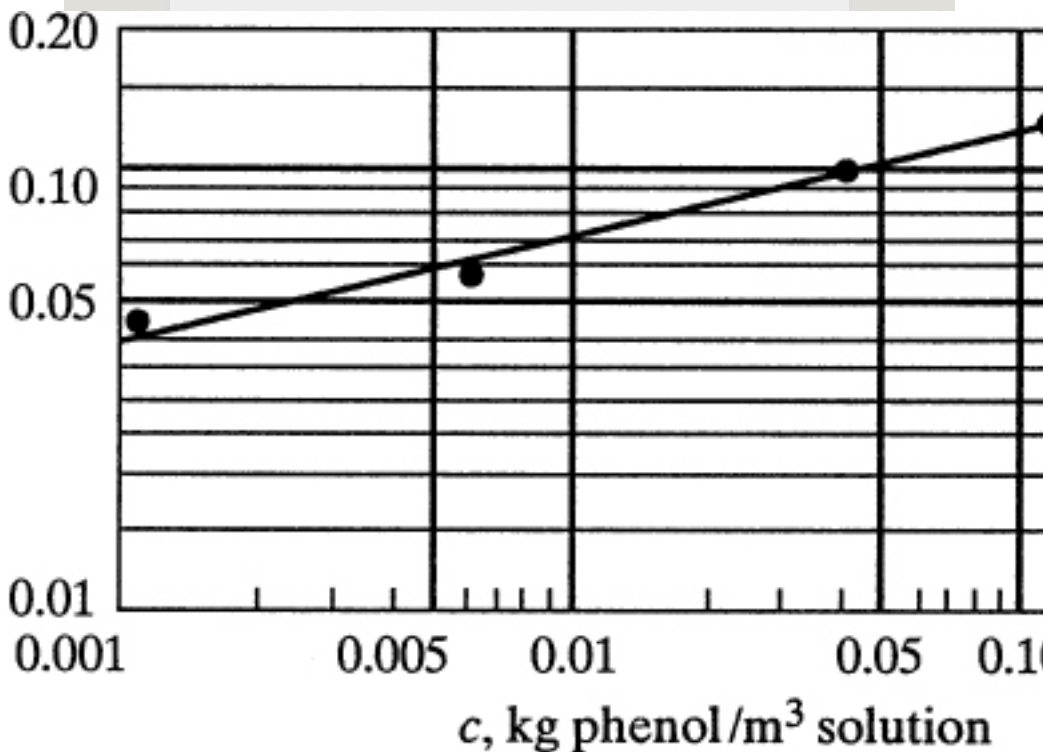


Figure 28.1-2. Plot of data for Example 28.1-1.

## 28.2 Batch Adsorption

Batch adsorption is often used to adsorb solutes from liquid solutions when the quantities treated are in small amounts, as in the pharmaceutical or other industries. As with many other processes, an equilibrium relation such as the Freundlich or Langmuir isotherm and a material balance are needed. The initial feed concentration is  $c^F$  and the final equilibrium concentration is  $c$ . Also, the initial concentration of the solute adsorbed on the solid is  $q^F$  and the final equilibrium value is  $q$ . The material balance on the adsorbate is

$$q^F M + c^F S = q M + c S \quad (28.2-1)$$

where  $M$  is the amount of adsorbent, kg;

and  $S$  is the volume of feed solution, m<sup>3</sup>.

When the variable  $q$  in Eq. (28.2-1) is plotted versus  $c$ , the result is a straight line. If the equilibrium isotherm is also plotted on the same graph, the intersection of both lines gives the final equilibrium values of  $q$  and  $c$ .

**EXAMPLE 28.2-1. Batch Adsorption on Activated Carbon**

A wastewater solution having a volume of 1.0 m<sup>3</sup> contains 0.21 kg phenol/m<sup>3</sup> of solution (0.21 g/L). A total of 1.40 kg of fresh granular activated carbon is added to the solution, which is then mixed thoroughly to reach equilibrium. Using the isotherm from Example 28.1-1, what are the final equilibrium values and what percent of phenol is extracted?

**Solution:** The given values are  $c_F = 0.21$  kg phenol/m<sup>3</sup>,  $S = 1.0$  m<sup>3</sup>,  $M = 1.40$  kg carbon, and  $q_F$  is assumed as zero. Substituting into Eq. (28.2-1),

$$0(1.40) + 0.21(1.0) = q(1.40) + c(1.0)$$

This straight-line equation is plotted in Fig. 28.2-1. The isotherm from Example 28.1-1 is also plotted in Fig. 28.2-1. At the intersection,  $q = 0.106$  kg phenol/kg carbon and  $c = 0.062$  kg phenol/m<sup>3</sup>. The percent of phenol extracted is

$$\% \text{ extracted} = c_F - c = 0.210 - 0.062 = 0.148 \quad \text{or} \quad 70.5\%$$

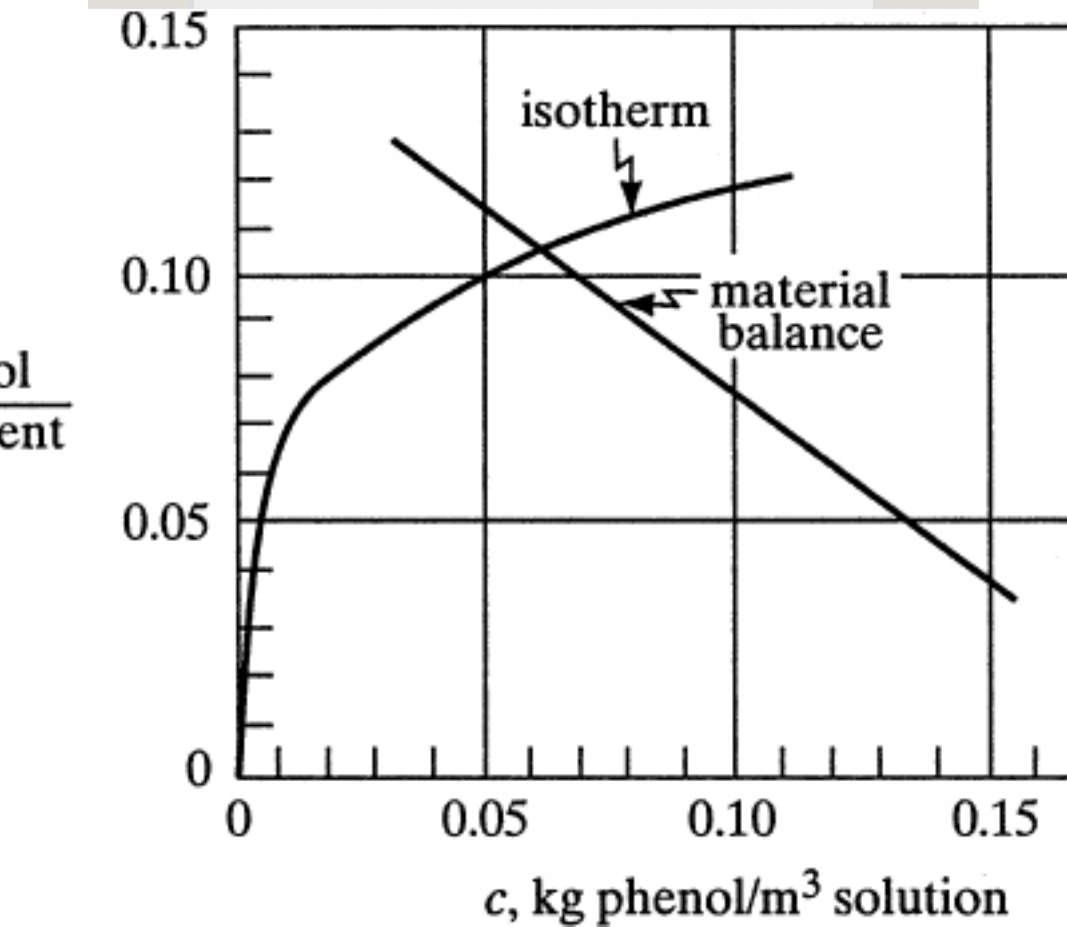


Figure 28.2-1. Solution to Example 28.2-1.

## 28.3 Design of Fixed-Bed Adsorption Columns

### 28.3A Introduction and Concentration Profiles

A widely used method for adsorption of solutes from liquid or gases employs a fixed bed of granular



particles. The fluid to be treated is usually passed down through the packed bed at a constant flow rate. The situation is more complex than that for a simple stirred-tank batch process that reaches equilibrium. Mass-transfer resistances are important in the fixed-bed process, and the process is unsteady state. The overall dynamics of the system determine the efficiency of the process, rather than just the equilibrium considerations.

The concentrations of the solute in the fluid phase and of the solid adsorbent phase change with time and with position in the fixed bed as adsorption proceeds. At the inlet to the bed, the solid is assumed to contain no solute at the start of the process. As the fluid first

comes in contact with the inlet of the bed, most of the mass transfer and adsorption takes place here. As the fluid passes through the bed, the concentration in this fluid drops very rapidly with distance in the bed and reaches zero well before the end of the bed is reached. The concentration profile at the start at time  $t_1$  is shown in Fig.

28.3-1a, where the concentration ratio  $c/c_0$  is plotted versus bed length. The fluid concentration  $c_0$  is the feed concentration and  $c$  is the fluid concentration at a point in the bed.

After a short time, the solid near the entrance to the tower is almost saturated, and most of the mass transfer and adsorption now takes place at a point slightly farther from the inlet. At a later time  $t_2$ , the profile or mass-transfer

zone where most of the concentration change takes place has moved farther down the bed. The concentration profiles shown are for the fluid phase. Concentration profiles for the concentration of adsorbates on the solid would be similar. The solid at the entrance would be nearly saturated, and this concentration would remain almost constant down to the mass-transfer zone, where it would drop off rapidly to almost zero. The dashed line for time  $t_3$  shows the concentration in the fluid phase in equilibrium with the solid. The difference in concentrations is the driving force for mass transfer.

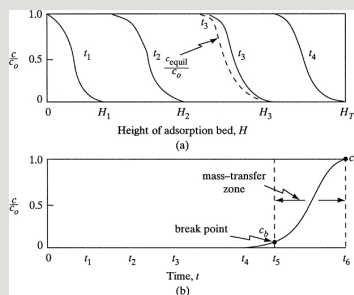


Figure 28.3-1. *Concentration profiles for adsorption in a fixed bed: (a) profiles at various positions and times in the bed, (b) breakthrough concentration profile in the fluid at the outlet of the bed.*

### **28.3B Breakthrough Concentration Curve**

As seen in Fig. 28.3-1a, the major part of the adsorption at any time takes place in a relatively narrow adsorption or *mass-transfer zone*. As the solution continues to flow, this mass-transfer zone, which is S-shaped, moves down the column. At a given time  $t_3$  in Fig. 28.3-1a, when almost half of the bed is saturated with solute, the outlet concentration is still approximately zero, as shown in Fig. 28.3-1b. This outlet concentration remains near zero until the mass-transfer zone starts to reach the tower outlet at time  $t_4$ . Then, the outlet concentration starts to rise and

at  $t_5$  the outlet concentration has risen to  $c_b$ , which is called the *break point*.

After the break-point time is reached, the concentration  $c$  rises very rapidly up to point  $c_d$ , which is the end of the breakthrough curve, where the bed is judged ineffective. The break-point concentration represents the maximum that can be discarded and is often taken as 0.01 to 0.05 for  $c_b/c_o$ . The value  $c_d/c_o$  is taken as the point where  $c_d$  is approximately equal to  $c_o$ .

For a narrow mass-transfer zone, the breakthrough curve is very steep and most of the bed capacity is used at the break point. This makes efficient use of the adsorbent and lowers energy costs for regeneration.

If the mass-transfer rate were infinitely fast and if no axial dispersion were present, the mass-transfer-zone width would be zero and the breakthrough curve would be a vertical line from  $c/c_o = 0$  to  $c/c_o = 1.0$ .

### **28.3C Mass-Transfer Zone**

As shown in Fig. 28.3-1a, on entering the bed, the concentration profile in the fluid starts to develop. For systems with a favorable isotherm, similar to the Freundlich and Langmuir isotherms (Fig. 28.1-1), which are concave downward (L1), the concentration profile in the mass-transfer zone soon acquires the typical S shape of the mass-transfer zone. Then, the mass-transfer zone is constant in height as it moves through the

column.

This constant height of the mass-transfer zone can then be used in scale-up when the height of the overall bed is large relative to the mass-transfer zone ( $L_1$ ,  $T_1$ ). Many industrial applications fall within these restrictions, which are applicable to adsorption from gases and liquids. Note that if the isotherm is linear or an unfavorable isotherm, the mass-transfer-zone width increases with bed length. A favorable isotherm for adsorption is unfavorable for effective regeneration (P1).

### **28.3D Capacity of Column and Scale-Up Design Method**

The mass-transfer-zone width and shape depend on the adsorption isotherm, flow rate, mass-transfer rate to the particles, and diffusion in

the pores. A number of theoretical methods have been published that predict the mass-transfer zone and concentration profiles in the bed.

The predicted results may be inaccurate because of many uncertainties due to flow patterns and correlations for predicting diffusion and mass transfer. Hence, experiments in laboratory scale are needed in order to scale up the results.

The total or stoichiometric capacity of the packed-bed tower, if the entire bed comes to equilibrium with the feed, can be shown to be proportional to the area between the curve and a line at  $c/c_o = 1.0$ , as shown in Fig. 28.3-2. The total shaded area represents the total or stoichiometric capacity of the bed as



follows (R2):

$$t_t = \int_0^\infty (1 - c/c_0) dt \quad (28.3-1)$$

where  $t_t$  is the time equivalent to the total or stoichiometric capacity. The usable capacity of the bed up to the break-point time  $t_b$  is the crosshatched area:

$$t_u = \int_0^{t_b} (1 - c/c_0) dt \quad (28.3-2)$$

where  $t_u$  is the time equivalent to the usable capacity or the time at which the effluent concentration reaches its maximum permissible level. The value of  $t_u$  is usually very close to that of  $t_b$ . Numerical integration of Eqs. (28.3-1) and (28.3-2) can be done using a spreadsheet.

The ratio  $t_u/t_t$  is the fraction of the total

bed capacity or length utilized up to the break point ( $C1, L1, M1$ ). Hence, for a total bed length of  $H_T$  m,  $H_B$  is the length of bed used up to the break point.

$$H_B = t_{utt} H_T \quad (28.3-3)$$

The length of unused bed  $H_{UNB}$  in m is then the unused fraction times the total length:

$$H_{UNB} = (1 - t_{utt}) H_T \quad (28.3-4)$$

The  $H_{UNB}$  represents the mass-transfer section or zone. It depends on the fluid velocity and is essentially independent of the total length of the column. The value of  $H_{UNB}$  may, therefore, be measured at the design velocity in a small-diameter laboratory column packed with the desired adsorbent. Then, the full-scale adsorber bed can be

designed simply by first calculating the length of bed needed to achieve the required usable capacity,  $HB$ , at the break point. The value of  $HB$  is directly proportional to  $t_b$ . Then, the length  $H_{UNB}$  of the mass-transfer section is simply added to the length  $HB$  needed to obtain the total length,  $HT$ :

$$HT = H_{UNB} + HB \quad (28.3-5)$$

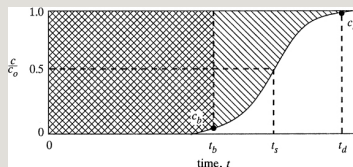


Figure 28.3-2. *Determination of column capacity from breakthrough curve.*

This design procedure is widely used; its validity depends on the conditions in the laboratory column being similar to those for the full-scale unit. The small-diameter unit must be well insulated to

be similar to the large-diameter tower, which operates adiabatically. The mass velocity in both units must be the same and the bed must be of sufficient length to contain a steady-state mass-transfer zone ( $L_1$ ). Axial dispersion or axial mixing may not be exactly the same in both towers, but if caution is exercised, this is a useful design method.

An approximate alternative procedure to use instead of integrating and obtaining areas is to assume that the breakthrough curve in Fig. 28.3-2 is symmetrical at  $c/c_o = 0.5$  and  $t_s$ . Then, the value of  $t_t$  in Eq. (28.3-1) is simply  $t_s$ . This assumes that the area below the curve between  $t_b$  and  $t_s$  is equal to the area above the curve between  $t_s$  and  $t_d$ .

A waste stream of alcohol vapor in air from a process was adsorbed by activated carbon particles in a packed bed having a diameter of 4 cm and length of 14 cm containing 79.2 g of carbon. The inlet gas stream having a concentration  $c_0$  of 600 ppm and a density of 0.00115 g/cm<sup>3</sup> entered the bed at a flow rate of 754 cm<sup>3</sup>/s. Data in Table 28.3-1 give the concentrations of the breakthrough curve. The break-point concentration is set at  $c/c_0 = 0.01$ . Do as follows:

- Determine the break-point time, the fraction of total capacity used up to the break point, and the length of the unused bed. Also, determine the saturation loading capacity of the carbon.
- If the break-point time required for a new column is 6.0 h, what is the new total length of the column required?

**Solution:** The data from Table 28.3-1 are plotted in Fig. 28.3-3. For part (a), for  $c/c_0 = 0.01$ , the break-point time is  $t_b = 3.65$  h from the graph. The value of  $t_d$  is approximately 6.95 h. Numerically or graphically integrating, the areas are  $A_1 = 3.65$  h and  $A_2 = 1.51$  h. Then, from Eq. (28.3-1), the time equivalent to the total or stoichiometric capacity of the bed is

$$t_t = \int_0^\infty (1 - c/c_0) dt = A_1 + A_2 = 3.65 + 1.51 = 5.16 \text{ h.}$$

Table 28.3-1. *Breakthrough Concentration for Example 28.3-1*

--	--

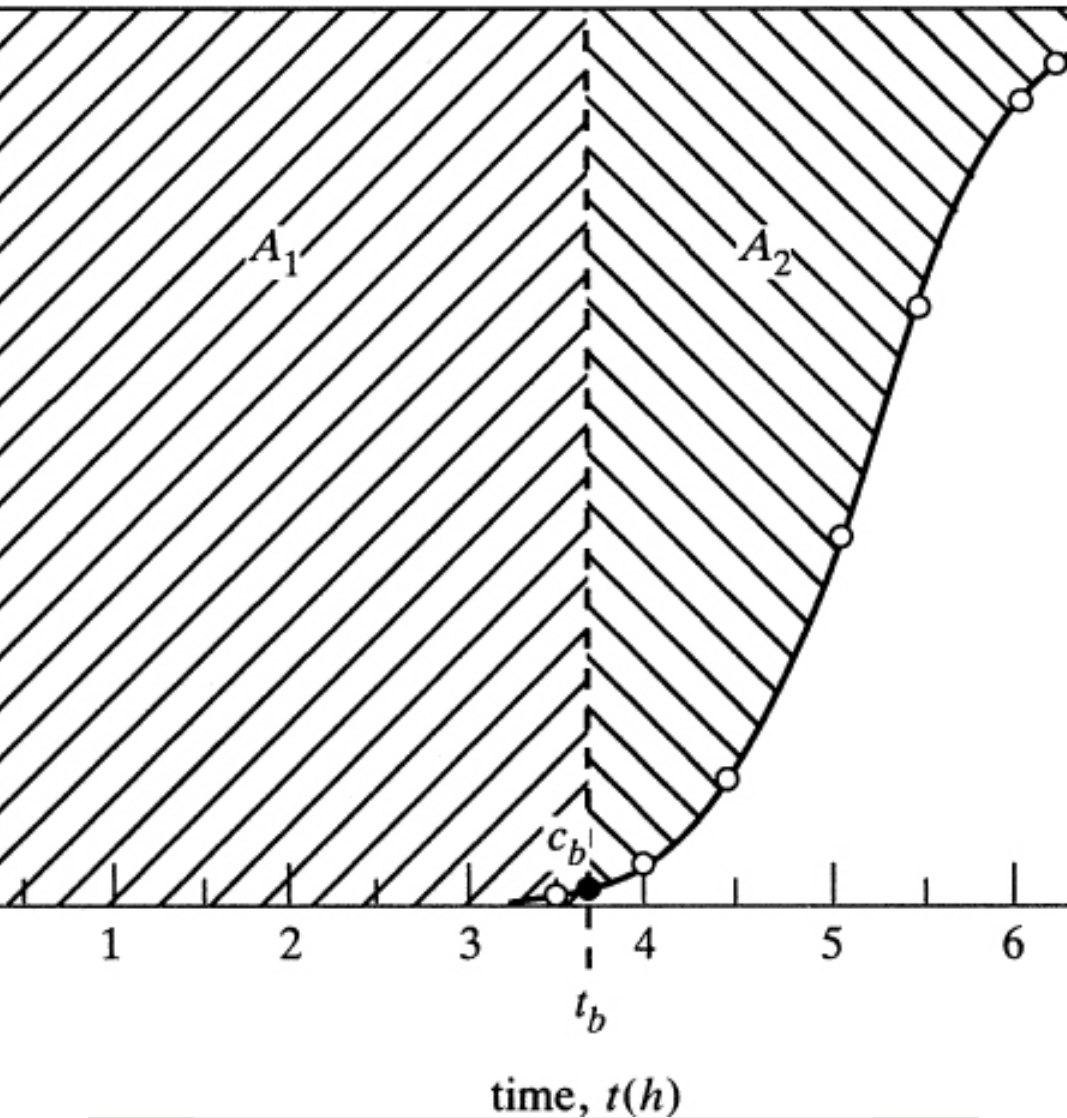


Figure 28.3-3. Breakthrough curve for Example 28.3-1.

Using Eq. (28.3-2), the time equivalent to the usable capacity of the bed up to the break-point time is,

$$t_u = \int_0^{t_b} (1 - c/c_0) dt = A_1 = 3.65h.$$

Hence, the fraction of total capacity used up to the break point is  $t_u/t = 3.65/5.16 = 0.707$ . From Eq. (28.3-3), the length of the used bed is  $H_B = 0.707(14) = 9.9$  cm. To

calculate the length of the unused bed from Eq. (28.3-4),

$$H_{UNB} = (1 - t_{\text{tutt}})HT = (1 - 0.707)14 = 4.1 \text{ cm}$$

For part (b), for a new  $t_b$  of 6.0 h, the new  $HB$  is obtained simply from the ratio of the break-point times multiplied by the old  $HB$ :

$$\begin{aligned} HB &= 6.03.65(9.9) = 16.3 \text{ cm} \\ HT &= HB \\ + H_{UNB} &= 16.3 + 4.1 = 20.4 \text{ cm} \end{aligned}$$

We determine the saturation capacity of the carbon:

$$\begin{aligned} \text{Air flow rate} &= (754 \text{ cm}^3/\text{s})(3600 \text{ s})(0.00115 \text{ g}/\text{cm}^3) = 3122 \text{ g air}/ \\ &\quad \text{h} \\ \text{Total alcohol adsorbed} &= (600 \text{ g alcohol}/106 \text{ g air}) \\ &\quad (3122 \text{ g air}/\text{h})(5.16 \text{ h}) = 9.67 \text{ g alcohol} \\ \text{Saturation capacity} &= 9.67 \text{ g alcohol}/79.2 \text{ g carbon} = 0.1220 \text{ g alcohol}/ \\ &\quad \text{g carbon} \end{aligned}$$

The fraction of the new bed used up to the break point is now  $16.3/20.4$ , or  $0.799$ .

In the scale-up, not only may it be necessary to change the column height, but the actual throughput of fluid may also be different from that used in the experimental laboratory unit. Since the mass velocity in the bed must remain constant for scale-up, the diameter of the bed should be adjusted to keep it constant.

Typical gas adsorption systems use

heights of fixed beds of about 0.3 to 1.5 m with downflow of the gas. Low superficial gas velocities of 15–50 cm/s (0.5–1.7 ft/s) are used. Adsorbent particle sizes range from about 4 to 50 mesh (0.3 to 5 mm). Pressure drops are low, only a few inches of water per foot of bed. The adsorption time is about 0.5 h up to 8 h. For liquids, the superficial velocity of the liquid in the bed is about 0.3 to 0.7 cm/s (4 to 10 gpm/ft<sup>2</sup>).

Practical bed depths usually need to be 5–10 times the length of the bed of the mass transfer zone to be economical (W1). The adsorption step usually uses downward flow in the bed. For desorption, the flow is usually upward for greater efficiency (S1).

### **28.3E Basic Models for Predicting Adsorption**



Adsorption in fixed beds is the most important method used for this process. A fixed or packed bed consists of a vertical cylindrical pipe filled or packed with the adsorbent particles. Adsorbers are mainly designed using laboratory data and the methods described in Section 28.3D. In this section, the basic equations for isothermal adsorption are described so that the fundamentals involved in this process can be better understood.

An unsteady-state solute material balance in the fluid is as follows for a section  $dz$  length of bed:

$$\begin{aligned} \varepsilon \partial c / \partial t + (1 - \varepsilon) p \partial q / \partial t = -v \partial c / \partial z \\ + E \partial^2 c / \partial z^2 \end{aligned} \quad (28.3-6)$$

where  $\varepsilon$  is the external void fraction of the bed;  $v$  is the superficial velocity in the empty bed, m/s;  $\rho_p$  is the density of particle, kg/m<sup>3</sup>; and  $E$  is an axial dispersion coefficient, m<sup>2</sup>/s. The first term represents the accumulation of solute in the liquid. The second term is the accumulation of solute in the solid. The third term represents the amount of solute flowing in by convection to the section  $dz$  of the bed minus that flowing out. The last term represents the axial dispersion of solute in the bed, which leads to mixing of the solute and solvent.

The second differential equation needed to describe this process relates the second term of Eq. (28.3-6) for accumulation of solute in the solid to the rate of external mass transfer of the

solute from the bulk solution to the particle and the diffusion and adsorption on the internal surface area. The actual physical adsorption is very rapid. The third equation is the equilibrium isotherm.

There are many solutions for these three equations that are nonlinear and coupled. These solutions frequently do not fit experimental results very well and will not be discussed here.

### **28.3F Processing Variables and Adsorption Cycles**

Large-scale adsorption processes can be divided into two broad classes. The first and most important is the cyclic batch system, in which the adsorption fixed bed is alternately saturated and then regenerated in a cyclic manner. The second is a

continuous flow system, which involves a continuous flow of adsorbent countercurrent to a flow of feed.

There are four basic methods in common use for the cyclic batch adsorption system using fixed beds. These methods differ from each other mainly in the means used to regenerate the adsorbent after the adsorption cycle. In general, these four basic methods operate with two or sometimes three fixed beds in parallel, one in the adsorption cycle and the other one or two in a desorbing cycle, to provide continuity of flow. After the first bed has completed the adsorption cycle, the flow is switched to the second newly regenerated bed for adsorption. The first bed is then regenerated by any of the

## following methods:

1. *Temperature-swing cycle*. This is also called the thermal-swing cycle. The spent adsorption bed is regenerated by heating it with embedded stream coils or with a hot purge-gas stream to remove the adsorbate. The elevation in temperature is used to shift the adsorption equilibrium curve and to affect regeneration of the adsorbent. Finally, the bed must be cooled so that it can be used for adsorption in the next cycle. The time for regeneration is generally a few hours or more.
2. *Pressure-swing cycle*. In this case, the bed is desorbed by reducing the pressure at essentially constant temperature and then purging the bed at this low pressure with a small fraction of the product stream. Reduction in pressure shifts the adsorption equilibrium and affects the regeneration of the adsorbent. This process for gases uses a very short cycle time for regeneration compared to that for the temperature-swing cycle.
3. *Inert-purge-gas stripping cycle*. In this cycle, the adsorbate is removed by passing a nonadsorbing or inert gas through the bed. This lowers the partial pressure or concentration around the particles and desorption occurs. Regeneration cycle times are usually only a few minutes.
4. *Displacement-purge cycle*. In this method, the pressure and temperature are kept essentially constant as in purge-gas stripping, but a gas or liquid is used that is adsorbed more strongly than the adsorbate and displaces the

adsorbate. Again, cycle times are usually only a few minutes.

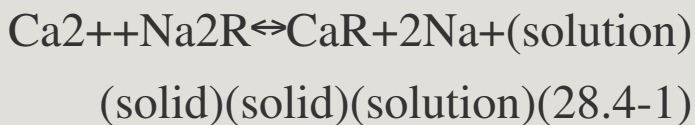
*Steam stripping* is often used in the regeneration of solvent-recovery systems utilizing activated-carbon adsorbent. This can be considered a combination of the temperature-swing cycle and the displacement-purge cycle.

## **28.4 Ion-Exchange Processes**

### **28.4A Introduction and Ion-Exchange Materials**

Ion-exchange processes are basically chemical reactions between ions in solution and ions in an insoluble solid phase. The techniques used in ion exchange so closely resemble those used in adsorption that for the majority of engineering purposes, ion exchange can be considered as a special case of adsorption.

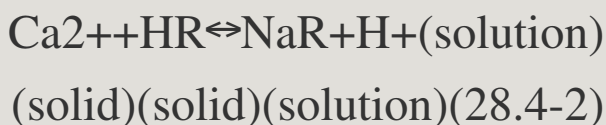
In ion exchange, certain ions are removed by the ion-exchange solid. Since electroneutrality must be maintained, the solid releases replacement ions to the solution. The first ion-exchange materials were naturally occurring porous sands called zeolites, which are cation exchangers. Positively charged ions in solution such as  $\text{Ca}^{2+}$  diffuse into the pores of the solid and exchange with the  $\text{Na}^+$  ions in the mineral:



where  $R$  represents the solid. This is the basis for “softening” water. To regenerate, a solution of  $\text{NaCl}$  is added, which drives the reversible reaction above to the left. Almost all of these

inorganic ion-exchange solids exchange only cations.

Most present-day ion-exchange solids are synthetic resins or polymers. Certain synthetic polymeric resins contain sulfonic, carboxylic, or phenolic groups. These anionic groups can exchange cations:



Here,  $R$  represents the solid resin. The  $\text{Na}^+$  in the solid resin can be exchanged with  $\text{H}^+$  or other cations.

Similar synthetic resins containing amine groups can be used to exchange anions and  $\text{OH}^-$  in solution:





$$-(\text{solution})(\text{solid})(\text{solid})(\text{solution})$$

$$(28.4-3)$$

#### 28.4B Equilibrium Relations in Ion Exchange

The ion-exchange isotherms have been developed using the law of mass action. For example, for the case of a simple ion-exchange reaction such as Eq. (28.4-2),  $HR$  and  $NaR$  represent the ion-exchange sites on the resin filled with a proton  $H^+$  and a sodium ion  $Na^+$ . It is assumed that all of the fixed number of sites are filled with  $H^+$  or  $Na^+$ . At equilibrium,

$$K = \frac{[NaR][H^+]}{[Na^+][HR]} \quad (28.4-4)$$

Since the total concentration of the ionic groups  $[R^-]$  on the resin is fixed (B2),

$$[R^-] = \text{constant} = [NaR] + [HR] \quad (28.4-5)$$

Combining Eqs. (28.4-4) and (28.4-5),

$$[\text{NaR}] = K[\text{R}^-][\text{Na}^+][\text{H}^+] + K[\text{Na}^+]$$

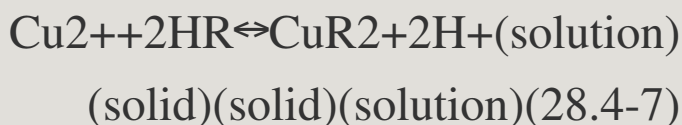
(28.4-6)

If the solution is buffered, so that  $[\text{H}^+]$  is constant, the equation above for sodium exchange or adsorption is similar to the Langmuir isotherm.

The ion-exchange process functions for strong acid or strong base exchangers by replacing the ions of a solution with ions such as  $\text{H}^+$  or  $\text{OH}^-$ . These replaced ions from the solution are taken up by the resin. Then, to regenerate the resin, a small amount of solution with a high concentration of  $\text{H}^+$  is used for cation exchangers or a high concentration of  $\text{OH}^-$  ions for anion exchangers. These high concentrations of  $\text{H}^+$  or  $\text{OH}^-$  for

regeneration shift the equilibrium to the left, making the regeneration process more favorable.

A typical ion-exchange process for the removal of metals from a solution is shown for a copper cation being removed from a stream containing dilute  $\text{CuSO}_4$  and  $\text{H}_2\text{SO}_4$ :



For regeneration, the bed of resin is contacted with a high concentration of  $\text{H}_2\text{SO}_4$  to shift the equilibrium to the left.

#### **28.4C Use of Equilibrium Relations and Relative-Molar-Selectivity Coefficients**

Convenient tables for relative-molar-selectivity coefficients  $K$  have been

prepared for various types of ion-exchange resins. Data are given in Table 28.4-1 for a polystyrene resin with 8% divinylbenzene (DVB) cross-linking (B1, P1) for strong-acid and strong-base resins. For cation exchangers, values are given for cation  $A$  entering the resin and displacing the cation  $\text{Li}^+$ , and for anion exchangers, values for anion  $A$  replacing  $\text{Cl}^-$ .

The equilibrium constant or selectivity coefficient for exchange of any two ions  $A$  and  $B$  can be approximated from Table 28.4-1 using values of  $K_A$  and  $K_B$ :

$$K_{A,B} = K_A / K_B \quad (28.4-8)$$

For example, for the reaction of cation  $\text{K}^+$  ( $A$ ) displacing cation  $\text{H}^+$  ( $B$ ),



Substituting into Eq. (28.4-8),  $K_{A,B} = K_A/K_B = 2.90/1.27 = 2.28$ .

For dilute solutions, activity coefficients are relatively constant and simple concentration units are used. For Eq. (28.4-9), the equilibrium constant is as follows:

Table 28.4-1. *Relative-Molar-Selectivity Coefficients K for Polystyrene Cation and Anion Exchangers with 8% DVB Cross-Linking (B1, P1)*

$$K_{A,B} = c_B q_A R c_A q_B R = (c_H^+) (q_K R) (c_K^+) (q_H R) \quad (28.4-10)$$

where, for the resin phase, concentrations  $q_{KR}$  and  $q_{HR}$  are in equivalents/L of the bulk bed volume of water-swelled resin, and for the liquid phase, concentrations  $c_{H+}$  and  $c_{K+}$  are in equivalents/L of the volume of solution.

The total concentration  $C$  in the liquid solution and the total concentration  $Q$  in the resin remain constant during the exchange process because of electroneutrality in Eq. (28.4-9). Then,

$$C=c_A+c_B, Q=q_{AR}+q_{BR} \quad (28.4-11)$$

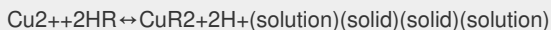
In the case of Eq. (28.4-7), where the ion  $Cu^{2+}$  (A) replaces  $H^+$  (B) and the charges are unequal,

$$\begin{aligned} K_{A,B} &= (c_B)^2 (q_{AR}^2) (c_A) \\ (q_{BR})^2 &= (c_{H+})^2 (q_{CuR}^2) (c_{Cu^{2+}}) \\ &\quad (q_{HR})^2 \quad (28.4-12) \end{aligned}$$

**EXAMPLE 28.4-1. Removal of  $\text{Cu}_{2+}$  Ion from Acid Solution by an Ion-Exchange Resin**

An acidic waste stream contains copper in solution that is being removed by a strong acid–cation resin. The cation  $\text{Cu}_{2+}$  (A) is displacing the cation  $\text{H}^+$  (B) in the resin. A polystyrene resin similar to that in Table 28.4-1 is being used. The total resin capacity  $Q$  is approximately 1.9 equivalents/L of wet bed volume. For a total concentration  $C$  of 0.10 N (0.10 equivalents/L) in the solution, calculate at equilibrium the total equivalents of  $\text{Cu}_{2+}$  in the resin when the concentration of  $\text{Cu}_{2+}$  in solution is 0.02 M (0.04 N).

**Solution:** The known values are  $C = 0.10$  N or equivalents/L of  $\text{Cu}_{2+}$  (A) and  $\text{H}^+$  (B) in solution, and  $Q = 1.9$  equivalents/L of A and B in the resin. The equilibrium relation is Eq. (28.4-7):



or,



From Table 28.4-1,  $K_A = K_{\text{Cu}^{2+}} = 3.85$  and  $K_B = K_{\text{H}^+} = 1.27$ . Then, from Eq. (28.4-8),

$$K_{A,B} = K_A/K_B = 3.85/1.27 = 3.03$$

Using Eq. (28.4-12),

$$K_{A,B} = \frac{(c_B)^2 (q_{AR_2})(c_A)(q_{BR})^2}{(c_{H^+})^2 (q_{CuR_2})(c_{Cu^{2+}})(q_{HR})^2}$$

From Eq. (28.4-11),  $C = 0.10$  equivalents/L  $= 2c_{\text{Cu}^{2+}} + c_{\text{H}^+}$ . Also,  $Q = 1.9 = q_{HR} + 2q_{\text{CuR}_2}$ . The values to substitute into Eq. (28.4-12) are  $K_{A,B} = 3.03$ ,  $q_{\text{CuR}_2} = 1.9/2 - q_{HR}/2$ ,  $c_{\text{Cu}^{2+}} = 0.02$ ,  $c_{\text{Cu}^{2+}} = 0.02$ , and  $c_{\text{H}^+} = 0.10 - 2c_{\text{Cu}^{2+}} = 0.10 - 0.04 = 0.06$ .

$$0.03 = \frac{(0.06)^2 (1.9/2 - q_{HR}/2)(0.02)(q_{HR})^2}{(q_{HR})^2}$$

Rearranging,

$$(q_{HR})^2 + 0.02970q_{HR} - 0.05644 = 0$$

Solving this quadratic equation,  $q_{HR} = 0.2232$ . Then,  $q_{\text{CuR}_2} = 1.9/2 - 0.2232/2 = 0.8384$ . Hence, the equivalents of

$\text{Cu}_{2+}$  in the resin is  $2(0.8384) = 1.677$  compared to a value of 1.9 when fully loaded with copper. The result shows that the removal of  $\text{Cu}_{2+}$  from the solution by the resin is highly favored.

## 28.4D Concentration Profiles and Breakthrough Curves

### *1. Basic models in ion exchange.*

The rate of ion exchange depends on the mass transfer of ions from the bulk solution to the particle surface, diffusion of the ions in the pores of the solid to the surface, exchange of the ions at the surface, and diffusion of the exchange ions back to the bulk solution. This is similar to adsorption. The differential equations derived are also very similar to those for adsorption. The design methods used for ion exchange and adsorption are similar.

### *2. Concentration profiles in packed beds.* Concentration profiles in packed



beds for ion exchangers are very similar to those given in Fig. 28.3-1a for adsorption. The typical S-shaped curves occur and pass through the bed. The major part of the ion exchange at any time takes place in a relatively narrow mass-transfer zone. This mass-transfer zone moves down the column. In Fig. 28.3-1b, the breakthrough curve is shown, which is similar for adsorption and ion exchange.

*3. Mass-transfer zone.* As the mass-transfer zone travels down the column, the height of this zone becomes constant. This behavior is generally characteristic in cases where the ion to be removed from the feed stream has a greater affinity for the solid resin than the ion originally present in the solid. The majority of industrial ion-exchange

processes fall in this category (M1).

This constant height of the mass-transfer zone can then be used for scale-up, similar to adsorption scale-up.

#### **28.4E Capacity of Columns and Scale-Up Design Method**

*1. Capacity of a column.* The design method for fixed-bed ion exchangers is quite similar to that used for adsorption processes. Theoretical predictions of concentration profiles, the mass-transfer zone, and mass transfer may be inaccurate because of uncertainties due to flow patterns and so forth. Hence, experiments using small packed-bed laboratory-scale columns are needed for scale-up.

The total stoichiometric capacity of the packed bed is the total shaded area in

the breakthrough curve in Fig. 28.3-2. The time  $t_t$  is the time equivalent to the total capacity:

$$t_t = \int_0^{\infty} (1 - c/c_o) dt \quad (28.3-1)$$

The usable capacity up to the break-point time  $t_b$  is the cross-hatched area from  $t = 0$  to  $t_b$ . Then,  $t_u$ , the time equivalent to the usable capacity, is

$$t_u = \int_0^{t_b} (1 - c/c_o) dt \quad (28.3-2)$$

Numerical integration of Eqs. (28.3-1) and (28.3-2) can also be done using spreadsheets. Then, the fraction of the total bed length or capacity utilized up to the break point is  $t_u/t_t$ . For a total bed length of  $H_T$  m,  $H_B$  is the length of the bed used up to the break point:

$$H_B = (t_u/t_t) H_T \quad (28.3-3)$$

The length of the mass-transfer section or unused bed  $H_{UNB}$  in m is then

$$H_{UNB} = (1 - t_u/t_t)HT \quad (28.3-4)$$

This  $H_{UNB}$  is essentially independent of the total column length. The experimental value of  $H_{UNB}$  is measured at the desired velocity in a small-diameter laboratory column. To design the full-scale column, the length of the bed  $H_B$  is calculated to achieve the desired capacity at the break point. Then, the total column length is

$$HT = H_{UNB} + H_B \quad (28.3-5)$$

The mass velocity of both the laboratory- and full-scale columns must be the same. The diameter of the large-scale column is calculated using the same given mass velocity.

2. *Typical process variables.* Some typical operating process variables are as follows: The laboratory column should be at least 2.5 cm in diameter and 0.3 m in length. Commercial liquid flow rates (W1) can be from 1 to 12 gpm/ft<sup>2</sup> (0.041–0.489 m/min) but are usually 6–8 gpm/ft<sup>2</sup> (0.244 – 0.326 m/min). Commercial columns are usually 1–3 m in height. Usually, a freeboard of 50% or more open space is needed to accommodate bed expansion when regenerant flow is upward.

The resin gel can swell due to exchange by about 10 to 20%. Particle sizes used can range from 0.2 mm to 1.0 mm.

Typical moisture contents of the resins vary from 50 to 70%. The equilibrium exchange capacities of strong-acid or strong-base exchange resins are

typically 3–5 meq/g of dry resin and 1–2 meq/ml of wet resin bed.

Regeneration flow rates are typically quite low, in the range of 0.5 to 5.0 bed volumes/h, in order to attain equilibrium while using minimum amounts of solution (W1). A bed volume is the total volume of the packed bed of resin as calculated from the column diameter and height of the packed bed.

Pressure drop can be predicted by using the equations for flow in packed beds. Typical pressure drops for beds are about 0.6 to 0.9 psi/ft height (13.6–20.4 kPa/m height) for flow rates of 6 to 8 gpm/ft<sup>2</sup>. Excessive pressure drops should be avoided, since the gel-resin particles can be deformed.

A useful method for correlating experimental breakthrough curves at different flow velocities and the mass-transfer zone is as follows: Instead of plotting  $c/c_o$  versus time  $t$ , as in Fig. 28.3-1b, a plot of  $c/c_o$  versus the number of bed volumes (BV) is made. Data for different flow velocities will then tend to fall on the same curve.

*3. Operating cycles.* The operating cycles for ion-exchange processes in a packed bed are more complicated than those for gas adsorption. These usually consist of the following four steps, with experimental data usually needed to define each operating time (S1, W1). (1) Downflow loading of the process feed for a proper time. At the end of loading, the bed voids are filled with feed solution. (2) Displacement of the feed

solution with upward flow of the regeneration solution. Thus, displacement of the occluded feed solution first occurs as a wave front. (3) Regeneration of the bed with continued upward flow of the regeneration solution. This occurs as a second wavefront. (4) Rinse upward to remove occluded regenerant from the bed. A rinse can be used instead of step (2) for recovering possibly valuable occluded process solution (W1).

For the actual design and for continuous feed flow, at least two columns are needed, so that one column is used to process the feed while the other is used for regeneration. When breakthrough occurs, the towers are switched. The total number of beds depends on the loading and regeneration times.



Alternatively, a three-column system can be used for better utilization of the columns. The feed enters column 2 and then column 3 in series while column 1 is being regenerated. When breakthrough occurs in column 3, column 2 is removed for regeneration. The feed is then rerouted and goes to column 3 and then to column 1.

## 28.5 Chapter Summary

### Batch Adsorption

The material balance on the adsorbate is

$$q_F M + c_F S = q_M + c_S \quad (28.2-1)$$

### Bed Height

The time  $t_t$  is the time equivalent to the total capacity:

$$t_t = \int_0^\infty (1 - c/c_o) dt \quad (28.3-1)$$

Then,  $t_u$ , the time equivalent to the usable capacity, is

$$t_u = \int_0^{t_b} (1 - c/c_o) dt \quad (28.3-2)$$

$H_B$  is the length of the bed used up to the break point:

$$H_B = (t_u/t_t) H_T \quad (28.3-3)$$

The length of the mass-transfer section or unused bed  $H_{UNB}$  in m is then

$$H_{UNB} = (1 - t_u/t_t) H_T \quad (28.3-4)$$

Then, the total column length is

$$H_T = H_{UNB} + H_B \quad (28.3-5)$$

## Problems

### **28.1-1. *Equilibrium Isotherm for Glucose Adsorption.*** Equilibrium

isotherm data for adsorption of glucose from an aqueous solution to activated alumina are as follows (H1):



Determine the isotherm that fits the data and provide the constants of the equation using the given units.

**Ans.** Langmuir isotherm,  $q = 0.145$   
 $c/(0.0174 + c)$

**28.2-1. Batch Adsorption for a Phenol Solution.** A wastewater solution having a volume of 2.5 m<sup>3</sup> contains 0.25 kg phenol/m<sup>3</sup> of solution. This solution is mixed thoroughly in a batch process with 3.0 kg of granular activated carbon until equilibrium is reached. Use the

isotherm from Example 28.2-1 and calculate the final equilibrium values and the percent phenol extracted.

**28.3-1. *Scale-Up of Laboratory Adsorption-Column Data.*** Using the break-point time and other results from Example 28.3-1, do as follows:

- The break-point time for a new column is to be 8.5 h. Calculate the new total length of the column required, the column diameter, and the fraction of total capacity used up to the break point. The flow rate is to remain constant at  $754 \text{ cm}^3/\text{s}$ .
- Use the same conditions as in part (a), but the flow rate is to be increased to  $2000 \text{ cm}^3/\text{s}$ .

**Ans.** (a)  $H_T = 27.2 \text{ cm}$ , 0.849 fraction; (b)  $D = 6.52 \text{ cm}$

**28.3-2. *Drying of Nitrogen and Scale-Up of a Column.*** Using molecular sieves, water vapor was

removed from nitrogen gas in a packed bed (C1) at  $28.3^{\circ}\text{C}$ . The column height was 0.268 m, with the bulk density of the solid bed being equal to  $712.8 \text{ kg/m}^3$ . The initial water concentration in the solid was  $0.01 \text{ kg water/kg solid}$  and the mass velocity of the nitrogen gas was  $4052 \text{ kg/m}^2 \cdot \text{h}$ . The initial water concentration in the gas was  $c_o = 926 \times 10^{-6} \text{ kg water/kg nitrogen}$ . The breakthrough data are as follows:



A value of  $c/c_o = 0.02$  is desired at the break point. Do as follows:

- Determine the break-point time, the fraction of total capacity used up to the break point, the length of the unused bed, and the saturation loading capacity of the solid.
- For a proposed column length  $H_T = 0.40 \text{ m}$ ,

calculate the break-point time and fraction of total capacity used.

**Ans.** (a)  $t_b = 9.58$  h, fraction used = 0.878

### **28.4-1. Scale-Up of an Ion-**

### **Exchange Column.**

An ion-exchange process using a resin to remove copper ions from an aqueous solution is conducted in a 1.0-in.-diameter column 1.2 ft high. The flow rate is 1.5 gph and the break point occurred at 7.0 min.

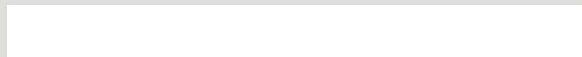
Integrating the breakthrough curve gives a ratio of usable capacity to total capacity of 0.60. Design a new tower that will be 3.0 ft high and operate at 4.5 gph. Calculate the new tower size and break-point time.

**Ans.**  $t_b = 24.5$  min,  $D = 1.732$  in.

**28.4-2. Height of a Tower in an Ion Exchange.** In a given run using a flow rate of  $0.2 \text{ m}^3/\text{h}$  in an ion-exchange tower with a column height of  $0.40 \text{ m}$ , the break point occurred at  $8.0 \text{ min}$ . The ratio of usable capacity to total equilibrium capacity is  $0.65$ . What is the height of a similar column operating for  $13.0 \text{ min}$  to the break point at the same flow rate?

**28.4-3. Ion Exchange of Copper in a Column.** An ion-exchange column containing  $99.3 \text{ g}$  of amberlite ion-exchange resin was used to remove  $\text{Cu}^{2+}$  from a solution where  $c_o = 0.18 \text{ M}$   $\text{CuSO}_4$ . The tower height =  $30.5 \text{ cm}$  and the diameter =  $2.59 \text{ cm}$ . The flow rate was  $1.37 \text{ cm}^3 \text{ solution/s}$  to the tower. The breakthrough data are

shown below:



The concentration desired at the break point is  $c/c_o = 0.010$ .

Determine the break-point time, the fraction of total capacity used up to the break point, the length of unused bed, and the saturation loading capacity of the solid.

#### ***28.4-4. Effect of Total***

#### ***Concentration on the Loading of Ion-Exchange Resin.***

Use the conditions of Example 28.4-1 for ion exchange of  $\text{Cu}_{2+}$  with  $\text{H}_{+}$ . However, determine the effect of total concentration in the solution on the loading of  $\text{Cu}_{2+}$  on the resin. Do this for a total concentration  $C$  of 0.010 N in the solution at equilibrium



instead of 0.10 N. Also, the concentration of  $\text{Cu}^{2+}$  in the solution is 0.002 M (0.004 N) instead of 0.02 M.

$$\text{Ans. } q_{\text{CuR}_2} = 0.9132 \text{ equiv/L}$$

### ***28.4-5. Equilibrium in an Ion***

***Exchange of  $\text{NH}_4^+$  for  $\text{H}^+$ .*** For the case where the cation  $\text{NH}_4^+$  (A) replaces  $\text{H}^+$  (B) in a polystyrene resin with 8% DVB, calculate the equilibrium constant  $K_{A,B}$ . The total resin capacity  $Q = 2.0$  equiv/L wet bed volume. The total concentration  $C = 0.20$  N in the solution. Calculate at equilibrium the equivalents of  $\text{NH}_4^+$  in the resin when the concentration of  $\text{NH}_4^+$  in solution is 0.04 N.

**Ans.**  $q_{\text{NH}_4R} = 0.6684 \text{ equiv/L}$

### References

### Notation

# Chapter 29. Crystallization and Particle Size Reduction

## 29.0 Chapter Objectives

On completion of this chapter, a student should be able to:

- Describe how crystallization is a solid–liquid separation process
- Identify industries where crystallization is used
- Explain why crystal size and shape uniformity is important
- Identify the seven classes of crystals in terms of axes and angles
- Explain when equilibrium occurs during crystallization
- Interpret data from a solubility curve
- Calculate the yield from a crystallization process
- Describe how heat and energy can affect the crystallization process

- Describe different types of crystallizers used in industry
- Explain the differences between homogeneous and contact nucleation
- Calculate crystal growth rates and growth coefficients
- Interpret data from a particle size distribution
- Use the MSMPR model to calculate grow rate and nucleation rate
- Explain why particle size reduction is often required in industry
- Describe the different methods by which particle size reduction may occur
- Calculate the energy and power associated with particle size reduction

## **29.1 Introduction to Crystallization**

### **29.1A Crystallization and Types of Crystals**

*1. Introduction.* Crystallization is a solid–liquid separation process in which mass transfer of a solute from the liquid solution to a pure solid crystalline phase occurs. An

important example is in the production of sucrose from sugar beets, where the sucrose is crystallized out from an aqueous solution. Other examples can be found in the pharmaceutical and food industries.

*Crystallization* is a process in which solid particles are formed from a homogeneous phase. This process can occur in the freezing of water to form ice, in the formation of snow particles from a vapor, in the formation of solid particles from a liquid melt, or in the formation of solid crystals from a liquid solution. The last process mentioned, crystallization from a solution, is the most important one commercially and will be considered in the present discussion. In crystallization, the

solution is concentrated and usually cooled until the solute concentration becomes greater than its solubility at that temperature. At that point, the solute comes out of the solution, forming crystals of approximately pure solute.

In commercial crystallization, not only are the yield and purity of the crystals important, but also the sizes and shapes of the crystals. It is often desirable that crystals be uniform in size. Size uniformity is desirable to minimize caking in the package, for ease of pouring, for ease in washing and filtering, and for uniform behavior when used. Sometimes large crystals are requested by the purchaser, even though smaller crystals are just as useful. Also, crystals of a certain shape are sometimes

required, such as needles rather than cubes.

2. *Types of crystal geometry.* A crystal can be defined as a solid composed of atoms, ions, or molecules that are arranged in an orderly and repetitive manner. It is a highly organized type of matter. The atoms, ions, or molecules are located in three-dimensional arrays or space lattices. The interatomic distances between these imaginary planes or space lattices in a crystal are measured by X-ray diffraction, as are the angles between these planes. The pattern or arrangement of these space lattices is repeated in all directions.

Crystals often appear as polyhedrons that have flat faces and sharp corners. The relative sizes of the faces and edges

of different crystals of the same material may differ greatly. However, the angles between the corresponding faces of all crystals of the same material are equal and are characteristic of that particular material. Therefore, crystals are classified on the basis of these interfacial angles.

There are seven classes of crystals, depending upon the arrangement of the axes to which the angles are referred:

1. Cubic system: three equal axes at right angles to each other
2. Tetragonal system: three axes at right angles to each other, one axis longer than the other two
3. Orthorhombic system: three axes at right angles to each other, all of different lengths
4. Hexagonal system: three equal axes in one plane at  $60^\circ$  to each other, and a fourth axis at right angles to this plane and not necessarily the same length



5. Monoclinic system: three unequal axes, two at right angles in a plane and a third at some angle to this plane
6. Triclinic system: three unequal axes at unequal angles to each other and not 30, 60, or 90°
7. Trigonal system: three equal and equally inclined axes

The relative development of a crystal's different types of faces may vary depending on the solute that is crystallizing. Sodium chloride crystallizes from aqueous solutions with cubic faces only. But if sodium chloride crystallizes from an aqueous solution with a given slight impurity present, the crystals will have octahedral faces. Both types of crystals, however, are in the cubic system. The crystallization in overall shapes of plates or needles has no relation to the type of crystal system and usually depends upon the process conditions under which the crystals are grown.

## 29.1B Equilibrium Solubility in Crystallization

In crystallization, equilibrium is attained when the solution or mother liquor is saturated. This is represented by a *solubility curve*.

Solubility is mainly dependent on temperature. Pressure has a negligible effect on solubility.

Solubility data are given in the form of curves where solubilities in some convenient units are plotted versus temperature. Tables of solubilities are given in many chemical handbooks (P1). Solubility curves for some typical salts in water are given later in Chapter 32 in Fig.

32.1-1. In general, the solubilities of most salts increase slightly or markedly with increasing temperature.

A very common type of curve can be seen in Fig. 32.1-1 for  $\text{KNO}_3$ , where the solubility increases markedly with temperature and there are no hydrates. Over the whole range of temperatures, the solid phase is  $\text{KNO}_3$ . The solubility of  $\text{NaCl}$  is marked by its small change with temperature. In solubility plots, the solubility data are ordinarily given as parts by weight of anhydrous material per 100 parts by weight of total solvent (i.e., water in many cases).

In Fig. 29.1-1, the solubility curve is shown for sodium thiosulfate,  $\text{Na}_2\text{S}_2\text{O}_3$ . The solubility increases rapidly with temperature, but there are definite breaks in the curve that indicate different hydrates. The stable phase up to  $48.2^\circ\text{C}$  is the pentahydrate  $\text{Na}_2\text{S}_2\text{O}_3 \cdot 5\text{H}_2\text{O}$ . This means that at concentrations

above the solubility line (up to  $48.2^{\circ}\text{C}$ ), the solid crystals formed are  $\text{Na}_2\text{S}_2\text{O}_3 \cdot 5\text{H}_2\text{O}$ . At concentrations below the solubility line, only a solution exists. From  $48.2$  to about  $65^{\circ}\text{C}$ , the stable phase is  $\text{Na}_2\text{S}_2\text{O}_3 \cdot 2\text{H}_2\text{O}$ . A half-hydrate is present between  $65$  to  $70^{\circ}\text{C}$ , and the anhydrous salt is the stable phase above  $70^{\circ}\text{C}$ .

### **29.1C Yields, Material, and Energy Balances in Crystallization**

*1. Yields and material balances in crystallization.* In many industrial crystallization processes, the solution (mother liquor) and the solid crystals are in contact for enough time to reach equilibrium. Hence, the mother liquor is saturated at the final temperature of the process, and the final concentration of the solute in the solution can be

obtained from the solubility curve. The yield of crystals from a crystallization process can then be calculated knowing the initial concentration of solute, the final temperature, and the solubility at this temperature.

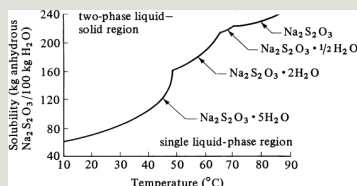


Figure 29.1-1. Solubility of sodium thiosulfate,  $\text{Na}_2\text{S}_2\text{O}_3$ , in water.

In some instances in commercial crystallization, the rate of crystal growth may be quite slow, due to a very viscous solution or a small surface of crystals exposed to the solution. Hence, some supersaturation may still exist, giving a lower yield of crystals than predicted.

In making the material balances, the calculations are straightforward when the solute crystals are anhydrous. Simple water and solute material balances are made. When the crystals are hydrated, some of the water in the solution is removed with the crystals as a hydrate.

**EXAMPLE 29.1-1. Yield of a Crystallization Process**

A salt solution weighing 10000 kg with 30 wt %  $\text{Na}_2\text{CO}_3$  is cooled to 293 K (20°C). The salt crystallizes as the decahydrate. What will be the yield of  $\text{Na}_2\text{CO}_3 \cdot 10\text{H}_2\text{O}$  crystals if the solubility is 21.5 kg anhydrous  $\text{Na}_2\text{CO}_3$ /100 kg of total water? Determine the yield for the following cases:

- Assume that no water is evaporated.
- Assume that 3% of the total weight of the solution is lost by evaporation of water in cooling.

**Solution:** The molecular weights are 106.0 for  $\text{Na}_2\text{CO}_3$ , 180.2 for  $10\text{H}_2\text{O}$ , and 286.2 for  $\text{Na}_2\text{CO}_3 \cdot 10\text{H}_2\text{O}$ . The process flow diagram is shown in Fig. 29.1-2, with  $W$  being kg  $\text{H}_2\text{O}$  evaporated,  $S$  kg being the solution (mother liquor), and  $C$  kg being the crystals of  $\text{Na}_2\text{CO}_3 \cdot 10\text{H}_2\text{O}$ . Making a material balance around the dashed-line box for water for part (a), where  $W = 0$ ,

$$0.70(10\,000) = 100 + 100 + 21.5(S) + 180.2/286.2(C) + 0(29.1-1)$$

where  $(180.2)/(286.2)$  is wt fraction of water in the crystals. Making a balance for  $\text{Na}_2\text{CO}_3$ ,

$$0.30(10\,000)=21.5100+21.5(S)+106.0286.2(C)+0(29.1-2)$$

Solving the two equations simultaneously,  $C = 6370$  kg of  $\text{Na}_2\text{CO}_3 \cdot 10\text{H}_2\text{O}$  crystals and  $S = 3630$  kg solution.

For part (b),  $W = 0.30(10\,000) = 300$  kg  $\text{H}_2\text{O}$ . Equation (29.1-1) becomes

$$0.70(10\,000)=100100+21.5(S)+180.2286.2(C)+300(29.1-3)$$

Equation (29.1-2) does not change, since no salt is in the  $W$  stream. Solving Eqs. (29.1-2) and (29.1-3) simultaneously,  $C = 6630$  kg of  $\text{Na}_2\text{CO}_3 \cdot 10\text{H}_2\text{O}$  crystals and  $S = 3070$  kg solution.

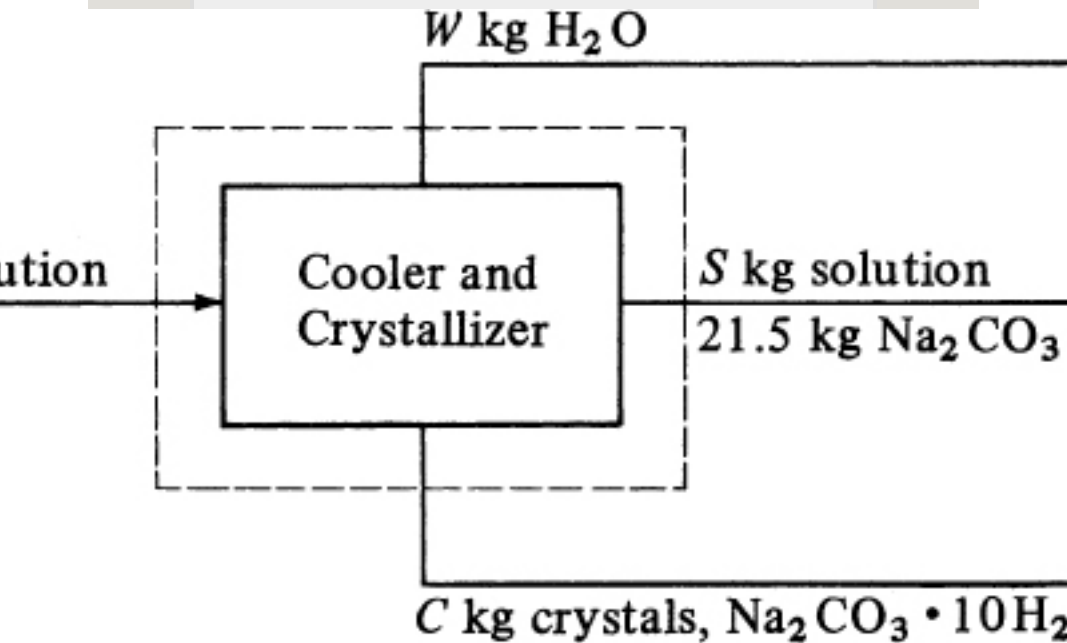


Figure 29.1-2. Process flow for crystallization in Example 29.1-1.

*2. Heat effects and heat balances in crystallization.* When a compound

whose solubility increases as temperature increases dissolves, there is an absorption of heat called the *heat of solution*. An evolution of heat occurs when a compound whose solubility decreases as temperature increases dissolves. For compounds whose solubility does not change with temperature dissolve, there is no heat evolution on dissolution. Most data on heats of solution are given as the change in enthalpy in kJ/kg mol (kcal/g mol) of solute occurring with the dissolution of 1 kg mol of the solid in a large amount of solvent at essentially infinite dilution.

In crystallization, the opposite of dissolution occurs. At equilibrium, the heat of crystallization is equal to the negative of the heat of solution at the same concentration in solution. If the



heat of dilution from saturation in the solution to infinite dilution is small, this can be neglected, and the negative of the heat of solution at infinite dilution can be used for the heat of crystallization. With many materials, this heat of dilution is small compared with the heat of solution, and this approximation is reasonably accurate. Heat-of-solution data are available in several references (P1).

Probably the most satisfactory method for calculating heat effects during a crystallization process is to use the enthalpy–concentration chart for the solution and the various solid phases that are present for the system.

However, only a few such charts are available, including the following systems: calcium chloride–water (H1),

magnesium sulfate–water (P2), and ferrous sulfate–water (K2). When such a chart is available, the following procedure is used: The enthalpy  $H_1$  of the entering solution at the initial temperature is read off the chart, where  $H_1$  is kJ (btu) for the total feed. The enthalpy  $H_2$  of the final mixture of crystals and mother liquor at the final temperature is also read off the chart. If some evaporation occurs, the enthalpy  $H_v$  of the water vapor is obtained from the steam tables. Then, the total heat absorbed  $q$  in kJ is

$$q=(H_2+H_v)-H_1 \quad (29.1-4)$$

If  $q$  is positive, heat must be added to the system. If it is negative, heat is evolved or given off.

A feed solution of 2268 kg at 327.6 K (54.4°C) containing 48.2 kg  $\text{MgSO}_4$ /100 kg total water is cooled to 293.2 K (20°C) where  $\text{MgSO}_4 \cdot 7\text{H}_2\text{O}$  crystals are removed. The solubility of the salt is 35.5 kg  $\text{MgSO}_4$ /100 kg total water (P1). The average heat capacity of the feed solution can be assumed as 2.93 kJ/kg · K (H1). The heat of solution at 291.2 K (18°C) is  $-13.31 \times 10^3$  kJ/kg mol  $\text{MgSO}_4 \cdot 7\text{H}_2\text{O}$  (P1). Calculate the yield of crystals and make a heat balance to determine the total heat absorbed,  $q$ , assuming that no water is vaporized.

**Solution:** Making a water balance and a balance for  $\text{MgSO}_4$  using equations similar to (29.1-1) and (29.1-2) in Example 29.1-1,  $C = 616.9$  kg  $\text{MgSO}_4 \cdot 7\text{H}_2\text{O}$  crystals and  $S = 1651.1$  kg solution.

To make a heat balance, a datum of 293.2 K (20°C) will be used. The molecular weight of  $\text{MgSO}_4 \cdot 7\text{H}_2\text{O}$  is 246.49. The enthalpy of the feed is  $H_1$ :

$$H_1 = 2268(327.6 - 293.2)(2.93) = 228\,600 \text{ kJ}$$

The heat of solution is  $-(13.31 \times 10^3)/246.49 = -54.0$  kJ/kg crystals. Then, the heat of crystallization is  $-(-54.0) = +54.0$  kJ/kg crystals, or  $54.0(616.9) = 33\,312$  kJ. This assumes that the value at 291.2 K is the same as at 293.2 K. The total heat absorbed,  $q$ , is

$$q = -228\,600 - 33\,312 = -261\,912 \text{ kJ} (-248\,240 \text{ btu})$$

Since  $q$  is negative, heat is given off and must be removed.

## 29.1D Equipment for Crystallization

*1. Introduction and classification of crystallizers.* Crystallizers may be classified according to whether they are batch or continuous in operation. Batch operation is done for certain

special applications. Continuous operation of crystallizers is generally preferred.

Crystallization cannot occur without *supersaturation*. A main function of any crystallizer is to cause a supersaturated solution to form. Crystallizing equipment can be classified according to the methods used to bring about supersaturation as follows: (1) supersaturation produced by cooling the solution with negligible evaporation—tank and batch-type crystallizers; (2) supersaturation produced by evaporation of the solvent with little or no cooling—evaporator–crystallizers and crystallizing evaporators; (3) supersaturation by combined cooling and evaporation in an adiabatic evaporator—vacuum crystallizers.

In crystallizers producing supersaturation by cooling, the substances must have a solubility curve that decreases markedly with temperature. This occurs for many substances and this method is commonly used. When the solubility curve changes little with temperature, as for common salt, evaporation of the solvent to produce supersaturation is often used. Sometimes evaporation with some cooling may be used. In the method of cooling adiabatically in a vacuum, a hot solution is introduced into a vacuum, where the solvent flashes or evaporates and the solution is cooled adiabatically. This method for producing supersaturation is the most important one for large-scale production.

In another method of classification of crystallizers, the equipment is classified according to the method of suspending the growing product crystals. Examples are crystallizers where the suspension is agitated in a tank, is circulated by a heat exchanger, or is circulated in a scraped surface exchanger.

An important difference between many commercial crystallizers is the manner in which the supersaturated liquid contacts the growing crystals. In one method, called the *circulating magma method*, the entire magma of crystals and supersaturated liquid is circulated through both the supersaturation and crystallization steps without separating the solid from the liquid into two streams. Crystallization and supersaturation are occurring together in

the presence of the crystals. In a second method, called the *circulating liquid method*, a separate stream of supersaturated liquid is passed through a fluidized bed of crystals, where the crystals grow and new ones form by nucleation. Then, the saturated liquid is passed through an evaporating or cooling region to produce supersaturation again for recycling.

2. *Tank crystallizers*. In tank crystallization, which is an old method still used in some specialized cases, hot saturated solutions are allowed to cool in open tanks. After a period of time, the mother liquor is drained and the crystals removed. Nucleation and the size of crystals are difficult to control. Crystals contain considerable amounts of occluded mother liquor. In some cases,

the tank is cooled by coils or a jacket and an agitator is used to improve the heat-transfer rate. However, crystals often build up on these surfaces. This type of crystallizer has limited application; it is sometimes used to produce certain fine chemicals and pharmaceutical products.

*3. Scraped surface crystallizers.* One type of scraped surface crystallizer is the Swenson–Walker crystallizer, which consists of an open trough 0.6 m wide with a semicircular bottom having a cooling jacket outside. A slow-speed spiral agitator rotates and suspends the growing crystals as it turns. The blades pass close to the wall and break off any deposits of crystals on the cooled wall. The product generally has a somewhat wide crystal-size distribution.



In the double-pipe scraped surface crystallizer, cooling water passes in the annular space. An internal agitator is fitted with spring-loaded scrapers that wipe the wall and provide good heat-transfer coefficients. This type is called a votator and is used in crystallizing ice cream and plasticizing margarine.

*4. Circulating-liquid evaporator–crystallizer.* In a combination evaporator–crystallizer, shown in Fig. 29.1-3a, supersaturation is generated by evaporation. The circulating liquid is drawn by the screw pump down inside the tube side of the condensing steam heater. The heated liquid then flows into the vapor space, where flash evaporation occurs, giving some supersaturation. The vapor leaving is condensed. The supersaturated liquid flows down the

downflow tube and then up through the bed of fluidized and agitated crystals, which are growing in size. The exiting saturated liquid then goes back as a recycle stream to the heater, where it is joined by the entering feed. The larger crystals settle out and a slurry of crystals and mother liquor is withdrawn as product. This type is also called the *Oslo crystallizer*.

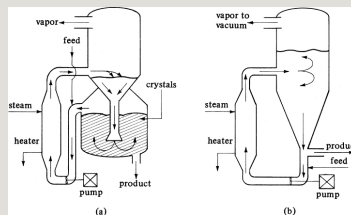


Figure 29.1-3. Types of crystallizers: (a) circulating-liquid evaporator-crystallizer, (b) circulating-magma vacuum-type crystallizer.

**5. Circulating-magma vacuum crystallizer.** In the circulating-magma vacuum-type crystallizer shown in Fig. 21.1-3b, the magma or suspension of

crystals is circulated out of the main body through a circulating pipe by a screw pump. The magma flows through a heater, where its temperature is raised 2–6 K. The heated liquor then mixes with body slurry and boiling occurs at the liquid surface. This causes supersaturation in the swirling liquid near the surface, which results in deposits on the swirling suspended crystals until they exit again via the circulating pipe. The vapors exit through the top. A steam-jet ejector provides the vacuum.

## **29.2 Crystallization Theory**

### **29.2A Introduction**

When crystallization occurs in a homogeneous mixture, a new solid phase is created. An understanding of the mechanisms by which crystals

form and then grow is helpful in designing and operating crystallizers. Much experimental and theoretical work has been done to help understand crystallization.

The overall process of crystallization from a supersaturated solution is considered to consist of the basic steps of nucleus formation, or nucleation, and of crystal growth. If the solution is free of all solid particles, whether foreign or of the crystallizing substance, then nucleus formation must first occur before crystal growth starts. New nuclei may continue to form while the nuclei present are growing. The driving force for the nucleation step as well as the growth step is supersaturation. These two steps do not occur in a saturated or undersaturated solution.

## 29.2B Nucleation Theories

*1. Solubility and crystal size.* In a solution at a given temperature, the thermodynamic difference between small and large particles or crystals is that the small particle has a significant amount of surface energy per unit mass, whereas the large particle does not. As a result, the solubility of a small crystal, of less than micrometer size, is greater than that of a larger-size crystal.

The ordinary solubility applies only to moderately large crystals. Hence, in a supersaturated solution, a small crystal can be in equilibrium. If a larger crystal is also present, the larger crystal will grow and the smaller crystal will dissolve. This effect of particle size is an important factor in nucleation.

2. *Homogeneous nucleation.* As a result of rapid random fluctuations of molecules in a homogeneous solution, the molecules may come together and associate into a cluster. This loose aggregate may quickly disappear. However, if the supersaturation is large enough, then sufficient particles may associate to form a nucleus, which can grow and become oriented into a fixed lattice to form a crystal. The number of particles needed to form a stable nucleus ranges up to a few hundred. In solutions with high supersaturation and no agitation, homogeneous nucleation may be important.

3. *Contact nucleation.* There are two types of contact nucleation. In the first type, the formation of new nuclei by contact nucleation is due to interference

of the contacting agent (walls of a container or agitator blades) with clusters of solute molecules becoming organized into the existing crystals and by actual breakage of microscopic growths on the surface of the growing crystals. In the second type, the formation of new nuclei occurs in collisions between crystals. The intensity of agitation is an important factor in contact nucleation.

This phenomenon of contact nucleation has been isolated and studied experimentally (C4) and a correlation has been developed. In practice, experimental data from an actual crystallizer are required for design.

*4. Nucleation in commercial crystallizers.* In commercial

crystallizers, supersaturation is low and agitation is used to keep the crystals suspended. At low supersaturation, the crystal growth rate is at the optimum for more-uniform crystals. The predominant mechanism is contact nucleation.

Homogeneous nucleation is largely absent because of the agitation and low supersaturation.

### **29.2C Rate of Crystal Growth and the $\Delta L$ Law**

*1. Rate of crystal growth and growth coefficients.* The rate of growth of a crystal face is the distance moved per unit time in a direction that is perpendicular to the face. Crystal growth is a layer-by-layer process, and since growth can occur only at the outer face of the crystal, the solute material must be transported to that face from the bulk of the



solution. The solute molecules reach the face by diffusion through the liquid phase. The usual mass-transfer coefficient  $k_y$  applies in this case. At the surface, the resistance to integration of the molecules into the space lattice at the face must be considered. This reaction at the surface occurs at a finite rate, and the overall process consists of two resistances in series. The solution must be supersaturated for the diffusion and interfacial steps to proceed.

The equation for mass transfer of solute A from the bulk solution of supersaturation concentration  $y_A$ , mole fraction of A, to the surface where the concentration is  $y'_A$ , is

$$N^{\text{--}}AA_i = k_y(y_A - y_{A'}) \quad (29.2-1)$$

where  $k_y$  is the mass-transfer coefficient in  $\text{kg mol/s} \cdot \text{m}^2 \text{ mol frac}$ ,  $N^{\text{--}}A$  is rate in  $\text{kg mol A/s}$ , and  $A_i$  is area in  $\text{m}^2$  of surface  $i$ . Assuming that the rate of reaction at the crystal surface is also dependent on the concentration difference,

$$N^{\text{--}}AA_i = k_s(y_{A'} - y_{Ae}) \quad (29.2-2)$$

where  $k_s$  is a surface-reaction coefficient in  $\text{kg mol/s} \cdot \text{m}^2 \text{ mol frac}$  and  $y_{Ae}$  is the saturation concentration. Combining Eqs. (29.2-1) and (29.2-2),

$$N^{\text{--}}AA_i = y_A - y_{Ae} \frac{1}{1/k_y + 1/k_s} = K(y_A - y_{Ae}) \quad (29.2-3)$$

where  $K$  is the overall transfer coefficient.

The mass-transfer coefficient  $k_y$  can be predicted by methods given in Section 21.4 for convective mass-transfer coefficients. When the mass-transfer coefficient  $k_y$  is very large, the surface reaction is controlling and  $1/k_y$  is negligible. Conversely, when the mass-transfer coefficient is very small, diffusional resistance is controlling. Surface-reaction coefficients and overall transfer coefficients have been measured and reported for a number of systems (B4, H2, P3, V1). Much of the information in the literature is not directly applicable, because the conditions of measurement differ greatly from those in a commercial crystallizer. Also, the velocities and the level of supersaturation in a system are difficult to determine and vary with the position of the circulating magma in the

crystallizer.

## *2. The $\Delta L$ law of crystal growth.*

McCabe (M4) has shown that all crystals that are geometrically similar and of the same material in the same solution grow at the same rate. Growth is measured as the increase in length  $\Delta L$ , in mm, in the linear dimension of one crystal. This increase in length is for geometrically corresponding distances on all crystals. This increase is independent of the initial size of the initial crystals, provided that all the crystals are subject to the same environmental conditions. This law follows from Eq. (29.2-3), where the overall transfer coefficient is the same for each face of all crystals.

Mathematically, this can be written as

$$\Delta L \Delta t = G(29.2-4)$$

where  $\Delta t$  is time in h and growth rate  $G$  is a constant in mm/h. Hence, if  $D_1$  is the linear dimension of a given crystal at time  $t_1$  and  $D_2$  at time  $t_2$ ,

$$\Delta L = D_2 - D_1 = G(t_2 - t_1)(29.2-5)$$

The total growth ( $D_2 - D_1$ ) or  $\Delta L$  is the same for all crystals.

The  $\Delta L$  law fails in cases where the crystals are given any different treatment based on size. It has been found to hold for many materials, particularly when the crystals are under 50 mesh in size (0.3 mm). Even though this law is not applicable in all cases, it is reasonably accurate in many situations.

## 29.2D Particle Size Distribution of Crystals

An important factor in the design of crystallization equipment is the expected particle size distribution of the crystals obtained. Usually, the dried crystals are screened to determine the particle sizes. The percent retained on different-size screens is recorded. The screens or sieves used are the Tyler standard screens, whose sieve or clear openings in mm are given in Appendix A.5-3.

The data are plotted as the particle diameter (sieve opening in screen) in mm versus the cumulative percent retained at that size on arithmetic probability paper. Data for urea particles from a typical crystallizer (B5) are shown in Fig. 29.2-1. Many types of

such data will show an approximate straight line for a large portion of the plot.

A common parameter used to characterize the size distribution is the coefficient of variation, CV, as a percent:

$$CV = 100 \frac{PD_{84\%} - PD_{16\%}}{PD_{50\%}} \quad (29.2-6)$$

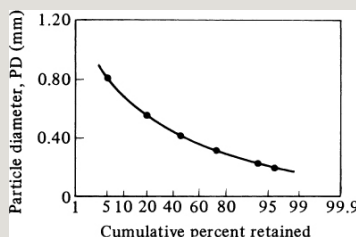


Figure 29.2-1. *Typical particle size distribution from a crystallizer.*  
 From R. C. Bennett and M. Van Buren, *Chem. Eng. Progr. Symp.*,  
**65**(95), 46 (1969).

where  $PD_{16\%}$  is the particle diameter at 16% retained. By giving the coefficient

of variation and mean particle diameter, a description of the particle size distribution is obtained if the line is approximately straight between 90 and 10%. For a product removed from a mixed-suspension crystallizer, the CV value is about 50% (R1). In a mixed-suspension system, the crystallizer is at steady state and contains a well-mixed-suspension magma with no product classification and no solids entering with the feed.

## **29.2E Model for Mixed Suspension–Mixed Product Removal Crystallizer**

### *1. Introduction and model*

*assumptions.* This model will be derived for a mixed suspension–mixed product removal (MSMPR) crystallizer, which is by far the most important type of crystallizer in use in industry today. Conditions



assumed are as follows: steady state, suspension completely mixed, no product classification, uniform concentration, no crystals in feed, and the  $\Delta L$  law of crystal growth applies. All continuous crystallizers have mixing by an agitator or by a pump. In ideal mixing, the effluent composition is the same as in the vessel. This is similar to a CSTR continuous-stirred tank reactor.

## *2. Crystal population-density function $n$ .*

To analyze data from a crystallizer, an overall theory must consider combining the effects of nucleation rate, growth rate, and material balance. Randolph and Larson (R1, R2, R3) derived such a model. They plotted the total cumulative number of crystals  $N$  per unit volume of suspension (usually 1 L of size and

smaller) versus this size  $L$ , as in Fig. 29.2-2. The slope  $dN/dL$  of this line is defined as the crystal population density  $n$ :

$$n = dN/dL \quad (29.2-7)$$

where  $n$  is the number of crystals/(L · mm) This characterizes the nuclear growth rate of this crystallizer. For this model, a relation between population density  $n$  and size  $L$  is desired.

This population density is obtained experimentally by screen analysis of the total crystal content of a given volume, such as 1.0 L of magma suspension. Each sieve fraction by weight is obtained by collection between two closely spaced and adjacent screens. Then,  $L_{av} = (L_1 + L_2)/2$ , where  $L_1$  and  $L_2$

are the openings in mm in the two adjacent screens. Also,  $\Delta L = (L_1 - L_2)$  where  $L_1$  is the size opening of the upper screen. Then, the volume of a particle  $v_p$  is

$$v_p = aL^3 \quad (29.2-8)$$

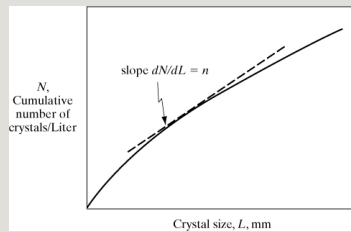


Figure 29.2-2. Determination of population density  $n$  of crystals.

where  $v_p$  is  $\text{mm}^3/\text{particle}$  and  $a$  is a constant shape factor. Knowing the total weight of the crystals in this fraction, the density  $\rho$  in  $\text{g}/\text{mm}^3$ , and the weight of each crystal, which is  $\rho v_p$ , the total number of crystals  $\Delta N$  is obtained for the size range  $\Delta L$ .

Then, rewriting Eq. (29.2-7) for this  $\Delta L$  size,

$$n = dN/dL \cong \Delta N/\Delta L \quad (29.2-9)$$

This method permits the calculation of  $n$  for each fraction collected in the screen analysis with an average size of  $L_{av}$  mm.

*3. Population material balance.* To make a population material balance in  $\Delta t$  time,  $\Delta n \Delta L$  crystals are withdrawn. Since the effluent composition in the outflow of  $Q$  L/h is the same as that in the crystallizer, then the ratio  $(\Delta n \Delta L)/(n \Delta L)$ , or fraction of particles withdrawn during  $\Delta t$  time, is the same as the volume ratio  $Q \Delta t$  withdrawn divided by the total volume  $V$  of the crystallizer. Hence,

$$-\Delta n \Delta L n \Delta L = Q \Delta t V \quad (29.2-10)$$

During this time period  $\Delta t$ , the growth  $\Delta L$  of a crystal is

$$\Delta L = G \Delta t \quad (29.2-11)$$

where  $G$  is growth rate in mm/h.

Combining Eqs. (29.2-10) and (29.2-11),

$$-\Delta n = Q \Delta L / V G \quad (29.2-12)$$

Letting  $\Delta L \rightarrow 0$ ,  $\Delta n \rightarrow 0$ , and integrating,

$$\int_{n_0}^n n \, dn = -1/G \tau \int_0^L L \, dL \quad (29.2-13)$$

$$\ln n = LG\tau + \ln n_0 \quad (29.2-14)$$

where  $n_0$  is the population of nuclei when  $L = 0$ ,  $n$  is the population when the size is  $L$ , and  $V/Q$  is the total retention or holdup time in h in the crystallizer. A plot of Eq. (29.2-14) of  $\ln$

$n$  versus  $L$  is a straight line with intercept  $n_0$  and slope  $-1/G\tau$ . If the line is not straight, this could be an indication of the violation of the  $\Delta L$  law. These calculations are well suited for being done with a computer spreadsheet.

*4. Average particle size and nucleation rate.* Further derivation of the population approach results in the equation for the average size  $L_a$  in mm of the mass distribution:

$$L_a = 3.67G\tau(29.2-15)$$

Here, 50% of the mass of the product is smaller or larger in size than this value. Also, the predominant particle size is given as

$$L_d = 3.00G\tau(29.2-16)$$

This predominant particle size means more of the mass is in this differential size interval than in any other size interval.

Another relation can be obtained from this model, which relates the nucleation rate  $B_0$  to the value of the zero-size particle population density  $n_0$  and the growth rate  $G$ . For the condition  $L \rightarrow 0$ , the limit of  $dN/dt$  (nucleation rate) can be written as

$$\lim_{L \rightarrow 0} \frac{dN}{dt} = \lim_{L \rightarrow 0} \frac{dN}{dL} \frac{dL}{dt} \quad (29.2-17)$$

However, when  $L \rightarrow 0$ , the slope  $dL/dt = G$ , the slope  $dN/dL = n_0$ , and  $B_0 = dN/dt$ . Hence,

$$B_0 = G n_0 \quad (29.2-18)$$

where  $B_0$  is nucleation rate in number of

nuclei/h · L.

*5. Prediction of cumulative weight fraction obtained.* The population equation can be used to perform a reverse calculation when only the values of  $G$  and  $\tau$  are known. The following equation has been derived from the population density function (L4):

$$(1-W_f) = e^{-x} \left( 1 + x + \frac{x^2}{2} + \frac{x^3}{6} \right) \quad (29.2-19)$$

where  $x = L/G\tau$ , and  $(1 - W_f)$  is the cumulative wt fraction at opening  $L$  mm, which is in the same form of results as from a screen analysis.

*6. Use of the population-model approach for process design.* The data for experimental crystal growth rate  $G$  and nucleation rate  $B_0$  obtained by



means of the population material balance are for one given set of conditions in the crystallizer. Then, additional experiments can be conducted to determine the effect of residence time  $\tau$  (production rate) and, possibly, the pump-around rate (mixing) on  $B_0$  and  $G$ . This is done until the desired distribution  $W_f$  from Eq. (29.2-19) is achieved. Or, in some cases, the goal may be for a desired dominant size  $L_d$  to be obtained. In many cases, as the residence time  $\tau$  is increased, the experimental growth rate  $G$  decreases. Additional useful references are (B6, C2, C4, L5, M2, P1, R4, S2).

**EXAMPLE 29.2-1. Growth and Nucleation Rates in an MSMPR Crystallizer**

Calculate the population density and nucleation growth rates for crystal samples of urea from a screen analysis. The slurry density (g of crystals) is 450 g/liter, the crystal shape factor  $a$  is 1.00, the crystal density  $\rho$  is 1.335 g/cm<sup>3</sup>, and the residence time  $\tau$  is 3.38 h. The screen analysis from reference (B5) is as follows:

**Solution:** The data above are tabulated in Table 29.2-1 using data from Appendix A.5-3. The value of  $L$  is the screen opening. For the 14–20 mesh portion,  $L_{av} = (1.168 + 0.833)/2 = 1.001$  mm and  $\Delta L = 1.168 - 0.833 = 0.335$  mm. For  $L_{av} = 1.001$  mm, using Eq. (29.2-8),  $u_p = aL_{3av} = 1.00(1.001)^3 = 1.003$  mm<sup>3</sup>/particle. The density  $\rho = 1.335$  g/cm<sup>3</sup> =  $1.335 \times 10^{-3}$  g/mm<sup>3</sup> and the mass/particle =  $\rho u_p = 1.335 \times 10^{-3}(1.003) = 1.339 \times 10^{-3}$  g. The total mass of crystals = (450 g/L) (0.044 wt frac).

Using Eq. (29.2-9) to calculate  $n$  for the 14–20 mesh size range,

$$n = \frac{\Delta N \Delta L}{(450 \text{ g/L})(\text{wt frac})\rho(aL)^3} = \frac{(450 \text{ g/L})(0.044)}{(1.335 \times 10^{-3} \text{ g/mm}^3)(100)} \\ (1001 \text{ mm})^3 (0.335 \text{ mm}) = 4.414 \times 10^4 \text{ number of crystals/L} \cdot \text{mm}$$

Then,  $\ln n = \ln 4.414 \times 10^4 = 10.695$ . For the 20–28 mesh size range,  $L_{av} = 0.711$  mm, and  $\Delta L = 0.244$ . Then,

$$n = \frac{(450)(0.144)(1.335 \times 10^{-3})(1.00)}{(0.711)^3 (0.244)} = 5.535 \times 10^5$$

Then,  $\ln n = 13.224$ . Other values are calculated in a similar manner using a computer spreadsheet and are given in Table 29.2-1.

The  $\ln n$  is plotted versus  $L$  in Fig. 29.2-3. The equation of this line is Eq. (29.2-14), where the slope is  $-9.12$  and the intercept = 19.79:

$$\ln n = -9.12L + 19.79 = -LG_T + \ln n_0$$

Table 29.2-1. *Data and Calculations for Example 29.2-1*

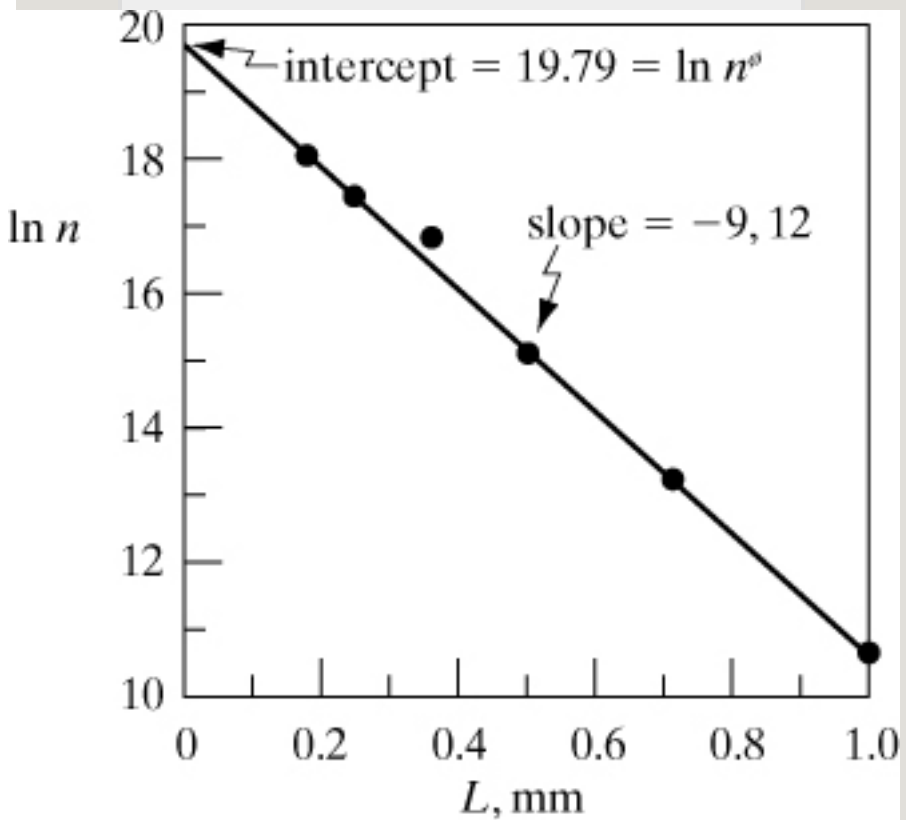


Figure 29.2-3. Plot of population density  $n$  versus length for Example 29.2-1.

The slope  $-9.12 = -1/Gr = -1/(G)(3.38)$ . Hence,  $G = 0.03244$  mm/h. The intercept  $\ln n_0 = 19.79$ . Hence,  $n_0 = 3.933 \times 10^8$ . From Eq. (29.2-18), the nucleation rate  $B_0$  is

$$B_0 = Gn_0 = 0.03244(3.933 \times 10^8) = 1.276 \times 10^7 \text{ nuclei/h} \cdot L$$

The average size is, from Eq. (29.2-15),  $L_a = 3.67Gr = 3.67(0.03244)(3.38) = 0.402$  mm. The predominant size, from Eq. (29.2-16), is  $L_d = 3.00Gr = 3.00(0.03244)(3.38) = 0.329$  mm.

## 29.3 Mechanical Size Reduction

### 29.3A Introduction

Many solid materials occur in sizes that are too large to be used and must be reduced. Often, the solids are reduced in size so that the separation of various ingredients can be carried out. In general, the terms *crushing* and *grinding* are used to signify the subdividing of large solid particles into smaller particles.

In the food-processing industry, a large number of food products are subjected to size reduction. Roller mills are used to grind wheat and rye into flour and to grind corn into cornmeal. Soybeans are rolled, pressed, and ground to produce oil and flour. Hammer mills are often used to produce potato flour and tapioca, as well as other types of flours. Sugar is ground to a finer product.

Grinding operations are very extensive in the ore-processing and cement industries. Copper ores, nickel and cobalt ores, and iron ores, for example, are ground before chemical processing. Limestone, marble, gypsum, and dolomite are ground to use as fillers in paper, paint, and rubber. Raw materials for the cement industry, such as lime, alumina, and silica, are ground on a very large scale.

Solids may be reduced in size by a number of methods. *Compression* or *crushing* is generally used for the reduction of hard solids to coarse particles, while *impact* results in coarse, medium, or fine particles. *Attrition* or *rubbing* yields fine products. *Cutting* is used to give specific sizes.

The feed-to-size reduction processes and the product are defined in terms of the particle size distribution. One common way to plot particle sizes is to plot particle diameter (sieve opening in a screen) in mm or  $\mu\text{m}$  versus the cumulative percent retained at that size. (Openings for various screen sizes are given in Appendix A.5.) Such a plot is given on arithmetic probability paper in Fig. 29.2-2.

Often, the plot is made as the cumulative amount, as percent smaller than the stated size, versus particle size, as shown in Fig. 29.3-1a. In Fig. 29.3-1b, the same data are plotted as a particle-distribution curve. The ordinate is obtained by taking the slopes of the 5- $\mu\text{m}$  intervals of Fig. 29.3-1a and

converting to percent by weight per  $\mu\text{m}$ . Complete particle size analysis is necessary for most comparisons and calculations.

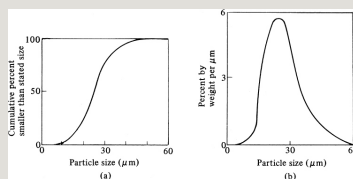


Figure 29.3-1. *Particle size distribution curves: (a) cumulative percent versus particle size, (b) percent by weight per  $\mu\text{m}$  versus particle size. From R. H. Perry and C. H. Chilton, Chemical Engineers' Handbook, 5th ed. New York: McGraw-Hill Book Company, 1973. With permission.*

### 29.3C Energy and Power Required in Size Reduction

*1. Introduction.* In size reduction of solids, feed materials of a solid are reduced to a smaller size by mechanical action. The materials are fractured; the particles of feed are first distorted and strained by the action of the size-reduction machine. This work to strain the particles is

first stored temporarily in the solid as strain energy. As additional force is added to the stressed particles, the strain energy exceeds a certain level and the material fractures into smaller pieces.

When the material fractures, new surface area is created. Each new unit area of surface requires a certain amount of energy. Some of the energy added is used to create the new surface, but a large portion of it appears as heat. The energy required for fracture is a complicated function of the type of material, its size and hardness, and other factors.

The magnitude of the mechanical force applied, the duration of the applied force, the type of force, such as



compression, shear, or impact, and other factors affect the extent and efficiency of the size-reduction process. The important factors in the size-reduction process are the amount of energy or power used and the particle size and new surface formed.

*2. Power required in size reduction.* The various theories or laws proposed for predicting power requirements for size reduction of solids do not apply well in practice. The most important ones will be discussed briefly. Part of the problem with these theories is estimating the theoretical amount of energy required to fracture and create new surface area. Approximate calculations give actual efficiencies of about 0.1 to 2%.

The theories derived depend on the

assumption that the energy  $E$  required to produce a change  $dX$  in a particle of size  $X$  is a power function of  $X$ :

$$dE/dX = -CX^n \quad (29.3-1)$$

where  $X$  is the size or diameter of a particle in mm, and  $n$  and  $C$  are constants, depending on the type and size of material and the type of machine.

Rittinger proposed a law that states that the work in crushing is proportional to the new surface created. This leads to a value of  $n = 2$  in Eq. (29.3-1), since area is proportional to length squared.

Integrating Eq. (29.3-1),

$$E = Cn^{-1}(X_2^{2n-1} - X_1^{2n-1}) \quad (29.3-2)$$

where  $X_1$  is the mean diameter of feed and  $X_2$  is the mean diameter of the

product. Since  $n = 2$  for Rittinger's equation, we obtain

$$E = KR(1/X_2 - 1/X_1) \quad (29.3-3)$$

where  $E$  is the work required to reduce a unit mass of feed from  $X_1$  to  $X_2$  and  $KR$  is a constant. The law implies that the same amount of energy is needed to reduce a material from 100 mm to 50 mm as is needed to reduce the same material from 50 mm to 33.3 mm. It has been found experimentally that this law has some validity in grinding fine powders.

Kick assumed that the energy required to reduce a material in size was directly proportional to the size-reduction ratio. This implies  $n = 1$  in Eq. (29.3-1), giving

$$E = C \ln X_1 X_2 = K \log X_1 X_2 \quad (29.3-4)$$

where  $K$  is a constant. This law implies that the same amount of energy is required to reduce a material from 100 mm to 50 mm as is needed to reduce the same material from 50 mm to 25 mm.

Recent data by Bond (B3) on correlating extensive experimental data suggest that the work required using a large-size feed is proportional to the square root of the surface/volume ratio of the product.

This corresponds to  $n = 1.5$  in Eq. (29.3-1), giving

$$E = K_B X_2 \quad (29.3-5)$$

where  $K_B$  is a constant. To use Eq. (14.4-5), Bond proposed a work index  $E_i$  as the work in kW · h/ton required to reduce a unit weight from a very large

size to 80% passing a 100- $\mu\text{m}$  screen. Then, the work  $E$  is the gross work required to reduce a unit weight of feed with 80% passing a diameter  $X_F$   $\mu\text{m}$  to a product with 80% passing a diameter  $X_P$   $\mu\text{m}$ .

Bond's final equation, in terms of English units, is

$$PT = 1.46 E_i (1/D_P - 1/D_F) \quad (29.3-6)$$

where  $P$  is hp,  $T$  is feed rate in tons/min,  $D_F$  is size of feed in ft, and  $D_P$  is product size in ft. Typical values of  $E_i$  for various types of materials are given in Perry and Green (P1) and by Bond (B3). Some typical values are bauxite ( $E_i = 9.45$ ), coal (11.37), potash salt (8.23), shale (16.4), and granite (14.39). These values should be multiplied by

## 1.34 for dry grinding.

### **EXAMPLE 29.3-1. Power Required by Bond's Theory to Crush Iron Ore**

It is desired to crush 10 ton/h of iron ore hematite. The size of the feed is such that 80% passes a 3-in. (76.2-mm) screen and 80% of the product is to pass a 18-in. (3.175-mm) screen. Calculate the gross power required. Use a work index  $E_i$  for iron ore hematite of 12.68 (P1).

**Solution:** The feed size is  $DF=3/12=0.250$  ft (76.2 mm) and the product size is  $DP=18/12=0.0104$  ft (3.175 mm). The feed rate is  $T = 10/60 = 0.167$  ton/min. Substituting into Eq. (29.3-6) and solving for  $P$ ,

$$P(0.167)=(1.46)(12.68)(100104-10250)P=(17.96 \text{ kW})$$

## 29.3D Equipment for Particle Size Reduction

### *1. Introduction and classification.*

Size-reduction equipment may be classified according to the way the forces are applied as follows:

between two surfaces, as in crushing and shearing; at one solid surface, as in impact; and by action of the surrounding medium, as in a colloid mill. A more practical classification is to divide the equipment into

crushers, grinders, fine grinders, and cutters.

2. *Jaw crushers*. Equipment for coarse reduction of large amounts of solids consists of slow-speed machines called *crushers*. Several types are in common use. In the first type, a jaw crusher, the material is fed between two heavy jaws or flat plates. As shown in the *Dodge crusher* in Fig. 29.3-2a, one jaw is fixed and the other is reciprocating and moves on a pivot point at the bottom. The jaw swings back and forth, pivoting at the bottom of the V. The material is gradually worked down into a narrower space, being crushed as it moves.

The *Blake crusher* in Fig. 29.3-2b is more commonly used, where the pivot point is at the top of the movable jaw.

The reduction ratios average about 8:1 in the Blake crusher. Jaw crushers are used mainly for the primary crushing of hard materials and are usually followed by other types of crushers.

*3. Gyratory crushers.* The *gyratory crusher* shown in Fig. 29.3-3a has, to a large extent, taken over in the field of large hard-ore and mineral-crushing applications. Basically, it is like a mortar-and-pestle crusher. The movable crushing head is shaped like an inverted truncated cone and is inside a truncated cone casing. The crushing head rotates eccentrically and the material being crushed is trapped between the outer fixed cone and the inner gyrating cone.



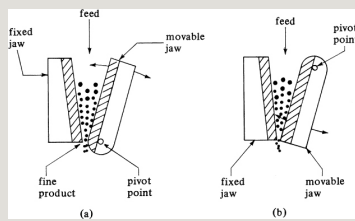


Figure 29.3-2. *Types of jaw crushers: (a) Dodge type, (b) Blake type.*

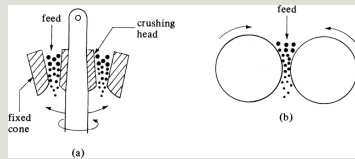


Figure 29.3-3. *Types of size-reduction equipment: (a) gyratory crusher, (b) roll crusher.*

**4. Roll crushers.** In Fig. 29.3-3b, a typical smooth *roll crusher* is shown. The rolls are rotated toward each other at the same or different speeds. Wear of the rolls is a serious problem. The reduction ratio varies from about 4:1 to 2.5:1. Single rolls are often used, rotating against a fixed surface, and corrugated and toothed rolls are also used. Many food products that are not

hard materials, such as flour, soybeans, and starch, are ground on rolls.

*5. Hammer mill grinders. Hammer mill devices* are used to reduce intermediate-size material to small sizes or to a powder. Often, the product from jaw and gyratory crushers is the feed to the hammer mill. In the hammer mill, a high-speed rotor turns inside a cylindrical casing. Sets of hammers are attached to pivot points at the outside of the rotor. The feed enters the top of the casing and the particles are broken as they fall through the cylinder. The material is broken by the impact of the hammers and pulverized into powder between the hammers and casing. The powder then passes through a grate or screen at the discharge end.

6. *Revolving grinding mills*. For the intermediate and fine reduction of materials, *revolving grinding mills* are often used. In such mills, a cylindrical or conical shell rotating on a horizontal axis is charged with a grinding medium such as steel, flint, or porcelain balls, or with steel rods. The size reduction is effected by the tumbling of the balls or rods on the material between them. In the revolving mill, the grinding elements are carried up the side of the shell and fall on the particles underneath. These mills may operate under wet or dry conditions.

Equipment for very fine grinding is highly specialized. In some cases, two flat disks are used, where one or both disks rotate and grind the material caught between the disks (P1).

## 29.4 Chapter Summary

In this chapter, we have introduced the concepts of crystallization and particle size reduction.

Crystallization was described as a solid–liquid separation process where solid particles are formed from a homogeneous liquid phase. Although the yield and purity of the crystals are important, size and shape uniformity is often equally desirable. To help classify the crystals that are formed, different types of crystal geometries were described.

During the crystallization process, it is necessary to understand the equilibrium solubility of the crystal to be formed. By understanding the equilibrium solubility and heat of crystallization, material and

energy balances can be performed to predict the composition of the product stream from a crystallizer. Multiple examples of batch and continuous crystallizers were provided for different types of industrial applications.

To help theoretically predict the solid attributes of the crystals formed in a crystallizer, an introduction to crystallization theory was provided. At the core of crystallization theory are several nucleation theories (e.g., homogenous nucleation, contact nucleation) that are dependent on the mass-transfer behavior and kinetic interactions between the solid and homogeneous fluid phases. To provide further insight into these theories, the rate of crystal growth and the  $\Delta L$  law of crystal growth were introduced and

given by:

$$\Delta L \Delta t = G(29.2-4)$$

As previously stated, an important property of the crystallization process is the particle size uniformity of the product stream. Particle size distributions were introduced as a way to describe the overall distribution of the product stream, including the mean particle size and standard deviation. Particle size distributions and the  $\Delta L$  law of crystal growth were linked together to develop a population balance model that could be used for mixed suspension–mixed product removal (MSMPR) crystallizers. These models were given by:

$$n = dN/dL \cong \Delta N \Delta L(29.2-9)$$

and

$$\ln n = LG\tau + \ln n_0 \quad (29.2-14)$$

The last part of this chapter focused on size reduction. Different techniques to reduce the particle size, such as milling, crushing, compression, attrition, and cutting were described. It was shown how these processes can influence the overall particle size distribution. Models that predicted the energy and power necessary to perform size reduction were also introduced. These included the Rittinger model:

$$E = KR(1/X_2 - 1/X_1) \quad (29.3-3)$$

and the Bond model:

$$E = KB1/X_2 \quad (29.3-5)$$

## Problems

**29.1-1. Crystallization of  $Ba(NO_3)_2$ .** A hot solution of  $Ba(NO_3)_2$  from an evaporator contains 30.6 kg  $Ba(NO_3)_2/100$  kg  $H_2O$  and goes to a crystallizer, where the solution is cooled and  $Ba(NO_3)_2$  crystallizes. On cooling, 10% of the original water present evaporates. For a feed solution of 100 kg total, calculate the following:

- The yield of crystals if the solution is cooled to 290 K ( $17^\circ C$ ), where the solubility is 8.6 kg  $Ba(NO_3)_2/100$  kg total water.
- The yield if the solution is cooled instead to 283 K, where the solubility is 7.0 kg  $Ba(NO_3)_2/100$  kg total water.

**Ans.** (a) 17.47 kg  $Ba(NO_3)_2$  crystals

**29.1-2. Dissolving and Subsequent Crystallization.** A batch of 1000 kg of KCl is dissolved in sufficient water to



make a saturated solution at 363 K, where the solubility is 35 wt % KCl in water. The solution is cooled to 293 K, at which temperature its solubility is 25.4 wt %.

- What is the weight of water required for the solution and the weight of the crystals of KCl obtained?
- What is the weight of the crystals obtained if 5% of the original water evaporates on cooling?

**Ans.** (a) 1857 kg water, 368 kg crystals;  
(b) 399 kg crystals

### **29.1-3. *Crystallization of $\text{MgSO}_4 \cdot 7\text{H}_2\text{O}$***

**7H<sub>2</sub>O.** A hot solution containing 1000 kg of  $\text{MgSO}_4$  and water having a concentration of 30 wt %  $\text{MgSO}_4$  is cooled to 288.8 K, where crystals of  $\text{MgSO}_4 \cdot 7\text{H}_2\text{O}$  are precipitated. The solubility at 288.8 K is 24.5 wt % anhydrous  $\text{MgSO}_4$  in the solution.

Calculate the yield of crystals obtained if 5% of the original water in the system evaporates on cooling.

**29.1-4. *Heat Balance in Crystallization.***

A feed solution of 10 000 lb<sub>m</sub> at 130°F containing 47.0 lb FeSO<sub>4</sub>/100 lb total water is cooled to 80°F, where FeSO<sub>4</sub> · 7H<sub>2</sub>O crystals are removed. The solubility of the salt is 30.5 lb FeSO<sub>4</sub>/100 lb total water (P1). The average heat capacity of the feed solution is 0.70 btu/lb<sub>m</sub> · °F. The heat of the solution at 18°C is –4.4 kcal/g mol (–18.4 kJ/mol) FeSO<sub>4</sub> · 7H<sub>2</sub>O (P1). Calculate the yield of crystals and make a heat balance. Assume that no water is vaporized.

**Ans.** 2750 lb<sub>m</sub> FeSO<sub>4</sub> · 7H<sub>2</sub>O crystals,  $q$   
= –428 300 btu (–451 900 kJ)

### ***29.1-5. Effect of Temperature on Yield and Heat Balance in Crystallization.***

Use the conditions given in Example 29.1-2, but the solution is cooled instead to 283.2 K, where the solubility is 30.9 kg  $\text{MgSO}_4$ /100 kg total water (P1).

Calculate the effect on yield and the heat absorbed by using 283.2 K instead of 293.2 K for the crystallization.

***29.2-1. Growth and Nucleation Rate in an MSMPR Crystallizer.*** Experimental data were obtained for an MSMPR crystallizer (S2). The slurry density is 169 g/L, the crystal density  $\rho$  is 1.65 g/ $\text{m}^3$ , the residence time  $\tau$  is 6.57 h, and the shape factor  $a$  is 0.98. The screen analysis of the crystals is as follows:

Using these data, do as follows:

- Calculate the population density, growth rate, and nucleation rate. Also, calculate the average size  $L_a$ .
- Using these calculated values, predict the cumulative weight fraction versus size  $L$  from the experimental value of  $G$  and  $\tau$ . Compare the predicted and experimental values.

**Ans.** (a)  $G = 0.01673$  mm/h; (b) For  $L = 0.589$  mm,  $(1 - W_f) = 0.218$

**29.2-2. Prediction of the Cumulative Weight Fraction of Crystals from the Growth Rate.** In Example 29.2-1, the growth rate  $G$  was determined to be 0.03244 mm/h for a residence time  $\tau$  of 3.38 h. Using these values, predict the cumulative weight fraction versus size  $L$ . Compare the predicted values with the experimental values.

**Ans.**  $L = 0.589$  mm,  $(1 - W_f) = 0.217$ ;  $L = 0.417$  mm,  $(1 - W_f) = 0.473$

**29.3-1. *Change in Power Requirements in Crushing.*** In crushing a certain ore, the feed is such that 80% is less than 50.8 mm in size, and the product size is such that 80% is less than 6.35 mm. The power required is 89.5 kW. What will be the power required using the same feed so that 80% is less than 3.18 mm? Use the Bond equation. (*Hint:* The work index  $E_i$  is unknown, but it can be determined using the original experimental data in terms of  $T$ . In the equation for the new size, the same unknowns appear. Dividing one equation by the other will eliminate these unknowns.)

**Ans.** 146.7 kW

**29.3-2. *Crushing of Phosphate Rock.*** It is desired to crush 100 ton/h of

phosphate rock from a feed size where 80% is less than 4 in. to a product where 80% is less than 18 in. The work index is 10.13 (P1).

- Calculate the power required.
- Calculate the power required to crush the product further to where 80% is less than 1000  $\mu\text{m}$ .

## References

## Notation

# Chapter 30. Settling, Sedimentation, and Centrifugation

## 30.0 Chapter Objectives

On completion of this chapter, a student should be able to:

- Explain why settling and sedimentation processes are different from filtration
- Provide examples of applications for settling, sedimentation, and centrifugal separation processes
- Explain the difference between free settling and hindered settling
- Identify and calculate the forces acting on a particle while it is in motion
- Calculate the particle Reynolds number
- Calculate the terminal velocity and drag coefficient for a single falling particle in different flow regimes
- Explain how wall effects could affect the settling

properties of particles

- Show how differential settling can be used to separate and classify solids of different particle sizes
- Calculate the sedimentation settling velocity and explain why it's different from the particle settling velocity
- Identify equipment used for settling, sedimentation, and centrifugal separation operations
- Identify and calculate the forces acting on particles during a centrifugal separation process
- Show how centrifugal settling can be used to separate and classify solids of different particle sizes
- Derive the governing equations of centrifugal filtration systems
- Explain the concept of a cyclone and how centrifugal forces govern its operation

## **30.1 Settling and Sedimentation in Particle–Fluid Separation**

### **30.1A Introduction**

During the process of filtration, solid particles are removed from a slurry by forcing the fluid through a filter



medium, which blocks the passage of the solid particles and allows the filtrate to pass through. In settling and sedimentation, however, the particles are separated from the fluid by gravitational forces acting on the particles.

Applications of settling and sedimentation include removal of solids from liquid sewage wastes, settling of crystals from the mother liquor, separation of a liquid–liquid mixture from a solvent-extraction stage in a settler, settling of solid food particles from a liquid food, and settling of a slurry from a soybean leaching process. The particles can be solid particles or liquid drops. The fluid can be a liquid or gas and it may be at rest or in motion.

In some processes of settling and sedimentation, the purpose is to remove the particles from the fluid stream so that the fluid is free of particle contaminants. In other processes, the particles are recovered as the product, as in recovery of the dispersed phase in liquid–liquid extraction. In some cases, the particles are suspended in fluids so that the particles can be separated into fractions differing in size or in density.

When a particle is at a sufficient distance from the walls of the container and from other particles so that its fall is not affected by them, the process is called *free settling*. Interference is less than 1% if the ratio of the particle diameter to the container diameter is less than 1:200 or if the particle concentration is less than 0.2 vol % in

the solution. When the particles are crowded, they settle at a lower rate and the process is called *hindered settling*. The separation of a dilute slurry or suspension by gravitational settling into a clear fluid and a slurry of higher solids content is called *sedimentation*.

### **30.1B Theory of Particle Movement Through a Fluid**

*1. Derivation of basic equations for rigid spheres.* Whenever a particle is moving through a fluid, a number of forces will be acting on the particle. First, a density difference is needed between the particle and the fluid. An external force of gravity is needed to impart motion to the particle. If the densities of the fluid and the particle are equal, the buoyant force on the particle will counterbalance the external force

and the particle will not move relative to the fluid.

For a rigid particle moving in a fluid, there are three forces acting on the body: gravity acting downward, buoyant force acting upward, and resistance or drag force acting in the opposite direction to the particle's motion.

We will consider a particle of mass  $m$  kg falling at a velocity  $v$  m/s relative to the fluid. The density of the solid particle is  $\rho_p$  kg/m<sup>3</sup> solid and that of the liquid is  $\rho$  kg/m<sup>3</sup> liquid. The buoyant force  $F_b$  in N on the particle is

$$F_b = m_p g - \rho V_p g \quad (30.1-1)$$

where  $m/\rho_p$  is the volume  $V_p$  in m<sup>3</sup> of the particle and  $g$  is the gravitational acceleration in m/s<sup>2</sup>.

The gravitation or external force  $F_g$  in N on the particle is

$$F_g = mg \quad (30.1-2)$$

The drag force  $F_D$  on a body in N may be derived from the fact that, as in the flow of fluids, the drag force or frictional resistance is proportional to the velocity head  $v^2/2$  of the fluid displaced by the moving body. This must be multiplied by the density of the fluid and by a significant area  $A$ , such as the projected area of the particle. This was defined previously in Eq. (6.1-2):

$$F_D = C_D v^2 \rho A \quad (30.1-3)$$

where the drag coefficient  $C_D$  is the proportionality constant and is dimensionless.

The resultant force on the body is then  $F_g - F_b - F_D$ . This resultant force must equal the force due to acceleration:

$$m \frac{dv}{dt} = F_g - F_b - F_D \quad (30.1-4)$$

Substituting Eqs. (30.1-1)–(30.1-3) into (30.1-4),

$$m \frac{dv}{dt} = mg - m\rho g \frac{C_D A v^2}{2\rho A} \quad (30.1-5)$$

If we start from the moment the body is released from its position of rest, the body's falling consists of two periods: the period of accelerated fall and the period of constant-velocity fall. The initial acceleration period is usually very short, on the order of a tenth of a second or so. Hence, the period of constant-velocity fall is the important one. The velocity is called the *free settling*

*velocity or terminal velocity  $v_t$ .*

To solve for the terminal velocity in Eq. (30.1-5),  $dv/dt = 0$  and the equation becomes

$$v_t = \frac{2g(\rho_p - \rho)m}{A\rho C_D} \quad (30.1-6)$$

For spherical particles,  $m = \pi D_p^3 \rho / 6$  and  $A = \pi D_p^2 / 4$ . Substituting these into Eq. (30.1-6), for spherical particles we obtain

$$v_t = \frac{4(\rho_p - \rho)gD_p^3}{3C_D\rho} \quad (30.1-7)$$

where  $v_t$  is m/s (ft/s),  $\rho$  is kg/m<sup>3</sup> (lb<sub>m</sub>/ft<sup>3</sup>),  $g$  is 9.80665 m/s<sup>2</sup> (32.174 ft/s<sup>2</sup>), and  $D_p$  is m (ft).

## *2. Drag coefficient for rigid spheres.*

The drag coefficient for rigid spheres has been shown to be a function of the

Reynolds number  $D_p v \rho / \mu$  of the sphere and is shown in Fig. 30.1-1. In the laminar-flow region, called the Stokes' law region for  $N_{Re} < 1$ , as discussed in Section 6.1B, the drag coefficient is

$$C_D = 24 / N_{Re} \quad (30.1-8)$$

where  $\mu$  is the viscosity of the liquid in  $\text{Pa} \cdot \text{s}$  or  $\text{kg/m} \cdot \text{s}$  ( $\text{lb}_m/\text{ft} \cdot \text{s}$ ). Substituting this into Eq. (30.1-7) for laminar flow,

$$v_t = g D_p^2 (\rho_p - \rho) / 18 \mu \quad (30.1-9)$$

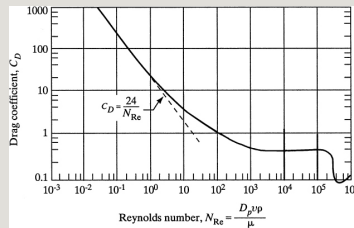


Figure 30.1-1. Drag coefficient for a rigid sphere.

For other shapes of particles, drag coefficients will differ from those given



in Fig. 30.1-1, and data are given in Fig. 6.1-2 and elsewhere (P1). In the turbulent Newton's law region above a Reynolds number of about 1000 to  $2.0 \times 10^5$ , the drag coefficient is approximately constant at  $C_D = 0.44$ .

Solution of Eq. (30.1-7) is by trial and error when the particle diameter is known and the terminal velocity is to be obtained, because  $C_D$  also depends upon the velocity  $v_t$ .

If the particles are quite small, Brownian motion is present. *Brownian motion* is the random motion imparted to the particle by collisions between the molecules of the fluid surrounding the particle and the particle. This movement of the particles in random directions tends to suppress the effect of gravity, so

settling of the particles may occur more slowly or not at all. At particle sizes of a few micrometers, the Brownian effect becomes appreciable, and at sizes of less than  $0.1\text{ }\mu\text{m}$ , the effect predominates. For very small particles, application of centrifugal force helps reduce the effect of Brownian motion.

**EXAMPLE 30.1-1. Settling Velocity of Oil Droplets**

Oil droplets having a diameter of  $20\text{ }\mu\text{m}$  ( $0.020\text{ mm}$ ) are to be settled from air at a temperature of  $37.8^\circ\text{C}$  ( $311\text{ K}$ ) and  $101.3\text{ kPa}$  pressure. The density of the oil is  $900\text{ kg/m}^3$ . Calculate the terminal settling velocity of the droplets.

**Solution:** The various knowns are  $D_p = 2.0 \times 10^{-5}\text{ m}$  and  $\rho_p = 900\text{ kg/m}^3$ . From **Appendix A.3**, for air at  $37.8^\circ\text{C}$ ,  $\rho = 1.137\text{ kg/m}^3$ ,  $\mu = 1.90 \times 10^{-5}\text{ Pa} \cdot \text{s}$ . The droplet will be assumed to be a rigid sphere.

The solution is trial and error since the velocity is unknown. Hence,  $C_D$  cannot be directly determined. The Reynolds number is as follows:

$$\begin{aligned} N_{Re} &= D_p v_t \rho / \mu = (2.0 \times 10^{-5})(v_t) \\ (1.137)1.90 \times 10^{-5} &= 1.197 v_t (30.1-10) \end{aligned}$$

For the first trial, assume that  $v_t = 0.305\text{ m/s}$ . Then,  $N_{Re} = 1.197(0.305) = 0.365$ . Substituting into Eq. (30.1-7) and solving for  $C_D$ ,

$$\begin{aligned} v_t &= 4(\rho_p - \rho)gD_p^3 / C_D \rho = 4(900 - 1.137)(9.8066)(20 \times 10^{-5}) \\ (3)C_D(1.137)c_D &= 0.2067 v_t^2 (30.1-11) \end{aligned}$$

Using  $v_t = 0.305 \text{ m/s}$ ,  $C_D = 0.2067/(0.305)^2 = 2.22$ .

Assuming that  $v_t = 0.0305 \text{ m/s}$ ,  $N_{Re} = 0.0365$  from Eq. (30.1-10) and  $C_D = 222$  from Eq. (30.1-11). For the third trial, assuming that  $v_t = 0.00305 \text{ m/s}$ ,  $N_{Re} = 0.00365$  and  $C_D = 22200$ . These three values calculated for  $N_{Re}$  and  $C_D$  are plotted on a graph similar to Fig. 30.1-1 and are shown in Fig. 30.1-2. It can be shown that the line through these points is a straight line. The intersection of this line and the drag-coefficient correlation line is the solution to the problem at  $N_{Re} = 0.012$ . The velocity can be calculated from the Reynolds number in Eq. (30.1-10):

$$N_{Re}=0.012=1.197v_tv_t=0.0100\text{m/s} \text{ (0.0328 ft/s)}$$

The particle is in the Reynolds number range less than 1, which is the laminar Stokes' law region. Alternatively, the velocity can be calculated by substituting into Eq. (30.1-9):

$$v_t=9.8066(2.0\times 10^{-5})^2(900-1.137)^{18}(1.90\times 10^{-5})=0.0103\text{m/s}$$

Note that Eq. (30.1-9) could not be used until it was determined that the particle fall was in the laminar region.

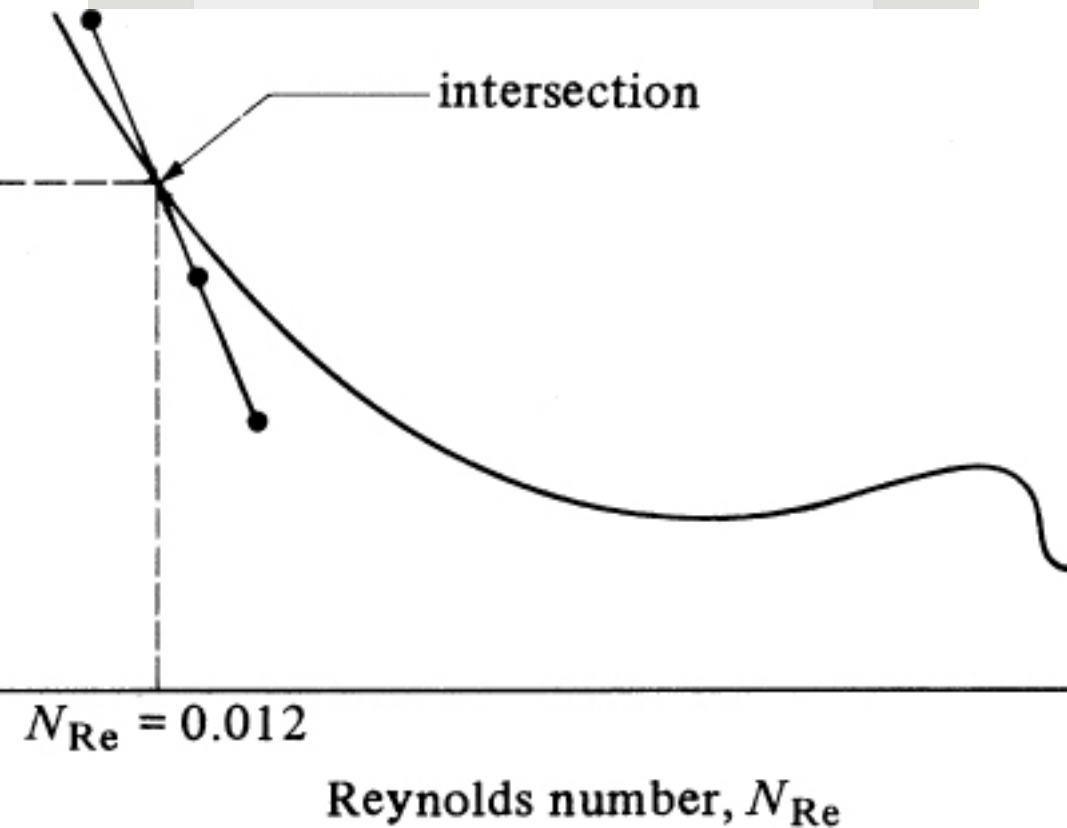


Figure 30.1-2. *Solution of Example 30.1-1 for settling velocity of a particle.*

For particles that are rigid but nonspherical, the drag depends upon the shape of the particle and the orientation of the particle with respect to its motion. Correlations of drag coefficients for particles of different shapes are given in a number of references (P1).

3. *Drag coefficients for nonrigid spheres.* When particles are nonrigid, internal circulation inside the particle and particle deformation can occur. Both of these effects affect the drag coefficient and terminal velocity. Drag coefficients for air bubbles rising in water are given in Perry and Green (P1), and for a Reynolds number less than about 50, the curve is the same as for rigid spheres in water.

For liquid drops in gases, the same drag relationship as for solid spherical particles is obtained up to a Reynolds number of about 100 (H1). Large drops will deform with an increase in drag. Small liquid drops in immiscible liquids behave like rigid spheres and the drag coefficient curve follows that for rigid spheres up to a Reynolds number of

about 10. Above this and up to a Reynolds number of 500, the terminal velocity is greater than that for solids because of internal circulation in the drop.

### **30.1C Hindered Settling**

For many cases of settling, a large number of particles are present and the surrounding particles interfere with the motion of individual particles. The velocity gradients surrounding each particle are affected by the close presence of other particles. The particles settling in the liquid displace the liquid, and an appreciable upward velocity of the liquid is generated. Hence, the velocity of the liquid is appreciably greater with respect to the particle than with respect to the settling

apparatus itself.

For such hindered flow, the settling velocity is less than would be calculated from Eq. (30.1-9) for Stokes' law. The true drag force is greater in the suspension because of the interference of the other particles. This higher effective viscosity of the mixture  $\mu_m$  is equal to the actual viscosity of the liquid itself,  $\mu$ , divided by an empirical correction factor,  $\psi_p$ , which depends upon  $\epsilon$ , the volume fraction of the slurry mixture occupied by the liquid (S1):

$$\mu_m = \mu \psi_p \quad (30.1-12)$$

where  $\psi_p$  is dimensionless and is as follows (S1):

$$\psi_p = 1101.82(1-\epsilon) \quad (30.1-13)$$

The density of the fluid phase effectively becomes the bulk density of the slurry  $\rho_m$ , which is as follows:

$$\rho_m = \epsilon \rho + (1 - \epsilon) \rho_p \quad (30.1-14)$$

where  $\rho_m$  is density of slurry in kg solid + liquid/m<sup>3</sup>. The density difference is now

$$\rho_p - \rho_m = \rho_p - [\epsilon \rho + (1 - \epsilon) \rho_p] = \epsilon (\rho_p - \rho) \quad (30.1-15)$$

The settling velocity,  $v_t$ , with respect to the apparatus is  $\epsilon$  times the velocity calculated by Stokes' law.

Substituting the mixture properties of  $\mu_m$  from Eq. (30.1-12) for  $\mu$  in Eq. (30.1-9), substituting  $(\rho_p - \rho_m)$  from Eq. (30.1-15) for  $(\rho_p - \rho)$ , and multiplying the result by  $\epsilon$  for the relative-velocity effect, Eq.



(30.1-9) becomes, for laminar settling,

$$v_t = g D_p^2 (\rho_p - \rho) / 18 \mu (\epsilon^2 \psi_p) \quad (30.1-16)$$

This is the velocity calculated from Eq. (30.1-9), multiplied by the correction factor  $(\epsilon^2 \psi_p)$ .

The Reynolds number is then based on the velocity relative to the fluid and is

$$N_{Re} = D_p v_t \rho_m \mu_m \epsilon = D_p^3 g (\rho_p - \rho) \rho_m \epsilon \psi_p / 18 \mu^2 \quad (30.1-17)$$

When the Reynolds number is less than 1, the settling is in the Stokes' law range. For Reynolds numbers above 1.0, see (P1). The effect of concentration is greater for nonspherical particles and angular particles (S1).

Calculate the settling velocity of glass spheres having a diameter of  $1.554 \times 10^{-4}$  m ( $5.10 \times 10^{-4}$  ft) in water at 293.2 K (20°C). The slurry contains 60 wt % solids. The density of the glass spheres is  $\rho_p = 2467$  kg/m<sup>3</sup> (154 lbm/ft<sup>3</sup>).

**Solution:** Density of water  $\rho = 988$  kg/m<sup>3</sup> (62.3 lbm/ft<sup>3</sup>), and viscosity of water  $\mu = 1.005 \times 10^{-3}$  Pa · s ( $6.72 \times 10^{-4}$  lbm/ft · s). To calculate the volume fraction  $\varepsilon$  of the liquid,

$$\varepsilon = 40 / 99840 / 998 + 60 / 2467 = 0.622$$

The bulk density of the slurry  $\rho_m$  according to Eq. (30.1-14) is

$$\rho_m = \varepsilon \rho + (1 - \varepsilon) \rho_p = 0.622(998) + (1 - 0.622)(2467) = 1553 \text{ kg/m}^3 \text{ (96.9 lbm/ft}^3\text{)}$$

Substituting into Eq. (30.1-13),

$$\psi \rho = 1101.82(1 - \varepsilon) = 1101.82(1 - 0.622) = 0.205$$

Substituting into Eq. (30.1-16), using SI and English units,

$$\begin{aligned} v_t &= 9.807(1.554 \times 10^{-4})^2(2467 - 998) \\ (0.6222 \times 0.205)^{18} (1.005 \times 10^{-3}) &= 1.525 \times 10^{-3} \text{ m} \\ s v_t &= 32.174(5.1 \times 10^{-4})^2(154 - 62.3) \\ (0.6222 \times 0.205)^{18} (6.72 \times 10^{-4}) &= 5.03 \times 10^{-3} \text{ ft/s} \end{aligned}$$

The Reynolds number is obtained by substituting into Eq. (30.1-17):

$$\begin{aligned} N_{Re} &= D_p v_t \rho_m \mu \varepsilon = D_p v_t \rho_m (\mu / \psi \rho) \varepsilon = (1.554 \times 10^{-4}) \\ (1.525 \times 10^{-3}) 1553 (1.005 \times 10^{-3} / 0.205) 0.622 &= 0.121 \end{aligned}$$

Hence, the settling is in the laminar range.

### 30.1D Wall Effect on Free Settling

When the diameter  $D_p$  of the particle becomes appreciable with respect to the diameter  $D_w$  of the container in which the settling is occurring, a

retarding effect known as the *wall effect* is exerted on the particle. The terminal settling velocity is reduced. In the case of settling in the Stokes' law regime, the computed terminal velocity can be multiplied by the following to allow for the wall effect (Z1) for  $D_p/D_w < 0.05$ :

$$k_W = 1 + 2.1(D_p/D_w)(30.1 - 18)$$

For a completely turbulent regime, the correction factor is

$$k_W' = 1 - (D_p/D_w)^2 [1 + (D_p/D_w)^4]^{1/2} \quad (30.1-19)$$

### **30.1E Differential Settling and Separation of Solids in Classification**

*1. Sink-and-float methods.* Devices for the separation of solid particles into several fractions based upon

their rates of flow or settling through fluids are known as *classifiers*. There are several separation methods for accomplishing this, namely, sink-and-float and differential settling. In the *sink-and-float method*, a liquid is used whose density is intermediate between that of the heavy or high-density material and that of the light-density material. In this liquid, the heavy particles will not float but settle out from the medium, while the light particles will float.

This method is independent of the sizes of the particles and depends only upon the relative densities of the two materials. This means the liquids used must have densities greater than water, since most solids have high densities. Unfortunately, few such liquids exist

that are cheap and noncorrosive. As a result, pseudoliquids are used, consisting of a suspension in water of very fine solid materials with high specific gravities, such as galena (specific gravity = 7.5) and magnetite (specific gravity = 5.17).

Hindered settling is used and the bulk density of the medium can be varied widely by varying the amount of the fine solid materials in the medium. Common applications of this technique are concentrating ore materials and cleaning coal. The fine solid materials in the medium are so small in diameter that their settling velocity is negligible, giving a relatively stable suspension.

*2. Differential settling methods.* The separation of solid particles into several

size fractions based upon their settling velocities in a particular medium is called *differential settling* or *classification*. The density of the medium is less than that of either of the two substances to be separated.

In differential settling, both light and heavy materials settle through the medium. A disadvantage of this method if the light and heavy materials both have a range of particle sizes is that the smaller heavy particles settle at the same terminal velocity as the larger light particles.

Suppose that we consider two different materials: a heavy-density material *A* (such as galena, with a specific gravity  $\rho_A = 7.5$ ) and a light-density material *B* (such as quartz, with a specific gravity

$\rho_B = 2.65$ ). The terminal settling velocity of components A and B, from Eq. (30.1-7), can be written as

$$v_{tA} = [4(\rho_p A - \rho)gD_{pA}^3 C_{DA} \rho]^{1/2} \quad (30.1-20)$$

$$v_{tB} = [4(\rho_p B - \rho)gD_{pB}^3 C_{DB} \rho]^{1/2} \quad (30.1-21)$$

For particles with equal settling velocities,  $v_{tA} = v_{tB}$  and we obtain, by equating Eq. (30.1-20) to Eq. (30.1-21), canceling terms, and squaring both sides,

$$(\rho_p A - \rho)D_{pA}^3 C_{DA} = (\rho_p B - \rho)D_{pB}^3 C_{DB} \quad (30.1-22)$$

or

$$D_{pA}^3 D_{pB} = \rho_p B - \rho \quad \rho_p A - \rho$$

$$\rho C_D A C_{DB} (30.1-23)$$

For particles that are essentially spheres at very high Reynolds numbers in the turbulent Newton's law region,  $C_D$  is constant and  $C_{DA} = C_{DB}$ , giving

$$D_p A D_p B = (\rho_p B - \rho) v_{tA}^2 / C_D (30.1-24)$$

For laminar Stokes' law settling,

$$D_p B = 24 \mu D_p B v_{tB} / C_D (30.1-25)$$

Substituting Eq. (30.1-25) into Eq. (30.1-23) and rearranging for Stokes' law settling, where  $v_{tA} = v_{tB}$ ,

$$D_p A D_p B = (\rho_p B - \rho) v_{tB}^2 / C_D (30.1-26)$$

For transition flow between laminar and



turbulent flow,

$$D_{pA} D_{pB} = (\rho_p B - \rho) / (\rho_p A - \rho)^{1/n} \quad \text{where } 12 < n < 1 \quad (30.1-27)$$

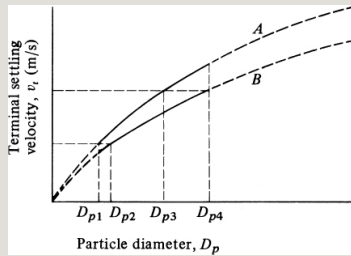


Figure 30.1-3. *Settling and separation of two materials, A and B, in Newton's law region.*

For particles settling in the turbulent range, Eq. (30.1-24) holds for equal settling velocities. For particles where  $D_{pA} = D_{pB}$  and settling is in the turbulent Newton's law region, combining Eqs. (30.1-20) and (30.1-21),

$$v_{tA} v_{tB} = (\rho_p A - \rho) / (\rho_p B - \rho)^{1/2} \quad (30.1-28)$$

If both A and B particles are settling in

the same medium, then Eqs. (30.1-24) and (30.1-28) can be used to make the plots given in Fig. 30.1-3 for the relation of velocity to diameter for  $A$  and  $B$ .

First, we consider a mixture of particles of materials  $A$  and  $B$  with a size range of  $D_{p1}$  to  $D_{p4}$  for both types of material. In the size range  $D_{p1}$  to  $D_{p2}$  in Fig. 30.1-3, a pure fraction of substance  $B$  can be obtained, since no particles of  $A$  settle as slowly. In the size range  $D_{p3}$  to  $D_{p4}$ , a pure fraction of  $A$  can be obtained, since no  $B$  particles settle as fast as the  $A$  particles in this size range. In the size range  $D_{p1}$  to  $D_{p3}$ ,  $A$  particles settle as rapidly as  $B$  particles in the size range  $D_{p2}$  to  $D_{p4}$ , forming a mixed fraction of  $A$  and  $B$ .

Increasing the density  $\rho$  of the medium

in Eq. (30.1-24), the numerator becomes smaller proportionately faster than the denominator, and the spread between  $D_{pA}$  and  $D_{pB}$  is increased. Somewhat similar curves are obtained in the Stokes' law region.

**EXAMPLE 30.1-3. Separation of a Mixture of Silica and Galena**

A mixture of silica (B) and galena (A) solid particles having a size range of  $5.21 \times 10^{-6}$  m to  $2.50 \times 10^{-5}$  m is to be separated by hydraulic classification using free-settling conditions in water at 293.2 K (B1). The specific gravity of silica is 2.65 and that of galena is 7.5. Calculate the size range of the various fractions obtained in the settling. If the settling is in the laminar region, the drag coefficients will be reasonably close to that for spheres.

**Solution:** The particle-size range is  $D_p = 5.21 \times 10^{-6}$  m to  $D_p = 2.50 \times 10^{-5}$  m. Densities are  $\rho_{pA} = 7.5(1000) = 7500$  kg/m<sup>3</sup>,  $\rho_{pB} = 2.65(1000) = 2650$  kg/m<sup>3</sup>,  $\rho = 998$  kg/m<sup>3</sup> for water at 293.2 K (20°C). The water viscosity  $\mu = 1.005 \times 10^{-3}$  Pa · s =  $1.005 \times 10^{-3}$  kg/m · s.

Assuming Stokes' law settling, Eq. (30.1-9) becomes as follows:

$$v_{tA} = g D_{pA}^2 (\rho_{pA} - \rho) / 18\mu \quad (30.1-29)$$

The largest Reynolds number occurs for the largest particle and the biggest density, where  $D_{pA} = 2.50 \times 10^{-5}$  m and  $\rho_{pA} = 7500$ . Substituting into Eq. (30.1-29),

$$v_A = 9.807 (2.50 \times 10^{-5})^2 (7500 - 998) / 18 (1.005 \times 10^{-3}) = 2.203 \times 10^{-3} \text{ m/s}$$

Substituting into the Reynolds number equation,

$$NRe = D_p A v_t A \mu = (2.50 \times 10^{-5}) \\ (2.203 \times 10^{-3}) 9981.005 \times 10^{-3} = 0.0547 (30.1 - 30)$$

Hence, the settling is in the Stokes' law region.

Referring to Fig. 30.1-3 and using the same nomenclature, the largest size is  $D_{p4} = 2.50 \times 10^{-5}$  m. The smallest size is  $D_{p1} = 5.21 \times 10^{-6}$  m. The pure fraction of *A* consists of  $D_{pA4} = 2.50 \times 10^{-5}$  m to  $D_{pA3}$ . The particles, having diameters  $D_{pA3}$  and  $D_{pB4}$ , are related by having equal settling velocities in Eq. (30.1-26). Substituting  $D_{pB4} = 2.50 \times 10^{-5}$  m into Eq. (30.1-26) and solving,

$$D_{pA3} 2.50 \times 10^{-5} = (2650 - 9987500 - 998)^{1/2} D_{pA3} = 1.260 \times 10^{-5} \text{ m}$$

The size range of pure *B* fraction is  $D_{pB2}$  to  $D_{pB1} = 5.21 \times 10^{-6}$  m. The diameter  $D_{pB2}$  is related to  $D_{pA1} = 5.21 \times 10^{-6}$  by Eq. (30.1-26) at equal settling velocities:

$$5.21 \times 10^{-6} D_{pB2} = (2650 - 9987500 - 998)^{1/2} D_{pB2} = 1.033 \times 10^{-5} \text{ m}$$

The three fractions recovered are as follows:

1. The size range of the first fraction of pure *A* (galena) is as follows:

$$D_{pA3} = 1.260 \times 10^{-5} \text{ m to } D_{pA4} = 2.50 \times 10^{-5} \text{ m}$$

2. The mixed-fraction size range is as follows:

$$D_{pB2} = 1.033 \times 10^{-5} \text{ m to } D_{pB4} = 2.50 \times 10^{-5} \text{ m } D_{pA1} = 5.21 \times 10^{-6} \text{ m to } D_{pA3} = 1.260 \times 10^{-5} \text{ m}$$

3. The size range of the third fraction of pure *B* (silica) is as follows:

$$D_{pB1} = 5.21 \times 10^{-6} \text{ m to } D_{pB2} = 1.033 \times 10^{-5} \text{ m}$$

## 30.1F Sedimentation and Thickening

### *1. Mechanisms of sedimentation.*

When a dilute slurry is settled by gravity into a clear fluid and a slurry

of higher solids concentration, the process is called *sedimentation* or sometimes *thickening*. To illustrate the method for determining settling velocities and the mechanisms of settling, a batch settling test is carried out by placing a uniform concentration of the slurry in a graduated cylinder. At the start, as shown in Fig. 30.1-4a, all the particles settle by free settling in suspension zone *B*. The particles in zone *B* settle at a uniform rate at the start, and a clear liquid zone *A* appears in Fig. 30.1-4b. The height  $z$  drops at a constant rate. Also, zone *D* begins to appear, which contains the settled particles at the bottom. Zone *C* is a transition layer whose solids content varies from that in zone *B* to that in zone *D*. After

further settling, zones  $B$  and  $C$  disappear, as shown in Fig. 30.1-4c. Then, compression first appears; this moment is called the *critical point*. During compression, liquid is expelled upward from zone  $D$  and the thickness of zone  $D$  decreases.

2. *Determination of settling velocity.* In Fig. 30.1-4d, the height  $z$  of the clear-liquid interface is plotted versus time. As shown, the velocity of settling, which is the slope of the line, is constant at first. The critical point is shown at point  $C$ . Since sludges vary greatly in their settling rates, experimental rates for each sludge are necessary. Kynch (K1) and Talmage and Fitch (T1) describe a method for predicting thickener sizes from the batch settling test.

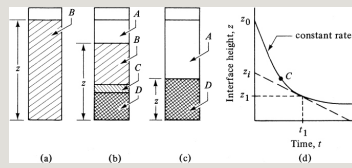


Figure 30.1-4. *Batch sedimentation results: (a) original uniform suspension, (b) zones of settling after a given time, (c) compression of zone D after zones B and C disappear, (d) clear liquid interface height  $z$  versus time of settling.*

The settling velocity  $v$  is determined by drawing a tangent to the curve in Fig. 30.1-4d at a given time  $t_1$ , with slope  $-dz/dt = v_1$ . At this point, the height is  $z_1$ , and  $z_i$  is the intercept of the tangent to the curve. Then,

$$v_1 = \frac{z_i - z_1}{t_1 - 0} \quad (30.1-31)$$

The concentration  $c_1$  is, therefore, the average concentration of the suspension if  $z_i$  is the height of this slurry. This is calculated by

$$c_1 z_i = c_0 z_0 \quad \text{or} \quad c_1 = \frac{z_0}{z_i} c_0 \quad (30.1-32)$$

where  $c_0$  is the original slurry concentration in  $\text{kg/m}^3$  at  $z_0$  height and  $t = 0$ . This is repeated for other times and a plot of settling velocity versus concentration is made. Further details of this and other methods of designing the thickener are given elsewhere (F1, F2, T1, P1). These and other methods in the literature are highly empirical and care should be exercised in their use.

### **30.1G Equipment for Settling and Sedimentation**

*1. Simple gravity settling tank.* In Fig. 30.1-5a, a simple gravity settler is shown for removing by settling a dispersed liquid phase from another phase. The velocity horizontally to the right must be slow enough to allow time for the smallest droplets to rise from the bottom to the interface, or from the top down to



the interface, and then coalesce.

In Fig. 30.1-5b, a gravity settling chamber is shown schematically. Dust-laden air enters at one end of a large, boxlike chamber. Particles settle toward the floor at their terminal settling velocities. The air must remain in the chamber a sufficient length of time (residence time) so that the particles reach the floor of the chamber. Knowing the throughput of the air stream through the chamber and the chamber size, the residence time of the air in the chamber can be calculated. The vertical height of the chamber must be small enough that this height, divided by the settling velocity, gives a time less than the residence time of the air.

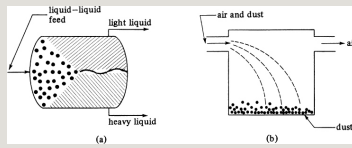


Figure 30.1-5. Gravity settling tanks: (a) settler for liquid-liquid dispersion, (b) dust-settling chambers.

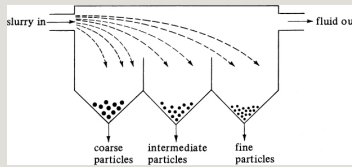


Figure 30.1-6. Simple gravity settling classifier.

**2. Equipment for classification.** The simplest type of classifier is one in which a large tank is subdivided into several sections, as shown in Fig. 30.1-6. A liquid slurry feed enters the tank containing a size range of solid particles. The larger, faster-settling particles settle to the bottom close to the entrance and the slower-settling particles settle to the bottom close to the exit. The linear velocity of the entering

feed decreases as a result of the enlargement of the cross-sectional area at the entrance. The vertical baffles in the tank allow for the collection of several fractions. The settling-velocity equations derived in this section hold.

*3. Spitzkasten classifier.* Another type of gravity settling chamber is the *Spitzkasten*, shown in Fig. 30.1-7, which consists of a series of conical vessels of increasing diameter in the direction of flow. The slurry enters the first vessel, where the largest and fastest-settling particles are separated. The overflow goes to the next vessel, where another separation occurs. This continues in the succeeding vessel or vessels. In each vessel, the velocity of upflowing inlet water is controlled to give the desired size range for each vessel.

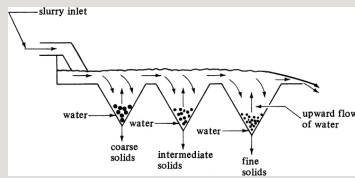


Figure 30.1-7. *Spitzkasten gravity settling chamber.*

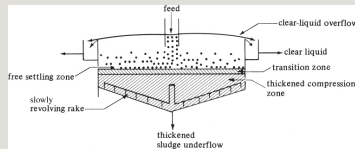


Figure 30.1-8. *Continuous thickener.*

**4. Sedimentation thickener.** The separation of a dilute slurry by gravitational settling into a clear fluid and a slurry of higher solids concentration is called *sedimentation*. Industrially, sedimentation operations are often carried out continuously in equipment called *thickeners*. A continuous thickener with a slowly revolving rake for removing the sludge or thickened slurry is shown in Fig. 30.1-8.

The slurry in Fig. 30.1-8 is fed at the center of the tank several feet below the surface of the liquid. Around the top edge of the tank is a clear-liquid-overflow outlet. The rake serves to scrape the sludge toward the center of the bottom for removal. This gentle stirring aids in removing water from the sludge.

In the thickener, the entering slurry spreads radially through the cross section of the thickener and the liquid flows upward and out the overflow. The solids settle in the upper zone by free settling. Below this dilute settling zone is the transition zone, in which the concentration of solids increases rapidly, and under that is the compression zone. A clear overflow can be obtained if the upward velocity of the

fluid in the dilute zone is less than the minimal terminal settling velocity of the solids in this zone.

The settling rates are quite slow in the thickened zone, which consists of a compression of the solids with liquid being forced upward through the solids. This is an extreme case of hindered settling. Equation (30.1-16) may be used to estimate the settling velocities, but the results can be in considerable error because of the agglomeration of particles. As a result, laboratory settling or sedimentation data must be used in the design of a thickener, as discussed previously in Section 30.1F.

## **30.2 Centrifugal Separation Processes**

### **30.2A Introduction**

*1. Centrifugal settling or sedimentation.* In Section 30.1, the processing methods of settling and sedimentation were discussed, where particles are separated from a fluid by gravitational forces acting on the particles. The particles were solid, gas, or liquid, and the fluid was a liquid or a gas. In this section, we discuss settling or separation of particles from a fluid by centrifugal forces acting on the particles.

The use of centrifuges increases the forces on particles manyfold. Hence, particles that will not settle readily or at all in gravity settlers can often be separated from fluids by centrifugal force. The high settling force means that practical rates of settling can be obtained with much smaller particles

than in gravity settlers. These high centrifugal forces do not change the relative settling velocities of small particles, but these forces do overcome the disturbing effects of Brownian motion and free convection currents.

Sometimes, gravity separation may be too slow because of the closeness of the densities of the particles and the fluid, or because of association forces holding the components together, as in emulsions. An example in the dairy industry is the separation of cream from whole milk, which produces skim milk. Gravity separation takes hours, while centrifugal separation is accomplished in minutes in a cream separator.

Centrifugal settling or separation is employed in many food industries, such as breweries, vegetable-oil processing,



fish-protein-concentrate processing, fruit-juice processing to remove cellular materials, and so on. Centrifugal separation is also used in drying crystals and for separating emulsions into their constituent liquids or a solid–liquid. The principles of centrifugal sedimentation are discussed in Sections 30.2B and 30.2C.

*2. Centrifugal filtration.* Centrifuges are also used in centrifugal filtration, where a centrifugal force is used instead of a pressure difference to cause the flow of slurry in a filter where a cake of solids builds up on a screen. The cake of granular solids from the slurry is deposited on a filter medium held in a rotating basket, washed, and then spun “dry.” Centrifuges and ordinary filters are competitive in most solid–liquid

separation problems. The principles of centrifugal filtration are discussed in Section 30.2E.

### **30.2B Forces Developed in Centrifugal Separation**

*1. Introduction.* Centrifugal separators make use of the common principle that an object whirled about an axis or center point at a constant radial distance from the point is acted on by a force. The object being whirled about the axis is constantly changing direction and is thus accelerating, even though the rotational speed is constant. This centripetal force acts in a direction toward the center of rotation.

If the object being rotated is a cylindrical container, the contents of fluid and solids exert an equal and

opposite force, called *centrifugal force*, outward to the walls of the container. This is the force that causes the settling or sedimentation of particles through a layer of liquid, or the filtration of a liquid through a bed of filter cake held inside a perforated rotating chamber.

In Fig. 30.2-1a, a cylindrical bowl is shown rotating, with a slurry feed of solid particles and liquid being admitted at the center. The feed enters and is immediately thrown outward to the walls of the container, as shown in Fig. 30.2-1b. The liquid and solids are now acted upon by the vertical gravitational force and the horizontal centrifugal force. The centrifugal force is usually so large that the force of gravity may be neglected. The liquid layer then assumes the equilibrium position, with the

surface almost vertical. The particles settle horizontally outward and press against the vertical bowl wall.

In Fig. 30.2-1c, two liquids having different densities are being separated by the centrifuge. The denser fluid will occupy the outer periphery, since the centrifugal force on it is greater.

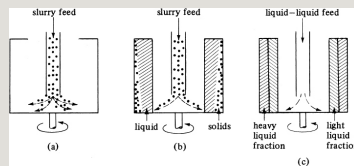


Figure 30.2-1. *Sketch of centrifugal separation: (a) initial slurry feed entering, (b) settling of solids from a liquid, (c) separation of two liquid fractions.*

2. *Equations for centrifugal force.* In circular motion, the acceleration due to the centrifugal force is

$$a_e = r\omega^2 \quad (30.2-1)$$

where  $a_e$  is the acceleration from a centrifugal force in  $\text{m/s}^2$  ( $\text{ft/s}^2$ ),  $r$  is the radial distance from the center of rotation in  $\text{m}$  ( $\text{ft}$ ), and  $\omega$  is the angular velocity in  $\text{rad/s}$ .

The centrifugal force  $F_c$  in  $\text{N}$  ( $\text{lbf}$ ) acting on the particle is given by

$$F_c = m a_e = m r \omega^2 \quad (\text{SI}) \quad F_c = m r \omega^2 g_c \quad (\text{English})$$

(30.2-2)

where  $g_c = 32.174 \text{ lb}_m \cdot \text{ft/lbf} \cdot \text{s}^2$ .

Since  $\omega = v/r$ , where  $v$  is the tangential velocity of the particle in  $\text{m/s}$  ( $\text{ft/s}$ ),

$$F_c = m r (v/r)^2 = m v^2 / r \quad (30.2-3)$$

Often, rotational speeds are given as  $N$   $\text{rev/min}$  and

$$\omega = 2\pi N/60 \quad (30.2-4)$$

$$N = 60v/2\pi r \quad (30.2-5)$$

Substituting Eq. (30.2-4) into Eq. (30.2-2),

$$F_{clbf} = mrgc(2\pi N/60)^2 = 0.000341 m r N^2 \quad (\text{English}) \quad (30.2-6)$$

By Eq. (30.1-2), the gravitational force on a particle is

$$F_g = mg \quad (30.1-2)$$

where  $g$  is the acceleration of gravity and is 9.80665 m/s<sup>2</sup>. In terms of gravitational force, the centrifugal force is as follows, by combining Eqs. (30.1-2), (30.2-2), and (30.2-3):

$$F_{clbf}/F_g = 0.000341 r N^2 / g \quad (\text{English})$$

Hence, the force developed in a centrifuge is  $r\omega^2/g$  or  $v^2/rg$  times as large as the gravitational force. This is often expressed as equivalent to a certain amount  $g$  forces.

**EXAMPLE 30.2-1. Force in a Centrifuge**

A centrifuge with a bowl radius of 0.1016 m (0.333 ft) is rotating at  $N = 1000$  rev/min.

- Calculate the centrifugal force developed in terms of gravity forces.
- Compare this force to that for a bowl with a radius of 0.2032 m rotating at the same rev/min.

**Solution:** For part (a),  $r = 0.1016$  m and  $N = 1000$ . Substituting into Eq. (30.2-7),

$$\begin{aligned} F_c/F_g &= 0.001118rN^2 = 0.001118(0.1016) \\ (1000)^2 &= 113.6 \text{ gravities or } g's \\ F_c/F_g &= 0.000341(0.333) \\ (1000)^2 &= 113.6 \end{aligned}$$

For part (b),  $r = 0.2032$  m. Substituting into Eq. (30.2-7),

$$F_c/F_g = 0.001118(0.2032)(1000)^2 = 227.2 \text{ gravities or } g's$$

### 30.2C Equations for Rates of Settling in Centrifuges

*1. General equation for settling.* If a

centrifuge is used for sedimentation (removal of particles by settling), a particle of a given size can be removed from the liquid in the bowl if there is sufficient residence time of the particle in the bowl for the particle to reach the wall. For a particle moving radially at its terminal settling velocity, the diameter of the smallest particle that can be removed can be calculated.

In Fig. 30.2-2, a schematic of a tubular-bowl centrifuge is shown. The feed enters at the bottom, and it is assumed that all the liquid moves upward at a uniform velocity, carrying solid particles with it. The particle is assumed to be moving radially at its terminal settling velocity  $v_t$ . The trajectory or path of the particle is shown in Fig.



30.2-2. A particle of a given size is removed from the liquid if sufficient residence time is available for the particle to reach the wall of the bowl, where it is held. The length of the bowl is  $b$  m.

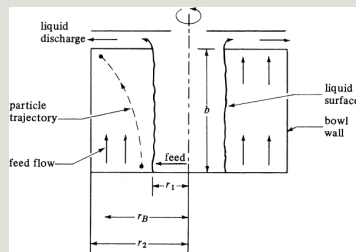


Figure 30.2-2. *Particle settling in a sedimenting tubular-bowl centrifuge.*

At the end of the residence time of the particle in the fluid, the particle is at a distance  $r_B$  from the axis of rotation. If  $r_B < r_2$ , then the particle leaves the bowl with the fluid. If  $r_B = r_2$ , the particle is deposited on the wall of the bowl and effectively removed from the liquid.

For settling in the Stokes' law range, the terminal settling velocity at a radius  $r$  is obtained by substituting Eq. (30.2-1) for the acceleration  $g$  into Eq. (30.1-9):

$$v_t = \frac{\omega^2 r D_p^2 (\rho_p - \rho)}{18\mu} \quad (30.2-8)$$

where  $v_t$  is settling velocity in the radial direction in m/s,  $D_p$  is particle diameter in  $m$ ,  $\rho_p$  is particle density in  $\text{kg/m}^3$ ,  $\rho$  is liquid density in  $\text{kg/m}^3$ , and  $\mu$  is liquid viscosity in  $\text{Pa} \cdot \text{s}$ . If hindered settling occurs, the right-hand side of Eq. (30.2-8) is multiplied by the factor  $(\epsilon_2 \psi_p)$  given in Eq. (30.1-16).

Since  $v_t = dr/dt$ , then Eq. (30.2-8) becomes

$$dt = \frac{18\mu\omega^2 (\rho_p - \rho) D_p^2}{r^2} dr \quad (30.2-9)$$

Integrating between the limits  $r = r_1$  at  $t$

$= 0$  and  $r = r_2$  at  $t = tT$ ,

$$tT = 18\mu\omega^2(\rho_p - \rho)D_p^2 \ln r_2/r_1 \quad (30.2-10)$$

The residence time  $tT$  is equal to the volume of liquid  $V$  m<sup>3</sup> in the bowl divided by the feed volumetric flow rate  $q$  in m<sup>3</sup>/s. The volume  $V = \pi b(r_2^2 - r_1^2)$ . Substituting into Eq. (30.2-10) and solving for  $q$ ,

$$\begin{aligned} q &= \omega^2(\rho_p - \rho)D_p^2 18\mu \ln(r_2/r_1) \\ (V) &= \omega^2(\rho_p - \rho)D_p^2 18\mu \ln(r_2/r_1) \\ &[\pi b(r_2^2 - r_1^2)] \quad (30.2-11) \end{aligned}$$

Particles having diameters smaller than that calculated from Eq. (30.2-11) will not reach the wall of the bowl and will go out with the exit liquid. Larger particles will reach the wall and be removed from the liquid.

A cut point or critical diameter  $D_{pc}$  can be defined as the diameter of a particle that reaches half the distance between  $r_1$  and  $r_2$ . This particle moves a distance of half the liquid layer or  $(r_2 - r_1)/2$  during the time this particle is in the centrifuge. The integration is then between  $r = (r_1 + r_2)/2$  at  $t = 0$  and  $r = r_2$  at  $t = tT$ . We then obtain

$$q_c = \omega^2 (\rho_p - \rho) D_{pc}^2 \frac{1}{8\mu} \ln \left[ \frac{2r_2}{(r_1 + r_2)} \right] (V) = \omega^2 (\rho_p - \rho) D_{pc}^2 \frac{1}{8\mu} \ln \left[ \frac{2r_2}{(r_1 + r_2)} \right] \left[ \pi b (r_2^2 - r_1^2) \right] \quad (30.2-12)$$

At this flow rate  $q_c$ , particles with a diameter greater than  $D_{pc}$  will predominantly settle to the wall and most of the smaller particles will remain in the liquid.

2. *Special case for settling.* For the special case where the thickness of the liquid layer is small compared to the radius, Eq. (30.2-8) can be written for a constant  $r \cong r_2$  and  $D_p = D_{pc}$  as follows:

$$v_t = \frac{\omega^2 r^2 D_{pc}^2 (\rho_p - \rho)}{18\mu} \quad (30.2-13)$$

The time of settling  $t_T$  is then as follows for the critical  $D_{pc}$  case:

$$t_T = \frac{V}{q_c} = \frac{(r_2^2 - r_1^2)/2}{v_t} \quad (30.2-14)$$

Substituting Eq. (30.2-13) into (30.2-14) and rearranging,

$$q_c = \frac{\omega^2 r^2 D_{pc}^2 (\rho_p - \rho)}{18\mu} \left[ \frac{(r_2^2 - r_1^2)}{2} \right] \quad (30.2-15)$$

The volume  $V$  can be expressed as

$$V \cong 2\pi r^2 (r_2 - r_1) b \quad (30.2-16)$$

Combining Eqs. (30.2-15) and (30.2-16),

$$q_c = 2\pi b r_2^2 \omega^2 D_p c^2 (\rho_p - \rho) / 9\mu \quad (30.2-17)$$

The analysis above is somewhat simplified. The pattern of flow of the fluid is actually more complicated. These equations can also be used for liquid–liquid systems where droplets of liquid migrate according to the equations and coalesce in the other liquid phase.

**EXAMPLE 30.2-2. Settling in a Centrifuge**

A viscous solution containing particles with a density  $\rho_p = 1461 \text{ kg/m}^3$  is to be clarified by centrifugation. The solution density  $\rho = 801 \text{ kg/m}^3$  and its viscosity is 100 cp. The centrifuge has a bowl with  $r_2 = 0.02225 \text{ m}$ ,  $r_1 = 0.00716 \text{ m}$ , and height  $b = 0.1970 \text{ m}$ . Calculate the critical particle diameter of the largest particles in the exit stream if  $N = 23000 \text{ rev/min}$  and the flow rate  $q = 0.002832 \text{ m}^3/\text{h}$ .

**Solution:** Using Eq. (30.2-4),

$$\omega = 2\pi N/60 = 2\pi(23000)/60 = 2410 \text{ rad/s}$$

The bowl volume  $V$  is

$$V = \pi b(r_2^2 - r_1^2) = \pi(0.1970)[(0.02225)^2 - (0.00716)^2] = 2.747 \times 10^{-4} \text{ m}^3$$

Viscosity  $\mu = 100 \times 10^{-3} = 0.100 \text{ Pa} \cdot \text{s} = 0.100 \text{ kg/m} \cdot \text{s}$ .

The flow rate  $q_c$  is

$$q_c = 0.0028323600 = 7.87 \times 10^{-7} \text{ m}^3/\text{s}$$

Substituting into Eq. (30.2-12) and solving for  $D_{pc}$ ,

$$q_c = 7.87 \times 10^{-7} = (2410)^2 (1461 - 801) D_{pc}^2 (2.747 \times 10^{-4})^{18} (0.100) \ln[2 \times 0.02225 / (0.00716 + 0.02225)] D_{pc} = 0.746 \times 10^{-6} \text{ m}$$

Substituting into Eq. (30.2-13) to obtain  $v_t$  and then calculating the Reynolds number, the settling is in the Stokes' law range.

*3. Sigma values and scale-up of centrifuges.* A useful physical characteristic of a tubular-bowl centrifuge can be derived by multiplying and dividing Eq. (30.2-12) by  $2g$  and then substituting Eq. (30.1-9) written for  $D_{pc}$  into Eq. (30.2-12) to obtain

$$q_c = 2(\rho_p - \rho)g D_{pc}^2 \frac{1}{18\mu\omega^2 V^2} \ln\left[\frac{2r_2^2}{(r_1 + r_2)}\right] = 2v_t \cdot \Sigma \quad (30.2-18)$$

where  $v_t$  is the terminal settling velocity

of the particle in a gravitational field and

$$\Sigma = \omega^2 V_2 g \ln[2r_2 / (r_1 + r_2)] = \omega^2 [\pi b (r_2^2 - r_1^2)] / 2g \ln[2r_2 / (r_1 + r_2)] \quad (30.2-19)$$

where  $\Sigma$  is a physical characteristic of the centrifuge and not of the fluid–particle system being separated. Using Eq. (30.2-17) for the special case of settling for a thin layer,

$$\Sigma = \omega^2 \pi b^2 r_2^2 g \quad (30.2-20)$$

The value of  $\Sigma$  is really the area in  $m^2$  of a gravitational settler that will have the same sedimentation characteristics as the centrifuge for the same feed rate. To scale up from a laboratory test of  $q_1$  and  $\Sigma_1$  to  $q_2$  (for  $v_{t1} = v_{t2}$ ),

$$q_1 \Sigma_1 = q_2 \Sigma_2 \quad (30.2-21)$$



This scale-up procedure is dependable for centrifuges of similar type and geometry, and if the centrifugal forces are within a factor of 2 from each other. If different configurations are involved, efficiency factors  $E$  should be used, where  $q_1/\Sigma_1 E_1 = q_2/\Sigma_2 E_2$ . These efficiencies must be determined experimentally, and values for different types of centrifuges are given elsewhere (F1, P1).

#### *4. Separation of liquids in a centrifuge.*

Liquid–liquid separations in which the liquids are immiscible but finely dispersed as in an emulsion are common operations in the food industry, among others. An example is the dairy industry, in which the emulsion of milk is separated into skim milk and cream. In these liquid–liquid separations, the

position of the outlet overflow weir in the centrifuge is very important, not only in controlling the volumetric holdup  $V$  in the centrifuge but also in determining whether a separation is actually made.

In Fig. 30.2-3, a tubular-bowl centrifuge is shown in which the centrifuge is separating two liquid phases, one a heavy liquid with density  $\rho_H$  kg/m<sup>3</sup> and the second a light liquid with density  $\rho_L$ . The distances shown are as follows:  $r_1$  is the radius to the surface of the light liquid layer,  $r_2$  is the radius to the liquid–liquid interface, and  $r_4$  is the radius to the surface of the heavy liquid downstream.

To locate the interface, a balance must be made of the pressures in the two

layers. The force on the fluid at distance  $r$  is, by Eq. (30.2-2),

$$F_c = mr\omega^2 \quad (30.2-2)$$

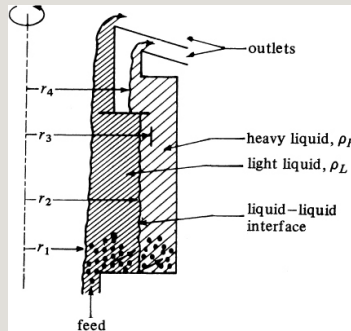


Figure 30.2-3. *Tubular bowl centrifuge for separating two liquid phases.*

The differential force across a thickness  $dr$  is

$$dF_c = dm r \omega^2 \quad (30.2-22)$$

But,

$$dm = [(2\pi r b) dr] \rho \quad (30.2-23)$$

where  $b$  is the height of the bowl in m and  $(2\pi r b)dr$  is the volume of fluid.

Substituting Eq. (30.2-23) into Eq. (30.2-22) and dividing both sides by the area  $A = 2\pi r b$ ,

$$dP = dF_c / A = \omega^2 \rho r dr \quad (30.2-24)$$

where  $P$  is pressure in N/m<sup>2</sup> (lbf/ft<sup>2</sup>).

Integrating Eq. (30.2-24) between  $r_1$  and  $r_2$ ,

$$P_2 - P_1 = \frac{\omega^2 \rho}{2} (r_2^2 - r_1^2) \quad (30.2-25)$$

Applying Eq. (30.2-25) to Fig. 30.2-3 and equating the pressure exerted by the light phase of thickness  $r_2 - r_1$  to the pressure exerted by the heavy phase of thickness  $r_2 - r_4$  at the liquid–liquid interface at  $r_2$ ,

$$\rho_H \omega^2 (r_2^2 - r_1^2) = \rho_L \omega^2 (r_2^2 - r_1^2) \quad (30.2-26)$$

Solving for  $r_2$ , the interface position,

$$r_2^2 = \frac{\rho_H r_1^2 - \rho_L r_1^2}{\rho_H - \rho_L} \quad (30.2-27)$$

The interface at  $r_2$  must be located at a radius smaller than  $r_3$  in Fig. 30.2-3.

**EXAMPLE 30.2-3. Location of the Interface in a Centrifuge**

In a vegetable-oil-refining process, an aqueous phase is being separated from the oil phase in a centrifuge. The density of the oil is 919.5 kg/m<sup>3</sup> and that of the aqueous phase is 980.3 kg/m<sup>3</sup>. The radius  $r_1$  for overflow of the light liquid has been set at 10.160 mm and the outlet for the heavy liquid is at 10.414 mm. Calculate the location of the interface in the centrifuge.

**Solution:** The densities are  $\rho_L = 919.5$  and  $\rho_H = 980.3$  kg/m<sup>3</sup>. Substituting into Eq. (30.2-27) and solving for  $r_2$ ,

$$r_2^2 = \frac{980.3(10.414)^2 - 919.5(10.160)^2}{980.3 - 919.5} = 13.75 \text{ mm}^2$$

## 30.2D Centrifuge Equipment for Sedimentation

1. *Tubular centrifuge.* A schematic of a *tubular-bowl centrifuge* is

shown in Fig. 30.2-3. The bowl is tall and has a narrow diameter, 100–150 mm. Such centrifuges, known as *supercentrifuges*, develop a force about 13000 times the force of gravity. Some narrow centrifuges, having a diameter of 75 mm and very high speeds of 60000 or so rev/min, are known as *ultracentrifuges*. Supercentrifuges are often used to separate liquid–liquid emulsions.

2. *Disk bowl centrifuge*. The *disk bowl centrifuge* shown in Fig. 30.2-4 is often used in liquid–liquid separations. The feed enters the actual compartment at the bottom and travels upward through vertically spaced feed holes, filling the spaces between the disks. The holes divide the vertical assembly into an inner section, where mostly light liquid

is present, and an outer section, where mainly heavy liquid is present. This dividing line is similar to an interface in a tubular centrifuge.

The heavy liquid flows beneath the underside of a disk to the periphery of the bowl. The light liquid flows over the upper side of the disks and toward the inner outlet. Any small amount of heavy solids is thrown to the outer wall.

Periodic cleaning is required to remove solids that are deposited. Disk bowl centrifuges are used in starch–gluten separations, concentrations of rubber latex, and cream separation. Details are given elsewhere (P1).

### **30.2E Centrifugal Filtration**

#### *1. Theory for centrifugal filtration.*

Theoretical predictions of filtration

rates in centrifugal filters have not been too successful. The filtration in centrifuges is more complicated than for ordinary filtration using pressure differences, since the areas for flow and driving force increase with distance from the axis, and the specific cake resistance may change markedly. Centrifuges for filtering are generally selected by scale-up from tests on a similar type of laboratory centrifuge using the slurry to be processed.

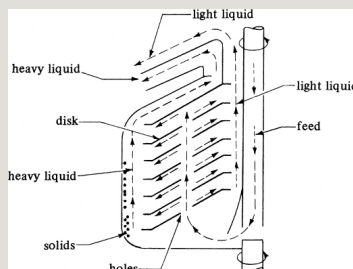


Figure 30.2-4. *Schematic of a disk bowl centrifuge.*

## The theory of constant-pressure



filtration discussed in Section 24.2B can be modified and used where centrifugal force causes the flow instead of an impressed pressure difference. The equation will be derived for the case where a cake has already been deposited, as shown in Fig. 30.2-5. The inside radius of the basket is  $r_2$ ,  $r_i$  is the inner radius of the face of the cake, and  $r_1$  is the inner radius of the liquid surface. We will assume that the cake is nearly incompressible so that an average value of  $\alpha$  can be used for the cake. Also, the flow is laminar. If we assume a thin cake in a large-diameter centrifuge, then the area  $A$  for flow is approximately constant. The velocity of the liquid is

$$v = \frac{q}{A} = \frac{dV}{A dt} \quad (30.2-28)$$

where  $q$  is the filtrate flow rate in  $\text{m}^3/\text{s}$  and  $v$  the velocity. Substituting Eq. (30.2-28) into (24.2-8),

$$-\Delta p = q\mu(m_c\alpha A^2 + R_m A) \quad (30.2-29)$$

where  $m_c = c_s V$ , the mass of cake in kg deposited on the filter.

For a hydraulic head of  $dz$  m, the pressure drop is

$$dp = \rho g dz \quad (30.2-30)$$

In a centrifugal field,  $g$  is replaced by  $r\omega^2$  from Eq. (30.2-1) and  $dz$  by  $dr$ .

Then,

$$dp = \rho r \omega^2 dr \quad (30.2-31)$$

Integrating between  $r_1$  and  $r_2$ ,

$$-\Delta p = \rho \omega^2 (r_2^2 - r_1^2) / 2 \quad (30.2-32)$$

Combining Eqs. (30.2-29) and (30.2-32), and solving for  $q$ ,

$$q = \rho \omega^2 (r_2^2 - r_1^2) / 2 \mu (m c \alpha A^2 + R_m A) \quad (30.2-33)$$

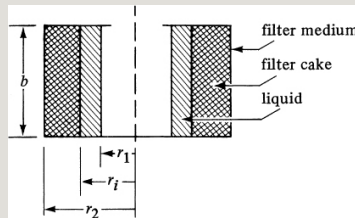


Figure 30.2-5. Physical arrangement for centrifugal filtration.

For the case where the flow area  $A$  varies considerably with the radius, the following equation has been derived (G1):

$$q = \rho \omega^2 (r_2^2 - r_1^2) / 2 \mu (m c \alpha A^{-L} A^{-a} + R_m A^2) \quad (30.2-34)$$

where  $A_2 = 2\pi r_2 b$  (area of filter medium),  $A_L = 2\pi b(r_2 - r_1)/\ln(r_2/r_1)$  (logarithmic cake area), and  $A_a = (r_1^2 - r_2^2)\pi b$  (arithmetic mean cake area). This equation holds for a cake of a given mass at a given time. It is not an integrated equation covering the whole filtration cycle.

## *2. Equipment for centrifugal filtration.*

In a centrifugal filter, slurry is fed continuously to a rotating basket that has a perforated wall and is covered with a filter cloth. The cake builds up on the surface of the filter medium to the desired thickness. Then, at the end of the filtration cycle, feed is stopped and wash liquid is added or sprayed onto the cake. Then, the wash liquid is stopped and the cake is spun as dry as possible. The motor is then shut off or slowed and

the basket allowed to rotate while the solids are discharged by a scraper knife, so that the solids drop through an opening in the basket floor. Finally, the filter medium is rinsed clean to complete the cycle. Usually, the batch cycle is completely automated. Automatic batch centrifugals have basket sizes up to about 1.2 m in diameter and usually rotate below 4000 rpm.

Continuous centrifugal filters are available with capacities up to about 25000 kg solids/h. Intermittently, the cake deposited on the filter medium is removed by being moved toward the discharge end by a pusher, which then retreats, allowing the cake to build up once more. As the cake is being pushed, it passes through a wash region. The filtrate and wash liquid are kept separate

by partitions in the collector. Details of different types of centrifugal filters are available (P1).

### **30.2F Gas–Solid Cyclone Separators**

*1. Introduction and equipment.* For separation of small solid particles or mist from gases, the most widely used type of equipment is the cyclone separator, shown in Fig. 30.2-6. The cyclone consists of a vertical cylinder with a conical bottom. The gas–solid particle mixture enters in a tangential inlet near the top. This gas–solid mixture enters in a rotating motion, and the vortex formed develops centrifugal force, which throws the particles radially toward the wall.

On entering, the air in the cyclone flows

downward in a spiral or vortex adjacent to the wall. When the air approaches the bottom of the cone, it spirals upward in a smaller spiral in the center of the cone and cylinder. Hence, a double vortex is present. The downward and upward spirals are in the same direction.

The particles are thrown toward the wall and fall downward, exiting out the bottom of the cone. A cyclone is a settling device in which the outward force on the particles at high tangential velocities is many times the force of gravity. Hence, cyclones accomplish much more effective separation than gravity settling chambers.

The centrifugal force in a cyclone ranges from about 5 times gravity in large, low-velocity units to 2500 times

gravity in small, high-resistance units. These devices are used often in many applications, such as in the spray-drying of foods, where the dried particles are removed by cyclones; in cleaning dust-laden air; and in removing mist droplets from gases. Cyclones offer one of the least expensive means of gas–particle separation. They are generally applicable in removing particles over 5  $\mu\text{m}$  in diameter from gases. For particles over 200  $\mu\text{m}$  in size, gravity settling chambers are often used. Wet-scrubber cyclones are sometimes used, where water is sprayed inside, helping to remove the solids.

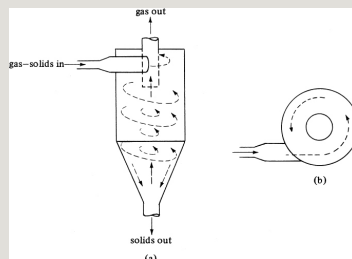




Figure 30.2-6. *Gas–solid cyclone separator: (a) side view, (b) top view.*

2. *Theory for cyclone separators.* It is assumed that particles on entering a cyclone quickly reach their terminal settling velocities. Particle sizes are usually so small that Stokes' law is considered valid. For centrifugal motion, the terminal radial velocity  $v_{tR}$  is given by Eq. (30.2-8), with  $v_{tR}$  being used for  $v_t$ :

$$v_{tR} = \frac{\omega^2 r D_p^2 (\rho_p - \rho)}{18\mu} \quad (30.2-35)$$

Since  $\omega = v_{\tan}/r$ , where  $v_{\tan}$  is tangential velocity of the particle at radius  $r$ , Eq. (30.2-35) becomes

$$v_{tR} = \frac{D_p^2 g (\rho_p - \rho)}{18\mu v_{\tan}^2} = \frac{v_t v_{\tan}^2 g r}{v_t v_{\tan}^2 g r} \quad (30.2-36)$$

where  $v_t$  is the gravitational terminal settling velocity  $v_t$  in Eq. (30.1-9).

The higher the terminal velocity  $v_t$ , the greater the radial velocity  $v_{tR}$  and the easier it should be to “settle” the particle at the walls. However, the evaluation of the radial velocity is difficult, since it is a function of gravitational terminal velocity, tangential velocity, and position radially and axially in the cyclone. Hence, the following empirical equation is often used (S2):

$$v_{tR} = b_1 D_p^2 (\rho_p - \rho) / 18 \mu r^n \quad (30.2-37)$$

where  $b_1$  and  $n$  are empirical constants.

### *3. Efficiency of collection in cyclones.*

Smaller particles have smaller settling velocities according to Eq. (30.2-37) and do not have time to reach the wall to

be collected. Hence, they leave with the exit air in a cyclone. Larger particles are more readily collected. The efficiency of separation for a given particle diameter is defined as the mass fraction of the size particles that are collected.

A typical collection-efficiency plot for a cyclone shows that the efficiency rises rapidly with particle size. The cut diameter  $D_{pc}$  is the diameter for which one-half of the mass of the entering particles is retained.

### **30.3 Chapter Summary**

In this chapter, we have introduced the concepts of settling, sedimentation, and centrifugal separation processes. All three processes involve the separation of a solid from the fluid phase. An

understanding of the forces acting on a moving particle is necessary to model these separation processes.

The main forces acting on a particle in motion are the gravitation force, buoyancy force, and drag force. When the forces balance out and the resultant acceleration is zero, the particle reaches its terminal velocity. This can be calculated using:

$$v_t = \frac{4(\rho_p - \rho)gD_p^3}{3CD_p} \quad (30.1-7)$$

or for laminar flow,

$$v_t = \frac{gD_p^2(\rho_p - \rho)}{18\mu} \quad (30.1-9)$$

To calculate the drag coefficient on a particle, it is necessary to know if it is in the Stokes' flow or Newton's law region. If the particle is in the Stokes'

flow regime, then it can be shown to be inversely proportional to the particle Reynolds number and given by

$$C_D = 24 D_p v_p / \mu = 24 N_{Re} (30.1 - 8)$$

If a large number of particles are settling at the same time, collisions may occur that influence the settling properties. This was described as hindered settling. Furthermore, if the column diameter in which a particle is settling is on the same order of magnitude as the particle size, wall effects may be noticed.

The settling properties of solids can be used to separate and classify solids based on particle size and density. These properties can be extended to highly concentrated slurries through the process of sedimentation. Sedimentation

is highly dependent on the concentration of solids in the slurry.

Centrifugal separation processes employ centrifugal forces as a means for separation. It is often necessary to calculate the angular and tangential velocities when calculating forces acting on the particles in these operations. Governing theories and models were provided for both centrifugal settling and filtration.

Finally, cyclone separators were introduced as equipment used for gas–solid separations. Cyclones are, in general, nonmechanical equipment that only uses centrifugal forces as a means to separated solids from gas–solid mixtures. Often, the grade efficiency, and not the overall efficiency, is used as

a way to classify the separation performance of a cyclone, as it is calculated based on particle size.

## Problems

**30.1-1. *Settling Velocity of a Coffee-Extract Particle.*** Solid spherical particles of coffee extract (F1) from a dryer having a diameter of  $400\ \mu\text{m}$  are falling through air at a temperature of  $422\ \text{K}$ . The density of the particles is  $1030\ \text{kg/m}^3$ . Calculate the terminal settling velocity and the distance of fall in  $5\ \text{s}$ . The pressure is  $101.32\ \text{kPa}$ .

**Ans.**  $v_t = 1.49\ \text{m/s}$ ,  $7.45\ \text{m}$  fall

**30.1-2. *Terminal Settling Velocity of Dust Particles.*** Calculate the terminal settling velocity of dust particles having

a diameter of  $60\text{ }\mu\text{m}$  in air at  $294.3\text{ K}$  and  $101.32\text{ kPa}$ . The dust particles can be considered spherical, with a density of  $1280\text{ kg/m}^3$ .

**Ans.**  $v_t = 0.1372\text{ m/s}$

**30.1-3. *Settling Velocity of Liquid Particles.*** Oil droplets having a diameter of  $200\text{ }\mu\text{m}$  are settling from still air at  $294.3\text{ K}$  and  $101.32\text{ kPa}$ . The density of the oil is  $900\text{ kg/m}^3$ . A settling chamber is  $0.457\text{ m}$  high. Calculate the terminal settling velocity. How long will it take the particles to settle? (*Note: If the Reynolds number is above about 100, the equations and form-drag correlation for rigid spheres cannot be used.*)

**30.1-4. *Settling Velocity of Quartz Particles in Water.*** Solid quartz



particles having a diameter of  $1000\ \mu\text{m}$  are settling from water at  $294.3\ \text{K}$ . The density of the spherical particles is  $2650\ \text{kg/m}^3$ . Calculate the terminal settling velocity of these particles.

**30.1-5. *Hindered Settling of Solid Particles.*** Solid spherical particles having a diameter of  $0.090\ \text{mm}$  and a solid density of  $2002\ \text{kg/m}^3$  are settling in a solution of water at  $26.7^\circ\text{C}$ . The volume fraction of the solids in the water is  $0.45$ . Calculate the settling velocity and the Reynolds number.

**30.1-6. *Settling of Quartz Particles in Hindered Settling.*** Particles of quartz having a diameter of  $0.127\ \text{mm}$  and a specific gravity of  $2.65$  are settling in water at  $293.2\ \text{K}$ . The volume fraction of the particles in the slurry mixture of

quartz and water is 0.25. Calculate the hindered settling velocity and the Reynolds number.

**30.1-7. *Density Effect on Settling Velocity and Diameter.*** Calculate the terminal settling velocity of a glass sphere 0.080 mm in diameter having a density of 2469 kg/m<sup>3</sup> in air at 300 K and 101.32 kPa. Also calculate the diameter of a sphalerite sphere having a specific gravity of 4.00 with the same terminal settling velocity.

**30.1-8. *Differential Settling of Particles.*** Repeat Example 30.1-3 for particles having a size range of  $1.27 \times 10^{-2}$  mm to  $5.08 \times 10^{-2}$  mm. Calculate the size range of the various fractions obtained using free settling conditions. Also calculate the value of the largest

Reynolds number occurring.

**30.1-9. *Separation by Settling.*** A mixture of galena and silica particles has a size range of 0.075–0.65 mm and is to be separated by a rising stream of water at 293.2 K. Use specific gravities from Example 30.1-3.

- To obtain an uncontaminated product of galena, what velocity of water flow is needed and what is the size range of the pure product?
- If another liquid, such as benzene, having a specific gravity of 0.85 and a viscosity of  $6.50 \times 10^{-4} \text{ Pa} \cdot \text{s}$  is used, what velocity is needed and what is the size range of the pure product?

**30.1-10. *Separation by the Sink-and-Float Method.*** Quartz having a specific gravity of 2.65 and hematite having a specific gravity of 5.1 are present in a mixture of particles. It is desired to separate them by a sink-and-float

method using a suspension of fine particles of ferrosilicon having a specific gravity of 6.7 in water. At what consistency in vol % ferrosilicon solids in water should the medium be maintained for the separation?

**30.1-11. *Batch Settling and Sedimentation Velocities.*** A batch settling test on a slurry gave the following results, where the height  $z$  in meters between the clear liquid and the suspended solids is given at time  $t$  hours:

The original slurry concentration is 250 kg/m<sup>3</sup> of slurry. Determine the velocities of settling and concentrations and make a plot of velocity versus concentration.

### **30.2-1. Comparison of Forces in**

**Centrifuges.** Two centrifuges rotate at the same peripheral velocity of  $53.34 \text{ m/s}$ . The first bowl has a radius of  $r_1 = 76.2 \text{ mm}$  and the second  $r_2 = 305 \text{ mm}$ . Calculate the rev/min and the centrifugal forces developed in each bowl.

**Ans.**  $N_1 = 6684 \text{ rev/min}$ ,  $N_2 = 1670 \text{ rev/min}$ ,  $3806 \text{ g's}$  in bowl 1;  $1951 \text{ g's}$  in bowl 2

### **30.2-2. Forces in a Centrifuge.**

A centrifuge bowl is spinning at a constant  $2000 \text{ rev/min}$ . What radius bowl is needed for the following?

- A force of  $455 \text{ g's}$ .
- A force four times that in part (a).

**Ans.** (a)  $r = 0.1017 \text{ m}$

**30.2-3. *Effect of Varying Centrifuge Dimensions and Speed.*** Repeat Example 30.2-2 but with the following changes:

- Reduce the rev/min to 10000 and double the outer-bowl radius  $r_2$  to 0.0445 m, keeping  $r_1 = 0.00716$  m.
- Keep all variables as in Example 30.2-2 but double the throughput.

**Ans.** (b)  $D_p = 1.747 \times 10^{-6}$  m

**30.2-4. *Centrifuging to Remove Food Particles.*** A dilute slurry contains small solid food particles having a diameter of  $5 \times 10^{-2}$  mm that are to be removed by centrifuging. The particle density is 1050 kg/m<sup>3</sup> and the solution density is 1000 kg/m<sup>3</sup>. The viscosity of the liquid is  $1.2 \times 10^{-3}$  Pa · s. A centrifuge at 3000 rev/min is to be used. The bowl dimensions are  $b = 100.1$  mm,  $r_1 = 5.00$

mm, and  $r_2 = 30.0$  mm. Calculate the expected flow rate in  $\text{m}^3/\text{s}$  just to remove these particles.

**30.2-5. *Effect of Oil Density on an Interface Location.*** Repeat Example 30.2-3, but for the case where the vegetable-oil density has been decreased to  $914.7 \text{ kg/m}^3$ .

**30.2-6. *Interface in Cream Separator.***

A cream-separator centrifuge has an outlet discharge radius  $r_1 = 50.8$  mm and outlet radius  $r_4 = 76.2$  mm. The density of the skim milk is  $1032 \text{ kg/m}^3$  and that of the cream is  $865 \text{ kg/m}^3$  (E1). Calculate the radius of the interface neutral zone.

**Ans.**  $r_2 = 150$  mm

**30.2-7. *Scale-Up and  $\Sigma$  Values of***

**Centrifuges.** For the conditions given in Example 30.2-2, do as follows:

- Calculate the  $\Sigma$  value.
- A new centrifuge having the following dimensions is to be used:  $r_2 = 0.0445$  m,  $r_1 = 0.01432$  m,  $b = 0.394$  m, and  $N = 26000$  rev/min. Calculate the new  $\Sigma$  value and scale up the flow rate using the same solution.

**Ans.** (a)  $\Sigma = 196.3 \text{ m}^2$

### **30.2-8. Centrifugal Filtration Process.**

A batch centrifugal filter similar to Fig. 30.2-5 has a bowl height  $b = 0.457$  m and  $r_2 = 0.381$  m and operates at 33.33 rev/s at 25.0°C. The filtrate is essentially water. At a given time in the cycle, the slurry and cake formed have the following properties:  $c_s = 60.0$  kg solids/m<sup>3</sup> filtrate,  $\varepsilon = 0.82$ ,  $\rho_p = 2002$  kg solids/m<sup>3</sup>, cake thickness = 0.152 m,  $\alpha = 6.38 \times 10^{10}$  m/kg,  $R_m = 8.53 \times 10^{10} \text{ m}^{-1}$ ,



$r_1 = 0.2032$  m. Calculate the rate of filtrate flow.

**Ans.**  $q = 6.11 \times 10^{-4} \text{ m}^3/\text{s}$

### References

### Notation

# Chapter 31. Leaching

## 31.0 Chapter Objectives

On completion of this chapter, a student should be able to:

- Describe the process of leaching and how it differs from liquid–liquid extraction
- Provide industrial examples of leaching processes
- Explain how the solid's material structure and the solute solubility can affect the rate of leaching
- Explain the general steps involved in modeling the rate of transfer during leaching
- Calculate the rate of leaching for both solution-controlled and diffusion-controlled processes
- Identify different types of equipment used for leaching processes
- Draw and interpret equilibrium diagrams for leaching
- Calculate solution concentrations using equilibrium diagrams for both single-state and countercurrent

## 31.1 Introduction and Equipment for Liquid–Solid Leaching

### 31.1A Leaching Processes

*1. Introduction.* Many biological, inorganic, and organic substances occur in a mixture of different components in a solid. In order to separate the desired solute constituent or remove an undesirable solute component from the solid phase, the solid is contacted with a liquid phase. The two phases are in intimate contact and the solute or solutes can diffuse from the solid to the liquid phase, resulting in a separation of the components originally in the solid. This separation process is called *liquid–solid leaching* or simply *leaching*.

The term *extraction* is also used to describe this separation process, although it also refers to liquid–liquid extraction. In leaching, when an undesirable component is removed from a solid with water, the process is called *washing*.

*2. Leaching processes for biological substances.* In the biological and food processing industries, many products are separated from their original natural structure by liquid–solid leaching. An important process, for example, is the leaching of sugar from sugar beets with hot water. In the production of vegetable oils, organic solvents such as hexane, acetone, and ether are used to extract the oil from peanuts, soybeans, flax seeds, castor beans, sunflower seeds, cotton seeds, tung meal, and halibut livers. In

the pharmaceutical industry, many different pharmaceutical products are obtained by leaching plant roots, leaves, and stems. For the production of soluble “instant” coffee, ground roasted coffee is leached with fresh water. Soluble tea is produced by water leaching of tea leaves. Tannin is removed from tree barks by leaching them with water.

*3. Leaching processes for inorganic and organic materials.* Leaching processes are used extensively in the metals-processing industries. The useful metals usually occur in mixtures with very large amounts of undesirable constituents, and leaching is used to remove the metals as soluble salts. Copper salts are dissolved or leached from ground ores containing other minerals by sulfuric acid or ammoniacal

solutions. Cobalt and nickel salts are leached from their ores by sulfuric acid–ammonia–oxygen mixtures. Gold is leached from its ore using an aqueous sodium cyanide solution. Sodium hydroxide is leached from a slurry of calcium carbonate and sodium hydroxide that is prepared by reacting  $\text{Na}_2\text{CO}_3$  with  $\text{Ca}(\text{OH})_2$ .

### **31.1B Preparation of Solids for Leaching**

#### *1. Inorganic and organic materials.*

The preparation method of a solid depends to a large extent upon the proportion of the soluble constituent present, its distribution throughout the original solid, the nature of the solid—that is, whether it is composed of plant cells or whether the soluble material is completely surrounded by a matrix of insoluble

matter—and the original particle size.

If the soluble material is surrounded by a matrix of insoluble matter, the solvent must diffuse inside to contact and dissolve the soluble material and then diffuse out. This occurs in many hydrometallurgical processes where metal salts are leached from mineral ores. In these cases, crushing and grinding of the ores is used to increase the rate of leaching, since the soluble portions are made more accessible to the solvent. If the soluble substance is in solid solution in the solid or is widely distributed throughout the whole solid, the solvent leaching action may form small channels. The passage of additional solvent is then made easier, and grinding to very small sizes may not

be needed. Grinding of the particles is not necessary if the soluble material is dissolved in solution adhering to the solid. Then, simple washing can be used, as in washing of chemical precipitates.

## *2. Animal and vegetable materials.*

Biological materials are cellular in structure and the soluble constituents are generally found inside the cells. The rate of leaching may be comparatively slow because the cell walls provide another resistance to diffusion. However, to grind the biological material sufficiently small to expose the contents of individual cells is impractical. Sugar beets are cut into thin, wedge-shaped slices for leaching so that the distance required for the water solvent to diffuse in order to reach individual cells is



reduced. The cells of the sugar beet are kept essentially intact so that sugar will diffuse through the semipermeable cell walls, while the undesirable albuminous and colloidal components cannot pass through the walls.

For the leaching of pharmaceutical products from leaves, stems, and roots, drying the material before extraction helps rupture the cell walls. Thus, the solvent can directly dissolve the solute. The cell walls of soybeans and many vegetable seeds are largely ruptured when the original materials are reduced in size to about 0.1 mm to 0.5 mm by rolling or flaking. Cells are smaller in size, but the walls are ruptured and the vegetable oil is easily accessible to the solvent.

### **31.1C Rates of Leaching**

*1. Introduction and general steps.* In the leaching of soluble materials from inside a particle by means of a solvent, the following general steps can occur in the overall process: The solvent must be transferred from the bulk solvent solution to the surface of the solid. Next, the solvent must penetrate or diffuse into the solid. The solute, which is found in the solid, dissolves into the solvent. The solute then diffuses through the solid solvent mixture to the surface of the particle. Finally, the solute is transferred to the bulk solution. The many different phenomena encountered make it virtually impracticable if not impossible to apply any one theory to the leaching action.

In general, the rate of transfer of the solvent from the bulk solution to the solid surface is quite rapid, while the rate of transfer of the solvent into the solid may be somewhat slow. These are not, in many cases, the rate-limiting steps in the overall leaching process. This solvent transfer usually occurs initially, when the particles are first contacted with the solvent. The dissolving of the solute into the solvent inside the solid may be a simple physical dissolution process or an actual chemical reaction that frees the solute for dissolution. Our knowledge of the dissolution process is limited and the mechanism may be different for each solid (K1).

The rate of diffusion of the solute through the solid and solvent to the

surface of the solid is often the controlling resistance in the overall leaching process and may depend on a number of different factors. If the solid is made up of an inert porous solid structure, with the solute and solvent in the pores in the solid, then the diffusion through the porous solid can be described by an effective diffusivity. To fully model the diffusion process, both the void fraction and the tortuosity are needed. This is described in Section 19.3C for diffusion in porous solids.

In biological or natural substances, additional complexity occurs because of the cells present. In the leaching of thin sugar-beet slices, about one-fifth of the cells are ruptured when the beets are sliced. The leaching of the sugar is then similar to a washing process (Y1). In the

remaining cells, sugar must diffuse out through the cell walls. The net result of the two transfer processes does not follow standard Fickian diffusion behavior with a constant effective diffusivity.

With soybeans, the whole beans cannot be leached effectively. Rolling and flaking the soybeans ruptures the cell walls so that the solvent can more easily penetrate them by capillary action. The diffusion rate of the soybean oil solute from the soybean flakes does not permit simple interpretation. A method for designing large-scale extractors involves using small-scale laboratory experiments (O2) with flakes.

The solute's resistance to mass transfer from the solid surface to the bulk

solvent is, in general, quite small compared to the resistance to diffusion within the solid (O1) itself. This has been found for leaching soybeans, where the degree of agitation of the external solvent has no appreciable effect on the extraction rate (Y1).

*2. Rate of leaching when dissolving a solid.* When a material is being dissolved from the solid to the solvent solution, however, the rate of mass transfer from the solid surface to the liquid is the controlling factor. There is essentially no resistance in the solid phase if it is a pure material. The equation for this can be derived as follows for a batch system and it can also be used for the case when diffusion in the solid is very rapid compared to mass transfer away from the particle.

The rate of mass transfer of solute  $A$  being dissolved to the solution of volume  $V \text{ m}^3$  is

$$N^{\circ}A = k_L(c_{AS} - c_A) \quad (31.1-1)$$

where  $N^{\circ}A$  is  $\text{kg mol}$  of  $A$  dissolving to the solution/s.  $A$  is the surface area of particles in  $\text{m}^2$ ,  $k_L$  is a mass-transfer coefficient in  $\text{m/s}$ ,  $c_{AS}$  is the saturation solubility of the solid solute  $A$  in the solution in  $\text{kg mol/m}^3$ , and  $c_A$  is the concentration of  $A$  in the solution at time  $t$  sec in  $\text{kg mol/m}^3$ . By performing a material balance, the rate of accumulation of  $A$  in the solution is equal to Eq. (31.1-1) times the area  $A$ :

$$V dc_A dt = N^{\circ}A = A k_L (c_{AS} - c_A) \quad (31.1-2)$$

Integrating from  $t = 0$  and  $c_A = c_{A0}$  to  $t =$

$t$  and  $c_A = c_A$

$$\int_{c_A=0}^{c_A=c_A} \frac{dc_A}{c_A - c_A} = -k_L A \int_0^t dt \quad (31.1-3)$$

$$c_A - c_A = c_A - c_A e^{-(k_L A/V)t} \quad (31.1-4)$$

The solution approaches a saturated condition exponentially. Often, the interfacial area  $A$  will increase during the extraction if the external surface becomes very irregular. If the soluble material forms a high proportion of the total solid, disintegration of the particles may occur. If the solid is completely dissolving, the interfacial area changes markedly. Also, the mass-transfer coefficient may then change.

If the particles are very small, the mass-transfer coefficient to the particle in an



agitated system can be predicted by using equations given in Section 21.4. For larger particles, which are usually present in leaching, equations for predicting the mass transfer coefficient  $k_L$  in agitated mixing vessels are given in Section 21.4 and reference (B1).

*3. Rate of leaching when diffusion in a solid is the controlling resistance.* In the case where unsteady-state diffusion in the solid is the controlling resistance in the leaching of the solute by an external solvent, the following approximations can be used: If the average diffusivity  $D_{A \text{ eff}}$  of solute  $A$  is approximately constant, then for extraction in a batch process, unsteady-state mass-transfer equations can be used, as discussed in Section 21.1. If the particle is approximately spherical, Fig. 14.3-13

can be used.

**EXAMPLE 31.1-1. Prediction of Time for Batch Leaching**

Particles having an average diameter of approximately 2.0 mm are leached in a batch-type apparatus with a large volume of solvent. The concentration of the solute A in the solvent is kept approximately constant. A time of 3.11 h is needed to leach 80% of the available solute from the solid. Assuming that diffusion in the solid is controlling and the effective diffusivity is constant, calculate the time of leaching if the particle size is reduced to 1.5 mm.

**Solution:** For 80% extraction, the fraction unextracted  $E_s$  is 0.20. Using Fig. 14.3-13 for a sphere, for  $E_s = 0.20$ , a value of  $DA_{\text{eff}}t/a^2 = 0.112$  is obtained, where  $DA_{\text{eff}}$  is the effective diffusivity in  $\text{mm}^2/\text{s}$ ,  $t$  is time in s, and  $a$  is radius in mm. For the same fraction  $E_s$ , the value of  $DA_{\text{eff}}t/a^2$  is constant for a different size. Hence,

$$t_2 = t_1 a_2^2 / a_1^2 \quad (31.1-5)$$

where  $t_2$  is the time for leaching with a particle size  $a_2$ . Substituting into Eq. (31.1-5),

$$t_2 = (3.11)(1.5/2)^2(2.0/2)^2 = 1.75 \text{ h}$$

#### *4. Methods of operation in leaching.*

There are a number of general methods of operation in the leaching of solids.

The operations can be carried out under batch or unsteady-state conditions as well as under continuous or steady-state

conditions. Both continuous and stagewise types of equipment are used in steady or unsteady-state operation.

In unsteady-state leaching, a method commonly used in the mineral industries is *in-place leaching*, where the solvent is allowed to percolate through the actual ore body. In other cases, the leach liquor is pumped over a pile of crushed ore and collected at the ground level as it drains from the heap. For example, copper is leached by sulfuric acid solutions from sulfide ores in this manner.

Crushed solids are often leached by percolation through stationary solid beds in a vessel with a perforated bottom to permit drainage of the solvent. The solids should not be too fine or a high

resistance to flow will be encountered. Sometimes, a number of tanks are used in series, called an *extraction battery*, and fresh solvent is fed to the solid that is nearest to completed extraction. The tanks can be open tanks or closed tanks called *diffusers*. The solvent flows through the tanks in series, being withdrawn from the freshly charged tank. This simulates a continuous countercurrent stage operation. As a tank is completely leached, a fresh charge is added to the tank at the other end. Multiple piping is used so that tanks do not have to be moved for countercurrent operation. This is often called the *Shanks system*. It is used widely in leaching sodium nitrate from ore, recovering tannins from barks and woods, and in the mineral industries and the sugar industry, as well as in other

processes.

In some processes, the crushed solid particles are moved continuously by bucket-type conveyors or screw conveyors. The solvent flows countercurrently to the moving bed.

Finely ground solids may be leached in agitated vessels or in thickeners. The process can be an unsteady-state batch or the vessels can be arranged in a series to obtain a countercurrent stage process.

### **31.1D Types of Equipment for Leaching**

*1. Fixed-bed leaching.* *Fixed-bed leaching* is used in the beet sugar industry and is also used for the extraction of tanning extracts from tanbark and the extraction of pharmaceuticals from barks and

seeds, as well as in other processes. In Fig. 31.1-1, a typical sugar-beet diffuser or extractor is shown. The cover is removable so that sugar-beet slices called *cossettes* can be dumped into the bed. Heated water at 344 K (71°C) to 350 K (77°C) flows into the bed to leach out the sugar. The leached sugar solution flows out the bottom into the next tank in series. Countercurrent operation is used in the Shanks system. The top and bottom covers are removable so that the leached beets can be removed and a fresh charge added. About 95% of the sugar in the beets is leached to yield an outlet solution from the system of about 12 wt %.

2. *Moving-bed leaching.* There are a

number of devices for stagewise countercurrent leaching where the bed or stage moves instead of being stationary. These are used widely in extracting oil from vegetable seeds such as cottonseeds, peanuts, and soybeans. The seeds are usually dehulled first, sometimes precooked, often partially dried, and rolled or flaked. Sometimes preliminary removal of oil is accomplished by expression. The solvents are usually petroleum products, such as hexane. The final solvent–vegetable solution, called *miscella*, may contain some finely divided solids.

In Fig. 31.1-2a, an enclosed moving-bed bucket elevator device is shown. This is called the *Bollman extractor*. Dry flakes or solids are added at the upper right side to a perforated basket or bucket. As

the buckets on the right side descend, they are leached by a dilute solution of oil in solvent called *half miscella*. This liquid percolates downward through the moving buckets and is collected at the bottom as the strong solution or *full miscella*. The buckets moving upward on the left are leached countercurrently by fresh solvent sprayed on the top bucket. The wet flakes are dumped as shown and removed continuously.

The *Hildebrandt extractor* in Fig. 31.1-2b consists of three screw conveyors arranged in a U shape. The solids are charged at the top right, conveyed downward, across the bottom, and then up the other leg. The solvent flows countercurrently.

3. *Agitated solid leaching*. When the



solid can be ground fine to about 200 mesh (0.074 mm), it can be kept in suspension by small amounts of agitation. Continuous countercurrent leaching can be accomplished by placing a number of agitators in series, with settling tanks or thickeners between each agitator.

Sometimes the thickeners themselves are used as combination contactor-agitators and settlers, as shown in Fig. 31.1-3. In this countercurrent-stage system, fresh solvent enters the first stage thickener as shown. The clear, settled liquid leaves and flows from stage to stage. The feed solids enter the last stage, where they are contacted with solvent from the previous stage and then enter the settler. The slowly rotating rake moves the solids to the bottom

discharge. The solids, together with some liquid, are pumped as a slurry to the next tank. If the contact is insufficient, a mixer can be installed between the settlers.

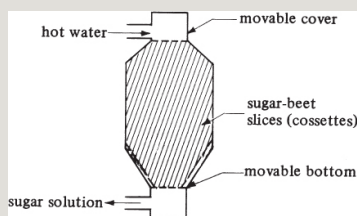


Figure 31.1-1. Typical fixed-bed apparatus for sugar-beet leaching.

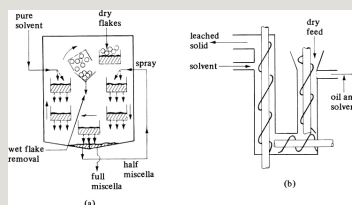


Figure 31.1-2. Equipment for moving-bed leaching: (a) Bollman bucket-type extractor, (b) Hildebrandt screw-conveyor extractor.

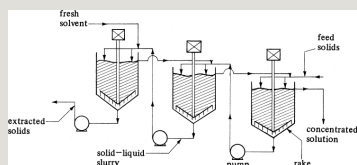


Figure 31.1-3. Countercurrent leaching using thickeners.

## 31.2 Equilibrium Relations and Single-Stage Leaching

### 31.2A Equilibrium Relations in Leaching

*1. Introduction.* To analyze single-stage and countercurrent-stage leaching, an operating-line equation or material-balance relation and the equilibrium relations between the two streams are needed, as in liquid–liquid extraction. It is assumed that the solute-free solid is insoluble in the solvent. In leaching, assuming there is sufficient solvent present so that all the solute in the entering solid can be dissolved into the liquid, equilibrium is reached when the solute is dissolved. Hence, all the solute is completely dissolved in the first stage. There is usually sufficient time for this to occur in the first stage.

It is also assumed that there is no adsorption of the solute by the solid in the leaching. This means that the solution in the liquid phase leaving a stage is the same as the solution that remains with the solid matrix in the settled slurry leaving the stage. In the settler in a stage, it is not possible or feasible to separate all the liquid from the solid. Hence, the settled solid leaving a stage always contains some liquid in which dissolved solute is present. This solid–liquid stream is called the *underflow* or *slurry stream*. Consequently, the concentration of oil or solute in the liquid or *overflow stream* is equal to the concentration of solute in the liquid solution accompanying the slurry or underflow stream. Hence, on an  $x$ - $y$  plot, the equilibrium line is on the  $45^\circ$  line.

The amount of solution retained with the solids in the settling portion of each stage may depend upon the viscosity and density of the liquid in which the solid is suspended. This, in turn, depends upon the concentration of the solute in the solution. Hence, experimental data must be obtained that show the variation of the amount and composition of solution retained in the solids as a function of the solute composition. These data should be obtained under conditions of concentrations, time, and temperature similar to those in the process for which the stage calculations are to be made.

## *2. Equilibrium diagrams for leaching.*

The equilibrium data can be plotted on the rectangular diagram as wt fraction for the three components: solute (A),

inert or leached solid ( $B$ ), and solvent ( $C$ ). The two phases are the overflow (liquid) phase and the underflow (slurry) phase. This method is discussed elsewhere (B2). Another convenient method of plotting the equilibrium data will be used instead, which is similar to the method discussed in the enthalpy–concentration plots in Section 26.7.

The concentration of inert or insoluble solid  $B$  in the solution mixture or in the slurry mixture can be expressed in kg ( $\text{lb}_m$ ) units:

$$N = \frac{\text{kg } B}{\text{kg } A}$$

$$\frac{\text{kg solid}}{\text{kg solution}} = \frac{\text{lb solid}}{\text{lb solution}} \quad (31.2-1)$$

There will be a value of  $N$  for the overflow where  $N = 0$ , and for the underflow  $N$  will have different values,

depending on the solute concentration in the liquid. The compositions of solute A in the liquid will be expressed as wt fractions:

$$x_A = \frac{\text{kg A}}{\text{kg A} + \text{kg C}}$$

$$= \frac{\text{kg solute}}{\text{kg solution (overflow liquid)}} \quad (31.2-2)$$

$$y_A = \frac{\text{kg A}}{\text{kg A} + \text{kg C}}$$

$$= \frac{\text{kg solute}}{\text{kg solution (liquid in slurry)}} \quad (31.2-3)$$

where  $x_A$  is the wt fraction of solute A in the overflow liquid and  $y_A$  is the wt fraction of A on a solid-*B*-free basis in the liquid associated with the slurry or underflow. For the entering solid feed to be leached,  $N$  is kg inert solid/kg solute A and  $y_A = 1.0$ . For pure entering solvent,  $N = 0$  and  $x_A = 0$ .

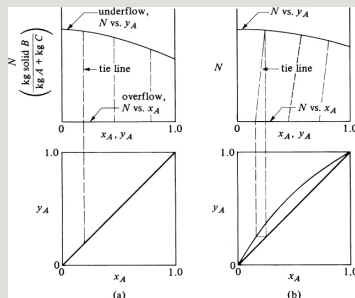


Figure 31.2-1. Several typical equilibrium diagrams: (a) case for vertical tie lines and  $y_A = x_A$ , (b) case where  $y_A \neq x_A$  for tie lines.

In Fig. 31.2-1a, a typical equilibrium diagram is shown, where solute A is infinitely soluble in solvent C, which would occur, for example, in the system soybean oil (A)–soybean inert solid meal (B)–hexane solvent (C). The upper curve of  $N$  versus  $y_A$  for the slurry underflow represents the separated solid under experimental conditions similar to the actual stage process. The bottom line of  $N$  versus  $x_A$ , where  $N = 0$  on the axis, represents the overflow liquid composition where all the solid has been removed. In some cases, small amounts



of solid may remain in the overflow. The tie lines are vertical, and on a  $y$ - $x$  diagram, the equilibrium line is  $y_A = x_A$  on the  $45^\circ$  line. In Fig. 31.2-1b, the tie lines are not vertical, which can result from insufficient contact time, so that all the solute is not dissolved; or from adsorption of solute  $A$  on the solid; or from the solute being soluble in the solid  $B$ .

If the underflow line of  $N$  versus  $y$  is straight and horizontal, the amount of liquid associated with the solid in the slurry is constant for all concentrations. This would mean that the underflow liquid rate is constant throughout the various stages as well as the overflow stream. This is a special case, which is sometimes approximated in practice.

In Fig. 31.2-2a, a single-stage leaching process is shown where  $V$  is kg/h (lbm/h) of overflow solution with composition  $x_A$ , and  $L$  is kg/h of liquid in the slurry solution with composition  $y_A$  based on a given flow rate  $B$  kg/h of dry, solute-free solid. The material-balance equations are almost identical to Eqs. (27.2-9)–(27.2-11) for single-stage liquid–liquid extraction and are as follows for a total solution balance (solute  $A$  + solvent  $C$ ), a component balance on  $A$ , and a solids balance on  $B$ , respectively:

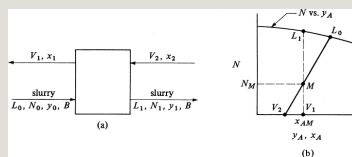


Figure 31.2-2. Process flow and material balance for single-stage leaching: (a) process flow, (b) material balance.

$$L_0 + V_2 = L_1 + V_1 = M \quad (31.2-4)$$

$$A_0 + V_2 x_{A2} = L_1 y_{A1} + V_1 x_{A1} = M x_{AM} \quad (31.2-5)$$

$$B = N_0 L_0 + 0 = N_1 L_1 + 0 = N_M M \quad (31.2-6)$$

where  $M$  is the total flow rate in kg  $A + C/h$  and  $x_{AM}$  and  $N_M$  are the coordinates of this point  $M$ . A balance on  $C$  is not needed, since  $x_A + x_C = 1.0$  and  $y_A + y_C = 1.0$ . As shown before,  $L_1 M V_1$  must lie on a straight line and  $L_0 M V_2$  must also lie on a straight line. This is shown in Fig. 31.2-2b. Also,  $L_1$  and  $V_1$  must lie on the vertical tie line. The point  $M$  is the intersection of the two lines. If  $L_0$  entering is the fresh solid feed to be leached with no solvent  $C$  present, it will be located above the  $N$ -versus- $y$  line in Fig. 31.2-2b.

## Soybeans

In a single-stage leaching of soybean oil from flaked soybeans with hexane, 100 kg of soybeans containing 20 wt % oil is leached with 100 kg of fresh hexane solvent. The value of  $N$  for the slurry underflow is essentially constant at 1.5 kg insoluble solid/kg solution retained. Calculate the amounts and compositions of the overflow  $V_1$  and the underflow slurry  $L_1$  leaving the stage.

**Solution:** The process flow diagram is the same as given in Fig. 31.2-2a. The known process variables are as follows: for the entering solvent flow,  $V_2 = 100$  kg,  $x_{A2} = 0$ ,  $x_{C2} = 1.0$ ; for the entering slurry stream,  $B = 100(1.0 - 0.2) = 80$  kg insoluble solid,  $L_0 = 100(1.0 - 0.8) = 20$  kg  $A$ ,  $N_0 = 80/20 = 4.0$  kg solid/kg solution,  $y_{A0} = 1.0$ .

To calculate the location of  $M$ , substituting into Eqs. (31.2-4), (31.2-5), and (31.2-6) and solving,

$$L_0 + V_2 = 20 + 100 = 120 \text{ kg} = M L_0 y_{A0} + V_2 x_{A2} = 20(1.0) + 100(0) = 120 x_{AM}$$

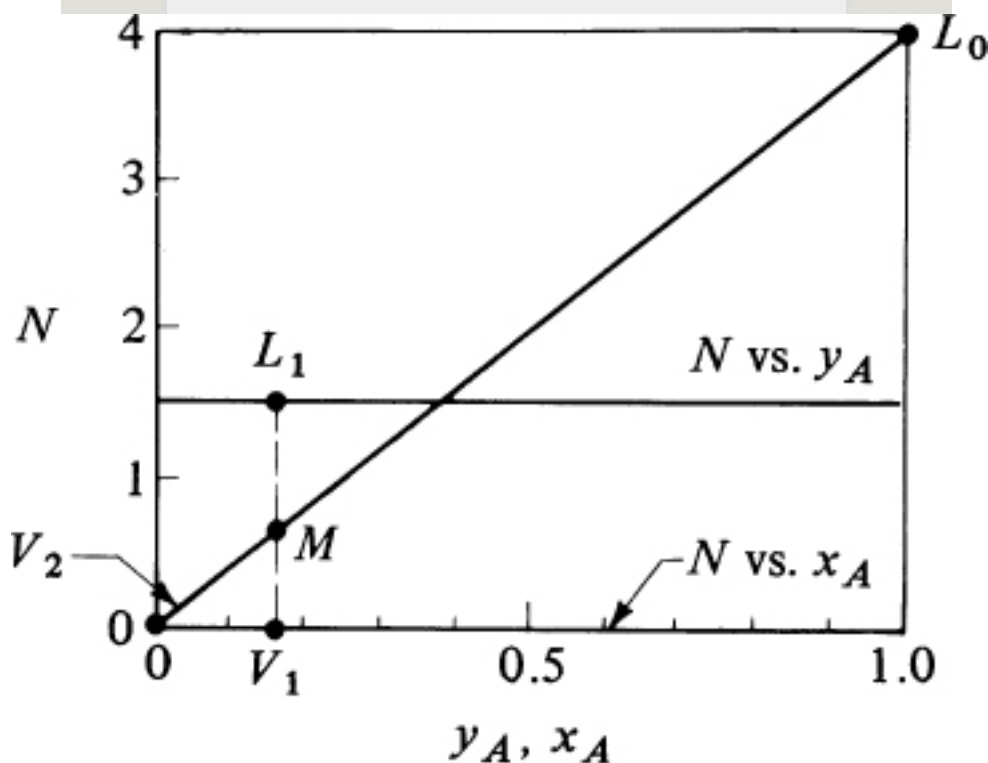


Figure 31.2-3. *Graphical solution of single-stage leaching for Example 31.2-1.*

Hence,  $x_{AM} = 0.167$ .

$$B = N_0 L_0 = 4.0(20) = 80 = N_M(120) \Rightarrow N_M = 0.667$$

The point  $M$  is plotted in Fig. 31.2-3 along with  $V_2$  and  $L_0$ . The vertical tie line is drawn locating  $L_1$  and  $V_1$  in equilibrium with each other. Then,  $N_1 = 1.5$ ,  $y_{A1} = 0.167$ ,  $x_{A1} = 0.167$ . Substituting into Eqs. (31.2-4) and (31.2-6), and solving or using the lever-arm rule,  $L_1 = 53.3$  kg and  $V_1 = 66.7$  kg.

## 31.3 Countercurrent Multistage Leaching

### 31.3A Introduction and Operating Line for Countercurrent Leaching

A process flow diagram for countercurrent multistage leaching is shown in Fig. 31.3-1 and is similar to Fig. 27.4-1 for liquid–liquid extraction. The ideal stages are numbered in the direction of the solids or underflow stream. The solvent (C)–solute (A) phase or  $V$  phase is the liquid phase that overflows continuously from stage to

stage countercurrent to the solid phase, dissolving solute as it moves along. The slurry phase  $L$  composed of inert solids ( $B$ ) and a liquid phase of  $A$  and  $C$  is the continuous underflow from each stage. Note that the composition of the  $V$  phase is denoted by  $x$  and the composition of the  $L$  phase by  $y$ , which is the reverse of that for liquid–liquid extraction.

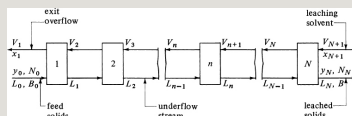


Figure 31.3-1. *Process flow for countercurrent multistage leaching.*

It is assumed that solid  $B$  is insoluble and is not lost in the liquid  $V$  phase. The flow rate of the solids is constant throughout the cascade of stages. As in single-stage leaching,  $V$  is kg/h (lbm/h)

of overflow solution and  $L$  is kg/h of liquid solution in the slurry retained by the solid.

In order to derive the operating-line equation, an overall balance and a component balance on solute  $A$  is made over the first  $n$  stages:

$$V_{n+1} + L_0 = V_1 + L_n \quad (31.3-1)$$

$$V_{n+1}x_n + L_0y_0 = V_1x_1 + L_ny_n \quad (31.3-2)$$

Solving for  $x_{n+1}$  and eliminating  $V_{n+1}$ ,

$$x_{n+1} = 1 + (V_1 - L_0)/L_n y_n + V_1 x_1 - L_0 x_0 / L_n + V_1 - L_0 \quad (31.3-3)$$

The operating-line equation (31.3-3), when plotted on an  $x$ - $y$  plot, passes through the terminal points  $x_1$ ,  $y_0$  and  $x_N$

+1,  $y_N$ .

In the leaching process, if the viscosity and density of the solution change appreciably with the solute ( $A$ ) concentration, the solids from the lower-numbered stages where solute concentrations are high may retain more liquid solution than the solids from the higher-numbered stages, where the solute concentration is dilute. Then  $L_n$ , the liquid retained in the solids underflow, will vary, and the slope of Eq. (31.3-3) will vary from stage to stage. This condition of variable underflow will be considered first. The overflow will also vary. If the amount of solution  $L_n$  retained by the solid is constant and independent of concentration, then constant underflow occurs. This simplifies somewhat the



stage-to-stage calculations. This case will be considered later.

### **31.3B Variable Underflow in Countercurrent Multistage Leaching**

The methods in this section are very similar to those used in Section 27.4B for countercurrent solvent extraction, where the  $L$  and  $V$  flow rates varied from stage to stage. Making an overall total solution (solute  $A$  + solvent  $C$ ) balance on the process shown in Fig. 31.3-1,

$$L_0 + V_{N+1} = L_N + V_1 = M \quad (31.3-4)$$

where  $M$  is the total mixture flow rate in kg  $A+C$ /h. Next, making a component balance on  $A$ ,

$$L_0 y_{A0} + V_{N+1} x_{A_{N+1}} = L_N y_{AN} + V_1 x_{A1} = M x_{AM} \quad (31.3-5)$$

Making a total solids balance on  $B$ ,

$$B = N_0 L_0 = N_N L_N = N_M M \quad (31.3-6)$$

where  $N_M$  and  $x_{AM}$  are the coordinates of point  $M$  shown in Fig. 31.3-2, which is the operating diagram for the process. As demonstrated previously,  $L_0 M V_{N+1}$  must lie on a straight line and  $V_1 M L_N$  must also lie on a straight line. Usually, the flows and compositions of  $L_0$  and  $V_{N+1}$  are known and the desired exit concentration  $y_{AN}$  is set. Then, the coordinates  $N_M$  and  $x_{AM}$  can be calculated from Eqs. (31.3-4)–(31.3-6) and point  $M$  plotted. Then,  $L_N$ ,  $M$ , and  $V_1$  must lie on one line, as shown in Fig. 31.3-2.

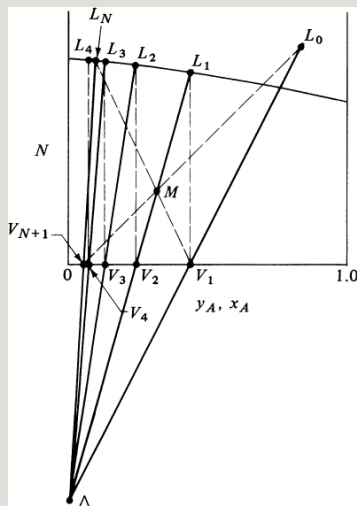


Figure 31.3-2. Number of stages for multistage countercurrent leaching.

In order to go stage by stage on Fig. 31.3-2, we must derive the operating-point equation. Making a total balance on stage 1 and then on stage  $n$ ,

$$L_0 + V_2 = L_1 + V_1 \quad (31.3-7)$$

$$L_{n-1} + V_{n+1} = L_n + V_n \quad (31.3-8)$$

Rearranging Eq. (31.3-7) for the difference flows  $\Delta$  in kg/h,

$$L_0 - V_1 = L_1 - V_2 = \Delta \quad (31.3-9)$$

This value  $\Delta$  is constant and also holds for Eq. (31.3-8) rearranged and for all stages:

$$\Delta = L_0 - V_1 = L_n - V_{n+1} = L_N - V_{N+1} = \dots \quad (31.3-10)$$

This can also be written for a balance on solute  $A$  to give

$$x_{AD} = \frac{L_0 y_{A0} - V_1 x_{A1}}{L_0 - V_1} = \frac{L_N y_{AN} - V_{N+1} x_{A,N+1}}{L_N - V_{N+1}} = \dots \quad (31.3-11)$$

where  $x_{A\Delta}$  is the  $x$  coordinate of the operating point  $\Delta$ . A balance made on solids gives

$$N\Delta = B L_0 - V_1 = N_0 L_0 - V_1 \quad (31.3-12)$$

where  $N_{\Delta}$  is the  $N$  coordinate of the operating point  $\Delta$ .

As shown in Section 27.4B,  $\Delta$  is the operating point. This point  $\Delta$  is located graphically in Fig. 31.3-2 as the intersection of lines  $L_0V_1$  and  $L_NV_{N+1}$ . From Eq. (31.3-10), we see that  $V_1$  is on a line between  $L_0$  and  $\Delta$ ,  $V_2$  is on a line between  $L_1$  and  $\Delta$ ,  $V_{n+1}$  is on a line between  $L_n$  and  $\Delta$ , and so on.

To graphically determine the number of stages, we start at  $L_0$  and draw line  $L_0\Delta$  to locate  $V_1$ . A tie line through  $V_1$  locates  $L_1$ . Line  $L_1\Delta$  is drawn given  $V_2$ . A tie line gives  $L_2$ . This is continued until the desired  $L_N$  is reached. In Fig. 31.3-2, about 3.5 stages are required.

**EXAMPLE 31.3-1. Countercurrent Leaching of Oil from Meal**

A continuous countercurrent multistage system is to be used to leach oil from meal by benzene solvent (B3). The process is to treat 2000 kg/h of inert solid meal (B) containing 800 kg oil (A) and also 50 kg benzene (C). The inlet flow per hour of fresh solvent mixture contains 1310 kg benzene and 20 kg oil. The leached solids are to contain 120 kg oil. Settling experiments similar to those in the actual extractor show that the solution retained depends upon the concentration of oil in the solution. The data (B3) are tabulated below as  $N$  kg inert solid  $B$ /kg solution and  $y_A$  kg oil  $A$ /kg solution:

--

Calculate the amounts and concentrations of the stream leaving the process and the number of stages required.

**Solution:** The underflow data from the table are plotted in Fig. 31.3-3 as  $N$  versus  $y_A$ . For the inlet solution with the untreated solid,  $L_0 = 800 + 50 = 850$  kg/h,  $y_{A0} = 800/(800 + 50) = 0.941$ ,  $B = 2000$  kg/h, and  $N_0 = 2000/(800 + 50) = 2.36$ . For the inlet leaching solvent,  $V_{N+1} = 1310 + 20 = 1330$  kg/h and  $x_{AN+1} = 20/1330 = 0.015$ . The points  $V_{N+1}$  and  $L_0$  are plotted.

The point  $L_N$  lies on the  $N$ -versus- $y_A$  line in Fig. 31.3-3. Also for this point, the ratio  $N_N/y_{AN} = (\text{kg solid/kg solution})/(\text{kg oil/kg solution}) = \text{kg solid/kg oil} = 2000/120 = 16.67$ . Hence, a dashed line through the origin at  $y_A = 0$  and  $N = 0$  is plotted with a slope of 16.67 and it intersects the  $N$ -versus- $y_A$  line at  $L_N$ . The coordinates of  $L_N$  at this intersection are  $N_N = 1.95$  kg solid/kg solution and  $y_{AN} = 0.118$  kg oil/kg solution.

Making an overall balance by substituting into Eq. (31.3-4) to determine point  $M$ ,

$$L_0 + V_{N+1} = 850 + 1330 = 2180 \text{ kg/h} = M$$

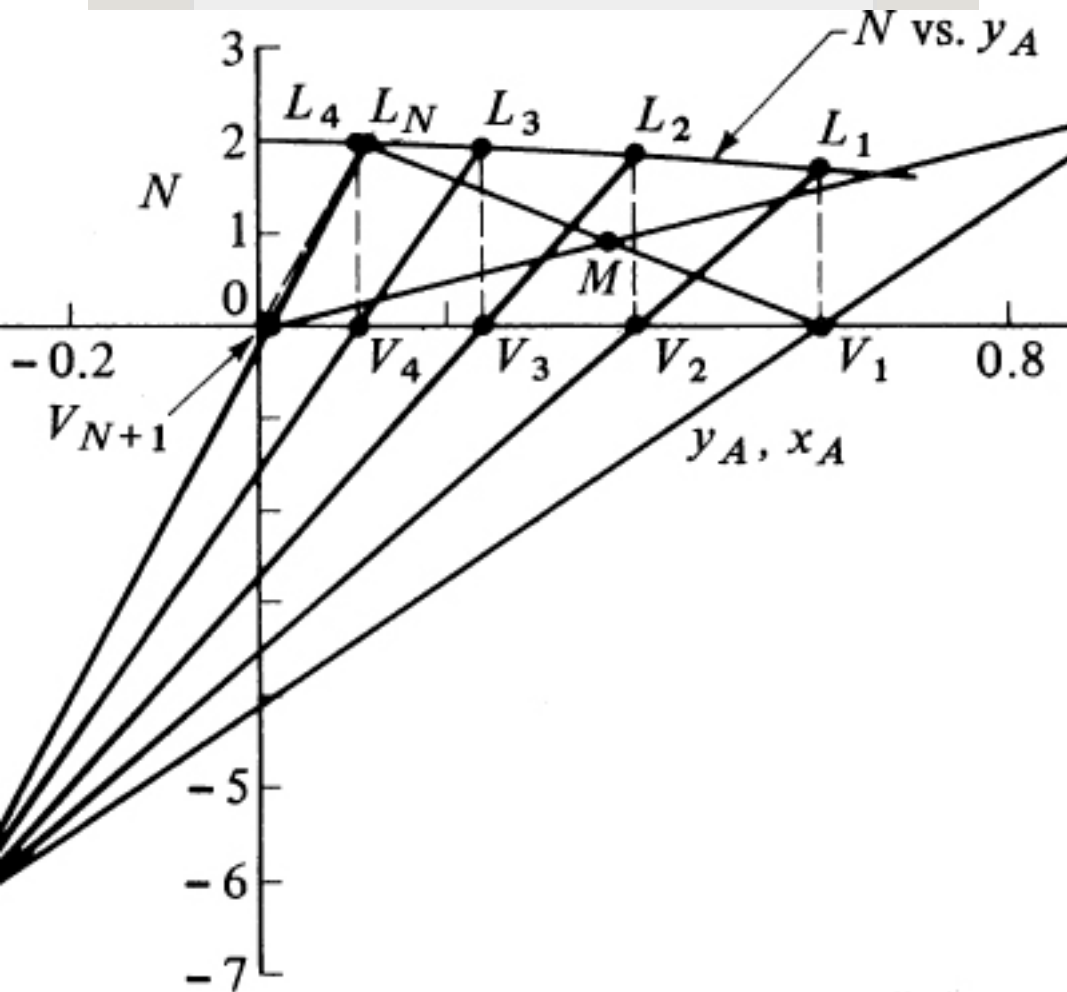


Figure 31.3-3. Graphical construction for number of stages for Example 31.3-1.

Substituting into Eq. (31.3-5) and solving,

$$L_0 y_{A0} + V_{N+1} x_{AN} + 1 = 850(0.941) + 1330(0.015) = 2180 x_{AM} \quad x_{AM} = 0.376$$

Substituting into Eq. (31.3-6) and solving,

$$B = 2000 = N M M = N M (2180) \quad N M = 0.918$$

The point  $M$  is plotted with the coordinates  $x_{AM} = 0.36$  and  $N_M = 0.918$  in Fig. 31.3-3. The line  $V_{N+1} M L_0$  is drawn, as is line  $L_N M$ , which intersects the abscissa at point  $V_1$  where

$$x_{A1} = 0.600.$$

The amounts of streams  $V_1$  and  $L_N$  are calculated by substituting into Eqs. (31.3-4) and (31.3-5), and solving simultaneously:

$$\begin{aligned} L_N + V_1 &= M = 2180 \text{ L N y A N} \\ + V_1 x_{A1} &= L_N(0.118) + V_1(0.600) = 2180(0.376) \end{aligned}$$

Hence,  $L_N = 1016$  kg solution/h in the outlet underflow stream and  $V_1 = 1164$  kg solution/h in the exit overflow stream. Alternatively, the amounts could have been calculated using the lever-arm rule.

The operating point  $\Delta$  is obtained as the intersection of lines  $L_0V_1$  and  $L_NV_{N+1}$  in Fig. 31.3-3. Its coordinates can also be calculated from Eqs. (31.3-11) and (31.3-12). The stages are stepped off as shown. The fourth stage for  $L_4$  is slightly past the desired  $L_N$ . Hence, about 3.9 stages are required.

### 31.3C Constant Underflow in Countercurrent Multistage Leaching

In this case, the liquid  $L_n$  retained in the underflow solids is constant from stage to stage. This means that a plot of  $N$  versus  $y_A$  is a horizontal straight line and  $N$  is constant. Then, the operating-line equation (31.3-3) is a straight line when plotted as  $y_A$  versus  $x_A$ . The equilibrium line can also be plotted on the same diagram.



In many cases, the equilibrium line may also be straight, with  $y_A = x_A$ . Special treatment must be given to the first stage, however, as  $L_0$  is generally not equal to  $L_n$ , since it contains little or no solvent. A separate material and equilibrium balance is made on stage 1 to obtain  $L_1$  and  $V_2$  (see Fig. 31.3-1). Then, the straight operating line can be used as well as the McCabe–Thiele method to step off the number of stages.

Since this procedure for constant underflow requires almost as many calculations as the general case for variable underflow, the general procedure can be used for constant underflow by simply using a horizontal line of  $N$  versus  $y_A$  in Fig. 31.3-2 and

stepping off the stages with the  $\Delta$  point.

### **31.4 Chapter Summary**

In this chapter, we have introduced the concepts of leaching. Leaching is a process by which a desired solute is extracted from the solid phase of another material. This process is different from liquid–liquid extraction, in that a solid phase is present. Leaching is a common process used to extract solutes in biological and pharmaceutical processes. In addition, it is also used to extract metal salts from ground ores.

The overall process of leaching is dependent on both the solubility of the desired solute, as well as the architectural structure of the solid itself.

The rate of leaching can be controlled by either the solubility or diffusion properties of the solute. The principles of convective mass transfer can be used to model the rate of leaching. Thus, the rate of leaching is dependent on the concentration profile, the surface area available for mass transfer, and the overall mass-transfer coefficient. Often, effective properties, such as effective diffusivity, are used in modeling the rate of leaching.

Many different types of equipment are available for leaching. The equipment may be classified in terms of the packing behavior of the solids.

Examples of leaching equipment include fixed-bed, moving-bed, and agitated vessels. The leaching process itself can also be classified as single-stage or

multi-stage, the latter of which is frequently operated countercurrently.

To predict the total amounts and concentrations of the solute during the leaching process, equilibrium diagrams can be developed for single-stage and countercurrent multistage processes.

The equilibrium diagrams are plots of inert solid concentration in the solution as a function of solute concentration. By performing a material balance on the process (both overall material balance and species material balance) and using the equilibrium diagrams, it is possible to calculate the concentration of solute in the exit streams.

## **Problems**

**31.1-1. *Effective Diffusivity in Leaching Particles.*** In Example 31.1-1,

a leaching time for the solid particle of 3.11 h is needed to remove 80% of the solute. Perform the following calculations:

- Using the experimental data, calculate the effective diffusivity,  $D_{A \text{ eff}}$ .
- Predict the time to leach 90% of the solute from the 2.0 mm particle.

**Ans.** (a)  $D_{A \text{ eff}} = 1.0 \times 10^{-5} \text{ mm}^2/\text{s}$ ; (b)  $t = 5.00 \text{ h}$

**31.2-1. *Leaching of Oil from Soybeans in a Single Stage.*** Repeat Example 31.2-1 for single-stage leaching of oil from soybeans. The 100 kg of soybeans contains 22 wt % oil and the solvent feed is 80 kg of solvent containing 3 wt % soybean oil.

**Ans.**  $L_1 = 52.0 \text{ kg}$ ,  $y_{A1} = 0.239$ ,  $V_1 = 50.0 \text{ kg}$ ,  $x_{A1} = 0.239$ ,  $N_1 = 1.5$

**31.2-2. *Leaching a Soybean Slurry in a Single Stage.*** A slurry of flaked soybeans weighing a total of 100 kg contains 75 kg of inert solids and 25 kg of solution with 10 wt % oil and 90 wt % solvent hexane. This slurry is contacted with 100 kg of pure hexane in a single stage so that the value of  $N$  for the outlet underflow is 1.5 kg insoluble solid/kg solution retained. Calculate the amounts and compositions of the overflow  $V_1$  and the underflow  $L_1$  leaving the stage.

**31.3-1. *Constant Underflow in Leaching Oil from Meal.*** Use the same conditions as given in Example 12.10-1, but assume constant underflow of  $N = 1.85$  kg solid/kg solution. Calculate the exit flows and compositions and the number of stages required. Compare

with Example 31.3-1.

**Ans.**  $y_{AN} = 0.111$ ,  $x_{A1} = 0.623$ , 4.3  
stages

**31.3-2. *Effect of Less Solvent Flow in Leaching Oil from Meal.*** Use the same conditions as given in Example 31.3-1, but the inlet fresh-solvent-mixture flow rate per hour is decreased by 10%, to 1179 kg of benzene and 18 kg of oil. Calculate the number of stages needed.

**31.3-3. *Countercurrent Multistage Washing of an Ore.*** A treated ore containing inert solid gangue and copper sulfate is to be leached in a countercurrent multistage extractor using pure water to leach the  $\text{CuSO}_4$ . The solid charge rate per hour consists of 10000 kg of inert gangue ( $B$ ), 1200

kg of  $\text{CuSO}_4$  (solute A), and 400 kg of water (C). The exit wash solution is to contain 92 wt % water and 8 wt %  $\text{CuSO}_4$ . A total of 95% of the  $\text{CuSO}_4$  in the inlet ore is to be recovered. The underflow is constant at  $N = 0.5$  kg inert gangue solid/kg aqueous solution. Calculate the number of stages required.

**Ans.** 9 stages,  $L_N = 20\,000$  kg/h,  $y_{AN} = 0.0030$ ,  $V_1 = 14\,250$  kg/h

### **31.3-4. *Countercurrent Multistage***

***Leaching of Halibut Livers.*** Fresh halibut livers containing 25.7 wt % oil are to be extracted with pure ethyl ether to remove 95% of the oil in a countercurrent multistage leaching process. The feed rate is 1000 kg of fresh livers per hour. The final exit overflow solution is to contain 70 wt %



oil. The retention of solution by the inert solids (oil-free liver) of the liver varies as follows (C1), where  $N$  is kg inert solid/kg solution retained and  $y_A$  is kg oil/kg solution:

Calculate the amounts and compositions of the exit streams and the total number of theoretical stages.

**31.3-5. Countercurrent Leaching of Flaked Soybeans.** Soybean flakes containing 22 wt % oil are to be leached in a countercurrent multistage process to contain 0.8 kg oil/100 kg inert solid using fresh and pure hexane solvent. For every 1000 kg soybeans, 1000 kg hexane is used. Experiments (S1) give the following retention of solution with the solids in the underflow, where  $N$  is

kg inert solid/kg solution retained and  
 $y_A$  is wt fraction of oil in solution:

Calculate the exit flows and  
compositions and the number of  
theoretical stages needed.

### References

### Notation

# Chapter 32. Evaporation

## 32.0 Chapter Objectives

On completion of this chapter, a student should be able to:

- Describe the process of evaporation
- Provide industrial examples of evaporation processes
- Describe the properties that can affect evaporation processes
- Identify different types of equipment used for evaporation processes and the methods by which they are used
- Explain how the overall heat transfer coefficient is calculated for evaporation
- Perform heat and material balances on evaporation units and processes
- Calculate the boiling point rise (BPR) of a solution using the Dühring Chart
- Determine the amount of steam required, the steam economy, and heat transfer surface area for evaporators

and multi-effect evaporators

- Describe the operation of condensers

## 32.1 Introduction

### 32.1A Purpose

In Section 15.6, we discussed the case of heat transfer to a boiling liquid. An important instance of this type of heat transfer frequently occurs in the process industries and is given the general name *evaporation*. In evaporation, the vapor from a boiling liquid solution is removed and a more concentrated solution remains. In the majority of cases, the separation process called evaporation refers to the removal of water from an aqueous solution.

Typical examples of evaporation are concentration of aqueous solutions of

sugar, sodium chloride, sodium hydroxide, glycerol, glue, milk, and orange juice. In these cases, the concentrated solution is the desired product and the evaporated water is normally discarded. In a few cases, water, which contains a small amount of minerals, is evaporated to give a solids-free water to be used as boiler feed, for special chemical processes or for other purposes. Evaporation processes to evaporate seawater to provide drinking water have been developed and used commercially. In some cases, the primary purpose of evaporation is to concentrate a solution so that upon cooling, salt crystals will form and be separated. This special evaporation process, termed *crystallization*, is discussed in Chapter 29.

The physical and chemical properties of the solution being concentrated and of the vapor being removed bear greatly on the type of evaporator used and the pressure and temperature of the process. Some of the properties that can affect the processing methods are discussed next.

*1. Concentration in the liquid.* Usually, the liquid feed to an evaporator is relatively dilute, so its viscosity is low, similar to that of water, and relatively high heat-transfer coefficients are obtained. As evaporation proceeds, the solution may become very concentrated and quite viscous, causing the heat-transfer coefficient to drop markedly. Adequate circulation and/or turbulence must be present to keep the coefficient

from becoming too low.

*2. Solubility.* As solutions are heated and the concentration of the solute or salt increases, the solubility limit of the material in solution may be exceeded and crystals may form. This may limit the maximum concentration in solution that can be obtained by evaporation. In Fig. 32.1-1, some solubilities of typical salts in water are shown as a function of temperature. In most cases, the solubility of the salt increases with temperature. This means that when a hot, concentrated solution from an evaporator is cooled to room temperature, crystallization may occur.

*3. Temperature sensitivity of materials.* Many products, especially food and other biological materials, may be

temperature-sensitive and degrade at higher temperatures or after prolonged heating. Such products include pharmaceuticals; foods such as milk, orange juice, and vegetable extracts; and fine organic chemicals. The amount of degradation is a function of the temperature and the length of time.

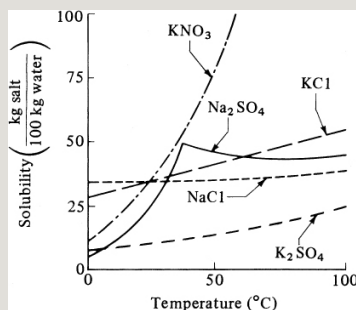


Figure 32.1-1. Solubility curves for some typical salts in water.

**4. Foaming or frothing.** In some cases, materials composed of caustic solutions, food solutions such as skim milk, and some fatty-acid solutions form a foam or froth during boiling. This foam



accompanies the vapor coming out of the evaporator and entrainment losses occur.

*5. Pressure and temperature.* The boiling point of the solution is related to the pressure of the system. The higher the operating pressure of the evaporator, the higher the temperature at boiling.

Also, as the concentration of the dissolved material in solution increases by evaporation, the temperature of boiling may rise. This phenomenon is called *boiling-point rise* or *elevation* and is discussed in Section 32.4. To keep the temperatures low in heat-sensitive materials, it is often necessary to operate under 1 atm pressure, that is, under vacuum.

*6. Scale deposition and materials of*

*construction*. Some solutions deposit solid materials called scale on the heating surfaces. These can be formed by decomposition products or by decreases in solubility. The result is that the overall heat-transfer coefficient decreases and the evaporator must eventually be cleaned. The materials used in construction of the evaporator should be chosen to minimize corrosion.

## **32.2 Types of Evaporation Equipment and Operation Methods**

### **32.2A General Types of Evaporators**

In evaporation, heat is added to a solution to vaporize the solvent, which is usually water. The heat is generally provided by the condensation of a vapor such as steam on one side of a metal surface, with the evaporating liquid on the

other side. The type of equipment used depends primarily on the configuration of the heat-transfer surface and on the means employed to provide agitation or circulation of the liquid. The general types of equipment are discussed below.

*1. Open kettle or pan.* The simplest evaporator consists of an open pan or kettle in which the liquid is boiled. The heat is supplied by condensation of steam in a jacket or in coils immersed in the liquid. In some cases, the kettle is direct-fired. These evaporators are inexpensive and simple to operate, but the heat economy is poor. In some cases, paddles or scrapers are used for agitation.

*2. Horizontal-tube natural circulation*

*evaporator*. The horizontal-tube natural circulation evaporator is shown in Fig. 32.2-1a. The horizontal bundle of heating tubes is similar to the bundle of tubes in a heat exchanger. The steam enters the tubes, where it condenses. The steam condensate leaves at the other end of the tubes. The boiling liquid solution covers the tubes. The vapor leaves the liquid surface, often goes through some de-entraining device such as a baffle to prevent carryover of liquid droplets, and exits at the top. This type of evaporator is relatively cheap and is used for nonviscous liquids with high heat-transfer coefficients and liquids that do not deposit scale. Since liquid circulation is poor, they are unsuitable for viscous liquids. In almost all cases, this evaporator and the types discussed below are operated continuously; that is,

the feed enters at a constant rate and the concentrate leaves at a constant rate.

### *3. Vertical-type natural circulation*

*evaporator.* In this type of evaporator, vertical rather than horizontal tubes are used; the liquid is inside the tubes and the steam condenses outside the tubes.

Because of boiling and decreases in density, the liquid rises in the tubes by natural circulation, as shown in Fig.

32.2-1b, and flows downward through a large, central open space or downcomer.

This natural circulation increases the heat-transfer coefficient. This type of evaporator is not used with viscous liquids. It is often called the *short-tube evaporator*. A variation is the basket type, where vertical tubes are used but the heating element is held suspended in the body so there is an annular open

space as the downcomer. In this way, it differs from the vertical natural circulation evaporator, which has a central instead of an annular open space as the downcomer. The basket type is widely used in the sugar, salt, and caustic-soda industries.

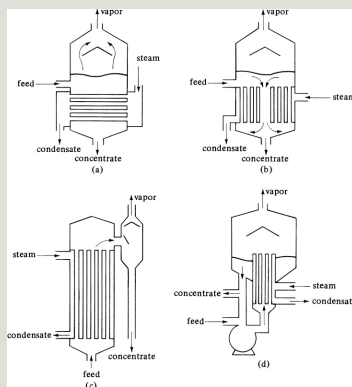


Figure 32.2-1. *Different types of evaporators: (a) horizontal-tube type, (b) vertical-tube type, (c) long-tube vertical type, (d) forced-circulation type.*

#### *4. Long-tube vertical-type evaporator.*

Since the heat-transfer coefficient on the steam side is very high compared to that on the evaporating-liquid side, high

liquid velocities are desirable. In a long-tube vertical-type evaporator, shown in Fig. 32.2-1c, the liquid is inside the tubes. The tubes are 3 to 10 m long and the formation of vapor bubbles inside the tubes causes a pumping action, which gives very high liquid velocities. Generally, the liquid passes through the tubes only once and is not recirculated. Contact times can be quite low in this type. In some cases, as when the ratio of feed to evaporation rate is low, natural recirculation of the product through the evaporator is effected by adding a large pipe connection between the outlet concentrate line and the feed line. This is widely used for producing condensed milk.

*5. Falling-film-type evaporator.* A variation on the long-tube-type

evaporator is the falling-film evaporator, wherein the liquid is fed to the top of the tubes and flows down the walls as a thin film. Vapor–liquid separation usually takes place at the bottom. This type is widely used for concentrating heat-sensitive materials such as orange juice and other fruit juices, because the holdup time is very small (5 to 10 s or more) and the heat-transfer coefficients are high.

#### *6. Forced-circulation-type evaporator.*

The liquid-film heat-transfer coefficient can be increased by pumping to cause forced circulation of the liquid inside the tubes. This could be done in the long-tube vertical type shown in Fig. 32.2-1c by adding a pipe connection shown with a pump between the outlet concentrate line and the feed line. In the forced-



circulation type, however, the vertical tubes are usually shorter than in the long-tube type, as shown in Fig.

32.2-1d. Additionally, in some cases a separate and external horizontal heat exchanger is used. This type of evaporator is very useful for viscous liquids.

*7. Agitated-film evaporator.* The main resistance to heat transfer in an evaporator is on the liquid side. One way to increase turbulence in this liquid film, and hence the heat-transfer coefficient, is by actual mechanical agitation of the film. This is done in a modified falling-film evaporator with only a single, large, jacketed tube containing an internal agitator. Liquid enters at the top of the tube and as it flows downward, it is spread out into a

turbulent film by the vertical agitator blades. The concentrated solution leaves at the bottom and vapor leaves through a separator and out the top. This type of evaporator is very useful with highly viscous materials, since the heat-transfer coefficient is greater than in forced-circulation evaporators. It is used with heat-sensitive viscous materials such as rubber latex, gelatin, antibiotics, and fruit juices. However, it has a high cost and small capacity. For interested readers, Perry and Green (P1) give more-detailed discussions and descriptions of evaporation equipment.

*8. Open-pan solar evaporator.* A very old yet still-viable process is solar evaporation in open pans. Saltwater is put in shallow open pans or troughs and allowed to evaporate slowly in the sun

to crystallize the salt.

### 32.2B Methods of Evaporator Operations

*1. Single-effect evaporators.* A simplified diagram of a single-stage or single-effect evaporator is given in Fig. 32.2-2. The feed enters at  $T_F$  K and saturated steam at  $T_s$  enters the heat-exchange section. Condensed steam leaves as condensate or drips. Since the solution in the evaporator is assumed to be completely mixed, the concentrated product and the solution in the evaporator have the same composition and temperature  $T_1$ , which is the boiling point of the solution. The temperature of the vapor is also  $T_1$ , since it is in equilibrium with the boiling solution. The pressure is  $P_1$ , which is

the vapor pressure of the solution at  $T_1$ .

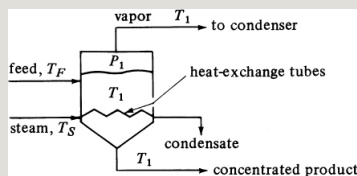


Figure 32.2-2. *Simplified diagram of single-effect evaporator.*

If the solution to be evaporated is assumed to be dilute and similar to water, then 1 kg of steam condensing will evaporate approximately 1 kg of vapor. This will hold if the feed entering has a temperature  $T_F$  near the boiling point.

The concept of an overall heat-transfer coefficient is used in the calculation of the rate of heat transfer in an evaporator. The general equation can be written as

$$q=UA \Delta T=UA(T_S-T_1)(32.2-1)$$

where  $q$  is the rate of heat transfer in W (btu/h),  $U$  is the overall heat-transfer coefficient in  $W/m^2 \cdot K$  (btu/h  $\cdot$  ft<sup>2</sup>  $\cdot$  °F),  $A$  is the heat transfer area in m<sup>2</sup> (ft<sup>2</sup>),  $T_s$  is the temperature of the condensing steam in K (°F), and  $T_1$  is the boiling point of the liquid in K (°F).

Single-effect evaporators are often used when the required capacity of operation is relatively small and/or the cost of steam is relatively cheap compared to the evaporator cost. However, for large-capacity operation, using more than one effect will markedly reduce steam costs.

*2. Forward-feed multiple-effect evaporators.* A single-effect evaporator, as shown in Fig. 32.2-2, is wasteful of energy since the latent heat of the vapor leaving is not used but is discarded.

Much of this latent heat, however, can be recovered and reused by employing a multiple-effect evaporator. A simplified diagram of a forward-feed triple-effect evaporation system is shown in Fig. 32.2-3.

If the feed to the first effect is near the boiling point at the pressure in the first effect, 1 kg of steam will evaporate almost 1 kg of water. The first effect operates at a temperature high enough so that the evaporated water serves as the heating medium to the second effect. Here, again, almost another kg of water is evaporated, which can then be used as the heating medium to the third effect. As a very rough approximation, almost 3 kg of water will be evaporated for 1 kg of steam in a three-effect evaporator. Hence, the *steam economy*, which is kg

vapor evaporated/kg steam used, is increased. This also holds approximately for more than three effects. However, the increased steam economy of a multiple-effect evaporator is gained at the expense of the initial cost of these evaporators.

In forward-feed operation, as shown in Fig. 32.2-3, the fresh feed is added to the first effect and flows to the next effect in the same direction as the vapor flow. This method of operation is used when the feed is hot or when the final concentrated product might be damaged at high temperatures. The boiling temperatures decrease from effect to effect. This means that if the first effect is at  $P_1 = 1$  atm abs pressure, the last effect will be under vacuum at a pressure  $P_3$ .

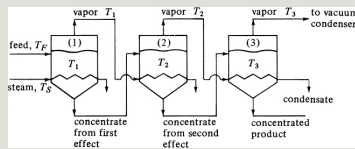


Figure 32.2-3. *Simplified diagram of forward-feed triple-effect evaporator.*

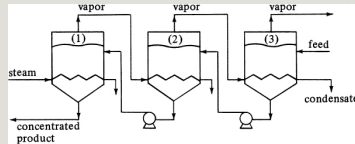


Figure 32.2-4. *Simplified diagram of backward-feed triple-effect evaporator.*

**3. Backward-feed multiple-effect evaporators.** In Fig. 32.2-4, the backward-feed operation for a triple-effect evaporator is shown; the fresh feed enters the last and coldest effect and continues on until the concentrated product leaves the first effect. This method of reverse feed is advantageous when the fresh feed is cold, since a smaller amount of liquid must be heated to the higher temperatures in the second



and first effects. However, liquid pumps must be used in each effect, since the flow is from low to high pressure. This reverse-feed method is also used when the concentrated product is highly viscous. The high temperatures in the early effects reduce the viscosity and give reasonable heat-transfer coefficients.

*4. Parallel-feed multiple-effect evaporators.* Parallel feed in multiple-effect evaporators involves the addition of fresh feed and the withdrawal of concentrated product from each effect. The vapor from each effect is still used to heat the next effect. This method of operation is mainly used when the feed is almost saturated and solid crystals are the product, as in the evaporation of brine to make salt.

### 32.3 Overall Heat-Transfer Coefficients in Evaporators

The overall heat-transfer coefficient  $U$  in an evaporator is composed of the steam-side condensing coefficient, which has a value of about  $5700 \text{ W/m}^2 \cdot \text{K}$  ( $1000 \text{ btu/h} \cdot \text{ft}^2 \cdot ^\circ\text{F}$ ); the metal wall, which has a high thermal conductivity and usually a negligible resistance; the resistance of the scale on the liquid side; and the liquid film coefficient, which is usually inside the tubes.

The steam-side condensing coefficient outside the tubes can be estimated using Eq. (15.6-20)–Eq. (15.6-26). The resistance due to scale formation usually cannot be predicted. Increasing the velocity of the liquid in the tubes greatly decreases the rate of scale formation,

which is one important advantage of forced-circulation evaporators. The scale may be salts, such as calcium sulfate or sodium sulfate, which decrease in solubility with an increase in temperature and hence tend to deposit on the hot tubes.

For forced-circulation evaporators, the coefficient  $h$  inside the tubes can be predicted if there is little or no vaporization inside the tube. The liquid hydrostatic head in the tubes prevents most boiling in the tubes. The standard equations for predicting the  $h$  value of liquids inside tubes can be used.

Velocities used often range from 2 to 5 m/s (7 to 15 ft/s). The heat-transfer coefficient can be predicted from Eq. (15.3-5), using a constant of 0.028 instead of 0.027 (B1). If there is some or

appreciable boiling in part or all of the tubes, use of the equation assuming no boiling will give conservative, safe results (P1).

For long-tube vertical natural-circulation evaporators, the heat-transfer coefficient is more difficult to predict, since there is a nonboiling zone in the bottom of the tubes and a boiling zone in the top. The length of the nonboiling zone depends on the heat transfer in the two zones and the pressure drop in the boiling two-phase zone. The film heat-transfer coefficient in the nonboiling zone can be estimated using Eq. (15.3-5) with a constant of 0.028. For the boiling two-phase zone, a number of equations are given by Perry and Green (P1).

For short-tube vertical evaporators, the

heat-transfer coefficients can be estimated by using the same methods as for long-tube vertical natural circulation evaporators. Horizontal-tube evaporators have heat-transfer coefficients on the same order of magnitude as short-tube vertical evaporators.

For the agitated-film evaporator, the heat-transfer coefficient may be estimated using Eq. (15.8-4) for a scraped-surface heat exchanger.

The methods given above are useful for actual evaporator design and/or for evaluating the effects of changes in operating conditions on the coefficients. In making preliminary designs or cost estimates, it is helpful to have available the overall heat-transfer coefficients

usually encountered in commercial practice. Some preliminary values and ranges of values for various types of evaporators are given in Table 32.3-1.

Table 32.3-1. *Typical Heat-Transfer Coefficients for Various Evaporators\**  
(B3, B4, L1, P1)

\*Generally, nonviscous liquids have the higher coefficients and viscous liquids the lower coefficients in the ranges given.

## 32.4 Calculation Methods for Single-Effect Evaporators

### 32.4A Heat and Material Balances for Evaporators

The basic equation for solving for the capacity of a single-effect evaporator is Eq. (32.2-1), which can be written as

$$q=UA \Delta T(32.4-1)$$

where  $\Delta T$  K ( $^{\circ}\text{F}$ ) is the difference in temperature between the condensing steam and the boiling liquid in the evaporator. In order to solve Eq. (32.4-1), the value of  $q$  in W (btu/h) must be determined by making a heat and material balance on the evaporator shown in Fig. 32.4-1. The feed to the evaporator is  $F$  kg/h (lb<sub>m</sub>/h), having a solids content of  $x_F$  mass fraction, temperature  $T_F$ , and enthalpy  $h_F$  J/kg (btu/lb<sub>m</sub>). Coming out is a concentrated liquid  $L$  kg/h (lb<sub>m</sub>/h) having a solids content of  $x_L$ , temperature  $T_1$ , and enthalpy  $h_L$ . The vapor  $V$  kg/h (lb<sub>m</sub>/h) is given off as pure solvent having a solids content of  $y_v = 0$ , temperature  $T_1$ , and enthalpy  $H_v$ . Saturated steam entering is  $S$  kg/h (lb<sub>m</sub>/h) and has a temperature of  $T_s$  and enthalpy of  $H_s$ . The condensed steam leaving of  $S$  kg/h is usually

assumed to be at  $T_s$ , the saturation temperature, with an enthalpy of  $h_s$ . This means that the steam gives off only its latent heat,  $\lambda$ , where

$$\lambda = H_S - h_S \quad (32.4-2)$$

Since the vapor  $V$  is in equilibrium with the liquid  $L$ , the temperatures of vapor and liquid are the same. Also, the pressure  $P_1$  is the saturation vapor pressure of the liquid of composition  $x_L$  at its boiling point  $T_1$ . (This assumes no boiling-point rise.)

For the material balance, since we are at steady state, the rate of mass in = rate of mass out. Then, for a total balance,

$$F = L + V \quad (32.4-3)$$

For a balance on the solute (solids)



alone,

$$FxF=LxL(32.4-4)$$

For the heat balance, since the total heat entering = total heat leaving,

$$\begin{aligned} \text{heat in feed} + \text{heat in steam} = & \text{heat in} \\ \text{concentrated liquid} + \text{heat in vapor} + & \\ \text{heat in condensed steam} & (32.4-5) \end{aligned}$$

This assumes no heat lost by radiation or convection. Substituting into Eq. (32.4-5),

$$Fh_F + SH_S = Lh_L + VH_V + Sh_S(32.4-6)$$

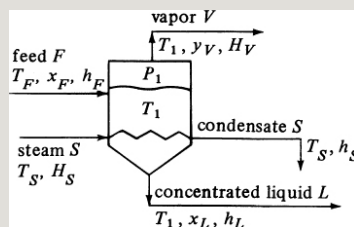


Figure 32.4-1. Heat and mass balance for single-effect evaporator.

Substituting Eq. (32.4-2) into (32.4-6),

$$Fh_F + S\lambda = Lh_L + Vh_V \quad (32.4-7)$$

The heat  $q$  transferred in the evaporator is then

$$q = S(H_S - h_S) = S\lambda \quad (32.4-8)$$

In Eq. (32.4-7), the latent heat  $\lambda$  of steam at the saturation temperature  $T_s$  can be obtained from the steam tables in Appendix A.2. However, the enthalpies of the feed and products are often not available; these enthalpy–concentration data are available for only a few substances in solution. Hence, some approximations are made in order to make a heat balance. These are as follows:

1. It can be demonstrated as an approximation that the latent

heat of evaporation of 1 kg mass of the water from an aqueous solution can be obtained from the steam tables using the temperature of the boiling solution  $T_1$  (exposed surface temperature) rather than the equilibrium temperature for pure water at  $P_1$ .

2. If the heat capacities  $c_p F$  of the liquid feed and  $c_p L$  of the product are known, they can be used to calculate the enthalpies. (This neglects heats of dilution, which in most cases are not known.)

**EXAMPLE 32.4-1. Heat-Transfer Area in a Single-Effect Evaporator**

A continuous single-effect evaporator concentrates 9072 kg/h of a 1.0 wt % salt solution entering at 311.0 K (37.8°C) to a final concentration of 1.5 wt %. The vapor space of the evaporator is at 101.325 kPa (1.0 atm abs) and the steam supplied is saturated at 143.3 kPa. The overall coefficient  $U = 1704 \text{ W/m}^2 \cdot \text{K}$ . Calculate the amounts of vapor and liquid product and the heat-transfer area required. Assume that the solution, since it is dilute, has the same boiling point as water.

**Solution:** The flow diagram is the same as in Fig. 32.4-1. For the material balance, substituting into Eq. (32.4-3),

$$F=L+V9072=L+V(32.4-3)$$

Substituting into Eq. (32.4-4) and solving,

$$FxF=LxL9072(0.01)=L(0.015)L=6048 \text{ kg/h of liquid}(32.4-4)$$

Substituting into Eq. (32.4-3) and solving,

$$V = 3024 \text{ kg/h of vapor}$$

The heat capacity of the feed is assumed to be  $c_p F = 4.14 \text{ kJ/kg} \cdot \text{K}$ . (Often, for feeds of inorganic salts in water, the  $c_p$  can be assumed to be approximately that of water alone.)

To make a heat balance using Eq. (32.4-7), it is convenient to select the boiling point of the dilute solution in the evaporator, which is assumed to be that of water at 101.32 kPa,  $T_1 = 373.2 \text{ K}$  ( $100^\circ\text{C}$ ), as the datum temperature. Then,  $H_v$  is simply the latent heat of water at 373.2 K, which from the steam tables in Appendix A.2 is 2257 kJ/kg (970.3 btu/lbm). The latent heat  $\lambda$  of the steam at 143.3 kPa [saturation temperature  $T_s = 383.2 \text{ K}$  ( $230^\circ\text{F}$ )] is 2230 kJ/kg (958.8 btu/lbm).

The enthalpy of the feed can be calculated from

$$h_F = c_p F (T_F - T_1) \quad (32.4-9)$$

Substituting into Eq. (32.4-7) with  $h_L = 0$ , since it is at the datum of 373.2 K,

$$\begin{aligned} & 9072(4.14) \\ (311.0 - 373.2) + S(2230) &= 6048(0) + 3024(2257) \\ S &= 4108 \text{ kg steam/h} \end{aligned}$$

The heat  $q$  transferred through the heating surface area  $A$  is, from Eq. (32.4-8),

$$\begin{aligned} q &= S(\lambda) = 4108(2230) \\ (1000/3600) &= 2\,544\,000 \text{ W} \quad (32.4-8) \end{aligned}$$

Substituting into Eq. (32.4-1), where  $\Delta T = T_s - T_1$ ,

$$q = 2544000 = UA \Delta T = 1704(A)(383.2 - 373.2)$$

Solving,  $A = 149.3 \text{ m}^2$ .

## 32.4B Effects of Processing Variables on Evaporator Operation

*1. Effect of feed temperature.* The inlet temperature of the feed has a significant effect on the operation of the evaporator. In Example 32.4-1,

the feed entering was at a temperature of 311.0 K, cold as compared to the boiling temperature of 373.2 K. About 14 of the steam used for heating was to bring the cold feed to the boiling point. Hence, only about 14 of the steam was left for vaporization of the feed. If the feed is under pressure and enters the evaporator at a temperature above the boiling point in the evaporator, additional vaporization is obtained by flashing part of the entering hot feed. Preheating the feed can reduce the size of evaporator heat-transfer area needed.

2. *Effect of pressure.* In Example 32.4-1, a pressure of 101.32 kPa abs was used in the vapor space of the evaporator. This set the boiling point of the solution

at 373.2 K and gave a  $\Delta T$  for use in Eq. (32.4-1) of  $383.2 - 373.2$ , or 10 K. In many cases, a larger  $\Delta T$  is desirable, since, as  $\Delta T$  increases, the heating-surface area  $A$  and the cost of the evaporator decrease. To reduce the pressure below 101.32 kPa, that is, to be under vacuum, a condenser and vacuum pump can be used. For example, if the pressure was reduced to 41.4 kPa, the boiling point of water will be 349.9 K and the new  $\Delta T$  will be  $383.2 - 349.9$ , or 33.3 K. A large decrease in heating-surface area would be obtained.

*3. Effect of steam pressure.* Using higher pressure, saturated steam increases  $\Delta T$ , which decreases the size and cost of the evaporator. However, high-pressure steam is more costly as well as often being more valuable as a

source of power elsewhere. Hence, overall economic balances are really needed to determine the optimum steam pressures.

### **32.4C Boiling-Point Rise of Solutions**

In the majority of cases in evaporation, the solutions are not dilute solutions such as those considered in Example 32.4-1. In most cases, the thermal properties of the solution being evaporated may differ considerably from those of water. The concentrations of the solutions are high enough that the heat capacity and boiling point are quite different from those for water.

For strong solutions of dissolved solutes, the boiling-point rise due to the solutes in the solution usually cannot be

predicted. However, a useful empirical law known as *Dühring's rule* can be applied. According to this rule, a straight line is obtained if the boiling point of a solution in °C or °F is plotted against the boiling point of pure water at the same pressure for a given concentration at different pressures. A different straight line is obtained for each given concentration. In Fig. 32.4-2, an example of a Dühring-line chart is given for solutions of sodium hydroxide in water. It is necessary to know the boiling point of a given solution at only two pressures to determine a line.

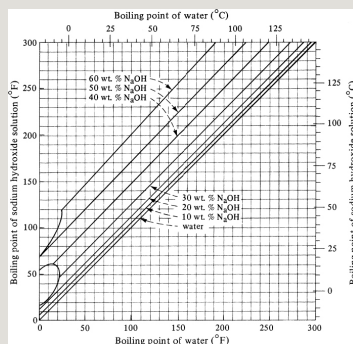




Figure 32.4-2. *Dühring lines for aqueous solutions of sodium hydroxide.*

**EXAMPLE 32.4-2. Use of a Dühring Chart for Boiling-Point Rise**

As an example of using the chart, the pressure in an evaporator is given as 25.6 kPa (3.72 psia) and a solution of 30% NaOH is being boiled. Determine the boiling temperature of the NaOH solution and the boiling-point rise (BPR) of the solution over that of water at the same pressure.

**Solution:** From the steam tables in Appendix A.2, the boiling point of water at 25.6 kPa is 65.6°C. From Fig. 32.4-2, for 65.6°C (150°F) and 30% NaOH, the boiling point of the NaOH solution is 79.5°C (175°F). The boiling-point rise is  $79.5 - 65.6 = 13.9^\circ\text{C}$  (25°F)

In Perry and Green (P1), a chart is given for estimating the boiling-point rise of a large number of common aqueous solutions used in chemical and biological processes. In addition to the common salts and solutes, such as  $\text{NaNO}_3$ ,  $\text{NaOH}$ ,  $\text{NaCl}$ , and  $\text{H}_2\text{SO}_4$ , the biological solutes sucrose, citric acid, kraft solution, and glycerol are given. These biological solutes have quite

small boiling-point-rise values compared to those of common salts.

### 32.4D Enthalpy–Concentration Charts of Solutions

If the heat of solution of the aqueous solution being concentrated in the evaporator is large, neglecting it could cause errors in the heat balances. This heat-of-solution phenomenon can be explained as follows: If pellets of NaOH are dissolved in a given amount of water, it is found that a considerable temperature rise occurs; that is, heat is evolved, called *heat of solution*. The amount of heat evolved depends on the type of substance and the amount of water used. Also, if a strong solution of NaOH is diluted to a lower concentration, heat is liberated. Conversely, if a solution is

concentrated from a low to a high concentration, heat must be added.

In Fig. 32.4-3, an enthalpy–concentration chart for NaOH is given (M1), where the enthalpy is in kJ/kg (btu/lbm) solution, temperature is in °C (°F), and concentration is in weight fraction NaOH in solution. Such enthalpy–concentration charts are usually not made for solutions having negligible heats of solution, since the heat capacities can be easily used to calculate enthalpies. Also, such charts are available for only a few solutions.

The enthalpy of the liquid water in Fig. 32.4-3 is referred to the same datum or reference state as in the steam tables, that is, liquid water at 0°C (273 K). This means that enthalpies from the figure

can be used with those in the steam tables. In Eq. (32.4-7), values for  $h_F$  and  $h_L$  can be taken from Fig. 32.4-3 and values for  $\lambda$  and  $H_V$  from the steam tables. The uses of Fig. 32.4-3 will be better understood from the following example.

**EXAMPLE 32.4-3. Evaporation of an NaOH Solution**

An evaporator is used to concentrate 4536 kg/h (10 000 lbm/h) of a 20% solution of NaOH in water entering at 60°C (140°F) to a product of 50% solids. The pressure of the saturated steam used is 172.4 kPa (25 psia) and the pressure in the vapor space of the evaporator is 11.7 kPa (1.7 psia). The overall heat-transfer coefficient is 1560 W/m<sup>2</sup> · K (275 btu/h · ft<sup>2</sup> · °F). Calculate the steam used, the steam economy in kg vaporized/kg steam used, and the heating surface area in m<sup>2</sup>.

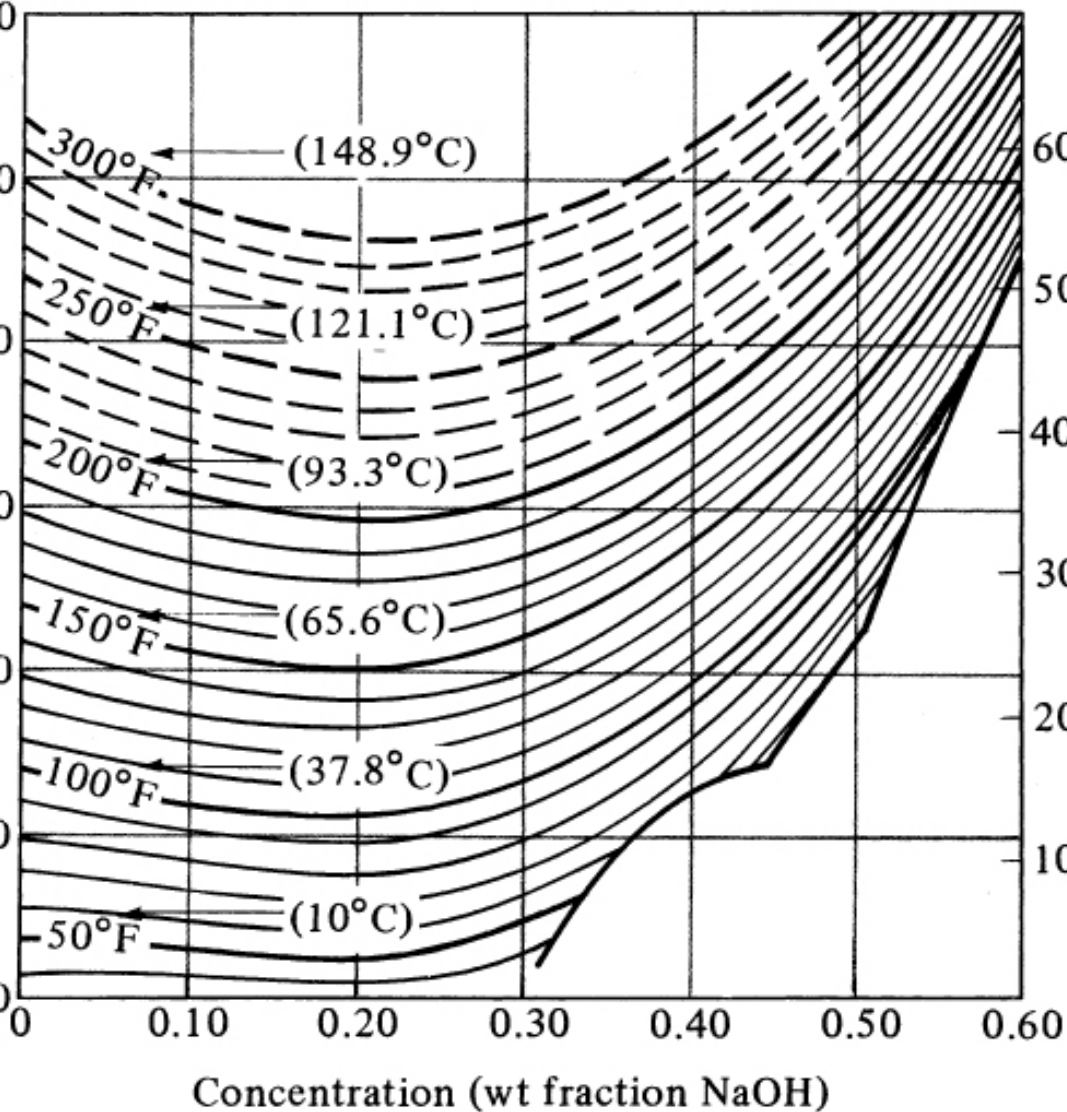


Figure 32.4-3. *Enthalpy-concentration chart for the system NaOH-water. [Reference state liquid water at 0°C (273 K) or 32°F.] From W. L. McCabe, Trans. A.I.Ch.E., 31, 129 (1935). With permission.*

**Solution:** The process flow diagram and nomenclature are the same as in Fig. 32.4-1. The given variables are  $F = 4536 \text{ kg/h}$ ,  $x_F = 0.20 \text{ wt fraction}$ ,  $T_F = 60^\circ\text{C}$ ,  $P_1 = 11.7 \text{ kPa}$ , steam pressure =  $172.4 \text{ kPa}$ , and  $x_L = 0.50 \text{ wt fraction}$ . For the overall material balance, substituting into Eq. (32.4-3),

$$F=4536=L+V(32.4-3)$$

Substituting into Eq. (32.4-4) and solving Eqs. (32.4-3) and (32.4-4) simultaneously,

$$FxF=LxL4536(0.20)=L(0.50)L=1814 \text{ kg/h} \quad V=2722 \text{ kg/h} \quad (32.4-4)$$

To determine the boiling point  $T_1$  of the 50% concentrated solution, we first obtain the boiling point of pure water at 11.7 kPa from the steam tables (Appendix A.2) as 48.9°C (120°F). From the Dühring chart, Fig. 32.4-2, for a boiling point of water of 48.9°C and 50% NaOH, the boiling point of the solution is  $T_1 = 89.5^\circ\text{C}$  (193°F). Hence,

$$\text{boiling-point rise} = T_1 - 48.9 = 89.5 - 48.9 = 40.6^\circ\text{C} (73^\circ\text{F})$$

From the enthalpy–concentration chart (Fig. 32.4-3), for 20% NaOH at 60°C (140°F),  $h_f = 214 \text{ kJ/kg}$  (92 btu/lbm). For 50% NaOH at 89.5°C (193°F),  $h_L = 505 \text{ kJ/kg}$  (217 btu/lbm).

For the superheated vapor  $V$  at 89.5°C (193°F) and 11.7 kPa [superheated 40.6°C (73°F) since the boiling point of water is 48.9°C (120°F) at 11.7 kPa], from the steam tables  $H_v = 2667 \text{ kJ/kg}$  (1147 btu/lbm). An alternative method for calculating the  $H_v$  is first to obtain the enthalpy of saturated vapor at 48.9°C (120°F) and 11.7 kPa of 2590 kJ/kg (1113.5 btu/lbm). Then, using a heat capacity of 1.884 kJ/kg · K for superheated steam with the superheat of (89.5 – 48.9)°C = (89.5 – 48.9) K,

$$H_v = 2590 + 1.884(89.5 - 48.9) = 2667 \text{ kJ/kg}$$

For the saturated steam at 172.4 kPa, the saturation temperature from the steam tables is 115.6°C (240°F) and the latent heat is  $\lambda = 2214 \text{ kJ/kg}$  (952 btu/lbm).

Substituting into Eq. (32.4-7) and solving for  $S$ ,

$$Fh_f + S\lambda = Lh_L + VH_v \\ 4535(214) + S(2214) = 1814(505) + 2722(2667) \\ S = 3255 \text{ kg steam/h} \quad (32.4-7)$$

Substituting into Eq. (32.4-8),

$$q = S\lambda = 3255(2214) = 2002 \text{ kW}$$

Substituting into Eq. (32.4-1) and solving,

$$2002(1000) = 1560(A)(115.6 - 89.5)$$

Hence,  $A = 49.2 \text{ m}^2$ . Also, steam economy =  $2722/3255 = 0.836$ .

## **32.5 Calculation Methods for Multiple-Effect Evaporators**

### **32.5A Introduction**

In evaporation of solutions in a single-effect evaporator, a major cost is the cost of the steam used to evaporate the water. A single-effect evaporator is wasteful in terms of steam costs, since the latent heat of the vapor leaving the evaporator is usually not used. To reduce this cost, multiple-effect evaporators are used that recover the latent heat of the vapor leaving and reuse it.

A three-effect evaporator, discussed briefly in Section 32.2B, is shown in

Fig. 32.2-3. In this system, each effect in itself acts as a single-effect evaporator. Raw steam is used as the heating medium to the first effect, which is boiling at temperature  $T_1$  and pressure  $P_1$ . The vapor removed from the first effect is then used as the heating medium, condensing in the second effect and vaporizing water at temperature  $T_2$  and pressure  $P_2$  in this effect. To transfer heat from the condensing vapor to the boiling liquid in this second effect, the boiling temperature  $T_2$  must be less than the condensing temperature. This means that the pressure  $P_2$  in the second effect is lower than  $P_1$  in the first effect. In a similar manner, vapor from the second effect is condensed in heating the third effect. Hence, pressure  $P_3$  is less than  $P_2$ . If the first effect is operating at 1 atm abs pressure, the



second and third effects will be under vacuum.

In the first effect, raw, dilute feed is added and is partly concentrated. Then, this partly concentrated liquid (Fig. 32.2-3) flows to the second evaporator in series, where it is further concentrated. This liquid from the second effect flows to the third effect for final concentration.

When a multiple-effect evaporator is at steady-state operation, the flow rates and rate of evaporation in each effect are constant. The pressures, temperatures, and internal flow rates are automatically kept constant by the steady-state operation of the process itself. To change the concentration in the final effect, the feed rate to the first effect

must be changed. The overall material balance made over the whole system and over each evaporator itself must be satisfied. If the final solution is too concentrated, the feed rate must be increased, and vice versa. Then, the final solution will reach a new steady state at the desired concentration.

### **32.5B Temperature Drops and Capacity of Multiple-Effect Evaporators**

*1. Temperature drops in multiple-effect evaporators.* The amount of heat transferred per hour in the first effect of a triple-effect evaporator with forward feed, as shown in Fig. 32.2-3, will be

$$q_1 = U_1 A_1 \Delta T_1 \quad (32.5-1)$$

where  $\Delta T_1$  is the difference between the condensing steam and the boiling point

of the liquid,  $T_s - T_1$ . Assuming that the solutions have no boiling-point rise and no heat of solution, and neglecting the sensible heat necessary to heat the feed to the boiling point, approximately all the latent heat of the condensing steam appears as latent heat in the vapor. This vapor then condenses in the second effect, giving up approximately the same amount of heat:

$$q_2 = U_2 A_2 \Delta T_2 \quad (32.5-2)$$

This same reasoning holds for  $q_3$ . Since  $q_1 = q_2 = q_3$ , then, approximately,

$$U_1 A_1 \Delta T_1 = U_2 A_2 \Delta T_2 = U_3 A_3 \Delta T_3 \quad (32.5-3)$$

In commercial practice, the areas in all effects are usually equal and

$$q A = U_1 \Delta T_1 = U_2 \Delta T_2 = U_3 \Delta T_3 \quad (32.5-4)$$

Hence, the temperature drops  $\Delta T$  in a multiple-effect evaporator are approximately inversely proportional to the values of  $U$ . Calling  $\sum \Delta T$  as follows for no boiling-point rise,

$$\sum \Delta T = \Delta T_1 + \Delta T_2 + \Delta T_3 = T_S - T_3 \quad (32.5-5)$$

Note that  $\Delta T_1^\circ\text{C} = \Delta T_1 \text{ K}$ ,  $\Delta T_2^\circ\text{C} = \Delta T_2 \text{ K}$ , and so on. Since  $\Delta T_1$  is proportional to  $1/U_1$ , then

$$\Delta T_1 = \sum \Delta T \frac{1/U_1}{1/U_1 + 1/U_2 + 1/U_3} \quad (32.5-6)$$

Similar equations can be written for  $\Delta T_2$  and  $\Delta T_3$ .

*2. Capacity of multiple-effect evaporators.* A rough estimate of the capacity of a three-effect evaporator

compared to a single-effect can be obtained by adding the value of  $q$  for each evaporator:

$$q_3 = U_1 A_1 \Delta T_1 + U_2 A_2 \Delta T_2 + U_3 A_3 \Delta T_3 \quad (32.5-7)$$

If we make the assumptions that the value of  $U$  is the same in each effect and that the values of  $A$  are equal, Eq. (32.5-7) becomes

$$q = UA(\Delta T_1 + \Delta T_2 + \Delta T_3) = UA\Delta T \quad (32.5-8)$$

where  $\Delta T = \sum \Delta T = \Delta T_1 + \Delta T_2 + \Delta T_3 = T_s - T_3$ .

If a single-effect evaporator is used with the same area  $A$ , the same value of  $U$ , and the same total temperature drop  $\Delta T$ , then

$$q = UA\Delta T \quad (32.5-9)$$

This, of course, gives the same capacity as for the multiple-effect evaporator.

Hence, the increase in steam economy obtained by using multiple-effect evaporators is obtained at the expense of reduced capacity.

### **32.5C Calculations for Multiple-Effect Evaporators**

In doing calculations for a multiple-effect evaporator system, the values to be obtained are usually the area of the heating surface in each effect, the kg of steam per hour to be supplied, and the amount of vapor leaving each effect, especially the last one.

The given or known values are usually as follows: (1) steam pressure to the first effect, (2) final pressure in the vapor space of the last effect, (3) feed conditions and flow to the first effect, (4) final

concentration in the liquid leaving the last effect, (5) physical properties such as enthalpies and/or heat capacities of the liquid and vapors, and (6) overall heat-transfer coefficients in each effect. Usually, the areas of each effect are assumed equal.

The calculations are done using material balances, heat balances, and the capacity equations  $q = UA\Delta T$  for each effect. A convenient way to solve these equations is by trial and error. The basic steps to follow are given in the next section for a triple-effect evaporator.

### **32.5D Step-by-Step Calculation Methods for Triple-Effect Evaporators**

1. From the known outlet concentration and pressure in the last effect, determine the boiling point in the last effect. (If a boiling-point rise is present, this can be determined from a Dühring-line plot.)

2. Determine the total amount of vapor evaporated by performing an overall material balance. For this first trial, apportion the total amount of vapor among the three effects. (Usually, equal amounts of vapor are produced in each effect, so that  $V_1 = V_2 = V_3$  is assumed for the first trial.) Make a total material balance on effects 1, 2, and 3 to obtain  $L_1$ ,  $L_2$ , and  $L_3$ . Then, calculate the solids concentration in each effect by a solids balance on each effect.
3. Using Eq. (32.5-6), estimate the temperature drops  $\Delta T_1$ ,  $\Delta T_2$ , and  $\Delta T_3$  in the three effects. Any effect that has an extra heating load, such as a cold feed, requires a proportionately larger  $\Delta T$ . Then, calculate the boiling point in each effect.

[If a boiling-point rise (BPR) in  $^{\circ}\text{C}$  is present, estimate the pressure in effects 1 and 2 and determine the BPR in each of the three effects. Only a crude pressure estimate is needed, since BPR is almost independent of pressure. Then, the  $\sum \Delta T$  available for heat transfer without the superheat is obtained by subtracting the sum of all three BPRs from the overall  $\Delta T$  of  $T_5 - T_3$  (saturation). Using Eq. (32.5-6), estimate  $\Delta T_1$ ,  $\Delta T_2$ , and  $\Delta T_3$ . Then, calculate the boiling point in each effect.]

4. Using heat and material balances in each effect, calculate the amount vaporized and the flows of liquid in each effect. If the amounts vaporized differ appreciably from those assumed in step 2, then steps 2, 3, and 4 can be repeated using the amounts of evaporation just calculated. (In step 2, only the solids balance is repeated.)



5. Calculate the value of  $q$  transferred in each effect. Using the rate equation  $q = UA\Delta T$  for each effect, calculate the areas  $A_1$ ,  $A_2$ , and  $A_3$ . Then, calculate the average value  $A_m$  by

$$A_m = \frac{A_1 + A_2 + A_3}{3} (32.5-10)$$

If these areas are reasonably close to each other, the calculations are complete and a second trial is not needed. If these areas are not almost equal, a second trial should be performed as follows.

6. To start trial 2, use the new values of  $L_1$ ,  $L_2$ ,  $L_3$ ,  $V_1$ ,  $V_2$ , and  $V_3$  calculated by the heat balances in step 4 and calculate the new solids concentration in each effect by a solids balance on each effect.

7. Obtain new values  $\Delta T_1'$ ,  $\Delta T_2'$ , and  $\Delta T_3'$  from

$$\Delta T_1' = \frac{\Delta T_1 A_1}{A_m} \quad \Delta T_2' = \frac{\Delta T_2 A_2}{A_m} \quad \Delta T_3' = \frac{\Delta T_3 A_3}{A_m} \quad (32.5-11)$$

The sum  $\Delta T_1' + \Delta T_2' + \Delta T_3'$  must equal the original  $\sum \Delta T$ . If not, proportionately readjust all  $\Delta T'$  values so that this is so. Then, calculate the boiling point in each effect.

[If a boiling-point rise is present, determine the new BPRs in the three effects using the new concentrations from step 6. To get a new value of  $\sum \Delta T$  available for heat transfer, subtract the sum of all three BPRs from the overall  $\Delta T$ . Calculate the new values of  $\Delta T'$  by Eq. (32.5-11). The sum of the  $\Delta T'$  values just calculated must be readjusted to the new  $\sum \Delta T$  value. Then, calculate the boiling point in each effect.] Step 7 is essentially a repeat of step 3 but

using Eq. (32.5-11) to obtain a better estimate of the  $\Delta T'$  values.

8. Using the new  $\Delta T'$  values from step 7, repeat the calculations starting with step 4. Two trials are usually sufficient so that the areas are reasonably close to being equal.

**EXAMPLE 32.5-1. Evaporation of a Sugar Solution in a Triple-Effect Evaporator**

A triple-effect forward-feed evaporator is being used to evaporate a sugar solution containing 10 wt % solids to a concentrated solution of 50%. The boiling-point rise of the solutions (independent of pressure) can be estimated from  $\text{BPR}^{\circ}\text{C} = 1.78x + 6.22x^2$  ( $\text{BPR}^{\circ}\text{F} = 3.2x + 11.2x^2$ ), where  $x$  is wt fraction of sugar in solution (K1). Saturated steam at 205.5 kPa (29.8 psia) [ $121.1^{\circ}\text{C}$  ( $250^{\circ}\text{F}$ ) saturation temperature] is being used. The pressure in the vapor space of the third effect is 13.4 kPa (1.94 psia). The feed rate is 22 680 kg/h (50 000 lb<sub>m</sub>/h) at  $26.7^{\circ}\text{C}$  ( $80^{\circ}\text{F}$ ). The heat capacity of the liquid solutions is (K1)  $c_p = 4.19 - 2.35x$  kJ/kg  $\cdot$  K ( $1.0 - 0.56x$  btu/lb<sub>m</sub>  $\cdot$   $^{\circ}\text{F}$ ). The heat of solution is considered to be negligible. The coefficients of heat transfer have been estimated as  $U_1 = 3123$ ,  $U_2 = 1987$ , and  $U_3 = 1136$  W/m<sup>2</sup>  $\cdot$  K, or 550, 350, and 200 btu/h  $\cdot$  ft<sup>2</sup>  $\cdot$   $^{\circ}\text{F}$ . If each effect has the same surface area, calculate the area, the steam rate used, and the steam economy.

**Solution:** The process flow diagram is given in Fig. 32.5-1. Following the eight steps outlined, the calculations are as follows:

*Step 1.* For 13.4 kPa (1.94 psia), the saturation temperature is  $51.67^{\circ}\text{C}$  ( $125^{\circ}\text{F}$ ) from the steam tables. Using the equation for BPR for evaporator number 3 with  $x = 0.5$ ,

$$\begin{aligned} \text{BPR}_3 &= 1.78x \\ &+ 6.22x^2 = 1.78(0.5) + 6.22(0.5)^2 = 2.45^{\circ}\text{C} (4.4^{\circ}\text{F}) \\ T_3 &= 51.67 + 2.45 = 54.12^{\circ}\text{C} (129.4^{\circ}\text{F}) \end{aligned}$$

*Step 2.* Making an overall and a solids balance to calculate the total amount vaporized ( $V_1 + V_2 + V_3$ ) and  $L_3$ ,

$$F=22680=L_3+(V_1+V_2+V_3) \quad Fx_F=22680(0.1)=L_3(0.5)+(V_1+V_2+V_3)$$

$$(0) L_3=4536 \text{ kg/h (10000 lbm/h)}$$

$$h) \text{ total vaporized}=(V_1+V_2+V_3)=18\,144 \text{ kg/h (40\,000 lbm/h)}$$

Assuming equal amount vaporized in each effect,  $V_1 = V_2 = V_3 = 6048 \text{ kg/h (13\,333 lbm/h)}$ . Making a total material balance on effects 1, 2, and 3 and solving,

$$(1) F=22680=V_1+L_1=6048+L_1, L_1=16632 \text{ kg/h (33667 lbm/h)}$$

$$(2) L_1=16632=V_2+L_2=6048+L_2, L_2=10584 (23334)$$

$$(3) L_2=10584=V_3+L_3=6048+L_3, L_3=4536 (10000)$$

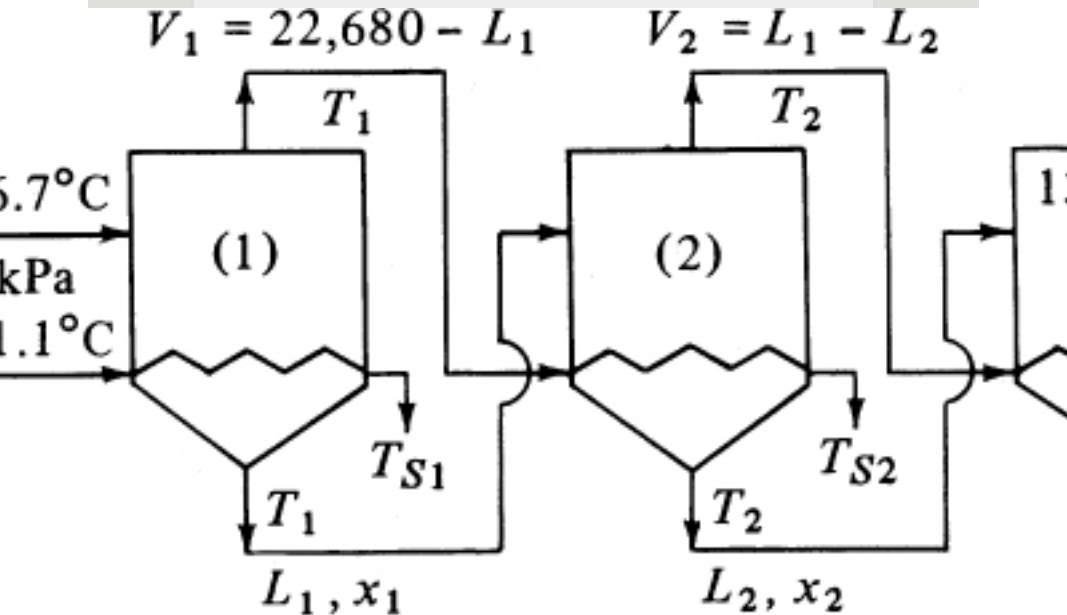


Figure 32.5-1. Flow diagram for triple-effect evaporation for Example 32.5-1.

Making a solids balance on effects 1, 2, and 3 and solving for  $x$ ,

$$(1) 22680(0.1)=L_1x_1=16632(x_1), x_1=0.136 \quad (2) 16632(0.136)=L_2x_2=10584(x_2), x_2=0.214$$

Step 3. The BPR in each effect is calculated as follows:

$$(1) \text{BPR}_1=1.78x_1+6.22x_1^2=1.78(0.136)+6.22(0.136)^2=0.36^\circ\text{C}(0.7^\circ\text{F})$$

$$(2) \text{BPR}_2=1.78(0.214)+6.22(0.214)^2=0.65^\circ\text{C}(12^\circ\text{F})$$

$$(3) \text{BPR}_3=1.78(0.5)+6.22(0.5)^2=2.45^\circ\text{C}(4.4^\circ\text{F})$$

$$\Sigma \Delta T \text{ available} = TS1 - T3(\text{saturation}) - (BPR1 + BPR2 + BPR3) = 121.1 - 51.67 - (0.36 + 0.65 + 2.45) = 65.97^\circ\text{C} (118.7^\circ\text{F})$$

Using Eq. (32.5-6) for  $\Delta T_1$  and similar equations for  $\Delta T_2$  and  $\Delta T_3$ ,

$$\Delta T_1 = \Sigma \Delta T_1 / (U_1 + 1/U_2 + 1/U_3) = (65.97) / (1/3123 + (1/1987) + (1/1136)) \Delta T_1 = 12.40^\circ\text{C} \quad \Delta T_2 = 19.50^\circ\text{C} \quad \Delta T_3 = 34.07^\circ\text{C} = 18.34^\circ\text{K}$$

However, since a cold feed enters effect number 1, this effect requires more heat. Increasing  $\Delta T_1$  and lowering  $\Delta T_2$  and  $\Delta T_3$  proportionately as a first estimate,

$$\Delta T_1 = 15.56^\circ\text{C} = 15.56^\circ\text{K} \quad \Delta T_2 = 18.34^\circ\text{C} = 18.34^\circ\text{K} \quad \Delta T_3 = 32.07^\circ\text{C} = 32.07^\circ\text{K}$$

To calculate the actual boiling point of the solution in each effect,

$$(1) T_1 = TS1 - \Delta T_1 = 121.1 - 15.56 = 105.54^\circ\text{C} \quad TS1 = 121.1^\circ\text{C} \text{ (condensing temperature of saturated steam to effect 1)} \\ \Delta T_2 = 105.54 - 0.36 - 18.34 = 86.84^\circ\text{C} \quad TS2 = T_1 - BPR1 = 105.54 - 0.36 = 105.18^\circ\text{C} \text{ (condensing temperature of saturated steam to effect 2)} \\ \Delta T_3 = 86.84 - 0.65 - 32.07 = 54.12^\circ\text{C} \quad TS3 = T_2 - BPR2 = 86.84 - 0.65 = 86.19^\circ\text{C} \text{ (condensing temperature of saturated steam to effect 3)}$$

The temperatures in the three effects are as follows:

$$\begin{matrix} T_{11} & T_{12} & T_{21} & T_{22} & T_{31} & T_{32} \\ (^\circ\text{C}) & (^\circ\text{C}) & (^\circ\text{C}) & (^\circ\text{C}) & (^\circ\text{C}) & (^\circ\text{C}) \\ \hline 121.1 & 105.54 & 105.18 & 86.19 & 54.12 & 51.67 \end{matrix}$$

Step 4. The heat capacity of the liquid in each effect is calculated from the equation  $c_p = 4.19 - 2.35x$ :

$$F: c_p = 4.19 - 2.35(0.1) = 3.955 \text{ kJ/kg}\cdot\text{K} \\ L1: c_p = 4.19 - 2.35(0.136) = 3.869 \text{ kJ/kg}\cdot\text{K} \\ L2: c_p = 4.19 - 2.35(0.214) = 3.684 \text{ kJ/kg}\cdot\text{K} \\ L3: c_p = 4.19 - 2.35(0.5) = 3.015 \text{ kJ/kg}\cdot\text{K}$$

The values of the enthalpy  $H$  of the various vapor streams relative to water at  $0^\circ\text{C}$  as a datum are obtained from the steam table as follows:

Effect 1:

$$H1 = HS2(\text{saturation enthalpy at } TS2) + 1.884(0.36^\circ\text{C superheat}) = 2621.3 \text{ kJ/kg} \\ H2 = HS1(\text{vapor saturation enthalpy}) - hS1(\text{liquid enthalpy at } TS1) = (2708 - 508) = 2200 \text{ kJ/kg} \\ \text{kg latent heat of condensation}$$

Effect 2:

$$H3 = HS3(\text{saturation enthalpy at } TS3) + 1.884(0.65^\circ\text{C superheat}) = 2654.4 \text{ kJ/kg} \\ H4 = HS2(\text{vapor saturation enthalpy}) - hS2(\text{liquid enthalpy at } TS2) = (2708 - 441) = 2267 \text{ kJ/kg}$$

Effect 3:

$$H5 = HS4(\text{saturation enthalpy at } TS4) + 1.884(2.45^\circ\text{C superheat}) = 2595.5 \text{ kJ/kg} \\ H6 = HS3(\text{vapor saturation enthalpy}) - hS3(\text{liquid enthalpy at } TS3) = (2708 - 108) = 2600 \text{ kJ/kg}$$

$$\text{kg} \lambda S3 = H2 - hS3 = 2655 - 361 = 2294 \text{ kJ/kg}$$

(Note that the superheat corrections in this example are small and could possibly have been neglected. However, the corrections were used to demonstrate the method of calculation.) Flow relations to be used in heat balances are

$$V1 = 22680 - L1, V2 = L1 - L2, V3 = L2 - 4536, L3 = 4536$$

Write a heat balance on each effect. Using  $0^\circ\text{C}$  as a datum, since the values of  $H$  of the vapors are relative to  $0^\circ\text{C}$  ( $32^\circ\text{F}$ ), and noting that  $(T_F - 0)^\circ\text{C} = (T_F - 0)^\circ\text{K}$  and  $(T_1 - 0)^\circ\text{C} = (T_1 - 0)^\circ\text{K}$ ,

$$(1) Fc_p(T_F - 0) + S\lambda S1 = L1c_p(T_1 - 0) + V1H1$$

Substituting the known values,

$$22680(3.955)(26.7 - 0) + S(2200) = L1(3.869)(105.54 - 0) + (22680 - L1)(2685)$$

$$(2) L1c_p(T_1 - 0) + V1\lambda S2 = L2c_p(T_2 - 0) + V2H2 \\ L1(3.869)(105.54 - 0) + (22680 - L1)(2244) = L2(3.684)(86.84 - 0) + (L1 - L2)(2655)$$

$$(3) L2c_p(T_2 - 0) + V2\lambda S3 = L3c_p(T_3 - 0) + V3H3 \\ L2(3.684)(86.84 - 0) + (L1 - L2)(2294) = 4536(3.015)(54.12 - 0) + (L2 - 4536)(2600)$$

Solving the last two equations simultaneously for  $L_1$  and  $L_2$ , and substituting into the first equation,

$$L1 = 17078 \text{ kg/}$$

$$hL2 = 11068 \quad L3 = 4536 \quad S = 8936 \quad V1 = 5602 \quad V2 = 6010 \quad V3 = 6532$$

The calculated values of  $V_1$ ,  $V_2$ , and  $V_3$  are close enough to the assumed values that steps 2, 3, and 4 do not need to be repeated. If the calculation was repeated, the calculated values of  $V_1$ ,  $V_2$ , and  $V_3$  will be used starting with step 2 and a solids balance in each effect will be made.

*Step 5.* Solving for the values of  $q$  in each effect and area,

$$q1 = S\lambda S1 = (89363600) \\ (2200 \times 1000) = 5.460 \times 10^6 \text{ W} \quad q2 = V1\lambda S2 = (56023600) \\ (2244 \times 1000) = 3.492 \times 10^6 \text{ W} \quad q3 = V2\lambda S3 = (60103600) \\ (2294 \times 1000) = 3.830 \times 10^6 \text{ W}$$

$$60 \times 1063123(15.56) = 112.4 \text{ m}^2 \quad A2 = q2U2\Delta T2 = 3.492 \times 1061987(18.34) = 95.8 \text{ m}^2 \quad A3 = q3U3\Delta T3 = 3.830 \times 1061136$$

The average area  $A_m = 104.4 \text{ m}^2$ . The areas differ from the average value by less than 10% and a second trial is not really necessary. However, a second trial will be made starting with step 6 to demonstrate the calculation methods used.

*Step 6.* Making a new solids balance on effects 1, 2, and 3, using the new  $L_1 = 17\,078$ ,  $L_2 = 11\,068$ , and  $L_3 = 4536$ , and solving for  $x$ ,

$$(1) 22680(0.1) = 17078(x_1), x_1 = 0.133$$

$$(2) 17078(0.133) = 11068(x_2), x_2 = 0.205$$

$$(3) 11068(0.205) = 4536(x_3), x_3 = 0.500 \text{ (check balance)}$$

*Step 7.* The new **BPR** in each effect is then

$$(1) \text{BPR}_1 = 1.78x_1 + 6.22x_2 = 1.78(0.133) + 6.22(0.133)^2 = 0.35^\circ\text{C}$$

$$(2) \text{BPR}_2 = 1.78(0.205) + 6.22(0.205)^2 = 0.63^\circ\text{C}$$

$$(3) \text{BPR}_3 = 1.78(0.5) + 6.22(0.5)^2 = 2.45^\circ\text{C}$$

$$\Sigma \Delta T \text{ available} = 121.1 - 51.67 - (0.35 + 0.63 + 2.45) = 66.00^\circ\text{C}$$

The new values for  $\Delta T$  are obtained using Eq. (32.5-11):

$$4 = 16.77^\circ\text{K} = 16.77^\circ\text{C} \quad \Delta T'_1 = \Delta T_2 A_2 A_m = 18.34(95.8)104.4 = 16.86^\circ\text{C} \quad \Delta T'_3 = \Delta T_3 A_3 A_m = 32.07(105.1)104.4 = 32.34^\circ\text{C}$$

These  $\Delta T'$  values are readjusted so that

$\Delta T'_1 = 16.77$ ,  $\Delta T'_2 = 16.87$ ,  $\Delta T'_3 = 32.36$ , and  $\Sigma \Delta T' = 16.77 + 16.87 + 32.36 = 66.00^\circ\text{C}$ . To calculate the actual boiling point of the solution in each effect,

$$(1) T_1 = \text{TS}_1 - \Delta T'_1 = 121.1 - 16.77 = 104.33^\circ\text{C}, \text{TS}_1 = 121.1^\circ\text{C}$$

$$(2) T_2 = T_1 - \text{BPR}_1 - \Delta T'_2 = 104.33 - 0.35 - 16.87 = 87.11^\circ\text{C} \quad \text{TS}_2 = T_1 - \text{BPR}_1 = 104.33 - 0.35 = 103.98^\circ\text{C}$$

$$(3) T_3 = T_2 - \text{BPR}_2 - \Delta T'_3 = 87.11 - 0.63 - 32.36 = 54.12^\circ\text{C} \quad \text{TS}_3 = T_2 - \text{BPR}_2 = 87.11 - 0.63 = 86.48^\circ\text{C}$$

*Step 8.* Following step 4, the heat capacity of the liquid is  $c_p = 4.19 - 2.35x$ :

$$F: c_p = 3.955 \text{ kJ/}$$

$$\text{kg} \cdot \text{KL} \quad 1: c_p = 4.19 - 2.35(0.133) = 3.877 \quad 2: c_p = 4.19 - 2.35(0.205) = 3.708 \quad 3: c_p = 3.015$$

The new values of the enthalpy  $H$  are as follows in each effect:

$$(1) H1 = HS2 + 1.884(^{\circ}\text{C superheat}) = 2682 + 1.884(0.35) = 2683 \text{ kJ/kg}$$

$$\lambda S1 = HS1 - hS1 = 2708 - 508 = 2200 \text{ kJ/kg}$$

$$(1) H2 = HS3 + 1.884(0.63) = 2654 + 1.884(0.63) = 2655 \text{ kJ/kg}$$

$$\lambda S2 = H1 - hS2 = 2683 - 440 = 2243 \text{ kJ/kg}$$

$$(3) H3 = HS4 + 1.884(2.45) = 2595 + 1.884(2.45) = 2600 \text{ kJ/kg}$$

$$\lambda S3 = H2 - hS3 = 2655 - 362 = 2293 \text{ kJ/kg}$$

Writing a heat balance on each effect,

$$(1) 22680(3.955)(26.7 - 0) + S(2200) = L1(3.877)$$

$$(104.33 - 0) + (22680 - L1)(2683)$$

$$(2) L1(3.877)(104.33 - 0) + (22680 - L1)(2243) = L2(3.708)$$

$$(87.11 - 0) + (L1 - L2)(2655)$$

$$(3) L2(3.708)(87.11 - 0) + (L1 - L2)(2693) = 4536(3.015)$$

$$(54.12 - 0) + (L2 - 4536)(2600)$$

Solving,

$$L1 = 17005 \text{ kg/h}$$

$$hL2 = 10952 \quad L3 = 4536 \quad S = 8960 \text{ (steam used)} \quad V1 = 5675 \quad V2 = 6053 \quad V3 = 6416$$

Note that these values from trial 2 differ very little from the trial 1 results. Following step 5, and solving for  $q$  in each effect and  $A$ ,

$$0(2000 \times 1000) = 5.476 \times 10^6 \quad Wq2 = V1\lambda S2 = 56753600(2243 \times 1000) = 3.539 \times 10^6 \quad Wq3 = V2\lambda S3 = 60533600(2293 \times 1000)$$

$$76 \times 1063123(16.77) = 104.6 \quad m2A2 = q2U2\Delta T2' = 3.539 \times 10^6 1987(16.87) = 105.6 \quad m2A3 = q3U3\Delta T3' = 3.855 \times 10^6 1130$$

The average area to use in each effect is  $A_m = 105.0 \text{ m}^2$ .

Note that this value of  $105.0 \text{ m}^2$  is quite close to the average value of  $104.4 \text{ m}^2$  from the first trial.

$$\text{steam economy} = V1 + V2 + V3S = 5675 + 6053 + 64168960 = 2.025$$

## 32.6 Condensers for Evaporators

### 32.6A Introduction

In multiple-effect evaporators, the

vapors from the last effect are usually leaving under vacuum, that is, at less than atmospheric pressure. These vapors must be condensed and discharged as a liquid at atmospheric pressure. This is done by using cooling water to condense the vapors. The condenser can be a surface condenser, where the vapor to be condensed and the cooling liquid are separated by a metal wall, or a direct-contact condenser, where the vapor and cooling liquid are mixed directly.

### **32.6B Surface Condensers**

*Surface condensers* are employed where actual mixing of the condensate with condenser cooling water is not desired. In general, they are shell-and-tube condensers, with



the vapor on the shell side and cooling water in multipass flow on the tube side. Noncondensable gases such as air,  $\text{CO}_2$ ,  $\text{N}_2$ , or another gas are usually present in the vapor stream. They may have entered as dissolved gases in the liquid feed or occur because of decomposition in the solutions. These noncondensable gases may be vented from any well-cooled point in the condenser. If the vapor being condensed is below atmospheric pressure, the condensed liquid leaving the surface condenser can be removed by pumping and the noncondensable gases can be removed by using a vacuum pump. Surface condensers are much more expensive and use more cooling water, so they are usually not used in cases where a direct-contact

condenser is suitable.

### **32.6C Direct-Contact Condensers**

In *direct-contact condensers*, cooling water directly contacts and condenses the vapors. One of the most common types of direct-contact condenser is the countercurrent barometric condenser shown in Fig. 32.6-1. The vapor enters the condenser and is condensed by rising upward against a shower of cooling water droplets. The condenser is located on top of a long discharge tailpipe. The condenser is high enough above the discharge point in the tailpipe that the water column established in the pipe more than compensates for the difference in pressure between the low absolute pressure in the condenser and the

atmosphere. The water can then discharge by gravity through a seal pot at the bottom. A height of about 10.4 m (34 ft) is used.

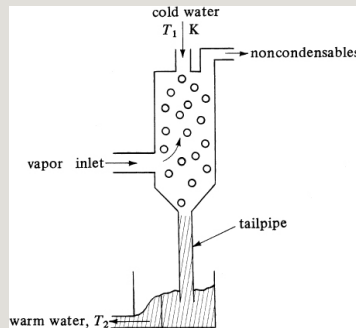


Figure 32.6-1. *Schematic of barometric condenser.*

The barometric condenser is inexpensive and economical of water consumption. It can maintain a vacuum corresponding to a saturated vapor temperature within about 2.8 K (5°F) of the water temperature leaving the condenser. For example, if the discharge water is at 316.5 K (110°F), the pressure corresponding to 316.5 + 2.8 or 319.3 K

is 10.1 kPa (1.47 psia).

The water consumption can be estimated by a simple heat balance for a barometric condenser. If the vapor flow to the condenser is  $V$  kg/h at temperature  $T_s$ , and the water flow is  $W$  kg/h at an entering temperature of  $T_1$  and a leaving temperature of  $T_2$ , the derivation is as follows:

$$VH_s + Wc_p(T_1 - 273.2) = (V + W)c_p(T_2 - 273.2) \quad (32.6-1)$$

where  $H_s$  is the enthalpy from the steam tables of the vapor at  $T_s$  K and the pressure in the vapor stream. Solving,

$$WV = \text{kg water} / \text{kg vapor} = \frac{H_s - c_p(T_2 - 273.2)}{c_p(T_2 - T_1)} \quad (32.6-2)$$

The noncondensable gases can be

removed from the condenser by a vacuum pump, either a mechanical pump or a steam-jet ejector. In the ejector, high-pressure steam enters a nozzle at high speed and entrains the noncondensable gases from the space under vacuum.

Another type of direct-contact condenser is the jet barometric condenser. High-velocity jets of water act as both a vapor condenser and an entrainer of the noncondensables out of the tail pipe. Jet condensers usually require more water than the more-common barometric condensers and are more difficult to throttle at low vapor rates.

## **32.7 Evaporation of Biological Materials**

### **32.7A Introduction and Properties of**

## Biological Materials

The evaporation of many biological materials frequently differs from the evaporation of inorganic materials such as NaCl and NaOH, and organic materials such as ethanol and acetic acid. Biological materials such as pharmaceuticals, milk, citrus juices, and vegetable extracts are usually quite heat-sensitive and often contain fine particles of suspended matter in solution. In addition, because of problems due to bacteria growth, the equipment must be designed for easy cleaning. Many biological materials in solution exhibit only a small boiling-point rise when concentrated. This is because suspended solids in a fine, dispersed form and dissolved solutes of large molecular weight contribute

little to this rise.

The amount of degradation of biological materials on evaporation is a function of the temperature and length of time. To keep the temperature low, the evaporation must be done under vacuum, which reduces the boiling point of the solution. To keep the time of contact low, the equipment must provide for a low holdup time (contact time) for the material being evaporated. Typical types of equipment used and some biological materials processed are listed below. Detailed descriptions of the equipment are given in Section 32.2.

1. Long-tube vertical evaporator: condensed milk
2. Falling-film evaporator: fruit juices
3. Agitated-film (wiped-film) evaporator: rubber latex, gelatin, antibiotics, fruit juices

4. Heat-pump cycle evaporator: fruit juices, milk, pharmaceuticals

### **32.7B Fruit Juices**

In the evaporation of fruit juices, such as orange juice, problems arise that are quite different from those associated with the evaporation of a typical salt such as NaCl. The fruit juices are heat-sensitive and the viscosity increases greatly as concentration increases. Also, solid suspended matter in fruit juices has a tendency to cling to the heating surface, thus causing overheating that leads to burning and spoilage of the matter (B2).

To reduce this tendency to stick and to reduce residence time, high rates of circulation over the heat-transfer surface are necessary. Since the material is heat-



sensitive, low-temperature operation is also necessary. Hence, a fruit-juice concentration plant usually employs a single rather than a multiple evaporation unit. Vacuum is used to reduce the temperature of evaporation.

A typical fruit juice evaporation system using the heat-pump cycle is shown in the literature (P1, C1); it employs low-temperature ammonia as the heating fluid. A frozen concentrated citrus-juice process is described by Charm (C1).

The process uses a multistage falling-film evaporator. A major fault of concentrated orange juice is a flat flavor due to the loss of volatile constituents during evaporation. To overcome this, a portion of the fresh pulpy juice bypasses the evaporation cycle and is blended with the evaporated concentrate.

### 32.7C Sugar Solutions

Sugar (sucrose) is obtained primarily from sugarcane and sugar beets.

Sugar tends to caramelize if kept at high temperatures for long periods (B2). The general tendency is to use short-tube evaporators of the natural circulation type. In the evaporation process for sugar solutions, a clear solution of sugar having a concentration of 10–13° Brix (10–13 wt %) is evaporated to 40–60° Brix (K1).

The feed is first preheated by exhaust steam and then typically enters a six-effect forward-feed evaporator system. The first effect operates at a pressure in the vapor space of the evaporator of about 207 kPa (30 psia) [121.1°C (250°F) saturation temperature] and the

last effect operates under vacuum at about 24 kPa (63.9°C saturation).

Examples of the relatively small boiling-point rise of sugar solutions and the heat capacity are given in Example 32.5-1.

### **32.7D Paper-Pulp Waste Liquors**

In the manufacture of paper pulp in the sulfate process, wood chips are digested or cooked and spent black liquor is obtained after washing the pulp. This solution contains primarily sodium carbonate and organic sulfide compounds. It is concentrated by evaporation in a six-effect system (K1).

## **32.8 Evaporation Using Vapor Recompression**

### **32.8A Introduction**

In the single-effect evaporator, the vapor from the unit is generally condensed and discarded. In the multiple-effect evaporator, the pressure in each succeeding effect is lowered so that the boiling point of the liquid is also lowered in each effect. Hence, there is a temperature difference created for the vapor from one effect to condense in the next effect and boil the liquid to form vapor.

In a single-effect vapor-recompression (sometimes called vapor-compression) evaporator, the vapor is compressed so that its condensing or saturation temperature is increased. This compressed vapor is returned to the heater, or steam chest, and condenses so that vapor is formed in the evaporator

(W1, Z1). In this manner, the latent heat of the vapor is used and not discarded. The two types of vapor-recompression units are the mechanical and the thermal.

### **32.8B Mechanical Vapor-Recompression Evaporator**

In a mechanical vapor-recompression evaporator, a conventional single-effect evaporator similar to that in Fig. 32.2-2 is used, as shown in Fig. 32.8-1. The cold feed is preheated by exchange with the hot outlet-liquid product and then flows to the unit. The vapor coming overhead does not go to a condenser but is sent to a centrifugal or positive-displacement compressor driven by an electric motor or steam. This compressed vapor or steam is sent back to the heat exchanger or

steam chest. The compressed vapor condenses at a temperature higher than the boiling point of the hot liquid in the effect, and a temperature difference is set up. Vapor is again generated and the cycle repeated.

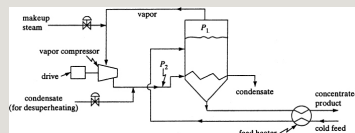


Figure 32.8-1. *Simplified process flow for mechanical vapor-recompression evaporator.*

Sometimes, it is necessary to add a small amount of makeup steam to the vapor line before the compressor (K2). Also, a small amount of condensate may be added to the compressed vapor to remove any superheat, if present. This is sometimes known as desuperheating.

Vapor-recompression units generally operate at low optimum-temperature differences of 5–10°C. Hence, large heat-transfer areas are needed. These units usually have higher capital costs than multiple-effect units because of their larger area and the costs of the relatively expensive compressor and drive unit. The main advantage of vapor-recompression units is their lower energy costs. Using the steam equivalent of the power to drive the compressor, the steam economy is equivalent to a multiple-effect evaporator of up to 10 or more units (Z1).

Some typical applications of mechanical vapor-recompression units are evaporation of seawater to give distilled water, evaporation of kraft black liquor in the paper industry (L2), evaporation

of heat-sensitive materials such as fruit juices, and crystallization of salts having inverse solubility curves, where the solubility decreases with increasing temperature (K2, M3).

Falling-film evaporators are well suited for vapor-recompression systems (W1) because they operate at low-temperature-difference values and have very little entrained liquid that can cause problems in the compressor. Vapor recompression has been used in distillation towers where the overhead vapor is recompressed and used in the reboiler as the heating medium (M2).

### **32.8C Thermal Vapor-Recompression Evaporator**

A steam jet can also be used to compress the vapor, in what is called a thermal vapor-recompression



evaporator. Its main disadvantages are the low efficiency of the steam jet, necessitating the removal of this excess heat, and the lack of flexibility to changes in process variables (M3). Steam jets are cheaper and more durable than mechanical compressors, and can more easily handle large volumes of low-pressure vapors.

## **32.9 Chapter Summary**

In this chapter, we have introduced the concepts of evaporation, a process by which water (or a solvent) is removed from a solution in order to make it more concentrated. Factors that can affect the evaporation process include: the initial liquid concentration, the solubility of the solute in the solvent,

the temperature sensitivity of the materials, the thermodynamic properties of the solution (pressure and temperature), and the the formation of foams, froths, and solute scale deposits. Many different types of evaporators are available in industry and their modes of operation can be single-effect or multi-effect.

In performing evaporation calculations and designing evaporation equipment, it is necessary to know the value of the overall heat-transfer coefficient. It is used to calculate the rate of heat transfer in an evaporator by using the following equation:

$$q=UA\Delta T=UA(TS-T1)(32.2-1)$$

The overall heat-transfer coefficient is composed of the steam-side coefficient, the wall thermal conductivity, the liquid film coefficient, and any additional resistances due to fouling and scaling. In order to calculate the heat-transfer coefficient, it is necessary to perform material and energy balances on the entire evaporation process. Once the heat-transfer coefficient and the operating temperatures are known, the heat-transfer surface area, the amount of steam required, and the steam economy can be calculated. During the evaporation process, often the boiling point of a solution can change due to its concentration. A Dühring chart can be used to predict the change in boiling point.

Solution techniques were provided to

perform calculations for multi-effect evaporators. Condensers were introduced as the equipment used to convert the evaporated water (or solvent) to the liquid phase. Examples of different types of condensers and vapor-compressors were provided. Finally, a discussion on the evaporation of biological materials, including fruit juices and pharmaceuticals, was provided.

## **Problems**

**32.4-1. *Heat-Transfer Coefficient in a Single-Effect Evaporator.*** A feed of 4535 kg/h of a 2.0 wt % salt solution at 311 K enters continuously a single-effect evaporator and is being concentrated to 3.0%. The evaporation is at atmospheric pressure and the area of the evaporator is 69.7 m<sup>2</sup>. Saturated

steam at 383.2 K is supplied for heating. Since the solution is dilute, it can be assumed to have the same boiling point as water. The heat capacity of the feed can be taken as  $c_p = 4.10 \text{ kJ/kg} \cdot \text{K}$ . Calculate the amounts of vapor and liquid product, and the overall heat-transfer coefficient  $U$ .

$$\text{Ans. } U = 1823 \text{ W/m}^2 \cdot \text{K}$$

**32.4-2. *Effects of Increased Feed Rate in an Evaporator.*** Using the same area, value of  $U$ , steam pressure, evaporator pressure, and feed temperature as in Problem 32.4-1, calculate the amounts of liquid and vapor leaving, and the liquid outlet concentration if the feed rate is increased to 6804 kg/h.

$$\text{Ans. } V = 1256 \text{ kg/h, } L = 5548 \text{ kg/h, } x_L =$$

### ***32.4-3. Effect of Evaporator Pressure on Capacity and Product Composition.***

Recalculate Example 32.4-1, but use an evaporator pressure of 41.4 kPa instead of 101.32 kPa abs. Use the same steam pressure, area  $A$ , and heat-transfer coefficient  $U$  in the calculations.

- Do this to obtain the new capacity or feed rate under these new conditions. The composition of the liquid product will be the same as before.
- Do this to obtain the new product composition if the feed rate is increased to 18 144 kg/h.

### ***32.4-4. Production of Distilled Water.***

An evaporator having an area of 83.6 m<sup>2</sup> and  $U = 2270 \text{ W/m}^2 \cdot \text{K}$  is used to produce distilled water for a boiler feed. Tap water having 400 ppm dissolved solids at 15.6°C is fed to the evaporator operating at 1 atm pressure abs.

Saturated steam at  $115.6^{\circ}\text{C}$  is available for use. Calculate the amount of distilled water produced per hour if the outlet liquid contains 800 ppm solids.

### **32.4-5. *Boiling-Point Rise of NaOH***

**Solutions.** Determine the boiling temperature of the solution and the boiling-point rise for the following cases:

- A 30% NaOH solution boiling in an evaporator at a pressure of 172.4 kPa (25 psia)
- A 60% NaOH solution boiling in an evaporator at a pressure of 3.45 kPa (0.50 psia)

**Ans.** (a) Boiling point =  $130.6^{\circ}\text{C}$ ,  
boiling-point rise =  $15^{\circ}\text{C}$

### **32.4-6. *Boiling-Point Rise of Biological***

**Solutes in Solutions.** Determine the boiling-point rise for the following solutions of biological solutes in water:

- A 30 wt % solution of citric acid in water boiling at 220°F (104.4°C)
- A 40 wt % solution of sucrose in water boiling at 220°F (104.4°C)

**Ans.** (a) Boiling-point rise = 2.2°F  
(1.22°C)

***32.4-7. Effect of Feed Temperature on Evaporating an NaOH Solution.***

A single-effect evaporator is concentrating a feed of 9072 kg/h of a 10 wt % solution of NaOH in water to a product of 50% solids. The pressure of the saturated steam used is 42 kPa (gage) and the pressure in the vapor space of the evaporator is 20 kPa (abs). The overall heat-transfer coefficient is 1988 W/m<sup>2</sup> · K. Calculate the steam used, the steam economy in kg vaporized/kg steam, and the area for the following feed conditions:



- Feed temperature of 288.8 K (15.6°C)
- Feed temperature of 322.1 K (48.9°C)

**Ans.** (a)  $S = 8959$  kg/h of steam,  $A = 296.9$  m<sup>2</sup>

**32.4-8. Heat-Transfer Coefficient to Evaporate NaOH.** In order to concentrate 4536 kg/h of an NaOH solution containing 10 wt % NaOH to a 20 wt % solution, a single-effect evaporator is being used, with an area of 37.6 m<sup>2</sup>. The feed enters at 21.1°C (294.3 K). Saturated steam at 110°C (383.2 K) is used for heating and the pressure in the vapor space of the evaporator is 51.7 kPa. Calculate the kg/h of steam used and the overall heat-transfer coefficient.

**32.4-9. Throughput of a Single-Effect Evaporator.** An evaporator is

concentrating  $F$  kg/h at 311 K of a 20 wt % solution of NaOH to 50%. The saturated steam used for heating is at 399.3 K. The pressure in the vapor space of the evaporator is 13.3 kPa abs. The overall coefficient is  $1420 \text{ W/m}^2 \cdot \text{K}$  and the area is  $86.4 \text{ m}^2$ . Calculate the feed rate  $F$  of the evaporator.

**Ans.**  $F = 9072 \text{ kg/h}$

### **32.4-10. *Surface Area and Steam***

#### ***Consumption of an Evaporator.*** A

single-effect evaporator is concentrating a feed solution of organic colloids from 5 to 50 wt %. The solution has a negligible boiling-point elevation. The heat capacity of the feed is  $c_p = 4.06 \text{ kJ/kg} \cdot \text{K}$  ( $0.97 \text{ btu/lb}_m \cdot ^\circ\text{F}$ ) and the feed enters at  $15.6^\circ\text{C}$  ( $60^\circ\text{F}$ ). Saturated steam at 101.32 kPa is available for heating,

and the pressure in the vapor space of the evaporator is 15.3 kPa. A total of 4536 kg/h (10 000 lb<sub>m</sub>/h) of water is to be evaporated. The overall heat-transfer coefficient is 1988 W/m<sup>2</sup> · K (350 btu/h · °F). What is the required surface area in m<sup>2</sup> and the steam consumption?

**32.4-11. *Evaporation of Tomato Juice Under Vacuum.*** Tomato juice having a concentration of 12 wt % solids is being concentrated to 25% solids in a film-type evaporator. The maximum allowable temperature for the tomato juice is 135°F, which will be the temperature of the product. The feed enters at 100°F. Saturated steam at 25 psia is used for heating. The overall heat-transfer coefficient  $U$  is 600 btu/h · ft<sup>2</sup> · °F and the area  $A$  is 50 ft<sup>2</sup>. The heat capacity of the feed  $c_p$  is estimated as

$0.95 \text{ btu/lb}_m \cdot ^\circ\text{F}$ . Neglect any boiling-point rise if present. Calculate the feed rate of tomato juice to the evaporator.

### **32.4-12. *Concentration of a Cane***

***Sugar Solution.*** For use in a food process, a single-effect evaporator is being used to concentrate a feed of  $10\,000 \text{ lb}_m/\text{h}$  of a cane sugar solution at  $80^\circ\text{F}$  and with a sugar content of  $15^\circ$  Brix (degrees Brix is wt % sugar) to  $30^\circ$  Brix. Saturated steam at  $240^\circ\text{F}$  is available for heating. The vapor space in the evaporator will be at 1 atm abs pressure. The overall  $U = 350 \text{ btu/h} \cdot \text{ft}^2 \cdot ^\circ\text{F}$  and the heat capacity of the feed is  $c_p = 0.91 \text{ btu/lb}_m \cdot ^\circ\text{F}$ . The boiling-point rise can be estimated from Example 32.5-1. The heat of solution can be considered negligible and thus neglected. Calculate the area required

for the evaporator and the amount of steam used per hour.

**Ans.** Boiling-point rise =  $2.0^{\circ}\text{F}$  ( $1.1^{\circ}\text{C}$ ).

$$A = 667 \text{ ft}^2 \text{ (} 62.0 \text{ m}^2 \text{)}$$

**32.5-1. Boiling Points in a Triple-Effect Evaporator.** A solution with a negligible boiling-point rise is being evaporated in a triple-effect evaporator using saturated steam at  $121.1^{\circ}\text{C}$  ( $394.3 \text{ K}$ ). The pressure in the vapor of the last effect is  $25.6 \text{ kPa abs}$ . The heat-transfer coefficients are  $U_1 = 2840$ ,  $U_2 = 1988$ , and  $U_3 = 1420 \text{ W/m}^2 \cdot \text{K}$ , the areas are equal. Estimate the boiling point in each of the evaporators.

**Ans.**  $T_1 = 108.6^{\circ}\text{C}$  ( $381.8 \text{ K}$ )

**32.5-2. Evaporation of a Sugar Solution in a Multiple-Effect**

**Evaporator.** A triple-effect evaporator with forward feed is evaporating a sugar solution with negligible boiling-point rise (less than 1.0 K, which will be neglected) and containing 5 wt % solids to 25% solids. Saturated steam at 205 kPa abs is being used. The pressure in the vapor space of the third effect is 13.65 kPa. The feed rate is 22 680 kg/h and the temperature 299.9 K. The liquid heat capacity is  $c_p = 4.19 - 2.35x$ , where  $c_p$  is in kJ/kg · K and  $x$  in wt fraction (K1). The heat-transfer coefficients are  $U_1 = 3123$ ,  $U_2 = 1987$ , and  $U_3 = 1136$  W/m<sup>2</sup> · K. Calculate the surface area of each effect if each effect has the same area, and the steam rate.

**Ans.** Area  $A = 99.1$  m<sup>2</sup>, steam rate  $S = 8972$  kg/h

### **32.5-3. *Evaporation in Double-Effect Reverse-Feed Evaporators.***

A feed containing 2 wt % dissolved organic solids in water is fed to two double-effect evaporators with reverse feed. The feed enters at 100°F and is concentrated to 25% solids. The boiling-point rise can be considered negligible, as can the heat of solution. Each evaporator has a 1000-ft<sup>2</sup> surface area, and the heat-transfer coefficients are  $U_1 = 500$  and  $U_2 = 700$  btu/h · ft<sup>2</sup> · °F. The feed enters evaporator number 2 and steam at 100 psia is fed to evaporator number 1. The pressure in the vapor space of evaporator number 2 is 0.98 psia.

Assume that the heat capacity of all liquid solutions is that of liquid water. Calculate the feed rate  $F$  and the product rate  $L_1$  of a solution containing 25% solids. (*Hint:* Assume a feed rate of, say,

$F = 1000 \text{ lb}_m/\text{h}$  and a value of  $T_1$ .

Calculate the area and  $T_1$ . Then, calculate the actual feed rate by multiplying 1000 by 1000/calculated area.)

**Ans.**  $F = 133\,800 \text{ lb}_m/\text{h}$  (60 691 kg/h),

$L_1 = 10\,700 \text{ lb}_m/\text{h}$  (4853 kg/h)

### **32.5-4. Concentration of NaOH**

#### ***Solution in a Triple-Effect Evaporator.***

A forced-circulation triple-effect evaporator using forward feed is to be used to concentrate a 10 wt % NaOH solution entering at  $37.8^\circ\text{C}$  to 50%. The steam used enters at 58.6 kPa gage. The absolute pressure in the vapor space of the third effect is 6.76 kPa. The feed rate is 13 608 kg/h. The heat-transfer coefficients are  $U_1 = 6246$ ,  $U_2 = 3407$ , and  $U_3 = 2271 \text{ W/m}^2 \cdot \text{K}$ . All effects



have the same area. Calculate the surface area and steam consumption.

**Ans.**  $A = 97.3 \text{ m}^2$ ,  $S = 5284 \text{ kg steam/h}$

**32.5-5. Triple-Effect Evaporator with Reverse Feed.** A feed rate of 20 410 kg/h of 10 wt % NaOH solution at 48.9°C is being concentrated in a triple-effect reverse-feed evaporator to produce a 50% solution. Saturated steam at 178.3°C is fed to the first evaporator and the pressure in the third effect is 10.34 kPa abs. The heat-transfer coefficient for each effect is assumed to be  $2840 \text{ W/m}^2 \cdot \text{K}$ . Calculate the heat-transfer area and the steam consumption rate.

**32.5-6. Evaporation of a Sugar Solution in a Double-Effect Evaporator.** A double-effect evaporator

with reverse feed is used to concentrate 4536 kg/h of a 10 wt % sugar solution to 50%. The feed enters the second effect at 37.8°C. Saturated steam at 115.6°C enters the first effect and the vapor from this effect is used to heat the second effect. The absolute pressure in the second effect is 13.65 kPa abs. The overall coefficients are  $U_1 = 2270$  and  $U_2 = 1705 \text{ W/m}^2 \cdot \text{K}$ . The heating areas for both effects are equal. Use boiling-point-rise and heat capacity data from Example 32.5-1. Calculate the area and steam consumption.

### ***32.6-1. Water Consumption and Pressure in a Barometric Condenser.***

The concentration of NaOH solution leaving the third effect of a triple-effect evaporator is 50 wt %. The vapor flow rate leaving is 5670 kg/h and this vapor

goes to a barometric condenser. The discharge water from the condenser leaves at  $40.5^{\circ}\text{C}$ . Assuming that the condenser can maintain a vacuum in the third effect that corresponds to a saturated vapor pressure of  $2.78^{\circ}\text{C}$  above  $40.5^{\circ}\text{C}$ , calculate the pressure in the third effect and the cooling-water flow to the condenser. The cooling water enters at  $29.5^{\circ}\text{C}$ . (*Note: The vapor leaving the evaporator will be superheated because of the boiling-point rise.*)

**Ans.** Pressure = 8.80 kPa abs,  $W = 306$   
200 kg water/h

## References

## Notation



# Chapter 33. Drying

## 33.0 Chapter Objectives

On completion of this chapter, a student should be able to:

- Explain the overall process of drying and provide examples of industrial applications
- List different types of drying equipment and explain how they work
- Calculate the humidity (moisture content) of an air-water vapor using vapor-pressure data, a humidity chart, and the wet bulb temperature
- Explain the concept of equilibrium moisture content in different materials
- Explain the difference between falling and constant drying-rate periods
- Use drying-rate curves to determine the falling and constant rate periods, as well as to calculate the required drying time for a process
- Calculate the required heat-transfer coefficients during

drying processes

- Use design equations to calculate the required drying time for various types of dryers
- Describe the process of freeze-drying and provide examples of applications
- Describe the process of sterilization and provide examples of biological applications
- Determine the thermal process time for sterilization using death-rate kinetics

## **33.1 Introduction and Methods of Drying**

### **33.1A Purposes of Drying**

The discussions of drying in this chapter are concerned with the removal of water from process materials and other substances. The term *drying* may be also used to refer to the removal of other organic liquids, such as benzene or organic solvents, from solids. Many of the types of equipment and calculation

methods discussed for the removal of water can also be used for the removal of organic liquids.

Drying generally means the removal of relatively small amounts of water from a material. Evaporation refers to the removal of relatively large amounts of water from material. In evaporation, the water is removed as vapor at its boiling point. In drying, the water is usually removed as a vapor by air.

In some cases, water may be removed mechanically from solid materials by means of filter presses, centrifuging, and other mechanical methods. Especially for the removal of water, this is usually cheaper than drying by thermal means. The moisture content of the final dried product varies depending upon the type

of product. Dried salt contains about 0.5% water, coal about 4%, and many food products about 5%. Drying is usually the final processing step before packaging and it makes many materials, such as soap powders and dyestuffs, more suitable for handling.

Drying or dehydration of biological materials, especially foods, is used as a preservation technique. Microorganisms that cause food spoilage and decay cannot grow and multiply in the absence of water. Also, many enzymes that cause chemical changes in food and other biological materials cannot function without water. When the water content is reduced below about 10 wt %, the microorganisms are not active. However, it is usually necessary to lower the moisture content below 5 wt



% in foods in order to preserve flavor and nutrition. Dried foods can be stored for extended periods of time.

Some biological materials and pharmaceuticals, which may not be heated for ordinary drying, may be freeze-dried, as discussed in Section 33.11. Also, in Section 33.12, the sterilization of foods and other biological materials is discussed, which is another method often employed to preserve such materials.

## **33.2 Equipment for Drying**

### **33.2A Tray Dryer**

In *tray dryers*, also called shelf, cabinet, or compartment dryers, the material, which may be a lumpy solid or a pasty solid, is spread uniformly on a metal tray to a depth

of 10 to 100 mm. A typical tray dryer, shown in Fig. 33.2-1, contains removable trays loaded in a cabinet.

Steam-heated air is recirculated by a fan over and parallel to the surface of the trays. Electrical heat is also used, especially for low heating loads. About 10 to 20% of the air passing over the trays is fresh air, the remainder being recirculated air.

After drying, the cabinet is opened and the trays are replaced with a new batch of trays. A modification of this type is the tray-truck type, where trays are loaded on trucks that are pushed into the dryer. This saves considerable time, since the trucks can be loaded and unloaded outside the dryer.

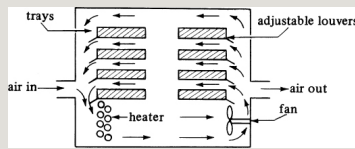


Figure 33.2-1. *Tray or shelf dryer.*

In the case of granular materials, the material can be loaded on screens, which form the bottom of each tray. Then, in this through-circulation dryer, heated air passes through the permeable bed, yielding shorter drying times because of the greater surface area exposed to the air.

### **33.2B Vacuum-Shelf Indirect Dryers**

*Vacuum-shelf dryers* are indirectly heated batch dryers similar to tray dryers. This type of dryer consists of a cabinet made of cast-iron or steel plates with tightly fitted doors so that it can be operated under vacuum. Hollow shelves of steel are fastened

permanently inside the chamber and are connected in parallel to inlet and outlet steam headers. The trays containing the solids to be dried rest on the hollow shelves. The heat is conducted through the metal walls and aided by radiation from the shelf above. For low-temperature operation, circulating warm water is used instead of steam for furnishing the heat to vaporize the moisture. The vapors usually pass to a condenser.

These dryers are used to dry expensive or temperature-sensitive or easily oxidizable materials. They are useful for handling materials with toxic or valuable solvents.

### **33.2C Continuous Tunnel Dryers**

*Continuous tunnel dryers* are often batch truck or tray compartments operated in series, as shown in Fig. 33.2-2a. The solids are placed on trays or on trucks, which move continuously through a tunnel with hot gases passing over the surface of each tray. The hot air flow can be countercurrent, cocurrent, or a combination. Many foods are dried in this way.

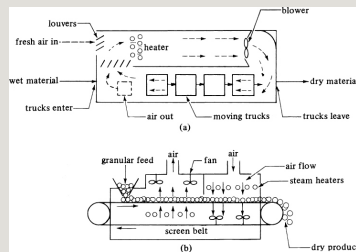


Figure 33.2-2. *Continuous tunnel dryers: (a) tunnel dryer trucks with countercurrent air flow, (b) through-circulation screen conveyor dryer.*

When granular particles of solids are to be dried, perforated or screen-belt

continuous conveyors are often used, as shown in Fig. 33.2-2b. The wet granular solids are conveyed as a layer that is 25 to about 150 mm deep on a screen or perforated apron while heated air is blown upward or downward through the bed. The dryer consists of several sections in series, each with a fan and heating coils. A portion of the air is exhausted to the atmosphere by a fan. In some cases, pasty materials can be preformed into cylinders and placed on the bed to be dried.

### **33.2D Rotary Dryers**

*A rotary dryer* consists of a hollow cylinder that is rotated and usually slightly inclined toward the outlet. The wet granular solids are fed at the high end, as shown in Fig. 33.2-3, and move through the shell as it

rotates. The heating shown is by direct contact with hot gases in countercurrent flow. In some cases, the heating is by indirect contact through the heated wall of the cylinder.

The granular particles move through the dryer a short distance before they are showered downward through the hot gases, as shown. Many other variations of this rotary dryer are available; these are discussed elsewhere (P1).

### **33.2E Drum Dryers**

A *drum dryer* consists of a heated metal roll, shown in Fig. 33.2-4, on the outside of which a thin layer of liquid or slurry is evaporated to dryness. The final dry solid is scraped off the roll, which revolves

slowly.

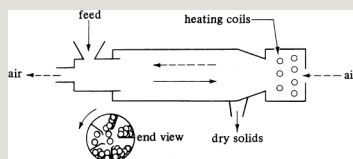


Figure 33.2-3. Schematic drawing of a direct-heat rotary dryer.

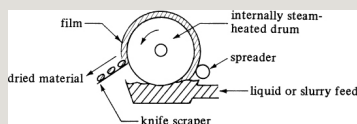


Figure 33.2-4. Rotary-drum dryer.

Drum dryers are suitable for handling slurries or pastes of solids in fine suspension and for solutions. The drum functions partly as an evaporator, as well as a dryer. Other variations of the single-drum type are twin rotating drums with dip feeding or with top feeding to the two drums. Potato slurry is dried using drum dryers to give potato flakes.



### 33.2F Spray Dryers

In a *spray dryer*, a liquid or slurry solution is sprayed into a hot gas stream in the form of a mist of fine droplets. The water is rapidly vaporized from the droplets, leaving particles of dry solid, which are separated from the gas stream. The flow of gas and liquid in the spray chamber may be countercurrent, cocurrent, or a combination.

The fine droplets are formed from the liquid feed by spray nozzles or high-speed rotating spray disks inside a cylindrical chamber, as shown in Fig. 33.2-5. It is necessary to ensure that the droplets or wet particles of solid do not strike and stick to solid surfaces before drying has taken place; hence, large chambers are used. The dried solids

leave at the bottom of the chamber through a screw conveyor. The exhaust gases flow through a cyclone separator to remove any fines. The particles produced are usually light and quite porous. For example, dried milk powder is made from spray-drying milk.

### **33.2G Drying Crops and Grains**

The grain from a harvest usually contains about 30 to 35% moisture. For safe storage for about 1 year, it should be dried to about 13 wt % moisture (H1). A typical continuous-flow dryer is shown in Fig. 33.2-6. In the drying bin, the thickness of the layer of grain, through which the hot air passes, is 0.5 m or less. Unheated air in the bottom section cools the dry grain before it leaves. Other types of crop dryers and

storage bins are described by Hall (H1).

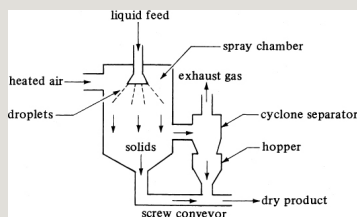


Figure 33.2-5. *Process flow diagram of spray-drying apparatus.*

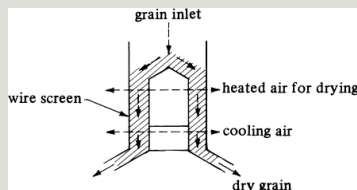


Figure 33.2-6. *Vertical continuous-flow grain dryer.*

## 33.3 Vapor Pressure of Water and Humidity

### 33.3A Vapor Pressure of Water

*1. Introduction.* In a number of the separation processes and transport processes, it is necessary to make calculations involving the properties of water vapor and air mixtures.

These calculations involve the knowledge of the concentration of water vapor in air under various conditions of temperature and pressure, the thermal properties of these mixtures, and the changes occurring when these mixtures are brought into contact with water or with wet solids in drying.

*Humidification* involves the transfer of water from the liquid phase into a gaseous mixture of air and water vapor. *Dehumidification* involves the reverse transfer, whereby water vapor is transferred from the vapor state to the liquid state. Humidification and dehumidification can also refer to vapor mixtures of materials such as benzene, but most practical applications occur with water. To better understand

humidity, it is first necessary to discuss the vapor pressure of water.

*2. Vapor pressure of water and physical states.* Pure water can exist in three different physical states: solid ice, liquid, and vapor. The physical state in which it exists depends on the pressure and temperature.

Figure 33.3-1 illustrates the various physical states of water and the pressure–temperature relationships at equilibrium. In Fig. 33.3-1, the regions of the solid, liquid, and vapor states are shown. Along the line *AB*, the liquid and vapor phases coexist. Along line *AC*, the ice and liquid phases coexist. Along line *AD*, the ice and vapor phases coexist. If ice at point (1) is heated at constant pressure, the temperature rises and the

physical condition is represented as moving horizontally. As the horizontal line crosses  $AC$ , the solid melts, and on crossing  $AB$ , the liquid vaporizes.

Moving from point (3) to point (4), ice sublimates (vaporizes) to a vapor without becoming a liquid.

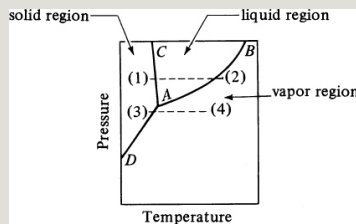


Figure 33.3-1. *Phase diagram for water.*

Liquid and vapor coexist in equilibrium along the line  $AB$ , which is the vapor-pressure line for water. Boiling occurs when the vapor pressure of the water is equal to the total pressure above the water surface. For example, at  $100^{\circ}\text{C}$  ( $212^{\circ}\text{F}$ ) the vapor pressure of water is  $101.3\text{ kPa}$  ( $1.0\text{ atm}$ ), and therefore it will

boil at 1 atm pressure. At  $65.6^{\circ}\text{C}$  ( $150^{\circ}\text{F}$ ), from the steam tables in Appendix A.2, the vapor pressure of water is 25.7 kPa (3.72 psia). Hence, at 25.7 kPa and  $65.6^{\circ}\text{C}$ , water will boil.

If a pan of water is held at  $65.6^{\circ}\text{C}$  in a room at 101.3 kPa abs pressure, the vapor pressure of water will again be 25.7 kPa. This illustrates an important property of the vapor pressure of water, which is not influenced by the presence of an inert gas such as air; that is, the vapor pressure of water is essentially independent of the total pressure of the system.

### **33.3B Humidity and Humidity Chart**

*1. Definition of humidity.* The humidity  $H$  of an air–water vapor mixture is defined as the kg of water

vapor contained in 1 kg of dry air.

The humidity so defined depends only on the partial pressure  $p_A$  of water vapor in the air and on the total pressure  $P$  (assumed throughout this chapter to be 101.325 kPa, 1.0 atm abs, or 760 mmHg). Using the molecular weight of water ( $A$ ) as 18.02 and of air as 28.97, the humidity  $H$  in kg H<sub>2</sub>O/kg dry air, or in English units as lb H<sub>2</sub>O/lb dry air, is as follows:

$$H = \frac{p_A P}{P - p_A} \times \frac{\text{kg H}_2\text{O}}{\text{kg dry air}} = \frac{p_A P}{P - p_A} \times \frac{18.02 \text{ kg H}_2\text{O}}{\text{kg mol H}_2\text{O}} \times \frac{1}{28.97 \text{ kg air}} \\ \text{kg mol air} \times 18.02 \text{ kg H}_2\text{O} / \text{kg mol H}_2\text{O} \times 1 / 28.97 \text{ kg air} \\ H = 18.02 \frac{p_A}{P - p_A} \quad (33.3-1)$$

Saturated air is air in which the water vapor is in equilibrium with liquid water at the given conditions of pressure and



temperature. In this mixture, the partial pressure of the water vapor in the air–water mixture is equal to the vapor pressure  $p_{AS}$  of pure water at the given temperature. Hence, the saturation humidity  $H_s$  is

$$H_s = 18.0228.97 p_{AS} / p_{AS} (33.3-2)$$

2. *Percentage humidity.* The percentage humidity  $HP$  is defined as 100 times the actual humidity  $H$  of the air divided by the humidity  $H_s$  if the air was saturated at the same temperature and pressure:

$$HP = 100 H / H_s (33.3-3)$$

3. *Percentage relative humidity.* The amount of saturation of an air–water vapor mixture is also given as percentage relative humidity  $HR$  using partial pressures:

$$H_R = 100 p_A / p_A S \quad (33.3-4)$$

Note that  $H_R \neq H_P$ , since  $H_P$  expressed in partial pressures by combining Eqs. (33.3-1), (33.3-2), and (33.3-3) is

$$H_P = 100 H_H S = (100) 18.022897 p_A P - p_A / 18.022897 p_A S P - p_A S = p_A p_A S P - p_A S P - p_A (100) \quad (33.3-5)$$

This, of course, is not the same as Eq. (33.3-4).

**EXAMPLE 33.3-1. Humidity from Vapor-Pressure Data**

The air in a room is at 26.7°C (80°F) and a pressure of 101.325 kPa, and contains water vapor with a partial pressure  $p_A = 2.76$  kPa. Calculate the following:

- Humidity,  $H$
- Saturation humidity,  $H_s$ , and percentage humidity,  $H_P$
- Percentage relative humidity,  $H_R$

**Solution:** From the steam tables at 26.7°C, the vapor pressure of water is  $p_{AS} = 3.50$  kPa (0.507 psia). Also,  $p_A = 2.76$  kPa and  $P = 101.3$  kPa (14.7 psia). For part (a), using Eq. (33.3-1),

$$H = 18.0228.97 p_A P -$$

$$p_A = 18.02(2.76)28.97(101.3 - 2.76) = 0.01742 \text{ Kg H}_2\text{O/Kg air}$$

For part (b), using Eq. (33.3-2), the saturation humidity is

$$H_S = 18.0228.97P_{AS}$$

$$-P_{AS} = 18.02(3.50)28.97(101.3 - 3.50) = 0.02226 \text{ kg H}_2\text{O/Kg air}$$

The percentage humidity, from Eq. (33.3-3), is

$$HP = 100H_S = 100(0.01742)0.02226 = 78.3\%$$

For part (c), from Eq. (33.3-4), the percentage relative humidity is

$$HR = 100p_A/p_{AS} = 100(2.76)3.50 = 78.9\%$$

*4. Dew point of an air–water vapor mixture.* The temperature at which a given mixture of air and water vapor would be saturated is called the *dew-point temperature* or simply the *dew point*. For example, at 26.7°C (80°F), the saturation vapor pressure of water is  $p_{AS} = 3.50 \text{ kPa}$  (0.507 psia). Hence, the dew point of a mixture containing water vapor having a partial pressure of 3.50 kPa is 26.7°C. If an air–water vapor mixture is at 37.8°C (often called the dry bulb temperature, since this is the

actual temperature a dry thermometer bulb would indicate in this mixture) and it contains water vapor of  $p_A = 3.50$  kPa, the mixture would not be saturated. On cooling to  $26.7^\circ\text{C}$ , the air would be saturated, that is, at the dew point. On further cooling, some water vapor would condense, since the partial pressure cannot be greater than the saturation vapor pressure.

*5. Humid heat of an air–water vapor mixture.* The humid heat  $c_s$  is the amount of heat in J (or kJ) required to raise the temperature of 1 kg of dry air plus the water vapor present by 1 K or  $1^\circ\text{C}$ . The heat capacity of air and water vapor can be assumed constant over the temperature ranges usually encountered at  $1.005$  kJ/kg dry air  $\cdot$  K and  $1.88$  kJ/kg water vapor  $\cdot$  K, respectively. Hence, for

SI and English units,

CS kJ/

Kg dry air · K = 1.005 + 1.88H (SI) CS btu/

lbm dry air · °F = 0.24 + 0.45H (Englis)

(33.3-6)

[*Note:* In some cases,  $c_s$  will be given as

$(1.005 + 1.88H)10^3 \text{ J/kg} \cdot \text{K}$ .]

*6. Humid volume of an air–water vapor*

*mixture.* The humid volume  $v_H$  is the

total volume in  $\text{m}^3$  of 1 kg of dry air

plus the vapor it contains at 101.325 kPa

(1.0 atm) abs pressure and the given gas

temperature. Using the ideal gas law,

$v_H \text{ m}^3/$

$(18.02H) = (2.83 \times 10^{-3} + 4.56 \times 10^{-3}H)T \text{ K } v_H \text{ ft}^3/$

$92T \cdot R(128.97 + 118.02H) = (0.0252 + 0.0405H)T$

$^\circ\text{R} (33.3-7)$

For a saturated air–water vapor mixture,  $H = H_S$ , and  $v_H$  is the saturated volume.

*7. Total enthalpy of an air–water vapor mixture.* The total enthalpy of 1 kg of air plus its water vapor is  $H_y$  J/kg or kJ/kg dry air. If  $T_0$  is the datum temperature chosen for both components, the total enthalpy is the sensible heat of the air–water vapor mixture plus the latent heat  $\lambda_0$  in J/kg or kJ/kg water vapor of the water vapor at  $T_0$ . Note that  $(T - T_0)^\circ\text{C} = (T - T_0)$  K and that this enthalpy is referred to liquid water.

$$\begin{aligned} H_y \text{ KJ/Kg dry air} &= C_S(T - T_0) + H\lambda_0 = (1.005 + 1.88H)(T - T_0^\circ\text{C}) + H\lambda_0 \\ H_y \text{ btu/lbm dry air} &= (0.24 + 0.45H)(T - T_0^\circ\text{F}) + H\lambda_0(33.3 - 8) \end{aligned}$$

If the total enthalpy is referred to a base temperature  $T_0$  of  $0^\circ\text{C}$  ( $32^\circ\text{F}$ ), the equation for  $H_y$  becomes

$$\begin{aligned} H_y \text{ KJ/Kg dry air} &= (1.005 + 1.88H) \\ &\quad (T^\circ\text{C} - 0) + 2501.4H \text{ (SI)} \\ H_y \text{ btu/lbm dry air} &= (0.24 + 0.45H)(T^\circ\text{F} \\ &\quad - 32) + 1075.4 \text{ (English)} \quad (33.3-9) \end{aligned}$$

8. *Humidity chart of air–water vapor mixtures.* A convenient chart of the properties of air–water vapor mixtures at 1.0 atm abs pressure is the humidity chart in Fig. 33.3-2. In this figure, the humidity  $H$  is plotted versus the actual temperature of the air–water vapor mixture (dry bulb temperature).

The curve marked 100% running upward to the right gives the saturation humidity  $H_s$  as a function of

temperature. In Example 33.3-1, for  $26.7^{\circ}\text{C}$ ,  $H_s$  was calculated as  $0.02226$  kg  $\text{H}_2\text{O}$ /kg air. Plotting this point for  $26.7^{\circ}\text{C}$  ( $80^{\circ}\text{F}$ ) and  $H_s = 0.02226$  on Fig. 33.3-2, it falls on the 100% saturated line.

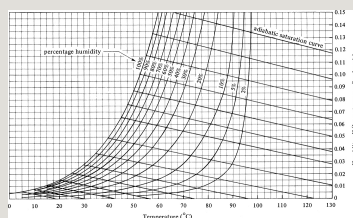


Figure 33.3-2. Humidity chart for mixtures of air and water vapor at a total pressure of  $101.325$  kPa ( $760$  mmHg). From R. E. Treybal, *Mass-Transfer Operations*, 3rd ed. New York: McGraw-Hill Book Company, 1980. With permission.

Any point below the saturation line represents unsaturated air–water vapor mixtures. The curved lines below the 100% saturation line and running upward to the right represent unsaturated mixtures of definite percentage humidity  $HP$ . Going



downward vertically from the saturation line at a given temperature, the line between 100% saturation and zero humidity  $H$  (the bottom horizontal line) is divided evenly into 10 increments of 10% each.

All the percentage humidity lines  $HP$  mentioned and the saturation humidity line  $HS$  can be calculated from the data for the vapor pressure of water.

**EXAMPLE 33.3-2. Use of a Humidity Chart**

Air entering a dryer has a temperature (dry bulb temperature) of  $60^{\circ}\text{C}$  ( $140^{\circ}\text{F}$ ) and a dew point of  $26.7^{\circ}\text{C}$  ( $80^{\circ}\text{F}$ ). Using the humidity chart, determine the actual humidity  $H$ , percentage humidity  $HP$ , humid heat  $cs$ , and humid volume  $v_H$  in SI and English units.

**Solution:** The dew point of  $26.7^{\circ}\text{C}$  is the temperature at which the given mixture is at 100% saturation. Starting at  $26.7^{\circ}\text{C}$  (Fig. 33.3-2), and drawing a vertical line until it intersects the line for 100% humidity, a humidity of  $H = 0.0225$  kg  $\text{H}_2\text{O}/\text{kg}$  dry air is read off the plot. This is the actual humidity of the air at  $60^{\circ}\text{C}$ . Stated in another way, if air at  $60^{\circ}\text{C}$  and with a humidity  $H = 0.0225$  is cooled, its dew point will be  $26.7^{\circ}\text{C}$ . In English units,  $H = 0.0225$  lb  $\text{H}_2\text{O}/\text{lb}$  dry air.

Locating this point where  $H = 0.0225$  and  $t = 60^{\circ}\text{C}$  on the chart, the percentage humidity  $HP$  is found to be 14%, by

linear interpolation vertically between the 10 and 20% lines.  
The humid heat for  $H = 0.0225$  is, from Eq. (33.3-6),

$$\begin{aligned}CS &= 1.005 + 1.88(0.0225) = 1.047 \text{ kJ/} \\ &\text{kg dry air} \cdot \text{K or } 1.047 \times 103 \text{ J/} \\ \text{Kg} \cdot \text{KCS} &= 0.24 + 0.45(0.0225) = 0.250 \text{ btu/} \\ &\text{lbm dry air} \cdot \text{F}^\circ (\text{English})\end{aligned}$$

The humid volume at  $60^\circ\text{C}$  ( $140^\circ\text{F}$ ), from Eq. (33.3-7), is

$$v_H = (2.83 \times 10^{-3} + 4.56 \times 10^{-3} \times 0.0225)(60 + 273) = 0.977 \text{ m}^3/\text{kg dry air}$$

In English units,

$$v_H = (0.0252 + 0.0405 \times 0.0225)(460 + 140) = 15.67 \text{ ft}^3/\text{lbm dry air}$$

### 33.3C Adiabatic Saturation Temperatures

Consider the process shown in Fig. 33.3-3, where the entering gas of an air–water vapor mixture is contacted with a spray of liquid water. The gas leaves having a different humidity and temperature, and the process is adiabatic. The water is recirculated, with some makeup water added.

The temperature of the water being recirculated reaches a steady-state temperature called the *adiabatic*

*saturation temperature,  $T_s$ .* If the entering gas at temperature  $T$  having a humidity of  $H$  is not saturated,  $T_s$  will be lower than  $T$ . If the contact between the entering gas and the spray of droplets is enough to bring the gas and liquid to equilibrium, the air leaving is saturated at  $T_s$ , and has a humidity  $H_s$ .

Writing an enthalpy balance (heat balance) over the process, a datum of  $T_s$  is used. The enthalpy of the makeup  $H_2O$  is then zero. This means that the total enthalpy of the entering gas mixture = enthalpy of the exiting gas mixture, or, using Eq. (33.3-8),

$$CS(T-T_s)+H\lambda S=cS(T_s-T_s)+H_s\lambda S \quad (33.3-10)$$

Or, rearranging, and using Eq. (33.3-6)

for  $cs$ ,

$$\begin{aligned} H - H_s T - T_s = \\ -cs\lambda_s = 1.005 + 1.88H\lambda_s(\text{SI}) \\ -T_s = 0.24 + 0.45H\lambda_s(\text{English}) \end{aligned} \quad (33.3-11)$$

Equation (33.3-11) is the equation of an adiabatic humidification curve when plotted on Fig. 33.3-2, which passes through the points  $H_s$  and  $T_s$  on the 100% saturation curve and through other points of  $H$  and  $T$ . These series of lines, running upward to the left, are called *adiabatic humidification lines* or *adiabatic saturation lines*. Since  $cs$  contains the term  $H$ , the adiabatic lines are not quite straight when plotted on the humidity chart.

If a given gas mixture at  $T_1$  and  $H_1$  is

contacted for a sufficiently long time in an adiabatic saturator, it will leave saturated at  $H_{S1}$  and  $T_{S1}$ . The values of  $H_{S1}$  and  $T_{S1}$  are determined by following the adiabatic saturation line going through point  $T_1, H_1$  until it intersects the 100% saturation line. If contact is not sufficient, the exiting mixture will be at a percentage saturation less than 100% but on the same line.

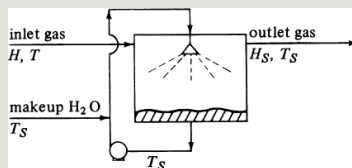


Figure 33.3-3. *Adiabatic air–water vapor saturator.*

#### **EXAMPLE 33.3-3. Adiabatic Saturation of Air**

An air stream at  $87.8^\circ\text{C}$  having a humidity  $H = 0.030$  kg  $\text{H}_2\text{O}/\text{kg}$  dry air is contacted in an adiabatic saturator with water. It is cooled and humidified to 90% saturation.

- What are the final values of  $H$  and  $T$ ?
- For 100% saturation, what will be the values of  $H$  and  $T$ ?

**Solution:** For part (a), the point  $H = 0.030$  and  $T = 87.8^\circ\text{C}$

is located on the humidity chart. The adiabatic saturation curve through this point is followed upward to the left until it intersects the 90% line at 42.5°C and  $H = 0.0500 \text{ kg H}_2\text{O/kg dry air}$ .

For part (b), the same line is followed to 100% saturation, where  $T = 40.5^\circ\text{C}$  and  $H = 0.0505 \text{ Kg H}_2\text{O/kg dry air}$ .

### 33.3D Wet Bulb Temperature

The adiabatic saturation temperature is the steady-state temperature attained when a large amount of water is contacted by the entering gas. The *wet bulb temperature* is the steady-state nonequilibrium temperature reached when a small amount of water is contacted under adiabatic conditions by a continuous stream of gas. Since the amount of liquid is small, the temperature and humidity of the gas are not changed, contrary to the case of adiabatic saturation, where the temperature and humidity of the gas are changed.

The method used to measure the wet bulb temperature is illustrated in Fig. 33.3-4, where a thermometer is covered by a wick or cloth. The wick is kept wet by water and is immersed in a flowing stream of air–water vapor having a temperature of  $T$  (dry bulb temperature) and humidity  $H$ . At steady-state, water is evaporating to the gas stream. The wick and water are cooled to  $T_w$  and stay at this constant temperature. The latent heat of evaporation is exactly balanced by the convective heat flowing from the gas stream at  $T$  to the wick at a lower temperature  $T_w$ .

A heat balance on the wick can be made. The datum temperature is taken at  $T_w$ . The amount of heat lost by vaporization, neglecting the small sensible heat change of the vaporized

liquid and radiation, is

$$q = M A N_A \lambda_W A \quad (33.3-12)$$

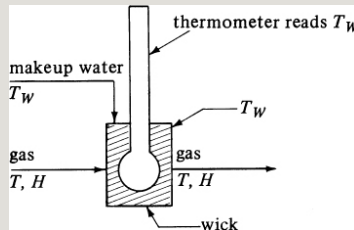


Figure 33.3-4. *Measurement of wet bulb temperature.*

where  $q$  is kW (kJ/s),  $MA$  is the molecular weight of water,  $N_A$  is kg mol H<sub>2</sub>O evaporating/s · m<sup>2</sup>,  $A$  is surface area m<sup>2</sup>, and  $\lambda_W$  is the latent heat of vaporization at  $T_W$  in kJ/kg H<sub>2</sub>O. In English units,  $q$  is btu/h,  $N_A$  is lb mol/h · ft<sup>2</sup>, and  $\lambda_W$  is btu/lb<sub>m</sub> H<sub>2</sub>O. The flux  $N_A$  is

$$N_A = K y' x B M (y_w - y) = k_y (y_w - y) \quad (33.3-13)$$



where  $Ky'$  is the mass-transfer coefficient in  $\text{kg mol/s} \cdot \text{m}^2 \cdot \text{mol frac}$ ,  $x_{BM}$  is the log mean inert mole fraction of the air,  $y_w$  is the mole fraction of water vapor in the gas at the surface, and  $y$  is the mole fraction in the gas. For a dilute mixture,  $x_{BM} \cong 1.0$  and  $k'y \cong k_y$ . The relation between  $H$  and  $y$  is

$$y = H/M_B + H/M_A \quad (33.3-14)$$

where  $M_B$  is the molecular weight of air and  $M_A$  the molecular weight of  $\text{H}_2\text{O}$ . Since  $H$  is small, as an approximation,

$$y \cong H/M_B \quad (33.3-15)$$

Substituting Eq. (33.3-15) into (33.3-13) and then substituting the resultant into Eq. (33.3-12),

$$q = M_B k_y \lambda_W (H_w - H) A \quad (33.3-16)$$

The rate of convective heat transfer from the gas stream at  $T$  to the wick at  $T_W$  is

$$q = h(T - T_W)A \quad (33.3-17)$$

where  $h$  is the heat-transfer coefficient in  $kW/m^2 \cdot K$  ( $btu/h \cdot ft^2 \cdot ^\circ F$ ).

Equating Eq. (33.3-16) to Eq. (33.3-17) and rearranging,

$$H - H_W - T_W = -h / MB_{ky} \lambda W \quad (33.3-18)$$

Experimental data on the value of  $h / MB_{ky}$ , called the *psychrometric ratio*, show that for water vapor–air mixtures, the value is approximately 0.96–1.005. Since this value is close to the value of  $c_s$  in Eq. (33.3-11), approximately 1.005, Eqs. (33.3-18) and (33.3-11) are almost the same. This means that the

adiabatic saturation lines can also be used for wet bulb lines with reasonable accuracy. (*Note:* This is only true for water vapor and not for other vapors, such as benzene.) Hence, the wet bulb determination is often used to measure the humidity of an air–water vapor mixture.

**EXAMPLE 33.3-4. Wet Bulb Temperature and Humidity**

A water vapor–air mixture having a dry bulb temperature of  $T = 60^\circ\text{C}$  is passed over a wet bulb, as shown in Fig. 33.3-4, and the wet bulb temperature obtained is  $T_w = 29.5^\circ\text{C}$ . What is the humidity of the mixture?

**Solution:** The wet bulb temperature of  $29.5^\circ\text{C}$  can be assumed to be the same as the adiabatic saturation temperature  $T_s$ , as discussed. Following the adiabatic saturation curve of  $29.5^\circ\text{C}$  until it reaches the dry bulb temperature of  $60^\circ\text{C}$ , the humidity is  $H = 0.0135 \text{ kg H}_2\text{O/kg dry air}$ .

## 33.4 Equilibrium Moisture Content of Materials

### 33.4A Introduction

As in other transfer processes, such as mass transfer, the process of

drying of materials must be approached from the viewpoint of the equilibrium relationships together with the rate relationships. In most of the drying apparatus discussed in Section 33.2, material is dried in contact with an air–water vapor mixture. The equilibrium relationships between the air–water vapor and the solid material will be discussed in this section.

An important variable in the drying of materials is the humidity of the air in contact with a solid of given moisture content. Suppose that a wet solid containing moisture is brought into contact with a stream of air having a constant humidity  $H$  and temperature  $T$ . A large excess of air is used, so its conditions remain constant. Eventually,

after exposure of the solid sufficiently long for equilibrium to be reached, the solid will attain a definite moisture content. This is known as the *equilibrium moisture content* of the material under the specified humidity and temperature of the air. The moisture content is usually expressed on a dry basis as kg of water per kg of moisture-free (bone-dry) solid or kg H<sub>2</sub>O/100 kg dry solid; in English units, it is expressed as lb H<sub>2</sub>O/100 lb dry solid.

For some solids, the value of the equilibrium moisture content depends on the direction from which equilibrium is approached. A different value for the equilibrium moisture content is obtained according to whether a wet sample is allowed to dry by desorption or a dry sample adsorbs moisture by adsorption.

For drying calculations, it is the desorption equilibrium that is the larger value and is of particular interest.

### **33.4B Experimental Data of Equilibrium Moisture Content for Inorganic and Biological Materials**

*1. Typical data for various materials.* If the material contains more moisture than its equilibrium value in contact with a gas of a given humidity and temperature, it will dry until it reaches its equilibrium value. If the material contains less moisture than its equilibrium value, it will adsorb water until it reaches its equilibrium value. For air having 0% humidity, the equilibrium moisture value of all materials is zero.

The equilibrium moisture content varies greatly with the type of material for any

given percent relative humidity, as shown in Fig. 33.4-1 for some typical materials at room temperature.

Nonporous insoluble solids tend to have equilibrium moisture contents that are quite low, as shown for glass wool and kaolin. Certain spongy, cellular materials of organic and biological origin generally show large equilibrium moisture contents. Examples of these in Fig. 33.4-1 are wool, leather, and wood.

*2. Typical food materials.* In Fig. 33-4.2, the equilibrium moisture contents for some typical food materials are plotted versus percent relative humidity. These biological materials also show large values for equilibrium moisture content. Data in this figure and in Fig. 33.4-1 for biological materials show that at high percent relative humidities of about 60

to 80%, the equilibrium moisture content increases very rapidly with increases in relative humidity.

In general, at low relative humidities, the equilibrium moisture content is greatest for food materials high in protein, starch, or other high-molecular-weight polymers and lower for food materials high in soluble solids.

Crystalline salts and sugars as well as fats generally adsorb small amounts of water.

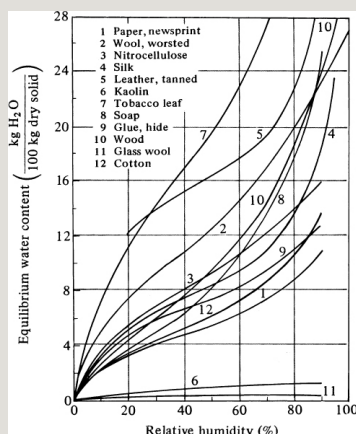


Figure 33.4-1. Typical equilibrium moisture contents of some solids at approximately 298 K (25°C). From National Research Council,



*3. Effect of temperature.* The equilibrium moisture content of a solid decreases somewhat with an increase in temperature. For example, for raw cotton at a relative humidity of 50%, the equilibrium moisture content decreased from 7.3 kg H<sub>2</sub>O/100 kg dry solid at 37.8°C (311 K) to about 5.3 at 93.3°C (366.5 K), a decrease of about 25%. Often, for moderate temperature ranges, the equilibrium moisture content will be assumed constant when experimental data are not available at different temperatures.

At present, theoretical understanding of the structure of solids and surface phenomena does not enable us to predict

the variation of equilibrium moisture content of various materials from first principles. However, by using models such as those used for adsorption isotherms of multilayers of molecules and others, attempts have been made to correlate experimental data. Henderson (H2) gives an empirical relationship between equilibrium moisture content and percent relative humidity for some agricultural materials. In general, empirical relationships are not available for most materials, and equilibrium moisture contents must be determined experimentally. Also, equilibrium moisture relationships often vary from sample to sample of the same kind of material.

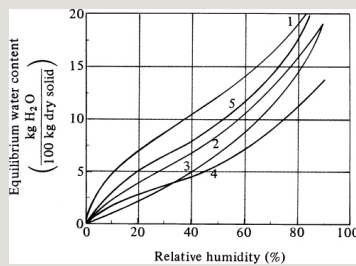


Figure 33.4-2. *Typical equilibrium moisture contents of some food materials at approximately 298 K (25°C): (1) macaroni, (2) flour, (3) bread, (4) crackers, (5) egg albumin. Curve (5) from ref. (E1). Curves (1) to (4) from National Research Council, International Critical Tables, vol. 2. New York: McGraw-Hill Book Company, 1929. Reproduced with permission of the National Academy of Sciences.*

### 33.4C Bound and Unbound Water in Solids

In Fig. 33.4-1, if the equilibrium moisture content of a given material is continued to its intersection with the 100% humidity line, the moisture is called *bound water*. This water in the solid exerts a vapor pressure less than that of liquid water at the same temperature. If such a material contains more water than indicated by intersection with the 100% humidity line, it can still exert a

vapor pressure only as high as that of ordinary water at the same temperature. This excess moisture content is called *unbound water*, and it is held primarily in the voids of the solid. Substances containing bound water are often called *hygroscopic materials*.

As an example, consider curve 10 for wood in Fig. 33.4-1. This intersects the curve for 100% humidity at about 30 kg H<sub>2</sub>O/100 kg dry solid. Any sample of wood containing less than 30 kg H<sub>2</sub>O/100 kg dry solid contains only bound water. If the wood sample contains 34 kg H<sub>2</sub>O/100 kg dry solid, 4 kg H<sub>2</sub>O will be unbound and 30 kg H<sub>2</sub>O bound per 100 kg dry solid.

The bound water in a substance may

exist under several different conditions. Moisture in cell or fiber walls may have solids dissolved in it and have a lower vapor pressure. Liquid water in capillaries with a very small diameter will exert a lowered vapor pressure because of the concave curvature of the surface. Water in natural organic materials is in chemical and physical–chemical combination.

#### **33.4D Free and Equilibrium Moisture of a Substance**

Free moisture content in a sample is the moisture above the equilibrium moisture content. This free moisture is the moisture that can be removed by drying under the given percent relative humidity. For example, in Fig. 33.4-1, silk has an equilibrium moisture content of 8.5 kg H<sub>2</sub>O/100 kg dry material in contact with air of

50% relative humidity and 25°C. If a sample contains 10 kg H<sub>2</sub>O/100 kg dry material, only 10.0 – 8.5, or 1.5, kg H<sub>2</sub>O/100 kg dry material is removable by drying; this is the free moisture of the sample under these drying conditions.

In many texts and references, the moisture content is given as percent moisture on a dry basis. This is exactly the same as the kg H<sub>2</sub>O/100 kg dry material multiplied by 100.

## **33.5 Rate-of-Drying Curves**

### **33.5A Introduction and Experimental Methods**

*1. Introduction.* In the drying of various types of process materials from one moisture content to another, it is usually desired to estimate the size of the dryer needed,

the various operating conditions of humidity and temperature for the air used, and the time needed to perform the amount of drying required. As discussed in Section 33.4, equilibrium moisture contents of various materials cannot be predicted and must be determined experimentally. Similarly, since our knowledge of the basic mechanisms of drying rates is quite incomplete, in most cases it is necessary to obtain some experimental measurements of those rates.

*2. Experimental determination of drying rate.* To experimentally determine the drying rate for a given material, a sample is usually placed on a tray. If it is a solid material, it should fill the tray so that only the top surface is exposed to

the drying air stream. By suspending the tray from a balance in a cabinet or duct through which the air is flowing, the loss in weight of moisture during drying can be determined at different intervals without interrupting the operation.

In doing batch-drying experiments, certain precautions should be observed to obtain usable data under conditions that closely resemble those to be used in the large-scale operations. The sample should not be too small in weight and should be supported in a tray or frame similar to the large-scale operation. The ratio of drying to nondrying surface (insulated surface) and the bed depth should be similar. The velocity, humidity, temperature, and direction of the air should be the same and should be constant to simulate drying under



constant-drying conditions.

### 33.5B Rate of Drying Curves for Constant-Drying Conditions

*1. Conversion of data to rate-of-drying curve.* Data obtained from a batch-drying experiment are usually obtained as  $W$  total weight of the wet solid (dry solid plus moisture) at different times  $t$  hours in the drying period. These data can be converted to rate-of-drying data in the following ways. First, the data are recalculated. If  $W$  is the weight of the wet solid in kg total water plus dry solid and  $W_s$  is the weight of the dry solid in kg,

$$X_t = \frac{W - W_s}{W_s}$$

$$X_t = \frac{\text{kg total water} - \text{kg dry solid}}{\text{kg dry solid}} \quad \left( \frac{\text{lb total water} - \text{lb dry solid}}{\text{lb dry solid}} \right)$$

$$(33.5-1)$$

For the given constant-drying conditions, the equilibrium moisture content  $X^*$  kg equilibrium moisture/kg dry solid is determined. Then, the free moisture content  $X$  in kg free water/kg dry solid is calculated for each value of  $X_t$ :

$$X = X_t - X^* \quad (33.5-2)$$

Using the data calculated from Eq. (33.5-2), a plot of free moisture content  $X$  versus time  $t$  in h is made, as in Fig. 33.5-1a. To obtain the rate-of-drying curve from this plot, the slopes of the tangents drawn to the curve in Fig. 33.5-1a can be measured, which give values of  $dX/dt$  at given values of  $t$ . The rate  $R$  is calculated for each point by

$$R = -LSA \frac{dX}{dt}$$

where  $R$  is drying rate in  $\text{kg H}_2\text{O}/\text{h} \cdot \text{m}^2$ ,  $Ls$  is  $\text{kg}$  of dry solid used, and  $A$  is exposed surface area for drying in  $\text{m}^2$ . In English units,  $R$  is  $\text{lb}_\text{m} \text{H}_2\text{O}/\text{h} \cdot \text{ft}^2$ ,  $Ls$  is  $\text{lb}_\text{m}$  of dry solid, and  $A$  is  $\text{ft}^2$ . For obtaining  $R$  from Fig. 33.5-1a, a value of  $Ls/A$  of  $21.5 \text{ kg}/\text{m}^2$  was used. The drying-rate curve is then obtained by plotting  $R$  versus the moisture content, as in Fig. 33.5-1b.

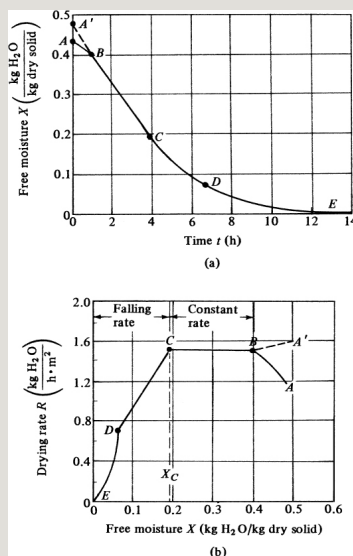


Figure 33.5-1. Typical drying-rate curve for constant-drying conditions: (a) plot of data as free moisture versus time, (b) rate of drying curve as rate versus free moisture content.

Another method for obtaining the rate-of-drying curve is to first calculate the weight loss  $\Delta X$  for a  $\Delta t$  time. For example, if  $X_1 = 0.350$  at a time  $t_1 = 1.68$  h and  $x_2 = 0.325$  at a time  $t_2 = 2.04$  h,  $\Delta X/\Delta t = (0.350 - 0.325)/(2.04 - 1.68)$ . Then, using Eq. (33.5-4) and  $Ls/A = 21.5$ ,

$$R =$$

$$-LSA\Delta X\Delta t = 21.5(0.350 - 0.325)(2.04 - 1.68) = 1.493$$

This rate  $R$  is the average over the period 1.68 to 2.04 h and should be plotted at the average concentration  $X = (0.350 + 0.325)/2 = 0.338$ .

*2. Plot of rate-of-drying curve.* In Fig. 33.5-1b, the rate-of-drying curve for constant-drying conditions is shown. At zero time, the initial free moisture

content is shown at point  $A$ . Initially, the solid is usually at a colder temperature than its ultimate temperature, and the evaporation rate will increase.

Eventually, at point  $B$ , the surface temperature rises to its equilibrium value. Alternatively, if the solid is quite hot to start with, the rate may start at point  $A'$ . This initial unsteady-state adjustment period is usually quite short and it is often ignored in the analysis of drying times.

In Fig. 33.5-1a, from point  $B$  to point  $C$ , the line is straight and hence the slope and rate are constant during this period. This *constant-rate-of-drying period* is shown as line  $BC$  in Fig. 33.5-1b.

At point  $C$  on both plots, the drying rate starts to decrease in the *falling-rate*

*period* until it reaches point *D*. In this first falling-rate period, the rate shown as line *CD* in Fig. 33.5-1b is often linear.

At point *D*, the rate of drying falls even more rapidly, until it reaches point *E*, where the equilibrium moisture content is  $X^*$  and  $X = X^* - X^* = 0$ . In some materials being dried, the region *CD* may be missing completely, or it may constitute all of the falling-rate period.

### **33.5C Drying in the Constant-Rate Period**

Drying of different solids under different constant conditions of drying will often give curves of different shapes in the falling-rate period, but in general, the two major portions of the drying-rate curve—constant-rate period and falling-rate

period—are present.

In the constant-rate drying period, the surface of the solid is initially very wet and a continuous film of water exists on the drying surface. This water is entirely unbound water and it acts as if the solid were not present. The rate of evaporation under the given air conditions is independent of the solid and is essentially the same as the rate from a free liquid surface. Increased roughness of the solid surface, however, may lead to higher rates than from a flat surface.

If the solid is porous, most of the water evaporated in the constant-rate period is supplied from the interior of the solid. This period continues only as long as the water is supplied to the surface as

fast as it is evaporated. Evaporation during this period is similar to that in determining the wet bulb temperature, and in the absence of heat transfer by radiation or conduction, the surface temperature is approximately the same as the wet bulb temperature.

### **33.5D Drying in the Falling-Rate Period**

Point *C* in Fig. 33.5-1b is at the *critical free moisture content*  $X_c$ . At this point, there is insufficient water on the surface to maintain a continuous film of water. The entire surface is no longer wetted, and the wetted area continually decreases in this first falling-rate period until the surface is completely dry, at point *D* in Fig. 33.5-1b.

The second falling-rate period begins at



point  $D$  when the surface is completely dry. The plane of evaporation slowly recedes from the surface. Heat for the evaporation is transferred through the solid to the zone of vaporization.

Vaporized water moves through the solid into the air stream.

In some cases, no sharp discontinuity occurs at point  $D$ , and the change from partially wetted to completely dry conditions at the surface is so gradual that no distinct change is detectable.

The amount of moisture removed in the falling-rate period may be relatively small, but the time required may be long. This can be seen in Fig. 33.5-1. The period  $BC$  for constant-rate drying lasts for about 3.0 h and reduces  $X$  from 0.40 to about 0.19, a reduction of 0.21

kg H<sub>2</sub>O/kg dry solid. The falling-rate period *CE* lasts about 9.0 h and reduces *X* only from 0.19 to 0.

### **33.5E Moisture Movements in Solids During Drying in the Falling-Rate Period**

When drying occurs by evaporation of moisture from the exposed surface of a solid, moisture must move from the depths of the solid to the surface. The mechanisms of this movement affect the drying during the constant-rate and falling-rate periods. Some of the theories advanced to explain the various types of falling-rate curves will be briefly reviewed.

*1. Liquid diffusion theory.* According to this theory, diffusion of liquid moisture occurs when there is a concentration difference between the depths of the solid and the surface. This method of

moisture transport is usually found in nonporous solids where single-phase solutions are formed with the moisture, such as in paste, soap, gelatin, and glue. It is also found in drying the last portions of moisture from clay, flour, wood, leather, paper, starches, and textiles. In drying many food materials, the movement of water in the falling-rate period also occurs by diffusion.

The shapes of the moisture-distribution curves in the solid at given times are qualitatively consistent with the unsteady-state diffusion equations given in Chapter 20. The moisture diffusivity  $D_{AB}$  usually decreases with decreased moisture content, so that the diffusivities are usually average values over the range of concentrations used. Materials drying in this way are usually said to be

drying by diffusion, although the actual mechanisms may be quite complicated. Since the rate of evaporation from the surface is quite fast, that is, the resistance is quite low compared to the diffusion rate through the solid in the falling-rate period, the moisture content at the surface is at the equilibrium value.

The shape of a diffusion-controlled curve in the falling-rate period is similar to Fig. 33.5-2a. If the initial constant-rate drying is quite high, the first falling-rate period of unsaturated surface evaporation may not appear. If the constant-rate drying is quite low, the period of unsaturated surface evaporation is usually present in region *CD* in Fig. 33.5-1b and the diffusion-controlled curve is in region *DE*. Equations for calculating drying in this

period where diffusion controls are given in Section 33.9. Also, Problem 20.1-4 for the drying of clay and Problem 20.1-6 for the drying of wood using diffusion theory are found in the Chapter 20 Problems.

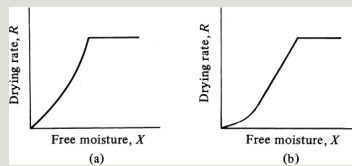


Figure 33.5-2. Typical drying-rate curves: (a) diffusion-controlled falling-rate period, (b) capillary-controlled falling-rate period in a fine porous solid.

## 2. Capillary movement in porous solids.

When granular and porous solids such as clays, sand, soil, paint pigments, and minerals are being dried, unbound or free moisture moves through the capillaries and voids of the solids by *capillary action*, not by diffusion. This mechanism, involving surface tension, is

similar to the movement of oil in a lamp wick.

A porous solid contains interconnecting pores and channels of varying pore sizes. As water is evaporated, a meniscus of liquid water is formed across each pore in the depths of the solid. This sets up capillary forces by the interfacial tension between the water and the solid. These capillary forces provide the driving force for moving water through the pores to the surface. Small pores develop greater forces than do large pores.

At the beginning of the falling-rate period at point *C* in Fig. 33.5-1b, the water is being brought to the surface by capillary action, but the surface layer of water starts to recede below the surface.

Air rushes in to fill the voids. As the water is continuously removed, a point is reached where there is insufficient water left to maintain continuous films across the pores, and the rate of drying suddenly decreases at the start of the second falling-rate period at point *D*. Then, the rate of water vapor diffusion in the pores and the rate of heat conduction in the solid may become the main factors in drying.

In fine pores in solids, the rate-of-drying curve in the second falling-rate period may conform to the diffusion law; the curve is concave upward, as shown in Fig. 33.5-2b. For very porous solids, such as a bed of sand, where the pores are large, the rate-of-drying curve in the second falling-rate period is often straight, and hence the diffusion

equations do not apply.

*3. Effect of shrinkage.* A factor often greatly affecting the drying rate is the shrinkage of the solid as moisture is removed. Rigid solids do not shrink appreciably, but colloidal and fibrous materials such as vegetables and other foodstuffs do undergo shrinkage. The most serious effect is that a hard layer may develop on the surface that is impervious to the flow of liquid or vapor moisture and thus slows the drying rate; examples are clay and soap. For many food products, if drying occurs at too high a temperature, a layer of closely packed, shrunken cells, which are sealed together, forms at the surface. This presents a barrier to moisture migration and is known as *case hardening*.

Another effect of shrinkage is to cause



the material to warp and change its structure. This can happen when drying wood.

To decrease these effects of shrinkage, it is sometimes desirable to dry with moist air. This decreases the rate of drying so that the effects of shrinkage on warping or hardening at the surface are greatly reduced.

### **33.6 Calculation Methods for a Constant-Rate Drying Period**

#### **33.6A Method for Using an Experimental Drying Curve**

*1. Introduction.* Probably the most important factor in drying calculations is the length of time required to dry a material from a given initial free moisture content  $X_1$  to a final moisture content  $X_2$ . For drying in the constant-rate period,

we can estimate the time needed by using experimental batch-drying curves or by using predicted mass- and heat-transfer coefficients.

*2. Method using a drying curve.* To estimate the time of drying for a given batch of material, the best method is based on actual experimental data obtained under conditions where the feed material, relative exposed surface area, gas velocity, temperature, and humidity are essentially the same as in the final drier. Then, the time required for the constant-rate period can be determined directly from the drying curve of free moisture content versus time.

**EXAMPLE 33.6-1. Time of Drying from a Drying Curve**

A solid whose drying curve is represented by Fig. 33.5-1a is to be dried from a free moisture content  $X_1 = 0.38$  kg H<sub>2</sub>O/kg dry solid to  $X_2 = 0.25$  kg H<sub>2</sub>O/kg dry solid. Estimate

the time required.

**Solution:** From Fig. 33.5-1a for  $X_1 = 0.38$ ,  $t_1$  is read off as 1.28 h. For  $X_2 = 0.25$ ,  $t_2 = 3.08$  h. Hence, the time required is

$$t = t_2 - t_1 = 3.08 - 1.28 = 1.80 \text{ h.}$$

*3. Method using a rate-of-drying curve for a constant-rate period.* Instead of using the drying curve, the rate-of-drying curve can be used. The drying rate  $R$  is defined by Eq. (33.5-3) as

$$R = -L S A \frac{dX}{dt} \quad (33.5-3)$$

This can be rearranged and integrated over the time interval for drying from  $X_1$  at  $t_1 = 0$  to  $X_2$  at  $t_2 = t$ :

$$t = \int_{t_1=0}^{t_2=t} dt = \frac{L S A}{R} \int_{X_2}^{X_1} dX \quad (33.6-1)$$

If the drying takes place within the constant-rate period, so that both  $X_1$  and  $X_2$  are greater than the critical moisture

content  $X_C$ , then  $R = \text{constant} = R_C$ .

Integrating Eq. (33.6-1) for the constant-rate period,

$$t = L \text{SARC}(X_1 - X_2) \quad (33.6-2)$$

**EXAMPLE 33.6-2. Drying Time from a Rate-of-Drying Curve**

Repeat Example 33.6-1 but use Eq. (33.6-2) and Fig. 33.5-1b.

**Solution:** As stated previously, a value of 21.5 for  $Ls/A$  was used to prepare Fig. 33.5-1b from 33.5-1a. From Fig. 33.5-1b,  $R_C = 1.51 \text{ kg H}_2\text{O/h} \cdot \text{m}^2$ . Substituting into Eq. (33.6-2),

$$t = L \text{SARC}(X_1 - X_2) = 21.5(1.51)(0.38 - 0.25) = 1.85 \text{ h}$$

This is close to the value of 1.80 h in Example 33.6-1.

### 33.6B Method Using Predicted Transfer Coefficients for Constant-Rate Period

*1. Introduction.* In the constant-rate period of drying, the surfaces of the grains of a solid in contact with a drying air flow remain completely wetted. As stated previously, the rate of evaporation of moisture under a

given set of air conditions is independent of the type of solid and is essentially the same as the rate of evaporation from a free liquid surface under the same conditions. However, surface roughness may increase the rate of evaporation.

During this constant-rate period, the solid is so wet that the water acts as if the solid were not there. The water evaporated from the surface is supplied from the interior of the solid. The rate of evaporation from a porous material occurs by the same mechanism as that occurring at a wet bulb thermometer, which is essentially constant-rate drying.

*2. Equations for predicting constant-rate drying.* Drying of a material occurs

by mass transfer of water vapor from the saturated surface of the material through an air film to the bulk gas phase or environment. The rate of moisture movement within the solid is sufficient to keep the surface saturated. The rate of removal of the water vapor (drying) is controlled by the rate of heat transfer to the evaporating surface, which furnishes the latent heat of evaporation for the liquid. At steady state, the rate of mass transfer balances the rate of heat transfer.

To derive the equation for drying, we neglect heat transfer by radiation to the solid surface and also assume no heat transfer by conduction from metal pans or surfaces. Conduction and radiation will be considered in Section 33.8. Assuming only heat transfer to the solid

surface by convection from the hot gas to the surface of the solid and mass transfer from the surface to the hot gas (Fig. 33.6-1), we can write equations that are the same as those for deriving the wet bulb temperature  $T_w$  in Eq. (33.3-18).

The rate of convective heat transfer  $q$  in W (J/s, btu/h) from the gas at  $T^\circ\text{C}$  ( $^\circ\text{F}$ ) to the surface of the solid at  $T_w^\circ\text{C}$ , where  $(T - T_w)^\circ\text{C} = (T - T_w) \text{ K}$ , is

$$q = h(T - T_w)A \quad (33.6-3)$$

where  $h$  is the heat-transfer coefficient in  $\text{W}/\text{m}^2 \cdot \text{K}$  ( $\text{btu}/\text{h} \cdot \text{ft}^2 \cdot ^\circ\text{F}$ ) and  $A$  is the exposed drying area in  $\text{m}^2$  ( $\text{ft}^2$ ). The equation of the flux of water vapor from the surface is the same as Eq. (33.3-13) and is

$$N_A = k_y(y_W - y) \quad (33.6-4)$$

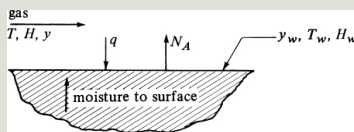


Figure 33.6-1. *Heat and mass transfer in constant-rate drying.*

Using the approximation from Eq. (33.3-15) and substituting into Eq. (33.6-4),

$$N_A = k_y M_B M_A (H_W - H) \quad (33.6-5)$$

The amount of heat needed to vaporize  $N_A$  kg mol/s · m<sup>2</sup> (lb mol/h · ft<sup>2</sup>) water, neglecting the small sensible heat changes, is the same as Eq. (33.3-12):

$$q = M_A N_A \lambda_W \quad (33.6-6)$$

where  $\lambda_W$  is the latent heat at  $T_W$  in J/kg (btu/lb<sub>m</sub>).



Equating Eqs. (33.6-3) and (33.6-6), and substituting Eq. (33.6-5) for  $N_A$ ,

$$RC = qA\lambda W = h(T - T_W)\lambda W = k_y M B (H W - H) \quad (33.6-7)$$

Equation (33.6-7) is identical to Eq. (33.3-16) for the wet bulb temperature. Hence, in the absence of heat transfer by conduction and radiation, the temperature of the solid is at the wet bulb temperature of the air during the constant-rate drying period. Thus, the rate of drying  $RC$  can be calculated using the heat-transfer equation  $h(T - T_W)/\lambda W$  or the mass transfer equation  $k_y M B (H W - H)$ . However, it has been found that using the heat-transfer equation (33.6-8) is more reliable, since an error in determining the interface temperature  $T_W$  at the surface affects the

driving force  $(T - T_w)$  much less than it affects  $(H_w - H)$ .

$$R_C \text{ Kg H}_2\text{O/h}\cdot\text{m}^2 = h\lambda W(T - T_w C^\circ) \\ (3600)(\text{SI}) \\ R_C \text{ lbm H}_2\text{O/h}\cdot\text{ft}^2 = h\lambda W(T - T_w F^\circ) \\ (\text{English}) \quad (33.6-8)$$

To predict  $R_C$  in Eq. (33.6-8), the heat-transfer coefficient must be known. For the case where the air is flowing parallel to the drying surface, Eq. (15.4-3) can be used for air. However, because the shape of the leading edge of the drying surface causes more turbulence, the following can be used for an air temperature of 45–150°C and a mass velocity  $G$  of 2450–29 300 kg/h · m<sup>2</sup> (500–6000 lbm/h · ft<sup>2</sup>) or a velocity of 0.61–7.6 m/s (2–25 ft/s):

$$204G^{0.8}(\text{SI})h=0.0128G^{0.8}(\text{English}) \quad (33.6-9)$$

where in SI units  $G$  is  $v\rho$  kg/h · m<sup>2</sup> and  $h$  is W/m<sup>2</sup> · K. In English units,  $G$  is in lb<sub>m</sub>/h · ft<sup>2</sup> and  $h$  in btu/h · ft<sup>2</sup> · °F. When air flows perpendicular to the surface for a  $G$  of 3900–19500 kg/h · m<sup>2</sup> or a velocity of 0.9–4.6 m/s (3–15 ft/s),

$$17G^{0.37}(\text{SI})h=0.37G^{0.37}(\text{English}) \quad (33.6-10)$$

Equations (33.6-8)–(33.6-10) can be used to estimate the rate of drying during the constant-rate period.

However, experimental measurements of the drying rate are preferred whenever possible.

To estimate the drying time during the constant-rate period, substituting Eq. (33.6-7) into (33.6-2),

$$t = LS\lambda W(X_1 - X_2)A_h(T - T_w) = LS(X_1 - X_2)A_k y_{MB}(H_w - H) \quad (33.6-11)$$

**EXAMPLE 33.6-3. Prediction of Constant-Rate Drying**

An insoluble wet granular material is dried in a pan  $0.457 \times 0.457$  m ( $1.5 \times 1.5$  ft) and 25.4 mm deep. The material is 25.4 mm deep in the pan, and the sides and bottom can all be considered to be insulated. Heat transfer is by convection from an air stream flowing parallel to the surface at a velocity of 6.1 m/s (20 ft/s). The air is at  $65.6^\circ\text{C}$  ( $150^\circ\text{F}$ ) and has a humidity of 0.010 kg  $\text{H}_2\text{O}$ /kg dry air. Estimate the rate of drying for the constant-rate period using SI and English units.

**Solution:** For a humidity  $H = 0.010$  and dry bulb temperature of  $65.6^\circ\text{C}$ , using the humidity chart from Fig. 33.3-2, the wet bulb temperature  $T_w$  is found to be  $28.9^\circ\text{C}$  ( $84^\circ\text{F}$ ) and  $H_w = 0.026$  by following the adiabatic saturation line (the same as the wet bulb line) to the saturated humidity. Using Eq. (33.3-7) to calculate the humid volume,

$$v_H = (2.83 \times 10^{-3} + 4.56 \times 10^{-3} H) T = (2.83 \times 10^{-3} + 4.56 \times 10^{-3} \times 0.01) (273 + 65.6) = 0.974 \text{ m}^3/\text{kg dry air}$$

The density for 1.0 kg dry air + 0.010 kg  $\text{H}_2\text{O}$  is

$$\rho = 1.0 + 0.010 / 0.974 = 1.037 \text{ kg/m}^3 (0.0647 \text{ lbm/ft}^3)$$

The mass velocity  $G$  is

$$G = u \rho = 6.1 (3600) (1.037) = 22,770 \text{ kg/h} \cdot \text{m}^2 \quad G = u \rho = 20 (3600) (0.0647) = 4660 \text{ lbm/h} \cdot \text{ft}^2$$

Using Eq. (33.6-9),

$$h = 0.0204 G^{0.8} = 0.0204 (22,770)^{0.8} = 62.45 \text{ W/m}^2 \cdot \text{K} \quad h = 0.0128 G^{0.8} = 0.0128 (4660)^{0.8} = 11.01 \text{ btu/h} \cdot \text{ft}^2 \cdot \text{F}^\circ$$

At  $T_w = 28.9^\circ\text{C}$  ( $84^\circ\text{F}$ ),  $\lambda_w = 2433 \text{ kJ/kg}$  ( $1046 \text{ btu/lbm}$ ) from the steam tables in Appendix A.2.

Substituting into Eq. (33.6-8) and noting that  $(65.6 - 28.9)^\circ\text{C} = (65.6 - 28.9) \text{ K}$ ,

$$RC = h\lambda w(T - T_w)(3600) = 62.452433 \times 1000(65.6 - 28.9) \\ (3600) = 3.39 \text{ kg/h} \cdot \text{m}^2 RC = 11.011046(150 - 84) = 0.695 \text{ lbm/h} \cdot \text{ft}^2$$

The total evaporation rate for a surface area of  $0.457 \times 0.457 \text{ m}^2$  is

$$\text{total rate} = RCA = 3.39(0.457 \times 0.457) = 0.708 \text{ kg H}_2\text{O/h} \\ h = 0.695(1.5 \times 1.5) = 1.564 \text{ lbm H}_2\text{O/h}$$

### 33.6C Effect of Process Variables on a Constant-Rate Period

As stated previously, experimental measurements of the drying rate are usually preferred over using the equations for prediction. However, these equations are quite helpful in predicting the effect of changing the drying-process variables when limited experimental data are available.

*1. Effect of air velocity.* When conduction and radiation heat transfer are not present, the rate  $RC$  of drying in the constant-rate region is proportional to  $h$  and hence to  $G^{0.8}$  as given by Eq.

(33.6-9) for air flow parallel to the surface. The effect of gas velocity is less important when radiation and conduction are present.

2. Effect of gas humidity. If the gas humidity  $H$  is decreased for a given  $T$  of the gas, then from the humidity chart the wet bulb temperature  $T_w$  will decrease. Then, using Eq. (33.6-7),  $R_c$  will increase. For example, if the original conditions are  $R_{c1}$ ,  $T_1$ ,  $T_{w1}$ ,  $H_1$ , and  $H_{w1}$ , then if  $H_1$  is changed to  $H_2$  and  $H_{w1}$  is changed to  $H_{w2}$ ,  $R_{c2}$  becomes

$$R_{c2} = R_{c1} \frac{T_1 - T_2}{T_1 - T_{w1}} \frac{H_{w1} - H_1}{H_{w2} - H_2} \quad (33.6-12)$$

However, since  $\lambda_{w1} \cong \lambda_{w2}$ ,

$$R_{c2} = R_{c1} \frac{T_1 - T_2}{T_1 - T_{w1}} \frac{H_{w1} - H_1}{H_{w2} - H_2} \quad (33.6-13)$$

3. *Effect of gas temperature.* If the gas temperature  $T$  is increased,  $T_w$  is also increased somewhat, but not as much as the increase in  $T$ . Hence,  $R_c$  increases as follows:

$$T_w^2 T_1 - T_w^1 = R_c (1 H_w^2 - H_2 H_w^1 - H_1) \quad (33.6-14)$$

4. *Effect of the thickness of a solid being dried.* For heat transfer by convection only, the rate  $R_c$  is independent of the thickness  $x_1$  of the solid. However, the time  $t$  for drying between fixed moisture contents  $X_1$  and  $X_2$  will be directly proportional to the thickness  $x_1$ . This is shown by Eq. (33.6-2), where increasing the thickness with a constant  $A$  will directly increase the amount of  $L$  s kg dry solid.

5. Experimental effect of process

variables. Experimental data tend to bear out the conclusions reached on the effects of material thickness, humidity, air velocity, and  $T - T_w$ .

### **33.7 Calculation Methods for the Falling-Rate Drying Period**

#### **33.7A Method Using Numerical Integration**

In the falling-rate drying period, as shown in Fig. 33.5-1b, the rate of drying  $R$  is not constant but decreases when drying proceeds past the critical free moisture content  $X_C$ . When the free moisture content  $X$  is zero, the rate drops to zero.

The drying time for any region between  $X_1$  and  $X_2$  has been given by Eq.

(33.6-1):

$$t = LSA \int_{X_2}^{X_1} \frac{dX}{R} \quad (33.6-1)$$



If the rate is constant, Eq. (33.6-1) can be integrated to give Eq. (33.6-2).

However, in the falling-rate period,  $R$  varies. For any shape of the falling-rate drying curve, Eq. (33.6-1) can be integrated by plotting  $1/R$  versus  $X$  and determining the area under the curve using graphical integration or numerical integration with a spreadsheet (see Section 1.8 for methods of numerical integration).

**EXAMPLE 33.7-1. Numerical Integration in the Falling-Rate Period**

A batch of wet solid whose drying-rate curve is represented by Fig. 33.5-1b is to be dried from a free moisture content of  $X_1 = 0.38$  kg H<sub>2</sub>O/kg dry solid to  $X_2 = 0.04$  kg H<sub>2</sub>O/kg dry solid. The weight of the dry solid is  $L_s = 399$  kg dry solid and  $A = 18.58$  m<sup>2</sup> of top drying surface. Calculate the time for drying. Note that  $L_s/A = 399/18.58 = 21.5$  kg/m<sup>2</sup>.

**Solution:** From Fig. 33.5-1b, the critical free moisture content is  $X_c = 0.195$  kg H<sub>2</sub>O/kg dry solid. Hence, the drying occurs in the constant-rate and falling-rate periods.

For the constant-rate period,  $X_1 = 0.38$  and  $X_2 = X_c = 0.195$ . From Fig. 33.5-1b,  $R_c = 1.51$  kg H<sub>2</sub>O/h · m<sup>2</sup>. Substituting into Eq. (33.6-2),

$$t = LSAR_c(X_1 - X_2) = 399(0.38 - 0.195)(18.58)(1.51) = 2.63h$$

For the falling-rate period, reading values of  $R$  for various values of  $X$  from Fig. 33.5-1b, the following table is prepared:

--

To determine this area by numerical integration using a spreadsheet, the calculations are given in the following table:

--

The area of the first rectangle is the average height  $(0.663 + 0.826)/2$ , or 0.745, times the width  $\Delta X$   $(0.195 - 0.150)$ , or 0.045, giving 0.0335. Other values are similarly calculated, giving a total of 0.1889.

Substituting into Eq. (33.6-1),

$$t = LSA \int_{X_1}^{X_2} dX R = 39918.58(0.1889) = 4.06 \text{ h}$$

The total time is  $2.63 + 4.06 = 6.69 \text{ h}$ .

### 33.7B Calculation Methods for Special Cases in Falling-Rate Region

In certain special cases in the falling-rate region, the equation for the time of drying, Eq. (33.6-1), can be integrated analytically.

*1. Rate is a linear function of  $X$ .* If both  $X_1$  and  $X_2$  are less than  $X_C$  and the rate  $R$  is linear in  $X$  over this region,

$$R=aX+b \quad (33.7-1)$$

where  $a$  is the slope of the line and  $b$  is a constant. Differentiating Eq. (33.7-1) gives  $dR = a dX$ . Substituting this into Eq. (33.6-1),

$$t = LSaA \int \frac{R_2}{R_1} \frac{dR}{R} = LSaA \ln \frac{R_1}{R_2} \quad (33.7-2)$$

Since  $R_1 = aX_1 + b$  and  $R_2 = aX_2 + b$ ,

$$a = \frac{R_1 - R_2}{X_1 - X_2} \quad (33.7-3)$$

Substituting Eq. (33.7-3) into (33.7-2),

$$t = LS(X_1 - X_2)A(R_1 - R_2) \ln \frac{R_1}{R_2} \quad (33.7-4)$$

*2. Rate is a linear function through origin.* In some cases, a straight line from the critical moisture content passing through the origin adequately

represents the whole falling-rate period. In Fig. 33.5-1b, this would be a straight line from  $C$  to  $E$  at the origin. Often, for lack of more detailed data, this assumption is made. Then, for a straight line through the origin, where the rate of drying is directly proportional to the free moisture content,

$$R = aX \quad (33.7-5)$$

Differentiating,  $dX = dR/a$ . Substituting into Eq. (33.6-1),

$$t = LSaA \int_{R_2}^{R_1} \frac{dR}{R^2} = LSaA \ln \frac{R_1}{R_2} \quad (33.7-6)$$

The slope  $a$  of the line is  $R_C/X_C$ , and for  $X_1 = X_C$  at  $R_1 = R_C$ ,

$$t = LSX_C A R_C \ln \frac{R_C}{R_2} \quad (33.7-7)$$

Noting also that  $R_C/R_2 = X_C/X_2$ ,

$$t = L S X C A R C \ln X C X_2 \quad (33.7-8)$$

or

$$R = R C X X C \quad (33.7-9)$$

**EXAMPLE 33.7-2. Approximation of Straight Line for the Falling-Rate Period**

Repeat Example 33.7-1, but as an approximation, assume a straight line for the rate  $R$  versus  $X$  through the origin from point  $X_c$  to  $X = 0$  for the falling-rate period.

**Solution:**  $R_c = 1.51 \text{ kg H}_2\text{O/h} \cdot \text{m}^2$  and  $X_c = 0.195$ . Drying in the falling-rate region is from  $X_c$  to  $X_2 = 0.040$ . Substituting into Eq. (33.7-8),

$$t = L S X C A R C \ln X C X_2 = 399(0.195)18.58(1.51) \ln 0.195/0.040 = 4.39 \text{ h}$$

This value of 4.39 h compares favorably with the value of 4.06 h obtained in Example 33.7-1 by numerical integration.

## 33.8 Combined Convection, Radiation, and Conduction Heat Transfer in the Constant-Rate Period

### 33.8A Introduction

In Section 33.6B, an equation was derived for predicting the rate of drying in the constant-rate period. Equation (33.6-7) was derived

assuming heat transfer to the solid by convection only from the surrounding air to the drying surface. Often, the drying is done in an enclosure, where the enclosure surface radiates heat to the drying solid. Also, in some cases the solid may be resting on a metal tray, and heat transfer by conduction through the metal to the bottom of the solid may occur.

### **33.8B Derivation of the Equation for Convection, Conduction, and Radiation**

In Fig. 33.8-1, a solid material being dried by a stream of air is shown. The total rate of heat transfer to the drying surface is

$$q = q_C + q_R + q_K \quad (33.8-1)$$

where  $q_C$  is the convective heat transfer

from the gas at  $T^{\circ}\text{C}$  to the solid surface at  $T_s^{\circ}\text{C}$  in W (J/s),  $q_R$  is the radiant heat transfer from the surface at  $T_R$  to  $T_s$  in W (J/s), and  $q_K$  is the rate of heat transfer by conduction from the bottom in W. The rate of convective heat transfer is similar to Eq. (33.6-3) and is as follows, where  $(T - T_s)^{\circ}\text{C} = (T - T_s)\text{K}$ :

$$q_C = h_C(T - T_s)A \quad (33.8-2)$$

where  $A$  is the exposed surface area in  $\text{m}^2$ . The radiant heat transfer is

$$q_R = h_R(T_R - T_s)A \quad (33.8-3)$$

where  $h_R$  is the radiant-heat-transfer coefficient defined by Eq. (12.6-10):

$$h_R = \varepsilon(5.676)(T_R 100)^4 - (T_s 100)^4 T_R - T_s \quad (12.6-10)$$

Note that in Eq. (12.6-10),  $T_R$  and  $T_S$  are in K. For the heat transfer by conduction from the bottom, the heat transfer is first by convection from the gas to the metal plate, then by conduction through the metal, and finally by conduction through the solid. Radiation to the bottom of the tray is often small if the tray is placed above another tray, and it will be neglected here. Also, if the gas temperatures are not too high, radiation from the top surface to the tray will be small. Hence, the heat by radiation should not be overemphasized. The heat by conduction is

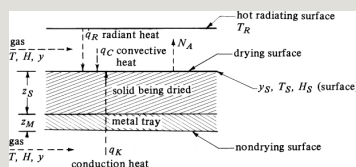


Figure 33.8-1. *Heat and mass transfer in drying a solid from the top surface.*



$$q_K = UK(T-T_S)A \quad (33.8-4)$$

$$UK = 1/h_C + z_M/k_M + z_S/k_S \quad (33.8-5)$$

where  $z_M$  is the metal thickness in m,  $k_M$  is the metal thermal conductivity in  $W/m \cdot K$ ,  $z_S$  is the solid thickness in m, and  $k_S$  is the solid thermal conductivity. The value of  $h_C$  in Eq. (33.8-4) is assumed to be the same as in Eq. (33.8-2).

The equation for the rate of mass transfer is similar to Eq. (33.6-5) and is

$$N_A = k_y M_B M_A (H_S - H) \quad (33.8-6)$$

Also, rewriting Eq. (33.6-6),

$$q = M_A N_A \lambda_S A \quad (33.8-7)$$

Combining Eqs. (33.8-1), (33.8-2), (33.8-3), (33.8-4), (33.8-6), and

(33.8-7),

$$RC=qA\lambda S=(hC+UK)(T-TS)+hR(TR-TS)\lambda S=k_yMB(HS-H)$$

(33.8-8)

This equation can be compared to Eq. (33.6-7), which gives the wet bulb temperature  $T_W$  when radiation and conduction are absent. Equation (33.8-8) gives surface temperature  $T_S$  greater than the wet bulb temperature  $T_W$ . Equation (33.8-8) must also intersect the saturated humidity line at  $T_S$  and  $H_S$ , and  $T_S > T_W$  and  $H_S > H_W$ . The equation must be solved by trial and error.

To facilitate solution of Eq. (33.8-8), it can be rearranged (T1) in the following way:

$$(HS-H)\lambda ShC/k_yMB=(1+UKhC)(T-$$

$$TS) + h_{Rh}C(TR - TS)(33.8-9)$$

The ratio  $hc/k_y M_B$  was shown in the wet bulb derivation of Eq. (33.3-18) to be approximately  $cs$  in Eq. (33.3-6):

$$cS = (1.005 + 1.88H)103 \text{ J/kg} \cdot \text{K} \quad (33.3-6)$$

**EXAMPLE 33.8-1. Constant-Rate Drying When Radiation, Conduction, and Convection Are Present**

An insoluble granular material wet with water is being dried in a pan  $0.457 \times 0.457$  m and 25.4 mm deep. The material is 25.4 mm deep in the metal pan, which has a metal bottom of thickness  $z_M = 0.610$  mm having a thermal conductivity  $k_M = 43.3 \text{ W/m} \cdot \text{K}$ . The thermal conductivity of the solid can be assumed as  $k_S = 0.865 \text{ W/m} \cdot \text{K}$ . Heat transfer is by convection from an air stream flowing parallel to the top drying surface and the bottom metal surface at a velocity of 6.1 m/s and having a temperature of 65.6°C and humidity  $H = 0.010 \text{ kg H}_2\text{O/kg dry air}$ . The top surface also receives direct radiation from steam-heated pipes whose surface temperature  $T_R = 93.3^\circ\text{C}$ . The emissivity of the solid is  $\epsilon = 0.92$ . Estimate the rate of drying for the constant-rate period.

**Solution:** Some of the given values are as follows:

$$T = 65.6^\circ\text{C} \quad cS = 0.0254 \text{ kJ/kg} \cdot \text{K} \quad k_M = 43.3 \text{ W/m} \cdot \text{K} \quad k_S = 0.865 \text{ W/m} \cdot \text{K} \quad z_M = 0.00061 \text{ m} \quad \epsilon = 0.92 \quad H = 0.010$$

The velocity, temperature, and humidity of the air are the same as in Example 33.6-3 and the convective coefficient was predicted as  $hc = 62.45 \text{ W/m}^2 \cdot \text{K}$ .

The solution of Eq. (33.8-9) is by trial and error. The temperature  $T_S$  will be above the wet bulb temperature of  $T_W = 28.9^\circ\text{C}$  and will be estimated as  $T_S = 32.2^\circ\text{C}$ . Then,  $\lambda_S = 2424 \text{ kJ/kg}$  from the steam tables. To predict  $h_R$  from

Eq. (12.6-10) for  $\varepsilon = 0.92$ ,  $T_1 = 93.3 + 273.2 = 366.5 \text{ K}$ , and  $T_2 = 32.2 + 273.2 = 305.4 \text{ K}$ ,

$$hR = (0.92)(5.676) \\ (366.5/100)^4 - (305.4/100)^4 = 7.96 \text{ W/m}^2\cdot\text{K}$$

Using Eq. (33.8-5),

$$UK = 11/hC + zM/kM + zS/ \\ kS = 11/62.45 + 0.00061/43.3 + 0.0254/0.865 = 22.04 \text{ W/m}^2\cdot\text{K}$$

From Eq. (33.3-6),

$$cS = (1.005 + 1.88H)103 = (1.005 + 1.88 \times 0.010)103 = 1.024 \times 103 \text{ J/kg}\cdot\text{K}$$

This can be substituted for  $(hc/k_y MB)$  into Eq. (33.8-9).

Also, substituting other knowns,

$$(HS - 0.01)\lambda S 1.024 \times 103 = (1 + 22.04/62.45)(65.6 - TS) + (7.96/62.45)(93.3 - TS) \\ TS = 1.353(65.6 - TS) + 0.1275(93.3 - TS) \quad (33.8-10)$$

For  $TS$  assumed as  $32.2^\circ\text{C}$ ,  $\lambda S = 2424 \times 103 \text{ J/kg}$ . From the humidity chart for  $TS = 32.2^\circ\text{C}$ , the saturation humidity  $HS = 0.031$ . Substituting into Eq. (33.8-10) and solving for  $TS$ ,

$$(0.031 - 0.010)(2424 \times 103)1.024 \times 103 = 1.353(65.6 - TS) + 0.1275(93.3 - TS) \\ TS = 34.4^\circ\text{C}$$

For the second trial, assuming that  $TS = 32.5^\circ\text{C}$ ,  $\lambda S = 2423 \times 103$ , and  $HS$  from the humidity chart at saturation is 0.032. Substituting into Eq. (33.8-10) while assuming that  $hR$  does not change appreciably, a value of  $TS = 32.8^\circ\text{C}$  is obtained. Hence, the final value is  $32.8^\circ\text{C}$ . This is  $3.9^\circ\text{C}$  greater than the wet bulb temperature of  $28.9^\circ\text{C}$  in Example 33.6-3, where radiation and conduction were absent.

Using Eq. (33.8-8),

$$RC = (hC + UK)(T - TS) + hR(TR - TS)\lambda S(3600) = (62.45 + 22.04) \\ (65.6 - 32.8) + 7.96(93.3 - 32.8)2423 \times 103(3600) = 4.83 \text{ kg/h}\cdot\text{m}^2$$

This compares favorably with  $3.39 \text{ kg/h} \cdot \text{m}^2$  for Example 33.6-3 for no radiation or conduction.

## 33.9 Drying in the Falling-Rate Period by Diffusion and Capillary Flow

### 33.9A Introduction

In the falling-rate period, the surface of the solid being dried is no longer completely wetted and the rate of drying steadily falls with time. In Section 33.7, empirical methods were used to predict the time of drying. In one method, the actual rate-of-drying curve was numerically or graphically integrated to determine the time of drying.

In another method, an approximately straight line from the critical free moisture content to the origin at zero free moisture was assumed. Here, the rate of drying was assumed to be a linear function of the free moisture content. The rate of drying  $R$  is defined

by Eq. (33.5-3):

$$R = -LSAdXdt \quad (33.5-3)$$

When  $R$  is a linear function of  $X$  in the falling-rate period,

$$R = aX \quad (33.7-5)$$

where  $a$  is a constant. Equating Eq. (33.7-5) to Eq. (33.5-3),

$$R = -LSAdXdt = aX \quad (33.9-1)$$

Rearranging,

$$dXdt = -aALSX \quad (33.9-2)$$

However, as mentioned briefly in Section 33.5E, in many instances the rate of moisture movement in the falling-rate period is governed by the

rate of internal movement of the liquid by liquid diffusion or by capillary movement. These two mechanisms of moisture movement and the theories related to experimental data in the falling-rate region will now be considered in more detail.

### **33.9B Liquid Diffusion of Moisture in Drying**

When liquid diffusion of moisture controls the rate of drying in the falling-rate period, the equations for diffusion described in Chapter 20 can be used. Using the concentrations as  $X$  kg free moisture/kg dry solid instead of kg mol moisture/m<sup>3</sup>, Fick's second law for unsteady-state diffusion, Eq. (20.1-10), can be written as

$$\frac{\partial X}{\partial t} = D_L \frac{\partial^2 X}{\partial x^2} \quad (33.9-3)$$

where  $D_L$  is the liquid diffusion coefficient in  $\text{m}^2/\text{h}$  and  $x$  is distance in the solid in  $\text{m}$ .

This type of diffusion is often characteristic of relatively slow drying in nongranular materials such as soap, gelatin, and glue, and in the later stages of drying of bound water in clay, wood, textiles, leather, paper, foods, starches, and other hydrophilic solids.

A major difficulty in analyzing diffusion drying data is that, at the start, the initial moisture distribution is not uniform throughout the solid if a drying period at constant rate precedes this falling-rate period. During diffusion-type drying, the resistance to mass transfer of water vapor from the surface is usually very small, and the diffusion in the solid



controls the rate of drying. Then, the moisture content at the surface is at the equilibrium value  $X^*$ . This means that the free moisture content  $X$  at the surface is essentially zero.

Assuming that the initial moisture distribution is uniform at  $t = 0$ , Eq. (33.9-3) may be integrated by the methods in Chapter 20 to give the following:

$$\frac{X_t - X^*}{X_1 - X^*} = \frac{X}{X_1} = 8\pi^2 \left[ e^{-\frac{1}{12} \frac{D t}{L^2}} + \frac{1}{9} e^{-9 \frac{D t}{L^2}} \left( \frac{\pi}{2} \frac{x_1}{L} \right)^2 + \frac{1}{25} e^{-25 \frac{D t}{L^2}} \left( \frac{\pi}{2} \frac{x_1}{L} \right)^2 + \dots \right] \quad (33.9-4)$$

where  $X$  = average free moisture content at time  $t$  h,  $X_1$  = initial free moisture content at  $t = 0$ ,  $X^*$  = equilibrium free moisture content,  $x_1 = 12$  the thickness of the slab when drying occurs from the

top and bottom parallel faces, and  $x_1 =$  total thickness of the slab if drying occurs only from the top face.

Equation (33.9-4) assumes that  $DL$  is constant, but  $DL$  is rarely constant; it varies with moisture content, temperature, and humidity. For long drying times, only the first term in Eq. (33.9-4) is significant, and the equation becomes

$$\frac{X - X_1}{X - X_C} = 8\pi^2 e^{-DLt(\pi/2x_1)^2} \quad (33.9-5)$$

Solving for the time of drying,

$$t = \frac{4x_1^2}{\pi^2 DL} \ln \frac{8(X - X_C)}{\pi(X - X_1)} \quad (33.9-6)$$

In this equation, if the diffusion mechanism starts at  $X = X_C$ , then  $X_1 = X_C$ . Differentiating Eq. (33.9-6) with respect to time and rearranging,

$$dX/dt = -\pi^2 D L X^4 / 12 (33.9-7)$$

Multiplying both sides by  $-Ls/A$ ,

$$R = -L S A dX/dt = \pi^2 L S D L^4 / 12 A X^4 \quad (33.9-8)$$

Hence, Eqs. (33.9-7) and (33.9-8) state that when internal diffusion controls for long periods of time, the rate of drying is directly proportional to the free moisture  $X$  and the liquid diffusivity, and that the rate of drying is inversely proportional to the thickness squared.

Or, stated as the time of drying between fixed moisture limits, the time varies directly as the square of the thickness. The drying rate should be independent of gas velocity and humidity.

**EXAMPLE 33.9-1. Drying Slabs of Wood When Diffusion of Moisture Controls**

The experimental average diffusion coefficient of moisture in a given wood is  $2.97 \times 10^{-6} \text{ m}^2/\text{h}$  ( $3.20 \times 10^{-5} \text{ ft}^2/\text{h}$ ). Large planks of wood 25.4 mm thick are dried from both sides by air having a humidity such that the equilibrium moisture content in the wood is  $X^* = 0.04 \text{ kg H}_2\text{O}/\text{kg dry wood}$ . The wood is to be dried from a total average moisture content of  $X_{t1} = 0.29$  to  $X_t = 0.09$ . Calculate the drying time required.

**Solution:** The free moisture content  $X_1 = X_{t1} - X^* = 0.29 - 0.04 = 0.25$ ,  $X = X_t - X^* = 0.09 - 0.04 = 0.05$ . The half-slab thickness  $x_1 = 25.4/(2 \times 1000) = 0.0127 \text{ m}$ . Substituting into Eq. (33.9-6),

$$t = 4 \times 12 \pi^2 D L \ln 8 X_1 \pi^2 X = 4(0.0127)^2 \pi^2 (2.97 \times 10^{-6}) \ln 8 \times 0.25 \pi^2 \times 0.05 = 30.8 \text{ h}$$

Alternatively, Fig. 14.3-13 for the average concentration in a slab can be used. The ordinate  $E_a = X/X_1 = 0.05/0.25 = 0.20$ . Reading off the plot a value of  $0.56 = DLt/x_1^2$ , substituting, and solving for  $t$ ,

$$t = x_1^2 (0.56) DL = (0.0127)^2 (0.56) 2.97 \times 10^{-6} = 30.4 \text{ h}$$

### 33.9C Capillary Movement of Moisture in Drying

If the pore sizes of the granular materials are suitable, water can flow from regions of high concentration to those of low concentration as a result of capillary action rather than by diffusion.

The capillary theory (P1) assumes that a packed bed of nonporous spheres

contains void spaces between the spheres called *pores*. As water is evaporated, capillary forces are set up by the interfacial tension between the water and the solid. These forces provide the driving force for moving the water through the pores to the drying surface.

A modified form of Poiseuille's equation for laminar flow can be used in conjunction with the capillary-force equation to derive an equation for the rate of drying when flow is by capillary movement. If the moisture movement follows the capillary-flow equations, the rate of drying  $R$  will vary linearly with  $X$ . Since the mechanism of evaporation during this period is the same as during the constant-rate period, the effects of the variables gas velocity, temperature

of the gas, humidity of the gas, and so on, will be the same as for the constant-rate drying period.

The defining equation for the rate of drying is

$$R = -LS \frac{dX}{dt} \quad (33.5-3)$$

For the rate  $R$  varying linearly with  $X$ , given previously,

$$R = R_C \frac{X - X_2}{X_1 - X_2} \quad (33.7-9)$$

$$t = \frac{LS}{R_C} \ln \frac{X_1 - X_2}{X - X_2} \quad (33.7-8)$$

We define  $t$  as the time when  $X = X_2$  and

$$LS = \frac{X_1 - X_2}{\rho_s} \quad (33.9-9)$$

where  $\rho_s$  = solid density kg dry solid/  
m<sup>3</sup>. Substituting Eq. (33.9-9) and  $X = X_2$

into Eq. (33.7-8),

$$t = \frac{x}{D} \frac{\rho S}{C_R C} \ln \frac{X_C}{X} \quad (33.9-10)$$

Substituting Eq. (33.6-7) for  $R_C$ ,

$$t = \frac{x}{D} \frac{\rho S \lambda W}{C h (T - T_W)} \ln \frac{X_C}{X} \quad (33.9-11)$$

Hence, Eqs. (33.9-10) and (33.9-11) state that when capillary flow controls in the falling-rate period, the rate of drying is inversely proportional to the thickness. The time of drying between fixed moisture limits varies directly as the thickness and depends upon the gas velocity, temperature, and humidity.

### **33.9D Comparison of Liquid Diffusion and Capillary Flow**

To determine the mechanism of drying in the falling-rate period, the

experimental data obtained for moisture content at various times using constant-drying conditions are often analyzed as follows: The *unaccomplished moisture change*, defined as the ratio of free moisture present in the solid after drying for  $t$  hours to the total free moisture content present at the start of the falling-rate period,  $X/X_C$ , is plotted versus time on semilog paper. If a straight line is obtained, such as curve B in Fig. 33.9-1 using the upper scale for the abscissa, then either Eqs. (33.9-4)–(33.9-6) for diffusion or Eqs. (33.9-10) and (33.9-11) for capillary flow are applicable.

If the equations for capillary flow apply, the slope of the falling-rate drying line



B in Fig. 33.9-1 is related to Eq. (33.9-10), which contains the constant drying rate  $RC$ . The value of  $RC$  is calculated from the measured slope of the line, which is  $-RC/x_1\rho_sX_C$ , and if it agrees with the experimental value of  $RC$  in the constant-drying period or the predicted value of  $RC$ , the moisture movement is by capillary flow.

If the values of  $RC$  do not agree, the moisture movement is by diffusion and the slope of line B in Fig. 33.9-1 from Eq. (33.9-6) should equal  $-\pi^2DL/4x_1^2$ . In actual practice, however, the diffusivity  $DL$  is usually less at small moisture contents than at large moisture contents, and an average value of  $DL$  is usually determined experimentally over the moisture range of interest. A plot of Eq. (33.9-4) is shown as line A, where

$\ln(X/X_1)$  or  $\ln(X/X_C)$  is plotted versus  $DLt/x^2$ . This is the same plot as Fig. 14.3-13 for a slab and shows a curvature in the line for values of  $X/X_C$  between 1.0 and 0.6, and a straight line for  $X/X_C < 0.6$ .

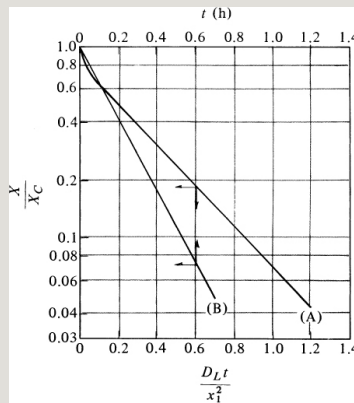


Figure 33.9-1. *Plot of equations for falling-rate period: (A) Eq. (33.9-4) for moisture movement by diffusion, (B) Eq. (33.9-10) for moisture movement by capillary flow. From R. H. Perry and C. H. Chilton, Chemical Engineers Handbook, 5th ed. New York: McGraw-Hill Book Company, 1973. With permission.*

When the experimental data show that the movement of moisture follows the diffusion law, the average experimental diffusivities can be calculated as follows

for different concentration ranges. A value of  $X/X_C$  is chosen at 0.4, for example. From an experimental plot similar to curve B, Fig. 33.9-1, the experimental value of  $t$  is obtained. From curve A at  $X/X_C = 0.4$ , the theoretical value of  $(DLt/x^2)_{\text{theor}}$  is obtained. Then, by substituting the known values of  $t$  and  $x_1$  into Eq. (33.9-12), the experimental average value of  $DL$  over the range  $X/X_C = 1.0 - 0.4$  is obtained:

$$DL = (DLt/x^2)_{\text{theor}} x_1^2 / t \quad (33.9-12)$$

This is repeated for various values of  $X/X_C$ . Values of  $DL$  obtained for  $X/X_C > 0.6$  are in error because of the curvature of line A.

Tapioca flour is obtained from drying and then milling the tapioca root. Experimental data on drying thin slices of the tapioca root 3 mm thick on both sides in the falling-rate period under constant-drying conditions are tabulated below. The time  $t = 0$  is the start of the falling-rate period.

--

It has been determined that the data do not follow the capillary-flow equations but appear to follow the diffusion equations. Plot the data as  $X/X_c$  versus  $t$  on semilog coordinates and determine the average diffusivity of the moisture up to a value of  $X/X_c = 0.20$ .

**Solution:** In Fig. 33.9-2, the data are plotted as  $X/X_c$  on the log scale versus  $t$  on a linear scale and a smooth curve is drawn through the data. At  $X/X_c = 0.20$ , a value of  $t = 1.02$  h is read off the plot. The value of  $x_1 = 3 \text{ mm}/2 = 1.5 \text{ mm}$  for drying from both sides. From Fig. 33.9-1, line A, for  $X/X_c = 0.20$ ,  $(DLt/x_1^2)_{\text{theor}} = 0.56$ . Then, substituting into Eq. (33.9-12),

$$DL = \frac{(DLt)_{\text{theor}} x_1^2}{t} = \frac{0.56 (1.5/1000)^2}{1.02 \times 3600} = 3.44 \times 10^{-10} \text{ m}^2/\text{s}$$

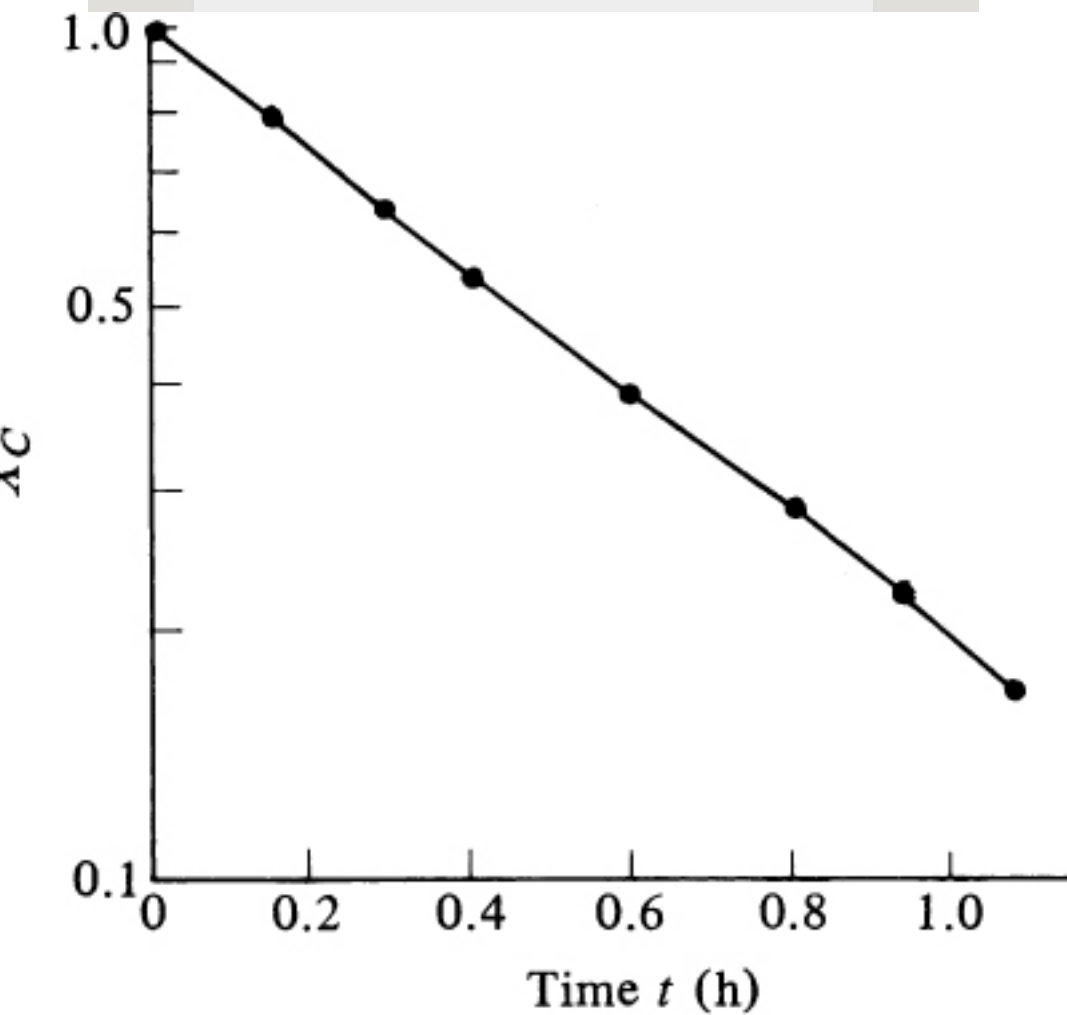


Figure 33.9-2. Plot of drying data for Example 33.9-2.

## 33.10 Equations for Various Types of Dryers

### 33.10A Through-Circulation Drying in Packed Beds

For through-circulation drying,

where the drying gas passes upward or downward through a bed of wet granular solids, both a constant-rate period and a falling-rate period of drying may result. Often, the granular solids are arranged on a screen so that the gas passes through the screen and through the open spaces or voids between the solid particles.

*1. Derivation of equations.* To derive the equations for this case, no heat losses will be assumed, so the system is adiabatic. The drying will be for unbound moisture in the wet granular solids. We shall consider a bed of uniform cross-sectional area  $A \text{ m}^2$ , where a gas flow of  $G \text{ kg dry gas/h} \cdot \text{m}^2$  cross section enters with a humidity of  $H_1$ . By performing a material balance on

the gas at a given time, the gas leaves the bed with a humidity  $H_2$ . The amount of water removed from the bed by the gas is equal to the rate of drying at this time:

$$R = G(H_2 - H_1) \quad (33.10-1)$$

where  $R = \text{kg H}_2\text{O/h} \cdot \text{m}^2$  cross section and  $G = \text{kg dry air/h} \cdot \text{m}^2$  cross section.

In Fig. 33.10-1, the gas enters at  $T_1$  and  $H_1$ , and leaves at  $T_2$  and  $H_2$ . Hence, the temperature  $T$  and humidity  $H$  both vary through the bed. Making a heat balance over the short section  $dz$  m of the bed,

$$dq = -Gc_s A dT \quad (33.10-2)$$

where  $A = \text{m}^2$  cross-sectional area,  $q$  is the heat-transfer rate in W (J/s), and  $c_s$  is the humid heat of the air–water vapor

mixture in Eq. (33.3-6). Note that  $G$  in this equation is in  $\text{kg/s} \cdot \text{m}^2$ . The heat transfer equation gives

$$dq = ha A dz(T - T_W) \quad (33.10-3)$$

where  $T_W$  = wet bulb temperature of the solid,  $h$  is the heat-transfer coefficient in  $\text{W/m}^2 \cdot \text{K}$ , and  $a$  is  $\text{m}^2$  surface area of solids/ $\text{m}^3$  bed volume. Equating Eq. (33.10-2) to Eq. (33.10-3), rearranging, and integrating,

$$haGcS \int_0^z dz = - \int_{T_1}^{T_2} \frac{dT}{T - T_W} \quad (33.10-4)$$

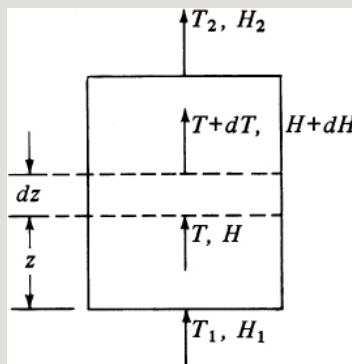




Figure 33.10-1. *Heat and material balances in a through-circulation dryer in a packed bed.*

$$hazGcS = \ln T_1 - TWT_2 - TW \quad (33.10-5)$$

where  $z$  = bed thickness =  $x_1$  m.

For the constant-rate period of drying by air flowing parallel to a surface, Eq. (33.6-11) was derived:

$$t = \frac{LS}{W} (X_1 - X_2) A_h (T - T_W) = \frac{LS}{W} (X_1 - X_2) A_k y_M B (H_W - H) \quad (33.6-11)$$

Using Eq. (33.9-9) and the definition of  $a$ , we obtain

$$LSA = \rho S a \quad (33.10-6)$$

Substituting Eq. (33.10-6) into Eq. (33.6-11) and setting  $X_2 = X_C$  for drying to  $X_C$ , we obtain the equation for through-circulation drying in the

constant-rate period:

$$t = \rho S l W (X_1 - X_C) a_h (T - T_W) = \rho S (X_1 - X_C) a_{ky} M_B (H_W - H) \quad (33.10-7)$$

In a similar manner, Eq. (33.7-8) for the falling-rate period, which assumes that  $R$  is proportional to  $X$ , becomes, for through-circulation drying,

$$t = \rho S l W X_C \ln(X_C/X) a_h (T - T_W) = \rho S X_C \ln(X_C/X) a_{ky} M_B (H_W - H) \quad (33.10-8)$$

Both Eqs. (33.10-7) and (33.10-8), however, hold for only one point in the bed in Fig. 33.10-1, since the temperature  $T$  of the gas varies throughout the bed. Hence, in a manner similar to the derivation in heat transfer, a log mean temperature difference can be used as an approximation for the

whole bed in place of  $T - T_w$  in Eqs. (33.10-7) and (33.10-8):

$$(T - T_w)_{LM} = (T_1 - T_w) - (T_2 - T_w) \ln \left| \frac{(T_1 - T_w)}{(T_2 - T_w)} \right| = T_1 - T_2 \ln \left| \frac{(T_1 - T_w)}{(T_2 - T_w)} \right| \quad (33.10-9)$$

Substituting Eq. (33.10-5) for the denominator of Eq. (33.10-9) and substituting the value of  $T_2$  from Eq. (33.10-5) into (33.10-9),

$$(T - T_w)_{LM} = (T_1 - T_w) (1 - e^{-haz/G_c S}) / G_c S \quad (33.10-10)$$

Substituting Eq. (33.10-10) into (33.10-7) for the constant-rate period and setting  $x_1 = z$ ,

$$t = \rho S \lambda W x_1 (X_1 - X_C) G_c S (T_1 - T_w) (1 - e^{-hax_1/G_c S}) \quad (33.10-11)$$

Similarly, for the falling-rate period, an approximate equation is obtained:

$$t = \frac{\rho_s \lambda W_x}{G_c S} \ln \left( \frac{X - X_c}{X - X^*} \right) \quad (33.10-12)$$

A major difficulty with the use of Eq. (33.10-12) is that the critical moisture content is not easily estimated. Different forms of Eqs. (33.10-11) and (33.10-12) can also be derived, using humidity instead of temperature ( $T_1$ ).

*2. Heat-transfer coefficients.* For through-circulation drying, where the gases pass through a bed of wet granular solids, the following equations for estimating  $h$  for adiabatic evaporation of water can be used (W1):

$$h = 0.59 D_p^{0.41} (T_g - T_w)^{0.75} \quad (33.10-13)$$

where  $h$  is in  $W/m^2 \cdot K$ ,  $D_p$  is the diameter in m of a sphere having the same surface area as the particle in the bed,  $G_t$  is the total mass velocity entering the bed in  $kg/h \cdot m^2$ , and  $\mu$  is the viscosity in  $kg/m \cdot h$ . In English units,  $h$  is  $btu/h \cdot ft^2 \cdot ^\circ F$ ,  $D_p$  is ft,  $G_t$  is  $lb_m/h \cdot ft^2$ , and  $\mu$  is  $lb_m/ft \cdot h$ .

3. *Geometry factors in a bed.* To determine the value of  $a$ ,  $m^2$  surface area/ $m^3$  of bed, in a packed bed for spherical particles having a diameter  $D_p$  m,

$$a=6(1-\epsilon)D_p(33.10-15)$$

where  $\epsilon$  is the void fraction in the bed. For cylindrical particles,

$$a=4(1-\epsilon)(h+0.5D_c)D_{ch}(33.10-16)$$

where  $D_c$  is diameter of cylinder in m and  $h$  is length of cylinder in m. The value of  $D_p$  to use for a cylinder in Eqs. (33.10-13) and (33.10-14) is the diameter of a sphere having the same surface area as the cylinder, as follows:

$$D_p=(D_{ch}+0.5D_c^2)^{1/2}(33.10-17)$$

*4. Equations for very fine particles.* The equations derived for the constant- and falling-rate periods in packed beds hold for particles of about 3–19 mm in diameter in shallow beds about 10–65 mm thick (T1). For very fine particles of 10–200 mesh (1.66–0.079 mm) and bed depth greater than 11 mm, the interfacial area  $a$  varies with the moisture content. Empirical expressions are available for

# estimating $a$ and the mass-transfer coefficient ( $T_1$ , $A_1$ ).

## **EXAMPLE 33.10-1. Through-Circulation Drying in a Bed**

A granular paste material is extruded into cylinders with a diameter of 6.35 mm and a length of 25.4 mm. The initial total moisture content  $X_{t1} = 1.0$  kg H<sub>2</sub>O/kg dry solid and the equilibrium moisture is  $X^* = 0.01$ . The density of the dry solid is 1602 kg/m<sup>3</sup> (100 lbm/ft<sup>3</sup>). The cylinders are packed on a screen to a depth of  $x_1 = 50.8$  mm. The bulk density of the dry solid in the bed is  $\rho_s = 641$  kg/m<sup>3</sup>. The inlet air has a humidity  $H_1 = 0.04$  kg H<sub>2</sub>O/kg dry air and a temperature  $T_1 = 121.1^\circ\text{C}$ . The gas superficial velocity is 0.811 m/s and the gas passes through the bed. The total critical moisture content is  $X_{tc} = 0.50$ . Calculate the total time necessary to dry the solids to  $X_t = 0.10$  kg H<sub>2</sub>O/kg dry solid.

**Solution:** For the solid,

$$\begin{aligned} X_1 &= X_{t1} - X^* = 1.00 - 0.01 = 0.99 \text{ kg H}_2\text{O/kg dry solid} \\ X_c &= X_{tc} - X^* = 0.50 - 0.01 = 0.49 \\ X &= X_t - X^* = 0.10 - 0.01 = 0.09 \end{aligned}$$

For the gas,  $T_1 = 121.1^\circ\text{C}$  and  $H_1 = 0.04$  kg H<sub>2</sub>O/kg dry air. The wet bulb temperature  $T_w = 47.2^\circ\text{C}$  and  $H_w = 0.074$ . The solid temperature is at  $T_w$  if radiation and conduction are neglected. The density of the entering air at  $121.1^\circ\text{C}$  and 1 atm is as follows:

$$\begin{aligned} \rho_H &= (2.83 \times 10^{-3} + 4.56 \times 10^{-3} \times 0.04) \\ &\quad (273 + 121.1) = 1.187 \text{ m}^3 / \\ \text{kg dry air} & (33.3 - 7) \rho = 1.00 + 0.04(1.187) = 0.876 \text{ kg dry} \\ &\quad \text{air} + \text{H}_2\text{O} / \text{m}^3 \end{aligned}$$

The mass velocity of the dry air is

$$G = v_p(1.01 + 0.04) = 0.811(3600)(0.876)(11.04) = 2459 \text{ kg dry air/h} \cdot \text{m}^2$$

Since the inlet  $H_1 = 0.040$  and the outlet will be less than 0.074, an approximate average  $H$  of 0.05 will be used to calculate the total average mass velocity. The approximate average  $G_t$  is

$$G_t = 2459 + 2459(0.05) = 2582 \text{ kg air} + \text{H}_2\text{O/h} \cdot \text{m}^2$$

For the packed bed, the void fraction  $\varepsilon$  is calculated as follows for 1 m<sup>3</sup> of bed containing solids plus voids. A total of 641 kg dry solid is present. The density of the dry solid is 1602 kg dry solid/m<sup>3</sup> solid. The volume of the solids in 1 m<sup>3</sup> of bed is then 641/1602, or 0.40 m<sup>3</sup> solid. Hence,  $\varepsilon = 1 - 0.40 = 0.60$ . The solid cylinder length  $h = 0.0254$  m. The diameter  $D_c = 0.00635$  m. Substituting into Eq. (33.10-16),

$$a = 4(1 - \varepsilon)(h + 0.5D_c)D_c h = 4(1.06) [0.0254 + 0.5(0.00635)](0.00635)(0.0254) = 283.5 \text{ m}^2 \text{ surface area/} \\ \text{m}^3 \text{ bed volume}$$

To calculate the diameter  $D_p$  of a sphere with the same area as the cylinder using Eq. (33.10-17),

$$D_p = (D_c h + 0.5D_c^2)^{1/2} = [0.00635 \times 0.0254 + 0.5(0.00635)^2]^{1/2} = 0.0135 \text{ m}$$

The bed thickness  $x_1 = 50.8 \text{ mm} = 0.0508 \text{ m}$ .

To calculate the heat-transfer coefficient, the Reynolds number is first calculated. Assuming an approximate average air temperature of 93.3°C, the viscosity of air is  $\mu = 2.15 \times 10^{-5} \text{ kg/m} \cdot \text{s} = 2.15 \times 10^{-5} (3600) = 7.74 \times 10^{-2} \text{ kg/m} \cdot \text{h}$ . The Reynolds number is

$$\text{NRe} = D_p G_t \mu = 0.0135(2582)7.74 \times 10^{-2} = 450$$

Using Eq. (33.10-13),

$$h = 0.151 G_t^{0.59} D_p^{0.41} = 0.151(2582)^{0.59} (0.0135)^{0.41} = 90.9 \text{ W/m}^2 \cdot \text{K}$$

For  $T_w = 47.2^\circ\text{C}$ ,  $\lambda_w = 2389 \text{ kJ/kg}$ , or  $2.389 \times 10^6 \text{ J/kg}$  (1027 btu/lb<sub>m</sub>), from the steam tables in Appendix A.2. The average humid heat, from Eq. (33.3-6), is

$$c_s = 1.005 + 1.88H = 1.005 + 1.88(0.05) = 1.099 \text{ kJ/kg dry air} \cdot \text{K} = 1.099 \times 10^3 \text{ J/kg} \cdot \text{K}$$

To calculate the time of drying for the constant-rate period using Eq. (33.10-11) and  $G = 2459/3600 = 0.6831 \text{ kg/s} \cdot \text{m}^2$ ,

$$t = \rho_s \lambda_w x_1 (X_1 - X_C) G_c S (T_1 - T_w) (1 - e^{-h a x_1 / G_c S}) = 641(2.389 \times 10^6)(0.0508)(0.99 - 0.49)(0.683)$$



$$\frac{(1.099 \times 10^3)(121.1 - 47.2)[1 - e^{-(90.9 \times 283.5 \times 0.0508)}]}{(0.683 \times 1.099 \times 10^3)} = 850 \text{ s} = 0.236 \text{ h}$$

For the time of drying for the falling-rate period, using Eq. (33.10-12),

$$t = \frac{\rho_s \lambda W x_1 X C \ln(XC/X) G_c S (T_1 - T_W) (1 - e^{-h a x_1 / G_c s})}{G_c s} = 641 (2.389 \times 10^6) (0.0508) (0.49) \ln(0.49/0.09) (0.6831) (1.099 \times 10^3) (121.1 - 47.2) [1 - e^{-(90.9 \times 283.5 \times 0.0508)}] / (0.683 \times 1.099 \times 10^3) = 1412 \text{ s} = 0.392 \text{ h}$$

total time  $t = 0.236 + 0.392 = 0.628 \text{ h}$

### 33.10B Tray Drying with Varying Air Conditions

For drying in a compartment or tray dryer where the air passes in parallel flow over the surface of the tray, the air conditions do not remain constant. Heat and material balances similar to those for through circulation must be made to determine the exit-gas temperature and humidity.

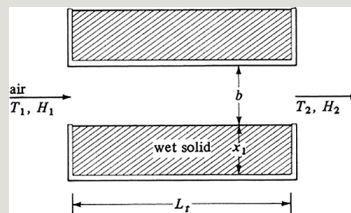


Figure 33.10-2. Heat and material balances in a tray dryer.

In Fig. 33.10-2, air is shown passing over a tray. It enters having a temperature of  $T_1$  and humidity  $H_1$  and leaves at  $T_2$  and  $H_2$ . The spacing between the trays is  $b$  m and dry air flow is  $G$  kg dry air/s  $\cdot$  m<sup>2</sup> cross-sectional area. Writing a heat balance over a length  $dL_t$  of tray for a section 1 m wide,

$$dq = GcS(1 \times b)dT \quad (33.10-18)$$

The heat-transfer equation is

$$dq = h(1 \times dL_t)(T - T_W) \quad (33.10-19)$$

Rearranging and integrating,

$$hL_t GcSb = \ln \frac{T_1 - T_W}{T_2 - T_W} \quad (33.10-20)$$

Defining a log mean temperature difference similar to Eq. (33.10-10) and

substituting into Eqs. (33.6-11) and (33.7-8), we obtain the following. For the constant-rate period,

$$t = \frac{1}{h} \left( \frac{L_s}{G_c} \right) \ln \left( \frac{X_1 - X_C}{X_1 - X} \right) \quad (33.10-21)$$

For the falling-rate period, an approximate equation is obtained:

$$t = \frac{1}{h} \left( \frac{L_s}{G_c} \right) \ln \left( \frac{X_C - X}{X_C - X_1} \right) \quad (33.10-22)$$

### 33.10C Material and Heat Balances for Continuous Dryers

*1. Simple heat and material balances.* In Fig. 33.10-3, a flow diagram is given for a continuous-type dryer where the drying gas flows countercurrently to the solids flow. The solid enters at a rate of  $L_s$  kg dry solid/h, having a free

moisture content  $X_1$  and a temperature  $T_{S1}$ . It leaves at  $X_2$  and  $T_{S2}$ . The gas enters at a rate  $G$  kg dry air/h, having a humidity  $H_2$  kg  $H_2O$ /kg dry air and a temperature of  $T_{G2}$ . The gas leaves at  $T_{G1}$  and  $H_1$ .

For a material balance on the moisture,

$$GH_2 + LSX_1 = GH_1 + LSX_2 \quad (33.10-23)$$

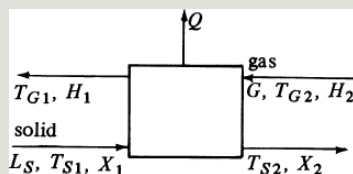


Figure 33.10-3. *Process flow for a countercurrent continuous dryer.*

For a heat balance, a datum of  $T_0^\circ\text{C}$  is selected. A convenient temperature is  $0^\circ\text{C}$  ( $32^\circ\text{F}$ ). The enthalpy of the wet solid is composed of the enthalpy of the dry solid plus that of the liquid as free

moisture. The heat of wetting is usually neglected. The enthalpy of the gas  $HG'$  in kJ/kg dry air is

$$HG' = c_S(T_G - T_0) + H\lambda_0 \quad (33.10-24)$$

where  $\lambda_0$  is the latent heat of water at  $T_0^\circ\text{C}$ , 2501 kJ/kg (1075.4 btu/lbm) at  $0^\circ\text{C}$ , and  $c_S$  is the humid heat, given as kJ/kg dry air  $\cdot$  K:

$$c_S = 1.005 + 1.88H \quad (33.3-6)$$

The enthalpy of the wet solid  $HS'$  in kJ/kg dry solid, where  $(T_S - T_0)^\circ\text{C} = (T_S - T_0) \text{ K}$ , is

$$HS' = c_{pS}(T_S - T_0) + Xc_{pA}(T_S - T_0) \quad (33.10-25)$$

where  $c_{pS}$  is the heat capacity of the dry solid in kJ/kg dry solid  $\cdot$  K, and  $c_{pA}$  is

the heat capacity of liquid moisture in  $\text{kJ/kg H}_2\text{O} \cdot \text{K}$ . The heat of wetting or adsorption is neglected.

A heat balance on the dryer is

$$\text{GHG2}' + L_s \text{HS1}' = \text{GHG1}' + L_s \text{HS2}' + Q(33.10-26)$$

where  $Q$  is the heat loss in the dryer in  $\text{kJ/h}$ . For an adiabatic process  $Q = 0$ , and if heat is added,  $Q$  is negative.

**EXAMPLE 33.10-2. Heat Balance on a Dryer**

A continuous countercurrent dryer is being used to dry  $453.6 \text{ kg dry solid/h}$  containing  $0.04 \text{ kg total moisture/kg dry solid}$  to a value of  $0.002 \text{ kg total moisture/kg dry solid}$ . The granular solid enters at  $26.7^\circ\text{C}$  and is to be discharged at  $62.8^\circ\text{C}$ . The dry solid has a heat capacity of  $1.465 \text{ kJ/kg} \cdot \text{K}$  that is assumed constant. Heating air enters at  $93.3^\circ\text{C}$ , having a humidity of  $0.010 \text{ kg H}_2\text{O/kg dry air}$ , and is to leave at  $37.8^\circ\text{C}$ . Calculate the air flow rate and the outlet humidity, assuming no heat losses in the dryer.

**Solution:** The flow diagram is given in Fig. 33.10-3. For the solid,  $L_s = 453.6 \text{ kg/h dry solid}$ ,  $c_{pS} = 1.465 \text{ kJ/kg dry solid} \cdot \text{K}$ ,  $X_1 = 0.040 \text{ kg H}_2\text{O/kg dry solid}$ ,  $c_{pA} = 4.187 \text{ kJ/kg H}_2\text{O} \cdot \text{K}$ ,  $T_{S1} = 26.7^\circ\text{C}$ ,  $T_{S2} = 62.8^\circ\text{C}$ ,  $X_2 = 0.002$ . (Note:  $X$  values used are  $X_t$  values.) For the gas,  $T_{G2} = 93.3^\circ\text{C}$ ,  $H_2 = 0.010 \text{ kg H}_2\text{O/kg dry air}$ , and  $T_{G1} = 37.8^\circ\text{C}$ .

Making a material balance on the moisture using Eq. (33.10-23),

$$GH_2 + LSX_1 = GH_1 + LSX_2 \quad G(0.010) + 453.6(0.040) = GH_1 + 453.6(0.002) \quad (33.10-27)$$

For the heat balance, the enthalpy of the entering gas at 93.3°C, using 0°C as a datum, is, by Eq. (33.10-24),  $\Delta T^\circ\text{C} = \Delta T\text{K}$  and  $\lambda_0 = 2501 \text{ kJ/kg}$ , from Table A.2-9:

$$HG_2' = cS(TG_2 - T_0) + H_2\lambda_0 = [1.005 + 1.88(0.010)](93.3 - 0) + 0.010(2501) = 120.5 \text{ kJ/kg dry air}$$

For the exit gas,

$$HG_1' = cS(TG_1 - T_0) + H_1\lambda_0 = (1.005 + 1.88H_1)(37.8 - 0) + H_1(2501) = 37.99 + 2572H_1$$

For the entering solid, using Eq. (33.10-25),

$$HS_1' = cpS(TS_1 - T_0) + X_1cpA(TS_1 - T_0) = 1.465(26.7 - 0) + 0.040(4.187)(26.7 - 0) = 43.59 \text{ kJ/}$$

$$\text{kg dry solid} \quad HS_2' = cpS(TS_2 - T_0) + X_2cpA(TS_2 - T_0) = 1.465(62.8 - 0) + 0.002(4.187)(62.8 - 0) = 92.53 \text{ kJ/kg}$$

Substituting into Eq. (33.10-26) for the heat balance with  $Q = 0$  for no heat loss,

$$G(120.5) + 453.6(43.59) = G(37.99 + 2572H_1) + 453.6(92.53) + 0 \quad (33.10-28)$$

Solving Eqs. (33.10-27) and (33.10-28) simultaneously,

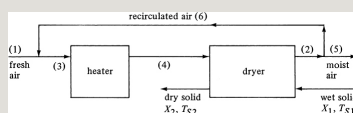
$$G = 1166 \text{ kg dry air/h} \quad H_1 = 0.0248 \text{ kg H}_2\text{O/kg dry air}$$

*2. Air recirculation in dryers.* In many dryers, it is desired to control the wet bulb temperature at which the drying of the solid occurs. Also, since steam costs are often important in heating the drying

air, recirculation of the drying air is sometimes used to reduce costs and control humidity. Part of the moist, hot air leaving the dryer is recirculated (recycled) and combined with the fresh air. This is shown in Fig. 33.10-4. Fresh air having a temperature  $T_{G1}$  and humidity  $H_1$  is mixed with recirculated air at  $T_{G2}$  and  $H_2$  to give air at  $T_{G3}$  and  $H_3$ . This mixture is heated to  $T_{G4}$  with  $H_4 = H_3$ . After drying, the air leaves at a lower temperature  $T_{G2}$  and a higher humidity  $H_2$ .

The following material balances on the water can be made. For a water balance on the heater, noting that  $H_6 = H_5 = H_2$ ,

$$G_1 H_1 + G_6 H_2 = (G_1 + G_6) H_4 \quad (33.10-29)$$





Making a water balance on the dryer,

$$(G_6)H_4 + L S X_1 = (G_1 + G_6)H_2 + L S C_2 \quad (33.10-30)$$

In a similar manner, heat balances can be made on the heater and dryer, and on the overall system.

### **33.10D Continuous Countercurrent Drying**

*1. Introduction and temperature profiles.* Drying continuously offers a number of advantages over batch drying. Smaller sizes of equipment can often be used, and the product has a more uniform moisture content. In a continuous dryer, the solid is moved through the dryer while it is in contact with a moving gas stream that may flow parallel or countercurrent to the solid. In

countercurrent adiabatic operation, the entering hot gas contacts the exiting solid, which has been dried. In parallel adiabatic operation, the entering hot gas contacts the entering wet solid.

In Fig. 33.10-5, typical temperature profiles of the gas  $T_G$  and the solid  $T_s$  are shown for a continuous countercurrent dryer. In the preheat zone, the solid is heated up to the wet bulb or adiabatic saturation temperature. Little evaporation occurs here and for low-temperature drying this zone is usually ignored. In the constant-rate zone, I, unbound and surface moisture are evaporated, and the temperature of the solid remains essentially constant at the adiabatic saturation temperature if heat is transferred by convection. The

rate of drying would be constant here but the gas temperature is changing, as well as the humidity. The moisture content falls to the critical value  $X_C$  at the end of this period.

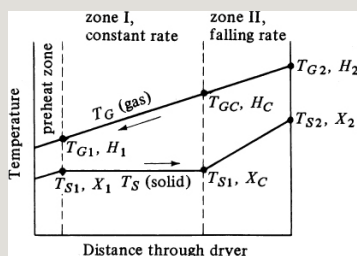


Figure 33.10-5. *Temperature profiles for a continuous countercurrent dryer.*

In zone II, unsaturated surface and bound moisture are evaporated and the solid is dried to its final value  $X_2$ . The humidity of the gas entering zone II is  $H_2$  and it rises to  $H_C$ . The material-balance equation (33.10-23) may be used to calculate  $H_C$  as follows:

$$LS(X_C - X_2) = G(H_C - H_2) \quad (33.10-31)$$

where  $Ls$  is kg dry solid/h and  $G$  is kg dry gas/h.

## 2. *Equation for the constant-rate period.*

The rate of drying in the constant-rate region in zone I would be constant if it were not for the varying gas conditions.

The rate of drying in this section is given by an equation similar to Eq. (33.6-7):

$$R = ky_M B(H_W - H) = h \lambda W(T_G - T_W) \quad (33.10-32)$$

The time for drying is given by Eq.

(33.6-1) using limits between  $X_1$  and  $X_C$ :

$$t = (A/Ls) \int_{X_C}^{X_1} dX / R \quad (33.10-33)$$

where  $A/Ls$  is the exposed drying surface m<sup>2</sup>/kg dry solid. Substituting Eq.

(33.10-32) into Eq. (33.10-33) and  $(G/Ls) dH$  for  $dX$ ,

$$t = \frac{GLS(LSA)}{1 \text{ kyMB}} \int_{H_C}^{H_W} \frac{dH}{H - H^*} \quad (33.10-34)$$

where  $G$  = kg dry air/h,  $Ls$  = kg dry solid/h, and  $A/Ls = m^2/\text{kg dry solid}$ . This can be integrated graphically or numerically.

For the case where  $T_W$  or  $H_W$  is constant for adiabatic drying, Eq. (33.10-34) can be integrated:

$$t = \frac{GLS(LSA)}{1 \text{ kyMB}} \ln \frac{H_W - H_C}{H - H^*} \quad (33.10-35)$$

The equation above can be modified by use of a log mean humidity difference:

$$\Delta H_{LM} = (H_W - H_C) - (H - H^*)$$

$$H1) \ln[(HW-HC)/(HW-H1)] = H1 - HC \ln[(HW-HC)/(HW-H1)] \quad (33.10-36)$$

Substituting Eq. (33.10-36) into Eq. (33.10-35), an alternative equation is obtained:

$$t = GLS(LSA) 1_{ky} MBH1 - HC \Delta HLM \quad (33.10-37)$$

From Eq. (33.10-31),  $H_C$  can be calculated as follows:

$$HC = H2 + LSG(XC - X2) \quad (33.10-38)$$

*3. Equation for falling-rate period.* For the situation where unsaturated surface drying occurs,  $HW$  is constant for adiabatic drying, the rate of drying is directly dependent upon  $X$  as in Eq. (33.7-9), and Eq. (33.10-32) applies:

$$R = RCXXC = k_y MB (HW - H) XXC \quad (33.10-39)$$

Substituting Eq. (33.10-39) into Eq. (33.6-1),

$$t = (LSA)XCk_yMB \int X^2XCdX(HW - H)X \quad (33.10-40)$$

Substituting  $G dH/Ls$  for  $dX$  and  $(H - H_2)G/Ls + X^2$  for  $X$ ,

$$t = GLS(LSA)XCk_yMB \int H^2HCdH(HW - H)[(H - H_2)G/Ls + X^2] \quad (33.10-41)$$

$$t = GLS(LSA)XCk_yMB \left[ \frac{1}{2}(HW - H_2)G/Ls + X^2 \ln XC(HW - H_2)X^2(HW - HC) \right] \quad (33.10-42)$$

Again, to calculate  $HC$ , Eq. (33.10-38) can be used.

These equations for the two periods can also be derived using the last part of Eq. (33.10-32) and temperatures instead of humidities.

## **33.11 Freeze-Drying of Biological Materials**

### **33.11A Introduction**

Certain food products, pharmaceuticals, and biological materials, which may not be heated even to moderate temperatures in ordinary drying, may be freeze-dried. The substance to be dried is usually frozen by exposure to very cold air. In freeze-drying, the water is removed as a vapor by sublimation from the frozen material in a vacuum chamber. After the moisture sublimates to a vapor, it is removed by mechanical vacuum



pumps or steam-jet ejectors.

As a rule, freeze-drying produces the highest-quality food product obtainable by any drying method. A prominent factor is the structural rigidity afforded by the frozen substance when sublimation occurs. This prevents collapse of the remaining porous structure after drying. When water is added later, the rehydrated product retains much of its original structural form. Freeze-drying of food and biological materials also has the advantage of little loss of flavor and aroma. The low temperatures involved minimize the degrading reactions that normally occur in ordinary drying processes. However, freeze-drying is an expensive form of dehydration for foods because of the slow drying rate and the

use of vacuum.

Since the vapor pressure of ice is very small, freeze-drying requires very low pressures or high vacuum. If the water were in a pure state, freeze-drying at or near  $0^{\circ}\text{C}$  (273 K) at a pressure of  $4580\text{ }\mu\text{m}$  ( $4.58\text{ mmHg abs}$ ) could be performed. (See Appendix A.2 for the properties of ice.) However, since the water usually exists in a solution or a combined state, the material must be cooled below  $0^{\circ}\text{C}$  to keep the water in the solid phase. Most freeze-drying is done at  $-10^{\circ}\text{C}$  (263 K) or lower at pressures of about  $2000\text{ }\mu\text{m}$  or less.

### **33.11B Derivation of Equations for Freeze-Drying**

In the freeze-drying process, the original substance is composed of a frozen core of material. As the ice

sublimes, the plane of sublimation, which started at the outside surface, recedes, and a porous shell of already-dried material remains. The heat for the latent heat of sublimation of 2838 kJ/kg (1220 btu/lbm) ice is usually conducted inward through the layer of dried material. In some cases, it is also conducted through the frozen layer from the rear. The vaporized water is transferred through the layer of dried material. Hence, heat and mass transfer are occurring simultaneously.

In Fig. 33.11-1, a material being freeze-dried is pictured. Heat by conduction, convection, and/or radiation from the gas phase reaches the dried surface and is then transferred by conduction to the

ice layer. In some cases, heat may also be conducted through the frozen material to reach the sublimation front or plane. The total drying time must be long enough that the final moisture content is below about 5 wt % to prevent degradation of the final material on storage. The maximum temperatures reached in the dried food and the frozen food must be low enough to keep degradation to a minimum.

The most widely used freeze-drying process is based on the heat of sublimation being supplied from the surrounding gases to the sample surface. Then, the heat is transferred by conduction through the dried material to the ice surface. A simplified model by Sandall et al. (S1) is shown in Fig. 33.11-2.

The heat flux to the surface of the material in Fig. 33.11-2 occurs by convection and, in the dry solid, by conduction to the sublimation surface. The heat flux to the surface is equal to that conducted through the dry solid, assuming pseudo-steady state:

$$q=h(T_e-T_s)=k\Delta L(T_s-T_f)(33.11-1)$$

where  $q$  is the heat flux in W (J/s),  $h$  is the external heat-transfer coefficient in  $\text{W/m}^2 \cdot \text{K}$ ,  $T_e$  is the external temperature of the gas in  $^{\circ}\text{C}$ ,  $T_s$  is the surface temperature of the dry solid in  $^{\circ}\text{C}$ ,  $T_f$  is the temperature of the sublimation front or ice layer in  $^{\circ}\text{C}$ ,  $k$  is the thermal conductivity of the dry solid in  $\text{W/m} \cdot \text{K}$ , and  $\Delta L$  is the thickness of the dry layer in m. Note that  $(T_s - T_f)^{\circ}\text{C} = (T_s - T_f) \text{ K}$ .

In a similar manner, the mass flux of the water vapor from the sublimation front is

$$N_A = D'RT\Delta L(p_{fw} - p_{sw}) = k_g(p_w - p_{ew}) \quad (33.11-2)$$

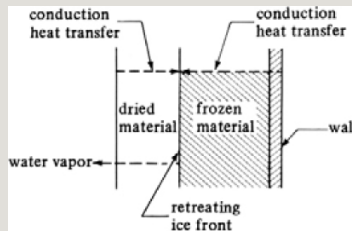


Figure 33.11-1. Heat and mass transfer in freeze-drying.

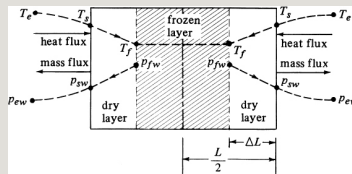


Figure 33.11-2. Model for uniformly retreating ice front in freeze-drying.

where  $N_A$  is the flux of water vapor in  $\text{kg mol/s} \cdot \text{m}^2$ ,  $k_g$  is the external mass-transfer coefficient in  $\text{kg mol/s} \cdot \text{m}^2 \cdot$

atm,  $p_{sw}$  is the partial pressure of water vapor at the surface in atm,  $p_{ew}$  is the partial pressure of water vapor in the external bulk gas phase in atm,  $T$  is the the average temperature in the dry layer,  $D'$  is an average effective diffusivity in the dry layer in m<sup>2</sup>/s, and  $p_{fw}$  is the partial pressure of water vapor in equilibrium with the sublimation ice front in atm.

Equation (33.11-1) can be rearranged to give

$$q = 11/h + \Delta L/k(T_e - T_f) \quad (33.11-3)$$

Also, Eq. (33.11-2) can be rearranged to give

$$N_A = 11/kg + RT\Delta L/D'(p_{fw} - p_{ew}) \quad (33.11-4)$$

The coefficients  $h$  and  $k_g$  are determined by the gas velocities and characteristics of the dryer and, hence, are constant.

The values of  $T_e$  and  $p_{ew}$  are set by the external operating conditions. The values of  $k$  and  $D'$  are determined by the nature of the dried material.

The heat flux and mass flux at pseudo-steady state are related by

$$q = \Delta H_s N_A \quad (33.11-5)$$

where  $\Delta H_s$  is the latent heat of sublimation of ice in J/kg mol. Also,  $p_{fw}$  is uniquely determined by  $T_f$ , since it is the equilibrium vapor pressure of ice at that temperature; or

$$p_{fw} = f(T_f) \quad (33.11-6)$$

Substituting Eqs. (33.11-3) and



(33.11-4) into Eq. (33.11-5),

$$\frac{1}{h} + \frac{\Delta L}{k}(T_e - T_f) = \frac{\Delta H_s}{k_g} + RT \frac{\Delta L}{D'}(p_{fw} - p_{ew}) \quad (33.11-7)$$

Also, substituting Eqs. (33.11-1) and (33.11-4) into Eq. (33.11-5),

$$\frac{1}{h} + \frac{\Delta L}{k}(T_s - T_f) = \frac{\Delta H_s}{k_g} + RT \frac{\Delta L}{D'}(p_{fw} - p_{ew}) \quad (33.11-8)$$

As  $T_e$  and, hence,  $T_s$  are raised to increase the rate of drying, two limits may possibly be reached. First, the outer surface temperature  $T_s$  cannot be allowed to go too high because of thermal damage. Second, the temperature  $T_f$  must be kept well below the melting point. For the situation where  $k/\Delta L$  is small compared to  $k_g$  and  $D'/RT \Delta L$ , the outer-surface temperature limit will be encountered first as  $T_s$  is

raised. To further increase the drying rate,  $k$  must be raised. Hence, the process is considered to be heat-transfer controlled. Most commercial freeze-drying processes are heat-transfer controlled (K1).

In order to solve the given equations,  $\Delta L$  is related to  $x$ , the fraction of the original free moisture remaining:

$$\Delta L = (1-x)L_2 \quad (33.11-9)$$

The rate of freeze-drying can be related to  $N_A$  by

$$N_A = L_2 M_A V_s (-dx/dt) \quad (33.11-10)$$

where  $M_A$  is the molecular weight of water,  $V_s$  is the volume of solid material occupied by a unit kg of water initially ( $V_s = 1/X_0 \rho_s$ ),  $X_0$  is the initial free

moisture content in kg H<sub>2</sub>O/kg dry solid, and  $\rho S$  is the bulk density of dry solid in kg/m<sup>3</sup>.

Combining Eqs. (33.11-3), (33.11-5), (33.11-9), and (33.11-10), we obtain, for heat transfer,

$$L/2 \Delta H_s M A V S (-dx/dt) = 1/h + (1-x)L/2k(T_e - T_f) \quad (33.11-11)$$

Similarly, for mass transfer,

$$L/2 M A V S (-dx/dt) = 1/k_g + RT(1-x)L/2D'(p_{fw} - p_{ew}) \quad (33.11-12)$$

Integrating Eq. (33.11-11) between the limits of  $t = 0$  at  $x_1 = 1.0$  and  $t = t$  at  $x_2 = x_2$ , the equation for the time of drying to  $x_2$  is as follows for  $h$  being very large (negligible external resistance):

$$t = \frac{L}{24kVS} \Delta H_s M_A (1 - x_2 - x_1^2 + x_2^2) \quad (33.11-13)$$

where  $\Delta H_s/M_A$  is the heat of sublimation in J/kg H<sub>2</sub>O. For  $x_2 = 0$ , the slab is completely dry.

Assuming that the physical properties and mass- and heat-transfer coefficients are known, Eq. (33.11-8) can be used to calculate the ice-sublimation temperature  $T_f$  when the environment temperature  $T_e$  and the environment partial pressure  $p_{ew}$  are set. Since  $h$  is very large,  $T_e \cong T_s$ . Then, Eq. (33.11-8) can be solved for  $T_f$ , since  $T_f$  and  $p_{ew}$  are related by the equilibrium-vapor-pressure relation, Eq. (33.11-6). In Eq. (33.11-8), the value to use for  $T$  can be approximated by  $(T_f + T_s)/2$ .

The uniformly retreating ice-front model was tested by Sandall et al. (S1) against actual freeze-drying data. The model satisfactorily predicted the drying times for removal of 65–90% of the total initial water (S1, K1). The temperature  $T_f$  of the sublimation interface did remain essentially constant as assumed in the derivation. However, during removal of the last 10–35% of the water, the drying rate slowed markedly and the actual time was considerably greater than the predicted time for this period.

The effective thermal conductivity  $k$  in the dried material has been found to vary significantly with the total pressure and with the type of gas present. Also, the type of material affects the value of  $k$  (S1, K1). The effective diffusivity  $D'$  of the dried material is a function of the

structure of the material, Knudsen diffusivity, and molecular diffusivity (K1).

### **33.12 Unsteady-State Thermal Processing and Sterilization of Biological Materials**

#### **33.12A Introduction**

Materials of biological origin are usually not as stable as most inorganic and some organic materials. Hence, it is necessary to use certain processing methods to preserve biological materials, especially foods. Physical and chemical processing methods of preservation, such as drying, smoking, salting, chilling, freezing, and heating, are commonly used. The freezing and chilling of foods were discussed in Section 14.5 as methods of slowing the spoilage of

biological materials. Also, in Section 33.11, freeze-drying of food and biological materials was discussed.

An important method is heat or thermal processing, whereby contaminating microorganisms that occur primarily on the outer surface of foods, causing spoilage and health problems, are destroyed. This leads to longer storage times for those foods and other biological materials. A common method of preservation is to heat-seal cans of food. Likewise, thermal processing is used to sterilize aqueous fermentation media to be used in fermentation processes so that organisms that do not survive are unable to compete with the material that is to be cultured.

The sterilization of food materials by

heating destroys bacteria, yeast, and molds that cause spoilage, and it also destroys pathogenic (disease-producing) organisms that may produce deadly toxins if not destroyed. The rate of destruction of microorganisms varies with the amount of heating and the type of organism. Some bacteria can exist in a vegetative growing form and in a dormant or spore form. The spore forms are much more resistant to heat. This mechanism of heat resistance is not clear.

For foods, it is necessary to kill essentially all the spores of *Clostridium botulinum*, which produces a deadly toxin. Complete sterility with respect to this spore is the purpose of thermal processing. Since *Cl. botulinum* is so dangerous and often difficult to use,



other spores, such as *Bacillus stearothermophilus*, which is a nonpathogenic organism of similar heat resistance, are often used for testing the heat-treating processes (A2).

Temperature has a great effect on the growth rate of microorganisms, which have no temperature-regulating mechanisms. Each organism has a certain optimal temperature range in which it grows best. If any microorganism is heated to a sufficiently high temperature for a sufficient time, it will be rendered sterile or killed.

The exact mechanism of thermal death of vegetative bacteria and spores is still somewhat uncertain. It is thought, however, to be due to the breakdown of enzymes that are essential to the

functioning of the living cell (B1).

### **33.12B Thermal Death-Rate Kinetics of Microorganisms**

The destruction of microorganisms by heating means loss of viability but not destruction in the physical sense. If it is assumed that inactivation of a single enzyme in a cell will inactivate the cell, then in a suspension of organisms of a single species at a constant temperature, the death rate can be expressed as a first-order kinetic equation (A2). The rate of destruction (number dying per unit time) is proportional to the number of organisms:

$$dN/dt = -kN \quad (33.12-1)$$

where  $N$  is the number of viable organisms at a given time,  $t$  is time in

min, and  $k$  is a reaction velocity constant in  $\text{min}^{-1}$ . The reaction velocity constant is a function of temperature and the type of microorganism.

After rearranging, Eq. (33.12-1) can be integrated as follows:

$$\int_{N_0}^N \frac{dN}{N} = - \int_{t=0}^t k dt \quad (33.12-2)$$

$$\ln \frac{N}{N_0} = -kt \quad (33.12-3)$$

where  $N_0$  is the original number of organisms at  $t = 0$  and  $N$  is the number at time  $t$ . Often,  $N_0$  is called the *contamination level* (the original number of contaminating microbes before sterilization) and  $N$  the sterility level. Equation (33.12-3) can also be written as

$$N = N_0 e^{-kt} \quad (33.12-4)$$

Sometimes, microbiologists use the term *decimal reduction time*  $D$ , which is the time in min during which the original number of viable microbes is reduced by 110. Substituting into Eq. (33.12-4),

$$N/N_0 = 1/10 = e^{-kD} \quad (33.12-5)$$

Taking the  $\log_{10}$  of both sides and solving for  $D$ ,

$$D = 2.303/k \quad (33.12-6)$$

Combining Eqs. (33.12-3) and (33.12-6),

$$t = D \log_{10} N_0/N \quad (33.12-7)$$

If the  $\log_{10}(N/N_0)$  is plotted versus  $t$ , a straight line should result from Eq. (33.12-3). Experimental data bear this out for vegetative cells and,

approximately, for spores. Data for the vegetative cell *E. coli* (A1) at constant temperature follow this logarithmic death-rate curve. Bacterial-spore plots occasionally deviate somewhat from the logarithmic rate of death, particularly during a short period immediately following exposure to heat. However, for thermal-processing purposes for use with spores such as *Cl. botulinum*, a logarithmic-type curve is used.

To experimentally measure the microbial death rate, the spore or cell suspension in a solution is usually sealed in a capillary or test tube. A number of these tubes are then suddenly dipped into a hot bath for a given time. Afterward, they are removed and immediately chilled. The number of viable organisms before and after

exposure to the high temperature is then usually determined biologically by means of a plate count.

The effect of temperature on the reaction-rate constant  $k$  may be expressed by an Arrhenius-type equation:

$$k = a e^{-E/RT} \quad (33.12-8)$$

where  $a$  = an empirical constant,  $R$  is the gas constant in  $\text{kJ/g mol} \cdot \text{K}$  ( $\text{cal/g} \cdot \text{mol} \cdot \text{K}$ ),  $T$  is the absolute temperature in  $\text{K}$ , and  $E$  is the activation energy in  $\text{kJ/g mol}$  ( $\text{cal/g mol}$ ). The value of  $E$  is in the range 210 to about 418  $\text{kJ/g mol}$  (50–100  $\text{kcal/g mol}$ ) for vegetative cells and spores (A2), and much lower for enzymes and vitamins.

Substituting Eq. (33.12-8) into (33.12-2)

and integrating,

$$\ln N_0/N = a \int_{t=0}^t e^{-E/RT} dt \quad (33.12-9)$$

At constant temperature  $T$ , Eq. (33.12-9) becomes (33.12-3). Since  $k$  is a function of temperature, the decimal reduction time  $D$ , which is related to  $k$  by Eq. (33.12-6), is also a function of temperature. Hence,  $D$  is often written as  $D_T$  to show that it is temperature-dependent.

### **33.12C Determination of Thermal Process Time for Sterilization**

For canned foods, *Cl. botulinum* is the primary organism to be reduced in number (S2). It has been established that the minimum adequate heating process should reduce the number of spores by a factor of  $10^{-12}$ . This means that,

since  $D$  is the time required to reduce the original number by  $10^{-1}$ , substituting  $N/N_0 = 10^{-12}$  into Eq. (33.12-4) and solving for  $t$ ,

$$t = 122.303k = 12D \quad (33.12-10)$$

Thus, the time  $t$  is equal to  $12D$  (often called the *12D concept*). In Eq. (33.12-10), this time to reduce the number by  $10^{-12}$  is called the *thermal death time*. Usually, the sterility level  $N$  is a number much less than one organism. These times do not represent complete sterilization but a mathematical concept that has been found empirically to give effective sterilization.

Experimental data for thermal death rates of *Cl. botulinum*, when plotted as



the decimal reduction time  $DT$  at a given  $T$  versus the temperature  $T$  in  $^{\circ}\text{F}$  on a semilog plot, give essentially straight lines over the range of temperatures used in food sterilization (S2). A typical thermal-destruction curve is shown in Fig. 33.12-1. Actually, by combining Eqs. (33.12-6) and (33.12-8), it can be shown that the plot of  $\log_{10}DT$  versus  $1/T$  ( $T$  in degrees absolute) is a straight line, but over small ranges of temperature a straight line is obtained when  $\log_{10}DT$  is plotted versus  $T^{\circ}\text{F}$  or  $^{\circ}\text{C}$ .

In Fig. 33.12-1, the term  $z$  represents the temperature range in  $^{\circ}\text{F}$  for a 10:1 change in  $DT$ . Since the plot is a straight line, the equation can be represented as

$$\log_{10}DT_2 - \log_{10}DT_1 = 1z(T_1 - T_2)$$

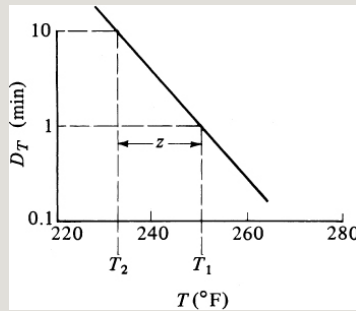


Figure 33.12-1. Thermal-destruction curve: plot of decimal reduction time versus temperature.

Letting  $T_1 = 250^\circ\text{F}$  ( $121.1^\circ\text{C}$ ), which is the standard temperature against which thermal processes are compared, and calling  $T_2 = T$ , Eq. (33.12-11) becomes

$$DT = D_{250} \times 10^{(250-T)/z} \quad (33.12-12)$$

For the organism *Cl. botulinum*, the experimental value of  $z = 18^\circ\text{F}$ . This means that each increase in temperature of  $18^\circ\text{F}$  ( $10^\circ\text{C}$ ) will increase the death rate by a factor of 10. This compares

with the factor of 2 for many chemical reactions for an 18°F increase in temperature.

Using Eq. (33.12-7),

$$t = DT \log_{10} \frac{N_0}{N} \quad (33.12-7)$$

Substituting  $T = 250^\circ\text{F}$  ( $121.1^\circ\text{C}$ ) as the standard temperature into this equation and substituting  $F_0$  for  $t$ ,

$$F_0 = D_{250} \log_{10} \frac{N_0}{N} \quad (33.12-13)$$

where the  $F_0$  value of a process is the time  $t$  in min at  $250^\circ\text{F}$  that will produce the same degree of sterilization as the given process at its temperature  $T$ .

Combining Eqs. (33.12-7), (33.12-12), and (33.12-13), the  $F_0$  of the given process at temperature  $T$  is

$$F_0 = t \cdot 10^{(T^\circ\text{F} - 250)/(z^\circ\text{F})}$$

(SI)  $F_0 = t \cdot 10^{(T^\circ\text{F} - 250)/(z^\circ\text{F})}$  (English)

(33.12-14)

This is the  $F_0$  value in min for the given thermal process at a given constant temperature  $T^\circ\text{F}$  and a given time  $t$  in min. Values for  $F_0$  and  $z$  for adequate sterilization of *Cl. botulinum* vary somewhat with the type of food. Data are tabulated by Stumbo (S2) and Charm (C2) for various foods and microorganisms.

The effects of different but successive sterilization processes in a given material are additive. Hence, for several different temperature stages  $T_1$ ,  $T_2$ , and so on, each having different times  $t_1$ ,  $t_2$ , ..., the  $F_0$  values for each stage are added to give the total  $F_0$ :

$$F_0 = t_1 \cdot 10^{(T_1 - 250)/z} + t_2 \cdot 10^{(T_2 - 250)/z} + \dots (\text{English}) (33.12-15)$$

**EXAMPLE 33.12-1. Sterilization of Cans of Food**

Cans of a given food were heated in a retort for sterilization. The  $F_0$  for *Cl. botulinum* in this type of food is 2.50 min and  $z = 18^\circ\text{F}$ . The temperatures in the center of a can (the slowest-heating region) were measured and were approximately as follows, where the average temperature during each time period is listed:  $t_1$  (0–20 min),  $T_1 = 160^\circ\text{F}$ ;  $t_2$  (20–40 min),  $T_2 = 210^\circ\text{F}$ ;  $t_3$  (40–73 min),  $T_3 = 230^\circ\text{F}$ . Determine if this sterilization process is adequate. Use English and SI units.

**Solution:** For the three time periods, the data are as follows:

0=20min,  $T_1 = 160^\circ\text{F}$  (71.1°C),  $z = 18^\circ\text{F}$  (10°C)  $t_2 = 40 - 20 = 20\text{min}$ ,  $T_2 = 210^\circ\text{F}$  (98.9°C)  $t_3 = 73 - 40 = 33\text{min}$ ,  $T_3 = 230^\circ\text{F}$  (110°C)

Substituting into Eq. (33.12-15) and solving, using English and SI units,

$$F_0 = t_1 \cdot 10^{(T_1 - 250)/z} + t_2 \cdot 10^{(T_2 - 250)/z} + t_3 \cdot 10^{(T_3 - 250)/z}$$

$$(20)10^{(160 - 250)/18} + (20)10^{(210 - 250)/18} + (33)10^{(230 - 250)/18} = 0.0020 + 0.1199 + 2.555 = 2.68 \text{ min (English)}$$

$$(20)10^{(71.1 - 121.1)/10} + (20)10^{(98.9 - 121.1)/10} + (33)10^{(110 - 121.1)/10} = 2.68 \text{ min (SI)}$$

Hence, this thermal processing is adequate, since only 2.50 min is needed for complete sterilization. Note that the time period at  $160^\circ\text{F}$  ( $71.1^\circ\text{C}$ ) contributes an insignificant amount to the final  $F_0$ . The major contribution is at  $230^\circ\text{F}$  ( $110^\circ\text{C}$ ), which is the highest temperature.

In the general case when cans of food are being sterilized in a retort, the temperature is not constant for a given time period but varies continuously with

time. Hence, Eq. (33.12-15) can be modified and written for a continuously varying temperature  $T$  by taking small time increments of  $dt$  min for each value of  $T$  and summing. The final equation is

$$F_0 = \int_{t=0}^{t_{10}} \frac{10(T - 250)}{(z_0 F) dt} \quad (\text{English}) \quad F_0 = \int_{t=0}^{t_{10}} \frac{10(T - 121.1)}{(z_0 C) dt} \quad (\text{SI}) \quad (33.12-16)$$

This equation can be used as follows:

Suppose that the temperature of a process is varying continuously and that a graph or table of values of  $T$  versus  $t$  is known or can be calculated by means of the unsteady-state methods given in Chapter 20. Equation (33.12-16) can be graphically integrated by plotting values of  $10(T - 250)/z$  versus  $t$  and taking the area under the curve. In most cases, a numerical integration is used to

determine  $F_0$ . (See Section 1.8 for methods of numerical integration.)

In many cases, the temperature of a process that is varying continuously with time is determined experimentally by measuring the temperature in the slowest-heating region. In cans, this is in the center of the can. The methods given in Chapter 20 for unsteady-state heating of short, fat cylinders by conduction can be used to predict the center temperature of the can as a function of time.

However, these predictions can be somewhat in error, since physical and thermal properties of foods are difficult to measure accurately and often can vary. Also, trapped air in the container and unknown convection effects can affect the accuracy of predictions.

**EXAMPLE 33.12-2. Thermal Process Evaluation by Numerical Integration**

In the sterilization of a canned purée, the temperature in the slowest-heating region (center) of the can was measured, giving the following time–temperature data for the heating and holding time. The cooling-time data will be neglected as a safety factor.



The  $F_0$  value of *Cl. botulinum* is 2.45 min and  $z$  is 18°F. Calculate the  $F_0$  value of the process above and determine if the sterilization is adequate.

**Solution:** In order to use Eq. (33.12-16), the values of  $10_{(T-250)/z}$  must be calculated for each time. For  $t = 0$  min,  $T = 80^\circ\text{F}$ ,  $z = 18^\circ\text{F}$ ,

$$10_{(T-250)/z} = 10_{(80-250)/18} = 3.6 \times 10^{-10}$$

For  $t = 15$  min,  $T = 165^\circ\text{F}$ ,

$$10_{(165-250)/18} = 0.0000189$$

For  $t = 25$  min,  $T = 201^\circ\text{F}$ ,

$$10_{(201-250)/18} = 0.00189$$

For  $t = 30$  min,

$$10_{(212.5-250)/18} = 0.00825$$

For  $t = 40$  min,

$$10_{(225-250)/18} = 0.0408$$

For  $t = 50$  min,

$$10_{(230.5-250)/18} = 0.0825$$

For  $t = 64$  min,

$$10_{(235-250)/18} = 0.1465$$



These calculated values are then used in Eq. (33.12-16) to perform a numerical integration to give  $F_0 = 2.50$  min. The process value of 2.50 min is greater than the required value of 2.45 min, and the sterilization is adequate.

### **33.12D Sterilization Methods Using Other Design Criteria**

In types of thermal processing that are not necessarily involved with the sterilization of foods, other types of design criteria are used. In foods, the minimum adequate heat process should reduce the number of spores by a factor of  $10^{-12}$ , that is,  $N/N_0 = 10^{-12}$ . However, in other batch-sterilization processes, such as in the sterilization of fermentation media, other criteria are often used. Often, the equation for  $k$ , the reaction velocity constant for the specific

organism to be used, is available:

$$k = a e^{-E/RT} \quad (33.12-8)$$

Then, Eq. (33.12-9) is written as

$$\nabla = \ln N_0/N = a \int_{t=0}^t e^{-E/RT} dt = \int_{t=0}^t k dt \quad (33.12-17)$$

where  $\nabla$  is the design criterion. Usually, the contamination level  $N_0$  is available and either the sterility level  $N$  or the time of sterilization at a given temperature is the unknown. In either case, a numerical or graphical integration is used to solve the problem.

In sterilization of food in a container, the time required to render the material safe is calculated at the slowest-heating region of the container (usually the center). Other regions of the container

are usually heated to higher temperatures and are overtreated.

Hence, another method used is based on the probability of survival in the whole container. These details are given by others (C2, S2). In still another processing method, a short-time, continuous-flow process is used instead of a batch process in a container (B2).

### **33.12E Pasteurization**

The term *pasteurization* is used today to apply to a mild heat treatment of foods that is less drastic than sterilization. It is used to kill organisms that are relatively low in thermal resistance compared to those that the more drastic sterilization processes are designed to eliminate. Pasteurization usually involves killing vegetative microorganisms

and not heat-resistant spores.

The most common process is the pasteurization of milk to kill *Mycobacterium tuberculosis*, which is a non-spore-forming bacterium. This pasteurization does not sterilize the milk but kills the *M. tuberculosis* and reduces the other bacterial count sufficiently so that the milk can be stored if refrigerated.

For the pasteurization of such foods as milk, fruit juices, and beer, the same mathematical and numerical procedures covered for sterilization processes in this section are used to accomplish the degree of sterilization desired in pasteurization (B1, S2). The times involved are much shorter and the temperatures used in pasteurization are

much lower. Generally, the  $F_0$  value is given as 150°F (65.6°C) or a similar temperature rather than 250°F as in sterilization. Also, the concept of the  $z$  value is employed, in which a rise in temperature of  $z$ °F will increase the death rate by a factor of 10. An  $F_0$  value written as F1509 means the  $F$  value at 150°F with a  $z$  value of 9°F (S2).

In pasteurizing milk, batch and continuous processes are used. United States health regulations specify two equivalent sets of conditions; in one, the milk is held at 145°F (62.8°C) for 30 min, and in the other, at 161°F (71.7°C) for 15 s.

The general equations used for pasteurization are similar to sterilization and can be written as follows. Rewriting

Eq. (33.12-13),

$$F_{T_1} z = D T_1 \log_{10} \frac{N_0}{N} \quad (33.12-18)$$

Rewriting Eq. (33.12-14),

$$F_{T_1} z = t \cdot 10^{(T - T_1)/z} \quad (33.12-19)$$

where  $T_1$  is the standard temperature being used, such as 150°F,  $z$  is the value of  $z$  in °F for a tenfold increase in death rate, and  $T$  is the temperature of the actual process.

**EXAMPLE 33.12-3. Pasteurization of Milk**

A typical  $F$  value given for the thermal processing of milk in a tubular heat exchanger is  $F_{150} = 9.0$  min, and  $D_{150} = 0.6$  min. Calculate the reduction in the number of viable cells under these conditions.

**Solution:** The  $z$  value is 9°F (5°C) and the temperature of the process is 150°F (65.6°C). Substituting into Eq. (33.12-18) and solving,

$$F_{150} = 9.0 = 0.6 \log_{10} \frac{N_0}{N} \quad N = 10^{15}$$

This gives a reduction in the number of viable cells of  $10^{15}$ .

## Constituents

Thermal processing is used to kill various undesirable microorganisms, but it also causes undesirable effects, such as the reduction of certain nutritional values. Ascorbic acid (vitamin C) and thiamin and riboflavin (vitamins B1 and B2) are partially destroyed by thermal processing. The reduction of these desirable constituents can also be given kinetic parameters such as  $F_0$  and  $z$  values in the same way as for sterilization and pasteurization. Examples and data are given by Charm (C2).

These same kinetic methods of thermal death rates can also be applied to predict the time for detecting a flavor change in a food product. Dietrich et al. (D1)

determined a curve for the number of days to detect a flavor change in frozen spinach versus the temperature of storage. The data followed Eq. (33.12-8) and a first-order kinetic relation.

### **33.13 Chapter Summary**

In this chapter, we have introduced the concepts of drying, as well as the processes of freeze-drying and sterilization. The process of drying involves the removal of moisture from a solid material. Although there are multiple mechanical approaches to removing moisture (e.g., filtration and centrifugation), this chapter focused primarily on thermal methods.

There are many types of equipment that can be used for drying. Often, this



equipment can be classified based on whether the drying process is batch or continuous. The following types of equipment were introduced: tray dryers, vaccum-shelf indirect dryers, continuous tunnel dryers, rotary dryers, drum dryers, and spray dryers.

In calculating the moisture conditions of a gas stream, it is necessary to know its humidity, or moisture content. This can be found by calculating the vapor pressure of water at a specific temperature, using a humidity chart, or determining both the dry-bulb and wet-bulb temperature of the water vapor–air mixture.

When drying solid materials, it is necessary to understand how moisture is stored in the material and how it diffuses

to the surface. Often, it is necessary to determine the equilibrium moisture content of solid materials, which is a function of relative humidity and temperature. Other moisture properties of solids that are also needed included the bound and unbound water in solids, and the free and equilibrium moisture of a substance.

The drying properties of materials can be graphically represented using rate-of-drying curves. There are two main types of these curves: free moisture content as a function of drying time, and drying rate as a function of free moisture content. From the latter curve, it is possible to graphically determine the constant-rate and falling-rate periods during the drying process. The constant-rate period is determined by the

unbound water at the surface of the material and the falling-rate period is determined by the diffusion of the liquid moisture through the solid material. Calculation methods were introduced to predict the drying time during both of these rate periods.

To predict the drying time required, many correlations to calculate the overall heat-transfer coefficient were provided. Additional thermodynamic and heat-transfer calculations were provided for drying in packed beds, tray drying, continuous dryers, and countercurrent dryers.

Finally, the processes of freeze-drying and sterilization were introduced. Freeze-drying is used in the food-processing industry to prevent the

degradation of the food product during drying. It is highly dependent on sublimation properties. Sterilization is used in the biological, pharmaceutical, and food-science industries to destroy bacteria and other pathogenic microorganisms. It can be modeled using thermal death-rate kinetics and the contamination-level requirements of the sterilization process.

## Problems

### **33.3-1. *Humidity from Vapor Pressure.***

The air in a room is at  $37.8^{\circ}\text{C}$  and a total pressure of 101.3 kPa abs containing water vapor with a partial pressure  $p_A = 3.59$  kPa. Calculate the following:

- Humidity
- Saturation humidity and percentage humidity
- Percentage relative humidity

### 33.3-2. *Percentage and Relative*

**Humidity.** The air in a room has a humidity  $H$  of 0.021 kg H<sub>2</sub>O/kg dry air at 32.2°C and 101.3 kPa abs pressure. Calculate the following:

- Percentage humidity  $HP$
- Percentage relative humidity  $HR$

**Ans.** (a)  $HP = 67.5\%$ ; (b)  $HR = 68.6\%$

**33.3-3. *Use of the Humidity Chart.*** The air entering a dryer has a temperature of 65.6°C (150°F) and a dew point of 15.6°C (60°F). Using the humidity chart, determine the actual humidity and percentage humidity. Calculate the humid volume of this mixture and also calculate  $cs$  using SI and English units.

**Ans.**  $H = 0.0113$  kg H<sub>2</sub>O/kg dry air,  $HP = 5.3\%$ ,  $cs = 1.026$  kJ/kg · K (0.245 btu/

$\text{lb}_m \cdot ^\circ\text{F})$ ,  $v_H = 0.976 \text{ m}^3 \text{ air} + \text{water}$   
vapor/kg dry air

**33.3-4. *Properties of Air to a Dryer.*** An air–water vapor mixture going to a drying process has a dry bulb temperature of  $57.2^\circ\text{C}$  and a humidity of  $0.030 \text{ kg H}_2\text{O/kg dry air}$ . Using the humidity chart and appropriate equations, determine the percentage humidity, saturation humidity at  $57.2^\circ\text{C}$ , dew point, humid heat, and humid volume.

### **33.3-5. *Adiabatic Saturation***

***Temperature.*** Air at  $82.2^\circ\text{C}$  having a humidity  $H = 0.0655 \text{ kg H}_2\text{O/kg dry air}$  is contacted in an adiabatic saturator with water. It leaves at 80% saturation.

- What are the final values of  $H$  and  $T^\circ\text{C}$ ?
- For 100% saturation, what would be the values of

$H$  and  $T$ ?

**Ans.** (a)  $H = 0.079 \text{ kg H}_2\text{O/kg dry air}$ ,  $T = 52.8^\circ\text{C}$

**33.3-6. *Adiabatic Saturation of Air.*** Air enters an adiabatic saturator having a temperature of  $76.7^\circ\text{C}$  and a dew-point temperature of  $40.6^\circ\text{C}$ . It leaves the saturator 90% saturated. What are the final values of  $H$  and  $T^\circ\text{C}$ ?

**33.3-7. *Humidity from Wet and Dry Bulb Temperatures.*** An air–water vapor mixture has a dry bulb temperature of  $65.6^\circ\text{C}$  and a wet bulb temperature of  $32.2^\circ\text{C}$ . What is the humidity of the mixture?

**Ans.**  $H = 0.0175 \text{ kg H}_2\text{O/kg dry air}$

**33.3-8. *Humidity and Wet Bulb***

**Temperature.** The humidity of an air–water vapor mixture is  $H = 0.030$  kg H<sub>2</sub>O/kg dry air. The dry bulb temperature of the mixture is 60°C. What is the wet bulb temperature?

**33.3-9. Dehumidification of Air.** Air having a dry bulb temperature of 37.8°C and a wet bulb temperature of 26.7°C is to be dried by first cooling to 15.6°C to condense water vapor and then heating to 23.9°C.

- Calculate the initial humidity and percentage humidity.
- Calculate the final humidity and percentage humidity. [*Hint:* Locate the initial point on the humidity chart. Then, go horizontally (cooling) to the 100% saturation line. Follow this line to 15.6°C. Then, go horizontally to the right to 23.9°C.]

**Ans.** (b)  $H = 0.0115$  kg H<sub>2</sub>O/kg dry air,  
 $HP = 60\%$



### **33.3-10. *Cooling and Dehumidifying***

**Air.** Air entering an adiabatic cooling chamber has a temperature of  $32.2^{\circ}\text{C}$  and a percentage humidity of 65%. It is cooled by a cold-water spray and saturated with water vapor in the chamber. After leaving, it is heated to  $23.9^{\circ}\text{C}$ . The final air has a percentage humidity of 40%.

- What is the initial humidity of the air?
- What is the final humidity after heating?

### **33.6-1. *Time for Drying in the***

***Constant-Rate Period.*** A batch of wet solid was dried on a tray dryer using constant-drying conditions and a thickness of material on the tray of 25.4 mm. Only the top surface was exposed. The drying rate during the constant-rate period was  $R = 2.05 \text{ kg H}_2\text{O/h} \cdot \text{m}^2$  ( $0.42 \text{ lb}_m \text{ H}_2\text{O/h} \cdot \text{ft}^2$ ). The ratio  $Ls/A$

used was  $24.4 \text{ kg dry solid/m}^2$  exposed surface ( $5.0 \text{ lb}_m \text{ dry solid/ft}^2$ ). The initial free moisture was  $X_1 = 0.55$  and the critical moisture content  $X_C = 0.22 \text{ kg free moisture/kg dry solid}$ .

Calculate the time to dry a batch of this material from  $X_1 = 0.45$  to  $X_2 = 0.30$  using the same drying conditions but a thickness of  $50.8 \text{ mm}$ , with drying from the top and bottom surfaces. (*Hint: First calculate  $Ls/A$  for this new case.*)

**Ans.**  $t = 1.785 \text{ h}$

### ***33.6-2. Prediction of the Effect of Process Variables on the Drying Rate.***

Using the conditions in Example 33.6-3 for the constant-rate drying period, do as follows:

- Predict the effect on  $RC$  if the air velocity is only

3.05 m/s.

- Predict the effect if the gas temperature is raised to  $76.7^{\circ}\text{C}$  and  $H$  remains the same.
- Predict the effect on the time  $t$  for drying between moisture contents  $X_1$  to  $X_2$  if the thickness of material dried is 38.1 mm instead of 25.4 mm and the drying is still in the constant-rate period.

**Ans.** (a)  $RC = 1.947 \text{ kg H}_2\text{O/h} \cdot \text{m}^2$   
( $0.399 \text{ lb}_m \text{ H}_2\text{O/h} \cdot \text{ft}^2$ ); (b)  $RC = 4.21 \text{ kg}$   
 $\text{H}_2\text{O/h} \cdot \text{m}^2$

**33.6-3. Prediction in Constant-Rate Drying Region.** A granular insoluble solid material wet with water is being dried in the constant-rate period in a pan  $0.61 \text{ m} \times 0.61 \text{ m}$  and the depth of material is 25.4 mm. The sides and bottom are insulated. Air flows parallel to the top drying surface at a velocity of 3.05 m/s and has a dry bulb temperature of  $60^{\circ}\text{C}$  and wet bulb temperature of  $29.4^{\circ}\text{C}$ . The pan contains 11.34 kg of

dry solid having a free moisture content of  $0.35 \text{ kg H}_2\text{O/kg dry solid}$ , and the material is to be dried in the constant-rate period to  $0.22 \text{ H}_2\text{O/kg dry solid}$ .

- Predict the drying rate and the time in hours needed.
- Predict the time needed if the depth of material is increased to  $44.5 \text{ mm}$ .

**33.6-4. *Drying a Filter Cake in the Constant-Rate Region.*** A wet filter cake in a pan  $1 \text{ ft} \times 1 \text{ ft}$  square and  $1 \text{ in.}$  thick is dried on the top surface with air at a wet bulb temperature of  $80^\circ\text{F}$  and a dry bulb temperature of  $120^\circ\text{F}$  flowing parallel to the surface at a velocity of  $2.5 \text{ ft/s}$ . The dry density of the cake is  $120 \text{ lb}_\text{m}/\text{ft}^3$  and the critical free moisture content is  $0.09 \text{ lb H}_2\text{O/lb dry solid}$ . How long will it take to dry the material from a free moisture content of  $0.20 \text{ lb H}_2\text{O/}$

lb dry material to the critical moisture content?

**Ans.**  $t = 13.3 \text{ h}$

**33.7-1. Numerical Integration for Drying in the Falling-Rate Region.** A wet solid is to be dried in a tray dryer under steady-state conditions from a free moisture content of  $X_1 = 0.40 \text{ kg H}_2\text{O/kg dry solid}$  to  $X_2 = 0.02 \text{ kg H}_2\text{O/kg dry solid}$ . The dry solid weight is  $99.8 \text{ kg dry solid}$  and the top surface area for drying is  $4.645 \text{ m}^2$ . The drying-rate curve can be represented by Fig. 33.5-1b.

- Calculate the time for drying using numerical integration in the falling-rate period.
- Repeat, but use a straight line through the origin for the drying rate in the falling-rate period.

**Ans.** (a)  $t(\text{constant rate}) = 2.91 \text{ h}$ ,

$$t(\text{falling rate}) = 6.65 \text{ h}, t(\text{total}) = 9.56 \text{ h}$$

### ***33.7-2. Drying Tests with a Foodstuff.***

In order to test the feasibility of drying a certain foodstuff, drying data were obtained in a tray dryer with air flow over the top exposed surface having an area of  $0.186 \text{ m}^2$ . The bone-dry sample weight was  $3.765 \text{ kg}$  dry solid. At equilibrium after a long period, the wet sample weight was  $3.955 \text{ kg H}_2\text{O} + \text{solid}$ . Hence,  $3.955 - 3.765$ , or  $0.190$ ,  $\text{kg}$  of equilibrium moisture was present. The following sample weights versus time were obtained in the drying test:

- Calculate the free moisture content  $X \text{ kg H}_2\text{O/kg}$  dry solid for each data point and plot  $X$  versus time. (*Hint: For 0 h,  $4.944 - 0.190 - 3.765 = 0.989 \text{ kg}$  free moisture in  $3.765 \text{ kg}$  dry solid. Hence,  $X = 0.989/3.765$ .)*

- Measure the slopes, calculate the drying rates  $R$  in  $\text{kg H}_2\text{O/h} \cdot \text{m}^2$ , and plot  $R$  versus  $X$ .
- Using this drying-rate curve, predict the total time to dry the sample from  $X = 0.20$  to  $X = 0.04$ . Use numerical integration for the falling-rate period. What are the drying rate  $R_C$  in the constant-rate period and  $X_C$ ?

**Ans.** (c)  $R_C = 0.996 \text{ kg H}_2\text{O/h} \cdot \text{m}^2$ ,  $X_C = 0.12$ ,  $t = 4.1 \text{ h}$  (total)

**33.7-3. Prediction of Drying Time.** A material was dried in a tray-type batch dryer using constant-drying conditions. When the initial free moisture content was  $0.28 \text{ kg free moisture/kg dry solid}$ ,  $6.0 \text{ h}$  was required to dry the material to a free moisture content of  $0.08 \text{ kg free moisture/kg dry solid}$ . The critical free moisture content is  $0.14$ . Assuming a drying rate in the falling-rate region, where the rate is a straight line from the critical point to the origin, predict the

time to dry a sample from a free moisture content of 0.33 to 0.04 kg free moisture/kg dry solid. (*Hint*: First, use the analytical equations for the constant-rate and the linear falling-rate periods with the known total time of 6.0 h. Then, use the same equations for the new conditions.)

**33.8-1. Drying Biological Material in Tray Dryer.** A granular biological material wet with water is being dried in a pan  $0.305 \times 0.305$  m and 38.1 mm deep. The material is 38.1 mm deep in the pan, which is insulated on the sides and bottom. Heat transfer is by convection from an air stream flowing parallel to the top surface at a velocity of 3.05 m/s, having a temperature of  $65.6^{\circ}\text{C}$  and humidity  $H = 0.010$  kg  $\text{H}_2\text{O}$ /kg dry air. The top surface receives



radiation from steam-heated pipes whose surface temperature  $T_R = 93.3^\circ\text{C}$ . The emissivity of the solid is  $\varepsilon = 0.95$ . It is desired to keep the surface temperature of the solid below  $32.2^\circ\text{C}$  so that decomposition will be kept low. Calculate the surface temperature and the rate of drying for the constant-rate period.

**Ans.**  $T_s = 31.3^\circ\text{C}$ ,  $R_C = 2.583 \text{ kg H}_2\text{O/h} \cdot \text{m}^2$

**33.8-2.** Drying When Radiation, Conduction, and Convection Are Present. A material is granular and wet with water and is being dried in a layer 25.4 mm deep in a batch-tray dryer pan. The pan has a metal bottom having a thermal conductivity of  $k_M = 43.3 \text{ W/m} \cdot \text{K}$  and a thickness of 1.59 mm. The

thermal conductivity of the solid is  $k_s = 1.125 \text{ W/m} \cdot \text{K}$ . The air flows parallel to the top exposed surface and the bottom metal at a velocity of  $3.05 \text{ m/s}$  and a temperature of  $60^\circ\text{C}$  and humidity  $H = 0.010 \text{ kg H}_2\text{O/kg dry solid}$ . Direct radiation heat from steam pipes having a surface temperature of  $104.4^\circ\text{C}$  falls on the exposed top surface, whose emissivity is  $0.94$ . Estimate the surface temperature and the drying rate for the constant-rate period.

### ***33.9-1. Diffusion Drying in Wood.***

Repeat Example 33.9-1 using the physical properties given but with the following changes:

- Calculate the time needed to dry the wood from a total moisture of  $0.22$  to  $0.13$ . Use Fig. 14.3-13.
- Calculate the time needed to dry planks of wood  $12.7 \text{ mm}$  thick from  $X_{t1} = 0.29$  to  $X_t = 0.09$ .

Compare with the time needed for a thickness of 25.4 mm.

**Ans.** (b)  $t = 7.60$  h (12.7 mm thick)

**33.9-2. *Diffusivity in Drying Tapioca Root.*** Using the data given in Example 33.9-2, determine the average diffusivity of the moisture up to a value of  $X/X_C = 0.50$ .

**33.9-3. *Diffusion Coefficient.***

Experimental drying data for a typical nonporous biological material obtained under constant-drying conditions in the falling-rate region are tabulated below.

--

Drying from one side occurs, with the material having a thickness of 10.1 mm. The data appear to follow the diffusion equation. Determine the average

diffusivity over the range  $X/X_C = 1.0 - 0.10$ .

**33.10-1. *Drying a Bed of Solids by Through Circulation.*** Repeat Example 33.10-1 for drying of a packed bed of wet cylinders by through circulation of the drying air. Use the same conditions except that the air velocity is 0.381 m/s.

**33.10-2. *Derivation of Equation for Through-Circulation Drying.*** Different forms of Eqs. (33.10-11) and (33.10-12) can be derived using humidity and mass-transfer equations rather than temperature and heat-transfer equations. This can be done by writing a mass-balance equation similar to Eq. (33.10-2) for a heat balance and a mass-transfer equation similar to Eq. (33.10-3).

- Derive the final equation for the time of drying in the constant-rate period using humidity and mass-transfer equations.
- Repeat for the falling-rate period.

$$\text{Ans. (a) } t = \frac{\rho_s x_1 (X_1 - X_C) G (H_W - H_1) (1 - e^{-k_y M_B a x_1 / G})}{k_y M_B a x_1 / G}$$

**33.10-3. *Through-Circulation Drying in the Constant-Rate Period.*** Spherical wet catalyst pellets having a diameter of 12.7 mm are being dried in a through-circulation dryer. The pellets are in a bed 63.5 mm thick on a screen. The solids are being dried by air entering with a superficial velocity of 0.914 m/s at 82.2°C and with a humidity  $H = 0.01$  kg H<sub>2</sub>O/kg dry air. The dry-solid density is determined as 1522 kg/m<sup>3</sup>, and the void fraction in the bed is 0.35. The initial free moisture content is 0.90 kg H<sub>2</sub>O/kg solid and the solids are to be

dried to a free moisture content of 0.45, which is above the critical free moisture content. Calculate the time for drying in this constant-rate period.

### **33.10-4. *Material and Heat Balances***

***on a Continuous Dryer.*** Repeat

Example 33.10-2, making heat and material balances, but with the

following changes. The solid enters at

15.6°C and leaves at 60°C. The gas

enters at 87.8°C and leaves at 32.2°C.

Heat losses from the dryer are estimated as 2931 W.

### **33.10-5. *Drying in a Continuous***

***Tunnel Dryer.*** A rate of feed of 700 lb<sub>m</sub>

dry solid/h containing a free moisture

content of  $X_1 = 0.4133$  lb H<sub>2</sub>O/lb dry

solid is to be dried to  $X_2 = 0.0374$  lb

H<sub>2</sub>O/lb dry solid in a continuous-

counterflow tunnel dryer. A flow of 13 280 lb<sub>m</sub> dry air/h enters at 203°F with an  $H_2 = 0.0562$  lb H<sub>2</sub>O/lb dry air. The stock enters at the wet bulb temperature of 119°F and remains essentially constant in temperature in the dryer. The saturation humidity at 119°F from the humidity chart is  $H_w = 0.0786$  lb H<sub>2</sub>O/lb dry air. The surface area available for drying is  $(A/Ls) = 0.30$  ft<sup>2</sup>/lb<sub>m</sub> dry solid.

A small-batch experiment was performed using approximately the same constant-drying conditions, air velocity, and temperature of the solid as in the continuous dryer. The equilibrium critical moisture content was found to be  $X_C = 0.0959$  lb H<sub>2</sub>O/lb dry solid, and the experimental value of  $k_y M_B$  was found as 30.15 lb<sub>m</sub>air/h · ft<sup>2</sup>. In the falling-rate period, the drying rate was directly

proportional to  $X$ .

For the continuous dryer, calculate the time in the dryer in the constant-rate zone and the falling-rate zone.

**Ans.**  $H_C = 0.0593$  lb H<sub>2</sub>O/lb dry air,  $H_1 = 0.0760$  lb H<sub>2</sub>O/lb dry air,  $t = 4.20$  h in the constant-rate zone;  $t = 0.47$  h in the falling-rate zone

**33.10-6. Air Recirculation in a Continuous Dryer.** The wet feed material to a continuous dryer contains 50 wt % water on a wet basis and is dried to 27 wt % by countercurrent air flow. The dried product leaves at the rate of 907.2 kg/h. Fresh air to the system is at 25.6°C and has a humidity of  $H = 0.007$  kg H<sub>2</sub>O/kg dry air. The moist air leaves the dryer at 37.8°C and



$H = 0.020$ , and part of it is recirculated and mixed with the fresh air before entering a heater. The heated mixed air enters the dryer at  $65.6^{\circ}\text{C}$  and  $H = 0.010$ . The solid enters at  $26.7^{\circ}\text{C}$  and leaves at  $26.7^{\circ}\text{C}$ . Calculate the fresh-air flow, the percent air leaving the dryer that is recycled, the heat added in the heater, and the heat loss from the dryer.

**Ans.** 32 094 kg fresh dry air/h, 23.08% recycled, 440.6 kW in heater

**33.12-1. *Sterilizing Canned Foods.*** In a sterilizing retort, cans of a given food were heated; the average temperature in the center of a can is approximately  $98.9^{\circ}\text{C}$  for the first 30 min. The average temperature for the next period is  $110^{\circ}\text{C}$ . If  $F_0$  for the spore organism is 2.50 min and  $z = 10^{\circ}\text{C}$ , calculate the

time of heating at  $110^{\circ}\text{C}$  to make the process safe.

**Ans.** 29.9 min

**33.12-2. *Temperature Effect on the Decimal Reduction Time.*** Prove by combining Eqs. (33.12-6) and (33.12-8) that a plot of  $\log_{10} DT$  versus  $1/T$  ( $T$  in degrees absolute) is a straight line.

**33.12-3. *Thermal Process Time for Pea Purée.*** For cans of pea purée,  $F_0 = 2.45$  min and  $z = 9.94^{\circ}\text{C}$  ( $^{\circ}\text{C}^2$ ). Neglecting heatup time, determine the process time for adequate sterilization at  $112.8^{\circ}\text{C}$  at the center of the can.

**Ans.**  $t = 16.76$  min

**33.12-4. *Process Time for Adequate Sterilization.*** The  $F_0$  value for a given

canned food is 2.80 min and  $z$  is  $18^{\circ}\text{F}$  ( $10^{\circ}\text{C}$ ). The center temperatures of a can of this food when heated in a retort were as follows for the time periods given:  $t_1$  (0–10 min),  $T_1 = 140^{\circ}\text{F}$ ;  $t_2$  (10–30 min),  $T_2 = 185^{\circ}\text{F}$ ;  $t_3$  (30–50 min),  $T_3 = 220^{\circ}\text{F}$ ;  $t_4$  (50–80 min),  $T_4 = 230^{\circ}\text{F}$ ;  $t_5$  (80–100 min),  $T_5 = 190^{\circ}\text{F}$ . Determine if adequate sterilization is obtained.

**33.12-5. Process Time and Numerical Integration.** The following time–temperature data were obtained for the heating, holding, and cooling of a canned food product in a retort, the temperature being measured in the center of the can:

The  $F_0$  value used is 2.60 min and  $z$  is  $18^{\circ}\text{F}$  ( $10^{\circ}\text{C}$ ). Calculate the  $F_0$  value for

this process and determine if the thermal processing is adequate. Use SI and English units.

### **33.12-6. Sterility Level of a**

**Fermentation Medium.** The aqueous medium in a fermentor is being sterilized and the time–temperature data obtained are as follows:



The reaction velocity constant  $k$  in  $\text{min}^{-1}$  for the contaminating bacterial spores can be represented as (A1)

$$k = 7.94 \times 10^{38} e^{-(68.7 \times 10^3)/1.987T}$$

where  $T = K$ . The contamination level  $N_0 = 1 \times 10^{12}$  spores. Calculate the sterility level  $N$  at the end and  $\nabla$ .

**33.12-7. Time for Pasteurization of Milk.** Calculate the time in min at  $62.8^{\circ}\text{C}$  for pasteurization of milk. The  $F_0$  value to be used at  $65.6^{\circ}\text{C}$  is 9.0 min. The  $z$  value is  $5^{\circ}\text{C}$ .

**Ans.**  $t = 32.7$  min

**33.12-8. Reduction in the Number of Viable Cells in Pasteurization.** In a given pasteurization process, the reduction in the number of viable cells used is  $10^{15}$  and the  $F_0$  value is 9.0 min. If the reduction is to be increased to  $10^{16}$  because of increased contamination, what would be the new  $F_0$  value?

### References

### Notation



## **Part 3: Appendixes**

## Appendix A.1. Fundamental Constants and Conversion Factors

Table A.1-1. *Gas Law Constant R*

--

Table A.1-2. *Volume and Density*

1 g mol ideal gas at 0°C, 760 mmHg  
= 22.4140 liters = 22 414 cm<sup>3</sup>

1 lb mol ideal gas at 0°C, 760  
mmHg = 359.05 ft<sup>3</sup>

1 kg mol ideal gas at 0°C, 760  
mmHg = 22.414 m<sup>3</sup>

Density of dry air at 0°C, 760 mmHg  
= 1.2929 g/liter = 0.080711 lb<sub>m</sub>/ft<sup>3</sup>



Molecular weight of air = 28.97 lb<sub>m</sub>/lb mol = 28.97 g/g mol

1 g/cm<sup>3</sup> = 62.43 lb<sub>m</sub>/ft<sup>3</sup> = 1000 kg/m<sup>3</sup>

1 g/cm<sup>3</sup> = 8.345 lb<sub>m</sub>/U.S gal

1 lb<sub>m</sub>/ft<sup>3</sup> = 16.0185 kg/m<sup>3</sup>

Table A.1-3. *Length*

1 in. = 2.540 cm

100 cm = 1 m (meter)

1 micron = 10<sup>-6</sup> m = 10<sup>-4</sup> cm = 10<sup>-3</sup> mm = 1 μm (micrometer)

1 Å (angstrom) = 10<sup>-10</sup> m = 10<sup>-4</sup> μm

1 mile = 5280 ft

$$1 \text{ m} = 3.2808 \text{ ft} = 39.37 \text{ in.}$$

Table A.1-4. *Mass*

$$1 \text{ lb}_m = 453.59 \text{ g} = 0.45359 \text{ kg}$$

$$1 \text{ lb}_m = 16 \text{ oz} = 7000 \text{ grains}$$

$$1 \text{ kg} = 1000 \text{ g} = 2.2046 \text{ lb}_m$$

$$1 \text{ ton (short)} = 2000 \text{ lb}_m$$

$$1 \text{ ton (long)} = 2240 \text{ lb}_m$$

$$1 \text{ ton (metric)} = 1000 \text{ kg}$$

Table A.1-5. *Standard Acceleration of Gravity*

$$g = 9.80665 \text{ m/s}^2$$

$$g = 980.665 \text{ cm/s}^2$$

$$g = 32.174 \text{ ft/s}^2$$

$$g_c \text{ (gravitational conversion factor)} = 32.1740 \text{ lb}_m \cdot \text{ft/lbf} \cdot \text{s}^2$$

$$= 980.665 \text{ g}_m \cdot \text{cm/gf} \cdot \text{s}^2$$

### Table A.1-6. *Volume*



### Table A.1-7. *Force*

$$1 \text{ g} \cdot \text{cm/s}^2 \text{ (dyn)} = 10^{-5} \text{ kg} \cdot \text{m/s}^2 = 10^{-5} \text{ N (newton)}$$

$$1 \text{ g} \cdot \text{cm/s}^2 = 7.2330 \times 10^{-5} \text{ lb}_m \cdot \text{ft/s}^2 \text{ (poundal)}$$

$$1 \text{ kg} \cdot \text{m/s}^2 = 1 \text{ N (newton)}$$

$$1 \text{ lbf} = 4.4482 \text{ N}$$

$$1 \text{ g} \cdot \text{cm/s}^2 = 2.2481 \times 10^{-6} \text{ lbf}$$

### Table A.1-8. *Pressure*

$$1 \text{ bar} = 1 \times 10^5 \text{ Pa (pascal)} = 1 \times 10^5 \text{ N/m}^2$$

$$1 \text{ psia} = 1 \text{ lbf/in.}^2$$

$$1 \text{ psia} = 2.0360 \text{ in. Hg at } 0^\circ\text{C}$$

$$1 \text{ psia} = 2.311 \text{ ft H}_2\text{O at } 70^\circ\text{F}$$

$$1 \text{ psia} = 51.715 \text{ mmHg at } 0^\circ\text{C} (\rho_{\text{Hg}} = 13.5955 \text{ g/cm}^3)$$

$$1 \text{ atm} = 14.696 \text{ psia} = 1.01325 \times 10^5 \text{ N/m}^2 = 1.01325 \text{ bar}$$

$$1 \text{ atm} = 760 \text{ mmHg at } 0^\circ\text{C} = 1.01325 \times 10^5 \text{ Pa} = 1.01325 \times 10^2 \text{ kPa}$$

$$1 \text{ atm} = 29.921 \text{ in. Hg at } 0^{\circ}\text{C}$$

$$1 \text{ atm} = 33.90 \text{ ft H}_2\text{O at } 4^{\circ}\text{C}$$

$$1 \text{ psia} = 6.89476 \times 10^4 \text{ g/cm} \cdot \text{s}^2$$

$$1 \text{ psia} = 6.89476 \times 10^4 \text{ dyn/cm}^2$$

$$1 \text{ dyn/cm}^2 = 2.0886 \times 10^{-3} \text{ lbf/ft}^2$$

$$1 \text{ psia} = 6.89476 \times 10^3 \text{ N/m}^2 = \\ 6.89476 \times 10^3 \text{ Pa}$$

$$1 \text{ lbf/ft}^2 = 4.7880 \times 10^2 \text{ dyn/cm}^2 = \\ 47.880 \text{ N/m}^2$$

$$1 \text{ mmHg (} 0^{\circ}\text{C)} = 1.333224 \times 10^2 \text{ N/} \\ \text{m}^2 = 0.1333224 \text{ kPa}$$

Table A.1-9. *Power*

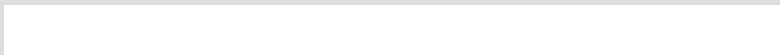


Table A.1-10. *Heat, Energy, Work*

$$1 \text{ J} = 1 \text{ N} \cdot \text{m} = 1 \text{ kg} \cdot \text{m}^2/\text{s}^2$$

$$1 \text{ kg} \cdot \text{m}^2/\text{s}^2 = 1 \text{ J (joule)} = 10^7 \text{ g} \cdot \text{cm}^2/\text{s}^2 \text{ (erg)}$$

$$1 \text{ btu} = 1055.06 \text{ J} = 1.05506 \text{ kJ}$$

$$1 \text{ btu} = 252.16 \text{ cal (thermochemical)}$$

$$1 \text{ kcal (thermochemical)} = 1000 \text{ cal} \\ = 4.1840 \text{ kJ}$$

$$1 \text{ cal (thermochemical)} = 4.1840 \text{ J}$$

$$1 \text{ cal (IT)} = 4.1868 \text{ J}$$

$$1 \text{ btu} = 251.996 \text{ cal (IT)}$$

$$1 \text{ btu} = 778.17 \text{ ft} \cdot \text{lbf}$$

$$1 \text{ hp} \cdot \text{h} = 0.7457 \text{ kW} \cdot \text{h}$$

$$1 \text{ hp} \cdot \text{h} = 2544.5 \text{ btu}$$

$$1 \text{ ft} \cdot \text{lbf} = 1.35582 \text{ J}$$

$$1 \text{ ft} \cdot \text{lbf/lb}_m = 2.9890 \text{ J/kg}$$

Table A.1-11. *Thermal Conductivity*

$$1 \text{ btu/h} \cdot \text{ft} \cdot ^\circ\text{F} = 4.1365 \times 10^{-3} \text{ cal/s} \\ \cdot \text{cm} \cdot ^\circ\text{C}$$

$$1 \text{ btu/h} \cdot \text{ft} \cdot ^\circ\text{F} = 1.73073 \text{ W/m} \cdot \text{K}$$

Table A.1-12. *Heat-Transfer Coefficient*

$$1 \text{ btu/h} \cdot \text{ft}^2 \cdot ^\circ\text{F} = 1.3571 \times 10^{-4} \text{ cal/s} \\ \cdot \text{cm}^2 \cdot ^\circ\text{C}$$

$$1 \text{ btu/h} \cdot \text{ft}^2 \cdot ^\circ\text{F} = 5.6783 \times 10^{-4} \text{ W/} \\ \text{cm}^2 \cdot ^\circ\text{C}$$

$$1 \text{ btu/h} \cdot \text{ft}^2 \cdot ^\circ\text{F} = 5.6783 \text{ W/m}^2 \cdot \text{K}$$

$$1 \text{ kcal/h} \cdot \text{m}^2 \cdot ^\circ\text{F} = 0.2048 \text{ btu/h} \cdot \text{ft}^2 \cdot ^\circ\text{F}$$

Table A.1-13. *Viscosity*

$$1 \text{ cp} = 10^{-2} \text{ g/cm} \cdot \text{s} \text{ (poise)}$$

$$1 \text{ cp} = 2.4191 \text{ lb}_\text{m}/\text{ft} \cdot \text{h}$$

$$1 \text{ cp} = 6.7197 \times 10^{-4} \text{ lb}_\text{m}/\text{ft} \cdot \text{s}$$

$$1 \text{ cp} = 10^{-3} \text{ Pa} \cdot \text{s} = 10^{-3} \text{ kg/m} \cdot \text{s} = 10^{-3} \text{ N} \cdot \text{s}/\text{m}^2$$

$$1 \text{ cp} = 2.0886 \times 10^{-5} \text{ lb}_\text{f} \cdot \text{s}/\text{ft}^2$$

$$1 \text{ Pa} \cdot \text{s} = 1 \text{ N} \cdot \text{s}/\text{m}^2 = 1 \text{ kg/m} \cdot \text{s} = 1000 \text{ cp} = 0.67197 \text{ lb}_\text{m}/\text{ft} \cdot \text{s}$$

Table A.1-14. *Diffusivity*

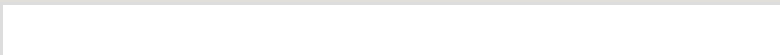




Table A.1-15. *Mass Flux and Molar Flux*

$$1 \text{ g/s} \cdot \text{cm}^2 = 7.3734 \times 10^3 \text{ lb}_\text{m}/\text{h} \cdot \text{ft}^2$$

$$1 \text{ g mol/s} \cdot \text{cm}^2 = 7.3734 \times 10^3 \text{ lb mol/h} \cdot \text{ft}^2$$

$$1 \text{ g mol/s} \cdot \text{cm}^2 = 10 \text{ kg mol/s} \cdot \text{m}^2 = 1 \times 10^4 \text{ g mol/s} \cdot \text{m}^2$$

$$1 \text{ lb mol/h} \cdot \text{ft}^2 = 1.3562 \times 10^{-3} \text{ kg mol/s} \cdot \text{m}^2$$

Table A.1-16. *Heat Flux and Heat Flow*

$$1 \text{ btu/h} \cdot \text{ft}^2 = 3.1546 \text{ W/m}^2$$

$$1 \text{ btu/h} = 0.29307 \text{ W}$$

$$1 \text{ cal/h} = 1.1622 \times 10^{-3} \text{ W}$$

Table A.1-17. *Heat Capacity and Enthalpy*

$$1 \text{ btu/lb}_m \cdot ^\circ\text{F} = 4.1868 \text{ kJ/kg} \cdot \text{K}$$

$$1 \text{ btu/lb}_m \cdot ^\circ\text{F} = 1.000 \text{ cal/g} \cdot ^\circ\text{C}$$

$$1 \text{ btu/lb}_m = 2326.0 \text{ J/kg}$$

$$1 \text{ ft} \cdot \text{lbf/lb}_m = 2.9890 \text{ J/kg}$$

$$1 \text{ cal (IT)/g} \cdot ^\circ\text{C} = 4.1868 \text{ kJ/kg} \cdot \text{K}$$

$$1 \text{ kcal/g mol} = 4.1840 \times 10^3 \text{ kJ/kg mol}$$

Table A.1-18. *Mass-Transfer Coefficient*

$$1 \text{ } k_c \text{ cm/s} = 10^{-2} \text{ m/s}$$

$$1 \text{ } k_c \text{ ft/h} = 8.4668 \times 10^{-5} \text{ m/s}$$

$$1 \text{ } k_x \text{ g mol/s} \cdot \text{cm}^2 \cdot \text{mol frac} = 10 \text{ kg}$$

$$\text{mol/s} \cdot \text{m}^2 \cdot \text{mol frac}$$

$$1 \text{ } k_x \text{ g mol/s} \cdot \text{cm}^2 \cdot \text{mol frac} = 1 \times 10^4 \text{ g mol/s} \cdot \text{m}^2 \cdot \text{mol frac}$$

$$1 \text{ } k_x \text{ lb mol/h} \cdot \text{ft}^2 \cdot \text{mol frac} = 1.3562 \times 10^{-3} \text{ kg mol/s} \cdot \text{m}^2 \cdot \text{mol frac}$$

$$1 \text{ } k_x \text{ a lb mol/h} \cdot \text{ft}^3 \cdot \text{mol frac} = 4.449 \times 10^{-3} \text{ kg mol/s} \cdot \text{m}^3 \cdot \text{mol frac}$$

$$1 \text{ } kG \text{ kg mol/s} \cdot \text{m}^2 \cdot \text{atm} = 0.98692 \times 10^{-5} \text{ kg mol/s} \cdot \text{m}^2 \cdot \text{Pa}$$

$$1 \text{ } kG \text{ a kg mol/s} \cdot \text{m}^3 \cdot \text{atm} = 0.98692 \times 10^{-5} \text{ kg mol/s} \cdot \text{m}^3 \cdot \text{Pa}$$

Table A.1-19. *Temperature*

$$0^\circ\text{C} = 32^\circ\text{F} \text{ (freezing point of water)}$$

$$1.0 \text{ K} = 1.0^\circ\text{C} = 1.8^\circ\text{F} = 1.8^\circ\text{R}$$

(Rankine)

$$^{\circ}\text{F} = 32 + 1.8 (^{\circ}\text{C})$$

$$^{\circ}\text{C} = (1/1.8)(^{\circ}\text{F} - 32)$$

$$^{\circ}\text{R} = ^{\circ}\text{F} + 459.67$$

$$\text{K} = ^{\circ}\text{C} + 273.15$$

$$100^{\circ}\text{C} = 212^{\circ}\text{F} = 373.15 \text{ K} = 671.67^{\circ}\text{R}$$

$$0^{\circ}\text{C} = 32^{\circ}\text{F} = 273.15 \text{ K} = 491.67^{\circ}\text{R}$$

$$-273.15^{\circ}\text{C} = -459.67^{\circ}\text{F} = 0 \text{ K} = 0^{\circ}\text{R}$$

(absolute zero)

## Appendix A.2. Physical Properties of Water

Table A.2-1. *Latent Heat of Water at 273.15 K (0°C)*

--	--

Source: O. A. Hougen, K. M. Watson, and R. A. Ragatz, *Chemical Process Principles*, Part I, 2nd ed. New York: John Wiley & Sons, Inc., 1954.

Latent heat of vaporization at 298.15 K (25°C)

--	--

Source: National Bureau of Standards, *Circular 500*.

Table A.2-2. *Vapor Pressure of Water*

--	--

Source: Physikalisch-technische, Reichsansalt, Holborn, Scheel, and Henning, *Wärmstabellen*. Brunswick, Germany: Friedrich Viewig and Son, 1909.

## Table A.2-3. *Density of Liquid Water*

--

*Source:* R. H. Perry and C. H. Chilton, *Chemical Engineers' Handbook*, 5th ed. New York: McGraw-Hill Book Company, 1973. With permission.

## Table A.2-4. *Viscosity of Liquid Water*

--

*Source:* Bingham, *Fluidity and Plasticity*. New York: McGraw-Hill Book Company, 1922. With permission.

## Table A.2-5. *Heat Capacity of Liquid Water at 101.325 kPa (1 Atm)*

--

*Source:* N. S. Osborne, H. F. Stimson, and D. C. Ginnings, *Bur. Standards J. Res.*, **23**, 197 (1939).

## Table A.2-6. *Thermal Conductivity of Liquid Water*

--

*Source:* D. L. Timrot and N. B. Vargaftik, *J. Tech. Phys.* (U.S.S.R.), **10**, 1063 (1940); 6th International Conference on the Properties of Steam,

Paris, 1964.

## Table A.2-7. *Vapor Pressure of Saturated Ice–Water Vapor and Heat of Sublimation*

--

Source: ASHRAE, *Handbook of Fundamentals*. New York: ASHRAE, 1972.

## Table A.2-8. *Heat Capacity of Ice*

--

Source: Adapted from ASHRAE, *Handbook of Fundamentals*. New York: ASHRAE, 1972.

## Table A.2-9a. *Properties of Saturated Steam and Water (Steam Table), SI Units*

--

Source: Data from ASME *Steam Tables, Compact Edition*, © 2006 ASME.

## Table A.2-9b. *Properties of Saturated*

# *Steam and Water (Steam Table), English Units*

Source: Data from ASME Steam Tables, Compact Edition, © 2006 ASME.

Table A.2-10a. *Properties of Superheated Steam (Steam Table), SI Units ( $v$ , specific volume  $m^3/kg$ ;  $H$ , enthalpy,  $kJ/kg$ ;  $s$ , entropy,  $kJ/kg \cdot K$ )*

Source: Data from ASME Steam Tables, Compact Edition, © 2006 ASME.

Table A.2-10b. *Properties of Superheated Steam (Steam Table), English Units ( $v$ , specific volume,  $ft^3/lbm$ ;  $H$ , enthalpy,  $btu/lbm$ ;  $s$ , entropy,  $btu/lbm \cdot ^\circ F$ )*



## Table A.2-11a. Heat-Transfer Properties of Liquid Water, SI Units

--

## Table A.2-11b. *Heat-Transfer Properties of Liquid Water, English Units*

--

## Table A.2-12a. *Heat-Transfer Properties of Water Vapor (Steam) at 101.32 kPa (1 Atm Abs), SI Units*

--

## Table A.2-12b. *Heat-Transfer Properties of Water Vapor (Steam) at 101.32 kPa (1 Atm Abs), English Units*

--

Source: D. L. Timrot and N. B. Vargaftik, *J. Tech. Phys.* (U.S.S.R.), **10**, 1063 (1940); R. H. Perry and C. H. Chilton, *Chemical Engineers' Handbook*, 5th ed. New York: McGraw-Hill Book Company, 1973; J. H. Keenan, F. G. Keyes, P. G. Hill, and J. G. Moore, *Steam Tables*. New York: John Wiley & Sons, Inc., 1969; National Research Council, *International Critical Tables*. New York: McGraw-Hill Book Company, 1929; L. S. Marks, *Mechanical Engineers' Handbook*, 5th ed. New York: McGraw-Hill Book Company, 1951.

## Appendix A.3. Physical Properties of Inorganic and Organic Compounds

Table A.3-1. *Standard Heats of Formation at 298.15 K (25°C) and 101.325 kPa (1 Atm Abs), (c) = crystalline, (g) = gas, (l) = liquid*

Source: J. H. Perry and C. H. Chilton, *Chemical Engineers' Handbook*, 5th ed. New York: McGraw-Hill Book Company, 1973; and O. A. Hougen, K. M. Watson, and R. A. Ragatz, *Chemical Process Principles*, Part I, 2nd ed. New York: John Wiley & Sons, Inc., 1954.

Table A.3-2. *Standard Heats of Combustion at 298.15 K (25°C) and 101.325 kPa (1 Atm Abs) (g) = gas, (l) = liquid, (s) = solid*

Source: R. H. Perry and C. H. Chilton, *Chemical Engineers' Handbook*,

5th ed. New York: McGraw-Hill Book Company, 1973; and O. A. Hougen, K. M. Watson, and R. A. Ragatz, *Chemical Process Principles, Part I*, 2nd ed. New York: John Wiley & Sons, Inc., 1954.

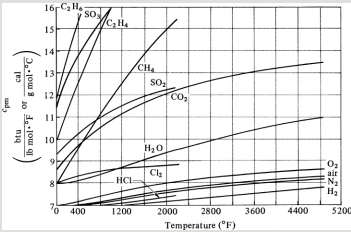


Figure A.3-1. Mean molar heat capacities from 77°F (25°C) to t°F at constant pressure of 101.325 kPa (1 atm abs). (From O. A. Hougen, K. M. Watson, and R. A. Ragatz, *Chemical Process Principles, Part I*, 2nd ed. New York: John Wiley & Sons, Inc., 1954. With permission.)

Table A.3-3a. *Physical Properties of Air at 101.325 kPa (1 Atm Abs), SI Units*

--

Table A.3-3b. *Physical Properties of Air at 101.325 kPa (1 Atm Abs), English Units*

--

Source: National Bureau of Standards, Circular **461C**, 1947; **564**, 1955; NBS–NACA, *Tables of Thermal Properties of Gases*, 1949; F. G. Keyes, *Trans. A.S.M.E.*, **73**, 590, 597 (1951); **74**, 1303 (1952); D. D. Wagman,

*Selected Values of Chemical Thermodynamic Properties.* Washington, D.C.: National Bureau of Standards, 1953.

### Table A.3-4. *Viscosity of Gases at 101.325 kPa (1 Atm Abs) [Viscosity in ( $\text{Pa} \cdot \text{s}$ ) $10^3$ , ( $\text{kg/m} \cdot \text{s}$ ) $10^3$ , or cp]*

*Source:* National Bureau of Standards, Circular **461C**, 1947; **564**, 1955; NBS–NACA, *Tables of Thermal Properties of Gases*, 1949; F. G. Keyes, *Trans. A.S.M.E.*, **73**, 590, 597 (1951); **74**, 1303 (1952); D. D. Wagman, *Selected Values of Chemical Thermodynamic Properties.* Washington, D.C.: National Bureau of Standards, 1953.

### Table A.3-5. *Thermal Conductivity of Gases at 101.325 kPa (1 Atm Abs)*

*Source:* National Bureau of Standards, Circular **461C**, 1947; **564**, 1955; NBS–NACA, *Table of Thermal Properties of Gases*, 1949; F. G. Keyes, *Trans. A.S.M.E.*, **73**, 590, 597 (1951); **74**, 1303 (1952); D. D. Wagman, *Selected Values of Chemical Thermodynamic Properties.* Washington, D.C.: National Bureau of Standards, 1953.

### Table A.3-6. *Heat Capacity of Gases at Constant Pressure at 101.325 kPa (1 Atm Abs)*

Source: National Bureau of Standards, Circular **461C**, 1947; **564**, 1955; NBS–NACA, *Tables of Thermal Properties of Gases*, 1949; F. G. Keyes, *Trans. A.S.M.E.*, **73**, 590, 597 (1951); **74**, 1303 (1952); D. D. Wagman, *Selected Values of Chemical Thermodynamic Properties*. Washington, D.C.: National Bureau of Standards, 1953.

# Table A.3-7. Prandtl Number of Gases at 101.325 kPa (1 Atm Abs)

Source: National Bureau of Standards, Circular **461C**, 1947; **564**, 1955; NBS–NACA, *Tables of Thermal Properties of Gases*, 1949; F. G. Keyes, *Trans. A.S.M.E.*, **73**, 590, 597 (1951); **74**, 1303 (1952); D. D. Wagman, *Selected Values of Chemical Thermodynamic Properties*. Washington, D.C.: National Bureau of Standards, 1953.

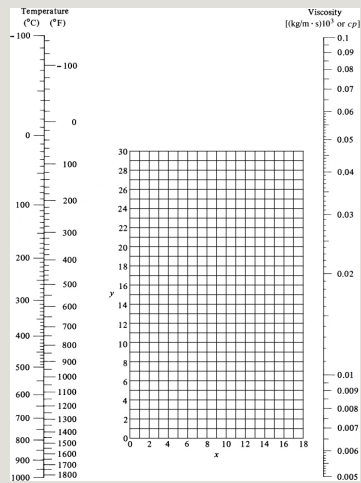


Figure A.3-2. Viscosities of gases at 101.325 kPa (1 atm abs). (From R. H. Perry and C. H. Chilton, *Chemical Engineers' Handbook*, 5th ed. New York: McGraw-Hill Book Company, 1973. With permission.) See Table

Table A.3-8. *Viscosities of Gases*  
(Coordinates for Use with Fig. A.3-2)

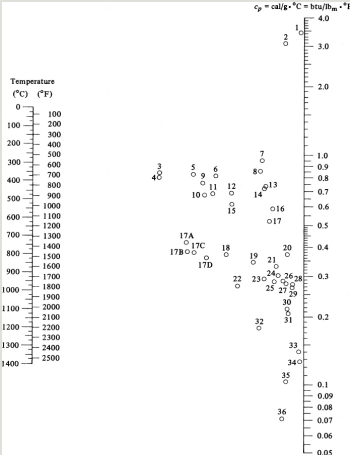


Figure A.3-3. Heat capacity of gases at constant pressure at 101.325 kPa (1 atm abs). (From R. H. Perry and C. H. Chilton, *Chemical Engineers' Handbook*, 5th ed. New York: McGraw-Hill Book Company, 1973. With permission.) See Table A.3-9 for use with Fig. A.3-3.

Table A.3-9. *Heat Capacity of Gases at Constant Pressure* (for Use with Fig. A.3-3)



## Table A.3-10. *Thermal Conductivities of Gases and Vapors at 101.325 kPa (1 Atm Abs); $k = W/m \cdot K$*

--

*Source:* (1) Moser, dissertation, Berlin, 1913; (2) F. G. Keyes, *Tech. Rept.* 37, Project Squid, Apr. 1, 1952; (3) W. B. Mann and B. G. Dickens, *Proc. Roy. Soc. (London)*, **A134**, 77 (1931); (4) *International Critical Tables*. New York: McGraw-Hill Book Company, 1929; (5) T. H. Chilton and R. P. Genereaux, personal communication, 1946; (6) A. Eucken, *Physik, Z.*, **12**, 1101 (1911); **14**, 324 (1913); (7) B. G. Dickens, *Proc. Roy. Soc. (London)*, **A143**, 517 (1934).

## Table A.3-11. *Heat Capacities of Liquids ( $c_p = kJ/kg \cdot K$ )*

--

*Source:* N. A. Lange, *Handbook of Chemistry*, 10th ed. New York: McGraw-Hill Book Company, 1967; National Research Council, *International Critical Tables*, Vol. V. New York: McGraw-Hill Book Company, 1929; R. H. Perry and C. H. Chilton, *Chemical Engineers' Handbook*, 5th ed. New York: McGraw-Hill Book Company, 1973.



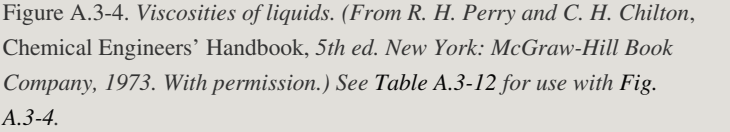


Table A.3-12. *Viscosities of Liquids*  
(Coordinates for Use with Fig. A.3-4)

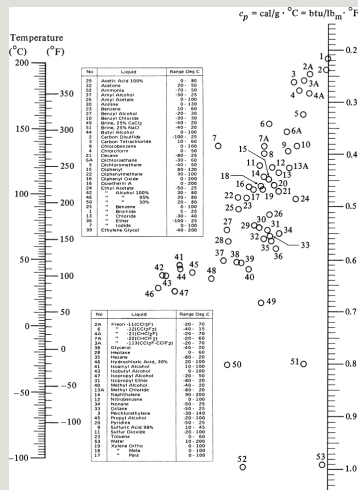


Figure A.3-5. Heat capacity of liquids. (From R. H. Perry and C. H. Chilton, *Chemical Engineers' Handbook*, 5th ed. New York: McGraw-Hill Book Company, 1973. With permission.)

## Table A.3-13. Thermal Conductivities of Liquids ( $k = W/m \cdot K$ )\*

\*A linear variation with temperature may be assumed between the temperature limits given.

Source: R. H. Perry and C. H. Chilton, *Chemical Engineers' Handbook*, 5th ed. New York: McGraw-Hill Book Company, 1973. With permission.

## Table A.3-14. Heat Capacities of Solids ( $c_p = kJ/kg \cdot K$ )

Source: R. H. Perry and C. H. Chilton, *Chemical Engineers' Handbook*, 5th ed. New York: McGraw-Hill Book Company, 1973; National Research Council, *International Critical Tables*, Vol. V. New York: McGraw-Hill Book Company, 1929; L. S. Marks, *Mechanical Engineers' Handbook*, 5th ed. New York: McGraw-Hill Book Company, 1951; F. Kreith, *Principles of Heat Transfer*, 2nd ed. Scranton, Pa.: International Textbook Co., 1965.

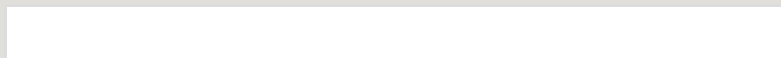
## Table A.3-15. *Thermal Conductivities of Building and Insulating Materials*



\*Room temperature when none is noted.

Source: L. S. Marks, *Mechanical Engineers' Handbook*, 5th ed. New York: McGraw-Hill Book Company, 1951; W. H. McAdams, *Heat Transmission*, 3rd ed. New York: McGraw-Hill Book Company, 1954; F. H. Norton, *Refractories*. New York: McGraw-Hill Book Company, 1949; National Research Council, *International Critical Tables*. New York: McGraw-Hill Book Company, 1929; M. S. Kersten, *Univ. Minn. Eng. Ex. Sta., Bull.* 28, June 1949; R. H. Heilman, *Ind. Eng. Chem.*, **28**, 782 (1936).

## Table A.3-16. *Thermal Conductivities, Densities, and Heat Capacities of Metals*



Source: L. S. Marks, *Mechanical Engineers' Handbook*, 5th ed. New York: McGraw-Hill Book Company, 1951; E. R. G. Eckert and R. M.

Drake, *Heat and Mass Transfer*, 2nd ed. New York: McGraw-Hill Book Company, 1959; R. H. Perry and C. H. Chilton, *Chemical Engineers' Handbook*, 5th ed. New York: McGraw-Hill Book Company, 1973; National Research Council, *International Critical Tables*. New York: McGraw-Hill Book Company, 1929.

## Table A.3-17. *Normal Total Emmissivities of Surfaces*

*Source:* R. H. Perry and C. H. Chilton, *Chemical Engineers' Handbook*, 5th ed. New York: McGraw-Hill Book Company, 1973; W. H. McAdams, *Heat Transmission*, 3rd ed. New York: McGraw-Hill Book Company, 1954; E. Schmidt, *Gesundh.-Ing. Beiheft*, **20**, Reihe 1, 1 (1927).

## Table A.3-18. *Henry's Law Constants for Gases in Water ( $H \times 10^{-4}$ )\**

\* $p_A = Hx_A$ ,  $p_A$  = partial pressure of A in gas in atm,  $x_A$  = mole fraction of A in liquid,  $H$  = Henry's law constant in atm/mole frac.

*Source:* National Research Council, *International Critical Tables*, Vol. III. New York: McGraw-Hill Book Company, 1929.

## Table A.3-19. *Equilibrium Data for SO<sub>2</sub>–Water System*

Source: T. K. Sherwood, *Ind. Eng. Chem.*, **17**, 745 (1925).

### Table A.3-20. *Equilibrium Data for Methanol–Water System*

Source: National Research Council, *International Critical Tables*, Vol. III. New York: McGraw-Hill Book Company, 1929.

### Table A.3-21. *Equilibrium Data for Acetone–Water System at 20°C (293 K)*

Source: T. K. Sherwood, *Absorption and Extraction*. New York: McGraw-Hill Book Company, 1937.

### Table A.3-22. *Equilibrium Data for Ammonia–Water System*

Source: J. H. Perry, *Chemical Engineers' Handbook*, 4th ed. New York: McGraw-Hill Book Company, 1963. With permission.

### Table A.3-23. *Equilibrium Data for*

## *Ethanol–Water System at 101.325 kPa (1 Atm)\**

\*Reference state for enthalpy is pure liquid at 273 K or 0°C.

*Source:* Data from L. W. Cornell and R. E. Montonna, *Ind. Eng. Chem.*, **25**, 1331 (1933); and W. A. Noyes and R. R. Warfel, *J. Am. Chem. Soc.*, **23**, 463 (1901), as given by G. G. Brown, *Unit Operations*. New York: John Wiley & Sons, Inc., 1950. With permission.

## *Table A.3-24. Acetic Acid–Water– Isopropyl Ether System, Liquid–Liquid Equilibria at 293 K or 20°C*

*Source:* *Trans. A.I.Ch.E.*, **36**, 601, 628 (1940). With permission.

## *Table A.3-25. Liquid–Liquid Equilibrium Data for Acetone–Water– Methyl Isobutyl Ketone (MIK) System at 298–299 K or 25–26°C*

*Source:* Reprinted with permission from D. F. Othmer, R. E. White, and

E. Trueger, *Ind. Eng. Chem.*, **33**, 1240 (1941). Copyright by the American Chemical Society.

## Appendix A.4. Physical Properties of Foods and Biological Materials

Table A.4-1. *Heat Capacities of Foods*  
(Average  $c_p$  273–373 K or 0–100°C)

--	--

--	--

Source: W. O. Ordinanz, *Food Ind.*, **18**, 101 (1946); G. A. Reidy, Department of Food Science. Michigan State University, 1968; S. E. Charm, *The Fundamentals of Food Engineering*, 2nd ed. Westport, Conn.: Avi Publishing Co., Inc., 1971; R. L. Earle, *Unit Operations in Food Processing*. Oxford: Pergamon Press, Inc., 1966; ASHRAE, *Handbook of Fundamentals*. New York: ASHRAE, 1972, 1967; H. C. Mannheim, M. P. Steinberg, and A. I. Nelson, *Food Technol.*, **9**, 556 (1955).

Table A.4-2. *Thermal Conductivities, Densities, and Viscosities of Foods*

--	--

Source: R. C. Weast, *Handbook of Chemistry and Physics*, 48th ed. Cleveland: Chemical Rubber Co., Inc., 1967; C. P. Lentz, *Food Technol.*,



**15**, 243 (1961); G. A. Reidy, Department of Food Science, Michigan State University, 1968; S. E. Charm, *The Fundamentals of Food Engineering*, 2nd ed. Westport, Conn.: Avi Publishing Co., Inc., 1971; R. Earle, *Unit Operations in Food Processing*. Oxford: Pergamon Press, 1966; R. H. Perry and C. H. Chilton, *Chemical Engineers' Handbook*, 5th ed. New York: McGraw-Hill Book Company, 1973; V. E. Sweat, *J. Food Sci.*, **39**, 1080 (1974).

## Appendix A.5. Properties of Pipes, Tubes, and Screens

Table A.5-1. *Dimensions of Standard Steel Pipe*

--

Table A.5-2. *Dimensions of Heat-Exchanger Tubes*

--

Table A.5-3. *Tyler Standard Screen Scale*

--

## Appendix A.6. Lennard-Jones Potentials as Determined from Viscosity Data

Source: E. Poling, J. M. Prausnitz, and J. P. O'Connell, *The Properties of Gases and Liquids*, 5th ed. New York: McGraw-Hill Education, 2000.

## Notation

SI units are given first (followed by English and/or cgs units).

*Greek letters*

## Index

### A

Absolute degrees, 8

Absolute pressure, 10

Absorption and stripping, 627

acetone in countercurrent stage towers,  
633–634

concentration profiles in interphase mass  
transfer, 637–638

countercurrent multiple-contact stages,  
631–633

countercurrent stage contact equations,  
634–636

description, 4–5

equilibrium relations, 636–637

equipment for, 646–649

film mass-transfer coefficients and  
interface concentrations, 638–642

gas–liquid equilibrium, 628–629

heat effects, 682–685

introduction, 645

mass-transfer coefficients and driving  
forces, 642–645

notation, 692–693

packed tower design

dilute gas mixtures, 662–667

introduction, 656–662

using transfer units, 668–672

packed towers

concentrated mixtures in, 675–679

mass-transfer coefficients, 679–682

pressure drop and flooding, 649–654

phase rule and equilibrium, 627–628

plate absorption towers, 654–656

problems, 686–691

of radiation by gas, 479–482

random-packed and structured packed  
tower efficiency, 672–674

references, 691–692

single-stage equilibrium contacts, 629–631

sulfur dioxide in tray towers, 655–656

summary, 685–686

Absorption carbon, void fraction for, 157

Absorptivity

and black bodies, 284–285, 462

gases, 480

radiation heat transfer, 468–469

Acceleration of gravity, 1108

Accumulation



conservation of mass, 13, 62

continuity equations, 199–200

energy balances, 68–69

mass balances, 64–66

momentum balances, 81–82, 86

steady-state heat transfer, 277

unsteady-state mass transfer diffusion,  
569

Acetic acid ( $\text{CH}_3\text{COOH}$ )

diffusion coefficient, 500

equilibrium data, 876–877, 885

ethanol–water systems, 1145

heat capacity, 1135

Acetic acid–water–isopropyl ether  
systems, liquid–liquid equilibria data  
for, 1146

Acetone ( $\text{CH}_3\text{COCH}_3$ )

absorption

in countercurrent stage towers, 633–634

in packed towers, 664–667

diffusion coefficient, 501

extraction from water with  
trichloroethane, 899–901

heat capacity, 1135

thermal conductivity, 1135

water system equilibrium data, 1144

Acetone–water–methyl isobutyl ketone  
systems, liquid–liquid equilibria data  
for, 1146

Acid solutions, cupric ion removal from,  
921–922

Activated alumina adsorbents, 908

Activated carbon

adsorbents, 908

batch adsorption on, 911

Adiabatic compression

flow, 128–129

gas-moving pumps, 175

Adiabatic saturation of air, 701

Adiabatic saturation temperatures

drying, 1046–1047

humidification, 700–701

Adiabatic water cooling, 705–706

Adsorption

adsorbents

equilibrium relations, 908–909

physical properties, 908

batch, 910–911

description, 5

fixed-bed adsorption columns, 912–917

introduction, 907–908

notation, 927

phenol in wastewater, 910

prediction models, 917

problems, 925–926

processing variables and cycles, 918

references, 926–927

summary, 924

Affinity laws for centrifugal pumps, 170

Agar

diffusion of urea in, 545–546

unsteady-state diffusion in, 573–574

Agitated-film evaporators

description, 1006

heat-transfer coefficients, 1009

Agitated solid leaching, 989–990

Agitation

equipment for, 177–179

flow number and circulation rate, 189

flow patterns, 179–180

heat transfer in, 427–430

mixing of powders, viscous materials,  
and pastes, 191–192

mixing times of miscible liquids, 186–  
189

notation, 195

power requirements

agitated vessels, 180–183

non-Newtonian fluids, 234–235

problems, 193–194

purposes, 176–177

references, 194–195

scale-up, 183–186

special systems, 189–190

summary, 192

turbine design, 180

Air

adiabatic saturation of, 701, 1047

carbon dioxide pressure in, 686

composition, 29

continuous dryer recirculation, 1081–  
1082

diffusion coefficients, 495

diffusion of water through, 523

diffusivity and permeability, 535

equilibrium stage contact, 630–631

gaseous membrane systems, 769

heat-transfer coefficient, 283

heating



by banks of tubes, 406–407

in turbulent flow, 396–397

molar heat capacity, 18–19, 267–268

physical properties, 1126

separation, 789–793

thermal conductivity, 280

tray drying with, 1078–1079

viscosity, 54

water-cooling towers, 710–711

Air bubbles in fermentation, 611–612

Air velocity in constant-rate drying  
period, 1061

Air–water vapor mixture

characteristics, 697–698

dew point, 1042

humid heat, 1043

wet bulb temperature, 703

Albumin, prediction of diffusivity of,  
507

Alcohols vapor-pressure data, 870

Aluminum (Al)

diffusivity and permeability, 535

emissivity, 286, 463

Ammonia (NH<sub>3</sub>)

absorption, 652–654

diffusion coefficient, 500

thermal conductivity, 1135

water system equilibrium data, 1144

Analytical equations

conduction, 318–320

countercurrent stage contact, 634–636

packed towers, 658–659, 670–672

Analytical methods for unsteady-state  
conduction, 337–339

Anchor agitators with no baffles, heat  
transfer in, 428

Angle valves, friction losses in, 117

Aniline heat capacity, 1135

Animal materials, leaching, 985

Anion exchangers, 920

Anionic groups in ion exchange, 919

Annulus laminar flow, 212–213

Anthracite coal void fractions, 157

Artificial kidneys, 750

Asymmetric membranes in gaseous systems

cocurrent flow equations, 784

concentration gradients, 779–780

countercurrent flow for air separation, 789–793

process flow patterns, 786

types, 760

Attrition of solids, 943

Average collision diameter in gas  
diffusion coefficients, 496

Average temperature in objects with  
negligible surface resistance, 354–355

Average velocity for mass balances

overview, 67–68

in turbulent flow, 98

Axial flow in three-blade propeller  
agitators, 177

Bacillus stearothermophilus, 1088

Backward-feed multiple-effect  
evaporators, 1008

Baffles in agitation, 180

Banks of tubes or cylinders, flow past  
convection heat transfer, 405–406  
heating air by, 406–407

Barometric condensers, 1026–1027

Basket type short-tube evaporators,  
1005

Batch adsorption, 910–911

Batch distillation, 815–817

Batch filters, 717

Batch leaching, time for, 987–988

Batch processes, filtration rate for, 725–726

Bed filters, 718

Beef, chilling, 368–369

Benzene ( $C_6H_6$ )

diffusion, 521

heat capacity, 1135

viscosity, 54

Benzene–toluene systems

boiling-point diagrams, 806–808

enthalpy-concentration plots, 842–844,  
846–850

rectification, 825–827

relative volatility, 814

Benzoic acid ( $C_7H_6O_2$ ) diffusion  
coefficient, 500

Berl saddles

absorption and distillation, 648, 810–  
811

liquid–liquid extraction, 882

packing factors, 651

shape factors, 155

Bernoulli equation

fluid flow measurements, 129

mechanical-energy balance, 79–81



Binary mixtures, continuity equations for, 510–511

Binding in diffusion, 505, 508

Bingham plastic fluids

flow rate, 231–232

time-independence, 221–222

velocity profiles, 230–231

Biological gels, diffusion in, 544–546

Biological materials

chilling and freezing, 366–372

equilibrium moisture content, 1049

evaporation, 1028–1029

freeze-drying, 1084–1088

leaching processes, 985

unsteady-state thermal processing and  
sterilization, 1088–1095

Biological solutes in liquids, diffusion  
of, 505–508

Biot number in unsteady-state heat  
transfer, 335

Black bodies

and absorptivity, 284–285

radiation heat transfer, 462–463, 466–  
467

view factors between, 470–474

Black planes, radiation heat transfer in, 468–469

Blake crushers, 946

Blake–Kozeny equation

fluids through filter cakes, 723

laminar flow, 152

Blasius  $1/7$ -power-law velocity profile, 262

Blasius solution for convection, 390–391

Blenders for agitation, 191

Blood, urea removal from, 750–751

Blowers for gas-moving pumps, 174

Body force in momentum balance, 83

Boiling

film, 417

mechanisms, 415–416

nucleate, 416–417

Boiling point

distillation diagrams, 806–808

evaporation, 1004

liquids, 12–13

multicomponent distillation, 854

temperature, 8

Boiling-point rise of evaporator

solutions, 1013–1014

Bollman extractors, 989–990

Boltzmann equation for gas diffusion coefficients, 496

Bond's theory, 944–945

Botulinum, 1088–1091

Bound water in solids, equilibrium moisture content of materials in, 1051

Boundary conditions

condensation, 420

conduction equation, 324–325

continuity equations, 197, 207

convective mass transfer, 614

fin efficiency, 433

laminar flow, 253, 614

potential flow, 242–243

shell momentum balance, 92, 94–95

slabs, 355–358

steady-state mass transfer

flat plates, 570

numerical methods, 551–554

special cases, 546–549

turbulent flow, 261

unsteady-state conduction

analytical methods, 338–339

convective, 363–365

unsteady-state mass transfer

diffusion, 571–572

numerical methods, 578–579

semi-infinite medium, 576

Boundary-layer flow, 250

convection, 392–393

laminar flow

heat transfer, 389–393

mass transfer, 613–615, 617

overview, 252–254

notation, 264

overview, 251–252

problems, 263–264

references, 264

summary, 263–264

turbulent flow

analysis, 260–263

nature and intensity, 254–260

wake formation, 252

Bourdon pressure gages, 46

Brake power

centrifugal fans, 172–173

pumps, 167, 170–171



Break points for fixed-bed adsorption columns, 913

Breakthrough curves

fixed-bed adsorption columns, 913

ion exchange, 922

Brownian motion in particle movement through fluids, 955

Btus, 17, 265–266

Bubble-cap trays, 646, 809

Bubble-point lines in distillation, 806

Bubbling fluidization in fluidized beds, 156

Bubbling velocity in fluidized beds, 161

Buckingham–Reiner equation, 231

Buckingham theorem

convection, 387–389

mass-transfer coefficients, 594

Buffer layer in turbulent flow, 260

Buffer zones in turbulent flow, 258

Building materials, thermal  
conductivities of, 1141

Bulk velocity for flow between parallel  
plates, 98

Burke–Plummer equation, 153

Butane

heat capacity, 1135

thermal conductivity, 280, 1135

Butter, conduction in, 342–343, 346

Butyl alcohol heat capacity, 1135

## **C**

Cabinet dryers, 1036

Calcium carbonate ( $\text{CaCO}_3$ ) filtration,  
726–727

Calories, 17, 265–266

Cans of food, sterilizing, 1092

Cans of pea purée, transient heat  
conduction in, 346

Capacitance in unsteady-state heat  
transfer, 335

## Capacity

centrifugal pumps, 170

fixed-bed adsorption columns, 913–917

ion exchange columns, 922–924

multiple-effect evaporators, 1018

## Capillaries

diffusion of gases in, 537–544

falling-rate drying by flow in, 1068–1073

flux ratios for diffusion of gases in, 541

metering of flow, 108–109

rate-of-drying curves, 1056

## Carbon (C)

combustion, 22, 270–271

void fractions, 157

## Carbon dioxide (CO<sub>2</sub>)

absorption film coefficients, 681–682

concentration in water, 687

diffusion coefficients, 495, 500

diffusivity and permeability, 535

equilibrium stage contact, 630–631

molar heat capacity, 18–19, 267–268

permeability in symmetric membranes,  
761

pressure in air, 686

viscosity, 54

Carbon monoxide (CO)

combustion, 25–26

molar heat capacity, 18–19, 267–268

thermal conductivity, 1135

Carman–Kozeny relation for fluids  
through filter cakes, 723

Case hardening in rate-of-drying curves,  
1056

Cassava root, drying, 31

Cations in ion exchange, 919–920

Cavitation with pumps, 168

Celsius ( $^{\circ}\text{C}$ ) scale, 6, 8

Centi (c) prefix, 6

Centimeters (cm), 7

Centrifugal compressors in gas-moving pumps, 174

Centrifugal fans, brake power of, 172–173

Centrifugal pumps, 169–171

Centrifugal separation processes

filtration, 967, 975–977

forces, 967–969

gas–solid cyclone separators, 977–979

introduction, 966–967

sedimentation equipment, 975

settling in, 969–974

Ceramic Raschig rings, 648, 810–811

Cgs system units, 6–7

Change-can mixers for agitation, 192

Chapman–Enskog model, 281–282

Characteristic curves for centrifugal pumps, 169–171

Characteristic mean beam length of absorbing gases, 479–480

Check valves, friction losses in, 117–118

Chemical reactions



material balances, 16–17

molecular diffusion plus convection,  
508–511

steady-state mass transfer boundary  
conditions, 548–549

Chilling and freezing of food and  
biological materials

dressed beef, 368–369

introduction, 366–368

meat, 371

Plank solution, 369–372

Chilton and Colburn *J*-factor analogy,  
598

Chlorine, thermal conductivity of, 1135

Chocolate, rheological constants, 231

Chromatography in gel permeation, 733

Circular fins for heat transfer, 431

Circular tubes, laminar flow in, 211–212

Circulating-liquid evaporator–  
crystallizers, 934–935

Circulating liquid method in  
crystallization, 934

Circulating magma method in  
crystallization, 933–934

Circulating-magma vacuum  
crystallizers, 935

Circulation rate in agitation, 189

Classification

convective heat transfer, 386

crystallizers, 933–934

filters, 717–721

membrane processes, 732–733

particle size reduction equipment, 945

separation processes, 4–5

settling and separation of solids, 959–  
963, 965

*Clostridium botulinum*, 1088

Coal, void fractions, 157

Coal dust, pulverized, 155

Coal slurry, rheological constants, 231

Coaxial cylinders, flow between, 213–215

Cocurrent flow in gaseous membrane systems, 779–787

Coefficient of variation for crystals, 937

Colburn  $J$  factor, 408

Collision diameter in gas diffusion coefficients, 496

Colloids, 505

Combined radiation and convection heat transfer, 290–291

## Combustion

carbon, 22, 270–271

fuel gases, 16–17

heat and material balance, 25–26, 274–275

heat of, 22, 1125

Compartment dryers, 1036

Complete-mixing model

gaseous membrane systems, 765–770

reverse osmosis, 746–747

Compressible fluids, 37

Compressible gases

adiabatic flow, 128–129

equations, 125–126

isothermal flow, 126–128

## Compression

gases in gas-moving pumps, 174–176

solids, 943

Compressors in gas-moving pumps, 174

Concentrated mixtures in packed  
towers, absorption in, 675–679

Concentrated solutions, packed towers  
for, 668

## Concentration

in evaporation, 1003

orange juice, 14

Concentration gradients in gaseous  
membrane systems, 779–780

Concentration polarization

reverse osmosis, 745

ultrafiltration, 737

Concentration profiles

fixed-bed adsorption columns, 912–913

interphase mass transfer, 637–638

ion exchange, 922

Concentration units for liquids, 10

Condensation

film-type, 419–422

mechanisms, 419

vertical tubes, 422–423

## Condensers

distillation, 836

evaporation, 1026–1027

McCabe–Thiele method, 841

## Conduction and conductivity

building and insulating materials, 1141

butter slabs, 342–343, 346

cans of pea purée, 346

combined with convection and overall



coefficients, 305–306

constant-rate drying period, 1065–1068

constants and conversion factors, 1110

foods, 1149–1150

gases, 1128, 1135

heat loss by, 306–308

liquids, 1140

metals, 1142

parallel materials, 289

shape factors, 317–318

stainless steel, 327

steady-state. *See* Steady-state

conduction

unsteady-state heat transfer, 333–334

vapors, 1135

water, 1115

Conduits, heat-transfer coefficient for,  
398

Conservation

of energy, 23, 271–272

of mass, 13, 62, 200

Constant density, continuity equations  
for, 200

Constant-drying conditions in rate-of-  
drying curves, 1052–1054

Constant molar overflow in distillation,  
812

Constant-pressure filtration, 725–731

Constant-rate drying periods

calculations, 1057–1062

continuous dryers, 1083

convection, conduction, and radiation,  
1065–1068

rate-of-drying curves, 1054

Constant-rate filtration, 731

Constants and conversion factors

diffusivity, 1111

force, 1109

gas law, 1107

heat, energy, and work, 1110

heat capacity and enthalpy, 1111

heat flux and heat flow, 1111

heat-transfer coefficient, 1110

length, 1108

mass, 1108

mass flux and molar flux, 1111

mass-transfer coefficients, 1111

power, 1109

pressure, 1109

standard acceleration of gravity, 1108

temperature, 1112

thermal conductivity, 1110

viscosity, 1110

volume and density, 1107–1108

Contact nucleation in crystallization,  
936

Contact resistance at interfaces, 312–  
313

Contamination level of microorganisms,  
1089

Continuity

binary mixture equations, 510–511

differential equations. *See* Differential

equations of flow

Continuous dryers

countercurrent drying, 1082–1084

material and heat balances, 1079–1082

tunnel, 1037–1038

Continuous multistage countercurrent  
extraction, 889–894

Continuous rotary filters, 721, 730–731

Contractions, friction losses in, 116–  
122, 226–227

Control surfaces, average velocity, 67–  
68

Control volume

boundary layers, 260–261, 392

convection heat transfer, 409

differential equations of continuity,  
196–197

energy balance, 68–70

macroscopic balances, 55

mass balances, 63–65

momentum balance, 81–84, 89–91, 93–  
94

steady-state heat transfer, 277–278

## Convection

agitated vessels, 427–430

boiling, 415–419

Buckingham method, 387–389

condensation, 419–423

constant-rate drying period, 1065–1068

cylinders with axis perpendicular to flow, 403–404

diffusion for gases, 492–493

dimensionless groups, 387

flow in packed beds, 408

flow parallel to flat plates, 402

flow past banks of tubes or cylinders, 405–406

flow past single spheres, 404

forced



description, 386

hot surfaces, 296

inside pipes, 394–402

outside various geometries, 402–407

heat exchangers

extended surface, 431–435

scraped-surface, 430–431

heat loss by, 306–308

introduction, 385–387

laminar flow and boundary-layer theory,  
389–393

mass transfer, 508

molecular diffusion and chemical reaction, 508–511

natural, 408–415

non-Newtonian fluids, 424–427

noncircular conduits, 398–400

notation, 442–443

numerical methods, 554–556

outside various geometries, 402–408

oven walls, 410–411

overview, 282–284

in pipes, 394–402

Prandtl mixing length and eddy thermal diffusivity, 393–394

problems, 437–441

radiation combined with, 290–291

references, 441–442

slab boundary conditions, 578–579

special heat-transfer coefficients, 427–435

summary, 436–437

unsteady-state mass transfer diffusion, 571–572

Convective boundary conditions,  
unsteady-state conduction with, 363–365

Convective mass transfer

air bubbles in fermentation, 611–612

dimensional analysis, 594–595

introduction, 586–587

laminar flow and boundary-layer theory,  
613–615

mass-transfer coefficients

dimensionless number, 595–596

experimental methods, 594

film theory, 591–592

from flat plates, 603–604

flow inside pipes, 601–602

flow outside solid surfaces, 602–603

flow past single cylinders, 610

flow past single spheres, 604–607

high flux conditions, 592–593

laminar flow, 598–601

liquid metals, 610

mass, heat, and momentum transfer,  
596–598

models, 616–617

packed beds, 607–610

types, 587–591

molecular diffusion, 490

notation, 623–624

Prandtl mixing length and turbulent  
eddy mass diffusivity, 615–616

problems, 619–622

references, 622–623

summary, 617–619

suspended particles, 610–613

vaporization, 590–591

## Conversions

conversion factors. *See* Constants and  
conversion factors

pressure to head of fluid, 43

## Cooling

copper fins, 403

spheres, 404

steel balls, 336

Cooling coils, tubing for, 302

Coordinate systems

continuity equations, 201–202

energy change, 376

liquid–liquid extraction, 875–876

motion equations, 206–207

shear-stress components for Newtonian fluids, 205

Copper (Cu)

cooling fins, 403

emissivity, 286, 463

Core regions in turbulent flow, 260

Coriolis force in motion equations, 207

Coriolis mass flow meters, 137

Countercurrent drying, 1082–1084

Countercurrent flow

gaseous membrane systems

air separation, 789–793

equations, 779–787

numerical methods, 787–788

permeation, 765

heat exchangers, 445, 447



rotary dryers, 1038

steady-state conduction, 308–309

Countercurrent multiple-contact stages,  
631–633

Countercurrent multistage leaching,  
994–999

Countercurrent process and overall  
balance in liquid–liquid extraction, 889–  
890

Countercurrent stage contact, analytical  
equations for, 634–636

Countercurrent-stage liquid–liquid  
extraction with immiscible liquids, 894–  
896

Countercurrent stage process, material

balance for, 890–891

Countercurrent stage towers, absorption of acetone in, 633–634

Counterdiffusion

convective mass transfer, 588

gases, 519–521

steady-state mass transfer, 529–530, 546

Coupling fittings, friction losses in, 117

Crank–Nicolson method for unsteady-state conduction, 366

Creeping flow in differential equations of motion, 246

Critical free moisture content in rate-of-

drying curves, 1055

Critical point in sedimentation, 963

Critical radius in electrical wire  
insulation, 312

Critical thickness in cylinder insulation,  
311

Critical velocity in fluid flow, 55

Crops, drying, 1039–1040

Cross-flow heat exchangers, 445–446

Cross-flow models

gaseous membrane systems

design, 775–779

equations, 773–775

microfiltration, 734

Cross-sectional areas, varying, diffusion through, 524–527

Crude oil

flow, 62–63

Keystone pipeline, 59

Crushed glass shape factors, 155

Crushers, 946–947

Dodge crushers, 946

Crushing solids, 942–943

Crystallization

crystals

growth rate, 936–937

size distribution, 937–938

types, 928–929

description, 5

equilibrium solubility, 930

equipment for, 933–935

heat balances, 932–933

mechanical size reduction, 942–947

mixed suspension–mixed product  
removal crystallizers, 938–942

notation, 950–951

nucleation theories, 935–936

potassium nitrate, 15–16

problems, 948–950

process steps, 935

references, 950

summary, 947–948

yields and material balances, 930–932

## Cubes

mean beam length for gas radiation, 480

shape factors, 155

Cubic system crystals, 929

Cumulative weight fraction in  
crystallization, 940

Cupric ion ( $\text{Cu}^{2+}$ ) removal from acid solutions, 921–922

Cutting solids, 943

Cycles, adsorption, 918

Cyclone separators, 977–979

Cylinders

average temperature charts, 354–355

axis perpendicular to flow, 403–404

characteristic dimension, 335

coaxial, flow between, 213–215

condensation on, 422–423

conduction

hollow, 301

multilayer, 303

two-dimensional, 352–354

unsteady-state, 346–348, 365–366

critical thickness of insulation for, 311

flow past

convection heat transfer, 405–406

convective mass transfer, 610

immersed objects, 148

heat generation in, 314–315

mean beam length for gas radiation, 480

natural convection from, 409–415



shape factors, 155, 317–318

surface area in packed beds of, 151

in tunnels, force on, 149

Cylindrical annulus in laminar flow,  
212–213

Cylindrical containers, rotating liquid in,  
215–216

Cylindrical coordinates

continuity equations for, 201

motion equations, 206

## **D**

Dalton's law for mixtures of ideal gases,  
11–12

Danckwerts penetration theory, 617

Darcy's empirical law for laminar flow,  
155–156

Days (d), 6

Dead-end filtration

introduction, 716–717

microfiltration flow model, 733–734

Death-rate kinetics of microorganisms,  
1089–1090

Decimal reduction time of  
microorganisms, 1089

Dehumidification

description, 695

drying, 1040

towers, 712

Dense-phase membranes

description, 779–784

symmetric, 760

Density

constants and conversion factors, 1107–  
1108

foods, 1149–1150

leaching, 995

liquids, 10

metals, 1142

motion equations of Newtonian fluids,  
204–207

water, 1114

Desuperheating, 1030

Dew point

air–water vapor mixture, 697, 1042

boiling-point diagrams, 806

drying, 1042

multicomponent distillation, 854

Dextrose ( $\text{C}_6\text{H}_{12}\text{O}_6$ ) diffusivity, 545

Dialysis

equipment for, 750

hemodialysis in artificial kidneys, 750

membrane separations, 732

process, 749–750

series resistances, 747–748

Diameter

particle mixtures, 155

pipe, 113–114

tray towers, 839–841

Dichlorine ( $\text{Cl}_2$ ) molar heat capacity, 19

Differential distillation, 815–817

Differential equations of energy change

derivation, 372–374

introduction, 372

special cases, 374–376

Differential equations of flow

continuity

derivation, 199–202

introduction, 196–197

notation, 249

between parallel plates, 207–210

stationary and rotating cylinders, 211–  
216

time derivatives and vector notation,  
197–199

motion

creeping flow, 246

ideal fluids, 241

introduction, 239–240

momentum transfer, 202–204

Newtonian fluid, 204–207

notation, 249

between parallel plates, 207–210

potential flow and velocity potential,  
241–245

problems, 247–248

stationary and rotating cylinders, 211–  
216

summary, 247

notation, 218–219

problems, 217–218

references, 218

summary, 216–217

time derivatives and vector notation,  
197–199

Differential pressure, 43–44

Differential settling and separation,  
959–963

Diffusers, leaching, 988

Diffusion

biological gels, 544–546

biological solutes in liquids, 505–508



ethanol through water, 530–531

falling-rate drying periods by, 1068–1073

gases

diffusion coefficients, 493–498

flux ratios, 541

Knudsen diffusion, 538–539

molecular, 519–527, 539

multicomponent, 527

plus convection, 492–493

porous solids and capillaries, 537–544, 732

transition-region, 539–541

in gels, 544–546

through packaging film, 534–535

tubes with path length change, 524

unsteady-state mass transfer

agar gel slabs, 573–574

basic equation, 568–570

flat plate with negligible surface  
resistance, 570–571

notation, 585

numerical methods, 577–582

problems, 583–584

references, 585

semi-infinite medium, 575–576

semi-infinite slabs, 574–575

summary, 582–583

various geometries, 571–572, 575

Diffusion coefficients

constants and conversion factors, 1111

dilute biological solutes, 506

dilute methanol in water, 513

electrolytes in liquids, 503–505

gases, 493–498

liquids, 498–500

solids, 535

tapioca root, 1073

Diffusion gradients in gaseous  
membrane systems, 764

Diffusion-type model for reverse  
osmosis, 740–742

Digital computers, unsteady-state  
conduction using, 362–363

Dilatant fluids

description, 222

velocity profiles, 229–230

Dilute gas mixtures in packed towers,  
662–664

Dilute methanol in water, diffusivity of,  
513

Dilute solutions, packed towers for,  
668–670

Dimensional analysis for convective  
mass transfer, 594–595

Dimensionally homogeneous equations,  
7–8

Dimensionless groups in convection,  
387

Dimensions

fluid statics, 37–38

force, 38–39

heat-exchanger tubes, 1152

steel pipe, 1151–1152

Direct-contact condensers, 1026–1027

Direct steam injection, rectification with, 834–836

Disk bowl centrifuges, 975

Disks

continuous rotary filters, 721

flow past, 148

Dispersion of gases and liquids in liquids, 189–190

Displacement-purge cycle in adsorption, 918

Dissolved oxygen concentration in water, 629

Distillation, 805

boiling-point, 806–808, 854–855

description, 4

dew point, 854–855

enriching section, 845–846

equilibrium, 814–815

equipment for, 646–649, 808–811

flash, 814–815, 854–855

flooding velocity and diameter of tray  
towers, 839–840

fractional, 814–815, 841–850

introduction, 813

McCabe–Thiele method

condenser and reboiler duties, 841

rectification, 831, 833–836

reflux ratios, 827–830

theoretical stages, 820–827

multicomponent, 851–862

notation, 872–873

phase rule and Raoult's law, 805–806

problems, 864–871

references, 871–872

with reflux, 814–815, 818–819, 855–862



relative volatility of vapor–liquid systems, 813–814

simple batch and differential distillation, 815–817

simple steam distillation, 817–818

single-stage equilibrium contact for vapor–liquid systems, 811–812

stripping section, 846, 850

summary, 862–864

tray efficiencies, 836–838

$x$ - $y$  plots, 806–808

Distribution coefficients for unsteady-state mass transfer diffusion, 580–582

Double-arm kneader mixers, 192

Double-cone blenders, 191

Double-helical-ribbon agitators, 179

Double-pipe heat exchangers, 444–445,  
454–458

Doughs in agitation, 191

Drag coefficient

flow past immersed objects, 146–147

nonrigid spheres, 957

particle movement through fluids, 954

rigid spheres, 954

Drag in boundary-layer flow, 251–254

Dressed beef, chilling, 368–369

Driving forces in absorption, 642–645

Dropwise condensation, 419

Drum dryers, 1038–1039

Drying

adiabatic saturation temperatures, 1046–  
1047

biological materials

freeze-drying, 1084–1088

unsteady-state thermal processing and  
sterilization, 1088–1095

constant-rate drying period

calculations, 1057–1062

convection, conduction, and radiation,  
1065–1068

continuous countercurrent, 1082–1084

crops and grains, 1039–1040

description, 4

equilibrium moisture content factor,  
1049–1052

equipment for, 1036–1040

falling-rate drying periods

calculations, 1062–1064

by diffusion and capillary flow, 1068–  
1073

humidity and humidity charts, 1041–

1045

material and heat balances, 1079–1082

notation, 1103–1104

problems, 1096–1102

purposes, 1035–1036

rate-of-drying curves, 1052–1057

references, 1102–1103

summary, 1096

through-circulation in packed beds,  
1074–1078

tray drying with varying air conditions,  
1078–1079

vapor pressure of water, 1040–1041

wet bulb temperature, 1047–1048

Dühring's rule, 1013–1014

Dynamic viscosity, 51

Dynes (dyn), 7

## **E**

Eddy thermal diffusivity, 393–394

Effectiveness of heat exchangers, 450–453

Efficiency

centrifugal pumps, 170

distillation trays, 836–838

electric motors for pumps, 168

fin, 432–435

gas–solid cyclone separators, 979

perforated-plate tower trays, 887

positive-displacement pumps, 172

random-packed and structured packed towers, 672–674

Elbow fittings, friction losses in, 117–118

Electric motor pump efficiency, 168

Electrical wire, insulating, 312

Electrodialysis for membrane separations, 732

Electrolytes in liquids, prediction of

diffusivities in, 503–505

Electromagnetic spectrum, 465–468

Elevation in evaporation, 1004

Emissive power in radiation heat transfer, 466–467

Emissivity

black bodies, 462–463

gases, 480–482

radiation, 285–286, 467, 470

surfaces, 1142

Enclosed spaces, natural convection in, 413–415

Energy



conservation of, 23, 271–272

constants and conversion factors, 1110

crystal size reduction, 944–945

Energy and heat units

heat capacity, 18–20, 266–269

heat of reaction, 21–23, 270–271

joules, calories, and btus, 17, 265–266

latent heat and steam tables, 20–21,  
269–270

Energy balance

applications, 73–75

equations, 69–70

flow calorimeters, 74–75

introduction, 68–69

kinetic-energy velocity correction  
factor, 71–73

mechanical-energy balance

Bernoulli equation, 79–81

compressible gas pipe flow, 125

friction losses, 118–122

overview, 75–79

pumping systems, 76–77

notation, 103–104

problems, 97–103

steady-state flow systems, 70–71

steam boilers, 73–74

summary, 96–97

Energy change, differential equations of,  
372–376

Engineering principles and units

classification of transport processes and  
separation processes, 3–5

conservation of energy and heat  
balances, 23–28

conservation of mass and material  
balances, 13–17

energy and heat units, 17–23

gas laws, 10–12

notation, 35

numerical methods for integration, 28–29

problems, 29–35

references, 35

summary, 29

temperatures and compositions, 8–10

unit systems, 6–8

vapor pressure, 12–13

English system units, 6–7

Enlargements, friction loss in, 88, 116

Enriching sections in distillation, 820–822, 833, 845–846

## Enthalpy

air–water vapor mixture, 698, 1043

constants and conversion factors, 1111

saturated steam, 1116–1119

water-cooling towers, 705, 709–710

## Enthalpy–concentration data

fractional distillation, 841–844, 846–850

single-effect evaporators, 1014–1016

Enthalpy–temperature–composition charts, 369

Entrance-region, effect on heat-transfer coefficient, 400

Entrance section of pipes, flows at, 123–125

Entropy in saturated steam, 1116–1119

Enzyme activity in food chilling and freezing, 367

Equal liquid motion in agitators, 183

Equal rates of mass transfer in agitators, 183

Equal suspension of solids in agitators, 183

Equations of change for continuity, 197

Equilibrium

absorption and stripping, 636–637

acetone–water systems, 1144

adsorbents, 908–909

ammonia–water systems, 1144

contact of vapor–liquid mixture, 812–813

crystallization solubility, 930

distillation, 814–815

gas–liquid, 628–629

ion exchange, 919–921

leaching, 990–992

liquid–liquid extraction, 875–878

methanol–water systems, 1144

moisture content in drying materials,  
1049–1052

multicomponent distillation, 852–853

and phase rule, 627–628

single-stage, 629–631

sulfur dioxide–water systems, 1143

Equimolar counterdiffusion

convective mass transfer, 588

film mass-transfer coefficients and  
interface concentrations, 638

in gases, 519–521

steady-state mass transfer, 529–530, 546



Erbar–Maddox correlation, 860

Ergs, 7

Ergun equation for flow in packed beds, 153

Ethane ( $\text{C}_2\text{H}_6$ )

molar heat capacity, 19, 269

thermal conductivity, 1135

Ethanol ( $\text{C}_2\text{H}_6\text{O}$ )

diffusion coefficient, 500

diffusion through water, 530–531

diffusivity, 545

heat capacity, 1135

thermal conductivity, 1135

vapor-pressure data, 870

water system equilibrium data, 1145

Ethyl ether ( $\text{C}_2\text{H}_5)_2\text{O}$  thermal  
conductivity, 1135

Ethylene ( $\text{C}_2\text{H}_4$ )

molar heat capacity, 19, 269

thermal conductivity, 1135

Euler equations

motion, 241

potential flow, 242

Evaporation

biological materials, 1028–1029

condensers, 1026–1027

description, 4

equipment for, 1004–1008

evaporators

heat-transfer coefficients, 1008–1009

multiple-effect. *See* Multiple-effect  
evaporators

single-effect. *See* Single-effect  
evaporators

introduction, 1002–1003

naphthalene spheres, 526

notation, 1034

problems, 1031–1034

processing factors, 1003–1004

references, 1034

summary, 1030–1031

vapor recompression, 1029–1030

Expansion of fluidized beds, 160–161

Expansions, friction losses in, 116–122,  
226–227

Experimental diffusivity data for gas  
diffusion coefficients, 494

Explicit method for unsteady-state  
conduction, 356

Extended surface heat exchangers, 431–

Extract layer in liquid–liquid extraction, 876

Extraction

leaching. *See* Leaching

liquid–liquid extraction. *See* Liquid–liquid extraction

## F

Fahrenheit (°F) temperature, 8

Falling-film evaporators

description, 1006

vapor recompression, 1030

## Falling films

diffusion in, 599–601

shell momentum balance, 93–96

velocity and thickness, 96

## Falling-rate drying periods

calculations, 1062–1064

diffusion and capillary flow in, 1068–1073

rate-of-drying curves, 1055–1057

## Fanning friction factor method

laminar flow, 110

turbulent flow, 111

Fans

brake power, 172–173

gas-moving pumps, 172

Feed

distillation

conditions, 823–824

multicomponent, feed-plate location,  
860

trays, 824–825

gas membrane systems, composition of,  
770

temperature, in evaporators, 1012

Feet, 7

Fenske total reflux equation, 859

Fermentation

air bubbles in, 611–612

media heating, 24–25, 272–274

Fick's law

alternate form, 560

diffusion of gases plus convection, 493

molecular diffusion

in gases, 520, 539

overview, 489–492

plus convection, 508–509

in solids, 531–536



unsteady-state diffusion, 1069

Film coefficients

convection, 386

heat-transfer, 283

and interface concentrations, 638–642

mass-transfer coefficients from, 644–645

packed towers, 660–662, 679–682

water-cooling towers, 707–710

Film theory for convective mass transfer, 591–592, 616–617

Film-type condensation, 419–423

Films

boiling region, 417

shell momentum balance, 93–96

Filter cakes, washing, 728–729

Filtration, 716

centrifugal, 967, 975–977

constant-pressure, 725–731

constant-rate, 731

dead-end, 716–717

equipment, 717–718

bed filters, 718

continuous rotary filters, 721

leaf filters, 720–721

plate-and-frame filter presses, 718–720

filter media and filter aids, 722

membrane separations. *See* Membrane separations

notation, 756–758

problems, 752–755

references, 755–756

summary, 751–752

Finite-difference numerical methods

gaseous membrane systems, 787–798

steady-state conduction, 320–325

Finned heat exchangers, 431–435

Fins

cooling, 403

heat transfer, 431

First law of thermodynamics, 68

Fischer Tropsch catalyst, 157

Fittings, friction losses in, 116–122,  
226–227

Fixed-bed adsorption columns

breakthrough concentration curves, 913

capacity of column and scale-up design  
method, 913–917

concentration profiles, 912–913

mass-transfer zones, 913

Fixed-bed leaching, 988–989

Flaked soybeans, 993–994

Flash distillation, 814–815, 855

Flat-blade turbine agitators, 428

Flat membranes, 762

Flat plates

convective mass transfer, 603–604

diffusion with negligible surface  
resistance, 570–571

flow over, 200–201

flow parallel to, 402

laminar boundary layer flow, 253–254

unsteady-state conduction in, 342–345

Flat slabs, conduction through, 299–300

Flexipac packing factors, 651

Flooding

distillation, 839–840

liquid–liquid extraction, 882

packed towers, 649–654, 883–886

Flow

Bingham plastic fluids, 231–232

boundary layer. *See* Boundary-layer flow

crude oil, 62–63

differential equations. *See* Differential equations of flow

fluidized beds, 156–161

gaseous membrane systems, 764–765

laminar. *See* Laminar flow

metering, 108–109

non-Newtonian fluid properties, 232–233

notation, 165

outside solid surfaces, 602–603

over flat plates, 200–201

packed beds, 150–156, 408

packed towers, 658

between parallel plates

bulk velocity for, 98

differential equations of, 207–210

parallel to flat plates, 402

past banks of tubes, 405–406

past immersed objects, 146–149

past single cylinders, 405–406, 610

past single spheres

convection heat transfer, 404

convective mass transfer, 604–607

pipes. *See* Pipe flows

problems, 162–164



references, 164

summary, 161–162

tank nozzles, 80–81

time-dependent fluids properties, 223–226

turbulent. *See* Turbulent flow

Flow calorimeters, 74–75

Flow field in stream function, 244

Flow-nozzle meters, 135

Flow number in agitation, 189

Flow patterns in agitation, 179–180

Flow systems in momentum balance

one direction, 83–84

two directions, 86–87

Fluid at constant density energy change,  
375

Fluid at constant pressure energy  
change, 375

Fluid dynamics, 37

Fluid mechanics, 37

Fluidized beds, 156–161

Fluids and fluid statics

fluid flow

differential equations. *See* Differential  
equations of flow

introduction, 54–55

laminar and turbulent flow, 55

notation, 60

problems, 58–59

references, 59–60

Reynolds number, 55–57

summary, 58

force, units, and dimensions, 37–38

head of, 42–43

introduction, 36–37

momentum transfer, 53

non-Newtonian. *See* Non-Newtonian

fluids

notation, 49

particle movement through, 953–957

pressure

through filter cakes, 722–724

measurements, 43–47

overview, 39–42

problems, 48–49

summary, 47

viscosity, 50–54

Flux

constants and conversion factors, 1111

convective mass transfer, 592–593

diffusion of gases in capillaries, 541

freeze-drying, 1085–1086

molecular diffusion plus convection,  
508–510

reverse osmosis equations, 740–743

shear stress, 53

ultrafiltration equations, 735–737

Flux ratio factor for molecular diffusion  
of gases, 539

Foaming in evaporation, 1004

Food and biological materials

can sterilization, 1092, 1094

chilling and freezing, 366–372

equilibrium moisture content of  
materials, 1049

heat capacities of, 1147–1149

thermal conductivities, densities, and  
viscosities, 1149–1150

## Force

centrifugal separation, 967–969

constants and conversion factors, 1109

on cylinders in tunnels, 149

English system, 7

fluid statics, 37–38

momentum balance, 81–83

SI system, 6

on submerged spheres, 149

units and dimensions, 38–39

viscous drag, 51

Forced-circulation evaporators

description, 1006

heat-transfer coefficients, 1009

Forced convection heat transfer

description, 386

hot surfaces, 296

inside pipes, 394–402

outside various geometries, 402–408

Form drag

boundary-layer flow, 251–252

flow past immersed objects, 146

Formaldehyde ( $\text{CH}_2\text{O}$ ) production, 32

Formation, heat of, 22

Formic acid ( $\text{CH}_2\text{O}_2$ )

diffusion coefficient, 500

heat capacity, 1135

Forward-feed multiple-effect  
evaporators, 1007–1008

Fouling factors in heat exchangers, 453–  
454

Fourier's equation



eddy thermal diffusivity, 394

fin efficiency, 432

Fourier's law

heat conduction, 278–279, 488

mass transfer, 487

steady-state conduction in two  
dimensions, 316

Fourier's second law for unsteady-state  
heat transfer, 374, 376

Fractional distillation

description, 814–815

enriching section, 845–846

enthalpy–concentration data, 841–844,

846–850

stripping section, 846, 850

Free convection, 386

Free jets striking fixed vanes,  
momentum balance, 89–90

Free moisture, 1051–1052

Free settling

description, 953

particle movement through fluids, 954

wall effect on, 959

Freeze-drying biological materials,  
1084–1088

Freezing

food and biological materials, 366–372

oranges, 380

Freezing point, 8

Freezing temperature in ground, 340–341

Freundlich isotherm equation, 909

Friction and friction loss

boundary-layer flow, 251–252

in expansion, contraction, and pipe fittings, 116–122

gas flow, 110–114

heat transfer effect on, 115–116

laminar flow, 107–110

momentum balance, 83

non-Newtonian fluids, 226–228

noncircular conduits, 123

sudden enlargements, 88

time-independent fluid flows, 225

turbulent flow, 110–114, 258

Frothing in evaporation, 1004

Fruit juices, evaporation of, 1028

Fuel gases, combustion of, 16–17

Full miscella, leaching, 989

Furnace enclosures, gas radiation to,  
480–481

Fusion, latent heat of, 20, 269

## **G**

Gage pressure

description, 10

fluids, 41

Galena and silica mixture, separation of,  
961–963

Gaps in non-Newtonian fluids flow, 233

Gas film coefficients for packed towers,  
681

Gas humidity in constant-rate drying  
period, 1061

Gas law constants, 11, 1107

Gas–liquid contactors in humidification,  
703

Gas–liquid systems

equilibrium, 628–629

single-stage equilibrium contact, 630–  
631

Gas mixtures in packed towers, 662–664

Gas-moving pumps

characteristics, 167–172

gas compression equations, 174–176

introduction, 166–167

machinery, 172–174

Gas permeation in membrane

separations, 732

Gas–solid cyclone separators, 977–979

Gas temperature in constant-rate drying period, 1061

Gaseous membrane systems, 759

cocurrent flow, 779–787

complete mixing model

design, 767–768

gas separation, 765–770

multicomponent mixtures, 770–773

countercurrent flow

air separation, 789–793

equations, 779–787

numerical methods, 787–798

cross-flow models, 773–779

equipment for, 762–764

flow in gas permeation, 764–765

membrane types, 760–762

notation, 803–804

permeability, 761–762

permeation, 759–765

problems, 799–802

references, 802

summary, 798–799



## Gases

combustion of, 16–17

concentrated mixtures in absorption  
tower design, 676–679

diffusion. *See* Diffusion

fouling coefficients, 453–454

heat capacity, 18–20, 1129, 1133–1134

Henry's law constants, 1143

ideal gas law, 10–11

ideal gas mixtures, 11–12

mass-transfer coefficients, 589

mixture composition, 12

molecular diffusion in, 519–527

packed bed flow, 153–154

Prandtl number, 1130

pressure drop and friction loss in, 110–114

radiation in

overview, 479–482

temperature measurement, 464–465

thermal conductivity, 281, 1128, 1135

viscosity of, 1127, 1131–1132

Gate valves, friction losses in, 117

Gauss–Seidel method, 324, 366

Gel permeation chromatography, 733

Gels

diffusion in, 544–546

polarization in ultrafiltration, 736–737

unsteady-state mass transfer diffusion,  
573–574

Gempak packing factors, 651

Giga (G) prefix, 6

Glass spheres, hindered settling of, 958–  
959

Globe valves, friction losses in, 118

Glycerol ( $\text{C}_3\text{H}_8\text{O}_3$ )

diffusivity, 545

heat capacity, 1135

viscosity, 54

Graetz number for heat transfer inside tubes, 424

Grains, drying, 1039–1040

Grams (g), 7

Graphical integration, numerical methods for, 29

Graphical method for two-dimensional conduction, 315–317

Grashof numbers

convection, 389

mass-transfer coefficients, 594

natural convection, 409–411, 413

## Gravity

centrifugal separation, 969

cgs system, 7

constants and conversion factors, 1108

English system, 7

momentum transfer, 203

particle movement through fluids, 953

SI system, 6

Gravity filters, 717

Gravity separators for immiscible liquids, 46–47

Gravity settling tanks, 964–965

Gray bodies

emissivity, 285

radiation heat transfer, 463, 468

radiation view factors, 476–477

Gray planes

radiation between, 477

radiation heat transfer, 469–470

Grinders, 947

Grinding solids, 942–943

Ground, freezing temperature in, 340–  
341

Growth rate of crystals, 936–937, 941–942

Gyratory crushers, 946–947

## H

Hagen–Poiseuille equation. *See also* Poiseuille's equation

gaseous membrane systems, 786

packed bed flow, 152

pressure drop and friction loss in laminar flow, 107, 110

viscosity of liquids, 139

Half miscella, leaching, 989

Hammer mill grinders, 947

Head of fluids, 42–43

## Heat

constants and conversion factors, 1110

convective mass transfer, 596–598

## Heat balances

continuous dryers, 1079–1082

crystallization, 932–933

description, 272

overview, 23–27, 272–276

single-effect evaporators, 1010–1012

## Heat capacity

constants and conversion factors, 1111



foods, 1147–1149

gases, 1129, 1133–1134

ice, 1116

liquids, 1135, 1139

metals, 1142

overview, 18–20, 266–269

solids, 1140

water, 1115

Heat effects

absorption, 682–685

crystallization, 932

Heat exchangers, 444

double-pipe, 454–458

effectiveness, 450–453

fouling factors and heat-transfer  
coefficients, 453–454

log-mean-temperature-difference  
correction factors, 447–449

notation, 460

problems, 459

references, 459

scraped-surface, 430–431

summary, 458–459

temperature correction factor, 449

tube dimensions, 1152

types, 444–446

## Heat flow

constants and conversion factors, 1111

insulated walls of cold rooms, 288–289

## Heat flux

constants and conversion factors, 1111

freeze-drying, 1085–1086

Heat generation in energy change, 375

## Heat loss

through convection, 283–284, 306–308

from fins, 434–435

from insulated pipes, 303–304

through insulating walls, 279–280

## Heat of combustion

description, 22, 270

material balances, 25–26

standard, 1125

## Heat of formation

description, 22, 270

standard, 1124

## Heat of reaction, 21–23, 270–271

## Heat of solution

crystallization, 932

single-effect evaporators, 1014

Heat of sublimation in saturated ice–  
water vapor, 1115

Heat transfer

combined radiation and convection,  
290–291

conduction and thermal conductivity,  
277–282

conduction through materials in parallel,  
289

conservation of energy, 271–272

convection. *See* Convection

description, 4

energy and heat units, 265–271

friction factor effect, 115–116

heat balance, 272–276

mass transfer, 487

notation, 298

pipes, 387–389

plane walls in series, 287–288

problems, 293–298

radiation, 284–287

references, 298

summary, 292–293

tubes, 424–427

water-cooling towers, 704–707

Heat-transfer area

and log mean temperature difference,  
310

single-effect evaporators, 1011–1012

Heat-transfer coefficients

constants and conversion factors, 1110

convection, 283–284, 427–435

entrance-region effect on, 400

evaporators, 1008–1009

finned tubes, 435

heat exchangers, 453–454

laminar flow inside pipes, 394–395

liquid metals, 400–401

noncircular conduits, 398

single-effect evaporators, 1007

through-circulation drying in packed  
beds, 1076

transition flow inside pipes, 397–398

Heat-transfer properties

liquid water, 1122

water vapor, 1123

Heating

air

by banks of tubes, 406–407



in turbulent flow, 396–397

fermentation media, 24–25

Heating jackets, agitated vessels with,  
427–429

Heavy keys in multicomponent  
distillation, 855

Height of transfer units in water-cooling  
towers, 711

Helical-ribbon agitators, 179, 428

Helical-screw impellers, 179

Helium (He)

diffusion coefficients, 495

diffusivity and permeability, 535

molecular diffusion in nitrogen, 490–492

in natural gas, 801

permeability in symmetric membranes, 761

transition-region diffusion, 542–543

Hemodialysis in artificial kidneys, 750

Henry's law

concentration profiles in interphase mass transfer, 637

gas–liquid equilibrium, 629

gases in water, 1143

HETP of random-packed and structured

packed towers, 672–674

HETS (height equivalent to a theoretical stage), 882, 888–889

Hexagonal system crystals, 929

Hexane thermal conductivity, 1135

Higbie penetration theory, 617

High flux conditions in convective mass transfer, 592–593

Hildebrandt extractors, 989–990

Hindered settling, 957–958

description, 953

glass spheres, 958–959

Hollow cylinders, conduction through,

Hollow-fiber membranes, 763–764

Hollow spheres, conduction through,  
304–305

Homogeneous nucleation in  
crystallization, 935–936

Homogeneous reactions in mass transfer  
boundary conditions, 549–550

Horizontal cylinders

condensation on, 422–423

film-condensation coefficients outside,  
423

natural convection from, 410, 412–413

Horizontal filters, continuous rotary, 721

Horizontal nozzles in momentum  
balance, 85–86

Horizontal plates, natural convection  
from, 410, 412–413

Horizontal-tube natural circulation  
evaporators, 1004

Horsepower of pumps in flow systems,  
77–79

Hot water, heat-transfer coefficients in  
jacketed vessels, 428

Hours (h), 6

Humid heat of air–water vapor mixture,  
697, 1043

Humidity and humidification processes,  
694

adiabatic saturation temperature, 700–  
701

charts

drying, 1041–1045

overview, 695–699

constant-rate drying period, 1061

dehumidification towers, 712

description, 1040

gas–liquid contactors, 703

notation, 714–715

problems, 712–714

references, 714

summary, 712

vapor pressure of water, 694–695

water-cooling towers. *See* Water-cooling towers

wet bulb temperature, 701–703, 1048

Hy-Pak packing factors, 651

Hydraulic radius in packed bed flow, 152

Hydrochloric acid (HCl)

diffusion coefficient, 500

heat capacity, 1135

Hydrogen (H<sub>2</sub>)

diffusion coefficient, 495, 500

diffusion through neoprene membranes,  
532–533

diffusivity and permeability, 535

heating, 266–267

Knudsen diffusivity, 538–539

molar heat capacity, 18–19, 267–268

permeability in symmetric membranes,  
761

thermal conductivity, 281

Hydrogen chloride (HCl) molar heat  
capacity, 19, 269

Hydrostatic pressure, 40



Hygroscopic materials, 1051

## I

Ice

heat capacity, 1116

thermal conductivity, 280

vapor pressure, 695

Ice–water vapor, vapor pressure of,  
1115

Ideal flow patterns in gaseous  
membrane systems, 764–765

Ideal fluids in differential equations of  
motion, 241

Ideal gas law, 10–11

Ideal gas mixtures, 11–12

Immersed objects, flow past, 146–149

Immiscible liquids

countercurrent-stage extraction with,  
894–896

gravity separators for, 46–47

Immiscible streams, countercurrent  
contact with, 632–633

Impact with solids, 943

Implicit numerical method for unsteady-  
state conduction, 366

In-place leaching, 988

Incompressible fluids, 37

Indirect dryers, 1037

Inert-purge-gas stripping cycle in adsorption, 918

Infinite black planes, view factors for, 468–469

Infinite parallel gray planes, view factors for, 469–470

Inorganic materials

equilibrium moisture content, 1049

leaching processes, 985

Instantaneous surface reaction in steady-state mass transfer, 547

Insulated boundary conditions for slabs, 357–358

Insulated pipes, heat loss from, 303–304

Insulated walls of cold rooms, heat flow through, 288–289

Insulating electrical wire, 312

Insulating materials, thermal conductivities of, 1141

Insulating walls, heat loss through, 279–280

Insulation for cylinders, critical thickness of, 311

Intalox metal type for absorption and distillation, 810–811

Integral analysis for convection, 392–393

Integral momentum balance in  
boundary-layer flow, 260–263

Integration, numerical methods for, 28–  
29

Intensity of turbulence, 255

Interaction and binding in diffusion, 505

Interfaces

centrifuges, 974

contact resistance at, 312–313

film mass-transfer coefficients, 638–642

interphase mass transfer, 640–642

Interfacial resistance, 637

Interfacial tension in liquid–liquid

extraction, 885–886

Internal energy in energy-balance equations, 69

Internal heat generation, conduction with, 313–315

Interphase mass transfer

concentration profiles, 637–638

interface compositions, 640–642

introduction, 636–637

Inviscid fluids, 241

Ion exchange

capacity of columns and scale-up design method, 922–924

concentration profiles and breakthrough curves, 922

cupric ion removal from acid solutions, 921–922

description, 5

equilibrium relations, 919–921

materials, 918–919

notation, 927

problems, 925–926

references, 926–927

summary, 924

Iron emissivity, 286, 463

Isopropyl ether equilibrium data, 876–

Isothermal compression

flow, 126–128

gas-moving pumps, 174

## J

Jacketed kettles, rate of heat transfer in,  
417–419

Jackets, agitated vessels with, 427–429

Jaeger Metal Tri-Pack for absorption  
and distillation, 810–811

Jaw crushers, 946

Jet barometric condensers, 1027



Joules (J)

cgs system, 7

description, 17, 265–266

English system, 7

SI system, 6

## K

Karr towers, 883, 888–889

Kelvin (K) units, 6, 8

Kettles, heat transfer rate in, 417–419

Keystone pipeline, 59

Kidneys, artificial, 750

Kilo (k) prefix, 6

Kilogram moles (kg mol), 6

Kilograms (kg), 6

Kinematic viscosity, 52

Kinetic energy

energy-balance equations, 69

laminar flow, 226–227

velocity correction factor, 71–73

Kirchhoff's law for radiation heat transfer, 462, 467–468

Kneader mixers, 192

Knudsen diffusion

gases, 538–539

hydrogen, 538–539

Knudsen equation

countercurrent stage contact, 635–636

gas transition-region diffusion, 539–541

## L

$\Delta L$  law of crystal growth, 937

Lactose ( $C_{12}H_{22}O_{11}$ ), oxidation of, 27–28, 275–276

Laminar flow

boundary-layer, 252–254

circular tubes, 211–212

convection, 389–392

convective mass transfer, 613–615

cylindrical annulus, 212–213

description, 51, 55

flow between parallel plates, 207–209

flow between vertical plates, 210

friction losses, 226–227

kinetic-energy velocity correction  
factor, 72

mass-transfer coefficients, 598–601

mixers, 190

momentum velocity correction factor,  
84–85

packed beds, 150–152

in pipes, heat-transfer coefficient for,  
394–395

pressure drop and friction loss in, 107–  
110

time-independent fluids, 223–226

in tubes, heat transfer in, 424–426

velocity profile in, 90–96

Langmuir isotherm equation, 909

Laplace's equation

conduction, 319

motion, 206

potential flow, 242–243

scalar fields, 199

Large flat plates, unsteady-state  
conduction in, 342–345

Latent heat

fusion, 20, 269

vaporization, 21, 269

water, 1113

Law of conservation of energy, 23, 271–  
272

Law of conservation of mass, 13, 200

Leaching, 984

countercurrent multistage, 994–999

equilibrium relations, 990–992

equipment for, 988–990

extraction batteries, 988

notation, 1001

preparation, 985–986

problems, 1000–1001

processes, 984–985

rates, 986–988

references, 1001

single-stage, 992–994

summary, 999

Leaf filters, 720–721

Length constants and conversion

factors, 1108

Lennard-Jones collision integral for thermal conductivity, 281

Lennard-Jones potentials

diffusion coefficients for gases, 496

from viscosity data, 1154–1155

Leveque solution for convective mass transfer, 599

Lever-arm rule for graphical addition, 878–880

Light keys in multicomponent distillation, 855

Lime from limestone, 294



Liquid diffusion of moisture in drying,  
1069–1070

Liquid diffusion theory for rate-of-drying curves, 1055–1056

Liquid film coefficients for packed towers, 681

Liquid film resistances in membrane diffusion, 748–749

Liquid–liquid equilibria

acetic acid–water–isopropyl ether  
systems, 1146

acetone–water–methyl isobutyl ketone  
systems, 1146

Liquid–liquid extraction, 874

acetone from water with trichloroethane,  
899–901

continuous multistage countercurrent  
extraction, 889–894

countercurrent-stage extraction with  
immiscible liquids, 894–896

description, 5

equilibrium relations, 875–878

equipment for, 880–881

mechanically agitated extraction towers,  
888–889

mixer–settlers, 881

notation, 905–906

problems, 902–905

processes overview, 874–875

references, 905

single-stage equilibrium extraction,  
878–880

summary, 901–902

towers

design, 896–898

mechanically agitated, 888–889

packed, 882–886, 898

perforated-plate, 886–887

pulsed packed, 887

spray, 881–882

## Liquid metals

convective mass transfer, 610

heat-transfer coefficient, 400–401

heat transfer inside tubes, 401–402

Liquid permeation in membrane separations, 732

Liquid–solid leaching, 5

## Liquid water

density, 1114

heat capacity, 1115

heat-transfer properties, 1122

thermal conductivity, 1115

viscosity, 1114

## Liquids

biological solutes in, diffusion of, 505–508

boiling point, 12–13

centrifugal separation, 973–974

diffusion coefficients, 498–500

fouling coefficients, 453

heat capacity, 1135, 1139

leaching. *See* Leaching

mass-transfer coefficients, 589

molecular diffusion in, 528–531

in packed beds, convective mass transfer, 609–610

prediction of diffusivity in, 500–503

shear stress, 52–53

thermal conductivities, 282, 1140

units, 10

vapor pressure of, 695

viscosity, 1136–1138

Loading point gas flow rate, 649

Local efficiency of distillation trays, 838

Log mean temperature difference

in conduction, 308–309

and heat-transfer area, 310

Log-mean-temperature-difference  
correction factors in heat exchangers,  
447–449

Long cylinders

flow past, 148

unsteady-state conduction in, 346–348

Long-tube vertical-type evaporators,  
1006, 1009

Longitudinal fins for heat transfer, 431

Lumped thermal capacitance in  
unsteady-state heat transfer, 335

## M

Mach number in fluid flow equations,  
129

Macroscopic behavior of fluids, 37

Magnetic flow meters, 137

Manometers, 44–45

Mass

cgs system, 7

conservation of, 13, 200

constants and conversion factors, 1108

convective mass transfer, 596–598

English system, 7

units, 8–9



Mass accumulation in continuity  
equations, 200

Mass balances

average velocity, 67–68, 98

control volume, 63–64

crude oil flow, 62–63

equations, 64–67

introduction, 62

notation, 103–104

problems, 97–103

stirred tanks, 66–67

summary, 96–97

Mass flux constants and conversion factors, 1111

Mass transfer

convective. *See* Convective mass transfer

description, 4

diffusion coefficients

gases, 493–498

liquids, 498–505

diffusion of biological solutes in liquids, 505–508

diffusion of gases plus convection, 492–493

examples, 489

introduction, 487–489

molecular diffusion plus convection,  
508–511

notation, 517–518

problems, 512–515

references, 515–517

steady-state. *See* Steady-state mass  
transfer

summary, 512

unsteady-state. *See* Unsteady-state mass  
transfer

Mass-transfer coefficients

in absorption, 642–645

constants and conversion factors, 1111

convective mass transfer. *See*

Convective mass transfer

and driving forces in absorption and stripping, 642–645

from film coefficients, 644–645

packed towers, 660–662

estimation, 679–682

liquid–liquid extraction in, 898

ultrafiltration, 738

water-cooling towers, 707–710

Mass-transfer zones

fixed-bed adsorption columns, 913

ion exchange, 922

Material balances

chemical reaction, 16–17

combustion, 25–26

continuous dryers, 1079–1082

countercurrent stage process, 890–891

crystallization, 930–932

crystals, 938

description, 13–15

recycle process, 15

single-effect evaporators, 1010–1012

# Materials

equilibrium moisture content of, in  
drying, 1049–1052

for evaporation, 1004

ion exchange, 918–919

in parallel, conduction through, 289

McCabe–Thiele method for distillation

condenser and reboiler duties, 841

rectification, 831, 833–836

reflux ratios, 827–830

theoretical stages, 820–827

tray efficiency diagrams, 838

Meal, oil from, 997–998

Mean diameter for particle mixtures,  
154–155

Mean molar heat capacities of gases,  
267–268

Mean surface renewal factor in  
convective mass transfer, 617

Measurements

crystal size, 943

gas temperature, 464–465

pipe flows

flow-nozzle meters, 135

miscellaneous meters, 136–137

orifice meters, 133–135

pitot tubes, 129–131

rotameters, 136

venturi meters, 131–133

pressure, 43–47

small liquid flows, 108–109

Meat, freezing, 371

Mechanical-energy balance

Bernoulli equation, 79–81

compressible gas pipe flow, 125

friction losses in, 118–122

overview, 75–79



pumping systems, 76–77

Mechanical-physical separations, 5

Mechanical vapor-recompression  
evaporators, 1029–1030

Mechanically agitated towers, 888–889

Mega (M) prefix, 6

Mellapak packing factors, 651

Membrane separations

description, 5

dialysis, 747–751

introduction, 732

membrane processes, 732–733

microfiltration, 733–734

notation, 756–758

permeability, 742–743

problems, 752–755

references, 755–756

reverse osmosis, 738–747

summary, 751–752

ultrafiltration, 734–738

## Membranes

gaseous. *See* Gaseous membrane systems

hydrogen diffusion through, 532–533

Mercury (Hg)

heat capacity, 1135

viscosity, 54

Metal Intalox (IMTP) packing factors,  
651

Metal Tri-Pack for absorption and  
distillation, 648, 810–811

Metal tubes, radiation to, 286–287, 464

Metals

convective mass transfer, 610

heat-transfer coefficient, 400–401

thermal conductivities, densities, and  
heat capacity, 1142

Metering of small liquid flows, 108–109

Meters (m), 6

Methane ( $\text{CH}_4$ )

compression of, 175–176

isothermal flow, 127

molar heat capacity, 18–19, 267–268

in natural gas, 801

permeability in symmetric membranes,  
761

reaction of, 22–23, 270–271

viscosity, 54

Methanol ( $\text{CH}_3\text{OH}$ )

diffusion coefficient, 500

diffusivity, 545

heat capacity, 1135

vapor-pressure data, 870

water system equilibrium data, 1144

Methylisobutyl ketone (MIBK)  
equilibrium data, 885

Micro ( $\mu$ ) prefix, 6

Microfiltration, 733–734

Microfluidics, 59

Microorganisms

food chilling and freezing, 367

thermal death-rate kinetics, 1089–1090

Milk

heating, 20, 269

pasteurization, 1095

thermal conductivity, 280

Milli (m) prefix, 6

Minimum bubbling velocity in fluidized beds, 161

Minimum concentration of reject stream in gaseous membrane systems, 770

Minimum reflux in distillation

McCabe–Thiele method, 828–830

multicomponent, 859–862

Minimum solvent rate in liquid–liquid extraction, 894

Minimum velocity in fluidized beds, 156–160

Minutes (min), 6

Miscella leaching, 989

Miscible liquids, mixing times of, 186–189

Mixed suspension–mixed product removal (MSMPR) crystallizers, 938–942

Mixer-settlers for liquid–liquid extraction, 881

Mixers in agitation, 191–192

Mixing, power requirements in, 234–235

Mixing times of miscible liquids, 186–189

Mixture composition of gases, 12

Mixture of silica and galena, separation of, 961–963

Modified Francis weir formula, 137

Moisture movements in rate-of-drying curves, 1055–1057

Molar flux constants and conversion factors, 1111

Molar heat capacities of gases, 18–20

Molarity, defined, 10



Mole fractions, 9

Mole units, 8–9

Molecular diffusion

with convection and chemical reaction,  
508–511

equations for momentum, heat, and  
mass transfer, 488

Fick's law, 488–492

in gases, 539

equimolar counterdiffusion, 519–521

multicomponent, 527

stagnant nondiffusion, 521–524

varying cross-sectional areas, 524–527

in liquids, 528–531

in solids, 531

Fick's law, 531–536

porous, 536–537

Molecular sieve zeolite adsorbents, 908

Molecular transport equation, 488

Molten chocolate rheological constants,  
231

Momentum balance

equations, 81–83

flow system in one direction, 83–84

flow system in two directions, 86–87

free jet striking fixed vanes, 89–90

horizontal nozzles, 85–86

notation, 103–104

pipe bends, 87

problems, 97–103

shell, 90–96

summary, 96–97

## Momentum transfer

convective mass transfer, 596–598

description, 4

differential equations, 202–204

fluids, 37, 53

processes, 487

Momentum velocity correction factor,  
84–85

Monoclinic system crystals, 929

Montz packing factors, 651

Motion, differential equations. *See*  
Differential equations of flow

Motionless mixers for agitation, 190

Motor efficiency of pumps, 168

Moving-bed leaching, 989

Multicomponent diffusion of gases, 527

Multicomponent distillation

boiling point, 854

dew point, 854

equilibrium data, 852–853

flash, 855

introduction, 851–852

key components, 855

total reflux, 855–859

Multicomponent mixtures in gaseous  
membrane systems, 770–773

Multilayer cylinders, steady-state  
conduction through, 303

Multiple-contact stages countercurrent,  
631–633

Multiple-effect evaporators

backward-feed, 1008

calculations, 1018–1026

capacity, 1018

forward-feed, 1007–1008

introduction, 1016–1017

parallel-feed, 1008

temperature drops, 1017

Multistage compression ratios for gas-moving pumps, 176

Multistage countercurrent extraction, 889–894

Multistage leaching, 994–999

Murphree tray efficiency in distillation,

837–839

*Mycobacterium tuberculosis*, 1094

## **N**

Nano (n) prefix, 6

Naphthalene spheres, 526

Natural circulation evaporators

description, 1004–1005

heat-transfer coefficients, 1009

Natural convection

description, 386

enclosed spaces, 414–415

introduction, 408–409

non-Newtonian fluids, 427

outside vertical planes, 388–389

simplified equation, 412–413

from various geometries, 409–415

vertical walls of ovens, 410–411

Natural gas

composition, 801

isothermal flow, 127

Navier–Stokes equations

boundary-layer flow, 252

differential equations, 239–240, 246



Newtonian fluids, 206

Negligible internal resistance, systems with, 334–337

Neoprene membranes, hydrogen diffusion through, 532–533

Nernst–Haskell equation for diffusion coefficients for liquids, 503

Net positive suction head required (NPSH) for pumps, 168–169

Newtonian fluids

motion equations, 204–207

shear-stress components, 205

Newtonian heating and cooling method, 335

Newtons

cgs system, 7

English system, 7

SI system, 6

Newton's equation for momentum transfer, 488

Newton's law of viscosity, 50–52

Newton's second law in momentum balance, 81–82

Nicotine ( $\text{C}_{10}\text{H}_{14}\text{N}_2$ ) with immiscible liquids, extraction of, 894–896

Nitric oxide (NO) molar heat capacity, 19, 269

Nitrobenzene ( $\text{C}_6\text{H}_5\text{NO}_2$ ) heat capacity,  
1135

Nitrogen ( $\text{N}_2$ )

diffusion coefficients, 495

diffusivity and permeability, 535

heating, 19–20

helium in, molecular diffusion of, 490–  
492

molar heat capacity, 18–19, 267–268

in natural gas, 801

permeability in symmetric membranes,  
761

thermal conductivity, 280

transition-region diffusion, 542–543

Non-Newtonian fluids, 220

description, 53–54

flow properties, 232–233

friction losses, 226–228

heat transfer inside tubes, 424–427

introduction, 424

natural convection, 427

notation, 238

power requirements in agitation and  
mixing, 234–235

problems, 236–237

references, 237–238

summary, 235–236

time-dependent, 222

time-independent, 221–226

types, 221

velocity profiles, 103, 229–232

viscoelastic, 223

Noncircular conduits

friction loss, 123

heat-transfer coefficient, 398

Nonisothermal absorption towers, heat  
balance in, 683–685

Nonrigid spheres, drag coefficient for, 957

Nor-Pac packing factors, 651

Norton Intalox packing factors, 651

Nozzles

flow rate in tanks, 80–81

momentum balance, 85–86

Nucleate boiling, 416–417

Nucleation rate in crystallization, 940–942

Nucleation theories in crystallization, 935–936

Numerical methods

falling-rate drying periods, 1062–1063

gaseous membrane systems, 787–798

for integration, 28–29

steady-state conduction in two  
dimensions using, 318–325

steady-state mass transfer, 550–556

thermal process evaluation, 1093

unsteady-state conduction, 355–366

unsteady-state mass transfer diffusion,  
577–582

Nusselt number

convection, 391

convective mass transfer, 605

mass-transfer analysis, 594

natural convection, 413

## **O**

### **Oil**

from meal, countercurrent leaching,  
997–998

metering flows, 134–135

Oil droplets settling velocity, 955–956

### **Olive oil**

thermal conductivity, 280

viscosity, 54

Open channels, pipe flows in, 137–138



Open kettle evaporators, 1004

Open-pan solar evaporators, 1006

Operating cycles in ion exchange, 923–924

Operating-line derivation

packed towers, 656–657

plate absorption towers, 654–655

Operating-line equation for immiscible liquids, 896–898

Operating reflux ratio in distillation

McCabe–Thiele method, 829

multicomponent, 859–862

Optimum reflux ratio for distillation,

Orange juice concentration, 14

Oranges, temperature in freezing weather, 380

Organic materials, leaching processes for, 985

Orifice meters, 133–135

Orthorhombic system crystals, 929

Oslo crystallizers, 935

Osmosis

membrane separations, 732

reverse. *See* Reverse osmosis

Osmotic pressure

solutions, 739

ultrafiltration, 735

Ostwald–de Waele equation, 222

Ovens, natural convection from, 410–411

Overall coefficients combined with convection and conduction, 305–306

Overall heat transfer in heat loss, 306–308

Overall tray efficiency in distillation, 837

Oxidation of lactose, 27–28, 275–276

Oxygen concentration, dissolved in water, 629

## Oxygen (O<sub>2</sub>)

absorption in fermentation, 611–612

diffusion coefficient, 500

diffusivity and permeability, 535

molar heat capacity, 18–19, 267–268

permeability in symmetric membranes,  
761

## P

Packaging film, diffusion through, 534–  
535

Packed beds

concentration profiles in, 922

convective mass transfer, 607–610

of cylinders, surface area in, 151

flow in, 150–156, 408

through-circulation drying in, 1074–1078

Packed towers

absorption and distillation

acetone, 664–667

concentrated mixtures in, 675–679

description, 647, 810

analytical equations, 658–660, 670–672

design, 656–672

dilute gas mixtures in, 662–664

film and overall mass-transfer  
coefficients, 660–662

limiting and optimum flow rate ratios,  
658

liquid–liquid extraction, 882–886, 898

mass-transfer coefficients, 679–682

operating-line derivation, 656–657

pressure drop and flooding, 649–654

transfer units, 668–672

Paddle agitators

description, 177–178

with no baffles, heat transfer in, 428

Paddle-wheel meters, 136

Pall rings

for absorption and distillation, 648,  
810–811

liquid–liquid extraction, 882

packing factors, 651

Pan evaporators, 1004

Paper-pulp waste liquors, evaporation  
of, 1029

Parallel black planes, radiation heat  
transfer in, 468–469

Parallel-counterflow heat exchangers,  
445–446

Parallel disks, radiation between, 474–476

Parallel-feed multiple-effect evaporators, 1008

Parallel gray planes

radiation between, 477

radiation heat transfer in, 469–470

Parallel plates

flow between

bulk velocity, 98

differential equations, 207–210

mean beam length for gas radiation, 480

Partial condensers in distillation, 836



Partial pressure and humidity, 696

Partial time derivatives in differential equations, 197

Particle-fluid separation. *See* Settling and sedimentation

Particle mixture flow in packed beds, 154–155

Particle movement through fluids, 953–957

Particulate fluidization, 156–157

Pascals (Pa), 6

Pastes in agitation, 191–192

Pasteurization, 1094–1095

Pea purée, transient heat conduction in, 346

Peclet number in convection, 401

Penetration theory for convective mass transfer, 617

Percentage humidity

description, 696

drying, 1041

Perforated-plate towers, 886–887

Performance of reverse osmosis, 744

Permeability

diffusion in solids, 533–535

gaseous membrane systems, 761–762

membrane separations, 742–743

reverse osmosis, 745

Permeance in gaseous membrane systems, 762

Permeation in gaseous membrane systems, 794–798

Perpendicular rectangles view factors, 478

Pharmaceuticals production, 985

Phase rule

distillation, 805–806

and equilibrium, 627–628

liquid–liquid extraction, 875–876

Phenol in wastewater, adsorption isotherm for, 910

Pipe flows

compressible gases, 125–130

convection in, 387–389

diameter calculations, 113–114

entrance section of pipes, 123–125

forced convection heat transfer inside, 394–402

heat loss from, 303–304

mass transfer, 601–602

measurements

flow-nozzle meters, 135

miscellaneous meters, 136–137

orifice meters, 133–135

pitot tubes, 129–131

rotameters, 136

venturi meters, 131–133

momentum balance in bends, 87

notation, 143–144

in open channels and weirs, 137–138

pipe sizing, 125

pressure drop and friction loss

in expansion, contraction, and pipe fittings, 116–122

gas flow, 114–115

heat transfer effects, 115–116

laminar flow, 107–110

noncircular conduits, 123

turbulent flow, 110–114

problems, 139–142

references, 142–143

Reynolds number, 57

shell momentum balance in, 91–93

summary, 138–139

velocity in steel pipes, 125

velocity profiles, 106–107

Pitot tubes, 129–131

Plait point in liquid–liquid extraction,  
876

Planck's equation for freezing, 369–372

Planck's law for radiation heat transfer,  
466–467

Plane walls

heat generation in, 313–314

in series, heat transfer through, 287–288

Planes to hemispheres, view factors  
from, 474

Plate-and-frame filter presses, 718–720

Plate towers

for absorption and distillation, 646,  
654–656

liquid–liquid extraction, 881

## Plates

distillation tray efficiency, 837

flat. *See* Flat plates

natural convection from, 410, 412–413

with negligible surface resistance,  
average temperature, 354–355

Point efficiency for distillation trays,  
838

Poiseuille's equation. *See also* Hagen-  
Poiseuille's equation



capillary flow, 1070

fluids through filter cakes, 722

Polarization in reverse osmosis, 745

Polystyrene cation, 920

Polytropic compression for gas-moving pumps, 176

Population-density function for crystals, 938

Population material balance for crystals, 938

Population-model approach for crystallization, 940

Pores in capillary flow, 1070

Porosity in particulate fluidization, 156–157

Porous silica, potassium chloride diffusion in, 536

Porous solids

capillary movement in, 1056

gas diffusion in, 537–544, 732

liquid diffusion in, 536–537

Positive displacement flow meters, 137

Positive-displacement pumps, 171–172

Potassium chloride (KCl)

diffusion coefficient, 500

diffusion in porous silica, 536

diffusivity, 503–505

Potassium nitrate ( $\text{KNO}_3$ )

crystallization, 15–16

solubility curve, 930

Potential energy in energy-balance equations, 69

Potential flow, 241–245

Potential function, velocities from, 244–245

Poundal units, 38

Powders in agitation, 191–192

Power

agitated vessels, 180–183

agitation and mixing of Non-Newtonian fluids, 234–235

constants and conversion factors, 1109

crystal size reduction, 944–945

pumps, 167

SI system, 6

Prandtl mixing length

convection, 393–394

convective mass transfer, 615–616

overview, 257–258

Prandtl number

convection, 386–387, 390–391, 395–396

convective mass transfer, 596–597, 605

gases, 1130

mass-transfer coefficients, 594

## Prediction

adsorption, 917

constant-rate drying period, 1060–1061

diffusivity

albumin, 507

with binding present, 508

biological solutes, 507

electrolytes in liquids, 503–505

gases, 494

liquids, 500–503

small solutes in protein solution, 507–508

mass-transfer film coefficients, 680–682

packed tower flooding, 883–885

reverse osmosis performance, 744

time for batch leaching, 987–988

## Pressure

compressible gas pipe flow, 125–126

constants and conversion factors, 1109

in evaporation, 1004

expressing, 10

flow rate, 79–80

fluid statics, 38

fluids, 39–42

and humidity, 696–697

measurements, 43–47

momentum balance, 83

pumps, 78

shell momentum balance in pipes, 91

SI system, 6

single-effect evaporators, 1012

standard conditions of, 11

storage tanks, 41–42

ultrafiltration, 735–736

vapor, 12–13

in vessels, 45–46

and viscosity, 54

Pressure drop

ammonia absorption, 652–654

fluidized beds, 157–158

fluids through filter cakes, 722–724

gas flow, 110–114

laminar flow, 107–110

packed bed flow, 153–154

packed tower absorption and stripping,



649–654

permeation effects, 794–798

power-law fluids, 225–226

turbulent flow, 110–114

Pressure ratio in gaseous membrane systems, 784–786

Pressure-swing cycle in adsorption, 918

Printing pigment rheological constants, 231

Processing variables

adsorption, 918

constant-rate drying period, 1061–1062

gaseous membrane systems, 784–785

ion exchange, 923–924

single-effect evaporators, 1012

ultrafiltration, 737–738

Propionic acid ( $\text{C}_3\text{H}_6\text{O}_2$ ) diffusion  
coefficient, 500

Pseudoplastic fluids

description, 222

velocity profiles, 229–230

Psychrometric ratio, 702–703, 1048

Pulsed packed towers, 883, 887

Pulsed sieve tray towers, 883, 887

Pumps

friction losses, 121

gas-moving

centrifugal, 169–171

characteristics, 167–172

gas compression equations, 174–176

introduction, 166–167

machinery, 172–174

horsepower in flow systems, 77–79

in mechanical-energy balance, 76–77

notation, 195

problems, 193–194

references, 194–195

summary, 192

## **R**

Radiation heat transfer

in absorbing gases, 479–482

basic equation, 461–463

basic mechanism, 284–286

combined with convection, 290–291

constant-rate drying period, 1065–1068

to furnace enclosures, 480–481

gas temperature measurement, 464–465

introduction, 461–462

to metal tubes, 286–287, 464

notation, 485–486

between parallel disks, 474–476

problems, 482–485

references, 485

to small objects, 286–287, 463–464

to small packages, 478

spectrum, 465–468

summary, 482

view factor derivations, 468–479

Raffinate layer in liquid–liquid  
extraction, 876

Random-packed towers, 672–674

Random packing for absorption and distillation, 647–652, 810

Random-walk process in molecular diffusion, 489

Rankine ( $^{\circ}\text{R}$ ) temperature, 8

Raoult's law

boiling-point diagrams, 806–808

distillation, 805–806, 813

Raschig rings

absorption and distillation, 810–811

liquid–liquid extraction, 882

packing factors, 651

shape factors, 155

Rate equations for water-cooling towers,  
704–707

Rate of accumulation in mass balances,  
65

Rate-of-drying curves, 1052

Rate of heat transfer in jacketed kettles,  
417–419

Rates, leaching, 986–988

Rayleigh equation for distillation, 816

Reboilers in distillation, 841

Reciprocating pumps, 171–172

Recompression in evaporation, 1029–

1030

Rectangular coordinates

liquid–liquid extraction, 876

motion equations, 206

Rectification in distillation

benzene–toluene mixtures, 825–827

description, 814–815

McCabe–Thiele method, 831, 833–836

Recycle process for material balances,  
15–16

Reflux in distillation

introduction, 818–819



McCabe–Thiele method, 820–825, 827–830

multicomponent, 855–859

Reject stream in gaseous membrane systems, 770

Relative humidity

description, 696

drying, 1041–1042

Relative-molar-selectivity coefficients in ion exchange, 920–921

Relative volatility

benzene–toluene systems, 814

vapor–liquid systems, 813–814

Reradiating walls, view factors for, 476

Resin adsorbents, 908

Resins for ion exchange, 918–919

Resistances

dialysis, 747–749

fluids through filter cakes, 724–725

gaseous membrane systems, 759–760

at interfaces, 312–313

Return bend fittings, friction losses in,  
117

Reverse osmosis

complete-mixing model, 746–747

concentration polarization, 745

equipment for, 745–746

flux equations, 740–743

introduction, 738–740

membrane separations, 732

operating variables, 743–744

permeability constants, 745

prediction of performance, 744

Revolving grinding mills, 947

Reynolds analogy for convective mass transfer, 596–597

Reynolds number

agitation, 180

boundary-layer flow, 251

convection, 386–387, 392, 397–399,  
428

convective mass transfer, 605–606,  
609–610

description, 55–56

differential equations of motion, 241,  
246

flow in fluidized beds, 157–158

flow in packed beds, 152–153

flow in pipes, 57, 106–107

flow past immersed objects, 147–148

fluid flow measurements

flow-nozzle meters, 135

venturi meters, 132

friction losses in mechanical-energy-  
balance equation, 119

heat transfer flow in packed beds, 408

hindered settling, 958

mass-transfer coefficients, 594–595

metering of small liquid flows, 109

particle movement through fluids, 954–  
955

power requirements for non-Newtonian  
fluids, 235

time-independent fluid flows, 225

turbulent flow

boundary layer, 263

friction factor, 111

friction losses, 227–228

intensity, 255

velocity distribution, 259

Reynolds stresses for turbulent flow,  
256

Rheological constants for Bingham  
plastic fluids, 230–231

Rheology, 54

Rheopectic fluids, 222

Rigid spheres, particle movement through, 953–956

Roll crushers, 947

Rotameters for fluid flow measurements, 136

Rotary blowers in gas-moving pumps, 174

Rotary dryers, 1038

Rotary pumps, 172

Rotating liquid in cylindrical containers, 215–216

Rotational speeds in centrifugal separation, 968

Rotational viscometers, 232–233

Rubbing solids, 943

Rubes, flow past banks of, 405–406

## **S**

Salt solutions, osmotic pressure of, 739–740

Sand

shape factors, 155

void fractions, 157

Saturated ice–water vapor pressure,  
1115

Saturated steam properties, 1116–1119

Saturation, adiabatic temperature, 700–701, 1046–1047



Scalars in differential equations of continuity, 198

Scale deposition in evaporation, 1004

Scale-up

agitators, 183–186

centrifugal separation, 972–973

fixed-bed adsorption columns, 913–917

ion exchange, 922–924

Scheibel towers, 883, 888

Schmidt method

slabs, 357, 577–578

unsteady-state conduction, 358–362

Schmidt number

convective mass transfer, 593, 596, 605, 610

gases, 497–498

Scraped surface crystallizers, 934

Scraped-surface heat exchangers, 430–431

Seconds (s)

cgs system, 7

SI system, 6

Sedimentation. *See* Settling and sedimentation

Selectivity coefficient in ion exchange,

920–921

Semi-infinite medium for unsteady-state mass transfer diffusion, 575–576

Semi-infinite slabs for unsteady-state mass transfer diffusion, 574–575

Semi-infinite solids for unsteady-state conduction, 339–340

Separation processes

centrifugal. *See* Centrifugal separation processes

classification, 4–5

gas

complete mixing model for, 765–770

cross-flow models, 773–779

membranes and permeabilities for, 760–765

membrane systems. *See* Membrane separations

Series resistances

dialysis, 747–748

gaseous membrane systems, 759–760

Settling and sedimentation

centrifugal separation processes. *See* Centrifugal separation processes

differential settling and separation of solids in classification, 959–963

equipment for, 964–966

hindered settling, 957–959

introduction, 953

notation, 982–983

particle movement through fluids, 953–957

problems, 980–982

references, 982

sedimentation and thickening, 963–964

summary, 979–980

velocity

oil droplets, 955–956

sedimentation, 963

wall effect on free settling, 959

Settling tanks, 964–965

Shanks leaching system, 988

Shape factors

flow in packed beds, 154–155

steady-state conduction in two  
dimensions using, 315–318

Shear stress

liquids, 52–53

Newtonian fluids, 204–205

non-Newtonian fluids, 103, 232

turbulent flow, 256

Shelf dryers, 1036

Shell-and-tube heat exchangers, 445

Shell momentum balance

falling films, 93–96

introduction, 90–91

pipes, 91–93

Sherwood number, 596, 605

Short cylinders, two-dimensional  
conduction in, 352–354

Short-tube evaporators, 1005, 1009

Shrinkage in rate-of-drying curves, 1056

SI system units, 6

Side streams, rectification towers with,  
834–835

Sieve tray towers, 883, 886–887

Sieve trays, 646, 808–809, 818

Sigma values for centrifugal separation,  
972–973

Silica and galena mixture, separation of,  
961–963

Silica gel adsorbents, 908

Simple batch distillation, 815–817

Simple steam distillation, 817–818

Simpson's rule for numerical



integration, 28–29

Single-effect evaporators

boiling-point rise of solutions, 1013–1014

description, 1006–1007

enthalpy-concentration charts of solutions, 1014–1016

heat and material balances, 1010–1012

processing variables, 1012

Single spheres, flow past, 404

Single-stage equilibrium contact

carbon dioxide–air–water, 630–631

gas–liquid systems, 630

overview, 629–630

for vapor–liquid systems, 811–812

Single-stage equilibrium extraction,  
878–880

Single-stage leaching, 992–994

Sink-and-float methods, 959

Size

crystals

average, 940

distribution, 937–938

measurements, 943

mechanical size reduction, 942–947

solubility, 935

pipes, 125

Skin drag

boundary-layer flow, 251–252

flow past immersed objects, 146

Slabs

agar gel, unsteady-state diffusion in,  
573–574

butter, conduction in, 342–343, 346

semi-infinite, unsteady-state diffusion  
in, 574–575

unsteady-state conduction, 355–357

unsteady-state molecular diffusion, 577–

wood, drying, 1070

Slugging in fluidized beds, 156

Slurry streams, leaching, 991

Small liquid flows, metering, 108–109

Small objects and packages, radiation  
to, 286–287, 463–464, 478

Small solutes in protein solution,  
diffusivity prediction of, 507–508

Sodium chloride (NaCl)

diffusivity, 545

heat capacity, 1135

osmotic pressure, 739–740, 744

solubility curve, 930

Sodium hydroxide ( $\text{NaOH}$ )

boiling point, 1014

evaporation in solutions, 1014–1016

weight fraction and mole fraction, 9

Sodium thiosulfate ( $\text{Na}_2\text{S}_2\text{O}_3$ ) solubility curve, 930

Solar evaporators, 1006

Solids

diffusion in, 536–537

energy change energy, 375

heat capacity, 1140

leaching. *See* Leaching

molecular diffusion in, 531–537

separation, in classification, 959–963

in series or parallel with convection,  
conduction through, 305–313

surface force in momentum balance, 83

thermal conductivity, 282

## Solubility

crystallization, 930, 935

evaporation, 1003

steady-state mass transfer, 533–534

Solutes, leaching, 986, 995

Solutions boiling-point rise in single-effect evaporators, 1013–1014

Solvent extraction

description, 874–875

phase amounts, 879–880

Solvent flows, 894, 897

Soybeans, 993–994

Special heat-transfer coefficients in convection, 427–435

Specific gravity of liquids, 10

Specific heat

description, 266

gases, 18–20

Specific volume in saturated steam,  
1116–1119

## Spheres

average temperature, 354–355

characteristic dimension, 335

convective mass transfer, 604–607

cooling, 404

diffusion from, 525–526

flow past, 148, 404

force on, 149

hindered settling, 958–959

mean beam length for gas radiation, 480



particle movement through, 953–957

steady-state conduction through, 304–305

unsteady-state conduction in, 349–351

Spherical coordinates

continuity equations, 201–202

motion equations, 206–207

shear-stress components for Newtonian fluids, 205

Sphericity in packed bed flow, 154–155

Spiral-wound membranes, 762–763

Spitzkasten classifiers, 965

Spray dryers, 1039

Spray towers, 881–883

Square rods, characteristic dimension of, 335

Stages

countercurrent extraction, 891–893

multicomponent distillation, 859–862

Stagnation points

flow past immersed objects, 147

fluid flow measurements, 129

Standard acceleration of gravity, 1108

Standard conditions of temperature and pressure (STP or SC), 11

Standard heats

combustion, 1125

formation, 1124

Stanton number, 596

Static pressure heads in gas-moving pumps, 172

Station mixers in agitation, 190

Stationary shell devices in agitation, 191

Steady-state conduction, 299

cooling coil tubes, 302

critical thickness of insulation for cylinders, 311

through flat slabs and walls, 299–300

through hollow cylinders, 301

through hollow spheres, 304–305

with internal heat generation, 313–315

log mean temperature difference, 308–310

multilayer cylinders, 303

notation, 331

problems, 327–330

references, 330–331

through solids in series or parallel with convection, 305–313

summary, 326

in two dimensions

using numerical methods, 318–325

using shape factors, 315–318

in two directions, 321–324

Steady-state flow systems in energy  
balance, 70–71

Steady-state heat transfer, 277–278

Steady-state mass transfer, 519

diffusion in biological gels, 544–546

diffusion of gases in porous solids and  
capillaries, 537–544

molecular diffusion

gases, 519–527

liquids, 528–531

solids, 531–537

notation, 567

numerical methods, 550–556

problems, 558–566

references, 566

special cases of general diffusion  
equation, 546–550

summary, 557–558

Steady-state processes, 13

Steam

distillation, 817–818

heat-transfer coefficient, 283, 428

properties, 1116–1120

water heated by, 398–400

Steam boilers, energy balance on, 73–74

Steam injection, rectification with, 833–836

Steam pressure in single-effect evaporators, 1012

Steam stripping in adsorption, 918

Steam tables, 20–21, 269–270

Steel balls, cooling, 336

Steel pipes

dimensions, 1151–1152

velocities in, 125

Stefan–Boltzmann equation, 463, 467

Stefan–Maxwell method, 527

Sterilization

biological materials, 1088–1095

cans of food, 1092, 1094

Stirred tanks mass balances, 66–67

Stockmayer potential for diffusion  
coefficients for gases, 496

Stokes–Einstein equation

diffusion coefficients for liquids, 500

diffusivities for biological solutes, 507

diffusivities in liquids, 500

Stokes's law



flow past immersed objects, 148

gas–solid cyclone separators, 978

hindered settling, 957

settling, 960

Storage tank pressure, 41–42

Straight line for falling-rate drying periods, 1064

Stream function, 240–241

flow field, 244

velocities from potential function, 244–245

Streamlines, 147, 240–243

Stripping. *See* Absorption and stripping

Stripping-column distillation, 831

Stripping factor in countercurrent stage contact, 635

Stripping sections for distillation

equations, 822–823

fractional, 846, 850

Stripping tower trays, 832

Structured packed towers

efficiency of, 672–674

liquid–liquid extraction, 883

Structured packing for absorption and distillation, 646–647, 809

packing factors, 651

pressure drop, 649–650

Submerged spheres, force on, 149

Substantial time derivatives in  
differential equations of continuity, 197

Sucrose ( $C_{12}H_{22}O_{11}$ ) diffusivity, 545

Suction lift of pumps, 168–169

Sudden enlargements, friction loss in,  
88

Sugar-beet leaching, 989

Sugar solutions in evaporation, 1018–  
1026, 1028–1029

Sulfur dioxide ( $SO_2$ )

absorption in tray towers, 655–656

molar heat capacity, 18–19, 269

thermal conductivity, 1135

viscosity, 54

water system equilibrium data, 1143

Sulfur trioxide ( $\text{SO}_3$ ) molar heat capacity, 19, 269

Sulfuric acid heat capacity, 1135

Sulzer packing factors, 651

Supercentrifuges, 975

Superheated steam, 1119–1121

Supersaturation in crystallization, 933, 936

Surface area in packed beds of

cylinders, 151

Surface condensers in evaporation, 1026

Surface conditions in unsteady-state  
mass transfer diffusion, 571–572

Surface diffusion in gases in porous  
solids, 544

Surface reactions in steady-state mass  
transfer, 547–548

Surfaces, emissivity of, 1142

Suspended particles in convective mass  
transfer, 610–613

Suspension of solids in agitation, 189

Symmetric membranes, 760, 785

Synthetic polymer adsorbents, 908

Systems, defined, 63

Systems with negligible internal resistance, unsteady-state heat transfer in, 334–337

## T

Tank crystallizers, 934

Tapioca flour, 31

Tapioca root diffusion coefficient, 1073

Tee fittings, friction losses in, 117–118

Temperature

adiabatic saturation, 700–701

constant-rate drying period, 1061

constants and conversion factors, 1112

drying, 1046–1048

English system, 7

equilibrium moisture content of  
materials, 1050

evaporation, 1004, 1027

expressing, 8

gases, radiation effects on, 464–465

and humidity, 696

objects with negligible surface  
resistance, 354–355

SI system, 6

single-effect evaporators, 1007, 1012

standard conditions of, 11

and viscosity, 54

water-cooling tower air stream, 711

water density, 1114

wet bulb, 701–703

Temperature correction factor for heat exchangers, 449

Temperature drops

in conduction, 308–309

multiple-effect evaporators, 1017

Temperature sensitivity of materials in evaporation, 1003



Temperature-swing cycles in adsorption, 918

Terminal velocity in particle movement through fluids, 954

Tetragonal system crystals, 929

Theoretical power in pumps, 167

Theoretical stages for distillation, 820–827

Thermal boundary layer for convection, 392–393

Thermal capacitance in unsteady-state heat transfer, 335

Thermal conductivity. *See* Conduction and conductivity

Thermal death-rate kinetics of  
microorganisms, 1089–1090

Thermal-gas mass flow meters, 137

Thermal processing and sterilization of  
biological materials, 1088–1095

Thermal radiation, 461

Thermal vapor-recompression  
evaporators, 1030

Thermochemistry, 21, 270

Thermodynamics, first law of, 68

Thermopane, 297

Thickeners in settling and  
sedimentation, 966

Thickening in sedimentation, 963–964

## Thickness

falling film velocity, 96

insulation for cylinders, 311

of solids, constant-rate drying period,  
1062

Thixotropic fluids, 222

Three-blade propeller agitators, 177

Three-dimensional systems, unsteady-  
state conduction in, 349, 352

Through-circulation drying in packed  
beds, 1074–1078

## Time

batch leaching, 987–988

drying, 1057–1058

filtration, 728–729

sterilization, 1090–1095

Time-dependent fluids, 222

Time derivatives in differential equations, 197–199

Time-independent fluids, 221–226

Toluene heat capacity, 1135

Tortuosity in diffusion

gases in porous solids, 544

liquids in porous solids, 536–537

Total amount of heat transferred in  
unsteady-state heat transfer, 337

Total cycle time in filtration, 728–729

Total enthalpy for air–water vapor  
mixture, 698, 1043

Total reflux in distillation

McCabe–Thiele method, 827–828, 830

multicomponent, 855–859

Total time derivatives in differential  
equations, 197

Towers

for ammonia absorption, diameter of,  
652–654

liquid–liquid extraction

design, 896–898

mechanically agitated, 888–889

packed, 882–886

perforated-plate, 886–887

spray, 881–882

multicomponent distillation, 851

packed. *See* Packed towers

plate

absorption and distillation, 646, 654–656

liquid–liquid extraction, 881

tray

absorption and distillation, 646

diameter, 839–841

efficiency, 673–674

sulfur dioxide absorption in, 655–656

water cooling. *See* Water-cooling towers

Transfer coefficients in constant-rate  
drying period, 1058

Transfer units

packed towers, 668–672

water-cooling towers, 711

Transient heat conduction in cans of pea  
purée, 346

Transition flow inside pipes, heat-transfer coefficient for, 394–395

Transition regions

convective mass transfer, 613

diffusion

gases, 539–541

helium and nitrogen, 542–543

Reynolds number, 56

Transverse fins for heat transfer, 431

Tray dryers

description, 1036

with varying air conditions, 1078–1079



Tray efficiency

distillation, 836–838

perforated-plate towers, 887

Tray towers

absorption and distillation, 646

diameter, 839–841

efficiency, 673–674

sulfur dioxide absorption, 655–656

Trays

absorption and distillation, 646

analytical equations for packed towers,  
658–660

description, 646

distillation columns, 818

efficiency, 836–838

liquid–liquid extraction, 898

location and number of, 824–825

overview, 808–809

plate absorption towers, 654–655

stripping towers, 832

Triangular coordinates for liquid–liquid extraction, 875–876

Trichloroethane with water, extraction of acetone from, 899–901

Triclinic system crystals, 929

Trigonal system crystals, 929

Triple-effect evaporator calculations,  
1018–1026

Tuberculosis, 1094

Tubes

banks of, heating air by, 406–407

circular, laminar flow in, 211–212

combined radiation and convection  
from, 290–291

condensation on, 422–423

convective mass transfer, 602

for cooling coils, 302

heat-exchanger, dimensions, 1152

liquid metals, heat transfer inside, 401–402

mean beam length for gas radiation, 480

with path length change, diffusion in, 524

radiation to, 464

time-independent fluid flows in, 225

Tubular centrifuges, 975

Tunnel dryers, 1037–1038

Tunnels, force on cylinders in, 149

Turbine agitators

description, 178–179

design, 180, 185–186

mixing times, 188–189

Turbine wheel meters, 136

Turboblowers for gas-moving pumps,  
174

Turbulent diffusion equations for  
momentum, heat, and mass transfer,  
488–489

Turbulent flow

analysis, 260–263

average velocity, 98

description, 51, 55

eddy mass diffusivity, 615–616

eddy thermal diffusivity, 393–394

friction losses, 227–228

heating of air in, 396–397

kinetic-energy velocity correction  
factor, 72–73

nature and intensity, 254–255

packed beds, 152–153

in pipes, convective mass transfer, 601

Prandtl mixing length, 257–258

pressure drop and friction loss in, 110–  
114

Reynolds stresses, 256

in tubes, heat transfer, 426–427

universal velocity distribution, 258–260

Turbulent mixers in convective mass transfer, 613

Turbulent regions in convective mass transfer, 587

Two-bulb method for gas diffusion coefficients, 493–494

Two dimensions

conduction

numerical methods, 318–325

shape factors, 315–318

in short cylinders, 352–354

unsteady-state, 349, 352

steady-state mass transfer numerical

methods, 550–556

Two directions, steady-state conduction  
in, 321–324

Two-fluid U tubes for pressure  
measurements, 45

Tyler standard screen scale, 1153

## U

U-tube manometers, 44–45

Ultracentrifuges, 975

Ultrafiltration

equipment for, 735

flux equations, 735–737



introduction, 734–735

process, 732

processing variables, 737–738

Unaccomplished moisture change in  
drying, 1071

Unbound water in solids, equilibrium  
moisture content of materials, 1051

Underflow streams in leaching, 991,  
995–999

Union fittings, friction losses in, 117

Units

cgs system, 6–7

dimensionally homogeneous equations,

7–8

energy and heat, 17–23

English system, 6–7

fluid statics, 37–38

force, 38–39

liquids, 10

mole, 8–9

SI system, 6

weight and mass, 8–9

Universal velocity distribution in  
turbulent flow, 258–260

Unsteady-state heat transfer

analytical methods, 337–339

basic equation, 332–334

chilling and freezing of food and  
biological materials, 366–372

conduction equation, 333–334

convective boundary conditions, 363–  
365

cylinders, 365–366

differential equation of energy change,  
372–376

with digital computers, 362–363

large flat plates, 342–345

long cylinders, 346–348

notation, 383–384

numerical finite-difference methods,  
355–366

problems, 378–383

references, 383

Schmidt method, 358–362

semi-infinite solids, 339–340

slabs, 355–357

spheres, 349–351

summary, 376–378

systems with negligible internal  
resistance, 334–337

two- and three-dimensional systems,

349, 352

Unsteady-state mass transfer, 568

diffusion. *See* Diffusion

notation, 585

problems, 583–584

references, 585

summary, 582–583

Unsteady-state thermal processing and  
sterilization of biological materials,  
1088–1095

Urea

diffusion coefficient, 500

diffusion in agar, 545–546

removal from blood, 750–751

## **v**

Vacuum-drum filters, 721

Vacuum-shelf indirect dryers, 1037

Valve-tray absorption towers, diameter of, 840–841

Valve trays, 646, 809

Valves, friction losses in, 117–118

van der Waals adsorption, 908

Vapor–liquid systems

equilibrium contact, 812–813

relative volatility, 813–814

single-stage equilibrium contact, 811–812

Vapor pressure

alcohols, 870

description, 12–13

humidity, 696–697, 1042

saturated ice–water vapor, 1115

water

drying, 1040–1041

introduction, 694–695

temperature factors, 1113

Vapor recompression in evaporation, 1029–1030

# Vaporization

convective mass transfer, 590–591

latent heat of, 21, 269

Vapors, thermal conductivities of, 1135

Variable-area flow meters, 136

Variable underflow in countercurrent  
multistage leaching, 995–998

Varying air conditions, tray drying with,  
1078–1079

Varying cross-sectional areas, diffusion  
through, 524–527

Varying temperature drop in  
conduction, 308–309



Vector notation in differential equations, 197–199

Vegetable materials, leaching, 985

Velocity

flow between parallel plates, 98

fluid measurements

orifice meters, 133–135

pitot tubes, 130–131

venturi meters, 131–133

in fluidized beds, 156–160

mass balances, 67–68

particle movement through fluids, 954

from potential function, 244–245

sedimentation, 963

in steel pipes, 125

turbulent flow, 258–260

Velocity potential, 241–245

Velocity profiles

laminar flow, 90–96

non-Newtonian fluids, 103, 229–232

pipe flows, 106

Venturi flow meters, 131–133

Vertical natural-circulation evaporators,  
1004–1005, 1009

## Vertical planes

natural convection from, 409–415

natural convection outside, 388–389

Vertical surfaces in film-type  
condensation, 419–422

Vertical tubes, condensation on, 422–  
423

Vertical walls of ovens, natural  
convection from, 410–411

## Vessels

heat transfer in, 430

pressure measurements, 45–46

View factor derivations in radiation heat

transfer, 468–479

Viscoelastic fluids, 221, 223

Viscometers, 232–233

Viscosity

agitators, 179

constants and conversion factors, 1110

fluids, 50–54

foods, 1149–1150

gases, 1127, 1131–1132

leaching, 995

Lennard-Jones potentials from, 1154–  
1155

liquids, 139, 1136–1138

motion equations of Newtonian fluids,  
204–207

water, 1114

Viscous flow, 55

Viscous forces, 51

Viscous materials in agitation, 191–192

Viscous sublayer in turbulent flow, 260

Visible radiation, 466

Voids in fluidized beds, 156–157

Volatility of vapor–liquid systems, 813–  
814

Volume

air–water vapor mixture, 697

constants and conversion factors, 1107–  
1108

von Kármán analogy for convective  
mass transfer, 598

von Kármán method in boundary-layer  
analysis, 260

Vortex-shedding flow meters, 137

Vorticity, 242

Votator heat exchangers, 430

## **W**

Wake formation in boundary-layer flow,  
252

Wall drag, 146

Wall effect on free settling, 959

## Walls

conduction through, 299–300

heat transfer through

cold rooms, 288–289

insulating walls, 279–280

plane walls in series, 287–288

radiation view factors, 476

## Washing

filter cakes, 728–729

in leaching, 984

Wastewater, phenol in, adsorption isotherm for, 910

Water

acetone equilibrium data, 1144

ammonia equilibrium data, 1144

carbon dioxide concentration in, 687

density, 1114

diffusion coefficient, 500

diffusion of ethanol through, 530–531

diffusion through stagnant, nondiffusing air, 523

diffusivity and permeability, 535

dilute methanol in, diffusivity of, 513



dissolved oxygen concentration in, 629

emissivity, 286, 463

equilibrium moisture content of  
materials, 1051

equilibrium stage contact, 630–631

ethanol equilibrium data, 1145

fouling coefficients, 453–454

heat capacity

of ice, 1116

and temperature, 1115

heat-transfer coefficient, 283

heat-transfer properties, 1123

heated by steam, 398–400

Henry's law for gases in, 1143

latent heat of, 1113

methanol equilibrium data, 1144

molar heat capacity, 18–19, 267–268

saturated steam properties, 1116–1119

sulfur dioxide equilibrium data, 1143

superheated steam, 1119–1121

thermal conductivity, 280, 282, 1115

with trichloroethane, extraction of  
acetone from, 899–901

vapor pressure

drying, 1040–1041

ice–water vapor, 1115

introduction, 694–695

temperature factors, 1113

viscosity, 54, 1114

Water-cooling towers

air streams, 711

calculations, 704–707

description, 703–704

height of transfer units, 711

minimum value of air flow, 710–711

Water meters, friction losses in, 117

Water vapor heat-transfer properties,  
1123

Watts (W), 6

Weight fractions, 9

Weight units, 8–9

Weirs, pipe flows in, 137–138

Wet bulb temperature

drying, 1047–1048

and humidity, 701–703

Wetted-wall towers, flow inside, 602

Wien's displacement law, 467

Wilke–Chang correlation, 501

Wilson and Geankoplis correlations,  
607

Windows, Thermopane, 297

Wire anemometers, 255

Wood, drying, 1070

Work constants and conversion factors,  
1110

Work required in pumps, 167

## **x**

*x*-*y* plots in distillation, 806–808

Xylene heat capacity, 1135

## **y**

Yields in crystallization, 930–932

## **z**

Zeolites

adsorbents, 908

ion exchange, 918–919



## Register Your Product at [informit.com/register](https://informit.com/register)

Access additional benefits and **save 35%** on your next purchase

- Automatically receive a coupon for 35% off your next purchase, valid for 30 days. Look for your code in your InformIT cart or the Manage Codes section of your account page.
- Download available product updates.
- Access bonus material if available.\*
- Check the box to hear from us and receive exclusive offers on new editions and related products.

*\*Registration benefits vary by product. Benefits will be listed on your account page under Registered Products.*

---

### InformIT.com—The Trusted Technology Learning Source

InformIT is the online home of information technology brands at Pearson, the world's foremost education company. At InformIT.com, you can:

- Shop our books, eBooks, software, and video training
- Take advantage of our special offers and promotions ([informit.com/promotions](https://informit.com/promotions))
- Sign up for special offers and content newsletter ([informit.com/newsletters](https://informit.com/newsletters))
- Access thousands of free chapters and video lessons



Connect with InformIT—Visit [informit.com/community](https://informit.com/community)



Addison-Wesley • Adobe Press • Cisco Press • Microsoft Press • Pearson IT Certification • Prentice Hall • Que • Sams • Peachpit Press

